Graham T. Smith

Machine Tool Metrology

An Industrial Handbook

Springer

Machine Tool Metrology

Graham T. Smith

Machine Tool Metrology

An Industrial Handbook

Springer

Graham T. Smith, MPhil (Brunel), Ph.D (Birmingham), CEng, FIMechE, FIET
Emeritus Professor Industrial Engineering & Metrology
Southampton Solent University
Hampshire, England

ISBN 978-3-319-25107-3 ISBN 978-3-319-25109-7 (eBook)
DOI 10.1007/978-3-319-25109-7

Library of Congress Control Number: 2015952765

Printed on acid-free paper

This Springer imprint is published by SpringerNature
The registered company is Springer International Publishing AG Switzerland

Publishing History

Previous books for Springer Verlag Publishing—by the Author:

- Advanced Machining: The Handbook of Cutting Technology (1989);
- CNC Machining Technology series (1993)
  - Book 1: Design, Development and CIM Strategies;
  - Book 2: Cutting, Fluids and Workholding Technologies;
  - Book 3: Part Programming Techniques;
- CNC Machining Technology—Comprehensive Library Edition (1993);
- Industrial Metrology—Surfaces and Roundness (2002);
- Cutting Tool Technology—Industrial Handbook (2008).

Preface

This book concerns itself with the key scientific disciplines of *Machine Tool Metrology*, which has long been considered something of a Black-art by many industrial users for this type of machine tool plant and associated metrology equipment. Invariably, a highly-productive machine tool situated in certain unenlightened production shops has, in fact, probably never actually been reverified, or recalibrated since the day of its original delivery and installation. Such a lack of any form of verification and metrological testing procedures in today's industrial climate of continuously-improving machined component quality and its accompanying lean-production methods seems somewhat unthinkable. Nonetheless, such a lack of subsequent testing is habitually the case in many of these workshops, being a somewhat dubious practice which seriously needs addressing. This lack of some form of basic assessment and to a certain extent indifferent attitude to calibration issues in general, is one of the major reasons for this current undertaking on machine tool metrology. Quick health checks are made both speedily and efficiently nowadays with pertinent software updates to significantly improve both the machine and its kinematic performance by specific adjustments to the machine's CNC controller. These diagnostic and remedial actions should be a mandatory activity in any industrial, or high-quality research environment, where exceedingly accurate and precise components must be consistently manufactured or tested. Just as important as the fact that such expensive and sophisticated machine tools need to be regularly verified and recalibrated, the associated metrological artefacts for this machine verification must also have measurement capability critically assessed periodically making them traceable to the relevant International Standards. Instruments and equipment such as laser interferometers, telescoping ballbars, precision artefacts, coordinate measuring machines, together with a wide range of metrological hand tools must also be subject to this periodic reverification, so that any potential likelihood of uncertainty of measurement is effectively minimised.

The current text herein concerning topics relating to *Machine Tool Metrology*, has been principally written for the industrial practitioner, rather than as a comprehensive academic work for perhaps an applied researcher—the latter of whom

would normally require significantly more in the way of specific mathematical content, scientific analyses and academic rigour. Within this current level of industrial content, significant and considerable usage has been made of the existing published literature and valid information obtained from a wide spectrum of manufacturers of plant, equipment and instrumentation. In order to make the overall text (hopefully) easier to both read and comprehend, any of the metrological and calibration subjects discussed herein have been to a certain extent deconstructed, where applicable, into simple bullet-pointed explanatory lists with certain facts and words being overly stressed, somewhat more than would usually be necessary. Moreover, the mathematical treatment in certain circumstances has also been intentionally over-simplified, as much as possible, and this level of arithmetic brevity has been utilised where it was considered to be absolutely necessary.

Significant use has been made of a voluminous amount of footnotes utilised throughout all of the chapters, which it is hoped adds some additional, but relevant detail to the subject currently being mentioned at that instance—within the text. Moreover, in many circumstances, briefly the background of the scientific contributor, or originator of the topic under discussion has been mentioned, to add some added-value to their intensive and often life-time's work. As can be seen, an extensive amount of photographic support has also been incorporated into this book, thus enhancing the comprehension to the reader of the facts being discussed at that time. Furthermore, just a brief sample of the applicable references are also included at the end of each chapter, for any readers requiring perhaps more detailed information on the topics covered within the text, together with the relevant appendices that may also offer some additional technical clarification on both validation and testing issues concerning these metrological and calibration topics. An abridged list has also been supplied of some of the international metrology addresses for a wide range of countries, relating to their respective Standards Organisations and Metrology Laboratories. Finally, the international companies that have supplied information in this current text are duly acknowledged and their addresses are produced alphabetically for further reference, also at the end of this book.

Birchington-on-Sea, Kent, England Graham T. Smith

Acknowledgements

First and foremost, I must sincerely thank my dear wife Brenda, for proofreading and correcting this text as much as she could (without engineering knowledge!) and also for giving me both the time and space to write this latest technical book. Furthermore, her exhaustive efforts in additional commenting on this current text, is most gratefully appreciated even if glossed over!

An industrially based book must inevitably rely on the information and photographic support provided by some of the world's leading industrial and metrological companies. First and foremost, I must give mention to all the highest quality technical expertise I have encountered over the years from Renishaw plc (Wotton-under-the-Edge, in England) for their previous technical discussions and informative training courses on both laser interferometry and telescoping ballbars following my previous university employer purchasing a large range of their calibration and metrology equipment. Moreover, Renishaw plc have unstintingly provided their relevant technical literature and valid photographic images, without which this work would have been impossible to otherwise adequately cover, or to have any significant and relevant depth. Likewise, I would also like to extend my sincere thanks to the many vastly experienced technical personnel at both Taylor-Hobson plc and Spectrum Metrology (both of Leicester, England) for practical information and yet more valid technical discussions concerning their world class and wide range of metrology equipment, optical instrumentation and electronic levels. Likewise, the technically innovative company Hexagon Metrology (GmbH) has also provided a considerable amount of valid metrological information, which has considerably enhanced the topics concerning testing procedures within this text—their help and cooperation here is very much appreciated. In a similar manner, I would also like to extend my appreciation to the world-class company Heidenhain (GB) Ltd., also to their parent-organisation in Traunreut, Germany, who have furnished me with considerable technical information, for subsequent inclusion in the book. There have been any number of impressive and knowledgeable scientists and engineers at The National Physical Laboratory (Teddington, London) that have been very supportive in their previous scientific discussions and have also provided their valid and pertinent informative guides, references and literature sources that

have been thoroughly utilised throughout the book. This level of NPL involvement was demonstrably utilised in my previous book *Industrial Metrology—Surfaces & Roundness* and once again, their relevant information/technical input here is really most appreciated.

Many of the foremost machine tool and metrology companies throughout the world have also willingly supplied information concerning their current products and technical literature, which has also been utilised and prominently exploited throughout the text. At the end of this book these associated companies' contact details are provided, for future reference. In a similar manner, I have invariably attempted to acknowledge the applied researchers' work utilised within this text—where it was applicable. As a consequence wherever practically possible, I have attempted to acknowledge their courtesy to me and support at the related point within either the text, or where I have included some of their photographic, or graphical images. Of some note, is the fact that I have personally produced many of the actual line diagrams/drawings utilised throughout this book. However, if there are any unintentional mistakes that have otherwise been unavoidably drafted in by myself, then the error is solely mine alone and should not be attributed to any of the companies, or research-based personnel mentioned herein.

Finally and very importantly, I would like to thank my long-term publishers *Springer Verlag* for their significant efforts in bringing this latest book to the published world. The author and Springer Verlag Publishing—both at their London headquarters and in Germany—have together had a very long and productive literary association covering more than 25 years, which has been an interesting mutual involvement for, I believe, all concerned.

Graham T. Smith

Contents

About the Author

Prof. Graham T. Smith initially began his production engineering career in the UK during the early 1960s, at a West Midlands company in England that manufactured precision automotive components by either Drop-forging, or Pressing (Smethwick Drop Forgings Ltd—part of GKN plc). At this GKN-based company, he became proficient in all aspects of precision engineering within a large commercial Die-shop in a heavy-duty toolmaking environment, becoming a fully skilled and practically qualified Toolmaker & Craftsman. In the late 1960s, he then relocated to the London area and worked for an aerospace company as a prototype toolmaker (Redifon Flight Simulation Ltd.) then later moved to an optical toolmaking company, working in an ultra-precision machine shop as a Jig-borer, Turner & Grinder (Merx Optical Co. Ltd.), whilst studying part-time for a Full Technological Certificate in Production Engineering. In the mid-1970s, the author was employed on a range of industrial contract-based work (Wolfson Materials Advisory Service) which was an applied research-based unit, working on a diverse series of short- and long-term engineering, metrology and metallurgical contracts. This Wolfson unit was located within campus of The University of Southampton. Whilst there, he also studied part-time for a Certificate of Advanced Study in Metallurgical Quality Control, which was then followed-up by a Master of Philosophy degree in Machinability, both of these post-graduate studies being undertaken at Brunel University (West London)—in the 1980s. While in the early 1990s, having secured an academic lecturing appointment at The University of Birmingham (Department of Mechanical Engineering), the author completed a Doctor of Philosophy degree in Machined Surface Integrity. Later, when employed at the Southampton Solent University in their Technology Research Centre, the author was instrumental in setting up a fully industrialised Flexible Manufacturing System (FMS).[1] Over the next decade, a considerable amount of applied

[1]This *Flexible Manufacturing System* (FMS)—developed by Cincinnati Milacron—was a sophisticated large-scale industrial installation comprised of an integrated range of both Slant-bed Turning and Vertical Machining Centres, equipped with adaptive control for both tool/work-probing (Renishaw), including a long-reach anthropometric six-axis Robot (Cincinnati Milacron T^3-776)—fitted with an adjustable back-to-back gripper for simultaneous load/unload component

and wide-ranging research programmes were undertaken on this FMS plant in conjunction with a new and purpose-built Metrology/Standards Laboratory, also on-campus. For many years, the author also acted as an engineering consultant for an international cutting fluid producer/distributor working as an industrial trouble-shooter (Castrol Industrial, Pangbourne) and at various companies throughout the UK in a similar vein. Further applied research entailed undertaking many other complex machinability/metrology short- and long-term duration projects for a range of industrial and aerospace companies, such as Guhring Tools plc, (Birmingham) and Rolls-Royce Aerospace plc (Filton, UK). Additionally during the past twenty plus years, the author has acted as an Expert Witness—in many notable engineering litigation cases, for a host of large international and UK-based industrial companies. During the early-1990s, Prof. Smith was one of the three original and founding members[2] of the now technically relevant international conference on Laser Metrology and Machine Performance (LAMDAMAP), which has continued to visit many academic venues throughout the UK. Of some note at the early stage in this conference's development, was the presence of the wide range of metrological research-based Keynote Speakers[3], who were invited to attend these events. Concurrent with this sequence of LAMDAMAP conferences, the author also founded and chaired the biennial series of international conferences on Industrial Tooling, which also began in the mid-1990s in the UK and has now been successfully staged within the USA—notably at Mississippi State University. Once again during each of these differing conference venues, a large tooling/metrology exhibition[4] concurrently took place, along with some exceptional invited Keynote Speakers being present.[5] The author

Footnote 1 (continued)

part handling facility, from a purpose-built tiered workstation. Furthermore, other associated equipment and plant included in this installation, was an integrated cantilever-type CMM (LK/Renishaw), plus an incorporated Optical tool-presetter (DeVlieg) for complete tool management of Sandvik Coromant's modular Block and Varilock cutting-tooling, with its part scheduling and automated FMS management, via an integrated Cincinnati Milacron Cell-controller.

[2]The other two original founding members of LAMDAMAP, were: Prof. A.D. Hope & Mr. D.M.S. Blackshaw.

[3]***LAMDAMAP Conference—Keynote Speakers*** have included: Jim Bryan (Los Alamos Laboratories, USA), Profs.: David Whitehouse (Warwick University, UK), Yoshiaki Kakino (Kyoto University, Japan), Pat Mckeown (Cranfield University, UK), Albert Franks and Graham Peggs (The NPL, UK), Sir David McMurtry (CEO, Renishaw plc), Dr. Wolfgang Knapp (ETH Zurich, IWF), plus many more such luminaries.

[4]***Industrial Tooling Conference—exhibitions***, were effectively organised and run by one of Prof. Smith's former academic colleagues: Prof. Guy Littlefair now, Head of Engineering at: *Deakin University*, Australia.

[5]***Industrial Tooling Conference—Keynote Speakers*** have included: Profs.: Milton C. Shaw (Arizona State University, USA); Ranga Komanduri (Oklahoma State University, USA); Ekkard Brinksmeier (IWT, University of Bremen, Germany); John T. Berry (Mississippi State University, USA), Dr. M. Eugene Merchant (Institute of Advanced Sciences, Cincinnati, USA); Michael L. Watts (Boeing Aircraft Corporation. Seattle, USA), to name just a few academic and industrial participants.

feels indebted/privileged to have known and learnt from such world leading academic and industrial authorities. This coupled to the vast range of influential industrial company delegates who also provided well-received presentations and papers at both of these series of conferences over several decades truly enhanced these respective proceedings. Professor Smith has lectured widely within the UK at industrial and exhibition venues, likewise across a diverse range of university campuses in both Europe and North America; moreover, he has continued to maintain close links in the related machine tool and metrology industries. He has also refereed submissions for The Machine Tool Technologies Association as a judge for the biennial MACH awards and has regularly undertaken book and journal reviews, as well as periodic technical articles for the Industrial Press. Furthermore, he has also produced some specific end-user products for a range of international companies, during last 50-plus years.

Chapter 1
Measurement and Machine Tools—An Introduction

"It is the Age of Machinery, in every outward sense of that word."
Thomas Carlyle
(Scottish Historian and Essayist)
[1795–1881]
(In: Signs the Times)

1.1 Why the Need for Accurate and Precise Machine Tools—a Brief History

The extensive development of early machine tools filled a need created by a buoyant textile industry during the early stages of the Industrial Revolution in England, this being in the middle-to-late 1700s. Until that time, most of the machinery was fabricated from, in the main, wrought iron and hardwood, the latter often including hard wooden gearing and shafts. With the inevitable increase in such mechanisation, it necessitated more robust metal parts—due to higher production demands and potential wear. So metal components were customarily now being manufactured from either cast or wrought iron, rather than the previous hardwood. The major advantage of cast iron was that it could be cast in complex and intricate shapes, holding its geometric form as it slowly cooled in its mould. This fact is a real benefit of utilising cast iron, due in the main from its unique metallurgical properties (i.e. primarily as a result of the formation of graphite flakes, which sets the geometric shape due to secondary expansion of said graphite flakes while cooling and still being pliable enough to follow the mould's internal contours) allowing larger components, typically engine cylinders and gears, to be readily founded. Large cast iron parts were difficult to work with by simply hand filing—for any form of accuracy and precision—but unfortunately due to their mechanical properties they could not be hammered into the desired dimensions. However, a red-hot wrought iron part could be successfully hammered into shape. So, at room temperature a wrought iron product might be worked with a file and chisel and, as such, could be made into somewhat rudimentary gears. This hand-working gear lacked

G.T. Smith, *Machine Tool Metrology*, DOI 10.1007/978-3-319-25109-7_1

any real involute tooth form, which was a necessity for its desired rotation, accuracy and precision, as was also the case when producing other complex parts—this technique being both a slow and expensive manufacturing process.

Due to these real and persistent industrial problems that needed to be addressed, namely the lack of capability in component precision and accuracy, coupled to the current level of manufacturing and production volumes during the Industrial Revolution, the stage was set for the early development of a machine tool industry. As a result of the already-mentioned manufacturing inadequacies, the milestone for the first machine tool development occurred in England, in 1774. This was when John Wilkinson built an accurate and precise boring machine that was employed for producing hydraulic cylinders for James Watt's steam engines—these steam engines were engaged in pumping out water from mining operations. In 1794, Oziel Wilkinson (i.e. no relation to the British boring machine developer just mentioned) in Pawtucket, USA, developed the first screw-cutting lathe, incorporating a slide rest with the original design being about 20-ft long (i.e. ≈6.5 m). Later in 1806, a smaller version of this Wilkinson lathe was produced in the USA, with the added benefit of an improved arrangement of the bearings, facilitating more accuracy for finish-turned workpieces. Here, the two bearing points were in line on the front of the prismatic way, while a third bearing rested on a slab-rib at the rear of the bed. So, once the front way had been made as straight as physically possible, the flat way could then be contoured—by a mechanic/fitter with a file—to minutely correct for any irregularities that remained in the prismatic way. Then, trial cuts on a test piece would be used to govern the file contouring. In this way, the unavoidable errors of handiwork were made to cancel out each other. This critical action allowed American mechanics/fitters of basic ability to produce an unlimited quantity of accurate and precise slide-rest lathes, which was unfortunately not the case in Europe, where highly skilled millwrights/fitters were needed to produce quality lathes, with the downside here being at much lower production volumes and higher cost. Later, still Wilkinson abandoned the use of rollers employed under the slide—in his original design—adding a hanging weight to compensate for the lighter weight of the slide-rest, stating that: "…it worked like a charm". Shortly, a major advancement in the accuracy and precision of machine tools can be credited to Henry Maudslay (1771–1831)—who produced the first engine lathe and index milling machine, which was then further refined by the introduction of the precision screwthread—by Joseph Whitworth in 1841. Prior to these machine tool developments, Maudslay had established the manufacture and use of Master-plane gauges in his workshop in London in 1809 (i.e. Maudslay, plus his co-worker Mr Field). While, Whitworth (1803–1887) built on the previous work of Maudslay (for whom he had previously worked) and developed the first truly flat surface plate. Whitworth's modified plate manufacturing technique had two notable requirements: first acting as a plane surface—a datum reference surface for measurement; while second providing a rigid surface—enabling flat and square planes, this being a major requirement when building orthogonal machine tool surfaces. The importance of a flat and rigid surface was not lost on Whitworth in 1840, when he then declared: "A true surface, instead of being in

common use, is almost unknown". Such a true datum surface required the use of three identical plates to be alternately lapped and scraped together (i.e. normally attained by the skilled fitter's controlled figure of eight motion of one plate on top of another—with engineer's blue smeared onto the top plate to indicate where the contact points of the bottom surface's high-spots occurred). As a consequence by scraping away these high-spots, it generated a flat surface—as each separate and alternate lapping plate cancelled out the geometric errors in each other. In this manner, master plane gauges were successfully developed. So, with the creation of Master plane gauges of such high accuracy and precision, all the critical components of machine tools, such as guiding surfaces for the machine's ways could then be compared against them and then scraped to the desired accuracy and precision demanded for a quality machine tool.

An important early development for machine tools included the: slide rest lathe; screw-cutting lathe; Turret lathe; and milling machine; together with the pattern-tracing lathe (shaper) and metal planer, that were all in use prior to 1840. Having such diverse machine tools now available enabled the decades-old objective of producing interchangeable parts—rather than building assemblies by selective assembly. This interchangeability of components allowed machine tools to be both fabricated and assembled significantly faster, offering the prospect of more readily available and affordable machine tools for industry. During the tragic time period of the American Civil War (1861–1865), another significant leap-forward in machine tool design occurred. The American Steven Morse solved the problem of having to file the grooves in twist drills with a new type of drill that had just recently been developed, by inventing a spiral milling capability on his newly designed universal milling machine (i.e. the first Toolroom machine tool). This universal mill had a knee-and-column configuration, which became the forerunner of today's conventional universal mills, albeit then powered by overhead belts and pulleys. In 1884, the Cincinnati Screw and Tap Company founded by Frederick Holz and George Mueller, initially making thread production tooling—with Holz acting as president of the company. Two years, later the company name was changed to that of the Cincinnati Milling Machine Company. Holz then redesigned and built the universal milling machine, by adding positive feed and repositioning the hand controls/levers into a more convenient ergonomic arrangement for better operator usage—very similar to today's conventional machine tools. In 1905, Fred A. Geier became Company President of, at the time, the world's largest producer of machine tools. Belt-driven machine tools were finally modified to incorporate their own individual motors in the early 1930s and both conventional lathes and milling machines produced pre-World War II would now be familiar to today's machinists. This introduction is an abridged summarising history of machine tool developments, which is only a basic snapshot of the overall developments of such machines. Many more companies undertook parallel design and development of their own products throughout the world, which could not be covered in this briefest of appraisals of some of the pioneering work undertaken throughout the last few hundred years.

1.2 The Early Historical Development of a Linear Measurements

In all probability, the oldest units of dimensional measurement employed in the ancient world were related to either one's body measurement—see Vitruvian man Fig. 1.1 (top), or to certain physical entities that were readily available in daily life—see Table 1.1.

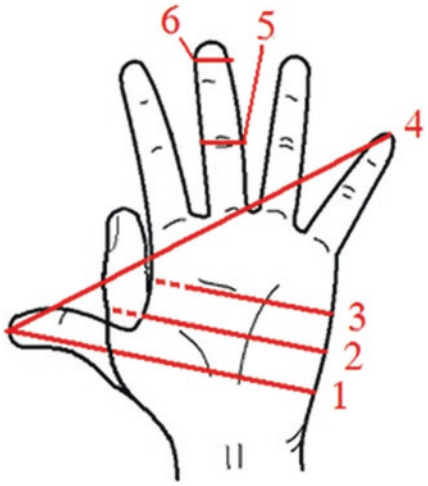

Ancient Egyptian length measurement, based on the physical characteristics of the hand—shown in Imperial units: Shaftment (1) = 6.5″, Hand (2) = 4″, Palm (3) = 3″, Span (4) = 9″, Finger (5) = 0.875″, Digit (6) = 0.75″, these are just some of the typical length measurements shown on a physical human hand

Table 1.1 Ancient Sumerian/[a]Akkadian—multiple-units of measurement

Basic length measurement in mesopotamia					
Unit	Cubic ratio	Ideal value (m)	Sumerian	Akkadian	Cuneiform
Grain	1/180	0.0025	še	uṭṭatu	Not shown
Finger	1/30	0.015	šu-si	ubānu	
Foot	2/3	0.333	šu-du$_3$-a	šīzu	
Cubit	1	0.497	kuš$_3$	ammatu	
Step	2	1.000	ĝiri$_3$	šēpu	
Reed	6	3.000	gi	qanû	
Rod	12	6.000	nindan	nindanu	

[a]The Akkadian Empire reached its political peak between the 24th and 22nd Centuries BC, following the conquests by its founder: Sargon of Akkad (2334–2279 BC). Under Sargon and his successors, Akkadian language was briefly imposed on neighbouring conquered states such as Elam. Akkad is regarded by many historians as the first initial empire in history

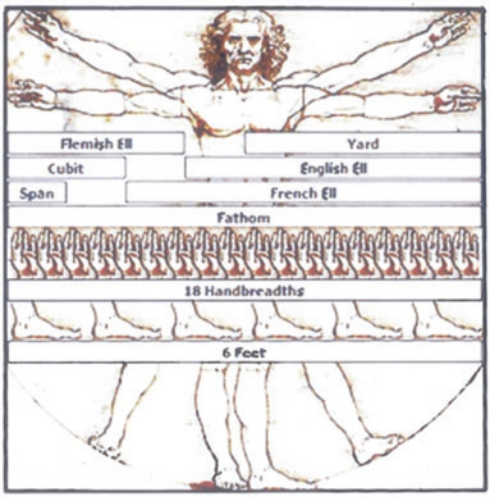

The Dimensional Measurement Services project provides industry high accuracy dimensional measurements within an internationally accepted quality system. Here, measurement of API Rotary Master Gauge on CMM. [Courtesy of The National Institute of Standards and Technology (NIST)]

The historical development of *Measurement Standards* varied – with *no* dimensional *correlation*, superimposed on the 'Vitruvian Man' (L. da Vinci). [Courtesy : Wikipedia]

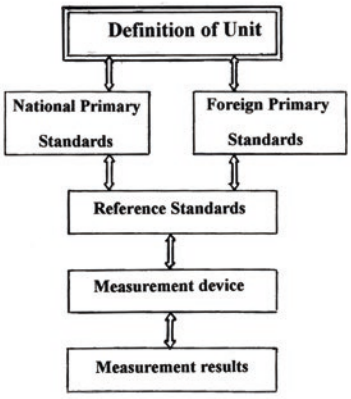

BIPM

ISO

NPL
National Physical Laboratory

NIST
National Institute of Standards and Technology
Technology Administration, U.S. Department of Commerce

PTB

Just a few of the active/leading countries Standards Organisations that adhere to the BIPM/ISO measurement & calibration philosophy

Flow-chart of *SI Units of Measurement* to the *National* & *International Standards.*

[Courtesy of National Physical Laboratory (NPL)]

Fig. 1.1 Until *dimensional measurement* was *'standardised', 'chaos reigned'*—with regard to any form of '*compatibility*'

In the Uruk Period of Sumer in ancient Mesopotamia—circa 4000 BC—the units of length are prefixed by the logogram DU, a convention of the archaic period counting system from which it was evolved. Here, basic length was utilised in architecture and field division and an abridged version of such linear measurement is shown in tabulated form in Table 1.1.

Virtually contemporary with these Mesopotamian cultures was that of the Old Kingdom of Ancient Egypt, which is the designation given to the period in the 3rd millennium BC when Egypt attained its first continuous peak of civilization (i.e. Third Dynasty through to the Sixth Dynasty: 2686–2181 BC). The basic form of length measurement developed at this time was the cubit,[1] this being the length obtained from the tip of the finger to the elbow (Fig. 1.1, top). The cubit was reproduced as an artefact across the length and breadth of Egypt, for comparison and standardisation throughout the Egyptian Empire. Moreover, the cubit could be subdivided into shorter units, such as the foot and hand (i.e. one hand equates to 4 in.—this latter term today being utilised for expressing the shoulder height of horses). Conversely, for architectural work a cubit can be extended by adding several cubits together to form the stride.

The great pyramid of Giza in Egypt (circa 2560 BC)—built for the Pharaoh Khufu (Old Kingdom)

[1]**The application of the Cubit**: it is well-known that the Great Pyramid of Giza, was built as a tomb for fourth dynasty Egyptian Pharaoh Khufu and was constructed over a 20-year period. Khufu's Vizier, Hemon, or Hemiunu, who is thought by some to be the actual architect. It is acknowledged that, after construction, the Great Pyramid was originally 280 Egyptian cubits tall, 146.5 m (480.6 ft), but with erosion and absence of its pyramidion, its present height is 138.8 m (455.4 ft). Each base side was 440 cubits, 230.4 m (755.9 ft) long. The mass of the pyramid has been estimated at ≈5.9 million tonnes. The volume, including an internal hillock, is roughly 2,500,000 m^3. The high accuracy of the pyramid's workmanship is such that the four sides of the base have an average error of only 58 mm in length. The base is horizontal and flat to within ± 15 mm. The sides of the square base are closely aligned to the four cardinal compass points (within 4 min of arc) based on true north (i.e. not magnetic north) and the finished base was squared to a mean corner error of only 12 s of arc.

This Egyptian stride had its equivalent in the Roman pace. Hence, a Roman pace, or double pace (i.e. in Latin: passus), was a measure of distance used in Ancient Rome. It was nominally the measure of a full-stride from the position of the heel when it is raised from the ground, to the point where the same heel is set down again at the end of the step. Accordingly, a distance can be paced-off by counting each time the same heel touches the ground, or, in other words, every other step. In Rome, this unit was standardised as two gradūs, or five Roman feet (i.e. approximately 1.48 m, or 58.1 English inches). There were 1000 passus (i.e. double pace) in one mille, and a mille was sometimes referred to as a mille passuum. This mille passuum differs from today's mile, being 5000 pedes (feet), or 4854 ft (i.e. of a 0.919 standard mile).

In England during the Saxon period, as early as 1000 AD the Saxon King Edgar kept a Yardstick[2] at Winchester as the official Standard of Measurement. However, it was not until the Norman period in the reign of King Richard I (popularly-known as Richard The Lionheart), that any form of standardisation of units of measurement was first documented. In his Assizes of Measures, in 1196, it was stated: "Throughout the realm there shall be the same yard of the same size and it should be of iron". This metallic artefact was the first permanent standard measure to be utilised in an attempt to control the vagaries of linear measurement. Following on from Richard's reign his brother King John, in 1215, was forced by the Norman Barons into producing the world's first great democratic document: The Magna Carta. In The Magna Carta, amongst all of the Rights for Freemen, it was also considered necessary to include more detailed units of standardised measurements—including those for both wine and beer! The yard, or ulna—as it was sometimes known, together with its linear subdivisions and aggregated divisions, came into existence during the Plantagenet reign of King Edward I (1272–1307). Here, it stated that: "It is ordained that three grains of barley, dry and round make an inch,[3] twelve inches make a foot, three feet make an ulna [yard], five and a half ulna make a perch[4] [rod], and forty perches in length and four perches in breadth make up an acre".

---

[2]**The Yardstick**—where the current term Yard was derived. Originates from the Saxon word gird, meaning the circumference of a person's waist—which at the time, was open to some variation in interpretation!

[3]**The Inch**: the measurement of the inch employing three dried barley grains—round and true—laid end-to-end, allowed the populace to have some consistency in their everyday level of accuracy and precision for Standards of Measurement. A vital criteria for many National forms of linear measurement—at that time period of history.

[4]**The Perch**, or **Rod** as it was known: was based upon the previous centuries of the Saxon-reign in England, which was a traditional Saxon land measure that still survived into the twenty first century. Although these Saxons had originally defined it as: "*The total length of the left feet of the first sixteen men to leave church on Sunday morning*". This somewhat distinctly vague statement, being open to considerable uncertainty in its length determination!

It is understood that in the reign of King Henry VII (1485–1509), he reverted back 350 years to obtain his dimensional standard—being a direct copy of King Edgar's Yardstick. In 1588, the Elizabethan yard, or ell as it was otherwise known, was once again based on a large man's stride. Alternatively, the measurement could be taken from the distance between a man's nose and his thumb when standing and stretching the arm, this technique was often used as a rudimentary form of length measurement by the clothing industry. Artefacts such as the Elizabethan yard were known as End standards, being engraved with an initial **E** and the Royal crown—to denote its universal acceptance in the country. Nonetheless, until 1824 this remained the legal and legitimate British Standard and was only superseded by an Act of Parliament under King George IV, when the Imperial Standard Yard[5] was introduced, to minimise the inaccuracies generally associated with linear measurement at the time. This Imperial yard had a relatively brief life (i.e. exactly 9 years and 198 days) as a comparative End standard, because in 1834 it was destroyed in the fire that swept through the old Houses of Parliament—while also destroying the complete building where it resided. Restoration of this linear end standard was undertaken from a metallic-alloy composition of: copper (16 parts); tin (2.5 parts) and zinc (1 part). It was colloquially known as Bronze No. 1[6] by its creator the Rev. Richard Sheepshanks, the principal design feature being that engraved gold plugs were recessed into the artefact at the plane of its neutral axis—to minimise flexure and hence any potential measurement inaccuracy. Duplicates of its exacting length dimensions were then made and they were legalised by Parliament in 1855, one example (below) being presented the Government of the United States of America in 1856.

[5]**The Imperial Standard Yard** (i.e. which is normally abbreviation: **yd**), this is a unit of length in both the Imperial and United States Customary Systems of Measurement. Historically, a Yard was also used in other systems of units. The Yard being exactly equal to 3 ft, or 36 inches in length. Under an agreement in 1959 between Australia, Canada, New Zealand, South Africa, with the United Kingdom and the United States, the yard (i.e. now known as the International yard in the United States), was legally defined to be exactly 0.9144 m.

[6]Sheepshanks's work was completed and published by his friend Sir G. B. Airy, the Astronomer Royal. In summary, what he had accomplished was this: Sheepshanks cast a number of bars of Baily's metal—as it was then known. Five selected bars were then accurately compared, with the existing scales, one of them (No. 1) being found to be as nearly as possible a Standard Yard in length at the prescribed legal temperature of 62 °F. It was stated that the new Standard yard should agree to the millionth part of an inch with the old one, but that, once fixed, it should be invariable. The yard is a rectangular bronze bar 38 in. long, with a 1-in. square section. One inch from either end is a 1/2-in. hole sunk to the centre line of the bar, and in the centre of each hole is a gold plug, set in flush with the bottom. On the face of each plug are inscribed three transverse lines about 0.01 in. apart, and two longitudinal lines about 0.02 in. apart, the whole resembling a three-barred gridiron in miniature. The lines are not more than 0.0005 in. wide. The legal yard is defined as being, when the bar is at a temperature of 62 °F., the interval between those portions of the central transverse lines included between the two longitudinal lines.

This actual Bronze Yard defined the Standard Yard of the United States of America from approximately 1857 until 1893, when the yard was then redefined in terms of the metre. It was constructed of the same material and dimensional form as the British Imperial Yard—legalised in 1855—and was subsequently presented to the USA, by Great Britain in 1856

1.2.1 The Historical Development of the Metre and the International Bureau of Weights and Measures (BIPM)

Across continental Europe, but most notably in France, parallel development was taking place creating the metric system—it had been known for sometime that a natural constant measurement value for the metre was essential. At this time (1791), the solution for the metre's appropriate length was developed from a portion (quadrant) of the circumferential line of longitude through the Earth, theoretically at sea level. For that reason, at the 1791 meeting of the French Academy of Sciences, the definition of the metre was stated as: "One ten millionth of the polar quadrant of the Earth passing through Paris". In more practical terms, what this meant was: of a theoretical line running from the true North Pole to the Equator—passing through Paris, representing a quarter of the Earth's circumference and, if this distance was scaled down to a ten millionth part of this linear length, the interval would represent a metre.

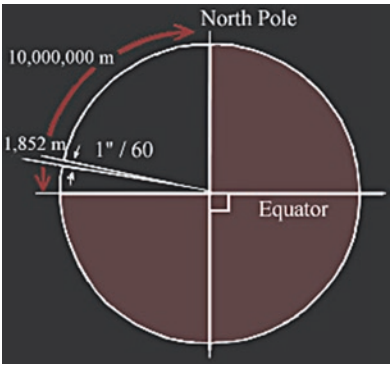

Length of a metre can be simply determined by circumferentially and linearly extending a quadrant of the Earth up to the North Pole (at sea-level), that at some stage passes through Paris (France). Where from the Earth's centre, a radial extension of one second of arc at this peripheral intersection, will equate to a measurement of 1/10,000,000 linear part

In order to determine the actual mathematical relationship for the metre, the Polar Quadrant Survey[7] was undertaken. A team of French surveyors was charged with the extremely challenging and difficult task of practically establishing this geometrical/linear relationship. The surveying took almost 6 years to complete, which was exacerbated by the war now raging between France and Spain. In practice, only a relatively small portion of the geographical terrain could be surveyed, namely between Dunkirk (France) to Barcelona (Spain), with the team leaders being split and converging together almost 6 years later, a truly amazing feat of scientific endeavour! Wherever possible, the surveyors attempted to minimise the effect of altitude, ideally taking measurements at sea level. Several of the team's surveyors—during this Franco-Spanish war, were charged as spies, nearly losing their heads in the process of the actual survey! The final outcome of this exacting and testing survey, being the 1799—Mètre des Archives.

[7]In 1791, the **French Academy of Sciences** selected the Meridional-definition over the Pendular-definition, because the force of gravity varies slightly over the surface of the Earth, which affects the period of a pendulum. To establish a universally accepted foundation for the definition of the metre, more accurate measurements of this meridian would have to be made. The French Academy of Sciences commissioned an expedition led by Jean Baptiste Joseph Delambre and Pierre Méchain, lasting from: 1792 to 1799. These surveyors measured the distance between a belfry in Dunkerque (Dunkirk) and Montjuïc castle in Barcelona, to estimate the length of the meridian arc through Dunkerque. This portion of the meridian, was assumed to be the same length as the Paris meridian, which was to serve as the basis for the length of the half meridian—connecting the North Pole with the Equator.

In 1875 in Paris, the Mètre Convention of participating nations established the International Bureau of Weights and Measures[8] (BIPM). In 1889, the physical metallurgy and design of measurement artefacts had been significantly improved from the rather crude previous designs and elementary metallurgical compositions, to those of more a uniform and inherently stable cross-section. In particular, of the 30 artefacts produced from the alloy platinum-iridium, No. 6 (as was at the time) was stringently tested and duly selected to replace its more primitive forerunner (i.e. Mètre des Archives). This new artefact was to become known as the International Prototype Metre[9]—see below. Many of these newly manufactured and uniformly French-made End standard artefacts were then distributed to countries around the world. In the United Kingdom it is worth mentioning the fact that the use of the metric system's Weights and Measures by trade and industry only became law in 1897, but even then it was not truly universally adopted without a certain reluctance, until 1971.

[8]The **International Bureau of Weights and Measures** (i.e. in French: **Bureau international des poids et mesures**), it is an **International Standards Organisation**, one of three such organisations established to maintain the International System of Units (SI)—under the terms of the Metre Convention (Convention du Mètre). The organisation is usually referred to by its French initials—**BIPM**. Accordingly, the BIPM was inaugurated on 20 May 1875, following the signing of the Metre Convention, a treaty among 51 nations (i.e. as of August 2008). It is based at the: Pavillon de Breteuil, Sèvres in France, situated on a 4.35 ha site (i.e. it was originally 2.52 ha), which was granted to the Bureau by the French Government in 1876, where it enjoys Extraterritorial status, this particular status that was clarified by the French decree No. 70-820 of: 9 September 1970.

[9]At the **BIPM** in Sèvres, France, is where they manufactured 30 prototype Line end standards of platinum-iridium. These bars had a modified **X** cross-section (see photographs), thus providing maximum rigidity, the Tresca section was named after the famous French Scientist: Henri Tresca—who proposed this geometry. Small elliptical areas on the central rib's upper surface were highly-polished with three transverse parallel ruled lines engraved, nominally 0.5 mm apart. The distance between the middle lines of each grouping, defined the standard length. As mentioned, Bar No. 6 was selected for the International Prototype Metre. The United Kingdom received bar No. 16, whereas in 1890, the United States of America received two National Prototype Metres: No's 21 and 27. When in 1893, the Mendenhall Order declared the metre to be the Fundamental length standard, with No. 27 becoming the Primary National Standard in the USA—for all length measurements and remained so, until 1960. The actual dimensional relationship between bar No. 27 and, that of the International Prototype Metre has been certified to be: $1\ \text{m} - 1.6\ \mu\text{m} + 8.657\ \mu\text{m}.T + 0.001\ \mu\text{m}.T^2 \pm 0.2\ \mu\text{m}$; with T being in °C. Moreover, it should also be noted that the inter-comparison between the International Prototype Metre and bar No. 27 yielded a probable error of $\pm 0.04\ \mu\text{m}$, while here, the probable uncertainty of the length of bar No. 27—at temperatures between 20 and 25 °C, was estimated by the BIPM to lie between: ± 0.1 and $\pm 0.2\ \mu\text{m}$.

The basic mechanical design and the geometric construction shape of the International Prototype Metre—circa 1889

1.2.2 Optical and Laser Length Measurement

In the previous section, the discussion was concerned with the historical development of a range of physical artefacts to determine length measurement. Several significant problems exist when utilising such conventional artefacts as the basis of comparative measurement, most notable among these difficulties being:

- **the inability to manufacture linear-based artefacts**—to reliable and matching lengths;
- **transferring these measurements accurately and precisely**—to employ these artefacts geographically, elsewhere around the world;
- **the instability of the artefact's material composition**—resulting from the entropy effects[10] of: loss of actual physical material (i.e. atomic weight)—with time, together with creep—as internal stresses are slowly-released—affecting its actual geometry;
- **component part accuracy and precision**—this fact, being coupled to the artefact's critical design tolerances which become tighter with chronological time, as a consequence requiring an even better means of establishing length.

This final observation was well-known to both designers and engineers of the past, but needed a new means to determine an even greater accuracy and precision

[10]**Entropy**: is a measure of the number of specific ways in which a system may be arranged, often taken to be a measure of disorder, or a measure of progressing towards what is termed: Thermodynamic equilibrium. Thus, this entropy of for example an isolated system, is one that basically never decreases, because isolated systems spontaneously-evolve towards its Thermodynamic equilibrium—which is the state of maximum entropy.

than was apparent utilising the International Prototype Metre and its other contemporary artefacts around the world. In order to minimise the major difficulties associated with metallic artefacts for standards, during the early-to-mid-twentieth century a truly natural standard was established for dimensional measurement, explicitly based upon the wavelength of light. Once the metre had been defined in terms of light wavelengths by an atomic discharge lamp-source, the necessary instrumentation could then be produced in any well-equipped metrology laboratory. In order to obtain an accurate determination of the metre in terms of the wavelength of light, a comprehensive testing programme was initiated—these tests occurring nine times—between 1892 and 1940 at various standards laboratories, for example, twice at the UK's National Physical Laboratory (The NPL)—in 1932 and 1935. Accordingly, the mean value of these nine test results became the basis of a new definition for the metre, thus: "The length equal to 1,650,763.73 wavelengths in a vacuum of the radiation … of krypton-86". In 1960, the metre was defined in this manner, thereby replacing the previous International Prototype Metre as the: Fundamental Standard of Measurement—being currently the achievable level of accuracy and precision at that time.

Ironically, at the same chronological time (i.e. in 1960), the first laser[11] was constructed and, by the mid-1970s lasers were routinely being utilised as Length standards. As a direct result, in 1983 the definition of the metre was redefined using the krypton-86 source, as: "The length of the path travelled by light in a vacuum during the time interval of 1/299,792,458 of a second". This metre length was achieved by employing iodine-stabilised helium-neon lasers (see photograph below) having a reproducibility with a fractional-uncertainty of 2.5 parts in 10^{11}. Although as a wavelength source this iodine-stabilised helium–neon laser has excellent physical/optical characteristics, in the near-future it should be possible to construct lasers with vastly superior wavelength accuracy. One of the main reasons why a new laser instrumental design is imperative is because the current iodine-stabilised helium–neon laser variety is somewhat limited by the fact that iodine molecules are at room temperature, colliding into each other, thus they tend to fluctuate in-and-out of the laser's beam. This relative molecular motion causes them to absorb laser light over a comparatively large range of wavelengths. The problem can be relatively simply rectified by substituting the iodine molecules with a single atom of a metal such as either ytterbium, or strontium. With such replacement atoms they are given an electrical charge—changing their characteristics into anions, which are held in an ion trap. Once the ion has been captured in

[11]The term **Laser**: refers to a device that emits light through a process of optical amplification based on the stimulated emission of electromagnetic radiation. Accordingly, the term laser originated (i.e. being invented in 1960) and was then referred to as an acronym for: **L**ight **A**mplification by **S**timulated **E**mission of **R**adiation. Lasers differ from other sources of light, because they emit light coherently. Consequently, its spatial coherence allows a laser to be focused to a minute and tight spot. Here, its spatial coherence also keeps a laser beam collimated over long distances, which is ideal for subsequent Laser interferometry and in this instance, for the instrumental-calibration of machine tools, CMMs and other such equipment.

Table 1.2 How the dimensional artefact accuracy has improved with time

Date	Definition of the metre	Accuracy of realisation of the metre from the definition of the period (mm)
1791	Based on the quarter meridian of the Earth	±0.06
1889	International prototype metre	±0.002
1960	First length quantum standard	±0.000007
1983	Speed of light	±0.0000007
2014	Speed of light, with improved He–Ne laser accuracy[a]	±0.00000002

Adapted from: The NPL (UK)
[a]In future, replaced by either: ytterbium/strontium laser source: ≤±0.0000000000002 mm

this manner, it can be cryogenically treated (i.e. cooled down), so that its temperature creates an almost stationary atomic motion and either **an** ultraviolet light, or blue laser will illuminate the ion. This single atom source can be considered as a considerable improvement for the wavelength-reference over that of the current technique, as it effectively absorbs light over a range of just one millionth that of iodine, which hopefully will offer the potential for a vastly improved laser performance in the future (Table 1.2).

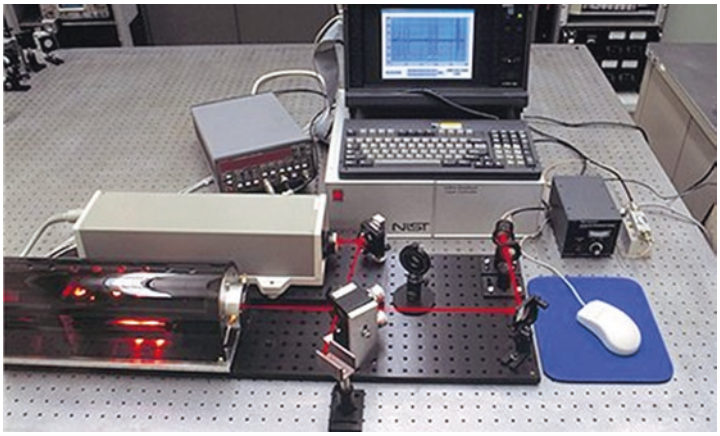

An advanced metrological setup for research activity into the iodine-stabilised helium–neon laser at The NPL (UK)

1.3 International Standards Laboratories—Why They Are Essential

Prior to discussing the philosophy and mechanism of traceable dimensional measurements and their calibration, it is worth briefly mentioning how just some of the technologically based countries achieve these objectives. Today, in terms

of dimensional measurements, leading technological countries around the world have their own standards organisations for fundamental and applied research and improvement of newly-developed measurement techniques, ensuring that their country conforms to international conventions, by maintaining records of current metrological practices, and so on. To somewhat expand on this national theme, just some of the major standards organisations include: The **International Bureau of Weights and Measures** (**BIPM**, Sevres, France); The **National Physical Laboratory** (**NPL**, Teddington, UK), The **National Institute of Standards and Technology** (**NIST**, at both Gaithersburg and Boulder, USA); **Physikalisch-Technische Bundesanstalt** (**PTB**, Braunschweig, Germany); these and many other countries cooperate to produce their own National Standards whilst helping to develop and adopt the Standards for the **International Organization for Standardization** (**ISO**).

1.3.1 What Is Traceability and Why Is It Necessary?

The term traceability[12] can be thought of as the property of the result of a measurement, not of an instrument, calibration report or that of a laboratory. Thus, it cannot be achieved by following any one particular procedure nor by utilising special equipment. Merely having an instrument calibrated, even by say the NIST/NPL/PTB/etc., is not enough to ensure that the measurement result obtained from that instrument becomes traceable. Hence, the measurement system by which these values are transferred, must be clearly understood and under control.

Traceability and Calibration

Measurement traceability[13] refers to such measurements that can then be related to a National Standard—like the metre, through a "…documented unbroken chain of calibrations…". For example in Fig. 1.1—the metre is the primary standard utilised to calibrate Reference Standards (i.e. secondary) that are normally situated within an accredited calibration laboratory. Subsequently, these reference standards are then next used to calibrate working standards, which may entail for instance, the calibration of a Company's Master Standards—these usually being retained within a company's standards laboratory. Hence, in the case of an industrial company's mechanical engineering reference measurements, i.e. its secondary

[12]**Traceability of measurements**—as a practice/philosophy: it has achieved global acceptance by the Metrology-community, as it is contained in the: **International Vocabulary of Basic and General Terms in Metrology**; **VIM**, **3rd edition, JCGM 200:2008**, this being: "The property of a measurement result (e.g. such as its length), whereby the result can be related to a reference through a documented unbroken chain of calibrations, each contributing to the measurement uncertainty".

[13]**Measurement traceability**: this refers to the unbroken chain of calibrations linking an instrument/artefact, or indeed a Standard, to its Primary Standard—see Figs. 1.2 and 7.1a.

standards and their associated Working standards, this could possibly be measuring instruments, or artefacts—typically Length bars, or Gauge blocks. Throughout any calibration process, instrument readings are compared to the certified values produced for a known reference standard and, as a result, these test results are then recorded in a suitable Calibration certificate. Consequently, if these measured results are consistent with the reference values, namely, the differences between them are within acceptable limits, then it is expected that no further action is deemed to be necessary. However, if the results are knowingly different, then certain specific calibration corrections must be applied to these test measurements made with the instrument or artefact. Occasionally, an instrument can be adjusted until it reads acceptably and these alterations are recorded on the certificate. In all of these inspection-cases of equipment calibration, every calibrating procedure must be accompanied by a statement of uncertainty—see Chapter Seven for more detail concerning these Measurement uncertainty issues.

In the case of many large industrial companies, they often have their own internal calibration hierarchies. As a consequence, such a company will calibrate/verify their instruments/artefacts—at appropriate intervals—by their own company's Working Standards against the Reference Standards, these having previously been calibrated by National Standards Organisations, such as those typically being for instance: PTB; NIST: The NPL; SNV; etc.; or via an accredited calibration laboratory. Something worthy of mentioning here is that for every calibration activity undertaken that is further down the traceability chain from that of the National Primary Standard, the level of uncertainty of measurement will proportionally increase—see below. Due to this fact, measurement uncertainty is calculated at each step of the traceability chain, this allows for an overall uncertainty for the whole chain to be calculated. Advisably, the optimum procedure is to shorten this chain as much as possible. This is usually undertaken by utilising each standard to calibrate many of the lower accuracy standards in parallel, rather than consecutively, thereby merely chaining them together. This traceability process is depicted in Fig. 1.2 and in a somewhat differing form below, where in this latter case, it has the distinct appearance of a pyramid-structure, with either one or two of the highest accuracy standards at the top employed to calibrate as many suitable standards—at the next level down. In a similar fashion, this pyramid structure allows for more and more Standards—at lower levels—to also be calibrated, as the pyramid widens. By this means, minimising the number of levels in the pyramid; henceforth, the length of the traceability chain is kept short, whilst simultaneously supporting a large number of standards at the lowest level of its traceability.

The superb & modern facilities at the National Physical Laboratory (Teddington), where the fundamental & applied research of measurements & Instrument/Artefact Calibration of Traceable Measurement is undertaken for the United Kingdom.

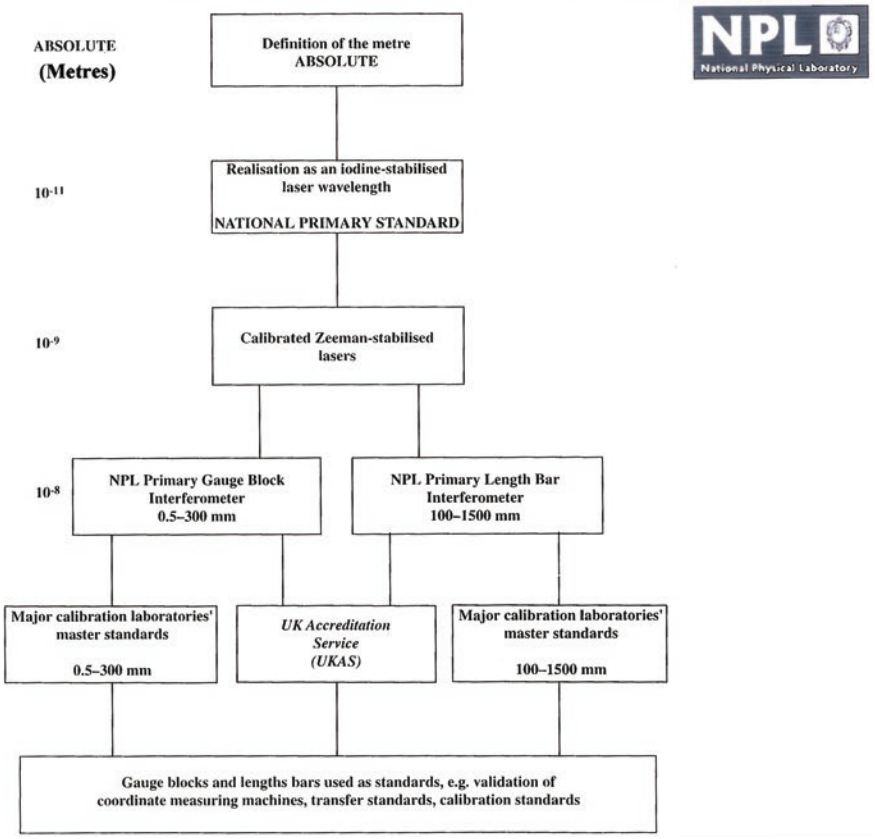

Fig. 1.2 The '*traceability of measurement chain*' for a range of *metrological artefacts* utilised in *machine tool calibration*

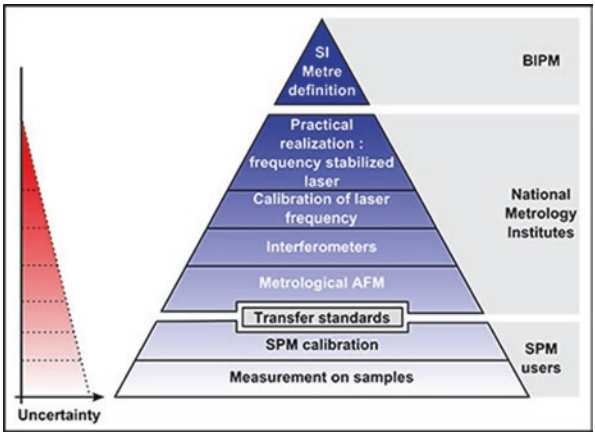

Traceability pyramid for the Metre and its potential calibrated uncertainties at differing measurement and calibration levels—illustrating how at lower levels this uncertainty proportionally increases [courtesy of: LNE (Laboratoire national de métrologie et d'essais, France) 2015]

Supporting a Claim of Traceability—Procedure to be Followed

It should be emphasised, that only the results of measurements and the values of Standards are traceable, which tends to infer that organisations cannot be traceable. Consequently, the provider of measurement results, or values of a Standard is responsible for supporting the claim of such traceability of these results, or values. This is so, whether that national provider might be: NMI; PTB; NIST; SFS; The NPL; etc.; or any another National Metrological Institute (NMI)—see a representative list of such NMI's at rear of this book. When supporting a claim of traceability, the provider—such as an industrial company—having a particular set of test measurement results, or values of a standard, must fully document the measurement process, or system utilised to establish the claim, providing a description of the chain of comparisons that were employed in establishing a connection to a particular stated reference standard. This documentary action means that there might be several common elements to all valid statements, or claims of traceability, such as a:

- **clearly defined certain quantity**—that has been measured;
- **comprehensive description of the system of measurement, or the working standard**—utilised to perform that measurement;
- **quantified measurement result, or value**—with its documented uncertainty;
- **wide-ranging specification of the particular reference at the time the measurement system, or comparison**—to its working standard;
- **measurement assurance program** (i.e. internally-driven)—that establishes the status of the measurement system, or the working standard being at all times pertinent to the claim of traceability;
- **measurement assurance program** (internal)—for instituting the prominence of the stated reference at the time that the measurement system, or comparison to its working standard occurred.

From these specific points listed above, it can be presumed that an internal measurement assurance program might be either quite simple or multi-faceted. The level, or exactitude to be determined normally depends on the level of uncertainty at issue and, what is desirable to demonstrate its traceable credibility. Therefore, the users of a specific test measurement result are responsible for determining what is acceptable to meet their company's needs. According to the internationally recognised metrological VIM-definition the term traceability is as previously mentioned, being a property of the result of a measurement, or the value of a Standard by which that result, or value is related to Standards and not to the National Metrological Institutions (NMI's). So to logically follow on, and as a simple example, the short phrase here (i.e. in this instance, specifically-relating to German metrological activities): Traceable to PTB, in its most correct sense, is basically shorthand for the: "Results of measurements that are traceable to reference standards developed and maintained by PTB".

1.3.2 Auditing Metrology: Artefacts, Instrumentation and Equipment

There are perhaps three main reasons for instigating Auditing by a company, these might be:

1. **an ISO 9000 assessment is conducted**—to ensure a company has the correct procedures for the type of manufacturing work undertaken and that they follow those procedures;
2. **an ISO 17025 assessment may be conducted**—to ensuring that procedures for any work undertaken monitors those procedures that provide the correct answers;
3. **a technical audit can be considered as an official examination of the company's: staff; laboratories; equipment; methods and procedures**—that are utilised during the actual measurement process.

In an audit, it is normal for a member of the management team to undertake an Internal audit, ensuring that the company's procedures/systems are detailed within the company's Quality Manual—certifying that they are being monitored and actually do work. From time-to-time, an External auditing exercise is also undertaken, in order to convince either an independent accreditation body, or a potential important customer, that the measurements reported are valid and the products, or services the company supplies and its manufactured goods, can be relied upon. When a Comprehensive audit of a company is instigated, it is anticipated that the actual process involves two distinct types of auditing procedure. These are namely: (i) a vertical audit; and (ii) a horizontal audit. In the following section, these types of auditing activities will now be considered in more detail.

Vertical Audit—Within a Company

Any vertical auditing necessitates that an approved technical assessor will normally select—at random—either, say, a measurement report, or more specifically for perhaps, calibration certification work that was produced by the company

being assessed. In either of these cases, the assessor, will then—in minute detail go through the whole process that was undertaken when producing that report. Here, the assessor scrutinises the written measurement procedure describing the measurements previously made, thus ensuring that the procedure was appropriate and up-to-date and that it had been complied with, in the correct manner. Here then, this technical assessor may question either the inspector, or metrologist, or indeed both, asking them to demonstrate a specific measurement procedure, to attempt to ascertain if the person understood their actual role in this inspection/validation/calibration activity. At this point, the actual data sheets and procedures are scrutinised with that of the raw data, plus any calculations produced that had been accurately recorded, then transferred to the measurement report, or certificate. Moreover, measurement dates are also noted and then a check and further examination of the environmental records would be made, ensuring that the company's facility had been functioning within the specified limits at the time of these measurements. So any artefacts and instrumentation, as well as other equipment utilised when performing these measurements are also checked, ensuring that each measuring item employed was itself within calibration during the time when the measurements were taken. Furthermore, checks on all of the applicable calibration certificates that were available, including certain corrections that had been applied—as deemed necessary—with a detailed analysis of the relevant uncertainty calculations, would also be expected at this time.

During the process of vertical auditing, the technical assessor would consider the general level of cleanliness/tidiness within the facility; this is often termed shine.[14] Furthermore, visual checks are also undertaken to establish if appropriate calibration stickers are applied to any measuring equipment and that the appropriate Reference Standards were utilised, which will also be scrutinised and noted. Moreover, all these types of auditing activities within the company would come under the general remit of a vertical audit.

Horizontal Audit—Within a Company

Horizontal auditing encompasses tracking particular processes from the beginning of any operation to its completion. This type of audit normally overlaps a number of the company's boundaries between distinct areas, functions or departments. Consequently, the technical auditors, for example, may decide that they need to examine in what manner a purchase order for certain metrological instrumentation is raised, then how it is processed within the company or in what way would any necessary calibration certificates be produced. As a result, an auditor could then observe and scrutinise that

[14]**Shine** (**Shine**, refers to the cleanliness and order of the actual plant, in its working environment.): is a term, which is derived from the Japanese maintenance philosophy of: **5S**. It is the name of a Workplace organisation method that utilises a list of five discrete Japanese words: Seiri (Sort), Seiton (Set-in-order), Seiso (Shine), Seiketsu (Standardise) and Shitsuke (Sustain). This **5S**-list describes how to organise an industrial workspace for efficiency and effectiveness: by identifying and storing the items used; maintaining the area and items; and sustaining the new-order. The decision making process is derived from a dialogue about standardisation, which builds an understanding among company's employees of how they should undertake the day-to-day work.

procedures exist in the company informing relevant staff what activities they are supposed to be carrying out, while checking to see that these procedures are complied with according to the stated objectives within the company's Quality manual.[15]

After the Audit

Once the preliminary auditing procedure has been accomplished, an internal review is normal, with any non-compliances highlighted being reported to the company's lead-assessor. This internal Audit review will then discuss points raised, in conjunction with either the quality manager, or laboratory head, or indeed both. This review enables a working schedule of agreed corrective actions to be instigated. The typical timeline for minor findings and their necessary actions can usually be resolved within a few weeks, or perhaps at worst in several months—depending upon on their level of severity—but any major problems encountered will have to be urgently resolved. Minor findings or non-compliances may include such details as: any typographical errors in a certificate; an out-of-date organisational chart; or simply, a missing calibration label. Moreover, if comparable minor non-compliances are found to exist across the whole company organisation, this can produce a more unacceptable quality risk. Major findings might comprise of inspectors utilising out-of-date calibration Standards. Here then, any actions arising from the use of redundant standards could cause a postponement of that activity until these standards have been recalibrated, recalling those certificates, or reports that had previously been issued since this standard's certification approval. Thus, quite serious implications might be the result, where some acceptable products may have been passed-off that were actually out-of-specification, namely, the company may have sold faulty items to their customer(s). This catastrophic action of selling faulty goods to the customer(s), could prove to be financially ruinous to the company, in terms of: loss of the company's good name; further contracts being declined; potential and expensive litigation; or all of these unfortunate events!

Credibility of an Audit

Prior to undertaking any form of inspection, verification or calibration activity, it is vital to ensure that all relevant artefacts, instrumentation and equipment for dimensional measurements are traceable to valid Reference Standards. A quality inspector, or metrologist, needs to fully comprehend the question of their credibility, so once dimensional measurements have been made, this inspector/metrologist must have the confidence that the results provided are correct to within the stated uncertainty values. In the future, if some technical qualms exist concerning the

[15]**Quality manual of ISO 9001:2008**: is at its simplest interpretation being an Internationally-recognised Standard for Quality Management. Thus, a Quality manual is a Management Standard, rather than just a simply a Quality Standard. The major benefit that ISO 9001 certification offers, is that it brings to most businesses the fact that by running the operation in the most effective way to improve their customer's satisfaction requirements, it also helps a company to understand and then to streamline their overall range of processes, and to improve their documentation for greater effectiveness and efficiency.

measurements taken, such inspected items may require re-measurement. Although, if these latest readings are still open to some degree of uncertainty, then perhaps it might be advisable to ask another qualified person to also re-inspect them. It is inevitable that very occasionally one can make a mistake, but the important point here is to minimise such errors and as a result, validating the overall audit's credibility.

As an aside, one of the major reasons why a quality assurance department is normally a distinct and separate department from that of a manufacturing department, is because otherwise say, a production manager might perhaps attempt to coerce the quality department to deliver certain quantities of inspected products at a particular date, which would otherwise be considered as unacceptable simply to meet an unattainable deadline. As a result of these management distinctions in authority, the production manager will not be able to exert any undue influence on the quality people—when checking the excellence of that product. These distinctions in departmental authorities and responsibilities, mean that product quality is paramount and this discrete arrangement, ensure that the company's credibility is not compromised.

1.3.3 National Metrological Research and Calibration Laboratories

Virtually every technological-based country in the world requires their own National Metrology Laboratories (NMIs)—see an abridged list of addresses at the rear of this book. Considerable research into both fundamental and applied metrological development has occurred through the endeavours of several of the leading-exponents in this scientific/metrological field. However, here—due to distinct space-restrictions—only a brief mention of just some of these advanced laboratories will show (historically), how such advanced metrological-research activities have arisen over time.

The National Physical Laboratory (NPL), Teddington, UK

In 1900, The NPL—shown with their newly-built laboratories in Fig. 1.2 (top)—was founded within the UK, with its first Director being: R.T. Glazebrock (FRS). Although the formal opening occurred in 1902, by the then Prince of Wales, who said in his formal opening remarks: "I believe that in the National Physical Laboratory we have the first instance of the State taking part in scientific research. The object of the scheme is, I understand, to bring scientific knowledge to bear practically upon our everyday industrial and commercial life, to break down the barrier between theory and practice, to effect a union between science and commerce". These very astute statements made by the Prince are still valid today for all such national metrological laboratories.

During the intervening 110 plus years, some notable achievements have been made by The NPL, with just a few of the significant advances and their approximate dates, being listed below:

- **1920**, the introduction of **Materials testing** and by this time, routine test work amounted to about 1000–1500 items per year covering a wide range: strength of materials tests, also the testing of the efficiency of engines and gears, etc.;
- **1935—Radar** was invented, and in February 1935, Robert Watson-Watt who then presented his report titled: "The Detection of Aircraft by Radio Methods", to the newly-formed committee for the scientific-survey of air defence. A basic trial followed employing the BBC's shortwave (~50 m wavelength) radio transmitter at Daventry against a Heyford Bomber. This trial was successful and resulting in the design and installation of a chain of radar stations along the East and South coast of England—just in time for the disastrous and tragic outbreak of WWII;
- **1946**—work began on the world's first **Automatic Computing Engine** (ACE), with the final improved version going into service in **1958**. The total cost of developing ACE at the time was £250,000, with the brilliant, but enigmatic Alan Turing[16]—being a member of a group being formed for the design, construction and use of a large automatic computing engine;
- **1955**—first accurate **Caesium Atomic Clock** was built. Here, Louis Essen developed this Caesium atomic clock, which led to the internationally agreed definition of the second being based on atomic time. Following a trip to the USA to see early versions of these atomic clocks, Essen then designed and built one that delivered much greater accuracy and stability, based on the transition of the caesium-133 atom. This atomic-clock still remains the fundamental standard today. In **2011**—the world's most accurate clock, The NPL's: **Caesium Fountain Atomic Clock**—known simply as: **NPL-CsF2**, was revealed to be the most accurate long-term timekeeper in the world—as it only loses, or gains just one second over 138 million years;
- during the last 50-odd intervening years to the present day, The NPL has designed, tested and built many ground-breaking and innovative scientific and metrological instruments and products and, in 2012—the world's first room-temperature Maser was designed and constructed. Scientists from The NPL

[16]**Alan M. Turing** OBE, FRS: (Born: 23 June 1912 in Paddington, London—died: 7 June 1954 in Wilmslow, Cheshire, England) was a brilliant and unique polymath: Mathematician, Logician, Cryptanalyst, Philosopher, Computer Scientist, Mathematical Biologist, being also a marathon-runner. Turing's undergraduate studies were from 1931 to 1934 at King's College, Cambridge, gaining first-class honours in Mathematics. In 1935 when at just 22, Turing was elected a Fellow at King's on the basis of a dissertation in which he proved the Central Limit Theorem—despite the fact that he had not known that it had already been proven! (i.e. in 1922, by: Jarl Waldemar Lindeberg). From September 1936 to July 1938, Turing studied under Alonzo Church at Princeton University (USA). Moreover, in this purely mathematical-work, he studied Cryptology and, he also built three of the four stages of an: electromechanical binary multiplier. After just two years (i.e. in June 1938), Turing obtained his Ph.D.—from Princeton. Dr Alan Turing was highly influential in the development of Computer Science, providing a formalisation of the concepts and of the algorithm for that of computation—with his so-called: Turing machine (These Turing machines are presently a central object of study in the Theory of Computation.) This actual machine, being considered a model of a general-purpose computer. Turing is now widely considered by many Scientists and Engineers, to be the father of: "Theoretical Computer Science and Artificial Intelligence".

demonstrated for the first time a solid-state MASER[17]—see below, capable of operating at room temperature, thus paving the way for its widespread-adoption. The actual team from both The NPL and Imperial College (London), have demonstrated masing in a solid-state device, working in air at room temperature, with no applied magnetic field. This fundamental and scientific breakthrough means that the cost to manufacture and then to operate such MASERs could be dramatically reduced, which could potentially lead to them becoming as widely utilised as today's Laser technology.

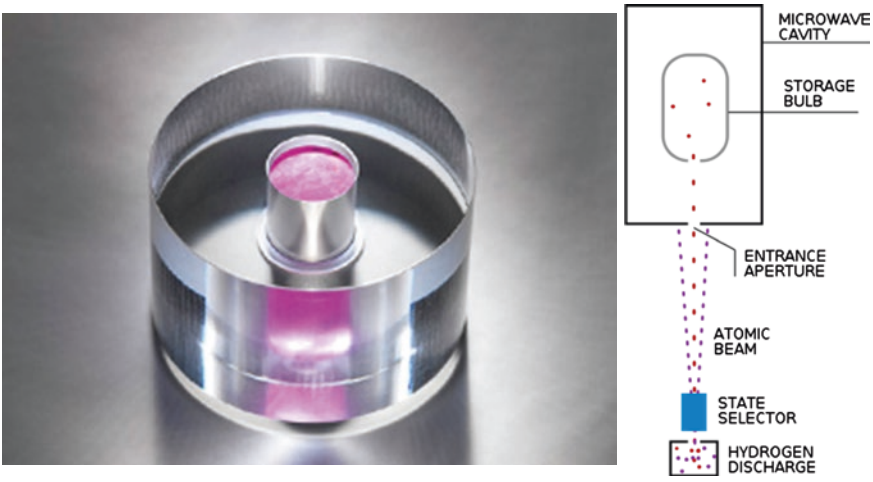

Hydrogen maser - which is currently (2015) The Atomic Frequency Standard.

The NPL-designed and built solid-state MASER (i.e. depicted on the left and, schematically on the right), could shortly be utilised in future laser-technological developments

The National Institute of Standards and Technology (NIST), Gaithersburg, USA

The **National Institute of Standards and Technology** (**NIST**) was known between the years 1901 until 1988 as: The **National Bureau of Standards** (**NBS**). However, acronym NIST (i.e. see Fig. 1.3, top), exists at several extensive

[17]A **maser** can be considered as an instrumental-device that produces coherent electromagnetic waves through amplification by stimulated emission. The actual term **maser**, has been derived from the acronym of **MASER**, meaning: **M**icrowave **A**mplification by **S**timulated **E**mission of **R**adiation. Of note, is that the lower-case usage arose from technological development having rendered the original definition imprecise, because contemporary masers emit electromagnetic waves and not just at microwave frequencies, but rather across a broader band of the electromagnetic spectrum. Hence, the Physicist Charles H. Townes, has suggested utilising the word molecular to replace microwave—for contemporary linguistic accuracy. Of some technical-note, was that the actual maser was originally first proposed and described by both: Nikolay Basov and Alexander Prokhorov—from The Lebedev Institute of Physics (USSR), at an: All-Union Conference on Radio-Spectroscopy, which was held in the then USSR, by The Academy of Sciences over 50 years ago—in May 1952.

Fig. 1.3 Many advanced technological countries have innovative research and calibration laboratories

sites within the United States and is one of the major Measurement Standards Laboratories in the world. Its National Metrological Institute (NMI), is a non-regulatory agency of the United States Department of Commerce. The Institute's official-mission is formalised to: "Promote U.S. innovation and industrial

competitiveness by advancing measurement science, standards, and technology in ways that enhance economic security and improve our quality of life".

By the close of the twentieth century in the USA, there were more than 700 federal laboratories, which is a stark contrast to the days when NIST stood-alone in concentrating on the Physical Sciences. However, NIST's influence continues to be as universal and crucial today. In fact, NIST's importance increases with the number of other federal laboratories, including both university and corporate research organisations, because many of their artefacts, instruments and measurements need to be traceable back to NIST's own Absolute Standards. This ability to be traceable to NIST, is because technological innovation and development, vitally depend more on measurements today, than at any previous time. One of NIST's past significant fundamental metrological innovations, relating to the optical interferometry development of the metre is shown below.

In 1951, NIST as it is now known, made this mercury lamp available to both science and industry as an ultimate Standard of Length. Here, the length measurements were based upon the circular interference fringes, which can clearly be seen being displayed on the background screen [courtesy of NIST (2015)]

By way of showing the depth and breadth of just one of NIST's fundamental research projects that was developed of late, is that of Atom-based Dimensional Metrology. The primary goal of this research project was to develop Intrinsic Calibration Standards—based upon the crystalline lattice. Hence, the ultimate limit for nanoscale-length metrology is the development of Intrinsic Calibration Standards, where the reference dimensions are founded upon the atomic spacing within an ordered, crystalline lattice. By means of techniques developed within this specific NIST research work, an advanced step height, line-width and pitch standards exhibiting picometre accuracy and precision[18] is now being developed, utilising an Ultra-high Vacuum Scanning Tunnelling Microscope (UHV-STM). Moreover, a NIST project goal here is to validate the use of atomic lattice spacing

[18]**Picometre**: is 1×10^{-12} m, which is in the region of the atomic dimensional size of a typical crystal lattice.

as a ruler through the comparison with interferometric length measurements such as those performed in the Molecular Measuring Machine. Such an atom-based dimensional metrology, will hopefully provide fundamental knowledge to develop the science of Metrology desirable to enable parallel, high-throughput, atomically precise manufacturing for NIST Standards development and for future industrial applications.

By way of an example of just some typical fundamental research work currently underway at NIST, is that of the already previously quoted Atom-based dimensional metrology, with its main objectives being:

- **to develop methods for repeatedly creating atomically sharp tungsten and alternative material tips and, then evaluating their atomic resolution imaging capabilities**—this minute metrological work includes a systematic evaluation of different crystalline materials capable of producing single atom tips, or atomic structures defined for high-resolution subnanometre imaging;

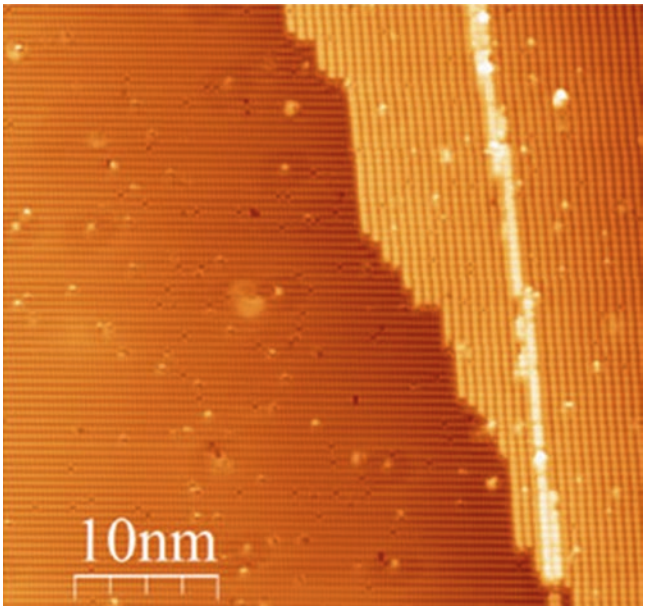

Scanning Tunnelling Microscope (STM) image shows two silicon (100) terraces and a single atomic step (i.e. with a minute height of 0.136 nm) between them. The STM patterned a single line on the right side of this atomic terrace [courtesy of NIST (2014)]

- **this current research requires a substantial effort to develop atomically ordered and large (i.e. >20 μm) silicon (100) surfaces for hydrogen termination**—by applying either the scanning probe STM, or AFM to create patterns on this hydrogen-passivated smooth surface and, with a suitable

oxidation process, a hard mask can be developed. Structures as small as 5 nm wide, having sub-nanometre thicknesses can now also be fabricated. Currently, these sections are not available commercially, for that reason it is essential to develop both suitable metrology for atomic resolution measurements and, the ability to fabricate and measure standards with atomic precision at this nanometric scale;

- by utilising the research facility of NanoFab at CNST[19] the development of a 'dry etching capability' to perform pattern transfer, for research/industrial applications—the patterns that are prepared by STM/AFM, can then be manufactured to thicknesses of just 1 atom and a Reactive Ion Etching (RIE) process, can enhance the vertical dimension to a more practical height of between 10 and 20 nm.

The Physikalisch-Technische Bundesanstalt (PTB)—Braunschweig, Germany

The PTB was originally founded in 1887 as the Physikalisch-Technische Reichsanstalt (PTR), which was the Physical and Technical Institute of the German Reich. The original objective of this organisation was to supervise and direct calibration and also establish Metrological Standards. The research areas have previously included Spectroscopy, Photometry, Electrical Engineering and Cryogenics. Instrumental in its original establishment were Werner von Siemens and Hermann von Helmholtz. Until 1934, the PTR was part of the Reichsinnenministerium (i.e. the Reich's Ministry of Interior Affairs), but after 1934, it became part of the Reichserziehungsministerium (i.e. the Reich's Ministry

[19]**NanoFab at CNST**, refers to: NIST's NanoFab laboratory at its Center for Nanoscale Science and Technology, which provides its researchers with state-of-the-art equipment, expert training and, a high level of flexibility to their current research and project work. Thus, the NanoFab laboratory also provides access to a wide variety of measurement and characterisation tools, technologies, with the appropriate expertise to NIST and its industrial and academic partners.

of Education). Previous incumbents of the Institute's Board of Directors have included Heinrich Konen and Walther Nernst circa 1930, together with Albert Einstein (1917–1933), Ludwig Prandtl and Max Planck, as well as other notable-representatives from a range of world-class companies, such as Siemens AG; Krupp; and Zeiss.

In a very short chronology from its commencement in **1887**, the PTR/PTB's fundamental milestones in its organisation, scientific and technical development, have included:

- **1898**—first legal tasks: realisation and maintenance of the electrical units, testing of a range of measuring instruments for electrical quantities;
- **1923**—incorporation of the Reichsanstalt für Maß und Gewicht (i.e. the Imperial Weights and Measures Office), supervising technical authority of the verification and testing offices, responsible for establishing and safeguarding all legal units;
- **1943**—after significant and heavy World War II damage, thus, it was essential to both rebuild and to relocate many the laboratories of the PTR—in **1945**;
- **1946**—the fundamental reconstruction of PTR in Berlin, as an agency for the Senate of West Berlin;
- **1950**—The Physikalisch-Technische Bundesanstalt (PTB) in Braunschweig, was then subsequently founded;
- **1953**—the incorporation of PTR in Berlin-Charlottenburg into the PTB, under the name of: Institut Berlin der PTB;
- **1977**—the State and Industry set up the Deutscher Kalibrierdienst (DKD)—which is the German Calibration Service, for the official authorisation of the certified calibration of Standards and Measuring-devices, under the supervision of the PTB;
- **1990**—the assumption of specified tasks in the Metrology sector, of the Amt für Standardisierung, Meßwesen und Warenprüfung (ASMW), which is an Agency for Standardisation, Metrology and Quality Control, German Democratic Republic (GDR);
- **2002**—the evaluation of PTB by an International Commission—with excellent results;
- **2007**—further evaluation of PTB by the German Council of Science and Humanities, by order of the German Federal Government—with once again, with excellent results.

The PTB has built upon its many diverse and significant advanced metrological research and calibration activities continuing to the present day with, for instance, just some of the extraordinary nanoimages from their previous work with AFM's being shown.

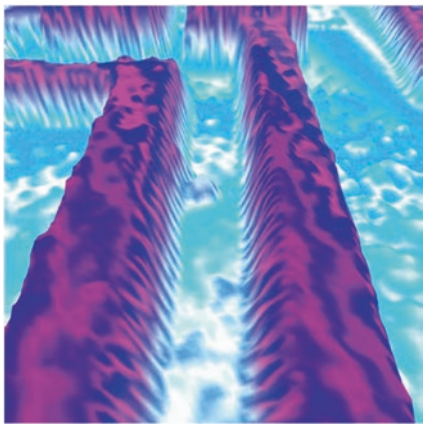

Atomic force photomicrograph: here the actual magnification is ≈×35,000, at capture, with the actual sample size being just ≈15 μm × 25 μm, by post-capture colourisation. This circuit-level image of a computer chip is a magnified-view from the sample. Thus, the blue water-like colouring symbolises the flow of information inside the microprocessor. The image-data was provided by the nanometrologist: Thorsten Dziomba, the post-capture colourisation was performed utilising: WS × M scanning probe microscopy software—for data visualisation [courtesy of: Hans U. Danzebrink and Anna-Maria Gleixner—Data Channels/Thorsten Dziomba—of the Physikalisch-Technische Bundesanstalt (PTB), Braunschweig, Germany (2007)]

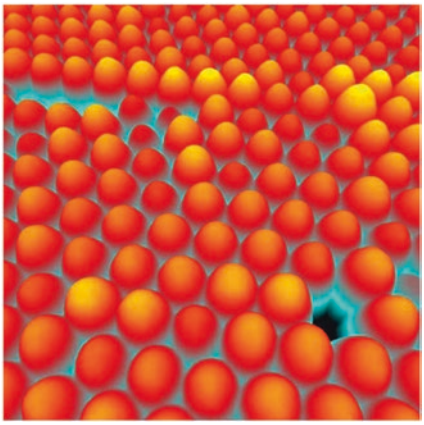

Atomic force photomicrograph: magnification was ≈×350,000 at capture, with a sample ≈1.5 μm × 2.5 μm in size; by post-capture colourisation. This image reveals dislocations in a photonic crystal arrangement of polystyrene nanospheres magnified from the sample. Here, the photonic crystals were grown as self-assembled structures from a colloidal solution. These nanospheres measure just ≈∅200 nm and are ≈300 times smaller than a human hair, but are still ≈500 times larger than actual atoms. Practically, photonic crystals can be utilised to control and manipulate the flow of light (e.g. in optical waveguides). In this instance, WS × M software was utilised to undertake the post-capture colourisation [courtesy of Hans U. Danzebrink—Aesthetic Imperfections and Physikalisch-Technische Bundesanstalt (PTB), Braunschweig, Germany—where: Thorsten Dziomba of PTB provided the image-data and furthermore, Dr. Frank Marlow of the Max-Planck-Institut für Kohlenforschung supplied the actual prepared sample for its subsequent photomicroscopy investigation and assessment (2008)]

These three world-class Metrological/Standards Laboratories briefly described, namely NPL, NIST and PTB are complemented by those in many other advanced technological countries, typically such as: Laboratoire national de métrologie et d'essais (LNE) in France; The National Metrology Institute of Japan (NMIJ); The National Measurement Institute (NMIA) in Australia; The Danish Institute of Fundamental Metrology (DFM); The National Institute of Metrology (NIM) in China, but due to text space requirements, it has not been possible here to cover all other countries valid and current fundamental and applied research work—in the highly focused field of advanced metrology development.

Commercial Metrology Laboratories

Virtually every country today has its own Commercial Metrology Laboratories—see an abridged list of them at rear of this book—such as those typically shown in Fig. 1.3 (i.e. within the UK—middle, and in Italy—bottom). These Metrology-laboratories would have some form of traceability, which for instance in the UK, would be from UKAS.[20] To show the scope of industrial metrology undertaken by a typical commercial laboratory, for instance within the UK (Fig. 1.3, middle), this particular metrology company offers two types of service: a laboratory-based calibration service for portable measuring instruments and an onsite calibration service for the larger types of instruments and equipment—for that of industrial companies. To show the scope of instruments and inspection/calibration testing for its internal calibration service, this particular metrological laboratory might include the Inspection and Testing of:

- Bore gauges and Setting rings;
- Optical parallels;
- Digimatic scales;
- Depth-, Snap- and Thickness-gauges;
- Combination sets, Steel rules and Bevel protractors;
- Bench centres, Squares and Cylindrical squares;
- Calibration testers;
- Types of Internal-, External- and Depth micrometres;
- Setting Standards;
- Vernier-, Dial- and Digimatic callipers;
- Height and Pin gauges;
- Dial gauges, Dial calliper gauges and Dial test indicators;
- Height, Square and Check Masters;

[20]**UKAS** is short for the: **U**nited **K**ingdom **A**ccreditation **S**ervice, which is the sole national accreditation body recognised by Government to assess, against: Internationally agreed Standards, together with organisations that provide certification, testing, inspection and calibration services. By an Accreditation from UKAS, this will demonstrate the competence, impartiality and performance capability of these Metrology-evaluators. UKAS is a non-profit-distributing private company, limited by guarantee. Although, UKAS is certainly independent of the UK Government, it is however, appointed as the national accreditation body by the: Accreditation Regulations 2009 (SI No 3155/2009) and the EU Regulation (EC) 765/2008. As such, it operates under a: "Memorandum of Understanding" with the Government through the Secretary of State for Business, Innovation and Skills.

- Gauge blocks and Accessories;
- Electronic and Bench Comparators.

In an **Onsite Calibration Service** (i.e. typically accredited by say, UKAS), it might include the testing of the following:

- Surface tables and Surface plates;
- CMM's—in various configurations;
- Microscopes and Projectors;
- Electronic and Optical comparators;
- Hardness testing machines.

Not only must the Commercial Metrology Laboratories conform to their individual country's Calibration Standards, such as previously mentioned concerning: UKAS in the UK, but they should also attain **ISO/IEC 17025**[21] competence. Additionally and apart from the documentation and procedures that need to be adhered to when attaining **ISO/IEC 17025**, the physical laboratory's Design enclosure parameters are expected to conform to the following:

- **temperature set point**: ±0.01–1.0 °C;
- **humidity set point**: ±1–5 % RH;
- **clean room**: ISO class 1 through class 8;
- **pressure**: positive, or negative;
- **air velocity**: 1–30 m min^{-1};
- **lighting**: 50, 100 FC.

Additionally, in some metrology laboratories, they may also include anti-static floors, with preferably no natural light straying in from windows, which might otherwise influence the overall measurement environment.

1.4 Machine Tool's Machining Capabilities

In the modern world, it is simply inconceivable that any highly accurate and precise product would be manufactured without the sophisticated-aid of CNC machining technology. Component dimensional tolerances together with their physical sizes can vary enormously, ranging from: nano-machined parts[22];

[21]**ISO/IEC 17025**: **General requirements for the competence of testing and calibration laboratories**: is the main **ISO/CASCO** Standard utilised by testing and calibration laboratories. It was originally known as: **ISO/IEC Guide 25**, with **ISO/IEC 17025** being initially issued by the International Organization for Standardization in 1999. There are many commonalities with the **ISO 9000** Standard, but **ISO/IEC 17025** is more specific in its requirements for competence. It applies directly to those organisations that produce testing and calibration results. After its initial release, a second version was instigated in 2005, once it was agreed that it needed to have its quality system words more closely aligned with the 2000 version of **ISO 9001**.

[22]**Nano-machining**: this is where either the component's size is in the region of 10^{-9} m, or for much larger parts, where its critical dimensions are toleranced within this nano-metric dimensional region.

Ultra-precision and micromachining; to General-purpose precision machining—where in this latter case, some truly massive components in the construction, aerospace and marine industries are invariably produced.

The challenge of nano-machining and component measurement

If one takes a closer look into the types of nano-machining challenges that exist when attempting to manufacture a component at this sub-micrometre range, then the problems of actual production have unique complications. The fact is, that because a miniscule D_{OC}[23] occurs, the circumstance of the normal honed cutting edges on most tooling cannot cope with such minute cuts, which causes the following condition, for instance, as the tool's edge is simply not sharp enough, it causes tool's edge to plough (i.e. ride-over the workpiece's surface) instead of cutting—a particular problem when machining very ductile workpiece materials. In such circumstances when say, turning in the nano-machining range, monolithic diamond tools[24] are invariably utilised—with the very sharp tool's diamond cutting edge specifically orientated so avoiding its natural fracture planes. When nano-machining at this level of precision and accuracy, namely at a few billionth parts of a metre (i.e. its D_{OC}), a wide range of process, environmental and machine tool influences are acknowledge, which must be minimised—more will be said on this topic later in this chapter. Simply controlling the tool placement and the actual machine tool slide's axis position, let alone the problem of component measurement, becomes a real challenge when operating at the nano-region of machining. To exacerbate the problem still further, it is anticipated that some components will shortly be machined within the pico-range (i.e. 10^{-12} m) in the near-future—this being true sub-atomic machining,[25] which will only be a possibility if the workpiece is cryogenically prepared (i.e. soaked at extremely low temperatures of ≤ -125 °C[26]). There are some major problems that exist at this infinitesimally small manufacturing level, as already mentioned above, but is compounded still further by the fact that thermodynamically, a material is inherently unstable, unless it is cryogenically treated. Today, laser-controlled slideways, coupled with a very stiff machine tool structural control loop are desirable for such machining operations, with precisely monitored and controlled ambient workshop laboratory

[23]The term: $\mathbf{D_{OC}}$, refers to the depth of cut taken when machining a component, or more specifically, when milling, or turning operations occur. Here when either turning/boring/facing-off, this cut-depth should more appropriately be known as the: undeformed chip thickness.

[24]**Monolithic diamond tooling**: utilises natural diamond, which will have the following typical characteristics of: Hardness ~8000 H_V; Density (ρ) 3515 kg m^{-3}; Compression strength 7000 MPa; with a Young's modulus (E), ≈930 GPa.

[25]For example and by way of a comparison, the typical **atomic radius** for just some much-employed elements that are frequently machined, are: carbon ~0.071 nm; iron ~0.0124 nm; with aluminium ~0.143 nm.

[26]**Cryogenic machining**: this is necessary for several reasons, firstly, to minimise the thermodynamic effect of the atomic lattice motion—at normal room temperature (i.e. 20 °C) and secondly, in order to minimise the effect of the coefficient of thermal expansion (α), which is caused by heat generated whilst cutting the part.

temperatures, plus anti-vibration floor-mountings being necessary, in order to attempt such an exacting machining-regime.

Ultra-Precision and Micromachining

In the last decade, the demand for accurate machining and precise assembled components, so that they have the capability to be located and aligned together in a much closer proximity has significantly increased. The term Ultra-precision machining is open to some debate as to what it actually entails. Does it refer to the manufacture of very small components (i.e. Fig. 1.4, top—left and right) or can it mean very large machined parts (i.e. Fig. 1.4, bottom) having its critical dimensions within this dimensional tolerance-range? CNC machining technology can achieve both of these requirements, with the appropriate quality, application and programming of suitable machine tools. In both of these cases of either: nano- and Ultra-precision machining, the challenge for the Metrologist is to determine whether the dimensions and tolerances for critical component features inspected were met. Here then is the actual dilemma, until a few years ago metrology equipment could be produced to an accuracy and precision of better than ten times that of the machined part. Conversely today, we are now at, or approaching the absolute limits of the physical capabilities of dimensional discrimination, namely, once the machined component has been produced. This then poses the real problem, how does one actually confirm the part's dimensional size, when the instruments and equipment currently employed have less dimensional size resolution than that of the machined workpiece? This critical and unresolved-problem is well-known to both manufacturing engineers and to that of metrologists; thus the manner in which this uncertainty of confirming the part's dimensional size has as yet, not been determined—to any technical level of satisfaction.

General Purpose Precision Machining

In the case of normally tolerated accurate and precise CNC machined parts, this metrology dilemma just mentioned above, concerning dimensional uncertainty issues is somewhat less challenging. By means of explaining what are the potential metrological problems that could arise, for example when attempting to machine the cylinder bores for the V20 engine block depicted in Fig. 1.4 (bottom) it might be worth considering this large casting's engine bores. Here, the Travelling Column Boring machine tool must be able to accurately position itself in the correct relationship for each individual bore to be machined, so each CNC axis must have very precise close-loop position monitoring control of the slideways to enable this to be achieved. Once the boring head's axes have been positioned over a respective bore to be machined, the boring operation can now commence, but even here some problems can arise. Typically, the boring head (be it single, twin, or tri-boring cutting edge inserts) must have been critically set to the correct bore's diameter—allowing for the desired tolerance requirements, prior to boring commencing. At this juncture, some potential positional uncertainties could arise in setting this bore diameter and its actual positional orientation to the respective unmachined bore.

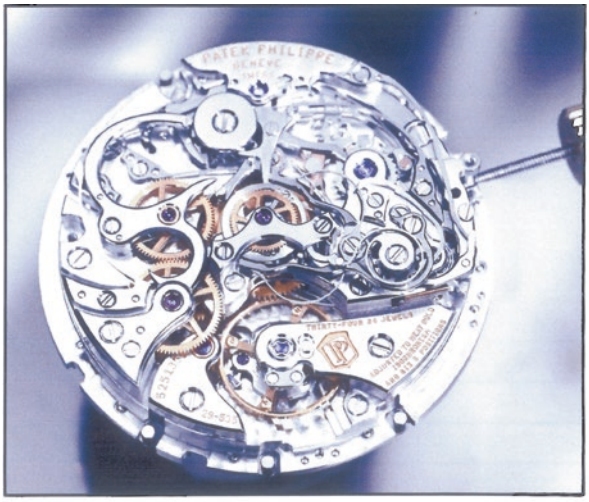

Micromachining to a positional accuracy of ≤ ±1 µm. [Courtesy of Cadence Inc. (USA)]

Ultra-high accurate & precise component assembly, such as required in intricate watch mechanisms, entail CNC machining technology to produce consistent & reliable parts.

[Courtesy of Patek Philippe (Switzerland)]

A *Travelling Column CNC (Vertical) Boring Machine*, machining a V20 engine block.

[Courtesy of Rottler (F109)/Premier Machinery Components (VIC, Australia)]

Fig. 1.4 The wide range and levels of sophisticated CNC machining technology today, can be found employed across such a diverse variety of industrial applications

Moreover, once these motions and tool settings have been established, then as the boring tool progresses down each bore's hole depth, other potential metrological problems could arise. The boring head's cutting inserts, might—as the edges progress around and down the bore—cause the following impending geometric

tolerance uncertainties, resulting from a range of tooling-rigidity and vibrational complications (e.g. chatter[27]) and tool wear-rates,[28] such as:

- **departures from roundness**[29]—ovality, or lobing (e.g. lobbing can occur in various geometric ways: 3-, 5-, 7-lobes, etc.);
- **harmonic behaviour**[30]—the undulations per revolution of the cutting edges—caused by deflection and chatter, can be superimposed onto the ovality, or roundness, or indeed onto each underlying harmonic, creating a complex roundness geometry;
- **cylindricity**[31]—this geometric error can often be present, most notably when boring the longer stroked engines;
- **coaxiality**[32] **and concentricity**[33]—both of these geometric errors could be present, when perhaps, a recessed counterboring operation is necessary.

It should be noted, that to a greater-or-lesser degree these geometric errors/uncertainties will always be present in a machined bore, including some others not stated here. Nevertheless, with judicious calibration of the machine tool and combining this with the appropriate cutting tool technology, coupled to the optimum feeds and speeds for boring, then at least some of these effects can be minimised. Once a bore has been bored out to its required diameter, it is often subjected to the secondary operation of cross-honing. Cross-honing heads are a complex operation of: rotational speed; oscillation speed; honing stroke length; together with honing stick pressure. This honing head rotation in combination with linear motion,

[27]**Chatter**: simply put, is a form of self-excited vibration introduced by a closed-loop force displacement response to cutting, which can be minimised by the astute use of the application of Stability-lobe diagrams—which is outside the remit of this book—see: Smith (2008).

[28]**Tool wear rates**: are a very complex topic and are affected by many machining and tooling parameters, being exacerbated by vibrational effects, during such machining operations.

[29]**Departures from roundness**: often commonly termed out-of-roundness, which is when the hole, or shaft feature tends to deviate from a true circle—this being the result of many machining-related factors.
NB The Least Squares Roundness (LSC) parameter, is often applied to determine the roundness of a component.

[30]**Harmonic behaviour**: is the product of a combination of factors, such as both the: tool-and-workpiece rigidity issues: coupled to any vibrational effects when machining.

[31]**Cylindricity**: this refers to two, or more roundness planes utilised to produce a cylinder, where the radial differences are at a minimum. Typical undesirable cylindricity geometry, could be a: bent; tapered; waisted; barrelled; or curved cylindrical profiles, or indeed, a combination of several of these cylindricity geometries.

[32]**Coaxiality**: this profile refers to the relationship of two cylinders, one of which is used as a datum. In this case, the datum cylinder is both square and concentric, but the secondary, or indeed yet more cylinders, are to be found perhaps, laying at an angle to this datum cylindrical axis.

[33]**Concentricity**: describes when the diameter of a geometrical circular feature—described by its profile centre—when rotated about that datum point (i.e. axis) is constant, as are any other diameters associated with this rotation.

creates a cross-honed pattern in the bore, correcting geometric imperfections, whilst improving oil-retention capabilities within the bore's cylinder.

1.5 Metrology Equipment Utilised for Basic Machine Tool Calibration Checks

In practical metrological measurements for the inspection and calibration work undertaken on machine tools, the use of equipment such as: Gauge blocks; Length bars; Angle gauges; Straightedges; Dial gauges; together with Dial test indicators forms the foundation for machine verification. Prior to discussing how this basic metrology equipment is utilised for calibration work, it may be a beneficial exercise to discuss each of these products in a little more detail.

1.5.1 Gauge Blocks

The original basis for the usage of Gauge blocks was developed by the Swedish inventor Carl Edvard Johansson. Johansson was employed in 1888 as an armourer-inspector by the state arsenal of Carl Gustafs stads Gevärsfaktori [Carl Gustaf Stad's Rifle Factory] in the town of Eskilstuna, Sweden. Johansson was concerned with the expensive tools for measuring parts for the Remington rifles then in production under licence at Carl Gustaf. When Sweden adopted a tailored-variant of the Mauser-carbine in 1894, Johansson was very eager concerning the chance to study Mauser's techniques of measuring. However, a visit by Johansson to the Mauser factory in Oberndorf am Neckar (Germany) proved to be somewhat of a disappointment. Whilst travelling on the train home, Johansson thought about the metrology and manufacturing problems for the rifle's production and his solution was to invent a set of blocks that could be combined to make up any dimensional measurement—within the limits of this set of blocks.

Johansson's ubiquitous Gauge block, also commonly known variously as: Gauge blocks, Johansson gauges, Slip-gauges, or simply Jo-blocks, are a system for creating accurate and precision lengths. An individual gauge block can be produced from either a metallic (e.g. WC), or ceramic-based material that has been precision ground and lapped to a specific and controlled thickness. Gauge blocks are available in sets of blocks, with a range of standard lengths—see Fig. 1.5a. In use, the

(a) A typical high-quality ceramic *Gauge Block* boxed set:

(b) Boxed set of highly accurate and precise *Length Bars* - the longer bars indicating their respective 'support points':

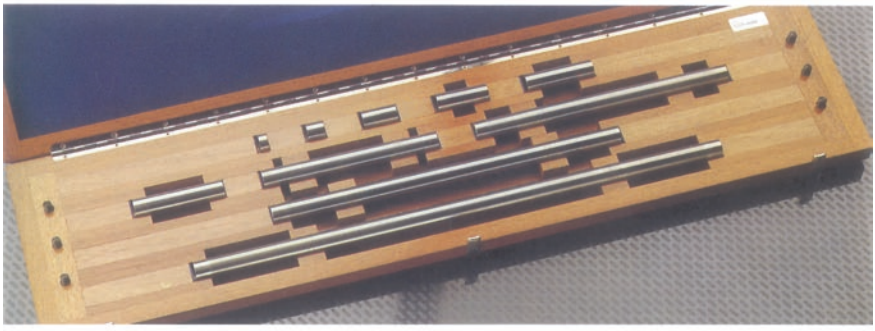

NB Detail of the 'Nichol Joint' for the connection of adjacent Length Bars:

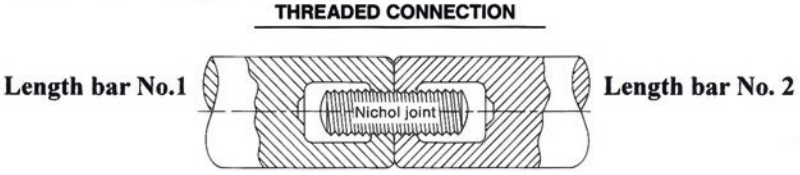

Fig. 1.5 Illustrates both *gauge block* and *length bar* sets—often in the past and occasionally presently, being employed for machine calibration work (courtesy of Tesa Metrology/Brown & Sharpe)

Table 1.3 Typical gauge block metrology applications, with their grades

Name	Applications	Grade
Workshop	Mounting tools and cutters	2
	Manufacturing gauges and calibrating instruments	1, or 2
Inspection	Setup of measuring devices	1, or 2
	Checking the accuracy of gauges and calibrating instruments	0, or 1
Calibration	Checking accuracy of gauge blocks for:	
	Workshop; Inspection; Accuracy of instruments	K, or 0
Reference	Checking accuracy of Gauge blocks for calibration and for academic research	K

Courtesy of Mitutoyo, Japan

blocks are stacked into a pile to make up a desired length.[34] A notable feature of Gauge blocks is that they can be amalgamated together with very little dimensional uncertainty—apart from each gauge's individual tolerance plus its associated wringing film (i.e. between each block). The blocks are joined by the combined action of sliding and a pressure-process called wringing (Fig. 1.7a), which causes their ultra-flat surfaces to adhere together.[35] As a result, a small number of gauge blocks can be utilised to create accurate lengths within a wide dimensional range. By utilising blocks from say, a large set of 105 blocks, one may create any of the required lengths up to its dimensional additive capacity—in 0.001 mm incremental-steps. The above Table 1.3, can be utilised as an approximate guide to select the appropriate gauge block grade according to usage (as specified by either the standards: **EN ISO 3650**; **BS4311**; and **JIS B 7506**), as indicated in the table below.

[34]When utilising metallic-based **Gauge blocks** in a pile as they are often known, in order to ensure wear is minimised on the opposite ends of the pile's outer faces, a good practice here is to use WC-protectors. Of some note is that by handling Gauge blocks, this increases their temperature and hence size, so they should be handled as little as possible and having been handled, one must then allow for subsequent stabilising—often termed its settling-time. Where calibrated measurements are being made to a high order of accuracy and precision, then a time of: 20 min per 25 mm length of gauge is normally recommended. During any form of handled measurement, it is best if all of the components utilised are left standing on for example, a cast iron surface plate, this provides a good heat-conductor, where it acts as a heat-sink dissipating any temperature differentials more rapidly. Cotton gloves (Fig. 1.7a), act as a basic thermal barrier to help to minimise the influence of thermal expansion of the component/artefact to be either measured, or calibrated, as a result of handling. Often when calibrating Gauge blocks that have been wrung onto a platen in the comparator, or an interferometer, then a transparent shield in front of one's face helps to reduce the effect that breath will have on any subsequent calibration measurements.

[35]Correctly wrung-together Gauge blocks may withstand a 330 N force—by the actual user. The exact wringing-mechanism is unknown, but it is believed to be a combination of these three effects: (i) air pressure, more specifically an applied pressure between the blocks causing the air to be squeezed-out at the Gauge block interface; (ii) surface tension from either any oil and water vapour that is present between the blocks; (iii) from molecular attraction occurring when two very flat surfaces are brought into contact. This attractive force (i.e. is not magnetic) causes Gauge blocks to adhere even without surface lubricants. Gauge blocks should then be de-wrung, to avoid any cold welding tendencies, shortly after their use.

The calibration of gauge blocks (e.g. typically shown in Fig. 1.7b, c) basically depends upon both their age and surface condition, with the older and worn blocks requiring more frequent calibration; characteristically, this should occur at least once per year. One technique often deployed for accurate and precise artefact verification/calibration is termed ANOVA gauge R&R,[36] or to be more specific: ANOVA gauge repeatability and reproducibility. This system is based upon a six-sigma methodology[37] which is a measurement systems analysis technique that practices an analysis of variance (ANOVA)—Random effects model, to assess a measurement system. The evaluation of a measurement system is not limited to just Gauges, but to all types of measuring instruments, test methods, plus other measurement systems. Specifically, ANOVA gauge R&R measures the amount of variability induced in measurements by the measurement system itself and compares it to the total variability observed to determine the feasibility of this measurement system. There are several constraints affecting a measurement system, these include:

- **measuring instruments**—the gauge, or instrument itself and all the gauge blocks, supports, fixtures, etc. The equipment's ease of use, any slackness among mating parts, and, zero-blocks, are all examples of these sources of variation in the measurement system;
- **operators** (i.e. personnel)—the abilities and/or discipline of a technical-based person who is required to follow written, or verbal instructions;
- **test inspection methods**—how the equipment to be utilised/verified/calibrated is set up, the specific test requirements, also including how this data is recorded, etc.;
- **specification**—the measurement is reported against a specification, or a reference value. So, the range, or the engineering tolerance does not affect its measurement, but is an important factor in evaluating the viability of the measurement system;
- **components**—some accurate and precise items are easier to be measured than others. A measurement system may be good for evaluating for example, a gauge block's length, but not for measuring material-compliant workpieces such as hard-rubberised component products.

In summary, there are basically two essential aspects of a gauge R&R, these are:

1. **Repeatability**—which is the variation in measurements taken by an individual, or instrument having the same/replicate item and under identical conditions;
2. **Reproducibility**—being the term utilised for the variation induced when different operators/instruments, or laboratories measure similar, or replicate parts.

[36]**ANOVA gauge R&R Study**: is a technique for determining the suitability of a Gauge, or Gauging-system for measuring a particular process. Every measurement taken will have some error associated with it, and if this error is large compared to the allowable range of values (i.e. its specific tolerance-band), the measuring device will frequently accept bad parts, while rejecting good ones.

[37]**Six-sigma methodology**: is a set of metaphorical tools and techniques/strategies which is normally utilised for process improvement, originally developed by Motorola in 1981. Six Sigma seeks to improve the quality of process outputs by identifying and removing the causes of these defects (errors) and then minimising variability in either the manufacturing and/or business processes.

In consequence, ANOVA gauge R&R is a significant feature within the overall Six Sigma methodology and, it is also often a specific/mandatory requirement for any type of: Production Part Approval Process (PPAP) documentation package.

1.5.2 Length Bars

When it becomes impractical to utilise Gauge blocks for longer length measurements, it is the normal practice to use Length Bars instead. These Length Bars are normally produced from high-carbon high-chromium steel [i.e. calibrated to: **ISO 3650 (1998)**; **BS EN ISO 3650 (1999)**, for **K**, **0**, or **1** grades], ensuring that the gauge faces are hardened to 64 H_{RC} (800 H_V). Typically, these Length Bars (Fig. 1.5b), have a round section of ∅30 mm for greater stability and ease of handling. Both of its ends are threaded and recessed and, precision lapped to meet with the stipulated Standards requirements of: finish, flatness, parallelism and gauge length.[38]

In order to calibrate Length Bars, the LBI1.5—Length Bar Interferometer (see below), was designed by The NPL, then manufactured by Hexagon Metrology to meet the requirement for calibrating longer type Length Standards at a Primary-level and with the best possible Measurement Uncertainty.[39] Accordingly, long-series Gauge blocks and Length Bars having lengths up to 1.5 m can be accommodated in this type of metrology equipment.

The NPL-designed/hexagon metrology manufactured (LBI1.5)—length bar interferometer (courtesy of The NPL/Hexagon Metrology)

[38]**Length bars** can be manufactured from differing materials and will normally produce the following expansion coefficients: steel and ceramic 11.7 ppm/°C; tungsten carbide 4.23 ppm/°C; chromium carbide 8.5 ppm/°C.

[39]**Length Measurement Uncertainty**, of: $\pm[0.045 + (0.06 \times L)]$ micrometres, where: '*L*' is in metres and this is possible, when the LBI1.5 (i.e. Length Bar Interferometer) is located within the correct environment.

In order to gain an appreciation of how Length Bar calibration equipment has been designed by The NPL, the essential features of this Length Bar Interferometer (i.e. shown in the photograph above and then schematically in Fig. 1.6a), are listed below:

- triple wavelength measurement for easier pre-classification of Length Standard size;
- three frequency stabilised laser light sources;
- phase-stepping optical system for high-precision length measurement and detailed analysis of Length Standard surface geometry;
- horizontal support of the Length Standard meets specification requirements;
- insulating and temperature controlled enclosure of the optical system;
- full and automatic measurement and compensation for ambient conditions;
- integrated and rapid Flatness and Length Variation measurement;
- automatic calculation and print-out of measurement results in inch, or metric units;
- flexible image-processing software for measurement of rectangular and square (i.e. Hoke) long-series gauge blocks and, round (i.e. British) Length Bars.

Support Points for Length Bars

The Airy support points are justly named after Sir George Airy,[40] who originally investigated the requirements for supporting precision Length Standards. These so-called Airy points are utilised for accurate and precision metrology measurement to support a Length Standard in such a way as to lessen its anticipated bending, or droop, while allowing the ends of the Length Bar to become parallel, or square (Fig. 1.6b, top). These Airy points are symmetrically arranged around the centre of the Length Bar and are separated by a distance that is equal to:

$$1/\sqrt{3} = 0.577L, \quad \text{or} \quad \text{approximately } 5/9\text{th of the total length of the Length Bar.}$$

It is normal to identify these Airy point positions by inscribed marks, or lines. Take for example, a 450-mm Length Bar, it would have an Airy point separation of 450 mm times 5/9 $\approx$ 250 mm. Consequently, a line, or more normally a pair of lines, would be engraved onto the gauge 100 mm in from each end. So, by supporting the Length Bar at these points, this will ensure that the calibrated length is attained. Alternatively, if this length Bar was not supported at the Airy points, then its measurement uncertainty would be increased.

The Bessel support points (i.e. after Friedrich William Bessel[41]), are the support positions for an evenly-loaded bar, where the droop for both the middle and

[40] **Sir George Biddell Airy** (1801–1892), was an English Mathematician/Astronomer, notably, he was the Astronomer Royal from 1835 to 1881, and from a metrology viewpoint, the instigator of the Airy support points.

[41] **Friedrich Wilhelm Bessel** (1784–1846) was a notable German Mathematician and an Astronomer, also he was the systematiser of the so-called Bessel functions and also developed the Bessell support points.

(a) A schematic diagram illustrating the *Laser Calibration* of *Length Bars*, under *controlled metrological conditions* in the laboratory.
[Courtesy of the National Physical Laboratory (UK)]

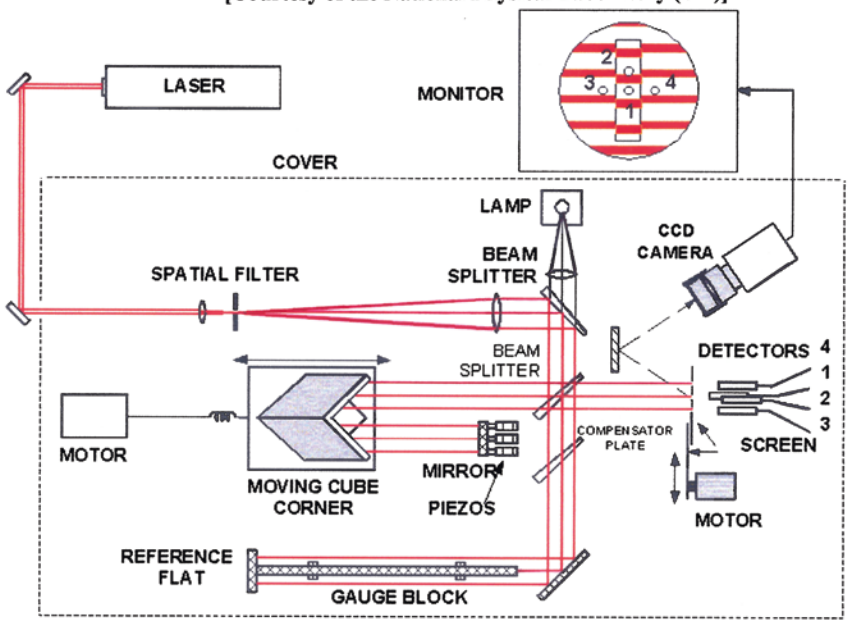

(b) Length Bar *Support points* (i.e. Airy & Bessel):

AIRY SUPPORT POINTS (ALLOW END-FACES TO BECOME PARALLEL):

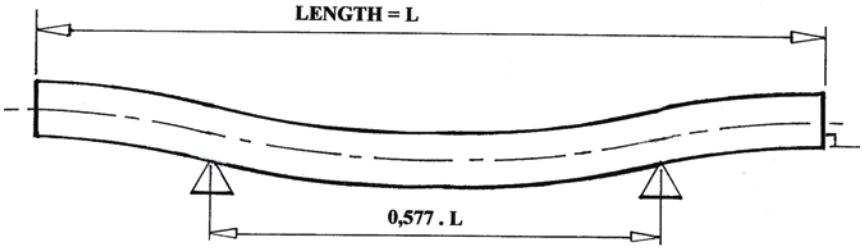

BESSELL SUPPORT POINTS (ALLOW POINTS OF MINIMUM DEFLECTION):

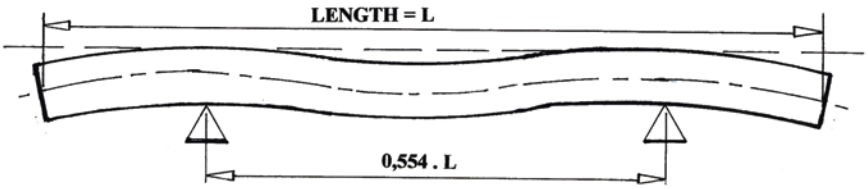

Fig. 1.6 *Length bars* have often been employed to calibrate machine tools

ends of the bar are at a minimum (i.e. termed its neutral axis). This support (Fig. 1.6b, bottom), often known as the points of minimum deflection, which is not valid for End Standards such as Length Bars, but can be utilised more effectively for the support points for flat metrology tables, or similar level items (Fig. 1.7).

1.5.3 Combination Angle Gauges

The original set of a combination of Angle Gauges was invented in 1939, by Dr G.A. Tomlinson[42] of The NPL. Currently, this type of combination set normally consists of a specific range of separate gauges, which may be utilised in conjunction with one square block and one parallel straight edge (see Fig. 1.8a). With this specific arrangement of a 15-piece combination set of Angle Gauges, it is possible to set up any angle to the nearest 2 s of arc (i.e. see Fig. 1.8b, c). In an identical way to gauge blocks, these high-quality angle Gauges are built up to give an angular dimension, of the required angle. Normally, these angle gauges are made of hardened alloy steel that are then seasoned (i.e. stabilised) carefully, thus ensuring permanence of their angular accuracy. The actual measuring faces are previously lapped and polished to a high degree of accuracy and flatness, similarly to that of gauge blocks. These angle gauges are approximately 75 mm long and 15 mm wide, with their faces being lapped to within 0.2 μm and having an included-angular tolerance of ±2 s of arc—between the two end faces.

Calibration of Angle Gauges by Interferometry

By this interferometry technique, the accuracy and precision of ≈0.1 s of arc in angular measurement is possible. It is normally assumed that these angle gauges have high degree of flatness on their working surfaces. The gauge length interferometer is normally utilised for such calibration purposes and the angle gauge—under test—is carefully wrung onto the platen. On viewing through the

[42]**Dr. George A. Tomlinson**: was a Principal Science Officer at The National Physical Laboratory (UK), he was Born: 7 January 1885 and died: 1 December 1944. Dr Tomlinson was educated at Nottingham High School, then progressing on to University College, Nottingham, where he took the degree of B.Sc. (London) in Engineering—obtaining first-class honours, while later completing a Ph.D. He was noted for his invention of Angle Gauges and also for a very early-form of surface texture instrumentation, known as the: Tomlinson Surface Meter. This particular instrument utilised a smoked glass screen for its surface-trace representation, via a mechanical/optical means for its magnification, then having obtained this smoked glass trace, it was then taken and further projected at ×50, or ×100 magnification for more accurate surface-examination. This metrology equipment, amongst many other notable contributions to the Science of Metrology, were also a significant feature of Dr Tomlinson's work.

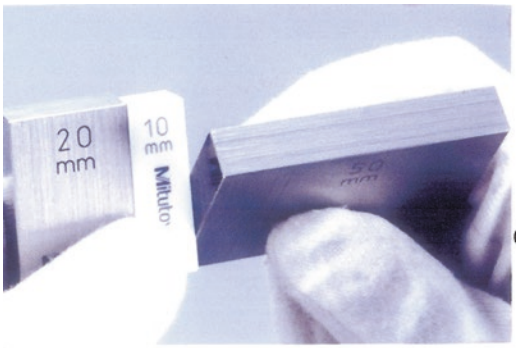

(a) *Gauge blocks* being *wrung-together*, while wearing/using *cotton gloves* to act as a *'heat -barrier'*, thereby minimising the potential *'Settling-time'*.
[Courtesy of Mitutoyo Metrology]

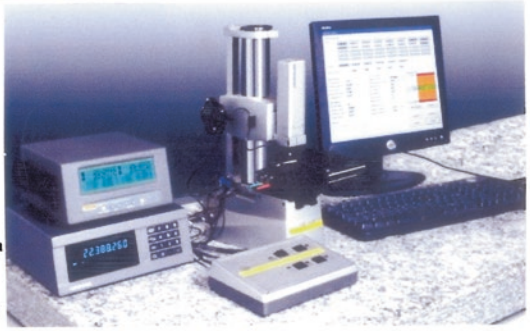

(b) Two *Gauge blocks* being placed onto a *Tesa UPD Gauge Block Comparator*, for *calibration*, prior to use.
[Courtesy of Tesa Metrology]

(c) Schematic diagram of the NPL Gauge Block Interferometer, calibrating 'blocks' to ISO 3650 – having been 'wrung' onto the platen.
[Courtesy of NPL/Tesa Metrology]

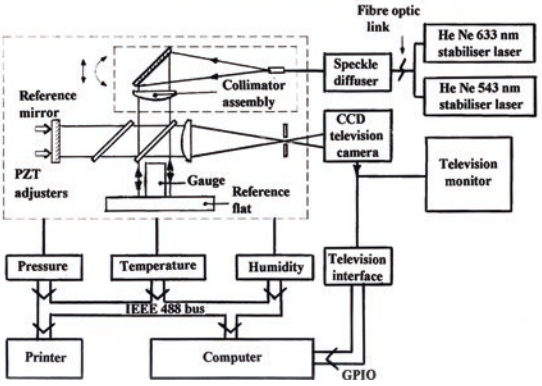

Fig. 1.7 The correct procedure for the preparation and calibration of gauge blocks to ISO 3650

instrument's eyepiece, interference patterns are seen consisting of straight, parallel and equally-spaced interference fringes. However, due to the angle between the surfaces, the pitch of the two sets of fringes will be different, so with suitable calculations, this difference can be found, thereby allowing the necessary calibration to be accurately and precisely achieved.

(a) A typical 15-piece Combination Angle gauge set:

(b) Combination Angle Gauge set consists of:

Unit Angle Gauge:	Accuracy:	
Size:	*Flatness:	Angle:
0.05 minutes 0.10 minutes 0.30 minutes 0.50 minutes 1 minute 3 minutes 9 minutes 27 minutes 1 degree 9 degrees 27 degrees 41 degrees Precision square Straight edge	0.2 μm	± 2 secs of arc

* Flatness of measuring faces

Coventry Gauge & Tool Matrix's 72-sided *Mirror polygon*, having a cumulative angular spread: +16,3/-5,9 arc seconds (Ø300 mm). [Courtesy of Hofstra Group, Ltd. Co. (NM, USA)]

(c) Example of combination angle gauge build-up for an included angle of: 24° 10′ 18″:

Angle gauge build-up to: 24° 10′ 18″
24° = 27° - 3°
10′ = 9′ + 1′
18″ = 0,3″
Angle = (27° - 3°) + (9′ + 1′ + 0,3″)
(i.e. without error)

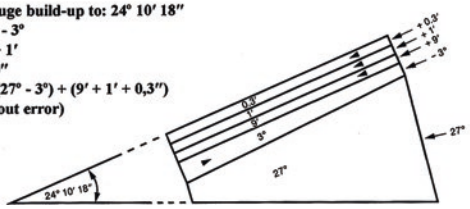

Fig. 1.8 Combination angle gauges (courtesy of Tesa Metrology/Brown & Sharpe)

1.5.4 Precision Polygons

For most normal metrology requirements, an optimum accurate and precise technique of circular division is possible, by the usage of Precision polygons. This technique can also be utilised for calibrating the circular-divided scales (i.e. with circles for optical-dividing equipment, such as rotary tables) amongst others.

In previous versions of a precision polygon, it usually consisted of a hardened and suitably stabilised piece of alloy steel—see Fig. 1.8b (right), having a number of optically flat and polished reflecting angular faces. These reflecting faces are normally machined then lapped flat to within 0.0001 mm. Their faces, or facets as they are also known, are normally exactly equal to the equi-spaced sub-divisions of a circle. Many of the Precision polygons of today are produced from fused silica, with a special aluminium protective coating—see below.

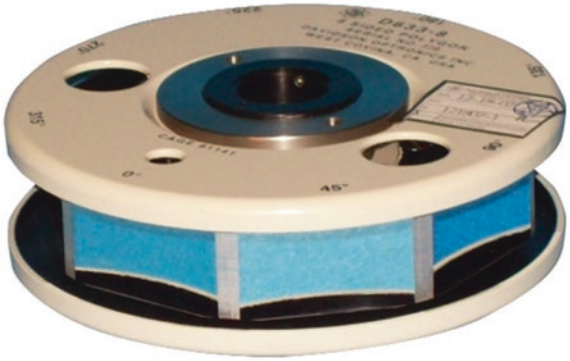

A typical Precision polygon, with its polygonal faces of fused silica—with a protective coating—available from 8 to 72 facets, having: flatness λ/10; accuracy ±5 arc seconds; with its calibration to 1/10 arc second [courtesy of Davidson Optronics, Covina, Ca. (USA)]

The largest metallic Precision polygon—shown in Fig. 1.8 (middle-right), usually has 72 faces at an included angular interval of 5°. However, normally a typical Precision polygon might have 12 sides at intervals of 30°, which is suitable for most types of inspection/ verification/calibration work. These polygons commonly have equiangular faces, but for certain special-purpose unequal angles can also be provided by the optical manufacturers. Precision polygons are generally made to be 15 mm thick and 75 mm across flats, with a central locating hole with smaller holes for mounting purposes. For handling convenience, usually the maximum overall size of precision polygons should not ideally exceed that of ∅300 mm—see Fig. 1.8 (middle-right).

Polygons are invariably utilised in conjunction with say, an Autocollimator—for further details see Chap. 3. Here, the polygon might be mounted on the indexing plate to be verified/calibrated, or a circular scale to be divided. The autocollimator is set to receive a reflection from any one of the faces of the Polygon and the reading is noted-down accordingly. Then the Polygon is rotated until the same reading is observed by the Autocollimator and thus obviously, the angle of the rotation will be equal to the angle between the Polygon faces. If this angle is previously known, then it is possible to divide the circle as well as undertake any required recalibration. The inherent accuracy of the technique, is due to the fact that no centring of the Polygon is necessary. Due to the variation in the distance of the reflector from the Autocollimator, it has no effect if the angular relationship

between the reflector and the optical axis of the Autocollimator, which is unaltered (i.e. the eccentricity of the Polygons cannot affect the angles between its faces, but can only affect the distance of succeeding-faces from Autocollimator). However, in practice it is found that the time spent in centring the Precision polygon is worthwhile, because it ensures that it is possible to avoid any potential errors caused by variations of Polygon form. A correction factor (i.e. the error of each polygon face from nominal) is normally supplied by the optical manufacturer.

1.5.5 Dial Gauges and Dial Test Indicators

The ubiquitous Dial Gauge, is usually available in two distinct types, namely as a:

(i) **plunger-type** (i.e. Fig. 1.9a, which here, features the mechanical version)—with the digital variety being shown below;
(ii) **lever type**[43] (i.e. Fig. 1.9b, c)—often referred to as a Dial test indictor.

These types of Dial Gauges are probably the most universal metrology instruments utilised in basic inspection/verification/calibration activities. In particular, the plunger-type mechanical Dial Gauge can be defined in the following manner: "As a measuring instrument with a contact point that is attached to a spindle and gears that moves a pointer on the dial. Dial indicators have graduations that are available for magnifying different readings of linear measurement values". In its most simple mechanical form, this universal Dial Gauge represents the type of instrument that many Machinists/Inspectors/Metrologists are familiar with for everyday basic measurements. A typical mechanical Dial Gauge[44] (Fig. 1.9a), consists of the following components such as the: plunger/sensor; bezel; indicating pointers; tool post and clamp; sensor button; and when utilised, a magnetic tool holder. The smaller sized indicators should be utilised to reduce what is termed, indicator bar sag.

Usually for any inspection/calibration-type of activity, a Dial Gauge should be selected that has ideally a minimum plunger-range of approximately 2.5 mm, whilst having at the very least, an accuracy of 0.001 mm division^{-1} (i.e. Fig. 1.9a, right). Often, this type of mechanical Dial Gauge is equipped with a longer plunger-motion (i.e. Fig. 1.9a, left). This latter type of mechanical Dial Gauge, normally consists of two distinct scales. One outer-larger scale which is often marked 0–100 in equal divisions (i.e. providing a total indicator movement of 1 mm of plunger motion per

[43] **ISO 9493:2010**: **Geometrical product specifications (GPS)**—Dimensional measuring equipment: Dial test indicators (lever type)—Design and metrological characteristics.

[44] **Dial Gauge—mechanical plunger-type**:
Accuracy according to **DIN 878: 2006-06 (E)—Geometrical product specifications (GPS)**—Mechanical dial gauges—Limits for metrological characteristics;
Dimensions—according to **DIN EN ISO 463: 2006-06 (E)—Geometrical Product Specifications (GPS)—Dimensional measuring equipment**—Design and metrological characteristics of mechanical dial gauges.

(a) Just a small range of mechanical Dial Gauges – used to verify / calibrate machine tools.

[Courtesy of CONTROLS s.r.l., Italy]

(b) A mechanical Dial Test Indicator (DTI) – used to verify / calibrate machine tools.

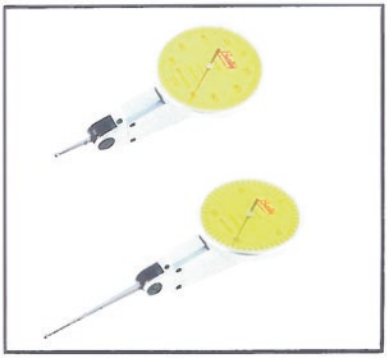

[Courtesy of Spear & Jackson Group, Sheffield, UK]

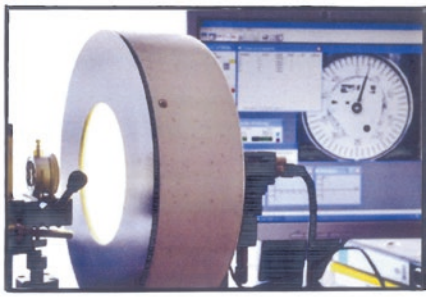

Dial gauge calibration – calibration with a 'deviation diagram and 'error' for ingoing-and-outgoing plunger motion, repeatability and hysteresis, according to DIN 878. [Courtesy of Käfer Messuhrenfabrik GmbH & Co. KG]

(c) Minimising the *Cosine Error* with 'tear-drop' pointer.

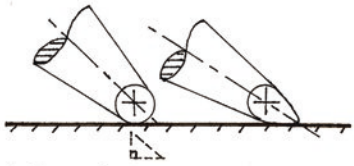

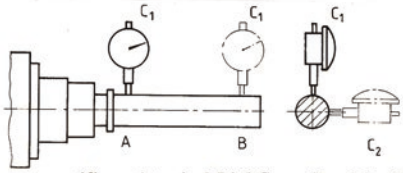

(d) A typical *Dial Gauge/Precision Test Mandrel* setup, for the assessment of a headstock spindle.

Fig. 1.9 Previously, *simple* metrology equipment was employed for machine tool calibration

revolution) and, an inset smaller second-scale marked usually from 0 to 25 divisions—this smaller-pointer relates and counts the number of revolutions rotated by the large-pointer, on the outer-scale—giving a total 25 mm of plunger-movement. When the plunger/sensor of the Dial Gauge is displaced upwards towards dial, then the needle on the dial will move clockwise; conversely, when plunger/sensor is moved downwards

away from the dial, then the needle on the Dial Gauge moves in an anti-clockwise direction. As a consequence, any Dial Gauge readings when the needle moves clockwise are positive, whereas when the needle moves anti-clockwise they are negative. The movement of the needle should be observed for clockwise, or anti-clockwise rotation throughout its motion to avoid any confusion of either positive, or negative signs.

Backlash Error

One should always check the indicator reading for any potential backlash-error. Here, the sensor is pressed and then released, whilst noting-down the Dial Gauge's reading, repeating this process at least two, or three more times. In every instance, if no backlash error is present in the dial gauge, then readings obtained should be identical. If these readings slightly differ, then one must change the dial gauge.

SAG calculation:

Dial gauges are usually available with standard mounting systems, such as for either:

- a single-gauge mounting;
- a double-gauge mounting.

Sometimes, depending on the plant/equipment to be aligned, certain modifications or extensions may be necessary in the arrangement of the mounting-system to undertake this alignment. If the length of the tool mounting holder is large, or any extensions are required for mounting a magnetic tool-holder, then there is more possibility of some sagging—due to the additional weight. When mounting the Dial Gauge and then inspecting with a Test Mandrel in say, a Turning centre's headstock—as shown in Fig. 1.9d—the Dial Gauge/Test Mandrel alignment procedure should be carefully performed so that the Dial Gauge's sensor-axis is both perpendicular and aligned to the axis to be inspected, thus ensuring that both sine and cosine errors[45] are effectively minimised. It is essential to calculate any potential sag in the Dial Gauge's assembly (i.e. Dial Gauge, plus its stand), before alignment testing occurs. For example, as a Dial Gauge's indicator is moved around the circumference of say a round shaft, it displays twice the difference between the projected centreline of the indicator's attachment point and the measured shaft centreline. This is true for both the vertical and horizontal readings. This difference is termed the Total indicator run-out (TIR). Accordingly, the sum of the vertical and horizontal readings, must be divided by two, to represent the actual differences in the two shaft centrelines, whilst remembering to observe the signs of the indicator readings closely, to prevent errors in these calculations. Thus, then the actual difference in shaft centre lines will be:

Offset in vertical plane = TIR (vertical)/2
Offset in horizontal plane = TIR (horizontal)/2

[45]**Sine and cosine errors**: the sensor perpendicularity to the intended workpiece axes, ensures that both sine and cosine errors are effectively minimised, otherwise this deviation from orthogonality (i.e. at 90°), will produce some significant measurement uncertainties.

A multi-functional Digital Dial Gauge (left), with: 12.5 mm measuring range: 0.01/0.005/0.002 mm reversible readings; 0.65–0.9 N measuring force; RS232C data output to bespoke software; plus C1-calibration. The Inspection set up (right)—according to ISO 17025—which can be employed to calibrate both Dial Gauges and Dial Test Indicators (courtesy of Mahr, Göttingen, GmbH)

Typical problems associated with mechanical-type Dial Gauges, might include:

- **that these indicators are prone to errors**—caused by inaccuracies that are magnified through the gear train;
  NB Often springs can be utilised by the instrument manufacturer to minimise any potential backlash in the rack-and-pinion, to reduce these errors;
- **the gears are small**—but friction can result in sticking, thus reducing accuracy;
- **the problem of backlash**—mentioned earlier, this will result in errors in these instruments. If the dial indicator is utilised to approach a dimension from two different opposing-sides, it will experience a form of mechanical-hysteresis that will bias the readings;
- **causes of this hysteresis**[46]—bending; strain; inertia; friction; together with play in the instrument.

[46]**Hysteresis**, can be defined as: "The difference in the indicated value for any particular input, when that input is approached in an increasing input direction, versus when approached from a decreasing direction". In Fig. 1.9 (right), is illustrated the calibration equipment, which produces a deviation diagram for the potential errors when determining: backlash; repeatability and hysteresis—according to **DIN 878**.
Perhaps a simpler-explanation hysteresis is that it usually arises because of strain energy stored in the system [i.e. for mechanical-plant, within the machine tool, by: slack bearings, gears, balls-crews, etc.] (Collett and Hope 1979).

When utilising Dial Test Indicators (i.e. lever-type), an in-built but very minute, although significant cosine error is present at the contact end of the ball-ended lever, that can be virtually eliminated by the simple geometric usage of a tear-drop shaped-pointer, as depicted schematically in the enlarged view shown in Fig. 1.9c.

These lever-type Digital Dial Test Indicators (above), are especially intended for use on either the shop floor, or in the inspection room. They are ideally-suited for comparative measurements and positional deviations of axial and run-out errors. They can achieve bidirectional measurements with automatic reversal, continuous clockwise pointer-rotation, whilst still providing error-free readings. These Digital DTIs are insensitive to magnetic fields, here in this version, with jewelled-movement (i.e. typically with 7 rubies), with the ball bearing lever system which can be swivelled-through an included angle of 240° (courtesy of Tesa/Hexagon Metrology)

1.5.6 Straightedges and Cylindrical Precision Mandrels

Straightedges

It is normal practice to check and verify the straightness and flatness of Straightedges in conjunction with calibrated surface plates and precision spirit levels. Straightedges can be produced from a variety of materials just some of which include: steel; cast iron; granite or Zerodur™. Steel Straightedges are usually available up to 2 m in length and may be rectangular in section with a bevelled edge. Whereas, cast iron Straightedges are normally made up to 3 m in length and are widely used for the testing of machine tool slideways. These cast iron straightedges are usually heavily ribbed and bow-shaped (i.e. often termed a camel-back construction, see photograph below—left) to prevent any potential distortions. They are usually provided with feet—invariably set at the Bessel points for minimum deflection.

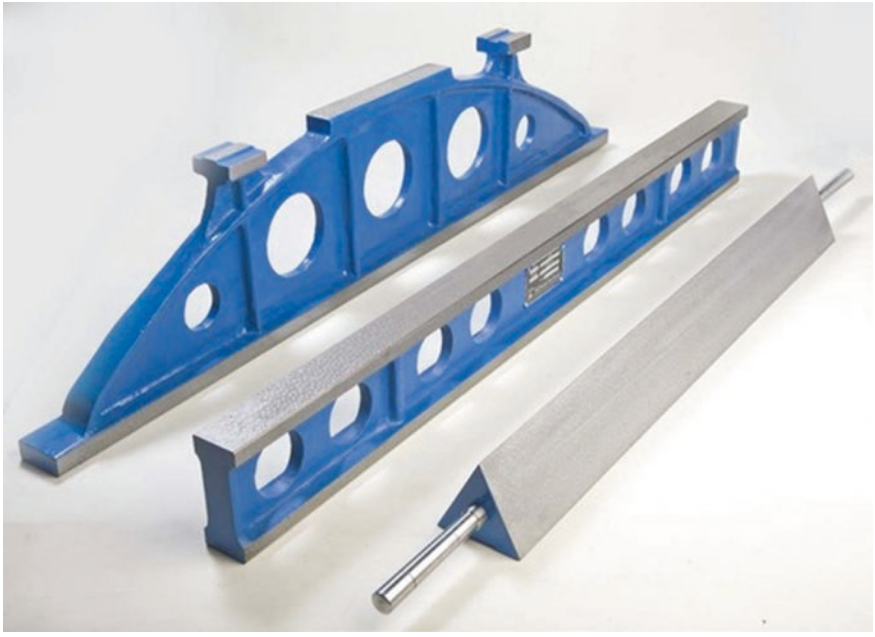

A typical range of high-quality cast iron Straightedge-geometries, illustrating the: Bow-shaped; I-section; and Triangular-section varieties (courtesy of Jash Precision Tools Limited, Madhya Pradesh, India)

In the illustration shown above, cast iron Straightedges of the bow-shaped and I-Section (i.e. parallel-type) in addition to a triangular type, that are normally available in Grades: 0, 1 and 2 accuracies, here being manufactured from flask-cooled grey iron casting (e.g. in the grade FG: 220 of IS: 210), having typical hardness values of a minimum 170 H_B, to: **ISO/IEC 17025** Standard. With such Straightedges, their critical surfaces have been completed with a final precision hand-scraped finish, to an accurate and precise flatness/straightness Standard. Bow-shaped Straightedges are usually available in lengths typically ranging from: 300 to 8000 mm.

The accuracy and precision of straightness of the working faces for Straightedges is tested by direct comparison with say, a master surface table**—**whose calibration data is already known. Here, two calibration-grade and equal-sized gauges blocks are situated on the surface table just below the Bessel support points, with the Straightedge on its working face being situated over these paired gauge blocks. Then, the gap (i.e. vertical-distance) between the lower working face of the straightedge and the datumed surface table, is measured at various points along its length by lightly and gently sliding-in gauge blocks of appropriate size, which gives an indication of the degree of parallelism along the length of straightedge.

Some important accuracy and precision requirements for these straightedges are:

- **its straightness tolerance—**of the working face;
- **the tolerance of parallelism—**of the working face;
- **the combined flatness and parallelism—**of the side faces;
- **the squareness of side faces—**to that of the working face.

Granite-based straightedges are often preferred for calibration activities for a number of reasons, such as their thermal stability and if they are accidently chipped, then the surface flatness is not compromised. This is because the fractured surface breaks below its working surface which means it does not create pile-up, which would cause a burr like that for example, in damaged steel, or cast iron, which might need further additional scraping to rectify this fault.

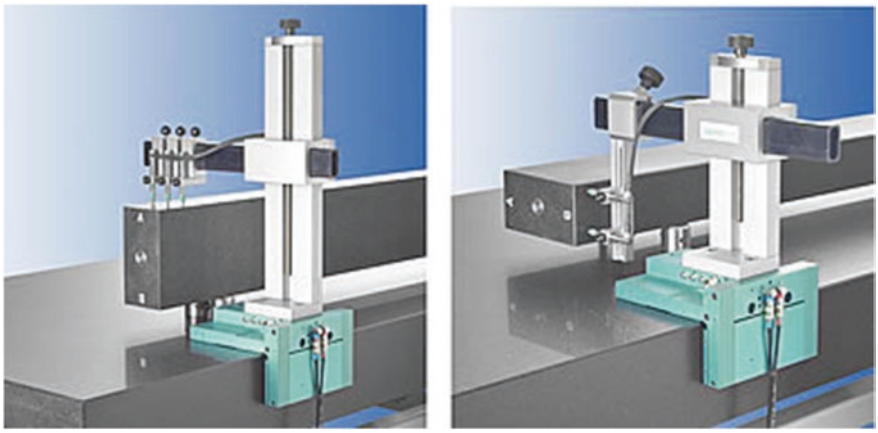

In the above photographs, is an exacting-calibration procedure for the overall inspection of a large granite Straightedge, for its length and breadth dimensions and its geometric characteristics

Utilising a calibrated granite Straightedge for inspection of a Horizontal Machining Centre's linear axis (courtesy of Kunz Precision AG, Zofingen, Switzerland)

Figure 1.10a, schematically depicts a calibrated I-sectioned Straightedge, being employed to inspect a surface's straightness to a reasonable level of accuracy and precision, while Fig. 1.10b, illustrates a simplified Laser-based optical-setup achieving an improved measurement uncertainty—more will be said on this subject in Chapter Two. Both of these techniques are ISO-recommended test procedures, for assessment of the straightness parameter.

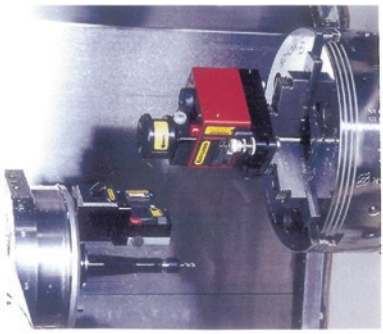

The 'Easy-Laser®' is an efficient measurement system for measuring/aligning machine tools, enabling: straightness, flatness, squareness, spindle pointing direction, level, etc, to be undertaken, with results documented & compared to ISO 10791-1 & -2 for machine tools.
Displayed resolution: 0,0001 mm
[Courtesy of Damaline (Sweden)]

(a) Using artefacts to inspect/calibrate a surface's straightness:

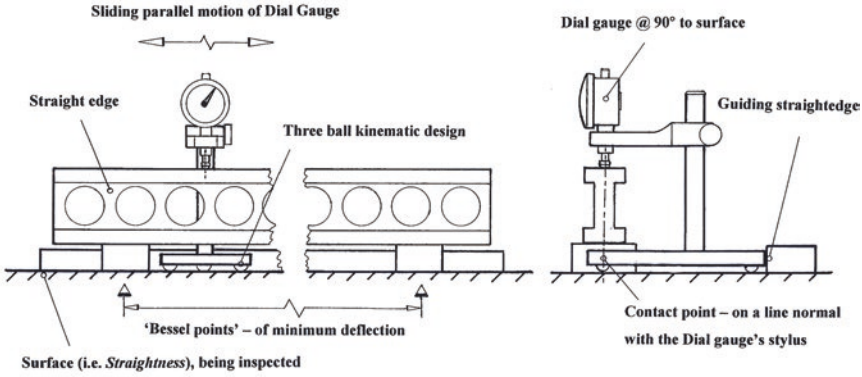

(b) Schematic diagram of Laser straightness calibration:

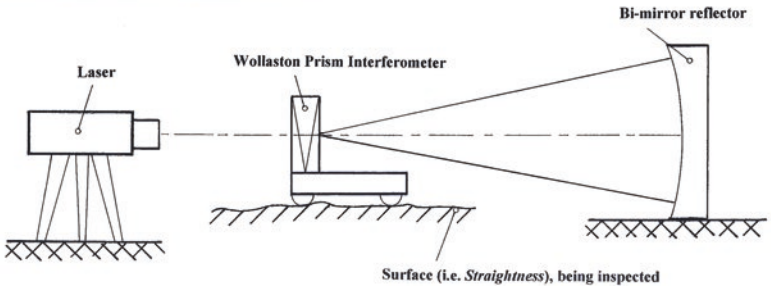

Fig. 1.10 Two ISO techniques for measuring the straightness parameter

A Zerodur™ Straightedge (i.e. being shown in Fig. 1.11) is seen here axis-calibrating a nanocentre lathe, having an inlet reflective metallic strip built into the straightedge—from where the measurements are taken. This type of straightedge material is produced in Germany by Schott Glass Technologies (i.e. since 1968), being made from lithium alumino-silicate glass ceramic. With its very low coefficient of thermal expansion, such Zerodur™ has many advantages for say, any

straightedge applications, as its coefficient of thermal expansion is somewhat less than that of borosilicate glass, which is an alternative, but cheaper solution for minimal measurement uncertainties—when related to this straightedge artefact.

The material Zerodur™ has both amorphous (i.e. vitreous) and crystalline components within its matrix, whereas its most important physical and mechanical properties are:

- **low thermal expansion** (i.e. $\approx 0.2 \times 10^{-7}$/K at 0–50 °C)—which is an order of magnitude better than that of fused quartz;
- **high 3-D homogeneity**—with few inclusions, bubbles and internal stria;
- **hardness values similar to borosilicate glass**—so that it can be ground and polished more easily than fused quartz;
- **high affinity for surface coatings**—enabling reflective surfaces to be readily coated;
- **low helium permeability**—enabling coatings to adhere satisfactorily;
- **non-porous material**—when compared to comparative sintered ceramics;
- **good chemical stability**—similar to that of fused quartz;
- **reasonable fracture toughness**—that is approximately 0.9 MPa. $m^{1/2}$.

Cylindrical Precision Mandrels

Cylindrical precision mandrels often have a self-holding taper and are also known as Inspection mandrels, which are utilised for calibrating both the alignment of machine tool's spindle axis and its run-out, such as for lathe headstocks—as depicted in Figs. 1.9d, 1.12 and 1.16 (top). Typically, Cylindrical taper mandrels (i.e. shown below—left), are usually made of hardened and stabilised alloy steel. Mandrels such as these, have accurate and precise ground and lapped protected centres for their precise-setup and ease of usage, with Morse tapers incorporated onto one end of the parallel test-shaft. These Taper mandrel's are self-holding[47] in their respective mating socket. In the examples of the ISO taper varieties, a tapped hole is often provided for fixing the mandrel with a threaded retaining pin. Straight/parallel mandrels (i.e. shown below—right) are also frequently known as Inspection mandrels and they are utilised for inspecting/calibrating for: concentricity; parallelism; and true-running of high-quality machined workpieces.

Mandrels mounted between centres, provide a reference straight line datum—joining the two points, namely between its two centres, facilitating the physical alignment checking of these centres. Parallel mandrels are also made of hardened

[47]**Self-holding tapers**: such as the ubiquitous Morse taper, this type of artefact being invented by Steven Morse in: East Bridgewater, Mass., USA—just after the onset of the American Civil War (i.e. 1861). Steven Morse was also famed for his major invention of the Twist drill, which has proved to be a significant improvement on the previous Spade-drill designs. Of note, is that Morse's drills have barely changed over the last 150 + years. Morse's self-holding taper angles only marginally-vary in included angle, depending upon its respective number (i.e. these No's normally ranging from: 0 to 6 in size). For example, a Morse No. 1 has an included angle of: 2°58′54″; whilst at the other extreme, the No. 6 is set to an angle of 2°59′12″. The advantage of these self-holding tapers, is that they can be suitably sleeved-together either up-and-down to fit the machine tool's holding-requirements, then simply released—by lightly-striking the slotted tang-fitment via a simple tapered-drift and mallet.

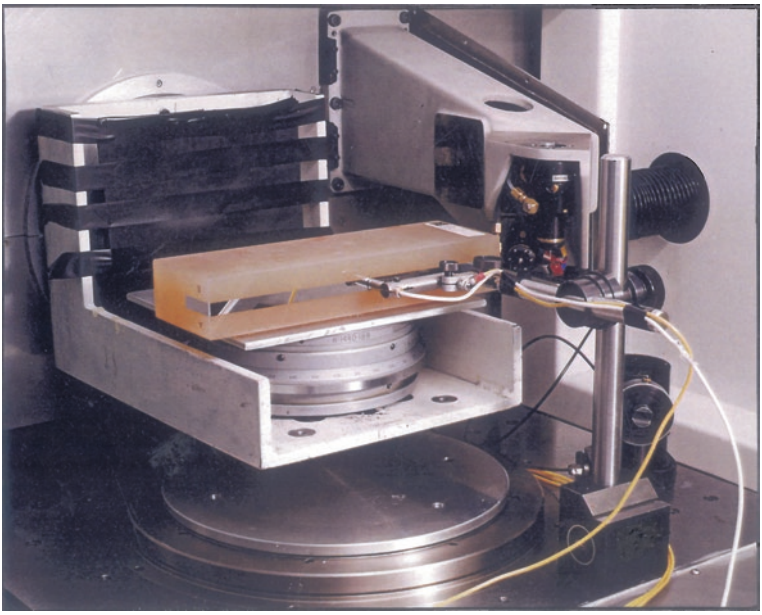

Fig. 1.11 Today, a '*zerodur*^{TM}' *straight edge* and *proximity sensor* can be utilised to calibrate a nanocentre's *X*-axis to a very high level of accuracy/precision, in a temperature-controlled machining environment (courtesy of Cranfield Precision/Atomic Weapons Establishment, Aldermaston)

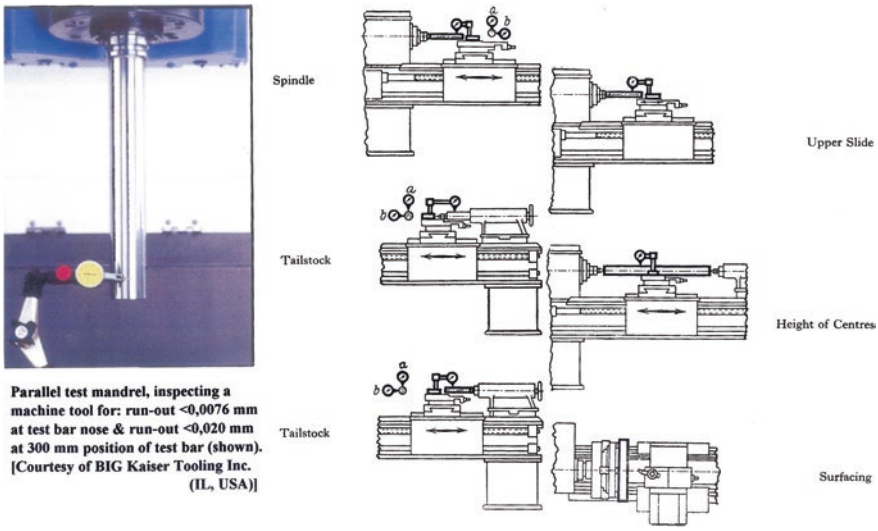

Fig. 1.12 Previously, *machine tool testing* was performed using: dial gauges, mandrels, gauge blocks, and straightedges, etc.

and stabilised alloy steel. Such mandrels incorporate cylindrically ground and lapped protected centres for easy usage, having a high degree of both accuracy and precision. Standard sizes and accuracy of these Straight and Taper mandrels are typically manufactured to: **ISO-2063:1962**. It is usual for manufacturers of both of these type of mandrels to supply them with standard taper fitments, characteristically, MT-2 to -4, or with an ISO fitment of 40, or 50. Taper mandrels, or Test arbors as they are also known—see Fig. 1.16 (top), usually range in diameters from: ∅40, or ∅50 mm and lengths ranging from: 300 to 600 mm, respectively.

Some typical versions of particular Taper test mandrels which can be utilised for the alignment/run-out verification of a machine spindle axis (*left*), whereas, the Straight mandrels, or Parallel mandrels (*right*) are also known as Inspection mandrels, these are also often employed for machine alignments (courtesy of Luthra Engineering Works, Haryana, India)

1.5.7 Precision- and Cylindrical Squares

Precision-Squares

Prior to any form of verification/calibration activity, it is essential to undertake a thorough calibration procedure on the actual artefact in question. This will entail the setting up and inspecting/verifying/calibrating of the Precision and Cylindrical squares in a disciplined and logical manner. This calibration can be achieved in any number of ways, but whatever technique is utilised, the calibration data results must be valid and their uncertainty issues must be clearly addressed.

Precision squares with a knife edge are particularly difficult to calibrate, as their knife edge chamfering creates problems in contact between the stylus attempting to calibrate the squareness of the edge itself. A solution can be found by adopting a measuring probe with a cylindrical touching surface that contacts the edge, as shown in the photograph below (left). Therefore, in this manner, the inner and outer leg of the precision square then can be accurately measured. To optimally fix the knife edge at 90° for calibration, an appropriate setup similar to that shown below (right) is necessary. Consequently, the precision (knife edge) square should be fastened onto an accurate and precise ground plate, such as this company's SQUARE-***base***™ with its clamping bracket, as illustrated. In order to ensure a consistent sideways positioning, it is also advisable to use the vacuum-injected alignment aid, such as again, this company's SQUARE-tool™. Here, the

required vacuum connection for this tool is already integrated within the squareness measurement device. For the concise recording of the calibrated measurement data, a bespoke PC analysis program, known as STRAIGHT-soft™ can then be employed that allows for both the straightness and squareness measurements to be readily obtained.

The calibration of typical knife-edged precision squares, requires both a cylindrical stylus (*above left*), inspecting both knife edges at one fixed setting (i.e. shown *below right*) (courtesy of Kunz Precision AG, Zofingen, Switzerland)

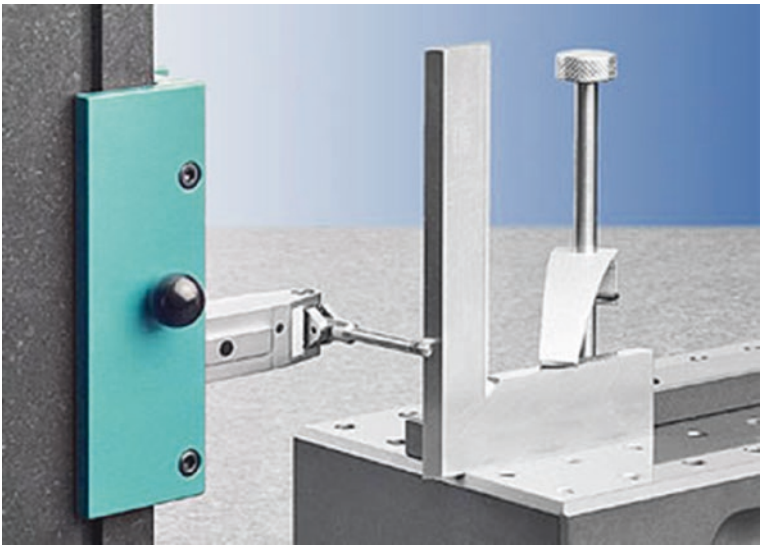

The calibration of hard stone (e.g. granite) Precision squares must also be carried out under controlled metrological conditions, according to the latest International Standards, as shown above

The calibrating procedure for a granite Precision square—which is precisely and accurately positioned, and situated on a CMM's table—while being metrologically validated (courtesy of Kunz Precision AG, Zofingen, Switzerland)

Cylindrical Squares

The use of Cylindrical squares in machine tool and CMM verification is somewhat unusual, as it is frequently the normal practice to utilise a calibrated Precision square, similar to those previously mentioned and depicted above. However, an alternative to this type of conventional square, is the Master Cylindrical square (shown below), as it has some distinct advantages when used for such squareness calibration; these are:

- **it is very stable in use—**due to its symmetrical footprint and significant weight;
- **it maintains both high accuracy and precision—**for any form of necessary squareness measurement;
- **due to the contact surface being a single-line cylindrical surface—**measurement data recorded has less uncertainty than various other squareness metrology techniques.

A typical standard range (i.e. abridged choice) of Master Cylindrical squares available from a specialist metrology manufacturing company, would exhibit the following range of: dimensional; tolerance; and weight parameters:

- ∅60 × 100 mm; parallelism ±2.5 μm; weight 3 kg;
- ∅100 × 300 mm; parallelism ±3.5 μm; weight 11 kg;
- ∅160 × 600 mm; parallelism ±5.0 μm; weight 47 kg;
- ∅240 × 1000 mm; parallelism ±7.0 μm; weight 155 kg;
- ∅300 × 2000 mm; parallelism ±12.0 μm; weight 340 kg.

This particular Master Cylindrical square is made from hardened alloy steel, with a chromium coating (courtesy of Obishi Keiki Seisakusho, Japan)

1.6 A Concise History of Machine Tool Calibration

Prior to the late 1870s, machine tools had in the main been designed and built with machined parts being produced by Selective Assembly. The mating components in the machine tool's structural assemblies were individually machined, then fitted together independently, thereby constructed on a fit-for-fit basis, rather than being from a conceptual philosophy and a more practical basis of Interchangeability—where all similar parts simply fit together within its design and build assembly. It was only when production volumes for such machine tools substantially increased in the manufacturing world, coupled to the serious demand for much higher levels of accuracy and precision, that some form of basic strategy for inspection and testing procedures needed to be formalised. In the major technological countries involved in increasing their machine tool product's quality levels, there was an industrial drive toward part tolerance fitments for machined components to become significantly tighter. Some form of basic inspection and testing procedures became a fundamental requirement, in order to present to their respective customer base a consistently high quality and reliable product, which could then be guaranteed and would comply with their current and future needs.

Such early machine tool criteria, was of significant interest to Dr Georg Schlesinger. He spent the majority of his working life developing techniques and methods for calibrating such a diverse range of machine tools and in the following section a résumé of just some of his career problems and notable achievements are précised herein.

Pioneering Machine Tool Testing Procedures of Georg Schlesinger (1874–1949)

The recognised founder of modern-day machine tool inspection and testing techniques and procedures was Dr Georg Schlesinger along with his applied research work. His original German book on the subject was entitled: Prüfbuch für Werkzeugmaschinen (basically translated as: Testing Machine Tools), which was first published in 1927, establishing a comprehensive series of acceptance test specifications for machine tools. In fact, Schlesinger was convinced of the importance of International Standardisation and, prior to the outbreak of WWII, he was an active member of the I.S.A. Committee 39 which was a forerunner to today's ISO Standards. In order to gain an understanding of the driving force behind Dr Schlesinger's work, it is worth taking a step-back, to look briefly at his somewhat tragic early life in Germany in both academia and industry and his later more settled and productive lifetime activities in other European countries.

After a one-year apprenticeship as a Mechanic (1891/1892) Schlesinger studied Mechanical Engineering at the Technical University of Charlottenburg (Germany). In 1897, he was hired as a Designer at the Berlin engineering firm of Ludwig Loewe, when in 1902, he became its Chief Designer. In February 1904, Schlesinger was now once again continuing his technical studies at the Charlottenburg Tech. University, where he completed his Ph.D. entitled (in English) The Fits in Mechanical Engineering. In July 1904, Schlesinger was awarded the Chair of Machine Tools and Manufacturing Processes—at the Technical University of Charlottenburg. By 1907, Schlesinger was then currently developing inspection testing techniques for a range of machine tools and in the same year he founded the engineering journal which is still published today: Werkstattstechnik, for whom he was the long-term editor.

Later, in his role as Head of Engineering at the Spandau Gun Factory, at Oberspree, Germany—during WWI—he was chiefly responsible for commissioning the weapons manufacture, plant and design. While at the factory at Spandau, Schlesinger developed, together with his colleague Ferdinand Sauerbruch, notable developments of some artificial arm and leg prostheses. By 1917, Schlesinger was a founder member of the Steering Committee of the newly founded **German Standards Committee** (**DIN**).

With the rise of National Socialism in Germany in the mid-to-late 1920s and as a Recognised Jew he was held in protective custody from April to November, 1933—under the dubious and flimsy pretext' of: "…alleged embezzlement; industrial espionage and treason". Ironically, his ex-student Otto Kienzle was appointed to his previous position, despite the fact that Schlesinger's charges had been rescinded by the Prussian Ministry for Science, Art and Education later that year. In January 1934, Schlesinger was given early retirement from the Charlottenburg

Technical University, with the incredible, but horrendous announcement that: "He was incapable of educating German engineers."

At this time, the Schlesinger family left Germany (1934), accepting a Visiting Professorship at Eidgenössiche Technische Hoshscule (E.T.H.) in Zurich (Switzerland), working with Professor Bickel, and the following year (1935) he was appointed Professor at the Universite Libre—in Brussels (Belgium). Moreover, Schlesinger continued his internationally recognised work on Standardisation of Testing Procedures and ironically, his book for the Berlin publishing house of Julius Springer—a two-volume reference work on Machine Tool Testing, first published in Germany, in 1936. Schlesinger had also continued his research work at the Universite Libre, until December 1938.

In 1939, Dr Schlesinger was then stripped of German citizenship and the same year, he and his whole family moved to England, where he became the Director of the specialised research laboratory at Loughborough, for the Production Engineering Research Institute. During WWII, he built-up and led a group at the Machine Tool Laboratory, within the College of Technology, Loughborough (1939–1944)—now known as Loughborough University.

The so-called Schlesinger Test Charts then standardised and formalised the manner in which machine tool inspection testing and verification procedures should be conducted—whilst utilising much of the previously explained metrology equipment. The specific and detailed Test charts illustrated the necessary metrology equipment that was required and how this should be arranged on the machine tool with the aid of simple-to-follow diagrams (see Fig. 1.12—typically showing a Centre-/Engine-lathe being partially inspected)—coupled with easy-to-read documentation, on how to conduct these calibration procedures, together with the anticipated permissible errors for each test performed. Much of Dr Schlesinger's standardised testing work is still valid even today and after his death in 1949, Professor F. Koenigsberger[48] amalgamated any of the slight discrepancies between the English and German versions of these Test Charts—for conventional machine tools (i.e. for non-CNC machines).

[48]**Professor Franz (Frank) Koenigsberger**, was born in Germany in 1907, where he studied under Professor Schlesinger at the University in Berlin. There were many Engineers that were influenced by Professor Schlesinger through his teaching, writing and research, but none more so than Professor Koenigsberger. After working as Schlesinger's private assistant, he also left Germany in 1935, to escape the ensuing atrocities of Hitler's Nazis. Koenigsberger then moved to Belgium where he worked for a Belgian Milling Machine Company—as a Chief Designer and Engineer, until 1938. He later moved to England, where Professor Koenigsberger was one of the founding members of: The CIRP (i.e. an International Academy of Production Engineering) and was then made President of CIRP. Furthermore, Koenigsberger was also President of the Manchester Association of Engineers. In 1959, he was the joint-founder along with his much respected-colleague: Professor Tobias—of: The University of Birmingham, for the Machine Tool Design and Research Conferences, now today, known by the long-running name for the MATADOR Conference—on Advanced Manufacturing. Professor Koenigsberger past-away in 1979.

Periodic Calibration

Most companies that produce machined products, will employ metrology/inspection equipment and diligently engage in some form of periodic calibration of this equipment. Normally these companies will keep sophisticated records, documenting the proof of such equipment calibration. This action is vital, although it does not prevent the production of poor quality machined components occurring on either inaccurate, or any un-calibrated machine tools. So, by including large-scale plant such as machine tools as part of any Gauging calibration database, or as an element in a Preventative maintenance program, this will result in significantly-improved machined work, with the added benefit of an overall lowering of the cost of improvement in quality. A secondary benefit of such machine tool/equipment calibration is one of an increased employee awareness of exactly how the machine tool geometry, coupled to a machined workpiece's accuracy and precision affects its level of product quality. Component accuracy and precision are often ambiguous terms, so to simply explain these important terms of workpiece quality parameters, they are illustrated in series of well-known Target-analogy schematic diagrams, depicted in Fig. 1.13. It is the normal practice for any form of periodic machine tool calibration to encompass both a combination of the machine's geometry and its accompanying accuracy and precision checks. It should also be mentioned here, that the machine tool's geometry can be considered as the relationship between the different moving members of the machine, such as its linear and rotational axes motions. This type of relative motion within the machine tool's volumetric envelope, is known by the term kinematics.[49] Correcting and rectifying the machine's geometry is also a precondition that must be achieved by means of periodic accuracy and precision validation inspection procedures. It is appreciated that accuracy is how closely an axis can be positioned to its CNC controller's programmed target value. While repeatability, or precision, can be thought of as its ability to return to an identical location, even if that position differs from the target value. Thus, the combination of the machine's geometry and linear accuracy, will contribute to any spacial, or volumetric accuracy for the machine tool.

[49]**Kinematics**: is the branch of Classical-mechanics that describes the motion of: points; bodies (objects); plus systems of bodies (i.e. groups of objects) without consideration of the causes of that motion. The actual term kinematics is widely utilised. It is the English version of A.M. Ampère's (**André-Marie Ampère** (Born: in Lyon: 20 January 1775—died: in Marseille, France: 10 June 1836). He was an eminent French Physicist and Mathematician, who is generally regarded as one of the main founders of the science of classical electromagnetism, which is normally referred to as simply: electrodynamics. Of note, is that the SI unit of measurement of electric current, the ampere, is named after him.) cinématique, from which Ampère constructed from the Greek: κίνημα, **kinema** (i.e. meaning: movement, or motion), which itself was derived from: κινεῖν, that is **kinein** (i.e. meaning: to move). Consequently, the study of **kinematics** is often referred to as the geometry of motion—however to read a more in-depth treatment of the subject, see further information regarding analytical dynamics. To describe machine tool motions—**kinematics**—they are primarily concerned with the studies the trajectories of points, lines and other geometric objects and their differential properties, such as both an axis velocity and its acceleration.

A range of highly accurate and precise machined components & assemblies. [Courtesy of RT Bearings Ltd, W.Midlands (UK)]

DEFINITIONS:

- **PRECISION:** *The closeness of the agreement between the results obtained by applying a defined procedure several times, under prescribed conditions.*
- **ACCURACY:** *The closeness to an observed quantity to the defined, or 'true' value.*

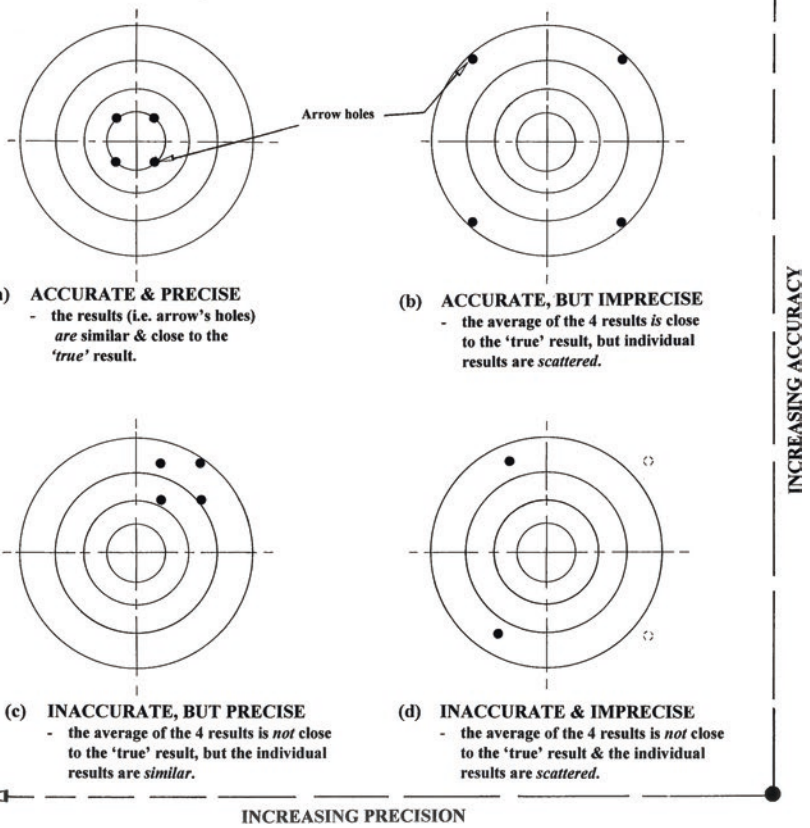

Fig. 1.13 The well-known '*target analogy*'—indicating the difference between accuracy and precision

There are three notable techniques for validating the periodic calibration of the machine tool:

1. specific procedures using standard metrology measuring equipment;
2. the in situ inspecting with a special gauge, or artefact, by utilising the machine's resident spindle touch-trigger probe (i.e. when fitted);
3. by utilising some form of Machining trials, for example, such as **NAS 979**—Composite cutting test (i.e. when milling the: circle diamond square geometry, for this test)—see Fig. 5.16.

The periodicity of any form of calibration of a machine tool is a matter of some considerable variation in its intended usage, which will be significantly influenced by some of the following parameters, such as the,

- **condition of the machine tool**—new, or old;
- **amount of its usage**—single-/double-/treble-shifts, exacerbated by a 24/7 practice;
- **critical tolerances that must be held**—open or closed limits on the machined parts;
- **materials to be machined**—good/poor machinability materials, such as brass, or latterly that of exotic aerospace alloys, respectively;
- **type of machining operations**—light/heavy cutting operations, compounded by such factors as continuous interrupted cutting/out-of-balance components, rather than by continuous cutting regimes;
- **workpiece loadings**—compounded by delicate parts and light loads, or heavy parts and robust cuts on components held on the machine tool;
- **temperature environment**—high and low ambient temperatures varying during the day and throughout the year, which can affect the production output of high accuracy and precision components.

These periodic calibration tests on the machine tools and CMM's, together with other equipment inspection procedures will be mentioned later in the relevant sections in the book. However, a qualified machine tool Technician, or more appropriately a Metrologist should be available, or at least consulted for details on how to perform such periodic calibration testing. Additionally, if excessive machine tool/CMM errors are found, then by periodic calibration of this plant, it will allow these errors/uncertainties to be diagnosed, then corrections can be taken to rectify any respective machine tool and instrumentation problems.

1.7 Notable Chronology in Machine Tool Testing

The historical development of both machine tool testing and its equipment has seen some major advancements since Dr Georg Schlesinger's early work previously mentioned, in metrological progress across almost a century's worth of applied research, in a diverse area of engineering and scientific specialisms. A

very-much abridged version of just some of these published milestones and timelines (i.e. up to the millennium) is briefly listed below for simple and easy reference—produced in Table 1.4.

Table 1.4 In this abridged list, just some of the valid and most significant advances/milestones in the specialised-field of: Machine Tool Metrology—up to the Millennium—are noted

Name	Description	≈Year
Schlesinger	Testing machine tools	1927
Tschirf	The straightedge reversal method	1941
Tlusty	Methods of testing machine tools	1959
Hewlett-Packard	Pioneered laser interferometry, based upon the 'Zeeman principle'	1966
American Machinist	Ball reversal, straightedge reversal, *Z*-slide parallelism to spindle axis	1967
American Machinist	Spindle accuracy of machine tools	1967
Loxham	The deterministic approach to predictable manufacture	1968
LLNL	International status for thermal error research for machine tools established	1969
Donaldson	Separating spindle error from test ball roundness error	1972
Taniguchi	Prediction of achievable accuracy of components	1974
Bryan	Simple method for testing measuring machines and machine tools	1981
Knapp	'Circular test' for machines	1983/87
Bryan	Telescoping ballbar (filed)—U.S. Patent No. 4,435,905	1984
Hicks/Guarini	CMM: diagonal displacement method	1985
Estler	Calibration and use of optical straightedges in the metrology of precision machines	1985
Hansen	Dynamic spindle analyzer	1988
Burdekin	Contisure ball bar	1988
ISO	ISO 230 Standards—test codes for machine tools	1990
Renishaw	Telescoping ballbar	1991
ANSI/ASME	Performance evaluation of machining centres	1992
LION/API	Rotating spindle analyzers	1992
Kakino	Telecoping ball bars (book)	1993
Nakazawa	Principles of precision engineering (book)	1994
Heidenhain	Grid encoder for machine tool calibration	1994
Martin	'Contouring test': utilising high speed and small radius	1995
Evans	Error correction/compensation of machine tools	1995
Ford/Postlethwaite	Accuracy improvement in CNC machining centres by: geometric/load/thermal error compensation	1999

1.8 Achievable Accuracy and Precision of Machine Tools

At the turn of the twentieth century, the terms relating to normal-/precision-/ultra-machining, had not yet been coined. As already alluded to, any components that had been machined were assembled and fitted together by a Selective assembly procedure on a fit-for-fit basis. By the time component Interchangeability had become the norm, somewhat later between WWI and II, there was a definite need to not only make consistent volume production parts to higher levels of tolerances, but their machined surface finish requirements had to be fundamentally upgraded, coupled to improved roundness characteristics—that was now proving to be essential. Obviously, these tolerance changes were a drastic overall enhancement in part machining capability, which was the case for any turned/ground/superfinished components. As the worldwide industrial demand increased for significantly better mating fits, the machine tools producing them also had to be manufactured to greater levels of accuracy and precision. This meant that by ≈1970, the critical tolerance requirements for Normal machining was generally agreed at ≈0.01 mm; Precision machining was established at ≈0.1 μm, while for Ultra-precision machining it was ≈0.01 μm. During the next thirty years, namely by the year 2000, this stringent tolerance requirement had markedly tightened and had subsequently been changed to Normal machining, which was now achievable at ≈1 μm; Precision machining was anticipated to be ≈0.01 μm; while for ultra-precision machining this was established to be ≈0.001 μm. In fact, this noticeable tightening of tolerances had already been predicted by Taniguchi in his thought-provoking and seminal work on Achievable Machining Accuracies in 1974—see the graph in Fig. 1.14. As a consequence Taniguchi not only correctly estimated that the driving force of much tighter tolerancing would be obligatory over the next few decades, but he also coined the term nano-machining to embrace this aspect of extremely close tolerance machining and performance requirements. Taniguchi's very informative chart for predicting this performance development time against the achievable accuracy (Fig. 1.14), has been well publicised over the years and it has proven to be a remarkably perceptive and accurate statement of fact.

It should be re-emphasised here once again, that nano-machining operations, are not simply concerned with minute components—where more-and-more parts are being manufactured to miniscule dimensions (Fig. 1.4 top)—but the term can also relate to much larger components that have their critical dimensions and surface texture tolerances produced to nano-metric sizes (see Fig. 1.15 top). In the exacting manufacturing nano-machining cases of either infinitesimal dimensional sizes or much larger parts having their own critically tight tolerances, they have created real challenges both now and in the future, in their actual machining and specific production operations and metrological requirements. The major problem here is that the so-called Golden rule of Metrology is now a distinctly redundant term! Reference to the Golden rule in the past meant that a measuring instrument was deemed to be up to 10 times more accurate that of the part tolerance being inspected, which understandably now cannot be achieved. This lack

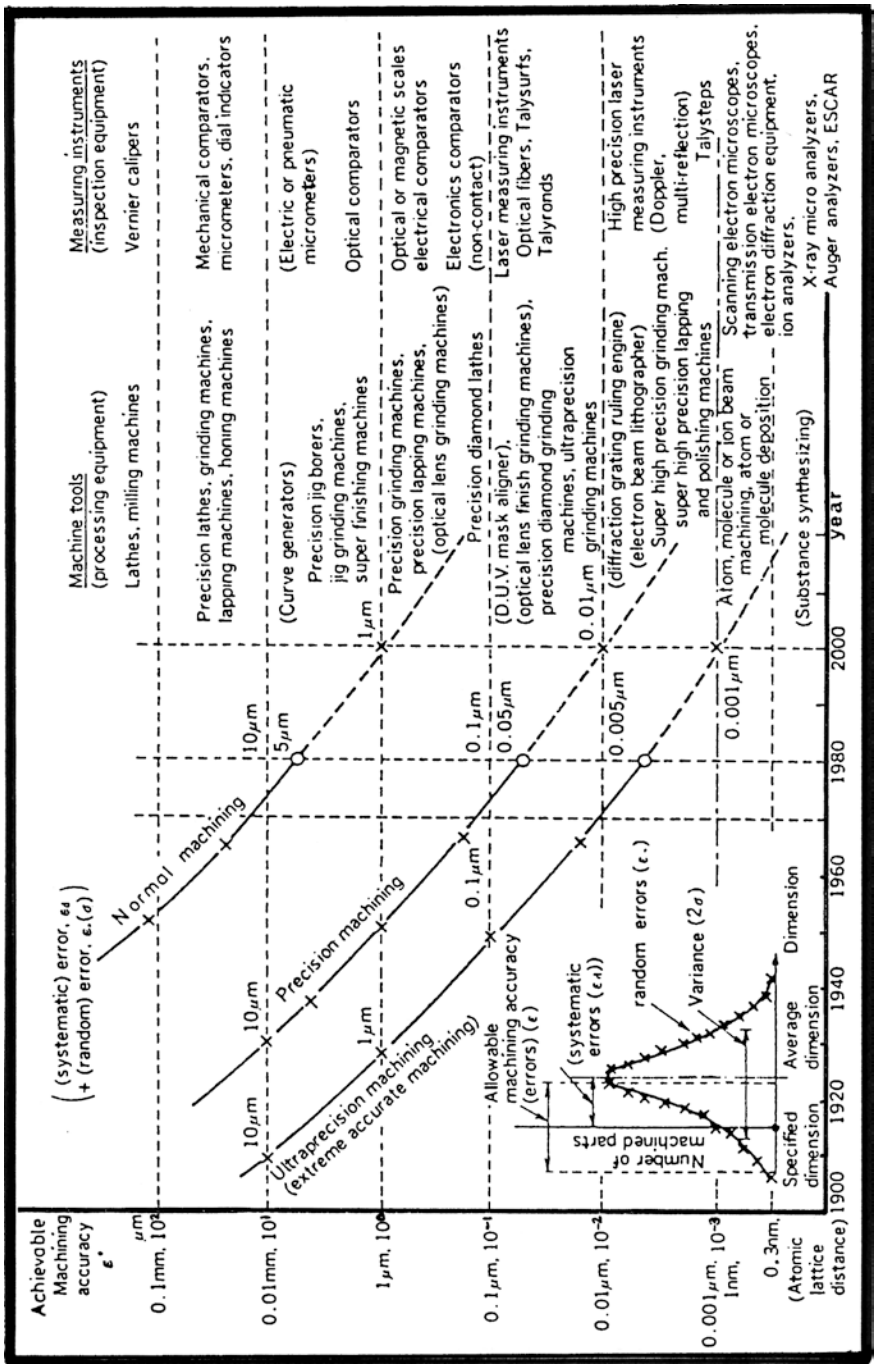

Fig. 1.14 The 'prediction' of achievable component accuracy and precision, over the next 25 years [*After* Taniguchi (1974)]

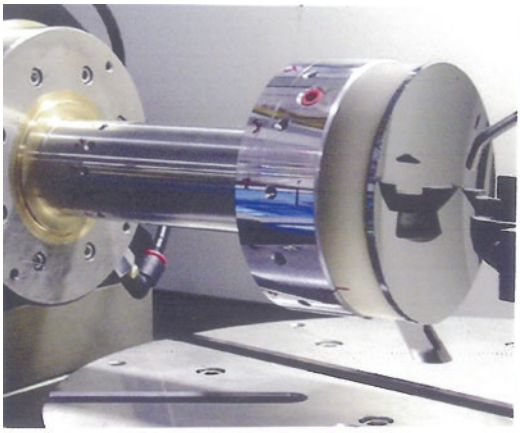

Ultra-precision machine systems support single point diamond turning operations. [Courtesy Moore Nanotechnology Systems]

A Germanium Lens being diamond turned on a Nanoform 250U, final surface texture of *Ra* 0,48 nm. [Courtesy of Ametek Precitech Inc. (USA)]

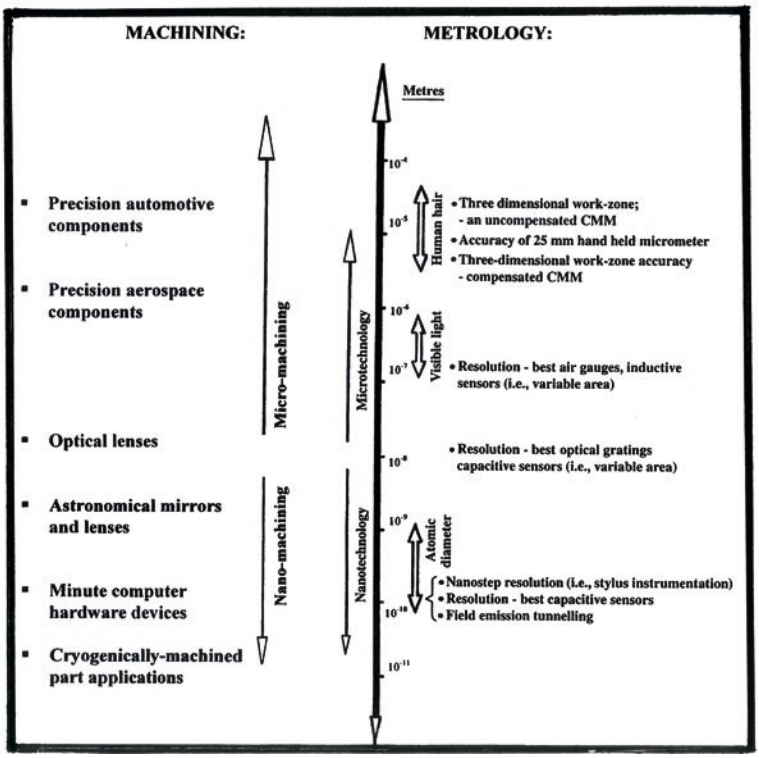

Fig. 1.15 The approximate relative size and scale metrological instrument assessment—for that of accurate and precision components (adapted from McKeown (1986)/Smith (2002))

of magnification of the difference between the part tolerance and the achievable accuracies of metrology equipment, explains why the Golden rule just cannot be adhered to for the miniscule tolerance boundaries that are currently being held, which will only be exacerbated still further in the future.

The simple schematic diagram illustrating Machining versus Metrology (Fig. 1.15) is now becoming a problem of real concern, because of this lack of scale in metrological magnification. It is shown to some effect in this Fig. 1.15, where the instrumentation simply cannot offer the required measurement solution that was once previously claimed—by the Golden rule. To emphasise this point still further, we are now approaching the absolute resolution for just about any form of instrumentation—at 10^{-10} m (i.e. the approximate atomic diameter), but presently the ultra-precision machine tools can now habitually machine at this level of precision and accuracy (Fig. 1.15 top). In fact, if one was to cryogenically freeze the workpiece (e.g. say, in a liquid nitrogen/methyl alcohol solution) and assuming the component can cope with this level of pre-stage chilling whilst utilising say, a monolithic (natural) diamond tool—within a nano-machine tool environment, then it should be possible to accomplish pico-machining operations (i.e. 10^{-12} m) within the near future. Moreover, there are still some significant technological challenges from a calibration viewpoint. Even simply validating the accuracy and resolution of such machine tool plant becomes a major technological stumbling block, as at the moment, today's commercial laser-based interferometers have a resolution of $\approx 1 \times 10^{-9}$ m.

Since the beginning of the twenty first century, there has been a momentous effort toward designing and producing components and indeed assemblies of exceedingly more infinitesimal size and miniaturisation than was previously the case. This increasing demand to be able to either locate and align mechanical components together in extreme and close proximity, or perhaps to offer improved operational functionality by providing an enhancement of power-to-weight ratios—is now a major requirement for electronic micro-circuitry. In the case of this latter parameter of typical adjacent circuit dimensions for nanometric electronic devices, they can have a proximity to each other of just $\leq$0.000005 mm (i.e. ≤ 5 nm $\equiv 5 \times 10^{-9}$ m). So, whether this type of incredibly small component assembly is either a minute mechanical device, or that of an infinitesimally small electronic device, this now presents some massive challenges for the whole of the ultra-precision manufacturing industries. Thus, to simply capture the part then to manipulate it into position, or just to supply equipment at this almost infinitesimally small size for our everyday usage, it has and will become, somewhat increasingly problematical—from the present day onward.

Pressing these points still further, attempting to comprehend the true dimensional size and scale of these exceedingly-miniature components and assemblies, a now rather redundant term such as a hair's breadth, was often quoted as an axiom of a very-minute dimensional size. By way of an illustration, in Fig. 1.16 the large circle has been schematically drawn to represent an actual hair's diameter and here, it is compared to another well-quoted term the Micrometre, or 10^{-6} m (i.e. often incorrectly termed a Micron, but for brevity's sake it is usually described as

Test arbors (i.e. Parallel Test Mandrels), are often used to inspect for machine tool spindle run-out.

[Courtesy of BIG Kaiser Tooling Inc (IL, USA)]

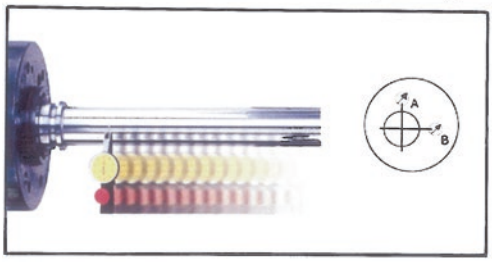

Deflection at A and B from nose to 300 mm (11.81") distance.

Less than 0,015 mm (0.0006").

Precision standard of BIG Daishowa Test Arbors	
Runout	0.002mm(.00008")
Roundness	0.001mm(.00004")
Cylindricity	0.003mm(.00012")
Roughness	Rz: 0.6mμ(.00002")
Taper contact	AT1
Diameter tol.	±0.005mm(.0002")

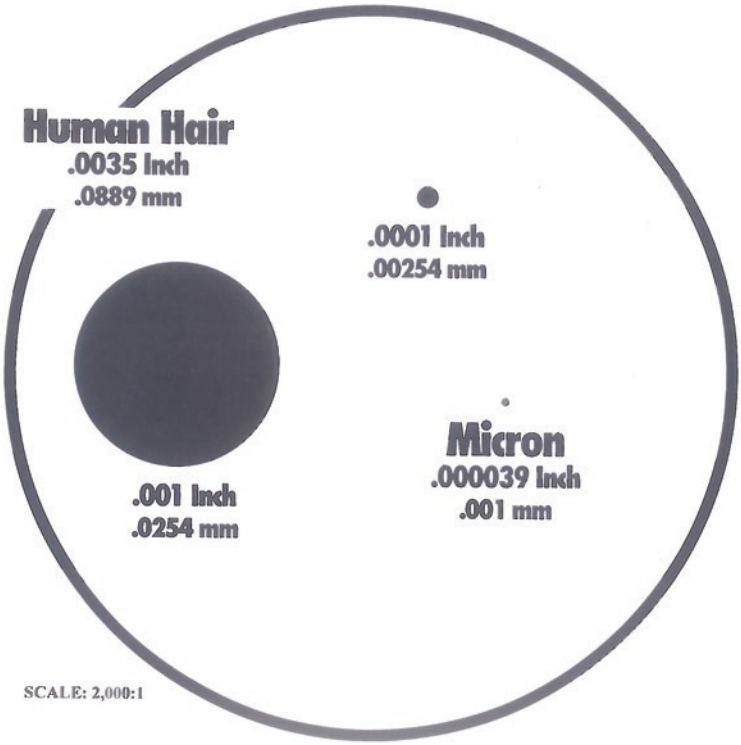

Fig. 1.16 The *comparative magnitudes* of dimensional size—against that of the width of a human hair

such!). Although even here with this hair-terminology axiom, an individual hair does not have a consistent diameter—as described (i.e. ∅0.0889 mm). As an aside and to take this argument a stage further, just over a decade ago, the author undertook a simple comparison test to establish a hair's actual diameter. So, a hair was

plucked from his head (i.e. one that he could not afford to miss!) plus four more from a group of his research colleagues; they were then placed within a Scanning Electron Microscope (SEM) chamber and a photomicrograph image was scaled-off for comparative measurement—this being achieved against the automatic measuring bar that appears in the photomicrograph in Fig. 1.17a, b. The surprise here—which is shown to good effect in Fig. 1.17a, was the variance between the five hairs selected; they varied quite considerably in their respective diameters, ranging from the smallest hair at ≈∅30 μm to the largest hair at ≈∅100 μm. What was also quite remarkable here—with this somewhat primitive comparison, was the fact that the diameter was singularly consistent along its length, regardless of the individual hair's diameter (Fig. 1.17b).

So, returning to Fig. 1.16 again, this diagram is somewhat misleading as a form of measurement criterion, as we can now appreciate that the difference of just a few microns can result in an excessively out-of-tolerance problem—when considering any form of calibration for ultra-precision manufacture.

1.9 Accuracy and Precision—Produced by a Machine Tool

When the calibration of a machine tool's accuracy and precision requires reverification, there are many interrelated factors that need to be established and wherever possible, being corrected, prior to its consequent metrological inspection procedure. To show just some of these potential measurement uncertainties that are likely to be present on a CNC machine tool, Figs. 1.18 and 1.19 present the major contributors to the majority of component inaccuracies. Just some of these potential inaccuracies (Figs. 1.18 and 1.19) that could influence component accuracy and precision—apart from the actual orthogonal axes themselves—will be mentioned later. These figures in general relate to the actual hardware of the machine tool, whilst the peripherals, namely pallets, tooling, probing and fixturing, recount the manner in which the machine itself was utilised, rather than the anticipated calibration errors for the actual machine.

Machine Tool

A machine tool when it is engaged in machining significant excess stock from components by roughing out, can produce a substantial volume of swarf,[50] see the

[50]**Swarf**: is the general term used to describe the volume of individual chips produced by cutting components on a machine tool. Individual chips—as has just been mentioned—can generate large volumes of swarf, with typically the chip's shape varying from, say: long continuous chips; or at the other extreme—by an automatic chip-breaking action—producing either tightly curled elemental chips, or discontinuous chips. Each chip geometry-type, will affect the chip-packing density [NB Lang's chip-packing ratio, is where it provides a means of establishing this packing-effect, this has been described elsewhere. Typical information can be found in: Smith (2008)] within the machine tool's volumetric-enclosure.

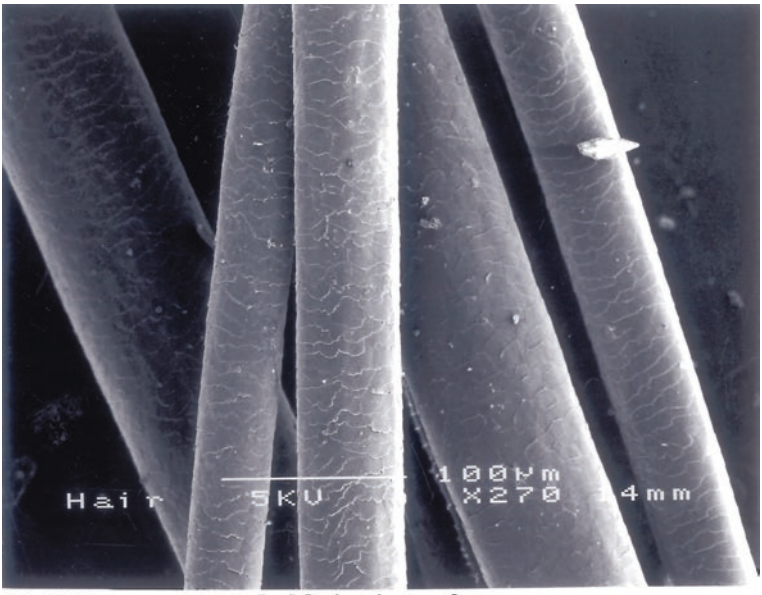

(a) Hairs vary remarkable in size - often used as a standard of minute measurement (magnification x270).

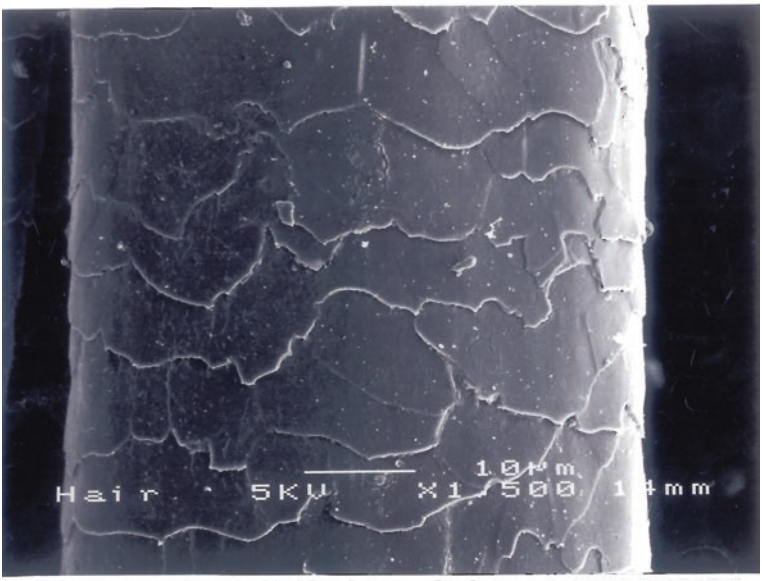

(b) Close-up of an individual strand of hair - illustrating good diametral consistency (magnification x1500).

Fig. 1.17 '*Hair size*'—with its *varying* diameter—has often been selected to illustrate the *magnitude* of *dimension size* (courtesy of JEOL (UK) Ltd)

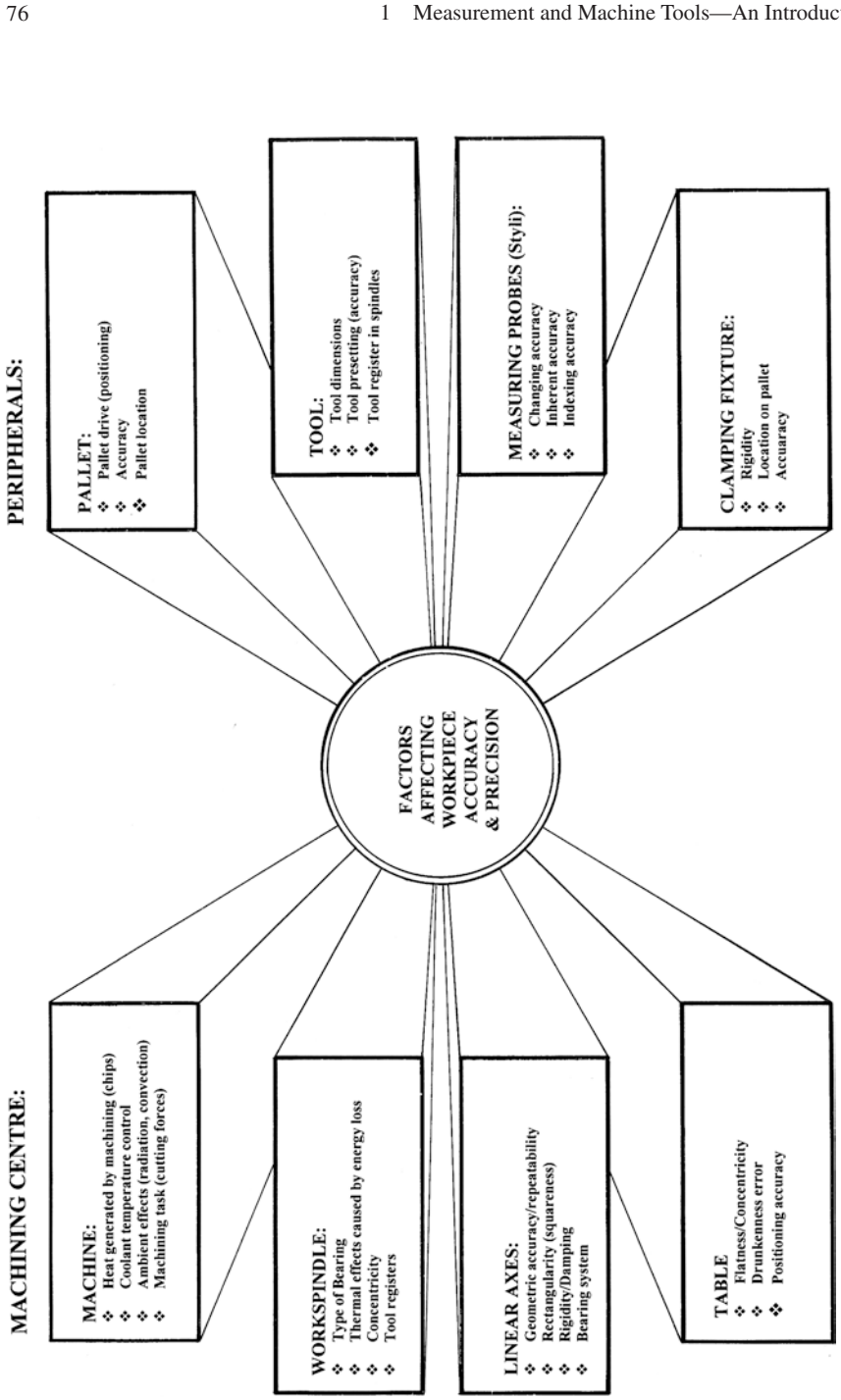

Fig. 1.18 The accuracy and precision produced by a machine tool (i.e. horizontal machining centre) will depend upon the machining centre and its peripherals (courtesy of Scharmann Machin Ltd.)

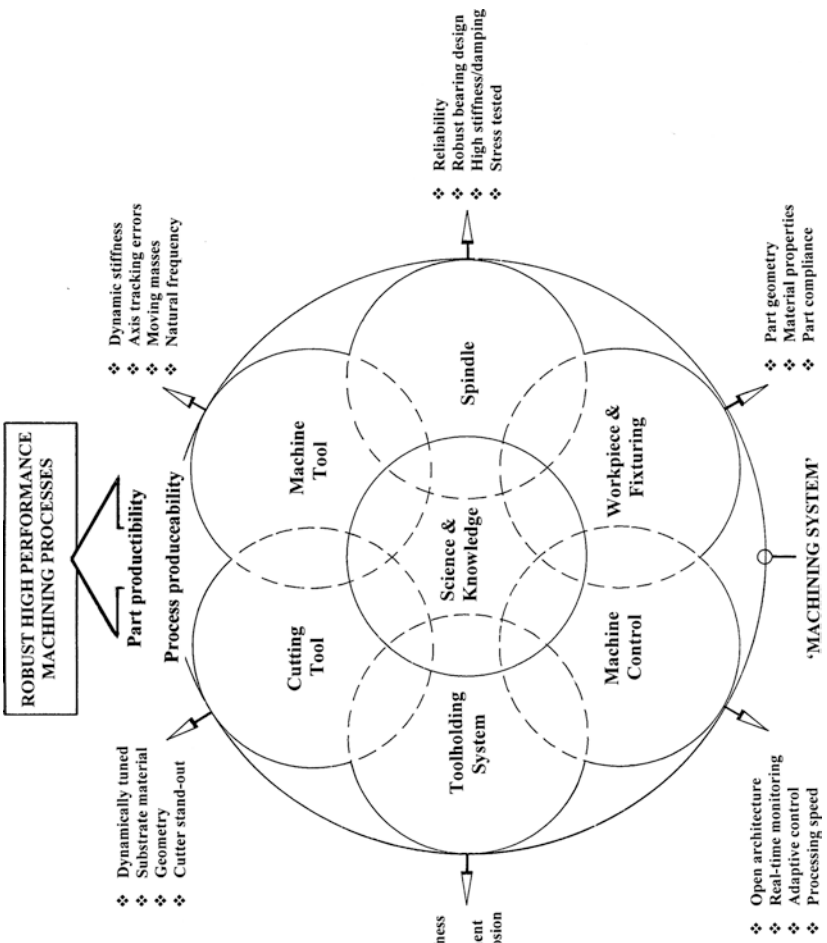

Fig. 1.19 The 'systems approach' to machining (courtesy of Boeing Commercial Airplane)

photograph below. If this swarf is allowed to accumulate in sufficient volume on the machine's table—as shown—or within the bed of the machine tool, or alternatively if it is not effectively removed from the machine by say, a swarf conveyor—it can potentially create thermal problems. Then, any heat generated in this vicinity can be considerable, hypothetically causing thermal gradients across the machine's structure, thereby inducing the likelihood of machine-element thermal expansion problems, which could potentially affect the machine's previous exercise in calibration. One obvious method of minimising the effects of swarf accumulation on a machine's table, is to utilise either a very-high-pressure coolant supply or a flood-coolant approach to such machining operations—this latter technique being depicted in the photograph below. Here, the vast-and-voluminous quantities of coolant will tend to flush these now otherwise stationary, but hot chips away, while yet another major benefit of flood-coolants is to simultaneously cool the chips down and in this manner, it will minimise the risk of any temperature differentials.

High volume of swarf generated by the CNC machine [courtesy of SolidCam Inc. (Newtown, PA, USA)]

Flood-coolant utilised to flush away any chips [courtesy of Fuchs Lubricants (UK) Plc]

When an uncontrolled machine shop temperature environment is the norm any differences in the ambient effects during the day—as temperatures tend to rise-and-fall—will have a deleterious effect on the entire machine tool. The temperature variation of the overall structure will be heavily influenced by the composition of its major structural elements, most notably when the major castings are produced from say, Malleable grey cast iron and to a lesser extent, by its Granitan[51] equivalent machine tool parts. Many modern-day machine shops that specialise

[51]**Granitan** Fritz Studer AG. (Switzerland), was the first company to develop this product, with its Granitan S-100 technology—in the early 1970s. This Granitan-based material, is a mixture of a reactable epoxy-resin binder—developed by Ciba-Geigy Ltd. (Switzerland), mixed with either high-quality granite, or gravel. Thus, Granitan produced with sand and gravel, was developed specifically for the requirements of machine tool structural parts: is an **epoxy granite**, also known as **synthetic granite**. It is a mixture of epoxy and granite commonly used as an alternative material for machine tool parts. Epoxy granite is utilised instead of cast iron and steel for

in the manufacture of close tolerance components, do not allow any daylight into the working environment. This lack of natural light is an unfortunate, but necessary compromise, as the radiation from, for example, a window onto part of the machine tool, will introduce differential expansions/contractions as the sun's rays reach the various exposed parts of the machine tool—having an undesirable effect on the calibrated machine. Moreover, even when convection currents are present in the workshop—as for instance, when doors are either opened or closed, this can influence the machine tool's calibration when machining ultra-precision components and should be minimised wherever practicable.

When the cutting forces are very high such as when roughing out superfluous bulk sections from the workpiece's stock, this can in extreme cases result in distortion through an elastic behaviour in the workpiece and upon release of such forces, they can affect part accuracy and precision. By modifying either the cutting operations, or its tooling, this can minimise such distortional effects, whilst improving component quality and reducing strain in the machine's structure, which reduces the need for the calibration intervals to be shortened. When the machine tool builder designs and constructs a new machine tool, factors such as its dynamic stiffness, natural frequency, the moving masses (i.e. its momentum[52]), plus likely axis tracking errors, are all mechanical parameters that are built into the overall build-quality, to improve machine excellence and reduce impending calibration occurrences.

Work spindle

The work spindle for a Machining Centre (as shown below), or headstock for a Turning Centre (Fig. 1.22), is the most important sub-assembly in the overall construction of a machine tool. This is because it is from here, that the workpiece's accuracy and precision is obtained whist machining. The whole spindle assembly is a very complex and sophisticated mechanism—illustrated below and, in Figs. 1.27, 6.1 and 6.2, with in many cases, process and condition monitoring sensors being incorporated into their respective design and build construction. Such important factors include spindle bearings—more will be said on this topic shortly—see Figs. 1.31 and 1.32, concentricity of rotating elements, thermal

Footnote 51 (continued)

better vibration damping, longer tool life and with lower assembly costs. Epoxy granite material has an internal damping factor up to ten times better than cast iron, with up to three times the superiority of natural granite, while being up to thirty times better than a steel fabricated structure. Epoxy granite is unaffected by coolants, it has an excellent long-term stability, with a markedly improved thermal stability and also having a high torsional and dynamic stiffness, coupled to an excellent noise absorption with negligible internal stresses present. Although, on the downside, an epoxy granite tends to be more costly to fabricate than its cast metallic-based equivalents.

[52]**Momentum**: in classical mechanics, it is more usually known as **Linear momentum**, or **Translational momentum** (i.e. SI unit: kg m/s, or equivalently, N s). Momentum, is the product of the mass and velocity of an object. Just like velocity, **Linear momentum** is a vector quantity, possessing both a direction, as well as a magnitude, namely: $p = mv$, where 'p' is momentum (N s); 'm' is mass (kg, or N); and 'v' is velocity (m/s).

effects reduced by the addition of heat-insulation plates (Fig. 1.27, top)—to decrease spindle growth, precise and accurate tool registers—fitment of tooling for a Machining Centre, or the location of workpieces on a Turning Centre. All these purposely designed features are necessary to minimise potential inaccuracy and imprecision in the production of high-quality components. Machine tool manufacturers pay particular attention to the design, construction, build quality and to the actual assembly of these expensive work spindles/headstocks, as frequent re-calibration would otherwise be necessary.

Whenever an unfortunate tool-crash accidently occurs during a particular machining operation, or a workpiece fixture is inadvertently struck while the axes are in rapid motion, this can necessitate at worst, a total rebuild of the spindle's assembly, or at best, realignment/recalibration of the machine tool. Such spindle crashes can be very costly indeed, apart from the anticipated production delays that they will inevitably create, while awaiting repair. Furthermore, an expensive cutting tool and its holder may also be ruined in this crash, or an irreplaceable workpiece might have to be scrapped. Under such ill-fated machining circumstances the result will inevitably mean that some considerable downtime[53] may result, leading to the spindle's bearings needing replacement, along with other attendant and costly repairs. The unanticipated downtime for these vital repairs, causes a significant loss of productivity and disruption to any job scheduling—within a company's Master schedule.

In the case of the spindle assembly—depicted below right—it is designed to decrease any transfer forces by decoupling and disconnecting the power transmission at the interface between the machine tool spindle and its motor—at the instant of a collision. This type of spindle protection is effective whether the impact is radial (i.e. if the spindle strikes some obstacle from the side—such as a fixture), or axial (i.e. when the spindle rapidly strikes something head-on, typically in a workpiece *Z*-axis crash). So, when impact is from the side, the protection system enables the spindle to tilt away from the collision—shown below (extreme right). When the impact is head on—shown below (middle right), the spindle compliance can tolerate this dynamic event by being pushed upward. When either type of disengagement behaviour occurs as a result of a crash, the built-in displacement sensors instantly trigger a controlled, but rapid deceleration of the feed axes, thereby bringing an axis motion to an immediate stop before an overload occurs. This instant reaction protects the shock-sensitive spindle components from potentially damaging forces of the impact/collision.

[53]**Down-time**: refers to periods when either the plant (i.e. here in this case, being the machine tool), or a related system is not available. The term: **Down-time**, or alternatively its **Outage-duration**, refers to a period of time that a system fails to provide, or to perform its primary-function. Terms such as: **reliability**, **availability**, **recovery**, or **unavailability,** are similarly-related concepts. Therefore, the plant's **unavailability** is the proportion of a timespan that it is unavailable, or for a system, this is known as being offline. It is normally a result of the system failing to function, because of an unplanned-event, or because of some routine maintenance procedures are deemed to be necessary. The term is most commonly applied for industrial environments in relation to failures in industrial production equipment. Some maintenance facilities will measure any downtime incurred during a work-shift, or by either an: 8; 12; or 24-h shift-period. Yet another common industrial practice, is to identify each down-time event, as having an: operational; electrical; or mechanical origin.

For this type of Spindle impact protection system, the internal magnets and springs can be adjusted to establish the necessary force and torque load limits that activate the protection system—when these preselected values are exceeded. Different limits can be set for both the radial and axial loads. Typically, mounting forces as high as 18 kN in the axial direction and, tilting moments as great as 2300 Nm—in case of a radial load, can be reached. Hence, after instantly responding to a collision, the spindle returns to its initial position within a tolerance of ≤5 μm. Furthermore, to prevent any potential deleterious workpiece particle ingress (i.e. debris/fines/etc.) into the spindle's intricate and precision assembly, the system's covers and seals have been designed specifically to keep out any harmful dust particles, chips and liquids.

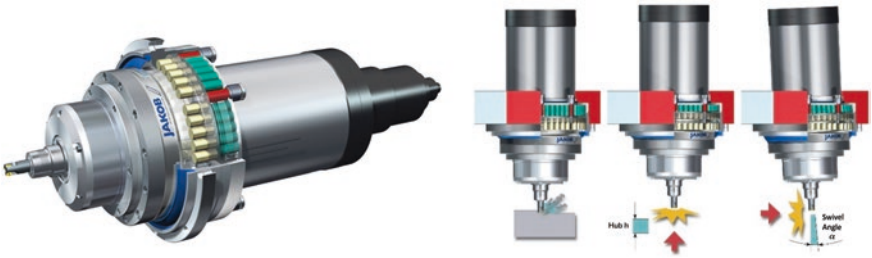

A representative machine tool spindle construction—partially sectioned (*left*) and in the three schematic views—shown on the *right*, illustrating the spindle's ability to withstand sudden tool-crashes/collisions [courtesy of Jakob Antriebtechnik (GmbH)]

Linear Axes—Table and Pallet

The linear axes of machine tools must all be geometrically accurate and precise having exacting orthogonality—often termed either squareness, or rectangularity to their complementary respective axes. Moreover, these machine tool axes must also provide highly efficient load bearing characteristics coupled to a low friction system, while maintaining consistent repeatability of their motional kinematics. The table (below left) or pallet on a Machining Centre must be both true and flat on stacked-up axes, being situated on top of each other (i.e. *X* and *Y*—vertical, or *X* and *Z*—horizontal configurations). Likewise, for a Turning Centre (below right) the Turret—offered as either a single, or as a twin co-axial configuration—see Fig. 1.22, is also stacked—but the axe designations will differ here—see the next section for further axes clarification. Calibration tests are not only undertaken to verify the straightness, squareness, etc. of respective axes, but additional inspection occurs for their table/turret flatness. If the table/pallet axis can be rotated, then some additional rotary checks here will need to be are carried out—for angular accuracy and precision.

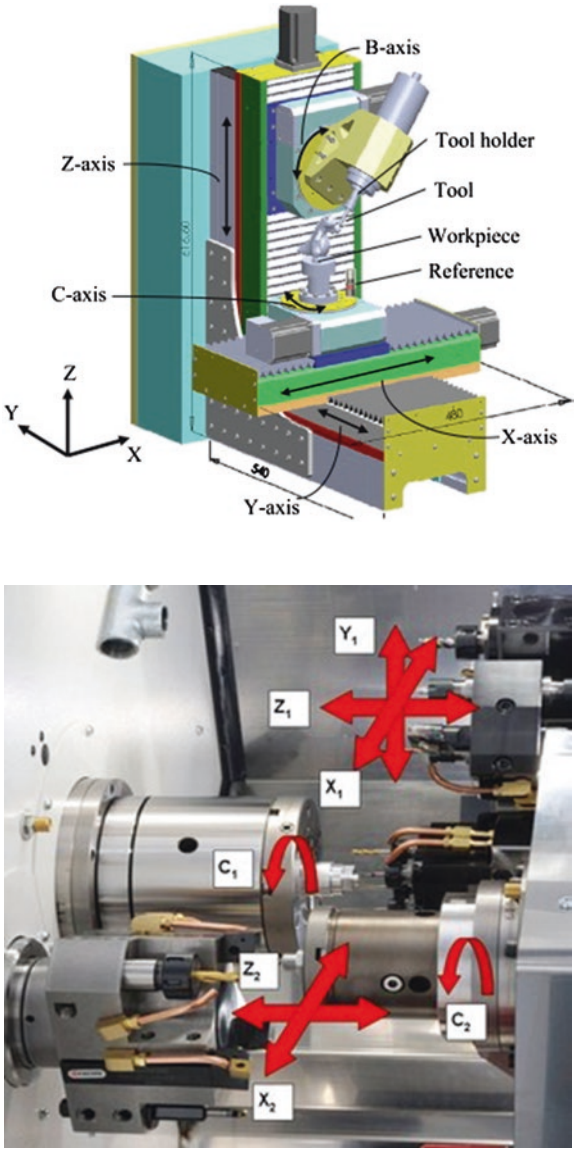

Axes classification: 5-axis vertical Machining Centre. Axes classification: Sliding-head Turning Centre (*after* Lin and Wu 2013) (courtesy of Citizen Machinery UK Ltd.)

1.10 Designation of Machine Tool Axes and Kinematics

In the following description of machine tool axes and kinematic designations/classifications, this description is not meant to be an exhaustive account of the wide-ranging and sometimes complex axes configurations, as these are more specifically indicated within the appropriately numbered and widely accepted ISO Standards that are currently available.

Axes and Motions

The general machine tool rules can be considered as follows:

- between the workpiece and cutting tool a relative motion has to be established to perform the machining operation, such motion occurs within a coordinate system;
- all CNC machine tools utilise an identical Standard for motional nomenclature, having the same coordinate system;
  NB This type of machine tool coordinate system has been historically standardised by the: **EIA 267-C**,[54] which is also in accordance with: **ISO 6983-1:2009**[55];
- the CNC programmer will always ensure and calculate any tool movements relative to the coordinate system, which is being linked to a stationary workpiece. It is irrelevant if on a real machine tool which has relative motions belonging to either the workpiece, or to the cutting tool.

The machine's coordinate system is defined by the Right-hand rule; see the diagram below. As a result and based on this system, the Right-hand rule establishes how the primary axis of a machine tool should be designated. The Sign conventions for axes motion have long been established by employing this Right hand rule. These axes conventions are based on the requirement to construct machine tool motional programs, in which the position of the tool in relation to the part (i.e. material) is defined; this is regardless of the kinematic arrangement of machine motion axes. In the simplest of terms, the primary axes of a machine tool are designated as '*X*', '*Y*', and '*Z*' (i.e. see Fig. 1.20). These axes can have either positive,

[54]**EIA 267-C—Axis and Motion Nomenclature for Numerically Controlled Machines (1990)**: this Standard defines a machine coordinate system and machine motion nomenclature for numerically controlled machines. The Standard applies to all numerically controlled machines, where it also defines a machine's movements, so that a programmer can describe machining operations without having to know whether the tool approaches the workpiece, or the workpiece approaches the tool.

[55]**ISO 6983-1:2009—Industrial Automation Systems and Integration for CNC machines**: this Standard specifies requirements and makes recommendations for data format/positioning, line motion and contouring control systems utilised in CNC machine tools, notably specifying the appropriate: G- and M-codes and so on—while having its origins within: **EIA RS274** (i.e. circa: ≈1950s).

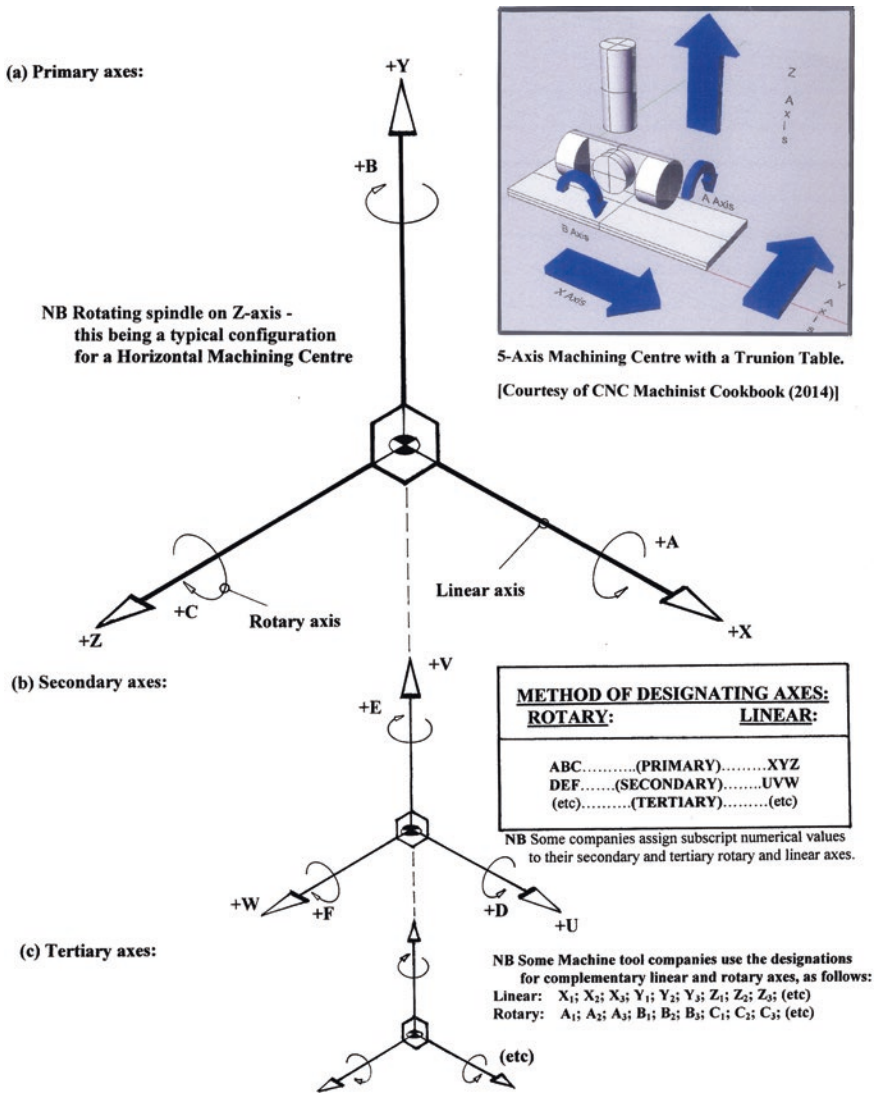

Fig. 1.20 Designation of machine axes for orthogonal machine tools

or negative axis values. By employing the Right-hand rule—for example on say, a vertical Machining Centre. The directions of the machine axes are relatively easy to remember with this rule. So, if one faces the machine and by holding one's right hand as shown below, with the middle finger in the direction of the tool axis ($+Z$) the thumb will point in the direction of the $+X$ axis and the forefinger (i.e. index-finger) in the direction of the $+Y$ axis.

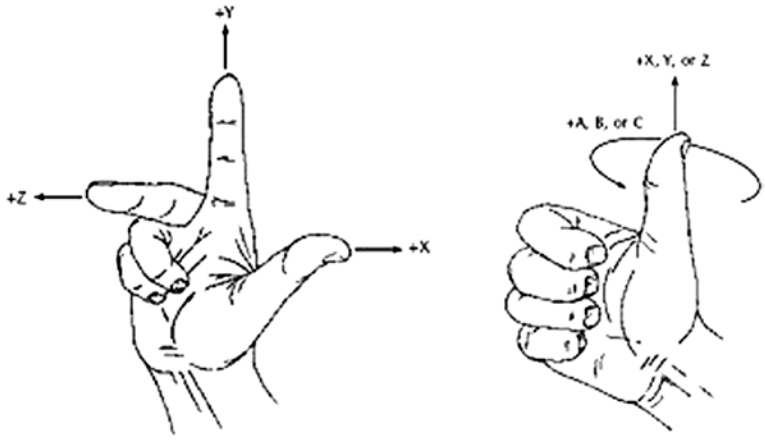

Simple, but valid practical methods for establishing this Right-hand rule: for designating the machine tool linear axes (*left*) and for its associated rotations (*right*)

The *Z*-axis is always parallel/coincident to the main spindle of the machine tool. It is irrelevant whether the spindle carries the workpiece, or its tooling, thus, the *Z*-axis can have either a vertical, or horizontal configuration. For example, on Machining Centres the spindle holds the rotating tooling, conversely, on Turning Centres the headstock spindle carries the rotating workpiece. So, any positive *Z*-movement of the axis will always result in an increase in the distance between the workpiece and the tool and vice versa. The *X*-axis motion is both horizontal and parallel to the workholding surface. If '*Z*' is horizontal, positive '*X*' is to the right looking from the spindle towards the workpiece. If '*Z*' is vertical, when looking from the spindle towards its supporting column, positive '*X*' is to the right. The *Y*-axis of motion is perpendicular to both the *X*- and *Z*-axes. Moreover, a positive '*Y*' is in the direction which would make a right-handed set of Cartesian coordinates. If there is more than one moving element in the same axis, the major one of these axes is called the primary axis as mentioned above (i.e. being designated as: '*X*'; '*Y*'; and '*Z*'). Furthermore, it is possible to obtain, '*U*', '*V*', and '*W*'—also in upper-case letters, while tertiary axes are also similarly represented in this manner (i.e. these classifications are depicted schematically, in Fig. 1.20).

One simple and convenient manner of establishing these associated Primary, Secondary, or Tertiary axes designations—together with their accompanying rotational designations, is by the use of the alphabet, as illustrated below:

A B C **D E F** **G H I**.....**R S T** **U V W** **X Y Z**

↓ ↓ ↓ ↓ ↓ ↓

Primary **Secondary** **Tertiary** ← **AXES** → **Tertiary** **Secondary** **Primary**

[← Rotational axes motions →] **[← Linear axes motions →]**

So, for example the designation/relationship between both the linear- and rotational axes, respectively, for these primary and secondary axes, would be:

$$\begin{array}{c} \mathrm{X\,Y\,Z\;\;U\,V\,W} \\ \downarrow \qquad \downarrow \\ \mathrm{A\,B\,C\;\;D\,E\,F} \end{array}$$

Some machine tool manufacturers might utilise the following designations—for their respective complementary linear and rotational axes (i.e. also see Fig. 1.20):

$$\text{Linear} : \mathrm{X_1;\ X_2;\ X_3;\ Y_1;\ Y_2;\ Y_3;\ Z_1;\ Z_2;\ Z_3;\ (etc.)}$$

$$\text{Rotary} : \mathrm{A_1;\ A_2;\ A_3;\ B_1;\ B_2;\ B_3;\ C_1;\ C_2;\ C_3;\ (etc.)}$$

Kinematics of a Machine Tool (Free-Body)

The so-called Free-body diagram of an entity (e.g. which is invariably a workpiece) in space without restriction of motion, possesses Six degrees of freedom for its linear motion. These linear motions will be: up-and-down, side-to-side, back-and forth (i.e. totalling six straight-line movements). Conversely, the rotational motions around individual linear axes are: yaw, pitch and roll (i.e. totalling 3 rotational movements). Each axis must be perpendicular to one another (i.e. totalling 3 squareness relationships). These kinematic translations will be linear motion along an axis, rotation about these axes, plus their squareness (i.e. orthogonally) for each axis with respect to one another, for say, a three-axis machine tool. This kinematic arrangement will then produce a total potential uncertainty in motion of 21 degrees of freedom (see the schematic diagram in Fig. 1.21), thus within the volumetric space for the machine tool, it must contain the following translational and rotational motions:

$$\mathbf{6}\,\text{linear} \times \mathbf{3}\,\text{rotational} + \mathbf{3}\,\text{squareness} = \mathbf{21}(\text{degrees of freedom}).$$

To fully calibrate a machine tool, all of these potential kinematic translational and rotational relationships must be verified, then corrected—if necessary—so that the machine will operate in a controlled accurate and precise manner. While another factor that must also be considered when operating machine tools is the actual workpiece's restraint and location[56] within the volumetric space of the machine tool, but this is only relevant in a machining operational context, so will not be further discussed in these circumstances.

[56]**Restraint and location** of the workpiece: which relates to its workholding method (e.g. clamping/fixturing arrangement, or simply holding/locating in a vice), together with the component's orientation with respect to the machine tool's axes alignments. Often a 3-2-1 kinematic clamping arrangement is utilised, thereby ensuring the part's exact location: on a fixture; on the table; or a pallet of for example, a Machining Centre.

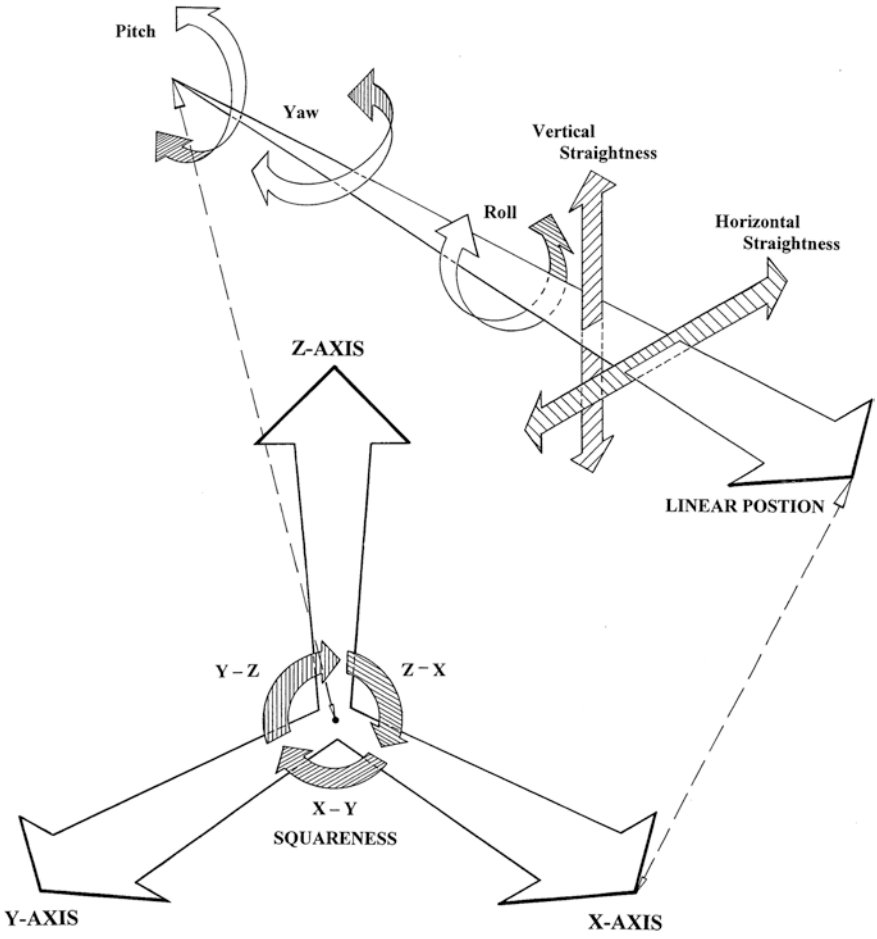

Fig. 1.21 The kinematics of an orthogonal machine tool

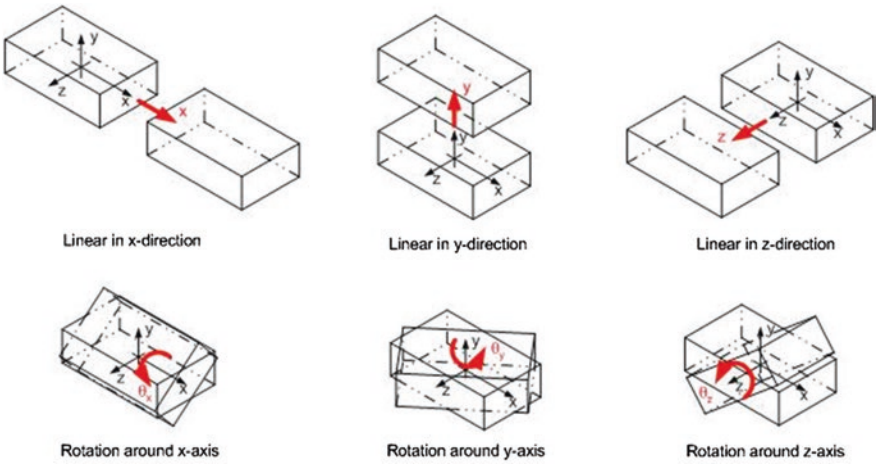

Some simple free-body diagrams, illustrating the potential kinematic motions on a typical machine tool

Expanding and elaborating on this kinematic theme still further, with regard to these 21 degrees of freedom, they can result in the following conditions for each type of motion, for the:

- **six linear motions**—these are the result of motional displacement, namely forward/backward for: $\pm X$; $\pm Y$; $\pm Z$ axes, that could introduce particular non-linearities (i.e. straightness uncertainty) into any potential slideway positioning;
- **three rotational motions**—namely, yaw, pitch and roll on each axis. Yaw is the side-to-side 'crabbing-motion' along the slideway. Pitch occurs through waviness in the slideway, introducing a backward and forward rocking (pitching) action, normal to the slideway, as the moving element traverses along the axis. Roll, may be introduced by two adjacent ways on this slideway not being coincident (i.e. laying within the same plane), causing an upward and downward rotational/pivoting action with respect to the line-of-sight along each axis, as the moving element traverses along its length;
- **three squareness errors**—these angular deviations result from the fact that each axis may not be perpendicular (i.e. square, or orthogonal) to one another.

Such kinematic machine-related uncertainties can be appreciably reduced by the application of either optical or laser-based calibration procedures and to a lesser extent, by verification employing artefact-based metrology techniques—although this latter technique is somewhat less precise, but can be significantly faster in many machine tool operational practices. There are numerous calibration procedures that can be utilised to restrict/prevent kinematic-motional uncertainties, including error-mapping techniques and dynamic-error compensation systems; this latter methodology utilises a real-time automated in-process control technique of machine tool adjustments—but is outside the scope of the current text.

1.11 Configurations of Machining and Turning Centres

1.11.1 Orthogonal Machine Tools

In the past the machine tool configurations for milling and turning operations could be divided into some distinct categories such as horizontal, or vertical spindle arrangement, but with either a straightforward turning, or milling operational production capability. Currently, machine tools are being designed and developed, with their constructional configurations being present in numerous and novel ways. For example, many Turning Centres now have milling capability due to driven/live (i.e. powered rotating) tooling and as such, they are often termed Mill/Turn Centres. While a significant number of Machining Centres can now have a turningcapability perhaps they could equally be entitled Turn/Mill machine tools? Furthermore, the state-of-the-art in these wide-ranging computer-aided manufacturing (CAM) developments means that both five- and six-axe machine tools are presently becoming increasingly more common in the Machining Centre variants. The kinematic consequences of these current machine tool configurations/trends will generate new demands and opportunities for the application of sophisticated tooling, meaning that:

- increased flexibility, in these machine tools and their machining applications will result;
- there will be significantly fewer machine and tooling set-ups to complete a component;
- reduced instability during the cutting process, as these machine tools are now much more rigid and, hence less prone to vibrational influences;
- due to both vastly increased rotational speeds coupled to more efficient cutting tools, it is now possible to utilise much longer tool lengths (i.e. tool loadings are significantly reduced), also meaning that less tool changes are now required;
- with the advent of increased cutter rotational speed, it is also possible to utilise smaller depth of cuts, while improving the finished machined surface texture—provided by the decreased step-over/pick-feed passes, to complete a milled surface feature.

1.11.2 Modular, or Reconfigurable Machine Tools

Over the past several decades, the design and development of many types of machine tools for high-volume industrial manufacture, has developed into two distinct categories, these are:

1. **General purpose machine tools**—that can be universally exploited for a very wide range of machined component manufacturing (e.g. notably being either configured variants of Machining, or Turning Centres);

2. **Specialised machine tool**—here, it has normally been designed for machining either exceedingly large batch volumes for part manufacturing of a specific type of part, or for a particular volume production process.

This latter category of Specialised machine tools can be considered to be very effective in their production output, although they do have some distinct disadvantages in terms of their overall manufacturing flexibility. One other major shortcoming is that if the product design for the machined component is modified, or indeed slightly changed, this may lead to the whole machine tool needing to be redesigned and then the line being totally rebuilt. While yet another problem is the bespoke, or custom-built machine tool, which normally has long lead-times for its design-and-build programme. The resolution to this extended development of a Specialist machine tool lead time, may be found in producing a Modular Machine Tool (MMT)—often known by the name Reconfigurable Machine Tool[57] (RMT); see the schematic flow diagram shown below. This RMT then allows for a customised machine tool that can be quickly redesigned and built from a library of modular components. Consequently, by utilising this library of standardised components, or modular sub-assemblies, it will lead to a novel, but discrete structural optimisation design problem, which must then be resolved. There are three specific phases to design and development of an RMT, namely:

1. **definition of the requirement that is undertaken by process planner according to change in production volume, or product design**—these requirements may be for its kinematics, power, or timing of the motion;
2. **reconfiguration generation can be achieved by a functional description of the machine tool**—utilising such mathematical tools as Screw theory and having a structural description with that of Graph theory—more will be mentioned on these tools below;
3. **evaluation of the generated machine tool configurations by utilising static, dynamic and kinematic analysis**—to eliminate any unfeasible configurations.

[57]**Reconfigurable Manufacturing System** (**RMS**) (The Reconfigurable Manufacturing System (RMS) as well as one of its specific components, which is the Reconfigurable Machine Tool (RMT), was invented in 1999 at the: Engineering Research Center for Reconfigurable Manufacturing Systems (ERC/RMS), at: The University of Michigan College of Engineering (USA). Ideally, in a typical Reconfigurable Manufacturing System it possesses six core RMS-characteristics, these are its: (i) Modularity; (ii) Integrability; (iii) Customised flexibility; (iv) Scalability; (v) Convertibility; also (vi) Diagnosability (i.e. see Koren et al. 1999). So, a typical RMS will have several of these characteristics, though not necessarily all of them. When possessing these characteristics, an RMS increases the speed of responsiveness of manufacturing systems to unpredicted events, such as for any sudden market-demand changes, or to unexpected machine tool failures.): can be defined as: "Designed at the outset for rapid change in its structure, as well as its hardware and software components, in order to quickly adjust its production capacity and functionality within a part family in response to sudden market changes, or intrinsic system change."

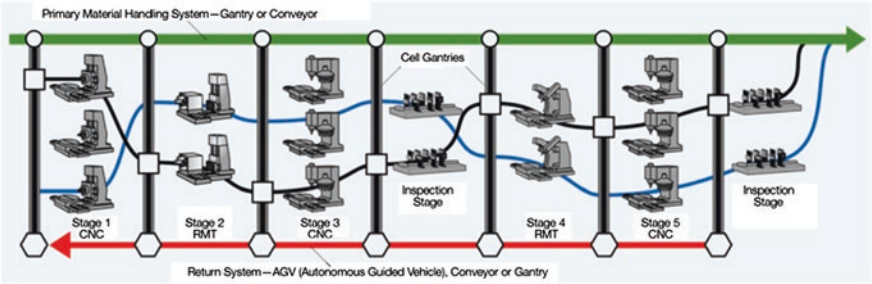

A schematic product's flow diagram of an RMS—incorporating Reconfigurable Machine Tools (RMT) [*After* USA artist—Rod Hill (1999)]

Mention was briefly made concerning the application of Screw theory (above), where this theory utilises three-dimensional motion of the rigid body by screw, to show the rotational and translational movements about an axis. The definition of the pitch of movement is translation motion divided by its rotation. The main disadvantage of employing concepts such as screw, expresses itself when we have just pure translation and no rotation, because in this case, the pitch becomes indefinite. A Homogeneous Transformation Matrix (HTM) demonstrates the displacement between the current position and the previous one. An HTM cannot show the nature of the motion, as one defines the translational and rotational motion task of machine tool according to its operation plan. This plan will include the machining operation type, cutter location and the Process plan for the new product volume, or perhaps new types of the products. Hence, by defining the HTM matrices from cutter location and then subsequently calculating displacement, one can obtain the dual vector of the motion and then one merges the motion in the same direction. To conclude, it is possible to have the final required motions needed to incorporate them within the machine tool. It should be noted that the actual mathematics behind such complex matrices, is beyond the current scope of this text, but can be found elsewhere within the references.

Accordingly, the structural description of the RMT, facilitates us in choosing the optimum modules to obtain the required machine tool movement. Thus, one can generate some structure configurations based on this type of description and consider the possibility of connection of the different modules, whilst making various types of configurations by means of Flow of Force[58] (FOF), then utilising a

[58]**Flow of Force** (FOF): this technique can be utilised to specify the order of the modules for different branches of tool and workpiece. By means of FOF, one can create different possible configurations of a machine tool, which can then fulfil the necessary motional requirements. Typically, two of the machine tool structures utilised by industry are: *XY*/*ZC* and *X*/*YZC*. These are simply alphabet symbols to show the moving parts of the machine in tool and, their respective work branches.

specific evaluation criteria to eliminate any of the unfeasible RMT configurations. A configuration generation by the Directed Graph Method (i.e. Graph theory—mentioned previously) enables the procedure of formation (i.e. by means of a directed graph), this being described as:

- **making the library of structural modules**—known as primitives needed to make different configurations, according to the required motions and to plan the process given by Process planner;
- **generating the single module complex units with a combination of primitive modules**—based on restriction of the connection of the vertices and directed edges in: Graph theory;
- **according to mainflow and regarding the tool, and subflow**—this relates to the workpiece Flow of force (FOF), where one can create different alternatives of machine configurations;
- **evaluation of the machine tool's configuration**—in terms of its kinematics, statics and dynamics.

1.11.3 Modular Machine Tool Construction

The majority of machine tools built today are based upon Modular design and build principles, with the model variants in their series requiring complementary dimensional and performance specifications together with a consistent approach to building the sub-assembly module designs—for this defined group. Therefore, a particular module in this machine tool series, must be standardised with regard to its functionality, or performance, while also including an interchangeability design factor to other respective modules within this series. Specifically, a group of standardised modules should be arranged in a uniform numerical series (i.e. concerning its volumetric dimensional specifications) whilst qualitatively maintaining an identical structural configuration.

In the machine tool photographs below, both Machining and Turning Centres are depicted here, both variants having been designed and constructed based upon these Modular design concepts, but in both cases they were manufactured in a volume production environment. This concept of modular manufacturing, enables the machine tool builder to optimise production volumes for any of its components that are manufactured, thereby permitting quite large batch sizes, which then leads to much lower costs per component part and a competitive overall pricing for its machine tool product ranges.

A typical range of commercially available CNC machine tools shown here are: Machining Centres (left), having: 12,000 rpm @ 22.4 kW vertical spindle; with 3 models in this range, but just two machine tools in the range are depicted here. Each series-type having a respective working area of: ≈920 × 460; ≈1375 × 640; ≈1625 × 710 (mm). Turning Centre models (right), each have: 4000 rpm @ 22.4 kW headstock spindle, comprising of just 2 models, these machines have a working area of: ≈240 swing × 1000 between centres (mm); ≈370 swing × 1525 between centres (mm)—with all of these machine tools being based upon Modular design concepts [courtesy of Haas Automation, Inc., Ca, (USA)—2015]

So, for a specific range of machine tools, only certain amount of sub-assembly items need to be changed in order to offer their prospective customer base either smaller, or larger capacity machine tools within a series. It is worth stating that perhaps for the Machining Centre variants (i.e. above—left) just described, there is probably less than 30 % difference on each machine which might be subject to any form of modification. For example, by typically just changing say, the table size, or increasing the capacity of the tool carousel, or by modifying guarding, but leaving the other structural elements unchanged such as its spindle assembly, electronics, CNC controller, etc., these latter items will be the same for each machine tool within this series. It follows that by using a modular approach to machine design and build, it allows a machine tool manufacturer to quickly respond to their customers manufacturing needs, or to compete with several of their competitors' newly-developed equivalent products in this targeted sales area.

Finally, with regard to a sustainable approach to this competitive problem of rapid and economic machine tool design and construction, it can be achieved by the modularisation of machine tools. If a machine tool manufacturer produces specific modules—often in Europe indicated by the German term Baugruppen[59]—each module provides certain functions in the build-up of the machine variants, which is usually determined in a specific customer's machining requirements. Then the process of constructing a bespoke machine tool from discrete modules, such as: small-to-large tables/beds, vertical/horizontal spindles, co-axial/single headstocks, small, or large capacity tooling carousels, one, or two turrets, etc., this customising assembly activity is known as bundling. As a result, with a bundling

[59]**Baugruppen**: this term is of German origin, which is primarily concerned with the development of: product ideas and concepts; design; design feasibility analyses; product protection for components and assemblies; and indeed, for complete products.

pricing strategy, this leads to an overall increase in terms of both revenue and profitability for the machine tool manufacturer.

1.11.4 Turning and Machining Centre Configurations

The plethora of both Turning and Machining Centre[60] configurations ranges from the relatively unsophisticated minimal two-axis machines, to complex multi-axes Mill/Turn Centres that are currently available, with just some of these variants being illustrated in Figs. 1.22 and 1.23. As can be visualised in Fig. 1.22, the co-axial spindled Mill/Turn centre has numerous linear/rotational axes, enabling it to either machine conventionally or to back-turn utilising its synchronised twin-spindle turning capability, also to mill component features, as necessary. A complex and sophisticated machine tool of this type requires, at the very least, a telescoping ballbar—periodic health check, but ideally this should be coupled with an annual laser calibration of its axes, thus ensuring that any high-quality machined component will be consistently manufactured.

In the case of the Mill/Turn centre illustrated in Fig. 1.23, the modularisation—previously discussed—can clearly be seen in this machine tool's concept of design and build. In the schematic Fig. 1.23a, it is possible for a customer to specify additional twin programmable steadies—shown on the left—or not, as in the case of the right-hand schematic diagram. In both cases (Fig. 1.23a), a co-axial synchronised spindle is employed—with variable positioning of tool turrets—allowing the option of either face, or back-turning operations independently, thereby significantly increasing production output from such a machine tool. The photograph shown in Fig. 1.23b illustrates the actual Mill/Turn Centre showing its flexible use of a programmable steady, with in-process part-probing/-interrogation—from one of the configurable turrets. Here, the same machine tool builder can offer customers a variety of machine tool configurations, based upon its generic slant-bed main casting, allowing not only a quick response to customer needs—for an almost bespoke machine—but also increasing the variety of machine tool variants within its current range.

Of note in the photograph in Fig. 1.23b and briefly mentioned above, is the fact that critical machined features can be probed in situ (i.e. as shown). This probing of the turned-part creates a feed-back loop to update the CNC controller's tool table, thereby compensating for such factors as tool wear (i.e. often termed drift). This tool wear condition is promoted as the tool's flank wear increases, causing either the turned diameter to marginally increase in its size, with successive parts manufactured, or conversely, for bored hole-features to accordingly decrease in size—with increased in-cut time usage. By using expensive and sophisticated

[60]**Turning and Machining Centres**, differ from either CNC Lathes/-Milling Machines, respectively, in that for both of these former cases they would be equipped with an automatic tool-changing ability, which their less-flexible CNC machining counterparts do not provide.

A micro-machined prismatic part, after machining on a: 5-axis Micro Milling Platform. [Courtesy of Microlution, Inc. (Chicago, USA)]

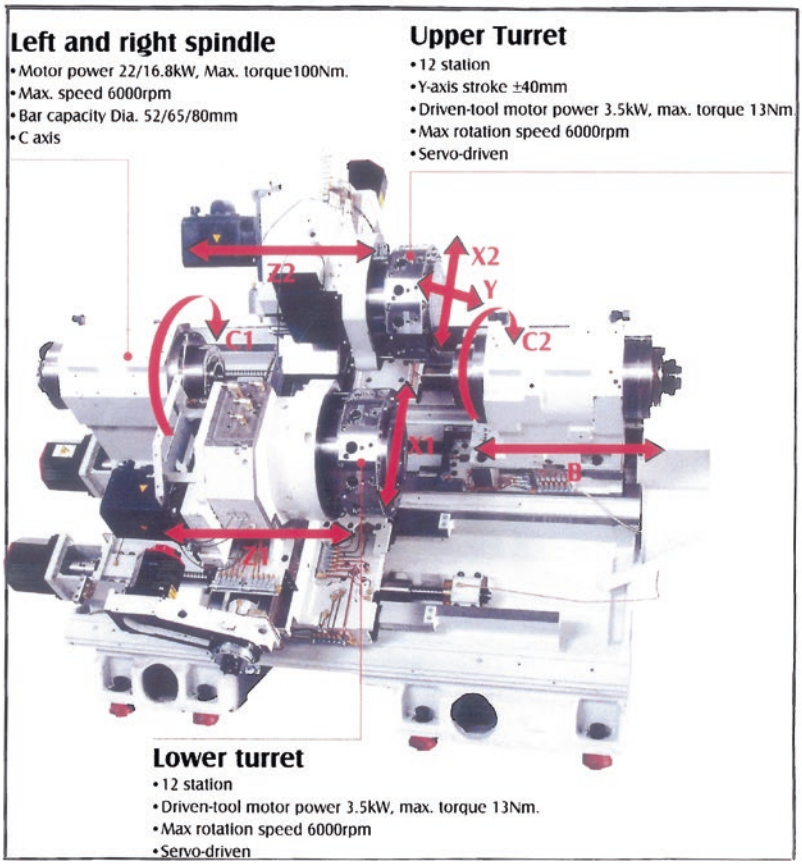

Fig. 1.22 A typical: *co-axial spindled mill/turn centre*, illustrating that each axis of the machine tool requires *periodic revalidation*—to ensure high quality production output throughout its 'working-life' [courtesy of Modern Tooling Ltd., Calgary, AB (Canada)]

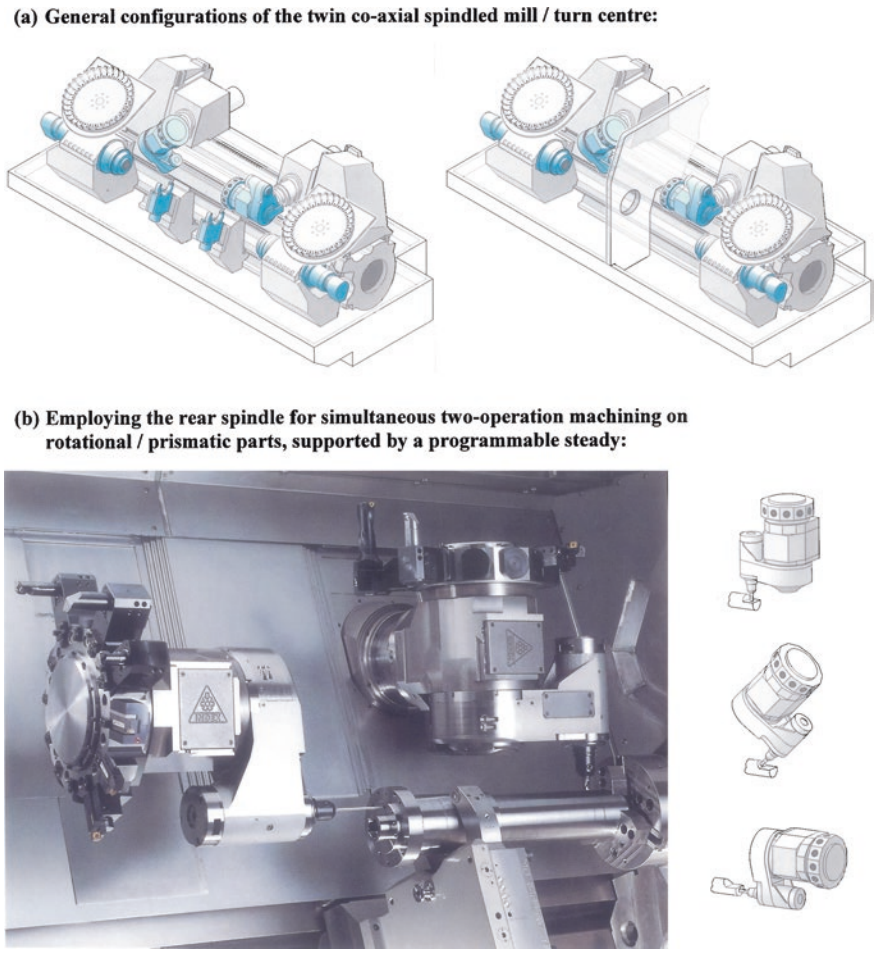

Fig. 1.23 A mill/turn (multi-axis) centre for increased production and high quality rotational/prismatic component manufacture (courtesy of Index-Werke GmbH)

machine tool plant such as these mentioned here, periodic calibration procedures will ensure quality production is consistently guaranteed.

By way of explanation of the wide and diverse types of machine tools that are available in a range of machining centres, such as the ones typically illustrated in Fig. 1.24, by just one of the major European machine tool builders, these machine configurations highlight the following machine tool characteristics:

- **a travelling column three axis vertical Machining Centre** (Fig. 1.24a)—here, it is fitted with linear-controlled axes, for exceptional linear acceleration/deceleration and rapid traverse speed. In this manner it can significantly decrease any non-productive cycle times whilst machining operations occur and, minimise

Fig. 1.24 Just some of the vast array of configurations of machining centres currently available (courtesy of Deckel Maho Gildemeister GmbH)

any potential servo-droop problems (i.e. promoting contouring errors) which is normally associated with this lag resulting from poor response time of the CNC controller and its axes;

- **a multi-axis Machining Centre** (Fig. 1.24b)—where the machine tool's table can be programmed to rotate to any required angle, or its variable-rotational head can be angularly rotated continuously in-cut. Likewise, with this in situ trunnion-table, it can also be orientated about its rotational axis, while continuously moving in the '*X*', '*Y*' and '*Z*' planes. This sophisticated multi-axis machine tool can be utilised to machine some exceedingly complex free-form curved component features, this requirement normally being programmed from cutting/geometry data via a DNC-link, from a bespoke CAD/CAM system;
- **the universal Machining Centre fitted with a high-speed spindle** (Fig. 1.24c)—which has a palletised rotational table and adjustable programmable spindle head. It can have automated pallet changing incorporated into the machine tool, for workpiece delivery as part of a flexible manufacturing cell/System (FMC/S). The high-speed spindle (HSM)—with a fast tool-changing head, enables cut-to-cut times to be minimised. Moreover, the HSM feature, which will enable the spindle-tooling to produce considerably lower cutting forces for a given feedrate when compared to normal rotational speed machining data. This higher rotational cutter speed has distinct production advantages, such as allowing for better machined surface finishes to be attained, coupled to increased tool lengths allowing for better length-to-diameter ratios, enabling smaller diameter cutters to be utilised, therefore necessitating less tool changes when machining certain part features, plus having an improved chip evacuation from the cutting vicinity.

In order to significantly increase the flexibility of Machining Centres, integrated FMC's have been developed—as depicted below—with an in situ robotic work-handling capability. This bespoke turn-key system has been fully industrial-hardened, eliminating any potential hard-/soft-ware clichés and robotic safety concerns (i.e. this is a fully-interlocked and guarded FMC), and the working footprint of this automated plant is very compact. Palletised workpiece fixtures—of known coordinate part datums—are located into their appropriate stacked shelf-slots, where the robotic arm can accurately and precisely move-and-place them, when required, within the working-volume of the Machining Centre. Not only can these palletised parts be scheduled as dictated by the company's Master schedule, but potential machined parts can be simply rescheduled—as demanded—according to the commands of the current production requirements. As with all such high-quality workpiece output from the FMC, the Machining Centre needs to be periodically calibrated, as will the in situ robotic arm, but more will be mentioned on these topics in the appropriate following chapters of this book.

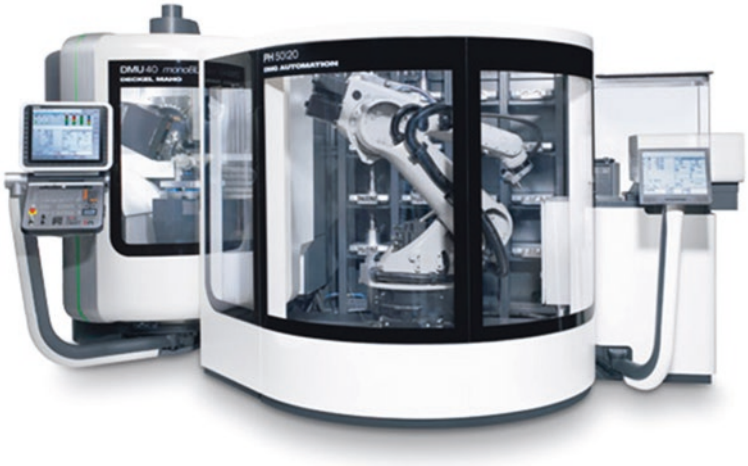

In order to increase automated productivity, but with a small working footprint, this highly-productive multi-axis Machining Centre is currently available. Here, this Flexible Manufacturing Cell (FMC) has within its small footprint, the incorporation of an integrated six-axis anthropometric robot, enabling robotic automation that can load/unload up to 20 work-pallets, the robot can also be specified with either a 50, or 200 kg weight-carrying capacity. The large palletised-storage capacity, allows for a range of highly-autonomous machining operations to be undertaken, with work scheduling and control being via the machine's DMG Job-Manager (courtesy of Deckel Maho Gildemeister GmbH—2015)

The travelling column vertical Machining Centre shown in Fig. 1.25, and as a rendition shown below, but with the guarding removed for clarity, has linear motor drives with very fast acceleration/decelerations. Of particular note with regard to these sophisticated machine tools, is the considerable amount of Artificial intelligence[61] (AI) that is now being incorporated within the machine's CNC controller. Just some of these latest 'AI' developments incorporated into its CNC controller by this particular machine tool builder are discussed below. This level of AI, will significantly influence the effectiveness of the machine's overall performance. This expanded AI discussion, is important to mention rather than simply discussing programming techniques that are based upon machining the actual workpiece because these topics are more than adequately mentioned elsewhere within the appropriate literature.

[61]**Artificial intelligence** (**AI**): this can be considered as the technology and a branch of Computer Science that studies and develops intelligent machines and software. The term, AI can be defined as: "The study and design of intelligent agents", where an intelligent agent, is a system that perceives its environment and takes actions that maximise its chances of success. John McCarthy (USA) (**Alan M. Turing**—see previous Footnote 16, also has a significant-claim for inventing the theory and much of the terminology associated with AI—which considerably predates the above.)—who some would say, coined the original AI term back in 1955, which was where he then adequately defined AI, as simply: "The science and engineering of making intelligent machines".

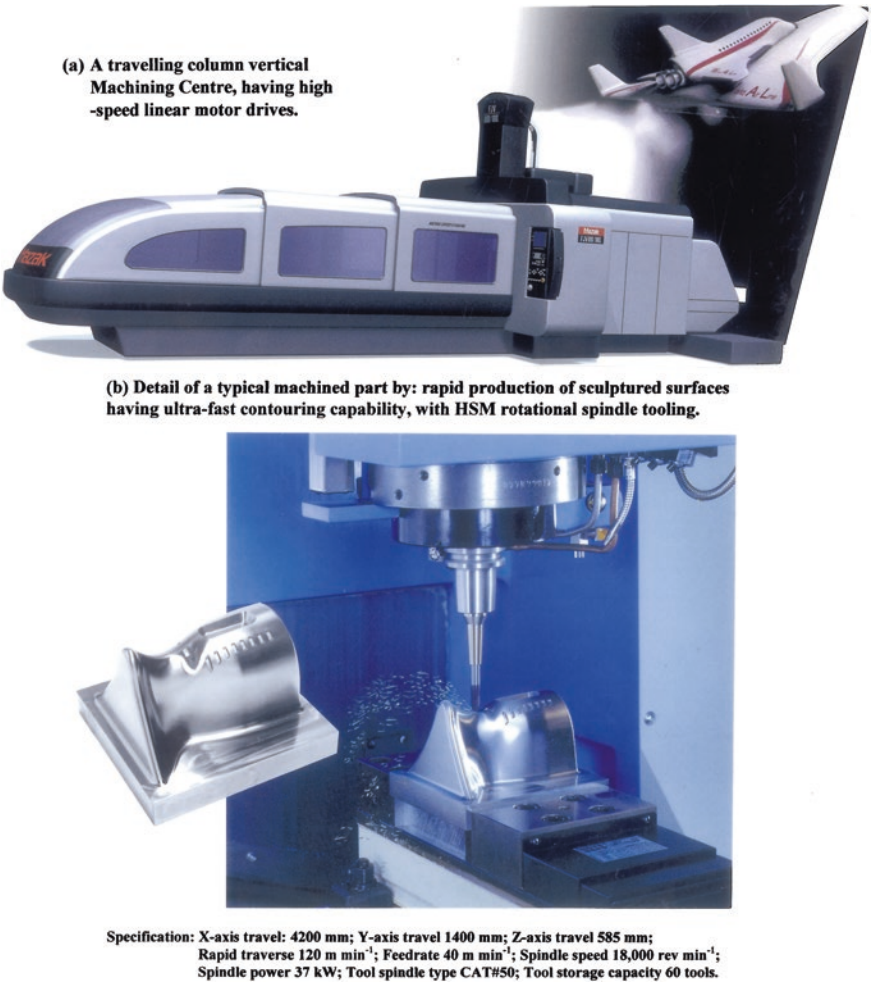

Fig. 1.25 A vertical machining centre equipped with *linear-driven slideways* and *high-speed machining* (HSM) capabilities, offers *rapid* cycle time reductions of production of *complex* accurate and precise machined components [courtesy of Yamazaki Mazak Corporation (Japan)]

1.11.5 CNC Controller Developments

The travelling column Machining Centre shown in Fig. 1.25, and in rendered-form below, incorporates into the latest version of its CNC controller a degree of AI, which the company terms its nervous system—as it seemingly has the ability to react to changes during its usage in the context of its operational machining environment. This seemingly high level of Artificial intelligence with its power

of synergy within the CNC controller, equips the machine tool with the following important advanced condition monitoring functions:

- **vibration minimisation**—via an Active vibration control, which means that any machine vibration promoted by axis movement (e.g. acceleration/deceleration) can considerably affect both the machining accuracy and precision with its machining time. This Active vibration control function will—during machining—dynamically dampen cutting tool nose vibration, enhancing an improved workpiece surface finish and minimise excessive tool nose wear rates, therefore extending the tool's life;
- **heat displacement control**—via an Intelligent thermal shield, so as the temperature of the machine tool changes due to its operation and the result of any ambient room temperature change, any unwanted-displacement will affect machined accuracy and precision. The Intelligent thermal shield will automatically compensate for such temperature variations, together with changes in spindle speed/slideway operation and in this manner stabilise machining accuracies. Additionally, to minimise heat-distortion—necessary for stable-machining accuracy, the machine elements that generate heat (e.g. spindle motors, ballscrews, etc.) are symmetrically-arranged within the overall machine tool. As a result, machine heat-displacement is of the order ≤ 8 μm—for a room temperature change of 8 °C. This minimising of such heat-effects on the machine tool stabilises the overall machine tool, for extended periods of usage;
- **machine interference prevention**—via an Intelligent safety shield; so when the operator manually moves the machine's axes, for either its setup, or for tool measurement, a synchronised 3-D model is depicted within the CNC's display screen—for checking of any impending machine interference. If any interference is detected, axes motions are immediately stopped; this protects the machine tool and allows for much faster setup times to be achieved;
- **verbal message system (VBS)**—via a Voice advisor that verbally informs which switches have been selected by the CNC operator and then advises caution when manually operating the machine tool. This VBS has the capacity to reduce CNC operator setup problems when selecting and moving linear and/or rotational axes. Moreover, the VBS states the following: when to add lubricants to the machine; at what time tool life is about to end; plus many more verbal-commands; enabling a smooth transition from manual to fully-automated machining control;
- **comprehensive spindle monitor**—via an Intelligent performance spindle, that will monitor a variety of vital spindle-related parameters by the strategically placed sensors housed within the spindle-assembly. Accordingly, by incorporating such sophisticated spindle monitoring, this reduces the potential spindle overload/damage and, in this manner, significantly minimising any production losses, due to potential downtime;
- **comprehensive maintenance control**—via an Intelligent maintenance support function that monitors the status of perishable-items within the machine tool, such as its: filtres; slideway cover wipes; etc., together with monitoring the

operational history of critical machine units. This type of information is vital in determining a preventative maintenance program, accordingly reducing unanticipated machine downtime. Other important features of this maintenance control system, include pop-up windows notifying the operator when replacement items are due, or at what time the next scheduled maintenance time will occur;

- **unbalanced table/chuck detection and analysis**—via an Intelligent balance analyser. If heavy fixtures/workpieces are loaded in an unbalanced-condition, then the machine's safe operation can be affected. This intelligent balance function analyses the balance problem, displaying the amount of weight and its location, highlighting how and where any re-balancing is required—to eliminate this potential unbalance condition. This system can also stop any workpiece rotation, if excessive vibration is detected.

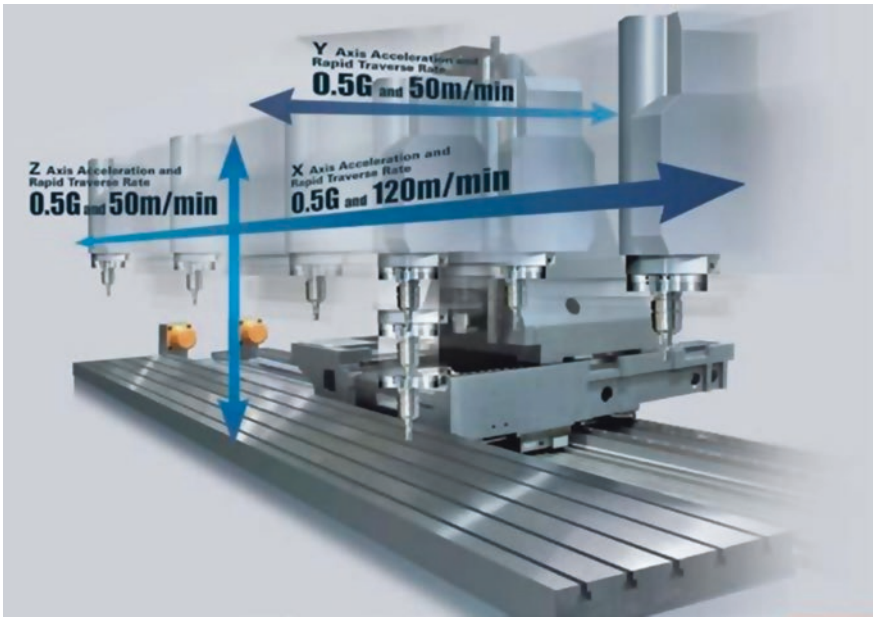

A travelling-column Machining Centre (rendered-diagram), illustrating that by being equipped with fast linear motor axes drives for rapid traverse rates and accelerations/decelerations, this will significantly minimise any non-productive idle-times, which might occur during the workpiece's machining cycle (courtesy of Yamazaki Mazak Corporation (Japan)—2015)

1.11.6 Non-orthogonal/Parallel Kinematic Machines (PKM)

So far, only some of the available designs and configurations of orthogonal machine tools have been fleetingly described, with these machine tools having axes that are perpendicular with respect to one another. Increasingly, however, there is yet another novel and inventive machine tool variant that has been

designed and developed with a very innovative type of axes configuration, logically termed non-orthogonal machine tools, or more generally known of late as parallel kinematic machines (PKMs).

Historically, in 1956, the first industrial application of PKMs must be credited to Gough,[62] but today this type of PKM is often known as a Stewart-platform. This type of supporting-platform was originally designed in 1956 to test automotive tyres. Since then, PKMs have mainly been utilised for dynamic platforms for flight test simulators and in selected robotic applications, due to the platform's specific advantages of a low moving-mass coupled to high dynamic performance. With the expansion of high-speed machining applications, these PKMs have become an alternative for some machine tool designs. In the case of a machine tool utilising a PKM-configuration, the tool is connected to the machine's base through several kinematic-chains—or support-legs—that are mounted in parallel. These support-legs are generally constructed of either telescopic-struts with fixed-node points, or alternatively with fixed length struts with gliding-node points. Parallel kinematic machines are often claimed to offer greater accuracy and precision over their serial (i.e. orthogonal) counterparts, offering high structural rigidity and improved dynamic capacity. Conversely, such a PKM-geometry generally suffers from a reduced operational workspace, due to the presence of internal-singularities, or from the potential problems of self-collisions. Nonetheless, apart from these potential technical-difficulties, Parallel Kinematic Machine tools are now attracting the scientific interest of a greater number of academic researchers and machine tool companies.

Following the first PKM-prototype that was exhibited in 1994 in the USA—during the IMTS in Chicago—by the machine tool company Giddings and Lewis, there have been many other PKM's designed and developed. However, with the introduction of this Giddings and Lewis Variax™ hexapod machine tool—shown in Fig. 1.26—there has been comparative study where it showed that certain parallel kinematic structures do have some potential and real advantages over their serial (i.e. orthogonal) counterparts. Despite this highly-publicised survey, it is worth mentioning that many industrial-based customers for machine tools are still not convinced by the potential benefits of such PKMs. As an example of the

[62]**Parallel kinematic machines (PKM)**: the first industrial application of PKMs was the Gough platform (Gough 1956–1957), designed in 1956 to simply test tyres. PKMs have then been utilised for many years in: Flight simulators; Robotic applications; etc.; because of their low moving-mass and high dynamic performance. Since the development of high-speed machining (HSM), these PKMs have become an interesting-alternative in machine tool design. Utilising a parallel manipulator in a mechanical system using several computer-controlled serial-chains to support a single platform, or an end effector. Probably, the best known parallel-manipulator is formed from six linear actuators, that support a movable-base for devices such as just mentioned, namely for flight simulators. This type of device is termed either a Stewart platform, or alternatively the Gough-Stewart platform in recognition of the Engineers who first designed and utilised them, but they are also additionally known as: Parallel robots.

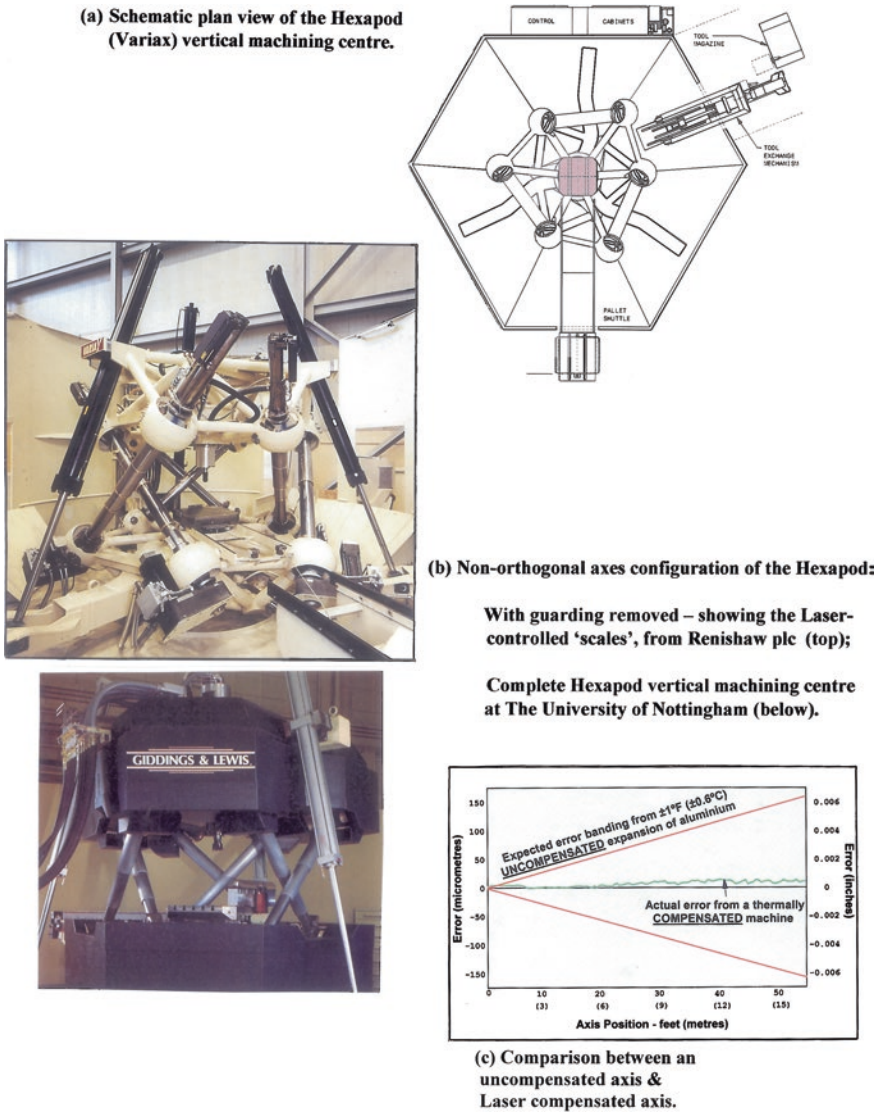

Fig. 1.26 A non-orthogonal vertical machining centre: 'hexapod' (Variax), equipped with laser-controlled axes positioning monitoring systems [courtesy of Giddings and Lewis Machine tools LLC (WI, USA)]

performance-comparison between a conventional five-axis machine tool and that of a PKM (i.e. the Variax™) depicted in Fig. 1.26, this particular PKM with its 630-mm square pallet has a capital cost that is competitive with an equivalent multi-axis orthogonal machine tool. Yet the Variax™, has a high structural integrity and rigidity of 175 Nm μm^{-1}; with a volumetric accuracy and precision of

≤10 μm; being equipped with a spindle power of 22 kW with a rotational speed range of between 100 and 15,000 rpm; while having a cutter inclination angle of 25° (max.); producing a chip-to-chip time of 6 s; with a pallet changeover time of 10 s; finally with a tool storage capacity of 50 tools. The actual structural-rigidity quoted for this PKM over its conventional counterpart is >500 %, due to the fact that all of the forces are in compression, or tension through the six legs of its space-frame. Hence, this PKM is very rapid in motion if it is compared to conventional machine tools with their individual Ballscrews. Such axis rapidity, is due to the low-mass being moved by all six Ballscrews working-together. There are many other claimed advantages for the PKM-type machine tools over their orthogonal counterparts, notably that their achievable volumetric accuracy is very close to that of a Coordinate Measuring Machine (CMM), because any error in each of the legs (i.e. axes) are averaged out, rather than stacked up, as is the case in conventional/orthogonal types of CNC machine tools.

Most industrial 3-axis machine tools have a PPP kinematic architecture[63] with orthogonal joint-axes originating along the '*X*', '*Y*' and '*Z*' perpendicular-directions. As a result, the motion of the tool in each of these directions will be linearly-related to the motion of one of the three actuated axes. Correspondingly, the performances (e.g. maximum speeds, forces, accuracy and rigidity) are uniformly-constant within most parts of its Cartesian workspace, which is often termed a parallelepiped. By way of comparison, the shared-features of most prevailing PKMs are a Cartesian workspace shape of complex geometry and with highly non-linear input/output relations. For most PKMs, the Jacobian matrix[64]—relating to the joint-rates and their output velocities is not constant and therefore is not isotropic. Consequently, the dynamic performance of the axes may vary considerably for different points in the Cartesian workspace and, for dissimilar directions at one given point, this tends to be a serious drawback for any potential machining applications. The mathematics for PKMs is somewhat-complex and as a result, will not be discussed in the present text, but this information is available in the literature concerning a PKM's kinematic motional control.

Since the initial commercial availability of the Giddings and Lewis Variax™ machine tool, there have been numerous newly-devised PKMs, one of which is shown below and will now be briefly mentioned. This ICON Tripod is a Parallel Kinematics Machine (PKM), created for 6-axis interpolation-operations either as a stand-alone unit, or integrated into a Flexible Machining Cell (FMC). Accordingly, the ICON Tripod provides very rigid machining capability with an extremely small

[63]**PPP kinematic architecture** (i.e. having a serial Precise Point Positioning): as with most industrial 3-axis machine tools, they have a PPP-kinematic architecture in conjunction with their orthogonal axes. The motion of the cutting tool's spindle in the space is quite simply related to the motion of the three actuated axes, with such machine tools often being termed: PPP-serial machines (i.e. having a regular Cartesian workspace shape and a uniform performance).

[64]**Jacobian matrix** (Carl Gustav Jacob Jacobi (Born: 10 December 1804 in Potsdam—died: 18 February 1851, Berlin): was a German Mathematician, who made some significant and fundamental contributions to the fields of: Elliptic functions, Dynamics, Differential equations, and to Number theory.): in mathematics this is principally-concerned with Vector-calculus, with this Jacobian matrix being the matrix of all first-order partial-derivatives of a vector-valued function.

machine tool footprint when compared to traditional machining centres. The rigidity of the PKM is due to the three-arm design. By centring the tooling head spindle, the machining-induced stresses are evenly displaced over a small area, rather than across the large machine base. The accuracy of this Tripod is due to its parallel kinematic design. Hence, axis motions on the '*X*-', '*Y*-', and '*Z*-axis', are performed by three parallel axes that hold rigidly tight, whilst still maintaining machine tool flexibility.

The 700S version of this PKM is shown below, which has a work-envelope of 800 mm × 800 mm × 400 mm, being equipped with a motor spindle of 18,000 rpm and 35 kW power and, having a rotary table size of 800 mm—with a zero-point clamping system.

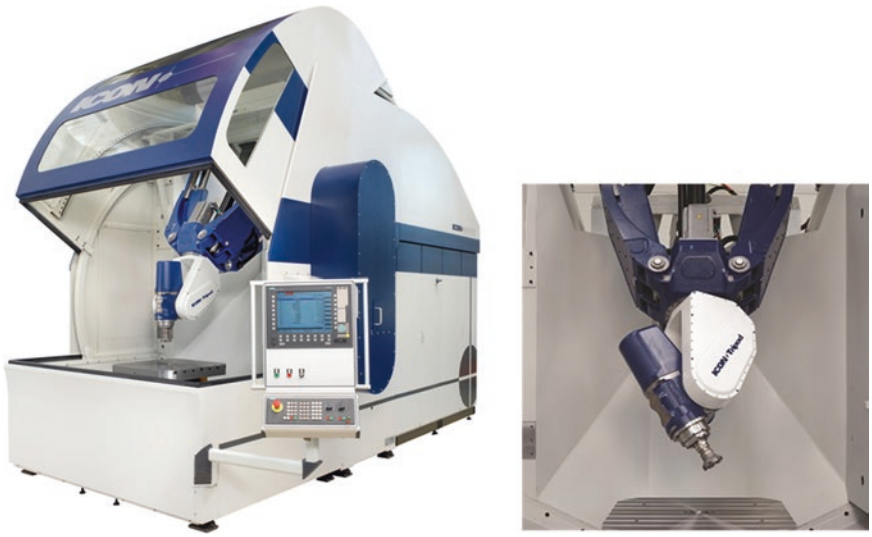

The ICON Tripod is a six-axis Parallel kinematic machine (PKM), which is currently equipped with a robust 18,000 rpm 35-kW spindle, for precise and accurate high-quality machining applications [courtesy of ICON Technologies, Division of Hydromat Inc. (St Louis, MO, USA)—2015]

The calibration of these PKM's is normally via some form of artefact-based instrumentation, such as Telescoping Ballbars and this type of volumetric verification technique will be mentioned in more detail in Chapter Four.

1.12 Major Elements in a Machine Tool's Construction

Most of today's CNC machine tools are designed and constructed from the principles of modular concepts—previously mentioned in Sect. 1.11.3, so in order to gain a clearer insight into the main reasons why such verification/calibration procedures are necessary, some of the major component assemblies will now be briefly reviewed.

1.12.1 Headstocks for Turning Centres and Spindles for Machining Centres

Belt-Driven and Direct-Drive Headstocks

The headstock on a turning centre should be thermally symmetrical in its design and construction, having the capacity to diminish potential turned workpiece distortion, whilst providing stable conditions for part accuracy and precision even in continuous high-speed machining operations. A typical partially sectioned belt-driven headstock is depicted in Fig. 1.27 (top-right). Here, within the cast headstock, the bearing configuration for the spindle is supported by high-speed angular contact bearings backed up by double-row cylindrical roller bearings in the front—close to its workholding region. While at the rear of the headstock, the spindle is supported by another set of double-row cylindrical roller bearings. This complex bearing configuration is provided to resist the axial cutting force in the *Z*-plane and the radial force in the *X*-plane, with these self-alignment angular contact bearings providing tremendous radial load capability. The tangential force—the major force produced when turning operations are undertaken on a workpiece—is also supported by this complex bearing support assembly within the headstock's main casting. In order to minimise the overall effect of thermal distortion of this headstock, heat insulation pads are strategically positioned within the assembly; these act as potential heat-sinks having the capacity to dissipate/remove heat generated by such continuous turning operations, thus reducing any potential displacement along the spindle's centreline. Moreover, the headstock's spindle-assembly has some lateral/compliant movement in the *Z*-plane. Controlled compliance is so designed to enable any heat that is generated during machining to force the spindle to grow away (i.e. by this controlled expansion) from the spindle nose and in this manner improve the overall turned-part quality.

Most belt-driven headstock spindles (Fig. 1.27) must of necessity have working clearances, however minimal, within their bearing assemblies—to provide the close running-fits required for rotation during turning operations. This bearing arrangement although a very rigid and precise assembly, will create some relative sinusoidal-movement (i.e. Fig. 1.27a), due to the radial force being exerted by the indispensable-tension that is required by the drive belts. This effective side-loading by the headstock's drive belts causes a regular harmonic rotational motion to the spindle as shown in Fig. 1.27b, which is then transferred to the workpiece when turning operations are carried out. The combination of these two regular cyclical actions produces a combined, but irregular resultant harmonic effect as depicted in Fig. 1.27c. This harmonic influence is then translated onto the workpiece's machined roundness, producing an irregular harmonic out-of-roundness[65] on the

[65]**Out-of-roundness** [For more information regarding Roundness assessment, see: Smith (2002)]: this term refers to the Departures from roundness of a workpiece, often termed undulations per revolution (upr). These upr harmonics are usually shown on a Polar chart (i.e. obtained from inspection on a Roundness Testing Machine), that has plotted the harmonic behaviour utilising one of four assessment techniques, with the most common being: Least Squares Circle (LSC).

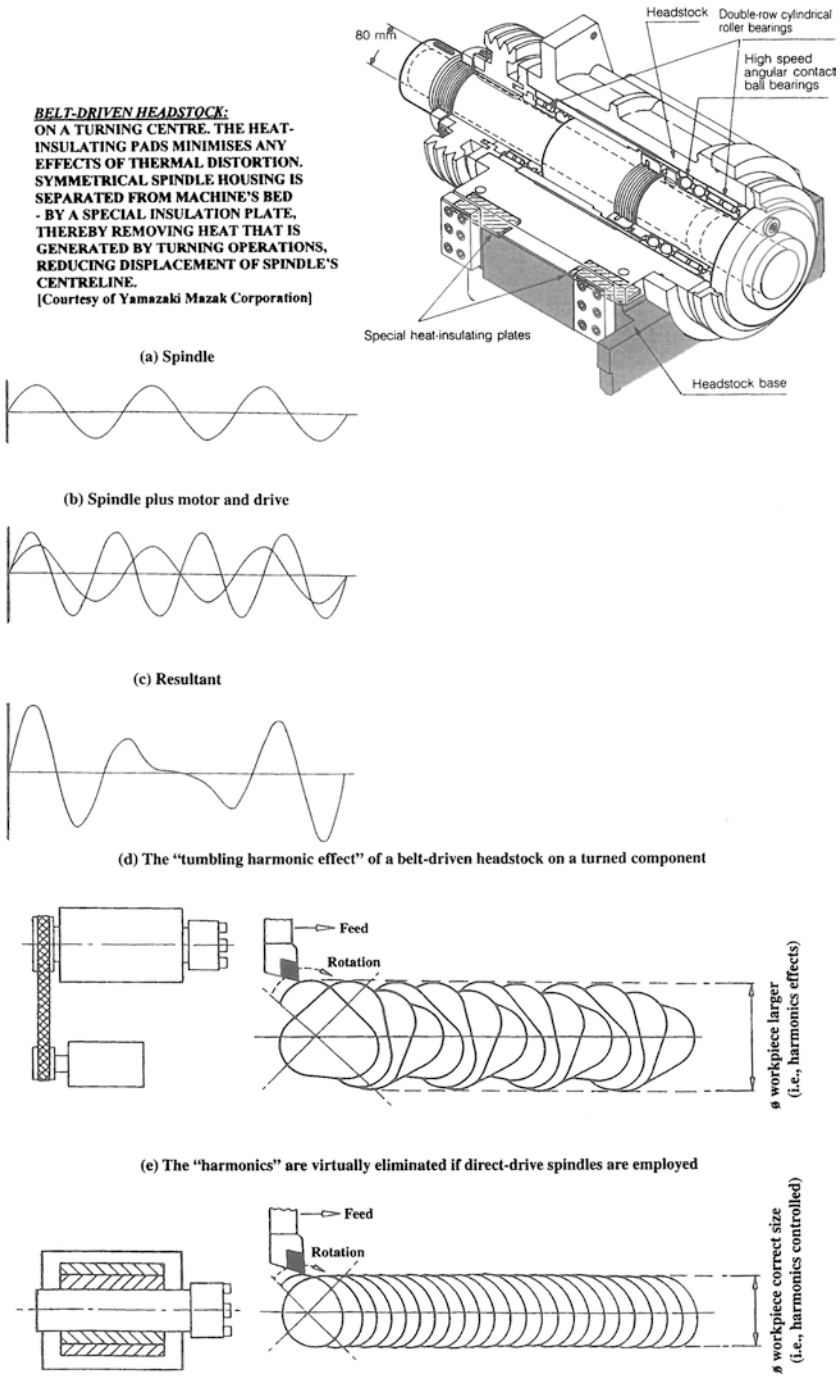

Fig. 1.27 On turning centres, utilising 'direct-drive' headstock spindles—for 'harmonic suppression', minimises machined roundness problems

Table 1.5 Harmonic behaviour related to either the component manufacturing process, or it measurement

Harmonic	Cause
1st (1 upr)	**Function of measurement**—only caused by the setting-up error on the instrument being used to measure the: Departures from roundness. The amplitude of this harmonic is equal to the eccentricity of the part, relative to the spindle axis of the roundness instrument
2nd (2 upr)	**Function of measurement, or manufacture**—this aspect of harmonics is generally termed Ovality and can be caused either by a setting-up error of the roundness instrument, or the part being machined out-of-square to its axis of rotation
3rd–7th (upr)	**Function of manufacture**—these harmonics are normally introduced by the workholding technique during manufacture. By way of illustration, if a three-jaw chuck was used to hold a relatively delicate part and excessive clamping force was employed, then upon machining and subsequent workpiece removal, a three-lobed part would be the result
15th and upwards	**Function of material and manufacture**—this aspect of harmonic behaviour is usually introduced to the part by either machine tool instability (i.e. self-excited vibration—chatter), or by the reaction of the materials utilised in the component's manufacture—cutting insert/toolholder, or lubricant (i.e. if any used)

NB The acronym 'upr' equates to: undulations per revolution
Sources Smith (2002)/Taylor Hobson (Leicester, UK)

completed machined part. The influence of this irregular harmonic rotation (i.e. Fig. 1.27c) can be gleaned from the schematic representation shown in Fig. 1.27d, where a repeating-series of tumbling three-lobed harmonic geometric shapes are reproduced on and along the turned workpiece. The irregular periodic nature of the rotational action provided by the belt-driven headstock is reproduced on the turned-workpiece by a series of kinematic combinations of the headstock rotation and the tool's linear motion. Hence, this type of Tumbling harmonic effect being supplied by the part's rotation, coupled with the longitudinal feed of the cutting tool along the part (i.e. Fig. 1.27d). If a direct-drive headstock configuration is utilised (i.e. Fig. 1.27e), then there is virtually no harmonic influence associated from the machine's headstock, resulting in more consistently turned workpieces. The harmonic behaviour that appears on the machined component is a function of both its manufacturing process and its post-machining inspection, as illustrated in Table 1.5.

Machining Centre—Spindle Bearings

Currently, most machining centre spindles are usually available up to a rotational speed of 15,000 rpm (i.e. see below) but ultra-high frequency magnetic spindles are now available with rotational speeds >100,000 rpm—see a typical active-type HSM spindle in Fig. 6.6 (top-right). These latter types of high-frequency spindles utilise active magnetic bearings for their spindle-alignment/support, but here, the power-availability will obviously be somewhat less than that of conventional spindles. In this brief review, only conventional ball/roller bearing-based spindles will be mentioned. Clearly, the importance of bearing design within the spindle's bearing system is critical to its rotational and machining performance. Simplistically-speaking,

these balls roll between the inner and outer alloy steel raceways. Often, the material utilised for ball bearings affects spindle temperature, vibration levels and ultimately the life of the spindle. Today, many spindle manufacturers are employing hybrid ceramic bearings, as they offer distinct advantages over equivalent steel ball bearings with these former bearings advantages being listed below.

Hybrid Ceramic Bearings—these will allow:

- **a reduction in the amount of mass**—with ceramic ball bearings they have ≤60 % of the mass if compared to that of their steel-balled equivalents. Regarding steel ball bearings that are rotated principally at high rotational speeds, the centrifugal forces will thrust the balls into the outer race, which may even begin to deform these actual ball shapes. So, as this type of ball bearing begins to deform, it causes it to wear faster, leading to a significant bearing deterioration. Conversely, ceramic balls have much less mass than their steel counterparts, allowing them to cope significantly better at an identical rotational speed. The practice of employing ceramic balls enables them to achieve 30 % higher rotational speeds—for a given ball bearing size, without foregoing bearing life;
- **cold welding elimination**—as ceramic balls are inert, they do not chemically react with the steel raceways, thus eliminating any impending cold welding, which can be the chief source of alloy steel bearing failure. The cold welding of steel bearings is a phenomenon that arises when microscopic particles of ball material cold weld to the raceway; this adhesion causes surface race wear. As a result, these minute cold welds actually promote surface cracks and then periodically fracture as the bearings rotate, creating surface roughness (i.e. this effect is often termed Brinelling[66]), which subsequently leads to unwarranted heat generation that results in the bearing's premature failure;
- **lower temperature operation**—occurs from the almost perfect spherical roundness of these ceramic balls. Consequently, these hybrid ceramic bearings can function at considerably lower temperatures than for steel ball bearings, resulting in a much longer life for the bearing's lubricant;
- **lower vibration levels**—bearing tests have shown that spindles utilising hybrid ceramic bearings, exhibit both a higher rigidity and improved natural frequencies to their alloy steel equivalents, making them less sensitive to vibration, leading to longer in-service life for the bearing lubricant.

[66]**Brinelling** (The term: Brinelling, being derived from the well-known: Brinell Hardness Test, which is where a hardened steel ball indentor is utilised, for comparison of hardness test measurements.): steel ball bearings are not usually specified for High-speed Machining (HSM) operations, because at approaching rotations of ≈20,000 rpm, this speed mechanically-sets the bearings upper rotational velocity for conventional spindle designs. As a result of these fast rotational speed effects, in combination with high centrifugal force, means that at: ≈80 m s^{-1} of ball rotational speed, these steel balls will lose contact with the journal walls. Hence, as a result of this loss-of-contact the hardened steel balls and accompanying raceways will rapidly wear out, causing the so-called Brinelling-effect within the raceway-track. This agitated ball motion creates: a poor circumferential track wear-pattern; track delamination; together with higher friction and increased temperatures leading to a major debilitation of spindle roundness modifications and a significant reduction in the bearing's service-life.

Turning and Machining Centres—types of spindles

The current range of machine tool spindle technology offers various techniques to rotate the spindle, such as belt-driven, gearing, plus either in-line and built-in motors. In the case of a Belt-driven spindle—shown for a Turning Centre's headstock in Figs. 1.27 (top-right) and 1.28a—the belt maintenance access and its replacement costs are important. Furthermore, if this belt type is utilised on Machining Centres, it will affect the noise level of the machine tool. So, where belt drives are necessary, then an improved designed belt having a herringbone design, tends to be quieter than normal belt types, due to the manner in which the herringbone arrangement disperses any trapped-air—while in rotary motion—thus reducing the overall noise effect. By way of comparison gear-driven spindles significantly add cost to the machine tool, making it noisier, whilst requiring more frequent maintenance than that of a typical belt-driven spindle.

Of late, the in-line spindle (i.e. often now known as a Direct-drive spindle—see Fig. 1.22 and schematically—in Fig. 1.27e) has been designed and constructed allowing the spindle to be directly coupled to the motor. These in-line/Direct-drive spindles can result in an excellent machined harmonics/surface texture, moreover they tend to be much smoother and quieter in operation. While yet another variant of the direct-drive spindle type is that of the built-in motorised spindle, here it literally means that the motor is built into the spindle assembly. These latter versions of machine tool direct-drive spindles are commonly utilised when much higher spindle speeds (i.e. $\geq$16,000 rpm) are necessary. Such a built-in motorised spindle tends to be much more costly when compared to the less complicated belt-driven spindle types. Irrespective of the type of spindle design utilised, the actual motor that rotates the spindle is vitally important. In the case of motors having two sets of windings—often known as Dual-wound spindle motors—they provide high cutting torque and offer very good material removal rates. Conversely, if a single-wound spindle motor is normally fitted, it offers a lower torque, which is sufficient for most machining applications, or where higher rotational speeds are not demanded.

Spindle Assemblies—Potential Problems

The fundamental problems associated with the maintenance operation of the machine tool's spindle are extraneous heat together with any debris and contaminants, in this latter case it is usually created by fines,[67] whilst coolant infiltrating

[67]**Fines** (Particles occurring within the bearing's oil/grease arise from a number of different sources. Contamination can enter the system during maintenance, through breathers, during oil top-offs, in the course of periodic oil changes and in other distinct ways. Wear-particles/Fines are generated during machine tool's operation. As mentioned, these wear particles can be the result of: contamination; improper lubrication; a change in the machine's operating-conditions; plus other contributory factors that may cause an unwanted metal-to-metal contact): these are microscopic work-hardened particles/debris usually produced when either removing stock material from: the workpiece; or by bearing delamination effects; or from other potential failure mechanisms. These fines are invariably minute, work-hardened particles and hence, they are quite abrasive in nature.
NB **Microscopic Particle Examination (MPE)**: can be usefully-employed to provide some form of Analytical Ferrography Analysis. This MPE is a comprehensive and detailed microscopic analysis of the solid Wear-particles/Fines that are captured within the oil/grease sample.

into the bearing system will also have a deleterious effect on this precision assembly. Previously, the most likely reason for a spindle's unanticipated end-point has been the bearing failure, in the main caused by contamination from one, or more of the following factors: coolant ingress; condensation; contamination or from chip damage. Essentially, the spindle temperature should remain stable and relatively cool, while ensuring that any contaminants are excluded. In most situations of spindle failure, contaminants have tended to enter the spindle assembly because of a particular seal's failure.

Many spindle manufacturers fit an air purge system[68] that utilises labyrinth seals,[69] while purging the seals with a positive air pressure to restrict contaminants ingress. Often a dual air purge system' has two ports—normally situated on the upper and lower spindle ends—so with this spindle design feature, it prevents ingress of virtually all of the contaminants into the assembly. Thermal stability of the spindle assembly where large fluctuations in temperature must be minimised, is yet another important factor that can present spindle problems. This temperature variation problem, where extraneous heat causes either the cast iron castings and/or the steel-based internal components to expand, creates unwanted spindle head growth—leading to minute, but unwanted *Z*-axis changes.

In order to minimise spindle assembly temperature variations, heat exchangers, or chillers (i.e. the latter being the most common type—see spindle assembly below) are invariably employed to keep the spindle stable and cool while controlling spindle growth. Chillers extend a spindle's life, thereby reducing head growth. These chillers—see the partially-sectioned rendition shown below—are typically utilised when operating long production cycles, or where high-duty stock removal cycles are demanded.

For extended high-speed applications, the incorporation of a thermal stabilisation system[70] that normally utilises a thermostat with an oil chiller, to automatically cool the spindle, becomes a necessity. Yet another contributing factor to

[68]**Air purge systems**: these are utilised to flush an electro-mechanical control instrumentation with clean air before it is turned on. This initial flushing (i.e. purging), ensures that the functionality of the equipment is not affected, or damaged by the contaminants from the surrounding environment. It is crucial that the design of the air purging system ensures that the flow of air does not draw in any contaminants from extraneous sources.

[69]**Labyrinth seals**: are a type of mechanical seal that provides a difficult sealant-path helping to prevent either: debris ingress, or leakage of the oil that is utilised to lubricate the bearings. These labyrinth seals are normally composed of several radial grooves that press tightly inside the housing, or alternatively inside a hole, so that the ingress/fluid has to pass through a long and difficult/convoluted path to enter, or escape from the spindle assembly.

[70]**Thermal stabilisation system**: for a typical CNC machine tool some form of a Thermal Stabilisation Package is invariably included, which would normally consist of a spindle-oil chiller this equipment being thermostatically controlled, enabling it to combat against any potential spindle-head growth when operating at high-rotational speeds. This type of installation being considered the optimum and most efficient manner to extend the HSM's spindle life, while also maintaining and preserving the overall performance accuracy/precision—when machining both accurate and complex part features.

spindle performance is that of the type of tooling employed during part manufacture. Furthermore, by the user utilising a poor tooling strategy of unbalanced tools; worn tools; and/or tools that are too long, these improper uses can have a significant effect on the longevity of whole spindle assembly.

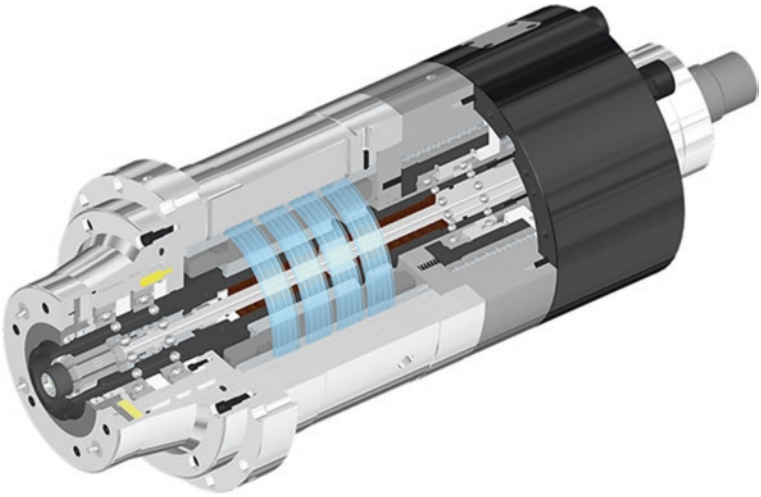

A notable and rendered schematic cutaway diagram of machine tool's spindle assembly—here, incorporating an integrated thermal chiller into the spindle's assembly [courtesy of Hyundai WIA Machine America Corp. (Carlstadt, NJ, USA)—2015]

1.12.2 CNC Conventional Drive Systems and Recirculating Ballscrews

CNC Machine Tool Conventional Drive Systems

Basic mechanical feed-drive system for CNC machine tools can be shown to vary immeasurably. Although the mechanical configuration of these feed-drive systems can, in the main, be standardised as schematically illustrated in the basic configuration shown in Fig. 1.28a. As a result, in the majority of these mechanical arrangements, the recirculating ballscrew is by far the most popular method for converting the rotary motion of the machine's servomotor into linear slide motion. This ballscrew is often just fixed in its axial direction of travel at only one end with its customarily preloaded angular contact bearings, which can contain the axial forces exerted by the machine's slide. Further, the servomotor and ballscrew drive are usually connected via a toothed-belt transmission and in this manner achieve a compact design, which is better adapted to the conventional slide's linear speed requirements—a variant of this arrangement is shown in Fig. 1.28a. A more sophisticated control loop system via a rotary encoder and ballscrew that also includes the servomotor, is depicted in Fig. 1.28b. Here, the basic configuration

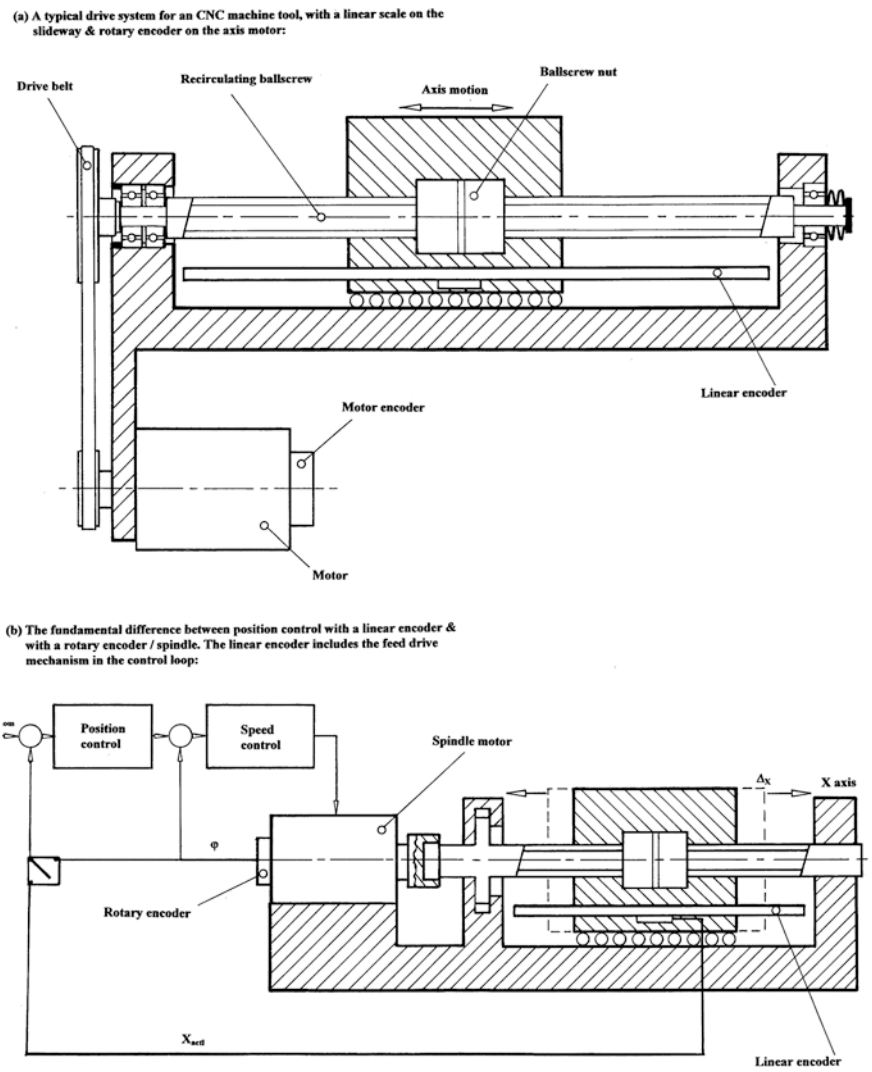

Fig. 1.28 Typical electromechanical drive systems for machine tools [courtesy of Heidenhain (GB) Ltd.]

shows there is no actual position control of the slide, because only the position of the servomotor's rotor is being monitored and controlled. In order to have the ability to extrapolate the slide's current position, the mechanical system between the servomotor and its slide must be known and, moreover, have the ability to reproduce exactly this mechanical transfer behaviour. A machine's positional control loop with for example a linear encoder fitted, will include its entire mechanical feed-drive system. Here, the linear encoder on the slide detects mechanical

transmission errors and these are then compensated for by the machine control unit.

Normally, there are basically two systems utilised to distinguish positional control, these are either: (i) direct measurement systems or (ii) indirect measurement systems. Likewise, there are also two main types of errors associated with a CNC machine tool slide, which are:

1. **kinematic errors**—these will occur in position measurement with a rotary encoder and its ballscrew, primarily resulting from the ballscrew's pitch error. This type of error directly influences the result of measurement, because the pitch of the ballscrew is utilised as a standard for linear measurement;
2. **reversal errors**—will result during motion of the slideway positioning from different directions. The causes of this error are its play (i.e. often more commonly known as backlash[71]) and elasticity in connection with induced frictional forces. Furthermore, this type of reversal error would normally occur via its so-called pitch-loss, resulting from a shift of the balls during the repositioning of the ballscrew drives. So, in the case of a two-point preloading of the ballscrew, this can usually lead to a reversal error magnitude of between 1 and 10 μm.

In order to minimise slide errors, some form of error compensation is practised with virtually all CNC controllers, as they are capable of compensating for both pitch errors and any accompanying reversal errors. Prior to determining the actual compensation values required in achieving error compensation, elaborate dimensional measurements are made utilising comparative measuring instrumentation, typically by employing equipment such as: laser interferometers; Alignment telescopes; Grid encoders; or from a range of metrological artefacts. Additionally, this undesirable reversal error is normally quite unstable over extended periods of time, requiring the machine's periodic reverification. The causes of this instability can include the initial running-in process of the ballscrews, coupled to changes in the frictional forces in the guideways. It is also notable, that when toothed-belt drives are fitted, they may also create significant positioning errors—with the course of time.

[71]**Backlash**: which is sometimes called either lash, or play, is the clearance, or lost motion in a mechanism caused by gaps between the mating-parts. Backlash can be simplistically-defined: "As the maximum distance through which one part of something can be moved without moving a connected part". One example, in the context of gears and gear trains, is the amount of involute clearance between meshing gear teeth. This backlash can be seen when the direction of movement is reversed and the slack, or lost-motion is taken-up before the reversal of motion is complete. Early types of CNCs were programmed to utilise the: "Always-approach-from-the-same-direction concept", but this is not the normal kinematic-action that is employed today. Although to a certain extent, backlash is unavoidable for nearly all reversing mechanical-couplings, but its effects can be virtually-negated, or compensated-for in many ballscrew-driven machine tool applications. The theoretical ideal would be zero-backlash, but in actual practice some minute backlash here, must always be tolerated, to prevent any form of ballscrew jamming. The main reasons for the presence of this ballscrew backlash might include: allowing for lubrication; manufacturing errors; deflection under load; as well as for thermal expansion.

The deformation of a machine tool's drive mechanism via a series of attendant forces can lead to the distortion of the feed-drive mechanisms occurring as a result of these inertial forces, resulting from: acceleration/deceleration of the slide; cutting process forces; plus changes in the frictional forces in the guideways. These unsolicited in-service factors, promote a shift in the actual axis slide location, relative to the position measured by the ballscrew and rotary encoder. Additionally, the forces of acceleration can create a mean axial rigidity of a feed-drive mechanism—as illustrated in Fig. 1.28a—which lies within the range of: 100–200 N μm^{-1} (i.e. when the distance between the ballnut and fixed bearing is 0.5 m and having a ballscrew of ∅40 mm). By way of illustration, if a machine tool's typical axis slide mass is of 500 kg and moves at a moderate acceleration of just 2 m s^{-2}, this will result in ballscrew deformations of between 5 and 10 μm, which cannot be recognised by the rotary encoder/ballscrew system. The current industry trend is toward accelerations of significantly higher ranges; these additional acceleration projection trends will inevitably result in increasingly larger ballscrew deformation values unless they are manufactured from stiffer and appropriately higher grade/specification materials.

Recirculating ballscrews have been one of the main topics mentioned above, which it is reasoned, now needs to some extent further clarification and discussion below, as they are a significantly vital element in any conventional CNC machine tool's axis drive.

Recirculating Ballscrews—A Brief Review and Nomenclature

Simplistically speaking, a recirculating ballscrew, like all accurate/precision screwthreads, is just a shaft with a helical groove, or grooves, that translates the rotational motion via the stationary mating ballnut, into linear motion—see Figs. 1.29 and 1.30 and below. Conversely, for example, in the case of a conventional screwthread—such as a leadscrew—the stationary half-nut will slide along on these synchronised rotating threads pulling the connecting piece (i.e. such as an attached cross-slide on a centre-/engine-lathe) with it, creating precise and accurate linear motion. In this manner, it is how a typical Acme-screwthread[72] form operates. Hence, this nut's sliding motion is quite easy to produce, although extremely inefficient, with ≈40 % of the input power being transferred to the

[72]**Acme screw thread**: these trapezoidal thread forms are screw thread profiles with trapezoidal outlines, which are the most common forms utilised for leadscrews (i.e. power-screws), by offering high strength and ease of manufacture. Acme forms are typically found where large loads, or high accuracies are required, as in the case of a leadscrew of a conventional lathe. The original trapezoidal thread form and still the one most commonly encountered worldwide, is the Acme thread form—developed circa 1885—as a profile well-suited to power-screws that has various advantages over the square thread, which had been the form of choice until then. It is easy to cut via either single-point screwcutting, or via threading—by a die—than the square thread. Moreover, the Acme form wears better than a square thread—because the wear can be compensated for—due to its 29° included angle taper, while it is stronger than a comparably sized square thread, making for smoother engagement of the half-nuts, on a conventional Centre-/Engine-lathe.

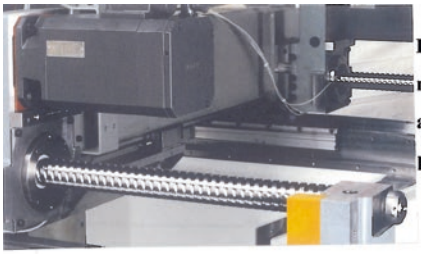

Fitting *'double ballscrews'* to this Machining Centre, minimises any potential *yawing* of the axis as it travels along its slideway, thereby decreasing any probable positional uncertainties of motion.
[Courtesy of Gebr. Heller Maschinenfabrik GmbH]

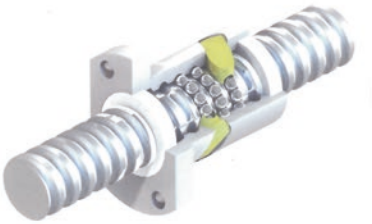

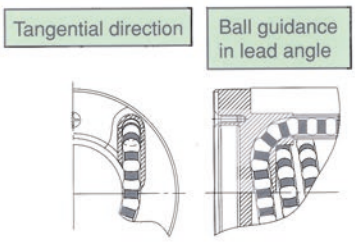

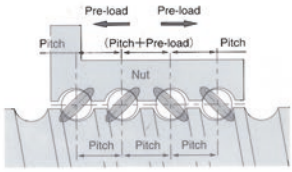

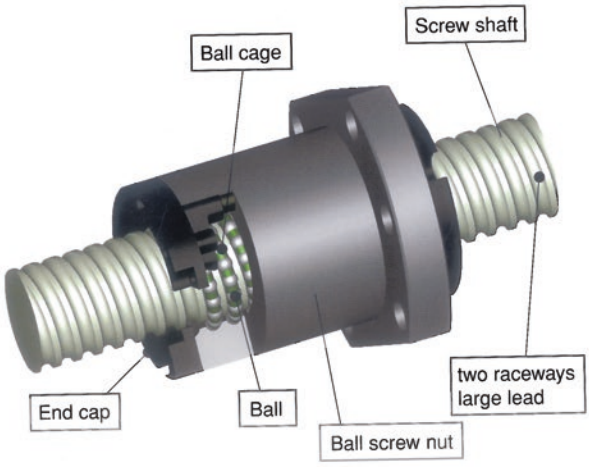

Fig. 1.29 Recirculating ballscrews construction for precise, accurate and repeatable performance (courtesy of THK Co., Ltd.)

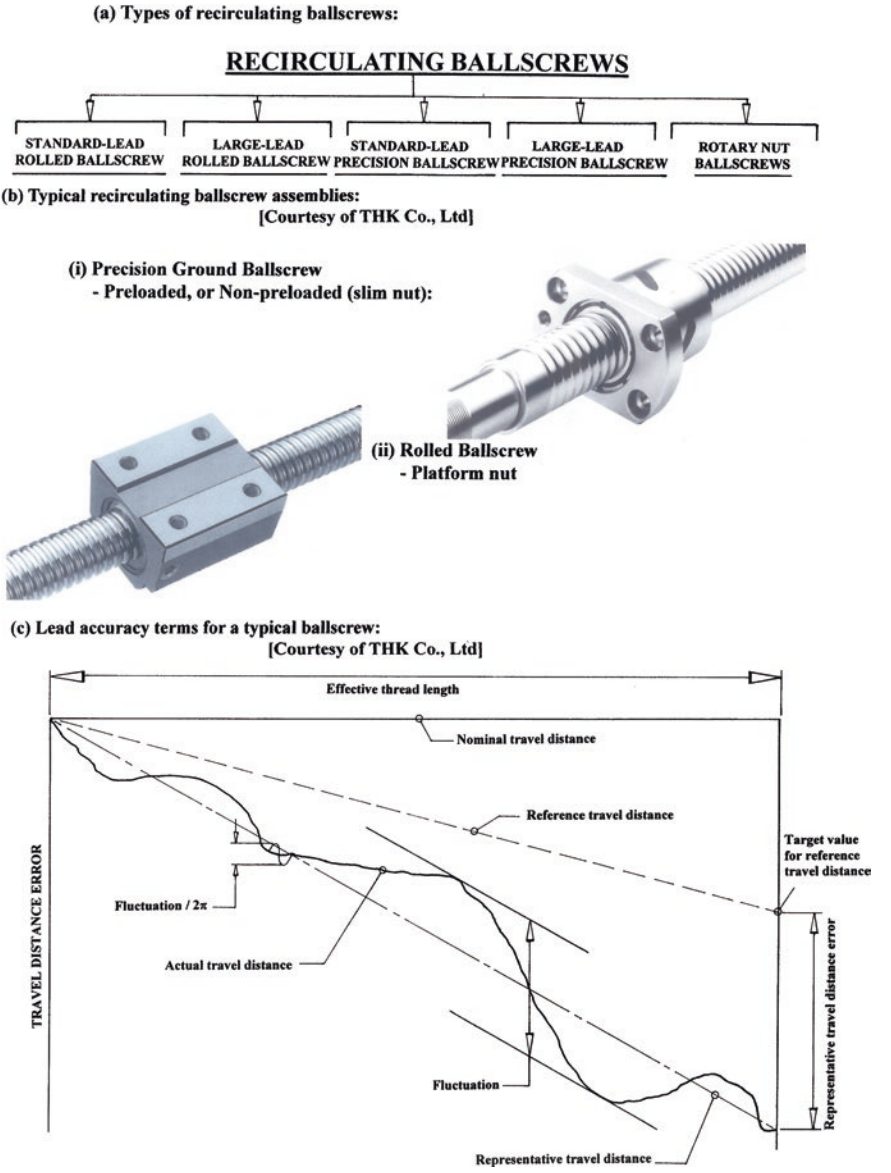

Fig. 1.30 Types of recirculating ballscrews—indicating a typical lead accuracy

workpiece. So, in order to improve the thread efficiency, this sliding contact must be substituted by rolling elements. In the case of recirculating ballscrews, they employ precision ball bearings usually within the ballnut's assembly which allows them to roll along the special screwthread geometry. A recirculating ballscrew assembly is based upon a Gothic arch (i.e. Ogival geometry) providing

point-contact between these mating balls and the screwthread and nut—see below. The assembly is so arranged that the ball's relative motion is restricted within a ballcage so they must recirculate—Fig. 1.29 (bottom and below)—or otherwise they would simply fall out of the ballnut! This ball arrangement within its assembly creates within the current designs for recirculating ballscrews efficiencies of $\geq$90 %. There are four major components of a ballscrew assembly, which include the: (i) ballscrew shaft; (ii) ballnut; (iii) ball bearings; and (iv) the seals/end caps (i.e. shown in Fig. 1.29—middle left/bottom). The actual ballscrew-threaded shaft is a long bar normally of the metallurgy high chrome-alloy steel[73] that has precise and accurate grooves formed into a helical pattern. In order to minimise any potential ballscrew twisting—or wind up—it has must have an inherent rigidity[74] of between 850 and 2000 N μm^{-1}, depending upon its machine tool application. Consequently, in the case of a ballscrew's design, certain factors affect its overall efficiency, these may well be:

- **ball groove design**—the most common groove style is in the form of a Gothic arch, as this Ogival groove geometry permits four points of contact at all times, so with these contact points the mating balls can be preloaded in any direction in that plane—see Fig. 1.29 middle right and below;
- **pitch circle diameter of balls**—namely, the pitch circle (dm), which is the diameter of a circle formed by the centre of recirculating balls. Here, this dm measurement being utilised for its maximum speed calculations;
- **nominal diameter**—represents the outside diameter of ballscrews, being utilised in measurement for ballscrew sizing, as this is convenient to measure;
- **root diameter**—is taken from the bottom of the groove, to the bottom of an adjacent groove, this being the smallest part of the ballscrew which is important for any critical speed calculations;
- **lead**—which is the distance the nut travels in one rotation. Hence, the larger the lead the faster the nut can travel as this lead will also determine the vertical maximum payload, together with the stopping power of the ballscrew. This fact is because the load angle will be steeper for greater leads—meaning that the amount of weight it can hold is somewhat lessened;

[73] **Ballscrew metallurgy**: utilises typically fully-hardened alloy steel: 100 Cr6–NFA 35.565, or its metallurgical equivalent—for a $\geq \varnothing 20$ mm Ballscrew. The hardness of the Ballscrew's contact surfaces is usually between 56 and 60 $H_R c$, depending on diameter, for standard Ballscrews.

[74] **Ballscrew rigidity**: can be obtained from typical Recirculating ballscrew manufacturer's charts and is normally-based upon the following Rigidity-value equation [i.e. If the Applied preload (Fa_o) is not 0.1 Ca, then the Rigidity-value (K_N) should be used] and can be obtained from the following expression:

$$K_N = K\left(Fa_o / 0.1\,Ca\right)^{1/3}$$

where: 'K' is in N μm^{-1}; 'Ca' is in kN; 'Fa_o' is the applied preload in N.

- **ball diameter**—relates to the diameter of the ball bearing that would fit into the groove with a preload of zero. This fact is utilised to calculate the diameter of the ball bearing that would give a certain preload, thus the bigger the balls are when compared to the nut and screw gap, the higher will be the preload.

Ballnut—type of nut and its ball recirculation

There are nominally three basic designs for the majority of ballscrew nuts, each type having a particular specialty; these types of ballnuts include:

1. **Profile Ball Groove**—being the most common type of ballnut—as it is relatively easy to manufacture and has a good and consistent performance. Its design simplicity makes this nut's production simple to mass produce, allowing it to adjust to fit most sizes, leads, and accompanying loads. Here, the balls are recirculated by tubes that pick up these ball bearings then deposit them back into the cycle. The number of rows of balls before they are recirculated is normally between 1.5 and 3.5 to keep the return tube size manageable and the subsequent re-balling easier;
2. **Ball Pitch Circle Diameter**—with this ballnut design it has a trimmer profile, because it does not require tubes to move the balls. Instead a deflector is utilised to bump the ball bearings into the previous track. This ball action means that there must be a deflector for every turn, with only one pitch circle per deflector. The ballnut design here is also inherently superior for smaller lead angles because the distance between the grooves is smaller and therefore making it much easier for the balls to jump. Consequently, this type of ballnut is more expensive to manufacture because more of the ball track is internalised and its application is limited by the lead;
3. **End Cap**—designs for ballnuts are usually specialised for use with high lead angles and multiple start thread applications. It is generally reserved for the aforementioned types of ballnuts, due to the fact that die moulds are required to produce them, thus increasing the manufacturing cost. Here, the number of ball rows per cycle is not limited in this recirculation ballnut design, as it is normal to have the whole nut recirculated with one cycle per start.

Multiple start thread Ballscrews[75]—see Fig. 1.29 (top), are often utilised when high-lead applications are demanded, allowing for additional balls to be in contact

[75]**Multiple-start thread ballscrews** (i.e. see Fig. 1.29, top): the lead being the distance travelled in one revolution of the Ballscrew, which is determined by the pitch times the number of starts, hence: Lead $= n \times p$. Where 'n' is number of starts; 'p' is the pitch (mm). For example, if the Ballscrew's pitch is 5 mm and the number of starts is 4, then the Ballscrew's lead equals 20 mm, being the linear distance moved in one complete revolution of this Ballscrew.

with the ballnut. Multiple-start threads are primarily employed on high-lead ballscrews because there is physically no room to situate them on small-lead ballscrews. End caps are also utilised for these ballscrews, because they use less space to recirculate the balls.

Ball Bearings—in Recirculating Ballscrews

A ball bearing's diameter must fit exactly into the helical groove and match with the ballscrew's shaft diameter. As a consequence, if the ball is too small there will be too much clearance space between threads—creating excessive backlash—conversely, if the balls are too big they can cause an interference fit—increasing friction and potential seizure. The crest between the grooves should ideally be flat, but not too large. Ball bearing loading is always present, so if there is no retainer between the balls similar to that found in the usual circular bearings, then the balls can become jammed when an undesirable ball-on-ball contact is made. This problem can be reduced by adding what is known as spacer balls. These spacer balls are slightly smaller balls and as such, they will spin between the main Load balls, but this will result in a reduction of the ballscrew's load capacity, because there are less Load balls present. Some manufacturers utilise a synthetic plastic cage that adds some desirable properties to any recirculating ball bearing application. This plastic cage prevents ball-on-ball contact and hence will obviously help by reducing friction and jamming, while increasing Recirculating ballscrew life.[76] Moreover, these cages have the added advantage of being able to trap oil and grease, thus helping to keep the ball bearings well-oiled.

[76]**Recirculating ballscrew life**: because of their very low frictional coefficients, this will significantly aid the ballscrew's accuracy and precision, as well as its longevity. The actual ballscrew life is determined by its intended: load; rotational speed; lead; plus ballscrew size. Typical values for ballscrew life are determined by either: 20,000 h of operation; 50,000 km travelled; or alternatively by ≥5 years of usage. Here, the basic load-rating (Ca), is utilised to calculate the life-span of a Ballscrew, when the nut is subjected to a load. The Axial directional load, is when revolving each set of identical Ballscrews, which will have a typical rating life-span of 90 % @ 106 rpm (i.e. 1,000,000 revolutions). From the basic load rating and axial directional load, the **life-span of a Ballscrew** is calculated using the following equation:

$$L = \left(\mathrm{Ca} / \mathrm{fw.Fa}\right)^3 \times 10^6$$

where '*L*' is the rated life span (revolutions); 'Ca' is the Basic load rating (*N*); 'Fa' is the Axial directional load (*N*); and 'Fw' is the load factor can be obtained from a relevant Ballscrew Table—from a Manufacturer. For example, values can range from: **1.0 to 1.2**—low velocities **≤0.25 m s^{-1}**; to **2.0–3.5**—high speed **>2.0 m s^{-1}**.

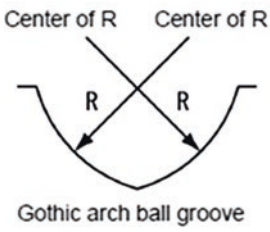

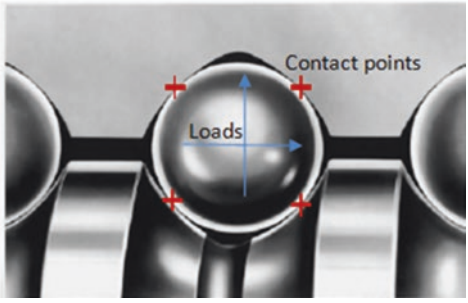

Cutaway photograph of a recirculating ballscrew and nut (*top*), with the Gothic arch thread geometry (*bottom left*), illustrating the contact points for a spherical ball situated between the ballscrew and its mating nut (*bottom right*)

Ballscrew Accuracy and Precision, Plus Lubrication and Maintenance

The inherent accuracy and precision is an essential component in a ballscrew's operation, as these ballscrews are utilised predominantly for the aspect of the dimensional characteristics. Moreover, the Lead error and mounting error are two calculated error parameters that are important considerations in the majority of ballscrew applications. Therefore, this lead error can be defined in two distinct ways, namely the:

1. difference between the expected length (L) and the actual length ($L \pm e$);
2. sum of all the e's ($\Sigma e = E$).

By way of an example, if the L value is 5 mm and the $e = \pm 0.005$ mm, the possible ballscrew length could range between 4995 and 5005 mm. The mounting error is instigated by the manner in which the ballscrew is supported and the installation of the ballnut. Possibly the three most anticipated ballscrew mounting errors will include: (i) bearing misalignment; (ii) coupling misalignment; (iii) nut misalignment. This unfortunate problem of a ballscrew mounting error can instigate the following conditions: increased noise; shorten its service life; plus it may cause some slide positioning errors.

Just some of the main types of these current recirculating ballscrews are listed in Fig. 1.30a, where many ballscrews at present tend to be rolled threads,[77] as they have considerably stronger thread forms than conventional machined threads (i.e. see both Fig. 1.30bi, bii). The major International Standards for these recirculating ballscrews are: **ISO 3408**; **DIN 69051**; **JIS B 1192-1997**, which are normally utilised in the selection and application of machine tool ballscrew systems. These standards for ballscrews define the following: performance ratings: accuracy grades; plus the dimensions of recirculating ballscrews and their accompanying ballnuts. Based upon the **ISO 3408**, there are ballscrew accuracy grades that range from: '1'—very high accuracy, through to '3.5'; with '7–10'—being lower accuracy grades. Moreover, if there is a requirement for an exact ballscrew positioning system, this generally requires one of the higher accuracy grade ranges, typically 3–5. The grades most commonly employed are ballscrew grades that are between 3.5 and 7. The actual accuracy grading reflects the precision of machining of these ballscrews, this being defined by the thread error over a 300 mm length. Even for the lowest ballscrew grades, they exhibit a tight tolerance limit, typically of 52 μm travel error. Whereas, Class 7 is the least accurate ballscrew, it can still be utilised in about 80 % of industrial applications. Conversely, Class 5 reduces these errors by half and suits precision slide positioning; moreover, Class 3 reduces this error by yet half again—giving extremely high precision, for example being utilised for most of the high-quality CNC machine tools of today. In Fig. 1.30c it shows the accuracy in this case for the ballscrew's lead, which is controlled in accordance with **JIS 1192-1997**, with its respective accuracy grades 'C0–C5' being defined in linearity and directionality, while grades C7–C10 is—in terms of travel distance error—in relation to 300 mm of travel. From a typical recirculating ballscrew's plot depicted in Fig. 1.30c, the indicated values relate to the following:

- **actual travel distance**—being error in its travel distance measured with a ballscrew;
- **reference travel distance**—is generally the same as nominal travel distance (NTD), but can be an intentionally corrected value of the NTD according to the intended use;

[77]**Rolled threads**: are the result of a chipless operation and occur due to the cold rolling production process. The process of thread-rolling, plastically-deforms the workpiece material to form the thread, meaning that the actual Ballscrew's grain-flow follows the thread's contours, creating a very much stronger thread than one that has been machined from wrought stock material, normally this latter machined-version will otherwise having directionality of grain-flow. Moreover, the rolling-operation is both cleaner (i.e. as there are no chips produced) and offers material-savings of the order of 15–20 %, by this rolling-application for a Recirculating ballscrew.

- **target value for reference travel distance**—here one might provide ballscrew tension to prevent this shaft from running out, or set the reference travel distance in a negative, or positive expansion/contraction from any external load, or temperature;
  NB In such circumstances, it is necessary to set a target value for the reference travel distance.
- **representative travel distance**—this is a straight line representing the tendency in actual travel distance and it is obtained by the least squares method from the curve that indicates this actual travel distance;
- **representative travel distance error** (i.e. in ±)—this is the distance between the representative travel distance and the reference travel distance;
- **fluctuation**—it is the maximum width of the actual travel distance between two straight lines, drawn in parallel with the representative travel distance;
- **fluctuation/ 2π**—which is a fluctuation in one revolution of the ballscrew shaft;
- **fluctuation/300**—this indicates a fluctuation against a given ballscrew thread length of 300 mm.

The ballscrew's preload is a predetermined load that is placed on a part—such as bolts, screws, bearings—before its operating load is applied. This actual preload of the ballscrew causes a controlled-induced elastic deformation that actually improves its operational performance. Accordingly, any elastic deformation will obviously change in shape—which is fully reversible—similar to the analogy of squishing a rubber ball. Hence, in the case of ballscrew applications, this preload is at the interface between the ballnut and ballscrew. Additionally, the ball bearings and both the ballnut and ballscrew grooves are all 'squished-together'. This basic 'squishing-action' has the advantage of eliminating both the backlash and also reducing deflection. Mentioning the term backlash in yet another distinct way, it can also be thought of as, "The amount of lost motion caused by looseness in the drive train which can cause slide placement errors". The ballscrew preload creates a tight fit, which is almost a transition fit for this ballnut, eliminating backlash. As a consequence, increased stiffness is instigated by the well-known mechanical property where a piece of steel is subjected to a tensile load; its cumulative elasticity becomes increasingly harder to deform. In consequence, this ballscrew preload eliminates the possibility of an easy deformation. Accordingly, a greater amount of force is subsequently required and obviously, a ballscrew must be supported so that the shaft can be freely rotated. Habitually, this support involves the use of roller bearings and their holding brackets. Sometimes for very long machine tool axes, a longer length of ballscrews will need to be supported for critical linear speed and to improve overall bending restraint. Therefore, some modified end machining may be necessary to fit the ballscrew into the bearing, or to attach it to the motor. So that the ballnut can linearly translate itself accurately and precisely, it must be kinematically restrained by its table axis alignment, together with its accompanying support from either the linear rails, or slideways.

The lubrication of the ballscrews is by either the recommended manufacturer's grease, or one of its approved oil specifications. It is normally recommended to

utilise grease for most regular machine tool applications. Reiterating that grease is preferred because it does not require any special lubricating system and as a consequence, much less grease is required than for an equivalent oil lubricant. Where oil takes preference over grease, is for use in most high-speed machining applications. Virtually, all ballscrews entail a certain degree of regular or periodic maintenance, although some specialty ballscrews do not require any maintenance at all. Any general maintenance activity should make sure that the rails/slideways are free of contaminates like: water; dirt; dust and any other forms of accompanying debris. The ballnut also requires to be periodically lubricated using either oil or grease. As previously mentioned, grease offers a lower overall performance but it is much more convenient and cheaper to use, while easier to maintain than oil—the latter necessitating a costly and sophisticated oil circulation system for the machine tool.

1.12.3 Machine Tool—Bearing Categories

Simplistically speaking, a bearing is a machine element that both locates and constrains relative motion between several moving parts, for solely the desired motion. For example, a bearing's design could provide for either the free linear movement of the moving component or for free rotation around a fixed axis. Alternatively, the bearing may prevent a motion by controlling the vectors of normal forces that bear on these moving parts. It is well known in both theory and practise that a considerable number of typical bearings facilitate the desired linear/rotational motion as much as possible by minimising any friction present. Bearings can be broadly classified according to the: type of operation; the motions allowed; or to the directions of the loads (forces) that are applied to such parts.

History of Bearings

Historically, the origination of the rolling bearings, was in the form of crudely shaped hardwood rollers. These basic bearings were employed for supporting and moving very heavy objects, with this rolling technique being seen from the antiquity of ancient civilisations such as that of the Egyptians. For example, in the colourful wall image exhibited below, depicting the moving of a massive stone figure—here on the wall in the tomb of Djehutihotep—it may even just predate the invention of the wheel. Leonardo da Vinci (circa 1500) incorporated some basic sketches of ball bearings in his design for a helicopter. However, Agostino Ramelli (1531–1610) was an Italian Engineer who designed the Book or Reading wheel and, first published drawings of roller and thrust bearings, despite the fact that captured, or caged, ball bearings were originally described by Galileo in the seventeenth century.

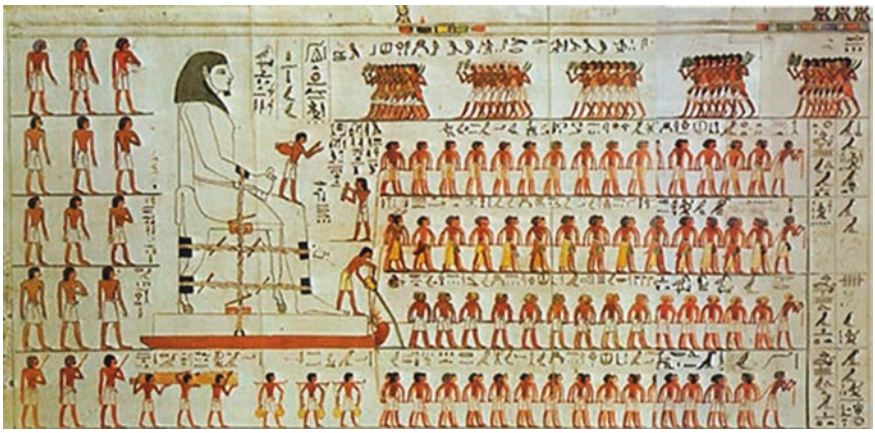

The famous scene from a wall painting in the tomb of Djehutihotep, he was one of the most powerful Nomarchs. Thus, Djehutihotep, lived in the reigns of the Middle Kingdom Pharaohs: Amenemhet II; Senusert II; also Senusert III (circa: 1932–1842 BC). He displayed—on the tomb's wall—this huge monolithic statue being transported from the quarries. The image shows a worker pouring water into the path of a sledge, which served to increase the stiffness of the sand, and probably reducing the forces needed to move this statue—by up to 50 % [*source* Terrence McCoy, The surprisingly simple way Egyptians moved massive pyramid stones without modern technology, Washington Post (USA), 2nd May 2014]

The first such rolling element bearing patent for what would become known as a ball race, was by Philip Vaughan of Carmarthen (Wales, UK) in 1794. Here, these early and basic plain and rolling element bearings were produced from hardwood and were quickly followed by the use of bronze. Over the years these bearings have been manufactured from a diverse range of materials that have included: ceramics; metals—bronze and steel; sapphire; glasses; and plastic derivatives (e.g. typically, nylon, polyoxymethylene, polytetrafluoroethylene, and UHMWPE, which are all being utilised in such bearings).

Probably the first really practical type of caged roller bearing assembly was invented in England by the outstanding Horologist/Artisan: John Harrison (1693–1776) for his very precise and accurate H3 Marine Chronograph (circa: 1740). This marvellous and exquisitely made time-keeping chronograph was employed for vital time-and-distance measurement by the Royal Navy for distance/time bearings in longitude; prior to his horological invention it had seemingly been thought of as an impossible task to achieve. At this time, 'Harrison's bearing' was utilised for a very limited angular oscillating motion, although he then utilised a similar bearing in a fully rotating application within the mechanism for a contemporaneous Regulator clock, all of these clocks that he both designed and personally made are still in operation—many also being fitted with jewelled-motional bearings.

A notable Parisian bicycle mechanic by the name of Jules Suriray was awarded the first ball bearing patent, in August 1869. Suriray, had these bearings fitted to the bicycle—built by French company Tribout and then ridden by the Englishman James Moore, who won the World's first bicycle road race, racing from Paris to Rouen—about 130 km (81 miles) distance, in November 1869.

In 1883 Friedrich Fischer—the founder of the well-known company FAG, invented an industrialised-production technique for milling and grinding balls of both equal size and exact roundness, instigating the basis for creation of today's vitally important bearing industry. Sven Wingquist (1907) is credited with the patented self-alignment ball bearing design of the well-known Swedish company SKF. Moreover, Henry Timken, had previously patented the tapered-roller bearing—in 1898—while by 1934, Erich Franke had also invented and patented the wire-race bearing. Franke's attention was on ensuring that the bearing's design would have a small cross section, which could then be integrated into intricate and closely designed bearing assemblies. Following cessation of WWII Erich Franke, in Germany, co-founded a company with Gerhard Heydrich, which was recognised as Franke and Heydrich KG—today it is simply known as Franke GmbH, and has the purpose of industrial development of wire race bearings. Furthermore, the applied research work by Richard Stribeck's extensive metallurgical research on ball bearing steels identified the now frequently utilised bearing alloy 100Cr6 (AISI 52100)—where Stribeck's original experimental work also highlighted the fact that: "… The coefficient of friction is a function of pressure".

In 1968, Bishop Wisecarver's co-founder Bud Wisecarver, had designed and then patented the creation of Vee groove bearing guide wheels—in 1972—these being a type of linear motion bearing, consisting of both an external and internal 90 degree Vee angle. Of more recent origin in the 1980s, the Pacific Bearing's founder Robert Schroeder invented the first bi-material plain bearing which was interchangeable in size with linear ball bearings. This bi-material bearing had a metal shell—which was often made from, aluminium; steel; or stainless steel, having a layer of teflon-based material being connected by a thin adhesive layer. Currently, machine tools' ball and roller bearings (i.e. typical of the ones shown below) are utilised in countless bearing applications that will include a rotating, or sliding component within their precision assemblies.

Just two examples some of the bearing manufacturing companies basic ranges of their rolling element bearings. These types of rolling element bearings are typically utilised in the construction of both rotating and sliding assemblies—being fitted into many CNC machine tools [courtesy of RAS Bearings Pvt. Ltd (Ahmedabad, Gujarat, India)—left/SKF Bearings (Gothenberg, Sweden)—right]

Rotating Bearing Selection

Generally speaking, the bearing type that is provisionally chosen for an application is selected based from a range of essential considerations, such as its: operating conditions; mounting configuration; ease of fitment/replacement; allowable space; as well as its cost and availability. Once these bearing parameters have been considered, then the bearing's size is chosen to satisfy the desired life requirement. Moreover, something intrinsic to the overall success of the selection procedure will be a number of additional factors, such as: fatigue life; noise and vibration; operating speed; wear rate; plus its grease life. These decisions and several other considerations for a rotating bearing's selection are shown in the flow diagram in Fig. 1.31.

Some of the foremost factors affecting a bearing's selection can include:

- **allowable bearing space**—for a rolling element bearing and its adjacent parts it is generally limited by the housing design limits. Generally, the shaft diameter is fixed—by the machine tool's design—hence a bearing is chosen by its bore size;
- **operating environment**—for a bearing, this will extend beyond ambient conditions of temperature, humidity and corrosiveness. These crucial factors must be considered in any selection procedure, with other decisions such as seizure resistance and its life, in combination with extreme heat effects and the vagaries of the periodicity of any lubrication strategy. However, recent developments in bearing technology can largely overcome many of these problems by employing a synergetic approach (i.e. by bringing together the materials, design, lubrication and sealing technologies);
- **load rating and bearing types**—namely, how high will be the axial and radial forces? Likewise, they are closely related in a manner that depends on the bearing design, as graphically illustrated in Fig. 1.32a. This chart highlights that when bearings of an identical dimension series are compared, roller bearings have a higher load capacity than ball bearing equivalents and are superior whenever shock loading may be prevalent. So, prior to designing any specific bearing arrangement, the size and proportions of the radial and axial loads and their direction need to be quantified, utilising equivalent loadings and cyclical load pattern calculations;
- **permissible speed and bearing types**—depend upon the maximum speed of a rolling bearing, plus its size, cage type, loads, heat dissipation and lubricating method. If one assumes that an oil bath lubrication method has been selected, the bearing types are generally arranged from high-to-low speeds, as indicated in Fig. 1.32b. Thus, the bearing speed is generally limited by the allowable operating temperature, which is a combination of friction (i.e. within the bearing) and heat input—potentially resulting from any adjoining structures;
- **misalignment of inner/outer rings and bearing types**—when specifying bearings, due consideration needs to be given to levels of bearing misalignments, as this condition is present if several factors occur, namely: deflection of the system caused by applied loads; dimensional/geometrical errors of the shaft, or

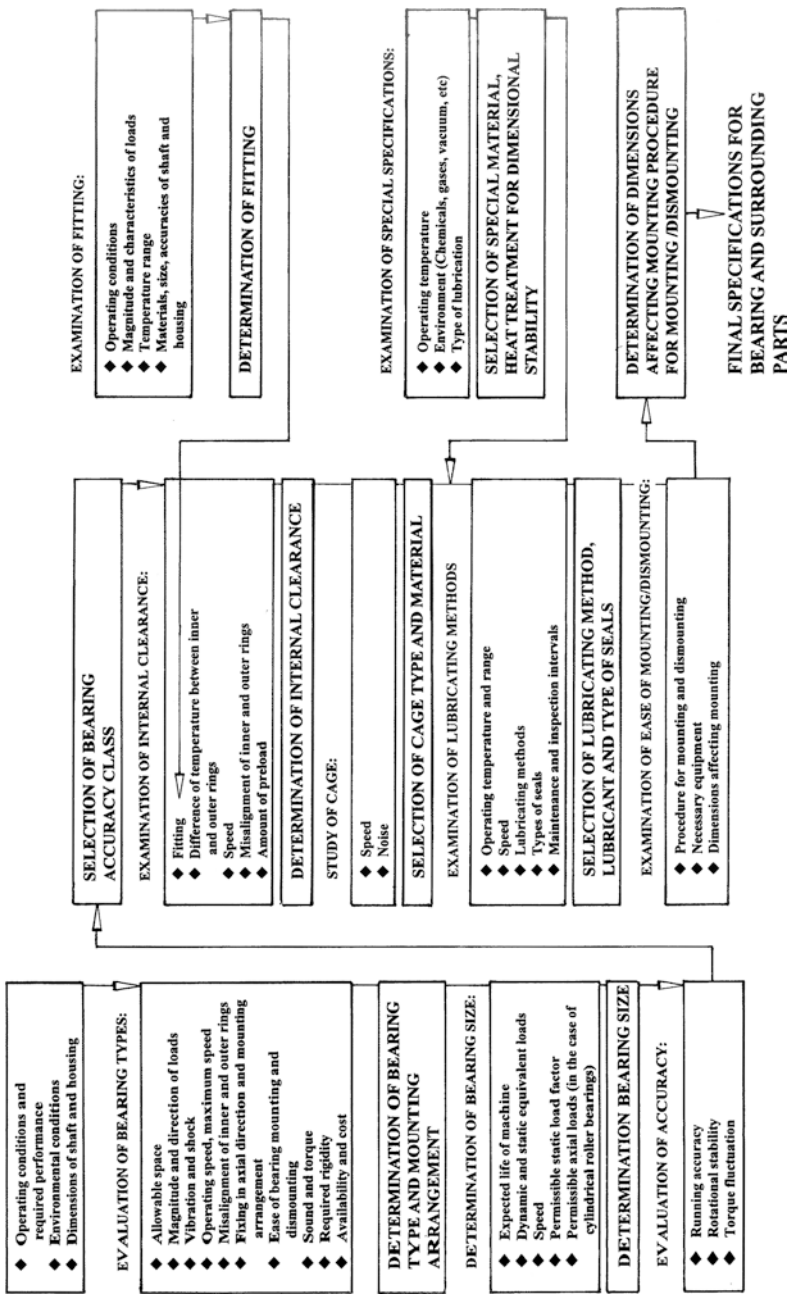

Fig. 1.31 Flowchart for rotating bearing selection procedure (adapted from Reed, Plant Engineer 2013/NSK)

(a) Relative load capacities for various types of rotating bearings.

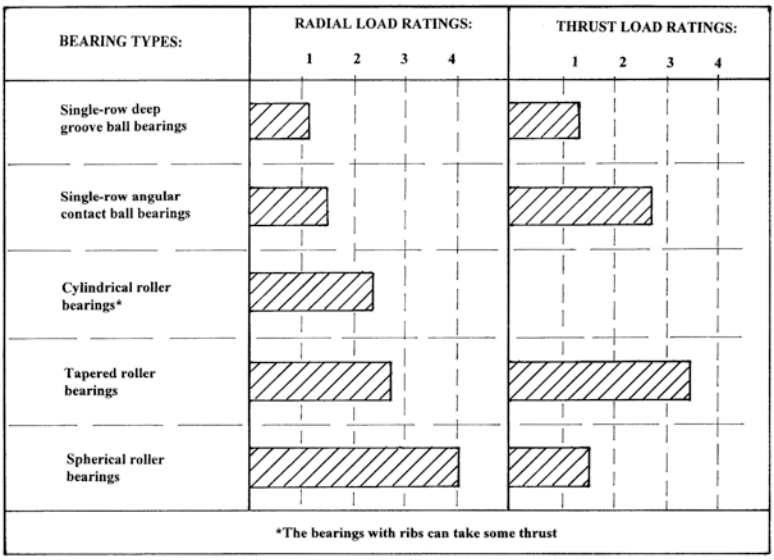

(b) Relative permissible rotational speeds for various rotating bearings.

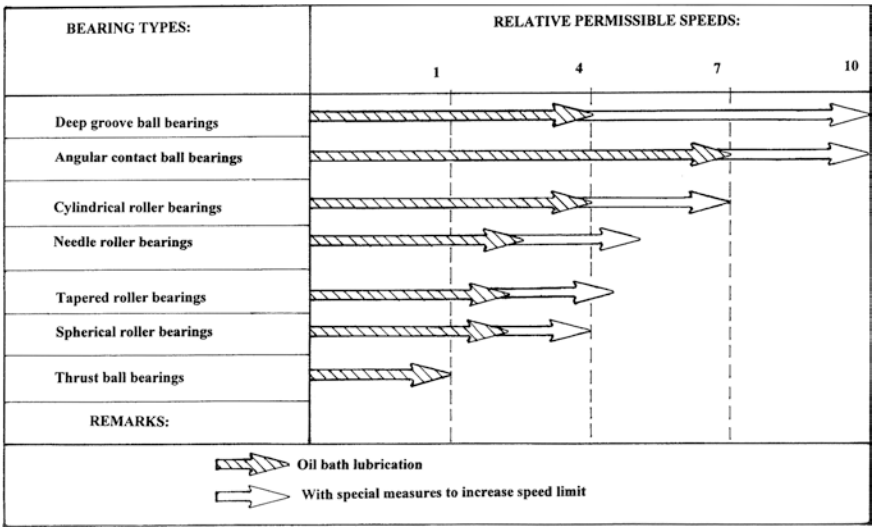

Fig. 1.32 The relative loading and speed comparisons for differing bearing types (adapted from Reed, Plant Engineer 2013/NSK)

its housing; plus mounting errors. Normally, the permissible level of this misalignment will vary—in conjunction with the type of bearing and its operating condition—but it is usually just a small angle, typically $\leq$0.0012 radians. If a large misalignment is anticipated, then self-aligning bearings or spherical roller bearings should be selected;

- **rigidity and bearing types**—if loads are imposed on a rolling element bearing, some elastic deformation occurs in the contact regions—between the rolling element and adjacent raceways. Bearing rigidity is determined by the ratio of bearing load to the amount of elastic deformation of the inner and outer rings, plus the rolling elements. Roller bearings are deflected less than their ball bearing equivalents, but if a predictably higher rigidity is anticipated, then the bearings are given a preload—meaning they have an interference fit;
- **low noise operation**—special emphasis is made in noise-reduction techniques[78] for greased bearings. Some of this bearing noise is caused by microscopic particles in the grease and in the additive packages, which can be reduced by up to 50 % if soluble, rather than solid additives are utilised;
- **minimising torque**—for rolling element bearings of the open varieties without seals they have low levels of torque, but when a high torque level is present, it can increase both heat generation and energy losses. So for example, by utilising deep-groove ball bearings, with super finishing[79] of the raceways, plus special pocket designs and newly developed high technology lubricants,[80] this ensures that minimal torque occurs;
- **running accuracy and bearing types**—being quantified in numerous ways and the specified class varies with each bearing type. For example, when the bearing's high-running accuracy is required, several bearing types can be utilised, such as: deep-groove ball bearings; angular contact bearings; or cylindrical roller bearings. For the main spindles of machine tools—requiring very high running accuracies, or high-speed rotational applications, high-precision bearings (i.e. class '5', '4', or '2') are utilised.

---

[78]**Rolling element noise levels**: in an in-service rotating ball bearing application, if a minute roundness error occurred in the actual balls, of for example $\geq$0.25 μm, this error would result in an increase in operational-noise level of $\approx$15 dBA. This rolling element ball error greatly increases the overall sound-level, which might have otherwise been caused by either track-wobble, or from the lack of shoulder-squareness.

[79]**Super-finishing operations** [Superfinishing operations were firstly-developed and then perfected in 1934, by the Chrysler Corporation (Detroit, USA).]: which are also known as: Micro-machining; or Micro-finishing. This production process is essentially Short-stroke honing, which is a metalworking process that improves both the surface finish and overall workpiece geometry. Super-finishing operations can be achieved by simply removing just the thinnest amorphous surface layer left by the previous production process, with an automated abrasive-stoning technique. Thus, this layer-removed is usually $\approx$1 μm thick. Super-finishing unlike Polishing, produces a superb mirror-finish to the component's surface, this being minutely-created by a miniscule cross-hatch patterning on the workpiece.

[80]**High-technology lubricants**: the lubricant being utilised will affect torque, so in order to minimise this in-service condition, greases combining polyester oil with a diurea thickener enable these additives, to achieve a significant torque-reduction effect in its bearings.

NB Other factors that influence bearing usage include: the seals and shields employed in the bearing's design; mounting and dismounting techniques for the bearings utilised by the maintenance fitter; together with the lubrication strategy adopted by the machine tool user.

Linear Rail Guideways

Linear guides that are invariably fitted to the cast members of machine tools, will be comprised of a mechanism in which hardened alloy steel balls are infinitely circulated to enable (theoretically) an endless stroke when operating these ball slides. Here, the balls roll along the ball groove formed in an accurate and precise hardened rail (e.g. typically rails are hardened to between 58 and 64 H_{RC}) where they are eventually scooped-up by the tip of an end cap. At this juncture, they are forced to change their circulating direction by the return guide of the end cap and guided to a circulating hole provided inside the ball slide. Once there—inside the ball slide—these balls continue to pass through the hole and are transported to the other end of this ball slide. In addition, these balls then go through the circulation circuit up to the tip at the other end cap, where they return once again to the ball grooves of rail and ball slide. In this manner, the balls repeat their endless circulation motion, as the machine's axis is moved along.

Linear rails[81] are available in basically two distinct forms, they are either round, or square/rectangular in their respective cross sections. For example, the criteria by a Machine Tool Design Engineer for choosing one linear guide rail type over another, is no different to that of choosing any other machine tool component.

In the case of the round rail technology—depicted below—it has been refined to near-perfection over the past 60 years, while square/rectangular profile rails have been in use for well-over 35 years. Both rail versions have definitely improved by their years of in-service practise, with most of the earlier inherent design problems being fully corrected. With the advances in Materials Engineering over recent decades, it has dramatically improved rail technology and company-specific engineers have configured this linear rail technology into somewhat of an exact science. However, most of the major technical hitches arise from linear rail misuse and/or misapplication. Some of the main reasons for such rail misapplication often derive from: a personal bias; prejudice; a miscalculation or simply an aesthetic judgment. These rather negative effects are mainly due to the fact that such rails present a relatively small linear profile, which although they might comply to the load, speed, and every other design requirement, when they are mounted onto the machine tool a misguided end-user might conclude that they look somewhat feeble and distinctly undersized, when this is definitely not the case to the discerning eye.

[81] **Linear ball bearing rails**: are normally manufactured to **ISO 10285**, where they are classified into 4 distinct groups—according to their external dimensions and tolerances.

A typical round rail linear bearing guide system, having approximately >200 times the service life, or 6 times the load-carrying capacity of conventional bearings, within the same guideway envelope [courtesy of SKF Group (Göteborg, Sweden)]

Square/Rectangular rails—shown partially sectioned below and in more detail in Figs. 1.33 and 1.34, were initially designed specifically for the machine tool industry. They have mainly replaced the machine's integrated hardened carriages and ways, which were integral areas of the machine bed for many previous machines—see Fig. 1.36 (top). Nonetheless, some traditional integrated carriages and ways are still necessary for very high accuracy and precision in certain submicron machining situations. In addition to initially being targeted for machine tools, such square/rectangular profile rail systems have currently displaced an assortment of round rail designs in some applications in the machine tool industry. A square/rectangular rail profile is generally much stiffer and more rigid than other linear guides, but they require straight, continuous support, having tight tolerances for both flatness and parallelism. However, these square/rectangular linear rails cannot span the widths for some larger machine tools, when compared to a pair of round linear rail equivalents. Although numerous machine tool manufacturers are accustomed to precision bed preparation, this rail-gapping limitation for square/rectangular linear guideways is generally not a problem. Machine tool manufacturers will habitually prefer the smaller, stiffer square/rectangular rail system instead of the round rail. Yet another distinction is that square/rectangular rails normally cost less, when higher load capacity for a limited space requirement is considered desirable. Conversely, the actual dimensional size of such rails might need to be increased, just because of its engineering aesthetics; otherwise, this square/rectangular rail may appear to be somewhat undersized and be perhaps deemed relatively too small in comparison to the rest of the machine tool's dimensions.

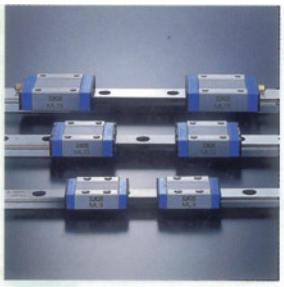

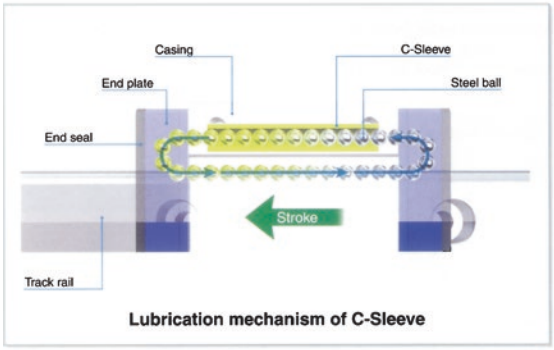

Lubrication mechanism of C-Sleeve

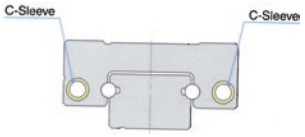

C-Sleeve Linear Way L

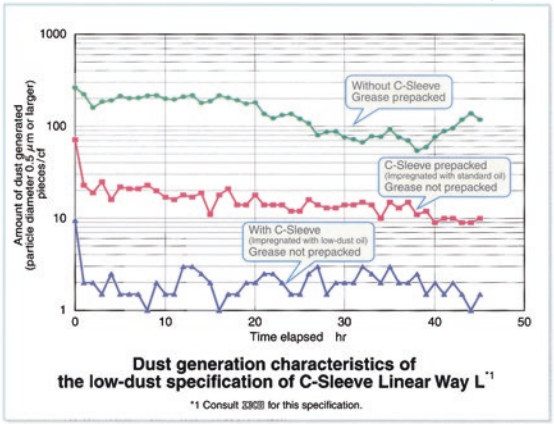

Dust generation characteristics of the low-dust specification of C-Sleeve Linear Way L*1

*1 Consult IKO for this specification.

Fig. 1.33 Design and construction of advanced linear ways for high-performance machines (courtesy of IKO Nippon Thompson Europe B.V.)

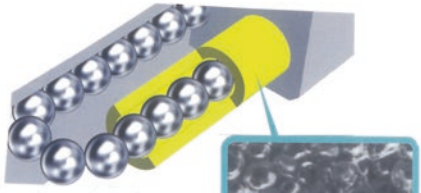

The lubrication sleeve based upon a porous sintered resin of fine mesh powder, impregnated with a large amount of lubricant:

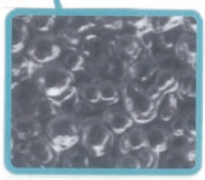

Texture of C-Sleeve (x 200)

Test conditions & results:

Durability test results of C-Sleeve Linear Way L

Test No.	Test condition			Test piece	Applied load (1) N	Test speed m/min	Acceleration/ Deceleration G	Calculated service life L km	Test results (conditions of test piece)
	C-Sleeve	Grease	Applied load						
①	Not used	Not prepacked	No load	LWL 9B	—	64	0.5	—	Damaged at 4.9 km due to insufficient lubrication
②	Used	Not prepacked	No load	ML 9	—	240	3.4	—	Still running after 80,000 km
						240	26	—	Still running after 30,000 km
③	Used	Not prepacked	Loaded	ML 9	0.1 *C*	120	1.7	50,000	Still running after 20,000 km
					0.4 *C*	64	0.5	780	Still running after 1,060 km

Note (1) : The applied load does not include the fixture weight.
Remark : ZKR standard is provided with grease prepacked.

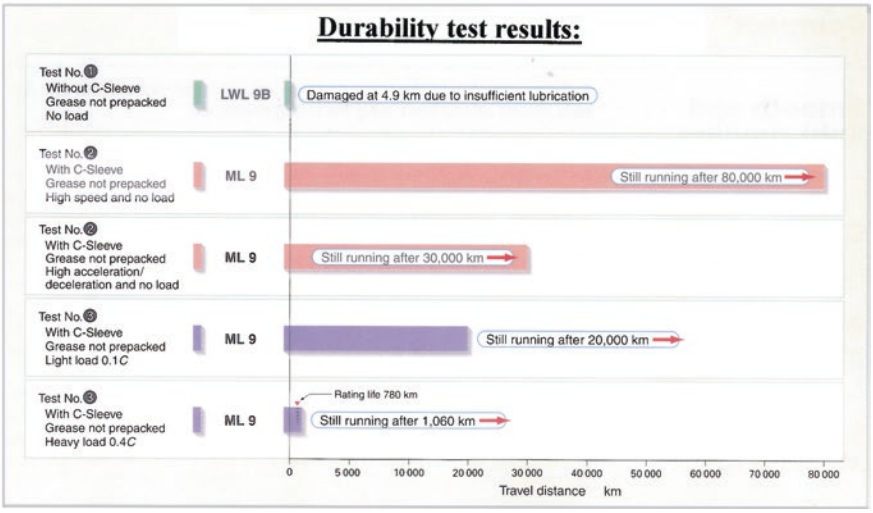

Fig. 1.34 Durability testing regime for linear ways under different working environment (courtesy of IKO Nippon Thompson Europe B.V.)

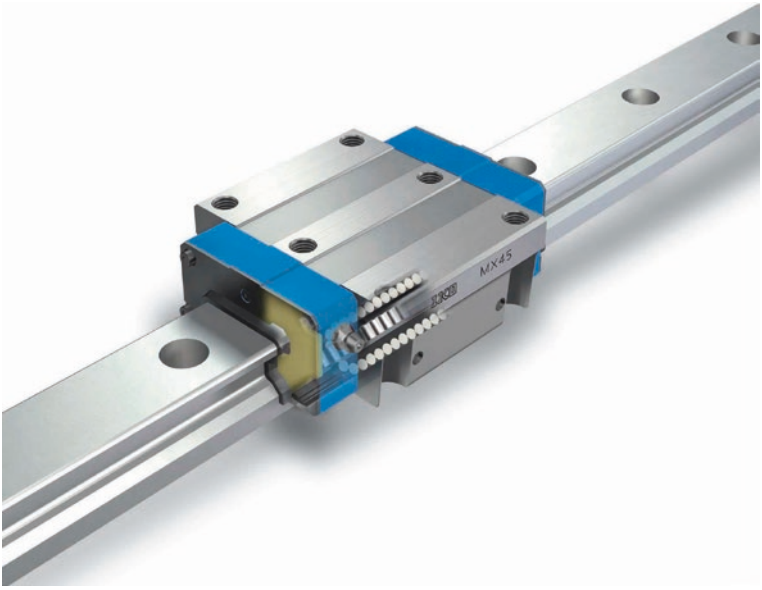

A typical square linear motion rolling guide, incorporating two rows of steel balls arranged in a four-point contact with the raceway—which can be fitted to CNC machine tool's linear axes (courtesy of IKO Nippon Thompson America)

The principal and distinct advantage of the square rail over its round rail counterpart is its very high positioning accuracy. Typically, a square rail has an order of magnitude of higher accuracy and precision to that of the comparable round rail, a property that is especially useful for quality: turning; milling and grinding applications. Characteristically, a square guiderail can achieve accuracies of between $\leq$5 and 25 μm over a linear length of >3 m, compared to that of 250 μm for round rails—over an identical distance. Further, square rails can accomplish this accuracy and precision for an instantaneous load, while for a single carriage and fitted with a solitary rail, it is considered better suited for this motion than a round rail. As a result of this metrological accuracy ability over a round linear rail, and because the square rail handles higher loads at high accuracy, most end users tolerate the somewhat less smoothness in operation than that to which a round rail supplies. Even though a single square profile linear rail unit can cope with instantaneous loads, it is not usually recommended. The norm is to utilise two or more of these square rail units as they have the ability to equalise the applied loads, or distribute the weight more uniformly—thus aiding the kinematic linear and rotational motional behaviour of such rails.

As mentioned, the Square rail has much higher load-life capacity, this feature being defined as, "The amount of load it survives travelling a specified distance". By way of example of this rating of load-life capacity, the Square rail can be expected to very easily carry a 20,000 N load over a distance of $\geq$100 km. Here, the rail's rolling element and its attendant rail wear will be minimal, because it

does not slide, but as its name implies, it has rolling contact. Many of the linear rail manufacturing companies undertake exhaustive testing regimes of their products, as depicted in Fig. 1.34. One of the major contributors to the extended life of linear type bearings is the lubrication system employed to lubricate its rolling elements. Here (i.e. Fig. 1.34, top), the capillary system[82] supplies lubricant via a porous resin C sleeve, or plate—having a steel backing which is formed, in this instance, from a sintered[83] fine resin powder and by impregnating—under a vacuum—a large amount of lubricant oil into its open pores. This action enables the supply of oil over an extended period of its service lifetime. The lubricant via capillary action is supplied and directed to the hardened steel balls as they circulate around the enclosed linear track (i.e. depicted in Figs. 1.33, middle left and 1.34, top).

A square rail's life primarily depends on the type of production environment in which it must reside, in conjunction with appropriate lubrication and maintenance strategies. If all these parameters are equal, then a round rail is somewhat more tolerant in actual usage, because its basic assembly is a more compliant package and as such is not as sensitive to slight machining and environmental variations. Equally, a square rail will be more sensitive to any form of rail debris, although it does have a higher capacity and resistance to impacts when in use on the machine tool, assuming these actual impacts do not affect its rolling elements.

Plain Bearings—With Hydrodynamic Lubrication

Whenever there is a specific requirement to fit plain bearings onto the large rotating masses within assemblies of huge machine tools (Fig. 1.35a) an appropriate lubrication system needs to be utilised and these systems can be categorised into three distinct classifications:

---

[82]**Capillary system**: it is well-known that all surfaces and interfaces of solids are loci of free-energy, whose universal-tendency is to decrease—due to the Second Law of Thermodynamics, leading to the phenomenon of both surface- and interfacial-tension. As a result, there will be a rise of liquid in a capillary, whose walls are wetted by this liquid and its depression in a capillary whose walls have no affinity for the liquid. The basic equation for depression, or capillary rise, is given by the following expression:

$$h = \frac{2T\cos\alpha}{r\gamma g}$$

where 'h' = height of capillary rise (cm); 'T' = surface tension (dyne/cm); 'α' = angle of 'wetting' (degrees); 'r' = radius of liquid (cm); 'γ' = density of liquid (g.cm^{-3}); 'g' = gravity acceleration (cm s^{-2}) (*source* Fang 2002).

[83]**Sintering**: or as it should more correctly be known as Powder Metallurgy (PM), which enables a diverse range of powder particulates to be: weighed-out; mixed; compacted (i.e. termed consolidation) in appropriate dies; then sintered (Sintering temperature values will depend on the main powder's physical melting temperature, and upon whether one is either Liquid-, or Solid-phase sintering.) in a furnace for a specified time and soaking-temperature; finally the pores between the particulants (i.e. pre-mixed metals), are then impregnated—by a secondary PM-processing technique. These processes can achieve the desired mechanical and metallurgical properties for the sintered compact, this being the term used to describe the completed final PM product. Occasionally, some secondary PM-machining may be required to hold exacting tolerances on critical features of these compacts.

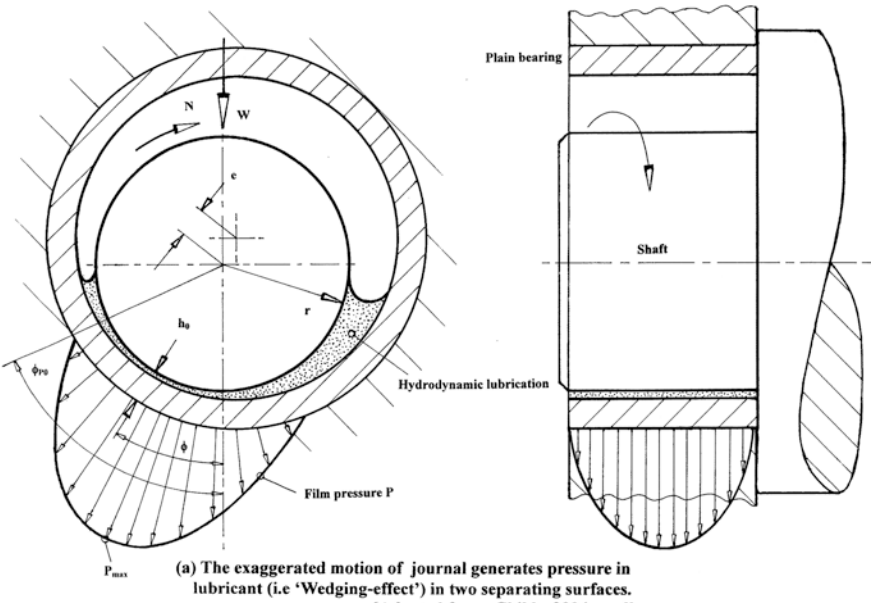

(a) The exaggerated motion of journal generates pressure in lubricant (i.e 'Wedging-effect') in two separating surfaces. [Adapted from: Childs, 2004, et al]

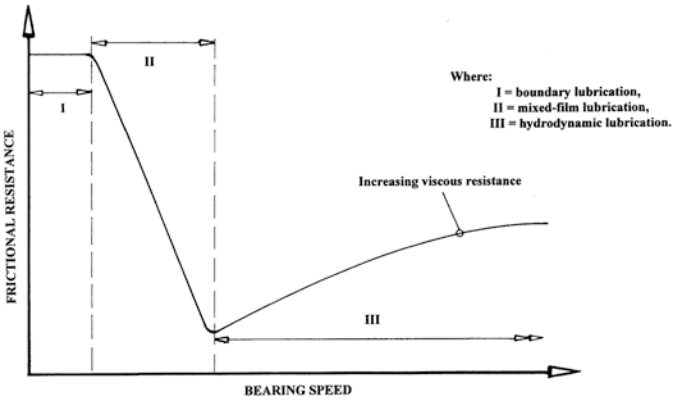

(b) Graphical representation of the transitions/variation of a plain bearing's frictional performance, associated with its lubricating effect and speed. [Adapted from: Childs, 2004 and Davies & Baker, 1987]

Fig. 1.35 Hydrodynamic lubrication occurring with plain bearings

1. **Class I**—here, the bearings require the application of a lubricant from an external source, such as either oil, or grease;
2. **Class II**—in this adaptation, the bearings that contain a lubricant are held within the walls (i.e. of the metallic matrix) of the bearing, such as: bronze; graphite; etc.; characteristically, these bearings call for an externally supplied lubricant to achieve maximum performance;

3. **Class III**—in this instance, the bearings are produced from materials that have the ability to internally retain the lubricant—typically via sintered bearings. This class of bearings is classically considered as self-lubricating and as such can operate without an external lubricant supply.

For the majority of plain bearings fitted to heavy-duty machine tools, there exist just three foremost types of lubrication; these are either: (i) Full-film condition; (ii) Mix, or Boundary condition; or (iii) Dry condition. In the case of full-film conditions, this is when the bearing's load is supported solely by a film of fluid lubricant—there being no contact between the two bearing surfaces. Whereas for mix or boundary conditions, the load is carried partially by direct surface contact and partly by a film forming between the two. Finally, a bearing in a dry condition has the full load being supported by surface-to-surface contact. As just described, fluid lubrication results in either a Full-film, or a boundary lubrication condition, thus, a correctly designed bearing system will decrease friction by eliminating any potential surface-to-surface contact between the journal and bearing through its fluid dynamic effects. As a general guide to a plain bearing's performance, this can be simplistically obtained by calculating the Bearing's modulus '*M*' which is defined in the following manner:

$$M = \mu.\nu / \rho$$

where 'μ' is the dynamic viscosity of the lubricant (centipoise 'cp') @ the operating temperature of the bearing; 'ν' is the linear velocity of the rotating journal (m s^{-1}); 'ρ' is the bearing pressure calculated on the bearing's projected area (MPa). NB 1 cp = 1000 Pa s.

A general rule of thumb design factor is the onset of thick-film lubrication, which occurs at a Bearing modulus (M) of 75.

Fluid bearings can be either hydrostatically or hydrodynamically lubricated. In the case of a hydrostatically lubricated bearing, it is usually lubricated by an external pump which continuously maintains a static amount of pressure. While in the case of a hydrodynamic bearing, the pressure in the oil film is sustained by the continuous rotation of the journal. Hydrostatic bearings only enter a hydrodynamic state when the journal is rotating. Hydrostatic bearings invariably utilise oil, conversely a hydrodynamic bearing may use either oil or grease. Hydrodynamic bearings necessitate greater detailing in their design and operation than a hydrostatic bearing. Further, these hydrodynamic bearings are also more susceptible to initial wear, because any lubrication does not occur until there is a partial rotation of the shaft. At slow rotational speeds, the lubrication may not attain complete separation between shaft and its bushing. As a result, hydrodynamic bearings may be aided by incorporating secondary bearings, which support the shaft during 'start-and-stop periods', thus protecting the fine-toleranced machined surfaces of these expensive journal bearings.

As a consequence, in the hydrodynamic state a lubrication wedge is formed, having the ability to lift the journal around its rotating centreline—see

Fig. 1.35a—which is due to the hydrodynamic pressure profile occurring with this cylindrical journal bearing. The journal also slightly shifts horizontally in the direction of rotation (depicted in Fig. 1.35a—left). The location of the journal is measured by its attitude angle. This angle is formed between the vertical and a line that crosses through the centre of the journal and the centre of the bearing and is termed the eccentricity ratio. This eccentricity is defined as, "The ratio of the distance of the centre of the journal from the centre of the bearing, to the overall radial clearance". Both the attitude angle and eccentricity ratio are dependent upon the following conditions of: rotation direction; speed of rotation; plus the load. In the case of hydrostatic bearings, the oil pressure will also have an effect on the eccentricity ratio. In electromagnetic equipment like motors, the electromagnetic forces can counteract gravitational loads, causing the journal to take up some unusual positions.

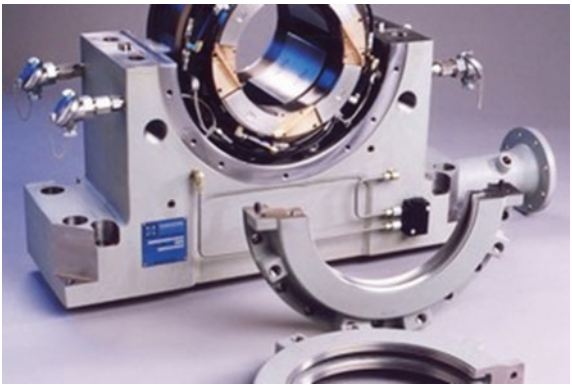

The partial assembly of the complex and intricate parts for an accurate and precise high-speed hydrodynamic bearing, prior to its machine tool installation [courtesy of John Crane (Manchester, England/Orion Corporation, USA)]

One distinct disadvantage specific to fluid-lubricated hydrodynamic journal bearings in high-speed machinery is termed its oil whirl, which is the result of self-excited vibration of the rotating journal. As a consequence, oil whirl is prevalent when the lubrication wedge becomes unstable, due to small disturbances of the journal resulting from reaction forces from the oil film causing further movement, initiating both the oil film and the journal to 'whirl' about the bearing's shell. Characteristically, this whirl frequency is usually $\approx$40 % of the journal rotating speed. In extreme situations, the oil whirl can lead to direct contact between the journal and the bearing and under such circumstances it can rapidly wear-out the bearing. Pursuing this theme still further, in some cases, the frequency of the whirl coincides with the critical rotational speed of the machine's shaft and under this condition it is known as oil whip. There is potential for this oil whip condition to be very destructive and expensive to the overall bearing assembly.

Any potential oil whirl circumstance can be prevented by a stabilising force being applied to the journal. Specific bearing designs strive to utilise a bearing geometry to either deliver an obstacle to this whirling fluid, or to provide a stabilising load to diminish whirl. One such bearing design is known as either a lemon or elliptical bore. In this elliptical bore design, specially prepared shims are installed between the two halves of the bearing housing, prior to the bore being machined to size. Later, after these shims have been removed, the bore bears a resemblance to a 'lemon-shape'—hence the alternative name. Shim removal decreases the clearance in one direction of the bore, while increasing the pre-load in that direction. The distinct disadvantage of this lemon shape design is its unfortunate lower load carrying capacity when compared to similar journal bearings. Such a lemon shape bore will still be susceptible to oil whirl at high rotational speeds; however, its production cost tends to be somewhat lower than an equivalent journal bearing.

If one considers the classical ZN/P curve, or Stribeck curve[84] as it is often known, shown in graphical form in Fig. 1.35b, there are three lubrication conditions—previously referred to (i.e. Boundary; Mixed film; plus Hydrodynamic lubrication)[85]—these being a function of the bearing's rotational speed. So, at rest or at slow shaft rotational speed, the journal will contact the lower face of the bearing—this condition is known as Boundary lubrication and considerable wear can occur during this time. Further, as shaft's rotation increases, oil is forced around by the shaft penetrating the gap between the shaft and the bearing, so that the shaft begins to float (i.e. rise) on a film of oil (see Fig. 1.35a)—this condition is termed thin-film lubrication. Here, the journal may occasionally contact the bearing particularly when a shock load occurs. At these low shaft rotations, only a

[84]**Stribeck curve**: it was named after the German Engineer: Professor Richard Stribeck (Historically, Professor Richard Stribeck (1861–1950), studied Mechanical Engineering in 1880 at the Technical University of Stuttgart in 1885, then later worked as a designer in Königsberg. In 1888, he became Professor in Stuttgart, and shortly afterward in 1890, he became Professor of Mechanical Engineering at the Technical University of Darmstadt. In 1893, Stribeck was appointed as a Professor at the Dresden Technical University. In 1896 he became head of the laboratory equipment of the university. In 1898 he was made Head of the Stribeck Physical Metallurgy Department of the Technical Institute and Director of the Centre for Scientific and Technical Studies—in Neubabelsberg. In 1902 he went on to describe the friction coefficient in lubricated bearings, now known as the Stribeck curve. From 1908, Stribeck worked for the company: Friedrich Krupp AG—in Essen and, in 1919 at: Robert Bosch GmbH—in Stuttgart. Moreover, Stribeck was a college friend of the famous and notable industrialist: Robert Bosch, with whom he remained for a joint-study at the: Royal Wuerttemberg in Stuttgart Polytechnic—this association being a lifelong-allegiance: who extensively studied and experimented with the changes in the amount of drag generated when two objects run together, called the friction coefficient. Hence, this friction begins with a minimal amount and then increases as movement occurs, but attains a specific, fixed value. Stribeck's experiments produced a chart measuring this trend and what is now known as the Stribeck Curve—in his honour.

[85]Alternative names are sometimes employed for these lubrication-states, of Mixed-film- and Hydrodynamic-lubrication, with these alternative terms are being known as either: Transition-/Thin-film-lubrication, or Thick-film lubrication, respectively.

moderate amount of wear may occur. Finally, at high rotational speed, this oil film thickness increases, causing the shaft to rise higher until a point is reached where the journal does not contact the bearing—this state is termed Hydrodynamic lubrication—where no wear/damage exists at this stage. It should also be noted that as the rotational speed is increased still further, the frictional resistance will also increase—as illustrated in Fig. 1.35b.

Lubricating oils that are utilised in journal bearings may necessitate cooling, if their operational temperature increases toward the upper range of its specification. Pressurised lubrication enables any metallic debris present to be filtered out and then flushed away from bearing. High-speed journal bearings are always lubricated with oil, rather than grease. The viscosity for a journal bearing can range between 20 and 1500 cSt, although the viscosity grade is dependent upon the bearing's shaft rotational speed; oil temperature: together with its associated load.

There are many reasons why a journal bearing might fail and a common mechanism being the loss of lubricant; here it is not so much a bearing's failure, as that of a system failure. While, the next most common failure mechanism that may be present is the result of fatigue damage and one of the most important considerations for the material lining bearings is that of its fatigue resistance.[86]

1.12.4 Constructional Elements for Machine Tools

Possibly the three most prevalent constructional materials presently utilised for major structural components of machine tools are cast iron castings, polymer composites, or steel weldments. The development of polymer composites offers the foremost capability in vibration damping capacity, with a disadvantage being that they have the poorest thermal conductivity. For the former reason, a polymer composite is often preferred for specific machine tool elements as its extra-mass damps vibration tendencies, which compensates for the relatively low modulus

[86]**Fatigue**, can be defined as: "The progressive and localised structural damage occurring when a material's are subjected to cyclic loading". Here, the nominal maximum stress values are somewhat less than the ultimate tensile stress limit, and can be less than the yield stress limit of the material. Normally, fatigue occurs when a material is subjected to a repeated series of loading/unloading conditions. So for example, in the case of a bearing's shaft, if these loads are above a certain threshold, this will instigate microscopic cracks forming at the stress-concentrators, typically at a surface imperfection, sharp corner, or at persistent slip-bands (PSBs), as well as at grain-boundary interfaces. Eventually a fatigue crack will reach a critical dimension—termed its critical crack length, when the structure will suddenly catastrophically fracture. The geometric shape of the component's structure will significantly affect its fatigue life, with: square holes; sharp corners; abrupt changes in cross-sections; such conditions will lead to elevated local stresses, whereupon enabling fatigue cracks to then be initiated. By contrast, round holes, or components having smooth transitions from small-to-large dimensions; or blended-fillets; these will minimise fatigue—by facilitating an increase the fatigue strength of the part's structure.

of elasticity. Conversely, often these polymer composites are not exploited for high-powered machine tools that have a small footprint (i.e. having small width-to-length ratios with respect to the machine's height). All three of these materials have been utilised in the design and construction of machines, meeting the necessary criteria for: inherent rigidity, shock/impact resistance, also—as mentioned—having a good vibration damping capacity. The ultimate selection of material is further affected by certain other parameters that include: overall cost, footprint/space requirements, plus their manufacturing and production lead-times.

Invariably, 'Meehanite™ grey cast iron castings'[87] continue as the principal choice for the production of machine tool structures—see Fig. 1.36—due to their comparatively low cost, ease of material sourcing, relatively good damping capacity coupled to high strength, while achieving a good capacity for surface hardening/machinability. Nonetheless, in certain circumstances, fabrications are customarily the favoured choice when low-volume production of large structures are necessary, mainly due to the otherwise high processing/moulding costs of comparable castings, coupled with complications of in-process quality control inherent in such very large castings. On the other hand, increasing emphasis is on high-speed machining and hard-part turning, with improved and consistent machining accuracies, better structural rigidity, along with an improvement in thermal stability and vibration damping of structural composites. These criteria are becoming major design considerations, ensuring that polymer composites have become the preferred choice. Contingent with these performance and cost requirements, the machine tool's base can be a composite—a combination of conventional castings with hardened ways, to enable strategically reinforcement within this composite element.

As a result of the existing market forces and competition within the machine tool industry, Value engineering (VE)[88] has become a noticeable factor in this challenging manufacturing environment. A key deliberation is to recognise the correct selection of structural member types for both the materials utilised and their inherent designs, as this will provide the optimum performance of the

[87]**Meehanite™ grey cast iron castings**: the process was developed in the late 1920s/early 1930s, by the: Ross Meehan foundry—in Chattanooga, Tennessee (USA). This patented-discovery (U.S. Patent 1,790,552—was issued to: Augustus F. Meehan—in January 1931, but in 1987, The Meehanite Metal Corporation was acquired by the: Finnish Foundry Group.) was based on the use of calcium silicide to inoculate irons melted in a controlled manner. This applied research work resulted in the development of cast irons of greater strength suitable for critical engineering applications, typified by machine tool structures. There are two basic materials covered by the majority of Meehanite™ specifications, these are: (i) flake [lamella] graphite, known as: Grey [Grey] irons; and the (ii) Nodular/Spheroidal graphite iron, sometimes termed: Ductile iron types- covered by a typical range of: **DIN 1691 GG25**, or **ISO 185/250/260** [etc.] specifications, according to metallurgy and its applications.

[88]**Value engineering** (VE): this activity can be considered as a systematic method to improve the value of: goods; products; and services; by utilising an examination of their functions. Usually the term: Value, is normally defined, as: "The ratio of function to cost". Consequently, Value can be increased by either improving the function, or reducing the cost, this being a primary tenet of Value engineering and that basic functions can be preserved and not be reduced, as a consequence of pursuing these value-improvements.

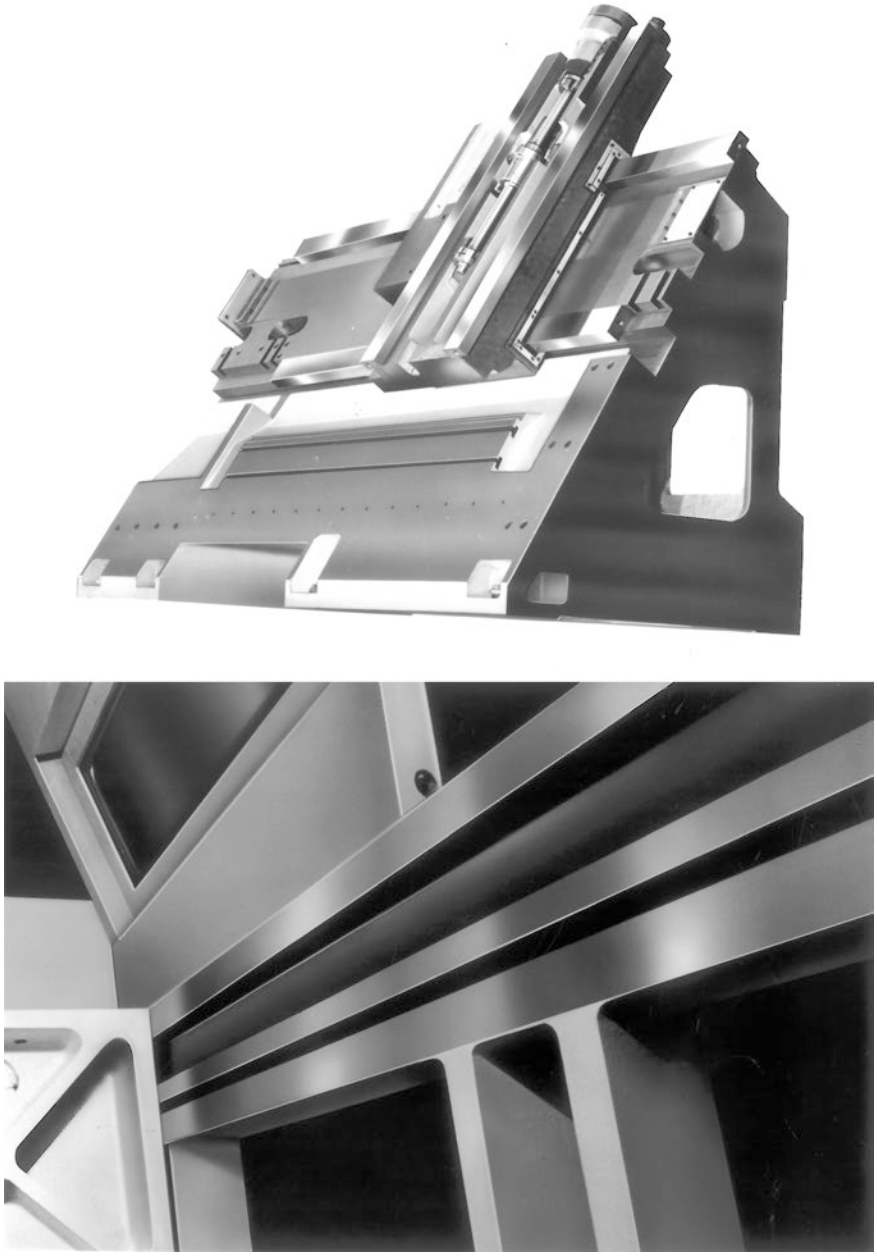

Fig. 1.36 The partial assembly of a slant-bed turning centre, having a box-like ribbed cast iron structure, with hardened ways (courtesy of Cincinnati Machine UK Ltd.)

machine tool, whilst minimising its cost. For that reason, alternative actions for evaluation criteria are necessary to determine different machine design elements, with an optimal cumulative impact on various technical, commercial and strategic requirements. Even though polymer composites offer superior damping—when compared to cast irons equivalents—they will also require highly exacting process and procedural controls for consistent cast quality. Moreover, by employing polymer composites, they provide a significant advantage of short lead-times from pour-to-casting assembly, while having equally excellent chemical and corrosion resistance, plus the ability of very low water absorption.

From the outset, conservable material damping coupled to static stability are mandatorily incorporated into machine tool design; invariably this is achieved by increasing the mass of components, while not affecting the casting's dynamic stiffness. In order to accomplish a comparison of differing machine tool cast materials and their effect on machine performance—for large structural machine tool elements, the subsequent criteria defines these significant features:

- **static stiffness under loading**—the chief structural components of machine tools bases, columns, carriages, as well as tables are comprised of relatively simple geometric shapes. For this analysis their geometries are simplified, by utilising rectangular beams, with their respective structural rigidities being characterised by bending stiffness in two planes and their torsional stiffness;
- **specific stiffness** (i.e. stiffness-to-mass ratio)—with specific stiffness this can be defined as, "Static-stiffness divided by the weight (or mass) of the component". Thus, the higher this specific value, the more efficient the use of the material within the component. Torsional compliance of a cast structure is normally the main contributor to the displacements within the cutting zone. Analyses of existing designs have revealed that for a specific geometry, torsional stiffness is considerably more sensitive to changes in the mass than both static and specific stiffnesses;
- **dynamic stiffness and damping dynamic stiffness**—such stiffness effects are directly related to the material's damping characteristics and is thus proportional to the static stiffness. For example, in a single degree of freedom system, it will exhibit a small damping ratio (i.e. $\zeta < 0.1$), Kdynamic $= 2\ \zeta$ Kstatic. Noting that dynamic stiffness is direction dependent and in appraising the cast structure, three different values are usually calculated that correspond to the three principal axes of a typical machine tool. Damping is material dependent, with its values being very close in different directions;
- **component's mass** (weight)—as a consequence, the effect of mass is encompassed in the above criteria when evaluating the component's structural response. Nonetheless, in isolation, the mass, or weight is a good substitution for the cost (i.e. namely for its material, processes, handling, plus its assembly). Consequently, when utilised as a benchmark, this casting's mass becomes the controlling factor in determining the overall cost of major structural components, although usually a cost limit is placed on its value.

What is worth mentioning in perhaps more detail, is the customary industrial practise utilised on most machine tools for the stacking of axes—see Fig. 1.36 (top)—and its result on the machine tool's damping characteristics. As more axes are placed on top of each other—for example here in Fig. 1.36 (top)—also in the case of the conventional configuration of the Mill/Turn Centre—shown below, with the *X*-axis situated on top of the *Z*-axis—these will change the overall damping capacity of the machine, due to the well-known rigidity rule,[89] which states that, "Rigidity decreases by the square of the distance".

This Rigidity rule explains why certain stacked axes that are normally twice as high as an alternative machine configuration, which makes them four times less rigid than their equivalent counterparts. Invariably, on very accurate and precise machine tools—required to manufacture ultra-precision components, these individual axis are often purposely designed to isolate each discrete axis with respect to one another—to overcome this debilitating stacking axes problem.

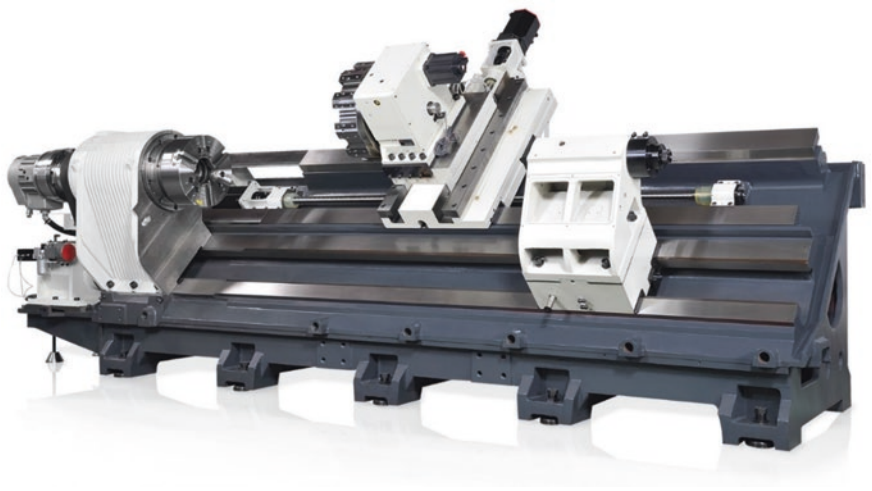

In this photograph, can be seen a partially completed assembly of a 45° slant bed Mill/Turn Centre, its main structural components are produced from Meehanite™ Cast Iron mono-block castings. Here, with this machine tool, the ways having been fully hardened, surface-ground, then they are hand-scraped. [courtesy of Chevalier Machinery (Sante Fe Springs, CA, USA)—2015]

[89]**Rigidity-rule**: thus as each machine tool axis is located and positioned on top of each (e.g. typically, the stacking of the *X*- and *Y*-axes on a Machining Centre, or *X*- and *Z*-axes on a Turning Centre), then the machine's rigidity decreases—by the: "Square of the distance". In fact somewhat contrary to this rigidity effect, is that the damping of a typical Meehanite cast iron bed in isolation, has a damping capacity of: ≈0.04 (log decrement), but when the complete machine tool has been assembled (i.e. see photograph above for a partially-assembled Mill/Turn Centre), then this damping capacity value now has significantly increased to: 0.25 (log decrement) (*source* Kalpakjian 1997).

A practical example and illustration of the current and abridged technical specification of a typical slant-bed Mill/Turn Centre is shown above. Here, the Mill/Turn Centre features a 380-mm chuck, having an ≈∅115 mm bar capacity, with a 770-mm swing over the bed, plus a turning diameter of ≈570 mm, with a turning length up to >2000 mm. This machine, with its ribbed 'Meehanite'™ Cast Iron mono-block casting, has previously been hardened, ground, then hand-scraped, to enable the slideways to minimise stick-slip, resist deflection and vibration—during heavy machining—thus ensuring stable end-to-end cutting of long shafts. Here, both the *X*- and *Z*-axes positioning accuracy is to ±5 μm, whilst the machine's repeatability is within ±2.5 μm.

This particular company's Mill/Turn Centre model is equipped with an impressive ≈45-kW digital direct spindle motor, with a two-speed gearbox that can generate up to ≥11 kN m of torque in its low-speed range, namely at 37 rpm. The 45° slant bed casting has a rigid box way structure—see this typical ribbed-/box-like arrangement in Fig. 1.36 (bottom)—with the bed also being fitted with an optional programmable tailstock. The machine is also equipped with a Tool eye setter—for automatic cutter offset compensation in situ in their respective tool turret pockets—plus touch-trigger probing—enabling critical part features to be interrogated, while further offering a reduction in work set-up times—keeping the non-machining idle times to a minimum. The 10 tool pocket position servo-indexing turret, allows a fast 0.5 s tool indexing time, whilst the live-/driven tooling facility provides a powerful milling capability—for prismatic part features, coupled to a standard ≈18.7-kW spindle motor that includes a two-speed gearbox, providing up to 478 Nm torque. Furthermore, such high power and torque capabilities enable this machine to tap a component with an M30 thread, or drill a hole of up to ∅50 mm into tough workpiece materials. The headstock's spindle has a full *C*-axis function, that can be programmed in 0.001° increment indexing.

Scraping of Machine Elements

At its most basic level, a hand scraper is utilised as a single-edged tool that is being employed to scrape unwanted metal from a surface—as shown below. This action is normally necessary where a surface requires to be 'trued'—corrected for the desired fit to a mating part, or when the surface needs to retain oil—often on a freshly ground machined surface, or simply when a decorative finish is required.

The name given to a highly skilled scraping operative is generally known in the trade as a Hand. Scraping is generally undertaken by employing a precision Master surface, typically either a surface plate/table, or a straightedge—as some form of a flatness standard. At this point in time, a typical straightedge can be considered as a small width surface plate, but of extreme accuracy and flatness.

A professional scraping tool will be a specially made manual handling tool—see the photograph below and those in Fig. 1.37—or perhaps a hand-operated powered scraping tool. Prior to use this Master surface is coated with a very thin and consistent coating of a material termed either Prussian blue or alternatively another substance known as Red marking compound. After thinly coating with either the blue or red compound over the Master, the workpiece/surface to be scraped and the Master are gently placed together—using simple gravity alone coupled to a gentle and controlled motion, enabling the high-spots on the

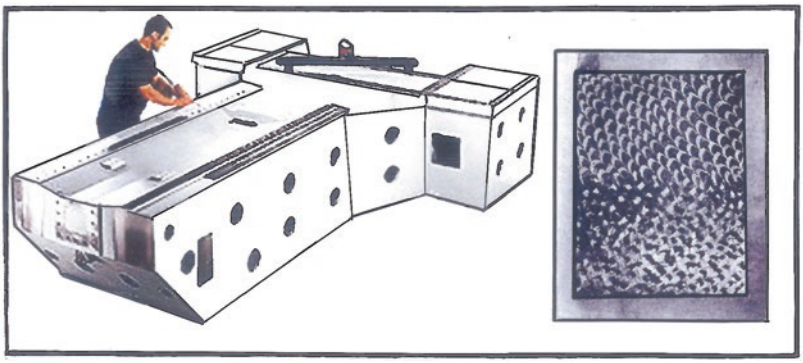

Scraping a large machine tool base (left), also illustrated (right) are just some of the differing scraping techniques (e.g. 'Frosting').

[Courtesy of the Scraping Community of India]

Fig. 1.37 The 'traditional' scraping technique for production of flat surfaces—which then reduces potential 'high-spots' on the casting's surface, while imparting a good lubrication surface condition on a machine tool's 'meehanite cast iron' base element, minimising 'stick-slip' for its moving members [courtesy of Yamazaki Mazak Corporation (Worcester, England)]

workpiece/surface to be highlighted by this dye from this coated Master. Once carefully separated, these high-spots are then prudently scraped-off the workpiece/surface. This application process is then successively repeated until there exists an even spread of high spots, usually totalling ≈60 % or more of the scraped surface area.[90] For example, an initial coarse scraping operation produces—in Imperial units—a resulting surface with between 5 and 10 points in.$^{-2}$; conversely, the action of Fine scraping yields 25 and 35 points in.$^{-2}$—see this former 'Coarse-scraping effect' illustrated below. If it is required the resultant scraped surface could then be Frosted (see Fig. 1.37, top right).

A surface that has been prepared by scraping, is generally considered to be superior in its overall accuracy/flatness to that produced by the manufacturing processes of either precision machining, or from surface grinding operations, although the lapping technique can equal, or often indeed exceed that of scraping, but this is normally only over smaller surface areas and for shorter linear distances. It should also be emphasised yet again, that both the Lapping and Grinding operations, do not achieve the long-distance flatness characteristics of a quality scraping operation, as both of these previous material removal actions act upon the entire workpiece surface rather than on the localised high or low spots on the part's surface area.

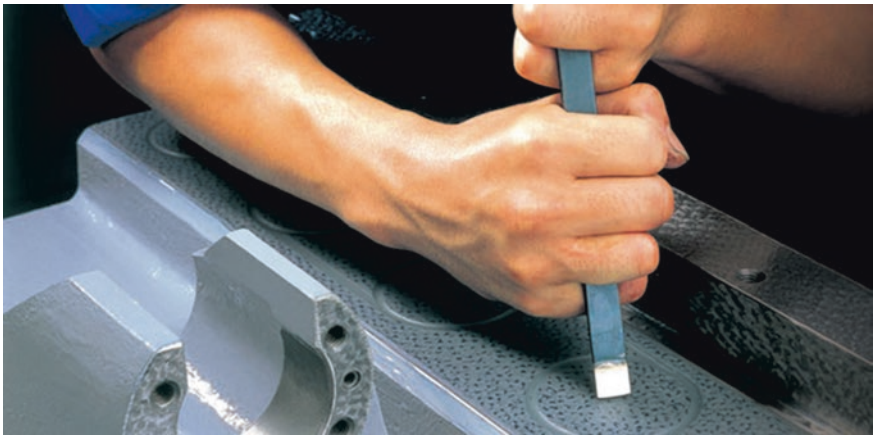

The highly skilled action of for example, the hand scraping of a casting's bearing surface will achieve the required: accuracy/flatness/pattern, via the desired number of high spots per centimetre^{-2}, or by alternatively the number per Imperial in.$^{-2}$ [courtesy of Yama Seiki USA INC, (Chino, CA)]

[90]The application of for example, Prussian blue from the Master surface to that of the workpiece/surface, should be achieved in as uniformly and consistent manner as possible. Some hands (i.e. the scraping operatives) will utilise a figure-of-eight motion when employing on either a blued surface plate, or a blued table—for a potential component-to-be-scraped flat from this surface. Here, the smoothly controlled continuous motion of the changing of direction when utilising a figure of eight action, imparts a much more uniformly-distributed amount of blue dye onto the high spots of the workpiece/surface to be scraped.

For any precision flat ground surfaces the applied lubricating oil film to bearing surfaces will lack the means to adhere to these very flat surfaces, particularly between two mating parts of exceptional surface finish. Hence, upon sliding motion, this deposited oil film will be swept away, leaving an interface of metal-to-metal contact and risking potential surface seizure. By a careful surface scraping procedure, this leaves the original high-quality surface still intact but provides numerous shallow depressions, where the residual oil film can be retained—allowing its depth and surface tension to be maintained. When the operation of scraping is utilised for this purpose, it can more accurately be known by several terms, such as frosting, spotting, feathering, or flaking (see Fig. 1.37, top right) as opposed to fully scraping an accurate and flat surface. Usually, a scraped workpiece surface is initially produced to a highly accurate flatness then this frosting is applied upon this surface—predominantly for its oil-retention capabilities. This oil-retention effect of frosting is somewhat controversial, as it is often claimed to minimise the so-called Stick-slip phenomenon,[91] resulting from an initial motion of a bearing machine member moving in a rather jerky fashion instead of moving/gliding smoothly. This stick-slip can instigate potential vibration and chatter to this otherwise smooth linear way motion. At this time, Frosting definitely increases the oil-retention potential, but can also have the negative effect of drastically reducing its total bearing area. Hence in this situation, there is virtually no possibility of achieving a hydrodynamic bearing performance on normal sliding machine ways—as the attendant axis velocity is far too low. In most cases, the ways operate under Boundary lubrication conditions, while at the highest linear speeds it might possibly achieve mixed lubrication—these lubrication conditions (see Fig. 1.35b) ensure that the application of the correct and enhanced oil additives are very important in axes way lubrication processes.

As mentioned, scraping by the skilled hand-operative produces distinctive patterns on the scraped surface—see Fig. 1.37 (top right)—with each hand-scraper operative being able to identify their own individual workmanship, almost like their own signature. The scraped-markings on the ways, distinctly indicate the

[91]**Stick-slip phenomenon**: which is also known as simply stick-slip, is the result of a spontaneous jerking-motion that can occur while two objects are in close contact and sliding over each other. However, there is a lack of understanding about this frictional phenomena, but the generally agreed upon view is that stick-slip behaviour results from common photon-modes (i.e. at the immediate interface between the substrate and the slider) that are pinned in an: "…undulating potential well-landscape…", that either un-pin (slip) and pin (stick), being primarily influenced by thermal-fluctuations. So, in the most basic of terms, Stick-slip can be simply described as: "Surfaces alternating between sticking to each other and sliding over each other, with a corresponding change in the force of friction". Typically, the static friction coefficient (i.e. a heuristic-number) between two surfaces is larger than the kinetic friction coefficient. If an applied force is large enough to overcome the static friction, then the reduction of the friction to that of kinetic friction, can cause a sudden-jump in the velocity of the movement, hence the term: Stick-slip.

level of precision in these ways. Unfortunately, in the case of some unscrupulous machine tool companies—where they are producing low-quality and -cost machines, they may artificially add this frosting to their machine ways, this being at best a superficial surface treatment that is designed to give the impression of high-quality scraped machine guide ways.

In many current machine tool manufacturing companies, scraping is undertaken by the use of a power-scraper, which has a reciprocating blade; this is often adjustable for its stroke length and number of strokes per minute.

Hand Scraping—The Essential Objectives

Hand scraping sets the foundation/datum surfaces for productive CNC machine tools, which is accomplished with the following intentions; that is to achieve:

- **accuracy**—scraping is undertaken to align critical components within, in some cases, nanometric levels of accuracy/precision—permitting both consistently held and exceedingly tight tolerances to be practically attained;
- **flatness**—for example, of between 8 and 10 contact points per in.$^{-2}$ (i.e. High spots—see photograph above) are created to prevent any surface rocking; moreover, adding balance when tightening down two mating machine element surfaces—this allows for a true flatness register between these mating parts (see diagram below—left);
- **oil pockets**—certain machine surfaces will have oil injected onto them—as the two surfaces intimately slide together. Accordingly by this previous scraping operation, it permits the creation of oil pockets—retaining residual oil on these bearing surfaces and allowing for a sliding/gliding motion. Deprived of these oil pockets, two flat surfaces will potentially stick together—creating an undesirable stick-slip condition;
- **appearance**—often the finishing touch of the scraping process is purely aesthetic. So, once the accuracy, flatness, and oil pockets have been produced, then these mating parts are design scraped—to achieve an attractive/cosmetic textured surface finish.

Supplementary to this process of hand scraping process, it was previously mentioned that it introduces the desired high and low spots on the mating surfaces of the CNC machine tool. Although it is often thought that truly flat surfaces would improve machining accuracy and precision, this is in fact not true. Further, it was also mentioned that two very flat surfaces in contact on the machine tool will virtually stick together, thus creating at best an inconsistency in its future machining characteristics. Besides, tight tolerances can only be attained by the addition of high and low-spots, that retain oil and facilitate sliding/gliding linear motion, rather than creating unwanted Stick-slip. As a result of introducing these additional contact points via high and low spots, this will also permit a degree of balance and subsequently create perfect surface-mating conditions. With truly flat surfaces, there is only one overall contact point, which can produce a

state of imbalance. In the case of bolted parts, hand scraping generates a tighter mating fit—see below (right), this condition being less likely to separate due to the result of the in-process material expansion/contraction—resulting from the potential thermal-flexing that can take place during the actual CNC machining processes.

The Casting, or Foundry production process[92] for the manufacture of large machine tool elements introduces some uncontrollable process variables into a final cast product, such as: small changes in the base materials; mould-release agent problems; variable temperature and environmental conditions—causing each component to have unique characteristics. Further, whilst being poured, the molten metal behaves in similar ways from one casting to the next—prior to its actual solidification. Once the casting has cooled sufficiently and been released from its constrained position in the mould, it can move and flex in a somewhat very unpredictable way. Thus, once the casting has been stabilised over a period time and machined, then a skilled Hand scraping operative can correct for any potential fluctuations in each machined individual casting—arising from aforementioned casting variables.

[92]**Foundry production processes**: these can be primarily-divided into two types of: (i) ferrous foundries; (ii) non-ferrous foundries. Basically, foundry processes involve making an accurate and precise pattern for the mould/core, extracting it, then in this cavity, melting and pouring the metal into the mould and finally removing the solidified casting and then finishing off this product (i.e. termed fettling). Although various processes will potentially differ in the number of steps required to make the final cast product. Thus as mentioned, for the metal casting process, it starts with creation of pattern for its mould. Metal that can be suitable cast and moulded, will be poured into this accurate and precise shaped mould cavity—where its hard-rammed running and feeding system has also been previously produced and then it is slowly-cooled. The form of metal being used and the shape of the final product required would also decide the material, which will be used to make the cast. A commonly used material here, is moulding-sand. While, both investment material techniques, also the use of metal moulds, etc., can also be employed. A variety of furnace types are utilised including: cupolas; electric arc; induction; hearth; reverberatory; or a crucible. Due to the different nature of metals, there are any number of varying-inputs that are required and they will differ, with a range of toxic wastes which are released from each type of casting metals and its associated processes. After the metal has been melted, it is gently poured into the mould-cast cavity and then allowed to cool and set. Of note is that silica sand with controlled moisture, oils and green sand are often mixed together to form a mould cavity, prior to the metal being poured into this cavity. Once the metal has sufficiently cooled, it is then easily-separated from the mould—often termed shake-out—prior to its fettling (i.e. removing feeders and the running system) and is ready for any subsequent machining, etc. Thus, this final machine tool cast member should now exhibit the desirable, but consistently small grain-size throughout its structure, while also exhibiting the required mechanical strength [*sources* TheMetalCasting.Com (2014)/Beeley (1982)].

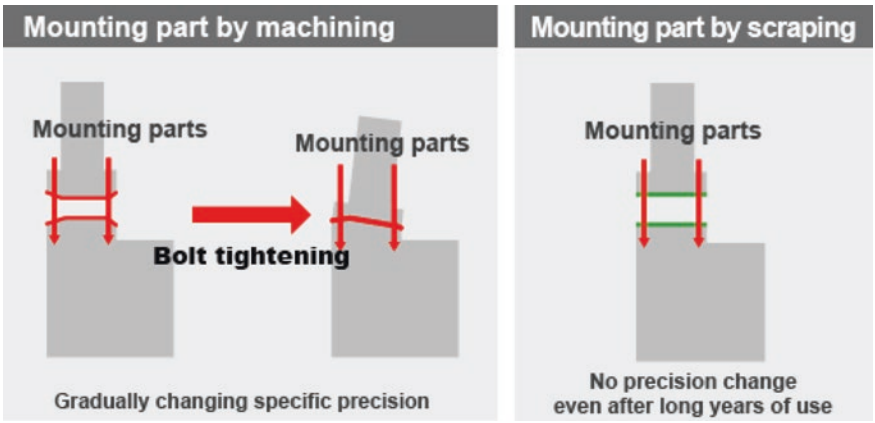

By subsequent hand scraping, this is necessary for the ultimate flatness between mating surfaces and to achieve perpendicularity on key components (above right), this being a most important procedure to accomplish for the required accuracy and durability on both Turning and Machining Centres [courtesy of YASDA PRECISION TOOLS K.K. (Japan)]

1.12.5 Linear Motor Drive Systems

In recent times and following the introduction of the Linear motor, there has been a massive increase in its manufacturing usage with some beneficial industrialised applications over several decades, most notably in the drive systems for CNC machine tools. In essence a linear motor is frequently described as a rotary motor that has been rolled-out flat, but with its principles of operation being identical. Here, the forcer (i.e. rotor) is constructed from coils of wires that are encapsulated in epoxy, while the track is fabricated by positioning magnets—usually high power rare earth magnets on steel—see the schematic representation of this arrangement in Fig. 1.38 (top). This forcer—of the motor—comprises the windings and a Hall-effect[93] board, together with a thermistor of thermal sensors to monitor temperature, as well as suitable electrical connections. It follows that in the case of rotary motors, the rotor and stator need rotary bearings to

[93]**Hall-effect** (This so-called Hall-effect was discovered by Dr Hall, whilst he was researching for a doctoral degree at the: Johns Hopkins University (Baltimore, Maryland, USA). Hall's exacting-measurements of the minute-effect produced in the apparatus he was utilising at the time, were considered by many to be an experimental 'tour de force', which was accomplished 18 years prior to that of the actual atom's electron being discovered.): is the production of a voltage difference—termed the Hall-voltage—across an electrical conductor, this being transverse to an electric current in the conductor and a magnetic field perpendicular to the current. This Hall-effect was named after the American Physicist and Engineer: Dr Edwin H. Hall (i.e. in 1879). Dr E.H. Hall was Born: 7 November 1855 in Gorham, Maine and died: 20 November 1938, in Cambridge, Massachusetts, USA. The Hall-coefficient can be defined as: "The ratio of the induced electric field to the product of the current density and the applied magnetic field". As a consequence, it is a characteristic of the material from which the conductor is made, since its value depends on the type, number, and properties of the charge carriers that constitute the current.

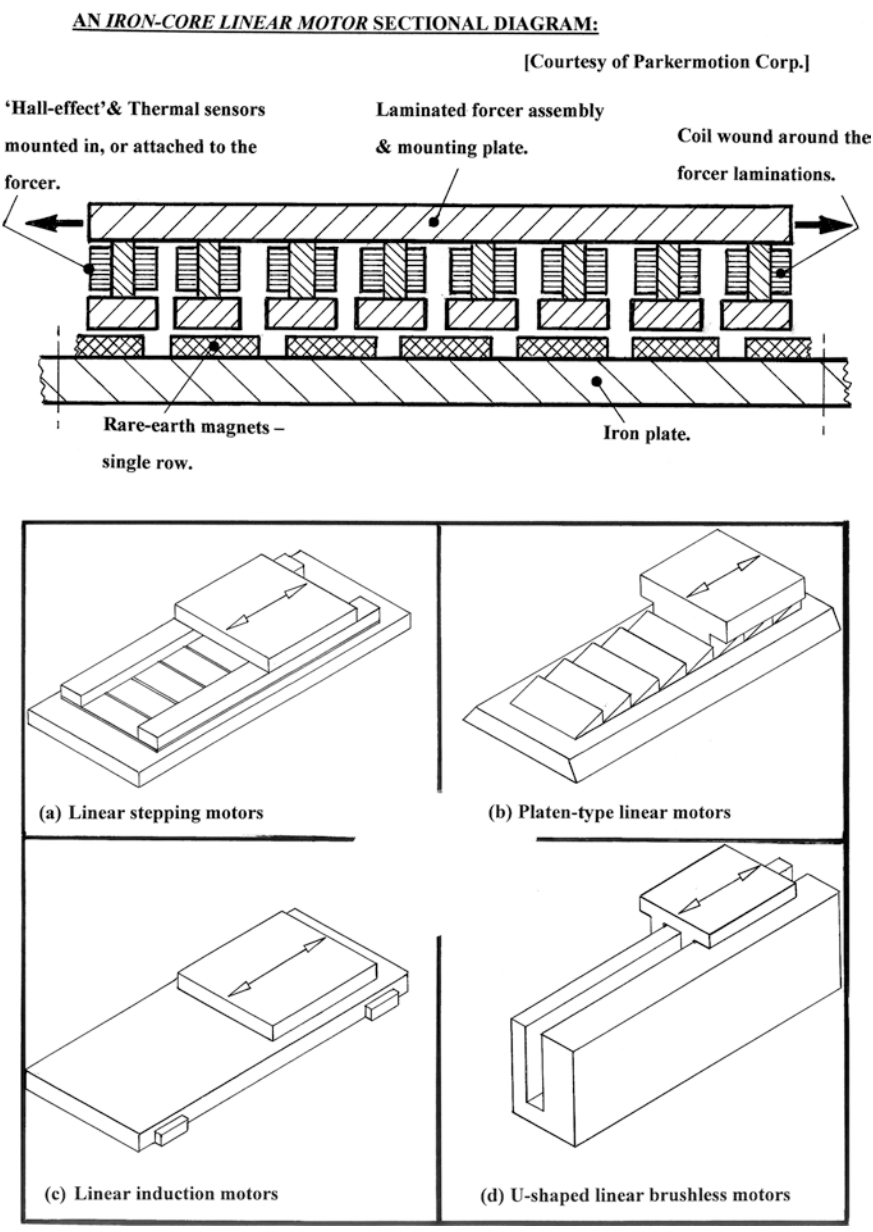

Fig. 1.38 Brushless permanent magnet (PM) motor technology and typical configurations for machine tools

support the rotor, whilst maintaining an air gap between the moving parts. Likewise linear motors normally require a set of matched linear guide rails to maintain the position of the forcer within this magnetic field of the magnet linear track. Encoders are mounted on rotors, as is the instance for similar rotary servomotors, to give positional feedback of the shaft, thus linear motors also require positional feedback in their linear motional directions. So, by employing a linear encoder, the axis position is directly measured at the load for increased accuracy of its load position; hence, the control for linear motors is indistinguishable from that of rotary motors. Equal to that of a brushless rotary motor, the forcer and track have no mechanical connection—no brushes. In contrast to that of rotary motors where the rotor revolves and the stator is held immobile, a linear motor system can operate with either the forcer, or the magnetic track moving (i.e. in many positioning system applications, they utilise a moving forcer and static track). A linear motor equipped with a moving forcer motor operates with the forcer weight being small compared with the load, although a cable management system with a high-flexure cable is a prerequisite. Accordingly, with a moving-track configuration, the motor must move both the load, plus the mass of the magnetic track, although here no cable management system is necessary. Comparable electromechanical principles occur, whether this motor is of a rotary, or linear construction. Moreover, the equivalent electromagnetic force that creates torque in a rotary motor, generates a force in its linear counterpart. As a result, the linear motor utilises the identical controls and programmable positioning, as with a rotary motor. A linear motor can be constructed in a number of configurations, such as a utilising a Flat type (i.e. with a Stepper motor), Platen type, Flat type (i.e. with an induction motor) or U-shaped channel (i.e. with a brushless motor)—see schematic Fig. 1.38 a–d, respectively. The linear motor configuration that is most suitable for a particular application will depend upon the actual desired specifications and its intended operating environment.

Linear motors can be considered as synchronous motors, where current is applied to the coil forming an electromagnet. This coil will then synchronise to the magnetic field generated by the permanent magnets in the magnet track. As a consequence, a force in the linear motor is generated—due to the comparative strength of these magnetic fields and the angle of their intentional misalignment. One type of linear shaft motor currently available consists of stationary, cylindrically wound coils and a smooth non-ferrous moving rod which has a series of rare earth iron boron (NIB) permanent magnets[94] inside, which are systematically

[94]**Rare-earth iron-boron (NIB) permanent magnets** (There are two principal types of Neodymium-magnet manufacturing methods, they are produced by either: (i) classical powder metallurgy, or via sintered magnetic processing; and by (ii) rapid solidification, or by the bonded magnet process.): a neodymium magnet (i.e. also known as: NdFeB, NIB, or Neo-magnet), is the most widely used type of rare earth magnet, that is a permanent magnet made from an alloy of: neodymium, iron and boron—to form: $Nd_2Fe_{14}B$, having a tetragonal crystalline structure. It was jointly-developed in 1982, by both: General Motors (USA) and: Sumitomo Special Metals (Japan). These neodymium magnets are the strongest type of permanent magnet that are commercially available today. They have replaced other types of magnets in many applications in modern products that require strong permanent magnets, such as in the industrial applications for linear motors for machine tool axes.

propulsed by both attractive and repulsive coil forces. In some cases, the round types of linear motors are offered with varying shaft diameters, typically ranging from: ∅4 mm up to ∅115 mm and with an output of extending from just: ≤1 N to >36,000 N.

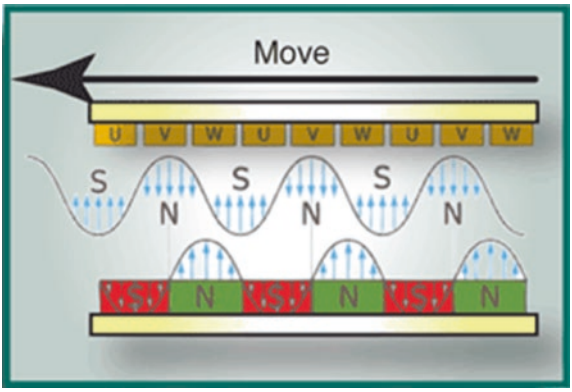

In the schematic diagram, is depicted the coil's synchronised magnetic field, which is generated by the permanent magnets in the magnet track of a linear motor—when fitted to a CNC machine tool [courtesy of Nippon Pulse America Inc. (Radford, Va, USA)]

Prior to the introduction of practical and inexpensive linear motors, all linear movement had to be fashioned from rotary machines by utilising ball, roller screws, or indeed with simple belts and pulleys. In many motor applications—where high loads are encountered and whenever the driven axis is in the vertical plane—the above mentioned techniques still remain possibly the best solution. However, linear motors can offer many distinct advantages over mechanical drive systems, such as very high and low speeds, fast acceleration, virtually zero maintenance—because there are no contacting parts (i.e. having air gaps present), plus high accuracy/precision—without attendant backlash. By achieving axis motion with a linear motor where gearing, couplings, or pulleys are unnecessary, this axis motion is highly practicable for many machine tool applications, where such complex drive components would otherwise tend to diminish the machine's performance and reduce its overall working life.

---

footnote 94 (continued)

NB Sintered Nd-magnets are prepared by the raw materials being melted in a furnace, then cast into a mould and cooled—to form ingots. These subsequent ingots are then pulverised and milled into minute particulates, then sieved for consistent particle size, in which they then undergo a process of Powder Metallurgy (PM) processing—normally by liquid-phase sintering—in which the powder is magnetically aligned into appropriate dense blocks. These blocks are then heat-treated, machined to the required shape, surface treated and magnetised, then fitted into an appropriate linear motor assembly—see Fig. 1.38 (top) (*source* Furlani et al. 2001).

Linear Motor—Sine Error

Non-contact linear shaft motors are incapable of mechanically binding when they are installed correctly. In this situation, the magnets in a linear shaft motor are centred; consequently this ensures that the air gap dimensions are non-critical. Here, the coil completely surrounds the magnet so any force produced is the net effect of the magnetic field. Accordingly, any variation in force is typically caused by air gap differences—usually due to misalignment, or inadequate machining practices being eliminated—thereby simplifying any alignment and device installation problems. Essentially, these characteristics are valid for all types of cylindrical non-contact linear motors. So the question that might be posed is: "What makes linear shaft motors different from any other linear motor designs?" The answer is simply due to its sine error, this being the phenomenon causing force variations in most non-contact linear motors. In the case of a Parallel linear motor drive system, when the separate coils' magnetic fields are perfectly aligned, together with the magnetic fields in all the magnetic tracks that are also perfectly aligned they can, in effect, become a single motor—without any differences of force generation. Conversely, any misalignment of coils or magnetic tracks may result in the angle of misalignment of magnetic fields in the motors and tends to fluctuate, thus creating different forces in each motor, so this force difference can cause what is termed binding. The sine error is the force difference created by a misalignment of coils or magnetic tracks—as calculated by the following expression:

$$F_{\text{dif}} = F_{\text{gen}} \times \sin\left(2\pi \times D_{\text{dif}} / \text{MP}_{\text{n–n}}\right)$$

where 'F_{dif}' = force difference between the two coils; 'F_{gen}' = force generated; 'D_{dif}' = length of misalignment; '$\text{MP}_{\text{n–n}}$' = north-to-north magnetic pitch.

Virtually all of the commercially available linear motors are arranged to have a north-to-north magnetic pitch of ≈25–60-mm long, with such a pitch being employed to reduce IR-losses, while improving the electrical time constant. Nevertheless, for example, a 1-mm misalignment in a motor which has a 30-mm N–N pitch will result in ≈21 % power loss. Conversely, linear shaft motors utilise a much longer north-to-north magnetic pitch—to reduce the effect of sine error, this being due to any accidental misalignment. Here, the same misalignment of 1 mm in a linear shaft motor with a 90-mm N–N pitch will result in just a 7 % loss of power.

An informative table for typical and various motional drive systems for CNC machine tools that are currently available—for direct comparison—is presented below—in Table 1.6.

In summary, an important benefit of eliminating the mechanical transmission components, includes the fact that no backlash will then be present. Besides, the machine tool's axis response can be ≥100 times quicker than for a mechanical transmission—thus minimising potential servo droop problems when contouring/profiling workpiece feature geometries. As has been mentioned, linear motors also function at very high speeds with exacting accuracy and precision; typically such

Table 1.6 Being a simple comparison of different types of the motional drive systems—for the majority of today's contemporary CNC machine tools

Contributions	Leadscrew	Ballscrew	Belt-drive	Linear-motor
Noise	Quiet	Noisy	Quiet	Moderate
Back-driving	Self-locking		Easy back-drive	
Backlash	Increases with wear	Constant	Increases with belt wear	Negligible
Repeatability	±0.005 mm	±0.005 mm	±0.004 mm	≤2 μm (best)
Duty-cycle	Max. 60 %		Max. 100 %	
Efficiency	Bronze bushing ≤ 40 %	≥90 %	≈90 %	90–95 %
Life	Short: high friction	Longer	Longer	Longest
Shock-loads	Higher	Lower	Low	Highest
Smoothness	Smoot: low speeds		Smooth at all speeds	Smoothest
Speeds	Low	High	Higher	Highest
Cost	~~££~~-Lowest	~~££~~-Lower	~~£££~~-Moderate	~~££££~~-Highest

Adapted from Johnson (1991) and Smith et al. (2008)

a linear drive system can achieve: ≥3 m s^{-1} with ≥1 μm resolution. Summarising the advantages of a linear motor drive system over that of conventional CNC machine tool drive systems—shown in Figs. 1.24a and 1.25 (fitted here to travelling column vertical Machining Centres) they:

- eliminate rotation—to that of translation mechanisms;
- offer zero backlash and fast response;
- produce high translatory speeds with great accuracy and precision;
- have a very fast response time.

1.12.6 Linear and Rotary Axis Positioning/Monitoring Systems

Recirculating Ballscrew—Thermal Stability and Control Problems

The thermal accuracy and precision of CNC machine tools is presently of increasing and critical importance, bearing in mind the widely varying operating conditions in many manufacturing production companies today. This factor is particularly relevant where the small production batches necessitate constantly changing machining tasks. Hence, under these quickly changing operational circumstances, a thermally stable condition cannot be readily accomplished. In a similar manner, the accuracy/precision of the first-off workpiece is now also becoming a critical feature for a company's profitability for its current and

future production orders. Furthermore, the continuous changes between machining operations such as drilling, and roughing and finishing milling operations, will also contribute to the variations in the machine tool's thermal condition. For example, during rough milling operations, high speed/velocity motions of the machine's slides are demanded, to obtain the desired volumes of stock removal and increased production rates, which will add to the thermal values $\geq$80 %, while conversely, values of $\leq$10 % will only be attained during any finish milling operations. Consequently, with these increasingly high accelerations/decelerations, coupled to the higher feedrates that are a necessary feature of manufacturing today for increased stock removal, this so-called rapid machining strategy, promotes some increased heating of the recirculating ballscrew, in the machine's linear feed drives.

In the last few decades there has been a significant development in high-speed machining (HSM) operational strategies by many machine tool builders and certain end-users. If recirculating ballscrew-driven systems are utilised for HSM, these mechanical drives will create additional limitations promoted by their critical speed of rotation. Subsequently, at this critical speed, a ballscrew starts to resonate[95] at its natural frequency—termed ballscrew whipping (i.e. potentially inducing some machining instability). Therefore this critical speed is proportional to the distance between the ballscrew's supports squared. Accordingly and in the worst-case assembly configuration,—this being for a very long and slender ballscrew-driven machine tool with wide supports—the ballscrew's resonating critical speed will be $\approx$2500 rev min^{-1}. In order to mitigate the problem of a ballscrew's high rotational speed—now being demanded for fast linear motions—high accelerations/decelerations in an HSM strategy mean that machine tool builders might utilise multi-start ballscrews (see Fig. 1.29, top, where in this case, matching twin 2-start recirculating ballscrews are fitted). So, with this variety of multi-start ballscrew arrangement, rotational speeds are halved. In order to alleviate this high-rotational speed problem with recirculating ballscrews that are attempting fast accelerations/decelerations,[96] linear-driven axes are often being fitted to specific HSM machine tools—see Sect. 1.12.5.

Yet still another problem that is associated with utilising recirculating ballscrews is the frequently mentioned term ballscrew wind-up. Here, the actual cutting

[95]**Resonant frequency**, this can be simply-defined as: "The frequency at which the magnitude ratio reaches a maximum value greater than unity".

[96]**Forces of acceleration**: for example the mean axial rigidity of a feed drive mechanism (e.g. see Fig. 1.28), lies within the range of: 100–200 N μm^{-1} (i.e. with the actual distance between the Ballnut and its fixed bearing of 0.5 m, with here in this case, being equipped with a Ballscrew mm). Therefore, in this type of machine tool configuration, on a typical CNC machine tool having slide of mass 500 kg and then operating under a moderate acceleration of just 2 m s^{-2}, this will result in deformations of between 5 and 10 μm, which in this instance, cannot be recognised by its rotary-encoder system. While the present machine tool trend is toward significantly higher accelerations/decelerations, this will unavoidably and then inevitably result in increasingly greater ballscrew deformation values.

forces create a slight twisting-rotation to the ballscrew, which is not positively identified and corrected by the attached rotary encoder thus creating a minute torsional effect inducing a potential positional measurement uncertainty in the slide's placement along its axis. Therefore, the CNC machine tool's slide positional measurement—employing highly accurate and precise linear encoders (see below) in the feed drives, plays a fundamental role in stabilising the thermal and mechanical behaviour—and hence accuracy and precision of these types of CNC machine tools.

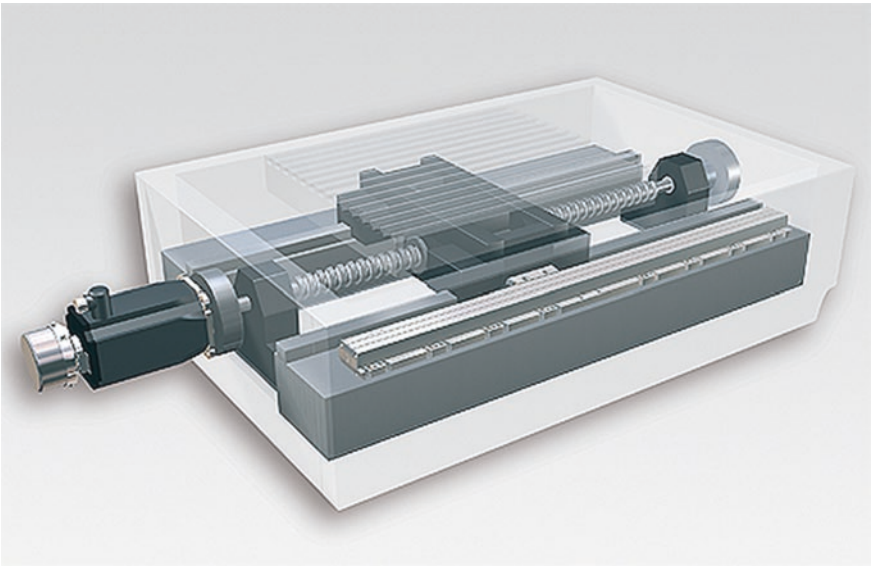

Utilising a linear encoder for a CNC machine tool slide's positional measurement, means that the control loop includes its feed mechanics—this often being referred to as a closed loop operation [courtesy of Heidenhain (Traunreut, Germany)]

A question that is often postulated is, "Should a company stipulate and specify, when purchasing a new CNC machine tool, the potential purchase of either a Rotary, or Linear-encoder system?". The fundamental problem involved with axis positional measurement when utilising a rotary encoder attached to the Recirculating ballscrew, is the thermal expansion created by this ballscrew in-service. In a small-batch machining environment, typical time constraints are usually of between one-to-two hours—or sometimes much less—of actual CNC usage. Hence, with the most utilised machine's axis, this ballscrew's thermal expansion can result in a positioning error of ≈100 μm magnitude—depending upon the nature and length of the actual CNC part program. This slide's positional uncertainty completely obliterates any thermally induced structural deformation and geometric errors produced within any machining and turning centres

configurations. Of note, is that after every new CNC part program machining operation of any level of reasonable complexity and length, the actual ballscrews will require ≈1 h to attain a thermally stable condition. This thermal growth condition will also apply for interruptions in the machining operational cycle.

By way of a practical rule of thumb for the thermal expansion of a ballscrew we can say that "Over the entire length of a cold Ballscrew of one metre in length, it will expect to grow by between ≈0.5 and 1 μm—after every double stroke of the slide". This potential thermal expansion will obviously accumulate, within certain time constraints.

Linear Axis Positioning/Monitoring Systems

In order to mitigate such thermal ballscrew fluctuations that have been created by the higher velocities/speeds of axes within the CNC machine tool, the role of linear encoders (below) for positional measurement becomes critically important for high-quality machined component output. Linear sensors and encoders are utilised regularly in CNC machine tool environments and high precision/accuracy equipment is employed to monitor the position, distance, direction and also speed of this type of industrial plant. Further, linear and rotary encoder types enable machine tool engineers to precisely control these kinematic motions by providing reliable feedback within the closed-loop process. In the main, optical rotary encoders are mostly deployed as a technique of transforming mechanical rotary motion into an electrical output—see Appendix 2. Usually, within this classification of encoders, there are three basic configurations; they are: (i) incremental; (ii) absolute or (iii) multi-turn absolute encoders. Such various types of encoders have comparable basic components where they function with the correspondingly similar basic principles. As a result, each of these encoder configurations offers a range of diverse performance characteristics, capabilities and, end-user benefits. So, within the CNC machine, its linear encoder is a form of sensor/transducer/readhead, which is paired with a scale that encodes the linear slide's position. At this time the sensor will read the linear scale in order to convert the encoded position into either an analogue, or digital signal, which can then be decoded into its actual linear position by the machine tool's motion controller.

It is customary to utilise an encoder that can be either of an incremental or absolute type. Slide motion can be established by the change in its relative position over time. The current versions of linear encoder technologies could include optical, magnetic, inductive, capacitive and eddy current variants. As a result, a sensor will read the linear scale in order to convert the encoded position into either an analogue or digital signal which can then be decoded into a discrete slide position, usually by some form of motion controller. So, this encoder may be either of an incremental or absolute variety, thus any slide motion can be determined by alteration in its position over time.

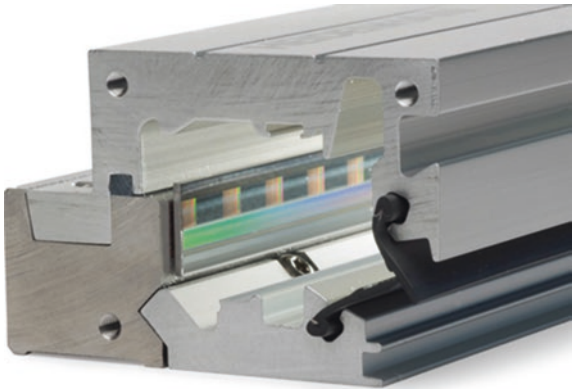

Shown above, can be seen a fully sealed linear encoder for CNC machine tools. Therefore from a grating period of 8 μm, the interferential measuring principle of the encoder generates scanning signals with a signal period of just 4 μm. These scanning signals are basically free of any harmonics and can be highly interpolated. The position error within one signal period, is typically $<\pm 0.04$ μm, this is equivalent to just <1 % of the signal period [courtesy of Heidenhain (Traunreut, Germany)]

Machine tool linear encoders are transducers that can utilise a variety of differing physical properties in order to achieve an encoded machine slide position. There are numerous types of linear encoders commercially available, with just some of which being listed below:

- **scale/reference based—**optical linear encoders of this type tend to dominate the high-resolution metrology/machine tool industrial market where they employ either shuttering/Moiré diffraction or holographic principles. Normally, the incremental scale periods can vary from 0.0001 to 0.00001 μm and after suitable interpolation, they can provide resolutions down to a nanometre.
  NB Typical light sources utilised may include: infrared LEDs, visible LEDs and miniature light bulbs as well as laser diodes;
- **magnetic**—magnetic linear encoders use either active (i.e. magnetised), or passive (i.e. variable reluctance) scales, with the position sensed by utilising: Sense coils, Hall effect, or Magneto-resistive readheads. Magnetic linear encoders have a more coarsely defined scale period than the equivalent optical encoders (e.g. typically being 0.0002 μm–2 mm) with a characteristic resolution in the order of ≤ 1 μm;
- **capacitive**—a capacitive linear encoder functions by sensing the capacitance between its reader and the machine's linear scale. A disadvantage here being the actual sensitivity to patchy debris, which could in this part of the slide's region, influence a change in the relative permitivity;
- **inductive**—inductive technology is unlike that of the capacitive encoders as they are simply unaffected by any form of contaminants. Typical of this type is the inductive measuring principle, being well-known as an Inductosyn;
- **Eddy current—**these Eddy current type digital encoders utilise a scale that is coded with high- and low-permeability non-magnetic materials, which is then detected and decoded by monitoring fluctuations in the inductance of an AC circuit that also includes an inductive coil sensor.

Output Signal Formats

As briefly and previously mentioned, most machine tool's linear encoders can have either an analogue, or digital output, thus:

- **analogue linear encoders**—these have been the normal industry standard, where the analogue output has sine and cosine quadrature signals. These outputs are normally transmitted differentially, thus improving their noise immunity. The quadrature sine/cosine signals can be simply monitored by an oscilloscope in its *X*–*Y* mode, to present a circular Lissajous figure.[97] The highest accuracy signals are attained when the Lissajous figure is circular—here having no gain/phase error and being perfectly centred. Most linear encoder systems utilise automatic circuitry to trim these error mechanisms. The overall accuracy and precision of these analogue linear encoders are a combination of both the scale accuracy and any errors introduced by the readhead. The scale contributions to the Error budget[98] include both linearity and slope—termed scaling factor error. Readhead error mechanisms are normally designated as either a cyclic error or Sub-divisional error (SDE), as they will repeat for every scale period. Conversely, the largest contributor to readhead inaccuracy is the signal offset, which is followed by its signal imbalance (i.e. ellipticity) and the phase error

[97]**Lissajous figures**: or mathematically, a **Lissajous curve** as it is also more commonly known, or indeed termed a **Bowditch curve**, which is the graphical representation of a system of parametric-equations, shown below:

$$x = A\ \sin(at + \delta), \quad y = B\ \sin(bt),$$

here, describing complex harmonic motion.

These types of curves were firstly-developed 200 years ago, by Nathaniel Bowditch (1815), while Jules Antoine Lissajous (Jules Antoine Lissajous was a noted French Mathematician—after whom Lissajous figures are named—he was Born: 4 March 1822, in Versailles—died: 24 June 1880, at Plombières-les-Bains, France). Lissajous invented the Lissajous apparatus, which was a device that creates the figures—that bear his name. In this apparatus, a beam of light is bounced off a mirror attached to a vibrating tuning fork and it is then reflected off a second mirror attached to a perpendicularly-oriented vibrating tuning fork (i.e. usually of a different pitch, creating a specific harmonic-interval), then onto a wall—resulting in a Lissajous figure. Of note, are that these Lissajous curves are enclosed by rectangular boundaries. This led to the invention of yet other inventive-apparatus, such as the: Harmonograph. Of note, was that Jules A. Lissajous, was educated at: The École Normale Supérieure, in France) (1857), explained such curves in greater detail—in his later work. The appearance of the Lissajous figure being highly-sensitive to the ratio a/b. For example, for a ratio of **1**, the Lissajous figure produced is an ellipse, but with special-cases including circles: ($A = B$, $\delta = \pi/2$ radians); also, lines: ($\delta = 0$). While another elementary Lissajous figure being parabola: ($a/b = 2$, $\delta = \pi/2$). Conversely, other a/b ratios produce somewhat more complicated curves, which are closed—but only if a/b is rational.

[98]**Error budgets**: these types of budgets are also termed either an Uncertainty budget, or alternatively, as Uncertainty analysis. Error budgets are a simple tool utilised for such processes having exacting-tolerances that are difficult to achieve. In engineering applications, these Error budgets were originally developed for: Diamond turning operations, where ultra-precise and accurate machined components were turned, usually with monolithic single-point diamond tooling. Although today, these Budgets are more widely-employed in the various fields of: Metrology; Optical manufacture, as well as in many other high-precision applications.

(i.e. when the quadrature signals are not being exactly 90° apart). Whereas the overall signal size will not affect a linear encoder's accuracy, the signal-to-noise ratio and its jitter performance could potentially degrade with smaller signals.

- **digital linear encoders**—many of the present variants of linear encoders interpolate the analogue sine/cosine signals in order to sub-divide the scale period, which will then provide a higher measurement resolution. Such interpolation process output is in the form of quadrature squarewaves, this being the distance between edges of the two channels of the resolution of the encoder. The reference mark or index pulse will be digitally processed in the form of a pulse, invariably of one-to-four units of resolution in width. The significant advantage of such encoders with a built-in interpolation and digital signal transmission is in improved noise immunity, although, with their high frequency, fast-edge speed signals they might tend to produce more emc emissions.

Absolute Reference Signals

Together with either analogue or digital incremental output signals, these linear encoders can provide absolute reference, or positioning signals. For example, with most types of incremental linear encoders, they can produce either an index, or reference mark pulse, consequently providing a datum position along the linear scale for use at either the machine tool's power-up stage, or after a loss of power. This index signal has to be able to identify its position within just one unique period of its scale, while its reference mark usually comprises of a single feature on the linear scale, such as an auto-correlator pattern (i.e. typically being that of a Barker code[99]), or a Chirp pattern.

---

[99] **Barker code**, or **Barker sequence**: can be considered as a finite sequence of N values of $+1$ and -1, as simply expressed as follows:

$$a_j \quad \text{for} \quad j = 1, 2, \ldots, N$$

with the ideal autocorrelation property, such that the offpeak (i.e. non-cyclic) autocorrelation coefficients are:

$$C_v = \sum_{j=1}^{N-v} a_j a_j + v \quad \text{where they are as small as possible:}$$

$$|C_v| \leq 1$$

thus, for all:

$$1 \leq v < N$$

There are only nine **Barker sequences** known, all of length '***N***', but at most, there could be even more, thus making it a possible for there to be 13 in total. In his original 1953 paper, R.H. Barker suggested sequences with the stronger condition of: $C_v \epsilon \{-1, 0\}$ but, here only four such sequences are known (*source* Barker 1953).

NB Whereas a **Chirp pattern**, is a signal in which the frequency either increases (i.e. up-chirp), or decreases (i.e. down-chirp) with time. Thus, in some sources, the term chirp is used interchangeably with a sweep-signal, moreover, it has also been called a: **Quadratic-phase signal** (*source* Abramowitz and Stegun 1972).

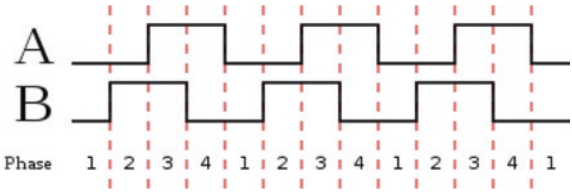

The simple schematic for the 'A' and 'B' quadrature channels (*source* Wikipedia et al. 2015)

Characteristically, the Distance coded reference marks (DCRM) are positioned onto the linear scale in a unique pattern permitting a minimal movement—symptomatically moving past two reference marks—to define the readhead's exact position. Multiple equally spaced reference marks can also be positioned onto this scale in a manner such that following its machine installation, the desired marker can either be precisely selected—usually via a magnet, optical means, or in the case of unwanted ones, they can be de-selected utilising either labels or by being simply painted over.

Absolute Code

By specifying suitably encoded scales such as multi-track, vernier, digital code or pseudo-random code, a linear encoder can establish its position without movement or needing to find a specific reference position. Accordingly, these absolute linear encoders will also communicate utilising serial communication protocols.

Limit Switches

There are various linear encoders, which can include the incorporation of built-in limit switches that are normally either optical, or magnetic in principle. At this point, often two limit switches are used, such as that occurs on the machine's power-up, where the controller can determine if the linear encoder is at the end-of-travel or in which direction to drive this actual machine tool's axis.

Protection and Arrangement of Linear Encoders

Linear encoders can be either of a fully enclosed, or open-type design. Furthermore, the enclosed linear encoders are mainly utilised for machine tool applications, as they often have to exist in very dirty and sometimes hostile environments. Such encoders typically comprise an all-encompassing aluminium extrusion that encloses either a glass or metal scale (i.e. typically, as shown previously above). Here, a flexible lip-seal will permit an internal, guided readhead to then read the linear scale. Accuracy and precision in this arrangement is somewhat limited due to some unwanted friction and hysteresis which is imposed by the mechanical arrangement. Whereas for scales having the highest accuracy and precision, they will necessitate the lowest measurement hysteresis in conjunction with the smallest frictional application; therefore, here it is usual to specify an open-type linear encoder. A variety of linear encoders may utilise either transmissive

(i.e. glass scale) or reflective scales, normally utilising either Ronchi,[100] or Phase grating varieties. These linear scales can use a range of materials for the respective scales, typically: chrome-on-glass; metal (e.g. stainless steel, gold-plated steel, Invar, etc.); ceramics (e.g. Zerodur™); or indeed certain plastics. These linear scales run the entire length of each of the machine's motional linear axis and may be self-supporting, thermally mastered to the substrate (i.e. via an adhesive, or adhesive tape); or alternatively track mounted. Track mounting can allow the linear scale to sustain its particular coefficient of thermal expansion,[101] thereby permitting large plant/equipment to be more easily broken down for ease of shipment.

Typical Design and Operation of Industrial-Based Linear Encoders for Machines

The workshop-hardened encoders that are utilised for industrial-based machines must provide effective motion control. So these motional systems necessitate the correct application of high-performance linear or rotary encoders. If the current metrological application demands a scale with an ultimate positioning

[100]**Ronchi test**: in 1923, the Italian Physicist Vasco Ronchi (**Vasco Ronchi**: (Born: 19 December 1897 in Florence—died: 31 October 1988) was a notable Italian Physicist who was known for his excellent work into Optics. As well as yet another distinguished Italian Physicist: Enrico Fermi, Ronchi was a student of the prominent Physicist: Luigi Puccianti. Ronchi, undertook his formal studies at: The Faculty of Physics, of the University of Pisa—in Italy, from 1915 to 1919 (*source* Ronchi 1923) published a description of the eponymous: **Ronchi test**, which is a variation of the: **Foucault knife-edge test** and in which, it utilises some simple equipment to test the essential quality of Optics. Thus, a **Ronchi-tester** would consists of the following apparatus: a light source; a diffuser; plus a Ronchi-grating. Here a Ronchi-grating, consists of a regular series of alternate dark and clear stripes.

[101]***Coefficient of thermal expansion***: thermal expansion can be considered as the tendency of matter to change in volume in response to a change in its temperature. Consequently, when a substance is heated, its atomic particles will proceed to move in a more vigorous manner and will thus normally maintain a greater average atomic separation. Moreover, any materials that tend to contract with increasing temperature are quite unusual; this effect is limited in size and will only occur within distinct temperature-ranges. Thus in the former case, the degree of a material's expansion, divided by the change in temperature—termed the material's **Coefficient of thermal expansion**, which will thus generally vary proportionally with its temperature, as given in the following the first approximation formula, which is both explained and given below:

Linear expansion:

To a first approximation, which is the change in length measurements of an object (i.e. its linear dimension—as opposed to for example, to its volumetric dimension), due to thermal expansion, which is related to temperature change by its linear expansion coefficient. Hence, it is the fractional-change in length per degree of temperature change and assuming a negligible-effect of pressure, which means it can then be simply-expressed as follows:

$$\alpha_L = 1/L\,\mathrm{d}L/\mathrm{d}T$$

where 'L' is a particular length measurement and, '$\mathrm{d}L/\mathrm{d}T$' is the rate of change of that linear dimension per unit change in temperature.

discrimination, in combination with both high accuracy/precision and reliability, the optimum solution might be for a non-contact optical linear encoder—see Figs. 1.39, 1.40 and 1.41. The industrial drive toward higher accuracy/precision has ensured that direct feedback linear encoders are often selected. Accordingly, with the widespread introduction of linear motors on machine tools (i.e. as mentioned in Sect. 1.12.5) and owing to their inherent speed/slide-positioning/simplicity, this has rendered the rotary encoder for many linear applications to be made virtually obsolete. Some innovative metrological suppliers of encoder systems, base their products on these Non-contact optical systems as they provide high resolution with zero mechanical hysteresis, while withstanding ingress by a variety of potential contaminants. The cause of this debris might typically be from light oils, dusts and other detritus, moreover these encoders will have a greater tolerance for any superficial scratches—without compromising the encoder's integrity. For ease of fitment to a machine tool such linear encoders (see Fig. 1.39) have a self-adhesive flexible gold-plated scale which has a lacquer coating—for handling/protection/ease of maintenance—while being tailored to each axis. The linear encoder can be up to 70 m in length, removing the need for drilling and tapping attachment, thus saving this additional installation time and further financial cost. Here, all readhead and interface combinations feature a setup LED, saving the extra costs that are normally associated with oscilloscope setup equipment. The encoder's various compact readheads are equipped with an integral interpolation facility, having a range of digital and analogue characteristics with outputs ranging from 5 μm to 50 nm being possible. This type of linear encoder is equipped with thermal matching of its scales, which then simplifies thermal compensation of the overall system. In the following text just some of the commercially available encoders will be described in more detail, in order to gain a specific comprehension of how such systems function and operate on CNC-based machines and for certain metrology equipment.

In the schematic diagram shown in Fig. 1.39, a linear encoder of an open non-contact optical configuration is illustrated, having filtering optics offering excellent signal stability of high-resolution operation. Each readhead has industry-standard analogue or square wave outputs, with a 20-μm analogue signal period (i.e. having a digital resolution ranging from just 5 μm to 50 nm). Upon its installation on the machine's axis, the setup LED lights up green when the optimum connection has been achieved. For this type of encoder, a reference mark and/or limit switch outputs can be fitted on all readhead models—this reference mark provides repeatable home or zero position, whilst the limit is employed as an end-of-travel indicator. As can be observed from Fig. 1.39, an infrared LED emits a light onto the angled scale facets, where it is then directed back into the readhead, through a transparent phase grating. This light passage produces sinusoidal interference fringes at the detection plane within the readhead. Here, the optical scheme averages the contributions from 80 scale facets and effectively filtres out signals of those not matching the scale period, thus ensuring signal stability even whenever the scale is either contaminated, or indeed, slightly damaged.

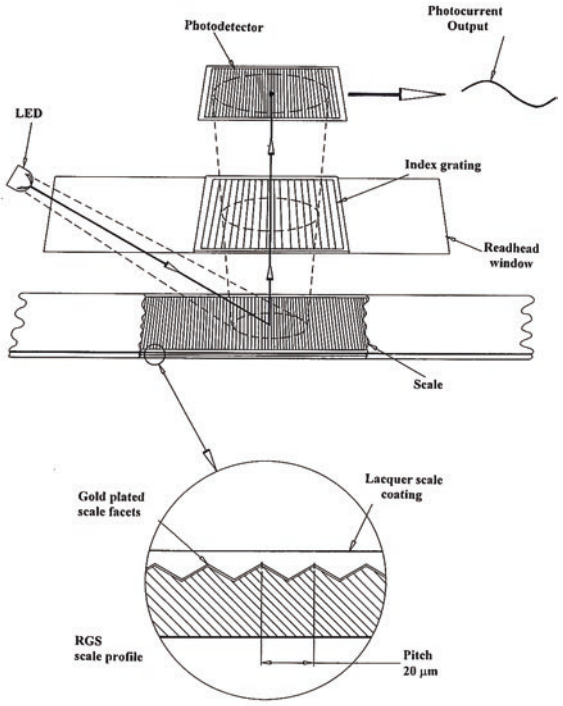

Fig. 1.39 A linear encoder of an open, non-contact optical configuration (courtesy of Renishaw plc)

Laser scale is based on technology utilised for laser calibration of machine tools, being widely known as *linear error compensation.* Theoretical accuracy for a laser calibration system is ±0.1 ppm (±0,025 µm). The scale uses the same principle - interferometry, but is 'packaged' for the machining environment. Beam strength, optical sensitivity, and other features have all been enhanced over a calibration laser to achieve high accuracy in an actual machining environment. The scale is shock rated to 35g, tolerates vibration of 10g at 3-300 Hz, and is sealed to: IP65 (NEMA 12/13).

[Courtesy of Renishaw plc]

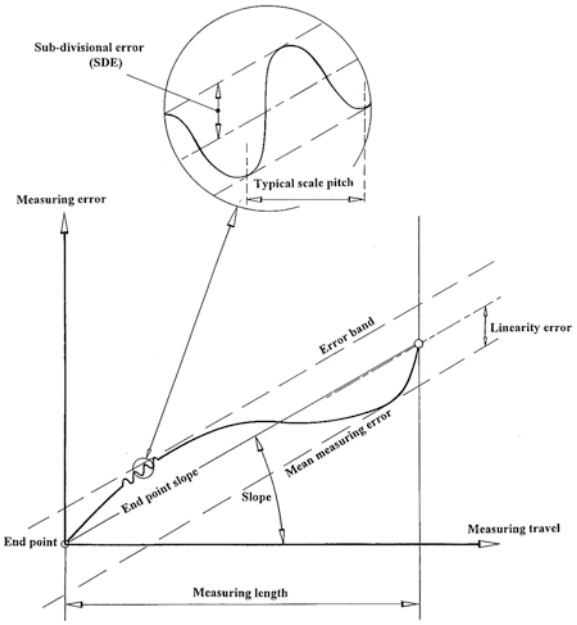

Fig. 1.40 Typical measuring errors occurring over the scale's measurement length (courtesy of Renishaw plc)

In encoders fitted to a machine's structure, the thermal characteristics often contribute a significant role in determining the overall measurement accuracy/precision—see Fig. 1.40. Therefore, as the self-adhesive backing scale is rigidly restrained at its ends (i.e. normally via epoxy-bonded end-clamps) it must forcibly match the thermal behaviour of the substrate (i.e. when attached to the machine's structural member) removing the need to compensate for yet another potential coefficient of expansion. In this situation, the low short-term errors are assured by the innovative optical design, typically producing $>\pm 0.15$ μm cyclic error, or as it is often termed Sub-divisional error (SDE). This detail is included within the linearity specification of ± 0.75 μm in 60 mm, or alternatively ± 3 μm in any metre length. These linear encoders are supplied in reels of these continuous lengths, which can then be precisely cut to the actual lengths required at the point of installation—with the minimum of axis preparation. Hence, the scale's installation on any axis becomes both quick and easy to achieve, by utilising the application tooling provided with the fitment kit, which then utilises the actual motion of the machine's axis to ensure its correct linear alignment. Finally, to complete the encoder's installation, the reference mark, limit switch actuators and end-clamps are then simply glued into place.

In Fig. 1.41 similar, but somewhat different from Fig. 1.39, is an Open non-contact optical system but here the obvious differences are readily apparent, in that the scale pitch has now been increased from 20 μm to that of 40 μm. This modified profile with a coarser facet design and pitch (see inset diagram in Fig. 1.41) allows for greater speed, coupled to more compliant tolerances when orientating the optical elements. In this optical configuration—displayed in Fig. 1.41, the

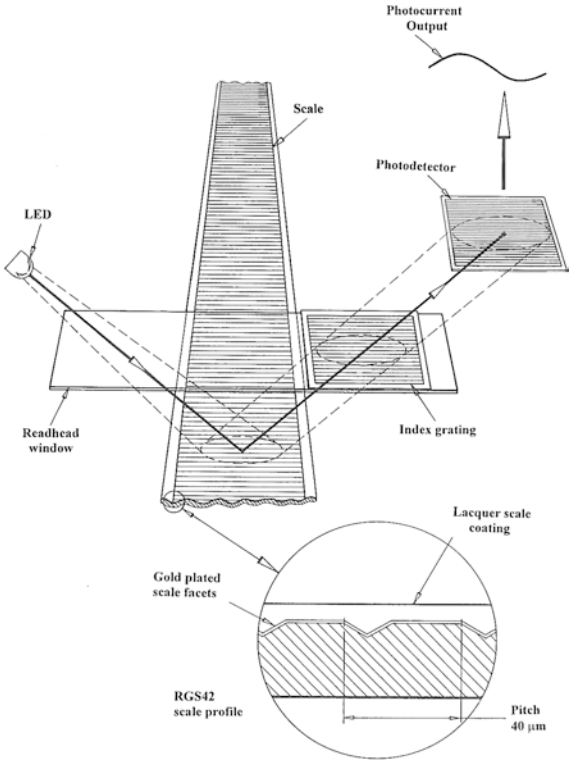

Fig. 1.41 A linear encoder of an open, non-contact optical configuration, with a faster operational speed (courtesy of Renishaw plc)

infrared LED emits light which is reflected from the scale face at 90° to the scale axis—rather than parallel to it—as depicted in Fig. 1.39; while the index grating is positioned identically to that of Fig. 1.39, thus producing its required sinusoidal interference fringes at the detection plane. By this differing optical arrangement, it facilitates the use of a variety of scale types, such as a:

- **gold-plated scale**—which is lacquer coated incorporating self-adhesive backing;
- **chrome-on-glass scale**—this version can be utilised where shorter lengths and an uncalibrated accuracy/precision is required, normally up to 1 m in length;
- **customer designed reflective etched linear and cylindrical steel scales**—this version can also be read by a range of differing readheads.

Of note, is that all of these readheads can maintain a low short-term error, typically having a cyclic error of just ±0.25 μm. The specific linearity of the linear encoder's scale is once again miniscule, being: ≤1 μm in any 60 mm and ≥±3 μm in any 1 m length.

Planar Encoders

One type of Planar encoder system is depicted in Fig. 1.42, where it features an *X*–*Y* readhead that is mounted directly onto the moving stage, with the position feedback being truly direct thus totally eliminating any possibility of either Abbé and orthogonality errors. This readhead has a small footprint enabling it to be easily integrated in a flexible range of mounting configurations. The readhead features a 1 V_{pp} analogue output with a remarkable level of Lissajous stability. This analogue output can be interpolated by a range of interface units, giving a digital output resolution to 0.1 μm. These planar encoders are perhaps an ideal installation for applications requiring high-speed direct positioning systems, offering accurate and precise positional feedback notably for Pick-&-place machine configurations.

The grid pattern (shown in schematically in plan-view and being the main diagram in Fig. 1.42) utilises a chess board-patterned chrome-on-glass grid-plate as

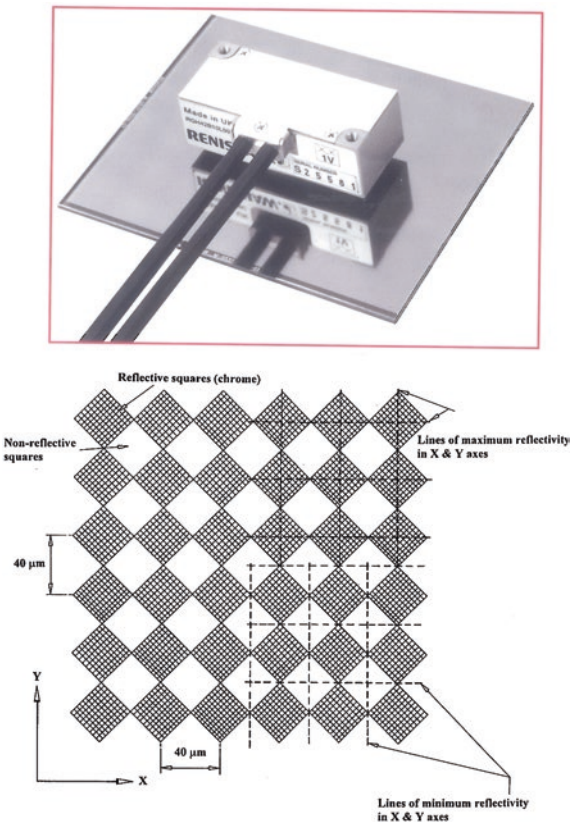

Fig. 1.42 Typical configuration of a planar encoder's grid pattern (courtesy of Renishaw plc)

the scale medium—these grids being of various dimensional sizes. Each optical element in the readhead will read the reflected light from the lines of maximum and minimum reflectivity. As a consequence, due to the accurate/precise pattern of reflective and non-reflective squares, these lines appear in both the *X*- and *Y*-axes, enabling them to be individually read by the two optical elements in the readhead—these being orientated at 90° to each other. Of note, is that this grid plate is manufactured from 1.5-mm thick fused silica glass, having a coefficient of thermal expansion of just 0.55 μm/m/°C. Thus, the chess board pattern chrome scale has a 40-μm pitch in both axis directions—matching the readhead optics—whilst having a standard measuring range of area 70 mm × 70 mm.

The actual readhead is comprised of two optical elements; in the body (i.e. separately reading the *X*- and *Y*-axes) signals being output via two separate cables—as illustrated in Fig. 1.42 (top). Typical readhead outputs conform to the 1 V_{pp} analogue standard—across a range of interpolators, giving digital square wave outputs ranging from 10 to 0.1 μm—in resolution. This interpolator also houses the setup LED. Here, the readhead can be mounted on both the top and side faces of the plant, with its actual ride height being established by the application of some plastic shimming. The planar readhead maintains low cyclic errors, typically ±0.25 μm, while the standard-sized grid pattern can resolve any machine motions down to just ±2 μm over its entire area.

Rotary and Angular Encoders

In Fig. 1.43, a range of industrial workshop-hardened Rotary/angular encoders scales are depicted. These particular rotary encoders can typically have an angular accuracy of ≥±10 s. Such angle encoders are found across a wide variety of machine tool applications that require precision angular measurement to accuracies within several arc seconds. Sub-assembly equipment positioned on CNC machine tools may also employ these rotary/angular encoders, including rotary tables, swivel heads—see Fig. 1.44b, as well as C-axes of Turning Centres—see Fig. 1.22.

Angle encoders can characteristically include the following mechanical design, such as: an encoder with an integral bearing, with a hollow shaft and integrated stator coupling. Due to the design and mounting of the stator coupling, it will absorb only that torque caused by friction in the bearing during angular acceleration of the rotating-shaft. This type of angle encoder will therefore provide excellent dynamic performance. With an integrated stator coupling, the specified system accuracy also includes the deviations from the shaft-coupling. Such types of encoders incorporate measuring standards of periodic structures, known as graduations—see Fig. 1.43. These graduations are applied to a glass—Fig. 1.43c—or alternatively to a steel substrate. Typically, the glass scales are utilised primarily in encoders for speeds up to 10,000 m min^{-1}. For encoders utilised for higher speed applications—up to 20,000 m min^{-1}—then steel drums are utilised. The scale substrate for large encoder diameters is normally a steel tape. These precision

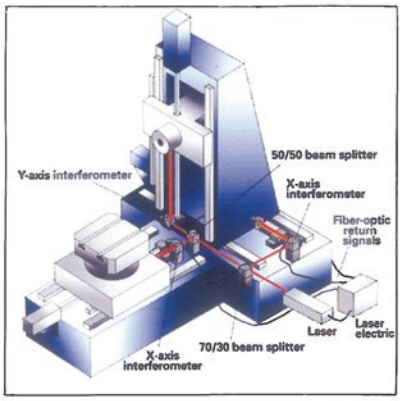

Laser-controlled slideways are now becoming available for machine tools. [Courtesy of C.D. Mize, Perry Automation Consulting Inc, Fl. (USA)]

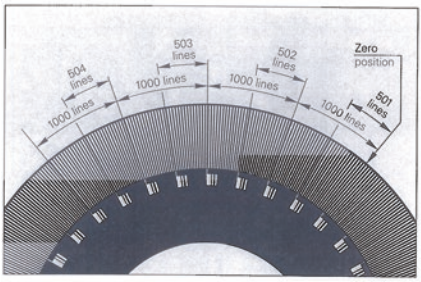

(a) Distance-coded reference marks on circular scale:

Line count z	Number of reference marks	Nominal increment I
90000	180	4°
45000	90	8°
36000	72	10°
18000	36	20°

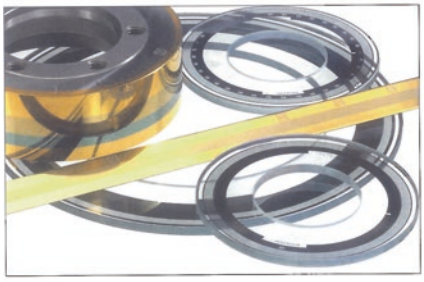

(b) Circular graduations of incremental angle encoders.

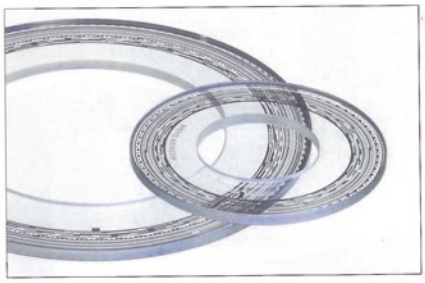

(c) Circular graduations of absolute angle encoders.

Fig. 1.43 Rotary/angular encoders for machine axis displacement (courtesy of Heidenhain (GB) Ltd.)

graduations are manufactured in various Photolithographic processes.[102] Graduations are fabricated from extremely hard chromium lines on glass, or gold-plated steel drums, matte-etched lines on gold-plated steel tape or three-dimensional structures etched into quartz glass. These photolithographic manufacturing processes can produce grating periods of between just 40 and 4 μm onto etched quartz glass—depending upon the etching medium (see Fig. 1.43b, c). As a consequence, these photolithographic processes permit very fine grating periods and are characterised by a high definition and homogeneity of the line edges—Fig. 1.43a. Together with the photoelectric-scanning method, this high-edge definition is a precondition for the high quality of the output signals. Absolute angle encoders, will feature multiple-coded graduation tracks (shown in Fig. 1.43c). The code arrangement provides the absolute position information, which is available immediately after machine's switch-on. The track with the finest grating structure is interpolated for the position value, while simultaneously it is utilised to generate an incremental signal.

In the case of a grating with an incremental measuring method (see Fig. 1.43b) the graduation consists of a periodic grating structure. The position information is acquired by counting the individual increments (i.e. measuring steps) from some particular point of origin. Since an absolute reference is required to ascertain positions, the scales or scale tapes are provided with an additional track that bears a reference mark—shown in Fig. 1.43a. The absolute position on the scale established by the reference mark is grated with exactly one measuring step. The reference mark must therefore be scanned to establish an absolute reference, or to find the last selected datum, while in certain situations this may require a rotation up to nearly 360°. Subsequently, in order to speed and simplify such reference runs, many encoders feature distance-coded reference marks—see Fig. 1.43a—which are multiple reference marks that are individually spaced according to a mathematical algorithm. Here, the consequent electronics will find the absolute reference after traversing two successive reference marks—meaning this is achieved after only a few degrees of traverse—see the Nominal increment I in the table (in Fig. 1.43a, right).

In the case of distance-coded reference marks (i.e. shown in Fig. 1.43a), the absolute reference is calculated by counting the signal-periods between two reference marks and, by utilising the following expression:

$$\alpha_1 = (\operatorname{abs} A - \operatorname{sgn} A - 1) \times I/2 + (\operatorname{sgn} A - \operatorname{sgn} D) \times \operatorname{abs} \mathrm{MRR}/2.$$

[102] **Photolithographic processes**, or **Photolithography**, but it can also be termed as: **Optical-lithography**, or indeed as: **UV-lithography**—which is a process used in micro-fabrication to pattern parts of a thin film, or the bulk of a substrate. Consequently, this **Photolithographic processes**, utilises light to transfer a geometric pattern from a photomask to a light-sensitive chemical photoresist, or simply resist—onto the substrate. Here, a series of chemical treatments will then either engrave the exposure-pattern into, or enable a deposition of a new material in the desired pattern upon, the material underneath the photo resist—to create this desired pattern (*source* Jaeger 2002).

where

$$A = 2 \times \text{abs}\,\text{MRR} - I \big/ \text{GP}.$$

'α_1' = Absolute angular position of the first traversed reference mark to the zero position in degrees; 'abs' = absolute value; 'sgn' = sign function ("+1" or "–1");
'MRR' = measured distance between the traversed reference marks in degrees;
'I' = nominal increment between two fixed reference marks (see table in Fig. 1.43);
'GP' = grating period (360°/line count); 'D' = direction of rotation (+1 or –1).

NB Rotation to the right (i.e. as seen from the shaft side of the angle encoder) gives "+1".

Many of the present day encoders operate using the principle of photoelectric-scanning. Photoelectric-scanning of a measuring standard is contact free and is therefore free from wear. This photoelectric-scanning technique can detect very fine lines of not more than a few micrometres wide, resulting in the generation of output signals with very small signal periods. In consequence, the finer the grating period of a measuring standard, the greater will be the effect of diffraction on photoelectric-scanning. In this particular company's product literature for the instrumentation shown in Fig. 1.43, two scanning principles are utilised with angle encoders, as either for an:

1. **Imaging scanning principle**—for grating periods from 10 to ≈70 μm;
2. **Interferential scanning principle**—which is employed for very fine graduations with grating periods of 4 μm.

Simplistically and in more detail for the former technique of the Imaging scanning principle, it functions by means of projected-light signal generation; here, two graduations with equal grating periods are moved relative to each other—these being the scale and the scanning-reticle. The carrier material of the scanning reticle is transparent, although the graduation on the measuring standard may be applied to a transparent, or reflective surface. Hence, when parallel light passes through a grating, light and dark surfaces are projected at a specific distance. At this distance, an index grating with the same grating period is located at this position. So, when the two gratings move relative to each other, the incident light is modulated. As a result, if the gaps in the gratings are aligned, light passes through them. If the lines of one grating coincide with the gaps of the other, then in this case, no light passes through. Photovoltaic cells convert these variations in light intensity into electrical signals. The specially-structured grating of the scanning reticle, filters the light current to generate nearly sinusoidal output signals. The smaller the period of the grating structure, the closer and more tightly toleranced the gap must be between the scanning reticle and the circular scale. The practical mounting tolerances for these encoders with the Imaging scanning principle are achieved with grating periods of 10 μm.

1.13 Finite Element Analysis (FEA) of Machine Tools

Introduction

Mathematically, the Finite Element Method (FEM) is a numerical technique for establishing approximate solutions to boundary value problems for differential equations. Techniques utilise variational methods (i.e. termed the Calculus of variations) to minimise an error function and produce a stable-solution. Analogous to the knowledge that connecting numerous miniscule straight lines—which can approximate a circle—FEM incorporates all the methods for connecting many simple element equations over many small sub-domains entitled finite elements to approximate a more complex equation over a larger domain. Consequently, Finite element Analysis (FEA) consists of a computer-generated model of a material or a design that is stressed and analysed for specific results. FEA is invariably utilised in a new product's design, or for certain aspects of existing product refinement. Subsequently, often FEA is employed by adapting an existing product, or when analysing a machine tool structure which is then exploited to qualify this product or structure for a potentially new service condition. In general, there are normally two distinct types of this variety of analysis being employed by industries today, namely:

1. **2-D modelling**—which conserves the simplicity of a basic design and then permits the analysis to be run on a relatively low-memory usage computer, although it has a tendency to yield somewhat less accurate results;
2. **3-D modelling**—with this application, it will generate more accurate and practical results, whilst effectively sacrificing the ability to run on all but the very fastest of computers.

Within each of these differing 2-D and 3-D modelling systems, the FEA programmer can insert numerous algorithms (i.e. functions) which may make the system perform and operate either linearly or non-linearly. The linear systems are significantly less complex and normally will not take into account any potential plastic deformation present. However, the more sophisticated non-linear systems do offer an interpretation for plastic deformation and many variants are also capable of testing a material to its complete destruction (i.e. to its catastrophic failure/fracture conditions).

Finite element Analysis (FEA) will utilise a complex system of interrelated-points that are termed **nodes**, which create a grid which is known as a **mesh** (see Fig. 1.44a and below). This mesh is then programmed to contain the material and structural properties, which can define how the structure will react to definitive loading conditions. It follows that nodes are then assigned at a specific density throughout the material, contingent with the anticipated stress-levels of a particular area. As a result, any of these anticipated high-stress regions that tend to receive relatively large amounts of stress, will customarily have a higher node-density than those which experience little, or indeed no apparent stress. Invariably,

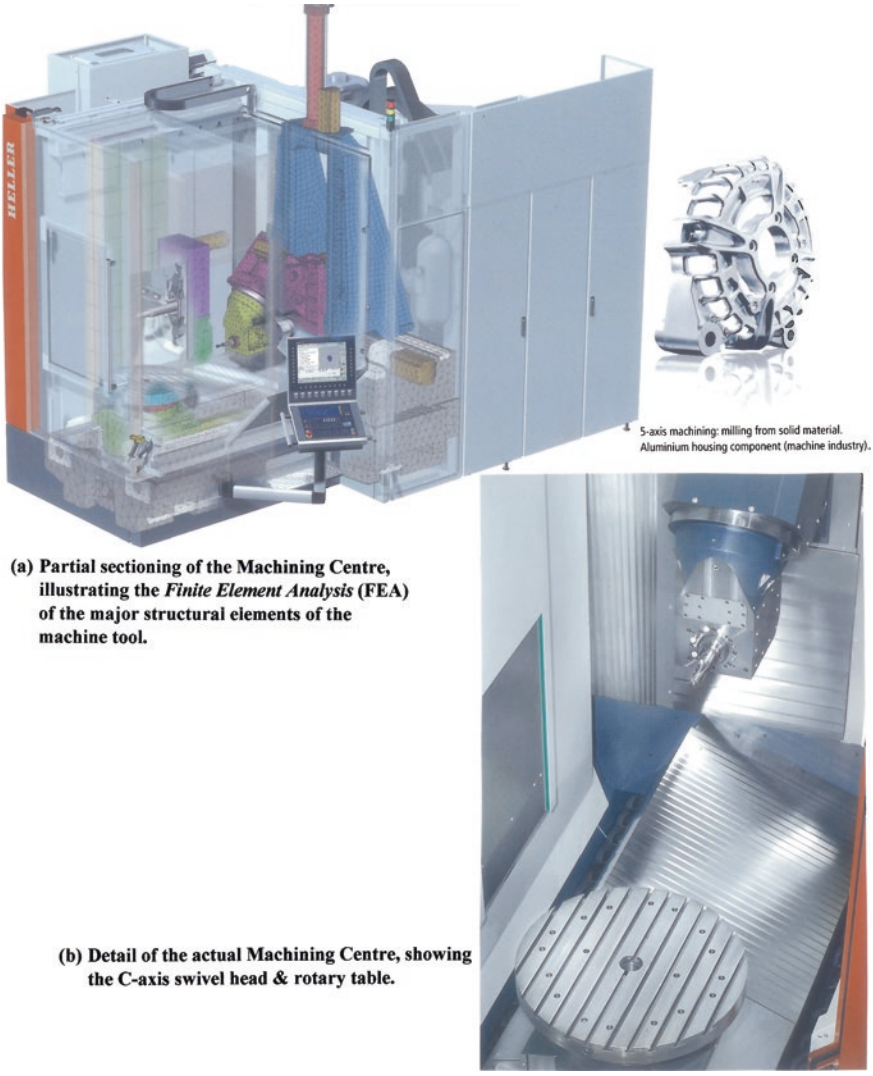

Fig. 1.44 A five-axes machining centre, with its main structure being constructed from an epoxy-resin concrete—for efficient vibration damping and thermal stability, fitted with an *C*-axis swivel head and integrated rotary table (courtesy of Gebr. Heller Maschinenfabrik GmbH)

these points of interest may typically consist of the fracture point of previously tested material, the positioning of fillet radii, any potential sharp corners, complex and multi-part detailing, together with any highly-stressed areas. An analogy for this mesh, is that it acts in a similar manner to that of a Spider's web, in that from each node, it will extend the mesh element to each of the adjacent nodes.

Accordingly, this web of vectors is what transmits the material properties to the object, creating the three node elements.[103]

1.13.1 FEA of CNC Machine Tools

In the cases of all types of CNC machine tools and CMMs, they are predisposed to exogenous effects, which invariably occur due to changeable environmental conditions—when there are large temperature variations taking place, most notably during day to night time shift patterns in companies, or across annual seasonal transitions. As a consequence, any actual thermal gradients will cause heat to flow throughout the machine's structure, resulting in non-linear structural deformations—occurring even if the machine is an in-cycle operation, or just residing in its static mode. Such environmentally stimulated deformations accumulate together with internally generated heat effects, resulting in significant displacement errors for machine tool functions over its longer time periods. For many manufacturing industries, any form of environmental testing is usually best avoided because of the associated extensive machine downtime necessary to empirically map this specific thermal relationship, which would be exacerbated by the associated cost to production.

In order to mitigate against any form of long-term environmental testing regimes, the technique of Offline thermal error modelling methodology utilising Finite element Analysis (FEA) significantly reduces the machine downtime necessary to establish the desired machine's thermal response. This so-called offline thermal error modelling technique creates an FEA model of the machine in which the initial thermal states of the real machine and a simulated machine model are matched. One of the major benefits of such an offline programme, is that the methodology determines the minimum experimental testing time necessary on

[103]**Three-node elements**: in the case of these three-node triangles (i.e. shown below in the meshed-model for a machine tool), where these nodes are all exterior and at any point within the element, the field-variable (i.e. which is computed only at these nodes), is described by the approximate mathematical-relationship of:

$$\Phi(x, y) = N_1(x, y)\Phi_1 + N_2(x, y)\Phi_2 + N_3(x, y)\Phi_3$$

where: Φ_1, Φ_2 and Φ_3 = the values of the field variables of the nodes; N_1, N_2 and N_3 = the interpolation functions (i.e. termed shape functions, or blending functions). Correspondingly, in FEA, these nodal values of the field-variable are treated as unknown constants that are to be determined.

NB The interpolation functions are most often given as polynomial forms of the independent variables, being derived to satisfy certain required conditions at these nodes. Of some significance, is the fact that the interpolation functions are predetermined, namely, they are known functions of the independent variables, as such, these functions describe the variation of the field variable within the actual finite element.

a machine, thus enabling a company's production management team to be fully informed of the cost to production of establishing this significant and crucial accuracy parameter. Possibly the most noteworthy contribution of such offline FEA work, is that thermal model calibration can be significantly reduced from say, several weeks, to a just a few hours.

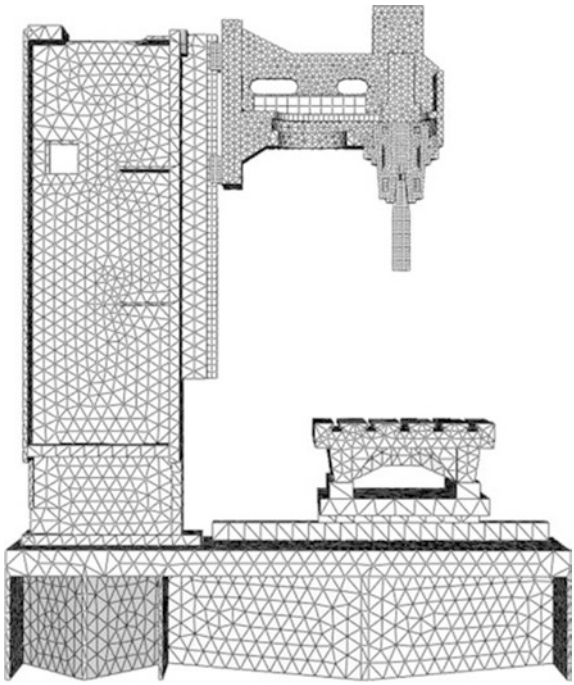

In this particular machine tool example, is shown a typical Finite Element Analysis (FEA) meshed model (i.e. illustrating its three node triangles), of a partially assembled vertical CNC machine tool's structure [*source* Mian, Fletcher, and Longstaff, Centre for Precision Technol., University of Huddersfield, (UK)]

1.13.2 Industrial Machine Tool Case Study in FEA—for a Machining Centre

The Present-Day Machine Tool Market

Currently, a popular orthogonal configuration of CNC machine tools for specific milling/drilling/boring/tapping operations—is considered by many end-users to be by means of the practical operational applications of a Vertical Machining

Centre (VMC). Within the UK ≈60 % of the machine tool market is made up of these variants. So one might ask, "Why would a major machine tool builder introduce yet another machine into this highly competitive environment?" One logical answer must be that this particular machine tool builder—discussed below—considers no other similarly-structured company is currently producing a machine that fulfils their existing and future customer's needs.

So, this potentially new Machining Centre (shown below) was targeted to enter the standard 40-taper VMC market, although the company's current products are best known for their high-end products of Horizontal Machining and Turning Centres. Accordingly, this builder has sought to improve its share of the VMC market in recent years. The majority of the 40-taper machine buyers will often undertake multifarious Spreadsheet comparisons of similar specifications and capabilities when considering purchasing a new machine—by consideration of the relative merits of each competitive machine tool.

Design and Construction of—VMC Machining Centre

This particular machine tool builder's in-house Design and Development Engineers, also considered the previously mentioned spreadsheet exercise; here, setting-out to design a machine tool that would more than match technical category by category that of their competitors—utilising the technique of Value Engineering and Analysis (VE/VA) ratings of comparable machines. Hence, this potentially newly specified machine was designed and engineered from the ground-up, utilising both computer-aided Design (CAD) together with a 3-D Finite Element Analysis (FEA)—mentioned in Sect. 1.13.1. This proposed machine tool design and build project was specifically conducted by the company's own Design Team at their Digital Technology Laboratory (i.e. within Mori Seiki's—Research and Development Facility) in Sacramento, California. These FEA/CAD analytical methods—see just the two illustrations below (left and right respectively)—designated the optimal bed thickness and rib shape and rib position, enabling them to maximise the actual stiffness, without adding any additional weight. This R&D effort helped the company to significantly improve the actual performance of the machine simultaneously reducing the initial machine's development cost.

Final Specification of—VMC Machining Centre

This orthogonal three-axis machine tool's final specification had an *X*-800 mm, *Y*-500 mm, and *Z*-500 mm of axes travel, which was more than adequate for the type of machining-work that typically occurs for this class of industrial plant. Significantly, most competitors' machines of a comparable working-volume utilise a greater footprint on the workshop floor. Further, the machine's worktable has been sited close to the front, so ergonomically speaking, it enabled the Machine tool operator to both setup and to reach the workpiece more readily inside the machine. The machine's enclosure covered the sides and top—to keep machined

chips and any coolant splash contained, yet the doors had adjustable top-panels so that when they were opened, any heavier workpieces could be simply-loaded by an overhead crane. Of significant note is that in operation, any small-improvement in its machine up-time is a major consideration.

This VMC machine-specification features a maximum spindle speed of 12,000 rpm, compared to the class average of between 7000 and 10,000 rpm. Here, the tool spindle utilises direct-drive gearless technology, providing acceleration to its full-speed in 0.97 s. Moreover, a 20,000-rpm spindle was also available as an option. The machine's top rapid traverse rate for all three axes is $\geq$40 m min^{-1}. In the automatic tool changer (ATC) the tool-to-tool changeover time is 1.0 s and likewise, the chip-to-chip time is just 2.6 s. Accuracy and precision were other major considerations, where the company pointed to features beyond built-in structural rigidity that minimises vibration, where this latter aspect is the primary factor that degrades accuracy/precision in any machine in a high-speed application. Thermal growth within the tool's spindle, which also affects its accuracy, was addressed by an optional compensation function. Of note, was a feature that included enhancing maintainability (i.e. the ease-of-maintenance) for these machines in the industrial-field. So that a reduction in the number of components in the ATC occurred, the magazine was also designed to have a direct-drive system rather than the more usual gear train. In order to circumvent worn timing belts on the *Z*-axis (i.e. tool's spindle axis) they were directly connected to its recirculating ballscrew. Lubricant distributors were positioned outside the machine, where they could be more readily reached, moreover, no electrical cables were located under the machine where they are difficult to check and repair—also further aiding maintenance. Some other features that were designed to reduce the environmental burden were also included, such as: oil-free roller-guides on the linear ways; an integral oil-bath; an ATC design to reduce consumption of lubricants; plus an automatic power cut-off that decreases electricity consumption. The CNC control panel utilised the company's own software MAPPS (Mori Advanced Programming Production System) as the interface. This interface is common among all the company's Machining Centres, where it incorporates features previously-requested by its end-users from around the world. Software options, such as CAPS-NET—for remote process logging and CAPS-DSN—for program transfer, provided connections to a factory Ethernet network. The company has conceded that this newly-designed Machining Centre will have its strongest-appeal to buyers that require it for both its quality and value, but not necessarily at the lowest price. They also contend that the productivity-potential of this machine will make it a strong-contender for the optimum return on the investment (ROI)—a compelling selling-factor.

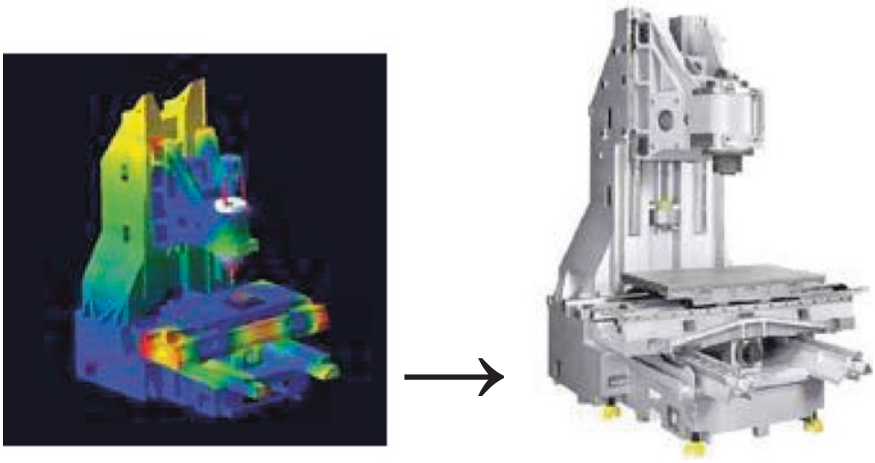

Left So, by utilising the technique of Finite element analysis (FEA), it has revealed the performance characteristics that could be improved through critical design changes—somewhat earlier than would otherwise be anticipated in the machine tool's development process. *Right* Castings for the column and base of this newly-built machine were analysed to maximise resistance to distortion from heavy machining forces. This machine tool company needed a much stronger and stiffer machine that could be taken into production quickly and economically [courtesy of Mori Seiki (Sacramento, Ca. USA)]

1.14 Basic Construction of Coordinate Measuring Machines (CMMs)

1.14.1 Introduction to the CMM

The Coordinate Measuring Machine (CMM)—is shown in just two variants of these sophisticated high-precision instruments in Fig. 1.45 and is a widely used metrology instrument for measuring the actual physical dimensional and geometrical characteristics of an inspected object. CMMs can be either manually controlled by CMM operators or they can be computer controlled—from a previously produced or generated inspection program. Component parts to be measured are accomplished by utilising some form of a probe that is normally attached to the CMMs moving axis. Such probes could be either: mechanical; optical; laser; or white light;—more details will be mentioned concerning probing in Sect. 1.14.3. These CMMs are highly accurate precision instruments, which obtain dimensional workpiece readings from its motional kinematics of six degrees of freedom, displaying such readings in a mathematical format.

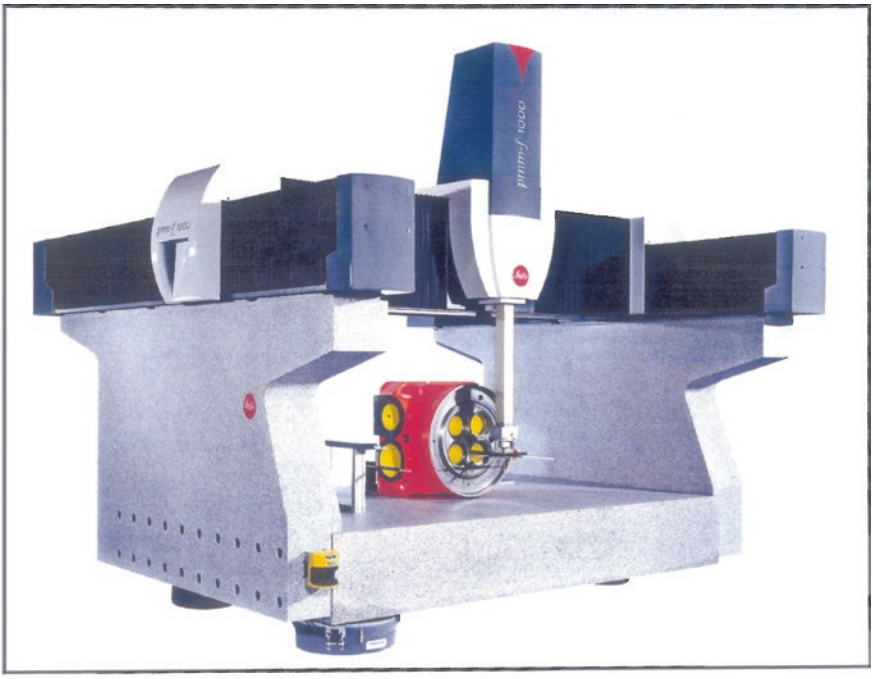

(a) ***Gantry-type CMM*****: at The Bremen Institute for Metrology, Automation and Quality Science (BIMAQ) - part of The University of Bremen (Germany). This Leitz PMM-F has a measurement volume of: 2,5 x 2 x 0,7 m – meaning, critical part features up to a diameter of 2,50 m can be measured highly accurately. NB: The *'maximum permissible error of indication'* (MPEE) for longitudinal measurements is: < 1,6 + L/400 µm - within a temperature range of 18 to 22 °C.**

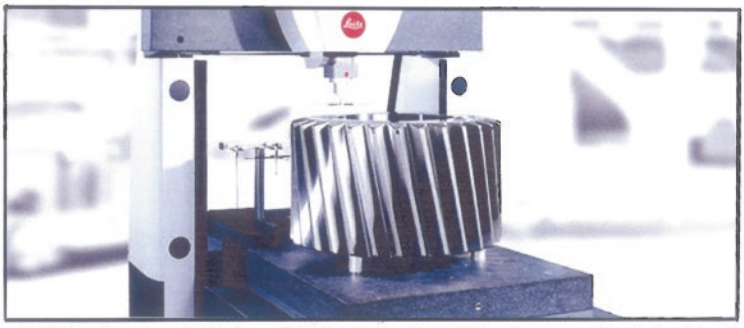

(b) ***Fixed bridge/moving table-type CMM*****: Leitz PMM-C – is versatile, but ultra-high precision CMM and gear metrology-checker.**

Fig. 1.45 Two variants of coordinate measuring machines (CMMs), interrogating parts—with their probing systems [courtesy of Hexagon Metrology (GmbH)]

Historically speaking, the first-representative CMM was developed by the Ferranti Company of Scotland during the late-1950s, due to the pressing-need to measure highly accurate and precise components in the company's own Military-portfolio, although at this time, the CMM was only equipped with two-controlled axes. The first truly commercial CMMs were based upon a three-axis model and was introduced in the 1960s, by the metrology company DEA—in Italy. These first industrialised CNC variants of CMMs made their presence felt during the early 1970s—typically by the Sheffield Company in the USA. Later in Germany, Leitz also designed and manufactured a 3 axis model with a high-quality fixed machine structure, but being equipped with a moving table.

An archetypal bridge type CMM is constructed about three orthogonal axes, namely: *X*-; *Y*-; with *Z*-axes, these are normally equipped with the probing head—see the diagrammatic arrangement shown in Fig. 1.46. Of some significant note, is at the time in a CMM's development, this important touch-trigger probe fitment was designed expressly for the then, newly developing CMM instrumentation—being an essential requirement to enable them to operate and fully realise their metrological-potential. These innovative probes were originally designed, built and tested in the 1970s, by the now Sir David R. McMurtry, the CEO at Renishaw plc (UK)—more will be said on this probing topic in Sect. 1.4.3.

In effect, a CMM normally has each axis orthogonal (i.e. at 90°) to one another, being configured in a characteristic three-dimensional coordinate system. Each of these linear axes also has a corresponding linear-scale system that specifies the exact location of the probe head on that axis. A CMM can be operated by a suitably qualified Inspector—under manual-control—or from within a fully automated CNC program. As a result of the latter case, the CMM will read the input from either a touch or scanning probe as directed within the automated and pre-defined CNC program. As a result, the CMM will then utilise these *X*-, *Y*- and *Z*-coordinates for each of these part-feature points, determining both the size and position of the inspected feature with micrometre precision and accuracy. Moreover, a CMM can also be exploited in the overall manufacturing/assembly processes, testing components, or assemblies against the company's design intent. For that reason, by precisely recording these *X*-, *Y*- and *Z*-coordinates of the measurement-target, dimensional points are then generated that are analysed—normally by bespoke regression-algorithms for the creation of part features. These points are usually collected by employing a probe which is—as previously mentioned—either manually-positioned by an experienced Inspector/Operator, or they can be automatically attained and measured by Direct Computer Control (DCC). Of note, is that a DCC can be repeatedly-programmed to measure whole-series of identical parts, so that it can be considered a CMM, in which it is a specialised-form of industrial robot—perhaps similar to the one featured below.

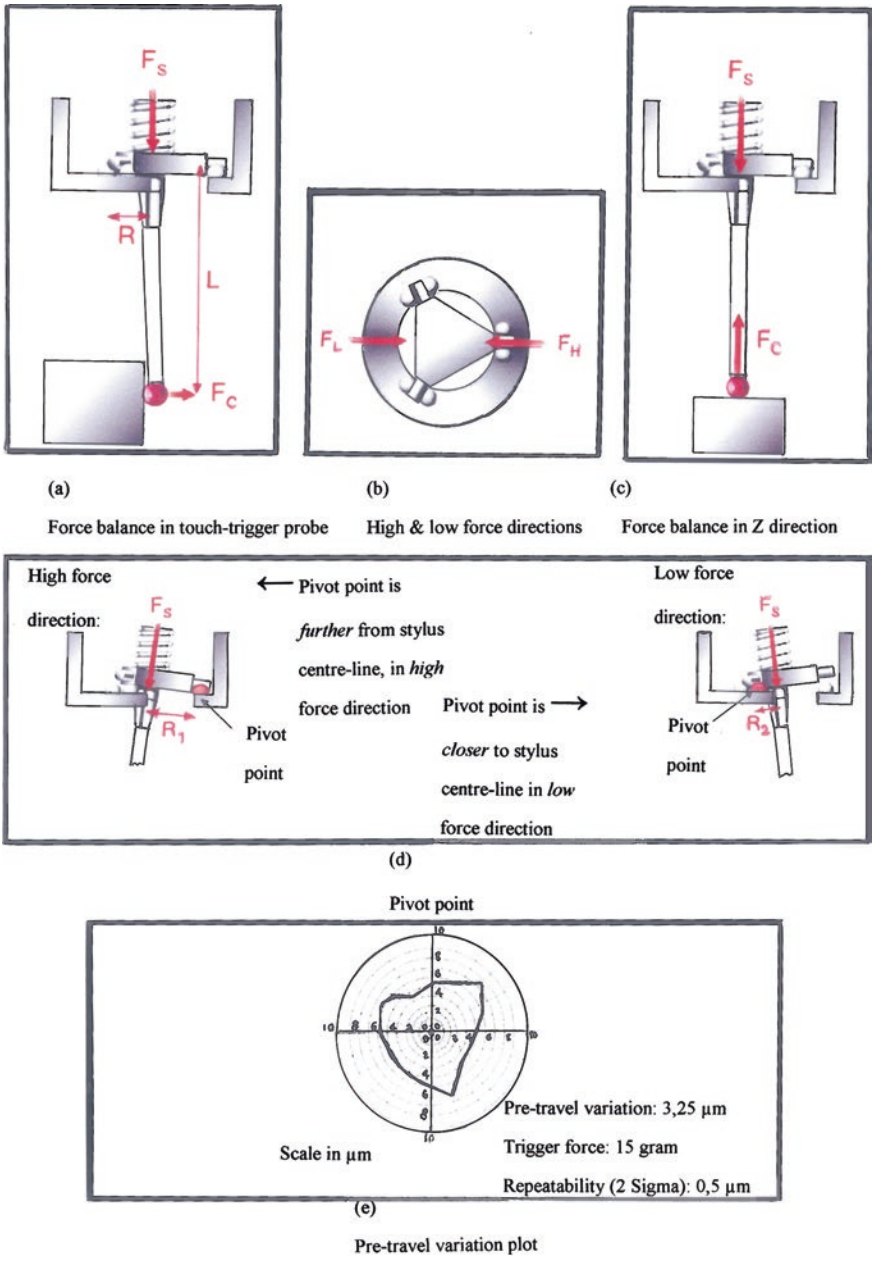

Fig. 1.46 Touch-trigger probe construction and its operation (courtesy of Renishaw plc)

A horizontal/cantilever-type arm CMM is shown above, that is equipped with the company's: HOLOS® NT freeform-surface and analysis software, having an accuracy of: $25 + L/100 \leq 60$ µm. At this time, it is being utilised to achieve automatic and full-measurement of the critical features for example, of a car's door, with an articulating and adjustable probe (courtesy of Zeiss Metrology GmbH)

1.14.2 CMM Construction

The most popular CMM configuration is probably the vertical gantry-/bridge-type superstructure variant. CMMs are frequently designed and configured with a fixed table, with two legs (i.e. columns) supporting its bridge, see two such variants in Fig. 1.45. Here, these CMMs are also arranged with all of the kinematic probe-motions being accomplished by the bridge's three-axis motions. However, with some other vertical bridge-assembly configurations, see Figs. 1.3 (bottom) and 5.20; the bridge can move freely along the granite table with one of the legs—often referred to as the inside leg—normally following a guide-rail which is precisely attached to one side of its granite table. Conversely, the opposite leg—usually termed its outside-leg—simply sits on this granite table while following the vertical surface contour. Yet, still another popular type of CMM configured variant employs a horizontal-cantilevered axes configuration, see above and Figs. 2.1bii and 2.2c.

It is customary to utilise air bearings for the kinematic linear-motions of the moveable-bridge, thus ensuring friction free travel. These air bearings utilise

compressed air, which is forced through a series of minute holes in a flat bearing surface, providing a smooth but controlled air cushion on which the CMM operates, enabling it to freely move in an almost frictionless manner. Hence this movement of, say, the bridge or a gantry along the granite table normally forms one axis of the *X*–*Y* plane. Likewise, the bridge/gantry will contain a carriage which then traverses the length between the inside and outside legs—forming either the *X*-, or *Y*-horizontal axis. The third axis of movement, namely the *Z*-axis, is usually provided by the addition of a vertical spindle that can move up-and-down through the centre of this carriage (bridge). The lightly-contacting Touch probe becomes the sensing device situated on the end of this vertical spindle. This linear kinematic arrangement of the movement of the *X*-, *Y*- and *Z*-axes, fully encompasses the CMM's so-called measuring envelope. Some types of CMMs are also equipped with an integral rotary table—see Fig. 5.20—also within the text in Chap. 5 concerning the Stereometric artefact CMM calibration. Such additional rotary table operational axes can enhance the usage and approachability of the measuring probe to more-complicated workpiece features. Although the fitment of a rotary table as a fourth-drive axis, does not in the main, influence the measurement of dimensions—which distinctly remains as a 3-D kinematic arrangement, it does, however, provide a degree of probing flexibility. In certain of the more sophisticated designs, some Touch probes are powered rotary devices, having programmable ability for the probe's stylus, being able to swivel vertically through $\geq 90°$, while also rotating through a full 360°.

1.14.3 CMM—Mechanical Probe

Initially as described, during the early development of mechanical probes for coordinate measurement (i.e. in the late-1960s) they were fitted into special holders on the end of the vertical spindle—termed its quill as it is often invariably known. These early stylus probes were somewhat basic in their design and construction. A typical stylus at that time, was produced by simply soldering a hardened ball, but of precise and accurate dimensions, onto the end of a shaft then fitting it into the quill. This probe's geometry and level of precision/accuracy was acceptable for measuring a wide range of flat; cylindrical; or spherical surfaces. Yet other styli types were often cylindrically/surface ground to specific geometric shapes, such as a quadrant probe—facilitating the measurement of special part features. These early and somewhat crude original styli were simply manually positioned by the Inspector/Operator against the workpiece feature, with the location in space being read via a 3-Axis digital readout (DRO) or, in the more sophisticated measuring-systems, being logged into simple computer software by means of, say, a foot switch, or similar type of triggering device. Here, these dimensional measurements were obtained by somewhat rudimentary physical contact methods, which were invariably unreliable as these CMMs were moved about their volumetric space—manually. At this juncture, each CMM operator might apply dissimilar amounts of pressure on the probe's stylus, or perhaps adopt differing techniques for a similar measured part feature.

Later in the CMM's development, a notable addition of electric motor drives provided powered control to these three linear axes. Hereafter, operators no longer had to manually control the CMM, but could drive each axis to the desired position on the part's feature, via a hand box, usually equipped with integral joysticks. This addition of a form of machine control of the CMM, meant that the measurement accuracy consistency and its associated precision improved markedly, notably coupled to the fact that the foremost invention at this time was the introduction of the Electronic touch trigger probe. As previously mentioned, the metrological-pioneer of this significant and novel advance in probe-design was by Sir David R. McMurtry successively forming and running a truly-innovative high technology international company now known worldwide as Renishaw plc. This original kinematic omnidirectional probe triggering-mechanism was still a contact-method. The probe head—see the schematics in Fig. 1.46—had controlled and lightly sprung-loaded arms connected to a precise and accurate steel-balled stylus—later modifications utilised a range of differing diameter ruby-balled styli (see the probe-contact schematic, below). The three individual stylus-arms—when at rest—were separately and kinematically-seated on two precision balls equally-spaced at 120° intervals around a flange (see Fig. 1.46b) but lightly-held in position by the controlled force of a compression spring (i.e. Fig. 1.46a, c). Accordingly, as the qualified-stylus gently touched the surface feature of the component, it was deflected (see Fig. 1.46d) and simultaneously electrically-triggered a signal with this *X*-; *Y*- and *Z*-coordinate dimensional information being registered within the computer software. Of note, was that some minute-lobing resulted from probing part features. Thus, these contact probes when originally tested produce this miniscule but significant lobing effect, as displayed on the pre-travel variation plot shown in Fig. 1.46e. Despite this somewhat slight-limitation in the probe's application, this was a true advance in probe-head operational procedure, overcoming the previous unreliable and inconsistent measurement errors produced by individual CMM operators, setting the scene for the introduction of fully CNC-operated CMMs, that are now presently utilised worldwide.

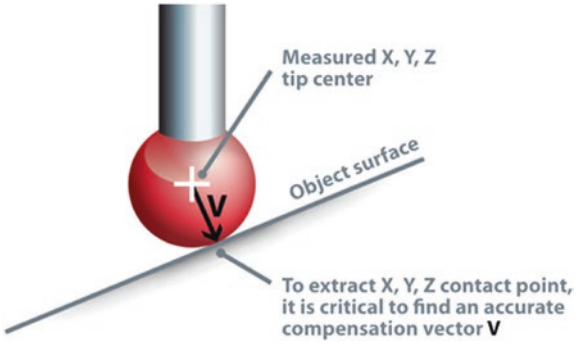

Single-point measurement utilising a contact-based touch probe: it has the points measured at the centre of a spherical tip which are not located on the part's surface. A critical aspect of utilising contact-based probing with a spherical probe tip, consists in computing true surface points from the measured tip centre points. This measurement process is termed: compensation [*source* InnovMetric Software Inc./3D Imaging and Modeling Group: National Research Council of Canada (2014)]

Parallel development of different probe types has been occurring, in particular for the enhancement by Optical probing utilising, for example, a lens-based CCD-system. These types of Optical probes move similarly to their equivalent mechanical types, but here they are aimed at the point of interest (i.e. the component feature) instead of touching the material. The captured surface image will be enclosed in the borders of a measuring window until the residue is adequate to contrast between the black-and-white zones. As a result, the dividing curve can be calculated to a specific point, which is the desired measuring point in space. This horizontal information on the CCD is two dimensional (i.e. in the *X* and *Y* plane) while the vertical location is the position of the complete probing system on the standard *Z*-drive—allowing for an entire 3D-probing facility to be undertaken (Figs. 1.47 and 1.48).

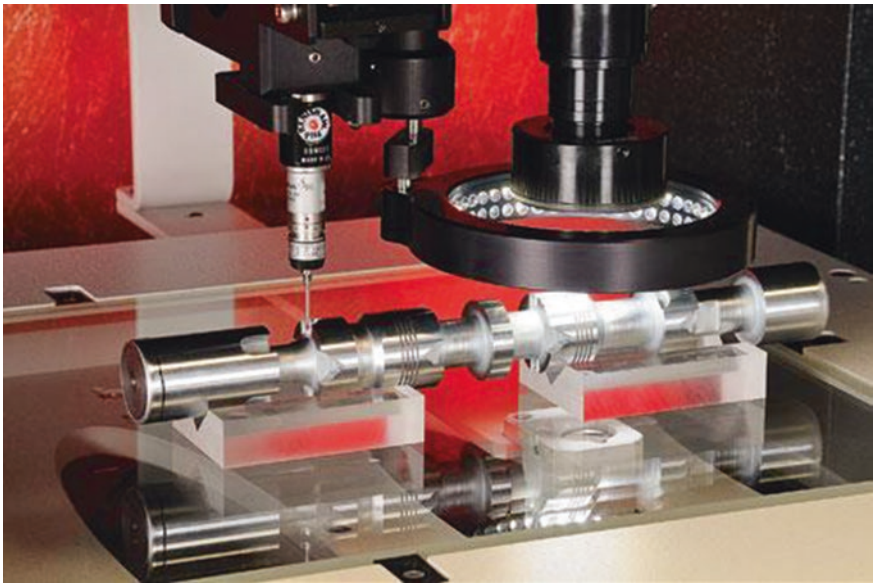

Photograph (*above*) illustrating both a Touch probe (*left*) and a non-contact video probe (*right*)—here, in a multi-sensor setup—for automated component inspection. The LED ring—shown here on the right—is where it illuminates critical component features for the camera [*source*; Parlee, K., Production Machining (2009)]

1.14.4 Recent CMM Probing Systems

A contact technique known as Scanning probing was developed that can either soft scan—at the so-called triggering position at specified intervals on a component's profile—or it can simply lightly drag along (i.e. again, soft-scanning) the component's surface taking continuous measurement points. This technique of CMM inspection, is normally more accurate and precise than some of the conventional

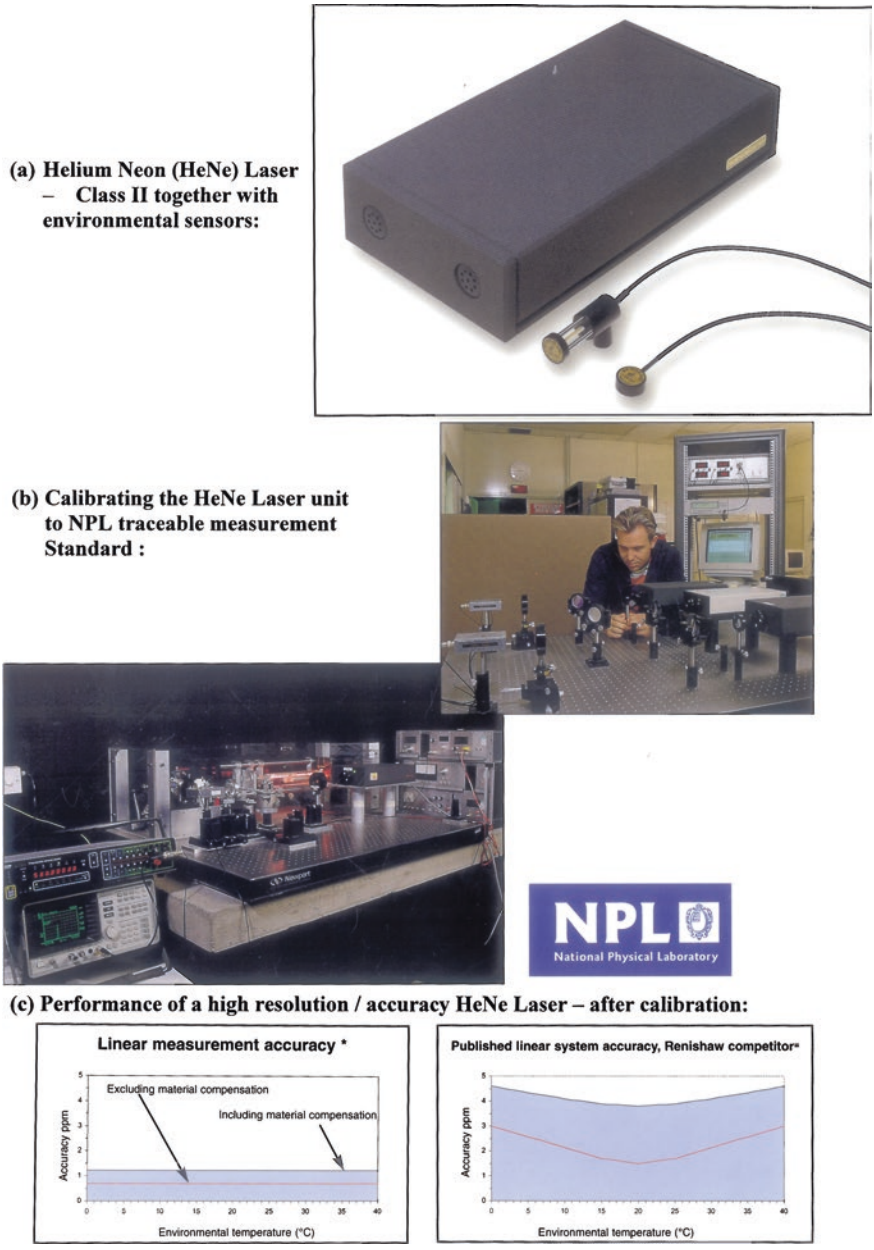

Fig. 1.47 Calibration of an HeNe laser system—incorporating an environmental compensation system (courtesy of Renishaw plc)

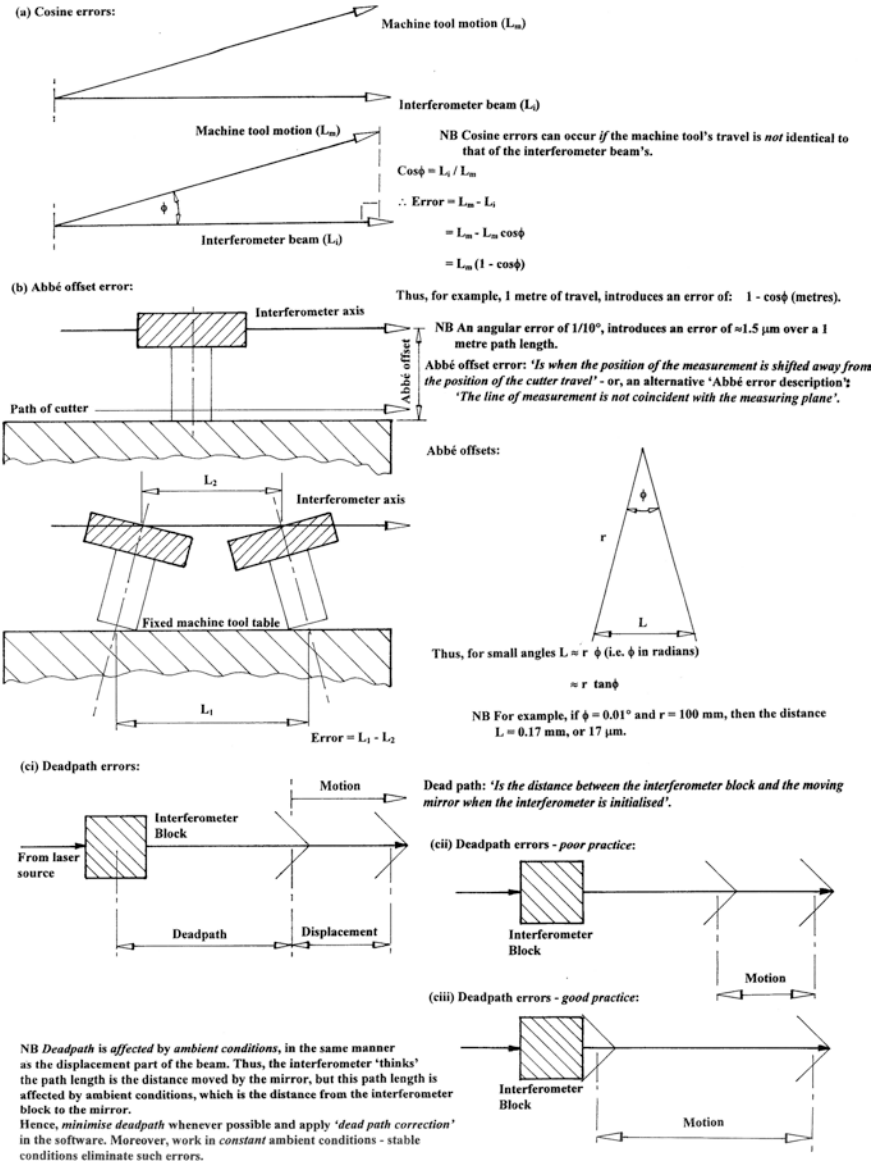

Fig. 1.48 Some error, or uncertainty sources which may be present during a calibration procedure (*source* Cross/NPL)

touch probe methods, while being significantly faster in the execution of the selected metrology task. Non-contact scanning probing was a slightly later addition to CMM development, which includes such techniques as high-speed Laser single-point triangulation—see below (right); Laser line scanning; as well as White light scanning, all

of which are now showing significant technological advancement. These techniques utilise either a laser beam, or white light[104]; which is projected against the surface of the part to be measured. Many thousands of coordinate data points can then be taken and utilised to not only check both size and position, but to also create a 3-D image of this part. This point-cloud data can then simply be transferred to suitable CAD software, creating a working 3-D model of the part. These types of optical scanners—see below (left)—can often be employed on either very soft, or delicate parts, as well as to facilitate that of Reverse engineering[105] activities.

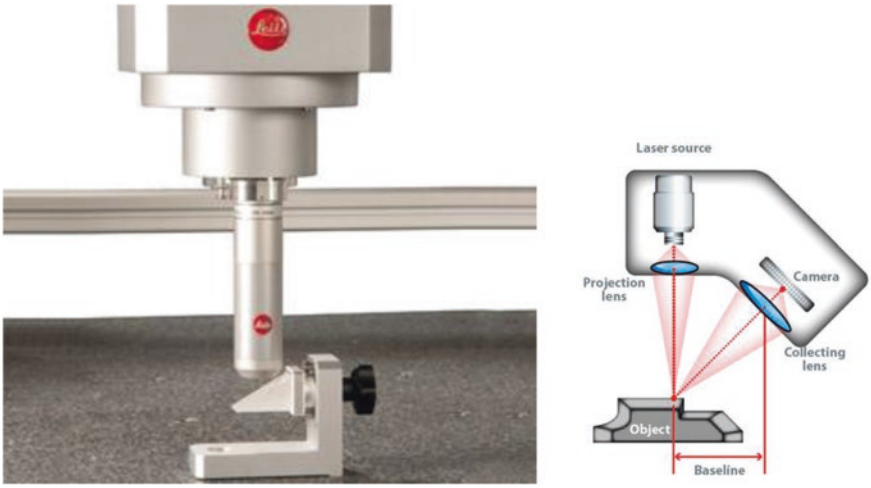

Left An Optical Sensor Probe—with lateral resolution for CMMs. It is especially suited for non-contact measurement of heavily inclined, sensitive, reflective, refractive, shiny, or transparent surfaces. This optical probe has a particularly wide beam acceptance angle of: 90° ± 40° (courtesy of Leitz/Hexagon Metrology). *Right* Triangulation-based Laser Digitisers: here, a laser beam is projected on the part's surface of interest. The reflected laser light is seen through a separate space-separated lens. This light is then focused (i.e. imaged) onto a camera. Thus the knowledge of both projection and collection angles relative to a baseline, will determine the dimensions of a triangle and hence, the coordinates of a point on that surface [*source* InnovMetric Software Inc./3D Imaging and Modeling Group: National Research Council of Canada (2013)]

[104]**White light**: refers to the apparently colourless light that occurs for example, in ordinary daylight. White light contains all the wavelengths of the visible spectrum at equal intensity. Conversely, monochromatic light is a wavelength that is composed of just one single colour, but it is confined to an extremely narrow spectral range.

[105]**Reverse Engineering**: can be defined as: "A process of discovering the technological principles of a device, object, or system through analysis of its structure, function and, operation". Reverse engineering often involves disassembling an item, or indeed, its assembly (e.g. for such as a mechanical device, or electronic component assemblies), then analysing it in detail for its components and actual operation, for either the purposes of: maintenance; to support creation of a new device; short of either using, or simply duplicating (i.e. without understanding) the original item.

1.14.5 Micro-Metrology Probes

In a relatively recent development in probing systems, the probes to be discussed here are concerned with microscale metrology applications. Today there are quite a number of commercially available CMMs which incorporate a microprobe being integrated into a CMM's metrology system. Considering that such CMMs are an excellent metrology platform—with nanometric scales—their operating principal limitation is one of a reliable and robust but capable micro-/nano-probe. Here, some of the challenges are for microscale-probing technologies that include the need for a high aspect ratio probe—providing the ability to access deep, narrow features but with extremely low probe contact forces. In this manner, the probe can avoid any damage to the high-precision surface—at this nanometre level. In addition, such a microscale probe can be susceptible to a range of specific environmental conditions, such as humidity; surface interactions—stiction[106] (i.e. notably caused by a range of factors, such as adhesion,[107] meniscus,[108] and/or the Van der Waals forces[109]).

---

[106]**Stiction**: can be simply defined as: "The static friction that needs to be overcome to enable relative motion of stationary objects in contact". Any solid objects pressing against each other, but not sliding, will require some threshold of force parallel to the surface of contact in order to overcome static-cohesion. Therefore, stiction is just a threshold value and not a continuous force. For example, where two planar-surfaces with areas below the micrometre range come into close proximity, they could possibly adhere together, thus at this minute-scale, the electrostatic and/or Van der Waals, plus the hydrogen bonding forces can become quite significant. Thus, the phenomenon where two such surfaces are being adhered together in this manner, is termed stiction.

[107]**Adhesion** can be simply-defined as: "The tendency of dissimilar particles, or surfaces to cling to one another". Conversely, the term **Cohesion**, refers to: "The tendency of similar, or identical particles, or surfaces to cling to one another". Consequently, the actual forces that promote either adhesion and cohesion are of several types, with the intermolecular-forces responsible for the function of various kinds of stickers and sticky-tape, which fall into the categories such as: chemical adhesion; dispersive adhesion; together with diffusive adhesion.

[108]**Meniscus**: which is a term is derived from the Greek language for the word crescent. Meniscus is defined as: "The curve in the upper surface of a liquid close to the surface of the container, or another object, caused by surface tension". Accordingly, meniscus can be either convex, or concave—depending on the liquid and the surface. A convex meniscus occurs when the particles in the liquid have a stronger attraction to each other (i.e. cohesion) than to the material of the item (i.e. adhesion). For example, this convex meniscus condition can occur, between mercury and glass in barometers and thermometers. Conversely, a concave meniscus occurs when the particles of the liquid are more strongly-attracted to the container than to each other, causing the liquid to climb the walls of the item. For example, this condition would normally occur between water and glass.

[109]**van der Waals forces**: in Physical Chemistry, they are sometimes termed: **van der Waals' interaction**, being attributed to the notable Dutch Scientist Johannes Diderik van der Waals (Johannes Diderik van der Waals, was an eminent Dutch Theoretical Physicist and Thermodynamicist, who was made famous for his work on an: equation of the state for both gases and liquids. Johannes Diderik van der Waals, was Born: 23 November 1837 in Leiden, Holland and died: 8 March 1923 in Amsterdam, Holland. He received his education in the Sciences, at: Leiden University (Holland)—obtaining a Ph.D. in September 1877. Moreover, van der Waals was appointed the first Professor of Physics, at the newly-founded: Municipal

These recent microscale probing technologies are necessary in achieving the desired level of exacting metrological discrimination, which can also include a scaled-down version of a conventional CMM such as the Small Coordinate Measuring Machine (SCMM) with enhanced design and sophisticated additional instrumentation—see Figs. 5.22 and 5.23; Optical probes; as well as Standing wave probes; amongst others (i.e. such as the one depicted in Fig. 5.24). Currently, it is exceedingly difficult, if not impossible, for optical technologies to be scaled small enough to inspect and measure a deep, narrow part-feature, particularly as optical resolution is limited by the wavelength of light. Certain designs of optical probes and/or laser probes can now be utilised, which will modify CMMs, making them at least comparable to that of high-quality measuring microscopes, or sophisticated multi-sensor measuring machines.

References

Journal and Conference Papers

Astin A.V. & Arnold Karo, H., *Refinement of values for the yard and the pound*, Washington DC: National Bureau of Standards, republished on National Geodetic Survey web site and the Federal Register (Doc. 59-5442, Filed, June 30, 1959, 8:45 a.m.)

Bazov, B.M., *Modular design of machine tools*, Russian Eng'g Research, Vol. 31 (11), 1084-1086, Nov., 2011.

Benes, J., *An industry evolves: lathes to computers*, American Machinist, 43-132, Aug. 1996.

Benes, J., *Probing the limits of metrology*, American Machinist, 34-39, Oct. 2006.

Brumfiel, G., *Microwave laser fulfils 60 years of promise*, in: Nature (2012).

Bryan, J. & McClure, E., *A study of thermal effects in manufacturing*, Lawrence Livermore UCRL-50194, 1967.

Bryan, J.B., *International status of thermal error research*, CIRP Annals 16, 1968.

Bryan, J.B., *A simple method for testing measuring machines and machine tools*, Precision Eng'g., 61, Vol. 4(2), 1981.

Burdekin, M., *Performance assessment of machine tools and co-ordinate measuring machines – some recent developments*, Proc. of LAMDAMAP V, 91-104, WIT Press, 2001.

Callaghan, R., *Methods for Establishing Machine Tool Performance Specifications from Part Tolerance Requirements*, Proc. of LAMDAMAP VI, WIT Press, 2003.

Footnote 109 (continued)

University of Amsterdam, later he was awarded the: Nobel Prize in Physics—in 1910.) These are rather complex interactions concerning the: sum of the attractive-, or repulsive-forces between molecules, or between parts of the same molecule, other than those due to: covalent bonds; the hydrogen bonds; the electrostatic interaction of ions with one another with neutral molecules, or charged molecules. The interaction term will also include: forces between two permanent dipoles (i.e. termed the Keesom-force); which is a force between a permanent dipole and a corresponding induced dipole (i.e. here it is known as the Debye force); or indeed, the force between two instantaneously-induced dipoles (i.e. where it is termed the London-dispersion force).

Chablat D., Wenger P. & Angeles J., *Conception Isotropique d'une morphologie parallèle: Application à l'usinage*, 3th Int. Conf. on Integrated Design and Manufacturing in Mechanical Engineering, Montreal, May 2000.

Chanal, H., Duc, E. & Ray, P., *Calibration Accuracy of a Parallel Structure Machine Tool with Respect to Machined Part Quality*, Advances in Integrated Design and Manufacturing in Mechanical Engineering II, 245-257, 2007.

Chi-Wei L., Yang-Kuei L. & Chih-Hsing C., *Dynamic Models and Design of Spindle-Bearing Systems of Machine Tools: A Review*, International J. of Precision Engineering and Manufacturing, Vol. 14 (3), 513-521, Mar. 2013.

Clerk-Maxwell, J., *Theory of Heat*, 10th ed. Longmans, Green and Co., 155–158, (1891).

Coordinate Measuring Machine History – Fifty Years of CMM History leading up to a Measuring Revolution, COORD3 Metrology, Internet accessed: 11th Nov. 2014.

Donmez, A., et al, *A general methodology for machine tool accuracy enhancement by error compensation*, Precision Eng'g., 0141-63591861040187-10, 1986.

Downs, M.J. & Nunn, J.W., *Verification of the subnanometric capability of an NPL differential plane mirror interferometer with a capacitance probe*, Measurement Science & Tech., Vol. 9, 1437-1440, 1998.

Ekinovic,S., Prcanovic, H. & Begovi, E., *Calibration of machine tools by means of laser measuring systems*, Asian Trans. on Eng'g, Vol. 2 (6), Jan. 2013.

Fletcher, S., Postlethwaite, S.R. & Ford, D.G., *Machine tool error identification and compensation advice system*, Proc. of LAMDAMAP IV, 323-334, WIT Press, 1999.

Ford, D.G. & Postlethwaite, S.R., *Error Compensation applied to high precision machinery*, Proc. of LAMDAMAP I, 105-112, Computational Mechanics Pub., 1993.

Franks, A., *Nanometric surface metrology at the National Physical Laboratory*, Nanotechnology, 2, 11-18, 1991.

Gough V. E., *Contribution to discussion of papers on research in automobile stability, control and tyre performance*, Proc. Auto Div. Inst. Mech. Eng,g., 1956-1957.

Gull, M., *Final acceptance test results for the Nanocentre 250*, Proc. of LAMDAMAP II, 13-26, Computational Mechanics Pub., 1995.

Gull, M., *An update on BSI and ISO Machine Tool Accuracy Standards*, Proc. of LAMDAMAP IV, 77-87, WIT Press, 1999.

Gull, M., *Developments in BSI and ISO machine tool accuracy standards*, Proc. of LAMDAMAP V, 221-232, 2001.

Gugger, M., *Getting to the bottom of chatter*, Cutting Tool Eng'g., 54-60, April, 2000.

Hahn, G. J., Hill, W. J., Hoerl, R. W. & Zinkgraf, S. A., *The Impact of Six Sigma Improvement - A Glimpse into the Future of Statistics*, The American Statistician, Vol. 53 (3), 208–215, 1999.

Hansen H.N., Carneiro, K., Haitjema, H. & De Chiffre, L., *Dimensional Micro and Nano Metrology*, CIRP Annals, 55 (2), 721-743, 2006.

Ibaraki, S., Iritani, T. & Matsushita, T., *Error map construction for rotary axes on five-axis machine tools by on-the-machine measurement using a touch-trigger probe*, Int. J. of Mach. Tools & Manuf., Vol. 29, 21-29, May 2013.

Johnson, M., *Achieving accuracy* [Linear motion], 17-18, Design Eng'g., Oct., 1991.

Kennedy, B., *Calming chatter – Strategies for minimising tool chatter*, Cutting Tool Eng'g., 28-35, July, 2004.

Knapp, W. & Schock, J., *Circular Test for high speed machining centres*, Proc. of LAMDAMAP II, 85-96, Computational Mechanics Pub., 1995.

Koren, Y., Jovane, F., Heisel, U., Moriwaki, T., Pritschow G., Ulsoy G., and Van Brussel H., *Reconfigurable Manufacturing Systems* (A Keynote Paper), Annals of the CIRP., Vol. 48(2), 6-12, Nov., 1999.

Koren Y. and Kota, S., *Reconfigurable Machine Tool*, US patent # 5,943,750; issue date: 8/31/1999.

Koren, Y. and Ulsoy, G., *Reconfigurable Manufacturing System Having a Method for Changing its Production Capacity*, US patent # 6,349,237; issue date: 2/19/2002.

Lamb, J., *Ultra-precision machining on a CNC Diamond Turning Lathe*, Proc. of Int. Conf. on Industrial Tooling, Molyneux Press Ltd. (London), 98-108, 1999.

Layer, H.P. & Tyler Estler, W., *Traceability of laser interferometric measurement*, NBS Technical Note 1248, June 1988.

Lee, E-S., Suh, S-H. & Shon, J-W., *A comprehensive method for calibration of volumetric positioning accuracy of CNC-machines*, Int. J. of Adv. Manufact. Technol., Vol. 14 (1), 43-49, 1998.

Lewis, A J, *Measurement of length, surface form and thermal expansion coefficient of length bars up to 1.5 m using multiple-wavelength phase-stepping interferometry*, Meas. Sci. Technol., Vol. 5, 694 – 703, 1994.

Lewis, A J, *Long-term study of gauge block interferometer performance and gauge block stability*, Metrologia, Vol. 47, 473-486, 2010.

Lin, M-T. & Wu, S-K., *Modeling and analysis of servo dynamics errors on measuring paths of five-axis machine tools*, Int. J. of Mach. Tools & Manuf., Vol. 66, 1-14, Mar. 2013.

McCarthy, J. & Hayes, P. J., *Some philosophical problems from the standpoint of artificial intelligence*, Machine Intelligence 4: 463–502, 1969.

Mian, N.S, Fletcher, S. & Longstaff, A.P., *Efficient estimation by FEA of machine tool distortion due to environmental temperature perturbations*, Precision Engineering, Vol. 37 (2), 372-379, April 2013.

Mobley, R. K., *Plant Engineer's Handbook* (5th Ed.), Pub. by: Butterworth-Heinemann (2001).

Moriwacki, T., *Trends in Recent Machine Tool Technologies*, NTN Technical Review, No. 74, 2006.

Page, Chester, H. and Vigoureux, Paul, eds., *The International Bureau of Weights and Measures 1875 - 1975: NBS Special Publication 420*. Washington, D.C.: National Bureau of Standards, 26–27, (20 May 1975).

Peggs, G.N., *Dimensional Metrology into the Millennium*, Proc. of LAMDAMAP V, 157-166, WIT Press, 2001.

Phelps, F. M., *Airy Points of a Meter Bar*, Amer. J. Physics Vol. 34 (5): 419-422, 1966.

Reed, M., *Better the devil you know?* [Bearing selection for machine tools], Plant Engineer, 10-12, Jan/Feb. 2003.

Rehsteiner, F., Neugebauer, R., Spiewak, S. & Wieland, F., *Putting parallel kinematics machines (PKM) to productive work*, Annals of CIRP, Vol. 48 (1), 345-350, 1999.

Ronchi V., *Le frange di combinazioni nello studio delle superficie e dei sistemi ottici*, Translation.: *Combination fringes in the study of surfaces and optical systems*, Rivista d'Ottica e Meccanica di precisione, Translation: Journal of Optics and Precision Mechanics, Vol. 2, 9–35, 1923.

Schwenke, H., Knapp, W., Haitjema, H. & Weckenmann, A., *Geometric error measurement and compensation of machines – An update*, CIRP Annals – Manufact. Technol., Vol. 57, 660-675, 2008.

Smith, G.T., *Condition monitoring for sub-micron machining on a turning centre*, Proc. of Comaden Int. Conf., IO Pub. Ltd., 146-150, 1991.

Smith, G.T., *Why the need for calibration?* Metalworking Production, Q5-Q8, 1998.

Smith, G.T., *Fight to the Finish* [Tool geometry & its effect on roundness & surface texture], Metalworking Production, 49-52, June, 2001.

Smith, R.R., McCrary, S.W. & Callahan, N.R, *Gauge Repeatability and Reproducibility Studies and Measurement System Analysis: A Multi-method Exploration of the State of Practice*, J. of Indust. Tech., Vol. 23 (1), Jan. 2007 through Mar. 2007.

Soori, M., Aerzoo, B. & Habibi, M., *Dimensional and geometrical errors of three-axis CNC milling machines in a virtual machining system*, Computer-Aided Design, Vol. 45 (11), 1306-1313, Nov. 2013.

Stewart, D., *A platform with six degree of freedom*, Proc. of the Inst. of Mech. Eng'g., Vol. 180, Part 1 (15), 371–386, 1965.

Stout, K., *How smooth is smooth? Surface measurements & their relevance in manufacturing*, Production Engr., 17-22, May, 1980.

Stout, K. & Johnson, A., *Nano-tronics: the role of the engineer in nanotechnology*, Korean J. of Prec. Eng'g., Oct. 1998.

Taniguchi, N., *On the basic concept of nanotechnology*, Proc. of ICPE, Tokyo, 1974.

Taniguchi, N., *Current status in and future trends of ultraprecision machining and ultrafine materials processing*, Annals of the CIRP, Vol. 32 (2), 573, 1983.

Taniguchi, N., *The state of the art of nanotechnology for processing of ultraprecision and ultrafine products*, Prec. Engrg., Vol. 16 (1), 5-24, 1994.

Varady, T., Martin, R. & Cox, J., *Reverse engineering of geometric models–an introduction*, Computer-Aided Design, **29** (4), 255–268, 1997.

Weck, M. & Staimer, D., *Parallel Kinematic Machine Tools – Current State and Future Potentials*, CIRP Annals - Manufacturing Technology, Vol. 51 (2), 671–683, 2002.

Wenger P., Gosselin C. & Maille, B., *A Comparative Study of Serial and Parallel Mechanism Topologies for Machine Tools*, Proc. PKM'99, 23-32, Milano, Italy, 1999.

Whitehouse, D.J., *Nanotechnology instrumentation*, Measurement & Control, Vol. 24, 37-46, Mar. 1991.

Whitehouse, D.J., *Surface measurement fidelity*, Proc. of LAMDAMAP IV, WIT Press, 267-276, 1999.

Xie, N., Li, A. & Xue, W., *Cooperative optimization of reconfigurable machine tool configurations and production process plan*, Chinese J. of Mech. Eng'g., Vol. 25 (5), 982-989, Sept. 2012.

Zhang, D., Chen, Y., Ai, W. & Zhou, Z., *Precision motion control of permanent magnet linear motors*, Int. J. of Adv. Manufact. Technology, Vol. 35, (3-4), 301-308, Dec. 2007.

Books, Booklets and Guides

Abramowitz, M. & Stegun, I.A., *Handbook of Mathematical Functions*, National Bureau of Standards, Dover Publications N.Y. (9th Ed.), 1972.

Acheson J., *Quality Control and Industrial Statistics*, fifth edition, Richard D. Irwin Inc., 1986.

ANSI/ASME B5.54-1992: *Methods for Performance Evaluation of Computer Numerically Controlled Machining Centers*, The American Society of Mechanical Engineers: New York, 1993.

Anthony, D.M., *Engineering Metrology*, Pergamon Press, 1986.

Arter, D.R., *Quality audits - for improved performance* (3rd Ed.), ASQ Quality Press Books, 2003.

ASME Draft B5.59-1: *Data Specification for Machine Tool Performance Tests*, and **ASME Draft B5.59-2**: *Data Specification for Properties of Machine Tools for Milling and Turning*, The American Society of Mechanical Engineers: New York, 2006.

Badadhe, A.M., *Metrology and Quality Control*, Technical Publications Pune, 2006.

Barker, R.H., *Group Synchronizing of Binary Digital Sequences*, Communication Theory, Butterworth Pub. (London), 273–287, 1953.

Beeley, P.R., *Foundry Technology*, Butterworth Pub., London, (1982).

Beginner's Guide to Measurement in Mechanical Engineering (Version 2), Joint: NPL Pub. / IMechE Pub., July 2013.

Ben-Naim, A., *Entropy Demystified*. World Scientific Pub., 2007.

Bently, D & Hatch, C., *Fundamentals of Rotating Machinery Diagnostics*, Pub. by: The Bently Pressurised Bearing Co., 2002.

Bewoor, A.K. & Kulkarni, V.A., *Metrology and Measurement*, Tata McGraw-Hill, 2009.

Braasch. J., *Position Measurement on Machine Tools: by Linear Encoder, or Ballscrew and Rotary Encoder*, Heidenhain Information Pub., 2013.

Bucher, J.L., *The Metrology Handbook*, ASQ Quality Press (Milwaukee, WI, USA), 2004.

Bureau International des Poids et Mesures. (n.d.), *The BIPM and the evolution of the definition of the metre*, 3 June 2006.

Busch, T., *Fundamentals of Dimensional Metrology –2nd Ed.*, Delmar Pub. Inc., 1989.
Chablat D., *Domaines d'unicité et parcourabilité pour les manipulateurs pleinement parallèles*, Thèse de Doctorat de l'Université de Nantes et de l'Ecole Centrale de Nantes, Nov., 1998.
Collett, C.V. & Hope, A.D., *Engineering Measurements*, Pitman Pub. Ltd. (London), 1979.
Czichos, H., Saito, T. & Smith, L.E., *Springer Handbook of Metrology & Testing*, Springer Pub. (Berlin), 2011.
Dagnall, H., *Let's Talk Roundness*, Taylor Hobson Pub., Nov. 1996.
Daney D., *Etalonnage géométrique des robots parallèles*, Thèse de Doctorat de l'Université de NiceSophia Antipolis, Février 2000.
Dawson, D.J., *Cylindricity and its measurement*, Int. J. Mach. Tools. & Manuf., 32 (1/2)247-253, 1992.
Doiron, T. & Beers, J., *The Gauge Block Handbook*, USA: Dimensional Metrology Group, US National Institute of Standards and Technology, 2009.
Eilam, E. & Chikofsky, E. J., *Reversing: Secrets of Reverse Engineering*, John Wiley & Sons, 2007.
Fang, H-Y., *Foundation Engineering Handbook* (2nd Ed.), Kluwer Academic Pub., Ma. USA (2002).
Flack, D. R. & Hannaford, J., *Measurement Good Practice Guide No. 80*, NPL Pub., January 2006.
Floud, R. C., *The British Machine Tool Industry, 1850-1914*, Cambridge University Press, 2006.
Furlani, E.P., et al. *Permanent Magnet and Electromechanical Devices: Materials, Analysis and Applications*, Academic Press, London (2001).
Gayler, J.F.W. & Shotbolt, C.R., *Metrology for Engineers – 5th Ed.*, Pub. Ltd., 1990.
Goldsmith, M., *A beginner's guide to measurement*, Measurement Good Practice Guide No. 118, NPL Pub., 2010.
Hirano, H., *5 Pillars of the Visual Workplace*, Cambridge, MA: Productivity Press, 1995.
Hodges, A., *Alan Turing: the enigma*, London: Burnett Books (London), 1983.
Hume, K., *A History of Engineering Metrology*, Mech. Eng'g Pub., 1980.
Hutton, D.V., *Fundamentals of Finite Element Analysis*, McGraw-Hill Pub. (NY), 2004.
International Standard **- ISO 841***: Industrial automation systems and integration — Numerical control of machines — Coordinate system and motion nomenclature*, 2nd Ed., International Organization for Standardization: Geneva, 2001.
International Standard **- ISO/CD 230/1.4**: *Test code for machine tools - Part 1: Geometric accuracy of machines operating under no-load or quasi-static conditions*, International Organization for Standardization: Geneva, 2006.
Ito, Y., *Modular Design for Machine Tools*, McGraw-Hill Pub., 2008.
Jaeger, R.C., *Lithography—Introduction to Microelectronic Fabrication* (2nd Ed.), Prentice Hall Pub. (USA), 2002.
Kalpakjian, S., *Manufacturing Processes for Engineering Materials – Third Ed.* Addison Wesley Pub. 1997.
Koetsier, T., *'Kinematics'*, in: *Companion Encyclopedia of the History and Philosophy of the Mathematical Sciences*, vol. 2, edited by Ivor Grattan-Guinness,Routledge, 994-1001, (1994).
Kummetz, J., *Getting the Best Accuracy out of Machine Tools* [Industrial article], Heidenhain, Traunreut, Germany, June 2013.
Laboratory Accreditation Bureau (Fort Wayne, IN, USA), ISO/IEC 17025, *Measurement Traceability*, 2009.
Leach, R., *Fundamental Principles of Engineering Nanotechnology (Micro & Nano Technologies)*, Elsevier Pub., 2009.
Leavitt, D., *The man who knew too much: Alan Turing and the invention of the computer*, Phoenix Pub., 2007.
Mummery, L., *Surface Texture Analysis – The Handbook*, Hommelwerke GmbH Pub., 1990.
NakaZawa, H., *Principles of Precision Engineering*, Oxford Univ. Press, 1994.
Nilsson, N., *The Quest for Artificial Intelligence: A History of Ideas and Achievements*, New York: Cambridge University Press, 2010.

Nyce, D.S., *Linear Position Sensors: Theory and Application*, John Wiley & Sons Inc. (New Jersey), 2003.
Placko, D. & French College of Metrology, *Metrology in Industry – The Key for Quality*, Pub. ISTE Ltd., 2006.
Redford, D.B. (Ed.), *The Oxford Encyclopaedia of Ancient Egypt*. Oxford University Press, 2001.
Unlock the hidden potential of your CMMs, White Paper, Renishaw plc, 2009.
Roe, Joseph Wickham (1916), *English and American Tool Builders*, New Haven, Connecticut: Yale University Press. Reprinted by McGraw-Hill, New York and London, 1926.
Rolt, L.T.C. (1965), *A Short History of Machine Tools*, Cambridge, Massachusetts, USA: MIT Press. Co-edition published as Rolt, L.T.C., 1965.
Romer, John *The Great Pyramid: Ancient Egypt Revisited*, Cambridge University Press, Cambridge, 2007.
Schijve, J., *Fatigue of Structures and Materials, 2nd Edition with Cd-Rom*, Springer Pub., 2009.
Schlesinger, G. *Testing Machine Tools* (7th Ed.), The Machinery Pub. Co. Ltd, 1966.
Smith, G.T., *CNC Machining Technology*, Springer Verlag Pub., 1993.
Smith, G.T., *Industrial Metrology – Surfaces and Roundness*, Springer Verlag, 2002.
Smith, G.T., *Cutting Tool Technology – Industrial Handbook*, Springer Pub. 2008
Smith, S. T. and D. G. Chetwynd, *Developments in Nanotechnology Vol. 2: Foundations of Ultra-precision Mechanism Design*, Taylor & Francis, 323 of 364, 1994.
Stout, K.J., *From Cubit to Nanometre – A history of Precision Measurement*, Penton Press, London, 1998.
Taylor, B.N. and Thompson, A. (Eds.), *The International System of Units (SI)*, United States version of the English text of the eighth edition (2006) of the International Bureau of Weights and Measures publication *Le Système International d' Unités (SI)* (Special Publication 330). Gaithersburg, MD: National Institute of Standards and Technology, 18 August 2008.
Thomas, G.G., *Engineering Metrology*, Butterrworths (London), 1974.
Tönshoff, N.: *Bundling and Pricing Strategies under Demand Uncertainty*; *International Machine Tool Industry Analysis*; in: *Modular Machine Tools*, Springer Pub., 1997.
Tönshoff, N., Fine, C.H. & Huchzermeier, A., *Bundling and Pricing of Modular Machine Tools Under Demand Uncertainty*, in: *Optimal Bundling*, Springer Pub., 1999.
Turing, S., *Alan M. Turing*, Centenary Edition - Cambridge University Press, 2012.
Valentino, J.V. & Goldenberg, J., *Introduction to Computer Numerical Control (CNC)*, (2nd Ed.), Prentice-Hall, Inc., 2000.
Whitehouse, D.J., *Handbook of Surface Metrology*, Inst. of Physics, Bristol (UK), 1994.
Whitehouse, D.J., *Surfaces and their Measurement*, Hermes Penton Press, 2002.
Woodbury, R. S., *Studies in the History of Machine Tools*, Cambridge, Massachusetts, USA, and London, England: MIT Press, 1972

Chapter 2
Laser Instrumentation and Calibration

"Shall I, the gnat that dances in the ray, dare to be reverent?"
Coventry Patmore
(British poet—and an Associate of the
Pre-Raphaelite Brotherhood)
[1823–1896]
(In Pysche's Discontent)

2.1 Introduction to Lasers

On a CNC machine tool, any basic or intricate machining process inevitably has some pre-requisite for some form of actual measurement. Both the accuracy and precision requirements for machined products are continuously increasing—see Fig. 1.14. As a consequence, this accuracy/precision level of machined components can be directly related to the machine tool's performance as it is utilised on a production line. Today, any form of competitiveness in the manufacture of products, coupled to an effective production line, will demand constant inspection of a machine tool's overall performance. Consequently, the CNC machine tools geometrical accuracy and precision is a foundation for the evaluation of such plant—according to their production and quality performance requirements. Of significant importance is the measurement and verification of a machine, via its periodic calibration.[1] In order to calibrate a machine tool, one well tried-and-tested but highly accurate and precise technique is by calibration utilising specially designed laser measuring systems. Lasers have been utilised for many years, mainly for the

[1]**Calibration**—the formal definition by **The International Bureau of Weights and Measures** (Paris, France) is an: "Operation that, under specified conditions, in a first step, establishes a relation between the quantity values with measurement uncertainties provided by measurement standards and corresponding indications with associated measurement uncertainties [of the calibrated instrument, or secondary standard] and, in a second step, uses this information to establish a relation for obtaining a measurement result from an indication".

G.T. Smith, *Machine Tool Metrology*, DOI 10.1007/978-3-319-25109-7_2

assessment of a diverse range of physical properties but principally for precise distance-measurement. As a result, an accurate and precise measurement can be achieved using laser beams, with lasers using interferometric-measurement being applicable for such machine tool and metrology equipment calibration.

Some basic facts concerning the application of a laser light source, will be that they are:

- **coherent**—having all the photons of a laser beam being in-phase with each other;
- **directional**—with all the photons being both parallel and directed;
- **monochromatic**—all photons have the same energy with the laser beam colour, depending upon the energy source that is utilised for the stimulation of atoms.

Accordingly, a laser can be considered as a concentrated beam of light, which normally possesses an enormous amount of energy. The term laser has already been mentioned in Chapter 1, but it is worth just re-emphasising once again, namely that the acronym **LASER** is derived from **L**aser **A**mplification by the **S**timulated **E**mission of **R**adiation, relating to energy from a stimulated source of light. Low-powered lasers are expressly utilised for laser measurements, due to the fact that a powerful laser source is unnecessary and could prove to be potentially destructive. Furthermore, such powerful lasers are somewhat dangerous if employed for any form of machine and instrument measurement/calibration. Laser measurement is fundamentally based on the principle of optical interferometry—of a basic beam and its return beam, which carries certain dimensional information. This return beam is normally reflected from a specially manufactured matched-optic such as an accurately positioned reflective mirror which is placed on an observed object, via an interferometric optical source—more will be said on this topic later in this chapter. The main problem during laser measurement assessment is one of laser beam stability. From the time when laser beam wavelength is utilised as a measuring-gauge, the influence of the environmental conditions, such as ambient temperature; humidity; thermal air-flow; plus other contributory factors; must be effectively and consistently controlled.

2.1.1 Why Is Calibration so Important?

Calibration can define the accuracy, precision, as well as the quality of measurements being recorded utilising specific plant and equipment. Hence, over time, there is a tendency for these results and its attendant-accuracy and precision to drift. This drifting is particularly noticeable when utilising certain levels of high-technologies, or measuring particular parameters such as exacting dimensional measurements, in association with changes in the local ambient temperature, humidity and to a lesser extent, by air-movement—typically by drafts and/or thermal air-currents. Accordingly, to be confident in the metrological results being measured, there is an on-going need to both service and maintain the calibration of equipment throughout

its lifetime for reliable, accurate, and repeatable measurements. The express goal of any form of calibration is to minimise any potential measurement uncertainty by ensuring the accuracy/precision of the test equipment, but in this case, by utilising the laser interferometer. Laser calibration when undertaken—see Fig. 1.47—will then have the capability to obviously quantify and control these undesirable error-sources, or uncertainties within measurement processes, maintaining them at an acceptable level.

One might ask the pertinent question, "What are the major objectives of calibration?" In essence, there are three foremost reasons for having both the industrial plant and metrological instruments calibrated, characteristically to:

1. **ensure** readings from the plant/instrument are consistent with other measurements;
2. **determine** the accuracy and precision of the plant/instrument readings;
3. **establish** the reliability of the plant/instrument—so that it can then be trusted.

2.1.2 Calibration of Laser Interferometers

Laser interferometer systems are widely employed in the manufacturing and metrology industries for direct precision measurement of length and displacement, particularly in relation to CNC machine tool and co-ordinate measuring machine (CMM) calibration.

Many technologically based countries have their own National Metrology Laboratories—see an abridged list of them at rear of this book, that can offer an end user/customer a laser calibration service, such as that provided by The NPL within the UK, or for certain industrial/metrology companies which are suitably accredited to undertake such calibration, or periodic re-calibration—see Fig. 1.47. Typically within the UK, The NPL offers a routine-service for the verification of interferometer system accuracy, which includes the following:

- calibration of a stabilised laser source wavelength;
- verification of displacement measurement—to 30 m;
- calibration of environmental compensation transducers;
- compensated system calibration—to 2 parts in 10^7;
- UKAS accreditation/ISO 9000 compliance.

Such essential periodic laser interferometer calibration confirms the traceability measurement chain to the absolute standard for the metre, as basically depicted in Fig. 1.2.

Typically, laser interferometers of the homo, or heterodyne-types, are frequently utilised by manufacturing industry at large, and in calibration laboratories for displacement-measurements in a very wide-range, from just 0.1 nm up to that of 50 m distance. The accurate and traceable operation of a laser interferometer requires calibrations and checks of several specific factors (i.e. see Table 2.1).

Table 2.1 The typical and maximum observed errors of either an representative industrial uncalibrated and unadjusted laser interferometer system

Quantity	Sensitivity/m	Typical error	Max. error
Wavelength	1	3.2×10^{-8} (relative)	7.1×10^{-8} (relative)
Pressure	−0.27 µm/hPa	1.7 hPa	−12 hPa
Air temp	0.96 µm/°C	0.16 °C	0.5 °C
Mat. temp	11.5 µm/°C	0.03 °C	0.3 °C

Source Centre for metrology and accreditation (MIKES), Espoo, Finland (2013)

Refractive Index of Air Compensation

A normal metrological practice is to establish the refractive index of air equation of a device, or by appropriate software, by comparing the calculated values to the values obtained from a commonly utilised updated Edlen equation

[Re: Bönsch, G., Metrologia, Vol. 35, 133–139 (1998)]

This specific value for the Edlen equation, for the reading of a commercial laser interferometer can be expressed as follows:

$$L_{20\,^\circ\mathrm{C}} = \frac{(D+\phi)\lambda_0/2}{n(t_{\mathrm{air}}, h, p)[1+\alpha(t_{\mathrm{mat}} - 20\,^\circ\mathrm{C})]}$$

where:

'D' is the integer amount of interference fringes;
'ϕ' is the fractional phase of the interference signal;
'λ_0' is the vacuum wavelength of laser light;

function '$n(t_{\mathrm{air}}, h, p)$', is for refractive index of air calculation with measured air; with: temperature, 't_{air}'; humidity, 'h'; and pressure, 'p'; are by corresponding sensors. Often commercial systems are also equipped with one, or several material temperature sensors, 't_{mat}', for thermal expansion compensation with expansion coefficient; 'α', of the material.

Realisation of the Metre and Vacuum Wavelength Calibration

The practical realisation of the definition of the metre, at the majority of countries National Standards Organisations, typically, such as at 'MIKES' in Finland, is obtained by:

- **an optical frequency combination, referenced to an atomic clock**—which is utilised to measure the absolute frequency of an iodine-stabilised He–Ne laser at 633 nm, this being operated according to the current international recommendations;
- **the vacuum wavelength of the iodine-stabilised laser**—which is calculated from the measured frequency and from the value for the speed of light in a vacuum.

As a result, the realisation of the metre is transferred to lasers utilised in interferometers, by calibrating their vacuum wavelength in beat-measurements with that of an iodine-stabilised (red) He–Ne laser.

Calibration of Sensors

As well as the actual laser interferometer, its associated-sensors (e.g. such as for temperature and material) will also need to be periodically calibrated, usually in the following manner:

- **air temperature sensors**—are compared against calibrated reference Pt100-sensors, inside a climate chamber;
- **pressure sensors**—are calibrated against a reference sensor typically utilising a piston cylinder to produce adjustable pressure;
- **humidity sensors**—are calibrated inside a climate chamber as a comparison to a reference humidity sensor;
- **material sensors**—of the instrument and reference Pt100-sensors, are attached to a steel block and inserted inside a climate chamber.

As a consequence of such a testing/calibration regime, if these sensors deviate considerably from the reference, then a correction is applied, or an adjustment is performed to them.

The Benefit of Calibration

In Table 2.2 is shown the radical improvement of uncertainty due to calibration for a characteristic commercial laser interferometer set-up. At this time, the uncertainty-calculation is undertaken for a typical commercially available interferometer system, although with the application of superior temperature-sensors then somewhat lower values of uncertainties could be achieved. This laser calibration will also provide traceability to the realisation of the metre, which guarantees conformity with other high-accuracy/precision dimensional measurements.

In summary, the periodic calibration of laser interferometers is:

- essential for accurate/precise and reliable measurements;
- necessary to achieve conformity with SI-metre (Standard), which definitely requires traceability that can only be achieved by its systematic calibration.

2.1.3 Laser Calibration—Potential Error and Uncertainty Sources

The main sources of error/uncertainty arising from the use of laser calibration systems is well known and documented and must be minimised if valid readings are to be obtained from the machine or equipment under test. The laser and interferometric measurement optics can provide remarkably high levels of linear resolution and precision. Nonetheless, it is the laser system's environmental compensation unit

Table 2.2 The uncertainty of a laser interferometer just prior to and after its calibration—with certain notable adjustments

Quantity system	Sensitivity coefficient		Uncalibrated system		Calibrated and adjusted system	
			Errors	Uncertainty contribution ($k = 1$)/μm	Errors	Uncertainty contribution ($k = 1$)/μm
$D + \phi$ (fringes)	1	n/a	5.0 nm	0.005	5 nm	0.005
λ_0 (wavelength)	1.6×10^6	L	0.02 pm	0.03L	0.003 pm	0.005L
n (refr. index)	1	L	1×10^{-7}	0.10L	3×10^{-8}	0.03L
t_{air} (air temp.)	-9.6×10^{-7}	1/K L	0.30 K	0.29L	0.05 K	0.05L
p (pressure)	2.7×10^{-9}	1/Pa L	170 Pa	0.46L	20 Pa	0.05L
α (coeff. exp.)	0.289	m K L	6×10^{-7}1/K	0.17L	6×10^{-7}1/K	0.17L
t_{mat} (mat.temp.)	-1.15×10^{-5}	1/K L	0.15 K	1.73L	0.025 K	0.29L
Combined standard uncertainty: Q(0.005; 1.8L)					Q(0.005; 0.34L)	

Where L is the measured distance in metres
Source Centre for metrology and accreditation (MIKES), Espoo, Finland (2013)

(i.e. often termed its weather-station) that is primarily responsible for the system's measurement accuracy and precision. This so-called weather-station, automatically compensates for the linear displacement readings from the laser on behalf of any variations in both the air refractive index[2] and material temperature.[3]

[2]**Refractive index of air**: because of the significance of refraction in both Optical-design and Metrology, the refractive index of air has been extensively-reported. Typically, the variations in atmospheric pressure, temperature and relative humidity, will alter the wavelength of a red 0.633 μm wavelength Helium Neon (He–Ne) laser, whose differences are normally quoted in parts per million (ppm). What is precisely known, is that the refractive index of a vacuum is exactly 1. The refractive index of what is termed Standard air (Standard air can be defined as: "The air with a pressure of 1013.25 mbar, at a temperature of 20 °C and, with a relative humidity of 50 %".), as seen by a He–Ne laser, is: ≈1.0002714. Consequently, a laser's wavelength in Standard air is: ≈271 ppm shorter than its actual vacuum wavelength.

[3]**Material temperature compensation**: in many situations this can be impractical and the dimensions have to be measured in situ. So that this can be successfully achieved, in for example, Renishaw's XL-80 laser interferometer system (i.e. see Figs. 2.1 and 2.2), which includes the capability to compensate for these linear readings, hence, by using a manually-entered Material expansion coefficient, plus the temperature from up to three material temperature sensors, this is successfully achieved and the process is termed: Material expansion compensation. The objective of the process here, is to estimate the linear laser readings that would have been obtained, if the measurements had been undertaken at the agreed: International Reference Temperature—of 20 °C.

Fig. 2.1 Portable laser measurement and calibration instrumentation (courtesy of Renishaw plc)

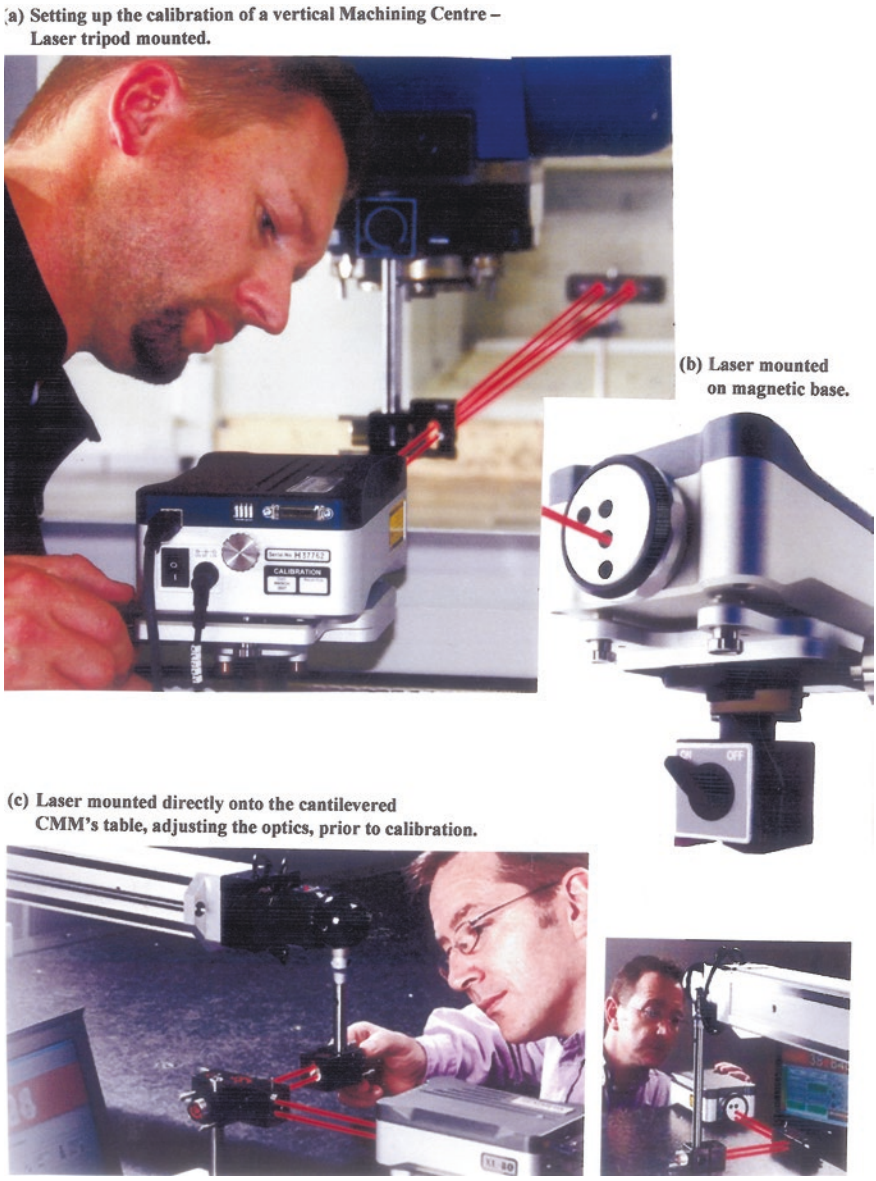

Fig. 2.2 Typical laser mounting configurations, prior to machine tool and CMM calibration trails (courtesy of Renishaw plc)

Just some of these significant values of uncertainty incurred when setting-up and utilising laser systems on machines, are the:

- **Cosine error** – this will be present if say, the machine tool's travel is not identical to that of the interferometer's beam (i.e. see Fig. 1.48a);
- **Abbé offset error**[4]—this is when the position of the laser measurement is shifted-away (i.e. offset), from the position of, say, the actual axis cutter's travel (i.e. see Fig. 1.48b);
- **Deadpath errors**[5]—are influenced by ambient conditions in the same manner as the displacement part of the beam. So, the interferometer reasons that the path length is the distance moved by the mirror, but in actuality this path length is affected by ambient conditions, thus being the distance from the interferometer block to the matched mirror (i.e. see Fig. 1.48ci, cii and ciii).

The equation, which is applicable to both air and material expansion compensation relating to linear laser readings, can be expressed as;

$$L = (1 - \alpha T) \,.\, \lambda_{\text{air}} \,.\, N \big/ 2$$

where:
'L' is the laser readout; 'N' is the number of laser fringes counted after the system was datumed; 'α' is the material expansion coefficient manually entered by the user; 'T' is the difference between the average material temperature and 20 °C; while, 'λ_{air}' is the current air refractive index—calculated using either the: Edlén-, or Ciddor-equations—from the air temperature, pressure and humidity.

---

[4]**The Abbé principle** was named after Dr E.K. Abbé, who stated that: "The measuring instrument is always to be so constructed that the distance being measured is a straight-line extension of the graduations on the scale that serves as the reference. … Should the measuring axis and that of the scale belong to two different axes, which are separated by a certain distance, then … the length being read off will be identical to the length being measured in general only when the moving system undergoes pure parallel motion, with no rotation. If the system undergoes a rotation between the initial and final settings, then the scale reading and the measured length are different".
Alternatively if this is somewhat too complex and confusing, then this **Abbé Offset**, can be simply stated as when: "The line of measurement is not coincident with the measuring plane". Dr Ernst Karl Abbé (Born: 23 January 1840 in Eisenach, Saxe-Weimar-Eisenach, Germany—died: 14 January 1905 in: Jena, Germany) was a notable German Physicist and Optical-scientist. Abbé was awarded his Ph.D. in Physics from The University of Göttingen, Germany—in 1861. In conjunction with both Otto Schott and Carl Zeiss, he laid the much toward the foundations of today's modern optical-developments and principles. Abbé was co-owner of Carl Zeiss AG, a respected German manufacturer of Research-microscopes, Astronomical-telescopes, Planetariums and for many other Optical-systems [source Galyer and Shotbolt (1990) and Smith et al. (2002)].

[5]**Deadpath errors**: in order for the equation (i.e. see the expression for 'L'), to effectively compensate linear measurements taken in unstable environments, it is important that 'N' (i.e. the fringe-count) nominally-reflects the separation between the optics in the measurement arm of the interferometer. For example, if the separation doubles, then 'N' should nominally double too and, when '$N = 0$'—the optics should be close together. This is easily achieved if the laser is datumed (i.e. with 'N' being set to '**0**') when the optics are close together. If these linear optics are not close together when the laser system is datumed and the environment subsequently changes, then the laser reading will show a small-drift in the datum position. This actual drift will often be comprised of two distinct components, these are: (i) an air deadpath error and, (ii) a material deadpath error.

Air Dead Path Error (E_{ADP})

With regard to the deadpath error (see Fig. 1.48ci) in the laser setup on the machine, effectively the system does not perceive that there is additional air in the measurement arm and as a result will not compensate for changes in the wavelength of the laser in that portion of the beam. As a consequence, the general equation for the air dead path error (E_{ADP}) is provided as follows;

$$E_{ADP} = D.(\lambda_{air} - \lambda_0)/\lambda_0$$

where:
'E_{ADP}' is the air dead path error; 'D' is the separation between the optics at datum (i.e. the dead path); 'λ_{air}' is the current laser wavelength; while, 'λ_0' was the laser wavelength—when the system was datumed.

For example, by utilising this equation and assuming alterations relative to Standard air, it is conceivable to estimate the dead path error per metre of air dead path. This alteration can be considered as follows:

- 0.27 μm error per mbar change in air pressure since datum;
- 0.96 μm error per °C change in air temperature since datum;
- 0.1 μm error per 10 % change in relative humidity since datum.

These specific readings clearly highlight that Air Dead Path Errors (E_{ADP}) are typically quite small and if the measurement arm optics are positioned such that 'D' is <10 mm when the system is datumed, then the air dead path error is negligible.

Material Dead Path Error (E_{MDP})

When considering once again the example shown by Fig. 1.48ci, the laser system is datumed where the encoder readout is 0.000 mm, but with a dead path separation as shown between the measurement arm optics. At this position the fringe count of '$N = 0$' is as expected, having the laser position readout at 0.000 mm. If one currently supposes that the temperature of the actual machine has now changed by +1 °C and then postulate that the material has an expansion coefficient of ≈10 ppm/°C, these effects will modify the measurement process. Moreover, this material expansion causes the measurement arm optics to move further apart by ≈10 ppm × D which instigates a 10 ppm increase in the number of waves that can now fit into the gap 'D' between the measurement optics. Accordingly, the fringe count 'N', will increase and the laser's position readout will drift-away from zero by 10 ppm × D. It should also be emphasised that this material dead path error is normally 10 times larger than the air dead path error produced by a 1 °C change in air temperature. Even if the environmental compensation unit has correctly calculated a new environment factor (EF), applying material expansion compensation will barely have any effect, since the fringe count is almost zero (i.e. instead of being 2D/EF). So in effect, the laser's system setup will not be able to distinguish that there is extra material in the measurement arm, consequently it will not compensate for its thermal expansion or contraction.

The general equation for Material Dead Path Error (E_{MDP}) is represented as follows:

$$E_{MDP} = D \,.\, \alpha \,.\, T$$

where:
'E_{MDP}' is the material dead path error; 'D' is the separation between the optics at datum (i.e. the dead path); 'α' is the linear coefficient of expansion of the material in the dead path; 'T' is the change in temperature of the material since the system was first datumed.

By way of practical example, if the material expansion coefficient is 10 ppm/°C, then the dead path error will be 10 μm per metre of material dead path per °C change in material temperature since its datuming. Clearly, this has exposed that these material dead path errors are potentially much more significant than its associated air dead path errors. This results from the materials in the dead path perhaps not being identical as the item being measured, so these temperatures may independently vary, ensuring that here, a simple software-correction is not a practical solution. In consequence, the optimum methodology herein—to lessen these undesirable conditions—is to apply good metrology practices, by minimising:

- **the material dead path**—by situating the setup of the laser's optics as closely and directly as possible to the point of metrological-interest;
- **any changes in material temperature during measurement**—by initially stabilising the temperature and/or promptly completing the measurements;
- **the optics separation (i.e. when the system is datumed)**—this should be made by utilising either a preset reading, or by employing a beam-splitter as the moving optic.

2.1.4 Introduction to Laser Machine Calibration

General Comments—Concerning CMMs and Machine Tools

The reliability of machine tools and CMMs has seen a marked-improvement, in particular, with respect to their inherent accuracy and precision, and of note, are the actual deviations in the machine tool accuracy/precision and subsequently how they affect the geometry of the machined workpiece, which may be due to a variety of technical reasons. Probable sources for this variation in these machines may include errors in the machine's geometry, due in part to the tolerances in their manufacture, construction and build/assembly of the separate machine parts, exacerbated by any deformation resulting from loads—whether they are either static or dynamic, or indeed both, via some form of thermal-deformation being present.

Laser Instrumentation and Equipment

Since the 1970s, laser interferometer systems have been employed for wide-ranging accuracy and precision calibration procedures, typically for a large range of CNC machine tools, co-ordinate measuring machines (CMMs) and other position-critical

systems. Typical of the latest-type of highly portable laser interferometer systems, is the one being illustrated in Figs. 2.1 and 2.2. Here, the major benefits of utilising these high-quality laser interferometers can be derived from their notable-characteristics, which are listed below, where they can exhibit:

- **high levels of consistent accuracy**—the system accuracy of ±0.5 ppm, is maintained throughout the laser system's operating range of: 0–40°C;
- **traceable interferometry**—having all the laser measurements, including straightness, angularity, etc., being interferometric in nature; these measurements are based upon the Internationally traceable Standard of the wavelength of laser light;
- **quick and secure alignments using a tripod-mounted laser**—with all alignments, these can be undertaken comfortably and safely outside the machine's envelope, so there will not be any loss in axis travel, nor will the instrument suffer from the effects of factors such as its cable-drag during the actual measurement process;
- **laser's optics designed for the workshop-hardened user**—because all of the optical-housings are manufactured from hard-anodised aluminium. Furthermore, when these optics are then coupled with a novel-designed beam-steerer[6] (i.e. see Fig. 2.1, bottom), this facilitates quick and assured laser beam alignments;
- **long range measurement**—this particular laser system facilitates linear measurements to be undertaken on any axes up to 80 m in length, or simultaneously measuring parallel axes—for dual-drive machines;
- **rotary axis calibration**—the combination of the laser with its associated Rotary Axis-calibrator (see Figs. 2.13, bottom and 2.14) can provide a fully automatic-technique of rotary axis calibration—on both multi-axes machine tools and for CMMs—the latter being equipped with a rotary table;
- **comprehensive laser software**—with Renishaw's bespoke-packages—which can support reporting to International Standards for its machine verification, along with other notable features such as linear position error correction and dynamic motion analysis.

This particular company's laser-products (Figs. 2.1 and 2.2) produce an extremely stable laser beam with a wavelength that is traceable back to National and International Standards, having the laser-frequency stability specified as: ±0.05 ppm over 1 year, or alternatively, ±0.02 ppm over just 1 h. This high-quality laser's performance is accomplished by dynamic thermal control of the laser-tube

[6]**Beam-steerer** (i.e. illustrated in Fig. 2.1, bottom): utilises simple-levers to rapidly align the laser beam in both the horizontal and vertical planes. This Beam-steerer was designed to enable both new and experienced users to speed through its: linear; angular; and straightness measurements—for laser interferometer calibration of machine tools and coordinate measuring machines (CMMs), plus other similar precision devices which may also require calibration. So, simply by the action of sliding horizontal, or vertical control levers, this steers the laser beam for rapid setup and alignment in both horizontal and vertical planes. This Beam-steerer can provide an angular beam sweep of: ±2° (i.e. ±35 mm m^{-1})—in both planes—for linear-axes up to 5 m long.

length—to within a few nanometres. Moreover, the laser's linear measurement accuracy is: ±0.5 ppm over the whole environmental range (i.e. from a temperature range of: 0–40 °C and across atmospheric pressures ranging from: 650 mbar to 1150 mbar). At this juncture, the laser readings are obtained at: 50 kHz, thus allowing a linear measurement speed of 4 m s^{-1} (maximum) with a linear resolution of 1 nm. This product's compact laser head is supplied with an independent compensator system—see Fig. 2.1a. Furthermore, it features an auxiliary analogue signal with quadrature output. Accordingly, the same socket will also accept a trigger-signal input for data-capture synchronisation, plus LED status-lights, which will indicate laser-status and its signal-strength, providing back-up to the software's on-screen indicators. This comprehensive laser specification, also includes a switchable long-range operational mode (i.e. ranging from 40 to 80 m in length).

Laser Sensor Integration

In association with the laser head (depicted in Figs. 2.1 and 2.2) are its complementary and purpose-built compensator unit, which is a crucial factor in the system's measurement accuracy and precision. This compensator features some intelligent-sensors that can process the readings at source, with the compensator having the ability to accurately measure: air temperature; air pressure; plus the relative humidity. Once these readings have been established, the compensator will then modify the nominal value of the laser-wavelength producing a true value. This newly established value is automatically undertaken and then refreshed—every 7 s—and at that moment it is then utilised in subsequent displacement-calculations, virtually eliminating any measurement errors resulting from these variations. Up to three material temperature sensors can also be attached to its accompanying compensator, thereby enabling linear measurements to be normalised to a standard material temperature of 20 °C. At this time it should be noted that both the air and material temperature sensors can be considered as intelligent, with integral-microprocessors to analyse and process these sensors' output, before sending its digital temperature values to the compensator—thus providing secure measurements.

Table 2.3 below shows the integrated laser-sensor's performance for this particular company's current commercial laser system, when they are coupled-up to the compensator unit and ultimately to that of the accompanying laser head—for controlled and accurate calibration readings.

Table 2.3 Typical values obtained for laser-sensor performance—for a representative commercial system

Sensor performance	Range	Accuracy
Material temperature	0–55°C	±0.1 °C
Air temperature	0–40 °C	±0.2 °C
Air pressure	650–1150 mbar	±1 mbar
Relative humidity (%)	0–95 %	±6 %RH

Courtesy of Renishaw plc

2.2 Methods of Machine Acceptance Tests—The Basis for Verification

In order to certify a high-degree of machine accuracy and precision, several measurement systems and processes have been produced, together with their appropriate published International Standards (see Appendix 1) governing machine tool acceptance tests. Procedures for machine acceptance consist of basically two types. These are either: (i) indirect; or (ii) direct processes; to identify a machine's properties. In the case of indirect machine accuracy identification, the trial workpieces are defined by the manufactured geometrical and formal characteristics utilising the machine tool to be tested drawing out deductions concerning machine accuracy/precision, these being based upon the deviations between the required and actual geometries. Here, these indirect processes are more easily matched to final functional tests to determine the accuracy/precision of a machine tool and as a result, are today considered as being the preferred method employed in acceptance tests. When these indirect acceptance criteria are not satisfactory, then direct processes will normally be applied for more detailed examinations. At this time, the direct determination of a machine's properties allows for the identification of so-called error-impacts. Consequently, these parameters are established directly on the machine, with the aid of suitable measurement instruments. Currently, tests of individual criteria, or discrete degrees of freedom can be undertaken, responding to more demanding machine accuracy/precision requirements. Where machine tools are configured with Serial cartesian kinematics, the results of test-measurements can be utilised to re-adjust the machine's performance. This theoretical re-adjustment is possible, as there is an indisputable-connection between the actual confirmation of each axis of the system coordinates for the workpiece and the corresponding actuation-axis of the machine tool.

The parallel kinematic machine tools (see a typically configuration, in Fig. 1.26) are calibrated after machine-assembly in a procedure which, in general, is considered as significantly more complex. With this kinematic-arrangement, it comprises of both the machine's parameter identification and error compensation. Moreover, such parameter identification serves the purpose of accurately determining the geometric parameters of these parallel kinematic machine tools (e.g. such as the actual leg-lengths, or its joint-positions) so the algorithms for the transformation of actuation and workpiece coordinates in such a machine control can be modelled with much greater-precision. Parameter identification serves the purpose of identifying, as directly as possible, the connection between the cause-and-effect of machine-errors, while also finding the decisive reasons underlying this actual error.

2.2.1 ISO 230 Machine Tool Standards—Previous and Current Calibration Procedures

Some of the earliest techniques for the calibration of machines (see the schematic diagrams shown in Fig. 2.3a, b) were quite time-consuming and somewhat

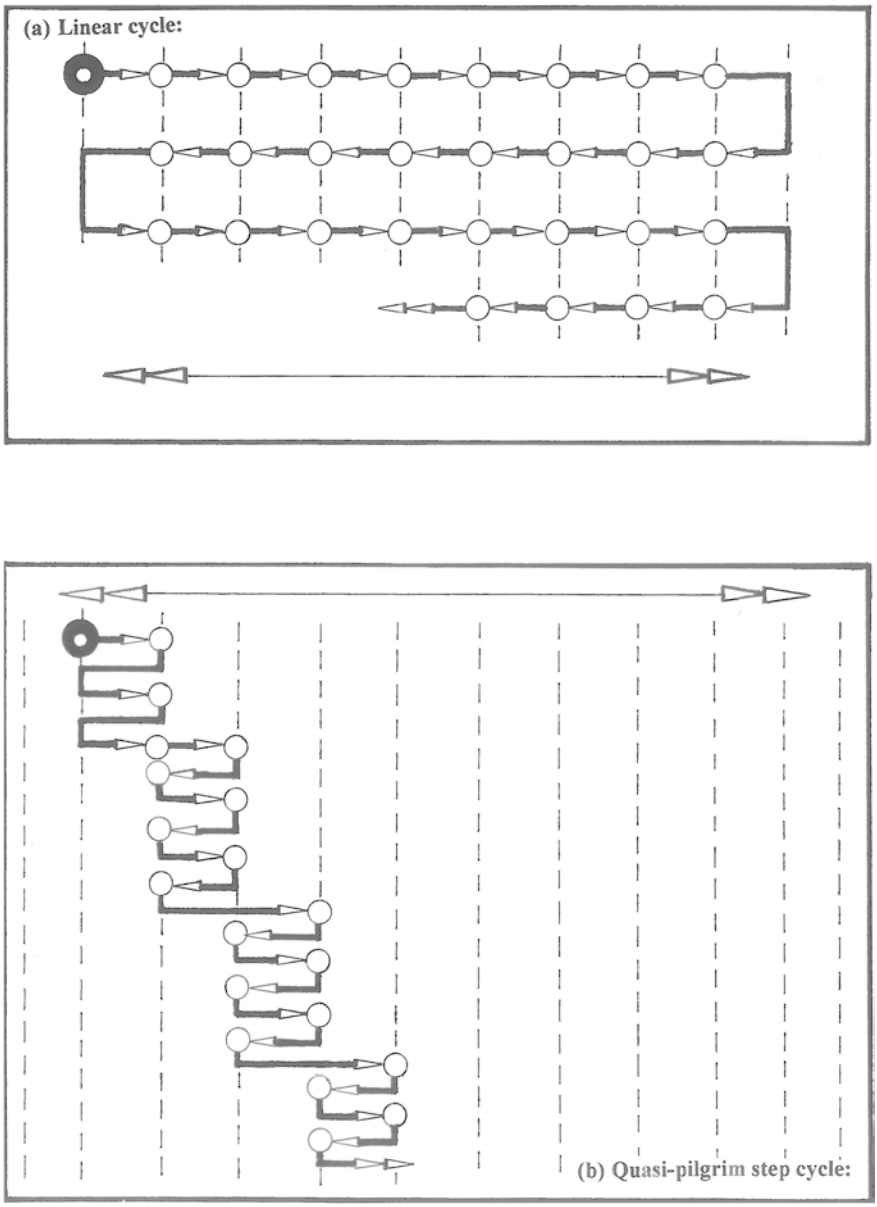

Fig. 2.3 Two types of *static step cycles* for machine tool calibration—previously employed

inefficient; this made them open to some degree of uncertainty in the readings obtained from such procedures. Here, in order to take static readings (i.e. by stop-and-go readings) along a particular axis—typically for straightness measurement—the original standard suggested that the linear motion for the target

positions—utilised in slide-calibration—moved either with the Linear cycle (i.e. Fig. 2.3a), or Quasi-pilgrim step cycle (i.e. Fig. 2.3b). By moving in this repetitive stop-start progressive manner over five bi-directional runs, the potential backlash would be effectively eliminated and its accompanying target-readings would by this procedure be averaged-out. Historically, of the **ISO 230-2** readings at that time, these two differing-techniques—for obtaining machine calibration—would have produced slightly differing results, so each linear-cycle was designated marginally differently, with the linear-cycle being denoted by the suffix 'L' and the quasi-pilgrim step cycle by suffix 'P'. Of note, was that this early standard did indeed state how when, as well as where, it was appropriate to take the calibration readings on a machine tool.

Today, the International Standards such as **ISO 230-series** have evolved from these previous standards that were already in use, in conjunction with the knowledge of current working-practices and with the awareness of the development in new technologies. Over the last several decades the **ISO 230-1 to 11** (parts) has been internationally adopted as the means to calibrate and validate vertical-spindled CNC machine tools, while **ISO 13041-1 to 8**[7] (parts) considers the testing of horizontal spindled machines—typified by that of turning Centres. For Co-ordinate Measuring Machines (CMM's) the equivalent standard here is **ISO 10360-1 to 6** (parts) which has also seen similar international-approval. Returning once again to the relevant **ISO 230-series** for machine tools equipped with vertical spindles, they can be simply described, in the following manner:

- **ISO 230-1: 2012 Part 1: Geometric accuracy of machines operating under no-load, or finishing conditions**—specifies methods for testing the accuracy of machine tools, operating either under no-load, or under quasi-static conditions, by means of geometric and machining tests. The methods can also be applied to other types of industrial machines. This Standard also covers power-driven machines, which can be used for machining metal; wood; etc.; by the removal of chips; or swarf material; or indeed by plastic deformation. However, it does not cover power-driven portable hand-tools. This **ISO 230-1** relates to the testing of geometric accuracy, but it is not applicable to the operational-testing of the machine tool for its: vibrations; stick-slip motion of components; etc.; nor to the checking of characteristics—such as speeds and feeds. Furthermore, it does not cover the geometric accuracy of high-speed machine motions—where its machining-forces are typically smaller than the acceleration-forces;

[7]**ISO 13041-1** for example, specifies with reference to: **ISO 230-1:1996**: the geometric tests on numerically controlled (NC) Turning machines and Turning Centres, of normal accuracy, with horizontal work-spindle(s). This Standard specifies the applicable-tolerances corresponding to the tests mentioned above; and goes on to explain different concepts, or configurations and common features of CNC Turning machines and Turning Centres. Moreover, the Standard also provides a terminology and designation of controlled axes. Here then, this **ISO 13041** also deals with verification of the accuracy of the machine. It does not apply to the operational-testing of machines (e.g. vibration, abnormal noise, stick-slip motion of components), nor to the machine's characteristics (e.g. speeds, feeds) as such, these checks are generally undertaken before testing the accuracy. For more information on the other parts of: **ISO 13041-series** of tests—see Appendix 1.

- **ISO 230-2: 2006 Part 2: Determination of accuracy and repeatability of positioning CNC machine tools**—the Standard specifies methods for testing and evaluating the accuracy and repeatability of the positioning of numerically controlled machine tool axes, by direct-measurement of individual axes on the machine. These methods apply equally to both its linear and rotary axes. However, when several axes are simultaneously under test, the methods do not apply. Here, **ISO 230-2** can be utilised for: type-testing; acceptance tests; comparison testing; periodic verification; machine compensation; etc. In this Standard, the methods involve repeat-measurements at each position. The related parameters of the test are defined and calculated, with their uncertainties being estimated—as described in: **ISO/TR 230-9:2005, Annex C**;
- **ISO 230-3: 2007 Part 3: Determination of thermal effects**—defines three distinct tests for the determination of thermal-effects on machine tools: (i) an environmental temperature variation error (ETVE) test; (ii) a test for thermal-distortion, caused by rotating-spindles; (iii) a test for thermal-distortion, resulting from moving linear axes. The test for thermal distortion caused by moving linear axes is applicable to computer numerically controlled (CNC) machines only and is expressly designed to quantify the effects of thermal expansion and contraction, together with the rotational-deformation of its structure. Hence, for practical reasons, it is applicable to machines with linear axes up to 2000 mm in length. If such tests are utilised for machines with axes longer than 2000 mm, then it will be necessary to choose a representative length of 2000 mm, but in the normal-range of each axis for the tests. These tests will correspond to that of drift-tests-according to **ISO/TR 16015** and then define the evaluation and the detailed procedure for such machine tools;
- **ISO 230-4: 2005 Part 4: Circular Test for CNC Machine Tools**—here, it specifies methods of testing and evaluating the bi-directional circular-deviation, as well as the mean bi-directional radial deviation, according to the circular-deviation and the radial-deviation of circular paths that are produced by the simultaneous movements of two linear axes. Thus, the standards objective, is to provide a method for the measurement of the contouring-performance of a CNC machine tool;
- **ISO 230-5: 2000 Part 5: Determination of the noise emission**—this part explains how, where, plus when noise-emissions are undertaken and the levels of acceptable-noise, also with the techniques and equipment utilised to establish these noise-levels;
- **ISO 230-6: 2002 Part 6: Diagonal displacement test**—specifies the actual diagonal displacement tests which allow the estimation of the volumetric-performance of a machine tool. The complete testing of the volumetric-performance of a machine tool is both a difficult and time-consuming process. Subsequently, diagonal displacement tests have been developed, that can reduce the time and cost associated with testing for the machine's volumetric performance. A diagonal displacement test is not in itself a truly diagnostic test, although conclusions of a diagnostic nature may sometimes be possible from these test results. In particular, when face diagonal tests are included, a direct

measurement of the axes squareness is also possible. Diagonal displacement tests on the body diagonals may be supplemented by tests in the complementary face diagonals, by tests parallel to the machine axes in accordance with **ISO 230-2**, or by the evaluation of the contouring-performance in the three coordinate planes, as defined in **ISO 230-4**. These types of diagonal displacement tests may be utilised for acceptance-purposes and as reassurance of machine performance—where parameters of the test are utilised as simply a comparison-index;

- **ISO 230-7: 2006 Part 7: Axes of rotation**—this Standard is primarily aimed at standardising methods of specification and test for the geometric accuracy of axes of rotation utilised in machine tools. Spindles, rotary heads and rotary and swivelling tables of machine tools will constitute axes of rotation, all of these having unintended-motions in space, as a result of multiple-sources of errors. Here, **ISO 230-7** encompasses the following properties of spindles axis of rotation error motion, together with speed-induced axis-shifts. The other additionally important properties of spindles will include, such factors as: thermally induced axis-shifts and environmental temperature variation-induced axis-shifts, both of which are dealt with in: **ISO 230-3**;
- **ISO 230-8: 2010 Part 8: Determination of vibration values**—this Standard is primarily concerned with the different types of vibration that can occur between the tool-holding part as well as the workpiece-holding part of a machine tool. (NB For simplicity, these features are generally referred to as simply the tool and workpiece, respectively.) These are vibrations that can adversely -influence the production of both an acceptable surface finish and an accurate workpiece. Here, the Standard is not aimed predominantly at personnel who have specialist expertise in vibration analysis and who would routinely undertake such work in research and development environments. However, the standard does not therefore replace relevant textbooks on the subject, but is normally intended for manufacturers and users alike, with general engineering knowledge—in order to enhance their understanding of the causes of vibration, by providing an overview of the pertinent background theory. **ISO 230-8**, will also provide basic information on measurement procedures for evaluating certain types of vibration problems that can beset a machine tool, such as:
  - vibrations occurring as a result of mechanical-unbalance;
  - vibrations generated by the operation of the machine's linear slides;
  - vibrations transmitted to the machine by external forces;
  - vibrations generated by the cutting process including self-excited vibrations—specifically chatter;
- **ISO 230-9: 2005 Part 9: Estimation of measurement uncertainty for machine tool tests according to ISO 230, basic equations**—this Standard will provide information on a possible estimation of the measurement uncertainties—for measurements according to **ISO 230**;
- **ISO 230-10: 2011 Part 10: Determination of the measuring performance of probing systems of a CNC machine tool**—is where it specifies test procedures to evaluate the measuring performance of contacting-probing systems

(i.e. utilised in a discrete-point probing-mode) being integrated with a numerically controlled machine tool. Moreover, it does not include other types of probing-systems, such as those used in a scanning-mode, or non-contacting probing-systems. Here, it should be noted that the evaluation of the performance of the machine tool being utilised as a coordinate measuring machine (CMM) is considered to be outside-the-scope of **ISO 230-10**;

- **ISO 230-11 [Standard in development: PD ISO/TR 230-11]: Part 11: Measuring instruments and their application to machine tool geometry tests**—this Standard's aspect will be concerned with that of measuring instruments. This standard in development is categorised in boring and milling, dividing and tool-workpiece holding devices, electrochemical machines, general, grinding and polishing, lathes, machining centres, manufacturing engineering, measurement; vibration and shock, numerically controlled machines, other specific equipment.

[Abridged details, courtesy of the ISO (2015)]

2.2.2 ISO 230—Laser Calibration Procedures on CNC Machine Tools

Before considering any laser calibration procedure on a CNC machine tool, it has already been mentioned that probably the greatest-uncertainty in most laser-measurements results from variations in its attendant environmental-conditions (e.g. these include air-temperature, air-pressure, also humidity) when compared to nominal values. Even relatively minor-variations in the ambient conditions will modify the laser-wavelength and consequently the resulting data-measurement reading. By the way of a practical example of this potential alteration in test conditions, if the following changes occurred, then they will increase laser wavelength by 0.25 ppm, such as 0.26 °C air-temperature increase, or a 0.93 mbar air-pressure decrease. Whenever such variations occur of temperature, humidity, plus pressure—from the nominal values—which are then combined, they can create a 20–30 ppm uncertainty in measurement (i.e. even if the test conditions remain stable during the whole test time-period). In order to mitigate against the undesirable variation in potential testing conditions, an Environmental compensation unit is normally included within the system, having some very accurate and precise environmental sensors, which will then compensate for these effects of the laser-wavelength. In the case of laser interferometer company's products, they will make great-efforts ensuring that their merchandise, such as their Compensation system and sensors—are highly accurate and precise across the entire operating-range of the system. It is this exacting-level of compensation that can typically maintain ±0.5 ppm linear measurement accuracy/precision from 0 to 40 °C ambient temperatures and, over the full air-pressure range, which thus ensures that reliable and traceable results are obtained from their sensors and instrumentation.

For many years the industry standard method of measuring CNC machine tool, or CMM performance, has been by utilising a free-standing laser, on a tripod, in combination with remote (i.e. separate) interferometer and reflector optics, these usually being mounted directly onto the machine table and into the spindle (i.e. see Figs. 2.1bi and 2.2a). The linear, angular (i.e. pitch and yaw), or straightness measurements between table and spindle, can then be separately commenced interferometrically, by utilising the appropriate choice of the system's interferometer optics. More recently, alternative systems have been introduced that depart from the above technique in one, or two significant areas, with these alternative calibration strategies being that they use:

1. **a linear interferometer optic that is combined with the laser-head** (i.e. either internally, or externally)—with the laser-head—in this case, being mounted directly onto the machine—rather than on its more-usual, separate tripod;
2. **remote electronic targets** (i.e. not interferometers)—these are utilised to measure: pitch; yaw; and straightness errors. With some laser systems, they can provide simultaneous 5-dimensional (i.e. 5D) measurements.

These alternative systems appear to suggest the benefits of easier set-up, increased portability and significantly reduced measurement time (i.e. particularly, if electronic targets and a linear interferometer are utilised to provide simultaneous linear, angular and straightness readouts). However, these more recently devised alternative techniques are often at the expense of both the machine's measurement accuracy and stability.

Comment will be made in the following extended-discussion on each type of measurement-mode, explaining the benefits of obtaining measurements interferometrically, but here, with a tripod-mounted laser system and by employing remote interferometer optics. Furthermore, these specific comments will then go on to consider the importance of the environmental compensation system—for its accompanying linear measurement accuracy.

There are number of distinct advantages in utilising a tripod-mounted laser with only the remote interferometer-optics mounted directly onto the machine, these being that the:

- **heat generated by the laser is isolated from the interferometer optics**—this allows the linear interferometer and reference arm to form the reference point from which all machine movement is measured. So any changes in the interferometer position or in the reference arm length, caused by thermal expansion/contraction, will degrade the accuracy of this measurement. In order to ensure that such changes are kept to an absolute minimum the laser system mimics good metrology principles, by ensuring that the heat of the laser source is distanced from that of the measurement-optics. Laser systems that employ an interferometer inside the laser-head, or have it mounted onto the front of this laser-head, do not follow these principles and as a result are likely to suffer from significant thermal-drift, both during laser warm-up as well as when ambient environment changes. Such thermal-drifting can have a magnitude of several orders of micrometres;

- **heat generated by the laser is remote from the machine under test**—typically, a Helium–Neon laser-head will dissipate >5 W of heat—with even more if it contains its integral power supplies. By situating a heat-source on, say, a small but high-accuracy machine, this action may cause a combined thermal-expansion and distortion of that machine. However, these effects are generally quite small but they can degrade the accuracy of results—at the micrometre-level of measurement. Consequently, by mounting the laser on a tripod, away from the machine, this will eliminate such heat-induced potentials;
- **laser-head does not obstruct axis movement**—if the laser-head is placed on the machine, its relative-size can often reduce the available range of travel of the axis under-test. Conversely, when the laser is mounted on a tripod, the only associated-items situated on the machine are its small interferometer optics, which will provide less-restriction in its axis-range of motion;
- **beam alignment adjustments can be undertaken outside the machine's envelope**—equally, if the laser is mounted inside the machine, all such laser-beam alignment adjustments have to be made inside the machine. A further restriction is that the machine's geometry and its machine guards, for any form of alignments, may make adjustments difficult to achieve. Certain laser systems allow adjustments to be made externally, by either utilising the tripod's stage-controls to move the laser, or internally—utilising a Beam-steering optic (see Fig. 2.1, bottom); this novel optical device being mounted directly onto the interferometer. Thus, a tripod-based laser allows the end user to choose the easiest method for calibration-testing—for the machine under-test;
- **there are no trailing cables inside the machine**—here, the laser-head requires power and signal cables, but in the case of the interferometer optics it does not. Subsequently, by mounting the laser on an external tripod with just the optics inside the machine, this avoids the need to route both the power- and signal-cables into the moving machine, preventing the expected problems of snagging, or dragging of these cables, which may cause either some damage, or a measurement error to occur.

Provided that any thermal drift has been eliminated (i.e. see first point above) then the accuracy of linear laser measurements will primarily depend on the performance of its integrated weather-station and not the laser-head. As a consequence, the accuracy of the weather-station sensors' over the full range of operation is a critical factor.

When undertaking either a full calibration, or verification procedure on a CNC machine tool, certain tests must be undertaken in accordance with the various **ISO 230—Parts**-see Sect. 2.2.1, these critical factors will be very briefly mentioned below:

- **linear positioning accuracy and repeatability of an axis**—the laser can measure the actual displacement moved along an axis and compare it against the displacement shown by the machine's axis encoders. This is the basis for error-compensation of machine tool CNCs—**see Appendix 3a**;
- **straightness of an axis**—both horizontal and vertical straightness of motion along an axis can be measured. Straightness-errors have a direct influence on

the machine and influence the cutter's path accuracy but, they are unlikely to be uniform along the entire axis of a machine's slide—**see Appendix 3b**;

- **squareness between axes**—these orthogonal axes of a machine tool need to be square to each-other, as well as accurate along their length. By utilising, say, a previously calibrated Optical-square and combining the two straightness-measurements, the squareness of two axes can be calculated precisely—**see Appendix 3c**;
- **flatness of a surface**—flatness of reference-tables (i.e. such as the machine tool's table) can be critical—as they are datum-surfaces for any potential measurement. This flatness-measurement enables a 3-D picture of its surface-form to be built-up—**see Appendix 3d**;
- **angular pitch and yaw of an axis**—these problems are common causes of positioning-errors. Even just a small error at the machine's spindle can cause a significant effect at the extended-position of the tool's tip, meaning that any interferometric-measurement must be fully traceable to International Standards—**see Appendix 3e**;
- **rotary axis/table angular positioning**—rotary axes are now becoming increasingly common features on multi-axis machine tools. Typically, a Rotary Axis Calibrator can provide for automatic data collection when utilised with a laser-head and its matched angular-optics—**see Appendix 3f**.

2.2.3 Laser Diagonal Displacement Test

The International **ISO 230-6** Standard specifies diagonal displacement tests—see Figs. 2.4, 2.5, 2.6 and 2.7 which allows the estimation of the volumetric-performance of a CNC machine tool. However, in some supplementary-topical work[8] on such testing, it was highlighted that under certain conditions, a machine can achieve a good result from the **ISO 230-6** and **B5.54 Diagonal Tests** even if this plant has a poor volumetric-performance. This positive-outcome is because changes in the lengths of the body-diagonals created by one source of error in the machine can be subsequently cancelled-out by the changes due to yet another source of error. This effect is illustrated by considering a volumetric capacity of $2 \times 1 \times 0.5$ m on an orthogonal machine tool. If the machine has no errors, then the body-diagonal measurement will show that, to the nearest micrometre, all four body-diagonals are exactly 2.291288 m long—this is derived from Pythagoras' theorem (see below). If one now supposes that this identical machine tool has a 25 μm m^{-1} over-travel error (i.e. a positive linear-error) in the motion of the *X*-axis, with a 100 μm m^{-1} under-travel (i.e. a negative linear-error) in the *Y*-axis motion but no error in the *Z*-axis, then under these set of conditions, the laser

[8]Chapman (2003).

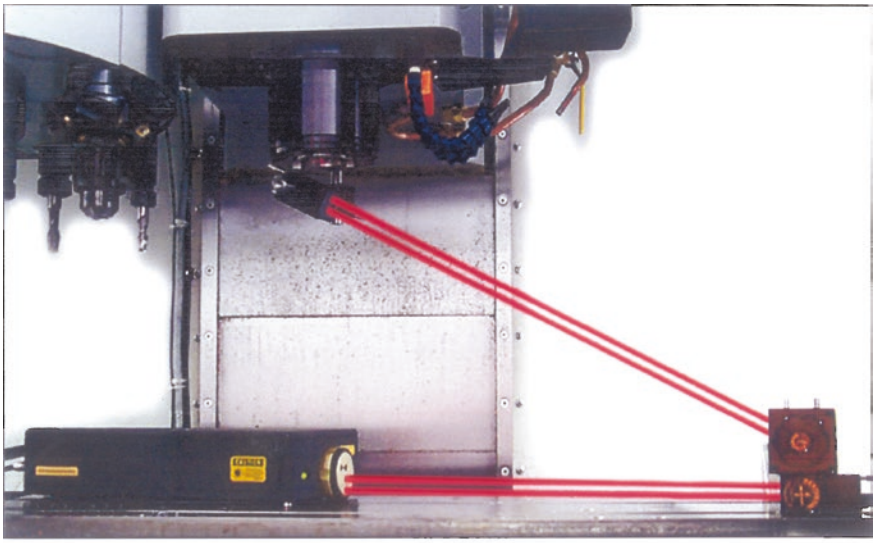

Laser diagonal test setup on a vertical Machining Centre.

[Courtesy of Renishaw plc]

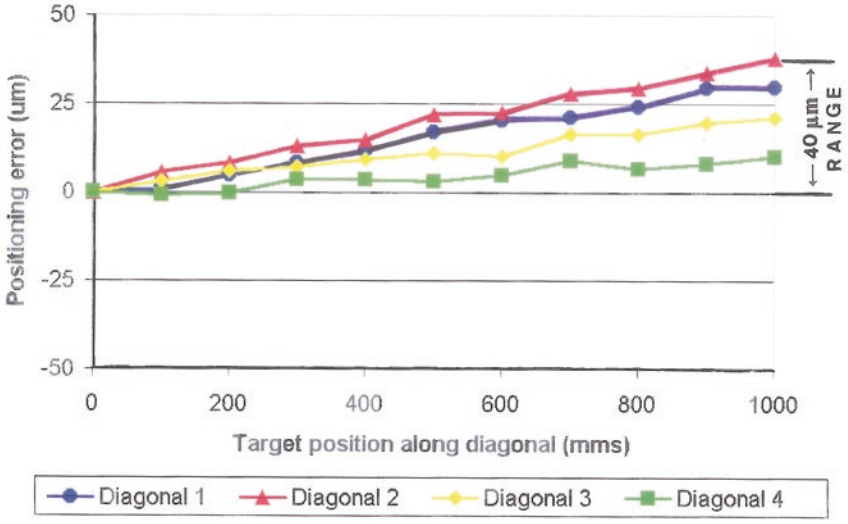

Typical B5.54 diagonal test results from a machine.

[Courtesy of Renishaw plc]

Fig. 2.4 The laser diagonal test on a machining centre and some typical test results

(a) The Laser Diagonal Test for Machining Centres are described in ISO 230-6 Standards, with the Laser interferometer being aligned to one of the four-body diagonals.

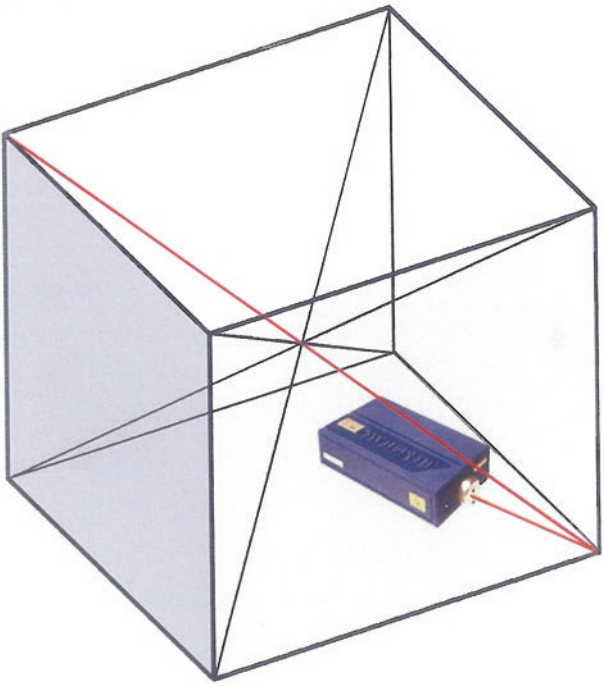

(b) A typical Laser Diagonal Test setup for a vertical Machining Centre.

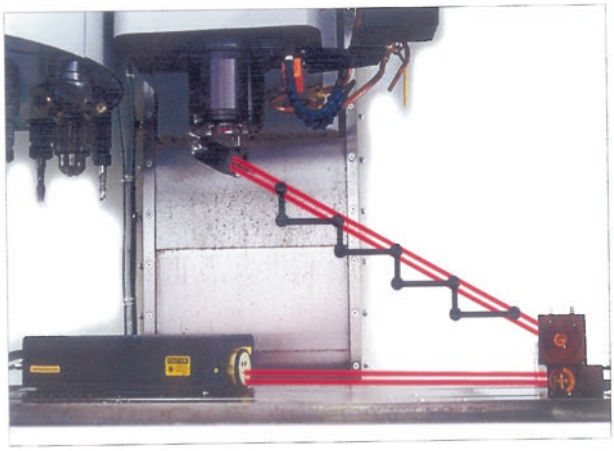

Fig. 2.5 The laser diagonal calibration setup for a typical machining centre (courtesy of ISO standards/Renishaw plc)

a) The *Laser Diagonal Test* - based upon the Standards: B5.54 and ISO230-6:

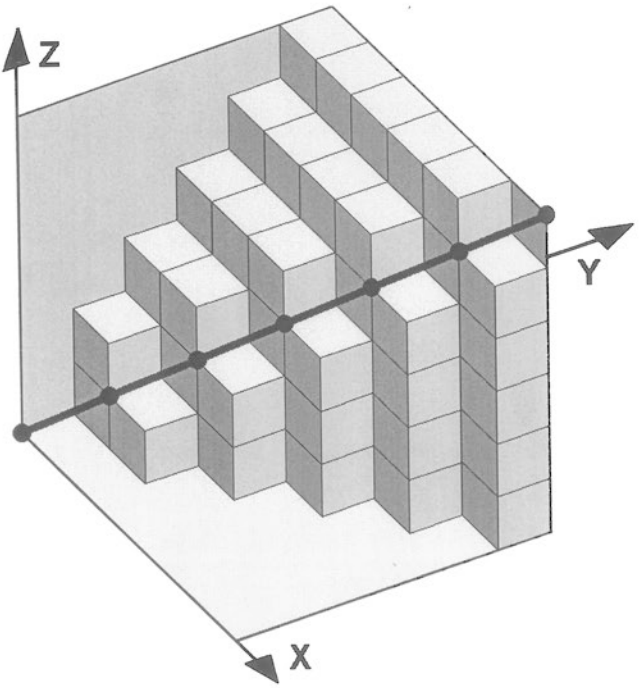

(b) The *Laser Step Diagonal Technique* - for orthogonal machine tool calibration:

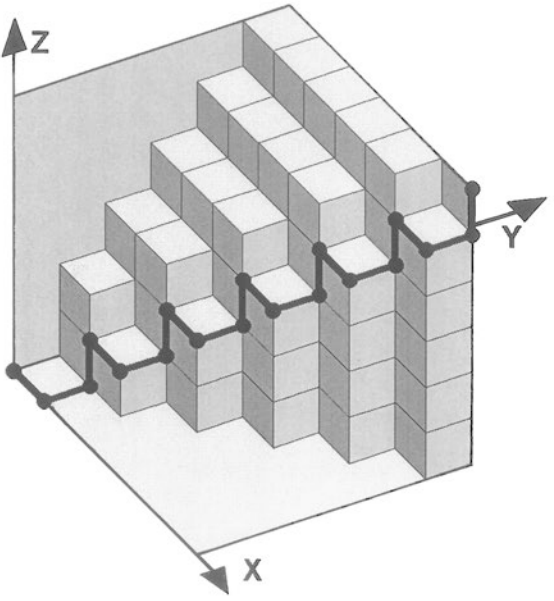

Fig. 2.6 Typical laser diagonal tests for orthogonal machine tools (courtesy of Renishaw plc)

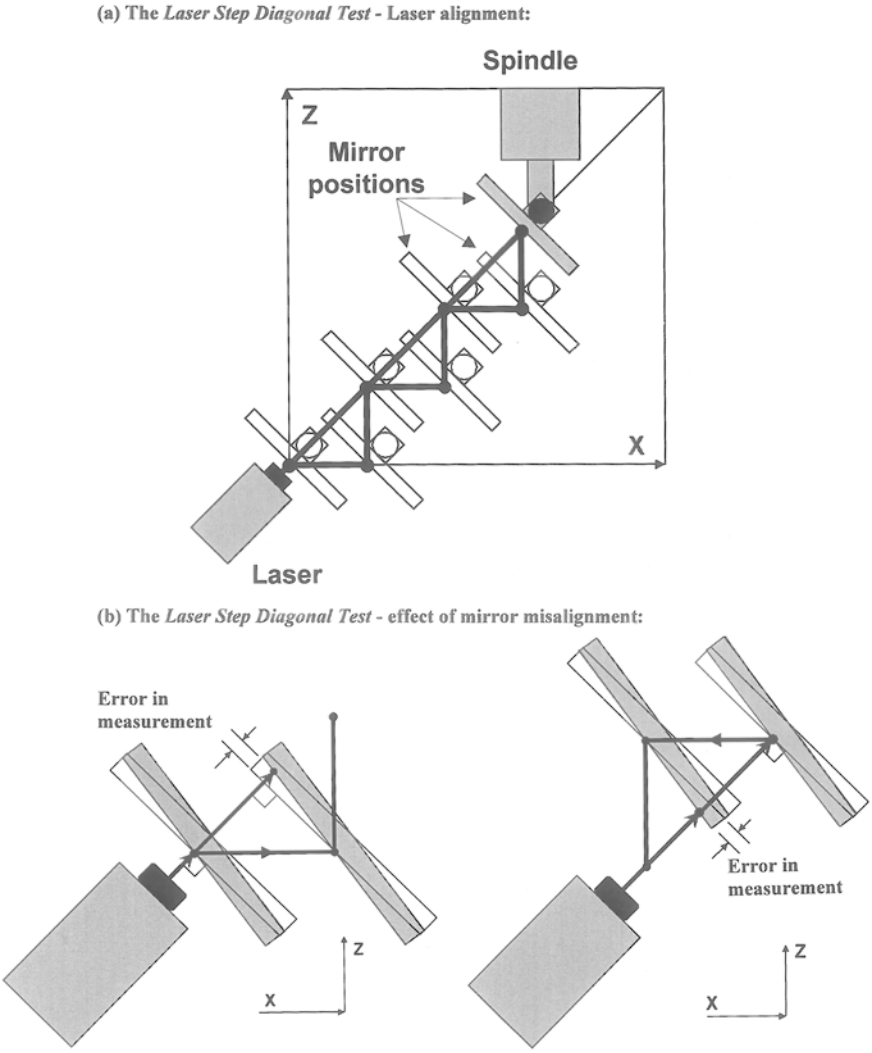

Fig. 2.7 Practicalities of the laser step diagonal testing arrangements (courtesy of Renishaw plc)

diagonal test will show that these diagonal lengths have changed by less than 0.1 μm and so, to the nearest-micrometre, they are still in effect 2.291288 m long—also derived from Pythagoras' theorem:

$$2.291288 = \sqrt{(2.000052 + 0.99992 + 0.52)}$$

Both the Standards **B5.54** and **ISO 230-6 Diagonal Tests** will indicate that the machine is still acceptable, even when this is undoubtedly not the case. The machine has a volumetric-error of >100 μm. It should also be noted that the

volumetric-error is defined in this situation as follows, "The length of the worst-case error vector between the target and the actual machine position anywhere within the machine volume". Laser measurement of overall diagonal-lengths and the results of these laser **B5.54** and **ISO 230-6 Diagonal Tests**, do not always give reliable-indication of volumetric-performance, so they should be interpreted with some caution. The act of undertaking any Diagonal-tests should not be utilised in isolation when comparing the actual volumetric-performance of machines. In order that reliable results are obtained, it is important to also undertake some supplementary tests,[9] such as for: linear accuracy; as well as pitch and yaw tests that are parallel to the *X*-, *Y*- and *Z*-axes. These additional tests are all succinctly defined in the **B5.54** and **ISO 230-Series** of Standards, although they are occasionally disregarded—to minimise actual calibration test-times.

Specific **Laser diagonal Tests** for Machining Centres are precisely described in **B5.54** and **ISO 230-6 Standards**. With such tests, a laser interferometer is utilised to measure the linear positioning accuracy of the machine as it proceeds along each of its four body diagonals in turn—see Figs. 2.4 (top) and 2.5a. The illustration (i.e. Fig. 2.4, top) shows a laser that is aligned (i.e. via a mirror) to one of four body-diagonals. A number of equi-spaced target positions—see Fig. 2.6a—are defined along each body-diagonal. Accordingly, the machine is then moved along this diagonal, from one target position to the next. Here, the laser will measure the linear-positioning errors at each target position. Moreover, measurements are taken in both the forward and reverse directions, and then they are averaged. Further measurements are then similarly repeated along each body-diagonal in turn. These laser diagonal test results can then be presented graphically—as depicted in a typical test run shown in Fig. 2.4 (bottom). In this **B5.54** test procedure, the diagonal positioning accuracy is quoted from the diagonal with the largest range of error-values where it is shown to be, in this example, 40 μm. By way of illustration and subsequent comprehension of these two important internationally applied standards, the following comments can be subsequently compared:

1. **American Standard B5.54: 1992**, states that, "The volumetric accuracy of a machine may be rapidly estimated by measuring the displacement accuracy of the machine along body diagonals";
2. **International Standard ISO 230-6: 2002**, states that, "The Diagonal displacement tests allow the estimation of the volumetric performance of a machine tool and, that these Diagonal displacement tests may be used for acceptance purposes and as reassurance of machine performance where parameters of the test are used as a comparison index".

[9]**ISO 230-6 Standard**: suggests additional tests to supplement the Body Diagonal Tests with such: tests on face-diagonals; tests parallel to the machine's axes; by either the well-known Circular test (i.e. see reference to Knapp, W.), or by Telescoping ballbar tests—see the Chap. 4 for details of this latter testing-regime.

In some contemporary applied research work at the company Renishaw plc and by others,[10] it has been shown that any estimates of volumetric, or machine performance which are based on these diagonal tests in isolation, may be considered as somewhat unreliable. To expand on this important unreliability-theme in some more detail, the results of a diagonal-test alone cannot be used as a reliable machine comparison-index. The potential weakness with this testing strategy—which has been reported for this diagonal test on a machine—can be comprehended more simply by considering a simple 2-D example, if one were to consider a perfect 1 m^2 planar machine, with the axes travel of the '*X*' and '*Y*' being both exactly 1 m and the machine which contains either no other positioning or geometric errors. So, simplistically, the length of both diagonals is given by Pythagoras' theorem,[11] as follows;

$$\text{Diagonal length} = \sqrt{\left(1^2 + 1^2\right)} = 1.4142136 \text{ m}$$

Now, let one imagine that the machine is somehow distorted, such that the *X*-axis over-travels by 25 μm m^{-1} and the *Y*-axis under-travels by 25 μm m^{-1}, of note is that these linear-positioning errors of this magnitude are relatively common in many machine tools, usually due to inaccuracies in the feedback-system (e.g. possibly the result of the original installation for the Ballscrew-tensioning/-preload and, possibly, resulting from any associated thermal-effects). Consequently, the length of the diagonals of this distorted-machine, are once again derived from Pythagoras' theorem, thus:

$$\text{Diagonal length} = \sqrt{\left(1.000025^2 + 0.999975^2\right)} = 1.4142136 \text{ m}$$

NB: here, the diagonal length appears unchanged, accordingly, for this test of a machine:

- diagonal length of perfect machine = 1.4142136 m;
- diagonal length of distorted machine = 1.4142136 m;
- thus, the diagonal lengths are the same ($\leq$ 0.001 μm);

[10] Ibaraki and Hata (2010). Plus, these findings confirmed once again the initial data obtained by: Chapman (2003).

[11] **Pythagoras' theorem**: in mathematics, the well-known **Pythagorean theorem** is an exacting-relationship in **Euclidean geometry**, being based upon the simple relationship of three sides of a right-angled triangle. It is a frequently applied geometric relationship, which simply-states: "That the square of the hypotenuse [i.e. the side opposite the right angle] is equal to the sum of the squares of the other two sides". This completely-reliable geometric-theorem was obviously-named after the Ancient Greek Mathematician: Pythagoras—who was Born on: Samos (Greece) in 570 BC, then died: in Metapontum (Italy) in 495 BC.

Table 2.4 Demonstrates the performance of three nominally identical 1 m^3 machine tools. Each machine tool has a different combination of linear-positioning errors in their respective axes (courtesy of Renishaw plc)

	Machine A	Machine B	Machine C
X axis linear error (um/m)	50	50	100
Y axis linear error (um/m)	50	0	−50
Z axis linear error (um/m)	−100	0	−25
B5.54 diagonal test result (um)	0	29	14
volumetric accuracy[a] (um)	122	50	115

[a]Volumetric-accuracy, can be defined as: "the length of the worst case error vector between the target and the actual machine position anywhere within the machine volume"

- that both the perfect and the distorted machine show identical results on a diagonal test, even though the distorted machine contains some distinct and mindful positioning-errors of >25 μm.

At this point, it might be considered that this test is somewhat of a special-case, which only occurs on, say, a 2-D machine tool if the error in the *X*-axis motion is exactly equal and opposite to the error in the *Y*-axis motion, but this is not the case; explaining this apparent-dilemma as follows: if any axis (or axes) shows an over-travel error whilst any another axis (or axes) shows an under-travel error, then their combined-effect on the body-diagonal length will normally cancel-out. These types of positional-errors are particularly common on machine tools. However, this problem will also occur on other orthogonal 3-D machine tools, as shown in Table 2.4.

From this Table 2.4 we note that there is a complete lack of correlation between the volumetric-accuracy of these machines and their diagonal test results. In the two extreme cases, machine A has the worst volumetric-accuracy, but displays no error on the diagonal test; while machine B has the best volumetric-accuracy, but shows the worst result for its diagonal test. Therefore, contrary to the statements in both **B5.54** and **ISO 230-6**, it now seems obvious that these laser diagonal test results do not provide a reliable estimate of volumetric accuracy, or performance—so cannot be utilised as a reliable comparison index between machines. However, what can be implied concerning these laser diagonal tests is that they do not provide a reliable method of measuring a machine's volumetric-accuracy but they can provide a good technique of measuring the squareness between any two axes.

In order to obtain the most accurate test results, it has also been suggested that to measure a face rather than the body diagonals will reduce the test time and as a result, will improve sensitivity. For example, if the two face diagonal lengths are designated as '*d*1' and '*d*2'—which are slightly distorted—then the machine squareness error (in radians) is given by:

$$\theta \approx \left(1 + m^2\right)(d1 - d2)/[m(d1 + d2)]$$

where: '*m*' = machine aspect-ratio.

The relative accuracy of a squareness result (i.e. angle) can be improved if:

- **the machine's axes are of similar lengths**—as this will improve sensitivity;
- **the test is quickly performed**—to minimise any thermal changes between measurement of each diagonal length;
- **results plotted graphically**—as it would show this squareness-effect of ±1 and ±5 ppm shifts in laser reading on the accuracy of squareness results for various aspect-ratio machine tools.

In addition, the accuracy of the squareness result (i.e. angle) is also enhanced if the diagonal-measurements both start and finish at identical '*X*', '*Y*', or '*Z*' coordinates. This measurement-strategy will ensure that the effects of other machine-errors are effectively eliminated. Furthermore, any potential backlash present, can be eradicated by always moving the axis in the same direction—before taking each reading. Under such ideal-conditions, it is possible to measure machine squareness within ±1 arcsecond. The technique is especially useful on much larger machine tools, where obvious access to an enormous mechanical reference square may prove to be distinctly restrictive.

In conclusion, one can make the following observations concerning such diagonal-testing applications … that these:

- **Laser Diagonal Tests**—can provide a quick and efficient technique of measuring a machine, as it moves-along a machine's diagonals;
- **Laser Diagonal Results**—can, with some care, be utilised to accurately establish the squareness errors between axes;
- **Laser Diagonal Measurements**—are sensitive to multiple machine error sources, nonetheless, it is possible for the effect of one error source on the diagonal to cancel another, thus, giving laser diagonal results that do not relate to the volumetric accuracy of the machine;
- **Laser Diagonal Testing**—when utilised in isolation, does not provide a reliable method of measuring machine volumetric-accuracy;
- **Laser Diagonal Testing Regimes**—offer a more reliable evaluation of machine performance, which should invariably be supplemented with other tests, typically by, Telescoping ballbar—Circular tests, together with conventional laser-calibration, by linear; angular; plus straightness tests; which are parallel to the machine's axes;
- **Machine Testing Techniques**—which are currently defined in both the American **B5.54** and **B5.57 Standards**, as well as in the **ISO 230-series** of International Standards.

2.2.4 Laser Step Diagonal Test

In relatively recent years, it has been proposed in a that the original Laser Diagonal Test can be suitably enhanced by using a Special Step-sequence to move between target positions on the body diagonals. This announced and modified

testing-technique is often known as either a step diagonal, or the vector method. In the original laser diagonal tests (i.e. as appropriately described in both the **B5.54** and **ISO230-6** Standards), the machine progresses movement of its *X*-, *Y*- and *Z*-axes simultaneously, to move in a straight-line between the target positions along each of its body-diagonals—see Figs. 2.4 (top), 2.5a and 2.6a. This compound-angled linear-motion is simply illustrated in Fig. 2.6a, which shows the target positions (i.e. here being depicted simply as black dots) along just one of the body diagonals. This laser-data is then recorded at each target-position, by utilising a laser linear interferometer, which is aligned along the diagonal and striking an aligned retro-reflector optic. A number of equi-spaced target-positions are defined along each body-diagonal. The machine is then moved along this diagonal, from one target position to the next. Simultaneously, the laser will then measure the linear-positioning error at each target-position. Measurements are taken in both the forward- and reverse-directions and these results are averaged. This measurement-strategy is then repeated along each of its body-diagonals in turn—as depicted in Fig. 2.5a. Results are typically presented graphically (i.e. as shown in the graph in Fig. 2.4, bottom). In **B5.54**, the diagonal-positioning accuracy is quoted from the diagonal with the largest-range of error-values—shown here (Fig. 2.4, bottom), where in this example, it was found to have a 40 μm range. Conversely, in the case of the step diagonal test, or vector test, the *X*-, *Y*- and *Z*-axes are moved individually (i.e. separately—one-axis-at-a-time)—as shown once again by the black-dots (i.e. see Figs. 2.5b and 2.6b) with laser-data recorded after the movement of each axis. This particular type of Stepped 3-D motion, will generate up to three times as much positional-data when compared to that of the Laser Diagonal Test. This motional-action being illustrated in Fig. 2.6b, which shows the effect of these additional target-positions.

It has been claimed by some investigators (i.e. see Footnote 10) that in addition to the original diagonal-displacement error results, the step diagonal method can also provide results for the: linear-accuracy; straightness; plus squareness; of the machine tool's *X*-, *Y*- and *Z*-axes. In order to undertake this specific test, the laser system is usually operated with a plane mirror reflector mounted onto the machine's spindle (i.e. see Fig. 2.5b). This laser-setup configuration of the mirror held in the machine's spindle, ensures that the laser-beam is always returned into the laser's return port as the machine zig-zags along the machine's diagonal (i.e. see Fig. 2.6b). However, in some more recent detailed analysis of the technique, it has been highlighted that there may be some fundamental flaws with this Laser Step Diagonal technique. The fundamental reasons for this deduction—concerning some specific flaws in this Step Diagonal Method, are suggested and listed below:

- **maintaining alignment of the laser beam**—so, as the machine moves along the stepped diagonal path, the laser is directed onto an angled plane mirror fixed to the machine spindle;
- **successive positions of the mirror**—are shown in Fig. 2.7a, as it is moved along the diagonal;
- **2-D schematic view**—here in Fig. 2.7a, is shown for simplicity;

- **laser beam**—is shown as having a straight path in Fig. 2.7a;
- **machine movement path**—is shown as a zig-zag black line (i.e. *X*, and *Z* linear motions);
- **laser beam and mirror are aligned perfectly**—thus, indicating that here, there are no: pitch-; yaw-; and roll-errors; in the machine, then the theory of operation is stated as follows:
  - when the *X*-axis moves, then the laser will measure the combined effect of errors in the linear and straightness motion of the *X*-axis;
  - when the *Y*-axis moves, then the laser will measure the combined effect of errors in the linear and straightness motion of the *Y*-axis;
  - thus, when the *Z*-axis moves, then the laser will measure the combined effect of errors in the linear and straightness motion of the *Z*-axis;
  - once data has been taken along all four body-diagonals, the individual contributions from the linear- and straightness-errors of each axis and the squareness-errors between the three orthogonal axes can, in theory, be calculated.

Nevertheless, there appears to be two fundamental complications here with the Step Diagonal Method, they are …:

1. when the vast-majority of orthogonal-based machine tools do have any significant types of: roll-; pitch-; and yaw-errors. These errors will influence the results, by introducing additional error terms which the proposed-calculation method does not unfortunately resolve;
2. when significant errors occur in the alignment of the plane-mirror and laser beam, which will introduce additional errors that cannot be separated-out from the linear-displacement errors in the *X*-, *Y*- and *Z*-axes of the machine tool.

In the following text, the problem with mirror alignment is explained in more detail in the circumstances of its actual usage. In Fig. 2.7b (left) the side-view of the laser-aligned to a body-diagonal of a 1:1:1 aspect ratio machine tool is shown. Here, the movement of a misaligned-mirror (i.e. presented in the diagram as a shaded-mirror) is compared with that of a perfectly aligned mirror (i.e. shown as simply a solid outline). Moreover, this mirror has been misaligned by a small angle about the *Y*-axis. Note, that in this schematic-diagram the mirror-misalignment has been somewhat exaggerated—for clarity. At this juncture, one can comprehend how this mirror-misalignment introduces an error into the laser-measurement. Consequently, as the machine moves along the *X* axis, the laser-beam will travel across this angled-mirror surface. Thus, the laser-reading is therefore affected by this mirror alignment, as well as by any linear- and straightness-errors in the axis. Furthermore, it might be thought that this specific error is very small; unfortunately this is not the case, because the error-accumulates. By way of a practical-example, if the plane mirror is misaligned by an angle of just 40 arcseconds, or 0.2 mm m^{-1}—this being a typical alignment-tolerance—and the *X*-axis step-size is set to 50 mm, then the laser will record an extra 7 μm of displacement during the *X*-axis step-movement. In isolation this induced-error may seem to some extent rather small, but because it occurs every time the *X*-axis moves,

therefore it can accumulate to a considerable error of 140 μm per metre—of *X*-axis travel! As a consequence, even a small amount of mirror-misalignment can accumulate—giving a very large measurement-error.

It has also been proposed—see Footnote 10—that because this error is constant it can be removed by appropriate software (e.g. by say either linear regression, or by slope-removal techniques, etc.). However, there are two specific-faults that have been reported with this approach, such that:

1. the error will only be constant if the angle of the mirror does not change—as it moves along the axis. On the other hand, if the machine contains any pitch- and yaw-errors, then the angle of the mirror will change, so that even with small changes in mirror alignment of a few arc seconds, this will have an unwanted and significant effect;
2. it is not possible to determine whether the error in laser readings is caused by mirror-misalignment or by a genuine progressive-linear over-travel in the axis motion. For that reason, the process of slope-removal will remove the effects of both and accordingly, it will eliminate one of the machine-errors the system is proposing to measure.

At this time one might take the view that by reversing the axis-movement sequence, it should be possible to separate the errors caused by mirror misalignment from any linear-travel errors in the machine's axis, but unfortunately this is not the case. Examples will follow showing the laser records additional movement despite the fact that the sequence has been reversed and the laser-beam has travelled onto the opposite side of the mirror—see Fig. 2.7b. Even though the Step diagonal technique cannot reliably measure the linear-positioning errors in a machine's axis, it can provide regular diagonal-displacement accuracy results in accordance with th: **B5.54** and **ISO230-6** Standards. Nonetheless, the technique has three distinct disadvantages, when compared utilising a regular linear laser interferometer and its accompanying retroreflector, such as:

1. an inaccurate alignment of the laser beam with the machine-diagonal combined with any misalignment of the mirror will cause small measurement-errors—where this effect is much smaller than that described-previously;
2. the test takes longer, because of the more complex machine tool part-programming routine and the additional target-positions required by such a testing-regime. This longer test time makes the actual test more prone to any environmental-fluctuations that may occur between the measurements of each diagonal;
3. the large angled-mirror assembly—when fitted to the machine-spindle limits the available *Z*-axis travel.

It should now be apparent from this previous discussion, that the Step Diagonal method does not give reliable linear positioning accuracy data for the machine's axes. Nonetheless, the technique can give reliable diagonal-displacement accuracy results, in accordance with **B5.54** and **ISO 230-6**—see Fig. 2.4 (bottom). It is therefore possible to estimate the diagonal length and squareness-errors and to

undertake a compensation to ensure the diagonal results are improved. Where one assumes that the diagonals are different lengths, then machine squareness can be adjusted, or compensated for utilising the cross-axis compensation parameters, until all four body-diagonals are the same length, although they may all still be either too long, or short. Once this compensation has been completed, then it is possible to apply a single and simple scaling-correction to the travels of all three linear-axes—ensuring that its body-diagonal lengths are also corrected. This type of remedial-action, will improve the **B5.54** and **ISO 230-6** test results. Although the diagonal test results have been improved by this operation, one might also pose the question, "Is it true that the machine's positioning-accuracy must have been improved too?" The answer here is a definitive no! Regrettably then, the combined weaknesses of the Step Diagonal Technique and **ISO 230-6**, or **B5.54 Diagonal Tests** when utilised in isolation, mean that the machine performance may have been degraded. This degradation is because the:

- **Step diagonal method**—does not give reliable linear positioning accuracy data for the machine's axes—as previously mentioned;
- **ISO 230-6 and B5.54 Diagonal Test results**—cannot detect the presence of complimentary linear positioning errors in two, or more axes.[12]

This is a specific technical problem, which is more adequately explained by the following theoretical test example:

If one considers a machine tool with a volumetric envelope of 1 m^3, which has perfect *X*- and *Y*-axes, but here in this case, the *Z*-axis over-travels by 100 $\mu m\ m^{-1}$, where all three axes are perfectly square to one another and contain no other errors, then diagonal results will indicate that all four body diagonals are too long—each body-diagonal is 1.732109 m long, instead of being 1.732051 m, thus having an error of +58 μm. Yet, any calculations utilised to remove these errors due to mirror misalignment in the step diagonal method will also extinguish any information about which of the machine's axes was responsible for this fault. Accordingly, the step diagonal technique will therefore fail to identify that the *Z*-axis alone was responsible for the problem, making correct linear-compensation impossible. However … it is now possible to apply compensation in order to improve the **B5.54**, or **ISO 230-6 Diagonal Test-results**; this can be achieved by simply applying a single $-33.3\ \mu m\ m^{-1}$ scale-factor correction to all three axes. This corrective action will produce a good diagonal test-result, but it will not have alleviated the problem with this machine tool, as the *Z*-axis still comprises of a significant linear-error of $+66.7\ \mu m\ m^{-1}$. However, for both the *X*- and *Y*-axes—which were originally perfect—they will, as a result, have a linear error of $-33.3\ \mu m/m$. After its compensation the machine's accuracy in the *X*-*Y* plane will now be seriously degraded, even though the **B5.54** and **ISO 230-6** body-diagonal

[12]**Complimentary linear positioning errors in two, or more axes**: this technical-information is more than adequately-described in some significant detail in the associated technical 'White-paper' company-documentation from Renishaw plc's—presentation, which is entitled: *Laser diagonal tests*.

results indicate that the machine tool has been improved. Therefore, these actual step diagonal tests have shown, that the:

- **sensitivity of the step diagonal method to mirror misalignment**—means that the method cannot be used in isolation to reliably determine the linear-positioning errors in a machine tool. Such errors should always be measured utilising conventional linear laser measurements, which are taken parallel to the machine's axes;
- **Step diagonal method**—can be utilised to give diagonal-positioning performance results, in accordance with **B5.54** and **ISO 230-6**. Moreover, this is not as accurate, or convenient as utilising a direct-diagonal measurement using a conventional linear interferometer and retro-reflector (i.e. as described in **B5.54**);
- **results from the Step diagonal test**—in isolation should not be used for linear-error compensation of a machine, even though the **B5.54**, or **ISO 230-6** results may show improvement, but the machine's positioning-accuracy may actually be worse.

Some additional and relevant comments on step diagonal testing have been provided by J.A. Soons—at NIST (i.e. The National Institute of Standards and Technology, USA) who has performed a detailed theoretical analysis of such tests. The results of this relevant work were presented at the LAMDAMAP 2005 International Conference within the UK and were published in its subsequent Proceedings, with the attendant abstract from this paper, stating that, "Our analysis confirms that setup errors in the alignment of the return mirror cause significant errors in the slope of the estimated positioning errors that cannot be detected from the (step-) diagonal measurements. Correction requires information on the slope of the positioning errors of two axes".

Step Diagonal Testing—Some Concluding Statements

It can now be justified—with some conviction—that there is some overwhelming-evidence that suggests that this step diagonal (vector) test method when utilised in isolation, cannot reliably-determine the linear-positioning errors in a machine tool. Moreover, any declarations to the contrary made by the originators of this step diagonal method in their previously published papers, are somewhat misinformed. Further, it has been adequately reported—see appropriate references at the rear of this chapter—that originators of the step diagonal (vector) test method have now developed some revised-software—to now address this previous problem. Accordingly, this recently modified-software will now allow the laser-user to take some additional but conventional linear laser measurements, parallel to two of the machine's *X*-, *Y*- and *Z*-axes, in order to determine the linear accuracies of all three axes. As a result, the requirement to take these additional linear measurements, which obviously now lengthens the time taken to calibrate a machine tool in this manner, has the effect of reducing somewhat one of the key benefits claimed (that it was a quicker testing procedure) for the introduction of step diagonal (vector) test method.

2.2.5 *Potential Errors—In Three Axes Machine Tools*

Introduction

Fundamentally, every machine tool-builder will list as part of a machine's specification, its accuracy and repeatability figures. What is generally not provided are the methods that were utilised to derive such test figures. The techniques used when defining a series of linear, straightness, squareness, rotary, etc. positioning methods within each Standard—was previously mentioned earlier in this chapter—but not all of these machine-builders will use the same standards. Not only do such machine tool-builders often use different Standards, but some do not consider all of the potential-errors that are likely to occur when considering their machine's accuracy and repeatability. Hence, the question one might readily ask is, "If this is so, what are these error-sources in a machine tool?" The following textural-dialogue attempts to expand on this error-based theme, briefly reviewing some of their significant causes in machine tools.

Types of Errors—Occurring in CNC Machine Tools

For a typical orthogonal horizontal Machining Centre, there are a range of problems associated with the actual position of a tool within its volumetric envelope, as depicted in the exaggerated diagram—shown in Fig. 2.8a. Not least of which, these types of errors will consist of:

- **positioning errors**—on each axis;
- **straightness**—of each perpendicular axes;
- **pitch, yaw** and **roll errors**—of each of the axes;
- **squareness errors**—between these orthogonal axes;
- **backlash errors** of each axis—except for the 21 kinematic errors[13];
- **contouring errors** of each axis—except for 21 kinematic errors (see Footnote 13).

In the previous section, it was argued that by utilising a conventional laser interferometer for measuring, say, the straightness—and squareness errors, it can require a prohibitive amount of calibration time—restricting the potential production usage of an expensive piece of plant (e.g. machine tool). This conventional laser technique, has led to the development of the body diagonal displacement method—which was also reviewed in Sect. 2.2.3, for a so-called speedy check, but having some attendant problems associated with it—as defined in the: **ASME B5.54**, or **ISO 230-6 Standards**—for this latter Standard, also see: Appendix 1.

[13]It has been previously-mentioned that a rigid body has 21 potential errors present—termed their degrees of freedom for a typical three-axes orthogonal machine tool (i.e. see Fig. 1.21). These potential errors will include three of each of the following error-types: linear displacement, vertical straightness, horizontal straightness, roll (angular), pitch (angular), yaw (angular), plus, squareness—between axes.

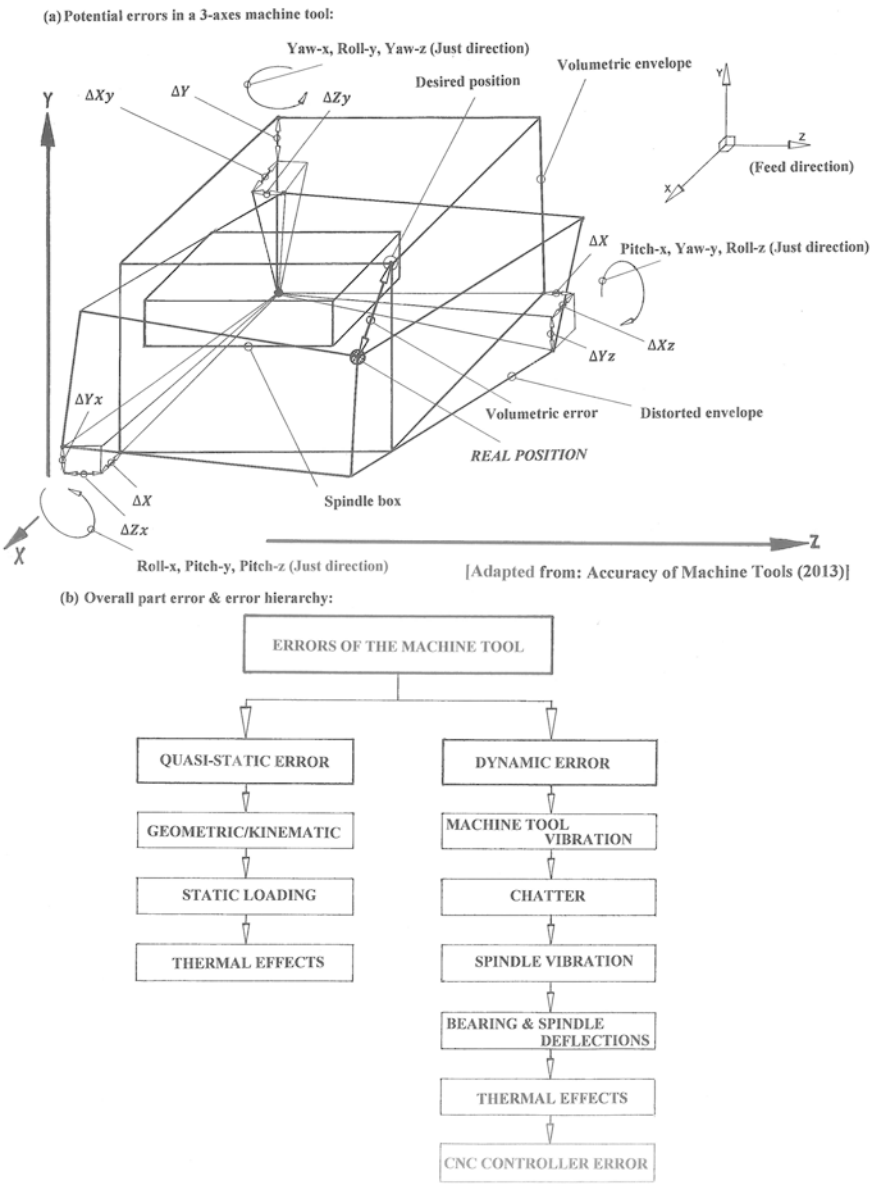

Fig. 2.8 Typical errors causing machine and tool positioning inaccuracies

Classification of Errors—For a CNC Machine Tool

For a CNC machine tool it is positioning for both accuracy and repeatability means that the machine is limited by a vast number of quasi-static errors and dynamic errors—as simplistically displayed in the flow-diagram, in Fig. 2.8b. Here, the

range of errors is quite enormous and can contain the following levels of uncertainty for the quasi-static errors, such as: geometric/kinematic errors of all components, load-induced (i.e. static) errors, thermal errors. The dynamic errors will usually consist of a range of machine-induced errors, as well as computational-errors, although the machine's resolution is limited by the quality of its sensors, quality of the control-system, frictional-effects—stick-and-slip effect (i.e. stiction), as well as by any potential backlash present. As a result, one might ask, "What are these error sources on a machine tool?" In the following-text these potential positioning-uncertainties (i.e. errors) and some other important factors shown in diagrammatic-form in Fig. 2.8b will be briefly mentioned. First, is a description of the range of quasi-static error sources, etc. then secondly, consideration of the influence on the machine of a variety of its dynamic errors, etc.—also to be found within a typical orthogonal CNC machine tool.

Quasi-static Machine Tool Errors—See Fig. 2.8b (left)

In terms of quasi-static errors, the geometric/kinematic errors are those errors that are present in a machine tool from its basic-design and original-build quality. These are unintentional built-in inaccuracies, which occur during the machine's assembly and are a result of the components and partial-assemblies utilised in the actual-build of the machine. Due to this machine tool assembly process, such errors can potentially form one of the greatest sources of machine tool inaccuracy. These error-sources originate from the purported quasi-static accuracy of working-surfaces that can move relative to one another. Consequently, the quasi-static accuracy of machined and lapped surfaces that axially travel relative to one another might result from either the linear-, or rotary-motion of axes, or from both of these effects. In the case of the linear-motion axis, they can exhibit: pitch; roll; yaw; straightness (i.e. two components); as well as linear displacement. While, for the rotary-motion of axes, they can have: radial-error motion (i.e. two components in fixed coordinate frame, plus one component in rotating-frame); axial-error motion; tilt-motion (i.e. two components); plus an angular-motion about the axis of rotation. Looking into these rotary-motions in more detail, one will note that the:

- **radial-error motion**—which is the positioning error of the rotary stage in the horizontal-direction, when the table is oriented in the horizontal plane. Here, the radial-runout can be theoretically defined as, "The total indicated reading [TIR] on a spherical ball positioned 50 mm above the table and centred on the axis of rotation";
- **axial-error motion**—is the error of the rotary-stage axis of rotation in the vertical direction when the stage is oriented in the horizontal plane. In this situation, the axial-runout is defined as, "The total indicated reading [TIR] on a spherical ball positioned 50 mm above the table and centred on the axis of rotation";

- **tilt-error motion**—is the relative wobble, which is defined as, "The angular error between the actual axis of rotation and the theoretical axis of rotation"—measured in arcseconds.[14]

Geometric/Kinematic Errors—see Fig. 2.8b (left)

Of particular note, is that the machine's geometric errors can be of a smooth and continuous nature while also demonstrating either some form of hysteresis, or random behaviour. These geometric errors of the machine tool are affected by influences such as the machine tool's surface straightness, surface texture (i.e. its roughness), bearing pre-loads, together with certain other influences, with just some of these errors sources being listed below:

- **hysteresis error**—this being considered as a deviation between the actual and commanded position of the programmed point, being created by elastic forces in the motion system. Hysteresis will also affect bi-directional repeatability;
- **backlash error**—which is an error in positioning initiated by the reversal of the axis travel direction. Backlash is the portion of the commanded motion that produces no change in position upon initial reversal of its travel direction, generally being the result of clearance between main elements within the drive-train (e.g. gears). Accordingly, as these clearances increase, the amount of input necessary to produce this required linear motion is proportionally greater. This increase in clearance, results in an amplification of the machine tool's backlash error. Backlash will also affect an axis repeatability, as listed below, affecting the machine's;
  - **uni-directional repeatability**—which refers to the repeatability when approached from the same direction. Uni-directional repeatability does not consider the effects of backlash;
  - **bi-directional repeatability**—specifies the repeatability when required from any direction and includes the effects of backlash;
- **feedback inaccuracy**—which will result from any imperfections in the operation of the machine's encoders, such as non-uniform division of the grating scale, or any imperfections in the photodetector signal, interpolator errors, axis-hysteresis, plus the levels of friction present;
- **noise**—this could affect the positioning-capabilities of, say, the rotary stage – when present on the machine tool.

[14]**Second of arc**—alternatively termed an **arcsecond**, or **arcsec**: is $^1/_{60}$ of an arc minute, $^1/_{3600}$ of a degree, $^1/_{1,296,000}$ of a circle, also $^\pi/_{648,000}$ (about $^1/_{206,265}$) of a radian. By way of a simple but practical and valid example of this minute angular relationship, is that it is approximately the angle-subtended by a U.S. dime-coin at a distance of 4 km (i.e. ≈2.5 miles). While yet another example of an **Arcsecond**, for a very useful general Rule of thumb, concerning an arcsecond and its relative distance, is that: **one arcsecond** (i.e. 1/3600°), when tilted through this angle over a length of one metre, has an approximate vertical height at its free-end position of: ≈5 μm.

In the case of these machine tool's kinematic errors, there are a number of factors that must be dutifully considered. Typically, these errors that may arise because of the:

- **kinematic errors**—which are the result of the relative motion \errors of several moving-machine components, that need to travel with precise functional requirements. Kinematic errors are particularly important as the result from the combined motion of different axes. Such errors occur during linear, circular, or other types of interpolation algorithms, but are more noticeable during any actual machining, such as the motion-errors due to alignment, the component's geometric shape thus resulting from the application of improper offsets—each of which, are thus creating translational-axes problems;
- **errors in an axis's trajectory**—being instigated by any misaligned/improperly tolerance/sized components in the assembly; squareness and parallelism between axes; error motions in a closed kinematic-chain; together with any potential external load-induced errors:

Static Errors—See Fig. 2.8b (left)

Of note, are that these static errors are often the result of:

- **errors due to deformation of machine components**—which consider any gravity load-induced errors (i.e. static errors); cutting/probing force induced-errors; plus axis acceleration load-induced errors;
- **errors due to uneven distribution of table-loading**—where a particularly heavy fixture and/or workpiece is positioned on an extreme end of the table's working volume, creating uneven loads and resulting in unwanted axes displacements.

Thermal Effects—See Fig. 2.8b (left)

A machine tool's thermal errors will account for between 40 and 70 % of the total dimensional and shape errors of a machined workpiece, in any manufactured form of precision engineering. It is well known (i.e. see appropriate references) that there are six sources of thermal influence that have been identified which will occur on a machine tool, these are:

1. heat from the machining process;
2. heat generated by the actual machine;
3. heating, or cooling provided by the machine's cooling-system(s);
4. heating-, or cooling influence of the machine-shop room;
5. the heat effect from people, working in the machine's vicinity;
6. thermal memory, from any previous machining environment.

If these heat-induced effects are prevalent on machine tools, then the question to be raised is, "What problems do they contribute to the accuracy and precision of machined parts, as a result of such thermal influences?" These valid points will now be described. Unwanted heat, causes relative expansion of the various elements of the machine tool, leading to inaccurate positioning of the cutting tool,

subsequently affecting the workpiece's machined-quality. Accordingly, errors due to spindle-growth, thermal expansion of the Recirculating ballscrews and thermal distortion of the machine's bed are invariably present. Consequently, as heat generation at the machine's contact-points is unavoidable; this source of error is one of the most difficult to effectively eliminate. In the manufacture of accurate and precise components, any error due to thermal-deformation of the machine elements will play a crucial role in limiting the accuracy and precision of the part produced by the machine. It is important to know both what and where the likely heat-sources are, that will contribute to the thermal errors on a machine tool within its operating-environment.

Just some of these thermal factors are the result of internal-heat sources caused by:

- a mean temperature other than 20 °C;
- thermal gradients in machine environment's, namely, resulting from its temperature variability;
- errors caused by thermal expansion of these vital machine tool elements, typically from: motors; bearings; the machining process; pumps; expansion of compressed fluids; plus temperature differentials in the actual coolant.

While some of the external heat sources that affect the machine tool are:

- mean temperature of the room/machine shop;
- solar-influences—typified by the sun shining through windows onto the exposed machine tool's elements;
- machine tool being situated in close-proximity to a hot-air vent;
- overhead-light sources, in the machine's vicinity;
- operator's body-heat.[15]

When machine tool builders design a new range of machines, their design strategies for this prospective plant, must address some important factors in order to alleviate these potential thermal influences. Typically, they would:

- isolate heat-sources and incorporate some form of temperature control system;
- maximise thermal-conductivity, or insulate against known heat-sources;
- combine at least one of above factors—by instituting machine thermal mapping in combination with its real-time error correction.

Accordingly, one might ask the pertinent question, "What are these thermal-sources?" Hence, these thermal effects must be known in order to mitigate against them within the machine tool. Characteristically, as the cutting speed increases

[15]**Body heat**: the actual amount of heat produced by a human-body will depend upon the individual, such as their respective: weight; plus their level of physical-activity. Accordingly, the total amount of heat produced over a period of time, is equal to the total calories-consumed, minus any useful mechanical-work being performed. For example, if a person consumes an average of 2400 kilo-calories per day, the average body heat produced is 100 kilo-calories per hour, or 116 W. So, ten people in a workshop, will produce the heat-equivalent of a typical single bar-element's output, from an electric-fire!

this creates heat, which impacts on both the machine's accuracy and repeatability. This simple fact, becomes more problematic with longer production cycle-times, plus it is exacerbated by higher speeds and feeds, but most notably, it is normally reduced by any high-speed machining (HSM) applications—due to the high passage of the cutter's edges through the yet-to-be-machined component's material stock. On the other hand, today, most techniques of thermal applications, will emphasise their efforts on keeping heat away from the workpiece, so that other areas—which are influenced by any likely thermal-distortion—are somewhat overlooked.

Thermal-stability can be maintained by an improved heat-dissipation throughout the machine's various components. Typical of this approach is in the machine's spindle's design, where:

- high-speed spindles can experience growth due to heat from friction, when rotating at high rpm's and may require longer saturation-periods before they stabilise;
- too much heat in the spindle will compromise accuracy and can potentially cause premature spindle-failure;
- one such notable spindle-builder, has designed a core-cooling system and an under-race lubrication system, that effectively cools the spindle from the inside-out—to minimise heat and growth for shorter saturation-periods of usage;
- the cooling system circulates in this (above) system, facilitating spindle oil through the centre of the rotating spindle. Hence, at high rotations, centrifugal force draws the lubricant outward through the spindle, by circulating through holes in the inner-bearing races—to both lubricate and chill these bearings.

While other notable thermal-sources on the machine tool are invariably from the Recirculating ballscrews,[16] where heat is present resulting from perhaps the high feedrate levels, this can be mitigated against by forcing chilled-oil through the ballscrew's core. Furthermore, the location and design of the machine's pumps, motors, hydraulics and magnetics, are key items in thermal heat reduction exercises. For example, on some Machining Centres they are designed so these ancillary—but vital—components are mounted at the rear of the machine within a so-called dead-air space, isolating them from the rest of the machine tool. To ensure this heat cannot impact upon the machine tool, a radiator cooling system is sometimes used to wrap-around the machining centre's column. The machine

[16]**Recirculating ballscrew/Ballnut—heat generated**: the moment for a ⌀40 mm Ballscrew having a 10 mm pitch was measured by Golz (Golz, Hans Ulrich, *Analyse, Modell-bildung und Optimierung des Betriebsverhaltens von Kugelgewindetrieben*, Dissertation: *University Karlsruhe*, Germany, 1990), for various preload-forces and rotational speeds. For example here, Golz found that with a typical preload of 3 kN, this results in a no-load, or frictional moment of between 0.5 and 1 N m. Meaning that the machine tool in a rapid traverse with a Ballscrew speed of 2000 rev min^{-1}, will produce between 100 and 200 W of frictional heat being generated by its associated Ballnut. Also see Fig. 6.18 (middle), for a thermographic snapshot image.

tool's actual workshop environment plays a significant role in the thermal characteristics within a machine shop. Although even with certain safeguards in place, the shop environment must be checked for external heat sources. Such hot-zones – as mentioned - can range from sunlight on the machine tool, to external heat on the shop floor, with any increase or decrease in temperature being appropriately dealt with in the working-environment. These unwanted ambient temperature fluctuations, can have a negative impact on machined component's accuracy and repeatability.

Dynamic Errors—In CNC Machine Tools—See Fig. 2.8b (right)

Once the machine tool is in motion and actually machining components, then the dynamic errors can be caused by either vibration/chatter, or by the control-processes, which can become significant. These particular problems along with other dynamic-factors relating to the CNC machine tool need to be considered, including:

- **vibration**—from the external environment, normally via the ground-based vibrational effects resulting from cutting processes and the influence of rotating masses;
- **control-system effects**—such as, algorithm-type induced programming-effects, stick-slip friction (i.e. stiction), varying-masses (i.e. rotating and linear motions) and its structural-stiffnesses—within the machine tool;
- **switching-amplifier's effects and servo-loop frequency changes**—which have the effect of exciting the natural mode of the machine;
- **calibration errors**—associated with mastering the actual machining process and the machine's sensors, influencing the intrinsic-accuracy of the machine tool, plus its linear-/circular-interpolation effects;
- **additional errors**—which could include, computational errors, namely, the errors introduced in the analysis-algorithms, rounding-off errors due to machine's hardware.
- **Cutting-force—Induced Errors**—See Fig. 2.8b (right)

The dynamic stiffness of all the components of the machine tool, typically the bed, column, etc., are within the respective cutting-loop that is responsible for errors caused as a result of cutting-action. The CNC machine tool stiffness is one of the major sources of error in metal/material-cutting machines—as the forces involved in the cutting action are considerable. As a result of these cutting forces, the relative position of the tool's tip with respect to the workpiece, varies on account of the volumetric distortion of the various elements of the machine—see Fig. 2.8a. Contingent on the structure's stiffness and under particular cutting conditions, the accuracy and precision of the machine tool could also considerably vary. For that reason, for a machine with a given stiffness, then it is obvious that a heavy-cut would generally produce more inaccurate components than if a lighter cut was programmed.

Errors Resulting From CNC Machine Tool's Motors—See Fig. 2.8b (right)

Of some note, are the dynamic errors induced by the machine's motors, which can result in a range of inaccuracies of programmed axes positioning and orientation; just some of these error-related factors are the result of:

- **positioning errors**—they are produced by errors in the position-detecting scale and the servo-system in the case of a closed-loop type system (i.e. having a linear-scale feedback type of CNC). While, for a semi-closed-loop type system (i.e. with a ballscrew/encoder feedback type of CNC) the errors are caused by the servo-control system and the ballscrew driving-mechanism (i.e. this effect being created by the ballnut/ballscrew and the coupling of the servo-motor assembly);
- **errors from motors**—as a result of the motor's angular-motion error, with the magnitude of this error being determined by the magnitudes of the moment, added to the sliders by gravity, the counterbalance force, ballscrew driving-force, plus the sliding-friction during the motion of these sliders. Moreover, the combination errors are also determined by the rigidity of the guideways that restrict the sliders. Furthermore, the inertial force should also be considered, when the acceleration of axis feed motion is very high.

Origins of Motion Errors—In CNC Machine Tools

There are a range of motion-induced errors that can occur on CNC machine tools, most notably the following list provides some of the major error-related motional-influences, like:

- **positioning errors**—resulting from any errors in the scaling-system;
- **uniform expansion**, or **contraction**—of the linear scale, cyclic error, also local error;
- **thermal expansion** and **distortion errors**—where temperature change causes the actual ballscrew to expand/grow, or via the temperature-gradient to distort the machine geometry, which also creates distinct positioning errors;
- **Ballscrew driving system**—significant errors can occur here;
- **Ballscrew uniform expansion**, or **contraction**—together with any attendant pitch error, ballscrew whirling-effects, lost motion, backlash, tilting of the thrust-bearing, errors in coupling assembly, transmission gears, or timing belts;
- **servo-control system**—can introduce some significant errors here;
- **'stiction'** (i.e. stick-motion) – often termed stick-slip errors, resulting from an inadequately defined pitch-error compensation, insufficient backlash compensation, reduction in the programmed-radius during circular-interpolation motion—due to response-lag (i.e. often termed servo-droop effects), mismatching of position loop-gain, as well as noise in the detectors';
- **straightness** and **squareness errors** of **guide ways**—these errors are caused when the guide way is not perfectly straight, usually resulting from the weight shifting (i.e. the machine's axis bending) or due to large-overhangs during extreme axis-travel (i.e. here, acting like a cantilever) which may lead to positioning errors;

- **angular motion errors**—resulting from straightness and parallelism errors of their respective guide-ways;
- **asymmetrical guide-way** and **ballscrew**—plus the effect of counter-balance, shift of weight, levitation of its slider.

Moreover, there are some additional error-categories that may also be present in the machine's positioning mechanism and in its feedrate errors, which can affect the CNC machine tool's operation, just some of these errors might include:

- **uniform expansion**, or **contraction**—(i.e. namely, of the first-order, and second-order)—of the ballscrews and the axes linear scales;
- **cyclic-error**—in a ballscrew; the linear-scale problems, presence of backlash/backlash compensation; as well as through inaccurate pitch-error compensation;
- **profile errors of guide way**—these are based upon: squareness-errors between two axes; straightness-errors; rolling of vertical axis; pitching of vertical axis; yawing of vertical axis; yawing of vertical axis with pre-compensated geometry; yawing of horizontal axis; plus the machine's parallelism error;
- **feedrate dependent errors**—that can include: lost motion; stick-slip; mismatching of position loop gain; decrease in radius of circular-interpolation motion—due to response lag in the servo-system; together with the levitation of sliders—possibly due to dynamic pressure.

It has been mentioned previously, but is still worth re-emphasising here, that machine design is key to the CNC machine tool's volumetric-accuracy. This crucial design element in the development of new machine tools, is normally based upon the builder's long experience in this specialised-field. Some considerable attention and significant attendant costs must furthermore be made to the appropriate depth of foundations in place, prior to the machine's installation. This latter factor is vitally important, prior to the siting and levelling of a new machine tool. As a consequence of having adequate foundations present, the machine must still be precisely levelled (i.e. see Fig. 3.17, top)—by appropriate levelling-systems. This siting and levelling is a crucial aspect of the machine's original commissioning, which will directly impinge upon its prospective operational performance—while having a significant impact on the machine's volumetric-accuracy.

2.3 ISO 10360 for Coordinate Measuring Machine (CMM) Calibration and Verification

The International Standard **ISO 10360** Acceptance and reverification tests for coordinate measuring machines (CMMs)—was established (1994) see Appendix 1. This standard defines the detailed test-procedures for the various applications of a CMM, typically for: length measurement, form inspection, measurements with and without a rotary table. Previously, some CMM manufacturers published specifications for their own CMM's according to the preceding German Standard

VDI/VDE 2617, or to that of the USA Standard **B89**. However, it is actual normal practise today, to adopt specifications according to **ISO 10360**, as only then can the performance of different CMMs from a variety of countries for their respective CMM-manufacturers, be adequately compared.

2.3.1 Coordinate Measuring Machine (CMM)—Fundamentals

Today, the ubiquitous CMM has, to a greater-degree, superseded the traditional hard-gauging systems,[17] with both process control and quality assurance in manufacturing operations increasingly dependent upon the performance of CMMs. During the last four decades, these CMMs have replaced old-style inspection techniques that usually employed gauges and fixtures and in the process, which have reduced the time and manpower required for these vital quality-control operations. CMMs enable one to inspect standard geometrical and linear dimensions, together with intricate components having special and complex features, such as: gear teeth (e.g. their involute tooth forms), cam-profiles, or air-foil and turbine-blade contours. Consequently, in a conventional manufacturing environment, each of these non-uniform contours/geometries, would have been both time-consuming in inspection procedures and required expensive and special metrological-instrumentation rather than today, a single multi-purpose CMM metrological testing machine.

A product's quality does not only depend on the excellence of the machine tools utilised for their actual manufacture, but it also heavily relies on the accuracy/precision and inherent-repeatability of these measuring/inspection devices. By way of an example, if a low-cost/performance turning centre is employed for part production in combination with a high-precision CMM, this arrangement can still guarantee good product quality; this is because only workpieces that are within tolerance can successfully pass this CMMs inspection. Equally, if an expensive and high-quality Mill/Turn Centre is operated in combination with a low-cost/accuracy conventional inspection device, this arrangement cannot always guarantee quality products. It is worth labouring the point still further, in that a certain percentage of out-of-tolerance components will always pass using a low-accuracy CMM for inspection; similarly, a certain percentage of parts within the tolerance

[17]**Hard-gauging systems**: thus a **Hard-gauge** is an extremely accurate and precise machined measurement gauge. Beginning with: **Gauge Blocks**, this type of **Hard gauge,** is associated with the Primary Standard—of dimensional metrology **(i.e. see chart—in Fig.** 1.2**)**. These artefacts are extremely accurate/precise and are utilised to perform verification on a range of hand measuring-tools and certain measurement equipment. Types of **Hard gauges** include: **Gauge Blocks—mentioned**; **Threaded, or Smooth Plug, or Ring Gauges (i.e. utilised as Limit-gauges for part-tolerances)**; **Pin Gauges**: **Angle Gauges**; **Bore Gauges**; also **Step Standards, plus many more variants**.

range will also be rejected.[18] Accordingly, selecting the correct CMM for the anticipated production output of parts is critical. CMM-uncertainties and accompanying test procedures have been more than adequately-described in **ISO 10360**—since 1994. In the case of **ISO 10360-2**, it specifies three types of uncertainties, they are for:

1. **volumetric length measuring uncertainty**—(MPEE);
2. **volumetric probing uncertainty**—(MPEP);
3. **volumetric scanning error**—(MPETHP).

Noting that the: MPE—is an acronym for: Maximum Permissible Error.

CMM Verification

For CMM verification, normally a set of five-calibrated gauge blocks—of differing lengths—is utilised to verify an MPEE—see Fig. 2.9a. These Gauge Blocks are then measured in seven different locations (i.e. for both their position and direction) within the CMMs measuring-volume for this so-called 'E-test'. Consequently, for each of these seven locations, the length of each of the five gauge blocks is measured three times, giving a grand total of 105 measurements. All of these 105 measurements must be within the stated-tolerance being specified by the CMM manufacturer. Furthermore, a precision calibrated sphere of between Ø10 and Ø50 mm—having its associated form and diameter certification utilised to verify a CMMs probing uncertainty (MPEP)—is colloquially termed a P-test—see Fig. 2.9b. The P-test consists of measuring 25 equally spaced points on this Calibration Sphere. Once this measurement task has been undertaken, the MPEP is computed by adding the absolute values of the minimum and maximum deviation from the radial form. Accordingly, the total measured form-deviation is the volumetric probing uncertainty, with the result being reported in micrometres (μm) and, all 25 probed points must be utilised in this calculation. While, the CMMs Scanning-performance—see Fig. 2.10a—is calculated by scanning a high-precision calibrated sphere on four exactly defined lines – as shown by the respective probing circles and partial arcs, but this is undertaken at a set speed of 10 mm s^{-1}. This probing-sequence will then produce the Total form deviation on all four lines, which is the MPETHP value—see Fig. 2.10b. Such an accurate and precise testing regime is very specific, both in terms of the CMMs definition and its actual execution.

[18]**Operating-characteristic**—is the result of a component production Sampling Plan. This type of Acceptance-sampling has utilised statistical-sampling to determine whether to accept, or reject a production-lot (i.e. batch) of material. It has previously been a common Quality Control technique utilised in industry and most notably for the military—for contracts and procurement. It is usually undertaken as products leave the factory, or in some cases even within the factory. Most often, a producer supplies a consumer a number of items and decision to accept, or reject the lot is made, by determining the number of defective-items in a sample from that lot. Thus, the lot is accepted if the number of defects falls below where the acceptance number occurs, or otherwise this lot is rejected. This is why inspection-strategies are critically-reviewed, away from tightened-inspection, to that of reduced-inspection procedures—whenever possible—to minimise quality-costs within the company.

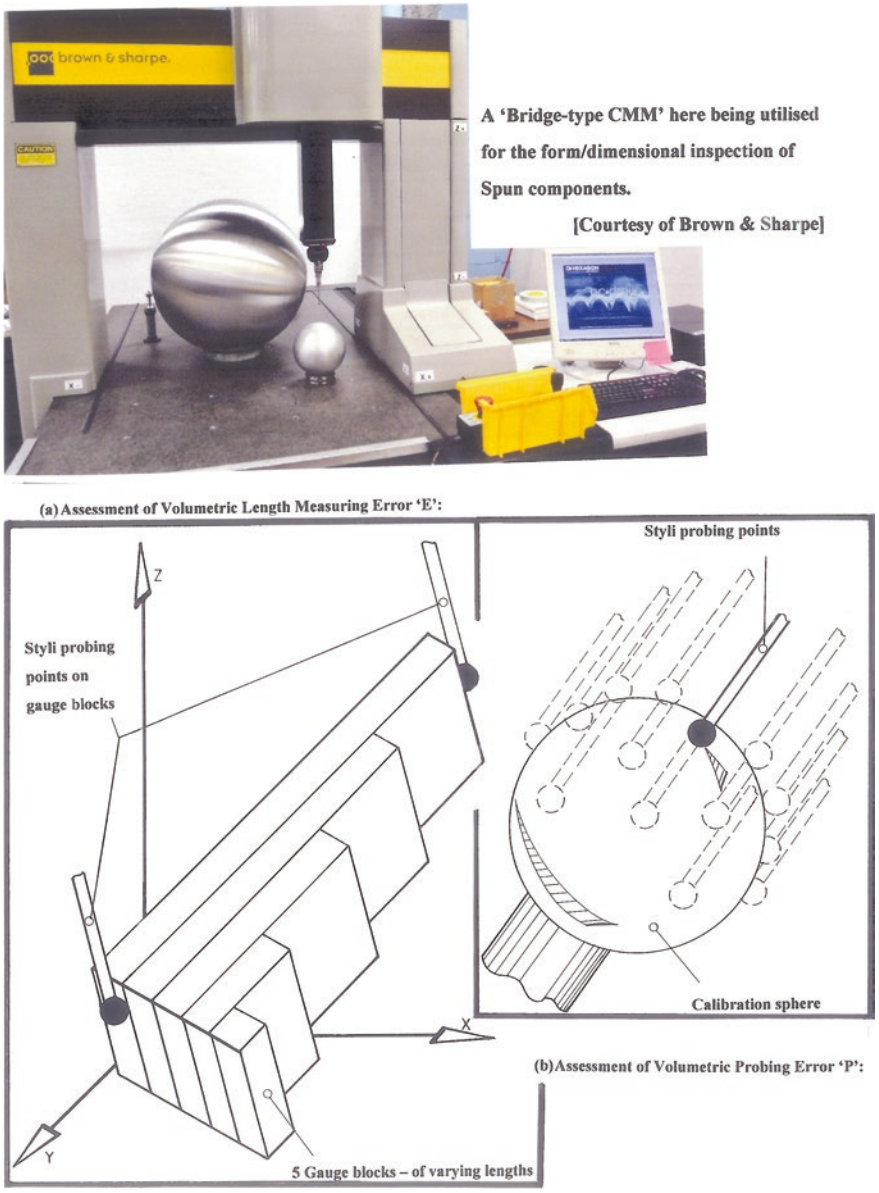

Fig. 2.9 Typical arrangement for assessing the volumetric probing errors '*E*' and '*P*' (adapted from: ISO 10360/Hexagon Metrology)

It is important to comprehend that a CMMs uncertainty under actual functioning circumstances could be larger than stated within the manufacturer's specifications. This difference in the CMMs performance, is because of a range of interrelated factors, such as the use of: probe extensions—either long, or slender

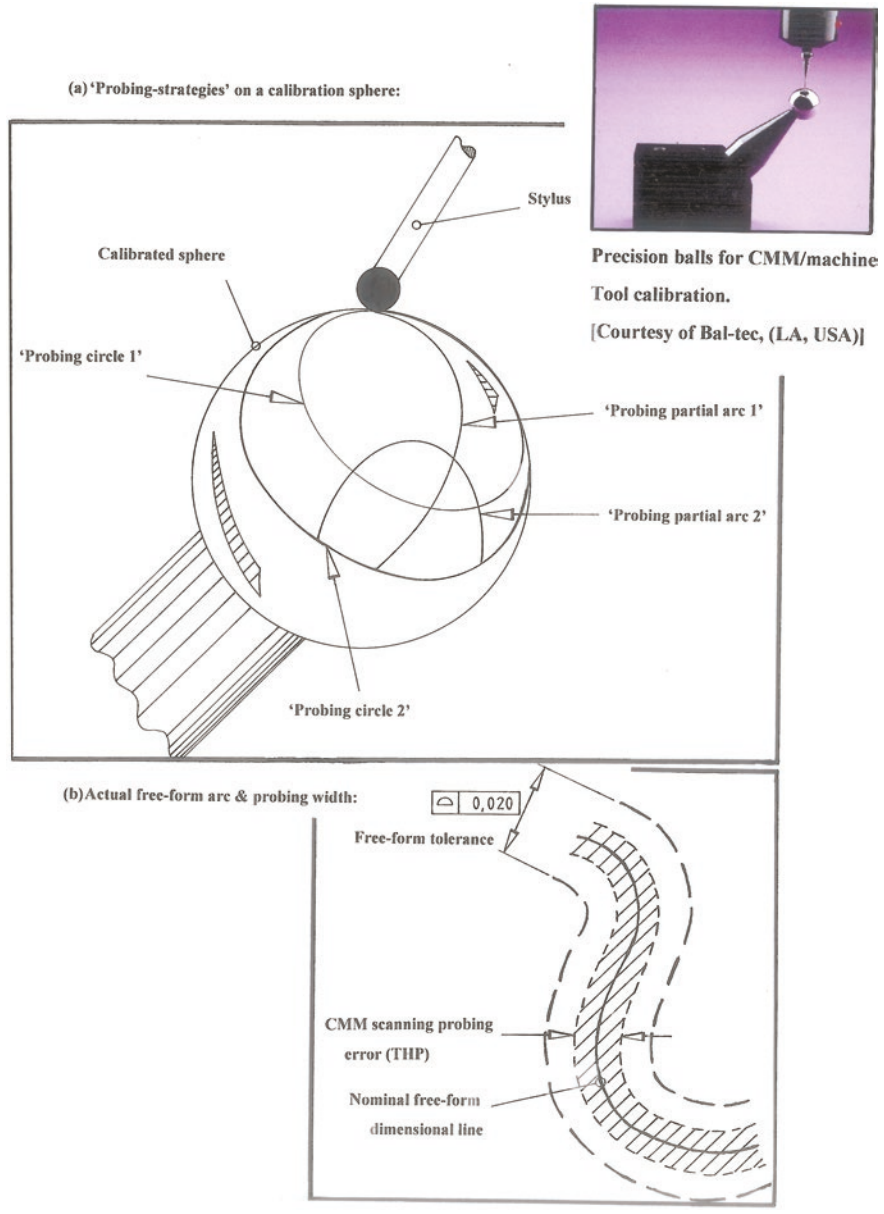

Fig. 2.10 Typical 'probing-strategies' when either 'qualifying a stylus', or 'scanning' a free-form profile (adapted from: ISO 10360/Hexagon Metrology)

probes; articulating probe heads; rotary tables[19]; ambient/CMM temperature changes; as well as any airborne contaminants within the working environment. By way of an example, MPEE and MPEP as specified, are actually determined by just one stylus fixed-directly into the probe head with no extensions and no rotation. Nevertheless, most intricate-geometry workpieces normally require some complex probe-configurations. Hence, a complex part geometry may necessitate the use of: several styli; probe-extensions; rotations of the probe; also possibly a probe-change during the inspection programme of critical component features. Since these probing-differences here are readily apparent, then the commonly accepted-practice is to apply a ratio of uncertainty to tolerance—when calculating a mandatory CMM specification. Therefore, this ratio may vary extensively, contingent upon the factors previously mentioned, also considering the complexity of the actual measurement task and the overall probing-process. Characteristic ratios of uncertainty can range from 1:3 to 1:20, but with values of between 1:5 and 1:10 being the most common. Accordingly, to maintain a 1:5 ratio of uncertainty to the part's tolerance, the CMM data-sheet specification, should be five times more accurate than that of the tightest tolerance inspected.

For just about all inspected parts, the CMMs must examine three-groups of features for: diameters/distances; positional tolerances; plus form tolerances. For this reason, an analysis of the mandatory-uncertainty must be accomplished for each of these three groups, hence:

1. **diameter/distance tolerances**—for example, must refer to the component drawing and location of the diameter for distances having the tightest tolerances. This is due to the length-dependency of its volumetric-uncertainty, where a greater tolerance on a very long feature may present more difficulty, than the opposite effect of a very tight tolerance on a small feature;
2. **positional tolerances**—these are usually defined by, say, a tolerance diameter, where only the radius is utilised to determine the deviation from the part's nominal-centre;
3. **form tolerances**—can include factors relating to the component's: roundness; flatness; straightness; cylindricity; as well as its profile form.

---

[19]**CMM—Rotary Table Calibration of the 4**th **Axis** (i.e. **ISO 10360—**Standard)**—**see Figs. 2.11 and 2.12, having the following - **Rotary table Errors**: Radial Error '**FR**'; Tangential Error '**FT**'; plus Axial Error '**FA**'.

CMM—Rotary Table Calibration—test procedure:

(i) fix spheres '**A**' and '**B**' on '**RT**'. (i.e. recommendation 'Δh' = 400, 'r' = 200 mm) (The errors of a rotary table generally increase with 'Δh', radius 'r' and table load.);
(ii) measure sphere '**B**' and set centre—point to zero (0,0,0);
(iii) measure sphere '**A**' in 14 positons, 7 positions from 0° to 720° and 7 positions from 720° to 0°;
(iv) measure sphere '**B**' in 14 positions, 7 from 0° to 720°, 7 from 720° to 0°, at the last position (28) measure sphere '**A**', one more time;
(v) calculate range of '**X**', '**Y**' and '**Z**' for '**A**' and '**B**';
(vi) Rotary table error: Radial '**FR**' = Max. range in '**X**' ('**A**', or '**B**');
(vii) Rotary table error: Tangential '**FT**' = Max. range in '**Y**' ('**A**', or '**B**');
(viii) Rotary table error: Axial '**FA**' = Max. range in **'Z**' ('**A**', or '**B**').

[Source: adapted from—Hexagon Metrology, GmbH (2014)].

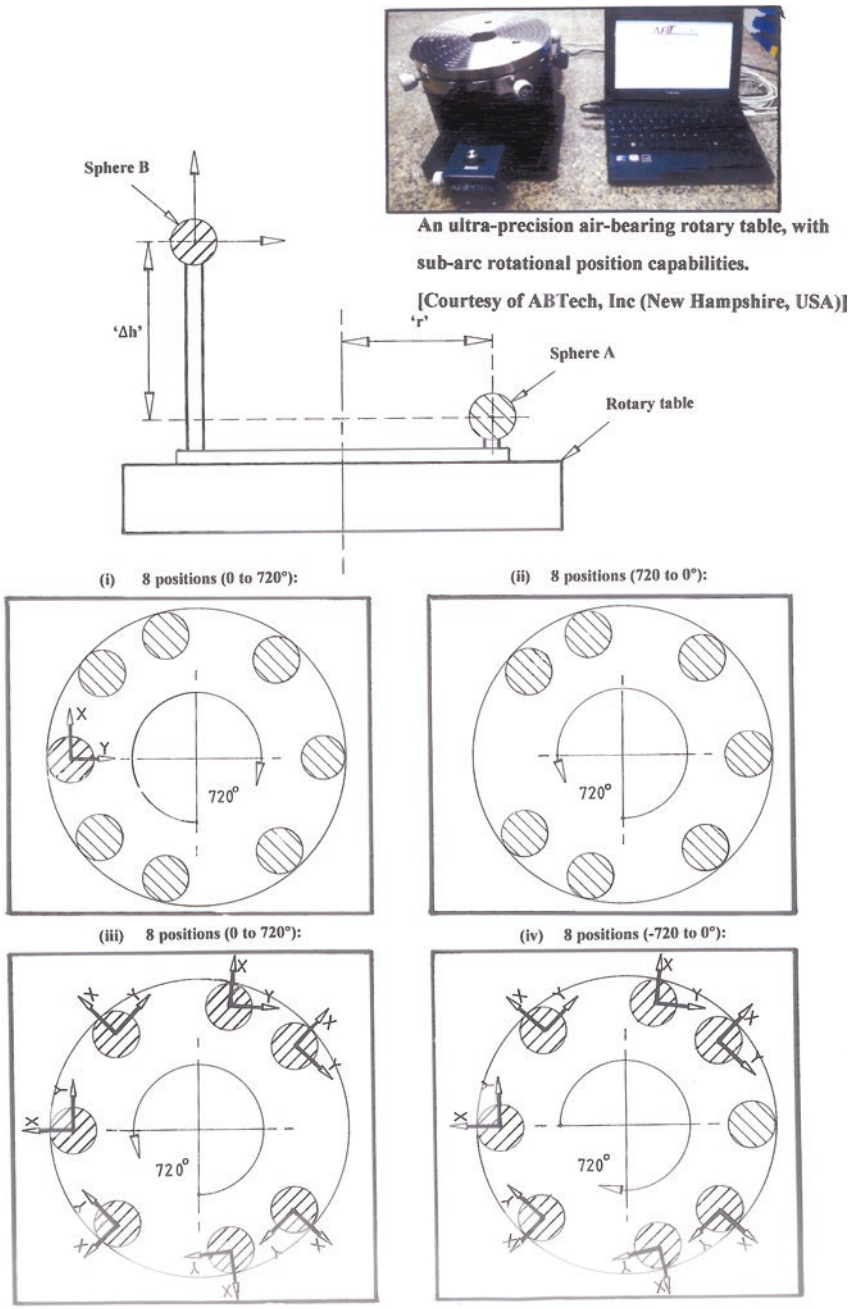

Fig. 2.11 A typical setup for the assessment of a rotary table (adapted from: ISO 10360/Hexagon Metrology)

3-D probing system - 'R-test' calibration, on a multi-axis vertical machining centre.
[After: B. Bringmann & W. Knapp (Inst. of Machine Tools & Manufacturing TH Zurich, Switzerland)]

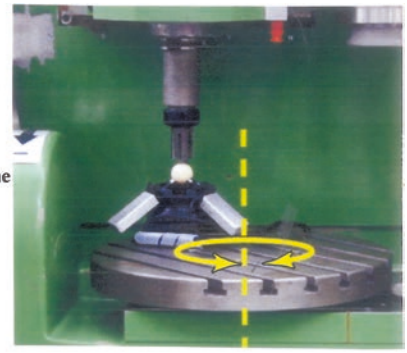

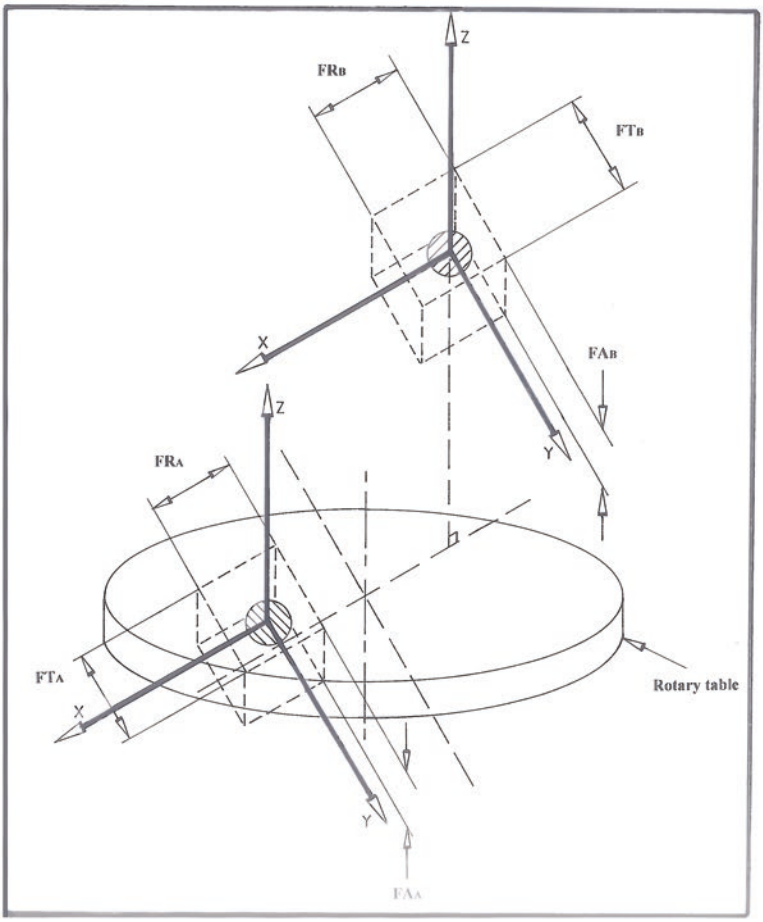

Fig. 2.12 General test procedure, with rotary table error (adapted from: ISO 10360/Hexagon Metrology)

2.3.2 CMM—Environmental Conditions

Metrological environmental conditions can have a serious effect on the prospective uncertainties of a CMM—in its present location. Accordingly, CMM-manufacturers normally stipulate the: temperature range; temperature variation per hour; temperature variation per day; also the temperature variation per metre; within which a specific CMM will ultimately achieve its performance specifications. These environmental variables must be considered when choosing its actual location site and ensuring that an appropriate CMM is supplied—being equipped with its necessary technical specification. Likewise, as also previously mentioned concerning adequate foundations—for machine tools—similarly, the CMM's floor-loadings must also be considered in a similar manner. Furthermore and additionally—in a CMM's case, the magnitude of anticipated floor vibration is an important consideration, to optimise its anticipated metrological performance. In addition, the majority of CMM-manufacturers supply details of the maximum vibration that such CMMs can withstand, while still meeting their stated technical specifications.

In certain situations, active or passive vibration damping-systems can be supplied that enable the CMM to be installed in distinctly challenging environments, enabling them to still perform to their published specifications. Of some note, is the often overlooked requirement of completing a Seismic vibration study—this being executed at the chosen CMM-installation site.

2.3.3 CMM Performance Standards

All current CMM-manufacturers can provide performance standards as the means to rate a CMM. Such standards are beneficial when equating different manufacturer's CMM products, to enable one to determine how well their current machine will inspect workpieces, while also ensuring that the machine operates correctly. There is a distinct range of different Standards of measurement for CMM calibration, although these opposing Standards can often create-confusion and a certain amount of misunderstanding for the CMM user. Of late, there are principally three primary standards that are invariably utilised to verify the accuracy and precision of a CMM's performance, these are **ASME B89.4.1**; **VDI/VDE 2617**; as well as the **ISO 10360-series**. The main differences between such Standards chiefly occurs in the number of tests utilised in evaluating CMMs and the manner in which performance specifications are written. For example, to evaluate the length-measuring performance, the **B89** Standard utilises multiple tests, while the **VDI/VDE 2617** utilises three tests; similarly **ISO 10360-series** also utilises three tests—but here, with one of these tests being for the probe. So, to represent a typical CMM performance-range of, say, the **B89**-specifications, this standard will consist of a single number. For example, a particular CMM could have a

B89—volumetric-performance specification of 0.010/325 mm. Here, the number after the slash represents the length of the ballbar measurement. This specification means that the range of measured lengths with the ballbar in its many positions is ≤10 μm. For the other CMM Standards, namely, the **VDI/VDE-** and **ISO**-specifications, they represent length-measuring performance as a formula. As a consequence, a CMM's volumetric performance, can be quantified in the **VDI/VDE** format, as follows:

$$U3 = 4 + 5L/1000.$$

where in this case the notation means that over the same measured 325 mm—length previously mentioned, there could be an error no larger than ±6 μm (i.e. actually 5.625 μm).

In all cases for the **VDI/VDE** and **ISO** Standards, they utilise measurements taken from a calibrated step gauge—see Chap. 5—or an equivalent set of calibrated gauge blocks (i.e. see Fig. 2.9a). Moreover, in the **VDI/VDE** Standard, this calibrated Step gauge is measured in three positions, which are:

1. **axial**—($U1$);
2. **planar**—($U2$);
3. **volumetric**—($U3$).

Hence, the differences between the measured lengths and the calibrated lengths of this Gauge are compared in the formula (i.e. for this **VDI/VDE**-specification), by:

$$U = a + b \times L/1000$$

where: the 'a' term is a value representing the error—when measuring a component part of zero-length; the terms 'b' and 'L' are divided by 1000, to represent the increase in error—being based on the length-measured; thus, the formula represents a line for zero measured length, which is its 'a' value. As an example of this, a 4 μm value—in the equation above (i.e. also, then see below), is where it goes up by a slope which is defined by the 'b' term. Further, this 'b' term is the number of micrometres that the error increases for every 1000 mm of 'L' length. Accordingly, the means that the error formula will then become:

$$U3 = 4 + 5L/1000 \text{ (i.e. for volumentric accuracy)},$$

which for zero measured-length, is 4 μm and for every additional metre of length measured it will become 5 μm larger. Often though, the specification is more generally stated as simply:

$$U3 = 4 + 5L.$$

The measurement approach is the identical for the **ISO** Standard, but in this specific case the formula will change to:

$$\text{MPE}_E = a + L/k$$

where: here the value of '*k*' is substituted for '*b*' value—from the **VDI/VDE** formula, this being divided into 1000. Here, there are no individual axial- and planar-specifications, as they are included in the volumetric '*E*' specification.

In the case of the **B89 Standard**, the basic test of a CMM's performance, includes five critical-measurements, these are for:

1. **multiple measurements of the position of a fixed ball**—the range (i.e. the largest minus smallest) is the machine's repeatability;
2. **measurements with a Step gauge, or by a laser**—in each axial direction, which determines the machine's linear accuracy;
3. **measurements of a ballbar**—at multiple-positions and orientations, within the machine's working-volume. This value is the machine's volumetric performance;
4. **measurement of the ballbar**—in four diagonal positions—in vertical planes. In each position, the ballbar is measured with two right-angle probe offsets and the difference in their measured lengths is determined. The differences are compared with an offset-probe performance specification;
5. **measurement of the length of a short Gauge block**—in four orientations. The measurement is compared with a bi-directional accuracy-measuring capability specification.

Probably, the most important topic being discussed at present—in both the USA-Committees and within the ISO-Standards Committees, is that while these performance tests provide an overall characterisation of a CMM's quality, they do not provide the CMM-user with sufficient information about how accurately a CMM can measure an actual feature. As a result of this quandary, Technical Standards Committees around the world are seeking to determine how to characterise what is termed Task-specific measurement uncertainty as a method of describing how accurately the CMM can perform a real measurement task.

2.4 Calibration of a Rotary Table—With a Rotary Indexer

The diagrammatic representation of an exploded view of a typical auxiliary 4th-axis rotary table is shown, for auxiliary-fitment to a CNC machine tool (i.e. Figure 2.13, middle). In this example, it is depicted as having a large-diameter, aluminium-bronze worm-gear, that can precisely mesh with a ground alloy steel-worm (i.e. here being hardened to 60 H_{Rc}) which is lubricated by submerging it in a synthetic oil bath. The apparent high precision indexing-accuracy is achieved in this indexer, by machining the worm gear while it is attached to its spindle, rather than the alternative, of assembling the finished worm-gear to a separate spindle—as might be the case with some other rotary-table manufacturers. Each assembled

Dual-Spindle Tilting 2-Axis Trunnion Rotary Table, with scale feedback on the A (tilting) axis.

[Courtesy of Haas Automation (USA)]

Exploded view of a Rotary Indexer, showing: 1-main body, 2-turntable platter, 3-bearings, 4-worm gear, 5-worm drive shaft, 6-brake disc & 7-motor enclosure.

[Courtesy of Haas Automation (USA)]

Rotary Axis Calibrator & Laser, plus its associated *Optics* can be used to *calibrate* a CNC *Rotary Indexer* for a machining centre, or *any* CNC machine tool's rotary axis. [Courtesy of Renishaw plc]

Fig. 2.13 A typical CNC rotary indexer and rotary axis calibrator

spindle is individually 'trammed-in' on a CNC Gear-hobber, to an accuracy of ≤2 μm run-out, then the worm-gear is precision cut. This particular two-stage gear-hobbing and shaving machining process,[20] will ensure high-concentricity between the large-diameter ball bearings and the worm-gear—minimising and assuring a bind-free operation. Rotary tables of this level of accuracy and precision, still require periodic recalibration of their angular-indexing[21] ability. So, in order to achieve this vital rotary table calibration, it is necessary to either statically, or dynamically calibrates this table periodically. In order to achieve this rotary-calibration, a Rotary axis calibrator (Fig. 2.13, bottom) can be utilised in conjunction with a laser—see Fig. 2.14a—which can achieve the necessary high-precision rotary table calibration, providing ±1 arcsecond angular measurement accuracy. Here, as shown in Fig. 2.14, the wireless operation and modular mounting system ensures suitability for a wide range of rotary axes calibration applications across a diverse range of CNC machine tool configurations.

A typical rotary axis calibrator setup is shown in the Machining Centre configuration in Fig. 2.14a. An angular reflector is mounted on top of the rotary axis calibrator, which in turn is also mounted on top of the machine tool's rotary table axis—in this case, it is an integral rotary table which is presently being calibrated. As the machining centre's axis, under test, is rotated from one target position to the next, the rotary axis calibrator is driven in the opposite direction in order to maintain alignment with that of the angular-interferometer. When the axis under test stops at each target-position, then the positioning-error is calculated by comparing this target-position, with the arithmetic-sum of the angular-readings from the laser interferometer and from that of the rotary axis calibrator. This specific rotary-action allows the calibration of the axis over a full 360°, or even over multiple-revolutions.

---

[20]**Gear-hobbing and Shaving machining processes**:
Gear hobbing—in basic terms: a Hobbing-machine is utilised, with two skew-spindles, one mounted with a blank workpiece and the other with the gashed-hob—having the desired gear-cutting tooth involute-geometry. The angle between that of the hob's spindle and the workpiece's spindle will vary, dependent upon the type of gear-tooth profile being produced. For example, if a Spur-gear (i.e. with straight-cut teeth) is being produced, then the hob is angled equal to the helix-angle of the hob; while if a Helical-gear is being produced (i.e. with helically-curved teeth), then this angle must be increased by an identical amount as to that of the helix-angle of the required helical-gear. Then these two shafts—one with hob and the other with the gear-blank—are then rotated at a previously-calculated and proportional-ratio, then the gear blank is cut (i.e. by feeding it across the hob at the desired depth), which determines the number of teeth on the blank.
Gear shaving—which is a technique for generating an improved tooth shape in gears of an involute-profile. By the action of a minute stock-removal process via Gear shaving, it may be used to improve the quality of meshing between two gears, or between a gear and its rack. So by this Gear shaving, it makes possible to vary the interaxial-distances within gear-transmission, providing a machining-solution for a number of important design problems.

[21]**Rotary table—angular indexing capability**: in Fig. 2.13, this typical full-axis rotary table can achieve an indexing: resolution of 0.001°; with an accuracy of ±15 arcseconds; plus a repeatability of 10 arcseconds.

(a) The *XR20-W Rotary Axis Calibrator*, situated on a multi-axes machining centre.

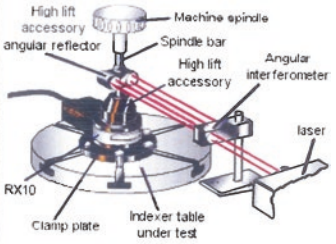

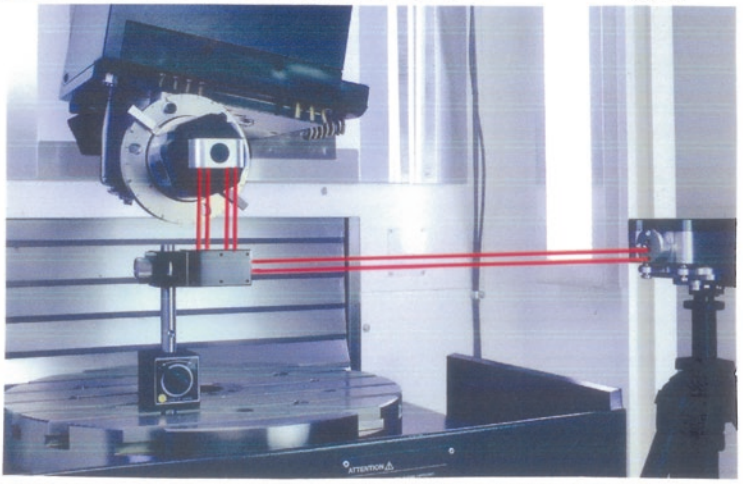

(b) Using the *XL-80 Laser Calibration System* in combination with the *XR20-W Rotary Axis Calibrator*, to undertake multi-axes calibration of the machine tool.

(c) Using the system described above, to calibrate a multi -axes mill/turn centre.

Fig. 2.14 Typical images of multi-axes laser calibration of machine tools (courtesy of Reinshaw plc)

One of the key benefits of utilising an angular-interferometer to provide the coupling between the counterrotating rotary axis calibrator and a stationary part of the axis under-test is that it is somewhat insensitive to small translation (i.e. side-to-side) movements of the reflector. This particular arrangement ensures that system alignment is much easier to achieve, by virtually eliminating a major potential source of angular-measurement error. For example, eccentrically mounting of a rotary axis calibrator, when being placed 1 mm from the centre of rotation of the axis under-test, will add $<\pm 0.5$ arcseconds of additional measurement error. By way of comparison, a Ø200 mm rotary-encoder disk, with external read-head, would have to be mounted to within 0.25 μm to achieve similar level of rotational-performance. Even a fully enclosed rotary encoder with its integral-bearings and sophisticated precision shaft-coupling, has to be mounted within ≈ 0.05 mm (i.e. a 40 times tighter-tolerance than that required by the rotary axis calibrator). On the other hand, keeping overall accuracy levels within ± 1 arcseconds, requires careful design and attention to detail to ensure that all of the possible error-sources are similarly controlled.

2.4.1 AxisSet™ Checkup—Utilised for Machine Tool Alignments

In order to achieve a cost-effective solution for checking the alignment and positioning performance of rotary axes, the AxisSet™ Checkup was developed—see Figs. 2.15b, c. Consequently, within just a few minutes of fitting this artefact to users of multi-axis, or multi-tasking (mill-turn) machines (i.e. here, typified by the CNC machine tool in Fig. 2.15a) it can efficiently identify and report on poor machine alignments and geometry that can cause extended process-setting times, as well as for checks on any non-conforming parts. The notable-features and accompanying-benefits of utilising this AxisSet™ Checkup device, are quite numerous and include the following:

- discrete reporting of the pivot-point on a CNC lathe/Turning Centre—line-error along linear axes (i.e. as commonly defined in CNCs);
- a reliable check and the ability to track any machine performance trends over time;
- enabling the measurement and reporting of critical-errors speedily and effectively;
- providing recommended correction-values for machine tool optimisation;
- increasing the confidence of the CNC-user, prior to critical features being machined;
- elimination of unplanned-downtime, which then reduces scrap levels and subsequently enables increased profits to be made;
- the ability to obtain both incremental and absolute reporting modes;

(a) The *machining* of a large *Hydro-impeller* situated on an integral *rotary table* on the Travelling Column CNC Milling Machine.
[Courtesy of Canyon Hydro (Deming, WA, USA)]

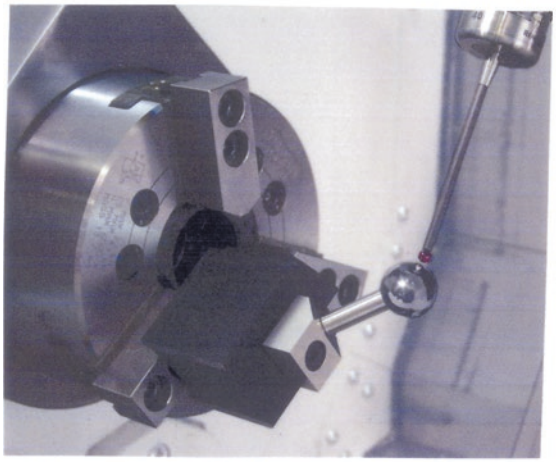

(b) Utilising the *AxisSet™ Checkup* on a Turning Centre with automatic probing routines to obtain performance data from a calibrated *Reference Artefact* – for the identification of poor *machine alignments*, prior to its *correction*.
[Courtesy of Renishaw plc]

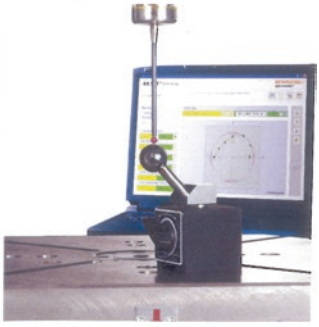

(c) Employing an *AxisSet™ Checkup* on a CNC Milling Machine's rotary table.
[Courtesy of Renishaw plc]

Fig. 2.15 In order to ensure that the CNC machine tool's rotary/*C*-axis, has the correct alignments, a quick and efficient artefact/probing routine can be exploited

- the system allows for user-selectable calculation methods—to establish pivot-points;
- displays of both form-error and the machine's swing-radius—where appropriate;
- the system can achieve automatic-import and backup—of multiple data sets.

AxisSet™ Checkup—Circular Plot—Software Overview

A graphical representation of rotary axis movement (i.e. see Fig. 2.15c—screen display), provides the user with a magnified view of errors in the machine path. Moreover, the actual tracking error gives an indication of the total effect of all measured errors, including both its centring and form errors. In particular, the definitions here will include:

- **Form Error**—which can be considered as, "The deviation of the measured points from a perfect curve";
- **Test Radius**—is, "The distance of measured points from the centre of rotation" (i.e. where the sphere is within the machine under-test);
- **Centring Error**—is, "The total error between the nominal and actual measured pivot point and represents the total magnitude of the pivot point error";
- ***X/Y/Z* Axis Component**—is, "The error between the nominal and actual pivot point, expressed along each relevant linear axis".

These specific definitions provide a practical understanding of what and where the errors are present within the machine tool, moreover, this also allows qualified-operators to correct these errors by updating CNC machine tool's parameter settings.

AxisSet™ Checkup—Angular Plot

Using the bespoke-software to produce an Angular Plot, it is then possible to understand the alignment of a rotary axis, then comparing it to its linear axes. This angular plot displays the rotary axis position against the linear axis, which is perpendicular to the axis of rotation and should of necessity, be stationary during the test. This linear axis here is also known as the static axis. As a consequence, any apparent movement of the static axis can be considered as the error caused by misalignment between the rotary axis and that of the static axis. Therefore, the maximum deviation of these errors is displayed as its tracking error.

2.5 Machine Tool Linear Axes—Factors Affecting Their Accuracy and Precision

An overall inaccuracy of machine tools, when they are machining components, can arise from a series of interrelated factors. Some quite significant problems can have an undue-influence on the machine's linear axes and their anticipated calibration, which could include inaccuracies due to:

- **geometric and kinematic machine tool inaccuracies**—affecting the linear ways, etc.;
- **internal stresses**—in the major machine tool's structural elements;
- **elastic deformation**—within the inherent rigidity (i.e. resulting from its lack of loop-stiffness) of the machine/tool/workpiece coupling resulting from the influence of cutting forces and other resistances;
- **thermal deformation of machine tool**—both internal and external thermal-effects;
- **wear and cutting forces**—resulting from the worn-tooling—increasing cutting forces, and as such, affecting these axes;
- **specific types of vibrations and some oscillation within the machine tool**—this is particularly apparent when machining at specific vibrational frequencies.

From this listing, probably the most important factor within a machine tool is that of its inherent machining accuracy and precision. Although, this accuracy and its accompanying measurement may be precise, but is it truly accurate? One technique in establishing the levels of accuracy of linear ways, is by statistical-methods. Here, the usual-approach is to use some form of statistical measures[22]—that are based upon well-established principles.

So, by utilising the **ISO 230-2** Standard, it is possible to employ it for the calibration and verification of, for example, the CNC machine tool positioning of its table. From Fig. 2.16, just one of the parameters that can readily establish the difference between the forward and backward linear series of runs along a measured-axis length, here termed its backlash, or alternatively, the uncorrected hysteresis error. Moreover, the **ISO 230-2** testing regime is targeted for both testing and evaluation of the accuracy and repeatability of positioning axes in CNC machine tools, by employing direct measurement of these axes. In this situation, the **ISO 230-2**-technique is equally applicable for either the machine's linear or rotary axes. The objective of these measurements under the **ISO 230-methodology**, is

[22]**Statistical measures**: which are often utilised in both machine tool and CMM calibration-techniques, being normally-based upon the following well-established principles, for their:

- **standard deviation**—known also as 'σ', which is a statistical measure of the precision in a '$\overline{x}$' (i.e. which is pronounced as: x-**bar)** series of repetitive 'x_i' measurements—with 'n', the number of data, while 'x_i' is each individual measurement and, the **mean** of all measurements;
- value 'x_i—$\overline{x}$' is called the **residual**—for each measurement.

Thus, it follows that:

$$\sigma = \sqrt{\sum_{i=1}^{n} (x_i - \overline{x})^2 \Big/ n - 1};$$

where:

$$\overline{x} = 1/n \sum_{i=1}^{n} x$$

to construct a compensatory curve and to then utilise this measured data to compensate for positioning-errors within these CNC machine tool's axes. In order to obtain the data necessary for the production of a graphical plot—similar to that shown in Fig. 2.16—these measurements are performed on the axis at a steady-state temperature. In accordance with requirements of **ISO 230-2**, the range of calibration of linear axes is invariably restricted. As a consequence, Fig. 2.16 displays the graphical representations of the results of accuracy and repeatability analysis

A large-scale Twin Column (LK) CMM
– with Horizontal Scanning Arms,
equipped with Digital Cross-scanner/laser
for Reverse Engineering comparison/validation.

[Courtesy of: Nikon Metrology/LK MSI/Warwick University]

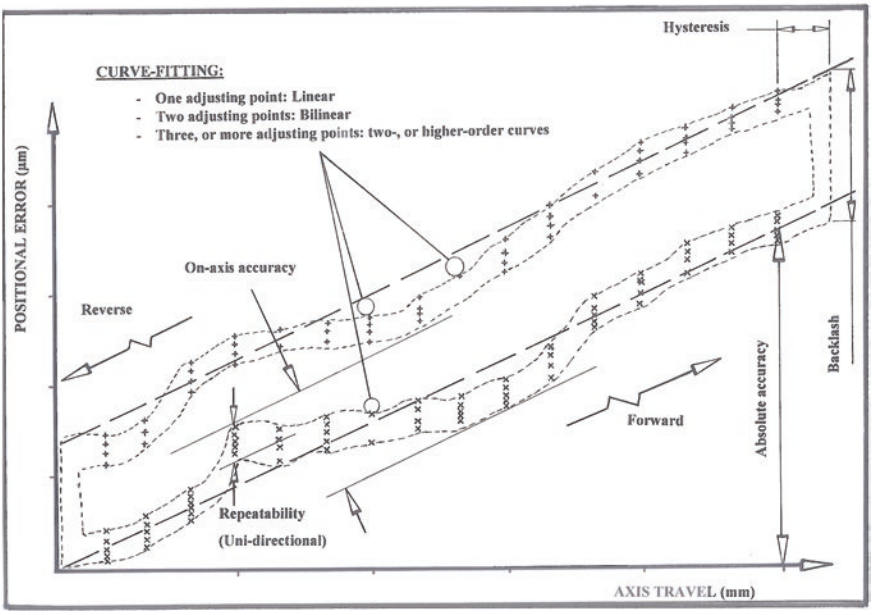

Fig. 2.16 A representative plot of a machine tool axis, illustrating: accuracy, repeatability and resolution (adapted from: ISO 10360/Hexagon Metrology)

of positioning on a typical axis, which highlights the additional parameters shown, that are also described in the **ISO 230-2**, these being evaluated by the envisioned calibration procedure—for the actual machine's table-positioning.

2.6 Laser Tracker—Instrumentation, Testing and Applications

The original Laser Tracker was patented in the USA in 1987—see the basic and schematic representation of it in Fig. 2.17. These now very-popular Trackers can be considered as Polar coordinate measuring systems, being capable of high-accuracy measurements over quite long linear distances. For example, in one of the systems now being utilised by The NPL, it can measure at distances of up to 40 m—to within discrete-accuracies of measurement of ±60 μm. Thus, in a Laser Tracker, it makes measurements of the positions via its Spherically mounted retro-reflectors (SMR's)—in terms of two angles—namely in the horizontal and vertical planes, which are measured using angular-scales mounted in the Tracker-mechanics, and distance (i.e. radius) to the SMR—by utilising a laser interferometer. By exploiting some relatively simple trigonometry, the Laser Tracker converts these obtained values into the usual cartesian coordinates (i.e. namely, into its *X*-; *Y*-; and *Z*-coordinates). Special-purpose tooling-fixtures allow the measurement of not just individual point locations, but also of surfaces such as for flatness and level, angles and squareness, surface form, as well as alignment between separate, or attached parts. By combining laser trackers with other measuring-systems, such as laser scanners, large objects with complex-surface features can be effectively and efficiently measured.

The metrological application of the laser tracker is especially useful for optical alignment—for three main reasons, these being:

1. **accuracy**—the current Laser Trackers can make measurements to ~10 μm accuracy without any special geometry, or data processing. By choosing advantageous geometry, calibrating repeating errors and by averaging random errors, the instrument's tracking allows it to measure to even tighter levels, of: <1 μm;
2. **flexibility**—the Laser Tracker can measure over a wide range of angles and distances. Moreover, a typical tracker can even measure through windows, thereby enabling the most difficult geometries to be measured with this type of instrument;
3. **ability to measure different optical spaces**—frequently optical systems incorporate fold mirrors to help with the system packaging. The laser tracker beam is also reflected by the mirrors, so the Tracker can determine optical-coordinates directly.

The relative merits of a laser tracker and its usage has been briefly mentioned above, but it needs re-stating once again, that they are utilised in wide-ranging metrological/calibration applications, some of which are simply depicted in

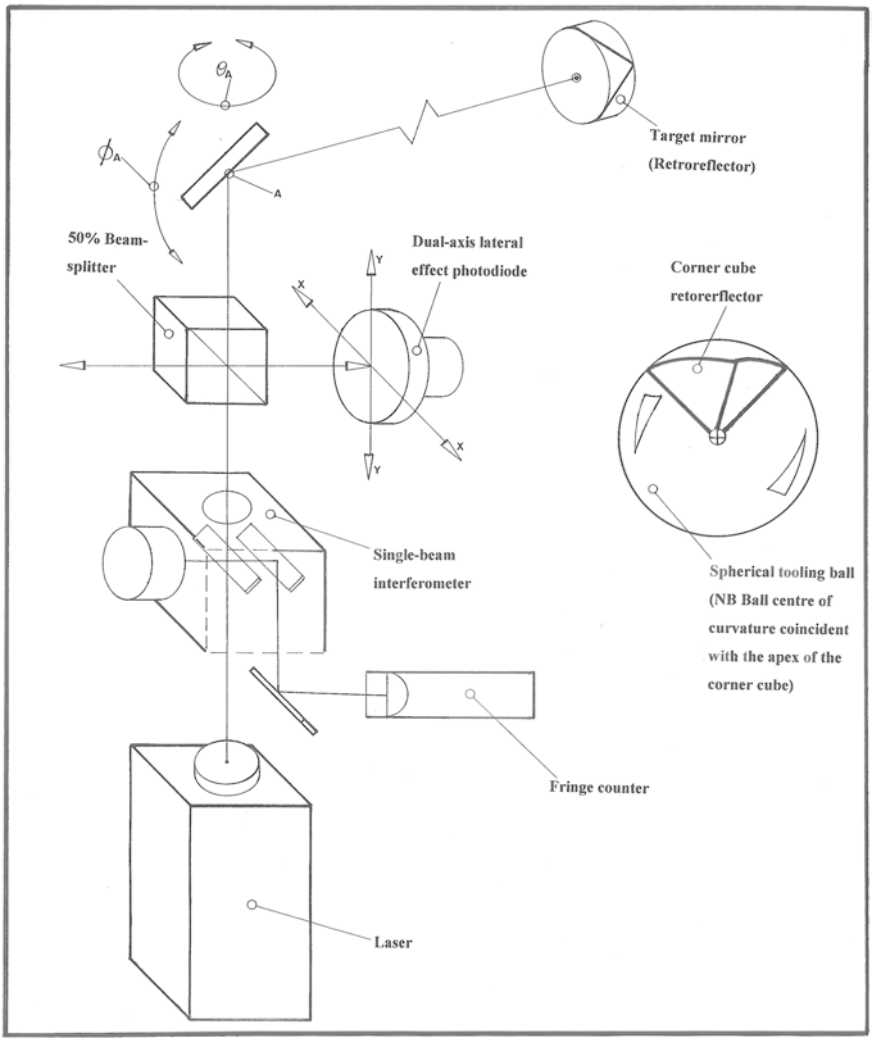

Fig. 2.17 An exploded view of the original *laser tracker* and its main components (*Source* US patent #4,714,339, in: proc. of SPIE vol. 6676 667760E-12)

Fig. 2.18—for various alignments and measurement of, say, large castings and for certain inspection procedures on alignments of machine tools. Typically, these trackers are often employed to ascertain and align the massive lengths of large aircraft wings—usually during final assembly. Accordingly, to take measurements with the tracker, the Inspector firstly sets-up a laser tracker on a tripod, with an unobstructed view of the object to be measured—see Fig. 2.18. Then the Inspector removes a target from the base of the tracker and carries it to the object, for certain regions of its features to be measured, moving smoothly to allow the laser

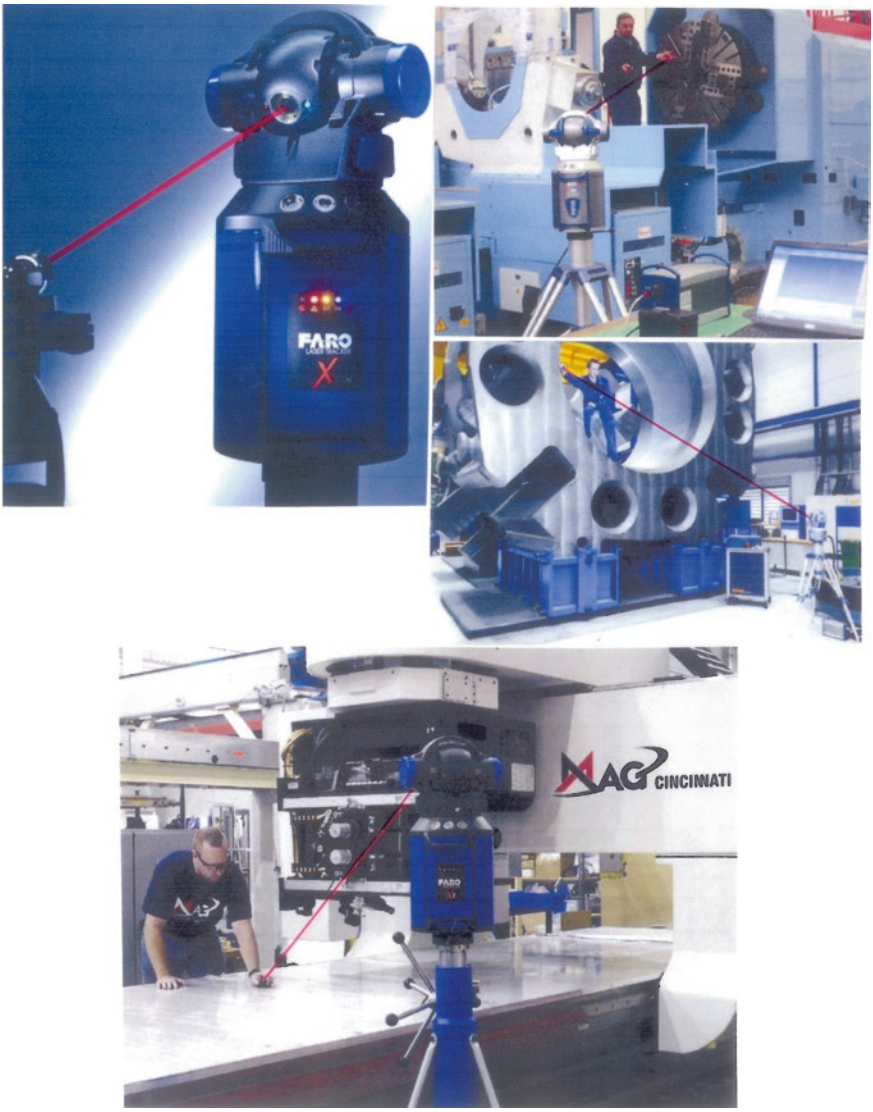

Fig. 2.18 Laser tracker applications can be wide-ranging in their inspection/calibration applications (courtesy of FARO Technologies Inc)

tracker to follow these movements of the target. During this procedure—as just mentioned—the Inspector individually places this target against the object, triggering-measurements to be taken at preselected points, sometimes utilising a remote control device. These direct-measurements can then be imported into different types of software to plot the relevant-points of interest, or to calculate deviation from the correct position. These targets are known as retroreflective, because

they reflect the laser beam back in the same direction it came from—in this case, back to the Laser Tracker. One type of target that is in common usage is the Spherically mounted retroreflectors (SMR)—often termed a spherical tooling ball, which resembles a ball-bearing with mirrored surfaces cut into it—see Fig. 2.17 (middle-right).

These laser trackers will also require periodic calibration, often by a country's National Institutions like the one which is typically provided by The NPL, which in this case utilises the seven tests prescribed in the **ASME B89.4.19** Standard—see below, in Sect. 2.6.1. These laser tracker tests are designed to exercise the tracker's measurement systems over a wide range of angles and distances, similar to those encountered in real-world usage. As a consequence, the Laser Tracker is subject to a configurations-test, which assesses the horizontal and angle encoder scale errors and eccentricities, together with its distance and displacement measuring systems. While the accompanying range-tests will verify the accuracy of the absolute distance meter (ADM), as well as the fringe counting performance of the laser interferometer (IFM)—if fitted.

2.6.1 Laser Tracker—Calibration Procedures

As mentioned in the previous Sect. 2.6 there are basically seven Laser Tracker test-procedures that are contained within the **ASME B89.4.19** Standard, which prescribes a series of repeated length-measurement tests for the verification of its IFM; its ADM; plus two-face tests: also the ranging-tests, which are undertaken in the following manner:

1. **horizontal length measurement system test**—in 9 configurations;
2. **vertical length measurement system test**—in 8 configurations;
3. **right diagonal length measurement system test**—in 8 configurations;
4. **left diagonal length measurement system test**—in 8 configurations;
5. **two-face system test measurement**—in 12 configurations;
6. **ranging tests**—for **IFM** and/or **ADM** up to 30 m;
7. **user-selected volumetric tests** —in 2 configurations.

These calibrated results from the Laser Tracker testing-regimes, are then reported against the performance specification (MPE-value)—these values being supplied by the particular laser tracker manufacturer. Additional calibration options, can also include laser wavelength calibration—with a comparison against Reference interferometer; plus its accompanying Weather station—for assessment (i.e. concerning testing it for temperature, humidity, also pressure).

2.6.2 Laser Tracker—Frequently Asked Questions

Invariably, some representative questions that are often raised concerning the practical usage and typical application of these laser trackers, might include:

- **What does it do?**—the Tracker can measure the three-dimensional location of a mobile-target with an accuracy of a few micrometres, over a range of tens of metres;
- **Why use this technique?**—Laser Trackers provide fast measurement of a target which can be moved almost anywhere within line-of-sight of its base-unit. A key factor in favour of the Tracker is the high relative-accuracy that can be achieved. Of note, is that these Trackers have largely superseded some of the more traditional measurement-techniques, such as by Theodolites, or conventional metrology tools in some instances as in the case of certain Auto-collimators, but more will be said concerning this optical-instrumentation—in Chap. 3;
- **What are Laser Trackers used for?**—these Trackers are often utilised for robot tracking, inspection and alignment; calibration tests, maintenance and testing procedures; aircraft manufacturing alignments; automotive jig-build and setup; verification of the design of manufactured structures; together with certain reverse Engineering applications;
- **Type of information gathered?**—data can vary from Raw 3-D coordinates; CAD models and surfaces; deformation and movement; Reverse Engineering-data; plus the tracking of moving objects;
- **How do these Laser Trackers work?**—Trackers operate by being based on the combination of two techniques: (i) a laser interferometer to measure relative distance; (ii) optical encoders to measure azimuth and elevation of a beam-steering mirror. Linear interferometers are a standard industrial measurement tool, working on the principle of light interference. In a standard Michelson interferometer setup, a coherent light source (i.e. from the laser) is split into two beams. One beam is used as a reference while the other beam is reflected-back from a mirror, or retro-reflector at some distance. This beam is then merged with the reference-beam, thereby producing interference. These interference-fringes are then counted as the external path-length changes. Since the wavelength of the laser is known and is highly stable, the distance can be calculated from the number of fringes. These devices are restricted to linear measurement. A Laser Tracker overcomes this limitation, by using a beam-steering mirror to direct the laser beam in a wide range of directions. The critical-task is for the beam to follow the movement of a retro-reflective target. This is achieved by a feedback loop. When the laser beam hits the retro-reflective target off-centre, it is reflected back, parallel to the incident beam, but will be displaced. A two-dimensional sensor will then measure this displacement, allowing the Tracker to adjust the beam-steering mirror to return the beam to its desired coaxial-state. Tracking mechanism—as described previously—is by using a corner-cube reflector. So, when the beam hits the centre of the target it returns without displacement, indicating the beam has hit the correct location. This mechanism

allows the laser beam to follow the movement of the target—by up to 5 m s^{-1}. Hence, the tracker follows a retro-reflective target, recording the distance; azimuth; plus its elevation. These polar co-ordinates are transformed into Cartesian coordinates, which can be centred anywhere in the measurement-space;

- **Laser trackers how do they operate?**—the operator simply walks around the object being measured, placing the retro-reflective target in positions to be recorded. Care must be taken not to break the beam from the laser tracker to the target, since the distance-count kept by the interferometer will be lost. If this happens, the target must be returned to a reference-position to reset the co-ordinate system. An additional feature is that some Trackers also have a secondary method of distance measurement that can be utilised to measure-arrays of mounted-targets. The tracker points the beam towards a given retro-reflector, and then a spiral-search pattern is used to establish a lock onto the hunted-target. The distance can then be measured without the interferometer and the process repeated. In this manner, a machine's structure, or assembly can be monitored for deformation, or movement without the Inspector being near the instrument. Alternatively, the Inspector can re-establish the interferometer-tracking once again, without going-back to the instrument. The accuracy of what is sometimes known as the absolute distance metre (ADM) is of the order of 50 μm. A camera can be utilised with at least one laser tracker, where the user can use a video-camera to view the object being measured and for the respective measurement-points to be selected. A hidden point device allows the user to measure using a small probe, instead of the relatively large spheres that typically range from 12.7 to 37.5 mm;
- **What are the benefits of this system?**—these benefits can include intuitive—here, an operator places the target anywhere a co-ordinate is required; fast—each data-point can be recorded in a few seconds; single-user—one device with an Inspector can record points working alone; range—typically over tens of metres, creating a large working volume; together with a reasonably large installed user-base in high-value operations;
- **What are the limitations of this system?**—the limitations include occlusion—this can only operate in line-of-sight, so by breaking the beam, it requires resetting the co-ordinate system; contact—the target must physically touch the measured-point; offset—must be recorded, with the co-ordinates being offset from the actual surface; target size—therefore the size of the retro-reflector limits the minimum radius of curvature measurable; static scene—the scene must remain static as the points are measured; environment—any changes in air temperature, pressure and humidity can affect measurements; cost—a Tracker is an expensive piece of equipment; portability—the Tracker is relatively large and heavy, making it unsuitable for some applications; ruggedness—the Tracker is a high precision piece of equipment and is unsuitable for use in many hazardous, dirty or unstable environments.

(Source (adapted): The questions and answers provided herein, plus for any further additional information, concerning these laser trackers, contact: **Optical Metrology Centre**, Bishop's Stortford, Herts, UK).

2.6.3 Laser Tracker—Machine-Based Research Applications

Machine Tool

In Fig. 2.19, is depicted a relatively new technique for the volumetric-verification of machine tools—in this case for a vertical machining centre. Beyond the consideration for a specific machine, a general verification methodology can be utilised to verify the number and movement of axes and by employing different techniques with a Laser Tracker. Therefore, a schematic and kinematic model—with the inclusion of the measurement system depending on the kinematics of the machine—can be achieved.

In this situation when utilising a laser tracker, the model describes the geometry and kinematics of an industrial machining centre, based upon a parametric synthetic data generator, which generates a test with known geometric errors and noise—enabling it to study different optimisation techniques and models. Likewise, dissimilar errors and identification techniques, plus volumetric verification models, can be obtained and analysed. This laser tracking research highlights the improvement that can occur in verification by considering optimisation-phases, the appropriateness of using new techniques of feedback and, the influence of optimisation-parameters. In this noted tracking research work, the use of Chebyshev polynomials[23] and its characteristics were employed, as well as a regression-function for the new verification model for the machine tool. Therefore, this newly developed Laser Tracking volumetric verification technique enables

[23]**Chebyshev polynomials**: are named after Pafnuty Lvovich Chebyshev, who was a brilliant Russian Mathematician (Born: 16 May 1821, Borovsk, died: 8 December 1894, Saint Petersburg, Russia). Chebyshev was educated at the Moscow State University. He introduced a sequence of orthogonal-polynomials which are related to: de Moivre's formula, which can be defined-recursively. One usually distinguishes between **Chebyshev polynomials—**of the first kind which are denoted 'T_n' and, **Chebyshev polynomials—**of the second kind, which are denoted 'U_n'. The letter 'T' is normally utilised, because of the alternative transliterations of the name Chebyshev—as Tchebycheff. These Chebyshev polynomials 'T_n', or 'U_n' are polynomials of degree 'n' and, the sequence of Chebyshev polynomials of either kind, composes a polynomial-sequence. As a consequence, these Chebyshev polynomials are polynomials with the largest possible leading-coefficient, but subject to the condition that their absolute value is bounded by the interval of: '1'. Hence, these Chebyshev polynomials are important in Approximation-theory, because the roots of these Chebyshev polynomials—of the first kind, which are also known as: Chebyshev-nodes, that are utilised as nodes in polynomial-interpolation. The resulting interpolation-polynomial, minimises the problem of what is termed Runge's-phenomenon (These various types of phenomenon and their associated equations, are somewhat outside the remit of the present metrological/calibration text, but are well-documented in the relevant and associated texts) and provides an approximation that is close to the polynomial of best approximation to a continuous-function under the maximum-norm. This approximation, then leads one directly to the method known as the: Clenshaw–Curtis quadrature (These various types of phenomenon and their associated equations, are somewhat outside the remit of the present metrological/calibration text, but are well-documented in the relevant and associated texts). So, in the study and usage of differential equations, they arise as the solution to these Chebyshev differential equations:

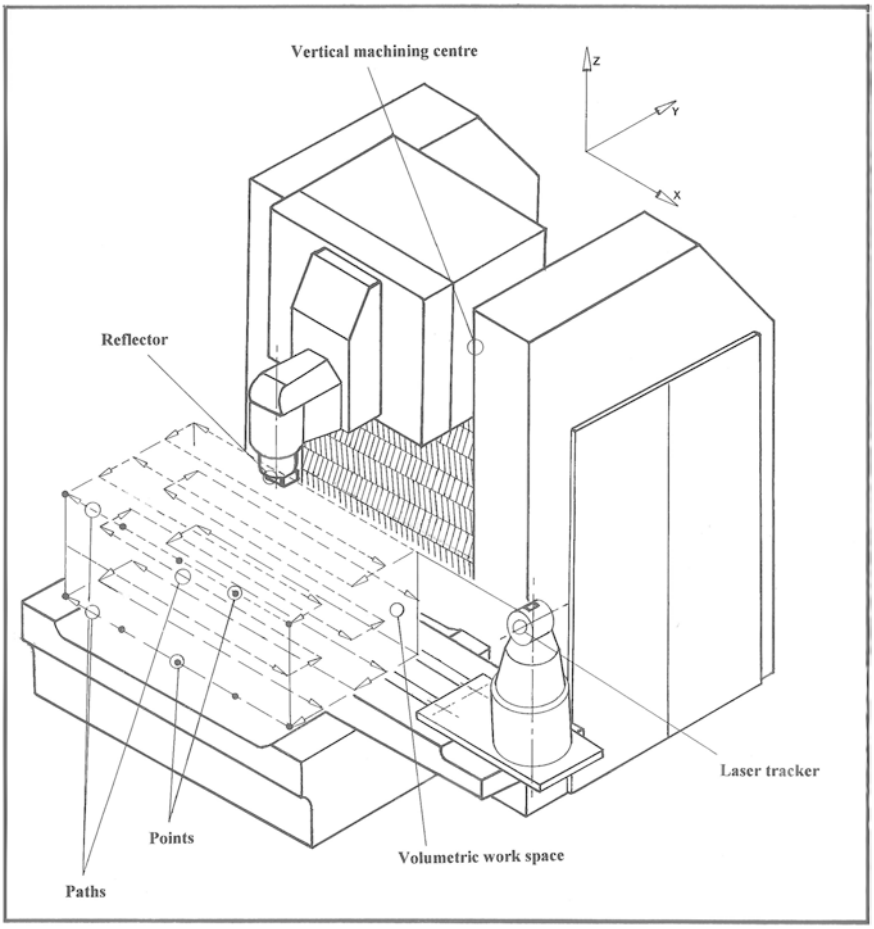

Fig. 2.19 The schematic arrangement for the volumetric verification of a machining centre *utilising laser tracking for the 'parametric generator test'* (Adapted from: Aguado, Samper, Santolaria and Aguilar, in: Int. J. Mach. Tools Manuf., Feb. 2012)

the characterisation of the different errors in the whole volumetric-workspace of the machine and in somewhat less time than by the more usually- employed direct laser and conventional optical verification methods.

Footnote 23 (continued)

$$\text{thus:} \quad \left(1 - x^2\right)y'' - xy' + n^2 y = 0$$

$$\text{and:} \quad \left(1 - x^2\right)y'' - 3xy' + n(n+2)y = 0$$

for the polynomials—of the first and second kind, respectively.
NB The above equations are special cases of the: Sturm–Liouville differential equation (These various types of phenomenon and their associated equations, are somewhat outside the remit of the present metrological/calibration text, but are well-documented in the relevant and associated texts).

Coordinate Measuring Machine

In Fig. 2.20 is schematically depicted a Laser Tracker, being employed for the technique of error-mapping a cantilevered CMM, based upon the concept that two-, or three-dimensional positions can be determined-exclusively from high-precision interferometric distance measurements, which is termed Multi-lateration. Here, all the relevant CMM distances are measured utilising a single conventional Tracker, with it being placed in four positions—see Fig. 2.20a. The CMM's errors are determined by creating a virtual-plate, which is comparable with a Ballplate—see Chap. 5 for more details of a typical Ballplate's geometry. The so-called virtual-plate is a set of reference positions, which are calculated from a large number of interferometric measured changes in length. As a consequence, a special-purpose optical retro-reflector unit (i.e. a turntable triple mirror) is mounted to the ram of the CMM, instead of the usual probing-head. In position, the laser tracker will then control the orientation of the triple-mirror, so that its open-side always points toward the direction of the laser beam. To achieve this relative mirror-motion, the mirror is rotated by a stepper motor, so that it prevents interruption of the interferometric signal, even when, for example the Tracker is located inside the bottom boundaries of this virtual-plate.

When mapping the CMM for its geometric errors, the machine moves the mirror into predefined positions in the horizontal and vertical planes—see Fig. 2.20a. When measuring in the horizontal plane for example, the Tracker at A is placed approximate to that plane for reasons of accuracy, and then it follows the movements of the CMM automatically. So, at position P_i for example, the CMM stops for between 5 and 10 s, until vibrations of the CMM have decayed—when the CMM's scales are read. The control programme of the Tracker automatically detects that the CMM has stopped, then it statically records the distance to the mirror. Thereafter, the Tracker once again changes into the dynamic measuring mode before the CMM starts to move the mirror to the next position to be measured. This motion-and-measurement activity continues until ≈50 points have been measured—forward and backward—taking <25 min—see Fig. 2.20c, d. After the first series of runs, it is necessary to reposition the Tracker to at least two other CMM-locations (i.e. B and C—see Fig. 2.20a)—it is normally beneficial to take a reading at the fourth position D, providing more accurate readings. The complete measurement process for the whole virtual-plane (i.e. over a relatively large surface area of 2 × 5 m)—see Fig. 2.20c—takes approximately 2 h, which will include the tracker-repositioning.

The evaluation procedure is based upon the measurement changes of lengths to a set of points from different positions, assuming that each set of changes of distances was sampled to the same set of pre-defined nominal positions—the mathematics and results of these tests are somewhat detailed and they appear in the appropriate reference at the end of this chapter. For this large CMM, its verification and full error-analysis is based upon the previously mentioned concept of Multi-lateration, which has proven to be quite a successful measurement

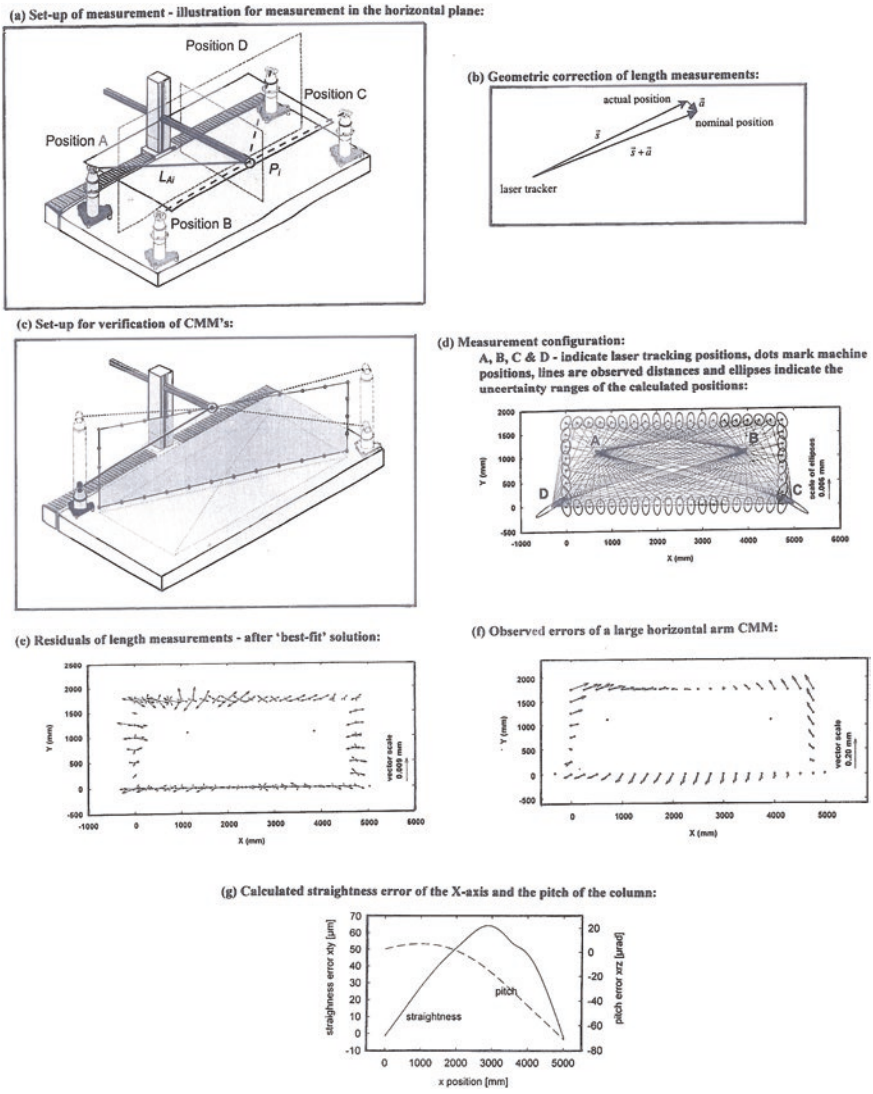

Fig. 2.20 The inspection of large-scale co-ordinate measuring machines (CMM's) by single multi-lateration, utilising a single laser tracker (After: Wendt, Schwenke, Bösemann and Dauke, 2003)

process—by employing the so-called Ballplate method, utilising a single Laser Tracker in this process—see Fig. 2.20. This measurement-technique allows one to systematically map all of the geometric errors for the CMM.

References

Journal and Conference Papers

Aguado, S., Samper, D., Santolaria, J. & Aguilar, J.J., *Identification strategy of error parameter in volumetric error compensation of machine tool based on laser tracker measurements*, Int. J. of Mach, Tools and Manufacture, Vol. 53 (1), 160-169, 2012.

Aguado, S., Samper, D., Santolaria, J. & Aguilar, J.J., *Machine Tool Rotary Axis Compensation Trough Volumetric Verification Using Laser Tracker*, Procedia Engineering, Vol. 63, 582-590, 2013.

Aguado, S., Santolaria, J., Samper, D. & Aguilar, J.J., *Influence of measurement noise and laser arrangement on measurement uncertainty of laser tracker multilateration in machine tool volumetric verification*, Precision Engineering, Vol. 37 (4), 929-943, Oct. 2013.

Bartscher, M., et al, *Artefact based traceability concept for large co-ordinate measuring machines*, Proc. of 9th Metrology Congress, Bordeaux (France), 158-161, 1999.

Birch. K.P. & Downs, M.J., *An updated Edlén equation for the refractive index of air*, Metrologia, Vol. 30, 155-162, 1993.

Birch, K.P. & Downs, M.J., *Correction to the updated Edlén equation for the refractive index of air*, Metrologia Vol. 31, 315-316, 1994.

Bridges, B., *How Laser Trackers Work*, Quality Digest, June 25, 2009.

Burge, J.H., Su, P., Zhao, C. & Zobrist, T., *Use of a commercial laser tracker for optical alignment*, Proc. of SPIE Vol. 6676 (66760E), 2007.

Burdekin, M., *Performance assessment of machine tools and co-ordinate measuring machines – some recent developments at UMIST*, Proc. of LAMDAMAP V Int. Conf., WIT Press, 91-104, 2001.

Callaghan, R., *Method for establishing machine tool performance specifications from part tolerance requirements*, Proc. of LAMDAMAP VI Int. Conf., WIT Press, 507-516, 2003.

Cedelnik, M., Sokovic, M. & Jurkovic, J., *Calibration and Checking the Geometrical Accuracy of a CNC Machine-Tool*, J. of Mech. Eng'g, Vol. 52 (11), 752-762, 2006.

Chapman, M.A.V., *Limitations of laser diagonal measurements*, Precision Engineering Vol. 27, 401–406, 2003.

Ciddor, P.E., *Refractive index of air: new equations for the visible and near infrared*, Appl. Optics, Vol. 35, 1566-1573, 1996.

Edlén, B., *The refractive index of air*, Metrologia, Vol. 2, 71-80, 1966.

Ekinovic, S., Prcanovic, H. & Begovic, E., *Calibration of machine tools by means of laser measuring systems*, Asian Transactions on Engineering, Vol. 2 (6), 17-21, Jan. 2013.

Gull, M., *Developments in BSI and ISO machine tool accuracy standards*, Proc. of LAMDAMAP III Int. Conf., 79-89, Computational Mechanics Pub., 1997.

Hale, L.C., *Principles and Techniques for Designing Precision Machines*, Doctor of Philosophy (Mechanical Engineering), Massachusetts Institute of Technology, 1999.

Hargreaves, B., *Measuring up*, Professional Eng'g., 71-73, April 2015.

Hof, A., *Theorie und Realisierung eines Abbé-Fehler-freien, selbst-kalibrierenden räumlichen Wegmeßsystems,* Fortschr. Ber. VDI Reihe 8, Nr. 134, VDI-Verlag, Düsseldorf, 1987.

Hong, C., Ibaraki, S. & Oyama, C., *Graphical presentation of error motions of rotary axes on a five-axis machine tool by static R-test with separating the influence of squareness errors of linear axes*, Int. J. of Mach. Tools and Manufact., Vol. 59, 24-33, Aug. 2012.

Ibaraki, S. & Hata, T., *A new formulation of laser step diagonal measurement – Three-dimensional measurement*, Precision Eng'g., Vol. 34, 515-525, 2010.

Iwasawa, K., Iwamaa, A. & Mitsui, K., *Development of a measuring method for several types of programmed tool paths for NC machine tools using a laser displacement interferometer and rotary encoder*, Prec. Eng,g, Vol.28, 399-408, 2004.

Knapp, W., *Test of the three-dimensional uncertainty of machine tools and measuring machines and its relation to the machine errors*, ETH Zurich, 459-464, 1993.

Knapp, W., *Interim checks for machine tools*, Proc. of LAMDAMAP III Int. Conf., Computational Mechanics Pub., 161-168, 1997.

Koelsch, J.R., *Should Laser Trackers be in your Arsenal of Metrological Tools?*, Quality Magazine, March 2012.

Kunzmann, H., Pteifer, T. & Flügge, J., *Scales vs. Laser Interferometers – Performances & Comparison of Two Measuring Systems*, Vol. 42 2), 753-767, 1993.

Kuric, I., Košinár, M. & Cisár, M., *Measurement and analysis of CNC machine tool*[s] *accuracy in different location*[s] *on work table*, Proceedings in Manufacturing Systems, Vol. 7 (4), 2012.

Lau K.C & Hocken, R.J., *Three and Five Axis Laser Tracking Systems*, United States Patent 4,714,339, 1987.

Longstaff, A.P., Fletcher, S. & Ford, D.G., *Practical experience of thermal testing with reference to ISO 230 Part 3*, Proc. of LAMDAMAP VI Int. Conf., WIT Press, 473-484, 2003.

Okafor, A.C & Ertekin, Y.M., *Vertical machining center accuracy characterization using laser interferometer, Part 1. Linear positional errors*, J. of Matls. Process. Technol., Vol. 105, 394-406, 2000.

Peták, T. & Kureková E., *Calibration of Biaxial NC positioning table*, Trans. of the VŠB – Tech. Univ. of Ostrava (Slovak Republic), Mechanical Series, Vol. LVIII (2), article No. 1922, 55-74, 2012.

Portable laser tracker measures large volumes accurately, Machine Design, Vol. 83 (14), 19, Aug. 25, 2011.

Santolaria, J., Majarena, A.C., Samper, D., Brau, A. & Velázquez, J., *Articulated Arm Coordinate Measuring Machine Calibration by Laser Tracker Multilateration*, The Scientific World Journal, Vol. 2014, Article ID 681853, 2014.

Schwenke H, et al., *Geometric error measurement and compensation of machines–An update*, Annals of the CIRP, Manufact. Technol., 57 (2), 660-675, 2008.

Smith, G.T., *Condition Monitoring of Machine Tools*, Chapter 9, in: Handbook of Condition Monitoring (1st Ed.), Elsevier Advanced Technology Pub., 170-207, 1996.

Soons, J.A., *Measuring the geometric errors of a hexapod machine tool*, Proc. of LAMDAMAP IV Int. Conf., WIT Press, 169-192, 1999.

Soons, J.A., *Analysis of the step-diagonal test*, Proc. of LAMDAMAP VII Int. Conf.,126-137, 2005.

Svoboda, O., *Volumetric positioning accuracy of a vertical machining center equipped with linear drives (evaluated by laser vector method)*, Proc. of LAMDAMAP VI Int. Conf., WIT Press, 141-150, 2003.

Svoboda, O., *Testing the diagonal measurement technique*, Precision Engineering, Vol. 30, 133-144, 2006.

Tomkinson, G., *Fitting laser interferometers to large machine tools as the primary positioning feedback system*, Proc. of LAMDAMAP III Int. Conf., Computational Mechanics Pub., 205-213, 1997.

Trapet, E. & Wäldele, F., *A reference object-based method to determine the parametric error components of co-ordinate measuring machines*, Measurement, Vol. 9, 17-21, 1991.

Ueno, S. & Matsumaru, S., *Evaluation of numerically controlled machine tool positioning accuracy*, Proc. of LAMDAMAP VI Int. Conf., WIT Press, 485-494, 2003.

Wendt, K., Schwenke, H., Bösemann, W. & Dauke, M., *Inspection of large CMMs by sequential multi-lateration using a single laser tracker*, Proc. of LAMDAMAP VI Int. Conf., WIT Press, 121-139, 2003.

Wang, C., *Laser vector measurement technique for the determination and compensation of volumetric positioning errors, Part 1: Basic theory*, Review of Scientific Instruments, Vol. 71 (10), October, 2000.

Wang, C. & Liotto, G., *A laser non-contact measurement of static positioning and dynamic contouring accuracy of a CNC machine tool*, Proceedings of the Measurement Science Conference, Los Angeles, 24-25, Jan. 2002.
Wang, C. Liotto, G., *A theoretical analysis of 4 body diagonal displacement measurement and step diagonal measurement*, Proc. of LAMDAMAP VI Int. Conf., WIT Press, 463-472, 2003.
Wang, C., *Machine tool calibration: standards and methods*, American Machinist, Jan. 2009.
Yin, J., Pan, F. & Li, M., *Accuracy Calibration of a Five Axis Gantry Machine Tool Using Laser Tracker*, International Conference on Convergence Information Technology, Vol.19, 2012.

Books, Booklets and Guides

AIA/NAS, NAS 979 Uniform Cutting Tests, *NAS Series Metal Cutting Equipment Specifications*, 1969.
ANSI/ASME B5.57, *Methods for Performance Evaluation of Computer Numerically Controlled (CNC) Lathes and Turning Centers*, 1998.
ANSI/ASME B5.54, *Methods for Performance Evaluation of Computer Numerically Controlled Machining Centers*, 2005.
ASTM E105: *Standard Practice for Probability Sampling of Materials*.
ASTM E122: *Standard Practice for Calculating Sample Size to Estimate, With a Specified Tolerable Error, the Average for Characteristic of a Lot, or Process*.
ASTM E141: *Standard Practice for Acceptance of Evidence Based on the Results of Probability Sampling*.
ASTM E1402: *Standard Terminology Relating to Sampling*.
ASTM E1994: *Standard Practice for Use of Process Oriented AOQL and LTPD Sampling Plans*.
ASTM E2234: *Standard Practice for Sampling a Stream of Product by Attributes Indexed by AQL*.
Bobroff, N. & Estler, W.T., *Interferometric Metrology*, Pub. by American Society for Precision Engineering, 1992.
Bucher, J.L., *The Metrology Handbook, Second Edition*, ASQ Quality Press, 2012.
Chapman, M.A.V., *Environmental compensation of linear laser interferometer readings*, Technical White Paper: TE329, Renishaw plc, 2013.
Chapman, M.A.V., Fergusson-Kelly, R. & Lee, W., *Interferometric straightness measurement and application to moving table machines*, Technical White Paper: TE325, Rensihaw plc, 2013.
Chapman, M.A.V., Fergusson-Kelly, R., Holloway, A. & Lee, W., *Interferometric angle measurement and the hardware options available from Renishaw*, Technical White Paper: TE326, Renishaw plc, 2013.
Crouch, S. & Skoog, D. A., *Principles of Instrumental Analysis*, Pub. by Pacific Grove: Brooks Cole, 2007.
Dotson, C., *Fundamentals of Dimensional Metrology*, Pub. by Thomson Delamar Learning 5th Ed. (2006), 6th Ed. (Feb. 2015).
Flack, D., CMM Verification, Good Practice Guide No. 42, NPL Publication.
Flack, D. & Hanniford, J., *Fundamental Good Practice in Dimensional Metrology*, Good Practice Guide No. 80, NPL Publication.
Galyer J.F.W. & Shotbolt, C.R., *Metrology for Engineers* (5th Ed.), Cassell Publishers Ltd., London, 1990.
Golz, H.U., *Analyse Modellbildung und Optimierung des Betriebsverhaltens von Kugelgewindetrieben*, Dissertation for the University of Karlsruhe, 1990.
Harihanan, P., *Basics of Interferometry*, Academic Press Inc. (Australia), 1991.
Hemming, B., *Measurement Traceability and Uncertainty in Machine Vision Applications*, MIKES Metrology, Espoo (Finland), 2007.

ISO 2859-1:1999: *Sampling procedures for inspection by attributes*.

JCGM 200:2008, *International vocabulary of metrology - Basic and general concepts and associated terms*, (VIM).

Kakino, Y., Ihara, Y. & Shinohara, A., *Accuracy inspection of NC machine tools by double ball bar method*, Ed. by Johannes Heidenhain (GmbH), Hanser Gardner Publications, Munich, 1993 .

Montgomery, D. C., *Statistical Quality Control: A Modern Introduction*, Wiley Pub., 2009.

Metrology Handbook - The Science of Measurement, Pub. by Mitutoyo, 2013.

Pennella, C.R., *Managing the Metrology System*, ASQC Quality Press - 2nd Ed. (USA).

Schmitt, T., *Modell der Wärmeübertragungsvorgänge in der mechanischen Struker von CNC-gesteuerten Vorschubsystemen*, Shaker publishing house, 1996.

Smith, G.T., *Industrial Metrology – Surfaces & Roundness*, Springer Verlag Pub., 2002.

Wilkening, G. & Koenders, L., *Nanoscale Calibration Standards and Methods: Dimensional and Related Measurements in the Micro and Nanometer Range*, Pub. by Wiley-VCH Verlag (GmbH), 2005.

Chapter 3
Optical Instrumentation for Machine Calibration

"*There's light enough for what I've got to do.*"
Charles Dickens.
(English Novelist).
[1812–1870].
(In: Oliver Twist, Ch. 47).

3.1 Basic Principles of Light

In the rudimentary study of optical principles based upon what is termed white light,[1] there is a very long history of development, dating back far into antiquity. Most of the original research into light was basically undertaken concerning early instrumentation, with these first rather crude optical instruments being somewhat rudimentarily built telescopes—*with distinctly poor lens quality, but they were* utilised for magnification of distant astronomical images. Conversely, at the other extreme a microscope was developed and utilised for magnifying very tiny images. Since the days of the inventors of the telescope and microscope, respectively, (these individuals being Galileo[2]

[1]**White light**: from electromagnetic radiation, is composed of a fairly even distribution of all of the frequencies in the visible range of the spectrum, but appearing white to the naked eye. The light from the Sun is nearly perfect white light, although the Sun does not itself appear white when viewed on Earth, due to the scattering of light with frequencies in the blue range by our atmosphere, leaving the Sun with a distinctive yellow colour. So that light that appears white to the eye, it is in effect, essentially composed of certain combinations of light with frequencies in the red, blue and green parts of the visible spectrum—see Fig. 6.16.

[2]**Galileo Galilei**: (Born: 15 February 1564—died: 8 January 1642), is often known as simply: **Galileo**. He was an Italian Polymath—physicist, mathematician, astronomer and philosopher—who played a significant and crucial role in the scientific revolution. Galileo's notable achievements include improvements to the telescope and consequent astronomical observations and moreover, he is known for his support of Copernicanism. Galileo has been rightly called: 'The Father of modern Observational Astronomy'.

G.T. Smith, *Machine Tool Metrology*, DOI 10.1007/978-3-319-25109-7_3

and Van Leeuwenhoek[3]) such optical instruments have greatly improved, having been extended in their optical applications and levels of sophistication over the intervening years. Their instrumental applications now have been expanded into other portions of the electromagnetic spectrum. However traditionally, if one focuses on the early twentieth century where there were two trains-of-thought concerning the fundamental physical properties of light, these were based upon either the:

1. **Wave nature of light**—advocated by the supporters of Huygen[4]. Huygen is particularly well known as an astronomer, physicist, probabilist, also to a lesser degree, as a horologist; although, Huygen is primarily remembered especially for his work on optical theories, most notably on the wave theory of light, which he first communicated in 1678—to the Paris Académie des Sciences. This wave theory was formerly published in 1690 in his work Traité de la lumière (Treatise on light). Huygens also refers to the work by Ignace-Gaston Pardies[5]—whose manuscript on optics helped him with his development of the wave theory.
2. **Particle nature of light**—which was supported by the optical research of Newton[6] and other notable scientists. Newton's seminal book Philosophiæ Naturalis Principia Mathematica (Mathematical Principles of Natural Philosophy) was first published in 1687. This fundamental treatise laid the foundations for much of our knowledge of classical mechanics. Newton also made pivotal contributions to that of optics and shares a degree of credit with Gottfried Leibniz[7] for the invention of infinitesimal calculus. Previously in 1666, Newton observed that the spectrum of colours exiting a prism was rectangular, even when the light's ray entering the prism was circular—thereby demonstrating that a prism will refract different colours at differing angles. This practical experimentation led Newton to conclude that colour is a property intrinsic to light—a point which had been somewhat debated over the intervening years. Furthermore, Newton also investigated the refraction of light,

[3]**Antonie Philips van Leeuwenhoek**: (Born: 24 October 1632—died: 26 August 1723) was from Delft (Netherlands) and was both a tradesman and scientist. He is commonly known as 'The Father of Microbiology'. Leeuwenhoek is considered to be the first microbiologist and is best known for his work on the improvement of the microscope, also for his original contributions towards the establishment of the science of Microbiology.

[4]**Christiaan Huygens**: FRS (Born: 14 April 1629—died: 8 July 1695). Huygens was a prominent Dutch mathematician and natural philosopher, being raised in The Hague (The Netherlands).

[5]**Ignace-Gaston Pardies**, *was a notable* French scientist (Born in Pau: 5 September 1636—died: 21 April 1673). Initially, he opposed Newton's 'Theory of refraction' and his letters, together with Newton's replies (i.e. which so satisfied Pardies, that he later withdrew his scientific objections), are found in the: Philosophical Transactions of the Royal Society—for 1672 and 1673.

[6]**Sir Isaac Newton FRS**: (Born in a village in Lincolnshire, England on: 25 December 1642—died: 20 March 1727). He was one of the truly eminent English physicists and mathematicians, who is now often widely regarded as one of the most influential scientists of all time—with his consummate work on a range of scientific endeavours.

[7]**Gottfried Wilhelm von Leibniz** (Born in Leipzig on: 1 July 1646—died: 14 November 1716). Leibniz was a German mathematician/philosopher and could be said to occupy a prominent place in the history of both Mathematics and in the history of Philosophy.

demonstrating that the multicoloured spectrum produced by a prism could be recomposed into white light by a lens and a second prism.

The relatively new and significant development of quantum mechanics (QM) is a branch of Physics which is concerned with physical phenomena at the truly microscopic scale of materials and their measurement, where the action is on the order of the Planck constant. Quantum mechanics departs from classical mechanics primarily at the quantum realm of atomic and subatomic length scales. It provides a mathematical description of much of the dual particle-like and wave-like behaviours and its interactions of energy and matter. It is the non-relativistic limit of quantum field theory (QFT) which was a theory developed slightly later, combining both quantum mechanics with that of relativity. QM allows one to understand that light has both wave and particulate properties, these being attributed to Planck[8] and his quantisation of black-body radiation. With the advent of our understanding of Quantum Mechanics we are able to comprehend—as just described—that light has both wave and particulate properties, while the fundamental work by Neils Bohr[9] resolved the Wave particle duality of light.

This whole scientific subject on recent developments in both quantum mechanics and the wave-like behaviour of light, is somewhat digressing and is basically beyond the scope of this current technical remit, but considerable literature and fundamental research are currently being undertaken in these important fields of

[8]**Max Karl Ernst Ludwig Planck**, FRS (Born: Kiel Duchy of Holstein, Germany on: 23 April 1858—died: 4 October 1947). Planck was an eminent German theoretical physicist who originated quantum theory, for which he won the Nobel Prize in Physics in 1918. Planck also developed many contributions to theoretical physics, although his fame primarily consists of his role as originator of the quantum theory. This work on quantum theory revolutionised human understanding of atomic and subatomic processes. In 1894, Planck focussed his attention on the problem of black-body radiation. This problem had been previously stated by Kirchhoff* in 1859, stating: 'How does the intensity of the electromagnetic radiation emitted by a black body [a perfect absorber, also known as a cavity radiator] depend on the frequency of the radiation [the colour of the light] and the temperature of the body?' Kirchhoff's central assumption behind his new derivation, presented to the DPG on: 14 December 1900, was the supposition, now known as the: Planck postulate, in that electromagnetic energy could be emitted only in quantised form, or alternatively, the energy could only be a multiple of an elementary unit, hence simply stated:

$$\mathbf{E} = \mathbf{h}\nu,$$

where '**h**' is Planck's constant, also known as—Planck's action quantum (i.e. he had already introduced this term in 1899), and 'ν' (i.e. the Greek letter nu) is the frequency of the radiation.

*__Gustav Robert Kirchhoff__ (Born: Könisberg, Kingdom of Prussia on: 12 March 1824—died: 17 October 1887). Kirchoff, was a well-respected German physicist who contributed to the fundamental understanding of: electrical circuits, spectroscopy and the point here of interest, being that Kirchhoff further investigated into the emission of black-body radiation—of heated objects.

[9]**Niels Henrik David Bohr** (Born: Copenhagen on: 7 October 1885—died: 18 November 1962). Bohr, was a prominent Danish Physicist, who made some really-fundamental contributions to our present understanding of the atomic structure and, to that of Quantum Theory—in this latter research work—for which, Bohr received the Nobel Prize in Physics, in 1922.

scientific study. However, in this current chapter, certain basic assumptions have to be made when dealing with the subject of optics, such as for those that are employed for machine calibration, namely:

- Parallax—this is a displacement or difference in the apparent position of an object viewed along two different lines-of-sight, being measured by either the angle, or semi-angle of inclination between those two lines. The term is derived from the Greek (parallaxis)—meaning alteration. Hence, any nearby objects have a larger parallax than more distant objects when observed from different positions, so parallax can be utilised to determine distances. Any measurements taken by viewing the position of a specific marker relative to something to be measured, are subject to parallax error, particularly when this marker is some distance away from the object of measurement and not viewed from the correct position. A similar error occurs when reading the position of a pointer against a scale in, say, an instrument such as either a mechanical comparator, or an analog multimetre. To assist the user in avoiding this potential parallax problem, the scale is sometimes printed above a narrow strip of mirror, and the user's eye is positioned so that the pointer obscures its own reflection. This simple optical relationship guarantees that the user's line-of-sight will be perpendicular to the mirror and therefore to the scale;
- **Reflection**—this is the result of a change in direction of a wavefront at an interface between two different media, so that this wavefront will return back into the medium from where it originated. Any reflection of light can be present as either specular (i.e. mirror-like) or diffuseX (i.e. retaining the energy, but losing the image)—depending upon the nature of the interface. Additionally, if the interface is between a dielectric and a conductor, the phase of the reflected wave is retained, otherwise if the interface is between two dielectrics, the phase may be retained, or inverted, depending on the indices of refraction. By way of explaining this type of phenomena but somewhat more succinctly, a mirror provides the most common example for specular light reflection and it will typically consist of a glass sheet with a metallic coating—where on this surface, the reflection actually occurs. Reflection is enhanced in metals by suppression of wave propagation beyond their skin depths. Reflection also exists at the surface of transparent media, such as water or glass. Consequently, if a light ray strikes a front-silvered mirror at an angular point, as a result it then becomes a reflected ray. So, by projecting an imaginary line that is normal, or perpendicular to this mirror, one can then measure the angle of incidence (i.e. denoted by '$\boldsymbol{\theta_i}$') and its angle of reflection (i.e. '$\boldsymbol{\theta_r}$'). Hence, the law of reflection simply states that: '$\boldsymbol{\theta_i = \theta_r}$', or in other words: 'The angle of incidence equals the angle of reflection'. As a matter of fact, the reflection of light may occur whenever light travels from a medium of a given refractive index, or when it travels into a medium with a different refractive index. Accordingly, in the most general case, a certain fraction of the light is reflected from the interface, while the remainder is refracted;
- **Refraction**—which results from the change in direction of a wave due to the change in its transmission medium. Refraction is essentially a surface phenomenon. This refraction phenomenon is principally concerned with the governance of the law of conservation of energy and momentum. Moreover, due to change

of the medium, the phase velocity of this wave is changed, but its frequency remains constant. This effect is most commonly observed when a wave passes from one medium to another, but at any angle other than that of either 90° or 0°. Refraction of light is the most commonly observed phenomenon, but any type of wave can refract when it interacts with a medium. Typical examples are when sound waves pass from one medium into another, or when certain waves of water move into different depths of water. Refraction is described by Snell's law[10] which states, 'That for a given pair of media and a wave with a single frequency, the ratio of the sines of the angle of incidence $\boldsymbol{\theta_1}$ and angle of refraction $\boldsymbol{\theta_2}$ is equivalent to the ratio of phase velocities ($\mathbf{v_1/v_2}$) in the two media, or equivalently, to the opposite ratio of the indices of refraction ($\mathbf{n_2/n_1}$)', such that:

$$\mathbf{\sin\theta_1/\sin\theta_2 = v_1/v_2 = n_2/n_1}$$

In optics, refraction is a phenomenon that often occurs when waves travel from one medium with a given refractive index to another, but here, at an oblique angle. At the boundary between the media, the wave's phase velocity is altered, usually by causing a change in its direction. Hence as a result, its wavelength increases, or decreases—although its frequency remains constant. For example, a light ray will refract as it enters and leaves glass, assuming there is a change in refractive index. Thus, a ray travelling along the normal (i.e. perpendicular to the boundary) will change speed, but not its direction. However, refraction will still occur in this case and as a consequence, by an understanding of this concept, it has led to the invention of lenses and ultimately to that of the refracting telescope.

Typically, the effect of refraction can be seen when looking into water, this is notable because air has a refractive index of ≈1,0003, while that of water will have a refractive index of ≈1,3330. By way of illustration, if someone looks at a straight object such as a rod, which is positioned at a slant and partially immersed in some still water, the rod will appear to be bent at the water's surface. This effect is due to the bending of light rays as they travel from the water to the air. Once these rays reach the eye, the eye then traces them back as straight lines (i.e. lines-of-sight). So, the lines-of-sight will intersect at a higher position than where the actual rays originated. This effect causes the immersed rod's shank to appear somewhat higher, while water would, respectively, seem to be shallow. Consequently, the depth that the water appears to be, when viewed from above, is known as its apparent depth. These fundamental optical principles are of some interest in the application of optical instrumentation utilised for such machine alignments and calibration procedures when verification is to be undertaken.

[10]**Snell's law***: this law is named after Dutch astronomer, Willebrord Snellius (Born: 13 June 1580, in Leiden, died: 30 October 1626, also in Leiden, The Netherlands). Snellius was educated at Leiden University, where he discovered this law—in 1621. In fact, the background to Snell's law, was originally and succinctly described by the now, obscure and notable Arabian scientist, Ibn Sahl—at the Baghdad Court (i.e. in AD984). Here then Sahl, in his original manuscript, being 'On Burning Mirrors and Lenses', is where he utilised this then unknown law, to derive lens shapes that could focus light, but Sahl also mentioned that this light existed without any geometric aberrations.

*Of note, is that Snell's law—which is also known as either Descartes' law, or even as the Snell–Descartes law, which then more accurately describes the law of refraction.

3.1.1 Optical Alignment—Basic Principles

The optical instrumentation equipment utilised in machine calibration/verification such as the range of clinometers, Talyvels and the autocollimator—shown in Fig. 3.1—are often overlooked and considered somewhat irrelevant by certain machine tool companies and end-users alike. However, this category of instrumentation has three unchallengeable and distinct attributes, namely: (i) they can magnify; (ii) they can apply reversal techniques; (iii) but also they have the ability to utilise gravity as a reference. Moreover, in all calibration procedures, optical instruments can validate a machine's straightness, flatness, squareness, plus its plumbness—this latter term refers to the machine's gravitational alignment. These purely optical instruments can utilise the phenomenon that a real image, which has been formed by its lens, can be treated as if it were an actual object, accordingly allowing it to then be magnified by its lens system. Customarily, graticules (i.e. both for the eyepiece and target) are normally visualised as graduated cross-wires—see Fig. 3.8b—being positioned in the plane of the image to be viewed, together with this image—by one's eye. For example, in the case of an alignment telescope, the point in the object where the centre of the cross-wires appears is on a theoretical line known as its line-of-sight[11] (L.O.S.), or alternatively it is sometimes termed as the line-of-collimation. This actual line-of-sight appears at first glance to be absolutely straight in undisturbed air, but this is not essentially the case, principally due to the effect of the Earth's curvature and air refraction—see Fig. 3.14. This metaphorical optical disparity becomes significant over longer distances, when taking readings for line-of-sight on very large machine structures with an optical alignment telescope, which is aimed at a strategically placed target—more will be said concerning these targets later—from which relevant measurements can be taken. The accuracy of these optical measurements is of the order of 1:200,000, or more specifically: $\leq$75 μm at 30 m.

Reversal techniques—for straightness measurements

In machine alignments in much of optical metrology, it is important to have the instrumental capability to be checked by the reversal technique. This reversal is a dimensional measurement procedure, which separates the errors of the reference,

[11]**Line-of-sight** (L.O.S.): is the basic reference for all measurements and it is necessary that the exact location of the line with reference to the object/work should be known, with great accuracy and precision. This is effected by arranging the line-of-sight to pass through two points of known height—from a mounting surface—these points being the equivalent of the centres of two (theoretical) spheres. Thus, the target is mounted in one sphere—with the centre of the pattern positioned exactly at the centre of this sphere—see Fig. 3.10b, conversely, the telescope is mounted in the other sphere and its position is adjusted by pivoting it in a spherical bearing—formed by the sphere and a conical mounting cup—see Fig. 11d and e. So, whatever is the tilt adjustment of the telescope, the line-of-sight which is concentric, will always pass through the centre of this sphere.

(a) A range of Clinometers & Talyvels (ie electronic levels) & instrumentation.

(b) Photoelectronic Autocollimator & Microptic Clinometer having a precision polygon attached.

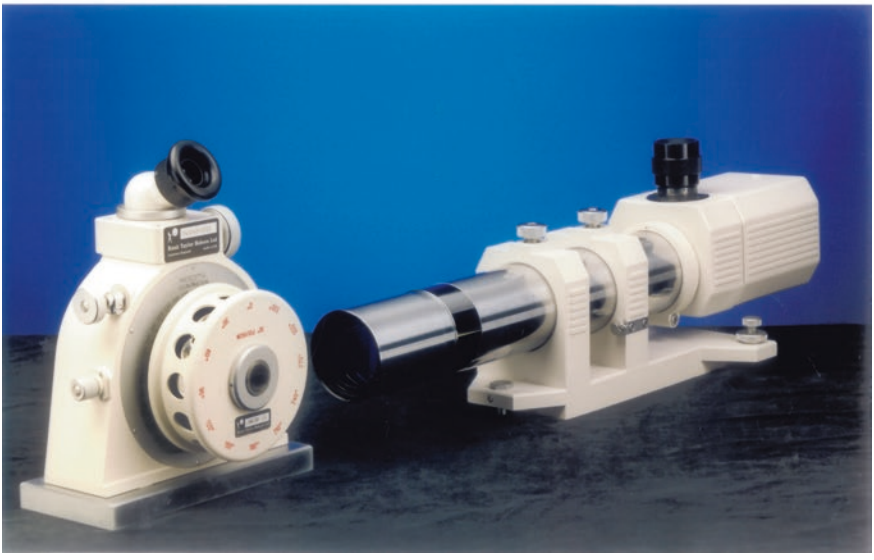

Fig. 3.1 A range of optical/electronic autocollimators, clinometers, Talyvels and polygons (courtesy of Spectrum Metrology)

from the errors that are present in the measurement artefact. The separation is customarily achieved by reversing the position of a reference object along with the sensitive direction of the instrument, then simply repeating a sequence of measurements—as a function of linear position or angle. Accordingly, reversal is a technique that allows the removal of residual machine errors and it relies on measuring the component in two specific orientations. In the first orientation, the machine error will add to the result, while in the second orientation the machine error subtracts from the result.

By way of example, in the first orientation if one measures the straightness of a line on a component, then what one is actually measuring is:

Workpiece straightness error + machine straightness error

Subsequently, in the second orientation, if one then turns the component over and, then measures down exactly the same line that was previously measured, then one obtains:

Workpiece straightness error − machine straightness error

Straightedge reversal

The technique of reversal can be demonstrated by utilising a precision metrological straightedge, to evaluate an axis' straightness. So, for example here in an experimental set-up, an indicator is mounted on, say, the travelling carriage in such a way that it is aligned in the direction of interest (i.e. usually orthogonal to the axis) and touching a straightedge mounted in the desired vicinity. If one now assumes that the machine slide straightness is given by a function '$M(x)$' and the departure of the straightedge is given by a function '$S(x)$', it is then possible to calculate the indicator output for this position by adding these two functions of '$M(x)$' and '$S(x)$' together and then calling it '$I_1(x)$'.

Thus

$$I_1(x) = M(x) + S(x).$$

Once satisfactorily completed, one then simply reverses the straightedge by rotating it about its long axis and remounting the indicator so that it is touching the straightedge, but it now has had its direction or sign reversed. This action is important to note, because now when one calculates the indicator output '$I_2(x)$', it is possible to see an apparent reversal of the machine axis; the ostensible lack of change in the straightedge output being despite the fact that this straightedge has been reversed. Thus

$$I_2(x) = -M(x) + S(x).$$

One can now go on to separate these terms by two simple equations, by adding them together and then taking the differences.

Thus $M(x) = I_1(x) - I_2(x)/2$,

$$\text{and} \qquad S(x) = I_1(x) + I_2(x)/2.$$

3.2 Autocollimation Principles

3.2.1 Basic Design of an Autocollimator

An optical, or visual autocollimator (see Fig. 3.2)—the latter term being more frequently used today—utilises white light with these instruments, being employed for the non-contact measurement of small angular displacements. Typically, such optical instruments are utilised to align axes/components, as well as to measure small deflections in either optical or mechanical systems. Accordingly, a visual autocollimator operates by projecting an image onto a target mirror/reflector—see Fig. 3.2c—which is then used to measure the deflection of the returned image against a graduated scale, either visually or by means of an electronic detector—such as in the case of the Photoelectronic/Digital autocollimator (see Fig. 3.3a). With the optical Autocollimator, it can quantify angles as small as 0.5 arcseconds, conversely with an electronic/digital autocollimator, this can be $\geq$100 times more accurate than the former instrument.

Visual autocollimators are invariably utilised for checking face parallelism, together with the basic angular orientation of optical polygons (see Fig. 3.3b), optical flats, optical wedges, etc. Due to their inherent greater measurement accuracy and precision, the electronic/digital autocollimators are normally utilised as a form of angular measurement standard, by monitoring any angular movement over perhaps long periods of time, whilst also checking the angular position repeatability—in certain mechanical systems. Specially designed servo autocollimators are a compact form of an electronic autocollimator, which can be utilised in high-speed servo feedback loops for precise and stable platform applications. As a consequence, an electronic autocollimator will typically be calibrated to read the actual mirror angle.

The principle method of operation of an optical autocollimator is where the optical set-up has a collimated beam (i.e. a beam of parallel light rays) that exits in an optical system, which is then subsequently reflected back into the same system by a plane mirror—see once again Fig. 3.2c. Consequently, an autocollimator can be employed for measuring small tilt angles of the target mirror—perhaps attached to a machine element requiring calibration/verification, or when testing the quality of an optical system, or indeed, when just simply being a part of this overall system. However, in the case of large aperture optics, they are usually tested with a Null corrector,[12] thus avoiding the production of a large plane mirror.

[12]**Null corrector**: this is an optical device utilised in the testing of large aspheric mirrors. Moreover, a spherical mirror of any size can be tested relatively easily utilising standard optical components such as: laser; mirrors; beam splitters, and converging lenses. One technique of achieving this is by employing a so-called Shack cube, but there are many other set-ups that are also possible. Thus, with this type of interferometer test, it generates a contour map of the deviation of the surface from a perfect sphere—with these contours in units of half the wavelength being utilised. This optical technique is termed a: null test, because when the mirror is perfect the result is null (i.e. there are no contours at all). However, if the result is not null, then the mirror

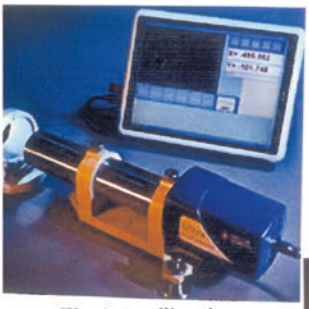

Windows ®-based software programs used with the digital autocollimators give graphical output of flatness, straightness, squareness, twist, also they can calibrate polygons with up to 72 faces. Visual autocollimators, or dual axis digital autocollimators are capable of measuring 0,01 second, equivalent to 50nm m^{-1}.

The Autocollimation range:

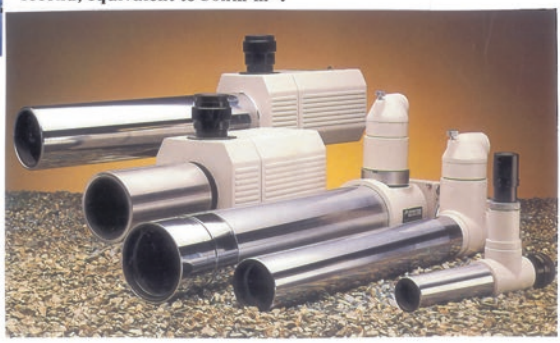

(a)

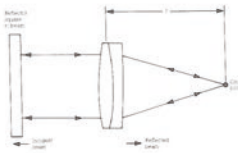

Light from the origin point 'O' is collimated (i.e. made parallel) by a high quality objective lens. If the collimated beam falls perpendicularly onto a plane reflecting surface, the light is reflected back along its original path and is brought to focus at a position coincident with the origin point - shown in Fig. (a).

(b)

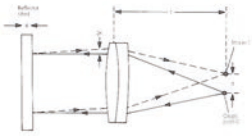

If the reflector is tilted through an angle 'θ' (Fig. b), the reflected beam is deflected through angle 2θ, with the image 'I' being laterally displaced from the origin 'O'.

The amount of displacement is given by: $d = 2\theta f$.
Where: f = focal length of lens,
θ = radians.

Given that 'f' is a known constant for the Autocollimator, measurement of the displacement 'd' enables the tilt 'θ' to be ascertained.

(c)

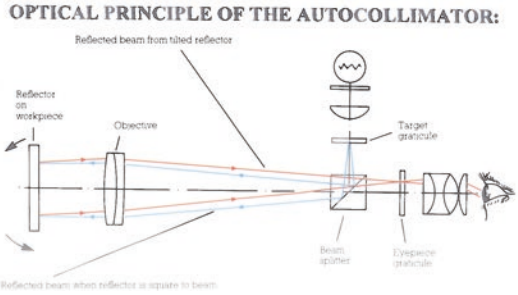

Fig. 3.2 The principles of autocollimation (courtesy of Spectrum Metrology)

Ultra Series dual-axis, digital autocollimator that incorporates the latest charge coupled device (CCD) technology and optical analysis software. The device automatically measures both X and Y directions at each measurement position along a slideway. Key features include a wide measurement range (1,800 seconds), high accuracy (0,2 seconds) and simple touchscreen operation.

(a) Optical arrangement for Photoelectronic Autocollimators:

NB Dual axis measurement with digital display

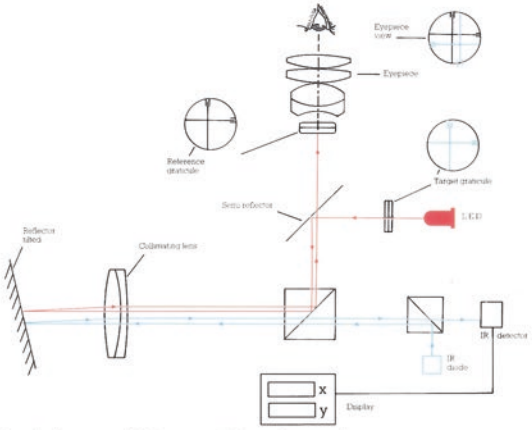

(b) Calibration of a Precision Polygon utilising two Photoelectronic Autocollimators - angularly displaced at the included angle of each polygon face.

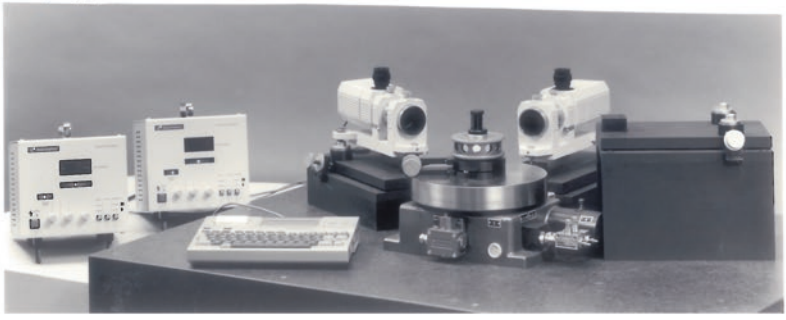

Fig. 3.3 Photoelectronic autocollimators can be utilised for calibration of precision polygons, which can then be typically employed for calibrating angular equipment such as rotary tables (courtesy of Spectrum Metrology)

3.2.2 Autocollimator—its Optical Operational Principle

Typically, the operating principle of an optical/visual autocollimator is for the light from an origin point to be collimated (i.e. made parallel) by a very high-quality objective lens. If the collimated beam falls perpendicularly onto a plane reflecting surface, the light is reflected back exactly along its original path and is brought to a focus at a point coincident with the origin point—see Fig. 3.2a. Subsequently, when the reflecting mirror is tilted through an angle (**θ**) the reflected beam is deflected through an angle '**2θ**'—which is a standard optical principle that is very well known, thus the image is displaced laterally from the origin—see Fig. 3.2b. At this point the amount of actual displacement is given by

$$d = 2\theta f$$

where '**f**' is the focal length of the lens; '**θ**' is in radians.

The light from an illuminated target graticule—being at the focus of an objective lens—is then directed towards the lens by a beam splitter—see Fig. 3.2c. After reflection by a mirror conveniently situated on the inspected element (i.e. namely the workpiece) the light will return through the autocollimator's optics and passes once again through the beam splitter, forming an image of the target graticule in the plane of an eyepiece graticule. Later, the eyepiece graticule and the reflected image of this target graticule are viewed (i.e. simultaneously) through the eyepiece. It should also be noted that the image of the target graticule is *always* seen in focus and at constant magnification in the eyepiece, this is regardless of the distance between the actual autocollimator and the reflecting surface/target. Nevertheless, at long working distances, where many visual autocollimator's are necessarily employed, only a small portion of the reflected target graticule may appear in the eyepiece, owing to the failure of the obliquely returning rays being able to enter the autocollimator's optics. This optical disparity of the returning rays will result in a somewhat restricted measuring range for this type of visual autocollimator.

Autocollimation can be utilised for highly specialised precision applications, such as when determining the focal length of a diverging lens. Here, a light source is accurately positioned at twice the focal length of a converging lens, but on one side and with a screen at the same distance on the other side, so that the image achieved for this light source is the sharpest possible. When this is accomplished, the screen is replaced with a mirror and the diverging lens is inserted between the converging lens and the light source at such a distance to the mirror, that the light returning through the diverging and converging lenses, produces a sharp image on

---

Footnote 12 (continued)

is not perfect and the subsequent pattern will show where any additional optical work should be carried out, as the mirror is then minutely repolished—to subsequently improve the mirror's overall configured geometry and hence, its optical performance. [*Source* Burge, J.H., *Advanced Techniques for Measuring Primary Mirrors for Astronomical Telescopes*, his Ph.D. – Thesis undertaken at: *The University of Arizona*, USA, 1993].

top of the luminous object. Hence this is the optical circumstance, when the beam hitting the mirror is collimated, thus the distance found will be the (negative) focal length of the diverging lens.

3.2.3 Digital Autocollimators

Probably the most popular form of autocollimation is by utilising a digital autocollimator—see typical examples of these autocollimators in Figs. 3.2 (top), 3.3 (top), 3.4 and 3.5 (top). These extremely sensitive accurate and precise metrology instruments are designed for minute angular displacement measurement and for suitable calibration/verification tasks. In operation, a digital autocollimator will use an electronic photodetector to detect the reflected beam. Such types of microradian autocollimators take advantage of the latest detector technology, which will include either advanced silicon-based photodetectors, or germanium-based detectors. A typical detector will be configured to send a signal to a microradian digital controller, which then digitises and processes the signal—normally utilising proprietary DSP-based electronics.[13] This type of processing will create a calibrated angular output which is traceable to an appropriate standard, such as that employed in the USA and established by NIST. The digital autocollimator's angular data is subsequently retrieved by, say, a touch screen LCD display—see Fig. 3.4a—which usually has either an RS-232 interface, or analog outputs which are normally all built into the controller. These digital autocollimators are suitable for many other applications, including that of the calibration of rotary tables (Fig. 3.4a), checking angle standards, remote-, or long-term angular monitoring, measurements of flatness (Fig. 3.5-top), or straightness, also providing angular feedback in servo-controlled systems. Such dual-axis digital autocollimators (Fig. 3.4) are invariably utilised on machines to quantify/measure:

- **angle**—typically the indexing accuracy of a head, or table—see Figs. 3.3b, 3.4a and 3.7b;

[13]**DSP-based electronics**: this is digital signal processing (DSP), which is the mathematical manipulation of an information signal to modify or improve it in some manner. Thus, the DSP is characterised by the representation of: discrete time, discrete frequency, or other discrete domain signals; by a sequence of numbers, or symbols and the processing of these signals. The principal objective of DSP is normally to: measure, filter and/or compress continuous real-world analog signals. First, conversion of the signal from an analog to a digital form, by a sampling requirement and then second, digitising it utilising an analog-to-digital converter (ADC), which then turns the analog signal into a stream of numbers. Although, it is often that the required output signal is another analog output signal, which subsequently necessitates a digital-to-analog converter (DAC). Moreover, even if this type of process is more complex than analog processing and has a discrete value range, the application of computational power to digital signal processing allows for many advantages over its analog counterpart, for processing in a range of applications, such as error detection and correction in transmission, as well as for data compression. [*Source* Stranneby, D. & Walker, W., *Digital Signal Processing and Applications* (2nd Ed.), Elsevier Pub., 2004.].

(a) Utilising an *Ultra Series dual-axis digital autocollimator* that incorporates the latest charge coupled device (CCD) technology and optical analysis software, to calibrate a *Rotary Table* with a *Precision Polygon* – evaluating any potential angular indexing errors.

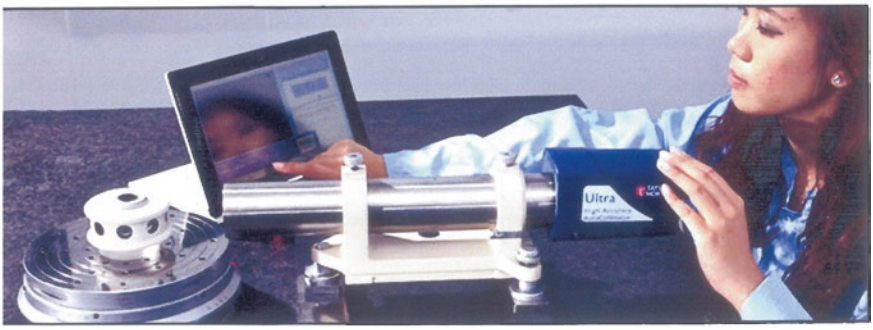

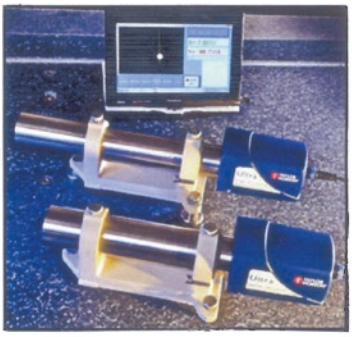

Autocollimator type:	Ultra High	Ultra
Accuracy:	0,1 sec (over entire range)	0,2 sec (over entire range)
Range of measurement:	300 sec	1800 sec
Direct reading to:	0,001 sec	0,001 sec

(b) Calibration chart for a Rotary Table - illustrating the exaggerated indexing errors present.

Typical values:
Minimum table X error: -1,50 sec,
Maximum table X error: 1,50 sec,
Minimum table Y error: -0,50 sec,
Maximum table Y error: 2,50 sec.

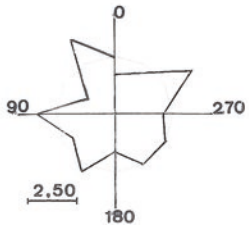

Fig. 3.4 A photoelectronic autocollimator being utilised in conjunction with a precision polygon, being employed for the metrological inspection of a precision rotary table, indicating on the calibration chart some typical results (courtesy of Spectrum Metrology)

- **straightness**—for example two axes of machine tool slide set-ups—see Figs. 3.5, 3.6 and 3.7a;
- **squareness**—typically the orthogonality between spindles-to-slideways—see Fig. 3.10d;
- **parallelism**—of slideways along their entire operational length.

For example, using a reflector (on a carriage) and dual axis autocollimator (Ultra autocollimator), up to 200 measuring steps can be taken for straightness checking, moving the reflector carriage along the slideway in equidistant steps. Any out-of-straightness in either of the two slideway surfaces X and Y (side and top of the slide) will cause the reflector carriage to change angle with respect to the autocollimator, and it is these changes which are measured and computed to determine the errors in straightness. The results are displayed in both tabular and graphical form - deviations from straightness in both axes are given in relation to either a least squares line, or ends zero.

Ultra Series dual-axis digital autocollimator – assessing a table's flatness:

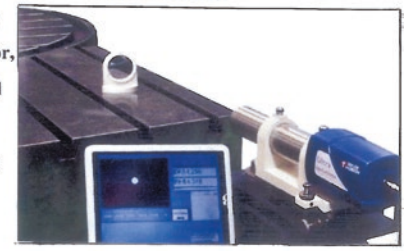

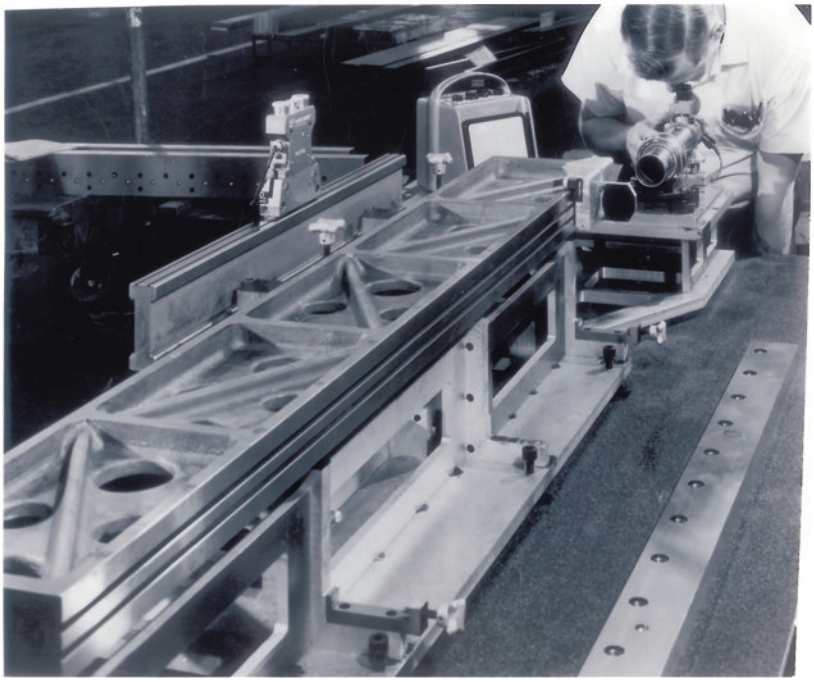

Fig. 3.5 Utilising an autocollimator in establishing a precision straightedge for a machine tool casting's reference surface in combination with the flatness assessment with a Talyvel (courtesy of Spectrum Metrology)

These relatively inexpensive dual-axis digital autocollimators are quite capable of measuring to $\leq$0.1 arcseconds, this measurement being equivalent to 0.5 nm m^{-1}. In all circumstances of autocollimation instrumentation, they are normally used in conjunction with either reflecting mirrors, or surfaces—see Fig. 3.6—for accurate and precise measurement of small angular deviations from a datum angle. In the

(a) The *Reflector* is an integral part of any Autocollimator system, necessitating adequate: flatness (0,08 μm); parallelism of faces (5 sec); reflectivity and diameter (ϕ50 mm):

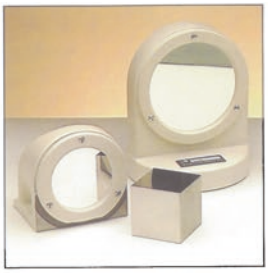

(b) A large *Reflector Carriage*, with glass-mounted reflector situated on an adjustable base - with side feet, for two-axis *Straightness* measurement of a machine tool's slideway:

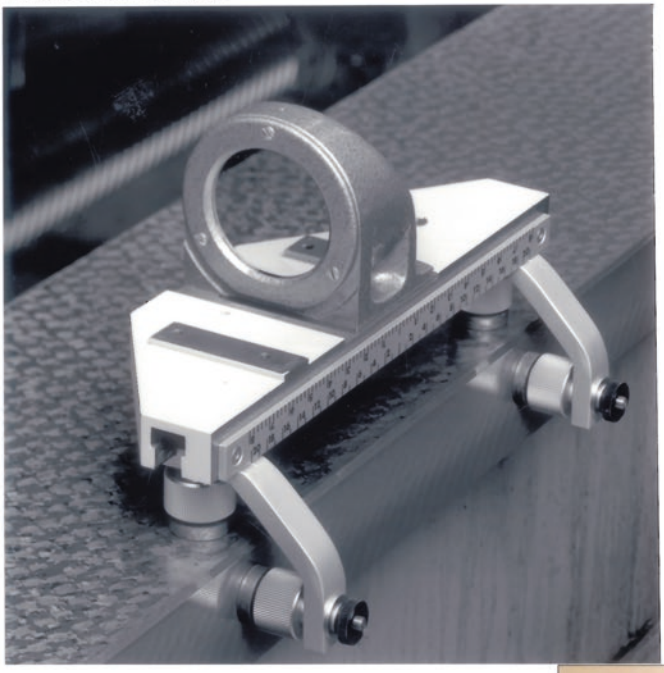

(c) A *Fixed Test Wedge*, can be utilised to quickly check the accuracy of the Autocollimator - it introduces a fixed angle of deviation (i.e. nominally 60 seconds), so by rotating the Wedge from its minimum to maximum deviation and comparing these values to Autocollimator's readings:

Fig. 3.6 Some typical reflectors and a carriage for autocollimation applications (courtesy of Spectrum Metrology)

(a) The simultaneous 2-axis straightness measurement of machine tool slideway.

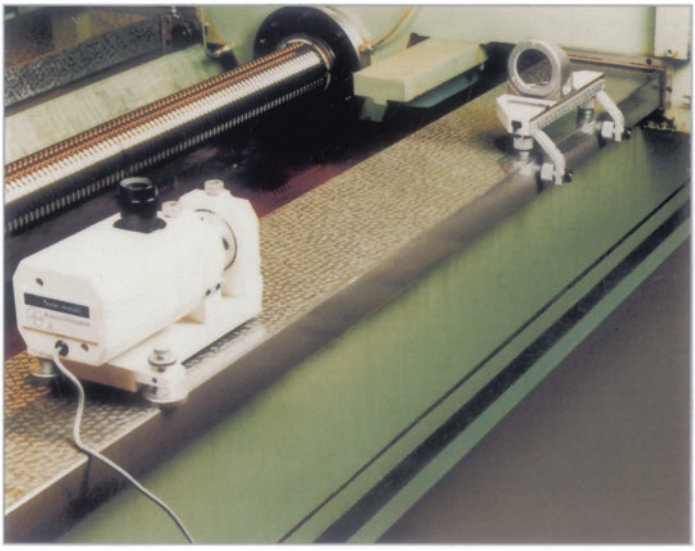

(b) Checking the angular indexing accuracy of a machine tool's rotary table, using an Autocollimator in conjunction with a Microptic Clinometer & associated Reflector in-situ.

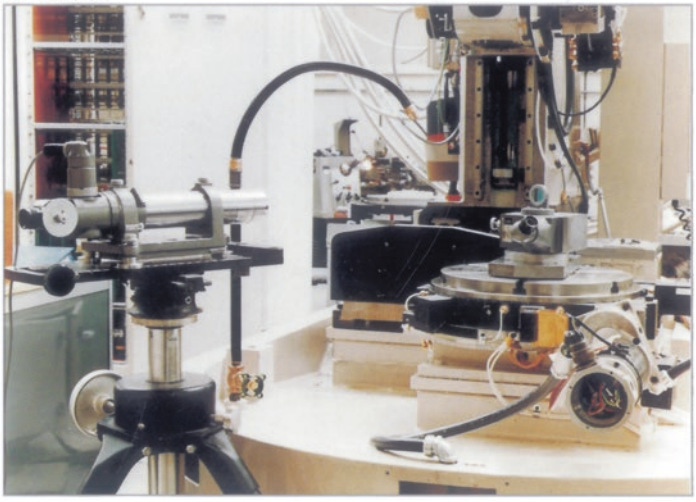

Fig. 3.7 Typical straightness and angular calibration tests employing optical techniques (courtesy of Spectrum Metrology)

case of the digital autocollimators shown in Figs. 3.2 (top) 3.4 (top) and 3.5 (top), they employ Windows™-based software programs, offering graphical output of flatness, straightness, squareness, also twist; as well as for polygon calibration—up

to 72 faces (i.e. Fig. 1.8 middle-right shows such a polygon and in actual practice in Fig. 3.4). This particular digital autocollimator utilises the latest CCD technology[14]—offering high accuracy and stability, with a laser-sighting aid for fast and simple set-up in combination with a tablet PC with integrated software. This sophisticated arrangement allows for measurement and analysis of a range of calibrating features necessary to fully exploit the overall inspection and validation procedures that are anticipated to be metrologically undertaken by various industries as well as in scientific research applications.

3.2.4 Precision Polygons for Angular Measurements

The application of precision polygons (Fig. 1.8 middle-right) for basic standards for angle measurement, is well known—see Figs. 3.3b and 3.4a—and they are normally utilised for such verification tasks and can either be calibrated in particular by the country's national standards laboratories, or independently calibrated with suitable metrology instrumentation. The uncertainty of measurement that is attainable with such polygons is largely dependent upon the geometry (i.e. its inherent flatness and squareness) of their angular reflecting faces and, to a certain extent on the optical errors of the autocollimator, together with any alignment errors occurring during sensing of the actual faces. The autocollimator with the multi-angular prism (i.e. precision polygon) angle measurement principle has long been considered as the most precise means of angular positional determination. This technique of angle determination remains the national angle reference in many countries. Consequently, the calibration of such features of the angular measurement, namely by the multi-angular prism/polygon can be considered as extremely important. As described, a typical multi-angular prism is a precision polygon having both accurate and precise flat mirror faces. As a result, the angle between the adjacent mirrored faces must not only be known, but must be very accurate and precise. Customarily, a multi-angular prism will consist of between 8 and 20 faces, or occasionally having either 24, 36, or even 72 faces (i.e. the latter being shown in Fig. 1.8 middle-right). The material that these multi-angular prisms/polygons are frequently made from, can range from hardened and stabilised alloy steels to that of stress-free quartz glass—as well as many other materials.

[14]**CCD technology** (The charge-coupled device (CCD), was invented in 1969, at the: AT&T Bell Laboratory (USA)—by: Willard Boyle and George E. Smith.): utilises a charge-coupled device (CCD), being a device for the movement of electrical charge, usually from within this device to a vicinity where the charge can be manipulated, for example by a conversion into a digital value. This conversion is achieved by shifting the signals between stages within the device—one at a time. CCDs move the charge between capacitive bins within the device, with the shift allowing for the transfer of charge between respective bins. The CCD is a major piece of technology in digital imaging. In a CCD image sensor, the pixels are represented by: p-doped MOS capacitors.

The angle between the faces of precision polygons is considered to be the reference angle and invariably this angular error value does not usually exceed 0.1 arcseconds. The main disadvantage of such a multi-angular prism is that positioning angles of the tested devices are normally equal to the angles between the polygon edges being measured. To achieve precise angular measurements, both the precision polygon and the autocollimator(s) being utilised in this calibration must themselves also be calibrated. These autocollimators are normally calibrated against small artefacts such as angle generators—of various constructions—this allowing for an appropriate calibration curve for each of these autocollimators to be acquired. In general, the systematic error sources for angular measurements performed by such autocollimators are the result of

- **the influence of the non-parallelism of beams**—resulting from the fact that the autocollimator was not focused to infinity;
- **some form of systematic error(s)**—perhaps of the CCD matrix;
- **errors resulting from**—the optical system of the autocollimator;
- **specific errors instigated by the CCD orientation**—which may be produced by the CCD matrix not being perpendicular to the actual beams.

The systematic errors of precision polygons are customarily caused by deviations of the angles between mirror faces; the pyramidality[15] of these mirror faces; or perhaps due to the flatness deviations[16]of the mirror faces.

3.2.5 Angular Calibration of a Precision Polygon

It has already been established in Sect. 3.2.4, that any errors or uncertainties in a precision polygon that are not known (e.g. if the Calibration certificate originally supplied with this artefact has been either lost, or mislaid), then in such circumstances, it is feasible to calibrate this polygon by utilising two autocollimators; the set-up which is typically configured being depicted in Fig. 3.3b. At this time, the polygon's errors are not known, but by employing two autocollimators in an angular configuration to produce reflections from adjacent polygon faces, this enables the errors to be successfully determined. For example, if an eight-sided polygon requires calibration—prior to use—then the two autocollimators are positioned at an included angle of 45° with respect to each other. So, if '$\boldsymbol{R_1}$' and '$\boldsymbol{R_2}$' are the

[15]The influence of **pyramidality** of mirror faces on the accuracy of angular measurement is not clearly defined, although that influence is distinctly present, there is still no unambiguous technique for elimination of these errors.

[16]The effect of **flatness deviation** of the mirror surfaces can be determined, although its influence on the measurements however, cannot be clearly evaluated and as such, these errors are not easily compensated. Moreover, a large number of approaches for reduction of mirror flatness deviation errors exist, but there is still no single unambiguous method that has been suggested. Whilst, deviations of angles between the mirror faces of the precision polygons can be undoubtedly determined, evaluated and quite simply corrected, by suitable measurement data processing.

readings taken on the autocollimators—identified as '**1**' and '**2**', respectively—with '***S***' being the angle between the normals of faces '***A***' and '***B***' and, '***T***' being the angle between these autocollimators, then by simple geometry we get

$$S + R_1 = T + R_2$$

or, alternatively, by transposition

$$S = T + (R_2 - R_1) \tag{i}$$

Therefore, to complete the polygon's geometrical faces for all values of 'S', 'T' and ('$R_2 - R_1$'), by addition, then

$$\sum S = \sum T + \sum (R_2 - R_1)$$

But, the value of '$\sum \boldsymbol{S} = 360°$', therefore

$$360 = \sum T + \sum (R_2 - R_1)$$

So, by dividing through by '***n***', this being the number of sides of the polygon, we get

$$360/n = \sum T/n + \sum (R_2 - R_1)/\mathbf{n}$$

Hence, a complete set of readings '$\sum(\boldsymbol{R_2 - R_1})$' can be established, enabling the value of '***T***' to be determined. Once found, '***T***' can be substituted back into equation (i), for each face, enabling the angle for each of these faces to be simply determined. Now, '360°/n' is the polygon's nominal angle and, '***T***' which is a constant, namely, the angle between the two autocollimators, then

$$\sum T/n = T.\mathbf{360}/n = T + \sum (R_2 - R_1)/n$$

or

$$T = \mathbf{360}/n - \sum (R_2 - R_1)/n$$

thus

$$\begin{aligned} T &= \mathbf{360}^\circ/n - \sum (R_2 - R_1)/\mathbf{n} \\ &= \mathbf{45}^\circ - \mathbf{25}'\mathbf{47.2}''/8 \end{aligned}$$

(i.e. the value of $25'47.2''$ is obtained from Table 3.11)

$$\begin{aligned} &= \mathbf{45}^\circ - \mathbf{3}'\mathbf{13.4}'' \\ S &= T + (R_2 - R_1) \\ &= \mathbf{45}^\circ - \sum (R_2 - R_1)/n + (R_2 - R_1) \end{aligned}$$

therefore

$$\text{Error} = (R_2 - R_1) - 3'13.4''$$

In Table 3.11 and for convenience, these calculations are more normally shown in tabular form as follows:

So, by employing this simple calculation, the precision polygon can be calibrated without due reference to an angular standard, with a remarkably high degree of accuracy and precision. The natural assumption here is that this calculation is based upon the known fact that a circle is a continuous function, namely, whatever the values of the individual polygon's angles, they exactly total to 360°.

3.2.6 Calibration of a Rotary Table

In many CNC machine tools and for some CMM's, they can utilise either an integral table (Fig. 5.20) or an auxiliary rotary table/indexer for either tilting and/or indexing the workpiece—see Fig. 3.7b. Consequently, a rotary table's positioning accuracy becomes an integral part of the machine's system accuracy. An autocollimator when utilised to measure angular errors of rotary tables/indexers will quantify the deviation from the nominal-angle—this being determined by the metrology artefact, which is usually some form of an angular master. Here, the angular master is normally a precision polygon or a very highly accurate index table. Such polygons are normally manufactured with regular angles between adjacent faces, but as can be seen from the previous Sect. 3.2.5, they are not perfectly regular, so a list of angular deviations is usually supplied in the form of a calibration chart. This chart's calibration accuracy and precision is customarily set to: $\geq$0.2 arcseconds.

In order to ensure an exact alignment of the calibrated precision polygon with that of the rotary table to be calibrated, it is the usual metrological practice to precisely locate the polygon on a suitable precision mandrel—see Chap. 1—within the bore of this rotary table, acting as a reference datum. Consequently, the inside diameter centreline is parallel to the polygon's faces and square to the rotary table's base—see Fig. 3.4a (i.e. here depicted utilising a Dual-axis digital autocollimator and an eight-sided precision polygon—to calibrate a rotary table). After an initial alignment with the autocollimator, one of the mirror faces of the polygon is rotated towards the autocollimator and zeroed, then the rotary table readout is also zeroed. During this subsequent inspection/calibration procedure, the rotary table is rotated until its readout is set to the nominal included angle of the adjacent face of the polygon. In this eight-sided polygon's case, 45° increments are necessary for its adjacent face-indexing calibration. Subsequently, the next face is angularly incremented—namely through yet another 45°—to that of the autocollimator, but if this angle is not identical, then the error can be read on the autocollimator. The rotary table must then be rotated to each of its successive polygon faces, until all angular face positions have been inspected, with at zero degrees, this rotary table should have rotated and returned to zero deviation. Of some note, is that the errors in the calibrated precision polygon—see Table 3.1—must be taken into account, when calibrating the angular indexing accuracy of this rotary table.

Table 3.1 Some typical tabulated optically obtained calibration values for a regular eight-sided precision polygons invariably utilised in rotary table verifications, etc.

Polygon faces viewed (°)	R_1		R_2		$(R_2 - R_1)$		Error
	Minutes	Seconds	Minutes	Seconds	Minutes	Seconds	Seconds
0–45	4	32.5	7	48.7	3	16.2	+2.8
45–90	5	15.3	8	33.8	3	18.5	+5.1
90–135	2	17.6	5	29.9	3	12.3	−1.1
135–180	4	52.1	8	07.2	3	15.1	+1.7
180–225	5	03.5	8	10.2	3	06.7	−6.7
225–270	4	22.9	7	41.0	3	18.1	+4.7
270–315	1	16.8	4	25.3	3	08.5	−5.9
315–0	4	18.9	7	30.7	3	11.8	−1.6
	Total: 25′47,2″						

After Galyer and Shotbolt (1990)

An alternative to calibrating with a precision polygon is to employ a suitable calibrated ultraprecision index table—for such rotary table inspection. Here, a typical index table's angular accuracy is just 0.25 arcseconds. As a consequence, a 360º position index table yields 1º resolution—with such index tables being available in any number of positions per revolution. To utilise an ultraprecise index table for rotary table inspection, a plane mirror is situated on the centre of rotation and parallel to this axis of rotation. This index table is suitably aligned in the same manner as described for the previous mentioned precision polygon. Accordingly, during the rotary table's inspection, this table is rotated, say, through an angle of 25º, while the ultraprecision index table is counter rotated, also by 25º. Consequently here, if the plane mirror is not exactly angularly aligned, then this error can be read on the autocollimator and the procedure follows a recognised technique—previously described for this table's overall angular calibration.

3.3 The Micro-optic Dual-Axis Autocollimator, or Angledekkor

The micro-optic dual-axis autocollimator (more often termed and simply known as the Angledekkor) is shown inspecting a constant deviation prism in Fig. 3.8a. This optical instrument is focused at infinity and contains a small illuminated graduated scale in the focal plane of the objective lens (i.e. its collimating lens). This scale, in its normal position, is outside the view of the microscope eyepiece. As a consequence, the illuminated scale is projected as a parallel beam by the collimating lens, which after striking a reflective working surface outside of the instrument is then refocused by the lens in the field of view of the eyepiece. In the field of view

Fig. 3.8 Micro-optic dual-axis autocollimator (courtesy of Spectrum Metrology)

of the microscope, there is another datum scale which is fixed across the centre of a screen and the reflected image of the illuminated scale is received at right angles to this fixed scale and the two scales in this position intersect each other, as depicted

in Fig. 3.8b. Consequently, the reading on the illuminated scale (i.e. its graticule) measures angular deviations from one axis at 90° to the optical axis, while the reading on the fixed datum scale measures the deviation about an axis mutually perpendicular to the other two. Stressing this point still further, any changes in angular position of the reflector in two planes, are indicated by changes in the point of intersection of these two scales. Readings obtained from these scales—with the use of a single micrometre adjustment—are then read to an angular accuracy of $\leq 1'$.

This Angledekkor has its overall optical system enclosed in a tube, which is usually mounted on a special-purpose slotted, fully adjustable angular bracket and located onto its flat integral surface plate—as seen in Fig. 3.8a. It is normal practice for this optical instrument to be supplied with a lapped flat and reflective base—as described—onto which all the objects requiring inspection are then placed, upon this datum surface. Invariably, the Angledekkor is universally employed as an optical comparator. Such an instrument measures by comparing the readings obtained from a known standard, such as either a suitably configured sine bar[17] or by combination angle gauges, the latter that are wrung together to achieve a desired angle—see Fig. 1.8—with that from the workpiece under test. Although the Angledekkor is not as truly accurate and precise as an instrument when compared to that of an actual autocollimator, it has a wider field of view, which is often necessary for the many and varied overall metrological applications undertaken and for general angular measurement.

3.3.1 Optical Squares and Prisms

Optical Squares

Habitually, for most forms of machine alignment in optical calibration work, an optical square has been particularly beneficial in deviating the line-of-sight by 90° from its original path. Many high precision optical instruments, especially, microscopes, autocollimators, angledekkors, etc., can exploit this optical capability.

[17]**Sine bar**: this artefact usually consists of a fully through-hardened, precision-ground body with two precision-ground cylinders fixed at the ends. The distance between the centres of the cylinders is exact—being accurately and precisely controlled—and the top surface of the sine bar is parallel to a line through the centres of the two rollers. It is standard metrological practise, to have the dimension between the two precision rollers chosen to be a whole number—for ease of later calculations—forming the hypotenuse of a triangle when in use. Sizes of these sine bars can range in length—this being determined by the centre distance between the rollers—as described, typically ranging from: 100 to 300 mm, or even greater. When a sine bar is placed on a level surface the flat-top's edge will be parallel to this datum surface. Consequently, if one roller is raised by a known distance, usually utilising say, a pile of Gauge blocks, then the top edge of the bar will be tilted by the same angular amount forming a reliable angle—that may be calculated by the simple application of the trigonometric relationship for sine of this angle, thus: Sin (θ) = Perpendicular/Hypotenuse, where **Perpendicular**—relate to the pile of gauge blocks (mm); **Hypotenuse** is the sine bar length, namely, the centre distance between the actual rollers (mm).

Essentially, an optical square is a pentagonal prism (i.e. a pentaprism[18]). Regardless of the angle at which the incident beam strikes the face of the prism, it is turned through 90° by internal reflection. Unlike a flat mirror, the accuracy and precision of a pentaprism is not affected by the errors present in the mounting arrangement. It is observed that any error in the mounting of the mirror, or in maintaining its base parallel in a fixed reference to the beam, is greatly magnified by the optical lever effect.[19] These two errors in combination may even be greater than the workpiece squareness error. This significant problem is usually overcome by employing an optical square. In the case of the optical path through an optical square, the incident ray is reflected internally from two faces and emerges from the square at exactly 90° to the incident light. This is indeed a remarkable optical property of the square. Furthermore, any slight deviation, or misalignment of the pentaprism does not affect the right angle movement of the light ray. Usually these optical squares are of two distinct types, being

1. **Integral fitting into instruments like telescopes**—wherein an optical square is factory fitted to ensure that the line-of-sight is perpendicular to the vertex;
2. **Supplied with necessary attachments for making adjustments to the line-of-sight**—this flexibility allows optical squares to be utilised in any number of metrological applications in optical metrology.

In Fig. 3.9b, the photograph illustrates the use of an optical square being utilised to test the straightness of both the slideways of the *X*- and *Y*-axes[20] for a highly accurate and precise CNC diamond turning machine tool, with a graphical representation of the measured data and accompanying results, being depicted in Fig. 3.9c. The squareness of the *X*-axis slideway with respect to a *Y*-axis slideway (see Footnote 20), or bed, is of utmost importance in the calibration of machine tools—otherwise significant machined workpiece geometric errors would result. The requirement at this time, for the specific optical configuration of the practical test set-up for straightness measurement being, in this particular case, a photoelectric autocollimator in conjunction with an optical square and a suitably positioned reflector. As a result, it is necessary to take a range of readings, initially with the reflector close by

[18]**Optical pentaprism**: it is normally a five-sided reflecting prism utilised to deviate a beam of light by a constant 90°, even if the entry beam is not at 90° to this prism. Thus, the beam reflects inside the prism twice, allowing the transmission of an image through a right angle without inverting it, or changing the image's handedness, as might be the case if an ordinary right angle prism, or mirror had been employed. So, any reflections inside the prism are not caused by total internal reflection, since the beams are incident at an angle less than the critical angle (i.e. the minimum angle for total internal reflection). Instead, the two faces are coated to provide mirror-like surfaces. Moreover, the two opposite transmitting faces are also often coated with an anti-reflection coating to reduce any spurious reflections. Furthermore, the fifth face of the prism is not employed optically, but truncates what would otherwise be an awkward angle joining the two mirrored faces.

[19]**Optical lever effect**: thus, an optical lever is normally a convenient device that is utilised to magnify a small displacement and in so doing, make possible an accurate measurement of this displacement.

[20]On most turning machine tools, this axis would normally be designated as the *Z*-axis.

(a) Inspecting a Pentagonal Prism using two Autocollimators.

(b) The calibration of a CNC Diamond Turning Lathe with a Photoelectric Autocollimator and a Pentagonal Prism.

(c) Typical graphical plot of machine's axis - for straightness.

Straightness plot:
Minimum value : (X) -2,73 µm (Y) -3,30 µm,
Maximum value : (X) 4,21 µm (Y) 2,91 µm,
Peak-to-Valley: (X) 6,94 µm (Y) 6,20 µm,
Slope: (X) 0,019 mm/m (Y) 0,017 mm/m.
Base length: 125,00 mm
Correction: Least squares

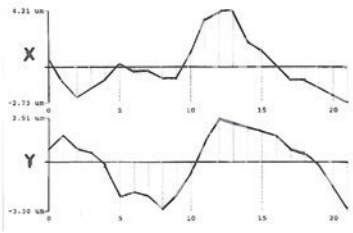

Fig. 3.9 Typical optical inspection and machine tool calibration—by photoelectronic autocollimation (courtesy of Spectrum Metrology)

the autocollimator and finally at the position furthest away—enabling a wide spread of graphical plotted data to be obtained—as shown in Fig. 3.9c. Then the machine can, if necessary, be corrected for any prospective out-of-tolerance slideway errors.

Constant Deviation Prism

A constant deviation prism enables both the projected and reflected beams to be turned through a right angle. It is therefore very suitable in machine alignment testing and checking, to determine whether its two surfaces are at right angles. This optical configuration is also more commonly known as an optical square—see the above comments. Moreover, the special property of this type of prism is that it always reflects a ray of light through the same angle, irrespective of the angle of incidence. In the prism, the reflecting surfaces are inclined at an angle of 45°. In view of that, as the ray is deflected through twice the angle between the reflectors, it will therefore be reflected through 90°. In actuality, the rays bend as they travel from rare-to-dense medium and similarly when exiting, but their optical effect is nullified and finally the beams are exactly at right angles.

Dowell Prism

This Dowell prism is invariably utilised to split up a single beam of light into two distinct beams, which are then exactly parallel but projected in opposite directions. The special feature of such a Dowell prism is that its construction is such that the two projected beams are parallel under any conditions of light transmission. Therefore, no particular setting of this Dowell prism is required when it is employed with, for example an Angledekkor—see Fig. 3.8a, b. This particular Dowell prism is very suitable for testing the parallelism of two faces[21] or surfaces. Since images from two surfaces will be seen simultaneously in the instrument's eyepiece, therefore enabling the error to be measured directly. This arrangement is often employed for use in assessing the axes alignments for the fixed and moving anvil faces, for micrometre callipers—also see Footnote 21.

3.4 Alignment Telescope–Principles of Alignment

Essentially, an alignment telescope—see Fig. 3.10a—having typical encasement of its optics, can also be recognised by some other less common names, such as a Linescope; or a Line-of-sight telescope. However in its basic form, the alignment

[21]**Parallelism of two faces**: here, the light from say the Angledekkor (i.e. shown in Fig. 3.8a), is divided into two parts by reflection at the faces by a Dowell prism (i.e. 90º split prism). So, each light path is directed towards one of the gauging faces—for example in an inspection configuration, thus here, their polished surfaces will act as suitable reflectors. The angle between the reflecting faces of this Dowell prism is precisely 90º, so that the two reflected beams are colinear. Therefore, for example in the case of inspecting a micrometre calliper, the light beams are reflected at the anvil face surfaces and re-enter the Angledekkor after a second reflection from the 90º prism. Consequently, each beam forms a reflected image of the scale and if the moving and fixed anvil faces are parallel, then these images coincide; otherwise the departure from parallelism is readily measured by reading the separation of the images against the fixed scale. Moreover, the squareness of the face of the micrometre spindle to that of the axis of rotation can also be verified, by measuring any displacement of the appropriate image as the spindle is rotated.

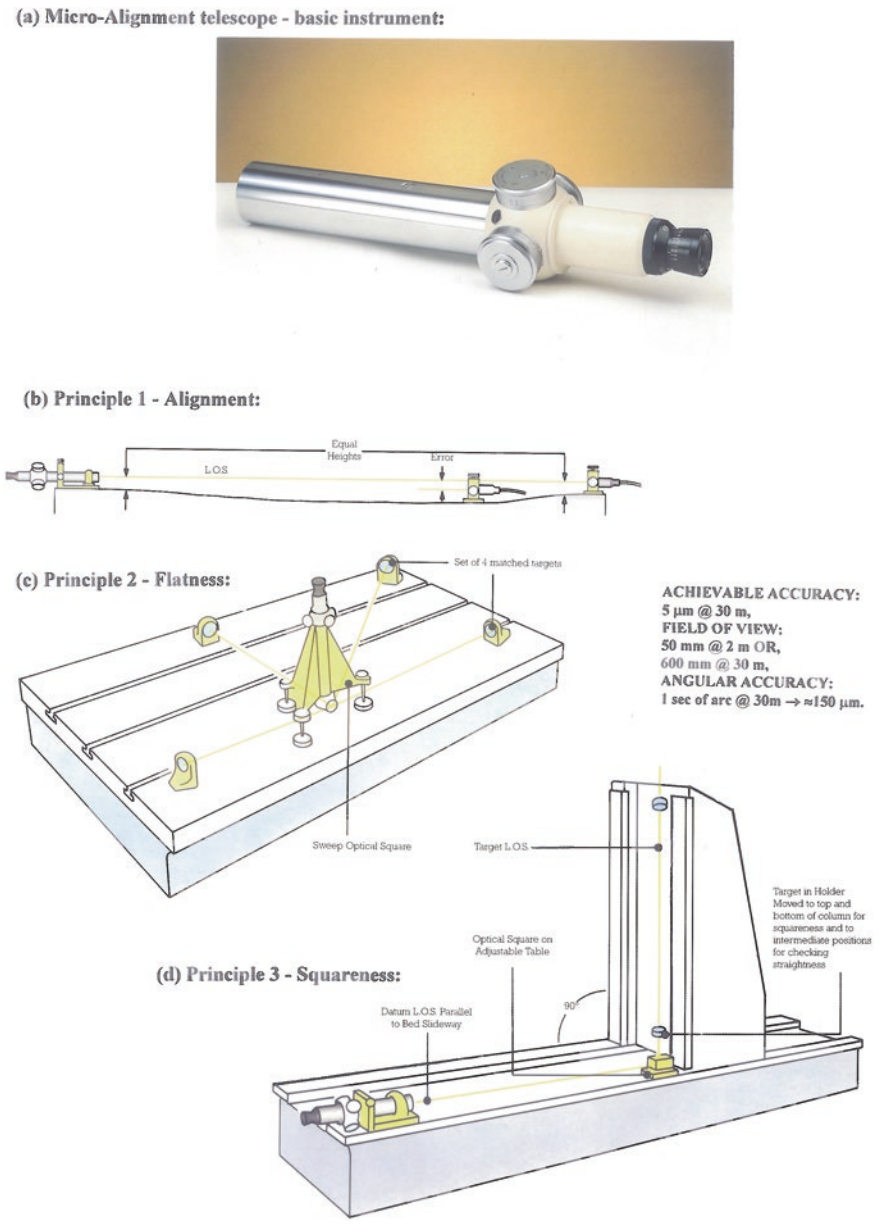

Fig. 3.10 Micro-alignment telescope—showing three of its principle features, for alignments flatness and squareness (courtesy of Spectrum Metrology)

telescope consists of two separate elements, a collimating unit and a focusing telescope; the body of each of which is cylindrically ground to a truly accurate and precise known outside diameter. Accordingly, each of these separate optical units can,

if necessary, be positioned and precisely located for widely spaced bearings and either fitted directly, or alternatively fitted by some precision bushing into these bearings, enabling sightings for basic alignment to be taken directly from the telescope unit to that of the collimating unit. It is customary for the collimating unit to contain the light source and condensers, in front of which is positioned a gracticle in the focal plane of the collimating lens—see Figs. 3.12 and 3.13 for views through the eyepiece of a standard circular auto-reflection target (i.e. as depicted in greater detail in Fig. 3.13a). The eyepiece within the telescope's body gives the principle means of magnification, ranging—for this instrument—from a standard ×34 magnification to an alternative higher ×43 magnification, although this latter eyepiece should only be utilised at lines-of-sight lengths of ≤6 m. Two micrometre drums are situated within the telescope unit—Fig. 3.10a—with the thimble being graduated with intervals of 0.02 mm—situated either side of the zero position and being click-stop adjustable. These two micrometre drums are set at 180° apart and when the alignment telescope is mounted—see Figs. 3.12 and 3.13—the focusing knob is normally positioned at 45° to the vertical (i.e. viewed from the eyepiece end—Fig. 3.11b). In this telescope orientation, the left-hand drum controls the movement of the line-of-sight in a horizontal plane, while the right-hand drum controls the movement in the vertical plane.[22] The movement of these micrometre drums is parallel to the direction of the cross-wires/-lines. For ease of use, these micrometre graduations are usually marked in red on one side of the zero, with black markings on the other side. This useful convenient colour arrangement enables the inspector to easily distinguish the two micrometre movement directions more readily, without introducing a need for a directional sense relative to the actual target.

LURD convention—for target directions when using alignment telescopes

In order to eliminate any inspector confusion in alignment telescope usage, one of the major telescope manufacturers has suggested the use of the LURD convention for all types of optical measurements, but specifically when utilising auto-reflection measurement—when recording, or writing down the micrometre readings. Accordingly, with the cross-lines vertical and horizontal with respect to the observer, having the left hand (upper) with the right hand (lower), the cross-lines being referenced here, so that the letters refer to: '***L***', '***U***', '***R***' and '***D***' (i.e. namely: ***L***eft, ***U***p, ***R***ight and ***D***own), respectively. By employing this simple, but logical LURD convention, then the following six basic orientation rules apply to the lignment telescope's usage:

1. a reading of the vertical micrometre must be preceded by either '***U***', or '***D***'—according to whether the target is either high, or low;
2. a reading of the horizontal micrometre must be preceded by either '***R***', or '***L***'—according to whether the target is to the right, or left of the centre;

[22]**Alignment telescope—micrometre adjustment**: with some care, the Operator/Inspector/Metrologist should be capable of obtaining repeat readings to within $^1/_5$ of a graduated micrometre drum division, namely, 0.004 mm (i.e. 4 μm)—on an aligned target being situated ≤3 m away.

Fig. 3.11 Micro-alignment telescope—indicating just some of the equipment shown currently available—for checking and setting straightness, alignment, vertically, parallelism, squareness and level (courtesy of Spectrum Metrology)

3. a zero reading can be preceded by either of the two letters indicating the direction of the cross-line[23];
4. it follows that neither '***U***' and '***D***', nor '***L***' and '***R***' can be utilised together, as such a combination will create an error;

[23]Exceptionally, a central position can be referred to merely as: '**0**;**0**'.

5. to ensure that this convention is unambiguous, the position of the telescope must be stated at the outset of the inspection/calibration procedure. For example, on say, a turning centre, one must state that the telescope is positioned at the tailstock end;
6. in addition, when vertical lines-of-sight are utilised, the position of one of the cross-lines: '***L***', '***U***', '***R***' and '***D***'; must be specified relative to the machine's orientation.

Alignment Telescope—general usage

As has been previously described above, the application of these alignment telescopes are invariably employed to establish and maintain the principal optical reference lines—when either undertaking periodic calibration, or during the initial installation of machines. Moreover, these reference lines can also be utilised by other instruments for a variety of alignment functions, characteristically to turn right angles from a reference line, or they may simply be employed as measurement references themselves—for example in a large engine bore's bearing straightness evaluation. In addition, such telescopes can generally provide all the important functions of: collimation/autocollimation as well as auto-reflection—see Sect. 3.4.2 for more details of these functions. An alignment telescope can be considered as an optical ruler with objects such as machines and instruments that are being aligned along a reference line (i.e. line-of-sight) then being metrologically assessed, with significantly higher accuracy and precision. As a consequence, the alignment telescope establishes precise reference lines-of-sight—see Fig. 3.10b. The telescope's focusing range has been mentioned and will range from zero to infinity. Here, the telescope's line-of-sight is the basic reference for all measurements, with the exact location of it being relative to the workpiece/machine, and must be known with great accuracy and precision. Of some note, is that with the aid of an alignment telescope it is only possible to observe the lateral displacement of a target, but *not* its angular displacement.

One of the main characteristics of an alignment telescope is that it is set to a finite range, while not emitting a parallel light beam (i.e. only at infinity will the outgoing beam be parallel).[24] A lateral displacement of the target(s) will be

[24]**Field of view**: this can be considered as the largest diameter that can be viewed through the alignment telescope and as such, will increase with the distance from the telescope. Some typical distance values for such telescopes are provided below:

Distance from telescope (m)	*Field of view* (mm)
0.3	18
3	74
15	320
30	600

NB The maximum distance between two objects while both remain in focus, is termed as its depth of field.*

observed with the aid of the alignment telescope. The effect of such a precise lateral displacement can be evaluated when viewing through the eyepiece of the telescope. In this configuration, both the centre intersection of the target and of the telescope's reticle will appear displaced. The target has no lateral displacement if the centre intersection point of the target and the centre of the crosshair reticle of the telescope coincide.

There are quite a wide range of basic measurement and optical principles available with these micro-alignment telescope systems, these include: (i) alignment/straightness—see Figs. 3.10b and 3.21a; (ii) flatness—see Figs. 3.10c and 3.21b; (iii) squareness/verticality—see Fig. 3.10d; (iv) parallelism—see Fig. 3.5; (v) as well as autocollimation; (vi) together with auto-reflection. Accordingly, as previously mentioned, the micro-alignment telescope generates a straight line-of-sight ranging from zero to infinity. This line-of-sight ability forms the basic reference from which all current measurements are taken. For example, to measure a machine tool's squareness a pentaprism (i.e. with an optical square mounted onto an adjustable table—see Fig. 3.10d) is utilised to deviate the straight line through exactly 90°. Of note, is that a similar configuration, but here, employing a rotating pentaprism (i.e. sweep optical square—see Fig. 3.10c) is utilised to generate a plane for the assessment of flatness measurement.

Alignment telescopes are designed to allow **autocollimation** and auto-reflection and as a consequence provide squareness and angular measurement utilising reflective mirror targets—see Figs. 3.12 and 3.13. Consequently, these micro-alignment telescopes, can be satisfactorily employed to set, check and verify a range of machine-based features, not least of which are typically alignment, squareness, straightness, flatness, parallelism, verticality, as well as for level. With its wide range of accessories—just some of which are depicted in Figs. 3.10, 3.11, 3.18 and 3.19—these micro-alignment telescopes form a unique and comprehensive system for establishing and solving alignment problems in a wide variety of machine and other associated metrological applications. As a result, a representative micro-alignment telescope system offers the following advantages when either inspecting or calibrating machines:

- **optical and mechanical axes alignment**—to $\leq$3 arcseconds and concentric within 6 μm;

Footnote 24 (continued)

*Hyperfocal distance—in both optics and photography: this is a distance beyond which all objects can be brought into an acceptable focus. There are two commonly utilised definitions, leading to values that differ only slightly, accordingly, the hyperfocal distance is the

1. closest distance at which a lens can be focused while keeping objects at infinity acceptably sharp. When the lens is focused at this distance, all objects at distances from half of the hyperfocal distance out to infinity will be acceptably sharp;
2. distance beyond which all objects are acceptably sharp, for a lens focused at infinity.

The distinction between the two meanings is rarely made, since they have almost identical values. The value computed according to the first definition exceeds that from the second, by just one focal length. Thus, the hyperfocal distance is the focus distance giving the maximum depth of field.

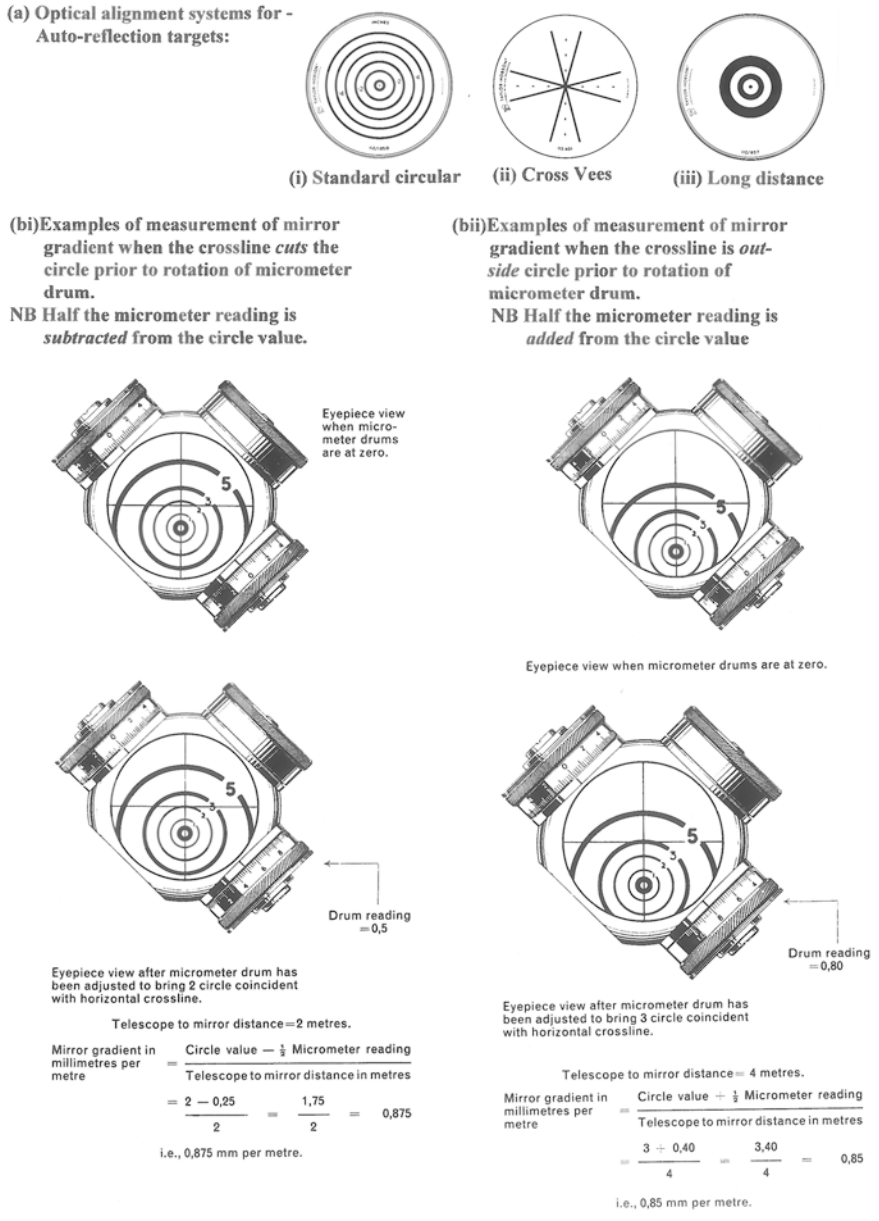

Fig. 3.12 Typical optical targets and the effect of readings taken within the eyepiece (courtesy of Spectrum Metrology)

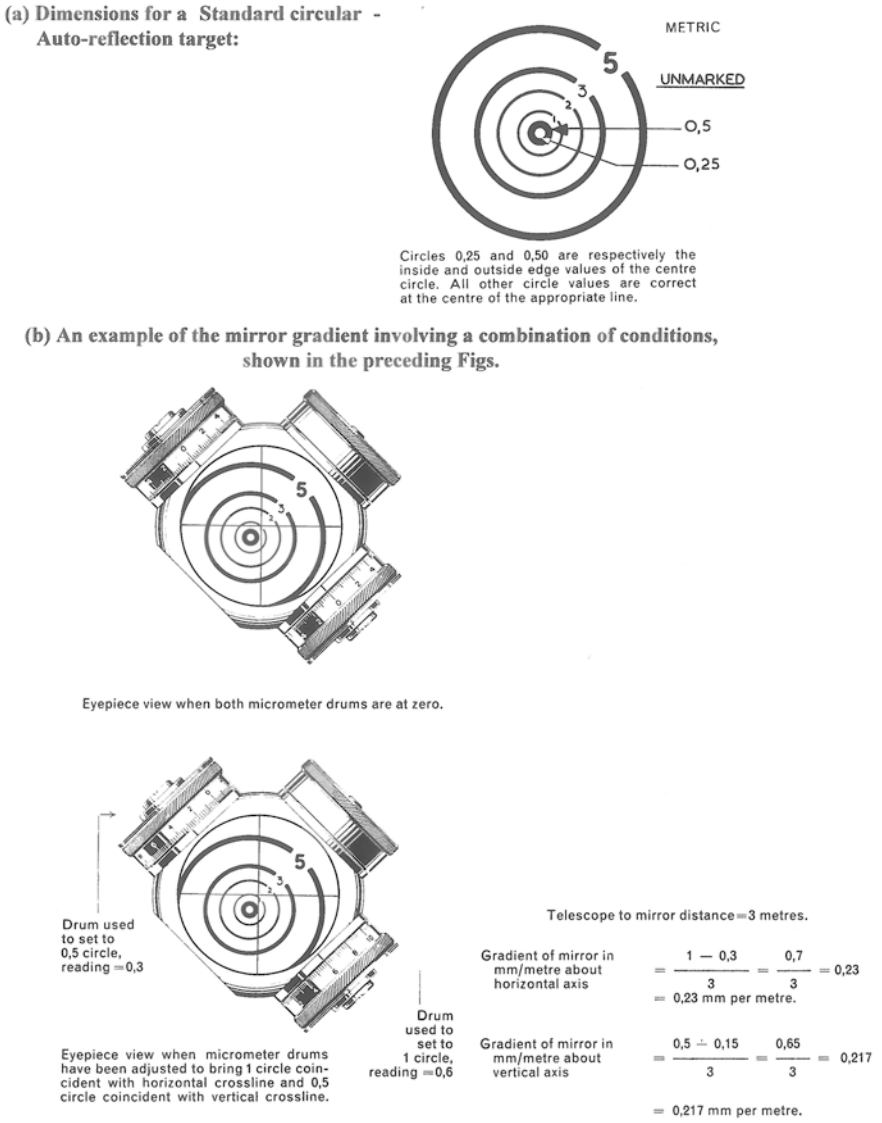

Fig. 3.13 Auto-reflection target dimensions and an example of a typical combination error (courtesy of Spectrum Metrology)

- **having an achievable accuracy and precision**—to ≤0.05 mm at 30 m;
- **having an extensive field of view of**—which ranges from 50 mm at 2 m or 600 mm at 30 m.

Although in this brief discussion one is principally concerned with machine and instrument calibration, a range of other optical applications for which the micro-alignment telescope can be satisfactorily employed are both wide and varied, which

this might include just some of the following: bore alignment inspection[25]—for main bearing alignment of large engines; turbine installation and maintenance; flatness checking and setting of bed plates—see Fig. 3.10c; weapon systems alignment and harmonisation; alignment of rollers of process machinery; aircraft jig setting and control; compressor installation and its maintenance; railway equipment assembly and set-up; shipbuilding repair and its maintenance; Earthmoving machinery and for general equipment alignment; plus portable machining system set-up and monitoring. For these diverse industrial and metrological applications, the micro-alignment telescope has now been shown with the ability to focus from zero to infinity, incorporating optical micrometres to measure deviations from an optical line-of-sight —in two directions and at right angles to each other.

Digital CCD system for micro-alignment telescope

In order to enhance either the inspector's, or operator's ease-of-usage of these types of telescopes, a digital CCD system can be connected to any of the alignment telescopes—see Fig. 3.11c. Such complete systems can be purchased with a new telescope, or as an accessory upgrade for existing micro-alignment telescopes when in use in the field. This system enhancement of an alignment telescope offers the following distinct advantages:

- **a clear digital output of both the *X*- and *Y*-axes**—thus minimising any potential operator error;
- **a graphical output**—which is also possible for professional reporting of results and storage of measurements;
- **consistent and repeatability of measurement**—which is also provided by this digital CCD system;
- **production of rapid calculation of results**—for quick-and-easy assessment of any measurements taken;
- **the system is ideal for automatic remote monitoring**—with measurement time interval input being controlled and adjusted by the inspector/operator;
- **the system offers typical accuracies of 5 μm up to 3 m**—which proportionally increases with respective distances, to that of 50 μm over 30 m.

This high-resolution CCD system with bespoke software has the ability to automatically sense the centre position of the targets, then calculates the displacement from

[25]**Bore alignment inspection**: so when the requirement is to refurbish say, a large diesel engine, it is important that the engine bores and the machining system are truly in-line before any boring operations commence. First, the engine bores are aligned—with any potential misalignment being viewed directly by the operator—making the adjustments by viewing with its digital CCD system by a CCTV camera, which is attached to the micro-alignment telescope's eyepiece. This type of sophisticated instrumentation set-up, not only eliminates the need for both a telescope operator and that of say, a second engineer—to adjust the bores—but it also means that in practice, the operator can make adjustments viewing directly any changes that must be made. Once all the bores are shown to be in-line with the micro-alignment telescope, this telescope is then left in situ, whilst the horizontal boring machine tool moves (i.e. is fed along the respective bores) and then subsequently bores along the same line for subsequent accurate/precision machining.

a set datum—ensuring a fast set-up time with repeatable readings, as well as digitally outputting the result. This latter characteristic of the system is particularly useful on large alignment projects such as for enormous machine tools, since a single operator can take measurements and adjustments along the machine tool's constructional elements, while the target is displayed on the monitor. As a consequence, the target readings are recorded along the large machine component element and can then be output as a graph/results table, or saved for further data analysis at a later time. Typically, the analysis of the results can offer advice on the necessary precise and accurate adjustment of the verification of the component under consideration to either ensure it is correct, or to bring it back into line quickly, while any distance measurements can also be obtained to within the accuracy/precision of just a few miniscule fractions of a millimetre. For convenience of use, the digital CCD system can be simply connected to a PC, laptop, or a tablet PC. In the current specification of the digital CCD system, it includes a normal operating range of between: 1 and 30 m; repetition of ≥2 μm accuracy; displacement using one target ≥2 % of displacement, or 5 μm—whichever is the greater; displacement using two targets ≥4 % of displacement, or 10 μm—whichever is the greater. Moreover, the distance measurement accuracy is 20 mm from 0 to 10 m, 25 mm from 10 to 20 m, and 30 mm from 20 to 30 m, with typical targets being standard, short and long range, plus virtual (i.e. see-through) targets, which are also normally available.

If a CCTV camera is also incorporated into the above digital CCD system, it provides just some of the following accompanying benefits: it will minimise eye fatigue; while eliminating any parallax error[26]; being easier and a more practical setting/adjustment of work by viewing from a monitor; enables a more comfortable viewing position of awkward measurement locations through the monitor; together with enabling the use of a high magnification lens—as a consequence of improving setting resolution. Furthermore, a miniature CCTV camera can also be fitted to the telescope eyepiece, to remotely view the target when working, for example, in particularly difficult or potential hostile locations. By viewing the target image on the monitor, any potential parallax problem is eliminated and the actual set-up can be completed more speedily, allowing the operator to adjust the machine tool, targets or fixtures, that may require adjustment/setting, without having to return to the telescope each time or perhaps rely on a second operator for their advice and directions. Moreover, this miniature CCTV camera can also allow a number of inspectors to observe the target image simultaneously, or alternatively, one inspector can view a series of connected telescopes—where applicable.

Further accessories—that have been briefly and previously mentioned—can augment the overall usage and performance of many types of these micro-alignment telescopes, in particular some of these useful additions for their enhancement can include a

[26]**Parallax error**: this is a displacement, or difference in the apparent position of an object viewed along two different lines-of-sight. It is measured by the angle, or semi-angle of inclination between those two lines. The term parallax as having been previously described, is a word derived from the Greek language parallaxis—meaning alteration. Consequently, any nearby objects will have a larger parallax than more distant objects—when observed from different positions—so this parallax effect can be utilised to determine distances.

- **right-angle eyepiece adaptor** (i.e. see Fig. 3.11b)—this 90º adapter enables the telescope to be viewed at right angles to the line-of-sight. It is especially useful where perhaps the space may be limited/cramped, or the sighting position would otherwise be inconvenient;
- **mounting telescope adjusting bracket** (i.e. see Figs. 3.11a, b)—this complementary precision bracket provides a fine azimuth and elevation adjustment for sighting the telescope, often employed in conjunction with a horizontal base, or a bore fixture;
- **plain cup** (i.e. see Figs. 3.11d, e)—it locates the mounting sphere on the horizontal base with its centre being exactly 76 mm from the base of the cup fixture—this spherical bearing ensures that the line-of-sight always passes through the centre of the sphere thereby giving a constant datum height;
- **setting the horizontal line**—for flatness/level incorporating a Talyvel 6 (Fig. 3.18a); or with Stride Base[27] (i.e. see Fig. 3.19b), or alternatively today this might be undertaken using wireless electronic level[28]—thus, by means of this Stride Base, a Talyvel can be mounted on the telescope barrel for accurate and precise setting horizontal lines-of-sight—see Fig. 3.18a;
- **Optical squares** (i.e. see Fig. 3.11e)—these squares are utilised to deviate the telescope's line-of-sight precisely by 90° within 1 arcsecond (i.e. ≈5 μm m^{-1}). Here, the 102 mm offset square is mounted on the barrel of the telescope. It can be rotated with the telescope, invariably where it is utilised to sweep out planes perpendicular to the telescope's reference line-of-sight. The square has a through-sighting facility, enabling the reference target to be viewed at all times;
- **alignment targets** (i.e. see Figs. 3.12 and 3.13)—these are parallel to ≤20 arcseconds which are normally used, but targets having a parallelism ≤2 arcseconds are also available as intermediate targets for through-sighting, thus, minimising possible sighting refraction errors.[29] Mirror targets are also utilised, when both alignment and squareness are checked concurrently, using either auto-reflection, or autocollimation.

[27]**Stride Base/Level**: it is normally utilised for establishing horizontal lines-of-sight, this is a precision level that is mounted directly on the telescope barrel—see Fig. 3.18a. Typical accuracies of ≤5 arcseconds are readily obtainable. NB A more detailed description of this Stride Level usage is given later in this chapter.

[28]**Talyvel 6 Wireless Electronic Precision Level**—see Fig. 3.20: is a proprietary instrument produced by a leading metrology instrument manufacturer. This Talyvel is a pendulum-transducer-type electronic level, which provides a digital reading in angular measurement, or as a gradient. Typical Talyvel accuracy setting is to: ≤0.2 arcsecond, or namely, 1 μm m^{-1}. NB A detailed description of this electronic level is given later in this chapter.

[29]Refraction errors: this is an error in the focusing of light by the eye and can be a frequent reason for reduced visual acuity. NB That one's eye that has *no* refractive error when viewing distant objects and as a result, it is said to have either emmetropia, or to be emmetropic—meaning the eye is in a state in which it can focus parallel rays of light (i.e. any light from distant objects) on the retina, without using any accommodation. Accordingly, a distant object in this case, is defined as an object being at 6 m away, or even further from the eye.

3.4.1 Targets for Autocollimators

A wide range of calibrated target types are available for use with a variety of autocollimators and their specific metrological usage; typically those shown in Figs. 3.12a and 3.13a are just a small sample of the types currently available. Notably, the standard target is normally utilised up to a distance of ≈30 m (i.e. Fig. 3.12ai) although it can be changed for other types, typically having either cross-vees (i.e. Fig. 3.12aii). Yet another type of target for even longer distance usage can be employed, this alternative fitment is necessary at great distance, where the standard concentric distance rings' will appear somewhat indistinct—so they are replaced by a more pronounced series of concentric target rings, as shown in Fig. 3.12aiii. The application of scales as targets[30] can also be quite effective for some inspection/verification procedures—in association with autocollimators. Of note, is that any intermediate target must of necessity, be visually transparent. Invariably, when a datum target is necessary in the inspection/calibration procedure, it is normal practice to employ a target illuminator, with obviously any additional intermediate target(s) which must also be transparent.

In principle, there are two general cases where the application of an alignment telescope is utilised, they both involve the ability to create a line-of-sight with this target, such that

1. **an intermediate target is used in conjunction with a datum target**—such as when the suitable bushed alignment telescope is employed for bore alignment of a large diesel engine—see Footnote 21—in this chapter. Here, at one extreme of the engine's casting, the bushed telescope is positioned in the bore, while at the other end the reflective datum target is situated. The transparent intermediate target can then be moved from the next adjacent bore by this datum target, then its readings recorded, with subsequent bore positions being further recorded as this intermediate target is moved successively and progressively towards the telescope's position, thus completing the inspection sequence. Yet another example of this multiple target arrangement is when inspecting a long bed turning centre/CNC lathe with an alignment telescope. Here, an accurate and precise line-of-sight has to be established along the machine's centre of rotation. By placing the instrument outside the machine,

[30]**Scales as targets**: although the special targets previously described have many advantages, there are particular applications in which a simple repeatable reference zero is all that is necessary. Under such circumstances, a scale can—with certain precautions—be utilised. Here, the scale should be *printed* onto *a flat surface*, but *not* either etched, or embossed into the scale. The specific reason for this printed scale is that the position of recessed marks appear to change with the angle of illumination. Moreover, this scale must be set parallel to one of the cross-lines. Furthermore, when this scale is initially viewed through the telescope, it may appear slightly tilted, hence, it must be accurately repositioned (e.g. marginally rotated) until it appears parallel to a cross-line. Of note, is that the scale's graduations can then be subdivided for greater accuracy and precision by the in situ micrometres.

this alignment telescope being positioned on a suitable adjustable tripod, then accurately situating a collimating target in the headstock, with a transparent intermediate target attached to say, the programmable cross-slide. This intermediate target is then CNC programmed to progressively travel along the bedway, gathering recorded data positional information as it successively moves from one stroke length end to the other (i.e. from, say, the headstock to the tailstock's end). If the tailstock—when it is fitted—cannot be easily removed it must remain in situ, then it is possible with suitable accessories, to locate the axis of the alignment telescope within this tailstock's bore;

2. **the instrumental arrangement is normally where only one target is used**—see Figs. 3.10b and 3.21a. Here, the reflective target is proportionally progressed along the intended line-of-sight—towards that of the alignment telescope, measuring both the deviations from straightness, and the consequent vertical displacements.

It should now have been comprehended that mounting these targets in association with the telescope, is a vitally important activity, as the location and orientation of this target with respect to the machine/workpiece/object must be critically known with some considerable accuracy and precision. Accordingly, a range of target-mounting accessories are currently available to assist in this inspection/verification operation. Yet another important criteria to consider when setting up this type of instrumental configuration, is the method of illuminating the target. If insufficient target illumination or alternatively too much glare occurs, these effects could interfere with the overall precision to which the inspector/operator can work, while additionally being somewhat tiring to this person in service.

3.4.2 Auto-reflection and Autocollimation

Auto-reflection

The various highly accurate and precise optical instruments previously mentioned, such as the autocollimators and alignment telescopes, can both be employed for auto-reflection. Auto-reflection refers to the principle that the image of an object seen in the mirror appears on the opposite side of this mirror, but equidistant from it and at a position in which the line joining the image and the object is normal to the mirror. Therefore when a telescope is utilised for auto-reflection, the object is the illuminated target (i.e. a typical auto-reflection target is like the one shown in Fig. 3.13a) on the cover glass of the telescope. Consequently, as the mirror is tilted with respect to this telescope's line-of-sight —similar to that depicted in Fig. 3.21a—the image of the target appears offset from the cross-lines (i.e. see Fig. 3.13b). Accordingly, as the mirror is rotated anticlockwise the image of the target moves towards the cross-lines until the mirror is normal to the line-of-sight. In this condition the target image will be shown to be centred on the cross-lines. Therefore, auto-reflection provides a

measurement technique for setting either squareness[31] (i.e. a typical configuration is depicted in Fig. 3.10d) or when measuring small gradients of tilt (i.e. similar to that shown in Fig. 3.21a).

So that the target is visible to the user, it must be illuminated by the insertion of a light source into the telescope—with a specially designed small lamphouse. This lamphouse is configured with a partially reflecting mirror, allowing the target to be illuminated from within the telescope, but without obscuring the line-of-sight through the telescope. This mirror can be either a plain surface-metallised mirror, or simply a mirror target. Of note, is that if the latter (i.e. the mirror target) is used, any ensuing displacements from the line-of-sight can be measured in the normal manner. The accuracy of the auto-reflection technique will depend among other factors such as the concentricity of the cover glass target, which has a tolerance of 0.025 mm.

Autocollimation

With optical instruments using the autocollimation technique, the setting or checking of a machine's squareness (i.e. shown in Fig. 3.10d) will utilise a lamphouse to illuminate the cross-lines, with the telescope being focused to infinity. Accordingly, from this telescope the rays of light are collimated (i.e. they are made parallel) and are successively reflected back along their own path from a mirror set square to this line-of-sight, forming a reverse image of the cross-lines, on the actual original cross-lines. A specific feature of the cross-line patterns is two pairs of short heavy lines—not shown—which produce a bold reverse image for precise setting. In consequence, if the mirror is slightly tilted, this cross-line image will be displaced. It is worth re-emphasising the point that when the telescope is focused at infinity the micrometres are then ineffective; thus they cannot be employed in the measurement process, hence, no graticule, or target—other than the cross-lines—are utilised for autocollimation. This means that the technique can only be employed to set an object for squareness, but not for its actual tilt, as this latter condition can be undertaken indirectly.

Due to the fact that the telescope cover glass is not used for autocollimation—this being a significant error source namely that of the cover glass tolerance,

[31]**Squaring-on reflector**: when either setting for squareness by that of auto-reflection, or autocollimation, the telescope target image cannot be seen in the eyepiece, until the mirror has been adjusted square to this telescope's axis: within ≈2.5 mm/300 mm. At distances up to 3 m, initial rough settings can be undertaken by open sighting using the telescope—with the naked eye. This operation can be achieved by the inspector/operator having their head in close proximity to that of the telescope, by looking along it to see the illuminated target image, thus enabling this image to be seen in the mirror. Although at increased distance, this technique becomes more difficult to accomplish, especially when a surrounding machine casting/framework might obstruct/obscure the field of view. Consequently, the squaring-on reflector (i.e. not shown) has been designed to assist in the preliminary setting of the object under test, by approximately enabling it to be squared to that of the line-of-sight from the telescope. Thus, now when the telescope is utilised for fine setting, the target image will be positioned within the field of view.

which is negated—and, as a consequence, autocollimation is capable of a slightly improved accuracy/precision to that of auto-reflection—specifically at distance of $\leq$1.5 m.

3.4.3 Calculating Mirror Gradients

When attempting to calculate the mirror gradients, the circular markings on the cover glass target (i.e. see Fig. 3.13a) correspond directly with the gradients of a tilted mirror (i.e. typically shown in Fig. 3.21a). Optical instrument manufacturers offer both imperial and metric units with such targets, with the latter indicating these gradients in millimetres per metre—if the mirror is positioned one metre from the telescope. Of particular note is that the inner and outer edges of the inner ring (i.e. shown in Fig. 3.13a) are calibrated positions, while the other values apply at the centre of the corresponding ring. The gradients at other mirror-to-telescope distances are proportional. Therefore, the

$$\textbf{Mirror gradient}\left(\text{mm m}^{-1}\right) = \textbf{circle value}/\textbf{telescope} - \textbf{to} - \textbf{mirror distance}(\text{m})$$

Typical schematic examples of these mirror gradients are illustrated in Figs. 3.12 and 3.13. So, in cases where the target circle or centre dot does not coincide with the cross-line, the telescope micrometre can be utilised in conjunction with the target to measure the gradient. Here, the appropriate micrometre drum is rotated—bringing the nearest circle (or alternatively if this displacement is slight, the pattern centre) onto the cross-line. Half the micrometre drum reading is either added to, or subtracted from, this circle value. The rule for either adding or subtracting values, can be established as follows, if the

1. cross-line *cuts* the circle prior to rotation of the micrometre drum, *subtract* the halved reading for the outside circle;
2. cross-line is *outside* the circle prior to rotation of the micrometre drum, *add* the halved reading to the circle value.

The tilt direction can be established by noting in which direction the target image is displaced, thus the edge of the mirror is then nearest to the telescope. In consequence, in Fig. 3.12 (bottom left/right diagrams) the mirror is inclined forward towards the telescope. This enables the LURD convention (i.e. see previous Sect. 3.4) to be applied to gradients. So, for example with the cross-lines vertical and horizontal, having a gradient of $\approx$R0.4 mm/300 mm, this would indicate that the mirror was tilted this amount with respect to the line-of-sight, with part of the mirror to the right of the line-of-sight—lying closer to the telescope. As a result, in order that the gradients measured and recorded in this manner are significant, the cross-lines must be visibly aligned with a known direction, such as the edge of the current object under scrutiny.

3.4.4 Effects of the Earth's Curvature and Atmospheric Refraction

Earth's curvature

In reality and based upon the human scale of measurement, the effective radius of the Earth's curvature can be considered as exceedingly small; this becomes to some extent more noticeable over much longer linear distances, especially when a line-of-sight configuration with the telescope is compared with a level surface set-up by a gravity-controlled instrument—like either a basic water level, or a simple plumb line. The intended length of surface set by reference to a level is curved (i.e. see Fig. 3.14a). As a consequence and metaphorically speaking, if a perfectly round sphere was placed on this curved surface, the sphere would not roll—because of the gravitational force that is acting upon it vertically at all points—likewise, a bubble level (i.e. see Sect. 3.5) at any position will indicate zero tilt. Then again, if this same surface is scrutinised with the telescope, any targets set at a varying range of distances will indicate that this surface is indeed, not flat.

Atmospheric refraction

In practice, the line-of-sight deviates from a straight line owing to refraction within the same atmosphere. It is well known that light travels in a straight line[32] through a medium of constant density. This statement is essentially valid in both theory and practise, although in practise there is normally some form of a density gradient in the atmosphere resulting from differential heating/cooling of the layers of air at varying heights above the Earth's surface. This will result in the bending of light rays—termed refraction—with an extreme example of this effect being seen in the formation of a mirage.[33] Of some importance is when the change in density is gradual whilst remaining constant, the line-of-sight through the atmosphere is a smooth curve and hence, with a target which appears to be at '**A**'—see Fig. 3.14a, it is actually located at '**B**'. So, if the heating or cooling effect fluctuates rapidly, the radius of curvature changes and the position of the target will appear to vary slightly. As a result, both of these effects of constant curvature due to a steady temperature gradient and the shimmer effect due to rapidly fluctuating

[32]**Light travelling in a straight line**: because this is due to the well-known path-of-least-resistance phenomena. This fact allows light to travel in a path which will make it travel this distance in the shortest time. Previously, this light's path was first postulated by the ancient Greek scientist: Euclid—in the year ≈300 BC. Moreover, it is obviously true that close to a massive object the light may appear to bend, but this is simply because '…mass-bends-space…'—although paradoxically, a straight line through curved space is still a straight line! So, the reason that light travels in a straight line is because a straight line is actually defined as the path taken by a beam of light.

[33]**Mirage**: this is a naturally occurring optical phenomenon in which light rays are bent to produce a displaced shimmering image of distant objects—such as often occurring on the horizon—in the heat of a desert, or perhaps when it is low in the sky. The word is derived from the French mirage, taken from the Latin language for mirari, meaning: 'To look at, to wonder at'. Of a somewhat diversionary note, is that this is the same language root, is where one can obtain both the terms for a: mirror, as well as for that of: to admire!.

(a) The influence of the Earth's curvature and atmospheric refraction on the Telescope's line-of-sight (L.O.S.), where:
DC is the shape of a surface set by gravity;
DA is the L.O.S. established by a Telescope at *D* in air - of constant density, or in a vacuum;
DB is the L.O.S. from a Telescope at *D* through air - having a constant vertical temperature gradient.

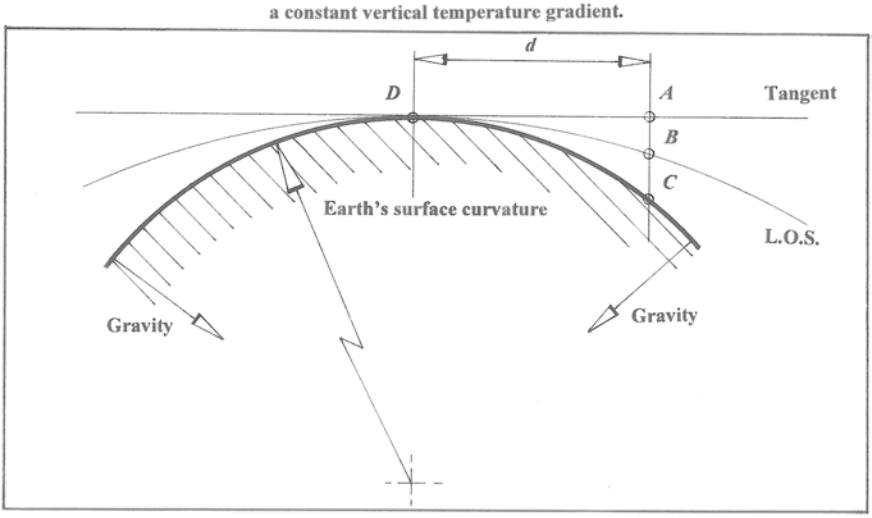

(b) Table of corrections for the curvature of the Earth and atmospheric refraction - in millimetres:

Distance *d* (in metres):	1 *AC*	2 *AB* (in millimetres)	3 *BC*
2.5	0.00056	0.000075	0.00049
5	0.0023	0.00030	0.0020
10	0.0090	0.0012	0.0078
25	0.056	0.0074	0.049
50	0.23	0.030	0.20
75	0.51	0.067	0.44
100	0.90	0.12	0.78

Fig. 3.14 The effect of both the curvature of the Earth and atmospheric refraction on telescope readings (courtesy of Spectrum Metrology)

air densities will seem to disappear when there is no temperature gradient across the line-of-sight, or if this line-of-sight is present in a vacuum.

The deviation of a level surface from the truly straight tangent to the Earth's surface is virtually constant and can be calculated. Accordingly, the deviation of a line-of-sight due to refraction in the atmosphere may be liable to vary with atmospheric conditions and as a consequence, only average values can be given. In Fig. 3.14b, a simple table of corrections for these values of deviations is given,

relating to differing linear distances (‘**d**’). **Column 1**—deviation of a line set by a gravity-controlled instrument, from a truly straight tangent to the Earth’s surface (i.e. ‘**AC**’ in Fig. 3.14a)—this can be regarded as accurate;**Column 2**—deviation of a line set by a telescope from the tangent (i.e. ‘**AB**’ in Fig. 3.14a)—this is subject to variation and here, only mean values are given;**Column 3**—deviation of a line set by a gravity-controlled instrument from the line-of-sight set by the telescope (i.e. ‘**BC**’ in Fig. 3.14a)—this is subject to variation and here, only mean values can be given.NB The values given in Column 3 are of the most practical importance, although if they are small, they can be neglected, otherwise they should be applied.

Protecting the line-of-sight

In essence, the telescope’s optical line-of-sight alignment must be protected against the following interferences:

- **currents of either hot or cold air**—here, the temperature gradients across the line-of-sight can cause refraction, or bending of a light beam, or alternatively currents of air at different temperatures will cause the image to shimmer—making it difficult to obtain an accurate measurement;

NB The effect of temperature gradients across the line-of-sight can be minimised if the actual cause can be found, such as that emanating from the heat from radiators; doors/windows open; ceiling fans operating; while in conditions of a slight shimmer, normally apparent over a much greater distance, then here, a perhaps long-distance target (i.e. one with a thicker and more pronounced pattern—Fig. 3.12aiii) may be helpful in such circumstances.

- **stray light**—this could enter the telescope reducing the contrast and making sighting more difficult to achieve;

NB This stray light effect can be minimised by painting the edge of apertures through which the line-of-sight passes dull black; by turning-off or shielding any bright lights that may inadvertently shine into the telescope it will also help; furthermore, by also shielding the telescope against the direct rays of the Sun, this can lessen these stray light effects.

- **obstructions**—a telescope should ideally receive light from the area of the target being examined, without any undue obstructions. So, when part of the light beam is obstructed by, for example, a protruding object into the optical path, some difficulty may be experienced during subsequent focussing—due to possible image shift.[34]

[34]**Image shift**: occurs on telescopes as a result of the mechanism utilised to obtain coarse focus. Thus, in an alignment telescope—which is a refractor type of optical instrument—the way to achieve focus and minimise this shift, is to move the eyepiece so that its focal point and that of the focal point of the telescope objective coincide.

NB For example, in some circumstances obstructions are more or less unavoidable, perhaps when a distant target is viewed through an intermediate one, or when the line-of-sight is established by a sweep optical square (i.e. see Fig. 3.10c) moving past just one of the feet of this square. Granting that providing the inspector/operator can determine the correct focus—under these conditions, then potentially no errors should be introduced.

- **condensation in the telescope**—this situation can be present within the telescope when it is transported from a slightly colder environment into that of the warmer atmosphere, for example, a machine shop or a metrology laboratory.

NB Such condensation will clear in a short time as the telescope approaches the ambient room temperature. This condensation can be reduced slightly by occasionally moving the focusing knob through its entire range—enabling any ambient warmer air to circulate within the telescope's body.

3.5 Precision Spirit Level

Historical background—invention of the spirit level

The principle design and original application of the basic spirit level was said to have been invented by the French Polymath, Melchisedech Thevenot (≈1620–1692). Thevenot being somewhat of an amateur scientist, was patron to many notable scientists and mathematicians of the day. He was both wealthy and well connected, latterly becoming the royal librarian to King Louis XIV of France. Thevenot probably invented the instrument prior to 2 February 1661. This actual and specific date for the spirit level's invention, can be exactly established from Thevenot's noted correspondence with the renowned Dutch scientist Christiaan Huygens. Moreover, after 1661, Thevenot circulated details of his invention to many others, namely to yet another significant British scientist/inventor, Robert Hooke in London, as well as to the Italian mathematician/scientist, Vincenzo Viviani in Florence. These earliest types of bubble levels—it was occasionally contended—did not become widespread in their practical usage until the beginning of the eighteenth century, with the original surviving examples being from that time. At somewhat of an earlier date in seventeenth century in France, Adrien Auzout[35] had recommended that the Académie Royale des Sciences take, '… Levels of the Thevenot type …', on its prospective expedition to Madagascar in 1666. It is more than likely that these earliest levels were utilised in France, and elsewhere, long before the turn of the seventeenth century. It should also be emphasised that Thevenot, the scientist, is

[35]**Adrien Auzout**: was a French astronomer (Born: in Rouen, France: 28 January 1622—died: 23 May 1691). Auzout made some significant contributions in telescope observations, including here—from a very valid and more notable metrological viewpoint—the perfection and use of the actual micrometre.

often confused with that of his nephew, the intrepid French traveller and explorer, Jean de Thevenot (1633 to 1667). Furthermore, there is some annectdotory evidence to suggest that both the scientists—namely Huygens and Hooke, later laid claim to this level's invention, although only within their own countries.

Modern development of precision spirit levels

A spirit level, or its alternative rather simplistic name the bubble level, is both an accurate and precision instrument designed to indicate whether a surface is either horizontal (level) or vertical (plumb). More basic early spirit levels had two banana-shaped curved glass vials at each viewing point and were quite complicated to actually use; although by the 1920s Henry Ziemann (the founder of the company Empire Level Manufacturing Corporation in the USA) was acknowledged to have invented the modern type of precision spirit level (i.e. see Standard: **AS2054:1977**)[36]—using its single vial. Such vials are in common use today, being equipped with a slightly curved glass tube, or for much greater accuracy/precision they are precisely hollow-ground thick-walled tubes—this tube being termed a vial—which are partly, but exactly filled with a liquid (e.g. these glass vials are produced in, for example the UK to **BS3509:1962**). This exact amount of liquid held within the vial is usually coloured spirit or alcohol, thus leaving a standardised bubble within this curved/hollow ground tube—see Fig. 3.15a.[37] At slight inclinations, the bubble will always travel away from the centre position, which is usually marked by precision graduations—as depicted in Fig. 3.15b. Typical fluids utilised in these vials include alcohols, such as ethanol, which are often preferred rather than water—due to water's higher surface tension effect.[38] As mentioned,

[36]**Precision Spirit Levels**: currently, there is no international standard agreement on this subject, within the: **ISO/TC 3**—Dimensional Metrology, nor does any appear likely for the foreseeable future. With this in mind, the Australian Standard: **AS2054: 1977**, is based upon the: Standard and account practices—previously specified within: BS958: **1968—Spirit Levels for Use in Precision Engineering**.

[37]**Glass vials**: it is recommended (i.e. within the UK in: **BS3509:1962—Specification for Spirit Level Vials**) that the dimensions of the glass vial should be such that at both ends of the bubble can always be read against a scale over an operating temperature range of: 10–40 ºC. To achieve this condition, it is also recommended that the alteration in bubble length for a temperature change of 1 ºC between 10 and 40 ºC, should not exceed 1 % of its actual length at: 27 ºC. This bubble's overall performance should be tested for its: sensitivity; consistency; roll error; sluggishness; total error; as well as for heat effects.

[38]**Surface tension effect**: the cohesive forces that are present among liquid molecules are responsible for the phenomenon of surface tension. Thus, in the bulk of the liquid, each molecule is pulled equally and in every direction by neighbouring liquid molecules—resulting in a net force of zero. However, molecules at the surface do not have adjacent molecules on all sides of them and therefore are pulled inwards, which creates some internal pressure and forces the liquid surfaces to contract to the minimal area. Consequently here, the surface tension is responsible for the shape of its liquid droplets. Although easily deformed, these droplets of say, that of water, tend to be pulled into a so-called spherical cap by the cohesive forces of the surface layer. In the absence of any other forces, including gravity, drops of virtually all liquids would be approximately spherical. This spherical shape minimises the necessary wall tension of the surface layer according to the Young–Laplace's law.* Moreover, because of the relatively high attraction of water molecules for each other, water has a high surface tension—producing a large spherical

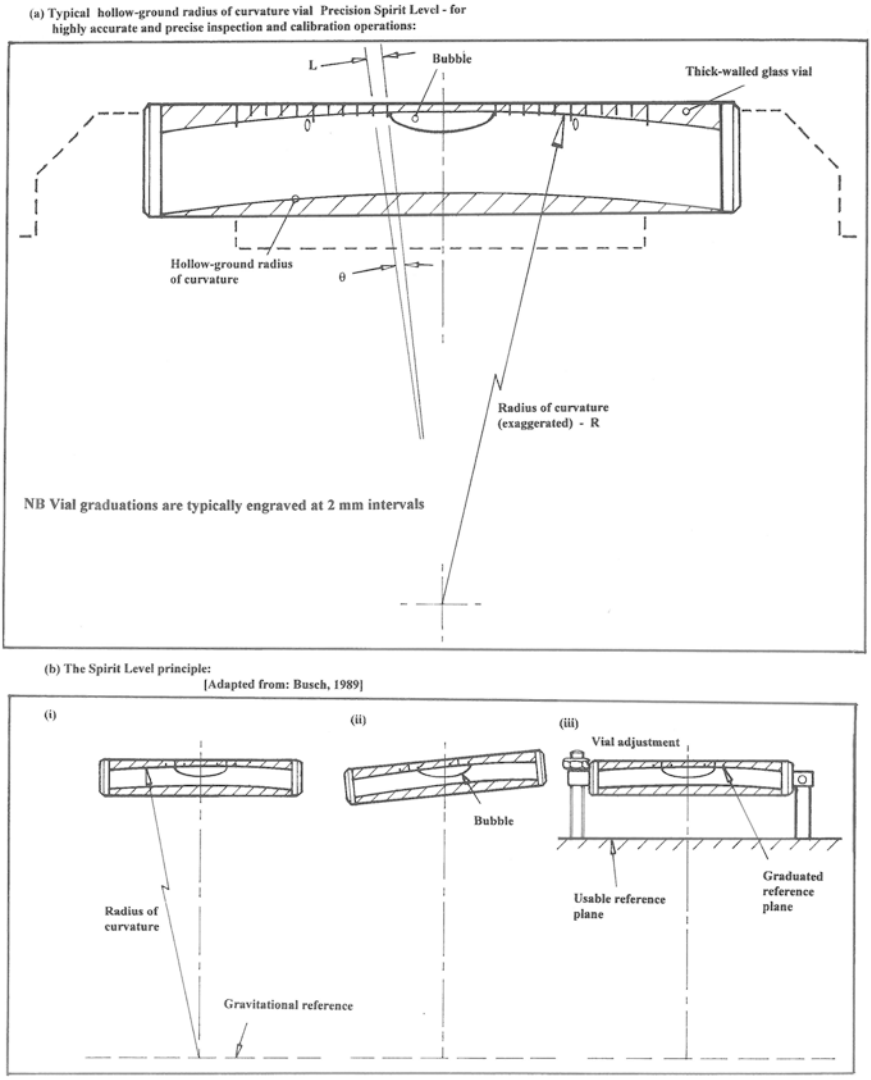

Fig. 3.15 The operating principle of the precision spirit level

---

Footnote 38 (continued)

cap (i.e. 72.8 mN m^{-1}—at 20 °C) compared to that of most other liquids. Of some note, is that surface tension and its accompanying wetability is an important factor in lubrication issues, which also influences the phenomenon of capillarity.

*__Young–Laplace equation__ (i.e. in Physics), which was derived as a nonlinear partial differential equation, that describes the capillary pressure difference sustained across the interface between two static fluids, such as water and air, due to the phenomenon of surface tension, or wall tension, although usage of the latter is only applicable if one assumes that its wall is very thin.

these alcohols have both low surface tension and viscosity, allowing the bubble to quickly travel within the vial and to settle accurately with minimal interference within the vial's glass internal surface. Yet another advantage of using alcohols is that the bubble can quickly reform if separated by an accidental jarring motion. Invariably, a colourant such as fluorescein is often utilised, this typically being of either a yellow or green colouration, which may be added to the liquid to increase the visibility of the bubble for the user—when in actual use.

To check the accuracy and repeatability of a basic spirit level, namely to assess whether the level can indicate if a truly horizontal surface is in fact level is of prime importance. To achieve this indication, the level must be positioned on both a flat and level surface, with the reading on the bubble's tube/vial being noted. This bubble reading indicates to what extent the surface is parallel to the horizontal plane—according to this level—which at this time is of unknown accuracy. The spirit level is then rotated through 180º—in the horizontal plane—with the bubble reading also being noted. As a consequence, if the level is accurate, it will indicate an identical bubble reading that had occurred for the previous orientation with respect to the horizontal plane. If a difference is present, then this will imply that the level is somewhat inaccurate. To achieve greater accuracy and precision of the bubble's positioning, some vial adjustment of this spirit level is performed. Hence once this is accomplished, by successively rotating the level and moving the bubble tube/vial, by adjusting it within its housing thereby taking up/adjusting to roughly half of this discrepancy until the magnitude of the reading remains constant when the level is successively flipped over (see Fig. 3.15ciii for a simplistic view of a typical vial adjustment screw/lock mechanism.) A similar procedure is applied to more sophisticated instruments, such as an engineer's precision level, and is adjusted as a matter of course each time the instrument is set up for metrological usage.

Sensitivity of the spirit level

The spirit level's sensitivity is a vitally important factor in the level's specification—with its actual accuracy dependent upon its sensitivity. Consequently, the sensitivity of a level is provided by either the change of angle, or gradient required to move the bubble by a discrete unit distance—see Fig. 3.15bii. If the bubble housing has graduated divisions (i.e. see Fig. 3.15a) then the sensitivity is the angle, or gradient change that swings the bubble by one of these calibrated divisions. This relationship—namely that of the bubble-to-scale—is often termed as its fiducial plane.[39] Typically, these graduations are normally spaced at 2 mm intervals, on an engineer's precision level, which also equates with the bubble movement of 2 mm, when the vial within the level is tilted by $\approx 0{,}005°$. As described, an engineer's precision level permits the levelling of objects to much greater accuracy than a basic plain spirit level. These engineer's precision levels

[39]**Fiducial plane**: this refers to a fiducial marker (i.e. graduation), which is graduated lines utilised in the field of view—for use as a point of reference, or a measurement.

are often utilised to level the beds of machine tools (i.e. see Fig. 3.17 top) or using bridging pieces/parallels[40] on machine tools, such levelling is normally employed to ensure that these machines can produce the expected production output, or for CMM's, inspect workpieces to the accuracy pre-built into such machines. The adjustable nature of this type of level means that they can also be utilised to measure the small and discrete inclinations of an object, if required.

The actual sensitivity of an engineer's precision level is dictated by the internal radius of the vial containing the liquid, in conjunction with the base length of its actual physical mount. This level has vial graduations separated by a linear distance of '$\boldsymbol{l}$', with the internal vial tube radius '$\boldsymbol{R}$'. Furthermore, one end of this vial tube is raised allowing it to move through an angle '$\boldsymbol{\theta}$', causing the bubble to also simultaneously move through **1** graduated division, thus

$$\theta \text{ radians} = l/R$$

Hence, if these graduations are engraved on the vial tube at 2 mm intervals—as depicted in Fig. 3.15a—and moreover represent 5 arcseconds, then

$$5 \text{ arcseconds} = 0.00002425 \text{ radians} = 2 \text{ mm} \big/ \text{R}$$

$$\text{R} = 2 \text{ mm} \big/ 0.00002425 = 82,474 \text{ mm}$$

or $R \approx 82.5$ m

By utilising this vial radius, which is then situated on a base mount whose length is exactly 250 mm, the height '$\boldsymbol{x}$' which one end must be raised for a 2 mm displacement/movement of the bubble is given by

$$0.00002425 \text{ radians} = x/250 \text{ m}$$

or $x = 0.006\ mm$ $(i.e.\ 6\ \mu m)$In a similar fashion, if the base length was reduced from 250 mm, this means that the sensitivity will be further increased. In addition and pressing this point, by reducing the base length from 250 mm to that of 125 mm—keeping the graduations identical (i.e. at 2 mm)—then each scale graduation will now represent just 0.003 mm or 3 μm. This latter value of vial sensitivity is quite high, and in many cases just 10 arcseconds per graduated vial division is normally quite sufficient.

In Table 3.2, typical vial radii have been tabulated, showing their respective angle-to-rise per vial division values.

[Adapted from: Busch, T. (1989)**]**

[40]**Bridging pieces/parallels**: are often employed on conventional flat-bed centre/engine lathes, or CNC lathes—when they are fitted with Vee-&-Flat ways, being an accurate and precisely ground parallel that can sit on just one Vee, then straddling to the adjacent Flat on the other way. They allow a precision engineer's level to then be situated on top of this bridging piece/parallel. Thus, this moveable assembly is then discretely and precisely moved along the bed, checking for its apparent: flatness, twist/wind, by this combination of bridging piece and level. Whereafter this whole assembly is then reversed and the other Vee-&-Flat can then be inspected in a similar operational fashion.

Table 3.2 Some typical relationships of a spirit level's: vial-curvature-to-angle-of-rise

Curve-to-angle rise relationship							
Radius in m:	525	209	105	52	35	17	0.28
Angles per division:							
Seconds	2	5	10	20	30	60	3600
Minutes						1	60
Degrees							1
Rise, mm/300 mm							
Per division	0.0254	0.0064	0.013	0.038	0.025	0.077	4.572

Some of these levels have Vee grooves machined along their bases, enabling them to precisely locate and sit on round bars, while remaining parallel with the bars' axes. These levels may also have smaller Vee's (i.e. cross-level grooves) to enable the second curved axis to also be approximately checked or corrected and to ensure the primary axis' bubbles are at the top of their vials—when the readings are actually noted.

An engineer's precision level—which usually has an accuracy/precision ratio of 1:24000 is often employed to check the levelling installation of precision machine tools in two axes. Flat-bed CNC lathes are normally manufactured with their base in a level plane and if the machine tool is not correctly installed, then level distortions in the structure will cause machining form errors to occur. Small CNC milling machines are invariably only roughly levelled, but their larger and heavier counterparts are installed accurately and then precisely levelled—see Fig. 3.17 (top). In the case of a hard-worn CNC lathe, it may have had a purposely induced slight twist that was introduced to the machine's bed to ensure that the machine now turns parallel—locally—to the spindle's axis. This deliberate and controlled distortion is achieved by twisting the bed by the maintenance personnel—where it is locally worn in a specific manner—to realign it to that of the spindle's axis; but this type of remedial action is the last resort prior to a total retrofit/rebuild, although, at this time most of these CNC lathes usually have several strategically positioned base levelling screws that are utilised to achieve this minute twisting effect. Generally, such a crude fix has limited utility for only part of the length of the cutting tool's carriage travel. It should be noted that any newly installed CNC lathe, habitually requires at least two or more further levelling trials as the machine castings tend to settle in once the original and initial machine levelling adjustments have been accomplished.

3.6 Optical Instrumentation—Clinometers

Clinometers—utilised in metrology

The traditional type of clinometer utilises the spirit level principle—previously described in Sect. 3.5. In this metrological application, the clinometer incorporates a spirit level which is mounted onto a rotary assembly member, which is then

carried within an instrument's housing—see Fig. 3.16a. In this precision metrology assembly, one face of the housing forms the base of the instrument. Situated within this housing is a circular scale that is incorporated with the angle of inclination of its rotary member carrying the level being relative to the datum base. By this means, the angle inspected can then be established by the in situ circular scale.

Precision Microptic Clinometer

The precision microptic clinometer is primarily utilised to determine the included angle of two adjacent faces of an object, such as when setting up either a workpiece or an angular fixture (e.g. an adjustable angle plate—see Fig. 3.16d). Accordingly and for angular setting purposes, the instrument's base is positioned on one face of the part to be set and then the rotary body is adjusted until a zero reading of the split bubble level (i.e. shown in Fig. 3.16b–left) is now obtained—as depicted in Fig. 3.16b (right). Having achieved this zero setting, the angle of rotation is then noted on the circular scale against the index. A second reading is then taken in a similar manner on the second face of the workpiece. Here, the included angle between the faces is the difference between these two readings. A precision microptic clinometer can also be used for checking/setting angular faces and the relief angles on large cutting tools and milling cutter inserts. Moreover, these types of clinometers can also be utilised for setting the angular orientation on dividing heads; adjusting/setting inclinable tables on say, a CNC jig-boring machine, as well as specific angular work setting requirements on CNC grinding machines.

The most commonly employed types of clinometers are those typically shown in Fig. 3.16a. Here in the case of a precision microptic clinometer, the highly accurate/precise circular glass scale is totally enclosed, with its graduations being divided up from 0° to 360°—normally at 10 min intervals. Subdivision of these 10 min intervals is also possible by utilising an optical micrometre. Consequently, a coarse scale is assigned with graduations being set every 10º, which is provided externally on the body for the coarse setting in basic work operations, or for just an approximate angular reading. For more specific and complex clinometer adjustments, a worm-based quadrant-setting arrangement is normally provided, so that angular readings of just 1 min are possible. However, in some types of clinometer designs, there is no bubble levelling facility, but instead, a graduated circle is supported on accurate ball bearings, this being so designed that when released, it always takes up the position being relative to the true vertical. Here, the reading is taken against the circle to a levelling accuracy of 1 arcsecond—with the aid of its incorporated vernier scale.

One of the special features of precision microptic clinometers is their ability to achieve a direct reading over a wide angular range, from 0° to 360°, having its optical reading system being totally enclosed with glass circles and easy-to-read scales, while having both the main and micrometre scales simultaneously visible in the eyepiece—see Fig. 3.16c. With this design of instrument, the external scale can also be adjusted for rapid coarse setting, with a slow-motion screw adjustment

(a) Typical construction of Clinometers (clockwise from bottom left): Pendulum Clinometer; Bubble Clinometer; Microptic Clinometer (reading to 10 seconds of arc); Microptic Clinometer (reading to ½ second of arc):

(b) Bubble unit incorporates a prismatic coincidence reader presenting both ends of the bubble as adjacent images in a split field of view - allowing precise levelling when two ends are coincident.

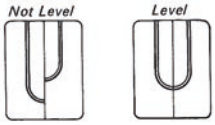

(c) Field of view through the illuminated eyepiece:

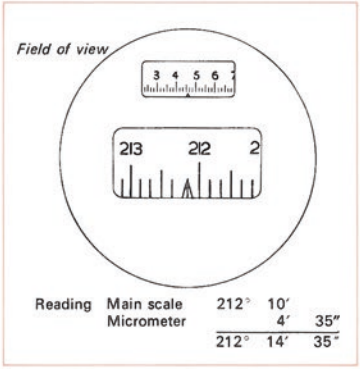

(d) Checking a workpiece angle using a Bubble Clinometer:

Fig. 3.16 Typical clinometer designs—utilised for either angular positional axis setting or workpiece checking (courtesy of Spectrum Metrology)

for its fine setting. The instrument's eyepiece is rotatable (i.e. shown on some of the clinometers in Fig. 3.16a) to allow for the most convenient optical viewing position, with the instrument as a whole, being fitted to a flat, hardened and ground steel base. Most variants of these precision microptic clinometers utilise a bubble unit (i.e. spirit level) with a prismatic coincidence reader, which presents both ends of the bubble as adjacent images in a split field of view—see Fig. 3.16b. When in use, as the clinometer's vial is levelled, these two half images move into coincidence—visually allowing appropriate sighting, ensuring that this bubble is exactly centred, without reference to any graduations—see Fig. 3.16b (right).

When determining the inclination of the clinometer, this bubble unit is simply levelled and the scales read off. In Fig. 3.16c, it is schematically depicted via the view through a more basic optical reader eyepiece, for its actual ease of clinometer reading/setting. However, there are more sophisticated optic configurations currently available, such as the following optical reader eyepiece, which has three apertures that can be seen within the eyepiece—not shown. Here, the upper aperture contains two pairs of double lines and two single lines. To set the clinometer's micrometre, the knob is turned until the single line is brought exactly central between the double lines. The scales can then be read with the required angle—this being the sum of the readings of the main scale and that of the micrometre scale. These double lines are imaged from one side of the circle, while the single ones are from a point diametrically opposite; by utilising the double lines as an index for the single line, any residual centring error of the circle is then cancelled out. These scales are illuminated by an integral low voltage lamp. The bubble unit is normally daylight illuminated, but a lamp is also provided in low light circumstances for alternative illumination. Normally, a locating face on the back of the clinometer allows the instrument to be used horizontally with, for example an accessory worktable or a reflector unit. The reference for this inclination is the bubble vial. In order to measure the inclination of a surface, the vial—to which the circle is attached—is turned until it is approximately level. Thereafter, the slow-motion screw is employed for a final adjustment to centre the bubble. To measure the angle between two surfaces, the clinometer is placed on each surface in turn and the difference in angle can then be calculated. The clinometer can also be utilised as a precision setting tool to set a tool head, or machine table and also an angle plate at a specific angle—as mentioned and once again shown in Fig. 3.16d.

Of more recent note, is the application of a compact digital inclinometer, which does not utilise a bubble level—as depicted in Fig. 3.17. This inclinometer is ideal for work in both metrological/inspection laboratories and for certain applications in the workshop, where one is setting up machine tools and fixtures. This type of digital inclinometer is a robustly constructed instrument that has been purposely designed for a clear and unambiguous simple reading. The system is ideal where a precision angle is to be determined—over a large angular range. All four quadrants of this instrument's system are precision machined, making it possible to measure angles from any of its relative sides.

Correct machine tool level and alignment is absolutely essential when maintaining long-term machine tool integrity and the ability to consistently produce quality parts.

[Courtesy of Konecranes Machine Tool Service (MTS)]

Technical Specifications:			
Settle time:	<5 seconds	Output:	RS485
Sensitivity:	0.02mm/m max	Battery:	AA 1.5V
Repeatability:	<0.1mm/m	Housing:	Aluminium hard anodised
Temp coefficient:	<0.01 deg/deg°C	Dimensions:	100x75x30mm
Working temperature:	0-40°C	Weight:	520g

Fig. 3.17 A digital inclinometer, highlighting its angular operation and technical specification (courtesy of Spectrum Metrology)

3.7 Talyvel—Precision Level

The ubiquitous company-based products known as Talyvel precision levels—see Figs. 3.18 and 3.19—can be utilised for measuring straightness, flatness or absolute level. Furthermore, this type of level can also function as a comparator to detect departures from a preset attitude—which may not necessarily be actually level. Incorporated within its compact, highly stable pendulum-type transducer, this level unit plus its rechargeable battery, or its mains-powered display unit, enables the instrument to provide rapid and simple reading of angular tilt and measurements, relative to gravity. The range of accessories for this and other versions of this level can include

- **Adjustable base** (i.e. see Fig. 3.19b)—this accessory can be set to the appropriate step interval length, being adjustable up to 200 mm in its length, for typical flatness measurement by either the grid, or union jack flatness test methods; also it can be utilised for straightness measurement. It provides a base for the Talyvel (i.e. as shown in Fig. 3.19b) with level units having self-aligning seating pads that are adjustable to a graduated scale. Base adjustment is provided for setting this level unit to its absolute horizontal. Additionally, this adjustable base can also be utilised for mounting an autocollimator reflector—not shown;
- **Block base** (i.e. see Fig. 3.18b)—this high-quality item has a 300 mm long base, allowing the vee groove in the level unit to be positioned along cylindrical objects (e.g. for the measurement of machine shafting). This block base has its 120° Vee-bearing faces surface-ground to a flatness $\leq$2.5 μm;
- **Box frame** (i.e. see Fig. 3.19a and 3.25)[41]—the measurement of inverted or vertical surfaces is facilitated by this 200 mm square box frame. Here, all bearing faces are surface-ground to a flatness $\leq$2.5 μm and with its adjacent faces all being square to $\leq$5 arcseconds (i.e. 0.025 mm m^{-1}). As standard, a pair of 120° Vee-bearing faces are provided on all of the adjacent faces and these are parallel to the base within the same tolerance;
- **Stride base** (i.e. see Fig. 3.18a)—this accessory permits the Talyvel to be mounted directly onto, say, an alignment telescope—as shown—to enable it to establish a truly horizontal line-of-sight reading;
- **Bubble vial**—not shown—this type of robust bubble vial can be mounted on any of the accessory bases described above, in place of the Talyvel's level unit, to provide a simple, cost-effective method of setting and checking both angle and level. It has a sensitivity of 5 arcseconds $division^{-1}$ (i.e. 0.025 mm m^{-1}). Adjustment for setting the level unit to absolute horizontal is provided for all these respective bases. Moreover, a further adjustment is provided, for eliminating any potential roll errors which can be significant, which is also included within this device.

In the case of the company's current Talyvel wireless electronic precision level system—shown in Fig. 3.20—it can be interfaced directly to a touch screen computer

[41] **Optical calibration of a Box Frame**: depicted in Fig. 3.25. Here, in this metrological configuration, it has an alignment telescope shown inspecting and verifying the squareness of the faces on this box frame, utilising a swivelling and self-aligning reflector, being situated on a previously highly accurate and precisely calibrated inspection beam.

(a) The *Stride Base*, enables the Talyvel to be mounted onto an *Alignment Telescope*, thereby establishing a truly *horizontal* line-of-sight (L.O.S.):

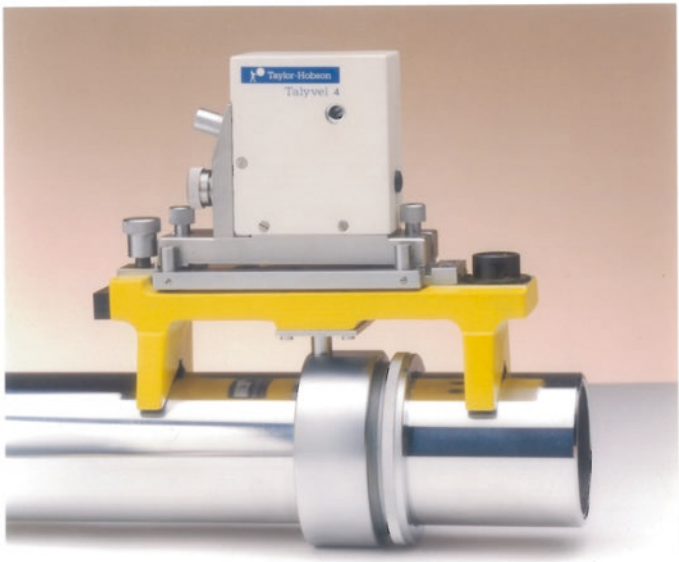

(b) The *Block Base*, is 300 mm in length, which with its inverted Vee, allows the Talyvel to be positioned on a machine tool's *cylindrical features*, or for other applications, etc, or it can be utilised for additional *Straightness* checks:

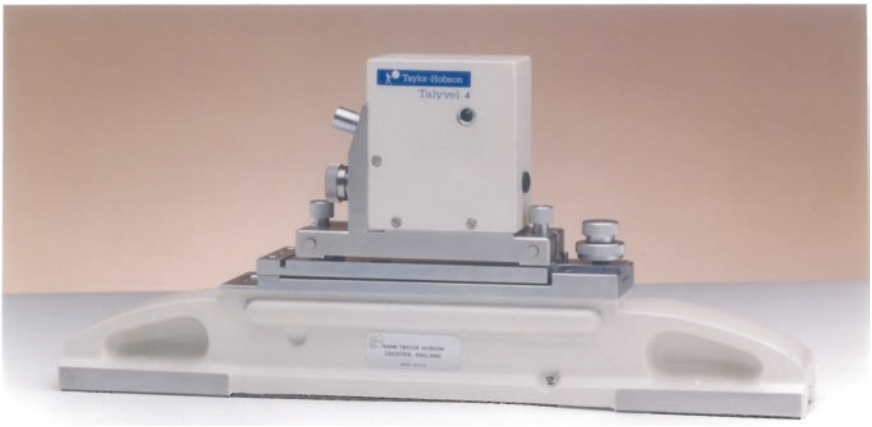

Fig. 3.18 Some practical accessories for the Talyvel (courtesy of Spectrum Metrology)

thus providing a versatile and precise measurement for a wide variety of industrial and optical engineering applications. These electronic Talyvel levels combine excellent accuracy, stability and repeatability with fast response. Weighing less than one kilogramme, the Talyvel 6 in its wireless mode, provides end-users with flexibility, in combination with both versatility and accuracy. This level instrument delivers

(a) The *Box Frame*, enables the *Talyvel* to be inverted, or facilitates assessment of vertical surfaces:

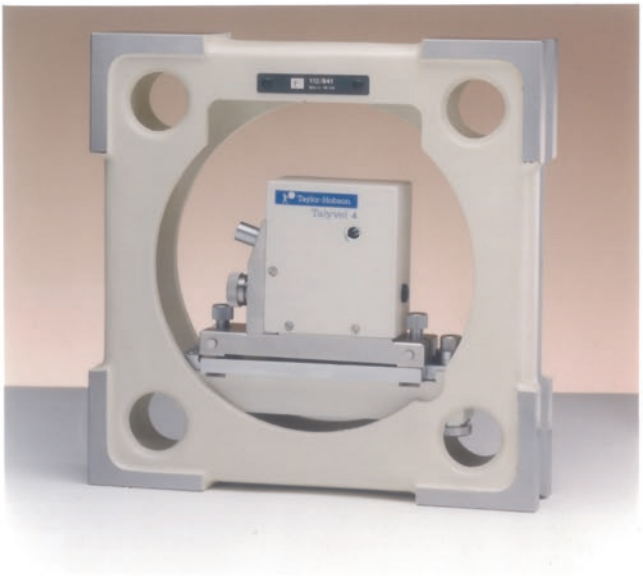

(b) The *Adjustable Base*, can be set to the appropriate step interval - in increments up to 200 mm, for *Flatness* measurement by either the Union Jack, or Grid methods, plus *Straightness* assessment:

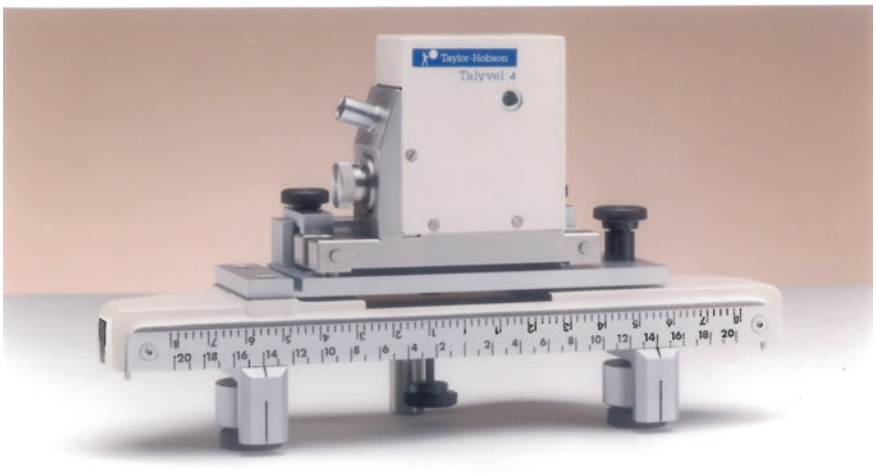

Fig. 3.19 Some more accessories for the Talyvel (courtesy of Spectrum Metrology)

a reading for the angle of tilt, with measurements relative to gravity and it is simple to both calibrate and operate. The level has an angular accuracy of just 0.2 arcseconds—over the centre of its measuring region. Moreover, this type of wireless

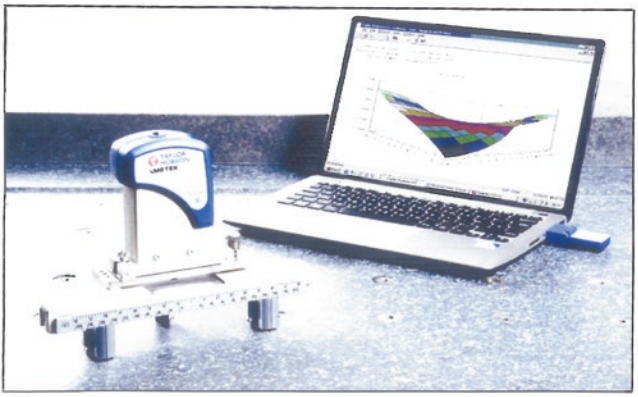

(a) Wireless Electronic Precision Level - used for measuring straightness, flatness, or absolute level, the Talyvel 6 interfaces directly to a touchscreen PC and can be used in wireless mode for complete flexibility – situated on an adjustable base.

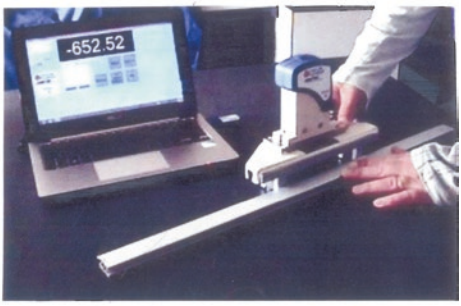

(c) Using Wireless Electronic Precision Level with an Adjustable Base unit to determine a table's flatness.

(b) Incorporating a highly stable pendulum transducer in the Level Unit and a rechargeable battery, the Talyvel 6 is simple to calibrate and operate, with a fast measurement response time and exceptional stability.

Fig. 3.20 A wireless electronic precision level (courtesy of Spectrum Metrology)

electronic precision level can be remotely positioned for particular hard-to-see visual obstructions, or for applications in exceptionally confined spaces. Once again, this level incorporates a pendulum-type transducer that can provide an exceptional measurement stability. This specific Talyvel 6 unit, has many metrological applications in particular for machine tools—for checking slideways for straightness and twist, or columns for squareness-to-slideways, as well as on surface tables/Plates—for their flatness assessment. It can also measure the settlement of particularly large machines. One of its most common uses is the ability to check the flatness of granite and cast iron tables—see Fig. 3.20c. Additionally, when utilised for measuring straightness, flatness or absolute level, the Talyvel 6 can also function as a comparator to detect departures from a preset altitude of inspected objects—that may not necessarily be actually level.

For some metrological inspection applications, two of these level units may be required—denoted here as 'A' and 'B' (i.e. shown in Fig. 3.20b) which can then be controlled from the single display unit providing a differential system for measuring the actual difference in the inclination of two surfaces, as well as their departure from absolute level. Hence, the display of results, from each level unit and their respective differential value, is determined by the switch selection of 'A', 'B' or by 'A-B'. This metrological application of differential levelling is of particular value in specific applications such as measuring the relative deflections while machines are in actual production and in the accurate assembly of precision machinery, furthermore for the monitoring twist, or deflection on exceptionally slowly tilting surfaces. The electrical zero adjustment operates on the display, from level unit A, and therefore also on any differential A-B applications. In summary, this type of wireless electronic precision level system, can provide

- **an optional differential system**—for comparative measurement;
- **a wireless dongle option**—with a distance range of up to 10 m;
- **highly stable pendulum-transducers**—having both a quick and efficient adjustment to gravity, or to absolute level;
- **high resolution and accuracy of 0.2 arcseconds**—over its central measuring range;
- **readings obtainable in both arcseconds, or gradient**—whichever is the most convenient method of assessment.

3.7.1 Software Programs—for Precision Electronic Levels

For these types of precision electronic levels, a full Windows™-based software package is currently available from the manufacturer, to support their existing wireless Talyvel. This package includes flatness measurement by either the union jack (i.e. Moody method[42])—see Fig. 3.22—or grid[43] methods, see Fig. 3.23,

[42]**Union Jack/Moody method—for flatness assessment**: this so-called Moody method (i.e. see Fig. 3.22), that was first proposed in 1955 by J.C. Moody (Of note, was that J.C. Moody was at the time—in 1955, working at the: Physical & Electrical Standards Dept., (Sandia Corp., Alburquerque, NM, USA)), which has since subsequently achieved wide acceptance. This Moody technique provides a relatively quick method of calibrating a surface table, or plate, with the results being presented as a contour plot along the eight measurement lines tested, in a format acceptable for certification. Although this technique does have one disadvantage, namely, that all of the points on each of the eight lines must be measured and plotted. This aspect of measurement can create problems in defining a foot spacing which will meet this requirement, particularly on a machine tool having Tee-slotted tables/surfaces—where the position of one or more slots may coincide with the required position of one of the feet of the flatness base.

[43]**Grid method—for flatness assessment**: with the so-called grid method (A disadvantage with both these grid methods, is that they require a reference plane to be defined. Conversely, the alternative technique, such as the Moody method is required, to define this reference plane.), any number of lines may be taken in two orthogonal directions across the surface. Here the grid method, whilst being of an incremental technique, requires that all points on a given line are

together with straightness measurement (i.e. including both twist and squareness) and the polygon angular indexing program. Furthermore, software for statistical filtering and edit facilities add to end-user confidence and flexibility of approach. Of note, is that the Moody Method (i.e. union jack) is considered by many as the industry standard for calculating surface plate flatness. The method provides a simple but accurate means of assessing flatness and has been employed in metrology applications for many years (Fig. 3.21).

Modern software and measuring instruments have improved the speed and accuracy of this Moody method. Invariably, one can use the Moody method to plot and analyse the surface table/plate flatness from measurements taken by electronic differential levels; or alternatively, by laser flatness measurement systems that are both NIST traceable and compliant also to that of **ISO-10012-1**.

Flatness program

The popular use of a surface table, or plate that is widely used as the datum plane for most measurements in either the metrology laboratory or the workshop inspection station has been very well documented over the years. The accuracy of any measurement data taken will be limited by knowledge of the flatness of these surface tables/plates. To ensure this metrological knowledge is up to date, it requires a datumed item's surface calibration to be normally performed at least once every 6 months. Specifications of surface flatness are generally expressed in either one, of two ways, namely, as the

1. **maximum allowable deviation** (i.e. plus & minus)—of any point in the surface from an ideal plane;
2. **maximum allowable separation**—of two parallel ideal planes, which entirely enclose the surface.

Flatness tolerances can vary from 1 to 250 μm—over the usable area of the surface table, or plate. Usually, some form of calculator program is applied, to reduce this surface table/plate flatness inspection data to a final and comprehensible form, with displays of this data normally being in the format of two parallel ideal planes. Accordingly, this type of numeric data plot program can display the data in either format—as previously discussed, flatness can be measured and displayed by employing either the union jack (i.e. Moody) method—see Fig. 3.22—or by the grid method—see Fig. 3.23. Here, a simple interactive menu-driven software displays an initial diagram of the surface to be measured—as shown in Figs. 3.22–3.24—together with surface generator lines coupled to instructions on the method of

Footnote 43 (continued)

measured, it is unnecessary to take measurements on all separate lines. Such measurement discretion allows any measurement lines to be configured to avoid particular obstructions (e.g. Tee slots, or fixture holes), or to provide greater detail in a given surface area. While, the alternative half grid method is a special case variation on the full grid method, where a number of measurement lines are taken in one direction (e.g. along the X-axis), but only the perimeter lines are utilised for the orthogonal direction.

(a) Measuring the *Straightness* of a precision surface utilising an Autocollimator with a Reflector Carriage:

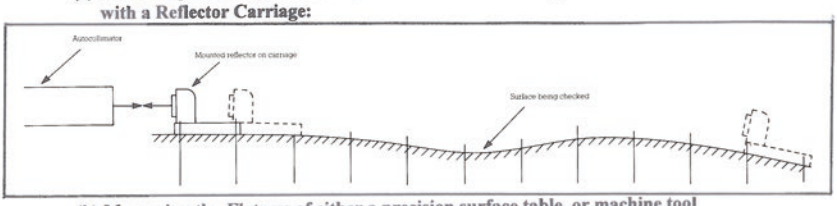

(b) Measuring the *Flatness* of either a precision surface table, or machine tool table using an Autocollimator, together with a Corner Reflector and Reflector Carriage:

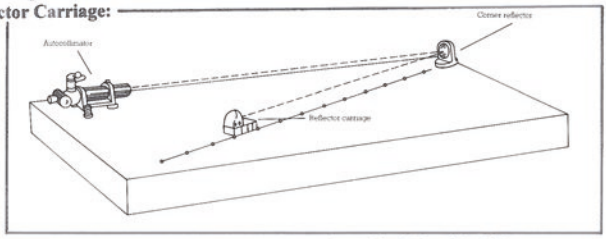

(c) A typical *Flatness* assessment - by Autocollimation - the Union Jack (i.e. Moody) method, for a precision Surface Table, employing the setup diagrammatically shown above in Fig. (b) :

Fig. 3.21 Illustrating some practical autocollimation operations for straightness and flatness inspection (courtesy of Spectrum Metrology)

entering surface data. For that reason, after the selected number of measuring steps have been entered, the program calculates and displays the shape of each generator line and the flatness of the surface. During actual measurement, readings can be automatically entered into the computer, normally by utilising in this instrument, the remote data entry lead. Once the computer has accepted these Talyvel readings, the values are displayed as arcseconds and then converted to micrometres, or if preferred, as millionths of an inch units for hard copy printout (i.e. as either μm,

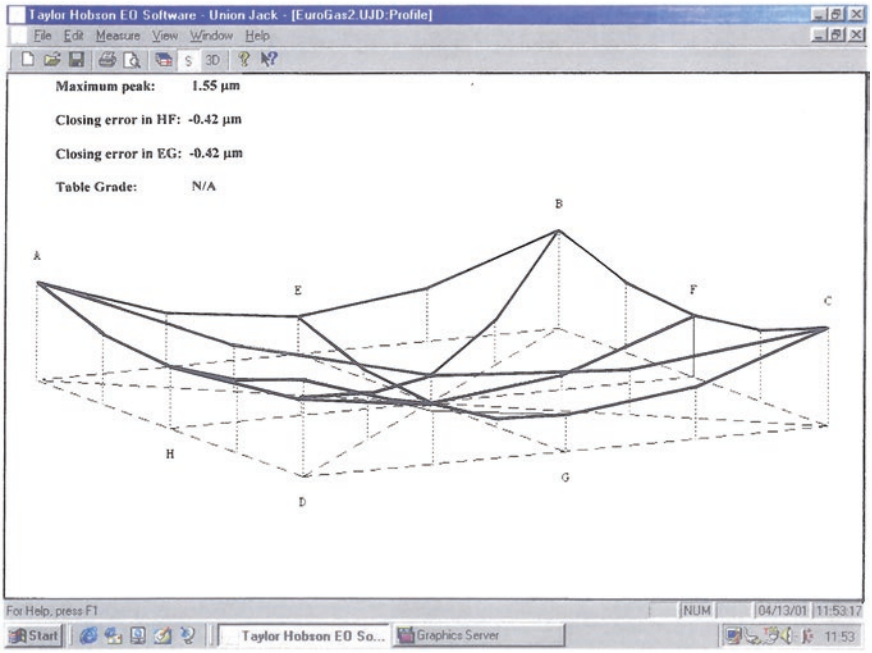

Fig. 3.22 A screen display of surface flatness by optical/Talyvel techniques—union jack method (courtesy of Spectrum Metrology)

or 0.000001 in, respectively). Measurement results of flatness are displayed and printed out as a graphical isometric diagram (Figs. 3.22 and 3.23) coupled to the printing of either a certificate or results list—as necessary. To comply with international standards, it is usual to produce a minimum-zone calculation to generate any flatness errors.

Straightness program

The Straightness program for verification procedures—see Fig. 3.24—will permit straightness measurement on components such as equipment and plant, for machine tool slideways, shafting and for rolls—although this latter inspection procedure is not discussed herein. The methods and procedure for use are similar to those previously described for flatness-measuring activities. Results are presented in both tabular form and also as a straightness graph—as depicted in Fig. 3.24. Both Twist and Squareness measurement are also available in this software package. Data analysis is to either an 'LSL',[44] or to other graphical/data analysis packages appropriate for these metrological results (Fig. 3.25).

[44]**Linden Scripting Language** (LSL): is built into this software as a three-dimensional modelling tool based on simple geometric shapes that allow residents to build virtual objects. There is also a procedural scripting language, which can be also utilised to add interactivity to these objects.

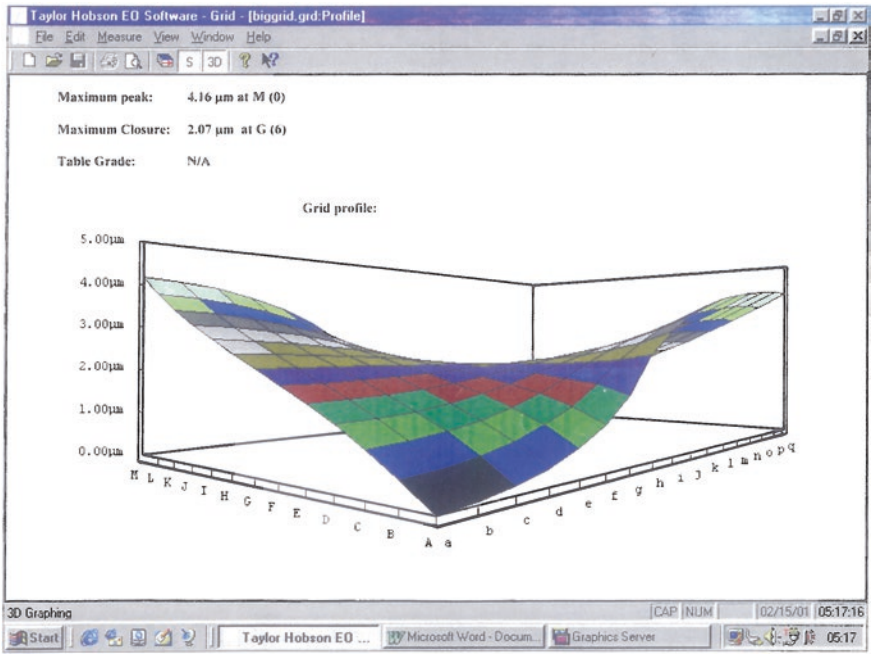

Fig. 3.23 A screen display of surface flatness by optical/Talyvel techniques—grid method (courtesy of Spectrum Metrology)

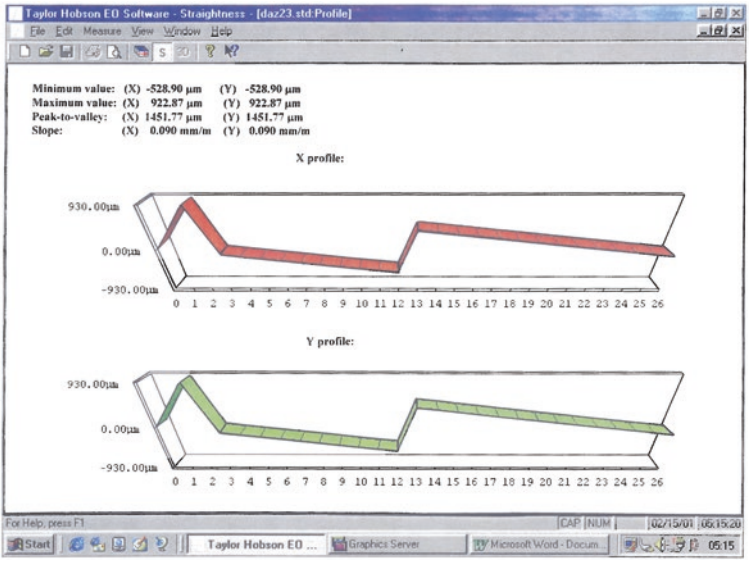

Fig. 3.24 A screen display of surface flatness by optical/Talyvel techniques—in the *x* & *y* planes (courtesy of Spectrum Metrology)

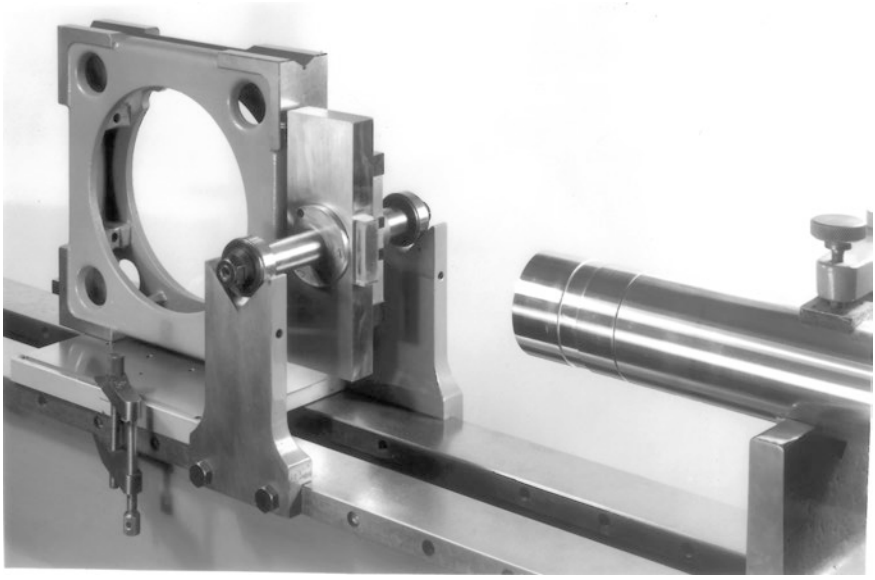

Fig. 3.25 The alignment telescope is inspecting and verifying the squareness of the faces on box frame, utilising a swivelling self-aligning reflector, situated on an inspection beam (courtesy of Spectrum Metrology)

Twist program

This Twist program—not shown—combines a single-line straightness measurement with a number of radial- or cross-measurements. All of these current software programs have the option of single, average or statistically filtered inputs.

References

Journals and conference papers

Arif Sanjid, M. & Chaudhary, K.P., *A novel multiple reflections technique to calibrate polygons and evaluation of its uncertainty of measurement*, in: MAPAN, Vol. 26 (1), 29-35. Mar. 2011.

Bručas, D., Giniotis, V., Augustinavičius, G. & Stepanovien, J., *Calibration of the multiangular prism (polygon)*, MECHANIKA, Vol. 4 (84), 2010.

Bručas, D., Giniotis, V., *Calibration of precision polygon/autocollimator measurement system*, J. of Physics: Conference Series, Vol. 238 (1), 2010.

Collyer, P.W., *Measurement of twist by autocollimation*, Optical Spectra—4th Quarter, 30-35, 1967.

Duis, W., et al, *Design and performance of a high accuracy automatic autocollimator*, Precision Engineering and Optomechanics, SPIE: Vol. 1167, 1989.

Estler, W.T., *Calibration and Use of Optical Straightedges in the Metrology of Precision Machines*, Optical Eng'g., Vol. 24 (3), 243-372, June 1985.

Fan, F.C., Wang, T.H., Wang, C.H. & Chen, H.M., *Development of an Abbé Error compensator for NC machine tools,* Proceed. of the: 37th Int. Matador Conf., Ed. by Hinduja, S. & Li, L., 105-108, 2012.

Fan, K-C., Yen, H-M. & Li., K-Y., *A New Concept of Volumetric Error Analysis of Machine Tools Based on Abbé Principle*, 3rd Int. Conf. on Design Engineering and Science, ICDES 2014, Pilsen, Czech Republic, 198-202, 2014.

Hermann, G. & Tomanyiczka K., *Autocollimator Calibration Using a Tangent Bar*, in: Intelligent Engineering and Informatics, Vol. 1, 321-330, 2012.

Just, A., Krause, M., Probst, R. & Wittekopf, R., *Calibration of high-resolution electronic autocollimators against an angle comparator*, Metrologia, 2003, Vol. 40, 288-294, 2003.

Kiyono, S., Zhang, S. & Uda, Y., *Self-calibration of precision angle sensor and polygon mirror*, Measurement, Vol. 21 (4), 125-136, Aug. 1997.

Mitrofanov, A.A, *Optical lever effect in optical instrument measurements*, Measurement Techniques, Vol. 24 (9), 737-739, Sept. 1981.

Moody, J.C., *How to Calibrate Surface Plates in Plant*, Tooling Engr., Vol. 35 (2), 15-21, Oct. 1955.

Muelaner J.E., Yang B.R., Davy C., Verma M.R. & Maropoulos, P.G., *Rapid Machine Tool Verification*, 8th Int. Conf. on Digital Enterprise Technol. - DET 2014- Disruptive Innovation in Manufacturing Engineering towards the 4th Industrial Revolution, Pub. by: ScienceDirect Procedia, CIRP 00 (2014) 000–000, 2014.

Olexa, R., *Keeping accuracy within reach*, Modern Machine Shop, 2005.

Osanna Öve, P.H., *Intelligent production metrology— A powerful tool for intelligent manufacturing*, Elektrotechnik und Informationstechnik, Vol. 114 (4), 162-168, April 1997.

Park, S-R., Hoang, T-K. & Yang, S-H., *A new optical measurement system for determining the geometrical errors of rotary axis of a 5-axis miniaturized machine tool*, J. of Mech. Science and Technology, Vol. 24 (1), 175-179, 2010.

Rahn, R.J., *It takes Three-point Specification to Insure Surface Plate Flatness*, Tooling & Prod., Vol. 20 (7), 123-125, Oct. 1954.

Ristonen T., Andersson, P.H. & Tikka, H., *Traceable flatness calibration with substitution method*, 16th Int. Congress of Metrology, published by EDP Sciences, 2013.

Ruiz, A.R.J., et al, *A Real-Time Tool Positioning Sensor for Machine Tools*, Vol. 9 (10), 7622-7647, In: Sensors, (Pub. On-line), Sept. 2009.

Shur, V.L., Lukin, A.Y., Shestopalov, T.N. & Popov, O.I., *Two-Coordinate Digital Autocollimator*, Measurement Techniques, Vol. 48 (9), 901-906, 2005.

Shur, V.L., Naidenov, A.S., Lukin, A.Y. & Leibengardt, G.I., *A liquid autocollimation refractometer*, Measurement Techniques, Vol. 49 (8), 815-819 Aug. 2006.

Taek, O.Y., *Design of precision angular indexing system for calibration of rotary tables*, J. of Mech. Science and Tech., Vol. 26 (3), 847-855, 2012.

Torng, J., Wang, C-H., Huang, Z-N. & Fan, K-C., *A novel dual-axis optoelectronic level with refraction principle*, Measurement Science and Technology, Vol. 24 (3), 2013.

Watanabe, T., Fujimoto, H., Nakayama, K., Kaji- tani, M. & Masuda, T., *Calibration of a polygon mirror by the rotary encoder calibration system*, XVII IMEKO World Congress, Dubrovnik, Croatia, 1890-1893, 2003.

Yandayana, T., *, Akgöza, S.A. & Haitjema, H., *A novel technique for calibration of polygon angles with non-integer subdivision of indexing table*, Precision Engineering, Vol. 26, 412-424, 2002.

Books, booklets and guides

Born, M. & Wolf, E., *Principles of Optics* (7th Ed.), Cambridge University Press, 2003.

Bucher, J.L., *The Metrology Handbook* (2nd Ed.), ASQ Quality Press, 2012.

Busch, T., *Fundamentals of Dimensional Metrology* (2nd Ed.), Delmar Pub. (USA), 1989.

de Silva, G.M.S., *Basic Metrology for ISO 9000 Certification*, Butterworth-Heinemann, 2002.
Flack, D., *Measurement Good Practice Guide No. 41- CMM Measurement Strategies*, NPL Pub., 2001.
Flack D. & Hannaford, J., *Measurement Good Practice Guide No. 80- Fundamental Good Practice in Dimensional Metrology*, NPL Pub., 2005.
Fulmar, I.H., *Dimensional Metrology*, NIST Pub. 265, 1966.
Galyer, J.F.W. & Shotbolt, C.R., *Metrology for Engineers* (5th Ed.), Cassell Pub. Ltd. (London), 1990.
Gåsvik, K.J., *Optical Metrology*, Wiley Pub., 2002.
Harding, K. (Ed.), *Handbook of Optical Dimensional Metrology*, CRC Press/Taylor & Francis Pub., 2013.
Kragh, H., *Niels Bohr and the quantum atom: the Bohr model of atomic structure*, 1913–1925. Oxford University Press, 2012.
Lehmann, B., *Practical Alignment Tools and Techniques*, TKT Engineering Inc. (USA).
Müller-Kirsten, H.J.W., *Introduction to Quantum Mechanics: Schrödinger Equation and Path Integral* (2nd ed.), World Scientific Pub., 2012.
Optical Alignment, Taylor-Hobson Pub., 1984.
Pickover, C.A., *Archimedes to Hawking: Laws of Science and the Great Minds Behind Them*, Oxford University Press, 2008.
Probst, R., *Measurement of Angle and Flatness Deviations of Polygon Prism Faces using a Phase-Shifting Interferometer*, VDI-Reports No. 1118, 173-178, 1994.
Thomas, G.G., *Engineering Metrology*, Butterworth & Co. Pub. (London), 1974.
Vloet, R.E.J.M., *Electronic Autocollimation*, Eindhoven University of Technology Faculty Mechanical Engineering Division Mechanical Production Technology and Automation Section- Precision Engineering, The Netherlands, WPA Report 310021, 1995.
Yoshizawa T. (Ed.), *Handbook of Optical Metrology: Principles and Applications*, CRC Press/ Taylor Francis Group Pub., 2009.

Chapter 4
Telescoping Ballbars and Other Diagnostic Instrumentation

"Everything that happens,
happens as it should,
and if you observe carefully'
you will find it to be so."
Marcus Aurelius Antoninus
(Roman Emperor and Philosopher)
[121–180 AD]
(In: Meditations, IV)

4.1 Telescoping Ballbars

4.1.1 Machine Tool Health Checks—The Reason Why They Are Necessary

Essentially, the machined quality of every single component produced on a CNC machine tool is highly dependent on the tangible machine's complete performance. Accordingly, if there are any potential problems with a machine tool, then the production output will inevitably result in perhaps some, perhaps all, defective machined components being produced under such serious circumstances. The reasons for this significant amount of part rejection may possibly be due to any number of reasons: its cosmetic appearance—with certain machining marks spoiling the finish; or an out-of-specification part—of critical tolerance features; or perhaps otherwise simply being unfit for its intended purpose. While actual subsequent inspection procedures, coupled to extra metrological investigation, plus any part rectification—will have a significant impact on company profitability; these aspects being conceivably due to certain:

- **wasted downtime**—affecting overall productivity;
- **higher piece part costs**—due to such non-productive activities;
- **delayed deliveries**—as a result of further investigation/rectification of these defects;

G.T. Smith, *Machine Tool Metrology*, DOI 10.1007/978-3-319-25109-7_4

- **dissatisfied customers**—due to actual due delivery-dates being either missed, or late, thereby affecting a company's production schedules.

Invariably, the traditional quality and inspection procedures can only identify problems after components have been produced, but this is far too late in the part's value-added manufacture. This, to a certain extent, of late realisation that a production problem exists, is especially true if one is manufacturing very high cost and complex critical tolerance components. These fundamental quality-related problems are exacerbated in combination with that of close tolerance part features and when high-volume machining operations occur there is little or no margin for such errors. Some of these component quality problems are conceivably due to human error, or resulting from tooling problems, which can be just some of the numerous reasons for this lack of part quality, but invariably the machine's poor positioning performance is habitually the major reason for a machined component's part rejection.

Today, all modern-day CNC machine tools have excellent technical specifications, but their overall manufacturing performance—even when new—may to a certain degree be compromised by such characteristics as: inadequate foundations; poor site location; or incorrect installation and plant-commissioning. After the machine tool has been initially installed, it can be subject to yet more vagaries in its production output, possibly resulting from excessive wear and tear, or via possible damage from tool crashes, as well as general misuse. This is why it is essential that a machine's overall production performance is regularly monitored and, just as importantly in many advanced shops, is the fact that the machine is normally health checked—by some efficient calibration and/or validation instrumentation, which can be undertaken just prior to beginning any part-manufacturing.

4.1.2 Telescoping Ballbars—Historical Development and Operation

The invention of the telescoping ballbar can be attributed to Jim Bryan—while working for the Lawrence Livermore Laboratories in California (USA).[1] In principle, one

[1]**Telescoping Ballbar**: the initial design concept and its structure for the telescoping ballbar was invented and described by James B. Bryan (James B. Bryan has been called: 'The founding-father of modern precision engineering'—(Manufacturing Engineering—a USA journal—by: Jim Lorincz, Senior Editor et al.). In 2002, Jim Bryan was honoured by the: European Society for Precision Engineering (Euspen), for: 'His tireless promotion of precision engineering philosophies, principles, innovations, practices, and standards through design, research, and teaching'. A registered Mechanical Engineer in the State of California since 1954, Jim began working at Lawrence Livermore National Laboratory (LLNL, CA, USA) in 1955, under Nobel laureate and Founding director: Ernest O. Lawrence. By the time he retired in 1986, Jim Bryan was Chief of Metrology, also with his significant contributions to precision engineering that were so diverse that one colleague has commented that picking the most notable one would depend upon whom you asked! While yet another professional colleague (i.e. Ben Taylor—of Renishaw plc) has described Jim Bryan: 'The world's most practical purist.') in the U.S. Patent No. 4,435,905—which was filed in 1984. Although prior to this date, some previous rigorous design and testing had been undertaken by Jim Bryan on his original ballbars, while at the Lawrence Livermore Laboratory (Ca., USA).

of the earlier commercial derivatives of this type of wired telescoping ballbar is shown in Fig. 4.1 (top) and schematically in operation in Fig. 4.2, with the initial ballbar set-up and its operation being described as follows. At the start, this previously calibrated ballbar (i.e. see Fig. 4.3, top-right) is attached to a machine tool using two kinematically designed sockets, which are magnetic, having hemispherical cavities accurately matching the size of the precision balls situated on either end of the actual ballbar. Here, one socket is situated on the machine's table, while the other is mounted into the spindle at the desired angular orientation—as shown in Fig. 4.1 (top). To utilise this ballbar arrangement for machine health checking, both the spindle and table are manually brought together (i.e. using the CNC machine's axis handwheel) but being separated by the radial distance of the required ballbar's length. Once in the desired position, these balls on each end of the ballbar are situated within their respective magnetic and kinematic sockets—in an unsprung position (i.e. with the ballbar not being under any form of tension). If any minor radial adjustment is necessary here, the compliant ballbar cup assembly—situated on the table socket—can be loosened and gently retightened to achieve desired accurate and precise untensioned fitment for this ballbar's length. Prior to taking any machine tool data, the bespoke software is programmed to move the ballbar radially inward by a millimetre—see Fig. 4.2b—to activate its in situ transducer. Then, this ballbar's software within the machine tool is programmed to move in anti-clockwise circle, using two predetermined axes—by circular interpolation, such as by its *X*- and *Y*-axis—see Figs. 4.2b, also 4.4 (top). The actual circular rotation, is for two complete rotational anti-clockwise radial circuits by this ballbar. Accordingly, in the first 180° of anti-clockwise motion—termed angular overshoot—is undertaken prior to any data capture, as the instrument sets and stabilises the ballbar's radial motional velocity. Then afterwards, a full interpolated circle occurs (i.e. during which time its data capture arc takes place) then finally yet another 180° angular overshoot occurs (i.e. to allow for any overrun to be negated—as the ballbar slows to a stop). Once these two complete anti-clockwise rotational motions have been undertaken, then the whole rotational operation is completely reversed and its clockwise readings are then subsequently captured—in an identical rotational manner—thus producing clockwise data. Consequently, if the CNC machine tool's axes are perfect, this circular motion by these interpolated axes would describe a true circle, as there will be no change in radial ballbar's length, or in its in situ LVDT[2] readings.

[2]**LVDT**: stands for a **L**inear **V**ariable **D**ifferential **T**ransformer by which it is often simply known as a differential transducer, this being a type of electrical transformer utilised for measuring linear displacement (position). These LVDT's are quite robust, absolute linear position/displacement transducers; which are inherently frictionless in operation, moreover, they have a virtually infinite cycle life when utilised correctly. As they are AC-operated, these LVDTs do not contain any electronics, although they can be designed to operate in both cryogenic temperatures, or in hot environments up to 650 °C. In operation, the LVDT converts a position, or linear displacement from a mechanical reference (e.g. zero, or null position) into a proportional electrical signal containing phase, for both direction and, amplitude—for distance information. The LVDT operation does not require an electrical contact between the moving part—the probe—and its coil assembly, but instead relies on an electromagnetic coupling.

QC10: Wired Ballbar System

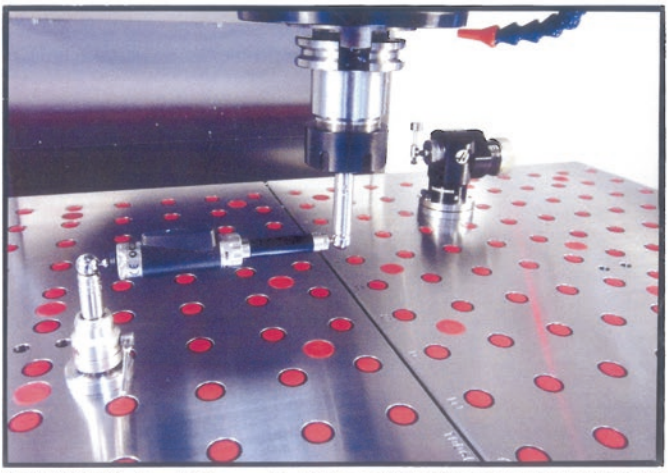

QC20-W: Wireless Ballbar undertaking a diagnostic check on a vertical Machining Centre.

Fig. 4.1 The telescoping ballbar for calibration/diagnostic assessment of machine tools (courtesy of Renishaw plc)

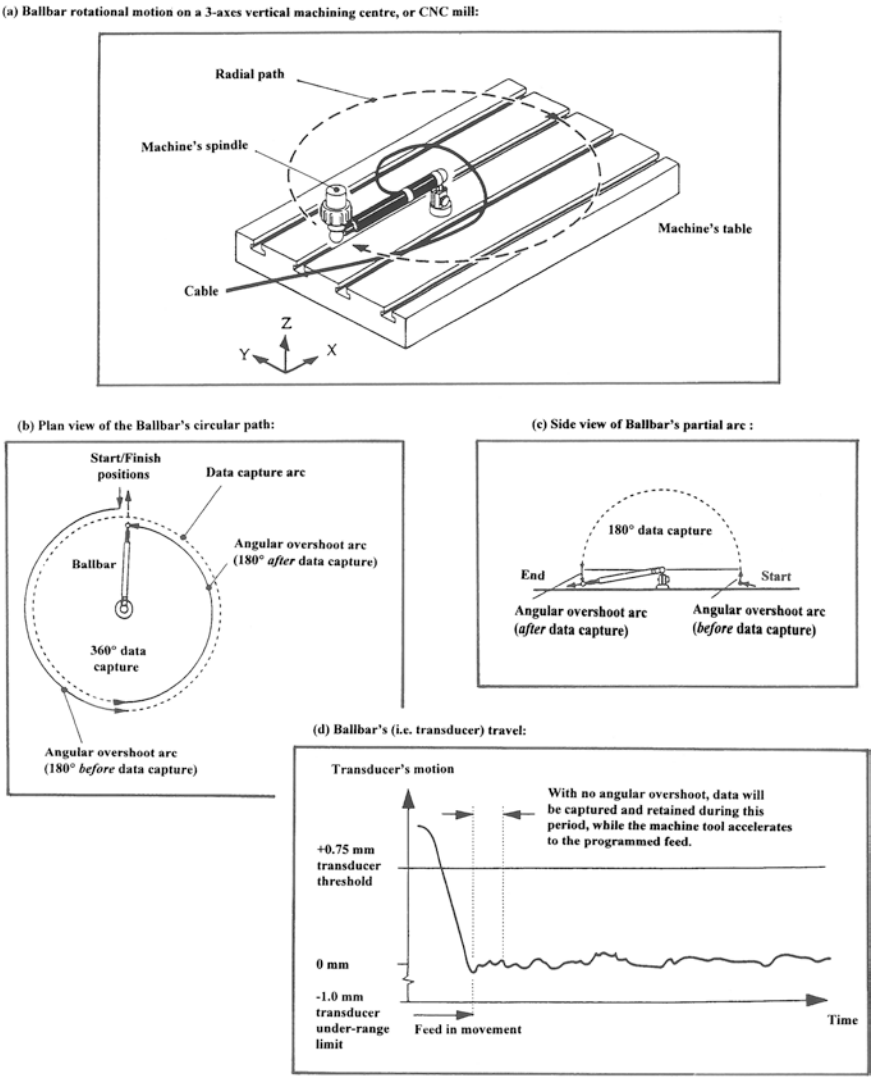

Fig. 4.2 Schematic representations of ballbar kinematic motions—for data capture and subsequent analysis (courtesy of Renishaw plc)

If, as is anticipated, the ballbar's reading displays some changes in its interpolated travel—see Figs. 4.2d, 4.4 and 4.6, this radial data provides significant diagnostic information about why the motion has not indeed been circular. As a consequence, the ballbar's reading is combined with that of the nominal machine position and with these radial changes in the ballbar's length; they are then displayed in a somewhat exaggerated and magnified scale—by the bespoke software,

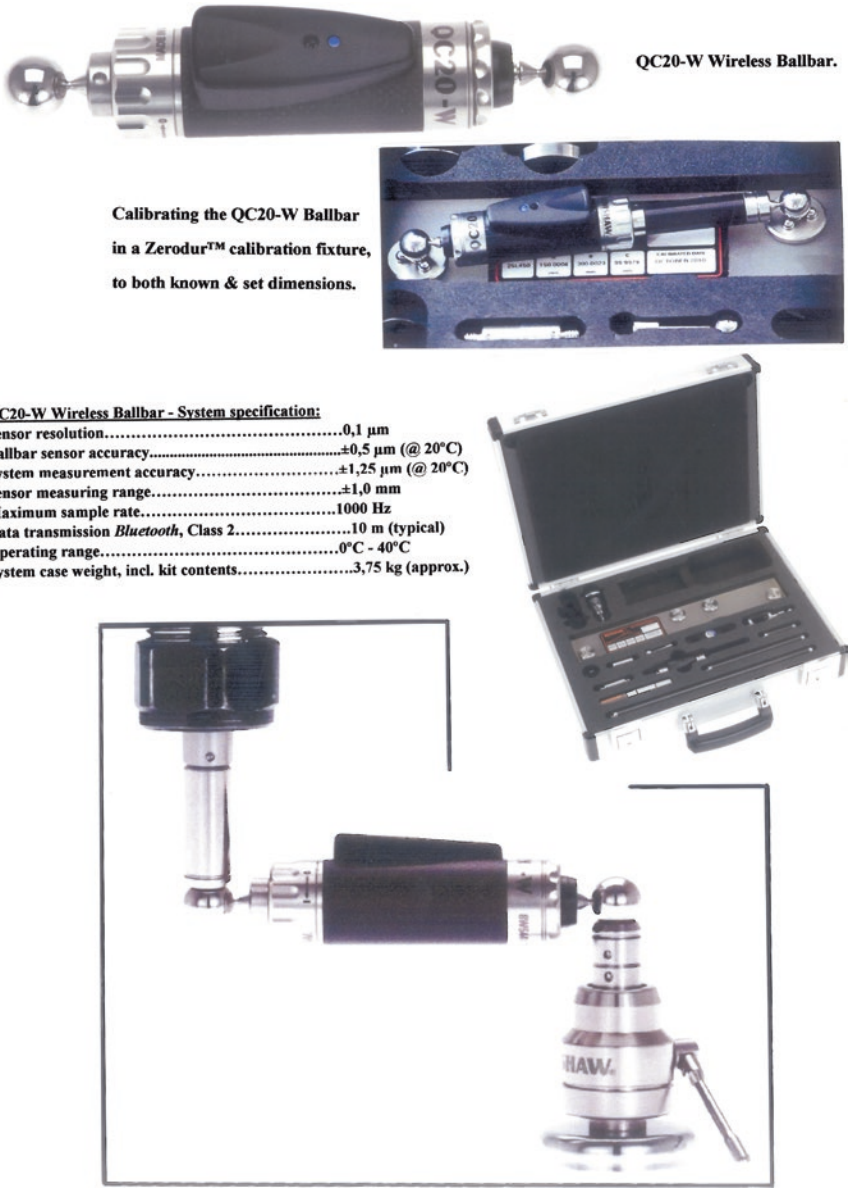

Fig. 4.3 A 'wireless ballbar' for the quick and efficient 'health checking' of a CNC machine tool (courtesy of Renishaw plc)

on what is termed a polar plot—see Figs. 4.4a and 4.6. Usually, if any backlash occurs, as might be the case with either a worn recirculating ball screw or perhaps due to a loss of ball nut preload, then there is a delay in the portion of the circular motion where the axis reversal occurs. Hence, the resulting polar plot indicates a distorted circle that appears to be both split and axially shifted (i.e. see Fig. 4.4b—this axial split/shift here, is just depicting one axis of backlash). Conversely, if the moving axes are not square to each other, then the ballbar's distorted measurement appears as an ellipse (i.e. see Figs. 4.4a and 4.6, bottom). The orientation of this elliptical plot resulting from the machine's non-squareness will not change when the machine is commanded to traverse this circular motion in either clockwise or anti-clockwise direction. Moreover, the ballbar measurement will also look identical to an ellipse error, if there is a scale error between these two axes. However in this situation, the orientation of the long axis of the ellipse shifts by 90°, depending on whether the circle is traversed in either the clockwise or anti-clockwise direction.

At the axis transition points, so-called servo-spikes are invariably present—for example, as a positive *X*-axis circular motion is reversed to a negative *X*-axis motion at the extreme of its axis rotational travel, during its controlled circular interpolation—see Fig. 4.4 (top). These servo-spikes occur at each axis transition point and can vary in their relative size (i.e. magnitude) for each axis—dependent upon the interpolation speed that has been programmed. Emphasising this fact still further, as the ballbar's rotational speed increases with higher programmed interpolated speeds, the actual height of these servo-spikes will also proportionally increase in size. Of some note is that any departure from a true circle—during such circular interpolation—will be represented as harmonic departure from roundness[3] (i.e. previously termed out-of-roundness) that could seriously affect the machine's in-service operational use. This action will result in any future machined component's rotational features not being round, particularly in, say, a criticallytoleranced assembly environment. See Appendix 4 for a visual troubleshooting guide and more details on telescoping ballbar roundness errors and their potential causes.

Due to the excellent diagnostic software capability of a telescoping ballbar for these quickly and efficiently taken health checks, it enables a CNC programmer/operator to see the characteristic appearances of many other kinds of machine tool errors: looseness of gibs; pitch error of the driving ball screw; plus any stick-slip present. The ballbar's measurement normally includes that of noise, but rarely exhibits only one type of error. Bespoke software helps by prioritising the combined polar plot measurement into the critical levels of significance for these machined component errors. Furthermore, any such measurements can be repeated using different

[3]**Departures from roundness**: this potential deviation from a true circle for the machined component which can be significant for a variety of reasons, not least of which is the problem of tolerance deviation and fitment of mating parts, in a precision assembly. More information can be gleaned on this and other roundness problems in the author's book, *Industrial Metrology—Surfaces and Roundness*, also by Springer Publishing (2002).

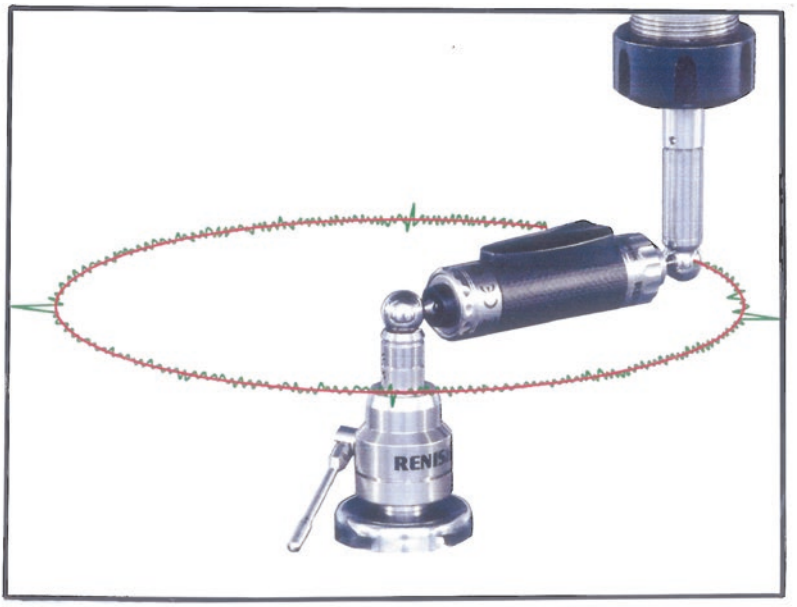

QC20-W Wireless Ballbar: illustrating the forward/reverse circular motion – when gathering thousands of data-points for subsequent machine tool diagnostics and the machine's rectification.

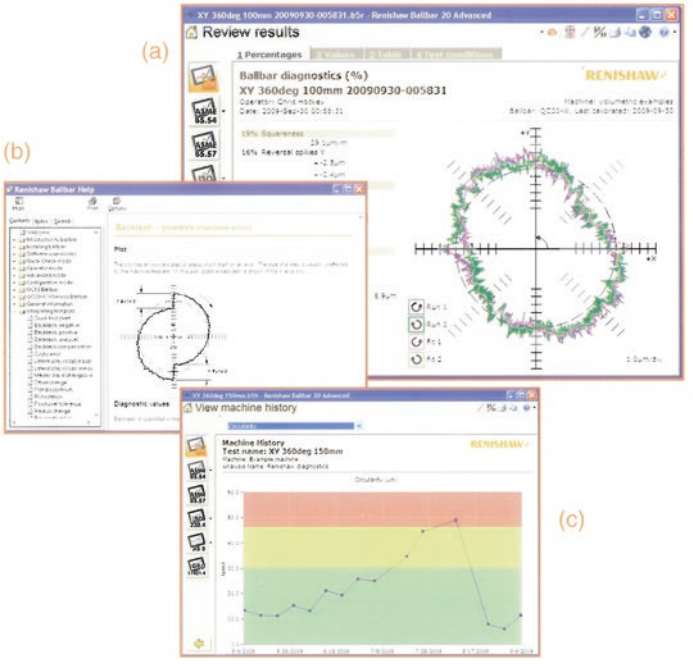

Fig. 4.4 A 'wireless ballbar's' kinematic motion, indicating just some of the diagnostic screens that can result from the speedy assessment of a machine tool (courtesy of Renishaw plc)

Partial arc tests of 100 mm & 150 mm can be carried out using the supplied central pivot.

Both partial arcs & circular motions can be achieved in a number of differing three-dimensional planes, typically: X-Y, X-Z, & Y-Z

Part of the *Small Circle Accessory Kit* (i.e. 50 mm): the calibration fixture being made from Zerodur™ , for the task of calibrating the *Small Circle Adaptor* prior to use.

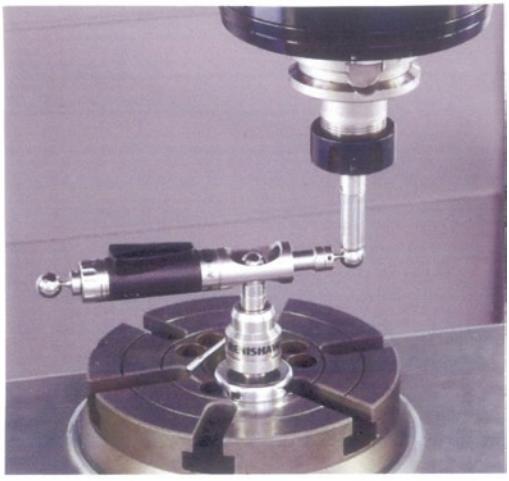

The *Small Circle Adaptor* (i.e. 50 mm) utilised in conjunction with the Wireless Ballbar on a vertical Machining Centre.

Fig. 4.5 The 'wireless ballbar' performing partial arc tests, also illustrating the small circle accessory kit arrangement and its zerodur™ calibration fixture (courtesy of Renishaw plc)

combinations of two machine axes and at any angular position (i.e. see Fig. 4.1), or simply as programmed partial arcs (i.e. see Figs. 4.2c and 4.5, top). The fundamental length of the ballbar can be easily changed by adding differing lengths of the non-moveable segments, for larger radial sweeps within the machine's volumetric envelope, or alternatively, the ballbar's radius can also be decreased in length, then recalibrated—as shown in Fig. 4.5 (bottom-left), prior to use (i.e. Fig. 4.5, bottom-right).

4.1.3 Telescoping Ballbar—In More Detail

As has been briefly described above, a telescoping ballbar can monitor a machine tool's spindle movement as its follows a programmed circular path, comparing its test path to that of a perfect circle. Therefore, a conventional telescoping ballbar consists of a telescopic bar—hence its name—having precision-machined magnetic balls and cup joints at either end; see this arrangement being typically illustrated in Fig. 4.1 (top). Regarding this assembled arrangement once again, the telescopic bar portion houses a high-accuracy position sensor, with one end of the ballbar being mounted via a magnetic cup to the machine bed, while the ball at its other end is attached to its associated magnetic cup in the machine's spindle—see Fig. 4.3 (bottom). This accurate and precise kinematic-mounting configuration allows the ballbar to transcribe, for example, a hemisphere-of-motion (see Fig. 4.5, top) and as such, this partial arc will determine the machine's dynamic positioning accuracy. Here, a ballbar has its internal sensor that contains two coils and a moving core and, in this manner, functions as per an LVDT. Consequently, as the ballbar's length changes—due to any radial variance during circular interpolation, this core will move inside these two external coils causing a change in the coil inductance. This inductance change is subsequently detected by sensor circuitry then it is converted to a positional readout with a resolution of 0,1 μm, having an accuracy of ±0,5 μm at 20 °C. With the earlier wired commercial ballbar type (shown in Fig. 4.1, top) there is only one wire connection, and it plugs directly—or via a USB adapter—into the RS232 port of any Windows™-based PC—with the machine tool previously having its associated ballbar software installed.

In an archetypal ballbar test, the ballbar might be assembled to sweep, say, a 150 mm radius, but for other tests the ballbar's radii can be changed, ranging from 50 mm (see Fig. 4.5, bottom-right) to that a larger radius of >1000 mm becomes possible. Different lengths of ballbar may be utilised to increase its sensitivity to particular machine tool-induced-errors. Accordingly, a longer radial ballbar length could be employed to increase sensitivity to geometry errors such as squareness; conversely a very small ballbar radius might be utilised to highlight any dynamic errors such as servo mismatch. A range of commercially available accessories can also be fitted to these ballbars—see Appendix 4—to enable them, for example, to be mounted between the spindle and turret on a slant-bed mill/turn centre; horizontal CNC lathes; also on vertical CNC turret lathes, or alternatively, on a wide range of machining centre configurations and their derivatives.

4.1.4 Ballbar Testing—Why the Need?

It is feasible for a ballbar test to take approximately 10–15 min to complete, which can be performed as a full circle; or partial arc; or indeed, at any angle and plane in: *X*–*Y*; *X*–*Z*; or *Y*–*Z* plane traces—as shown for example, in Fig. 4.5

(top-right). Once the ballbar's initial software installation on the machine tool has been accomplished, this permits the machine to be programmed to drive its spindle in a circular path having a radius equal to the length of the ballbar. As a consequence, this ballbar tracks the spindle's movement to within ±0.5 μm, with weight errors based on these measured values, then converting this ballbar data into an error-exaggerating polar plot of the machine's actual movement. As a result, an experienced CNC user can simply identify every error in the machine from this plot. Within the bespoke software, sophisticated algorithms for the ballbar can also produce a comprehensive diagnostic report that enumerates up to 22 different dynamic and geometric error values, then ranking them in order of error importance. Moreover, the overall positioning capability, or true position, of the machine is also calculated. Reports from such ballbar tests can also be produced in accordance with a wide range of international standards, these being typified by such standards such as **ISO 230-4; ASME B5.54**, etc.

It is vital in today's highly productive precision engineering environment to regularly monitor all of a company's CNC machine tools' performance parameters—with some form of diagnostic instrumentation, such as that produced and exemplified by these ballbar tests. Immediately any non-conformance in machined components becomes apparent, the CNC operator should set up and conduct a ballbar diagnostic test. Such testing of a vertical machining centre, will check up to 14 different geometric parameters in each of the three machine planes tested: *X-Y*; *X-Z* and *Y-Z*. Hence, any potential errors resulting from this ballbar testing will be quickly identified, which can then be efficiently corrected by the company's maintenance personnel. Additionally, periodic and random ballbar checks help reduce any unscheduled downtime, by tracking trends in a particular machine's performance. Therefore, any axis-related problems can be speedily identified before a machine tool degrades in its performance, which enables vital and necessary scheduled repairs to be efficiently undertaken, rather than creating a specific production crisis in its machined output. It has been well documented that the ballbar has significantly reduced the time needed to complete routine preventive maintenance. Furthermore, the ballbar data permits the maintenance technician to determine the true extent of any corrective action a machine may require. Invariably, the machine tool just simply requires a few minor adjustments than would otherwise normally be scheduled. It was mentioned earlier—see Fig. 1.21—that a typical three-axis machine tool is subject to 21 degrees of freedom (i.e. deviations that include linear positioning, pitch; yaw, roll, straightness, as well as squareness—between these axes). All of these error uncertainties can have a detrimental effect on the machine's overall positioning accuracy and, as such, on the quality of any machined parts produced. The potential for extra manufacturing problems will increase when considering the additional dynamic effects as the machine moves, and the coordination required to produce smooth machine interpolated motion is affected.

The degradation of the CNC machine tool's positioning accuracy is not always apparent until this machine begins to produce some component features that are

tending to drift toward out-of-tolerance, or at the more extreme circumstance, producing complete rejected machined components. As a result, it is desirable to have a process to enable control of the machine tool allowing a CNC operator to decide whether a particular problem requires immediate attention, or if it can be attended to later—during perhaps, a scheduled maintenance window. However, in all such cases, this type of diagnostic checking of CNC machine tools should be mandatory prior to a company's actual shift commencing; thus machining high-quality parts, beginning at the shift's start and from the outset. With so many mitigating and interrelated factors to be considered, any technical solution has to be simple to use, quick to undertake, while delivering easily understood results, with the minimum disruption and cost to a business, hence, the popularity and wide-spread use of the application of these ballbar diagnostic health checks.

4.1.5 Wireless Telescoping Ballbar

The commercially available wireless telescoping ballbar—shown in Figs. 4.1 (bottom), 4.3, 4.4 and 4.5—includes and incorporates the application of Bluetooth™ wireless technology. This latest derivative version of ballbar instrumentation—which is now unfettered by wires—unlike earlier wired versions of these ballbars (i.e. see Figs. 4.1, top and 4.2.) Both ballbar types have had a significant influence of late, on CNC machine diagnostic testing. Many current end-users believe that this latest wired ballbar variant offers significant advantages over the previous wired ballbar product. Bluetooth™ wireless technology has been considerably simplified and made much more consistent, the action and operation of ballbar testing in a machine tool's three orthogonal planes. A single and simple hardware set-up produces efficient and fast testing, with the ability to produce a representative volumetric measurement of positioning accuracy. Checking machine user trends, with regular repeatable testing, is fundamental to effectively tracking changes in machine tool error sources over time. Therefore, a comprehensive machine tool history function can produce a quick and simple way to examine the complex and significant data records produced. This efficient data analysis enables the CNC programmer to see if problems are developing, and in this manner, schedule an early preventative maintenance (PM) strategy—if necessary—in a more targeted and timely manner. Consequently, by fixing any problems before they become critical, this will minimise the potential machined part scrap rates, reduce downtime and as a result, minimise any associated production and maintenance costs. As described, ballbar testing is also included in a number of current international standards for machine tool accuracy testing, including **ASME B5.54** and **ISO 230-4**. So, the data collected by the ballbar, is employed to calculate overall measures of positioning accuracy (e.g. circularity, circular deviation, etc.) which can then be displayed graphically, as well as in numeric format to aid and support efficient machine tool diagnosis—see Figs. 4.4a–c, also 4.6.

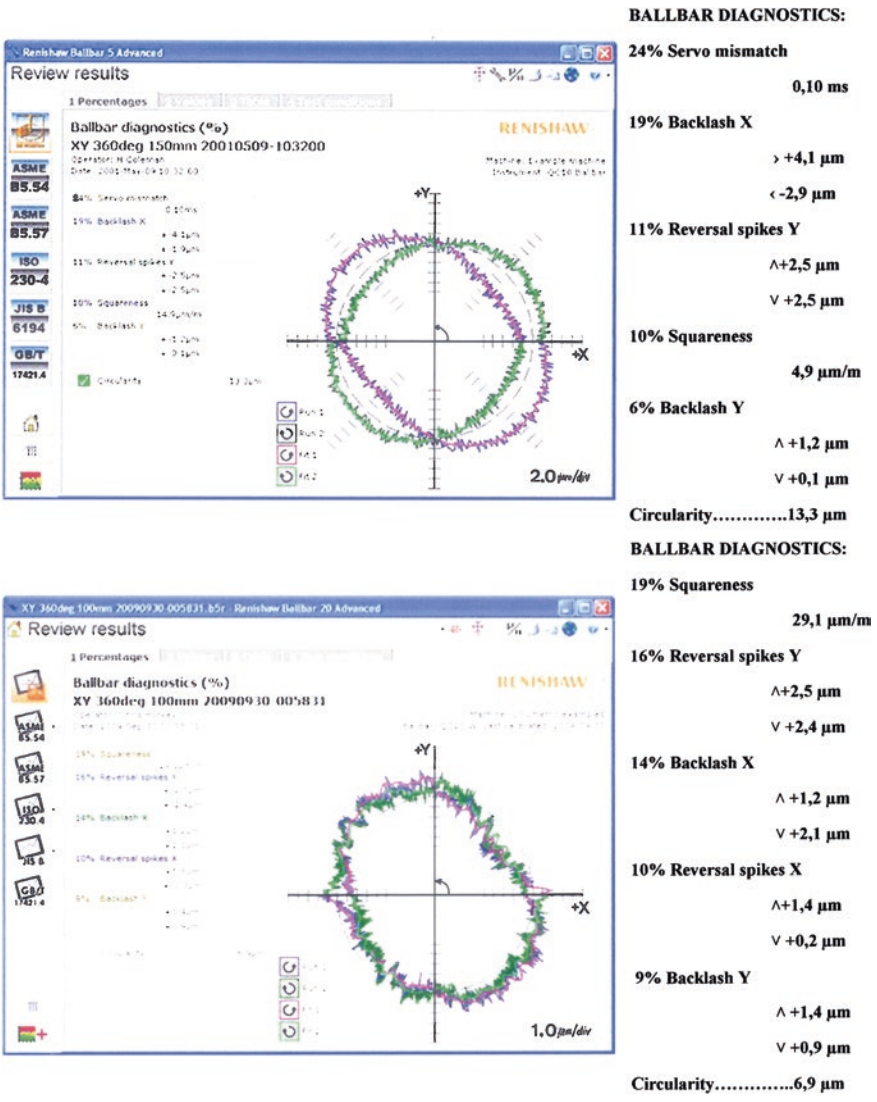

Fig. 4.6 Typical examples of vertical machining centre ballbar plots, illustrating the severity of motion error causes (courtesy of Renishaw plc)

With this latest commercial wireless telescoping ballbar, it is supplied as a complete kit-in-a-case (i.e. shown in Fig. 4.3—middle-right)—providing this comprehensive ballbar kit with both a powerful and a portable solution—just requiring a PC prior to beginning any form of diagnostic testing. The Ballbar's software then

guides the CNC machine tool user through its circular test program, via a simple four-step process, as follows:

1. **set-up**—this action being both quick and easily undertaken, here, with the ballbar being mounted between two repeatable magnetic joints;
2. **capture**—thus, the machine tool performs two consecutive circular arcs (e.g. anti-clockwise and clockwise) in any one of the machine's test planes (i.e. *X–Y*, *Y–Z*, *Z–X*) and very accurately records and measures any variations in the test circle radius, traced by the machine during this test;
3. **analyse**—after testing, the bespoke ballbar software will then analyse the measured data producing results in accordance with various international standards (e.g. typically to: **ISO 230-4** and **ASME B5.54**);
4. **diagnose**—thus, finally a unique and comprehensive diagnostic report will also give the end-user an overall assessment of machine performance (e.g. its circularity, when circular interpolating), but in addition, it provides an automatic diagnosis of up to 15 specific machine-positioning errors. Here, each error is then ranked according to its significance to the overall machine performance—alongside its actual error value. Typically, this whole verification and testing process becomes a very powerful diagnosis tool, which becomes the choice of many of the world's leading machine tool builders and manufacturing companies for their standard test report format.

After this four-step sequence of ballbar test procedure has been undertaken, fixing the machine tool from data obtained from the diagnosis report is achieved in a logical manner, as follows:

(a) not only does the ballbar test rank individual machine errors, but by utilising the hot links to the ballbar's system manual, one can comprehend these typical machining faults;
(b) related to these faults, the user manual will even suggest some possible machine tool fixes, which can then be utilised on the machine in question.

NB Even with this level of diagnostic ability, a CNC user can still be faced with many alternative strategies to get the machine tool to within the manufacturer's and the standard's required specification.

The subsequent choices that an end-user makes, will depend on the machine tool configuration and what resources are currently available to that company. However, by utilising an integrated simulator package, these end-users can access the results file, to see the What-if combinations of likely error-fixes which will produce an overall improvement in the machine's performance. This level of simulated decision-making, allows end-users to make an informed decision on the best course of action, whether that is by an in-house correction; contracted-in machine maintenance; or even moving prospective production operations to an alternative and previously verified machine tool.

4.1.6 Telescoping Ballbar—A Closer Examination of Machine Tool Inaccuracies

As has been previously described, diagnostic testing with a telescoping ballbar for machine tool verification can reveal a number of machine-related problems. Below, are listed just some of the potential common errors to be found through ballbar testing of a machine tool—these errors being typically shown on exaggerated ballbar plots:

- **Axis reversal spikes** (i.e. see Appendix 4i—Fig. A.12)—when an axis is driven in one direction and then has to reverse and move in the opposite direction, instead of reversing smoothly, it may pause momentarily at the turnaround point. This effect gives the impression of short spikes that appear at 90° on each axis reversal point—for an orthogonal machine tool;
- **Scale mismatch** (i.e. see Appendix 4ii—Fig. A.13)—this type of error is shown as an oval plot, being extended along one axis. Perhaps here, one of the machine's axes is either over-travelling or under-travelling relative to the other. Conceivably, one axis could be feeding too far, or perhaps the other axis is not feeding far enough, possibly because of a variety of reasons, such as, either the result of a faulty ball screw, or its actual over-heating—also see Fig. 6.18 (middle);
- **Backlash step** (i.e. see both Appendices 4iii and 4iv—Figs. A.14 and A.15)—which is usually presented as the plot showing a step along one axis, that indicates the lost motion resulting from this backlash. Here, an outward step could suggest play in the drive system, while an inward step may indicate hysteresis in the CNC's encoder. Moreover, either step type could be caused by play in the machine's guideways;
- **Stick-slip** (i.e. see Appendix 4v—Fig. A.16)—which is the result of noise produced when friction causes one axis to stick when it is fed at a very low motional rate. So as a result, if left unchecked, this type of error could prevent the machine from producing an acceptable machined surface finish;
- **Squareness** (i.e. see Appendix 4vi—Fig. A.17)—this error geometry is shown as an oval ballbar plot, usually occurring when orthogonal axes are no longer moving at 90°, relative to one another. This type of error may possibly be due to a bent axis, or some other form of axis misalignment. This squareness error ovality on the plot will tilt it at 45° with respect to the two axes, remaining in the same position regardless of the direction of travel of the ballbar (i.e. whether it is moving in CW, or ACW motions);
- **Servo mismatch** (i.e. see Appendix 4vii—Fig. A.18)—this error is depicted as an oval plot which is tilted by 45°; however unlike the previous squareness plot, it does not stay in the same orientation. Here, the plot shifts back and forth by 90°, depending on the direction of axis travel. This switching error, indicates mismatched servo-gains in the CNC, causing the axis with the higher gain to lead the other, while ensuring that a precise circular interpolation motion is impossible to achieve;

- **Cyclic error** (i.e. see Appendix 4viii—Fig. A.19)—this error is shown as a plot with waviness that varies in amplitude and reaches its maximum amplitude at axis reversal. This type of machine error is normally caused by either a flaw in the axis leadscrew, or from its previous leadscrew-mounting;
- **Machine vibration** (i.e. see Appendix 4ix—Fig. A.20)—this type of error is characterised by noise on the ballbar plot (i.e. vibration) where it reaches a maximum when the vibration is aligned with the ballbar. Of note, is that its amplitude can vary around the plot, although the frequency does not;
- **Master/slave** (i.e. not shown in Appendix 4)—this is a changeover error that often results on CNC machine tools, when they can only interpolate one axis at a time. Varying the speed of the master axis while the slave axis follows can generate arcs. This changeover error produces a complex plot having 45° saw-like appearance coupled to equi-pitched steps, which can make any form of precision machining of circular features virtually impossible to achieve.

4.1.7 Ballbars—Other Instrumental Variations

Double Ballbar (DBB)

The double ballbar (DBB) instrumentation enables rapid tests for the measurement of the motion error on a range of machines, such as machining and turning centres, or other types of plant which are driven by a CNC controller—having the programming ability of circular interpolation motion. A typical DBB commercial instrument is schematically shown and partially sectioned in Fig. 4.7 (top). It consists of a sealed, self-guided linear encoder with a pushrod, and has a magnetic table-mounting socket, which is attached to the machine's table, with an identical magnetic spindle-mounting socket that is clamped into the machine tool's spindle—as shown in Fig. 4.7 (bottom). Thus, the linear encoder is held into the correct orientation/position by its magnetic bearings on these two mounting sockets. This assembled arrangement permits measurement of, for example, radial deviations from the circular path, in all three working planes of an orthogonal three-axis CNC machine tool. This particular DBB is supplied with calibrated extension bars with radii of the following lengths: 150, 200 and 300 mm—to be registered prior to use. Here, the measured data are downloaded into a PC with a bespoke counter-card, where the data receives further processing, via the supplied evaluation programs. Once data are processed, the amount of error, such as either circular or radial deviation, is then automatically determined in conformance with such international standards typified as **ISO 230-4**.

The measuring instrument (i.e. DBB) records the physical points on a circular curve, which then either enlarges the extension, or contraction of the DBB ballbar showing data in polar coordinates, known here, as a motion error trace. This trace is then analysed and the volumetric accuracy is speedily evaluated. Historically, some very valuable work concerning the phenomena in utilising a DBB and its

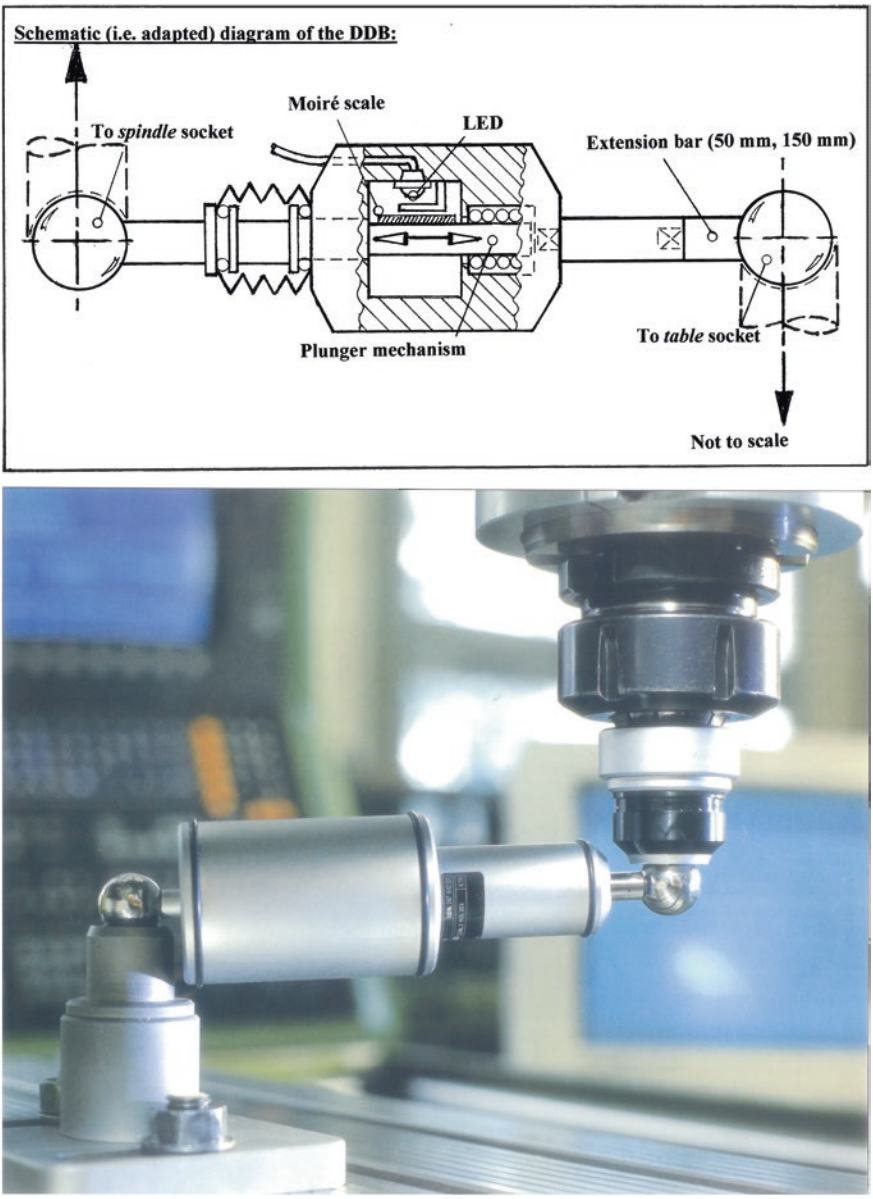

Fig. 4.7 The double acting ballbar on the table of an CNC machine tool (courtesy of Heidenhain (G.B.) Ltd.)

associated measurements, was undertaken and studied in the machine tool laboratory in Japan by Prof. Y. Kakino et al.—during the late 1980s; most of their later ballbar studies and applied work being based upon previous research—see the relevant references and accompanying book title, at rear of this chapter. There are several variants of the basic design of a DBB currently commercially available to the machine tool users, which can fulfil similar analysis to the one mentioned herein.

Laser Ballbar (LDDM)

The laser ballbar (LDDM) is a relatively recent machine tool calibration technique, its operation being based upon a single-aperture Laser Doppler Displacement Meter (LDDM). The foremost features are that the measurement is non-contact; where the circular path radii can be varied continuously, ranging from: 1 to 150 mm; with the linear accuracy being traceable to NIST. Here, the LDDM's feedrate is up to 4 m s^{-1}; having a data capture rate of $\leq$1000 data s^{-1}; further, the actual feedrate, velocity, plus its acceleration can also be determined. This type of LDDM is based upon the scientific principle of Dopplermetry.[4] In effect, when a laser beam is reflected from a target, the Doppler frequency shift is proportional to the velocity. Since the frequency shift is the change of the phase and the velocity is the change of the position, therefore after integration—with respect to time—the Doppler phase shift will be proportional to the position. So, once this phase has been measured, its actual position can be determined. One of the positive advantages of this type of LDDM is that it has both flexibility and is compact to use—see this setup in Fig. 4.8. Accordingly, it is possible to fit two interferometers into one laser head, or to reduce these two apertures with an output beam aperture and a receiving beam aperture, down to just one aperture; both the output laser beam and the receiving laser beam will share the same aperture. Due to the configuration of this single-aperture optical arrangement, it is possible to use a flat mirror as the target, thus tolerating a large

[4]**Doppler effect**, or as it is also known—**Doppler shift**: is named after the Austrian physicist and mathematician Christian Doppler (Christian Andreas Doppler (Born: Salzburg, Austria on 29 November 1803—died: Venice, Italy on: 17 March 1853). In this research work, Doppler postulated his principle—which was later coined as the Doppler effect, that the observed frequency of a wave depends on the relative speed of the source and the observer, and Doppler attempted to utilise this concept for explaining the respective colours occurring in binary stars.), who proposed this effect in 1842—in Prague. Fundamentally, this so-called Doppler effect, being the change in frequency of a wave, or another periodic event, for an observer who appears to be moving relative to its source. These relative changes in frequency can be best explained as follows: when the source of the waves is moving toward the observer, each successive wave-crest is emitted from a position closer to the observer than the previous wave. So, each wave will take slightly less time to reach the observer than the previous wave. Hence, the time between the arrival of successive wave-crests at the observer is subsequently reduced, causing an increase in the frequency. While they are travelling, the distance between successive wavefronts is reduced; so these waves tend to bunch together and additionally—from the observer's position—instigating to one's hearing, a higher tone. Conversely, if the source of waves is moving away from this observer, then each successive wave is emitted from a position farther from that of the observer—than the previous wave—so the arrival time between any such waves is increased. So, the distance between the successive wavefronts is proportionally increased, meaning the waves will be spread out and additionally, from the observer's viewpoint, instigating to one's hearing, a lower tonal effect.

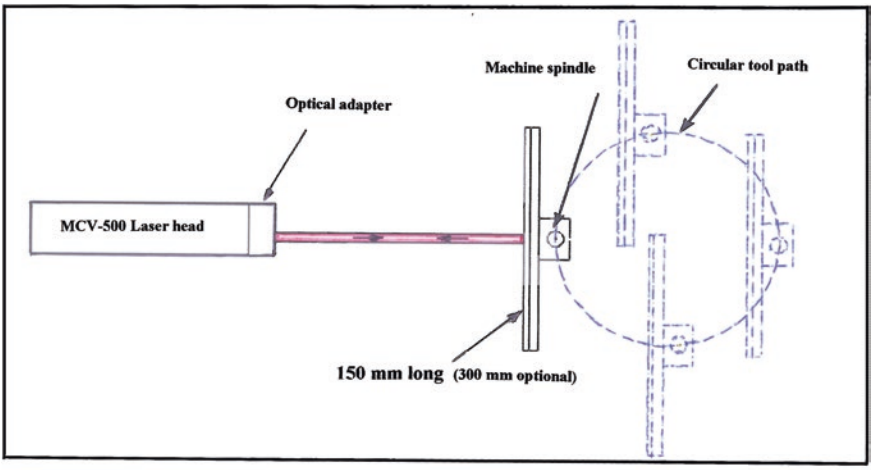

(a) Schematic arrangement of a *'Laser/ballbar'* circular test procedure.

(b) A *'Laser/Ball-bar'* circular test being conducted on a CNC Turret mill.

Fig. 4.8 A laser/ballbar testing configuration for a range of CNC machine tools (courtesy of Optodyne, Inc. (Compton, CA, USA))

lateral displacement. As schematically depicted in Fig. 4.8a, the laser is shown pointing perpendicular to the flat mirror, this being mounted into the machine's spindle. The spindle—in a non-rotating mode—moves along a path via a programmed circular interpolation, the flat mirror remains perpendicular to the laser beam, with the displacement along the laser beam direction being measured—even with a quite large lateral movement. Consequently, by repeating the same measurement in the direction 90° from the previous measurement, but with the same spindle motion, the displacement along the laser beam direction can once again be measured. Assuming this spindle motion is repeatable, the data obtained from these two measurements can be combined to generate the actual circular path.

The discrete hardware required for this commercial laser/ballbar is as follows: an MCV-500 single-aperture laser calibration system; with an optical adapter having a flat mirror target with a mount; plus a PC interface card; coupled to a notebook PC with Windows™-software installed. A typical CNC machine tool configuration and set-up of this type of laser/ballbar is shown in Fig. 4.8b. So, in the case of interpolating with a small radius, or alternatively, when utilising a high-feedrate circular test, but here under these differing conditions, it is necessary to have a high data capture rate. Moreover, with a special PCMCIA interface card,[5] a data rate up to 1000 data s^{-1} can be realistically achieved. For example, characteristically for a polar plot of a measured circular path having a radius of 100 mm, with a feedrate of 1000 mm min^{-1}, it necessitates a sampling rate of 30 s^{-1}. Furthermore, an ASCII output data file[6] can also be generated for external data processing, or for further investigative diagnostic activities.

Laser/ballbars create an established two-dimensional measurement, with principally both that of the *X*- and *Y*-axes coordinates being measured to generate a circular path. On the other hand, the telescoping ballbar could be considered as

[5]**PCMCIA interface Card** (It was originally designed as a standard for memory expansion cards—for computer storage. The existence of a usable general standard for notebook peripherals led to many kinds of devices being made available, these being based upon its form factor, including network cards, modems, also for hard disks.): accordingly, in computing terminology, this **PC Card** is a form factor peripheral interface, which was originally designed for laptops. It was originally introduced as a **PCMCIA Card**; the **PC Card standard**—as well as its successors—such as the **CardBus** that were defined and developed by the Personal Computer Memory Card International Association (i.e. PCMCIA).

[6]**ASCII output data file**: hence, any data files can be stored in one of two distinct ways:
(i) **Text file**—(i.e. also termed an **ASCII file**), stores information in ASCII characters, with this text file containing visible characters. Here, one can see the contents of file on the monitor, or edit it utilising any of the text editors. So, in a text file, each line of text is terminated, (i.e. delimited) with a special character known as an end-of-line (EOL) character. In these text files, some internal translations take place when this EOL character is either read or written;
(ii) **Binary file**—this is a file that contains data being in the same format in which the information is held in memory (i.e. in a binary form). Accordingly, in a binary file, there is no delimiter for a line. Furthermore, no translations occur in binary files and, as a result, binary files are both faster and easier for a programmer to read and write, than the alternative text files this is as long as the file does not need to be read, otherwise it might need to be ported to a different type of system. Hence, these binary files are the optimum manner to store any program information.

a form of one-dimensional measurement, essentially here with only the radius changes along the angular positions being measured. At this time, these actual angular positions are not measured, but are calculated by assuming the machine feedrate is a constant. Accordingly, with the application of a two-dimensional laser/ballbar measurement, it can provide some important dynamic information, such as the feedrate, tangential velocity, also acceleration. Moreover, the tool paths are not limited to just a circular path, for example tool paths with decreasing radius, or even a shallow spiral path are entirely possible to assess by this instrumentation. Any such laser/ballbar measurement is non-contact, and as a consequence of this, the circular path enables many revolutions to be easily measured. What is more, the radius of this circular path can be continuously varied. As previously described and further emphasised, the laser/ballbar employs a laser displacement meter for the measurement, and as a result, the accuracy is very high, typically in the region of 1 ppm—which is also traceable to NIST. Conversely, the telescoping ballbars utilise a transducer for its measurement, thus these instrumental accuracies tend to be slightly lower, and as such require periodic re-calibration—while also being sensitive to any ambient temperature changes. While yet another factor of significance is that since a laser displacement meter is employed in the laser/ballbar, this laser meter can also be utilised for linear calibration of the machine tool, enabling the generation of a compensation file. What is of some significance is that two sets of measurements with two specific set-ups are required for the laser/ballbar to generate the circular path, when compared to that of its telescoping ballbar commercial competitor, where only one set-up and just one set of measurements are necessary.

In order to reduce the setup time of the laser/ballbar, a steering mirror and optical adapter are also provided in its instrumental kit to facilitate the initial alignment and to increase its adaptability for any misalignment tolerance. A typical laser/ballbar set-up time is usually less than 10 min. In Table 4.1, a performance comparison is displayed, as a means of evaluation between both a laser/ballbar and the telescoping ballbar.

In summary, to evaluate or to simply optimise the performance of any CNC machine tool, it is imperative to assess both its static-positioning errors—see an example of this wired ballbar operation in Fig. A.24, as well as the dynamic tool path errors—also see an example in Fig. A.25. Various types of laser interferometers, telescoping ballbars or a LDDM can be utilised to check for any static positional errors and to generate a compensation file for the actual CNC's controller, thus markedly improving its machining performance. This performance improvement is achieved by these commercially available telescoping ballbars, or alternatively laser/ballbars, which can be employed to quickly assess the machine tool's dynamic characteristics such as servo mismatch, axis reversal spikes, backlash, scale mismatch, squareness errors, vibrations, etc. For example, in the case of a laser/ballbar, or its equivalent commercial instrumentation, it can be employed to optimise the machine performance by both generating a static displacement compensation file and for the dynamic tuning of the machine tool's servo-controllers.

Table 4.1 A simple performance comparison between two instrumental competing systems, namely the laser/ballbar and the telescoping ballbar

Performance	Laser/ballbar	Telescoping ballbar
Measurement sensor	Laser Doppler displacement sensor (LDDM)	Transducer
Measurement method	Measure *X*- and *Y*-coordinates to generate the circular path	Measure the radius changes along angular positions on a circular path
	Basically a two-dimensional measurement	Angular positions not measured
		Basically one-dimensional measurement
Sensor calibration	Linear accuracy is traceable to NIST	Transducer needs periodic calibration to NPL
Sensor range	Up to a few metres	Up to a few millimetres
Non-contact measurement	Yes	No
Radius of circular path	Continuously variable from 1 mm to 150 mm	Fixed radius with increments of 50 mm
Measured feedrate	Yes	No
Sampling rate	1000 data s^{-1}	250 data s^{-1}
Maximum feedrate	Up to 240 m min^{-1}	Up to a few m min^{-1}

Source Adapted from information provided from Wang and Griffin

4.2 Grid Encoders and Linear Comparator Systems

Grid Encoders

A grid encoder system is exhibited in both Figs. 4.9 and 4.10 and has the capability to dynamically test the contouring accuracy of CNC-controlled machine tools. For example, the grid encoder can perform a circular interpolation test with continuously adjustable radii ranging from 115 mm down to just 1 μm—at feedrates up to 80 m min^{-1}—see Fig. 4.10 (top). Furthermore, these types of grid encoders can also perform free-form tests—in two axes. The advantages of these kinds of grids include the fact that they are a form of contact-free measurement, which eliminates the influence of factors such as the ball bearings which are invariably utilised with the DBB tests, such was previously mentioned in Sect. 4.1.7. Similarly, the error resulting from the machine's geometry has no influence on the results of circular- nterpolation tests—with very small radii.

The grid encoder instrumental assembly consists of a grid plate with a circular encoded area of $\approx \varnothing 1400\,\text{mm}$ with a waffle-type graduation, which is embedded into a mounting base—see Fig. 4.9 (top)—as well as a scanning head—shown in Fig. 4.9 (bottom). The encoded area also employs diffraction-based technology, but slightly different to that of the linear comparator equivalent—depicted in Fig. 4.11. The big difference here is that this plate is encoded bi-directionally—that is, one

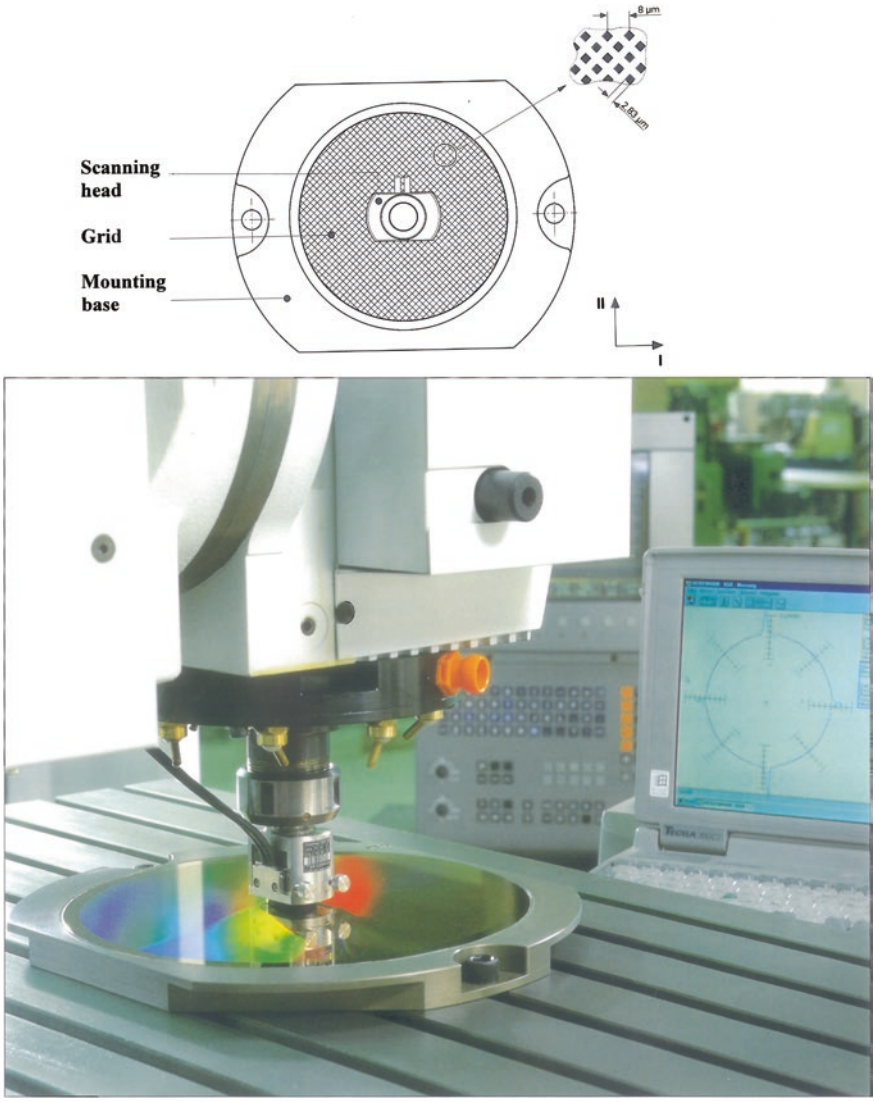

Fig. 4.9 A grid encoder system for calibrating two axes of an CNC machine tool (courtesy of Heidenhain (G.B.) Ltd.)

measuring standard can detect any movement in two directions simultaneously. It can potentially read around 2D corners. The grid's surface is somewhat similar to that of a chessboard (Fig. 4.9, top) but with its equivalent white squares being slightly higher than the corresponding black squares. Of course, these squares are not actually either white or black although nonetheless they are in fact produced with a structure which is more like a lattice coating, but covered with a protective

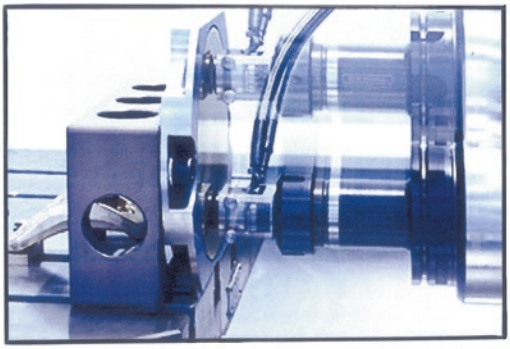

Utilising a *Grid encoder* for circularity testing at 115 mm radius to within 1 μm, at a feedrate of 80 m min^{-1}.
[Courtesy of WZLRTHAACHEN]

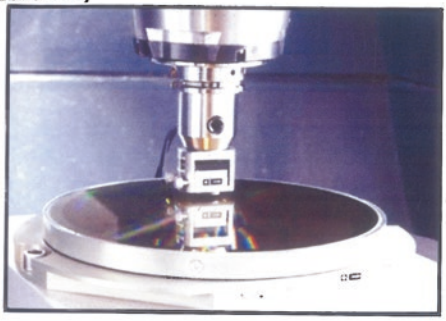

A *Grid encoder* being utilised to validate the potential sources of errors/uncertainties on a vertical Machining Centre when programmed by circular interpolation.

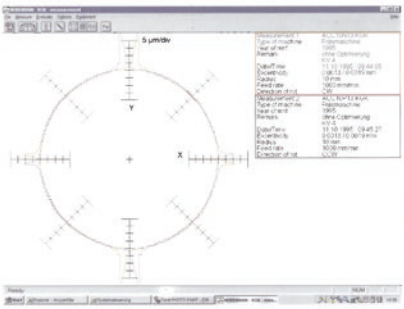

Standard display mode 'Circle large': the most conspicuous deviation results from reversal error at the quadrant transitions and the difference between clockwise and counter-clockwise traverse. Here, the machine tool was equipped with linear encoders.

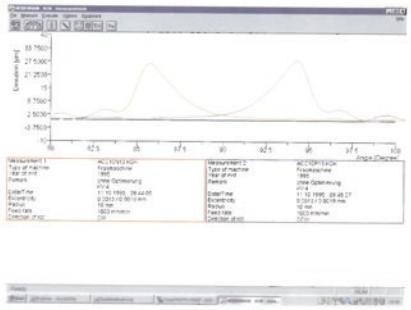

'Linear large' display mode.

Fig. 4.10 Motion error traces from both the circular interpolation and 'linearlarge' tests, on an CNC machine centre (courtesy of Heidenhain (G.B.) Ltd.)

material. Hence, the raised portions of this grid encoder, in combination with a spindle-mounted non-contact scanning head, can provide very accurate 2D measurements of $\leq \pm 2$ μm. This physical relationship allows for any 2D movement over the grid to be detected and then recorded accurately.

Throughout machine tool measurement—see Fig. 4.10 (top)—the scanning head moves just above and over the grid plate without making any form of mechanical contact. For machine tool set-up, the mounting base is fixed on the workpiece-holding element (e.g. such as the table of a machining centre—see Figs. 4.9, bottom and 4.10, middle-right) and then it is aligned. The instrument's scanning head is mounted in the locked toolholding element (e.g. namely that of the spindle of a machining centre) and is also approximately aligned. Typically and in practice, some spacer foil is often uiltised to set the scanning gap to an accurate and precise height of $\approx 0.5 \pm 0.05$ mm. Afterward, a finer setting is then attained by turning a set of adjustment screws on the scanning head, to optimise the measuring-signals displayed with the aid of the instrument's ACCOM evaluation software. For each of the two perpendicular machine tool axis directions, the grid encoder outputs two 90°-phase-shifted signals—with a signal period of 4 μm. These measuring-signals are then sent to a PC for further data processing, where it can subdivide the sinusoidal measuring-signals which is 4096-fold (i.e. achieving a signal sub-division)—to provide measuring-steps down to ≈1 nm—in each of the machine's axes. The bespoke software evaluates the measured values in accordance with the **ISO 230-4** standard. The ACCOM software makes it very simple to program for either a circular interpolation test, or any type of programmed free-form tests. The ACCOM evaluation software will also prompt the user for all the necessary parameter information and then generates the corresponding CNC program, which can be immediately loaded into its CNC controller through its communications interfaces (i.e. either by serial or Ethernet TCP/IP).

At this time, the circular interpolation program allows the scanner head to move over the surface of the grid plate, in exactly the same manner as for that of a circular contour check. Indeed, this grid encoder can perform the circular contour check just as easily as its equivalent ballbar instrumentation. Furthermore, it can also detect some additional errors that are perhaps much subtle for many of the equivalent commercial ballbar test instrumentation. The question one might pose here is, 'Why is this so?' Consider this example: on any CNC machine tool running a programmed circle, some mechanical errors on an axis become larger as the radius is increased—this being simply a matter of its proportional geometry. For example, a 0.025 mm pitch-down error over 1000 mm of travel is naturally less at the 200 mm point, which in turn, is even less at the 250 mm point, and so on. Hence, at some point along the radius, this pitch-down error becomes so small that it is somewhat hard to actually detect. Accordingly, if one agrees to this in principle, then it would be reasonable to assume that any errors caused by other machine tool sources could easily be obscured within the larger errors triggered by the additional magnitude of machine tool's geometry. That is exactly where the ability of this grid encoder starts to show some tangible and positive benefits, because it is not physically limited to the mechanical radius of, say, a ballbar with smaller circles, as these can be programmed to trace a path over the grid plate. Any potential mechanical errors that show clearly at large radii will become more difficult to determine on these small interpolated circles and the errors that are now present can be traced to the CNC itself, or to its associated electronics. By way of further

example, these excessive lead or lag errors, gain adjustments and interpolation problems can be considered as being the controller problems, not just as machine tool mechanical problems; although such control problems will have an effect on the movement of the machine tool and in optimising control. Grid encoders can demonstrate this aspect as physical evidence and not just as either a voltage, or an amperage value on a meter. Succinctly one might say that there is simply no other commercially available instrumental device—currently—that can portray these latter type of errors as a discrete movement within the machine tool.

Irrespective of the measuring instrument, the measuring data acquisition and accompanying analysis software is also extremely important. With any subsequent machine tool inspection/verification, there are many data computations that must be performed to ensure that the collected data are as relevant and useful as possible. Fortunately, the instrument's bespoke software makes it relatively easy to use, where it can run on a PC—in its Windows™ environment. Moreover, for these instrumental devices mentioned above, a counter-card is required for the PC running this bespoke software, which functions as an interface for the incoming measuring-signals. In the case of this ACCOM software for the grid encoder, these values—as mentioned—are in accordance with the **ISO 230-4** standard. The instrument's software also makes it relatively easy to program such routines as circular interpolation tests, curved path tests, as well as more simple controlled machine tool movements. Here, the program prompts the user for all the necessary parameter information and then generates the corresponding CNC program, which is then downloaded to the machine's CNC controller.

Therefore, yet another technical question that could be posed is, 'Will such machine tool inspection tests tell one everything needed to be known about a particular manufacturing process?'—but the answer here is that it is distinctly unlikely. This is because there are many other interrelated factors that must be accounted for when ensuring that the components produced on a machine tool are within acceptable tolerance limits, material considerations, tooling, fixturing, feeds and speeds, plus many more technical respects. By obtaining a clear indication of the machine's contouring performance, this will indicate how inherently capable this particular machine tool is at achieving the required levels of accuracy and precision from the outset, while pointing out many other machine tool correctable error factors.

Linear Comparator System

The linear comparator system set-up—is shown in Fig. 4.11—which is actually just a high-quality linear-scale having the physical construction based upon a robust U-shape channel geometry—of exceptionally high-toleranced and -quality steel. Here, this channel has precision graduations positioned in the bottom of its 'U-channel'—see Fig. 4.11 (top-right). Now, rather than utilising a typical transmission-based technology, these graduations are primarily designed around a special type of diffraction technology. This linear comparator is available in lengths up to one metre, having an accuracy of ≤ 1 μm, and accordingly it is equal to some types of the basic machine inspection lasers—over the same length. This linear comparator system is not intended to measure larger sized machines

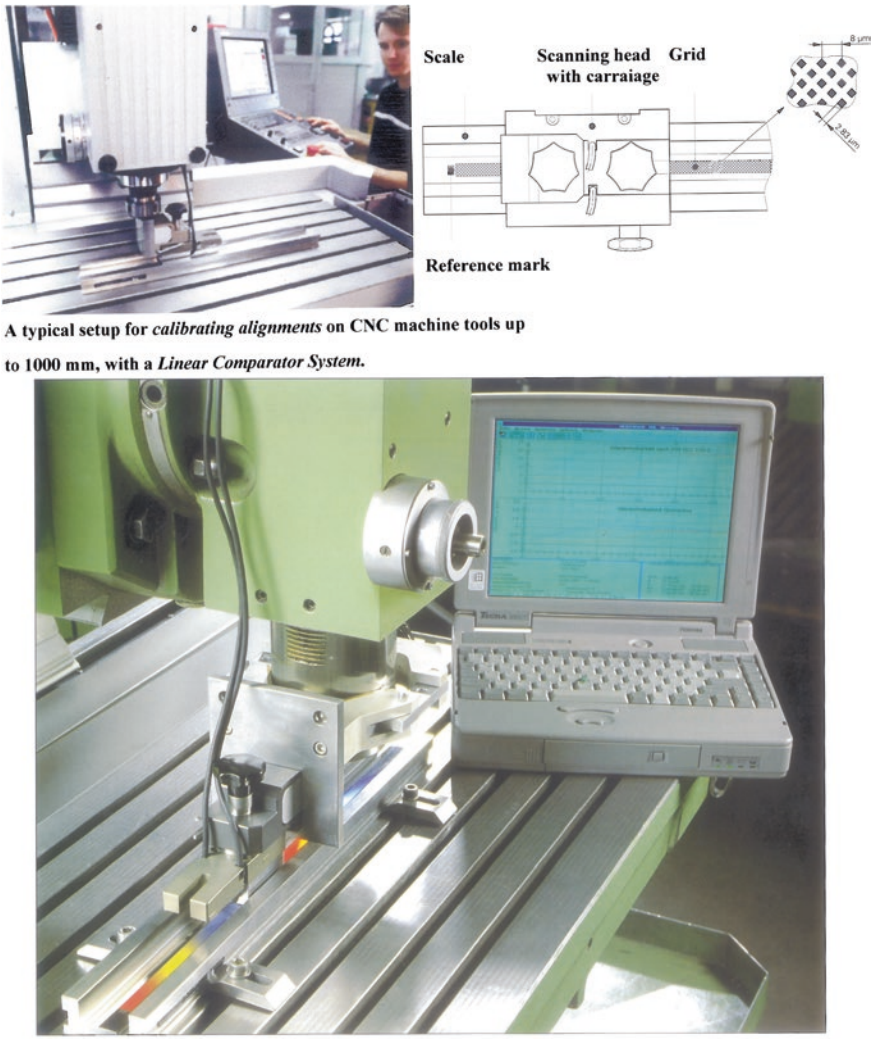

Fig. 4.11 A comparator system postioned on the table of a CNC milling machine (courtesy of Heidenhain (G.B.) Ltd.)

(e.g. normally having >2000 mm of axis travel), but it is beneficial for smaller machine tools and especially many types of machining centres. In many verification-type tests, this instrument can be utilised as a direct substitute for a laser for the linear displacement accuracy test. Simplistically, the linear displacement accuracy check is one of the four tests that are required in the one-day test procedure—as defined by **ASME**—where users will find it to be accurate, convenient, fast and economical—when it is compared to some alternative types of instrumental measurement technologies.

To operate this linear comparator system, the steel scale assembly is placed on the work surface (typically on the machine tool's table) aligning it to the machine's linear axis, then the scanning unit is affixed to the spindle—see Fig. 4.11 (bottom). Here, a specially made carriage has been configured so that the scanning head can be magnetically attached to a clamp on the machine's spindle. Once this physical arrangement has been undertaken, the scanning unit is then released and in consequence, exhibits non-contact between that of the linear scale, nor with that of the scanning unit. Next, the machine's axis measurement occurs—via a programmed motion of this axis—and the bespoke software accordingly performs specific and routine calculations. The entire machine tool validation process occurs in ≈15 min per axis. Apart from this linear displacement accuracy check, this artefact's technology can also be utilised for linear repeatability checks—for axes ranging from 1000 to 2000 mm, utilising a simple form of a consecutive step-and-repeat process for the axis length being assessed.

4.3 Rotary Analyzer System and Calibration Rings

Rotary Axis Analyzer System ('R-Gage')—for Machine Tools

The five-axis machine tool rotary axis checking ystem with its wired probe is depicted in Fig. 4.12 (top), which can be considered as an in-depth analysis and diagnostics instrument for calibrating a machine tool's rotary and linear axes. Thus, this so-called R-Gage is a calibration metrology instrument utilised to gather positional data information for CNC machine tools having both linear and rotary axes. It employs a three-axis kinematic probe (shown in Fig. 4.12, top-right) and a precision master ball to determine the positioning location (being partially shown in situ, in Fig. 4.12, top-left) and relationship errors between moving axes. The system is typically applied to three-, four-, or five-axis vertical, or horizontal machining centres, but can also be utilised on either a mill/turn centre, as well as on a wide range of multi-tasking CNC machines.

Where there is simultaneous linear and rotary motion, the true positioning accuracy of the tool relative to the workpiece is where it becomes considerably harder to determine this action. As a consequence, this R-Gage can establish the true position error by measuring the deviation from a commanded path. Consequently, for any machine tool developers and maintenance operatives alike, it can quantify a machine's performance in real-time with the possibility of establishing both its static and dynamic measurements. The probe's basic configuration allows high-accuracy 3D measurements to determine equally the location and the squareness of either an integral or auxiliary fitment rotary table. This calibration instrument has either a wired or wireless probe fitted to the rotary axis analyzer, with the location of a master ball being accurately determined in the three dimensions, namely *X*-, *Y*-, as well as the *Z*-axes, simultaneously. The probing system can measure the actual position of the master ball's centre point. This master ball

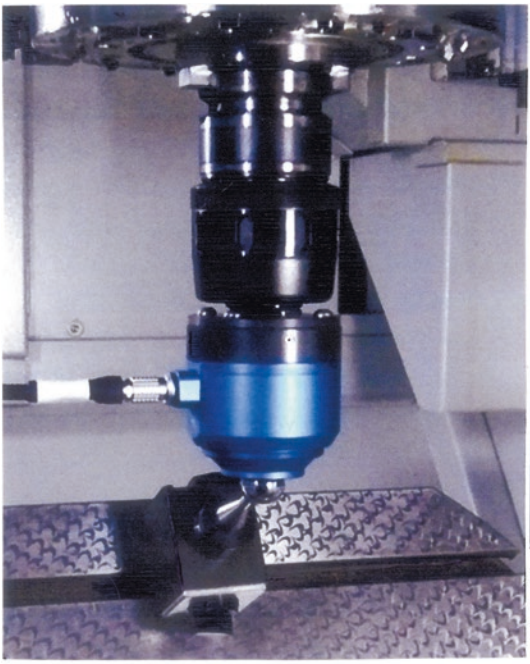

5-axis Rotary Analyzer System (i.e. 'R-test') on a Machining Centre.
[Courtesy of IQL, East Hartford, CT (USA)]

Kinematic seating for 'R-test' ball.
[Courtesy of IBS Precision Engineering, Eindhoven, The Netherlands]

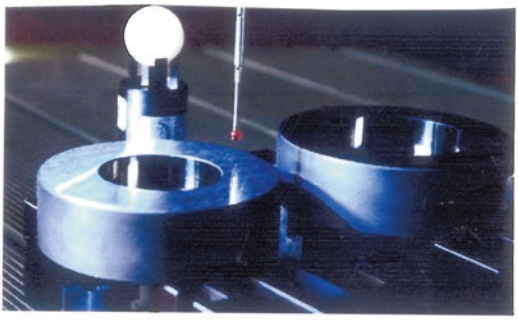

Calibrating machine tools with Calibration Rings.
[Courtesy of Tampere University of Technology (Finland)]

Fig. 4.12 Utilising a 'rotary analyzer system' and 'calibration rings' to calibrate machine tools

is customarily located on the non-rotating part of the machine—as typically shown in Fig. 4.12 (top-left). The probe is mounted on the rotating part of the machine tool but here, this probe is normally stationary within the spindle. After its use in machine verification, its data gathering readings are then displayed on a PC near to the machine, with this testing regime being performed either statically or dynamically.

While this rotary axis checking system verification device can give both position and orientation information, it can also be utilised as a simple go-/no-go device. Here, the bespoke software enables a CNC user to establish a baseline condition. The rotary axis analyzer system can then be applied periodically, although the diagnostic strategy adopted can be either, at the start of each shift, or once per week, or once per month; or how often the maintenance schedule dictates it is necessary. This type of scheduled periodic in-service maintenance application will highlight whether the machine has remained within an acceptable performance range, or if any corrective action needs to be taken prior to executing the desired manufacturing processes.

The rotary axis analyzer system measuring criteria are normally utilised in establishing:

- **machine acceptance**—the instrument is a very efficient tool when performing a machine acceptance test, verifying the kinematic accuracy and precision of the machine tool. Different kinematic tests can be defined, but most commonly they are the tests according to: **ISO 10791-6**[7]—which defines circular motion by either simultaneous three- or five-axis control. In the case of three-axis control, the accuracy of a circular trajectory is verified when the circular interpolation motion of two linear axes is synchronised with that of the rotation of a rotary axis—at constant speed. Equally, with five-axis control, the accuracy of these circular trajectories are verified when the circular interpolation motion with three linear axes and two rotary axes are controlled simultaneously while at constant feedrate;
- **rotary table position and compensation**—with a simple measurement, the actual location of a rotary table can be determined with a high degree of accuracy (i.e. with a measuring uncertainty of the wired probe being <0.6 μm and that of the wireless probe being to <1.0 μm). The machine tool is programmed to incrementally step through the range of the rotary axis, with the linear axes following the motion. After each step, the machine is paused and a measuring data point is taken. The probe measures the actual machine's location in 3D simultaneously. Based upon this static measurement procedure, the rotary axis analyzer's software determines the location of the rotary table, plus the actual squareness of this table. The results are directly presented in the machine's coordinate system and can then be applied to correct the machine's kinematic model that presently resides within the machine's CNC controller. A subsequent repeat of this measurement test will reveal if the improvement of the machine's positioning behaviour has been achieved;
- **dynamic analysis**—these dynamic measurements are performed by this metrological instrument to reveal the machine's accuracy of the paths described by

[7]**ISO 10791-6 Test conditions for Machining Centres—Accuracy of feeds, speeds and interpolations:** it will differ between three different machine types of configurations: (i) swivel-head machines; (ii) rotating table machines, (iii) trunnion machines; as well as for machines equipped with either swivel-heads, or rotary tables combined. All these machine configurations can be measured with this rotary axis analyzer system.

the simultaneous movement of two or more CNC linear and rotary axes. In this case, measuring data points are taken 'on-the-fly' (i.e. in dynamic motion). The dynamic rotary axis analyzer measurement is an advanced measurement technique showing the machine's accuracy, with all motional axes included in the measurement. This measurement assessment provides the machine tool with the anticipated accuracy and precision one would expect when making high-quality machined components. Both machine tool developers and many professional maintenance providers alike can quantify a machine's performance in real-time, with both of these static and dynamic measurement tests.

Summarising this rotary axis checking system (Fig. 4.12, top), it can measure the real position of the master ball centre point, which is conveniently mounted on the non-rotating part of the machine—such as its table. The probe is fixed to the rotating part of the machine—but here with its spindle stationary—and after testing, its diagnostic data being displayed accordingly on a PC near to the machine—in accordance with **ISO 10791-6**.

4.4 Calibration Spheres and Rings—for CMMs

A CMM is a very complex integral metrological device with many internal components that one cannot see (i.e. a typical, but highly sophisticated, CMM is shown in Fig. 1.45a) which could potentially be in various unanticipated stages of disrepair resulting from either it being damaged and worn or simply in an out-of-adjustment state. Although here, if one assumes that this CMM is in an as-new status, then its qualified probe provides the expected measurement results, based upon the manufacture's product specifications and in so doing delivers a baseline for any subsequent and succeeding measurements. A newly installed and calibrated CMM with its qualified probe forms an overall measurement system which is both tight and well balanced with its accuracy and repeatability being certified by the manufacturer and presented for a company's records—in the form of a calibration certificate. A simple set of numerical values gives one an expected range of where the CMM users own measurements should fall, when measuring any calibrated artefacts of known size, as when qualifying with calibration ring gauges—depicted in Fig. 4.12 (bottom). Today, the majority of CMMs are calibrated, or reverified, to one of two international standard specifications, such as the **ASME B89**, or **ISO 10360-2**.[8]

[8]**ISO 10360-2:2009—Geometrical product specifications (GPS)—Acceptance and reverification tests for coordinate measuring machines (CMM)—Part 2: CMMs used for measuring linear dimensions**. Here, this standard specifies the acceptance tests for verifying the performance of a coordinate measuring machine (CMM) utilised for measuring linear dimensions—as stated by the manufacturer. Moreover, it also specifies the reverification tests that enable the user to periodically reverify the performance of the CMM. These acceptance and reverification tests given in this **ISO 10360-2:2009** standard, which are applicable only to Cartesian-type CMMs—using contacting probing systems of any type—but operating in the discrete point probing mode.

By way of example, if a CMM was calibrated to the **ASME B89-specification**, then it will have one numerical value for repeatability. Explaining this criterion in more detail, if the number is, for example 0.004 mm (i.e. 4 μm), this numerical value means that when measuring a certified sphere its location measurement should repeat to ≤0.004 mm. Conversely, if this CMM was calibrated to **ISO 10360-2**, it has a numerical value for the probing test, typically being, for example 0.0025 mm value. This number is termed its baseline probing uncertainty being 0.0025 mm (2.5 μm), and this standard states that the probing error of 25 points, measured on a certified sphere, does not exceed this value. This use of strict terminology is similar to that of both its sphericity and size deviation—from the certified diameter. As a consequence, if this CMM has been certified to **ISO 10360-2** when it is required to measure a certified calibration ring, its diameter deviation and roundness should comply to within ≤2.5 μm.

One of the most important and basic tests performed on any CMM is a check of its probing set-up. Simply by qualifying the probe set-up, as one would normally undertake for any given inspection project—see Fig. 2.9b—then it is necessary to create an appropriate inspection routine in the automatic mode within the CNC controller on the CMM to measure that same calibration sphere—see Fig. 2.10—with at least 25 points and 4 rows, but with the same probe angle. Then, repeat this identical measurement three or more times and with the probing-results from this previous testing regime, they should all lie within the baseline range—as discussed earlier. If not, then some further metrological investigation and testing is required. Should these subsequent test results fall outside the acceptable limits, then one must work backwards through the probing set-up to attempt to diagnose this actual probing problem; beginning this probing diagnosis with the qualification sphere confirming the diameter is as specified in the CMM's software and assessing that it matches the certified diameter of the sphere. Next, it is always advisable to double check the actual probe's stylus is actually seated and situated within its holder correctly. Confirm that this probe is so and that it is tightly secured, also that it matches the diameter and length specified within the CMM software. These relatively simple and precautionary steps resolve the most common problems that are likely to occur and luckily the most inexpensive to fix—concerning most CMM accuracy/repeatability issues. Once these actual potential variables of probe uncertainty have been confirmed and then adequately addressed, it is then possible for one to re-run the sphere program—to see if these metrological issues have been fully resolved.

If by following the previous precautionary diagnostic steps, but here, it did not resolve the problem, then potentially it can become somewhat expensive if it is necessary that a damaged, or worn-out probe needs subsequent replacement. Accordingly, if the working probe has non-interchangeable modules (i.e. similar to that of some commercial company's products, such as types TP-2 or TESAStar-p) initially check the connection to the probe head is basically tight, then confirm it is not sticking (i.e. when its probe is triggered) or has some excessively leaking oil

present. Moreover, it is also advisable to check and adjust the probe's touch trigger force is within the manufacturer's technical specification, with either a strain-gauge arrangement, or a special purpose triggering unit. Although if either of the two previous symptoms arise, namely sticking or leaking, then the best advice is to replace this whole probe unit and then go on to investigate the CMM's software. Once the CMM user has confirmed everything tested for this CMM was within acceptable limits, then basically re-run the sphere program to see if these probing issues have been successfully resolved.

ISO 10012:2003—Measurement Management Systems—Requirements for Measurement Processes and Measuring Equipment

The adoption of, say, **ISO 10012:2003** by an industrial company, will provide commonality in dimensional measurement, while providing a guide to the implementation of this standard for manufacturers. The actual standard specifies generic requirements and provides guidance for the management of measurement processes, as well as metrological confirmation of measuring equipment utilised to support and demonstrate compliance with metrological requirements. As a consequence, this standard specifies quality management requirements of a measurement management system, which can then be used by an organisation performing measurements as part of the overall management system and to ensure metrological requirements are met.

It should be made clear here that this **ISO 10012:2003** is not intended to be used as a requisite for demonstrating conformance with, say, **ISO 9001**,[9] or **ISO 14001**[10]; or to any other standard for that matter. So, interested parties can agree to use this **ISO 10012**:**2003** as an input for satisfying measurement management system requirements in certification activities. Other standards and guides exist for particular elements that affect measurement results, for example, the details of measurement methods, the competence of personnel or for any form of inter-laboratory comparisons.

[9]**ISO 9001** (**ISO 9001**, which is the arguably the most popular of the international management system standards and, is currently being revised by the ISO Committee with the final publication anticipated towards the end of 2015.) is a certified quality management system (QMS) for companies/organisations who want to prove their ability to consistently provide products and services that meet the needs of their customers and for other relevant stakeholders.

[10]**ISO 14000** (While, **ISO 14001**—in this series—is an internationally accepted standard that outlines how to put an effective environmental management system into place. This standard is designed to help companies/businesses remain commercially successful without overlooking environmental responsibilities. It can also help a company to expand while reducing the environmental impact of this growth. Accordingly, an **ISO 14001** system provides the framework to allow a company to meet increasingly high customer expectations of corporate responsibility, as well as legal, or regulatory requirements.) is a family of standards that has been developed relating to environmental management that exists to help companies/organisations, to: (a) minimise how their operations (processes, etc.) negatively affect the environment (i.e., cause adverse changes to air, water or land); (b) comply with applicable laws, regulations and other environmentally oriented requirements, and (c) continually improve—in the above circumstances.

References

Journals and conference papers

Abbaszadeh-Mir, Y., Mayer, J.R.R., Cloutier, G. & Fortin, C., *Theory and simulation for the identification of the link geometric errors for a five-axis machine tool using a telescoping magnetic ball-bar*, Int. J. Prod. Res., Vol. 40 (18), 4781-4797, 2002.

Acko, B., *Calibration of Measuring Instruments on a Coordinate Measuring Machine*, Advances in Production Engineering Management (APEM – Journal), Vol. 2 (3), 127-134, 2007.

Blackshaw, D.M.S., *Machine tool accuracy and repeatability – a new approach with the revision of ISO 230-2*, Proc. of LAMDAMAP III, Computational Mechanics Pub., 91-100, 1997.

Bringmann, B. & Knapp, W., *Machine tool calibration: Geometric test uncertainty depends on machine tool performance*, Precision Eng'g., Vol. 33 (4), 524–529, Oct. 2009.

Bryan, J.B., *A simple method for testing measuring machines and machine tools – Part 1: Principles and application*, Precision Eng'g, Vol. 4 (2), 61-69, April 1982.

Bryan, J.B., *A simple method for testing measuring machines and machine tools – Part 2: Construction details*, Precision Eng'g, Vol. 4 (3), 125-138, July 1982.

Burdekin, M. & Park, J., *Contisure – a computer aided system for assessing the contouring accuracy of NC machine tools*, Proceed. of 27th Int. MATADOR Conf., April 1988.

Cauchick Miguel, P.A., King, T. & Abackerli, A.J., *CMM touch trigger performance verification using a probe test apparatus*, J. Braz. Soc. Mech. Sci. & Eng. Vol. 25 (2), Rio de Janeiro, April/June 2003.

Florussen, G.H.J., Delbressine, F.L.M. & Schellekens, P.H.J., *Accuracy Analysis of multi-axis machines using double Ballbar*, Proceedings on: Improving Machine Tool Performance, Vol. 2, 533-543, July 1998.

Glos, R., *Do-It-Yourself Machine Inspection*, Modern Machine Shop, Jan. 1996.

Hadzistevic, M., Strbac, B., Budak, I., Vukelic, D.J. & Hodolic, J., *Analysis of the Operator Influence on the Accuracy of the Calibration Styli Results in CMM*, Annals of DAAAM for 2011 and, Proc. of the 22nd Int. DAAAM Symposium, Vol. 22 (1), 1665-1666, 2011.

Hargreaves, B., *Measuring Up*, Professional Eng'g., 71-73, April 2015.

Hermann, G., *Geometric Error Correction in Coordinate Measurement*, Acta Polytechnica Hungarica, Vol. 4 (1), 47-62, 2007.

Ibaraki, S., Sawada, M., Matsubara, A. & Matsushita, T., *Machining tests to identify kinematic errors on five-axis machine tools*, Precision Eng'g., Vol. 34 (3), 387-398, 2010.

Ihara, Y., *Ball Bar Measurement on Machine Tools with Rotary Axes*, Int. J. Automation Technol., Vol. 6 (2), 180-187, 2012.

Kakino, Y., Ihara, Y. & Nakatsu, Y., *Measurement of motion errors of NC machine tools and diagnosis of their origins by using telescoping magnetic Ballbar method*, CIRP Annals, Vol. 36 (1), 377-380, Berne, Jan. 1987.

Kakino, Y., Ibaraki, S., Yamaji, I., Ogawa, K. & Ota, H., *Measurement of Motion Accuracies of Five-axis Machine Tools by Using the Double Ball Bar Method DBB5*, Proc. of 2008 Int. Sym. on Flexible Automation, 2008.

Kao, J.Y., Yeh, Z.M., Tarng, Y.S. & Lin, Y.S., *A study of backlash on the motion accuracy of CNC lathes*, Int. J. Mach. Tools Manufact., Vol. 36 (5), 539-550, 1996.

Knapp, K., *Test of the Three-dimensional Uncertainty of Machine Tools and Measuring Machines and its relation to the Machine Errors*, Annals of the CIRP, Vol. 32 (1), 459-464, 1983.

Küng, A. & Meli, F., *Self calibration method for 3D roundness of spheres using an ultraprecision coordinate measuring machine*, Proc. of 5th Euspen Int. Conf. – Montpellier, France, Vol. 1, May 2005.

Kunzmann, H. & Wäldele, F., *On Testing Coordinate Measuring Machines (CMM) with Kinematic Reference Standards (KRS)*, Annals of the CIRP, Vol. 32 (1), 465, 468, 1983.

Lai, J.M., Liao, J.S. & Chieng, W.H., *Modeling and analysis of nonlinear guideway for double-ball bar (DBB) measurement and diagnosis*, Int. J. of Mach. Tools Manuf., Vol. 37 (5), 687–707, 1997.

Lee, D-M., Cha, Y-T. & Yang, S-H., *Analysis of eccentricity in the ball bar measurement*, J. of Mech. Science and Technol., Vol. 24, 271-274, 2010.

Lei, W.T., Sung, M.P., Liu, W.L. & Chuang, Y.C., *Double ballbar test for the rotary axes of five-axis CNC machine tools*, Int. J. of Mach. Tools Manuf., Vol. 47 (2), 273–285, 2007.

Lei, W.T., Paung, I.M. & Yu, C.C., *Total ballbar dynamic tests for five-axis CNC machine tools*, Int. J. of Mach. Tools and Manuf., Vol. 49 (6), 488–499, 2009.

Lotze, W., *Circle form test for testing of coordinate measuring machines and machine tools*, Proc. Int. Symp. on Metrol. for Quality Control in Prod., 289-293, Tokyo, 1984.

Marin, D. & Predincea, N., *Circular Path for CNC Machine Tools*, Proc. in Manufact. Systems, Vol. 8 (1), 29 – 34, 2013.

Matano, K & Ihara, Y., *Ball bar measurement of five-axis conical movement*, Proc. of LAMDAMAP VIII, 34-43, 2007.

Matúš Beňo, Marek Zvončan, Martin Kováč, Jozef Peterka, *Circular Interpolation and Positioning Accuracy Deviation Measurement on Five Axis Machine Tools with Different Structures*, Tehnički vjesnik 20 (3), 479-484, 2013.

Mayer, J., Mir, Y. & Fortin, C., *Calibration of a five-axis machine tool for position independent geometric error parameters using a telescoping magnetic ball bar*, in: Proc. of 33rd Int. MATADOR Conf., 13275–14280, Manchester, UK, July 2000.

NAS979, *Uniform Cutting Tests – NAS series, metal cutting equipment specifications*, 34-37, 1969.

Nubiola, A., Slamani, M. & Bonev, I.A., *A new method for measuring a large set of poses with a single telescoping ballbar*, Precision Engineering, Vol. 37 (2), 451–460, April 2013.

Pahk, H.J., Kim, Y.S. & Moon, J.H., *New technique for volumetric error assessment of CNC machine tools incorporating Ballbar measurement and 3D Volumetric error model*, Int. J. of Mach. Tools & Manufact., Vol. 37, 1583-1596, Nov. 1997.

Painter, P.R., Smith, G.T. & Hope, A.D., *Performance Evaluation of a Machining Centre using Laser Interferometry and Artifact-based Techniques*, Proc. of FAIM'92, CRC Press, Inc. (NY), 962-974, 1992.

Rodríguez-Ibáñez, D., Alonso, J. & Antonio Quiroga, J., *Squareness error calibration of a CMM for quality control of ophthalmic lenses*, Int J. Adv. Manuf. Technol., Vol. 68, 487–493. 2013.

Shafie, S., Chiles, V., Jenkinson, D. & Blackshaw, D.M.S., *Static and dynamic measurements of machine tools*, Proc. of LAMDAMAP III, Computational Mechanics Pub., 215-227, 1997.

Smith, G.T., Hope, A.D., Painter, P.R. & Blackshaw, D.M.S., *The Assessment of Machining & Turning Centres, using Artifact-based Techniques*, Proc. of LAMDAMAP I, Computational Mechanics Pub., 275-286, 1993.

Smith, G.T., *Inspection of Components Manufactured on a Machining Centre, by On- and Off-line Techniques*, Proc. of FAIM'96, Begell House, Inc. (NY), 216-224, 1996.

Smith, S., Measuring machine errors with a ball bar, Vol. 64 (4), Cutting Tool Eng'g., April 2003.

Srinivasa, N., Ziegert, J.C. & Mize, C.D., *Spindle thermal drift measurement using the laser ball bar*, Precision Eng'g., Vol. 18 (2/3), 118-128, April/May 1996.

Tarng, Y.S. & Cheng, H.E., *An investigation of stick-slip friction on the contouring accuracy of NC machine tools*, Int. J. Mach. Tools Manufact., Vol. 35 (4), 565-576, 1995.

The Ins and Outs of Ballbar Calibration, Quality Magazine, May 5, 2003.

Ueno, S. & Matsumaru, S., *Evaluation of numerically controlled machine tool positioning accuracy*, Proc. of LAMDAMAP VI, WIT Press., 485-494, 2003.

Wang, M., Hu, J. & Zan, T., *Kinematic error separation on five-axis NC machine tool based on telescoping double ball bar*, Frontiers of Mechanical Engineering in China, Vol. 5 (4), 431-437, Dec. 2010.

Wang, S.M., Yu, H.J. & Chen, D.F., *A Ball-Bar Based Error Measurement Method for a RRTTT-Type Five-Axis Machine Tool*, Advanced Materials Research, Vol. 126, 785-790, Aug. 2010.

Wang, W., Zhang, Y. & Yang, J., *Double Ballbar Measurement for Identifying Kinematic Errors of Rotary Axes on Five-Axis Machine Tools*, Advances in Mechanical Engineering, Vol. 2013, Article ID 198487, Sept. 2013.

Weikert S, *R-Test, a New Device for Accuracy Measurements on Five Axis Machine Tools*, The CIRP Annals, Vol. 53, 429-432, 2004.

Xiang, S., Yang, J. & Zhang, Y., *Using a double ball bar to identify position-independent geometric errors on the rotary axes of five-axis machine tools*, Int. J. of Advanced Manufact. Technol., Nov. 2013

Zargarbashi, S.H.H. & Mayer, J.R.R., *Assessment of machine tool trunnion axis motion error, using magnetic double ball bar*, Int. J. of Mach. Tools Manufact., Vol. 46 (14), 1823–1834, 2006.

Books, booklets and guides

Bosch, J,A., *Coordinate Measuring Machines and Systems*, CRC Press, 1995.

Donmez, M.A., *A general methodology for machine tool accuracy enhancement: Theory, application & implementation*, Ph.D diss., Purdue University, West Lafayette, IN, USA, 1985.

Eden, A., *The search for Christian Doppler*, Springer-Verlag Pub. (Wien), 1992.

Jalote, P., *CMM in Practice: Processes for Executing Software Projects at Infosys*, Addison-Wesley Professional Pub., 2000.

Kakino, Y., Ihara, Y. & Shinohara, A., *Accuracy Inspection of NC Machine Tools by Double Ball Bar Method*, Hanser/GardnerPublications, Inc. (Cincinnati, Ohio), 1993.

Mize, C.D., Ziegert, J.C., Pardue, R. & Zurcher, N., *Spatial measurement accuracy tests of the laser ball-bar*, Report for CRADA No. Y-1293-02244: between Martin Marietta Energy Systems & Tetra Precision Inc., Aug. 1994.

Parmar, K.L., *Development and Use of a Telescoping Magnetic Ball Bar for Checking the Contouring Performance of Machine Tools*, Pub. by: University of North Carolina at Charlotte, 1992.

Paulk, M.C., *The Capability Maturity Model: Guidelines for Improving the Software Process* [i.e. for CMM's], Addison-Wesley Pub., 1995.

Weck, M., *Handbook of Machine Tools - Vol. 3*, Pub.: John Wiley & Son Ltd, Chichester, UK, 1984.

Chapter 5
Artefacts for Machine Verification

"There is a very good saying that if triangles invented a god, they would make him three-sided."
Charles, Baron de Montesquieu
(French Writer and Historian)
[1689–1755]
(In: Lettres persanes 59)

5.1 Introduction to Artefact Verification—For Interim CMM Checks

In order for product quality to be significantly improved with time, the use and metrological application of the ubiquitous Coordinate Measuring Machines (CMMs)—a universal metrology instrument—must have their accuracy and precision regularly monitored and verified, with stated performance levels substantiated against accepted International Standards; often this is termed Interim-checking. Consequently, this verification testing procedure is undertaken to ISO 10360-2, which specifies a wide range of mechanical artefacts for such CMM performance verification. With the introduction of CMM technology, an obvious question that regularly arises and was succinctly suggested by Knapp et al. (1991), where it was stated, "How can a user of a CMM test the accuracy specified and guaranteed by the supplier after installation of the machine and later, during the years of operation?" Here, it seems somewhat obvious that standardised testing methods are necessary, to examine a typical CMM's performance and the development of accurate and efficient techniques for verifying such high value-added capital equipment.

G.T. Smith, *Machine Tool Metrology*, DOI 10.1007/978-3-319-25109-7_5

5.1.1 An Introduction to CMM Error Sources

The typical error sources found in CMM measurements might be categorised as follows:

- **Spatial errors**—these are errors in the measured position of a point on the part's surface being determined by the accuracy of the components assembled in the CMM—such as: its guideways; the measurement scales fitted; type of probing system and its associated qualification sphere; the external environment in which the CMM operates—ambient temperature, temperature gradients, humidity and vibration; typical probing strategy adopted—the magnitude and direction of the probe force, the type of probe stylus utilised and the measuring speed of this probe; plus the part's geometric characteristics; also in addition to its known—elasticity, surface texture, hardness and component's mass;
- **Computational errors**—these errors are found in the estimated dimensions and form deviations of the workpiece being determined by the CMM software—employed to estimate the geometry of the workpiece; the correctness of the CMM's computer; the number and relative position of measured points; as well as the degree to which the part-geometry differs from its ideal geometric form;
- **Geometric errors**—in CMMs, these are either measured directly, typically by laser interferometers coupled to their specialist optics, or indirectly by techniques typified by sequential multi-lateration. After the geometric errors have been measured, the errors present can then be utilised to error-correct the machine.

Previously, it was established that these notable CMM geometric errors were shown to be the 21 sources of kinematic error. Such error sources in the machine components are due to either the CMM's imperfect manufacturing, or alignment problems during its initial assembly.

5.1.2 ISO 10360 and CMM Performance

The CMM performance verification guidelines and tests are based on sampling the length measurement capability of the instrument, determining whether its performance conforms to the manufacturer's stated maximum permissible error of length measurement (see Maximum permissible error of indication of a CMM—for size measurement). Further, the calibration tests will only allow a statement to be made about the overall length-measurement capability of the CMM; this limitation is due to the complicated way in which errors combine. Therefore, the sampled length measurement uncertainty cannot really be considered as representative of all the possible measurement tasks that the CMM is capable of performing. The central-question that must be asked is, does one either, "Calibrate, or verify a CMM?" The three words that are often confusingly interchanged when

considering CMMs and to avoid any future confusion, the correct terminology relating to them, are listed below:

1. **Qualification**—of its stylus/probing system, this being the task that is undertaken on a day-to-day basis to determine the effective radius of the stylus tip;
2. **Verification**—typically for a CMM, this is a task undertaken at planned periodic intervals (i.e. often annually) to determine if the CMM still meets the manufacturer's specification;
3. **Calibration**—which is a CMM task which is normally undertaken upon its installation, when it is necessary to determine the magnitude of all the 21 kinematic error sources.[1]

ISO 10360-2—Objectives

The **ISO 10360-2** tests—see more information in Appendix 1c—have three technical objectives being listed within this standard, namely, to test the

1. **error of indication of a calibrated test length using a probing system**—without any RAM axis stylus tip offset;
2. **error of indication of a calibrated test length using a probing system**—with a specified RAM axis stylus tip offset;
3. **repeatability**—of measuring a calibrated test length.

Major benefits accrue from a testing regime, with the measured results having direct traceability to the unit of length (i.e. metre) and providing information on how the CMM will perform on similar length measurements. Here, then, the **ISO 10360-2 Standard** specifies typical performance requirements that can be assigned by the manufacturer, or the user, for their CMM. Additionally, this CMM standard identifies the manner of execution of such acceptance and reverification tests, demonstrating the stated requirements, rules for proving conformance, together with applications for which the acceptance and reverification tests can be utilised.

ISO 10360—Overview

In the current-interpretation of **ISO 10360-2:2009**, it describes in some detail the following testing procedures, these being the:

- **Acceptance test**—this test verifies that both the performance of the CMM and that of its probing system is as stated by the manufacturer of the machine. Hence, an acceptance test is always undertaken during the installation of the machine;
- **Reverification test**—this test enables the end-user to reverify the CMM and its associated probing system, but in this instance, on a periodic basis according to the user's requirements and actual usage-conditions for this particular machine;
- **Interim check**—this metrological check enables the end-user to determine whether the CMM and its accompanying probing system are operating correctly—between any regular reverification tests.

[1]NB Often this metrological-activity being referred to as: Error-mapping a CMM.

Previously, one of the main objectives of this **ISO 10360 Standard** was to enable the end-user to carry out these tests in the most efficient manner, allowing the user to freely specify the test locations and/or orientations anywhere within the machine's working volume. However, these previous testing procedures did not imply an omission, or lack of care in formulating the standard, but moreover, it ensured that the supplier of the measuring system could not truly optimise the CMM's performance. Nonetheless, in the current standard it distinctly lists four required positions, plus three default positions, with additional recommended requirements for any high aspect-ratio CMMs. These acceptance and verification tests for CMMs are essentially length-measuring tasks, ensuring that the tests now closely conform to frequently performed measurement procedures undertaken by an end-user. Here, the probing error test is carried out at acceptance and reverification, which is designed to assess any potential probing errors associated with any probing systems that are currently operating in the discrete point measuring mode. Since it is virtually impossible to isolate such probing errors from its machine errors, or to some additional system errors, which have both static and dynamic origins inherent within the CMM (e.g. due to the CMM's servo system) they will also be measured by this more rigorous test. To reiterate, the CMM performance verification, namely acceptance testing, reverification tests, plus interim checks will not guarantee actual traceability of measurement for all measurement tasks that the CMM performs. Nonetheless, the current version of the Standard recognises that in an industrial environment, such tests and checks are presently the closest approximation to traceability available to the CMM-user.

ISO 10360—Latest Interpretation

This latest assessment method principle can be utilised to calibrate a test length—being traceable to the metre. Moreover, it establishes whether the CMM is capable of measuring within the stated maximum permissible error of length measurement for a CMM, with a specified ram axis stylus tip offset—having both zero offset and 150 mm offset. Previously, the former **ISO 10360 Standard** specified no offset. Currently, the calibrated test length may now be by either a Ballbar or Laser interferometer system—see previous chapters for more details—while formerly, the single stylus probing test that appeared in **ISO 10360-2:2001**, does not occur in the current version of **ISO 10360-2**. This actual test has been relocated to the **ISO 10360-5 Section**, thus replacing **ISO 10360-5:2000**. Furthermore, **ISO/PAS 12868** has now been prepared to allow the single stylus probing test to be available, until the publication of the new edition of **ISO 10360-5**, whereas **ISO 10360-5:2010** has recently been published and **ISO/PAS 12868:2009**, has been cancelled.

ISO 10360—Its Limitations

In **ISO 10360-2** test, the number of measurements standardised is a compromise between its attention to detail and practical and economical implementation. As a consequence, two separate tests are undertaken on the same CMM, even if one assumes there is a time-invariant, which could potentially create different problems, such as probing errors, length measurement errors, plus several more error sources. These tests are primarily for the following reasons, being the choice of

test locations and the CMM's environmental conditions plus its repeatability. Such limitations originate from the definition of the test, which specifies the number of different repeated measurements, allowing this test to be performed just once—thus meeting the manufacturer's environmental specifications. Justification for this is a compromise to ensure that the test is economically feasible, being based upon educated experience in that most CMM performance is determined by such a test, with the awareness that a more all-embracing coverage would only be achieved at prohibitive cost for such test implementation.

5.1.3 Material Standard of Size and CMM Accuracy

The **ISO 10360 Standard** defines the following conditions of a Material standard as, "A material measure reproducing a traceable value of a dimensional quantity of a feature". Moreover, this standard also defines a Material standard of size as, "A material standard reproducing a feature of size." In previous versions of the **ISO 10360 Standard**, it was strongly recommended that this Material standard should be either a Step gauge (i.e. see Figs. 5.1, 5.2, 5.3, 5.4, 5.5 and 5.6), or alternatively, an End/Length bar (i.e. see Fig. 1.5b), otherwise a series of Gauge blocks (i.e. see Figs. 1.5a and 2.9a), conforming to **ISO 3650**.[2] Here, the Material standard of size has to contain two or more nominally parallel planes, with the distance between these planes being correctly and precisely specified. In Figs. 5.2, 5.3, 5.4, 5.5 and 5.6, Step gauges are shown verifying CMMs. **ISO 10360-2:2009** now utilises terminology concerning the calibrated test length. With bidirectional measurements verification can make use of a Gauge block, Step gauge, Ballbar or Laser interferometer, so long as the probing directions are in opposition at either end of the calibrated test length. Any unidirectional measurements can be undertaken so long as they are supplemented with those of bi-directional measurements. Accordingly, suitable calibrated test lengths can be acquired from Step gauges, Ballbars and Laser interferometers, by either unidirectional probing, or Laser interferometers without contact probing. The Material standard of size employed for such testing must itself be calibrated. Here, the influence of the uncertainty of calibration must be considered and any calibration procedures must be traceable to the relevant International Standard.

CMMs—How Accurate Are They?

In the case of a major CMM manufacturer, the improvement in the machine's thermal stability has enabled them to significantly increase their working temperature accuracy range. In particular, on this company's previous CMM models—see

[2]**ISO 3650—Geometrical Product Specifications (GPS)**, refers to length standard Gauge blocks: Thus, the International Standard specifies vital design and metrology features of Gauge blocks—having rectangular cross-sections—and a nominal length 'l_n', ranging from: 0.5 to 1000 mm. Limit deviations and associated tolerances are stated for Calibration grade '*K*', as well as for grades: '0', '1' and '2'—for a variety of measurement requirements.

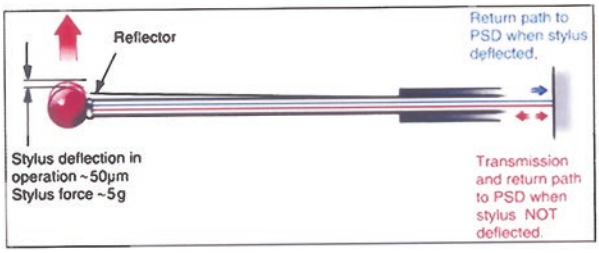

Laser beam inside the hollow stylus is used to detect the exact position of the stylus' tip. [Source: M.Albert, Modern Machine Shop (2006)]

(a) Temperature Variable Accuracy (TVA) for differing measuring environments:

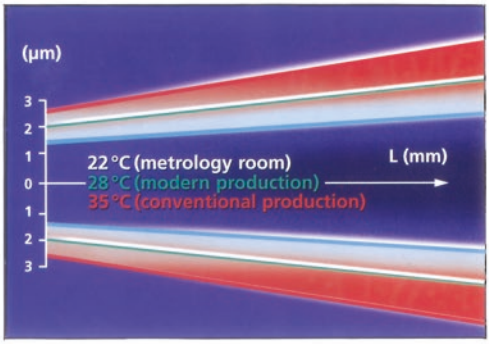

(b) Comparison of TVA under differing measurement conditions:

Case 1: Metrology room.....22 °C.....MPE_E = 1,7 µm + L / 286

Case 2: Modern production.....28 °C.....MPE_E = 2,0 µm + L / 244

Case 3: Conventional production.....35 °C.....MPE_E = 2,35 µm + L / 195

(c) An accurate & precise artefact employed in the calibrated assessment of a Bridge-type CNC CMM:

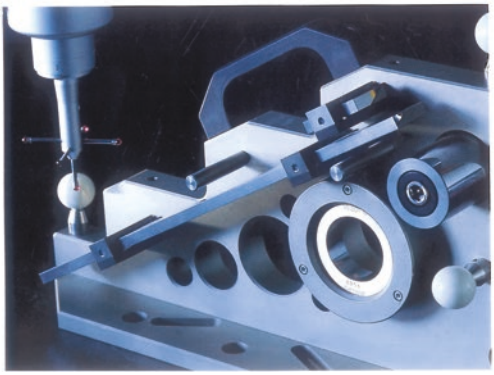

Fig. 5.1 The calibration of a coordinate measuring machine and its associated artefact, is dependent upon the environment utilised during the assessment (courtesy of Carl Zeiss Limited)

(a) Step Gauge rig situated on a bridge-type CMM, for verifying the accuracy and precision of Step Gauges:

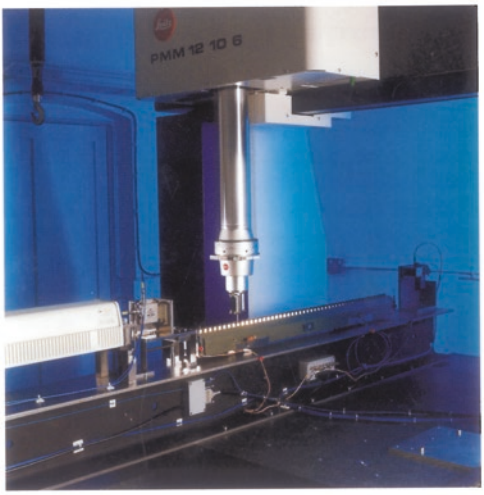

(b) Detail of touch-trigger probe about to inspect one of the steps on a 1000 mm Step Gauge:

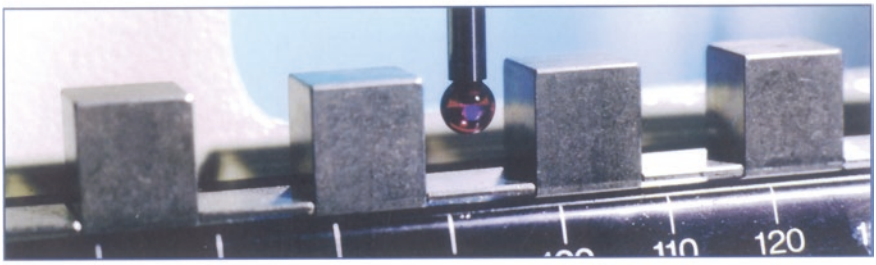

NB Calibration accuracy of ± (0,2 + 0,8L) µm - at the 95% confidence limit.
Where: L = length of artefact (m).

Fig. 5.2 Step-gauges are standard reference artefacts that can be employed to verify the performance of coordinate measuring machines (CMMs) (courtesy of Centre of Length Metrology, NPL)

Fig. 1.45a for such a CMM—the accuracy was guaranteed within the range: 18–22 °C, but with technologically advanced materials and redesign, they can now guarantee this latest version of the CMM, at an increased temperature range of: 15–35 °C. All types of CMMs are internationally calibrated to operate and function correctly at their optimum temperature performance, this being at 20 °C. Any ambient temperatures that exceed this exact temperature level can cause structural

(a) Precision Step Gauge situated on a Coordinate Measuring Machine (CMM):

(b) Step Gauge shown spanning the major diagonal of the working envelope on a CNC milling machine, equipped with Touch-trigger Probing:

(c) Step Gauge shown lying horizontally aligned along the X-axis of the CNC machine's rotary table, equipped with Touch-trigger Probing:

(d) Step Gauge with a swivel support and base, shown at various angular inclinations:

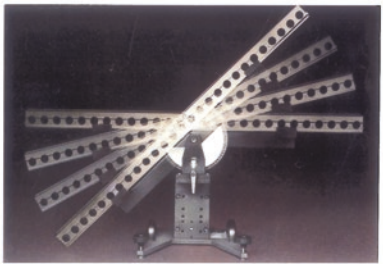

Fig. 5.3 Step gauges can be employed to monitor/calibrate both machine tools and coordinate measuring machines (CMMs) (courtesy of Kolb & Baumann GmbH & Co. KG)

changes to the machine's structural-components, while adversely affecting the CMM's accuracy and precision. Therefore, many of today's CMM manufacturers will utilise strategically positioned temperature sensors on each of their guideways to monitor, then correct for any temperature changes. Additionally, some CMMs

(a) An individual gauge block obliquely orientated in three-dimensions on the table of an CMM, showing the outside machine dimension (L_e) being measured:

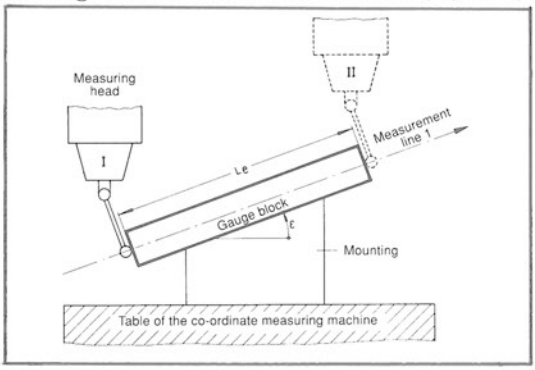

(b) Castellated Step Gauge obliquely orientated in three-dimensions on the table of an CMM, with an outside length (L_e) being measured:

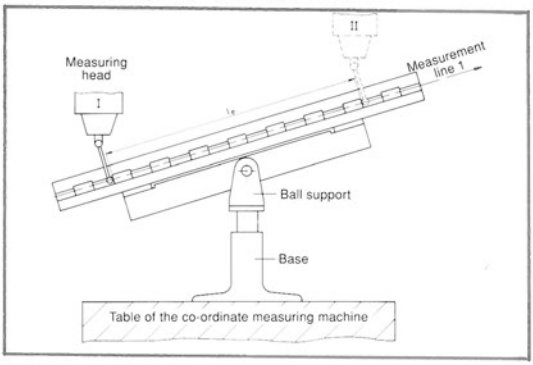

(c) Step Gauge obliquely orientated in three-dimensions on the table of an CMM, illustrating measurement of an inside dimension (L_i), of an outside dimension (L_s), or of the position (L_p) of a gauge face as a distance from the datum face:

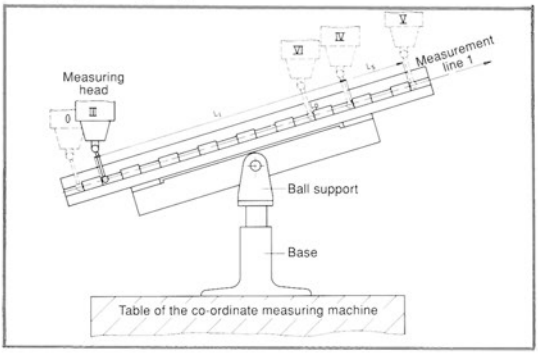

Fig. 5.4 Schematic representation of gauge block and step gauge usage-in three-dimensions (courtesy of Kolb & Baumann GmbH & Co. KG)

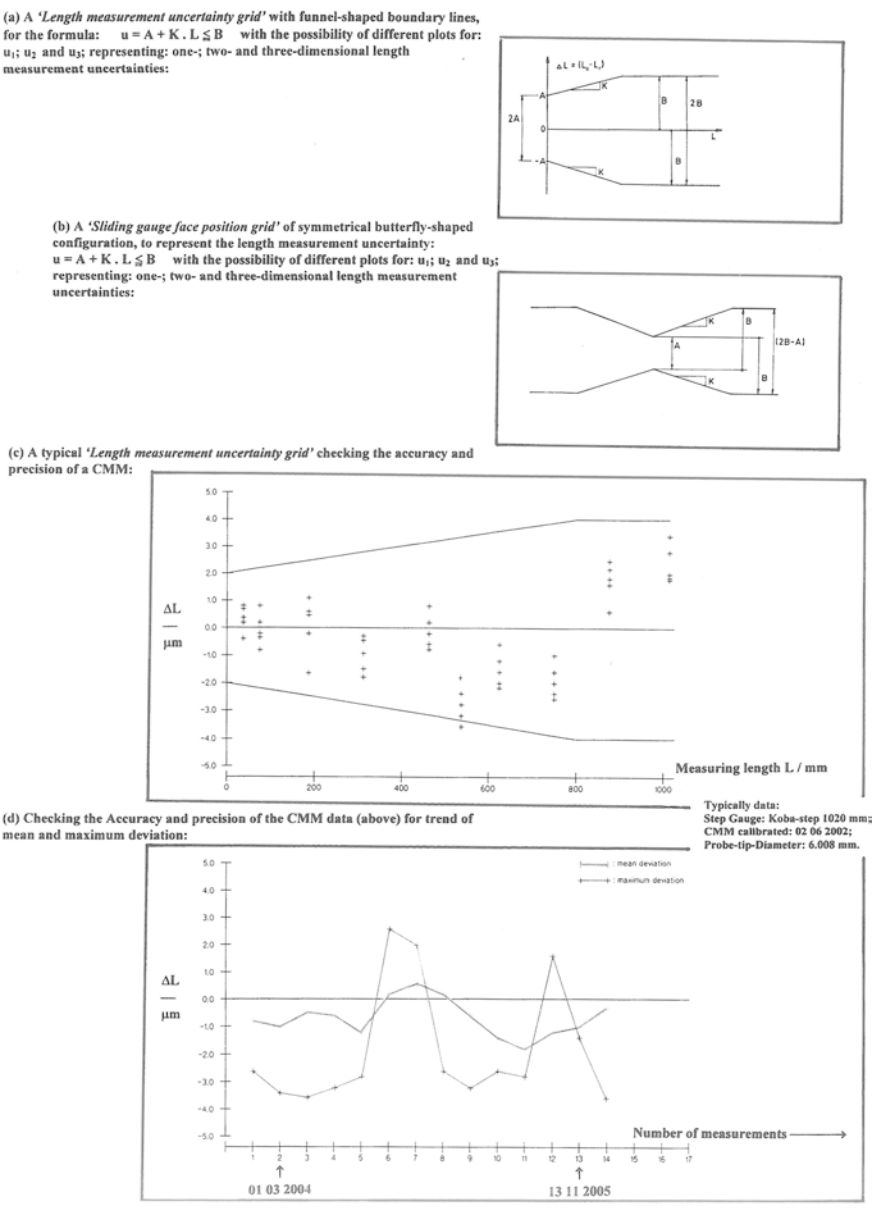

Fig. 5.5 Establishing the measurement uncertainty of a coordinate measuring machine (courtesy of Kolb & Baumann GmbH & Co. KG)

have a temperature probe that can be included in the tool changer, which can measure the temperature of the actual part and then compensate for certain temperature ranges by up to ±20 °C. As a result, when these CMM temperatures vary,

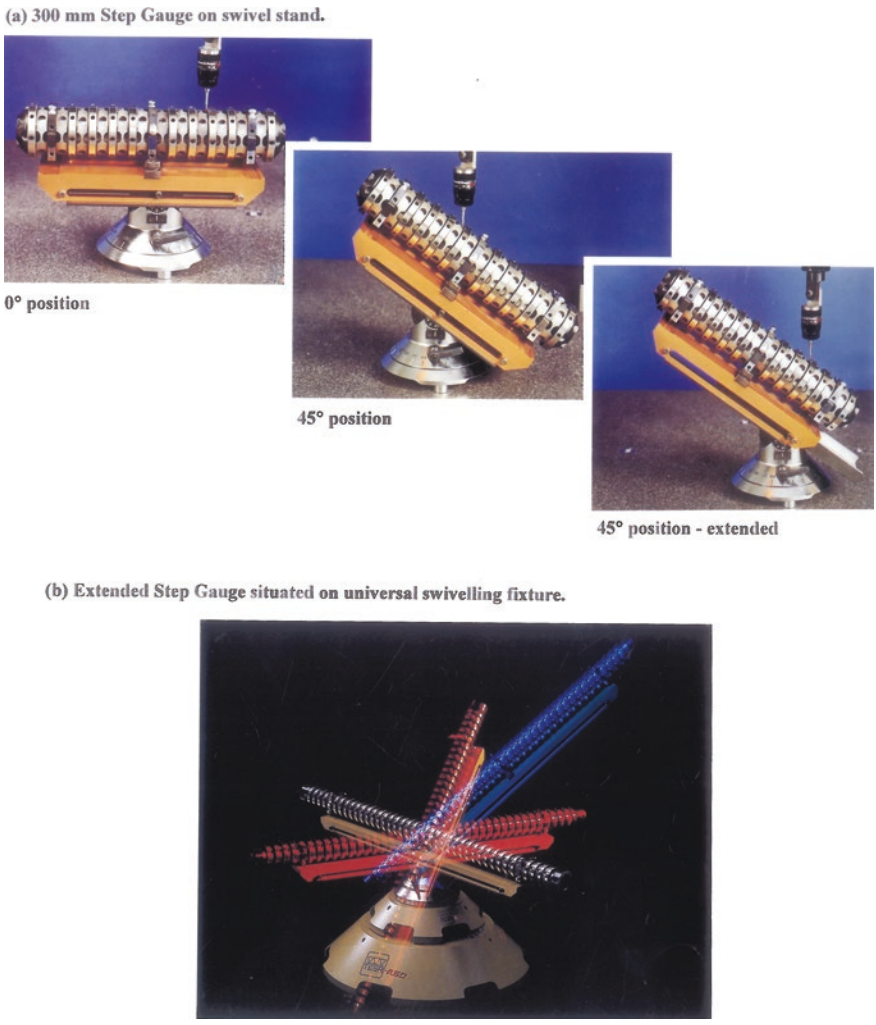

Fig. 5.6 Step gauges can be utilised for volumetric calibration of machine tools and CMMS (courtesy of Tesa RSD/Brown and Sharpe)

for whatever reasons, then the changes are filtered through an appropriate algorithm and the measurement results are compensated to that degree.

In various CMMs, they are accurate within the specified temperature range, but the question is, "How accurate are they really within that range?" One leading CMM company defined the temperature accuracy specification, allowing the user to know exactly how precise the machine is, even as this temperature imperceptibly changes. In this particular CMM manufacturer's case, they introduced the term Temperature Variable Accuracy (TVA) that demonstrates how accurate the CMM is performing,

whilst still measuring up to 35 °C and, by knowing this temperature affect, the CMM can then reduce its measurement uncertainty—see Fig. 5.1a, b. While this CMM manufacturing company is on record as stating that, "On a standard machine, we provide the temperature spec in which we guarantee a certain measuring uncertainty". Furthermore, they then go on to say, "When we build a machine at a perfect 20°, the machine only uses maybe 25 % of the total tolerance range of error. When we go to the high end spec we are still going to be within that bandwidth, but we don't know exactly how accurate it is. With the TVA, you know exactly what you can expect in terms of measuring uncertainty, because you know exactly where it is going to be at a given temperature". [Source: Carl Zeiss Ltd. (2014)].

It seems somewhat obvious that the coefficient of thermal expansion (CTE)[3] will vary for different materials that either a CMM is manufactured from, or its calibration artefacts, in this latter case, typically for Gauge blocks, which are used in many cases for CMM verification.

5.1.4 CMM—Length Measurement and Maximum Permissible Errors

In the case of an error of indication for a CMM with regard to size measurement (i.e. its length measurement error) this is the error with which the size of the material standard can be established by the CMM. Accordingly, here, a measurement taken through the two opposing points on an artefact, or workpiece, along two nominally parallel planes, normal to one of these planes, necessitates the probing head to approach such points from opposite directions. Any length measurement error of a CMM, can be expressed in micrometres (μm) and is denoted by the symbol: 'E_L'.

For the maximum permissible error of indication of a CMM for size measurement, the term: '$E_{\mathrm{MPE},\,L}$' is defined as the extreme value of the error of indication of a CMM for size measurement 'E_L' permitted by the specifications and regulations for a CMM. Consequently, the maximum permissible error of indication of a CMM for length measurement error (i.e. '$E_{L,\,\mathrm{MPE}}$') can be defined in one of the three following expressions:

[3]**Coefficient of thermal expansion (CTE)**: this is how much the workpiece material changes its size for a given temperature change, consequently it is known as the: Coefficient of linear thermal expansion. Typically, the CTE of a material such as steel, is normally-expressed as: 11.6×10^{-6} °C^{-1}. Hence, to correct for a length @ 20 °C, one will use the following equation:

$$L_{20} = L_T + (20 - T) \cdot \alpha \cdot L_T$$

Where: 'L' is length (mm); 'T' is the temperature at which the length was measured (°C); 'α' is the coefficient of thermal expansion (no units).
NB If the calibrated test length is not of a normal CTE material (e.g. $\alpha < 2 \times 10^{-6}$ °C^{-1}), then the corresponding $E_{0,\mathrm{MPE}}$ and $E_{150,\,\mathrm{MPE}}$ values, are designated with an asterisk (*). For example, $E_{0,\,\mathrm{MPE}}$* and an explanatory note is usually provided, giving both the material and its CTE.

Table 5.1 Typical symbols that have been historically employed in CMM measurements—in ISO 10360

Meaning	2009	2001	1995
Length measurement error	E_L	E	ΔL
Repeatability range of the length measurement error	R_0	–	–
Maximum permissible error of length measurement	$E_{L,\,\mathrm{MPE}}$	MPE_E	E
Maximum permissible limit of the repeatability range	$R_{0,\,\mathrm{MPL}}$	–	–
Single stylus form error	P_{FTU}	P	$r_{\max} - r_{\min}$
Maximum permissible single stylus form error	$P_{\mathrm{FTU,\,MPE}}$	MPE_P	R

Source Flack, D. @ The NPL (July 2011)

1. $E_{L,\,\mathrm{MPE}} = \pm$ minimum of $(A + L/K)$ and B;
2. $E_{L,\,\mathrm{MPE}} = \pm(A + L/K)$;
3. $E_{L,\,\mathrm{MPE}} = \pm B$.

Where: 'A' is a positive constant expressed in μm and supplied by the manufacturer; 'K' is a dimensionless positive constant supplied by the manufacturer; 'L' is the measured size, in mm; 'B' is the maximum permissible error '$E_{\mathrm{MPE},\,L}$' in μm, as stated by the CMM manufacturer.

These expressions can be applied to any location and/or orientation of the Material standard of size—within the CMM's measuring volume. Measurements must be undertaken by utilising the three axes of the CMM, with the expressions applying for any position and orientation of the material standard within the CMM's working envelope. The maximum permissible error of length measurement '$E_{L,\,\mathrm{MPE}}$' is newly defined as: "The extreme value of the 'length measurement error' ('E_L'), permitted by specifications". In the case of **ISO 10360-2**, the values of: '$L = 0$' mm, and '$L = 150$' mm (i.e. namely the default values) are specified. Of some note it is that a maximum permissible error (**MPE**) rather than a maximum permissible limit (**MPL**) specification, is employed when the test measurements determine errors, therefore testing an **MPE** specification necessitates the practical use of calibrated artefacts.

In the **ISO 10360 Standard**, designated symbols have been utilised historically, with just some of these being presented in Table 5.1 (above).

With the examples of the use of these CMM symbols they can also include: 'E_0'—the length measurement error with minimum offset (i.e. being as small as possible); '$E_{0,\,\mathrm{MPE}}$'—maximum permissible error of length measurement with minimal offset; '$E_{150,\,\mathrm{MPE}}$'—maximum permissible error of length measurement with RAM axis stylus tip offset of 150 mm.

5.2 Purpose-Made Artefacts—Testpieces

Purpose-made artefacts (i.e. metrology-testpieces) are specifically designed to duplicate both the type and orientation of workpiece features, which are routinely found and employed on CMMs. The major advantages of utilising such Purpose-made

artefacts are that they can stringently test the probing- and software-capabilities of the specific CMM utilised. These so-called testpieces are employed to exhaustively examine the CMM, within its normal working-volume; although in the case of machines equipped with pallet systems, this may entail artefact-repositioning—in some situations, perhaps up to several times. There are a number of disadvantages when utilising these testpieces, in that if the measurement task changes—for some technical/metrological reason, then a new variety of such a testpiece may now be required. While yet another shortcoming could be that the prospective testpiece is somewhat difficult to both manufacture and measure to the high accuracy demanded, or alternatively, it might simply be too costly to calibrate. Sometimes, a high-quality calibrated replica of the actual workpiece article that is normally measured might also be utilised. In this instance, the term high quality would normally refer to it having an excellent surface finish and accurate/precise part-geometry that will not in fact, significantly affect the part's uncertainty of measurement. Moreover, such Purpose-made artefacts, should ideally be both thermally and dimensionally stable.

In Fig. 5.1c, the photograph depicts a complex and sophisticated metrological-testpiece, which is produced by a well-known CMM manufacturer. Additionally, it can be positioned within the CMM's volume in several differing testpiece-orientations. As mentioned, in reality, a testpiece can be simply just a typical workpiece that is measured on the CMM, but it is labelled as such and can only be utilised for this type of CMM verification. Normally, it is recommended that this testpiece is measured several times immediately after a comprehensive CMM verification and then subsequently at defined periodic intervals.

5.3 General Artefacts for CMM Verification

There are a quite and diverse range of highly specialised and purpose-built artefacts—ranging in both their size and accuracy/precision—that are currently available for the verification of CMMs. Due to limitations in this current text, only some of these artefacts can be highlighted within the following section.

5.3.1 Step Gauge—Its Calibration

Typical mechanical reference artefacts such as Step gauges can provide a cheap and effective way of assessing the performance of CMMs—for its length measuring task. These Step gauges are particularly valid when performing the formal performance verification procedures described in many National, or International Standard specifications, notably in: **BS EN ISO 10360-2:2009**.[4]

[4]**BS EN ISO 10360-2:2009—Geometrical product specifications (GPS)**. **Acceptance and reverification tests for coordinate measuring machines (CMM)**. This is the full-titled designation for CMM's utilised for measuring linear dimensions.

With the introduction of the **BS EN ISO 14253-1:2013**[5] decision-rules have significant implications for users choosing suitable reference artefacts for CMM verification. This is because this recently revised standard gives explicit guidance on the measured part's pass/fail criteria. These criteria take and then consider the uncertainty of the verification process, which consequently depends on both the uncertainty in the calibration of the reference artefact, together with the control of the machine's working-environment. Normally, there is a high level of uncertainty associated with reference artefacts, which reduces the conformance zone assigned to the CMM. As a consequence, it is considered distinctly desirable to have the best possible calibration of an artefact.

International Standards Organisations such as typified by The NPL—within the UK—have a state-of-the-art closed-controlled room, which has been developed expressly for a semi-automated Step gauge calibration system, which utilises laser interferometry when achieving the smallest uncertainty for calibration of these Step gauges. Within this metrology facility, a range of differing length Step gauges up to 1500 mm long can be calibrated. Measurements are made on the Step gauge's central length as well as its face parallelism—see Fig. 5.2a—with here, the UKAS calibration certificate stating the distance between the centre of the faces highlighting any faces where the parallelism measurements show some cause for concern—see Fig. 5.2b. The Calibration and Measurement Capability (CMC),[6] this being expressed as an expanded uncertainty ($k = 2$) for a particular Step-gauge, will depend upon the length of this gauge and its overall quality of manufacture. Typically, for example, a 1000 mm Step gauge can be calibrated with an expanded uncertainty of 0.34 μm—much more will be mentioned concerning the factors concerning the uncertainty of measurement and will be provided in Chap. 7.

5.3.2 Step Gauge—For Verification of the Accuracy of CMMs

When considering the operation of industrial metrology, the actual physical bodies of known length that can be contacted by mechanical sensors, are extremely important as Reference standards—when actually measuring a metrological instrument's geometrical parameters. Such reference standards have become essential for assessing the accuracy of either two-or three-axis CMMs—which employs such mechanical sensors. So, by checking these length measurements, any uncertainty has proven to be both a highly informative and an economical method for the acceptance testing and on-going monitoring of CMMs. Invariably, high-quality artefacts such as the Step gauge can be utilised in an enormous variety of ways. For example, they

[5]**BS EN ISO 14253-1:2013—Geometrical product specifications (GPS)**. **Inspection by measurement of workpieces and measuring equipment**. Decision-rules for proving conformity, or nonconformity with specification.

[6]**Calibration and Measurement Capability (CMC)**: thus, this CMC expressed as an expanded uncertainty of ($k = 2$), which is given by the following equation: $(0.1 + 0.000236 \cdot L)$ μm. Where: L is the length in mm.

have the advantages of either uni-, or bidirectional, targeting and enabling measurements from all the gauge faces along a line-of-measurement in succession, while requiring only the briefest of time for setup/preparation and measurement. Any localised errors can simply be detected in the CMM and characteristics can be derived for the individual coordinate axes of the machine—see Fig. 5.3.

With the assistance of the length measurement uncertainty, the manufacturer, or an end-user can specify and check the accuracy of a CMM to establish its suitability for length measurement. In dimensional metrology, this fundamental task is of particular importance due to the fact that in practice, the majority of measuring requirements are for the verification of lengths. Therefore, Length measurement uncertainty is defined by a range of International Standards, typically such as **VDI/VDE 2617 Part 2.1**,[7] which states the uncertainty with which a CMM allows the precisely known distance between two points on two mutually parallel gauge faces situated in succession along a line-of-measurement to be remeasured. In Fig. 5.4a is illustrated a typical measurement of this kind, here having an individual parallel Gauge block with an outside length 'L_e', being arranged obliquely in three dimensions and whose length is then remeasured by successive contacts with this Gauge block, having the Probe head in positions 'I' and 'II'. Likewise, with this type of linear measurement on a more sophisticated type of Castellated Step Gauge—see Fig. 5.4a, b showing the dimensional spacings of different kinds for undertaking test measurement—all of which can be obtained simultaneously, as follows:

- **Outside dimension** 'l_e'—for example, with the Probe head in positions 'I' and 'II', as shown in Fig. 5.4b;
- **Inside dimension** 'L_i'—for example, with Probe head in positions 'III' and 'IV', as shown in Fig. 5.4c;
- **Rear-face to rear-face dimension** 'L_s'—for example, with Probe head in positions 'III' and 'V', as shown in Fig. 5.4c;
- **Front-face to front-face dimension** 'L_p'—for example, with Probe head in positions 'VI' and 'IV', as shown in Fig. 5.4c;
- **Positional length** ('L_p' **of a gauge face from the datum gauge face**)—for example, with Probe head in positions 'VI' and 'IV', as shown in Fig. 5.4c.

The schematic illustrations shown in Fig. 5.4 show some of the options available for each type and size of spacing with this Step gauge. In consequence and in magnitude, the differences between, for example, the length value of 'L_a' could be indicated by the following: the CMM; its printout; or being displayed by its output processor; as well as the true value 'L_r' of the measurement uncertainty 'U'. What this means is that a value such as 'L_a' can be both larger and smaller than 'L_r'. Hence, the value of the length measurement uncertainty, is normally derived from the form of a length-dependent formula, as follows:

$$U = A + K \cdot L \leq B.$$

[7] **VDI/VDE 2617 Part 2.1**—***Accuracy of coordinate measuring machines***: parameters and their reverification—Code of practice for the application of **DIN EN ISO 10360-2** for length measurement 2012-07.

At this time, a distinction should be made between the term '$U1$'—specified for one-dimensional test measurements along a coordinate axis (i.e. with terms 'A_1, K_1 and B_1') while the term '$U2$' for two-dimensional test measurements made diagonally in a coordinate plane (i.e. with terms 'A_2, K_2 and B_2') and the term '$U3$' for three-dimensional test measurements made diagonally in the three-dimensional space defined by the coordinates (i.e. here with terms 'A_3, K_3 and B_3').

Graphical Representation and Analysis—Length Measurement Uncertainty Plot

When considering the purposes of graphical analysis with these Step gauges, the differences '$\Delta L = L_a - L_r$' are found and plotted—with the correct signs for the individual measured lengths and runs in a length measurement uncertainty grid (i.e. see Fig. 5.5a). Now, the top and bottom boundary lines produce a funnel-shaped outline with the neck of the funnel measuring '$2A$'—which is where 'A' equals the figure specified by manufacturer for length measurement uncertainty irrespective of length. At this juncture, 95 % of all the test measurements must lie within, or on the actual boundaries. Accordingly, a quantitative analysis can be undertaken simply by counting the number of measurements which lie outside these boundary lines.

Gauge Face Position Plot

Utilising this type of Castellated Step Gauge, it is also possible to test the positions 'L_p' of the gauge faces—as distances from the datum face. Here, if the relevant length errors 'ΔL_p' being given by position measurement in accordance with the **VDI guideline 2617—Part 3**, are entered in a plot, then it is possible to see both the position of the test length and also the sequence if, for example, these measurement points in a run are connected by straight lines. With a set of individual Gauge blocks this is not possible, because they do not have any true common reference point and more importantly they are not positioned on a measurement line.

In measurement data analysis, use is made of a gauge face position grid (i.e. depicted in Fig. 5.5b—this being similar to the length measurement uncertainty grid). The outline here is symmetrical and similar in shape to that of say, a butterfly, with a width across the waist of '$1A$'. The parameters in this case, correspond to the appropriate figures: 'A_1, K_1 and B_1' and so on. As a result, as this grid is moved along the measured length 'L', at least 95 % of all the measurements must always lie within, or on the boundary lines, meaning that all the measurement points must be consistent, no matter the position of the actual waist. This fact will ensure that any pairing of two gauge faces (e.g. even from different measurement runs) in the form of outside, inside, or face-to-face dimensions, will also lie inside the funnel of the length measurement uncertainty grid—see Fig. 5.5c. Accordingly, this grid forms a combined graphic expression of both the equations given above for all points of measurement.

Comparison Between the Test Standards: Length Bars, Gauge Blocks and Step Gauges

Separately, from that of any Step gauge, the Reference standards by which lengths are known with the greatest accuracy and precision are those of parallel Length bars. These Length bars—metrologically speaking—are, however, relatively flexible and must to be mounted at the Airy points (i.e. mentioned earlier, being set at the symmetrical spacing of: $0.57735 \cdot L$) so that they are relatively free of subsequent bending moments—if this parallelism of the gauge faces is to be maintained. In the case of the use of Gauge blocks for the individual test lengths, they can be individually placed one behind the other for shorter lengths and next to one another for longer lengths. However, when this is carried out, there is no method of obtaining the different gauge points along a line-of-measurement, which are necessary for specific measurement, or calibration purposes.

Usually, the Step gauge is of castellated configuration—see Figs. 5.2, 5.3 and 5.4—thus within its structure a large number of forward and backward gauge faces are lined-up along a single line-of-measurement. In this physical arrangement, the line-of-measurement is identical for measurements between any faces and the position of the workpiece—its orientation of the carrying body has to be determined once to find this line (i.e. see Fig. 5.4). With such Step gauges, there are numerous possible combinations in various positional orientations—see Fig. 5.3d—along the measurement line. In the case of the Step gauge depicted in Fig. 5.3, the actual number of different interface dimensions for this gauge—having 26 equi-spaced castellations (i.e. with a nominal size of length: 1020 mm) is theoretically: 1326. A special feature of this particular Step gauge, is the fact that the actual gauge points are situated on the neutral-axis of the carrying body, meaning that there are no first-order changes in its length if this Step gauge's bending state slightly changes. In such a configuration of the carrying body, the fact that the line-of-measurement is situated on this neutral axis prevents any increase in the distance between the gauge faces at the points where the carrying body is supported; accordingly, preventing these faces from moving closer together at intervening points. With this Step gauge design (i.e. Figs. 5.3 and 5.4) which is neutral in bending moment, it has Cylindrical Gauge blocks that are individually fixed in position situated within an internal longitudinal groove formed in a rugged steel carrying body of square section (i.e. of side length: 55 mm)—shown in Fig. 5.3. The axis of the Cylindrical Gauge blocks is situated on the neutral axis of the carrying body which is non-aligned in bending, as they form a series extremely accurate and precise castellations. The geometric arrangement has been adopted by this Step gauge manufacturer to provide high-protection for these gauge faces. The design of the Step-gauge can be mounted in a wide variety of orientations due to the mechanical strength of the carrying body and the fact that these lengths virtually do not vary if there are changes in the bending to which it is subject—as shown in Fig. 5.3. For example, it can be cantilevered with a so-called zero position support, or with support at the Bessel points—as previously described.

Step Gauge Accessories

There are a range of Step-gauge accessories available which are necessary to fully exploit this artefact, such as when requiring Swivel-support—see Fig. 5.3d—with the base allowing the gauge body to be mounted on the CMM in such a way as to be free of torsion. A Swivel-support of this kind produces a particularly stable connection between the Step gauge and the CMM's table (i.e. being shown on both a CMM—Fig. 5.3a, a conventional machine tool—Fig. 5.3b; plus a CNC vertical Machining Centre—Fig. 5.3c). The combination of this Step gauge and its accessories, produces a comprehensive system for creating an overall check on the CMM. One particularly notable feature is that the procedure of checking the CMM can be undertaken fully automatically with a CNC-controlled machine.

Traceability and Recalibration

The acceptance or rejection of a CMM may depend on the outcome of the length measurement uncertainty test, therefore it is always advisable to use officially calibrated testing equipment in order to avoid unexpected results and any misinterpretations—see Fig. 5.2. In the case of the Step gauge shown in Fig. 5.3, it is available with both a **DKD calibration certificate** (i.e. provided by the German Calibration Service–DKD) as well as a Works calibration certificate. With this Castellated Step Gauge, the length measurement uncertainties which can currently be achieved with such a 1020 mm artefact are:

- **DKD**: $U = 0.10\ \mu m + 0.5 \cdot 10^{-6}\ L \geq 0.12\ \mu m$;
- **Works Calibration**: $U = 0.3\ \mu m + 0.8 \cdot 10^{-6} \cdot L$ (length).

As one would expect with all the various measurement Standards, this particular Step gauge should normally be recalibrated after usage over a certain period of time. Typically, the manufacturer's recommended recalibration intervals are that the first recalibration occurs after one-to-two years, with each successive recalibration being subsequently at intervals of two-to-three years, this action being dependent upon its overall usage—see Fig. 5.5d.

In Fig. 5.6 can be seen yet another type of Step gauge configuration. Here, it is shown situated on a bridge-type CMM for verification purposes, by probing the precision steps on this Step-gauge. The universally adjustable stand it resides upon allows for a range of differing orientations of this configured Step-gauge—see Fig. 5.6a. However, an extended version of this same gauge geometry is shown in Fig. 5.6b for greater coverage of a machine's volumetric envelope together with its various angular orientations.

5.3.3 Machine Checking Gauge (MCG)

In today's modern manufacturing environments, many end-users require a simpler technique of monitoring accuracy and precision at regular intervals between the full calibration of their machines, or rapidly and efficiently after a collision. By utilising

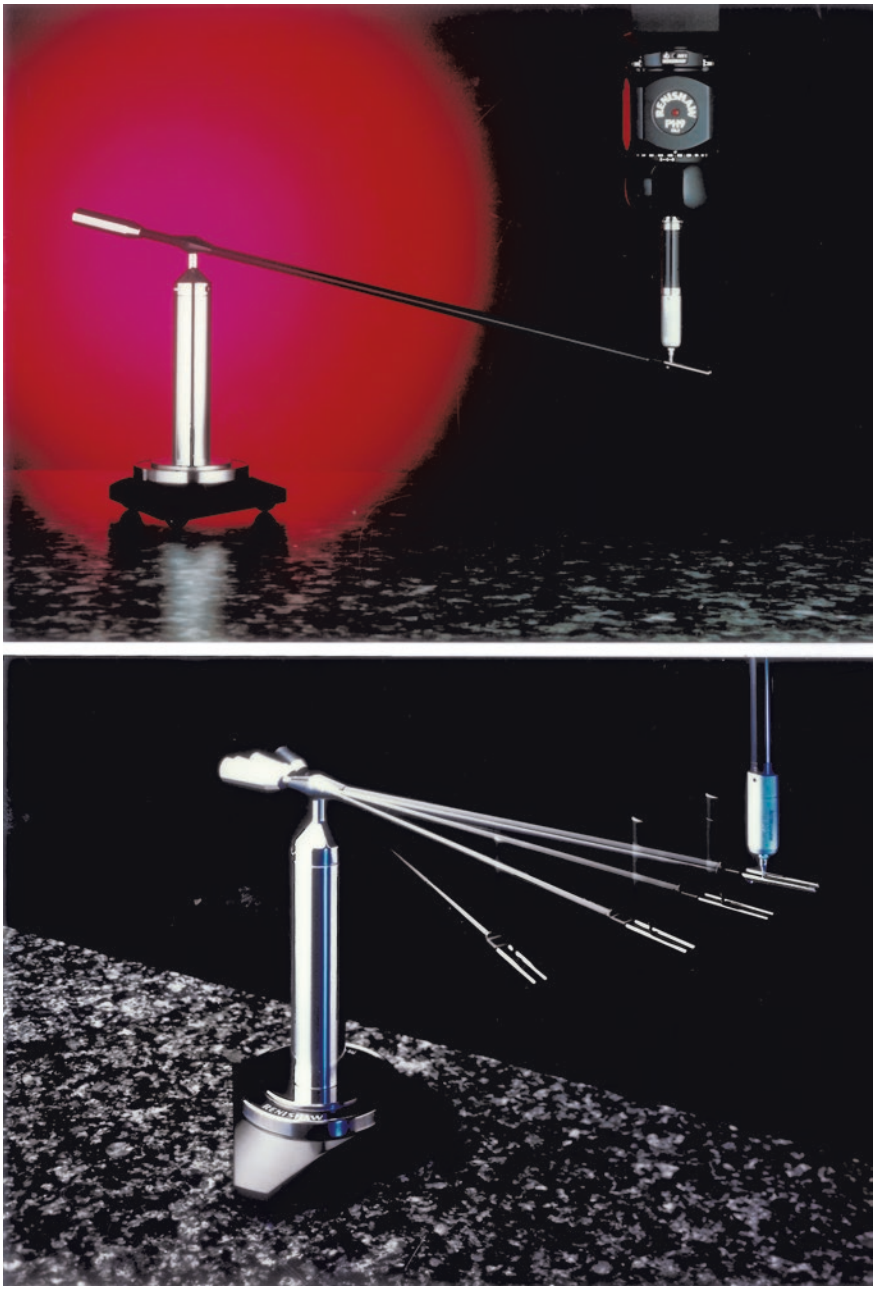

Fig. 5.7 A machine checking gauge (MCG) assessing a range of volumetric and repeatability factors of on a coordinate measuring machine (CMM) (courtesy of Renishaw plc)

metrology equipment such as the Machine Checking Gauge (MCG—see Fig. 5.7) for its volumetric accuracy, the verification can be efficiently and speedily established. The results of obtaining such probing measurement data, provides assurance that these measurements being taken on the CMM will be both accurate and precise, or alternatively, they can provide conclusive proof that servicing, or recalibration work is indeed necessary. This MCG verification process is both prompt and cost effective. As a result, the MCG with its range of pillar heights and arm lengths, mean that volumetric accuracy can be checked on either quite large as well as small volumetric CMMs. This MCG complies with the major International Standards and specifically with the British Standard **BS EN ISO 10360-2**.

Invariably, most CMMs are characteristically subjected to an annual service and recalibration by its original equipment manufacturer, or perhaps from a third-party independent calibration company. Inspection is usually undertaken to a definitive procedure, which is defined within a recognised Standard, typically by Standards such as the **ISO**, **ASME** or **VDI/VDE**. These tests necessitate the use of fixed length Ball-ended bars; Step gauges; as well as Laser measurement systems. The measurement data can subsequently be utilised to modify the CMM controller's electronic error map and in this manner it will restore the machine within traceable and quantified accuracy specifications. This overall verification operation is a well-recognised procedure being an essential and periodic verification task, but without artefacts such as the MCG, it would otherwise be both time-consuming and costly.

The majority of CMM-users have need of a simpler technique of monitoring accuracy and precision at regular intervals, between these overall comprehensive checks, or as previously mentioned after either a probe or axis collision with, for example, a workpiece/fixture. The MCG enables CMM-users to commence a 20-min interim-verification of the volumetric accuracy to **ISO 10360-2**. These ensuing measurement results, provide assurance that measurements taken on the CMM are accurate and precise, or alternatively, give conclusive proof that either servicing, or recalibration work is necessary.

MCG—Principle of Operation

The counterbalanced arm, as depicted in Fig. 5.7, has a kinematic seat which precisely sits on a precision ruby ball, this being located on the top of an adjustable tower. As a result, the kinematic seat permits very accurate arm-pivoting, both horizontally through 360° and vertically through ±45° of angular motion—see Fig. 5.8a (middle-right). At the end of this counterbalanced arm is a second kinematic location, which is formed by two parallel rods, with the tungsten carbide ball of the arm and the probe stylus ball—shown in Fig. 5.7 (bottom). This configuration allows the counterbalance-arm to sweep through a volumetric truncated-spherical outline of radius '*R*' about this kinematic pivot location—also depicted in Fig. 5.8a (middle-right). The counterbalanced arm assembly is balanced to provide a permanent and biased-downforce of 2 g at the measuring end, allowing precise arm movement, but without false-triggering of the probe. The probe is moved to its required position—within

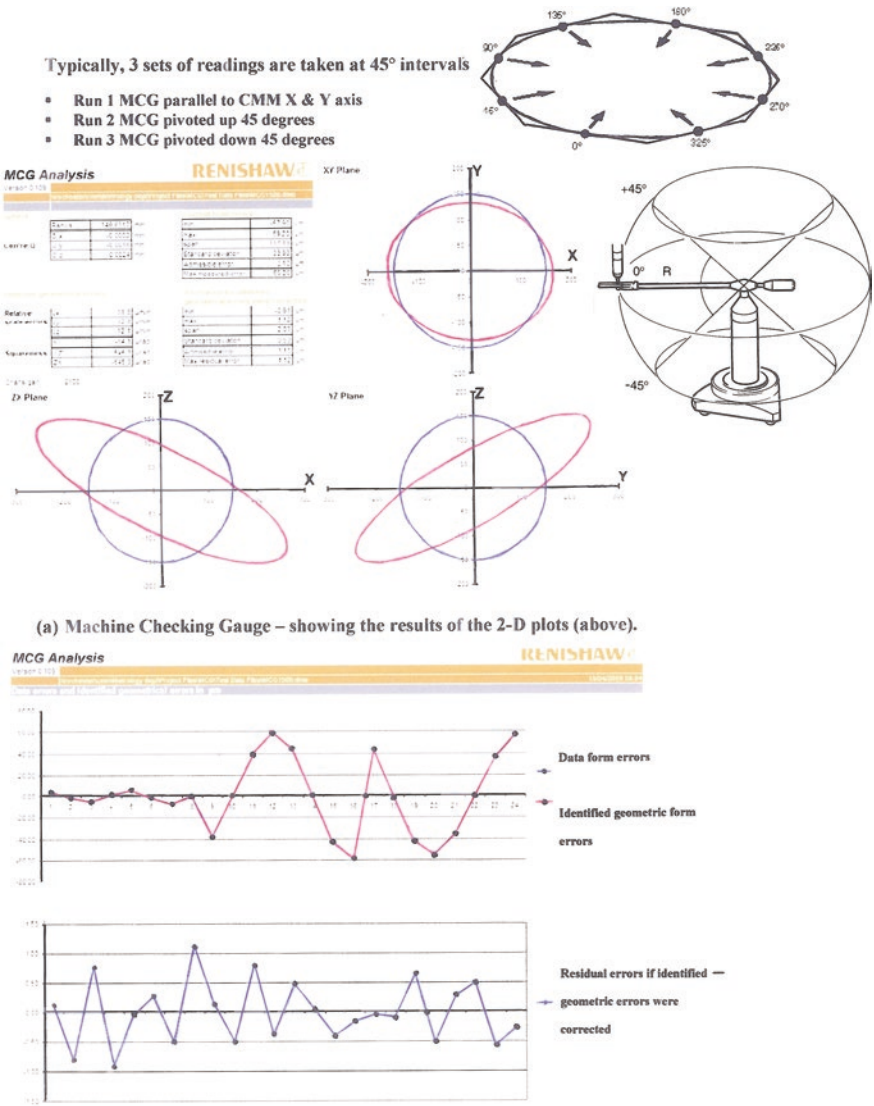

Fig. 5.8 Volumetric calibration of a CMM with the MCG (courtesy of Renishaw plc)

its confined volumetric space and then radially moved towards the pivot position, where it will trigger a reading at this kinematic location, resulting in the radius at this point in space being measured. Meanwhile, this counterbalanced arm is of a constant radius '*R*', so any deviation from '*R*' being an indication of the volumetric measuring

performance of the CMM for that volume swept by the arm. Subsequent repetition of a sequence of readings will check the system for its repeatability. Consequently, the volumetric measuring performance is the maximum error between any two points in a desired plane, this being over any distance within the full measuring volume. In the case of horizontal/cantilevered arm CMMs, the probe is mounted at 90° to this arm.

The MCG permits for the end-user to collect data from the CMM immediately following its installation, or when the annual calibration is designated to be carried out. Furthermore, periodic checks of the CMM with the MCG can be compared to that of the original data with this current MCG-data, to monitor any change, or notable trends in the CMM's performance. As might be anticipated, one year between CMM calibration is really too long in today's quality-focused manufacturing society and in addition, multiple-user CMMs—particularly those installed in front-line production environments—can experience more frequent accidental crashes that can disturb the CMM's geometry and potentially affect its future metrological accuracy and precision. As recently discussed, the CMM probe's stylus slots into the end of what is, in effect, a reference Ballbar, hence, the probe effectively traps and carries the bar with it around a spherical path; the desired motion coming from a CMM part program. Here, radial readings are then taken at different positions and the range of readings indicates the volumetric measuring performance of the CMM—see Fig. 5.8 (top). Therefore, the repetition of a sequence of MCG readings checks the system for its repeatability. As a consequence, the volumetric measuring performance is the maximum error between any two points in any plane, over a prescribed distance within the full measuring volume. Of note, is that with each MCG-provided, special calibrated styli are supplied.

Taking Measurements When Using the Online Machine Checking Gauge Service

By utilising the MCG coupled with Renishaw's online MCG service,[8] the application of the MCG can be achieved in three stages, thus enabling measurement, analysis and tracking the volumetric performance of a CMM, as follows:

1. **Creating an MCG test program to run on the CMM**—here, a DMIS program is generated enabling the setup of specific parameters required for the test. This testing on the CMM generates a set of measurement results;
2. **Analysis of the MCG test results**—the MCG test generates a set of measurement results—in a DMIS-format. This operation can be achieved by uploading from the Renishaw-website, enabling measurement data to be analysed online—with appropriate guidance allowing an accurate interpretation of this data—see Fig. 5.8a;
3. **Storage and retrieval of previous results to spot trends**—the MCG test data can be stored online and then retrieved at a later date, allowing identification of any changes in the performance of this CMM over time—see Fig. 5.8b.

[8]**Online machine checking gauge service**: here, Renishaw have simplified the implementation of utilising a Machine Checking Gauge, by providing an Online machine checking gauge (MCG) service, which can be found at the respective Renishaw website at: www.renishaw.com.

Taking Measurements When not Using the Online Machine Checking Gauge Service

Typically, three sets of measurement readings are taken per MCG position, with each run comprising of just eight points taken at 45° intervals—see Fig. 5.8 (top) as follows:

1. **Run 1**—MCG parallel to CMM *X* and *Y* axis;
2. **Run 2**—MCG pivoted up 45°;
3. **Run 3**—MCG pivoted down 45°.

In more detail—see Fig. 5.8a—the kinematic motions of the MCG when taking measurement readings on the CMM are provided below:

1. **Arm elevation** 0°—measurement of the arm radius '*R*' at 45° intervals in the horizontal plane (i.e. a total of eight measurements)[9];
2. **Arm elevation** −45°—measurement of the arm radius '*R*' at 45° intervals in the horizontal plane (i.e. a total of eight measurements) (see Footnote 9);
3. **Arm elevation** +45°—measurement of the arm radius '*R*' at 45° intervals in the horizontal plane (i.e. a total of eight measurements) (see Footnote 9);
4. **Repeat steps 1 to 3 (twice to obtain repeatability measurements)**—this provides a total of 72 (i.e. 3 × 24) measurements for evaluation of volumetric measuring performance and system repeatability;
5. **Remove the counterbalanced arm carefully and re-datum the pivot ball using a minimum of ten readings**—if the pivot ball centre has moved significantly more than the maximum measured repeatability, re-datum the pivot ball ensuring that the;

a. seating faces between the pivot, pillars and baseplates are perfectly clean and that these parts are firmly tightened;
b. stated pillar thermal stabilising period (i.e. 2 min minimum) is observed;
c. utmost care should be undertaken when placing the counterbalanced arm on the pivot.

With the fast-paced global manufacturing economy today, the objective of equipment support is to minimise downtime. In order to achieve this aim, the integration and implementation of a series of effective technology-based tools allows for a rapid diagnosis and an effective remedy to any reported metrological issues. By utilising MCG-Tools—this is a Microsoft Excel™ workbook that manages the MCG—where it allows the user to generate a DMIS-part program in order to execute the MCG test on a CMM. It can then import the MCG-data to analyse and identify whether geometrical errors exist on the CMM.

The results from every MCG test can be archived in order to follow the evolution of the geometry of a CMM over time. Here, the MCG-Tools analyses the form error of the sphere that is generated by the MCG arm, by taking points around

[9]As shown in Fig. 5.8a (middle-right).

its pivot and identifies six of the main CMM geometrical errors, namely: three squareness errors and three relative scale errors.

The data analysis initially best—fits a sphere onto the MCG points—which identifies a best-fitted centre and radius. Further, from this best-fitted sphere, the form errors that are the radial deviation from the best-fitted spherical surface are then analysed in order to identify the CMM geometrical errors. This form error analysis is also a linear best-fit of the effect of the CMM errors onto the MCG points. This data identifies the three squareness errors of the CMM as well as its three relative scale errors. The MCG-Tools spreadsheet provides all the necessary features for one to create a DMIS-part program that runs in MODUS metrology software. At this juncture, the MCG-Tools import a results file created during the program run and then reports various metrology characteristics of this CMM. These results correlate directly with the maximum error between two points and determine the volumetric accuracy of a CMM. Over time, the volumetric accuracy of a CMM will change and the MCG-Tools spreadsheet maintains a historical overview with changes spotted through trend-analysis. The MCG and MCG Tools is a powerful reporting tool, not a calibration tool. The greatest benefit of this MCG product is to report the current state of a CMM allowing a user to perform preventative maintenance before problems arise.

Volumetric Performance—In Summary

As described, the counterbalanced arm of known and calibrated length is located at one end on a stationary freestanding pivot positioned on the CMM's table. The pivot allows the arm to rotate very accurately through 360° horizontally and ±45° vertically. When purchased, each MCG comes with six arms, ranging from 101 to 685 mm in length, as well as pillars supplied in heights of 72–235 mm. The other end of the arm is comprised of two parallel guide rods with sufficient clearance between them to allow the CMM probe to move towards the pivot position, taking a radius measurement as the probe stylus ball contacts a ball attached to the end of the arm. Thus, as this arm is a known length, any discrepancy between this length and the measured CMM value can be calculated.

To conform to **ISO 10360-2 Standard** and to once more reiterate the MCG's motional-operation, this MCG test must be performed at set positions around a spherical path of movement. Here, a standard test provides for eight measurements at each of 0°, 45° and −45° arm elevation, giving a total of 24 points. The data-gathering process is then repeated three times to allow for machine repeatability,[10] NB The only distinct disadvantage of using the MCG, is that it can only be utilised on a CMM to vector in a truncated-circular volumetric space—within the total machine's volumetric envelope. producing a total of 72 measured results in all. As the volumetric measuring performance of the CMM is the maximum error between any two points in any plane over any distance within the full measuring volume, the verification-test can be performed at multiple strategic-locations across the machine's table. The

[10]**MCG—machine repeatability**: the repetition of a sequence of readings by this MCG, will check the CMM's repeatability and the total gauge error to a claimed ±0.5 μm.

analysis page of MCG-Tools subsequently presents a detailed analysis of MCG results. In this instance, the first part displays the analysed result along with three 2-D plots. At this time, there is a plot for each principal plane of the machine, namely in the *XY* plane, the *YZ* plane, as well as the *ZX* plane. The result of the identified CMM errors on the MCG arm length is plotted—with the effect being magnified by a gain.

5.4 Ball- and Hole-Plates

As previously recommended within the **ISO 10360 Standard**, it is strongly recommended that a CMM should be checked regularly during the times between its periodic reverification—known colloquially as Interim checks. Depending on the actual measurement tasks required, the most pertinent of the following commonly used artefacts should normally be chosen for such Interim checks—see Table 5.2—where it indicates some conventional metrological equipment for verification of comparisons of standards of length to be employed on Machine Tools and also indicates problems in their usage on today's CMMs. Some examples of such artefacts used in this manner are given below:

Table 5 2 A simple comparison of some of the various material standards of length, for basic metrology artefacts, with their notable features and possible drawbacks

Standard	Features
Length bars	Accuracy $\leq$0.5 μm m^{-1}
	Only one length per bar
	Easily damaged
	Can become separated, or lost
Gauge blocks	Accuracy $\leq$0.5 μm m^{-1}
	Only one length per bar
	Easy to setup multiple arrangements
	Requires supporting structure
	More rigid than length bars
	Easily damaged
	Can become separated, or lost
Step gauges	Accuracy $\leq$1.0 μm m^{-1}
	Multiplicity of length
	Uni-, or bidirectional
	Very rigid
	Easily supported
	More robust
	Cannot become separated
	Individual steps prone to move

adapted from [Flack, D. @ The NPL—UK (July 2011)]

- **a purpose-made test piece**—that has features representing typical geometrical shapes, which is dimensionally stable, mechanically robust, and has a surface finish/texture that does not significantly affect its likely uncertainty of measurement—see Fig. 5.1c for a commercially available artefact that fulfils these metrological criteria;
- **A 3-D Ball-plate**—for either machine, or probing verification—the latter of such being accomplished as shown in Fig. 5.9;
- **Ball**-, or **Hole-plate**—for verification tasks on either CMM, or machine tool—with the former being exhibited in Fig. 5.10 on a machine tool, while the latter is shown in Fig. 5.11 (bottom) for a CMM;
- **A circular artefact** (e.g. such as Calibration Rings)—an example of which is shown in Fig. 4.12 (bottom);
- **A bar that can be kinematically located between a fixed reference sphere and the CMM probe stylus sphere**.

Interim Checks—Using a Ball and Hole-Plates

There are numerous configured Ball-plates that are currently available for machine verification, which are both metrologically stable and very rugged in their construction—see Fig. 5.11 for a typical artefact. A slight disadvantage is that they can be very heavy, with the larger Ball-plate and stand being shown in Fig. 5.11. Often with these larger versions, they require two people to lift and accurately position them both on-and-off the machine. Of note, is that the equivalent Hole plates tend to be much lighter than the corresponding Ball-plates of similar sizes. Here, the actual measurement task is one that is only necessary in practice periodically and which necessitates reliable and workshop-hardened software to compute the actual ball-centres—see Fig. 5.11 (top-right). Furthermore, as its ball-centres are being measured, this artefact will not discover any probe qualification-related problems—unless each of these individual balls has been previously calibrated for size. This type of commercially available Ball-plate can be accessed by the machine's probe, from both sides of the artefact—as shown in Fig. 5.11 (bottom-left). Ball-plates can be measured in various artefact orientations on the machine. In certain situations, the CMM-user may wish to perform an interim test such that the results can be compared to the manufacturer's specifications. Therefore, in these checks, a calibrated test length should be employed and the measurement procedures described in Standards such as **ISO 10360** must be rigorously followed. So that the time is minimised when performing an interim test, often an abbreviated test procedure can be undertaken, where it is recommended that such checks should concentrate on those test positions that will most commonly reveal potential problems with this kinematically configured CMM. Such an example of an abbreviated test might be the measurement of a single long test length in each of the machine's body-diagonals. This testing procedure will normally reveal CMM errors with more distinct accuracy than would otherwise be the case, typically for measurements of five test lengths along a specific CMM axis. Each of the machine-induced errors from the interim test should be somewhat less than those of the corresponding specification,

A range of calibration reference balls – with & without stems, utilised on CMM s.

[Courtesy of Spheric Trafalgar Ltd (Ashington West Sussex, UK)]

Fig. 5.9 The calibration of a CMM, utilising a '3-D ball-plate'—where the major benefit being here to have differing sphere positions/heights—supplied on a purpose-built fixture, when calibrating the equipment (courtesy of Renishaw plc)

for example the Measurement error 'E_0'; Maximum permissible error 'MPE'; etc. This check verifies that the actual test was conducted according to the procedures stated in relevant Standards, such as that of **ISO 10360**, while ensuring that the environmental conditions are within those stated by the CMM manufacturer.

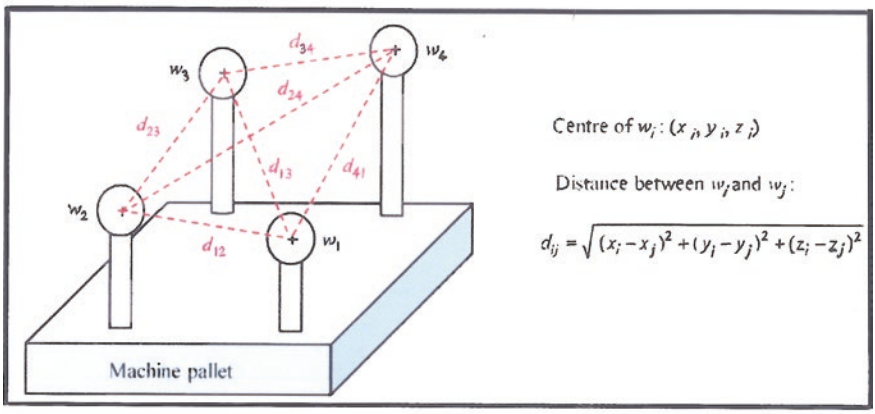

Geometry definition of a *Four-ball artefact*.

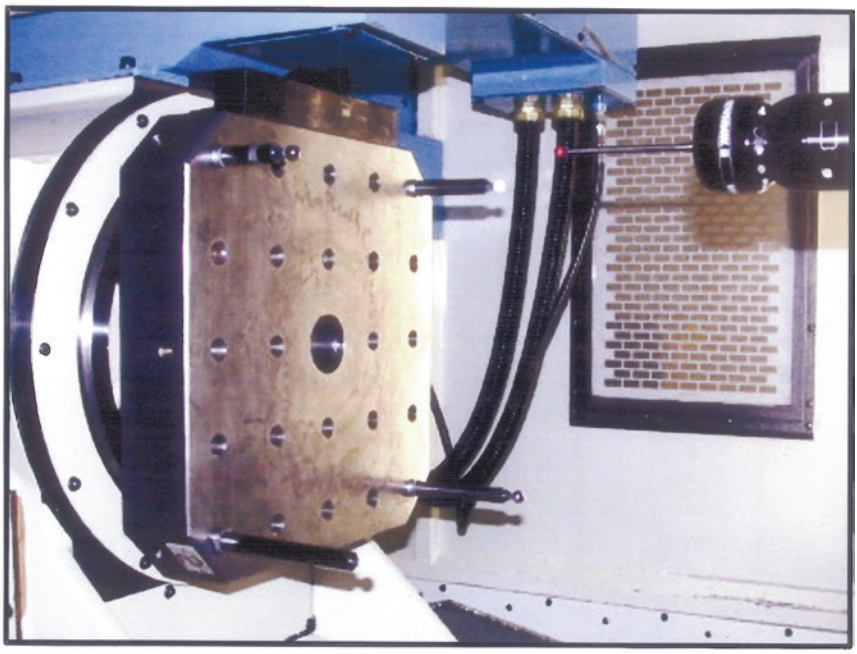

A *Four-ball artefact* configuration on a five-axis horizontal machine.

Fig. 5.10 A four-ball artefact for volumetric distortion assessment of a (*horizontal*) five-axis machining centre (*Source* T. Erkan, J.R. René Mayer, Y. Dupont École Polytechnique (Montreal)/ Pratt & Whitney (QC) Canada)

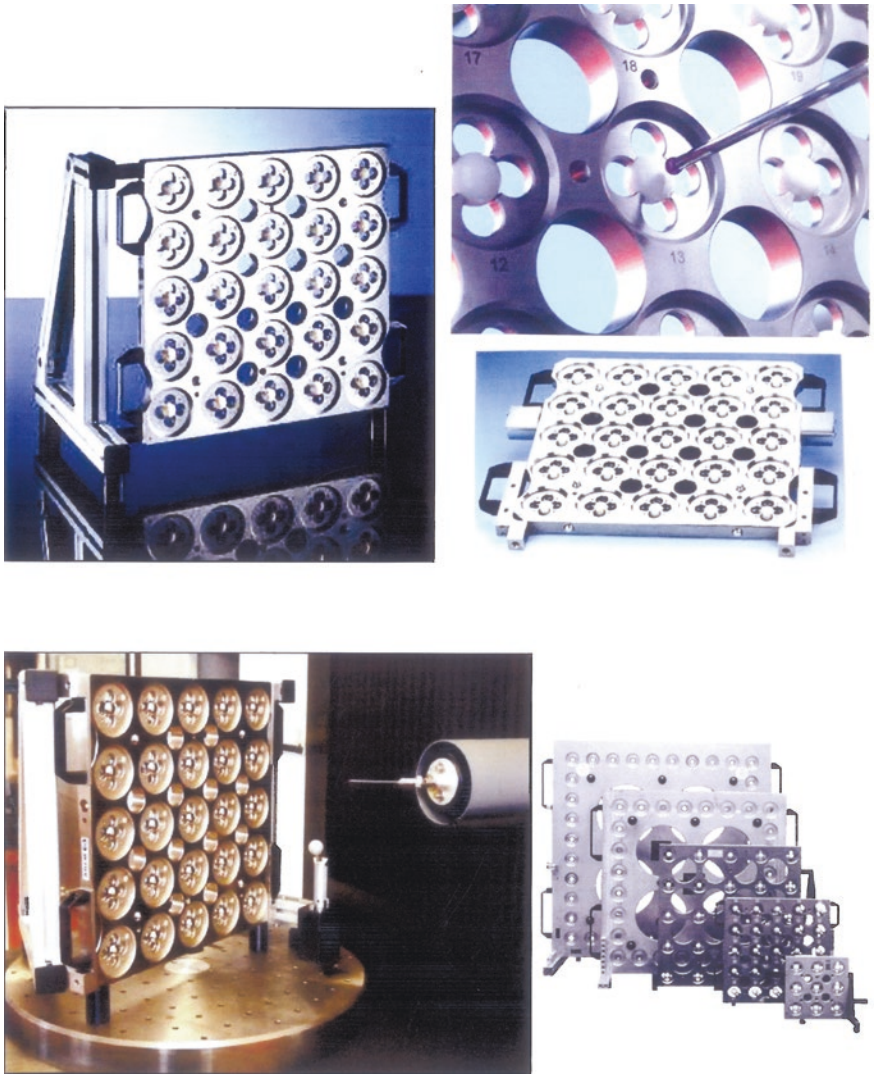

Fig. 5.11 The 'ballplate' is an artefact that enables significant coverage of many CMMs volumetric envelopes [courtesy of Retter Automation and Measurement (GmbH)]

5.4.1 The 3-D Ball-Plates

Introduction

There are a large number of procedures for CMM performance machine verification. In general, they are normally based upon sampling the length measurement capability of a CMM. During that verification process, the artefact is checked as to

whether the length measurement errors lay within the defined limits. For the purpose of testing the capability of the machine to measure lengths with enough accuracy and precision, two different concepts are normally recommended, these are:

1. **ISO 10360—concept** (i.e. also accepted in **VDI/VDE 2617 guidelines**)—here, the tests are performed utilising different calibrated artefacts, thereby test measurements determine errors (i.e. the errors of indication of CMM at measuring lengths);
2. **ASME B89.1.12M-1990—concept**—here, the results of test measurements are not errors, but are a range of the indicated results obtained by only one measurement length (i.e. volumetric tests). In this manner, the use of calibrated artefacts is not required, i.e. "…the performance of the machine and its geometry is assessed, independent of conformance to international length standards" [Source: Bringmann and Kung (2005)]. Hence, such measurements on calibrated artefacts, in this case, need to be undertaken only in order to provide traceability.

Based on one or the other of the concepts above, these verification tests are performed using different length measurement standards (artefacts). Such artefacts can also be sub-divided in accordance with arrangements of their measurement features (e.g. their plane surfaces, cylinders, or spheres) within their volumetric space, or into either their linear (i.e. one-dimensional), two-dimensional or three-dimensional characteristics.

With the advent of highly sophisticated multi-axes machine tools, there are some different approaches for metrological evaluations of these machines. Typically, a five-axis machine tool can be utilised in the machining of either large/complex monolithic parts, or small intricate high-precision components. Such a multi-axis machine's ability to orientate the cutting tool relative to the workpiece's surface, offers a significant reduction in the number of setups required. Machining and measurement strategies adopted have varied quite considerably with this type of expensive plant, which might include:

- **measuring the individual axes**—by bringing specialised instrumentation (i.e. previously alluded to) within the machine's volumetric envelope which demands human intervention, thus requiring specific personnel, while reducing the machine production down-time;
- **On-machine probing of an artefact as a reference part**—to obtain the machine's volumetric status. One solution that has been proposed, was a Cube-array artefact being composed of eight cubes to quickly assess the positioning errors of a multi-axis machine tool. This artefact was calibrated on a CMM and then subsequently installed on the machine tool;
- **Pseudo 3-D artefact**—by mounting a 2-D Ball-plate in different locations, the objective here being for the prompt testing and calibration of machine tools; CMMs; as well as for robots; normally with at least three linear axes;
- **Development of a technique to transfer the accuracy of a CMM to a machine tool by measuring a part with fiducials both on a CMM and on a machine tool**—however, storage and transportation of such artefacts are the major-drawbacks in a production environment;

- **Reconfigurable uncalibrated artefact**—this artefact was designed to exploit the on-machine probing capability to perform a rapid volumetric assessment of the machine. This particular artefact was composed of independent (unconnected) master balls, mounted on the ends of rods of different lengths forming 3-D artefacts—see a similar arrangement in Figs. 5.9 and 5.10 (top). A representative basic artefact assembly—when fixtured onto a machine tool, is composed of an arrangement of master balls, situated upon varying length rods and inserts, which is depicted on a machine in Fig. 5.10 (bottom).

Reconfigurable Uncalibrated Artefact

This latter Reconfigurable uncalibrated artefact's goals are in facilitating its integration and subsequent verification within the machine tool. The most significant characteristic of this particular 3-D artefact is its reconfigurability. It has been designed and manufactured from a range of adjustable master balls, which are located within the machine's working and probing envelope. The actual rods of varying length are screwed directly into the standard threaded fixturing holes of the machine's pallet. Accordingly, the actual machine pallet then becomes an integral part of this artefact. In Fig. 5.10 (bottom) is depicted an example of reconfigurability of this artefact, in this instance being composed of four balls—of differing heights, mounted on a pallet in a five axis horizontal Machining Centre.

This 3-D reconfigurable artefact highlights the fact that when initially fitted onto the machine tool it will be presently uncalibrated, as its inherent design philosophy hinders precise knowledge of its actual geometry. As a consequence, a mathematical model was developed to assign values to the linear setup errors of each ball and the probe's tip, so that their impact on the volumetric errors can be removed. The actual positions of the master balls and that of the stylus tip, deviate from their nominal positions by small values termed setup errors. Consequently, the ball centre data obtained from on-machine probing includes not only the effect of these machine errors, but those also of the setup errors. A mathematical model was developed in order to assign values to the setup errors in an attempt to explain the measured ball centre data. Hence, this model consists of three Cartesian setup errors for each of the master balls and another three for the probe. For example, with an artefact composed of four master balls, there are 15 error parameters in total—this information is fully explained in specific detail being provided in the Erkan et al. (2011) reference, at the end of this chapter. As previously described, these verification-tests were performed on a five-axis machine tool, with the identified artefact geometry being validated on a CMM. In this artefact's verification, the worst-case difference between the CMM measurements and estimated ball-to-ball distance was shown to be 7.4 μm. These results indicate that specific geometric setup errors can be assigned to the artefact and stylus tip, in order to minimise/eliminate their effects from the machine probing results, thus allowing some of the machine volumetric errors to be exposed for machine verification purposes.

5.4.2 Ball- and Cube-Tetrahedrons

With regard to the use of commercially available Ball-tetrahedrons (Fig. 5.12a) and Cube-tetrahedrons (Fig. 5.12b) for CMM verification, they provide the CMM-user with a good choice between very fast, but precise and simple volumetric check, against that of an exhaustive and a very thorough verification—with other types of artefacts taking more time and preparation in their setup and programming. Considering these examples shown are the standard type of Ball-tetrahedron with edge connectors of steel and being of a very compact design, these edge connectors do not significantly contribute to the thermal expansion coefficient of the overall size of the tetrahedron. Moreover, their configuration ensures very good accessibility for CMM probing operations. Usually, performing an interim check with such a cube can be achieved in approximately 45 min in total—when employed on normal bridge-type CMMs (i.e. shown schematically in Fig. 5.12c). Therefore, the length measurement errors can be verified for over 200 different derivations of measurement lines in three-dimensional space with an appropriately qualified probe stylus. For a full volumetric assessment check where the cube is accurately positioned on the CMM's table, the more exhaustive verification of **ISO 10360-2 Standard** can also be undertaken.

In the case of larger volume CMMs, for subsequent verification, they necessitate that the Cube-tetrahedron has to be measured, which entails more probing positions. Nonetheless, with the Quick Check-T data and its accompanying software analysis package, which is currently available for these Ball-tetrahedron artefacts, it evaluates the length measurement errors and machine geometry parameters, using measurement data obtained with this tetrahedron—see Fig. 5.12 (top-right). Here, the length measurement errors are recorded as the difference between measured and calibrated ball distances (i.e. with the appropriate sign convention). The CMM's actual machine geometry errors include the scale factors of: *X*; *Y*; and *Z*; as well as squareness errors between the axis planes, namely: *Y*-to-*X*; *Z*-to-*X*; and *Z*-to-*Y*. Here, one may store these measurement results in a history sheet, then review any changes of the CMM over time—in a similar manner to that of an SPC process control chart. Data are normally entered by simply copy-pasting—as there are only six values to be transferred from the CMM-user surface, to that of the Quick Check-T-user surface. Of note is that, usually only the last numerical digits change from any periodic time interval between CMM checks. Once all data have been entered, pressing the appropriate button on a PC, namely here the add results to history, enables the current history sheet to be amended by a new record line, with all data needed for a thorough traceability update. Supplementary software activities mean that the three graphics displays are also amended (i.e. specifically for position; squareness; as well as for maximum length error). Normally, tetrahedron artefacts are measured in the manner in which they are revealed in the photograph shown in Fig. 5.12a, meaning that one of its corners will be pointing in the CMM's ram direction (i.e. namely in '*Z*', this being depicted in Fig. 5.12a, top-right) in the case of the triangular equilateral Ball-tetrahedron.

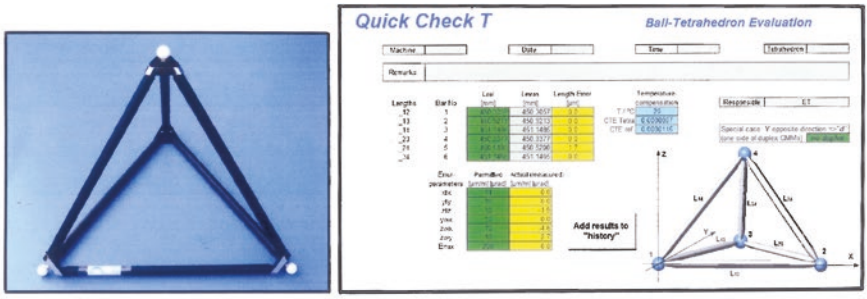

(a) The *'Ball Tetrahedron'* is an efficient way to validate results from a CMM.

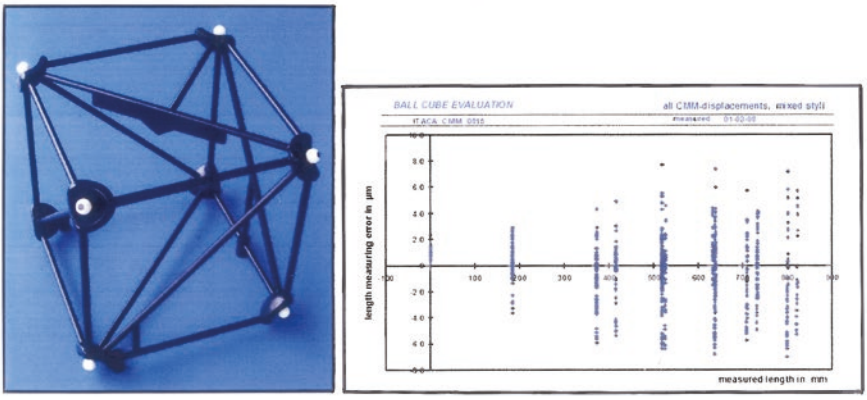

(b) *'BallCubes'* can be employed to obtain CMM displacements efficiently.

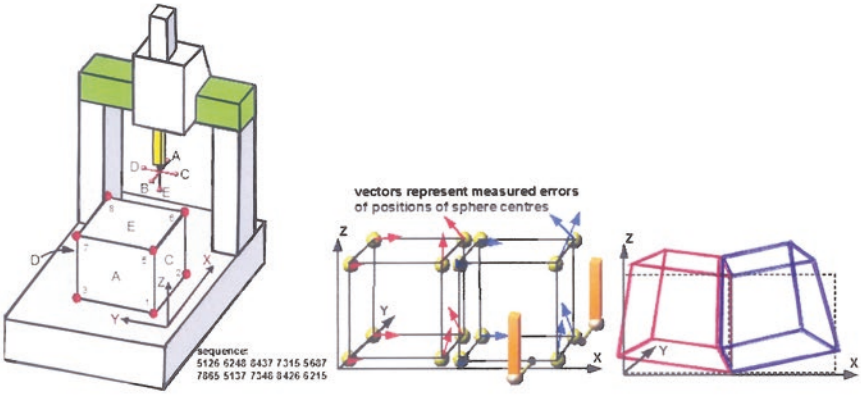

(c) CMM 'probing sequence' for volumetric calibration of a either a 'Bridge-type' (shown), or 'Cantilever-type' CMM.

Fig. 5.12 Both 'ball tetrahedrons' and 'ballcubes' can be utilised to validate CMMs—to ISO 10360-2 [courtesy of Trapet Precision Engineering (Sarria, Spain)]

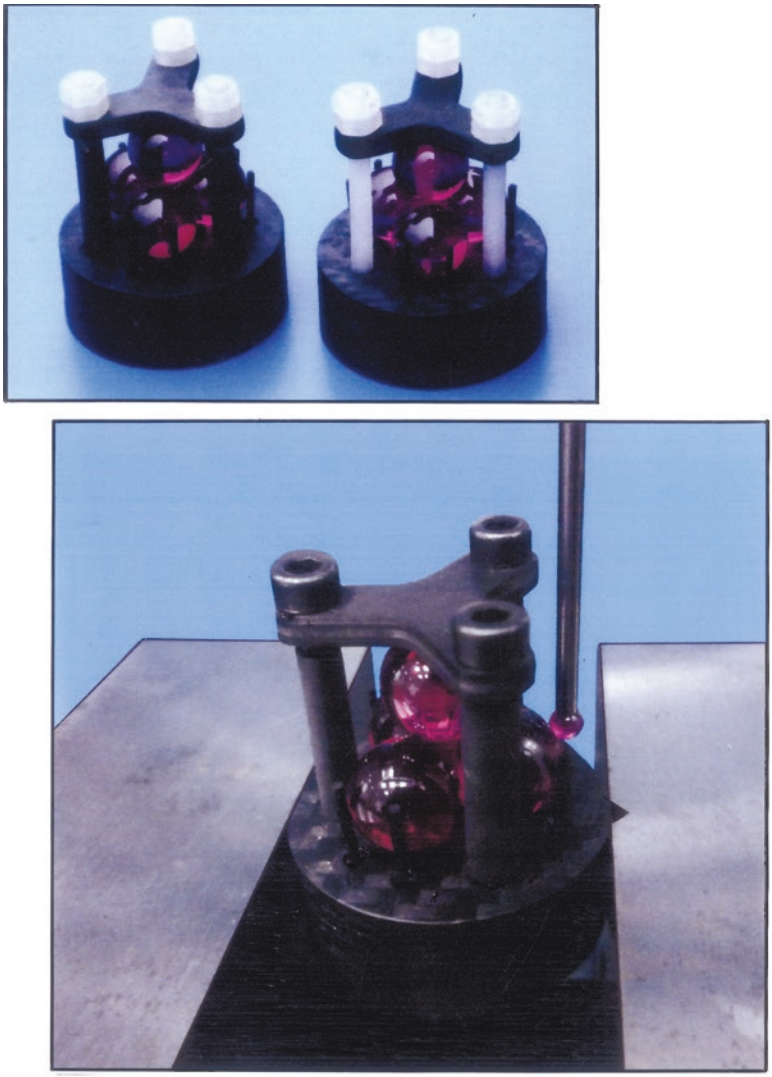

Fig. 5.13 An CMM artefact: the touching-ball tetrahedron for tomography [courtesy of Trapet Precision Engineering (Sarria, Spain)]

With regard to verification of CNC machine tools, they usually require a very large tetrahedron design—to adequately cover much of their machine's volumetric envelope; therefore, in these circumstances, it calls for the application of a so-called Virtual Tetrahedron. This virtual artefact is basically a Ball-plate with three balls that are measured in three different orientations, yielding the same dimensional information as the measurement of a tetrahedron in just one orientation. The Ball-plate's geometry is just a simple equilateral, thus the sides of a tetrahedron are emulated and in so doing, enabling use of the same evaluation spreadsheet as for a real tetrahedron.

In Fig. 5.13, a different measurement probing technique has been utilised on the CMM, with it here being depicted is a miniature Touching-ball-tetrahedron, which is based upon a geometrical arrangement of ∅10 mm touching-balls. These four highly accurate and uniform spherical ruby balls are very lightly pressed together by a known and controlled spring force—so that a somewhat minimal diametral-distortion of these ruby spheres is present. In this geometrical arrangement, these touching-balls form a very reproducible tetrahedron array—without the necessity of an adhesive being required to maintain this assembled configuration. The CMM probing calibration operation is performed on the individual balls–being shown in Fig. 5.13 (bottom). In this Touching-ball-tetrahedron design, only carbon fibre composite, plastic screws, tubes and ruby balls are utilised, which affords an excellent resolution to this test artefact, as the balls' distances will only start to slowly thermally grow a miniscule amount from zero—making them an ideal artefact for small-scale CMM verification.

5.5 Large Reference Artefact—For Large-Scale CMM Verification

Introduction

At The NPL in the UK, a major step was embarked on in establishing the traceability of measurements undertaken by CMMs, which involved the comparison of measurements of a specially designed artefact with the certain calibration information associated with this object. The metrological approach is explicit in the **ISO 10360-2 Standard**, enabling a procedure for determining the length measuring capability of a CMM from measurements of calibrated length artefacts, these are usually: Gauge blocks, Length Bars and Step gauges. Granting that this Standard applies most directly to CMMs with operating axes of ≤1 m, its underlying principles apply to coordinate measuring systems with working volumes of any proportions. To establish verification according to this **ISO 10360-2 Standard**, it necessitated:

- **a reference artefact**—whose length is no less than 66 % of the longest space diagonal within the working volume;
- **an artefact having a known calibration uncertainty**—which was no greater than 20 % of the error of indication for this CMM—see Fig. 5.14b;
- **artefact measurements of the length**—which are undertaken along seven distinct measuring lines.

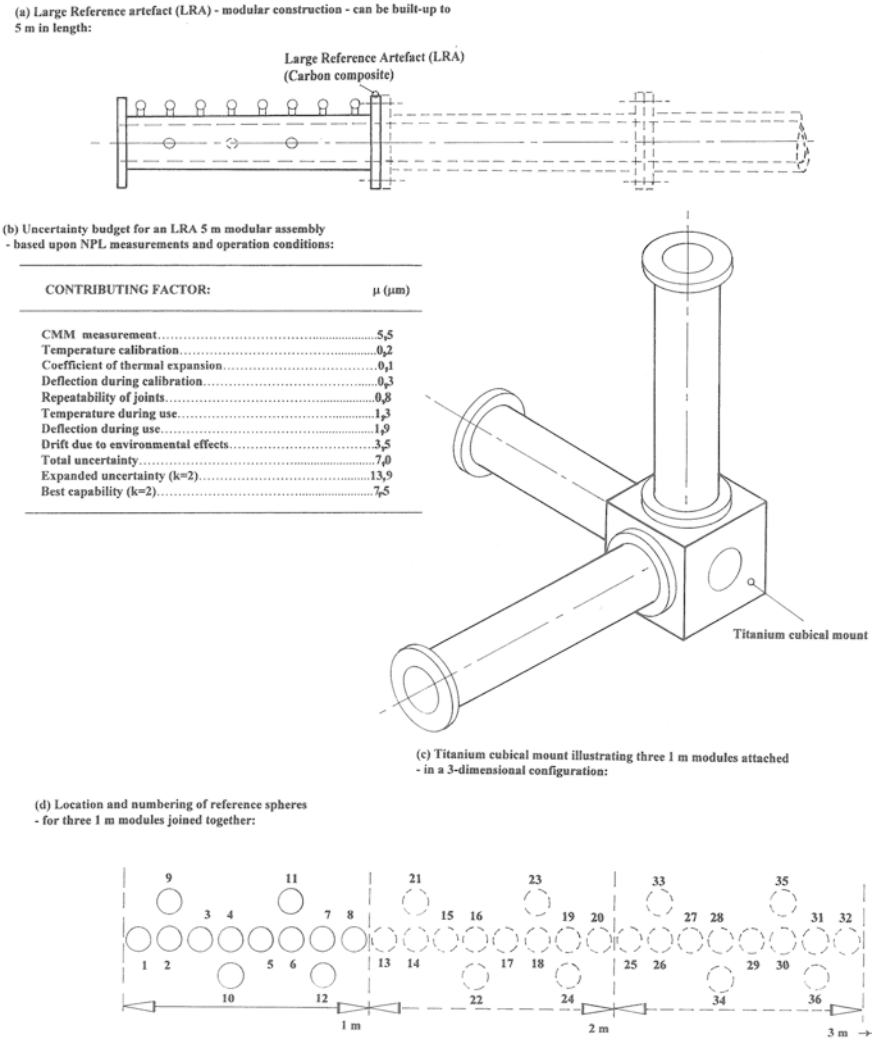

Fig. 5.14 Large reference artefact (LRA) for coordinate measuring machine (CMM) verification [*Source* Centre of Length Measurement (NPL)—Corta et al. (1998)]

This verification technique for large CMMs, is only limited by the ability to provide an artefact that can be accurately calibrated and stably positioned within the machine's working volume; despite the fact that characteristically Step gauges and Gauge blocks are of up to one metre in length, when suitably calibrated, which can be considered as not uncommon. The construction of very much longer artefacts with comparable accuracy and practicality presents significant difficulties, which must be overcome in order to be both usable and practicable.

5.5.1 Large Reference Artefact (LRA)—Design and Construction

The NPL (UK) in the 1990s made an initial design decision to construct an artefact of carbon-composite materials and in so-doing, providing rigidity while at the same time keeping this artefact lightweight. In order to meet the modularity requirement for general metrological usage, the artefact was constructed from modular tubular sections as schematically shown in Fig. 5.14a. During the construction of this tubular form, the carbon fibres were layered unidirectionally and aligned with the tube's axis. Furthermore, an additional layer of fibre material was wrapped around the tube at 90° to the tube axis, which helped to control the ovality of each individual completed tube. These individual tubes utilised for the LRA are 1 m in length—with four of them having been made, and a further two of 0.5 m in length were also constructed. This range of individual lengths of size, allowed for the verification of the performance of CMMs with its largest dimensions up to 5 m in 0.5 m incremental steps. Moreover, it is also possible in principle, to add even further length sections to this LRA. In Fig. 5.14a, three of the modules of the LRA are schematically represented, being joined together in a linear assembly. Upon each module are depicted eight reference spheres, which are fixed to the measuring stations on top of each cylindrical section, with similar spheres being attached to the sides of the artefact.

Here, the actual requirement for modularity introduced the problem of how each of these modules could be joined together? For practical reasons, the NPL decided that each tube had to have a flange of laminated construction bonded to each of its ends. These actual flanges are manufactured from sheets of carbon fibre, each being laid at a different orientation and pressed over a former, requiring their uniform thicknesses to be built up in layers. The alignment and connection of the each of these modules was achieved by using semi-kinematic flange joints. The concept of utilising pure kinematic connections was disregarded, as it was considered that such kinematic connections would not provide the required rigidity and might also be subject to damage during actual usage. The operation of the flange features was as follows, the mating faces are precision ground so that they are flat and also square to the tube axis, meaning that when bolted together these assembled modules would have no axial freedom to movement. On one end of a module, the flange has two precision-ground holes located on a diameter, with the upper hole fitted with one half of a conical bush and the lower hole with a tooling dowel-pin that protrudes approximately 12 mm. The mating flange on the adjoining module has two corresponding holes and here, the upper hole is fitted with the other half of the conical bush with the lower hole having a precision ground parallel bush, which has a transition fit for the protruding tooling dowel-pin—with ≈5 μm clearance. This tooling dowel-pin was manufactured so that it can only locate across the equatorial plane of the bush, thus allowing only an insignificant movement in the vertical direction.

Throughout LRA assembly operation, the two mating flanges are brought together so that the tooling dowel-pin locates in the parallel bush. Hence, the two

halves of the conical bush are then connected by means of a conical bolt, which has been lapped to be an exact fit with the flanges in contact. Finally, the flanges are fitted together—using a controlled torque wrench setting of 12 Nm, by three equi-spaced MID bolts. Moreover, these bolts played no part in the location of the flanges, but merely held the modules together. This cone-&-bolt assembly fixed the vertical degree of freedom of the flanges and the tooling dowel-pin and its parallel bush prevented any significant rotation.

In Fig. 5.14c, a cubical base station is depicted, where it has been designed and manufactured from titanium to which each of the tubular sections can be attached. Utilising this base station, a reference artefact can be assembled in a range of configurations, such as for an: L-; T-; or X-shaped 2-dimensional artefact, or in the latter assembly, as a 3-dimensional artefact of various configurations (i.e. the latter type of configuration being illustrated in Fig. 5.14c). There are eight measuring stations mounted axially, being 125 mm apart on each 1 m module, and four on each 0.5 m module, in line with a generator of the cylinder. These measuring stations are positioned symmetrically such that the 125 mm spacing is in alignment across the flanged joints—see Fig. 5.14d. These stations consist of titanium platforms bonded to the tube and are designed to carry a range of reference surfaces, such as: steps—Gauge blocks; Cylindrical-dowels or Spheres. The complete assembled LRA, can hold a considerable number of reference surfaces, that can be utilised to define calibrated lengths associated with this artefact (i.e. as shown in Fig. 5.14d).

5.5.2 Large Reference Artefact—Reference Surfaces

The unique LRA construction has the primary function of providing a stable structure to convey reference features, which in turn are comprised of multiple reference surfaces. As a consequence, a number of design options were considered by The NPL, such as:

- **Steps**—the Step gauge is an important artefact in verifying CMMs with moderate working volumes, which is an obvious choice for the reference surfaces on the LRA—where steps with two, or more flat surfaces are employed, for example when using Gauge blocks. The corresponding calibration information is a set of distances between selected planes, these being nominally parallel faces.

The main advantages of this choice are that it:

(i) represents a simple extension of Step gauge principles familiar to users;
(ii) allows for simple, bidirectional probing strategies, a requirement of the current version of **ISO 10360-2**.

The main disadvantages are that:

(i) these steps have to be mounted accurately to achieve parallelism between faces;
(ii) the calibrated distances represent only 1-dimensional information;

(iii) the steps cannot be used easily to define calibration information if the artefact is configured as a 2- or 3-dimensional artefact using the base station;
(iv) any bending of the artefact will affect the parallelism of the faces—as well as the distance between the faces.

- **Reference spheres** (i.e. termed Tooling balls)—with their high sphericity they are readily commercially available and have long been utilised in CMM verification as the reference surfaces for Ball-plates.

The main advantages of this choice are that:

(i) no special mounting alignment is required. The only requirement here is that the location of the spheres is known accurately enough for the CMMs CNC programming;
(ii) the calibration information can be in terms of the inter-ball distances (i.e. 3-dimensional) as positions in some fixed frame of reference. This applies equally to: 1-; 2-; or 3-dimensional configurations of the artefact;
(iii) spheres can be probed in a range of differing orientations.

The main disadvantages are that the:

(i) calibration information depends on calculations of the sphere centre coordinates, however, reliable algorithms and software are available for this task;
(ii) measurements are not truly bidirectional, which is of less importance for large volume CMMs where probing-errors are likely to be small compared to the geometrical errors.

In the example of this LRA, each of these measuring station carries a grade 25 silicon nitride sphere (i.e. having a ± 1 μm sphericity) of ∅20 mm. In addition to the eight reference features on each 1 m module, there are four auxiliary spheres, or in the case of the 0.5 m module, two auxiliary spheres—see Fig. 5.14d. These auxiliary spheres are of the same design configuration as the main spheres, but lies one in each of the planes that pass through the centre of every other of the main spheres and are radial to the tube—see both Fig. 5.14a, d. With respect to the line of these measuring stations, the auxiliary spheres are mounted alternately at $+90°$ and $-90°$. These auxiliary measurement spheres are an essential feature of the modules, because they enable a calibration of the artefact to be performed on a standard sized CMM and allow the measurements of the individual modules to be combined—see Fig. 5.15a. Moreover, they can also be regarded as reference features utilised to define additional calibration information. The use of carbon composites, titanium and ceramic materials throughout the artefact's overall construction, has ensured that the LRA is of modest weight, with the complete assembled 5 m artefact including reference features, weighing <25 kg.

(a) Two LRA modules of a 5-metre long lightweight artefact in the process of being calibrated - sphere positions - on a Bridge-type CMM:

(b) Summary of experimental results of LRA undertaken at a French car manufacturer with a large CMM, having two cantilever arms, with a working volume of: 6 m x 1,4 m x 1,7 m - according to ISO 10360:

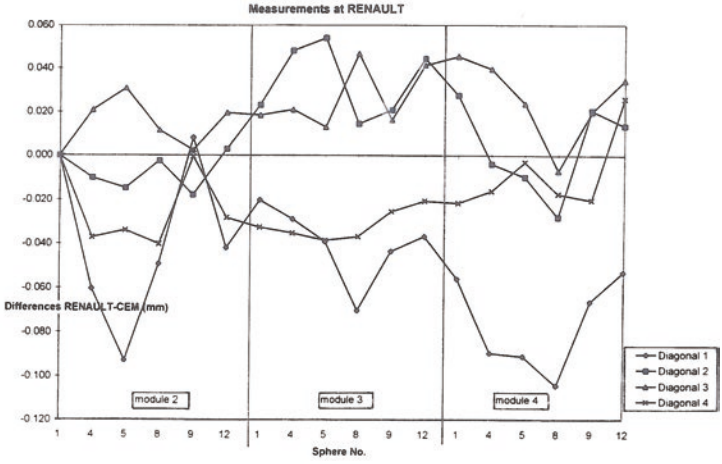

NB The 3 m LRA was positioned at an angle of 30° - along the four space diagonals of its working volume, with the LRA measured three times.

Fig. 5.15 The large reference artefact (LRA) utilised for verification of large working-volume CMMs [*Source* Centre of Length Measurement (NPL)—Corta et al. (1998)]

5.5.3 *Large Reference Artefact—Artefact Positioning, Alignment and Testing*

Yet another major factor in this LRA's design system is its mounting, with the artefact being mounted on a substructure carried by one central light and stable pillar on a triangular base. This base has three retractable wheels that enable the artefact to move easily on the CMM table—the LRA being shown in situ in Fig. 5.15a, where it is positioned on a Bridge-type CMM. The pillar can either be attached rigidly to the CMM table, or weighed down using lead masses. The column allows the artefact to be lowered, raised and orientated at any angle. In this instance, the main supporting substructure can be assembled using two or three aluminium sections depending on the length of the artefact to be mounted. This artefact is mounted on the substructure using clamps, which attach to the flanges at each end of the artefact; additionally, the artefact can also be suspended vertically using the same equipment. This LRA design system arrangement, is capable of orientating the artefact in all the relative positions suitable for CMM verification according to **ISO 10360-2** procedures.

In exhaustive testing of the LRA, the stability of the support has been verified using a gauge attached to one end of the support to measure any change in position. It was also reported in these verification procedures, that no change was detected—at the micrometre level—over a duration of many hours. Since the tooling balls are situated off the neutral axis of the tube and when the tube inevitably bends due to gravitational loading, the inter-sphere spacing will vary with: angle; support condition; as well as its length. By way of closely controlled experimentation and the application of FEA (i.e. finite element analysis) it has been shown that bending only introduces significant changes in inter-sphere spacing for lengths greater than 2 m. Accordingly and in order to minimise these bending effects, a mechanical–optical alignment procedure has been implemented to determine the straight condition for any arbitrary length of artefact and then supporting this artefact in such a manner that the centre sag is within 0.1 mm of this straight condition. This correction application was sufficient to allow for an accurate rectification of the inter-sphere distances using finite element analysis.

An international program of LRA industrial testing was undertaken by the French car company Renault, at their automotive plant in Valladolid—in Spain. Here, the CMM had two cantilever arms and a working-volume of: 6 m × 1.4 m × 1.7 m. In this instance, the assembled 3 m LRA was positioned at an angle of 30° along the four space-diagonals of the CMM's working-volume. The artefact was measured three times in each orientation, with six spheres on each module being measured, using five probing-points. Typically, a commercially available Renishaw-probe was employed, with a ∅3 mm ball-ended stylus. A summary of the LRA-probing results is given in Fig. 5.15b. This graphical measurement data shows the differences between the distances from the first sphere to the other spheres, determined from each of the measurements along four diagonals and the

distances determined by CEM-calibration.[11] Of note, was that these latter-distances are not corrected for artefact deflection, with the correct distances differing by up to 5 μm. The LRA results showed that there are certain differences of the order of 100 μm between the diagonal measurements (i.e. independently of any calibration).

5.5.4 Large Reference Artefact—Summary and Concluding Remarks

The verification of the length measurement capabilities of large CMMs according to the principles of **ISO 10360-2** necessitates a length artefact that is structurally stable, capable of defining accurately calibrated lengths and easily supported and positioned. This LRA is of reconfigurable modular design, being up to five metres long, with each 1 m module made from tubular sections of carbon-composite materials. The use of carbon composite tubular sections has meant that the artefact is exceptionally light yet very rigid. Due to its modular design and construction, the artefact lengths can be simply disconnected, making it both easy to transport and store. In summary, the Large Reference Artefact has the following metrological-attributes:

- **each module has silicon nitride reference spheres**—these are spaced uniformly along a measuring line, with the calibrated lengths being specified in terms of the distances between these reference spheres;
- **each module has precision-ground flanges**—which are also made from carbon fibre, that allow the modules to be joined together semi-kinematically, with the fit of each joint being highly repeatable in terms of variations in the distances between pairs of spheres, with one on each side of the modular LRA-joint;
- **an innovative calibration strategy**—utilising repositioning methods and software, which has been designed allowing the complete five metre assembly to be calibrated using a CMM with a longest working axis of $\leq$500 mm. These modules and the joins of pairs of modules are calibrated in run, with positional calibration software being employed to determine the geometry of the complete assembly;
- **the LRA was independently calibrated by three EURAMET laboratories**—producing an expanded uncertainty ($k = 2$) for the length of the five metre assembly, with a typical calibration of the order of 0.010 mm (i.e. the uncertainty here, will depend somewhat on the CMM performing the measurements, its operating conditions, etc.). Hence, the contribution to this uncertainty budget from the repeatability trials of the joins, was estimated to be $\leq$2 μm;
- **equipment for supporting and repositioning the artefact**—this overall and total NPL-design and construction of the LRA, enabled verification of a CMM;
- **artefact and positioning equipment**—was successfully tested in the verification of large CMMs according to the principles of **ISO 10360-2**.

[11]**CEM**—LRA calibration was jointly-undertaken at the: **Centro Español de Metrología** (CEM) in Madrid, Spain, which is one of the International Partnerships of the Metrology Standards Organisations of EURAMET.

In conclusion, this uniquely designed LRA, was both originally designed and constructed by The NPL, where it reflected the requirements of its design philosophy and calibration methodology, being reconfigurable, while providing a generic template for large-scale reference length artefacts. With this template, the verification of the length measuring capabilities of large CMMs can be implemented in practice.

5.6 Machinable-Artefacts for Machine Tool Verification

When initially purchasing a new CNC machine tool, it is considered common practice—during the actual commissioning-stage—to have at least one testpiece machined to prove-out the accuracy and precision performance of this machine. Of note, is that this type of machined testpiece is not actually used to calibrate the machine tool, but rather for just its acceptance purpose and for perhaps a machine performance check during any periodic re-verification.

5.6.1 Introduction to Machinable Testpiece Standards

The International Organisation of Standardisation (ISO) has published a standard which designates the test conditions for Machining Centres. Here, **ISO 10791-7**, defines the accuracy of such finished machinable testpieces. There are two distinct testpieces which are considered in this Standard, the first being for a positioning and contouring testpiece, whereas the second is a face milling testpiece. The former test is for checking of the geometric properties of Machining Centres—with the maximum numbers of axes that need to act simultaneously to cut this testpiece being just two. The German company NC-Gesellschaft, has previously published a recommendation for workpieces for high speed cutting (HSC) having similar machining features described in the ISO Standard, but with these NC-G recommendations, it features testing the influence of different feedrates of the machine tool and the actual machining operation utilising three simultaneous translational axes. At the EMO Hannover Show of 2005 NC-Gesellschaft presented yet another recommendation, describing a testpiece to be machined with up to five simultaneous axes. The interpretation of the testpiece quality here, is not by means of quantitative measurements and comparison with tolerances, as in the other prescribed machined testpieces, but rather by qualitative assessment—mostly by optical means, with the interpretation of certain features for its various form of elements. Additionally, NC-Gesellschaft gave indications for the causes of possible machining errors. Accordingly, the usage of this machinable testpiece is well-suited for the periodic testing of machines and in particular, for tests after there has been a machine-crash.

In the latter half of the twentieth century, the Aerospace Industries Association of America, Inc. (AIA) published a National Aerospace Standard (**NAS 979**) describing uniform cutting tests—see Fig. 5.16—for a generic schematic representation of this machinable artefact. In this **NAS 979** machinable testpiece, various cutting test

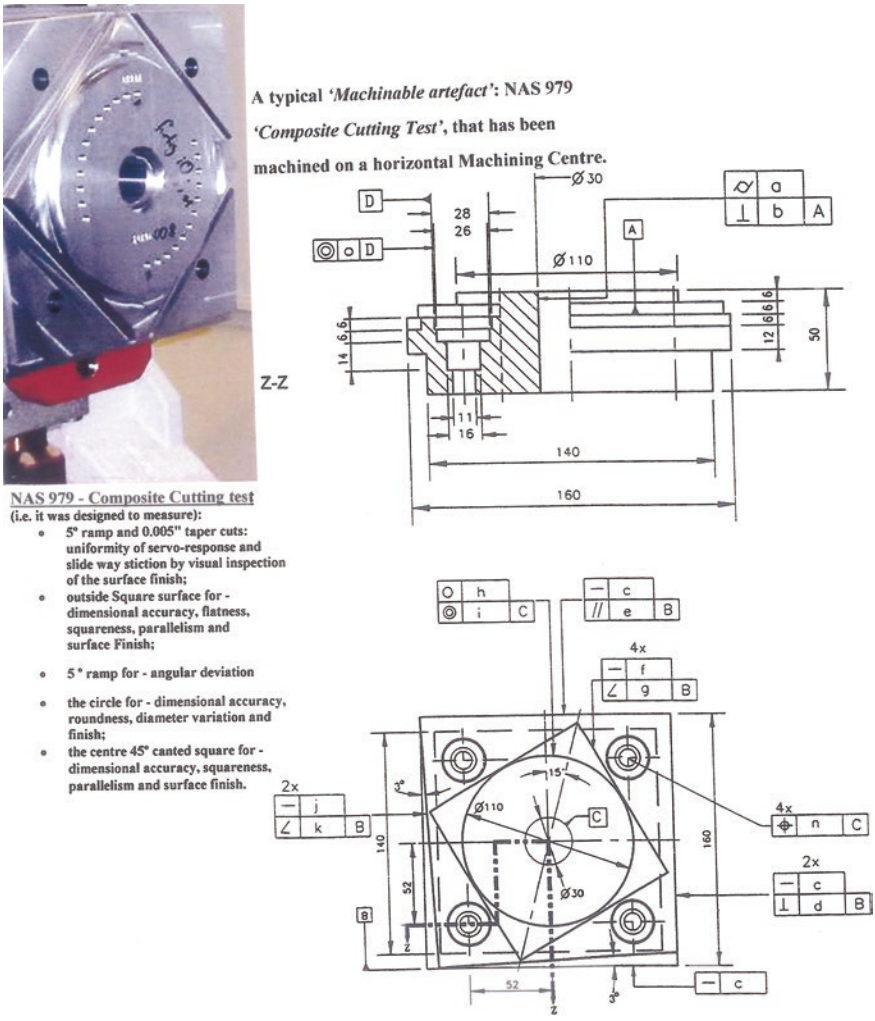

Fig. 5.16 Small-sized machining testpiece for machine capability assessment

features were specifically described for use in evaluating machine tools that at the time were being procured for the aerospace manufacturing industry. Some of these cutting tests also included machinable elements similar to the ones described by **ISO 10791-7**. Within the Boeing Aircraft Company, it had its own Equipment Design and Asset Acquisition Standards, which included the Profile cone frustum cutting test—derived from **NAS 979**. The description of the Boeing-test was not enhanced, but typical tolerance requirements are defined as being ten times tighter than presented in the original **NAS 979 Standard**. After machining, no tolerance was specified for the surface texture as it is in **NAS 979**, where a value is stated for

the maximum finish in Roughness Height Reading[12] (i.e. RHR—which is in units of micro-inches). Moreover, the American Society of Mechanical Engineers (ASME) also made reference to this **NAS 979 Standard**, for simultaneous five axis machined testpieces. Furthermore, if the text of the **NAS 979** is critically reviewed, it has unfortunately some machine tool-related problems associated with it, such as:

- **concerning the actual machine tool being tested**—it mentions that it should have very large cutting tool spindle, which invariably is not the case;
- **the cutter's path is somewhat ambiguous**—although within the text it is written that, '…all five axes should be moved…'; even if in effect, just four simultaneous axis movements are enough to perform this test;
- **while noting the machining testing sequence**—it states that, '…the *Z*-axis shall move 1 in. [25.4 mm] minimum…'—as a consequence, the tool's centre point does not actually trace a circular path, but that of an ellipse.

Relating to the above-mentioned reasons concerning this **NAS 979** tests, many machine tool builders and their customers undertake a 'Cone frustum cutting test' by applying specific machining test conditions to any such machining trials.

5.6.2 Artefact Stereometry—For Dynamic Machine Tool and Comparative Assessment

Introduction

In order to gain a more detailed understanding of the total aspect of machine tool calibration, coupled to the verification by machinable-artefacts, an applied research program of work was carried out, which is reported in the following sections for a typical Machining Centre. However, prior to this discussion, a machinable artefact having: prismatic; rotational; as well as positional features; has been described in the previous section concerning the **NAS 979 Standard Test** (i.e. shown in Fig. 5.16) which has long been employed by the industry to establish an overall machine tool's machining capability. Despite this previous adoption of the **NAS 979** machining test by industry-at-large, it does have several more significant limitationsand these are that the:

- **overall dimensional artefact's size is relatively small**—when compared to that of the volumetric envelope of a typical Machining Centre;
- **circular features cannot be directly compared to that of diagnostic instrumentation**—typically the Ballbar, as the diameter of this rotational feature differs somewhat from that of standard lengths of Ballbar rotational sizes;

[12]**Roughness Height Reading** (**RHR**): here, this RHR value of for example: 35 micro-inches, corresponds to a total height of the profile '*Rt*' of 0.9 μm. The '*Rt*' surface texture parameter is the total height of the profile, based upon the amplitude parameters of peak-to-valley readings from the surface trace—for more specific details see: *Industrial Metrology—Surfaces and Roundness* (Smith 2002).

- **weight of the artefact does not realistically compare (i.e. in the loaded state) to any workpieces normally placed on the machine's table**—meaning that the true machine tool loading-conditions are not directly comparable.

With these machinable testpiece limitations in mind, it was considered worthwhile to design and develop a new artefact with a totally different machining and verification strategy for such machine tools, but in this instance, being under more realistic loaded conditions. Moreover, this newly developed artefact would be directly comparable to that of the Ballbar and certain other metrological instrumentation, but with a larger volumetric size and increased weight, but also having the capacity for reuse of the machinable parts of this artefact's assembly—thus keeping the overall artefact's cost down. This newly designed partially machinable artefact was based upon the concept of Stereometry,[13] which is schematically depicted in Fig. 5.17.

5.6.3 Stereometric Artefact—Conceptual Design

The term Stereometry is a concept in machine tool verification that has often been either dismissed, or simply overlooked, but it is concerned with the volumetric content of a range of geometric shapes. However, this volumetric concept can be carefully integrated into a single artefact—see Fig. 5.17. In this manner, it can be employed for verification and diagnostic works on machine tools such as Machining Centres—see Fig. 5.19. Here (i.e. in Fig. 5.17), the cylindrical volume was represented by three machinable aerospace-grade aluminium disks (i.e. grade: 2017F—produced from 6 mm sheet, but just slightly larger in diameter at: >∅ 300 mm), with each disk accurately and precisely located on a hardened and cylindrically ground mandrel. Each of the three disks are set 100 mm apart in height and after circular interpolation milling these disks were exactly ∅300 mm—see Fig. 5.19a. The ∅10 mm holes in each disk, namely 1 (bottom); 2 (middle); and 3 (top); (i.e. shown in Fig. 5.17) were also produced by circular interpolation, where this geometry represented a swept right-circular conic frustum having an included angle of 22½°; this arrangement being the result of producing four equi-spaced holes at various positions on each disk. This is achieved by starting with the bottom disk in situ (i.e. disk 1) and slot-drilling four holes, then stopping the machine and fitting the middle disk (i.e. disk 2) and slot-drilling four holes, once again stopping the machine, then fitting disk 3, and finally slot-drilling the remaining four holes. Each hole was offset when looked at in plan-view, producing an Isosceles triangular relationships, across the three disks—see Fig. 5.17 (bottom). Moreover, in this

[13]**Stereometry**: in mathematics, is the term for solid geometry that was the traditional name for the geometry of three-dimensional Euclidean space, but for all practical purposes it was based upon the kind of space in which we [i.e. Man] exists. Thus, Stereometry concept was instigated following the further-development of plane geometry. Accordingly, Stereometry deals with the measurements of volumes of various solid geometrical figures including a: cylinder; circular cone; truncated cone (i.e. termed a frustum); sphere; as well as for prisms.

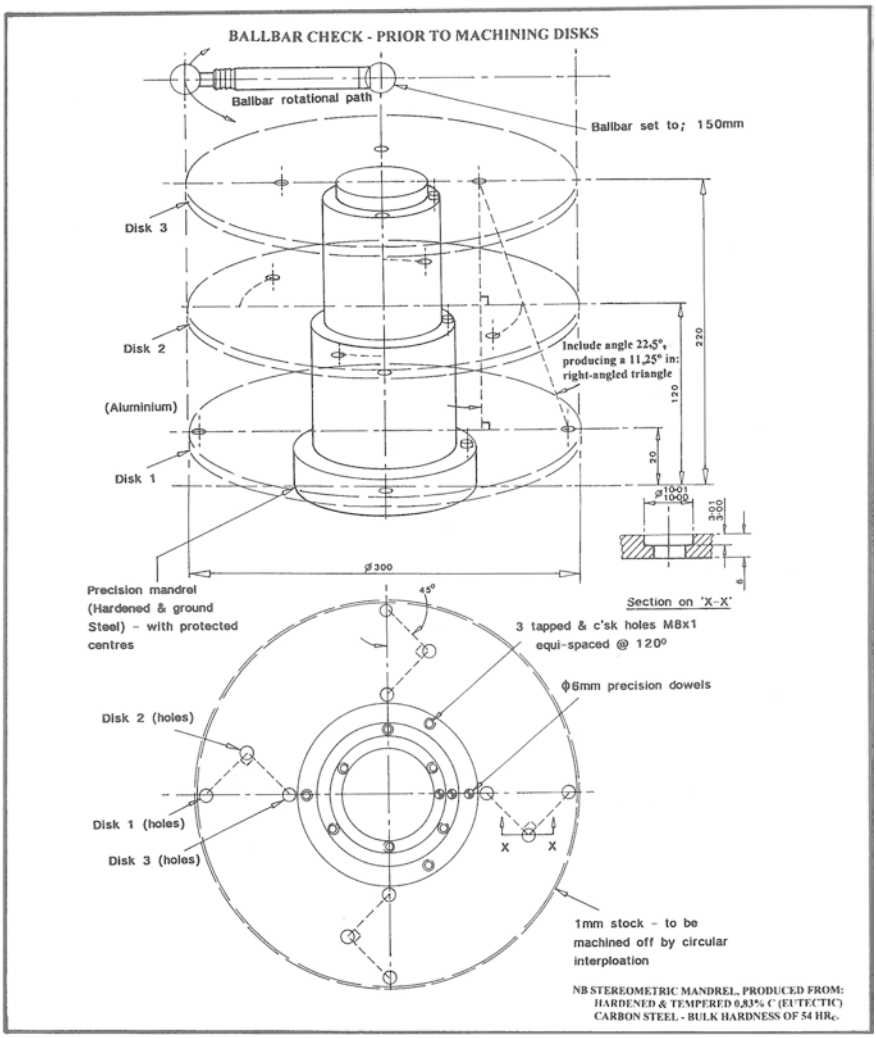

Fig. 5.17 The geometry of the stereometric artefact, designed for the volumetric and positional uncertainties on machining centres, by: high-speed machining (HSM) interpolation of machinable disks [*Source* Smith et al. (2001)]

plan-view, it can also be seen that these individual holes are set at an angular relationship of 90° equi-spaced apart—across the three disk heights. These geometric and volumetric relationships were intrinsically set and datumed to the previously machined centrally located slot in the base of precision mandrel, while each disk was individually located on ∅6 mm precision dowel pins—as shown in Fig. 5.17. This strict orientation-relationship between each disk and their precise and accurate location on the mandrel meant that the volumetric-relationship remained constant and in situ, for this Stereometric artefact, even when this whole assembly was removed from the machine tool for subsequent metrological analysis.

5.6.4 Stereometric Artefact—Machining Trials

Prior to the Stereometric artefact having its machinable disks milled along their peripheries, the initial test machine—this being a Cincinnati Milacron Sabre 500 with Fanuc OM CNC controller—was fully diagnostically calibrated. This actual calibration was undertaken by Laser interferometry; coupled with long-term dynamic thermal monitoring of its duty-cycles, in both the loaded and unloaded condition, as well as by verification using Ballbar assessment—see Fig. 5.18. Prior to discussing the actual machining of the disks, it is worth taking a few moments to consider the precision cylindrical mandrel that accurately and precisely locates each disk in the desired orientation, with respect to the machine tool's axes. This mandrel body, shown in the photographs in Figs. 5.19 and 5.20, was produced from eutectic steel,[14] which after through-hardening and then stabilising to obtain a bulk hardness of 54 HR_C, was precision cylindrically ground on the three register diameters, with the top and bottom mandrel faces surface ground flat and square with respect to these diameters. Previous to the heat treatment and grinding operations, precision dowelling datums (i.e. ∅6 mm holes) were accurately and

[14]**Eutectic steel—metallurgical details**: this grade of steel is often termed: Silver-steel, due to its bright and shiny appearance when it is compared to that of other grades of plain carbon steels. In brief and from a simplistic-metallurgical viewpoint, this 0.83 wt% carbon content steel is known as a eutectic steel (A eutectic metallurgical structure is a two-phase microstructure resulting from the solidification of a liquid having a eutectic composition: the phases exist as fine lamellae that alternate with one another), as it relates to the eutectic composition derived from the iron-carbon thermal equilibrium diagram (TED). It has a 100 % pearlitic structure (i.e. having metallographic brilliance, or iridescence), when suitably etched and viewed under a microscope exhibiting fine alternate layers of Fe_3C and Fe. Thus, to harden eutectic steel, its temperature is raised to slightly above the arrest point (i.e. normally reportedly-set at: 723 °C). So that it is possible to harden it, this eutectic steel's temperature is usually raised slightly higher to ≈765 °C, into the γ-solid solution (i.e. austenitic region) an soaked, then it can be rapidly-quenched and agitated usually in water to strictly-minimise carbon atomic diffusion [i.e. this is normally undertaken at faster than the critical cooling velocity (CCV), at >1000 °C s^{-1}]. After quenching, these carbon atoms are now effectively-fixed—even though they are not intrinsically-part of the atomic lattice structure. This quenching-process and subsequent carbon entrapment, creates intense local strains that block any form of dislocation-movement. Accordingly, the resulting metallurgical structure is both hard and extremely strong, but it is also very brittle and being somewhat unstable. Microscopically, the hardened structure appears as a "…random and chaotic array of needles…", being completely different from the original pearlitic structure. This so-called needle-like structure is formed by the trapped carbon atoms within the iron crystal lattice, which is termed: martensite. Thus, the degree of bulk hardness of in this case, the precision mandrel after quenching, being proportional to its actual lattice-strain. After hardening (Through-hardening did not occur in this instance, due to the interrelated factors of the steel's: Ruling-section and its Mass-effect; plus this lack of through-hardening can be realised by considering the influence of the CCV on the Time-Temperture-Transformation (T-T-T) graph), the mandrel required tempering, which is a controlled heat treatment process (i.e. usually undertaken between 200 and 300 °C), to allow some of the trapped carbon atoms to escape from their interstitial-spaces between the distorted lattice structure, so releasing some of this strain-energy, where they eventually form particles of cementite. [Sources: Thelning (1975), Alexander et al. (1985), Callister et al. (2003)].

(a) Comprehensive Laser and Thermal mapping of a vertical machining centre:

(b) Detail of Y-axis Laser calibration, with thermocouple placement(s) - the latter for medium-term thermal monitoring / data-logging information:

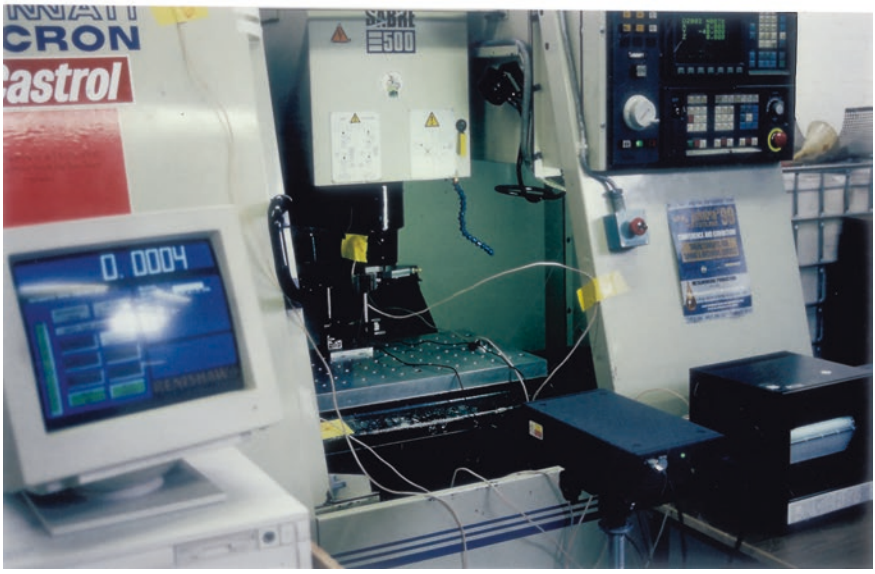

Fig. 5.18 Calibration of a vertical machining centre, prior to high-speed machining trials on a stereometric artefact [after: Smith et al. (2001)]

(a) Stereometric artefact's final disk being machined – high-speed machining (HSM) @ 20,000 rev min^{-1} by circular interpolation:

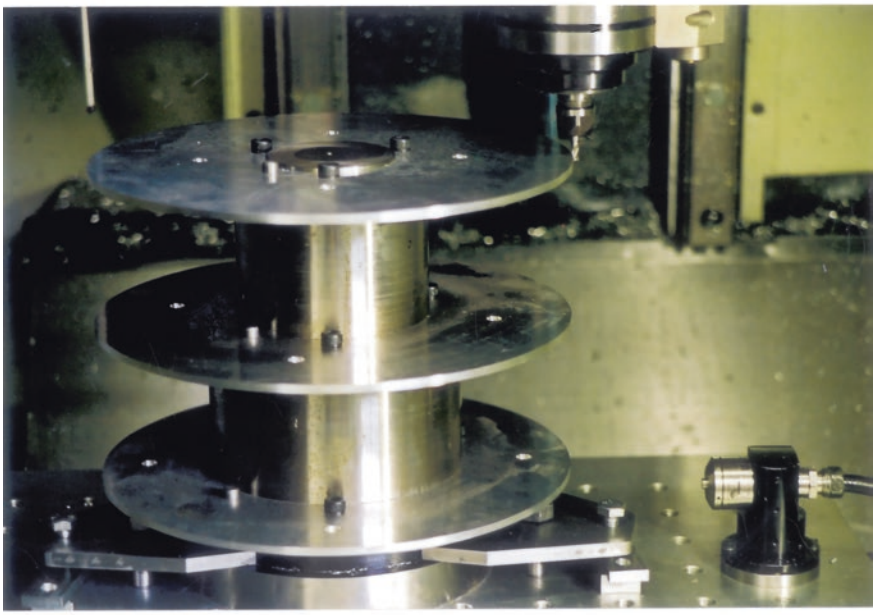

(b) Triangulated hole positions @ quadrant angular displacement - being HSM slot-drilled and opened-out to ϕ10 mm - by circular interpolation:

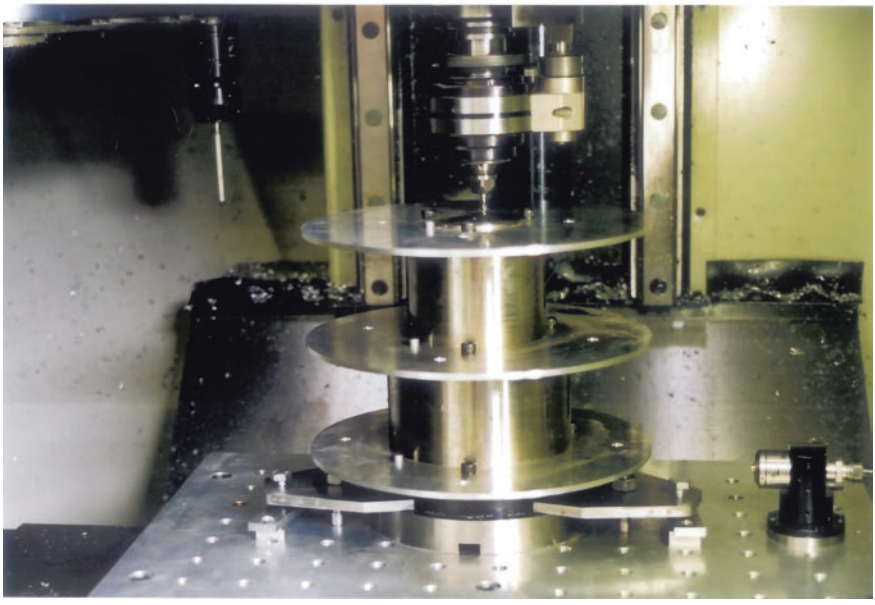

Fig. 5.19 The high-speed machining trials on machinable aerospace aluminium disks for a stereometric artefact [after: Smith et al. (2001)]

precisely drilled and reamed, then 3-equi-spaced tapped clamping holes for each disk (i.e. M8 × 1) along with a surface ground central datuming-orientation slot in the base of the mandrel. These various datums and more specifically the base's datum-slot, allowed all of the artefact's features to be correctly orientated with respect to the geometry of the machine's axes—see Figs. 5.19b and 5.20b.

Several unique features were introduced into the machining portions of this Stereometric artefact, which included:

- the aerospace-grade aluminium disks machined to ∅300 mm, being peripheral milled by high-speed milling (HSM). This HSM, enabled these disks to be directly compared to the radial path of the Ballbar—see Fig. 5.17 (top) previously utilised for this machine's diagnostic machine tool assessment, thus ensuring that some degree of correlation occurred between them;
- the three *Z*-plane disk heights of: 70; 170 and 270 mm; (i.e. the respective disk heights being the only modification from the original design—depicted in Fig. 5.17) coincided with both the *X*-*Y* plane table positions and the vertical heights utilised for the three respective Ballbar plots, creating a reasonably large swept cylindrical volumetric envelope (i.e. indicated in Fig. 5.17). Moreover, this artefact was also designed to be orientated to coincide with the start-and-finish positions of these Ballbar's polar traces;
- at the four quadrants, the four circular interpolated holes (i.e. ∅10 mm) on each disk—see Fig. 5.17—were geometrically positioned to form a three-dimensional Isosceles triangle at these respective three heights—with the first and third holes relating to the axes transition points in the *X*- and *Y*-axes, respectively. Thus, each of the interpolated milled holes in the face of the separate disk's produced the geometric Stereometry of a swept right-circular conic frustum, having an included angle of 22½°—when the angular orientation in the middle disk was software-aligned to produce a straight line relationship between the holes—see Figs. 5.17 and 5.21b;
- the overall combined weight of the mandrel and this disk-assembly was 38 kg; accordingly, this could be considered as a realistic loaded condition for the machine tool to operate under from a practical sense and in this manner, mimic the machine's operational performance under actual industrial/production conditions.

In order to minimise the milling forces and potential distortion on these machinable disks, HSM was employed, by utilising a spindle-mounted speed increaser[15]—see Fig. 5.19. The Speed-increaser utilised a ∅6 mm high-performance slot drill with quick-flute angle (i.e. being made from Tungsten carbide with PCD

[15]**Speed-increasers**: these are auxiliary spindle-adaptors that are fitted directly into the machine tool's spindle. These increasers act as a means of multiplying the rotational speed of the machine's spindle, by employing a fixed-relationship geared head. Here, the one shown was a 'Speed-increaser' that had a 3:1 gearing ratio, equating to a top rotational speed of 18,000 rev min^{-1}, when the machine was operating at its maximum 6000 rev min^{-1} speed, but other 'Speed-increasers' could also peripheral mill > 20,000 rev min^{-1}, with a 4:1 geared head.

(a) CNC 4-axis CMM inspecting the machinable disks on the Stereometric artefact while in-situ and in the correct angular orientation:

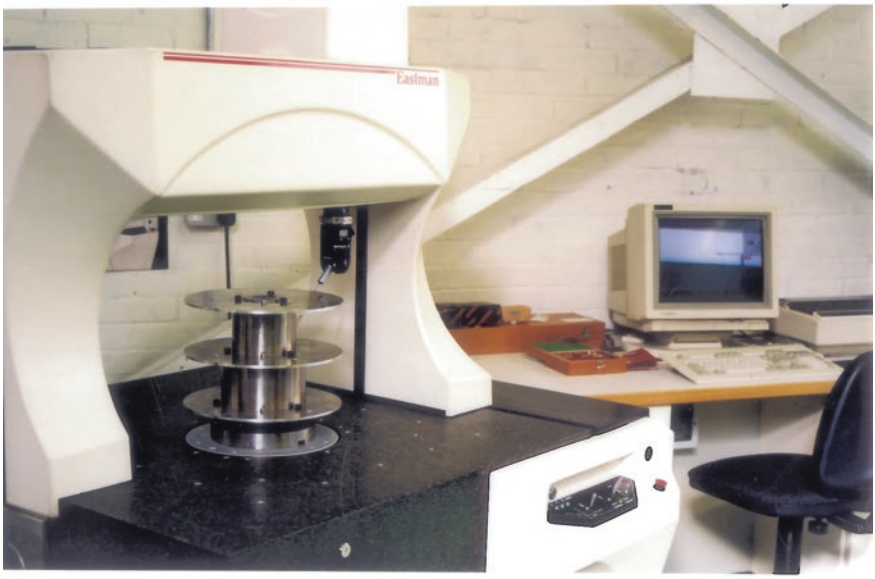

(b) An automatic probing cycle of the 'artefact's' diameter and the three-dimensional quadrant hole positions on the disks, using an analogue probe:

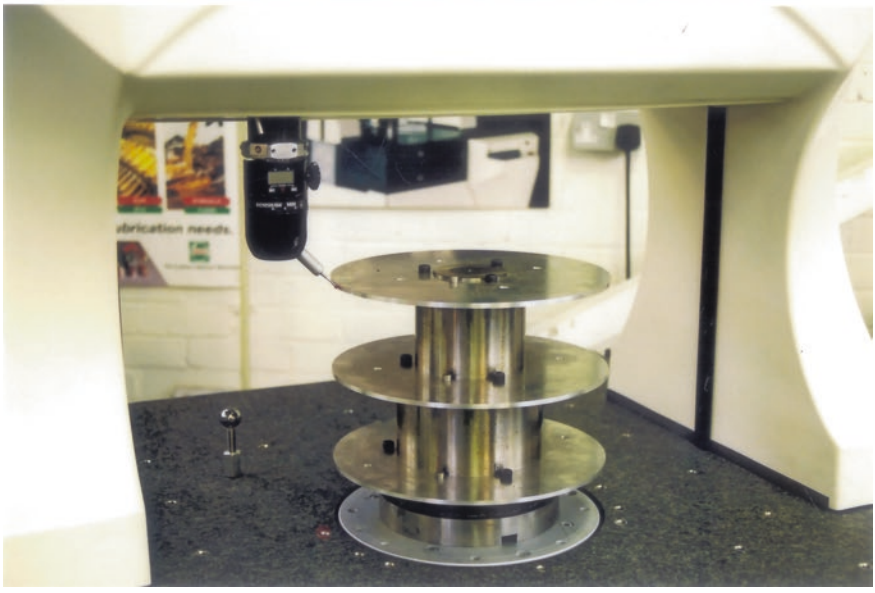

Fig. 5.20 An CMM inspection procedure of the machinable disks in situ on the stereometric artefact [after: Smith et al. (2001)]

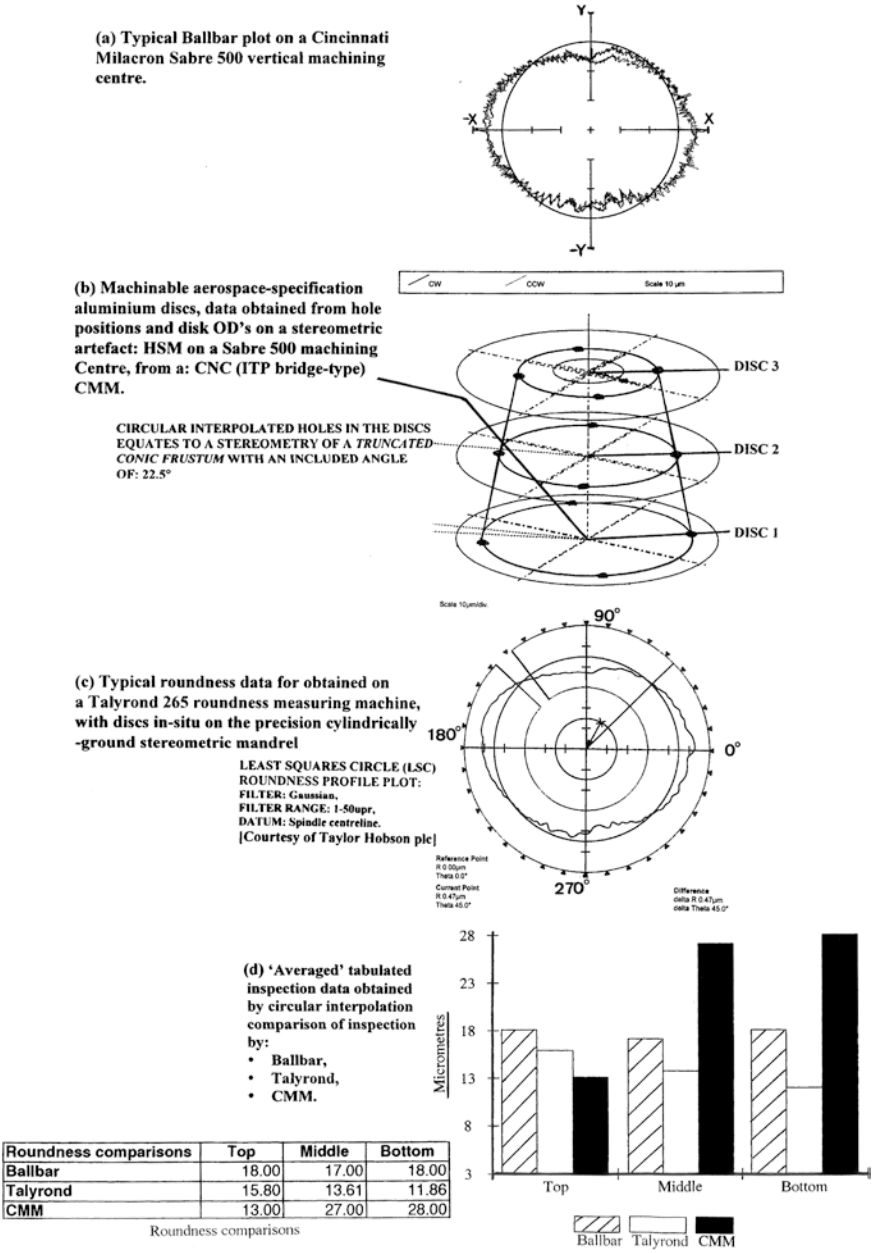

Roundness comparisons	Top	Middle	Bottom
Ballbar	18.00	17.00	18.00
Talyrond	15.80	13.61	11.86
CMM	13.00	27.00	28.00

Fig. 5.21 Data obtained from machining a stereometric artefact [*Source* Smith et al. (2001)]

multi-coating[16])—allowing the tool to both drill-down 3 mm depth into the disk surface and then scroll-out by circular interpolation milling for the disk's hole diameters to ∅10 mm—see Fig. 5.17, i.e. showing a cross-section of the hole's details in Section on *X*-*X*. This HSM was undertaken at 20,000 rev min^{-1} and notably, the peripheral milling occurred with a circular interpolation feed of 750 mm min^{-1}, with an excess disk stock of 1 mm, meaning that the cutting tool loading was exceedingly small.

5.6.5 Stereometric Artefact—Machined and Metrological Results

After HSM of all of these machinable disks features by circular interpolation on the vertical Machining Centre, the complete artefact with these disks still in situ was carefully removed from the machine tool. It was then automatically inspected for quadrant hole positioning and disk diameters—in the exact same orientation as they were manufactured on the Machining Centre. This metrological inspection was undertaken on an Eastman/ITP four axis bridge-type CNC Coordinate Measuring Machine—see Fig. 5.20. This particular CMM had previously been: Laser-calibrated; thermally error-mapped; then also verified with a Machine Checking Gauge, prior to the artefact undertaking an automated-inspection procedure—enabling this CMM to produce some realistic measurement data. Once CMM data acquisition had been successfully accomplished, the complete artefact assembly was then inspected on a Taylor Hobson Talyrond 265 Roundness Testing Machine within a fully air-conditioned and metrological laboratory environment. Each of these disks were machined for their individual roundness parameter of Least Squares Circle[17] (LSC), as well as the overall

[16]**PCD multi-coatings—on cutting tools**: this Polycrystalline diamond (PCD) coating is normally formed in a large High Temperature-High Pressure (HT-HP) press, as a synthetic diamond-like coating on a backing of tungsten carbide. Typically, this PCD coating is normally produced by sintering many micro-size single diamond crystals at high temperature and high pressure by either a: Physical Vapour Deposition (PVD); or Chemical Vapour Deposition (CVD) process. Therefore this specific PCD coating has very high hardness, good fracture toughness coupled with excellent thermal stability. NB Polycrystalline diamonds are normally synthesised from graphite under: ≧15 GPa and @ 2300 to 2500 C (i.e. here they consist of fine grains of: 10–30 nm in size—in crystalline layers), having very high Knoop hardness (Hk ≧ 120 GPa). [Sources: Sumiya and Irifune (2008), Smith (2008)].

[17]**Least Squares Reference Circle** (i.e. LSC1): can be defined as: "A line, or figure fitted to any data such that the sum of the squares of the departure of the data from that line, or figure is a minimum". This is also the line that divides the roundness profile's trace into equal minimum areas. NB This LSC1 is the most commonly-used Reference circle. The term: out-of-roundness, or more specifically: departures-from-roundness as it is should now be known, is then expressed in terms of the maximum departure of the profile from the LSC1 (i.e. the highest peak to the lowest valley—on the polar plot). [Source: Smith (2002)].

disk's Cylindricity[18] being assessed, with the averaging of results of three trials, so that the combined results from the Ballbar, CMM and Talyrond are displayed in Fig. 5.21d.

When a comparison is made of these results from the three individual and completely differing metrological inspection procedures, namely: Ballbar, CMM and Talyrond, they exhibit some degree of metrological consistency. For example, a 15 μm variation (i.e. range) is indicated from the top-to-bottom disks, but they also show a mean value of ≈22.7 μm dispersion of results by the CMM. The Talyrond polar plots (i.e. LSC), also produced some consistent roundness results, ranging from <4 μm and having a mean value of ≈14 μm. Conversely, the smallest variability occurred with the Ballbar, producing a range of just 1 μm, with a mean value of ≈17.6 μm—at these three *Z*-axis heights. Prior to discussing why the CMM results significantly varied from those obtained from the Ballbar and Talyrond, it is worth visually looking at a comparison between the general profile shapes of typical polar plots that were produced by these Ballbar and Talyrond metrology instruments. In Fig. 5.21a (right), a representative polar plot from a Ballbar is shown and likewise in Fig. 5.21c (right) for the Talyrond a typical polar plot is also depicted. Here, their respective profiled shape geometries, in terms of their respective harmonics[19] are remarkably alike, illustrating the same generally similar elliptical shape combined with its identical axis orientation.

---

[18]***Cylindricity***: can be defined as: "The minimum radial separation of 2 cylinders, coaxial with the fitted reference axis, which totally enclose the measured data." NB A working definition for cylindricity, might be: "If a perfectly flat plate is inclined at a shallow angle and a parallel cylindrical component is rolled down this plate. If the component is a truly round cylinder, then as it rolls, there should be no discernible radial/longitudinal motion apparent." [Sources: Dagnall (1996) and Smith (2002)].

[19]**Harmonics—of departures from roundness—of components**: thus, by using harmonic analysis one can establish what actually creates the lobing conditions on the inspected part. Generally, there are three major contributors to the lobing condition, these are the:

(i) **first harmonic**—which is called the fundamental sinusoid. Its actual wavelength is the entire length of the circumference (i.e. over 360°) and it measures geometry errors that repeat once per revolution. These types of errors tend to be the result of an eccentric-error, such as by the operator inadvertently placing the part off-centre when it is initially setup in the machine;

(ii) **second harmonic**—this measures errors that repeat twice per revolution, so its wavelength is one half the fundamental wavelength (i.e. over 180°). These second harmonic problems are invariably the result of an out-of-squareness condition in either the: machine tool; its fixture; or resulting from the actual measurement setup;

(iii) **third harmonic**—this measures errors that repeat three times per revolution. Hence, its wavelength is one third of the fundamental wavelength (i.e. over 120°). Thus, in the same vein, then the **Nth harmonic**, will be a sinusoid whose wavelength is the fundamental wavelength divided by '*N*'. Moreover, the third and higher harmonics problems are often the result of workpiece clamping, a particular aspect of the manufacturing process, or otherwise resulting from the various sources of induced vibration—whilst machining. For example in the former clamping-situation, a three-point chuck is apt to produce an odd number of equi-spaced lobes on the machined roundness profile. [Source: Schuetz (2007)].

Returning to the CMM results only a few data-points are utilised to obtain a measured diameter and its profile, conversely, with both the Ballbar and Talyrond alike, they literally take thousands of actual data-points to obtain the polar plotted profile. When the CMM touches each machinable disk's profile with its touch-trigger probe, this specific coordinate's data could have been obtained at the extreme of the elliptical shape, namely at its major and minor diameters—see Fig. 7.6. Such a variation in both the range and discrepancies in the CMM measurements, when compared to the data obtained by either the Ballbar and Talyrond, may possibly account for such diversity—in this instance.

The four ∅10 mm holes in each disk produced by HSM utilising circular interpolation at their respective quadrant positions (i.e. see Figs. 5.17 and 5.21b), are given in tabulated data form shown in Table 5.3—in terms of their positional accuracy and radial change from their theoretical centres.

From the ∅10 mm data given in Table 5.3 for the radial change for each disk, for the top, middle, and bottom disks, it was: 46; 45 and 42 μm; respectively, giving a positional uncertainty of 4 μm. Equally, if the difference is considered for the three stacked disks with respect to their angular relationships to each other, at: 0°; 90°; 180° and 270°; then their angular positional changes are: 46; 26; 32 and 49 μm; respectively, giving a positional uncertainty of 23 μm. This general interpolated milled-hole positional uncertainty is still relatively small considering that in this case, each hole's position is on a different *Z*-axis plane—spanning a dimensional height of 200 mm. If one considers the grand mean for both cases, then they have a positional uncertainty of just 1 μm, which for a vertical Machining Centre that at the time of testing was three years old, is quite exceptional—having by now, undertaken considerable industrial machinability trials for both the automotive and aerospace industries. Admittedly, this particular machine tool had previously been both Laser-calibrated and Ballbar-diagnostically corrected—thus showing the true relevance of such calibration to resolve and minimise any current machine- and process-errors, which might currently be present within the actual machine tool.

Table 5.3 The ∅10 mm hole positional deviations for the frustum—based upon the three-dimensional Isosceles triangle—in the machinable disks at the four quadrant positions (i.e. from the theoretical), in terms of their actual radial change

Position of holes	Top disk	Middle disk	Bottom disk	Range	Mean	Grand mean
0°	987	941	969	46	966	↓
90°	978	952	953	26	961	**972**
180°	1014	986	982	32	994	
270°	968	946	995	49	965	
Range	46	45	42			
Mean	987	956	975			
Grand mean	→	**973**				

Numerical values in: μm
Source Smith et al. (2001)

The initial verification work using the Stereometric artefact, has shown—Fig. 5.21—that its overall positional ability when utilised for HSM analysis coupled to accuracy and precision assessment in combination with machine tool diagnostics, has some degree of metrological-success. Here, then, the actual physical weight of this artefact when verifying the machine's capabilities, would tend to exacerbate any axis geometry and positioning problems for such a machine tool, which provides a realistic measure of the machine tool's machining and positional performance in-service.

5.7 Small Coordinate Measuring Machine (SCMM)

Introduction

It is acknowledged that any object greater than a few centimetres in size can be habitually inspected by conventional CMMs, where they can realistically achieve uncertainties of several micrometres. On the other hand, objects that range from a few micrometres down to say, a nanometre, cannot be realistically inspected even on very highly sophisticated CMMs, as in this latter case, the measuring capabilities of nanometrology instrumentation is in effect, mandatory. The problem with any of these nanometrology instruments—which despite their undoubtedly excellent uncertainty performance—is that they cannot measure component parts as large as a few centimetres in size. Likewise at present, there are no 3-D CMMs that can achieve micrometre uncertainties for these complex measurands. So, in order to address this problem, The NPL within the UK, has developed a metrological instrument with a working-volume of 50 mm^3, with an uncertainty within the range of: 50–150 nm. At this juncture, this SCMM instrument can be effectively considered as a miniature CMM, which can successfully operate in full 3-D, but can also be programmed in a similar fashion to a conventional CMM, where in use it has achieved some remarkable metrological results.

5.7.1 Small Coordinate Measuring Machine—Design Requirements

With the SCMM situated within its host CMM (i.e. see photograph in Fig. 5.22a, with its schematic design being represented in Fig. 5.23a where the design requirements were essentially based upon three distinct aspects; these were the instrument's: (i) accuracy (i.e. uncertainty); (ii) working volume (iii) coupled to its traceability. Regarding the instrument's accuracy, it had to achieve a volumetric uncertainty sufficiently small enough to enable sub-micrometre measurements to be made, when considering the Standards requirements of both **ISO 10360** and

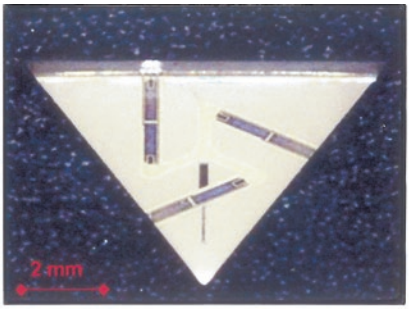

The NPL has developed a novel micro-scale CMM probe that aims to reduce the measurement uncertainty of micro-CMM's to below 100 nanometres, or 0,0001 millimetres. The probe consists of a three-legged flexure device and a micro-stylus with a spherical tip. Each flexure is 2 mm long, 0,2 mm wide and around 0,02 mm thick. The stylus is 2 mm long and 0,2 mm in diameter with a ϕ0,07 mm spherical tip. The probe is a MEMS device (micro-electrical mechanical system). It has built-in piezoelectric film coated onto the flexures so they act as sensors and actuators, allowing the device to vibrate away from measurement surfaces and counteract surface forces that are very strong at these tiny distances. The vibration also allows the probe to operate in a non-contact mode. *This micro-scale CMM probe was designed at The NPL and built in Germany at TU Braunschweig (Sept. 2012).*

(a) The Small Coordinate Measuring Machine (SCMM), situated within a–bridge-type CMM:

(b) Simultaneous head and interferometer data X-axis (i.e. uncorrected for gain and offset):

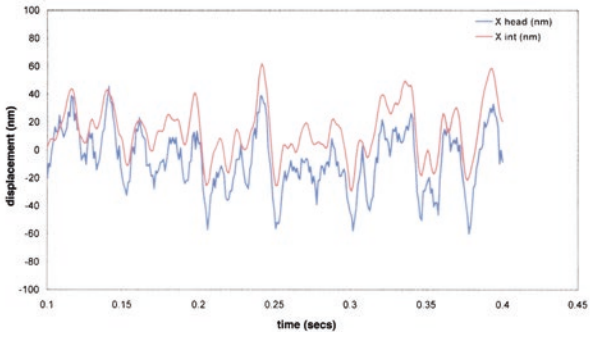

Fig. 5.22 Small coordinate measuring machine (SCMM)—for the highly accurate and precise measurements of miniature components and features [*Source* Centre of Length Measurement (NPL)]

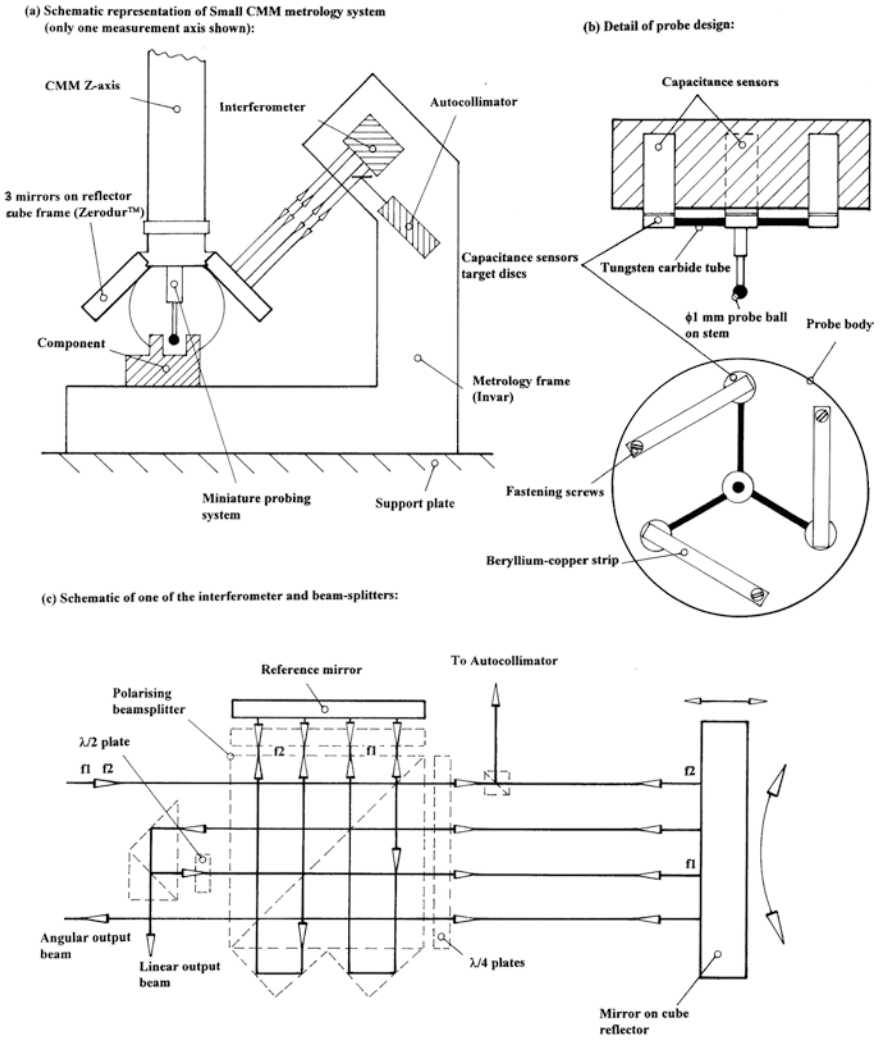

Fig. 5.23 Schematic details of the 'small coordinate measuring machine' (SCMM) [*Source* Centre of Length Measurement (NPL)/Lewis et al. (2001)]

ISO 14253.[20] Accordingly, at The NPL it set a design target of 50 nm volumetric uncertainty, for a working volume of 50 mm^3. Here, the specific requirement was for an accuracy of: $\geq$1 part in 10^6, in conjunction with the needs for traceable-metrology. In order to minimise the actual SCMM's development time,

[20]**ISO 14253 Standard**: where this Standard establishes the rules for determining the conformity, or nonconformity with a given tolerance for a characteristic of a workpiece, or a population of workpieces, as well as for the limits of maximum permissible errors for a metrological characteristic of measuring equipment, taking into account its specific measurement uncertainty.

commercial interferometers were employed (i.e. such as the Zygo ZMI2000 range), having 0.31 nm resolution with a linear displacement of 0.005 arcsecond resolution—for the angular rotations. Three such interferometers monitor the six degrees of freedom (i.e. three displacements and three rotations) for the probe system, via direct measurement of these displacements/rotations by three commercial mirrors mounted on the probe assembly (i.e. see Fig. 5.23a)—being termed a reflector cube. The interferometer enables a long range displacement (i.e. 50 mm) of this reflector cube to be measured to nanometric accuracy, having direct traceability via the calibrated laser wavelength. The reflector cube with its accompanying metrology frame—the fixed structure of the SCMM—is manufactured from Invar® for thermal stability.[21] The probe system has a fully 3-D analogue probe motion, achieved by designing and utilising a low-force probe, having displacement-sensing based on capacitance gauging. These capacitance transducers are calibrated against the interferometers to achieve their respective traceability, with the overall metrology system being schematically displayed in Fig. 5.23a, with details of the probe shown in Fig. 5.23b.

5.7.2 Small Coordinate Measuring Machine—Interferometers, Autocollimators and Probe Design

In Fig. 5.23c is depicted just one of the SCMM's three interferometers. These interferometers, as mentioned, measure the displacement and angular rotation—rather than absolute angle. Consequently, at The NPL, it was necessary to incorporate an additional absolute angle measurement system and for this aspect, autocollimators were utilised. Here, each autocollimator utilises a laser beam, which is split from the interferometer's primary linear measurement beam. These autocollimators act as a four-quadrant photo-detector, which senses two-axis

[21] **Invar**®—for *thermal stability*: where it is also known generically as: **FeNi36** (i.e. **64FeNi** in the USA), which is a nickel–iron alloy, being notable for its uniquely low coefficient of thermal expansion (i.e. CTE, or 'α'). Like other nickel/iron compositions, Invar is a solid solution; being a single-phase alloy, consisting of ≈36 % Ni and 64 % Fe. Typical common grades of Invar have an 'α' (i.e. at temperatures of between 20 and 100 °C) of about $1.2 \times 10^{-6}\ K^{-1}$ (i.e. 1.2 ppm/°C), while as a direct-comparison, plain carbon steels have values of around 11–15 ppm. Extra-pure grades (i.e. with <0.1 % Co), can readily produce values as low as 0.62–0.65 ppm/°C. Some Invar formulations display negative thermal expansion (NTE) characteristics. Although Invar exhibits high dimensional stability over a range of temperatures, it does have a propensity to creep. The actual name Invar is derived from the word *invariable*, referring to its lack of expansion, or contraction with temperature changes. Invar was invented in 1896, by Swiss scientist Charles Édouard Guillaume. In 1920, Guillaume received the Nobel Prize in Physics for this discovery of Invar, which enabled notable improvements in many and various types of scientific instruments.

displacements of the beam across the detector's surface. After calibration, the detectors function as two axis autocollimators, providing absolute angle information that is employed during the alignment and self-calibration of the system. The small beam-splitter directs the beam to one of the autocollimators—as illustrated in Fig. 5.23c. The detector electronics for the autocollimators and counter-cards for the interferometers, are contained remotely from the instrument, preventing any undesirable thermal-related problems.

With this SCMM instrument, the probe is a critical component in its usage, as it actually contacts the object under test—see Fig. 5.23b. Accordingly, the probe must be lightweight—to minimise any dynamic probing-forces, while exhibiting low stiffness, so that any resulting static probe forces are also minimised despite the fact that here, the probe offers no directional bias. Such a probe prevents the miniscule probe's tip from potentially damaging minute components whilst the probing-process occurs, allowing true 3-D probing—in any arbitrary direction. This probe's mechanical design was based upon that of Pril et al. (1997); with the capacitance sensing aspect—as utilised by Yang et al. (1998). In Fig. 5.23b, part of the main probe's system is schematically illustrated, with the probe-flexures being made from beryllium-copper strips, having cross-links produced from tungsten carbide, which are also shown in Fig. 5.23b. The moving portion of this probe assembly has a mass of just ≈370 mg and exhibits a stiffness of ≈10 Nm^{-1}—in all axes. This probe's working range is 20 μm and if its deflection is 10 μm, this corresponds to an actual probing force of just 0.1 mN. The styli for this probe's ball-point can be changed, ranging from ∅0.3 to ∅1 mm (i.e. this latter stylus is shown in Fig. 5.23b)—depending upon the metrological application. The probe's sensing elements are three miniature capacitance gauges—also shown in Fig. 5.23b—with each sensor mounted behind a ∅3 mm aluminium target disc, this being held in situ by the probe's cross-links. With this probe configuration, any motion of the probe ball causes one, or more of the gaps between the capacitance sensors and its associated target discs to change. Therefore, by elementary trigonometry, this probe motion relates these changes in the three capacitance readings to resolve motion along the conventional three Cartesian axes—see Fig. 5.22b. Probe calibration is achieved by probing along five orthogonal directions, namely: $+X$; $-X$; $+Y$; $-Y$ and $-Z$; whilst simultaneously monitoring the interferometer outputs. In this manner, the probe's motion is calibrated with traceability via the laser wavelength. Here, any inhomogeneities of the probe's motion and the anticipated sphericity errors of the probe tip, can be mapped by measuring against a known reference sphere. This traceable calibration of the analogue probe's 3-D functions, produces a 3 nm resolution, with a 10 μm range and sub-mN probing force. Of some significant note is that in recent years, this probe's design has been markedly improved in its fundamental probing potential, see further details of this design configuration in the photograph and its accompanying caption in Fig. 5.22 (top).

Much more could be said concerning the self-calibration and alignment of this SCMM, together with the Host CMM and the control software, but this is more fully described within the supplied references, regarding this SCMM instrument—at the end of the chapter. However, it is worth mentioning the step height standard

that has been accurately and precisely measured by this SCMM. Thus, this step height standard was manufactured as a chromium-layer on top of a Zerodur™–substrate, with the chromium coating providing a uniformly reflective surface. Here, the step's height is just 200 nm—when it was measured by optical techniques. Consequently, this SCMM could routinely and precisely measure and verify this minute step height, indicating the usefulness and validity of the actual instrument, but also showing its metrological potential across a wide range of miniscule component features on a range of ultra-precision parts.

5.8 A Novel 3-D-Nano Touch Probe—For an Ultra-Precision CMM

Introduction

During the past few years, the metrological capabilities of CMMs have become very versatile and widespread metrology tools, with today's CMMs being able to efficiently perform very complex measurement tasks. However, in industry-at-large with the on-going miniaturisation in the fields of mechanical and optical production, there is a new demand for highly accurate geometrical measurements on minute components. Accordingly, any new metrological instrumentation should be designed and developed to have low measurement uncertainties and be able to probe objects with their minute spheres, while utilising very low contact forces. Until the present day, the main limiting factor for the application of CMMs on small components was mainly restricted to the probe-head technology; therefore, new metrological developments are now becoming increasingly urgent for such ultra-precision tasks.

Expressly manufactured for a CMM, the novel 3-D-nano Touch Probe—shown in Fig. 5.24 (top), has exchangeable probes with spheres in the range from: ∅0.1 to ∅0.3 mm, exhibiting very low probing forces of: ≤0.5 mN. This actual 3-D probing-device—Fig. 5.24 (top)—is based on parallel kinematics with flexure hinges, being structurally-manufactured out of a single piece of high-grade aluminium. With this probe configuration, all rotational movements of the probing sphere are restricted, thus enabling the remaining potential translational motion to be separated into its X, Y and Z components, each of which are then measured by an inductive sensor. All the probe's axes have the same orientation with respect to gravity. The probe stiffness is isotropic in nature, with a value of only 20 mN mm^{-1}, while the effective moving mass is ≈7 g. In some early experimental work, with this 3-D-nano Touch Probe, specific and controlled test procedures were performed on a linear measuring machine equipped with a laser interferometer. At this time, the standard deviation of repeated probing-measurements for example, was for the difference between left and right probing on a 5 mm Gauge block and was in the order of 5 nm—see Fig. 5.24 (bottom-right).

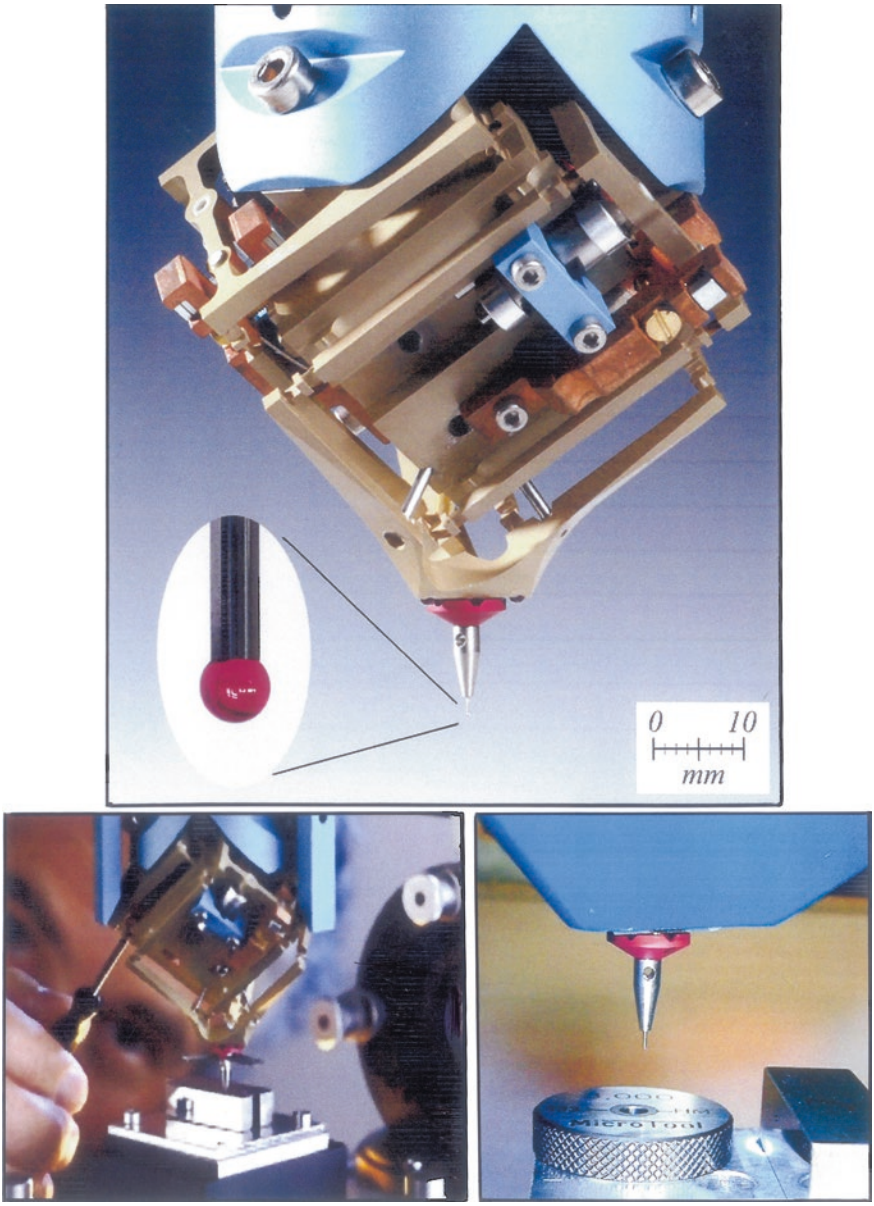

Fig. 5.24 A '3D-Nanotouch probe', for an ultra-precision CMM—for the inspection of minute components [courtesy of Mecartex (Switzerland)]

5.8.1 Probing Force and Surface Damage

The point of contact between the probing sphere and the sample test surface should be obtained by measuring probe deflections at several CMM positions. This test permits extrapolation to zero-deflection, where the contact force is zero. This very low probing force is an important factor for a nano-probe, as the actual plastic deformation on say, the indentation of the surface of an aluminium part-feature after probing with a conventional CMM probe—introduces maximal-admissible probing forces for various sphere diameters of 1000 MPa contact pressure in the immediate vicinity of contact. As can be gleaned from the previous statement, these relatively large probing forces of conventional probe systems could create damage to the workpiece's surface and consequently falsify the measurement result. Typically, if an Atomic Force Microscope (AFM) image of such a plastic surface deformation on an aluminium testpiece was investigated, then when probed with a conventional 3-D touch probe with a sphere of ∅0.6 mm, this would result in a surface indentation having a 330 nm depth. Whereas, if a probe sphere of ∅0.1 mm was utilised, but without leaving any permanent surface indentation, the probing-force must be ≈100 times smaller than that with today's commercial probe systems. This probing-phenomenon means that the probing system stiffness has to be exceedingly small, for example, of the order: 20 mN mm^{-1}, however, still allowing some probe deflection at these low forces. The probing stiffness design and construction criteria, is even more critical with respect to dynamic forces that act when the probing sphere strikes the surface upon its first contact. Hence, the effective moving mass also needs to be as small as possible, to allow reasonable probing approach speeds.

5.8.2 The 3-D-Nano Touch Probe—Constructional Details

This actual 3-D-nano Touch Probe, is based upon parallelograms and flexure hinges having a new kinematic structure that was designed for the probe-head—see Fig. 5.24 (top). This structure leaves the probing sphere with exactly three degrees of freedom. The rotational movements are blocked and the translational motion is separated in its *X*, *Y* and *Z* components, which as previously mentioned, are each measured by an inductive sensor. All axes have the same orientation with respect to gravity and provide identical probing forces in all directions. As a consequence, the main part of the structure is manufactured out of a single piece of aluminium—produced by utilising electro-discharge machining (EDM). For that reason, the most critical and integral part does not need to be assembled. The flexure hinges have a thickness of only 60 μm resulting in an actual stiffness of: 20 mN/mm. Hence, the effective moving mass here is just: 7 g. Due to the low stiffness the deformation caused by gravity needs to be compensated; therefore for this purpose, an adjustable system with permanent magnets was developed.

The measurement range was set to: ±0.2 mm, while the mechanical limits allow a range of: ±0.5 mm; while, the probing element is magnetically attached to the head and positioned by means of three balls in three grooves. The magnetic holding of the probing element allows an easy replacement and acts also as a mechanical fuse. Therefore, the handling of this highly sensitive device remains quite easy to achieve in-service. A small moving mass is important to keep the dynamic contact forces low while maintaining reasonable approach speeds. Some later model calculations have shown that the effective mass (7 g) of the probe is still rather too high. Thus, a small additional mechanical filter element was developed to reduce the effect of dynamic forces. Its stiffness is almost equal in all directions and roughly 100 times higher than that of the probe-head, but it has a very low effective mass, giving a typical approach velocity of: 1 mm/s.

Experimental Results

The overall performance of this new probe can only be measured on a CMM with equal or better performance than the probe itself. However, at the time of writing this abridged review of the probe, research work was shown to be lacking assessment by an ultra-precision CMM. Consequently, the first experiments with this new 3-D-nano Touch Probe were performed on a linear measuring machine (LMM), being equipped with a laser interferometer. In this manner only probing in a horizontal plane could be made and verified. However, due to the special orientation of the probe coordinate system, all three sensors of the probe-head were involved in these test measurements. Here, this test consisted of probing a known and calibrated 5 mm gauge block on its left and right side—see Fig. 5.24 (bottom-right). The difference between the two points minus the gauge block length is the probe constant, which is essentially the sphere diameter. The repeatability of this probe-constant is an important parameter for a 3-D-nano Touch Probe. In experimental-evaluations, the standard deviation of five such measurements was always in the order of 5 nm. This value includes interferometer noise and machine instability—such as vibration and drift—moreover, for large probe deflections up to 150 μm the linearity of the probe signal was shown to remain very good with this newly designed probe configuration.

In conclusion

A new 3-D-nano Touch Probe for CMMs with exchangeable probes and low probing forces was developed and as such, a patent has now been filed. This innovative probing-design is based on parallel kinematics with flexure hinges—with the first test measurements recorded being deemed very successful. This actual probe, with its probing forces <0.5 mN, has a repeatability which was in the order of: ≈5 nm. In the near future, for the full characterisation of this probe, it will require a CMM with comparable metrological performance, therefore, it was reportedly planned to incorporate the probe-head into a new ultra-precision CMM at METAS. The

primary metrological objective here, being to offer calibration and measurement services for very small/minute parts, up to a size of about 50 mm—at a later date.

5.9 Robotic Arms

Introduction

Invariably, many Industrial robot arm[22] configurations are based upon multi-axes articulated arms. Characteristically, examples can include SCARA robots—often utilised for efficient assembly type-work; while Cartesian coordinate robots, Articulated arm robots (i.e. sometimes termed: Anthropometric robots) as well as Gantry-type robots, will tend to be employed for a wide range of automation/manipulation-tasks. Generally speaking, most types of the current robots can be categorised as a robotic-arm (i.e. 'manipulator' in the Standard **ISO 8373:2012**). These kinematically configured robots exhibit varying degrees of autonomy, such as:

- some robots are programmed to authentically undertake specific repetitive actions without variation and to a high degree of accuracy. These robotic actions are determined by programmed routines that specify the following: direction; acceleration; velocity; deceleration; and distance of a series of coordinated motions—during such motion;
- while other types of robotic varieties are much more flexible as to the orientation of the object/workpiece on which they are operating, or even the task that has to be performed on the object itself. The robot may even need to identify the object's geometry/shape, its orientation, etc.—prior to beginning the set programmed-task. Today, some form of Artificial Intelligence (AI),[23] is now becoming an increasingly-important factor in any form of automation for these modern industrial robots.

[22]**Industrial robot**: this has been defined and stated by the ISO (**ISO 8373:2012—*Robotic and Robotic Devices***) as: "An automatically controlled, reprogrammable, multi-purpose manipulator programmable in three, or more axes". Conversely, the field of robotics may be more practically defined as: "The study, design and use of robot systems for manufacturing".

[23]**Artificial Intelligence (AI)**: this AI-acronym has already been described—also see the significant work by Alan Turing, but once again, here it can be defined as: "The intelligence exhibited by machines, or software, and the branch of computer science that develops machines and software with intelligence". Today, many of the current AI-researchers, together with accompanying robotics textbooks, define the field as: "The study and design of intelligent agents", where an intelligent-agent is a system that perceives its environment and takes actions that maximise its chances of success. Whereas previously back in 1955, John McCarthy in the USA, was first person to coin the actual AI-term, where he definied it simply as: "The science and engineering of making intelligent machines".

5.9.1 Industrial Robotics—Their Historical Development

Probably the earliest known form of industrial robot, which conforms to the current ISO standard definition, was that invented by 'Bill' Griffith P. Taylor back in 1937 and then subsequently published in the: Meccano Magazine (March, 1938). This small and primitive crane-like device was constructed almost entirely by utilising simple Meccano components (i.e. bolted and assembled pre-made toy parts) with each axes being powered by just a small electric motor. With this configuration, five axes of movement were possible, including Grab and Grab-rotation—by the gripper/end-effector. The automation was attained by utilising the well-known technique of punched paper tape—to energise its solenoids, which could then facilitate the movement of the actual crane's control levers. It was really the applied and fundamental work of George Devol who instigated the first true robotics patents in 1954 (i.e. these being granted in 1961). Back in 1956, the first commercial company to produce an industrial robot of practical use and significant importance was from within the USA, by Unimation, Inc.—this company being founded by George Devol and Joseph F. Engelberger—and here the robot's design and construction was based upon Devol's original patents. These early designed and manufactured Unimation robots were also known as Programmable Transfer Machines (PTM's)—as initially their main working practice was to simply transfer objects from one-point-to-another, typically over distances of up to 4 m.

At this time the robot's axis motions utilised hydraulic-actuators, which were programmed in joint-coordinates (i.e. the angles of the various joints were stored during a teaching phase and then replayed in actual operation). It has been reported that these robots were positionally accurate to: $\leq$2.5 mm. Of particular note, is that accuracy here is not usually an appropriate measurement in robotics, as their positional performance is normally evaluated in terms of their repeatability. Somewhat later, Unimation licenced their robotic technology to Kawasaki Heavy Industries (Japan) as well as to GKN (UK) where the actual manufacturing of these robots was carried out. At that time, Unimation's only major competitor—for a considerable period of time—was from Cincinnati Milacron Inc. (Ohio, USA), although this robotic manufacturing production environment radically changed in the late 1970s, when several of the big Japanese corporations began producing comparable industrial robots. By 1969, Victor Scheinman (at Stanford University, Ca., USA) had invented the so-called Stanford-arm, which was a six axis articulated robot—electrically powered, being designed to permit an arm-solution to its operation. This new robot design and configuration, allowed it to precisely follow arbitrary paths in space—within its working envelope, thus increasing robotic potential usage to the more sophisticated applications such as: assembly; welding; adhesive bonding; also paint-spraying activities, plus many more operations. Later on, Scheinman went on to design a different robotic-arm for the MIT AI Laboratory (USA), where it was termed the MIT-arm. After receiving a fellowship from Unimation to develop his robotic-designs, Scheinman sold these future-designs to Unimation, who then developed them still further, with

financial support from General Motors, who later marketed this new robot as the Programmable Universal Machine for Assembly (PUMA)—one version seen here in Fig. 5.25b—with this PUMA's end-effector being attached to a Partially cubed calibration device.

In Europe during the early 1970s, industrial robotics was quickly developed, typically by such companies as ABB Robotics (Sweden)—see Fig. 5.25a—as well as KUKA Robotics (Germany)—see Fig. 6.15 (top)—who introduced their own robots to the market by 1973. Of note, was that ABB Robotics (formerly known as: ASEA) presented their IRB 6 robot, which was among the world's first commercially available industrial robots having an all-electric microprocessor-controlled robotic-arm. Likewise, in 1973, KUKA Robotics introduced an industrial robot, known as FAMULUS, which was also an Articulated-robot having six electromechanically driven axes.

In the USA, in the late 1970s, several companies entered this fast-developing robotics-field, such as, General Electric (GE) and General Motors (GM), who then formed joint-ventures with both Japanese FANUC Robotics and with FANUC Ltd. At this time, in the USA, some local startup companies also became involved in robotics, which included both Automatix and Adept Technology, Inc. At the height of the robot-boom (i.e. notably around the mid-1980s) the Westinghouse Electric Corporation had acquired Unimation for $107 million. Later, in 1988, Westinghouse sold Unimation to Stäubli Faverges SCA (a French company) which has manufactured Articulated-robots for wide-ranging industrial and clean-room applications, and by 2004, Stäubli bought the robotics division of Bosch (Germany). Today, only a few non-Japanese companies have ultimately managed to survive in this highly competitive market; typically just some of the major robotic manufacturers are currently: Adept Technology (USA), Fanuc Corporation (Japan), Stäubli-Unimation (France) and the Swedish/Swiss company ABB (Asea Brown Boveri), plus the highly industrialised German company KUKA Robotics and, in a similar manner, the Italian robotic company Comau.

5.9.2 Defining Robotic Parameters

There are any number of differing methods and techniques to actually define most configurations of industrial robotic arms, some of which might include the:

- **number of axes**—the minimum of two-axes are necessary to reach any point in a plane; but three axes are required to reach any point in space, so to fully control the orientation of the end of the robotic-arm—termed its wrist—then normally a further three axes are mandatory, these being termed its: yaw; pitch; and roll;
- **degrees of freedom**—this is usually equivalent to the number of robotic axes;
- **working envelope**—this is the volumetric region of space that this physical configuration of robotic articulation can effectively reach;

(a) Calibrating a six-axis industrial robot for both rotary/linear positioning performance, using a Renishaw Ballbar, with extensions. [After: M. Slamani, A. Nubiola & I. Bonev, AME, École de technoloie supérieure, Quebec, Canada (2012)]

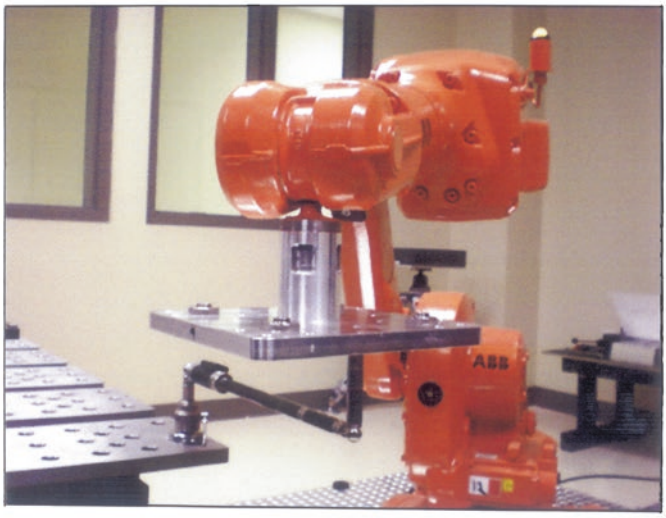

(b) Six-axis anthropometric robotic calibration, utilising a partial-cubed kinematic device, fitted to the end-effector's flange – about to enter a strained-gauged kinematicly-designed cubic artefact. [Courtesy of Southampton Solent University/G.T. Smith (1994)]

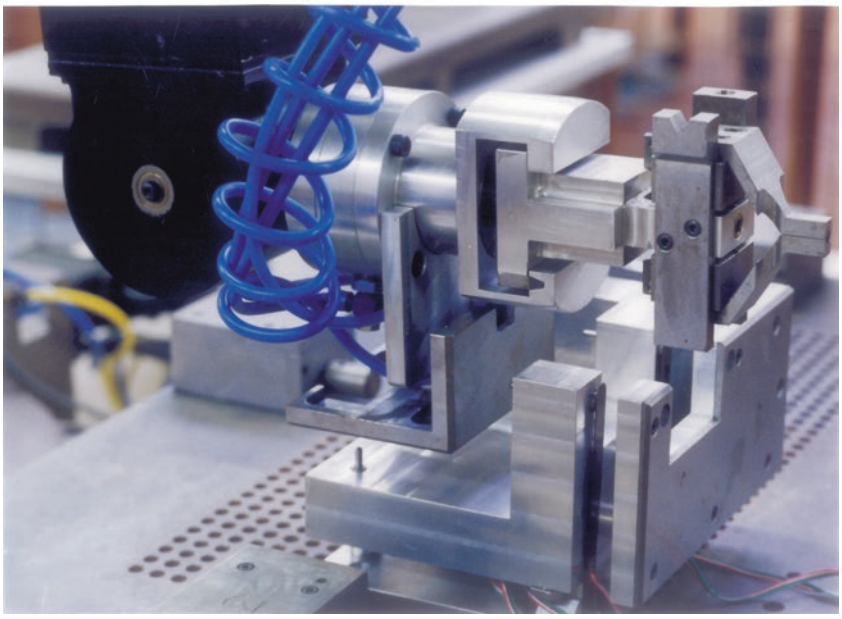

Fig. 5.25 Calibrating multi-axis robots with artefacts

- **kinematics**—which in robotic-terms, is primarily concerned with the arm's actual arrangement of its rigid members and joints in the robot, which determines the robot's conceivable motions.
  NB The actual classes of robot-kinematics will include many differing types, typically these are: Articulated (i.e. Anthropometric); Cartesian; Parallel; SCARA; and Parallel Kinematic Mechanisms (PKMs);
- **carrying capacity, or payload**—this is how much weight the actual robot can lift, which should also include the weight of its gripper/end-effector;
- **speed**—this is its dynamic-motion, being concerned with how fast a robot can position the end of its arm.
  NB Speed could be defined in several ways, by terms such as its: angular-speed; linear speed of each axis; or as a compound-speed; but specifically, the speed of the end of the arm when all of its axes are continuously moving;
- **acceleration**—this is how quickly the arm's axis can accelerate,
  NB The limiting factor of a robot is that it may not be able to reach its specified maximum speed for movements over just a short distance, or if a complex and variable-path requires frequent changes of direction;
- **accuracy**—this is how closely a robot can reach its commanded-position.
  NB When the absolute position of the robot is measured and then compared to the commanded-position, this error is a measure of its accuracy; although this accuracy, can be improved with some form of external-sensing, such as when incorporating a vision system, or by Infrared-sensing. Other factors affecting the robotic arm's accuracy might be the result of varying its speed and position within the working-envelope of these axes with its intended payload;
- **repeatability**—this term relates to how well, or repeatable, the robot will return to a programmed position,
  NB; however—as mentioned—this repeatability should not be confused with its accuracy. For example, the robotic-arm might be programmed to go to certain *X*, *Y* and *Z* coordinate positions in space, but here, if it gets to only within 1 mm of that position, this would be the robot's accuracy, although this positional-accuracy can be significantly improved by previous axes calibration—which will now be mentioned in the following section.

5.9.3 Robotic Calibration

The activity concerned with robot calibration, can be defined as, "The process of determining the actual values of kinematic and dynamic parameters of an industrial robot [IR]". These kinematic parameters designate the robot's relative position and orientation of its links and joints, while the dynamic parameters describe the arm and joint masses—as well as its internal friction. Accordingly, it seems somewhat obvious that a calibrated robot has a much higher absolute positioning accuracy than an identical uncalibrated robot. Specifically, the real position of the

robot's end-effector would normally correspond much better to the position calculated from the mathematical model of that robot. As a consequence, a robot's absolute positioning accuracy is, for the most part, relevant in connection with robot exchangeability and for offline programming in any form of precision working-applications. Furthermore, robotic calibration is predominantly concerned with calibrating its tools and the attendant workpieces in its so-called cell calibration configuration, which can help to minimise any potential/occurring inaccuracies and thus, improve the overall production process security.

In **SS ISO 9283:2012**,[24] this Standard sets different performance criteria for an industrial robot, where it suggests certain test procedures in order to obtain appropriate robotic parameter values. Here, the significant criteria and probably the most commonly utilised are the robot's accuracy of pose (AP), together with its repeatability of pose (RP). Robotic repeatability is singularly important when the robot is manually moved towards its command-positions (i.e. during its Teach-In-mode). If, for example, the robot program is generated by the more usual 3-D simulation package (i.e. often termed: Offline programming), then its absolute accuracy is vital. Both of these factors are generally influenced in a negative way by the robot's kinematic-factors, the joint-offsets and deviations in joint-lengths and angles between the individual robot links being particularly affected.

The problems of robotic errors produced by these pose-measurements can be significantly minimised by what is termed: numerical-optimisation. In the case of a robot's kinematic calibration, a complete kinematical model of the geometric structure must be developed, whose parameters can then be calculated by mathematical-optimisation. Consequently, the robot's common system-behaviour can be described with the Vector model function, plus its input- and output-vectors. Here, the robotic-variables of: '**k**'; '**l**'; '**m**' and '**n**'; with their respective-derivatives, can describe the dimensions of the single-vector spaces. The minimisation of the residual-error '**r**' for the purpose of identification of the optimal parameter vector '**p**', occurs, from the difference between its output vectors by utilising the Euclidean-norm. When attempting to solve many of the robot's kinematical optimisation problems, then the least squares descent techniques can be satisfactorily employed, typically by utilising a Modified quasi-Newton method. These particular and notable robotic analysis techniques are somewhat outside the current textural-remit, but this type of procedure supplies corrected kinematical parameters for the robotic device, which can then be used to update the system

[24]**SS ISO 9283:2012, IDT**: **Manipulating industrial robots—Performance criteria and related test methods**. This actual Standard describes methods of specifying and testing the following wide-range of performance characteristics of manipulating industrial robots, namely its: pose-accuracy and pose-repeatability; multi-directional pose-accuracy variation; distance accuracy and distance repeatability; position stabilisation time; position overshoot; drift of pose-characteristics; exchangeability; path accuracy and path repeatability; path accuracy on reorientation; cornering deviations; path velocity characteristics; minimum posing time; static compliance; as well as its weaving deviations.

variables within the controller, in order to adapt the current robot model to that of its real kinematics. An obvious point worth mentioning here, is that the positioning accuracy of industrial robots varies by: robot manufacturer; its age and usage; the robot-type; plus its axes-configuration. Hence, the magnitude of the robotic-error between the actual and desired positions can range-widely from: $\leq$0.1 to >2 mm—in certain cases. Consequently, by utilising kinematic calibration, these robotic-errors can invariably be reduced to: $\leq$1 mm, in most industrial automation cases.

In certain industrial applications, there is something of a trend developing toward the substitution of CNC machine tools and other specialised-machines with that of fully programmable high accuracy/repeatability multi-axes industrial robots. Today, this slowly developing take-up and replacement by robots for certain specified manufacturing tasks, whose accuracy demands can be fulfilled by these calibrated robots, is likely to continue. By the correct application of efficient calibration methods, it is possible with modern industrial robots and more particularly for those of the type with Parallel kinematic manipulators, to achieve an accuracy-of-pose of: $\leq$0.1 mm. This is expected to endure and increase into the near-future, as a result and in order to improve this robotic-exchangeability, the ability to simplify any offline program activities will enable new and highly precise robotic applications to be successfully utilised.

5.9.4 Robotic Calibration Devices and Techniques

It has been well-documented in the relevant robotic-literature, that $\approx$97 % of most robot's positional errors are due to the error in its zero position (i.e. its home-position), which can mean that a full calibration is not always necessary. Accordingly, the technique of remastering can be accomplished by returning the robot to this home position and then simply resetting its encoder values. This simple technique is habitually performed by the robot manufacturer before it is shipped to the end-user. Moreover, the robotic supplier could also recommend that this remastering process is repeated on a regular basis—beginning with its initial installation. There are a considerable number of traditional techniques of programming that involve utilising a robot's Teach-pendant. Under these circumstances the robot's end-user does not depend on the accuracy of the manipulator, but simply relies solely on its repeatability. Nonetheless, as these industrial robotic applications become more widely accepted; then, end-users will expect that an industrial robot is both accurate as well as repeatable. After remastering a robot, if it does not provide the end-user with the required accuracy/repeatability for the industrial-application, then it must be recalibrated.

Typically, most effective robotic calibration techniques will compare the actual Teach-point positions, with measurements relating to the tool/gripper and to that of an independent 3-D measuring device/artefact. This comparison enables the robot's DH-parameters[25] within the mathematical model to be modified, so that the actual distance between where the robot assumes it is and, where overall accuracy of the robot's actual position truly is can then be minimised. This so-called modified model—of the robot's controller, will depend upon the complexity of the actual calibration technique.

With the advent of advances in Offline programming (OLP) software packages, they now have the capacity to update the robot model within the software—thereby matching the parameters recorded from calibrating the actual robot. In addition, a robot's calibration can also be accomplished utilising both contact and non-contact probing methods. Invariably the non-contact techniques include utilising either: laser proximity-sensors: beam-breakers; high-resolution cameras; visual servo-ing; or many more techniques. Such non-contact methods can provide the robot with high accuracies, but they have a tendency to be relatively expensive to accomplish. This fact is due to the expense when acquiring this type of calibration equipment, as well as the time required for setup and interfacing with that of the robot controller. This means that the so-called cost drivers in industry ensure that robotic-users have to incorporate much less sophisticated and the somewhat cruder techniques of contact methods for their subsequent robotic calibration. These contact techniques might include the use of a wide range of dummy-parts, compliant-devices, precision-styli or other artefact-based techniques, some of which will now be briefly mentioned below.

---

[25]**DH-parameters**: or more fully termed as the Denavit–Hartenberg parameters. These are the four parameters associated with a particular convention for attaching reference-frames to the links of either a spatial-kinematic chain, or in this case, for a robot-manipulator. In 1955, Jacques Denavit and Richard Hartenberg introduced this convention in order to standardise the coordinate frames for spatial-linkages. While in 1981, Richard Paul demonstrated its value for the kinematic-analysis of robotic system. Thus, the commonly utilised convention for selecting frames-of-reference in robotics applications is the: Denavit and Hartenberg (D–H) convention. In this convention, coordinate frames are attached to the joints between two links—such that one transformation is associated with the joint, [Z], and the second is associated with the link [X]. Consequently, the coordinate transformations along a serial-robot consisting of 'n' links form the kinematics-equations of the robot, are thus:

$$[T] = [Z_1][X_1][Z_2][X_2] \ldots [X_{n-1}][Z_n]$$

Where: [$\boldsymbol{T}$] is the transformation locating the end-link.
So, in order to determine the coordinate transformations [Z] and [X], the joints connecting the links are modelled as either hinged, or sliding-joints, each of which have a unique line 'S' in space that forms the joint-axis and define the relative movement of the two links. For example, for a typical serial-robot it is normally characterised by a sequence six of lines, such as: S_i, $i = 1,\ldots, 6$, one for each joint in the robot. For each sequence of lines: 'S_i' and 'S_{i+1}', there is a common normal line: '$A_{i,i+1}$'. The system of six joint axes: 'S_i' and five common normal lines: '$A_{i,i+1}$' form the kinematic-skeleton of the typical six degrees of freedom in a serial-robot. As a consequence of their research, Denavit and Hartenberg, have subsequently introduced the convention that Z-coordinate axes are assigned to the joint axes: 'S_i', while the X-coordinate axes are also assigned to the common normals '$A_{i,i+1}$'.

Telescoping Ballbar—For Robotic Calibration

Figure 5.25a depicts a Telescoping Ballbar (i.e. the Ballbar model here is a QC20-W Ballbar produced by the company Renishaw plc; having Bluetooth™ wireless-technology), which is kinematically affixed to a worktable platen at one end and attached to an Articulated arm on a six-axis robot's end-effector at the other end (i.e. in this case, the robot model was an ABB IRB 1600-6/1.45). This Ballbar's sensor accuracy at 20 °C is ±0.5 μm—with a measuring range which is limited to just ±1.0 mm. In these calibration trials the end-effector weighed ≈2 kg and was utilised in all of the Ballbar tests that were undertaken. During the robotic-testing procedure, the Ballbar's circular tests were performed—in both clockwise (CW) and anti-clockwise (ACW) directions, with differing Ballbar-radii, of 100, 150, as well as at 300 mm, with constant feedrates utilising the robot's Tool Centre Point[26] (TCP) operational-mode, with linear-velocities ranging from: 20 to 700 mm s^{-1}. Here, the coordinates of the measurement point (i.e. from the centre of the tool-cup) with respect to the robot's flange reference-frame, was set at: ≈0; 65; and 149 mm. Prior to beginning any Telescoping Ballbar testing, the robot was initially warmed-up by repeating the actual circular-trajectories for 1 h—from its cold startup (i.e. with the laboratory's ambient temperature at that time, being 21 °C).

These circular tests were performed on this particular six-axis Articulated arm industrial robot, which highlighted the robot's servo-dynamic errors that have a significant impact on its contouring-errors, causing out-of-roundness and potentially some large radius sized-errors. These test comparisons with a Telescoping Ballbar, being performed at different TCP rotational speeds, indicated that the robot's geometric errors are dominant at low TCP speeds, which has a significant impact on its circular contouring errors. Here, the robot's dynamic errors are present as vibrations, being obviously more dominant at high TCP speeds for small circular-contouring radii, achieving 25 % of the total-error at a TCP-rotation of 700 mm s^{-1}. The robotic results have also indicated that the tested-robot exhibited significant radius size-errors. With these specific Ballbar tests, the research-approach for the modelling and prediction of these radius size-errors was developed, this being based on both the experimental data and statistical testing procedures. Therefore, the developed-model was fitted utilising this experimental data and then its kinematic performance was checked, by comparing the model predictions to additional sets of data, which are dissimilar from those utilised for identification. The Ballbar results from these particular robotic-trials, has demonstrated that the model which was developed was able to predict 98–99 % of its radius size-error.

[26]**Tool Centre Point** (**TCP**): when undertaking the robotic calibration procedure, the robot is calibrated up to the last axis—termed the flange—which enables one to calculate the positions of all the robot's axes during any complex movement. When a tool is mounted on the final axis (i.e. on the robot's flange), the robot needs to know the actual position of the active-point of the tool's positioned here, which is invariably-known as its: Tool Centre Point (TCP).

Therefore in summary, by employing a Telescoping Ballbar, which is an excellent instrument for measuring both the static and dynamic performance of an industrial robot, it thus provided the techniques required towards the verification-information necessary to then potentially calibrate these types of multi-axis robots.

Robotic Calibration Cube—For Home Positioning

A very common and historically tried-and-tested calibration technique is to locate the robot's manipulator at its home-position, which usually necessitates that it is positioned with all joint-angles specified to a value of either zero, or at 90°. For large industrial robots, this home-position must be repeatable to $\leq$0.2 mm, in its cartesian space at the end-point of the robot. Utilising robot-kinematics, the cartesian requirement can be transformed into joint-angle repeatability of just 0.01°. Consequently, to obtain a significant improvement in the robot's home calibration, this can be found by three separate techniques, these are by:

1. **relative calibration**—this is an expensive process which requires each component in the robotic structure to be defined relative to the previous component. Accuracies from such relative-calibrations can vary to a certain degree, being based upon the accuracy of these robotic components;
2. **optimal calibration**—this utilises a measurement combined with kinematic-models of the robot, to measure numerous positions of the robot—in its envelope, and then correct any errors present in the structure. Accuracy from optimal calibration can vary to some extent, being based upon the robot's positions and its kinematic model;
3. **level-based calibration**—this calibrating-process employs simple electronic levels (i.e. typically Inclinometers) to easily orientate each component of the robot structure with respect to its angle—this data being read by the Inclinometer.

In order to practically validate the robot's home-position, a technique of utilising an artefact of an Open-/Partial-cube is conveniently situated (i.e. permanently) on the robot's flange which is then nested into a kinematic-fixture—situated at another convenient position within the working envelope of the robot (see Fig. 5.25b for a close-up photograph of the robot's-approach into this kinematic-fixture). Here, within this integrated robotic-cell, it was specifically built to assemble small precision-made reduction-gearboxes, with its interchangeable robotic gripper, which could change all of its robotic tooling from a purpose built tool store, then automatically and accurately assemble these gearbox components and finally bolt them together at completion. The Partial-cube when nesting in the mating fixture (i.e. see Fig. 5.25b) was positioned by the standardised kinematic

principle of: 3-2-1-location. That is, the sensors were contact-type strain-gauged devices, with three situated at one internal face, two at another face, with the final face having just one sensor—thereby defining the exact corner datum point (i.e. its defined home position). The kinematic-fixture enabled a closed-loop feedback into the robot's controller (for linkage positional error adjustment, as necessary). This type of configuration/calibration allowed a true home-position to be established for the robot either during the end-effector's (i.e. gripper) change-over, or after the completion of the gearbox assembly task. In this manner, the robot's actual positioning within its volumetric envelope was always known, thus enabling this complex-precision robotic operation to be successfully achieved in-service.

5.10 Parallel Kinematic Mechanism (PKM)—Equator™ Gauge

Introduction

With the launch of the metrology instrument/artefact known as the Parallel Kinematic Mechanism-based machine (PKM) also being commercially known as the Equator™ Gauge (i.e. see Fig. 5.26), it has been specifically targeted at an industrial user-market said to be potentially worth ≈$3 billion per annum—this model being just the start of a range of related-products. This type of PKM-equipment seems somewhat different to many other types of metrological instruments, because it is neither a CMM, nor a hard-gauging artefact. Such configuration of these PKMs, are most easily explained by stating that when compared to machine tools, or indeed CMMs, they do not have mutually perpendicular axes; furthermore, their axes are not connected in either a serial-chain, nor stacked one-upon-the-other.

This specific PKM-instrument, has three distinct axes—being either extending, or contracting struts—all of which must be moved in order to position the vertically inclined probe body and its attached stylus, which can be positioned either vertically, or indeed cranked—in any coordinate axis position in: '*X*'; '*Y*'; as well as '*Z*' axes. For example, the PKM's platform (see Fig. 5.26a) to which the axes and probe body holding a Renishaw SP25 scanning-probe are connected—is efficiently constrained to remain parallel to this base surface, by means of two struts associated with each axis. These two accurately and precisely positioned struts are there to help prevent the platform from any form of actual twisting, or tilting as the axes are either being extended or contracted (i.e. consequently these struts are necessary for controlling the other—rotational—three degrees-of-freedom, namely the: '*A*'; '*B*' also '*C*' rotations; about the instrument's linear coordinates of its: '*X*'; '*Y*' and '*Z*' axes, respectively).

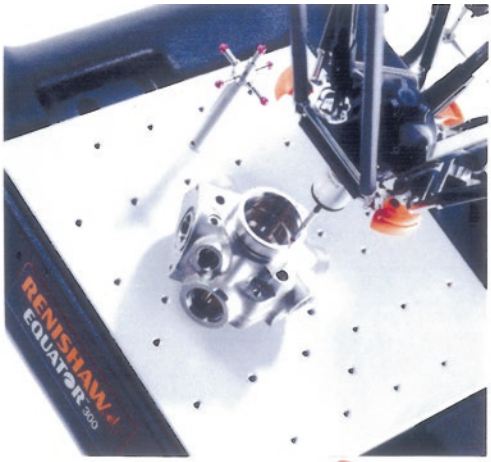

(a) Details of the: table, machined component & probes, on *Renishaw's Equator™ Gauge*, offering extremely fast gauging of critical component features.

(b) The *Renishaw Equator™ Gauge*, is a *parallel kinematic mechanism-based machine*, allowing a diverse range of component parts to be gauged, with a range of probes from its in-built probing facility.

Fig. 5.26 The parallel kinematic mechanism-based machine: equator^{TM}, that can complete in terms of both: speed of operation and versatility, with 'hard-gauging' techniques (courtesy of Renishaw plc)

5.10.1 Theory of Operation—Of the PKM

The underlying principle of operation for this Programmable-gauge (see Fig. 5.26) is to utilise flexible bespoke-software to drive this PKM, thus providing versatility for varying product designs. In prior attempts at such flexible-gauging to retool hardware—for example by utilising linear variable differential transformers (LVDTs)—in order to gauge a family of similar parts an instrument's flexibility tended to be limited and was normally at the cost of significant setup time and lost throughput. This latest Programmable-gauge differentiates itself from many other types of retoolable-gauging, in that it has been reconfigured for completely different part measurements and the metrology process can also be automated, which vastly reduces overall setup time.

On the latest PKM-design the gauging and reconfiguration are simultaneously achieved by moving a single-sensor around the part, in a similar manner to that of a CMM; although here, any particular part-features and tolerance dimensions are programmed and its operation can be totally automated. Traditional hard-gauging has a limited inherent accuracy but has good repeatability (see a typical Receiver-gauge version in Fig. 7.2b). At this present time, the PKM normally has the accuracy obtained by zeroing a Master part's individual touch-and-scan points to that of the nominal, as if each point was an LVDT in its own right. Unlike that of traditional gauges—which are typically either GO and NO-GO or specified as Pass and Fail—the quantitative dimensional reporting is readily available due to the nature of software-driven inspection. Consequently, by measuring a Master part on a CMM, that CMM's accuracy and its associated process capability potential, is then simply transferred to this Programmable-gauge through a known set of offsets. Here, the process control possibilities of just one single CMM can be effectively scaled through an arrangement of a series of multiple-versions of these Programmable-gauges and can offer the cost, robustness, and throughput advantages of all types of traditional gauging techniques.

A fundamental property of this PKM-instrument is its closed-loop force-path—as there are no cantilevered-forces within the structure itself as would be the case for an open-loop vertical Machining Centre. These PKMs are therefore very stiff structures indeed, accordingly having a high stiffness-to-weight ratio. For that reason, this Equator™ Gauge can be considered as being thermally neutral—meaning that any structural thermal growth is symmetrical, due to the use of matched materials in its overall construction.

The first product launched in this PKM-range, was the Equator 300 (see Fig. 5.26) having a working envelope of the following dimensions: ∅300 mm by 150 mm high, which has measurement uncertainty of: $\geq \pm 2$ μm. This unique PKM-instrument is intended to replace many bespoke hard-gauging applications in a full production industrial environment. The cost of a typical PKM, is financially comparable to that of most hard-gauging systems, but moreover, it is easily and infinitely reconfigurable

The target industrial applications for such a PKM-instrument, are in the medium-to-high volume manufacturing processes, typically found in the automotive sector—for example when measuring conrods/pistons, or for domestic markets—for white goods component inspection, as well as in the medical fields—typically for surgical implants/instruments, also it will find metrological applications in the aerospace industries—more notably for their blade-manufacturing operations. This programmable-gauge has also been envisaged as part of an automated setup, when the parts handling is via productive robot cell configuration—such as if efficient and speedy automatic-offset updates might need to employed. Furthermore, this Equator™ Gauge can also quickly change between differing parts, due to its inherent flexibility obtained from its attached six-stylus probing rack—see Fig. 5.26b.

5.10.2 Calibrating This PKM

Prior to looking in more detail as to how this PKM instrument functions in a metrological application, and being considered as a comparator, its initial calibration must be discussed. In this instance, the term calibration should be more appropriately retitled as Mastering, which can be undertaken in either one, or two specific ways, by means of a:

1. **Calibrated master part**—in this case, the actual master has nominal dimensions for all those component features to be measured;
2. **Production part**—in this instance, where the component's actual dimensions will be more than likely to deviate from the nominal and as such, it subsequently becomes the accredited Master.

Whichever artefact measurement technique employed for its PKM-verification, the part is firstly measured on a conventional CMM in a temperature-controlled environment (i.e. establishing its actual traceability–to International Standards) with the subsequent CMM's measurement results output as an ASCII text file for these specific measured data-points. This data is then input into the Equator™ Gauge's software (i.e. having been developed by Renishaw plc and it is known as MODUS) and then compared against its CAD nominal data (i.e. here in a DMIS-format) which has also been fed into the PKM's computer. This bespoke-computer software results in the creation of offsets from the nominal, but where the actual measured data-points are not nominal. This PKM-instrument will then measure the Master part—at any temperature—having previously established its position via datum features, thus zeroing the system. After this metrological-action of Remastering, the measurement uncertainty will now be close to 2 μm—for this programmable-gauge. Any subsequent part measurement necessitates that the component parts are placed in virtually the same position—to the nearest millimetre—by locating the parts on a very high accuracy palletised system, which is also available from the supplier. From this time, the actual Remastering needs to occur at periodic intervals—related to process

tolerance limits and due to any changes in ambient temperature (i.e. concerning the part's thermal-growth). Here, it is important to stress that any measurements on this PKM-instrument, are compared data-point-for-data-point with that of the original CMM's data-points—even when inspecting for any workpiece swept-surfaces. This fact is true, even where CMMs are not utilising Renishaw's own controller, or are not programmed via the MODUS-software—but they must run the same measurement script. This data-point level of operation is vital, for the metrological instrument to be able to operate correctly.

In summary for this Renishaw Equator™ Gauge, it can be stated that it is a truly Programmable-gauge being constructed upon a parallel kinematic platform with a scanning tactile probe, which makes it a versatile alternative to the majority of conventional Custom-gauging practices, offering inspection of an unprecedented variety of many manufactured high-quality parts. This PKM-system features working-volume in its '*X*', '*Y*' and '*Z*' axes for component part dimensions, which might typically be: ∅300 mm by 150 mm—having a comparison-uncertainty ±2 μm; with a maximum scanning speed 100 mm s^{-1}; while having a fixturing requirement of ±1 mm; with an electrical supply of single-phase 100–240 V; but here, it does not require any air-supply. This programmable-gauge weighs between 25 and 27 kg, dependent on the model's arrangement, so it can be deemed as portable—but with some care in its handling. The high-data capture-rates for a part's rapid form measurement enable thousands of such points to be collected during 3-D-scanning, with the industry-standard Renishaw SP25 probe. Such PKM-measurement results are a reliable form of metrology, which compares remarkably favourably against that of conventional-gauging, enabling an effective technique for that of component form measurement. Every data-point can be utilised for comparative measurement. So, just one PKM-instrument can perform the same function as thousands of DTI's; LVDT's; or by that of handheld-instruments. As a consequence, any requirement for Remastering is swiftly performed as when, for example, measuring a production part and it immediately compensates for any possible thermal effects, returning data-collected to the shop floor—being the equivalent to that obtained in a temperature-controlled quality room. This programmable-gauge—as mentioned—can be considered as a cost-effective alternative and invariably should replace equivalent manual measurement, which can greatly increase throughput and reduce scrap-rates, at a fraction of the cost of a custom-gauging system with its related and costly fixturing requirements.

5.11 Articulated Arm CMM (AACMM)

Introduction

In recent years, there have been many advances in conventional CMM technology, including the development of several portable CMMs. Accordingly, these portable CMMs, can provide many of the benefits of traditional CMMs, but with some

added flexibility. Articulated Arm CMMs (AACMM)[27]—see Fig. 5.27—are also known by the derivative-names of: Portable CMMs (PCMM) or even as Articulated Arm CMMs. These metrology instruments are lightweight and can therefore be utilised virtually anywhere—wherever some form of accurate and precise measurement is demanded. Specifically, the AACMM can be moved to the part for its inspection, hence, the term portable. Under these inspection-circumstances, a controlled environment is unnecessary, as the instrument's operation is very simple. These portable metrology instruments provide highly accurate and reliable results, with the added-benefit of being robust enough to work in a wide-range of working-environments. Such Portable CMMs are considerably much less expensive to purchase than a conventional, more sophisticated CMM, although this latter-type of CMM metrology equipment, has the distinct advantage of being significantly more precise and indeed accurate in usage.

Rapid Shop Floor Inspection

Invariably, within the modern production shop floor environment when utilising AACMMs there are three significant factors that need to be considered when implementing some form of rapid shop floor inspection, these being for:

1. **suitable hardware**—today, in order to conduct inspection on the shop floor, invariably some form of PCMM is necessary, although here there might be several other metrology options, but the common choice in, say, a small machine shop might be to use an Articulated Arm CMM—equipped with contact probe (see Fig. 5.28, top). It is normal practice to temporarily mount the PCMM on any firm and rigid surface—prior to its use—as shown in Fig. 5.28 (bottom).

[27]**Articulated Arm CMMs** (**AACMM**): these have also often been termed a ROMER Arm (The original design for the ROMER arm was based on: US patent 3,944,798—filed in 1974 by Homer Eaton, one of ROMER's-founders, while working at the company: Eaton Leonard. At that time, this early Measuring-arm was intended solely for the measurement of complex-bent tube geometry. Later, Eaton teamed-up with a prospective-colleague: Romain Graiger—to create: ROMER SARL (France), to produce Portable measuring arms—for general-purpose industrial measuring applications. Accordingly, the word **ROMER** originates from a combination of the two founders' names: i.e. **Rom**ain Grainger and Hom**er** Eaton). This typical Portable CMM, or another alternative name being an Articulated Arm CMM, is commercially-produced by: Faro Technologies, Inc, who were involved in the design of the original ROMER arm in the 1980's. It was conceived to solve the problem of how to measure large objects such as aircraft and automotive bodies, without moving them to a dedicated measuring laboratory. Thus, a CMM that precisely measures an object in a 3-D coordinate system that is often utilised in comparison with that of a Computer-aided Design (CAD) model. This Portable CMM is normally a manual measuring device, with the arm operating in 3-D space with either 6, or 7 joints, comprising six degrees of freedom (i.e. 6DoF). Which means that the arm can move in three-dimensional space: linearly—forward/backward; up/down; left/right; combined with rotations about these three perpendicular axes (i.e. for its roll, yaw and pitch). The movement along each of the three axes is independent of each other, also being independent of the rotation about any of these axes, thus, truly-comprising of the six degrees of freedom. The physical-arrangement of an AACMM, is very similar to that of the biology of a human arm, with its wrist, forearm, elbow—as depicted and operated in the case of the well-known Faro-arm example—shown in Figs. 5.27 and 5.28.

Fig. 5.27 The archetypal 'personal coordinate measuring machine', is normally justified as: a portable, cost-effective and three-dimensional gauge, for speedy assessment of components, etc. (courtesy of FARO Technologies Inc.)

These lightweight-metrological instruments can be easily transported anywhere within the shop. Such Arms have highly mobile joints that let the Inspector, or even Machinist utilise the equipment—see Figs. 5.27 and 5.28 (top), enabling PCMMs to extend and rotate the measurement-probe into virtually every component feature, such as its: channels; bores; or pockets; or any other types of

Inspecting critical dimensional features of an accurate & precise turned component employing an 'articulated arm'. [Courtesy of FARO Technologies Inc]

Calibrating an *'Articulated arm'*, by utilising a previously referenced and calibrated artefact.

Fig. 5.28 An 'articulated arm CMM' prior to use, requires verification against a calibrated artefact [courtesy of the National Physical Laboratory (UK)]

inspected part-features. Usually these Arms have a reach of between: 0.8 and 2 m, although they are not restricted by the physical size limits that are common with conventional stationary CMMs—making them extremely versatile inspection tools;

2. **appropriate software**—is a mandatory-requirement, so that it can receive all of the necessary and valid information emanating from inspection by this Arm. In its most basic mode of operation, this bespoke-software will log and report measurement data taken with the Arm. However, the major advantage here is in

both the time and efficiency gains, which occur when the software's full functionality is employed. At this time, the PCCM-software can create prompted-inspection plans, as either datums, or features that are selected while in its teach mode. Moreover, this software will also provide real-time inspection data with visual, on-screen references—to really expedite the overall inspection process, furthermore, it can import a CAD reference model for direct comparison of the manufactured part—to its actual design intent;

3. **quality specification and inspection plan**—the inspection work can be undertaken by referencing a part's engineering drawings. Although this approach works acceptably, the inspection process becomes much quicker when that measurement data is assigned to a digital reference within the PCMM's-software.

5.11.1 Articulated Arm CMMs—In More Detail

Most types of Articulated arm CMMs will determine and record the location of its probe in 3-D space and then report the inspection results through suitable-software—as mentioned in Sect. 5.11. As a result and in order to calculate the position of the probe's tip, the rotational angle of each joint and the length of each segment in the arm must be known—having a radial reach when extended, which typically ranges from: 0.8 to 2 m. The measurement angle of each rotating-joint within the arm is determined by utilising optical rotary-encoders. These high-quality encoders count rotations incrementally, via the detection of accurately spaced lines on a glass grating disc. Once counted, the software then converts these counts into angular-changes. Such Arms—as mentioned—typically have either 6, or 7 axes of rotation, which means the instrument can move throughout a very wide range of physical orientations.

A typical Articulated Arm CMM (AACMM)—is depicted in Fig. 5.27—which can be considered as a high-quality metrology instrument of multi-DoF (i.e. having typically 6 degrees of freedom—6DoF), which is modelled according to the structure of human joints; with a series of linkages being connected by rotating joints. In a comparison with traditional CMMs, the AACMM has the notable-features of small size, lightweight, large measurement range, while being flexible and can be utilised in just about any industrial site. As a consequence, with these unique-advantages the AACMM has been utilised in the fields of: Mould design; Product quality online testing; as well as in the inspection of equipment for maintenance and assembly; plus in situ machine tool component inspection—see Fig. 5.28 (top). At this point, the accuracy of structural parameters is the main influencing-factor to the measurement accuracy of AACMMs, with the structural parameter identification being one of the main measures to improve the accuracy of them. The Arm calibration is an integrated-process of four distinct steps including: (i) modelling; (ii) measurement; (iii) parameter identification; plus its (iv)

error-compensation. The selection of the appropriate kinematic model and its calibration model is the premise of calibration of any AACMM and, by subsequent processing of the data of calibration for structural parameter identification achieves the overall calibration of a typical AACMM. In parameter identification, the linearly related structural parameters can result in a so-called Jacobian matrix,[28] which is mathematically singular, thus its solution is not the required structural parameters one expects, so the linearly related structural parameters must be determined, before identification.

In order to achieve precise inspection measurements on a part, the touch trigger probes on conventional and stationary CMMs will require controlled speeds when coming in contact with the part's surface—slowing the approach to any part-feature being measured, which will inevitably increase overall inspection time. Moreover, if this approach is not exactly along the '*X*', '*Y*' or '*Z*' axes, some additional time will be added to the overall process for probe-angle calibration. To precisely establish an accurate probe compensation in association with its spatial orientation when adding either the: fourth-; or fifth-DoF, every probe angle that will be utilised to measure a part must also be calibrated to that of a Master sphere.

The probe-angles on these stationary CMMs can pose a challenge beyond the time necessary to calibrate them. Since additional DoFs are gained with an indexing-head, here the probe-angle is normally adjustable in: 7.5° increments up to 105°—from the vertical. This restriction on the CMM's probing, can limit potential access to certain part-features. As a consequence, CMMs often need custom-holding fixtures to position and orientate a part, to enable the probe direct-access to a part feature of interest, while for many component parts, multiple fixtures are expensive, but sometimes necessary additions. Conversely, in the case of an Articulated Arm—see Figs. 5.27 and 5.28—the probe approaches the part at any angle without slowing-down as it nears the surface; this action eliminates the probe-angle calibration and the n eed for custom holding fixtures. For large items and structures requiring inspection, these PCMMs can take on other forms, such as utilising either lasers (see Fig. 5.27, top-right) and that of infrared light. Additionally, the long-range PCMMs can capture measurements up to distances of 100 m, while in many industrial applications Laser-trackers are the most common form of long-range PCMMs, which were previously described and illustrated—see Figs. 2.17, 2.18, 2.19 and 2.20.

[28] **Jacobian matrix** (**Carl Gustav Jacob Jacobi**, (Born: 10 December 1804 in Potsdam—died: 18 February 1851 in Berlin, then part of the: Kingdom of Prussia), he was a notable German Mathematician, who made some fundamental contributions to that of: Elliptic functions; Dynamics; Differential equations; also to Number theory): so in Vector calculus, this so-called: **Jacobian matrix**, can be considered as the matrix of all first-order partial derivatives of a vector-valued function. This mathematical work generalises the gradient of a scalar-valued function of multiple-variables, which itself takes a broad view of the derivative of a scalar-valued function of a single-variable. In other words, the Jacobian—for a scalar-valued multi-variable function—is the gradient and that of a scalar-valued function of single-variable, this being simply its derivative. Here, the Jacobian can also be generally thought of as describing the amount of: stretching; rotating; or transforming; that a transformation imposes locally.

5.11.2 Verification of Articulated Arm CMM (AACMM)

In the UK, at The National Physical Laboratory (The NPL) a verification service is offered for Articulate Arm CMMs to the **ASME B89 4.22** Standard—this currently being utilised by the majority of these Arm-manufacturers—see Fig. 5.28 (bottom—left and right). Once verified, an Articulated Arm, or Portable CMM, can achieve uncertainties of just a few tens of micrometres and are principally employed in industry for inspecting parts, and more importantly, in many of today's reverse engineering processes. Unlike traditional inspection equipment, AACMMs allow the measurement system to come to the part being inspected, and as such, these metrological instruments are becoming an increasingly common sight next to assembly lines in high technology factories in a diverse range of industries such as aerospace and automotive, moreover, they are also now being employed in motorsport.

The NPL has become one of the first calibration services within the UK to offer this verification of Articulated arm CMMs to the Internationally recognised and frequently employed **ASME B89 4.22** Standard. This particular Standard has become the basis of the manufacturer's certification, while recently a UK-application has been made for UKAS-accreditation of this calibration service.

Within The NPL, its Engineering Measurement Team has designed and constructed a specialised calibration facility—for these types of PCMM-devices, being based upon the calibration measurements obtained by utilising a highly stable precision-engineered granite structure—weighing around four tonnes (see Fig. 5.28, bottom). This heavy and substantial granite base, supports both the instrument being tested and a pair of calibrated length artefacts manufactured from carbon fibre tubes, these materials being selected for their lightness, stiffness and low coefficient of thermal expansion. These particular tubular-metrological artefacts are 2.4 m long and are positioned and located on kinematic-mounts, bolted onto this stable granite base structure. Each artefact has 19 magnetic-nests defining all possible measurement positions for Articulated Arms that can range in size from about <1 to 4 m in length—see Fig. 5.28 (bottom).

The NPL has manufactured and assembled these calibrated artefacts, including the bonding of these actual nests to the tubes. Following artefact calibration by both a highly sophisticated CMM and a Laser-tracker, each nest was found to have been both set and positioned extremely accurately and precisely. As these AACMMs are invariably utilised on the shop floor, The NPL's Calibration Service has to be both efficient and fast, to minimise any potential company production downtime. Accordingly, The NPL has written some bespoke-software for guiding the operator through the calibration testing process, enabling them to both record and analyse the measurement data taken and then to automatically generate the necessary and valid certification—for the appropriate verification of their AACMM.

References

Journals and Conference Papers

Beyer, L. & Wulfsberg, J., *Practical Robot Calibration with ROSY*, in: Robotica, Vol. 22, 505–512, 2004.

Bringmann, B. & Kung, A., *A measuring artefact for true 3D machine testing and calibration*, Annals of CIRP - Manufacturing Technology, Vol. 54 (1), 471-474, 2005.

Busch, K., Trapet, E. & Wäldele, F., *Simple Interim Check of Large Coordinate Measuring Machines*, European Prod. Eng'g., Vol. 18, 3-4, 1994.

Chen, W., Xu, X., Dai, P., Chen, Y. & Jiang, Z., *Granite Step Gauge: A New Device for Error Measurement on CNC Machine Tools*, in: Advanced Materials Research (Volumes 472 - 475), 328-331, Feb. 2012.

Conrad, K.L. & Shiakolas, P.S., *Robotic Calibration Issues: Accuracy, Repeatability and Calibration*, Proc. of the 8th Mediterranean Conference on Control & Automation (MED 2000), Rio, Patras, GREECE, 17-19 July 2000.

Cox, M.G., Forbes, A.B. & Peggs, G.N., *CMM verification and grading*, NPL Report CLM 1, National Physical Laboratory, Teddington, UK, 1997.

Cox, M.G., Cross, N.R., Flack, D.R., Forbes, A.B. & Peggs, G.N., *Measurement of artefacts using repositioning methods*, NPL Report CLM 2, National Physical Laboratory, Teddington, UK, 1998.

Cox, M.G., Forbes, A.B., Harris, P.M., & Peggs, G.N., *Determining CMM behaviour from measurements of standard artefacts*, NPL Report CISE 15/98, National Physical Laboratory, Teddington, UK, 1998.

De Aquino Silva, J.B., Hocken, R.J., Miller, J.A., Caskey, G.W. & Ramu, P., *Approach for uncertainty analysis and error evaluation of four-axis coordinate measuring machines*, Int. J. of Adv. Manufact. Tech., Vol. 41 (11-12), 1130-1139, 2009.

Denavit, J. & Hartenberg, R.S., *A kinematic notation for lower-pair mechanisms based on matrices*, Trans. ASME J. Appl. Mech., Vol. 23, 215–221, 1955.

Elatta, A.Y., Gen, L.P., Zhi, F.L., Daoyuan Y. & Fei, L., *An Overview of Robot Calibration*, Information Technology Journal, Vol. 3 (1), 74-78, 2004.

Erkan, T., Mayer, R. & Dupont, Y., *Reconfigurable uncalibrated 3D ball artefact for five-axis machine volumetric check*, Proc. of the 9th Int. Conf. and Exhibition on laser metrology, machine tool, CMM and robotic performance – Proc. of LAMDAMAP 2009, London (UK), June/July 2009.

Erkan, T. & Mayer, J.R.R., *A cluster analysis applied to volumetric errors of five-axis machine tools obtained by probing an uncalibrated artefact*, Annals of CIRP – Manufacturing Technology, Vol. 59(1), 539-542, 2010.

Erkan, T., Mayer, J.R.R. & Dupont, Y., *Volumetric distortion assessment of a five-axis machine by probing a 3D reconfigurable uncalibrated master ball artefact*, Precision Eng'g., Vol. 35, 116-125, 2011.

Fang, C. & Butler, D.L., *An innovative method for coordinate measuring machine one-dimensional self-calibration with simplified experimental process*, Rev Sci Instrum., Vol. 84 (5), May 2013.

Forbes, A.B. & Peggs, G.N., *A large reference artefact for CMM verification*, Proc. of LAMDAMAP III, Computational Mechanics Pub., 393-400, 1997.

Hamana, H., Tominaga, M., Ozaki, M. & Furutani, R., *Calibration of Articulated Arm Coordinate Measuring Machine Considering Measuring Posture*, Int. J. of Automation Technology, Vol.5 (2) 109-114, 2011.

Hope, A.D. & Blackshaw, D.M.S., *The application of artefacts and lasers to perform verification of coordinate measuring machines*, Proc. of LAMDAMAP V, WIT Press., 117-126, 2001.

Knapp, W., Tschudi, U. & Bucher, A., *Comparison of different artefacts for interim coordinate-measuring machine checking: a report from the Swiss Standards Committee*, Precision Eng'g., Vol. 13 (4), 277-291, 1991.

Knapp, W., *Interim Checks for Machine Tools*, Proc. of LAMDAMAP III, Computational Mechanics Pub., 161-168, 1997.

Knebel, R., *Scanning for better results* [Concerning probing-points for roundness on a CMM], 76-78, Nov. 1999.

Kruth, J-P., Zhou, L., Van den Bergh, C. & Vanherck, P., *A Method for Squareness Error Verification on a Coordinate Measuring Machine*, Int. J. of Adv. Manuf. Technol., Vol. 21 (10-11), 874-878, July 2003.

Kunzmann, H., Trapet, E. & Waeldele, F., *A Uniform Concept for Calibration, Acceptance Test, and Periodic Inspection of CMMs using Reference Objects*, Annals of CIRP, Vol. 39(1), 561-564, 1990.

Lewis, A., Oldfield, S. & Peggs, G.N., *The NPL Small CMM – 3-D measurement of small features*, Proc. of LAMDAMAP V, WIT Press, 197-207, 2001.

Liu, P. & Fu, J., *Modeling method for mechanism configuration of the articulated industrial robot*, Advanced Materials Research, Vol. 694-7, 1696-1699, May 2013.

Mao, X., Hanmin Shi, B.L., Xi Li, H.L. & Li, P., *Error measurement and assemble error correction of a 3D-step-gauge*, Frontiers of Mechanical Engineering in China, Vol. 2 (4), 388-393, Oct. 2007.

Mutilba, U., Kortaberria, G., Olarra, A., Gutiérrez, A., Gomez-Acedo, E. & Zubieta, M., *Performance Calibration of Articulated Arm Coordinate Measuring Machine*, Procedia Engineering, Vol. 63, 720–727, 2013.

Nardelli, V.C. & Donatell, G.C., *A Simple Solution to Interim Check of Coordinate Measuring Machines*, XVIII IMEKO World Congress - Metrology for a Sustainable Development Rio de Janeiro, Brazil, Sept. 2006.

Nguyen, H-N., Zhou, J. & Kang, H-J., *A new Full Pose Measurement Method for Robot Calibration*, in: Sensors (Basel), Vol. 37 (7), 9132-9147, July 2013.

Nubiola, A, & Bonev, I.A., *Absolute robot calibration with a single telescoping ballbar*, Precision Engineering, Vol. 38 (3), 472-480, 2014.

Omari, M., Ajao, D., Kampmann, G.G. & Schmadel, I., *Machine Tool Accuracy Quick Check in Automotive Tool and Die Manufacture*, Annals of the CIRP, Vol. 56 (1), 2007.

Osawa1, S., Sato, O. & Takatsuji, T., *Project for supporting Japanese local public metrology institutes in the field of a coordi-nate metrology*, The 10th International Symposium of Measurement Technology and Intelligent Instruments, Japan, June 29 to July 2011.

Pahk, H. & Kim, J., *Development of computer aided calibration module for CMMs and machine tools using a compensated step gauge*, KSME Journal, Vol. 7(2), 158-164, June 1993.

Peggs, G.N., *Creating a Standards Infrastructure for Coordinate Measurement Technology in the UK*, Annals of CIRP, Vol. 38(1), 521-523, 1989.

Peggs, G.N., *Developing Standards for CMMs*, Quality Today, S1-S3, 1998.

Pril, W.O., Struik, K.G. & Schellekens, P.H.J., *Development of 2D probing system with nanometer resolution*, Proc. of 16th ASPE, 438-442, 1997.

Quality Digest, *The New Face of Automation - High-speed, comparative gauging system makes cell integration possible* [Parallel Kinematic Mechanism], Oct. 2013.

Ran, H., Liu, S. & Zhang, H., *Articulated Arm Length Calibration for Cantilever Coordinate Measuring Machine*, Applied Mechanics & Materials, Vol. 333-5, 77-80, 2013.

Ruijl, T., Franse, J. & van Eijk, J., *Ultra precision CMM aiming for the ultimate concept*, Proc. of 2nd Euspen Int. Conf. (Turin, Italy), 234-237, May 2001.

Russell, S.J. & Norvig, P., *Artificial Intelligence: A Modern Approach* (2nd Ed.), Upper Saddle River, New Jersey: Prentice Hall, 2003.

Sagar, P., *When the last several microns count*, S12-S14, July 1998.

Saundry, L., *Standards and traceability*, Quality Today, S38-S40, July, 1998.

Schuetz, G., *Harmonic Analysis* [Concerning machined roundness of components], Modern Machine Shop, Jan. 2007.

Scott, P., *Fundaments of measurement for testing software in computationally-intensive metrology,* Proc. of LAMDAMAP XI, The University of Huddersfield (UK), 2015.
Sims, C., Hope, A.D, Smith, G.T. & Gull, M., *Correlation of machine tool and CMM accuracy and precision*, Proc. of LAMDAMAP IV, WIT Press, 389-402, 1999.
Singh, J., Hughes, M. & Petzing, J.N., *Investigating the volumetric performance of multi-axis measurement arms*, Proc. of LAMDAMAP VI, WIT Press, 131-139, 2003.
Slamani, M., Nubiola, A. & Bonev, I., *Assessment of the Positioning Performance of an Industrial Robot*, Industrial Robot, Vol. 39 (1), 57–68, 2012.
Slamani, M., Nubiola, A. & Bonev, I., *Effect of Servo Systems on the Contouring Errors in Industrial Robots*, Trans. of the Canadian Soc. for Mech. Eng'g., Vol. 36 (1), 83-96, 2012.
Smith, G.T., Sims, C., Hope, A.D. & Gull, M., *A stereometric artefact for volumetric calibration of machining centres*, Proc. of LAMDAMAP V, WIT Press, 51-58, 2001.
Sumiya, H. & Irifune, T., *Microstructure and Mechanical Properties of High- Hardness Nano-Polycrystalline Diamonds*, SEI Technical Review, No. 66, 85-91, April 2008.
Tagiyev, N. & Alizade, R., *A Forward and Reverse Displacement Analysis for a 6-DOF In-Parallel Manipulator*, Mech. Mach. Theory, Vol. 29 (1), 115–124, 1994.
Takeshima, H. & Ihara, Y., *Finished Test Piece Example for Five axis Machining Centers*, Proc. of the 5th Int. Conf. on Leading Edge Manufacturing in 21st century (LEM21), 123-126, 2009.
Trapet, E. & Franke, M., *The Ball Cube Method for CMM Interim Checks*, Workshop on Traceability of Coordinate Measuring Machines, PTB Braunschweig, 9 & 10 Oct. 1997.
Trevelyan, J. P., *Robot Calibration with a Kalman Filter*, Presentation at Int. Conf. on Advanced Robotics and Computer Vision (ICARCV96), Singapore 1996.
Wang, X.Y., Liu, S.G., Zhang, G.X., Wang, B. & Guo, L.F., *Calibration Technology of the Articulated Arm Flexible CMM*, Engineering Materials, Vol. 318-2, 161-164, 2008.
Weckenmann, A. & Petrovic, N., *Conceptualization of Comparative Measurements of Artefacts Intended for Inspection of CMM Length Measuring Capability*, 4th Research/Expert Conf. with Int. Participations, 'QUALITY 2005', Fojnica, B&H, Nov., 2005.
Woody, B.A., Smith, K.S., Hocken, R.J. & Miller, J.A., *A technique for enhancing machine tool accuracy by transferring the metrology reference from the machine tool to the workpiece*, J. of Manufact. Science and Eng'g., Trans. of ASME, Vol. 129 (3), 636-643, 2007.
Yang, S., Li, S., Kaiser, M.J. & Kwun, F.H., *A probe for the measurement of diameters and form error of small holes*, Meas. Sci. Technol., Vol. 9, 1365-1368, 1998.
Ziegert, J. & Mize, C., *The laser ball bar: a new instrument for machine tool metrology*, Precision Engineering, Vol.16 (4), 259-267, 1994.

Books, Booklets and Guides

* The actual researchers involved from their work at various research organisations.
Alexander, W.O., Davies, G.J., Reynolds, K.A. & Bradbury, E.J., *Essential Metallurgy for Engineers*, Van Nostrand Reinhold Pub. (UK), 1985.
ANSI/ASME B89: *Methods for Performance Evaluation of Coordinate Measuring Machines*, The American Society for Mechanical Engineering, New York, 1990.
ANSI/ASME B5.54:1992, *Methods for Performance Evaluation of Computer Numerically Controlled Machining Centers*, The American Society of Mechanical Engineers, New York, 1992.
ASME B89.4.22-2004: *Methods for performance evaluation of articulated arm coordinate measuring machines*, 2004.
Boeing, D38553-4:1999, *Testing and Acceptance - 1999,* BCAG Equipment Design and Asset Acquisition Standards (EDAAS), 1999.
Bosch, J.A., *Coordinate Measuring Machines and Systems*, Marcel Dekker, INC. New York, 1995.
Bossoni, S., *Geometric and Dynamic Evaluation and Optimization of Machining Centers*, for the degree of: Dr. sc. ETH Zürich, Diss. ETH No. 18382, 2009.

Bossoni, S., *Geometric and Dynamic Evaluation and Optimization of Machining Centers*, Zürcher Schriften zur Produktionstechnik, Fortschritt-Berichte VDI Reihe 2 Nr. 672. Düsseldorf: VDI-Verlag, 2009.

Buice, E.S., *Implementation of Dynamic Positioning Machine for nano-scale Engineering*, PhD Dissertation, The University of North Carolina at Charlotte, 2007.

Butler, B.P., Forbes, A.B. & Kenward, P.K., *Position Calibration Software: Fortran implementation of algorithms to determine frame of reference from measurements of registration points*, NPL Report CISE 14/98, National Physical Laboratory, Teddington, UK, 1998.

Callister, Jr., W.D., *Materials Science and Engineering – An Introduction* (6th Ed.), John Wiley & Sons, Inc., 2003.

Colestock, H., *Industrial Robotics – Selection, Design& Maintenance*, McGraw-Hill Pub., 2005.

Corta, R., Cox, M.G., Cross, N.R., Dotson, J.R., Flack, D.R., Forbes, A.B., O'Donnell, J., Peggs, G.N. & Prieto, E., *A large reference artefact for CMM verification*, NPL Report CLM 6 (PDB: 1301), May 1998.

Cubero, S. (Ed.), *Industrial Robotics: Theory, Modelling and Control*, Pub. by: Pro Literatur Verlag, Germany / ARS, Austria, Dec. 2006.

Dagnall, H., *Let's Talk Roundness*, (3rd Ed.), Taylor Hobson Pub., Nov. 1996.

Flack, D.R., Measurement Good Practice Guide No. 42 - CMM Verification, National Physical Laboratory Pub.,.

Forbes, A.B., *Least squares best fit geometric elements*, NPL Report DITC 140/89,National Physical Laboratory, Teddington, UK, 1998.

Hazewinkel, M. (Ed.), '*Jacobian*' - *Encyclopedia of Mathematics*, Springer Pub., 2001.

ISO 10791-7:1998(E), *Test conditions for machining centres - Part 7: Accuracy of a finished test piece*, *International Standard*, International Organization for Standardization, Geneva, Switzerland, 1998.

ISO 9283 - *Manipulating industrial robots*. *Performance criteria and related test methods*, (Geneva) 1998.

JIS B 7440-1987: *Test Code for Accuracy of Coordinate Measuring Machines*, by: Japanese Standards Association.

Koba-step: *Precision Step gauge, plus data-analysis software – equals - a complete system for monitoring coordinate measuring machines*, by: Kolb & Baumann GmbH & Co., (DE-63741 Aschaffenburg, Daimlerstr. 24, Germany), 2009.

Luger, G. & Stubblefield, W., *Artificial Intelligence: Structures and Strategies for Complex Problem Solving* (5th Ed.), The Benjamin/Cummings Pub. Co., Inc., 2004.

Meli, F., Bieri, M., Thalmann, R., Fracheboud, M.*, Breguet, J-M.*, Clavel, R.* & Bottinelli, S.**, *Novel 3D analogue probe with a small sphere and low measurement force*, Swiss Federal Office of Metrology and Accreditation (METAS)/**Mecartex/*Institut de Production et Robotique (IPR-LSRO), Switzerland, 2014.

NAS 979:1969, *Uniform Cutting Tests - NAS Series Metal Cutting Specification*, Aerospace Industries Association of America, Inc. (AIA), 1969.

NCG 2005 - *NCG-Prufwerkstuck fur die 5-Achs-Simultan-Frasbearbeitung*, [NCG test piece for 5-axis-simulataneous milling], NC-Gesellschaft, 2005.

NF E11-150: *Accuracy of Coordinate Measuring Machines*, France, 1986.

Paul, R., *Robot manipulators: mathematics, programming, and control: the computer control of robot manipulators*. Cambridge, MA: MIT Press, 1981.

Quinn, T., *From Artefacts to Atoms: The BIPM and the Search for Ultimate Measurement Standards*, Oxford University Press, 2012.

Smith, G.T., *Industrial Metrology – Surfaces and Roundness*, Springer Verlag Pub., 2002.

Smith, G.T., *Cutting Tool Technology – Industrial Handbook*, Springer Verlag Pub., 2008.

Thelning, K-E., *Steel and its Heat Treatment – Bofors Handbook*, Butterworths Pub., 1975.

VDI/VDE 2617 – Parts 1 to 5: *Accuracy of Coordinate Measuring Machines*, Dusseldorf, Germany, 1986-1991.

VDI/VDE 2617 Part 9: *Acceptance and reverification test for articulated arm measuring machines*, 2009.

Chapter 6
Machine Tool Performance: Spindle Analysis; Corrosion and Condition Monitoring; Thermography

"I like work; it fascinates me.
I can sit and look at it for hours.
I love to keep it by me;
the idea of getting rid of it nearly breaks my heart".
Jerome K. Jerome
(British Dramatist and Humourist)
[1859–1927]
(In: Three Men in a Boat, Ch. 15)

6.1 Machine Tool Spindle Analysis

Introduction

Throughout the prevailing last few decades, CNC machine tools have been developed to become highly flexible manufacturing plant, being capable of performing a very wide range of programmed machining tasks. At this time, a machine tool spindle or its equivalent headstock are crucially important precision component assemblies in all of these types of machines, where they are employed to undertake a vast range of high-quality machining operations, these sub-assemblies being seen partially sectioned in Fig. 6.1a, b respectively. Such consistently manufactured part quality machined components and their associated product assemblies, require part finishing via a range of production processes. These might be: turning; milling; drilling; tapping; reaming; plus various additional surface/cylindrical grinding processes and so on, to accomplish their final prismatic and rotational shapes so as to be within the specified design tolerances and quoted surface finish requirements.

In principle, the machine tool's spindle is normally a motor-driven shaft that both positions and transmits power to a cutting tool (Fig. 6.1a) or accurately and precisely holds and locates a workpiece (Fig. 6.1b). Usually, the majority of conventional

G.T. Smith, *Machine Tool Metrology*, DOI 10.1007/978-3-319-25109-7_6

(a)

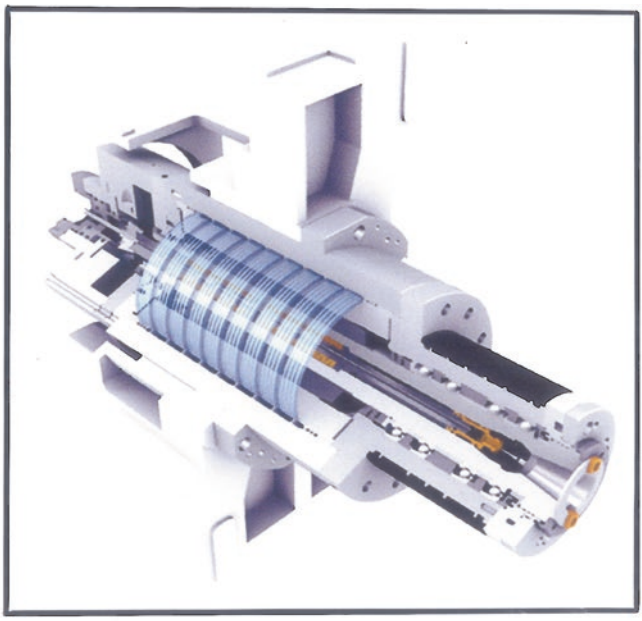

Horizontal Machining Centre spindle, with: HSK-63 spindle taper; 15,000 rev min^{-1} rotational speed; having 25 kW spindle power.

(b)

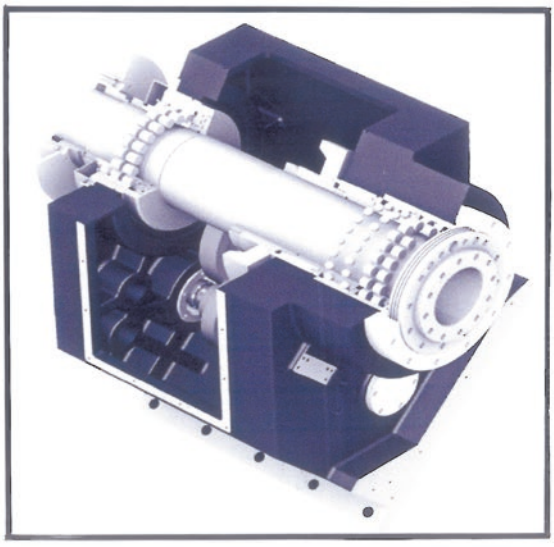

Turning Centre headstock (Heavy-duty), with: 44.8 kW power; +7 kNm spindle torque; having a ϕ320 mm spindle bore.

Fig. 6.1 Partial sections of a machining centre's spindle and a turning centre's headstock [courtesy of Hyundai WIA America (Carlstadt, NJ, USA)]

machine tool spindles—equipped with their rolling element bearings,[1] can operate at rotational speeds of up to 20,000 rev min^{-1}, which if unintentionally damaged in any way, can have a direct impact on the machine's efficiency, accuracy and overall workpiece productivity. Consequently, a high-speed spindle that will be utilised in stock material removal on a machine tool must be designed to provide its required design performance features, which customarily include the:

- **necessary spindle power**—at either peak and/or continuous cutting operations;
- **maximum spindle load**—in the tangential, axial and radial directions;
- **maximum spindle speed**—applicable for the desired machining operations;
- **wide speed range**—allowing an extensive range of materials to be machined and a widespread range of associated tooling that can be utilised;
- **belt-driven spindle, or integral motor spindle designs**—whichever is appropriate for the machine's manufacturing requirements;
- **spindle tooling: fitment; style; size and capacity for its ATC**[2]—normally these toolholder variables being applicable to either Machining, or Mill/Turn Centres.

6.1.1 Design Trends in Machine Tool Spindles

Of late, there are some specific trends that have emerged in both the engineering design and development of machine tool spindle, which have indicated there are three predominant types of spindle configurations that can be tailored to different machining application needs, these are for:

1. **low-cost machine tools, or those with high torque**—here, the conventional belt-driven spindle assembly units are usually preferred. Frequently these belt-driven spindle units are to be found on heavy duty CNC Turning Centres and CNC lathes—see Figs. 1.28a and 6.1b, where cost issues are invariably the decisive features in their final selection and usage;
2. **general-purpose applications that demand flexibility and an automatic spindle change**—under these circumstances the spindle units coupled to matched motors are the norm. These coupled motor designs, can respond to the customer requirements for high productivity, they are also beneficial where there is limited space for the spindle where high flexibility in case of its servicing and improved dynamic performance is a requirement. This type of spindle

[1]**Rolling element bearings**: at a rotational speed of approximately >20,000 rev min^{-1}, the conventional type of ball bearings become detached (i.e. they lose contact) with their adjacent journal walls—due to this high-rotation affecting centrifugal forces in this region. As a result, this may cause damage to the adjacent raceways by the ball's action of its so-called Brinelling-effect.

[2]**ATC**; this refers to the **A**utomatic **T**ool **C**hanger, which can normally be a rotary carousel, or large-capacity chain-driven magazine, but other automated tool-holding configurations are also utilised by machine tool builders.

design is now being applied to new machine tool concepts and existing standard machine tools with asynchronous motors, having both excellent torque and high-speed characteristics. These spindle units with coupled motors can actually offer a flexible approach to design, as a result of their method of connection—see typically Fig. 1.27;

3. **medium and high-performance machine tools, high-speed and high-power systems**—the motorised spindle unit is today usually the preferred design option—see Fig. 6.2. Currently this type of motorised spindle unit can incorporate asynchronous, or synchronous motor technology facilitating spindle speeds >20,000 rev min^{-1} and even beyond that to +80,000 rev min^{-1}—see Fig. 6.6 (top-right). This latter type of integral spindle design can respond to customer demands for higher productivity and enhanced workpiece quality. Typical applications for these self-contained spindle units, or cartridges as they are sometimes known, might include Machining Centres—see Figs. 1.25 and 1.26, CNC Milling machine tools and Coaxial Spindled Mill/Turn Centres—see Figs. 1.22 and 1.23—for machining applications in the aerospace industry, or indeed, for many grinding machine tools, as well as for pickup and high-performance CNC lathes.

The well-established world-class company SKF, launched a range of new bearing products and solutions for the machine tool industry that could be fitted to an integral high-speed spindle—typified by the one centrally illustrated in Fig. 6.2.

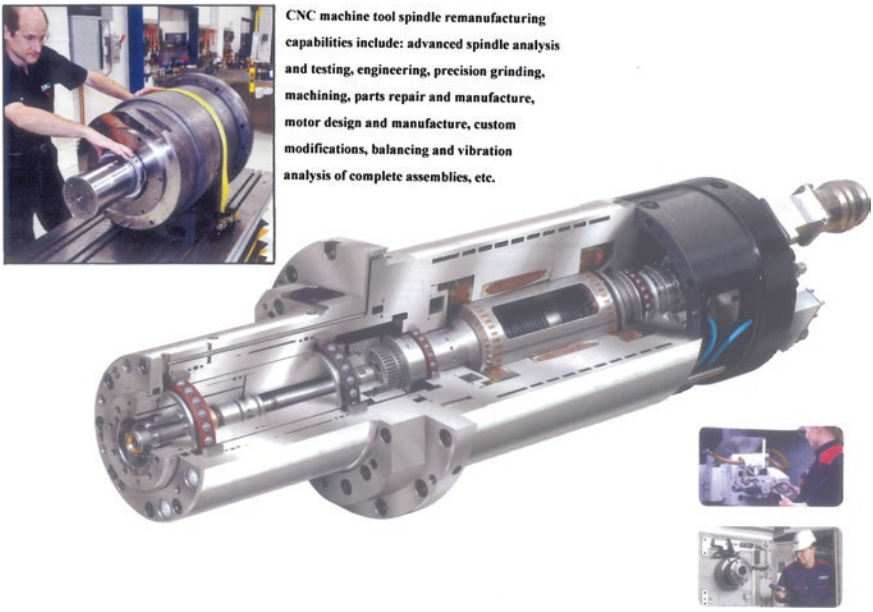

Fig. 6.2 A typical illustration of the partial sectioning of a customer's high-performance machine tool spindle, having the appropriate bearing arrangements and spindle locations illustrated—for efficient HSM rotational performance (courtesy of SKF USA Inc.)

These bearing products included a series of high-precision ball and roller bearings, such as sealed angular contact ball bearings, silicon nitride cylindrical roller bearings and nitralloy (i.e. produced from a special steel alloy)—for exceptionally high rotational performance. This current bearing range also included hybrid bearings with different sizes of ceramic balls. With regard to the current machine tool applications, these specialist bearing-based companies can provide sophisticated and high-technology bearing maintenance programmes that are coupled to specific technical solutions, which can provide:

- purposely built support bearings and bearing units, for example in screw drives;
- specific lock-nut designs for many of these high-performance spindles;
- novel spindle lubrication systems, having technical engineering solutions for precision measuring and spindle monitoring across a full range of complex spindle designs;
- spindle maintenance programmes, which can include the spindle's total refurbishment, for all brands of current and many previous spindle systems.

Understandably, the high-speed spindle's bearings are a key factor in all machine tool applications and as a consequence the bearings have to cope with: temperature differences; expansion of inner rings; reduced contact-angles; as well as high axial- and radial loads—during in-service machining operations. The latest generation of angular contact ball bearings has both new raceway geometry coupled with their integrated and novel cage design, which can result in both higher spindle stiffness and less noise than their bearing predecessors. Currently, the latest types of oval cage pockets are an example that is designed to accommodate any ball excursion (i.e. its relative ball motion) within the bearing. In conjunction with this new type of bearing design, the angular contact ball bearings have benefited recently from SKF's technical efforts to improve the overall bearing's material performance. This recent applied research and testing regime, has included a steel grade that can now offer enhanced bearing kinetics and improved cage materials, whose mechanical properties include higher strength, plus the ability to allow grease and oil to adhere properly during their subsequent rotational operation. Moreover, these latest bearing surface profiles with enhanced quality, will also contribute to both lower wear and less noise than many of the current conventional types of bearings.

As mentioned, standard machine tool spindles are usually supplied as either belt-driven, or motorised, these latter versions being available as either a cartridge, or block unit. This type of spindle's standard bearing product range, can include high-frequency milling cartridge/grinding spindles—see Fig. 6.6 (top-right)—designed for applications that require exceptionally high operating rotational speeds at relatively low torques and loads. Customarily, these derivative spindles of active magnetic bearing types are preferred in high-precision machines, where the rotational application speeds are considerably much higher than appropriate for the more usual rolling element bearings.

6.1.2 Machine Tool Spindle Failure Modes

With respect to any expensive, critical and key machine tool asset such as a machine's spindle, it can potentially fail for any number of in-service reasons, which may be due to: contaminants; loss/increase of pre loads; because of a number of lubrication issues; also from improper care and maintenance; or even utilising an inappropriate spindle design for a given machining application. End-users can help to mitigate these unanticipated problems and related spindle usage issues, by understanding the key question of, "How and why spindles can fail…?" and, in the process, help keep their spindles up-and-running—as originally intended.

Spindle Failure—Common Causes

There are quite a number of specific causes for why an expensive machine tool spindle might prematurely fail, just some of which are listed below, including:

- **normal fatigue wear of spindle components**—this is a significant cause of failure that can be expected over time. Spindle components are typically subject to deterioration, because of the: wear on the shaft's front, -rear, as well as its -main housings; a range of bearing failure modes; stator failure; rotor failure; problems with the tool's finger assembly; drawbar springs—affecting its pull-stud pressure; spacer problems; encoder errors; as well as its front shaft nut and cap—see cutaway assembly in Figs. 6.1a and 6.2. If any of these spindle-related parts exhibit signs of early wear rates, faults or some form of damage, these critical components should be either immediately repaired or replaced;
- **spindle contaminants**—these contaminants can affect shafts and/or bearings, which might include any undesirable foreign substances ranging from: coolant and condensation, to debris ingress of fines/chips, grinding swarf, as well as the result of other forms of debris from the stock material being machined. As a consequence, proper spindle seal installation and its accompanying periodic maintenance can help to significantly minimise these contaminant risks;
- **improper lubrication**—this lubrication problem can considerably increase wear, while generating excessive heat and result in higher than required operating temperatures. These effects can limit spindle speed and power, while reducing energy efficiency. Therefore, by supplying the approved lubricant in the correct amount and at the right time, this will be imperative for the spindle's longevity. Any lubricants utilised on the plant, should always be of highest-quality, properly specified, as well as previously stored for the application, while being clean and free from moisture or any other form of contaminants. Neither too much nor too little lubricant should be applied and lubricant containers, plus all transmission lines should be inspected, to rule out any pre-existing contaminants. Moreover, in the case of air/oil lubrication systems, clean and dry air is crucial for prolonged spindle life. Additionally, any lubricant can be subject to some form of chemical breakdown while in-service and as such, should be regularly monitored to confirm its integrity;

- **mishandling bearings**—which is another frequently encountered cause of a spindle's premature breakdown. For example, any radial-/axial impacts—known colloquially as tool crashes—to a spindle's shaft can cause run-out/concentricity issues—see Figs. 6.3a, 6.5 and 6.6. Moreover, any form of Brinelling, or permanent denting to the raceway's tracks, will subsequently result in very rapid deterioration of a spindle's precision bearings and hence, its performance. Machine tool spindles should be properly handled and protected from any undesirable vibrations and any other potentially adverse influences, to help keep this expensive plant performing—as it was intended.

In summary, there is no shortage of potential causes that can result in premature/catastrophic spindle failures, these problems being the result of a range of spindle-related factors—see Figs. 6.3b and 6.4. Others influences that might result in premature spindle failure, could include: overloads, or improper preload on bearings, spindle imbalance, tool change errors, improper maintenance and repair,[3] but there are many more potential spindle failure sources (i.e. shown graphically displayed in Fig. 6.4—for the main causes of such failure). Here, the main spindle unit is shown to be one of the machine tool components that is most susceptible to damage during any form of collision. As depicted in this histogram/pie chart in Fig. 6.4, it has been reported that 60 % of the damage caused to the main spindle unit are from these actual collisions. Of note, is that the rolling element bearings, are among the machine spindle components most affected by such undesirable collision forces. Due to the relatively small contact surface areas between the races (i.e. both inner- and outer raceways) and the rolling elements, the maximum allowable interface pressure is invariably exceeded when these collision forces are too high, which can deform, or damage the rolling elements and the races. In addition, the tool interface and tool clamping system may also be subject to additional damage and as a result might also need to be repaired upon strip down.

Spindle Service Life—Extension

Habitually, CNC machine tool operators have an important part to play, by facilitating optimal spindle performance, while enabling an extension of the spindle's service life. For example, these machine spindles must always be correctly

[3]**Improper maintenance and repair**: during spindle disassembly, the bearings must be extracted correctly, by utilising a controlled removal action from, for example using bearing pullers (i.e. see Fig. 6.6b), to ensure that any form of bearing damage during its removal is at best, then minimised. After this bearing's inspection, or when assembling/fitting new bearings, if possible, press fit the bearing into its housing. This bearing fitment is undertaken by employing just a uniform and controlled pressure by circumferential and even loading of the bearing's non-moveable portion of the race in this vicinity. If this bearing mounting is forced by say, an uneven shock-loading fitment—into its register shoulder/position within the respective housing/spindle by any other means, this will inevitable result in bearing damage. For example, through the uneven striking of this replacement rotating bearing with a mallet, this action may potentially create premature Brinelling of the raceways, which could significantly affect its rotational efficiency and might normally result in premature bearing failure when it is in-service.

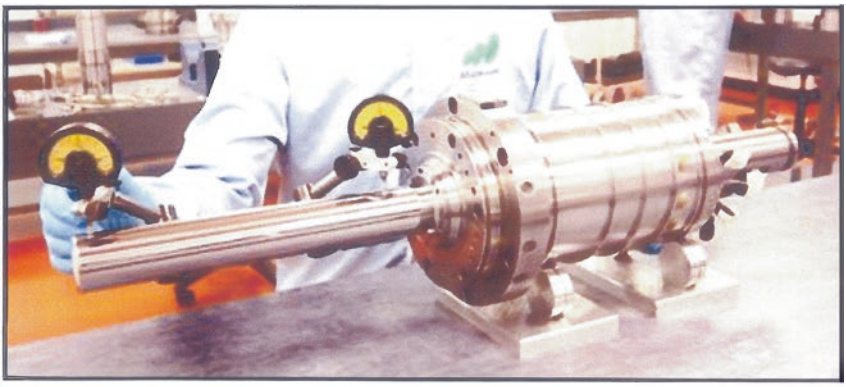

(a) Inspecting and calibrating a re-built high-speed spindle for alignment, run-out and concentricity, within the company's Spindle Clean Room Facility.
[Courtesy of Matsuura Machinery Ltd (Coalville, Leicestershire, UK)]

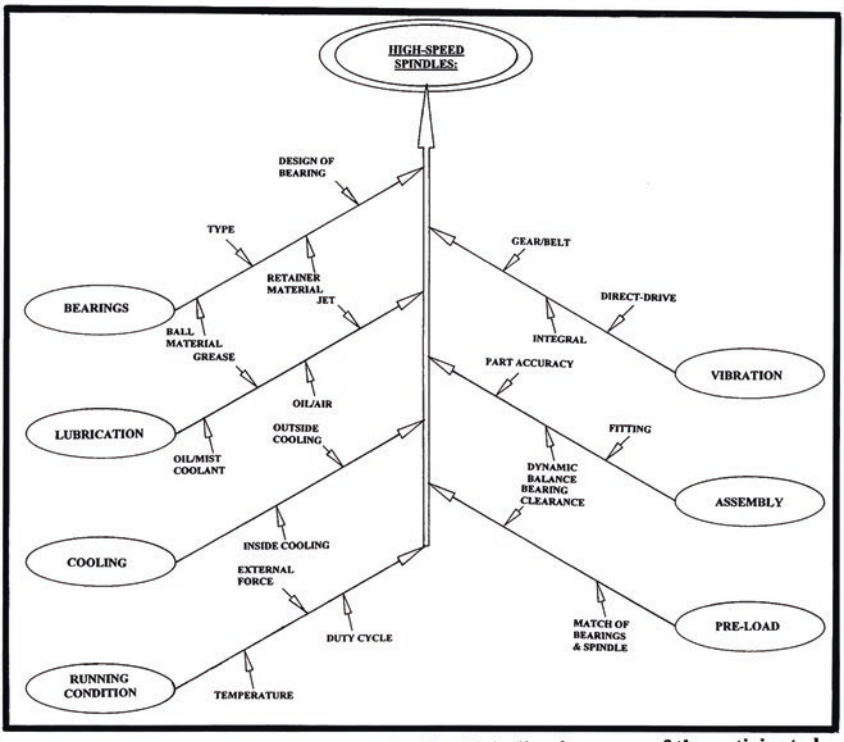

(b) An 'Ishikawa diagram' (i.e. 'Cause-&-effect'), indicating some of the anticipated considerations for the components of high-speed spindles.
[Courtesy of Yamazaki Mazak Corporation (Japan)]

Fig. 6.3 A refurbished machine tool spindle and UHSM spindle cartridge: listing of the factors affecting such a spindle's design and its operation

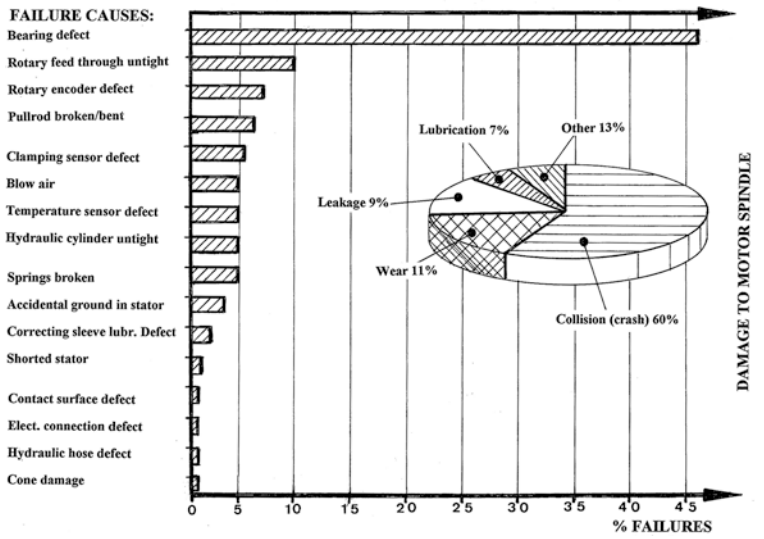

Fig. 6.4 The failure causes and damages of motor spindles [*source* Design World (Aug. 2012)]

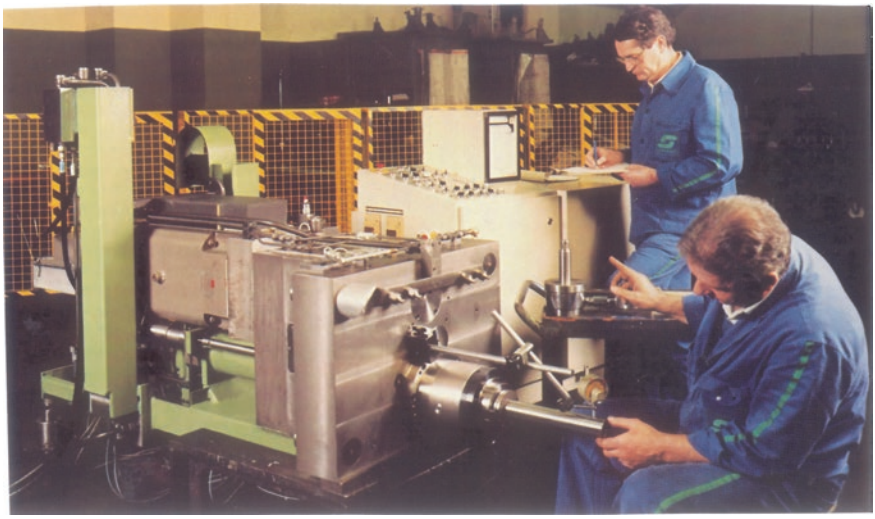

Fig. 6.5 Test bench for sub-assembly of machine spindles for machining centres, employing precision mandrels and dial gauges (courtesy of Dörries Scharmann Ltd.)

balanced. As a consequence, when a spindle assembly rotates during machining operations, any potential imbalance in these rotating components creates centrifugal force—which will increase exponentially with its rotational speed. As a result of this force increase, coupled to excessive and potentially troublesome vibration,

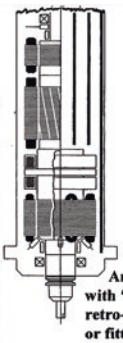

An ultra-fast high-frequency spindle cartridge, with 'active' magnetic bearings, that can be retro-fitted to a conventional CNC machining centre, or fitted to new machine tools.
Spindle specification:
80, 000 rev min^{-1} - spindle rotational speed;
10 kW - spindle power;
SKI 25 - taper fitment.
NB Other spindle cartridges can be fitted with differing: rotational, power and fitment characteristics.
[Courtesy of IBAG, Switzerland]

(a) Systematic rolling bearing monitoring with suitable diagnosis tools, makes it possible for: planned, condition-related maintenance, with short machine down-times, thus increasing productivity and reducing costs. Vibrations in the spindle are recorded at the machine and then analysed either immediately on site, or when conveniently later on - for full diagnostic interpretation.

[Courtesy of Schaeffler Technologies GmbH & Co. KG (Herzogenaurach, Germany)]

(b) Bearing pullers are necessary for various types of pulls, whether they are for: external, internal and even blind pulling. The range includes mechanical, hydraulic and hydraulically-assisted pullers for easy application of high withdrawal forces. Here, being pictured removing a Turning Centre headstock's bearings.

[Courtesy of SKF USA Inc – North American HQ (Lansdale, PA, USA)]

Fig. 6.6 In-situ bearing maintenance and partial stripdown of machine tool spindles

which will inevitably follow, this will result in poor machining efficiency and attendant machined surface finish, which will create a difficulty when attempting to hold close work tolerances.

The causes of a spindle's imbalance may be inherent in its initial design, meaning that the spindle may not even have been appropriately balanced from the outset,

or it might just have been damaged, or intentionally modified by the end-user. As a result, by expressly calculating a spindle's balance tolerance,[4] this information can provide an acceptable range for its intended machining operational performance. This dynamic balance process will designate the intended operating speed and then specify the maximum allowable imbalance within the rotational speed parameters. Dynamic balancing within the tolerance range can help avoid these problems, while optimising spindle performance and accuracy. Any spindle vibration should be within normal parameters. So, excessive, or abnormal machine vibration will often indicate there is a spindle problem and if this is the case, the spindle should undergo at the very minimum, an inspection check—see Figs. 6.2 and 6.3a.

During actual usage, a CNC machine tool operator should make every effort to protect the spindle(s) from coolant ingress. Such spindle contamination from intense and pressurised coolant spray, or via high-pressure flood coolant application, can washaway the grease, or oil from the bearings and attack the spindle's shaft; motor, as well as its electronics. Coolant should preferably be directed at the tool/workpiece, but if at all possible, always away from the machine's spindle. By monitoring the spindle's operating temperature for any potential fluctuations, this can suggest an early warning sign of its impending premature spindle failure. Once the normal operating temperature for an application is ascertained, it can be rather helpful to record the baseline temperatures for the spindle's front and rear bearings for comparison—raising the possibility of an immediate and remedial maintenance action, if this condition worsens. Some other useful best practice tips to help extend the spindle's life, which might possibly include:

- **listening for unusual and/or noticeable audible noise**—as a potential alarm about the spindle's impending vibrational trouble—see Fig. 6.6a;
- **keeping a clean and proper oil flow**—by supplying clean and dry compressed air to the spindle, this will minimise oil contamination within the rotating elements;
- **monitoring feeds and speeds**—arriving at the optimum combination for the given machining application.

[4]**Calculating a spindle's balance tolerance** [For more details on the subject of: Cutter/Spindle Imbalance also on information concerning that of HSM, see: Smith (2008)]: this is normally the result of non-uniform rotating masses within the spindle (i.e. usually created by the out-of-balance tooling), this out-of-balance can be simply determined graphically from a chart for: Milling Cutter Imbalance (in rev min^{-1}) versus Centre of Gravity Displacement (in μm). This calculation of spindle imbalance being based upon the: **ANSI S2.19-1989** Standard, or its equivalents, such as: **ISO:1940:1**; or **ISO:1290G**, which is as usually expressed as below:

$$\text{Unbalance:} \quad U = \frac{9549 \times \text{M} \times \text{G}}{N} \quad \text{(i.e. in units of: g-mm)}$$

$$\text{Force:} \quad F = U\left(\frac{N}{9549}\right)^2 \quad \text{(i.e. in: } N\text{)}$$

where: U = allowable unbalance (g-mm); 9549 = a constant; M = mass, or weight of the total cutter assembly (kg); G = preselected balance tolerance: derived from the graph, in: **ANSI S2.19-1989** Standard.

Spindle Service Provider—Vetting

A typical professional spindle service provider, would normally possess an in-depth technical knowledge of the required appropriate maintenance procedures, enabling them to perform efficient and comprehensive repairs and rebuilds to previously damaged machine spindles. This machine tool maintenance company's engineering facilities should be equipped with a wide range of in-house technical capabilities and engineering support, which might include the full engineering capability of: correct maintenance stripdown and build procedures; high-quality machining capabilities; precision cylindrical and surface grinding; honing—as necessary; together with other forms of appropriate manufacturing engineering and metrology. Here, the company's knowledge and specialised experience should include all factors relating to these spindles, such as: information concerning the current and previous commercial spindle brands; typical assembly configurations; coupled to their own in-house machining capabilities; all of the former factors being an essential prerequisite; plus an in-depth knowledge of potential spindle defects and their root causes. As a consequence, when delivering a company's machine tool spindle to an outside expert for its attendant remanufacturing, there are certain best practice procedures, that must be considered, which would normally include the following:

- **spindles**—the spindle service company should carefully disassemble it in a dedicated area, or preferably in a Clean room facility (Fig. 6.3a) to maintain a high level of quality control. Their in-house maintenance technicians should look for signs of: spindle crashes; bearing/seal contamination; lack of lubrication; possible misuse; or any other apparent signs of failure. As a result of this in-depth inspection, once a spindle has been completely disassembled, each component should be cleaned then polished to remove any signs of surface rust, or damaged high spots, prior to its actual rebuild;
- **disassembled spindles**—these spindles should be taken to an inspection area, where the company's trained maintenance technicians can analyse each individual component for their: size—to see if it is still within its stated tolerance; run-out; alignment; roundness, and parallelism—see Figs. 6.3a and 6.5. At this time, an ensuing detailed report can then be generated for any subsequent remedial action;
- **areas for grinding operations**—this machine tool facility should ideally be climate-controlled and suitably calibrated grinding machines should be capable of cylindrically/surface grinding—to very precise and accurate tolerances;
- **remedial maintenance work**—the spindles should then be reassembled in a dedicated area, or a clean room (i.e. see once again, Fig. 6.3a)—utilising the highest technological quality precision bearings in its reassembly, that are equal to, or even better than the originals they are replacing—see Fig. 6.2 (top-left);
- **after careful reassembly followed by stringent Metrological inspection**—see Figs. 6.2, 6.3a and 6.5—the spindles should be tested by being brought up to their operating rotational speed (i.e. by controlled incremental speed increases) within a clean testing area. Such tests will verify that the rotational speed can be achieved; vibration levels are minimal—see Fig. 6.6a; temperature gradients

are acceptable; as well as its critical run-outs are within specification (i.e. see Figs. 6.8, 6.9 and 6.10). By monitoring spindles for all of these critically important operating parameters, such machine tool spindles can then be ultimately returned to their original specifications, or may indeed be somewhat better now that they have been fully rebuilt.

Finally, the apparent health of a machine's spindle will have a direct impact on the operational performance of the overall machine tool. As a consequence, if a spindle's health fails—for whatever reason—then a suitable Specialised service provider for this type of spindle work (i.e. see a typical example of such a specialist provider in Fig. 6.2)—who can demonstrate a track record of experience and as such, can become true partners with their customers is essential. Such a specialist spindle company, can offer appropriate diagnoses and realistic remedies for returning these spindles to desired levels of performance and their anticipated longevity when once again rebuilt and back in-service within the machine tool.

6.1.3 Complete Machine Tool Retrofits and Rebuilds

For certain machine tool companies, the term Retrofit[5] normally refers to simply an upgrade to just their CNC controller, but this is generally not the case. In the practical example of a typical Turning Centre's complete Re-engineering and its subsequent calibration, just some of the details of the overall essential maintenance work, when completely overhauling such capital plant is depicted in Fig. 6.7. Nonetheless, when just a CNC controller's upgrade is required, it should also include new servomotors; drives; magnetics (i.e. motor starters, breakers, solid-state relays, etc.); together with a complete rewiring of the machine tool. Typically, a thoroughly undertaken maintenance and servicing operation for a machine's rebuild costs in the region of ≈30 % of the price of a new equivalent machine tool, so the potential retrofit candidate must—of necessity—be mechanically sound to justify this level of investment. At this time, either the OEM, or reputable machine tool rebuilder, as previously mentioned and depicted in Fig. 6.7, can provide a complete mechanical and electrical assessment of a machine tool. This older CNC machine tool undergoing just a retrofit operation, will have a new CNC controller

[5]**Retrofitting** [For most industrial manufacturers, machine tools represent significant capital investments and they must maintain their viability for many years in-service. So, by upgrading to the latest control technologies and a full machine tool refurbishment—via a total CNC Re-engineering, or Retrofit, this is one way many companies can extend the productive life of their machine tools. This appropriate maintenance action, will: decrease the mean time between failure (MTBF) and its associated mean time to repair (MTTR); also is will lower energy costs, reduce cycle times; whilst achieving a new level of manufacturing its accompanying data accessibility. (*Source* CNC Engineering, Inc., Enfield, CT 06082, USA)]: basically refers to the addition of new technology, or new features to older machine tool systems. Here, the production of these retrofit parts is necessary in manufacture, when the design of a large assembly such as a machine tool, is either changed, or revised in some manner.

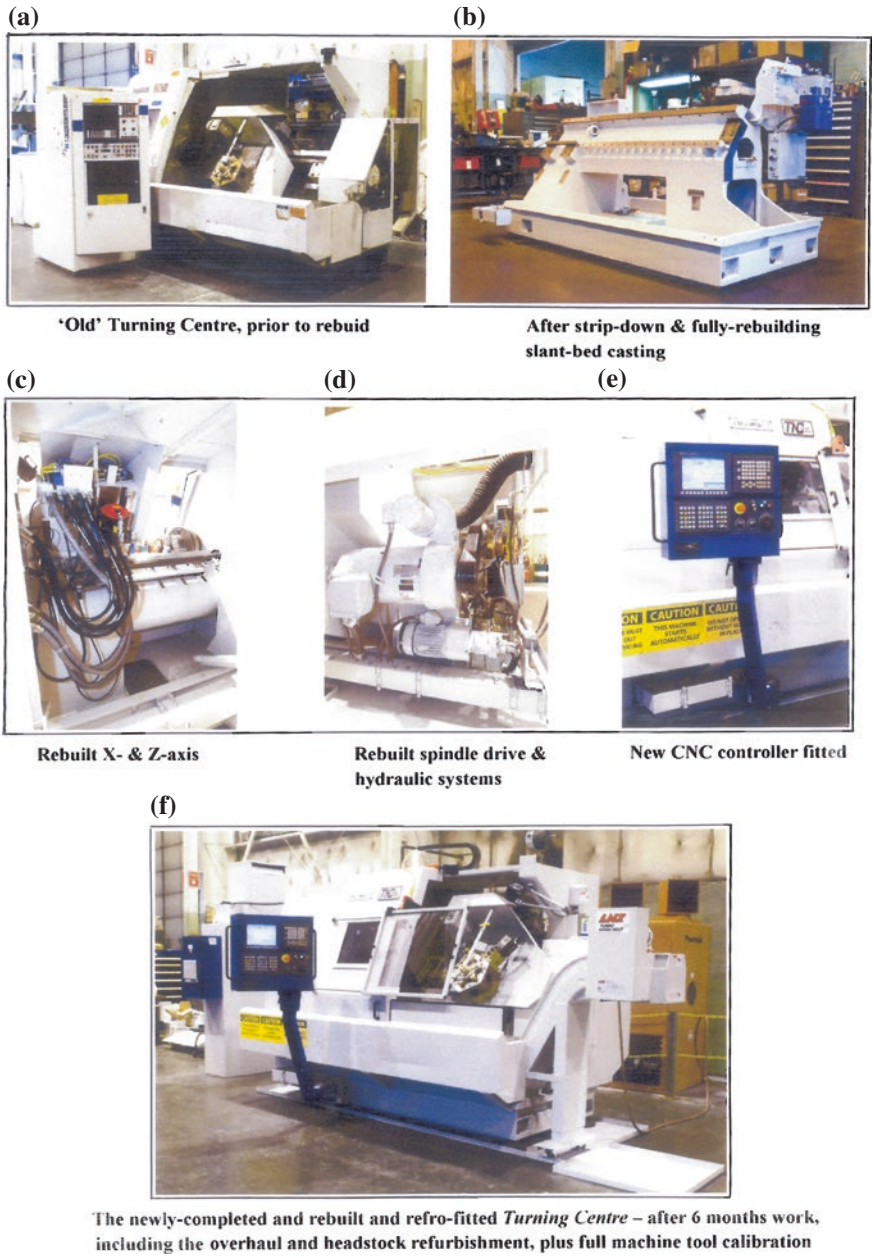

Fig. 6.7 The complete 're-engineering' and calibration of a turning centre [courtesy of Peiffer Machine Services (Mt. Aetna, PA, USA)]

installed and associated peripherals—see Fig. 6.7e—which will incorporate many advanced features that were not available at the time the original machine was purchased. Although with even just a less costly retrofit—plus new servos and drives rather than a complete re-engineering—with this new CNC controller it will now have a faster data processing speed capability, which means a quicker acceleration/deceleration rate of its axes motions, coupled to greater positioning accuracy and precision. The latest CNC capabilities are a major reason why it is essential to upgrade many other associated machine tool attributes, such as servomotors; drives; and their magnetics; hydraulic systems; etc.—during a complete re-engineering. Subsequently, if by failing to upgrade the entire system, this will mean that the end-user will not truly realise the full benefits of this new CNC fitment.

On many of the older CNC controllers, they will not have the latest peripheral-/host computer communication capabilities, while any new CNCs can provide a variety of communication options. Furthermore, today's machine controls also have built-in computer diagnostics to assist the CNC operator/programmer and the maintenance personnel when machine problem troubleshooting, such as when having perhaps a tooling problem present; or if a programming error keeps occurring; alternatively when a specific type of machine fault arises. Moreover, a dedicated CNC controller will just simply run the machine tool, while the newer types of PC-based CNC units, can simultaneously run both the machine programme and other associated software. Both types of CNC have advantages and disadvantages, therefore, a company potentially embarking on an expensive re-engineering/retrofit, should have a familiarisation for each potentially new CNC controller regarding its speed; programming features; memory and graphics capabilities; prior to selecting a specific new controller, which is definitely an advisable user strategy.

Servos, Drives and Wiring

In recent times, the predominant servomotor that tends to be installed on either a new, or upgraded machine tool is that of the brushless AC motor type. This motor has an excellent power-to-size ratio requiring little or no maintenance. Some dedicated CNC controllers, mandate the use of both digital servomotors and matched drives, these being an excellent combination in order to upgrade the control. The subsequent drive tuning on a digital system can be undertaken, via the control screen, with specific soft parameters—as there is no manual tuning here being necessary. The communications/connections between the machine's drive and its CNC are usually either by means of serial, or fibre optics, both of these communications being a faster and more reliable process than by utilising analogue connections. In certain cases, some control and drive manufacturers have joined forces in an effort to develop digital interfaces, which can then be utilised with PC-based systems. Even if many successful retrofits are completed without replacing the original magnetics system (i.e. its motor-starter, fuses, disconnects, relays, etc.) it is not normally recommended. A big advantage of having a new CNC controller, is

that the servomotors and drives are significantly smaller than their earlier generation counterparts. Likewise, the newer magnetics panels are also much smaller, so they will occupy less floor space. It is also highly recommended by any reputable machine tool rebuilder, that completely replacing the machine's wiring is advisable, as by this rewiring operation, it also ensures that the machine meets the latest standards for its electrical codes—within that country of operation.

In the current manufacturing environment, with the demand for higher spindle rotational speeds, this then raises the retrofitting issue of whether to replace the spindle motor and its associated drive. The limiting factor for increasing spindle speed is basically mechanical, as one cannot simply fit a 6000 rev min^{-1} motor in its place on a Turning Centre's headstock—instead of the original 1800 rev min^{-1} motor, without causing some irreparable damage to the machine's transmission. Nevertheless unlike servomotors, there are certain instances where it makes financial sense to rebuild the original DC motor and then to match it to a new digital DC drive. Generally, it is advisable keep a DC system that is for instance >22.5 kW power rated and only replace one that is <22.5 kW with typically a brushless AC system, making sure that due consideration here is made for the base motor speed, which is an important detail. Older types of DC spindle motors normally have base speeds that can range from just 500–850 rev min^{-1}, with their top speeds being 2500–3000 rev min^{-1}. The base speed of a brushless AC motor is normally in the region of 1500 rev min^{-1}, with maximum speeds as high as 10,000 rev min^{-1}. Consequently, if the base speed of the AC motor is three times the old DC motor, then at the original base speed, an AC motor will only generate one-third of the old DC motor's rated power. One technique to overcome this lack of power problem, is to change the gear train/pulley ratios. Then again, if the motor is directly coupled to the spindle, some necessary engineering work will be needed to make the brushless AC system generate the same low-speed torque and power characteristics.

Rebuilding a Complete CNC Machine Tool

Customarily when the machine tool industry refers to a rebuild, it generally means that all the mechanical components of the machine are to be cleaned, inspected and then reassembled utilising either new, or re-machined components. As previously mentioned with a rebuild, a rebuilt CNC machine of this complexity, costs approximately one-third the price of an equivalent new machine. Generally, the ideal candidates for a rebuild are machines that are <10 years old that still have a reliable CNC with servomotors and a spindle motor and drives that do not need upgrading. Further, it is necessary to make sure that any components that have not been replaced are still readily available and will continue to be supported for the expected life of the machine's rebuild. Therefore, any major mechanical upgrade to a machine tool, should always include the replacement of all bearings and seals, to the OEM specifications. Additionally, the spindle assembly, or cartridge, and/or its headstock, should be completely disassembled and inspected, with all internal

bearings being replaced, including the fitting of precision class spindle bearings—see Figs. 6.2 and 6.3a. Moreover, all transmission gears should be inspected for tooth involute, flank wear and localised cracking, with their accompanying shafts also being critically inspected for tolerances, straightness and cylindricity. On Machining Centres, the main spindle itself should normally be cylindrically reground, with the spindle taper and its face also being cylindrically reground and then inspected to the OEM specifications—see Fig. 6.3a. In the case of the Machining Centre's drawbar, this should be rebuilt, including replacing all its clamping springs. CNC lathe spindles must be inspected for tolerances, straightness and cylindricity, with the integral taper being carefully inspected and, if necessary, cylindrically taper reground with fitment of new high-quality bearings. The final spindle reassembly should always follow the OEM-specification for correct and permissible run-out and endplay—see Figs. 6.3a and 6.5. It may be possible that damage to the spindle/headstock will be too severe to repair, but that becomes an unknown problem, until it is completely disassembled and then critically inspected. Fortunately, many of today's OEMs will manufacture additional parts for stock replacement, most notably for their spindle assemblies and cartridges.

Yet another mechanical subsystem that often requires to be rebuilt is that of the machine tool's Way system. The work undertaken here is critical to ensure that the machine meets its original accuracy and precision specifications. Customarily, there are two primary Way systems utilised by the machine tool industry; they are either Box ways—shown in Fig. 1.36, or Linear guides—typically illustrated in Fig. 1.33. Accordingly, if the machine tool has Box ways, they need to be visually inspected for severe scoring and then bulk hardness tested for their bearing face surface hardnesses. The majority of new Box ways have an average hardness of between 50 and 63 H_{Rc}—usually to a depth ranging from: 3 to 3.5 mm. These respective Ways should be surface ground flat, perpendicular and parallel, within <5 μm TIR, while also having a Ra of ≈0.8 μm (surface texture). This level of accuracy and precision of the Ways, is usually obtained by surface grinding them on a specialised machine tool, such as a high-precision Slideway bed grinder—see Fig. 6.14. As a consequence, following this indispensable regrinding operation, the Ways should have no less than a 1.25 mm depth of surface hardness still present, to ensure a reasonable amount of in-service Way longevity. Of further note, is that if a Way has scoring below this necessary depth of hardness, it may have to be scrapped—see Fig. 1.37—that is if it cannot be re-hardened—by a localised Induction-hardening operation. Invariably, the Way system is an integral part of the casting—see Fig. 1.36 (bottom) which has been previously induction hardened to the required depth, although if high wear occurs here, it can sometimes be repaired, but this is not usually a prudent strategy. Some OEMs make their hardened Ways removable, allowing these disassembled ways to be finish ground separately away from the machine. The reground way should then be correctly reinstalled and at that time, a further surface grinding operation is necessary in situ, to ensure its highest possible accuracy and precision.

Many of these integral hardened steel Box ways—see Fig. 1.36 (bottom)—can incorporate one of three prevalent modified slideway techniques, these are by utilising:

1. **low-friction material, such as Turcite**,[6] **or Multifil**[7]—this is probably the most popular and inexpensive slide improvement technique. Here, the existing material is removed from the slide, then new material is glued in place and the slide is finally hand scraped onto these new Ways. An alternate Way technique, is to machine the base surfaces of the slideway to accept a wear strip, then a Multifil tape strip is glued to a piece of spring steel—so that it can be removed for fitting. In this instance, future replacement of the wear strip becomes much easier to deal with, because the slideway does not now need to be removed;
2. **slide system incorporating linear roller bearings**—with the roller bearings being placed side by side in a cage that resembles a tank track (sometimes termed: Tychoways)—see Fig. 1.33. If the Box ways are made from cast iron rather than steel (Fig. 1.36, bottom) then they can be reworked by hand scraping and mating the Way to its accompanying slide, until it reaches the desired accuracy/precision of the original OEM specification. There are at least three potential and distinct disadvantages to this approach, these being:
   (i) the effect of the machine tool's feed rate. So, by this metal-to-metal slideway restoration technique, it means that the slide cannot be driven at any rapid feed rates, which means it is usually limited to: $\geq$10 m min^{-1};
   (ii) this type of Way system is prone to damage from debris contamination, usually in the form of work-hardened metal chips/fines that get between the slide and its mated way, potentially causing severe scoring that can significantly reduce machine accuracy;
   (iii) unfortunately nowadays, the skilled operation of hand scraping of Ways is something of a rapidly disappearing skill (see Fig. 1.37). If a company offers this specific scraping service, one must need to be absolutely sure that the retrofitting company concerned can offer a comprehensive contract to rebuild this machine and knows it is competent with respect to scraping of the machine's Ways;

[6]**Low friction material**: such as **Turcite™** is a glued-on bearing material frequently utilised for the restoration of Way-bearing surfaces in machine tools undergoing a major rebuild. This Turcite™ material, has certain low friction characteristics, and because one will normally machine the Way surfaces to restore linearity and geometry the machine, if carefully undertaken, it can then be reassembled as per the original way, together with its subsequent recalibration and its accompanying new alignments and geometries.

[7]**Low friction tape**: such as **Multifil™**, is a patented tape-bearing material, normally commercially supplied up to $\approx$300 mm wide and between 0.38 and 3.2 mm thick, of varying lengths. For example, with the Multifil 426 product, it has is low-friction bearing tape (i.e. consisting of PTFE, plus a proprietary filler system, being of a greased water process fluid) which will—when fitted correctly—be able to up to a certain degree, correct for many of previous the Way system inaccuracies.

3. **hydrostatic system slideways**—these Ways are often found on very much larger machine tools—see Fig. 2.15a. With this heavy duty slideway transmission design, the slide rides on an incompressible film of oil at all times—similar to that shown in the graph in Fig. 1.35b (i.e. depicted for Hydrodynamic lubrication). When rebuilding a hydrostatic system, all of the pressure-compensating valves must be replaced and the slide should be checked for a correct fit to the Way system and then it is scraped—as necessary. At present, the majority of modern CNC machine tools use some form of Linear guideways—one such type being typically and previously illustrated in Fig. 1.33. As described, concerning these Tychoways and their alternative variants, usually a linear guide system consists of a pair of rails. Each rail rides on two, or more bearing packs that are often termed trucks—as are illustrated in Fig. 1.33—attached to a Machining Centre's table, or its cross-slide member. However, if these rails are still in good condition, they can be reused after basic maintenance has been performed; although unlike Box-ways (Fig. 1.36) these Linear guides cannot be reground. Linear-guide rails and their trucks will basically wear as a complete system. Accordingly, if replacement is necessary, it is important to insist that both the rails and their accompanying trucks are also replaced.

The CNC machine tool's recirculating ballscrews are of prime concern for its positional axis accuracy and precision and as such, they can be very expensive to replace—see Figs. 1.29 and 1.30. Fortunately, many types of Ballscrews can be rebuilt at least once, or sometimes even twice—depending on the amount of wear, or actual damage that must be corrected. This type of Ballscrew rebuilding service would normally be outsourced by contracted machine rebuilders, to specific companies/shops that specialise in the production and subsequent remanufacture of such Ballscrews. This Re-engineering process requires that the Ballscrew and its accompanying Ballnut are disassembled and then critically inspected for a variety of issues, such as its tolerances, surface texture, hardness, corrosion (i.e. rust) and wear. After this detailed inspection, it can then be determined if a Ballscrew repair is a possibility. A precision reground Ballscrew will then be returned and fitted with a new Ballnut, while the bearing journals are also inspected and repaired—as necessary. Once these vital tasks have been completed, the Ballscrew is then reinstalled and pressurised to minimise any potential backlash—by means of its new thrust bearings. Then the complete system is finally inspected and the Ballscrew assembly is checked for accuracy/precision to ensure its correct height; parallelism; also its run-out in situ. If a Ballscrew-repair is not either possible, or indeed feasible, then one should be aware that the equivalent replacement with new Ballscrews can have a lead time of between 8 and 10 weeks.

Fluid Checks on Machine Tools

Many of the current larger range of CNC machine tools operate with some form of hydraulic systems present. Accordingly, from either an ongoing maintenance-, or rebuilding strategy, such a machine's hydraulic fluid reservoir should be thoroughly cleaned during any form of rebuilding work. Here then, its hydraulic pump

and motor should either be rebuilt, or replaced, along with any of its necessary filters, or strainers. Additionally, the flexible hydraulic hoses and couplings must also be replaced, although the solenoid valves of a hydraulic system do not usually mechanically fail, but their burnt-out coil is the typical failure element in many such cases. Consequently, the decision to replace these components during a machine rebuild is usually determined by assessing the Risk of obsolescence and whether these types of specific valves have been prone to frequent failure in the past, by looking into the machine tool's previous service history.

Undoubtedly the single most important fluid system on any CNC machine is its central lubrication system. In any rebuild, all of the flexible lubrication lines must be replaced and the entire system of its metal lines must then be flushed through and then pressure tested for leaks, along with the pump—which it is always essential to replace as a matter of priority. Usually, there are two types of Central lubrication systems fitted to such plant currently present on the majority of CNC machine tools, these are the:

1. **One-line resistance system**—consisting of a low-pressure pump that sends a single line of lubricant directly into a manifold. Here, the multiple lines that exit this manifold are then routed to individual lubrication points throughout the entire machine tool. A metering unit in each of the lines serves to regulate the rate of oil flow, while a small orifice in the metering unit supplies the correct amount of oil for a given lubrication point. These units are available in various sizes, based upon the amount of oil that is needed, however, all of these metering units must of necessity, be replaced;
2. **Progressive-type lubrication system**—which will normally utilise a very high oil high pressure (i.e. $\leq$20 MPa) usually with an air over oil pump with individual feeder blocks that contain spools. As a result, each time the pump piston is activated, these spools are then linearly displaced in their respective blocks, precisely controlling the amount of oil that reaches each actual lubrication point. At this time, a block can sense if a spool has not linearly shifted and as a consequence, sends a lubrication alarm to the machine's CNC-controller. This type of Progressive lubrication system can be completely flushed through, inspected and then reused.

   NB If this particular type of CNC machine tool spends the majority of its productive life machining cast iron or other types of highly abrasive materials, and if it is only equipped with the previously discussed one-line system, then due consideration should be made to converting it to the more superior progressive-type system.

Final Machine Tool Reassembly

With the total re-engineering overhaul of a CNC machine tool, the reassembly of these refurbished large individual machine components begins at its base, by having its correct levelling carried out, as shown in Fig. 3.17 (top). Therefore, as this controlled rebuilding of major structural elements now takes place, there is distinct weight shift occurring as each additional structural component (e.g. such as its table; spindle; column, etc.) is added to the original base unit. Here, there is a risk of an accuracy uncertainty error, which will be significantly reduced if the

machine's level is then subject to periodic and further rechecking, after each major component is added to this machine base—see typically such metrological activities in Fig. 3.10d. Moreover, the machine's geometric alignments should be determined utilising the OEM's specification procedures and tolerances. Appropriate axis alignments—during rebuilds, include a static check that can be performed with a range of artefacts, typified by the use of granite squares; electronic levels; or dynamically—by laser instrumentation, etc. The various Standards of today's demand correct machine tool axes-alignments, which will also include its dynamic check with a system that provides a computer-generated analysis of the accuracy/precision of the machine tool in motion. Typically here, the procedure of either a Ballbar-, or Laser test, will ensure that the individual axes are correctly aligned and compensated for and that the relationships between these axes in motion are also now both accurate and precise.

As previously described, the most comprehensive type of machine tool upgrade is known as re-engineering—see Fig. 6.7. This all-inclusive re-engineering combines everything involved in both a retrofit and rebuild. Additionally, any vital remanufacturing operation will probably include certain design changes that will then improve the machine's overall performance—beyond that of its original OEM specifications. These large-scale machine improvements may well include a significant increase in its rapid traverse and attendant machining feed rates, often coupled with extended axis travels and higher spindle rotational speeds—as applicable, after this re-engineering.

At ≈50 % cost of a comparably equipped new machine, any form of re-engineering is only worthwhile when a new replacement machine would be likely to cost in the region of ≥$400,000 (US). By way of example, a typical retrofit that includes a CNC controller, servomotors and its drives, will normally take between 4 and 8 weeks to complete. Most CNC control manufacturers have delivery schedules in the 4-to-6-week range, thus a control-only retrofit will be slightly quicker to achieve. However, the delivery for a complete rebuild should customarily range between 12 and 16 weeks duration, depending on the extent of the damage and wear to the original machine tool. Conversely, the re-engineering of a machine tool can take between 5 and 7 months from the time the machine was originally shipped, until it returns once again to the user company's shop floor ready once again for the demands of full production.

Machine Tool Documentation—Prior to Rebuilds

When considering undertaking a typical machine-rebuild, the initial writing of a machine tool's documentation becomes a critical element of any such machine upgrade. At this time, the lack of appropriate accurate and complete machine tool documentation can turn a good-intentioned retrofit; rebuild; or even re-engineering-activity; into a potential disaster when the first significant technical problem occurs. At a basic minimum, the CNC machine tool's documentation should include the following essential five elements: (i) high-voltage schematics; (ii) all of the input and output diagrams; (iii) complete servo/spindle wiring schematics (i.e. which will include all pinouts—on the plugs); (iv) physical machine-view

engineering drawings; (v) plus the OEM's operator manual. Finally, it is suggested that the last piece of machine-related documentation may perhaps be somewhat controversial, so here, it is necessary to ensure that the actual technical requirements are distinctly spelt out within the contract. Here then, no potential machine tool upgrade is really complete without a fully cross-referenced Ladder- or Soft logic diagram.[8] However, some OEMs and third-party specialists believe that this is their proprietary information, but a machine tool rebuilder cannot effectively troubleshoot any CNC machine tool rebuild without this additional and essential information. As a further advisory note, it is suggested that all of the machine tool's documentation should be provided, in several distinct formats, to the contracted machine rebuilder.

Prior to work commencing by this now-contracted machine tool rebuilder, a customer should insist on a hard copy with a digital backup of the all the work to be undertaken, written in a commonly available format that can be stored, duplicated or reprinted in-house. At the time of the ongoing contractual work programme, a considerable amount of a user company's capital can have been spent in the initial machine-rebuilding exercise. So it is important—prior to any commencement—for a prospective customer to interview all of the operators and maintenance mechanics at the rebuilders factory, to expose any known problems with its intended machine performance rebuild, before any work is subsequently contracted. Thus, in the joint written agreement between these two parties, the customer and builder must distinctly spell out the specific performance problems that could be expected to be eliminated—by whatever machine tool upgrade work that is selected. Here, the majority of competent machine-rebuilding firms will provide a historical list of industrial references and offer to show their prospective customer actual machine tools that they have previously and recently successfully upgraded.

---

[8]**Ladder-** or **Soft logic diagrams**: these previous Ladder logic diagrams were originally a written method to document the design and construction of relay racks—as utilised in manufacturing and process control. Each device in the relay rack would then be represented by a symbol on the Ladder diagram with connections between those devices shown. Additionally, other items external to the relay rack such as pumps, heaters, and so forth, would also be shown on this Ladder diagram. Although these diagrams have been originally utilised when logic could only be implemented using switches and electromechanical relays, the term Ladder logic was only latterly adopted with the advent of: Solid-state programmable logic. Thus, Ladder-logic has now evolved into an actual programming language that represents a programme by a graphical diagram, being based on the circuit diagrams of relay logic hardware. This latest form of Ladder-logic is nowadays utilised to develop software for: programmable logic controllers (PLCs)—utilised in industrial control applications. This Ladder logic name, is derived from the observation that programmes in this language resemble ladders, with two vertical rails and a series of horizontal rungs between them. Such types of Ladder diagrams were initially the only available notation for recording programmable controller programmes. Today, some other forms—utilising these techniques—are now Standardised in: **IEC 61131-3**. Thus, **IEC 61131-3** [i.e. is the third part (of 8)] of the: **Open International Standard IEC 61131**—for programmable logic controllers, and was first published in December 1993 by the IEC. The current Standard (i.e. in its 3rd edition—at time of writing of this text), was then published in February 2013.

Finally, by way of a somewhat cautionary note to anyone potentially embarking on a CNC machine tool refurbishment as opposed to that of a more expensive rebuild/re-engineering contract with a specialist in this field, one should always be very wary of the R term that is invariably and often glibly used today for Refurbishment. In many of these so-called Refurbished machine tools, they have received little more than simply a superficial, "Bath and a paint job!"—to coin the phrase.

6.2 Monitoring and Diagnostics of Machine Tool Spindles

Introduction

In the existing manufacturing economic climate, as has been described in the previous section, a strong case has been made for the essential maintenance of machine tool spindles by either re-engineering, or at the very least, attempting to repair spindles when they fail. Likewise, an outright spindle replacement strategy may sometimes be necessary, but often the desired course of action will be to facilitate the spindle's return to service both as speedily and reliably as possible. Additionally, any inherent factors affecting the spindle's delivery times, costs and productivity issues will determine the correct route to pursue in each case. Of late, typically the average lead time for the delivery of a totally new replacement spindle can be in the region of $\leq$24 weeks, while either its spindle repair, or alternatively simply by reconditioning a spindle these less comprehensive maintenance activities can normally be achieved in $\approx$3 weeks. The cost for a new machine's spindle, can sometimes be triple the price of a remanufactured unit and additionally, the company's investment in this remanufacturing approach will involve only the components that need to be replaced and their actual fitment, but without the higher costs associated with purchasing an entirely new spindle. Furthermore, any worn or crashed spindles can often be remanufactured many times, without any adverse consequences. Furthermore, any technological upgrades to, say, new types of bearings, are always possible at this time, upon its initial stripdown then followed by a careful rebuild.

Spindle monitoring and its associated diagnostics are now becoming especially important because of the ever-increasing extension of plant warranty periods. There is a specific need to continuously monitor and control the operations in machine tools in order to reduce unscheduled downtimes and to meet safety requirements in such machine tools. Several specialist companies offer appropriate Sensor technology that provide monitoring and diagnostics of the spindle and consequently to that of the machining process. It has been recently estimated by SKF in the USA, that the global machine tool spindle market has been appraised to be worth more than $1 billion (US). Furthermore, at least half of this cost can be directly related to spindle maintenance and refurbishment actions.

6.2.1 Spindle Monitoring Instrumentation—For Machine Tools

With the ever-increasing drive towards sophisticated technologies and the intensive care requirement concerning spindle monitoring, which is now becoming important for a variety of reasons, these activities will optimistically be succinctly explained in the following CNC machine tool spindle-related sections.

6.2.2 Thermal Distortion—At the Spindle

In any type of machine tool's spindle its thermal growth is the largest single source of machining problems, this condition being directly related to machining certain component part feature locations or any type of hole and pocket depth difficulties. As a consequence the spindle drives are distinct heat sources, which as a result will transfer heat to other cooler sections of the machine tool. This well known form of heat transfer causes transient thermal variations (i.e. temperature variables being uneven heating at different portions of the machine tool's structure) which results in potential distortion and bending within the machine's structure. Such heat-induced distortions cause the spindle to alter while either misaligning the cutting tool or workpiece—depending on whether the machine is either a Machining or Turning Centre. Such distortions can be particularly problematic in Gantry-type machine tool configurations, because of the large vertical distance from the Gantry structure to the tooling—this effect is shown in Fig. 2.18 (bottom) where a Gantry-type Machining Centre is depicted. At the tool's point, any distortion in a machine tool's gantry is significantly magnified at the maximum limit of its extended travel distance. It should be emphasised that although thermal distortions could occur in all configurations of machine tools, those machines which have been designed symmetrically, or indeed that are constructed to minimise these attendant heat loads—with either spindle cooling jackets (i.e. see Fig. 6.1a) or special heat-insulating plates (i.e. see Fig. 1.27, top-right) are less susceptible to such thermal heat sources.

The problem of thermal distortion can arise in machine elements that are not even in close proximity to the spindle, possibly via thermal cycling in their axes by the recirculating ballscrews. These somewhat remote heat sources have been reported in practice even when the Ballscrew is equipped with internal fluid cooling. Here, the internal coolant can also be the basis for the Ballscrew to thermal cycle, creating definite localised expansion and contraction, thus moving the workpiece in a manner suggesting that the spindle's positioning is affected by such thermally induced effects. One technique that has been shown to minimise this potential motional effect by its respective Ballscrews, is by the tightening of the

coolant temperature deadband from, for example, an original 2 °C zone, to a fraction of a degree, which can potentially resolve, or at worst minimise this thermally induced problem.

6.2.3 Spindle Error Motions

It has been previously widely reported that there are up to six different motions possible by the machine tool's spindle. These kinematic motions include pure rotation around the spindle's axis (i.e. its *Z*-axis) this being considered as the desired motion, plus certain undesirable motions in five other directions, explicitly by: *X*; *Y*; *Z*; plus tilting along both the *X* and *Y* axes—these latter five motions being considered under such circumstances as potential errors/uncertainties. Measurements of spindle tilt allow this error to be calculated then another measurement is taken, which is particularly useful for extrapolating the potential error of, for example a boring bar that would otherwise be too long to measure at its actual tool point. Consequently, these types of spindle errors may be classified under four distinct headings to distinguish their specific root causes, or their real effect on the part's machined quality. As a consequence, these spindle error sources could include just some of the following conditions:

1. **drift**—which is generally a relatively slow change that occurs over time, resulting from some form of external influence, such as ambient temperature variation, causing a positional change in the tool's point;
2. **shift**—being an abrupt change in an operating parameter, as a result of some change in the system, typified by a speed change or an air pressure variation, for example on that of an air bearing spindle. This shift is particularly relevant in high-speed machining that involves significant increases in centrifugal force on the spindle's rotating components, with these increased speed changes causing bearing elements to affect the tool's position—causing this tool's point to be minutely repositioned;
3. **synchronous error motion**—which will repeat every revolution of the spindle. In a typical spindle error plot of these types of errors, it shows lobes that can occur either once, twice or alternatively by multiple lobing per revolution. Such synchronous error motion—also termed its Departure from roundness—in roundness assessment metrology, predicts the ability to, for instance, bore a round hole or turn a cylindrical and round part. Here, the tool will tend to cut a workpiece with the same number of lobes as exhibited in its synchronous error motion plot. Obviously a spindle will normally run true until it begins to operate at its resonant speed, which usually results in excessive vibration. Synchronous error motion plots—exhibited at differing spindle speeds—can highlight these resonant speeds, enabling a CNC operator to modify the tight band of resonant-speed activation enabling them to be avoided;

4. **asynchronous error motions**—as their designation suggests, these motions are not synchronised with the spindle rotation, and thus do not repeat at successive spindle rotations. These types of error motions are characterised by a certain fuzziness of the spindle's polar plot—see Fig. 6.10a, b—which are also directly related to both the machined part's lobing and its accompanying surface texture. Moreover, these asynchronous error motions can develop as a result of an interaction of spindle–bearing elements that are rotating at different speeds, typified by its specific rolling elements; rolling element retainer; the cages; plus the bearing races. Furthermore, if some heavy plant—such as a loaded Forklift truck or similar—continually passes by the machine tool when in-cut, this can result in asynchronous errors by the non-structural parts of the machine, typified by its hydraulic-, or coolant pumps.

6.3 Spindle Error Analyser (SEA) Instrumentation

A characteristic Spindle Error Analyser (SEA) system, which is commercially available as both hard- and software packages for measuring and analysing the accuracy of spindles on machine tools—is depicted in Figs. 6.8, 6.9 and 6.10. The SEA system can effectively evaluate the majority of CNC machines, such as: CNC milling machines; Machining Centres; CNC lathes; Turning Centres; Mill/Turn Centres; as well as CNC boring machines; together with many types of manual machines. This type of SEA hardware—a specific example of which is shown in Fig. 6.8a—would normally utilise non-contact capacitance gauges to collect the necessary spindle data and use proprietary software to analyse and display the test results (i.e. as typically shown in Fig. 6.8b). With this SEA instrumentation, the following spindle performance measurement data can be efficiently collected and then analysed to evaluate its:

- radial rotating sensitive direction;
- radial fixed sensitive direction;
- axial error motion;
- 5-probe thermal stability—monitoring up to seven temperature sensors;
- temperature variation error;
- FFT frequency analysis;
- target reversal.

Additionally, this bespoke software can compare two files or equate current data to previous specific data from a file by overlaying their respective plots. All software displays are obtained in real time (i.e. being updated once per second) and any four types of graphical representations can then be displayed simultaneously in a four-quadrant arrangement—see Fig. 6.8a (i.e. the screen display), or as any single display which can then be viewed as a full screen.

(a)

A 5-sensor *Spindle Error Analyser* being utilised on a vertical *Machining Centre*, with the instrument's measurements conforming to ISO 230-3/-7 Standards.

(b)

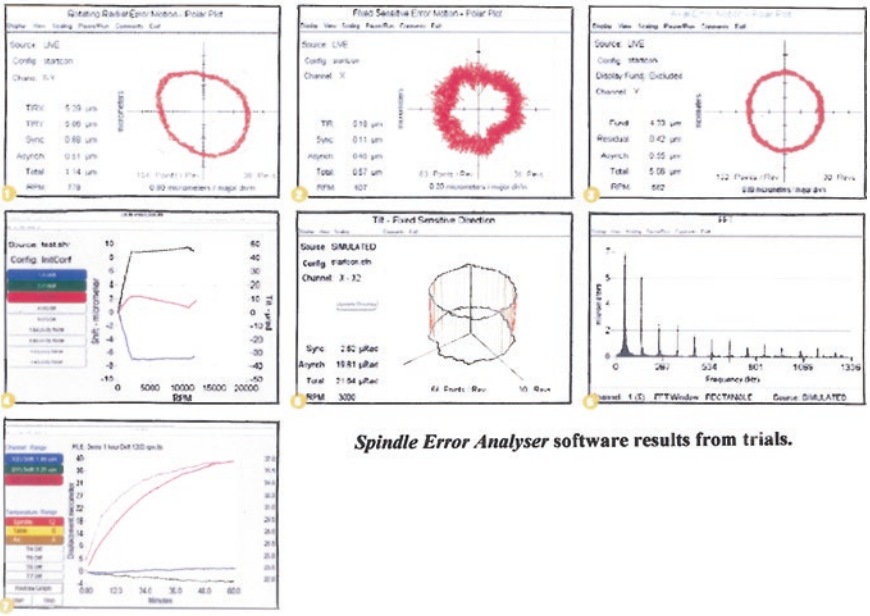

***Spindle Error Analyser* software results from trials.**

Fig. 6.8 A spindle error analyser enables the real-time capture of any spindle errors on machine tools [courtesy of IBS Precision Engineering BV (Eindhoven, The Netherlands)]

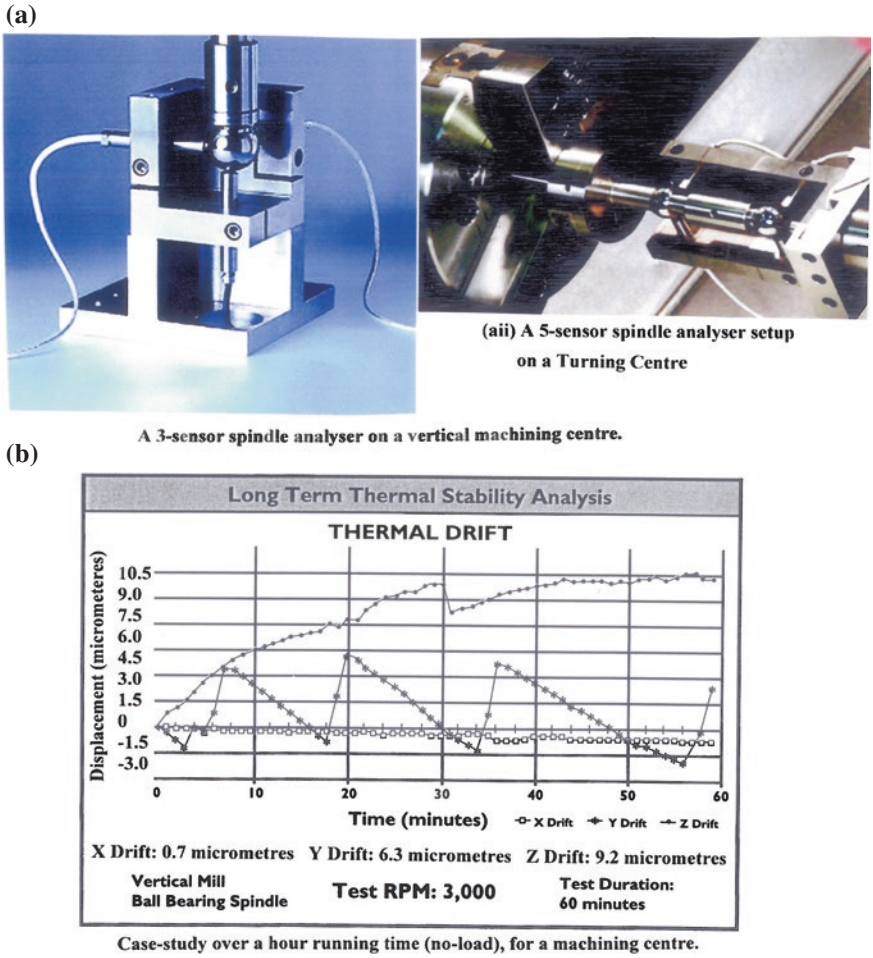

Fig. 6.9 Machine tool spindle (3-sensor) analysis system, with typical data capture for thermal stability analysis (courtesy of Lion Precision)

Spindle Monitoring—Capacitance Probes

The example of the SEA shown here (Fig. 6.8a) has been configured to measure a rotating spindle at its normal range of operating speeds. To obtain an accurate representation of the spindle error, it is necessary to acquire rotating data from the spindle position at various operational rotating speeds. For instance here, the actual sensing technique must be of non-contact in nature to provide realistic and accurate measurements. Accordingly, the commercial instrumentation described herein, is an example of an SEA system that utilises capacitance-sensing technology, as this type of technology is uniquely able to meet the demanding requirements of spindle measurement.

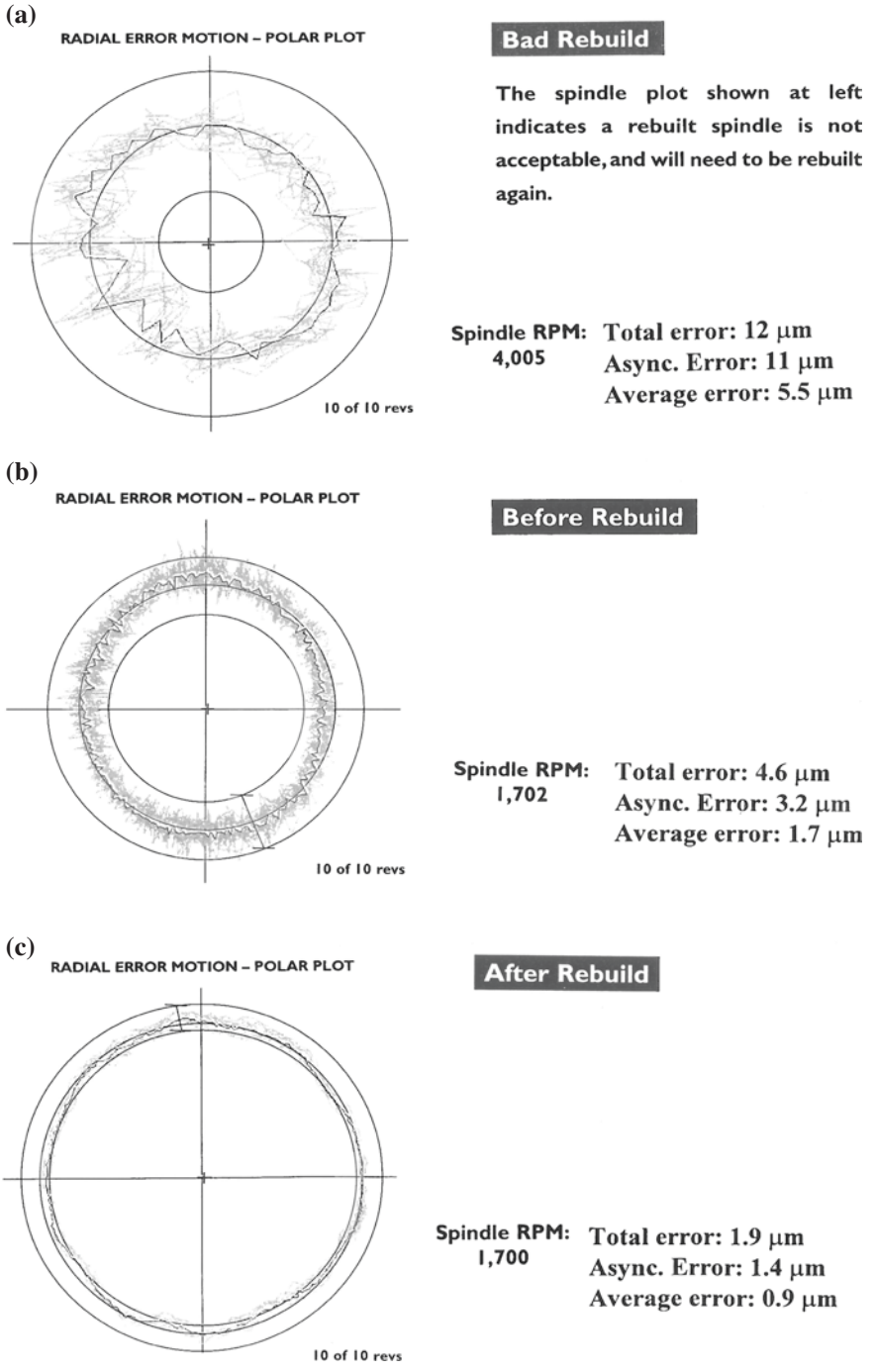

Fig. 6.10 Machine tool spindle error plots, illustrating spindle condition (courtesy of Lion Precision)

In the relevant Standard: **ANSI B5.54:1992**: Methods for Performance Evaluations on CNC Machining Centers, it states within Sect. 10.13 that, "… the only suitable indicators for spindle error measurement are high bandwidth capacitance gages … [which] shall have a bandwidth of at least 10 kHz or higher".

Capacitance Gauging Versus Eddy Current Gauging

With some alternative commercial SEA counterparts, they may conceivably employ the techniques termed either that of Eddy current gauging,[9] or Inductive sensing. With these spindle sensor systems, a magnetic field is generated around a coil (which is often imbedded in a solid probe). Consequently, when the rotating spindle is inserted into this sensing field, the resulting changes in the magnetic field are detected as the basis for this SEA, which measures the distance between the probe and the spindle.

In the case of Capacitance gauging[10] there are several advantages over the alternative Eddy current gauging, which most notably is that capacitance:

- is insensitive to metal alloy variations;
- is not affected by variations in the surface;
- it allows measuring equipment to be readily calibrated in an approved calibration laboratory and can be traceable to an International Standard.

By way of an example, if two spindle plots are compared for the results of measuring an identical rotating spindle utilising either an Eddy current or capacitance probe, then the Eddy current probe will interact with the target material and as such, give potentially inaccurate results. Whereas, the alternative capacitance probe actually detects this air gap between the probe and target, thus the measurement is not affected by any material variation. For these and other unspecified reasons not described herein, the **ANSI B5.54:1992** Standard does not include either Eddy current, or Inductive gauges as an acceptable sensing technology for this type of spindle error measurement.

---

[9]**Eddy current gauging** (**Eddy currents** (i.e. also called **Foucault currents**), are circular electric currents induced within conductors by a changing magnetic field in the conductor, being due to: Faraday's—Law of Induction. The well-known French Physicist [Jean Bernard] Léon Foucault (Born: 18 September 1819, in Paris, France—died: 11 February 1868, in Paris, France), has been credited with having discovered Eddy currents—in September 1855): utilises **Electromagnetic induction** (**Electromagnetic induction**: is the production of an electromotive force across a conductor when it is exposed to a varying magnetic field. As previously mentioned, it was mathematically described by Faraday in his: Law of Induction, which was named after the English Scientist who contributed to the fields of: Electromagnetism and Electrochemistry. Here, Faraday's main discoveries specifically included those of: Electromagnetic induction, Diamagnetism and Electrolysis. Michael Faraday (Born: 22 September 1791, Newington Butts—died: 25 August 1867 at Hampton Court Palace, Molesey, England). Faraday, has been generally credited with the discovery of: Induction—in 1831) to detect any either any probable errors or potential flaws.

[10]**Capacitance gauging** (The term: **Capacitance**, which is an electrical property, this being created by applying an electrical charge to two conductive objects with an associated gap between them): this type of gauge utilises a non-contact device, capable of high-resolution measurement of the position and/or change of position of any conductive target.

6.3.1 *Spindle Error Analyser—The Master Target and Its Fixtures—Spindle Hardware*

In this instance, the Master target and its fixture are mounted on the machine tool spindle and will provide the reference surface for measurements taken by this SEA system—see Figs. 6.8a and 6.9a. With this SEA system, there are several different configurations of Master targets and their fixtures that are currently commercially available, such as an adjustable:

- single ∅25 mm Master ball fixture—see Fig. 6.9a;
- dual ∅25 mm Master ball fixture—see Figs. 6.8a and 6.9aii;
- single ∅12.5 mm Master ball fixture—not shown;
- other targets (e.g. Gauge pin, etc.)—not shown.

A typical Master ball fixture consists of a precision ball mounted onto a fixture that allows an operator to adjust the eccentricity (run-out) of the ball, when it is mounted into a machine's spindle—see Fig. 6.9a. This physical arrangement provides a reference surface for the measurements taken by the SEA system. The diameter of the ball and the manner of its adjustment will vary with the specific industrial application. In general, the higher the speed, the smaller the ball and fixture. These balls have a typical and miniscule roundness error of just ≤0125 μm. This effective roundness provides a suitable reference for all but the most accurate rotating fluid-bearing spindles. In certain spindle monitoring applications, a different type of Master fixture (i.e. rather than utilising just a ball) may be more applicable. Here, some applications may require the use of a cylindrical target—not depicted—although this is not a preferred target, but may occasionally be necessary. However, in all cases it is fundamental that the system includes a Master target of known roundness and is equipped with some form of an eccentricity adjustment mechanism.

A probe holder is a mechanical fixture that holds probes in a specific and precision geometrical relationship, so that an axis of rotation (i.e. from the spindle) can actually be measured. This particular probe holder variant, establishes the reference coordinate system from which all measurements are taken. There are several types of probe holders that can be employed—as previously mentioned—which can be adapted to suit various spindle monitoring situations, these include a:

- **three-probe nest adaptor**—illustrated in Fig. 6.9a;
- **five-probe nest adapter**—illustrated in Fig. 6.8a;
- **lathe fixture adaptor**—illustrated in Fig. 6.9aii;
- **individual probe mounts**—not shown.

Where feasible, the simplest and easiest probe holder to use is a single unit probe nest that mounts onto the machine's table and holds either three-, or five probes—in the appropriate orientation. Machining Centres and CNC milling machines, or similar, generally have a flat table (see Fig. 6.8a) or a similar flat-palletised arrangement, onto which a probe nest can be readily mounted, with these probe nests being well suited to such machine configurations.

As previously described in Footnote 10, capacitance probes measure the air gap between the probe and the target by detecting a change in capacitance as the air

gap changes. The SEA can be of either: one-; two-; three-; or five-probe systems, which are utilised to measure rotating machine tool spindles. The probes utilised here, are typically cylindrical and have a ∅9.53 mm. The sensing tip is surrounded by a concentric guard ring, which prevents sensing of targets that might be adjacent to this probe. A cylindrical stainless steel shell provides the mounting surface for the probe. These probes have a built-in sensor to detect temperature at the measurement point and during probe calibration, the electronics are adjusted so that the signal output does not vary with temperature. The actual measuring range of a spindle probe is affected by two distinct factors, these are: (i) area of the sensing tip; (ii) sensitivity of its calibration. A larger area of the sensing tip increases the range of the probe measurement, and accordingly the probe driver and probe are calibrated to either a single-, or dual sensitivity. This high-sensitivity level can normally be employed for synchronous- and asynchronous errors, because they are generally quite small, while its lower sensitivity can be utilised for thermal drift errors—because these errors might be up to ten times larger.

6.3.2 Spindle Error Analyser—Spindle Software

In the example of the hardware system previously mentioned, it has an SEA software that utilises several simple conventions that make it more readily usable, such as:

- **quadrant displays**—the SEA starts with four display panels in four quadrants on the screen—see Fig. 6.8a (i.e. inset on its monitor screen). Each quadrant displays a selected view of the current data, for example a probe meter; rotating radial display; oscilloscope; and FFT; which may all be active and showing live data—from its data acquisition card. Selecting this menu item in any quadrant, brings up a list of displays that can be shown in that quadrant. Since a display can only exist in one quadrant at a time, the menu selections for these displays that are currently active in the four quadrants are suitably dimmed out. Any other display choice in the menu list can also be selected and this results in the display in the quadrant changing to the selected display;
- **SEA main menu**—the main menu here, is exhibited across the top of the screen, where it is fixed, and as such does not change when the displays are changed. As with most versions of Windows™-based programmes, one can select a main menu option and, then displays it in a suitable pull-down menu.

6.3.3 SEA—Thermal Drift—Resulting from Expansion of Materials

Any modifications that occur in the structure of a machine tool come about quite slowly, these are generally thermal in nature. All materials have a coefficient of

thermal expansion—understandably making them longer when hot and shorter when cold. The temperature variation can be caused by external sources, such as: ambient room temperature changes; coolant flooding; lighting; or internal sources (i.e. heat generated by motors and bearings). Any thermal expansion and contraction in the machine can cause errors in a part feature's location. In fact, the largest single source of error in commercial machine tools today is that of its thermally induced error, from either the environment or internally by generated heat. Any configuration of machine tool does not change as a result of temperature in a uniform manner. Parts of the machine exposed to heat sources, such as a spindle motor, will become warmer while other regions of the machine tool will remain at its ambient temperature. These distinct thermal gradients cause distortions of the structure, which result in errors many times larger than the expansion coefficient of the material.

6.3.4 SEA—Thermal Tests

In the representative case study depicted in Fig. 6.9b, the variation in the machine tool's temperature here is the major cause of its positioning error. This thermal drift graph suggests at least three significant technical questions that need to be addressed, such as:

1. "How long does it take for the machine tool to stabilise?"
2. "How much *Z*-axis growth does the machine produce at top spindle speed?"
3. "How far displaced has the machine become, because of distortion in the machine tool structure?"

So in Fig. 6.9b, the thermal test shows that the *X*-axis is relatively consistent with time, but the *Y*-axis has displayed repetitive cyclical behaviour, while the *Z*-axis has simply progressively grown with time. These distinct tool positioning drifting actions of both the *Y* and *Z* axes would need to be further investigated, to establish their actual causes, so that some form of rectification can be achieved … thus, subsequently demonstrating that the largest single source of error in commercial machine tools today is this thermally induced error—from either the environment, or by some form of internally generated heat.

Temperature Variation Error (TVE)—For a Non-rotating Spindle

This Temperature Variation Error (TVE) can be tested for movement in the spindle relative to the mounting system due to ambient temperature changes. This static thermal test is performed without spindle rotation and with power to the machine turned off. Moreover, due to the slow-changing nature of ambient temperature and the time required for the thermal mass of a machine tool to soak out to the ambient temperature, these types of tests tend to be of long duration—with around 24 hours being a typical testing time period.

This type of static rotation of the machine tool spindle measurement, is performed with a probe situated in the *X*-, *Y*-, and *Z* axes. As a result of the axial

movement with temperature, it is usually many times larger than the radial movement, thus, a larger range, lower sensitivity probe may be utilised in the *Z*-axis. The change in each axis over time can then be plotted with temperature information from these temperature sensors—if they are utilised.

6.3.5 SEA—How Spindle Measurement Data is Displayed

In this current commercially available system, the display of data in the SEA polar plots and its other graphs—see Fig. 6.8b—enables an operator to obtain a clear understanding of how to read the displayed data, maximising the benefits of such a system. Just some of these typical SEA plots might include:

- **Polar plots**—here, the test data from rotating measurements is usually displayed with a polar plot showing target position at successive angular locations on consecutive rotations and is evaluated in a similar custom to that of the roundness plot for a machined part. From this representation of data the various error motions can be computed and displayed, with the calculated values being listed next to the polar plot;
- **Least Squares Circle (LSC)**—the calculation of rotational error motions is based upon the radii of circles that define the ideal and actual motion of a rotating spindle. The spindle measurement data is processed through a well-known mathematical procedure termed least squares fitting. This generates a perfect circle that best describes the data represented. In the calculation of some error motions, other circles are drawn relative to the LSC and it is the relationship of their radii that describes the error motion value. The radius of the LSC in radial measurements is generated by the intentional eccentricity of the target. Here, the LSC radius is further manipulated in the software when the display range is changed, but it is only utilised to adjust the appearance of the plot and to establish the plot centre. In radial measurements, the actual radius of the LSC is not related to error motion. There is no target eccentricity in the Z-axis. In axial measurements, the LSC is determined by real error motion only and therefore, its radius is a measurement of such error motion;
- **Error motion calculations**—there are several different types of error motion in a machine tool's spindle. The SEA here, has the capability to measure, interpret and display all the types listed—within the applicable standards.

6.3.6 SEA—Spindle Error Plots: For Analysis and Rectification of Bearings

In Fig. 6.10, the polar plots for this commercial system, show how the actual SEA system has the ability to evaluate both a new and rebuilt machine tool spindle's

condition. In the spindle error indicated on the polar plot depicted in Fig. 6.10a, it illustrates that a very badly rebuilt machine tool spindle is simply not acceptable in this condition. Poor spindle performance is in the main, largely the result of significant radial variability, with here, the total error: 12 μm @ 4005 rev min^{-1}, which would severely compromise any cutting tool's machining performance. Conversely, in Fig. 6.10b, a well-worn spindle assembly is depicted prior to its rebuild, having a total error of: 4.6 μm @ 1702 rev min^{-1}. After correct refurbishment and rebuilding, the spindle's error has now been drastically reduced to a total error of: 1.9 μm @ 1700 rev min^{-1}—see Fig. 6.10c. Visually the difference between these two latter polar plots (shown in Fig. 6.10a, b, respectively) is quite astounding, in that both the asynchronous- and average errors have virtually disappeared, see Fig. 6.10c, making it as new and ready to perform significant machining in-service.

As an aside, it is a well known fact by any competent CNC machinist worldwide and familiar with their older and heavily utilised machine tools that certain machine spindles will run smoother and produce better machined roundness on workpieces if they are rotated at its so-called sweet spot. Equally and just as important, is that the quality of parts produced will also be affected if the spindle is rotated at its opposing sour spot. By utilising an SEA system, significant information can be obtained from such rotational analysis, allowing certain speed ranges to be selected that would optimise the present status of the spindle's condition, prior to its potential rebuild—before it is called for refurbishment at a later date.

Much more could also be mentioned concerning these important SEA systems, but with limited textural space, it is hoped that an appreciation of such commercially available instrumentation and its associated software, has been gleaned from this brief review of the spindle error analysis topic.

6.4 Corrosion—Basic Concepts

Introduction

The topic concerning Corrosion is a very complex scientific discipline, which would usually require considerable technical discussion and scope to adequately cover the subject, therefore it is only briefly reviewed herein. Accordingly, the term Corrosion can be considered as, "The gradual destruction of materials [normally metals], by a chemical reaction with its environment"—often in the presence of water—see Fig. 6.11a. In its most basic form, this means electrochemical oxidation of metals in reaction with an oxidant, such as oxygen. The actual term known as Rusting, is the result of the formation of iron oxides, which is a well-known and documented example of electrochemical corrosion. This type of metallic damage typically produces oxide(s) or salt(s) forming in the original metal. Moreover, corrosion can also be present in materials other than metals, such as ceramics or polymers, although here, in this context, it is more commonly known

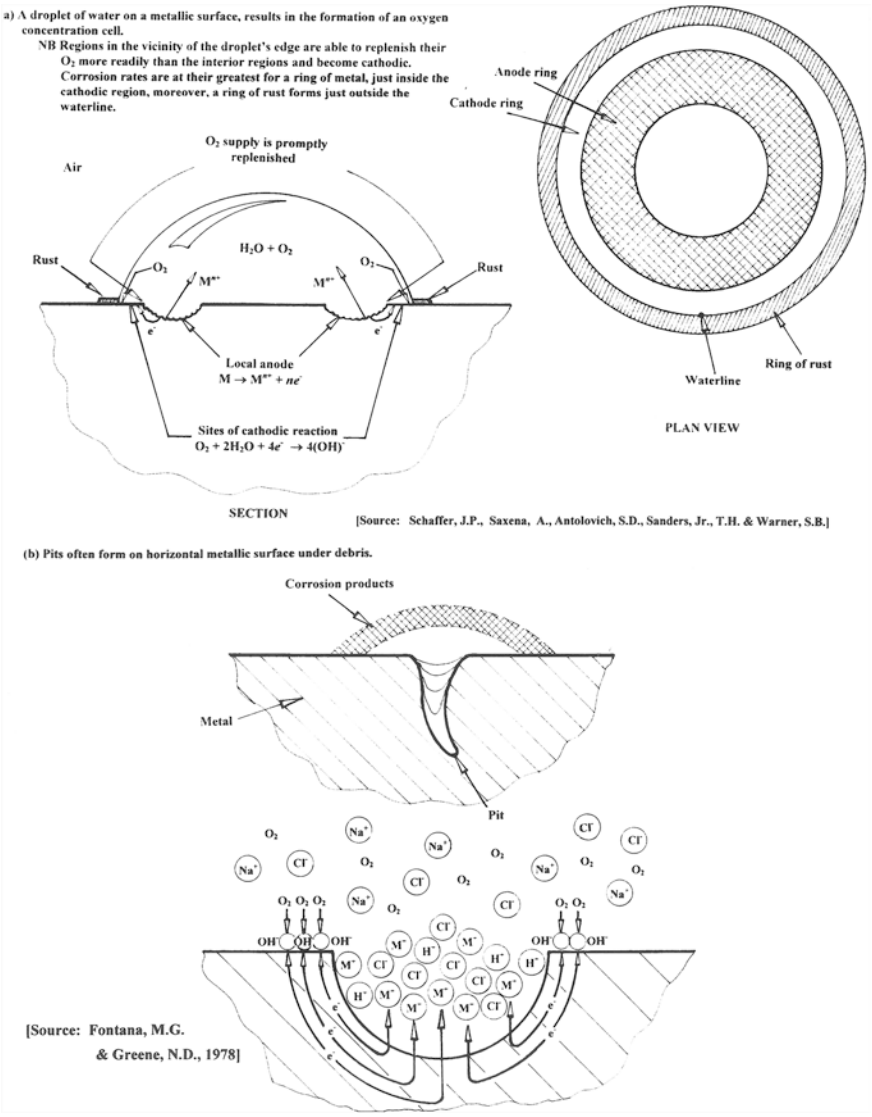

Fig. 6.11 The action of a water droplet and the corrosion mechanism on a metallic surface, plus the growth of a corrosive pit in the presence of water and debris

by the term 'Degradation'. Any form of corrosion will degrade the beneficial properties of materials and structures including their: strength; appearance; as well as its permeability to liquids and gases. A considerable number of structural alloys corrode merely from exposure to moisture in the atmosphere, but the process can be strongly affected by exposure to certain substances. Typically, corrosion can be concentrated locally to form a pit—see Fig. 6.11b—or crack/crevice—see

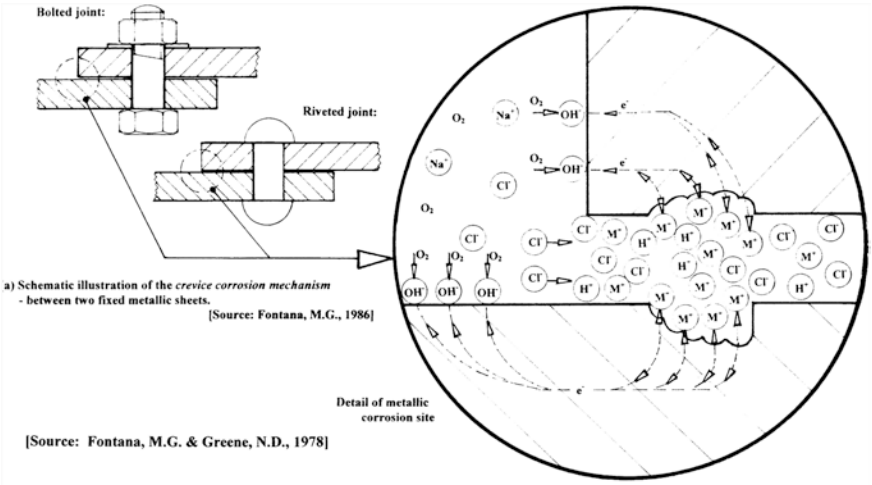

(b) The 'standard' *electromotive force (emf) series* together with the *galvanic series* - for an 'indirect comparison':
[Adapted from: Fontana, M.G., 1986]

←*electromotive force (emf) series*→ Electrode reaction:	Standard electrode potential V^0(V):	Condition:	←*galvanic series*→
		↑	
$Au^{3+}+3e^- \rightarrow Au$	+1.420	**Inceasingly inert (Cathodic)**	Platinum
$O_2+4H^++4e^- \rightarrow 2H_2O$	+1.229		Gold
$Pt^{2+}+2e^- \rightarrow Pt$	~+1.200		Graphite
$Ag^++e^- \rightarrow Ag$	+0.800		Titanium
$Fe^{3+}+e^- \rightarrow Fe^{2+}$	+0.771		Silver
$O_2+2H_2O+4e^- \rightarrow 4(OH^-)$	+0.401		316 Stainless steel-passive
$Cu^{2+}+2e^- \rightarrow Cu$	+0.340		304 Stainless steel-passive
$2H^++2e^- \rightarrow H_2$	0.000		Inconel (80Ni-13Cr-7Fe)
$Pb^{2+}+2e^- \rightarrow Pb$	-0.126		Nickel-passive
$Sn^{2+}+2e^- \rightarrow Sn$	-0.136		Monel (70Ni-30Cu)
$Ni^{2+}+2e^- \rightarrow Ni$	-0.250		Copper-nickel alloys
$Co^{2+}+2e^- \rightarrow Co$	-0.277		Bronzes (Cu-Sn alloys)
$Cd^{2+}+2e^- \rightarrow Cd$	-0.403		Copper
$Fe^{2+}+2e^- \rightarrow Fe$	-0.440		Brasses (Cu-Zn alloys)
$Cr^{3+}+3e^- \rightarrow Cr$	-0.744		Inconel-active
$Zn^{2+}+2e^- \rightarrow Zn$	-0.763	**Increasingly active (Anodic)**	Nickel-active
$Al^{3+}+3e^- \rightarrow Al$	-1.662		316 Stainless steel-active
$Mg^{2+}+2e^- \rightarrow Mg$	-2.363		304 Stainless steel-active
$Na^++e^- \rightarrow Na$	-2.714		Cast iron
$K^++e^- \rightarrow K$	-2.924		Iron and Steel
			Aluminium
			Cadmium
			Commercially pure Aluminium
			Zinc
			Magnesium and Mag-alloys

Fig. 6.12 Crevice corrosion resulting from metallic materials in intimate contact, also listing some abridged tables of the electromotive force and galvanic series

Fig. 6.12a—moreover, it can extend across a wide surface area, being either more, or less uniform when corroding such metallic surfaces. The fact that corrosion is a diffusion controlled process and it usually occurs on exposed and untreated surfaces, has enabled techniques to be developed to reduce this deterioration on the exposed surface. Such corrosion inhibitors include passivation and chromate conversion, which can increase a material's corrosion resistance.

Galvanic corrosion occurs when two different metals having a physical or electrical contact with each other are then immersed in a common electrolyte—see

Fig. 6.12b. Alternatively, this galvanic corrosion can also occur when an identical metal is exposed to electrolytes with different concentrations. In a characteristic galvanic couple, the more active metal (i.e. the anode) corrodes at an accelerated rate and the more noble metal (i.e. the cathode) will corrode at a retarded rate, but if they are immersed separately, then each metal corrodes at its own distinct rate. The corrosion-based question one might pose, is, "What type of metal[s] is one to specify and use?" This clarification is readily determined by following the much simplified listing of the galvanic series—as illustrated in Fig. 6.12b (right). For example, Zinc is often utilised as a sacrificial anode for steel structures—particularly in maritime environments. Accordingly, galvanic corrosion is of major interest to the marine industry, or indeed any industry where water containing salts will be in contact with pipes, or metal structures such as in machine tools that are subjected to water-based coolants in their various forms and strengths. The factors such as relative size of an anode, the types of metals involved and their operating conditions (i.e. temperature, humidity, salinity, etc.) will also affect galvanic corrosion rates. The surface area ratio of the anode to cathode will have a direct effect on the corrosion rates of the materials. As mentioned, this galvanic corrosion is often prevented by the use of precisely and accurately placed and distributed sacrificial anodes, within this physical corrosion environment.

Galvanic Series

In a specified environment (i.e. where the standard medium is aerated, at room temperature by salt water) one metal will be either more noble, or more active than others, this fact being based upon how strongly its ions are bound to the surface—see Fig. 6.12b (left). As a result, if two metals in electrical contact share the same electrons, by a simple tug-of-war analogy at each surface, generating a competition for free electrons between the two materials. Utilising the electrolyte as a host for the flow of ions in the same direction, the noble metal will then take electrons from the active one. The resulting mass flow, or electrical current, can be measured to establish a hierarchy of materials in the medium of interest. This metallic hierarchy is known as the galvanic series (with an abridged listing depicted in Fig. 6.12b, right) and is useful in predicting and understanding corrosion. This type of corrosion reduction technique is expensive to actually operate, but offers the maximum protection against such corrosion. However, some corrosion mechanisms are less visible and as such become somewhat unpredictable in nature.

6.4.1 Understanding Metallic Corrosion—In Brief

Corrosion Reactions

So far, from the introductory remarks, dialogue has been primarily concerned with basic corrosion and the knowledge that this process produces a new and less desirable material from that of the original metal, which can result in a loss of function

of the component, or system. In this instance, the corrosion product exhibited most commonly is termed Rust—which forms on the surface of untreated steel and by some means converts a steel into rust. As a result, the question raised is, "What are these reactions enabling this degradation to occur?" and for this corrosion to happen, the major component in steel being iron (i.e. Fe) undergoes a number of simple changes at the surface of a component. Initially,

$$\mathrm{Fe} \rightarrow \mathrm{Fen}^{+} + n\,\text{electrons}$$

Here, an iron atom can lose some electrons and become a positively charged ion, allowing it to bond to other groups of atoms that are themselves negatively charged. Additionally, it is also known that wet steel rusts to give a variant of iron oxide, so the other part of the reaction must involve water (H_2O) and oxygen (O_2), as indicated below:

$$\mathrm{O_2} + 2\mathrm{H_2O} + 4\mathrm{e}^{-} \rightarrow 4\mathrm{OH}^{-}$$

This chemical reaction is valid, as it produces a negatively charged material that can combine with the iron and electrons that are produced in the first reaction and are used-up. Therefore in clarification, one can ignore these electrons and now rewrite this expression simply as follows:

$$2\mathrm{Fe} + \mathrm{O_2} + 2\mathrm{H_2O} \rightarrow 2\mathrm{Fe(OH)_2}$$

Here then, the: **Iron** + **Oxygen** with **Water** → **Iron hydroxide**, which is the resultant chemical change. Moreover, oxygen can dissolve quite readily in water and thereby react with the iron hydroxide, such that:

$$4\mathrm{Fe(OH)_2} + \mathrm{O_2} \rightarrow 2\mathrm{H_2O_3} + \mathrm{H_2O}$$

Namely, that: **Iron hydroxide** + **Oxygen** → **Water** + **Hydrated iron oxide**, which will then characteristically produce, what is known as: brown rust.

The following five basic steps will help to simply and then explain this complex metallic corrosion process, where:

1. **ions are involved and need a medium to move in**—normally water;
2. **oxygen is involved**—which needs to be supplied;
3. **the metal has to be able to give up electrons**—to start the process;
4. **a new material is formed**—this may react again, or could be protective of the original metal;
5. **a series of simple steps are involved**—requiring a driving force to achieve this corrosion process.

Within this chemical corrosion process, the most important fact is that by interfering with the above-listed steps the corrosion reaction is allowed to be either completely stopped, or at the very least slowed to a manageable rate.

Uniform Corrosion

It has been well documented that ≈30 % of metallic failures are the direct result of uniform corrosion and as the name suggests, this occurs over the majority of the surface

of a metal at a steady and often predictable rate. Although such corrosion is visually unsightly, its predictability facilitates easy control, with the most basic technique being to make the material either thick, or substantial enough to function for the lifetime of the component. So as mentioned, this Uniform corrosion can be either slowed down, or indeed stopped, by utilising the five rudimentary actions listed below, to:

1. **slow down, or stop the movement of electrons by**:
   (a) coating the surface with a non-conducting medium such as paint, lacquer, or oil;
   (b) reducing the conductivity of the solution in contact with the metal and in an extreme case—would be to keep it dry, while washing away any conductive pollutants regularly;
   (c) applying a current to the material (e.g. one technique is by the established procedure of cathodic protection);
2. **slow down, or stop oxygen from reaching the surface**—which is difficult to undertake completely, but here, certain specific coatings can help;
3. **prevent the metal from giving up electrons**—by using a more corrosion-resistant metal higher in the electrochemical series. Here, the use of a sacrificial coating which gives up its electrons more easily than the metal being protected, is preferable—by applying either cathodic protection, or by utilising corrosion inhibitors;
4. **select a metal that forms an oxide**—here, one utilises a metallurgy that is both protective and stops the reaction;
5. **control, with consideration of environmental and thermal factors**—which is also essential in diminishing any form of uniform corrosion.

Localised corrosion

In a similar manner to that concerning uniform corrosion, it is also known that ≈70 % of metallic failures are the consequences of localised corrosion, which can be a great deal more severe than any form of Uniform corrosion. Generally, this is because the failure occurs without warning and usually after a surprisingly short period of use, or exposure. The application of these five basic facts—listed above—needs much greater thought and technical insight to achieve the desired effect—in this instance.

Galvanic Corrosion

This concept of Galvanic corrosion can take place when two different metals are situated in contact with each other and where one metal has a greater willingness to give up its electrons, rather than the other. There are three special features of this galvanic corrosion mechanism, which are necessary for such corrosion to occur, these are:

1. that the metals need to be in contact—electrically;
2. one metal needs to be significantly superior at giving up its electrons than the other;
3. an additional path for ion and electron movement is necessary.

Any form of prevention of this galvanic corrosion problem, is based upon one or more of the three listed features below, by:

1. breaking the electrical contact—by utilising perhaps, plastic insulators or coatings between the metals;
2. selecting metals close together in the galvanic series—see those in the abridged list in Fig. 6.12b (right);
3. preventing ion movement by coating the junction with an impermeable material, or ensuring that the environment is dry and any liquids cannot be trapped.

Pitting Corrosion

Pitting corrosion occurs in materials that would normally have a protective film, such as a corrosion product or when a coating breaks down. At this point, the exposed metal surface gives up electrons easily and the reaction initiates tiny pits with localised chemistry supporting this rapid attack (Fig. 6.11b). The control of this pitting can be safeguarded by the following remedial actions:

- **selecting a corrosion-resistant material**—to minimise any electron activity;
- **ensuring a high enough flow velocity of fluids in contact with the material, or by frequent washing**—this will help to slow down the pitting activity;
- **control of the chemistry of fluids and use of inhibitors**—this will also tend to minimise the tendency for electron flow;
- **use of a protective coating**—this coating should inhibit all pitting effects if it is totally uniform in its coverage;
- **maintaining the material's own protective film**—which is typically the case, for instance, when utilising for example, stainless steels.

NB Although these pits are normally very small, they can act as crack initiators in certain stressed components, or those where the residual stresses have resulted from a previous primary-forming operation (e.g. rolling, casting, forging, etc.)—which can lead to an undesirable case of stress corrosion cracking.

Selective Corrosion Attack

The type of corrosion category termed selective corrosion attack, manifests itself in alloys such as brass, when one metallic component, or phase, is more susceptible to attack than another and as such it will tend to corrode preferentially—leaving a porous material product that will later simply crumble. This unwanted selective corrosion attack can be best avoided by the selection of a resistant metallic material, although some other forms of corrosion-inhibiting techniques can be just as effective, such as by simply: coating the material; reducing the aggressiveness of the environment; or by utilising some form of cathodic protection.

Stray Current Corrosion

Stray current corrosion becomes apparent when a direct current flows through an unintended path and the flow of electrons supports this type of corrosion. A form of stray-current corrosion can also occur in flowing or stationary fluids. The most effective remedies for such corrosion, involve controlling the current by:

- insulating the structure to be protected, or the source of current;
- earthing sources and/or the structure to be protected;
- applying cathodic protection;
- utilising sacrificial targets.

6.4.2 Machine Tool Spalling—of Bearings and Gears

In 1995 at The Massachusetts Institute of Technology (MIT) Ernest Rabinowicz—a retired Emeritus Professor—suggested that ≈70 % of machine tools should be removed from service, due to the degradation of their mechanical surfaces. This type of surface degradation could be present as a result of: corrosive; abrasive; adhesive; erosive; fatigue-induced wear; categories of debilitating regimes. A clear comprehension of how these wear regimes can develop will assist any lubrication technician in understanding the importance of their role in improving machine tool reliability. As a consequence, a knowledge and understanding of bearing and gearing surface degradation leading to corrosion for pitting and spalling[11] can address the nature of its subsurface material degradation—see Fig. 6.13b, c. In the comments given below, an introduction to the influence of filtration and use of solid-film additives, which can promote surface degradation and how one can also improve reliability will be briefly addressed.

6.4.3 Bearing Failure Modes—With Hard Particle Lubricant Contamination

Whenever any Elastohydrodynamic (EHD) lubrication regimes occur, they are statistically more problematic for contaminant particles to enter the contact patch (i.e. the interface)—between two mating surfaces, because of the squeeze effect at these non-conformal contacts. Additionally, their minimum film thicknesses tend

[11]**Spalling** or, **Galling**, which can be simply defined as: "A form of wear caused by adhesion between sliding surfaces"—such Galling is a form of adhesive wear. While this term spalling, is caused by macroscopic transfer of material between metallic surfaces, during transverse motion (i.e. normally, a sliding action). Spalling frequently occurs whenever metal surfaces are in contact, sliding against each other, especially when there is poor lubrication. Thus, spalling often occurs in: high load, low-speed applications; although it can also be present in high-speed applications with very little loads. Spalling is a common problem in bearings, hydraulic cylinders and many other industrial operations. Moreover, spalling is a distinctive from either gouging, or scratching, in that spalling involves the visible transfer of material as it is adhesively pulled from one surface (i.e. being mechanically spalled), leaving it adhered to another surface in the form of a raised work-hardened deposit. Unlike other forms of wear, spalling is usually not a gradual process, but occurs both quickly and spreads rapidly—as these raised deposits exacerbate and induce acceleration of yet more of this Spalling conditional effect.

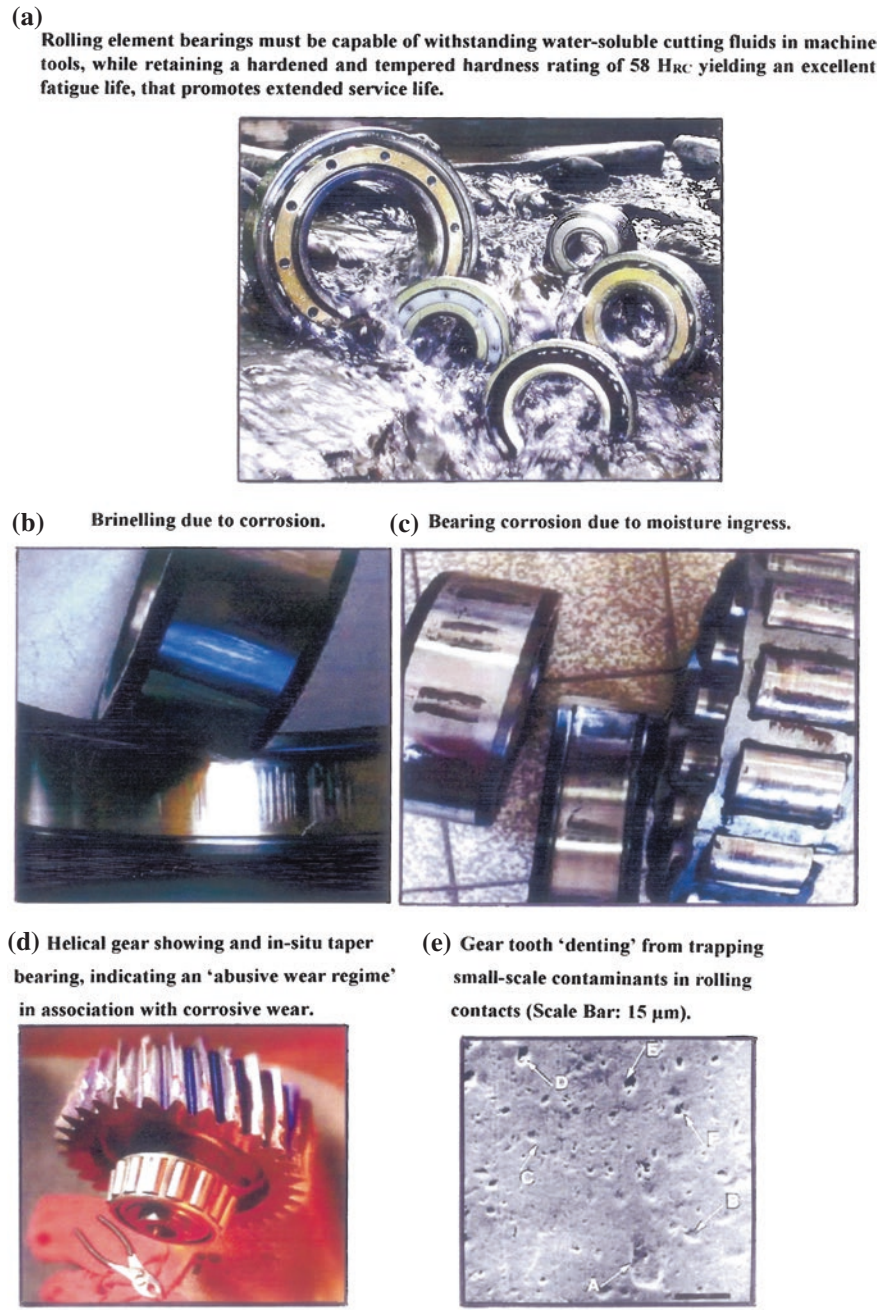

Fig. 6.13 Bearing and gear corrosion in machine tools [*source* Kuhnell, B.T. (Monash University, Australia) 2004]

to be much smaller (i.e. geometrically) than for hydrodynamic lubrication films—these being typically just 5 μm compared to 100 μm, respectively. Conversely, offsetting this to some degree, is the phenomenon that the viscosity of lubricants is pressure-dependent, and as a result by increasing pressure this will also increase the fluid viscosity. In many machine tool applications with typical rolling bearing contacts, the viscosity can increase by a magnitude of $\times 1000$—for a pressure rise of just 300 MPa—this being quite possible for such Hertzian contacts.[12] This increased viscosity due to pressure, has greater capacity to trap and hold contaminant particles within the contact region. In any form of EHD lubrication of all Hertzian-contacts—including that of a machine tool's rolling element bearings—the lubricating film thickness must be approximately three times the combined surface roughness of the contacting component parts, to circumvent any asperity intersection and boundary lubrication. All of these rolling element bearings—see Fig. 6.13a—are manufactured with finely cylindrically ground and polished surfaces, so that the EHD film thicknesses will adequately satisfy this requirement.

In some previous metallographical/metallurgical examinations—by Kuhnell (2004) of rolling element bearing failures—stringent tests were undertaken with the intention of determining the precise origins of their failures. In the majority of these bearing failure cases, there was direct evidence of a surface defect-initiated spall, where the contact surface was destroyed by spall propagation and/or was to some extent camouflaged by specific secondary spall debris damage. In these investigative tests, the bearings were critically investigated and thought to be the result of subsurface-initiated failure (i.e. subsurface cracking) where Kuhnell carefully took metallographic cross sections through this spall region. However, these examinations failed to determine conditions such as: faulty microstructure; non-metallic inclusions; or carbide agglomeration—that would conclusively verify their subsurface origin. Here, under microscopic examination of the shape and depth of this spall, it generally gave the best indication of the most probable failure mode. Moreover in some further testing by Kuhnell, the mechanism of surface spall initiation appeared to change with lubricant filter size. It was also noted in this applied research work, that Point surface-originated spalls, could be characterised by a shallow, arrowhead pattern which appeared to be the most prevalent in the case of utilising a 3 μm (absolute) lubricant filter, in such tests.

[12]**Hertzian-contacts** [The original work in **Contact mechanics** dates back to 1882, with the publication of the seminal paper: *On the contact of elastic solids* (i.e. Ueber die Berührung fester elastischer Körper)—by **Heinrich Rudolf Hertz**—who was an eminent German Physicist (Born: in Hamburg on 22 February 1857, whose then untimely death by—Wegener's granulomatosis—occurred at the age of 36, when Hertz was living in Bonn, Germany—on 1 January 1894)], as it is known as within the discipline of Contact mechanics: which is the study of the deformation of solids that touch each other at one, or more points. The physical and mathematical formulation of the subject is built upon the principles Mechanics of Materials and Continuum mechanics and focuses on computations involving: elastic; viscoelastic; as well as plastic bodies in static, or dynamic contact. Accordingly, the central aspects in any form of Contact mechanics, are the actual pressures and adhesion acting perpendicular to the contacting bodies' surfaces—this being the normal direction—plus the frictional stresses acting tangentially between these surfaces.

(a)

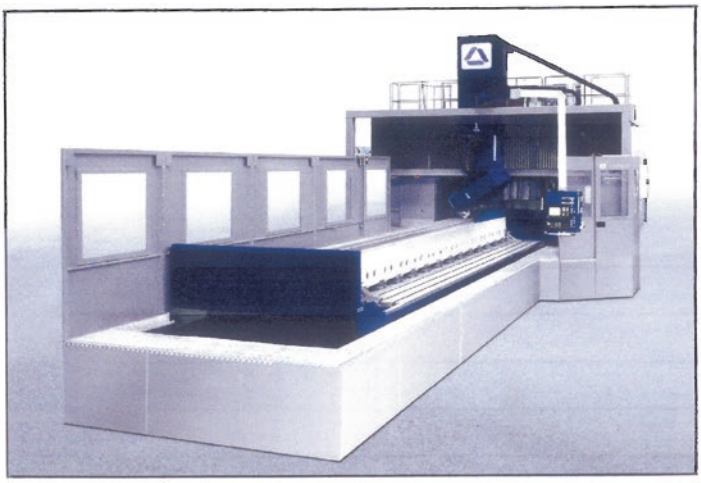

Double column slideway grinding machine tool **with either fixed, or mobile cross rail and tangential and/or universal wheelheads. Applications include: machine tool beds and guideways and high precision heavy-duty and large components.**

(b)

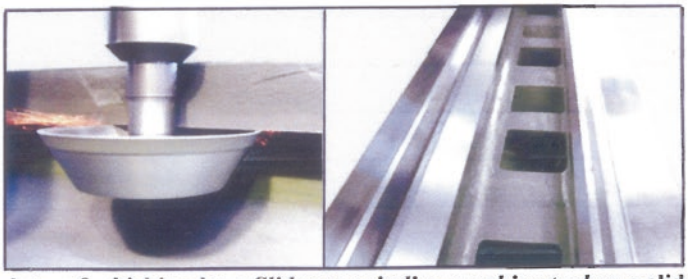

Complete refurbishing by a *Slideway grinding machine tool* on a slideway.

(c)

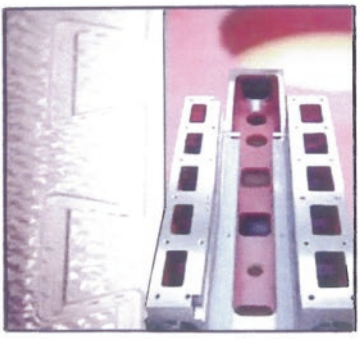

Completely Re-engineered, reground and scraped machine tool bed.

Fig. 6.14 Any damaged, or corrosion machine tools beds and slideways can be completely refurbished by a slideway grinding machine tool [courtesy of DANOBAT GROUP (Spain)]

Micro pitting results from debris particles interrupting the elasto-hydrodynamic film and this was most prevalent in these tests when utilising 49 μm lubricant filtration. In the circumstances of the influence of debris dents—shown in Fig. 6.13e—these are significantly larger than the absolute pore size of the filter and were occasionally found on suspended (i.e. in clean oil) test bearings, indicating that the debris particles can be generated within the bearing assembly itself. However, the number of these particles and their potential to initiate fatigue has been judged to be relatively small in comparison to debris ingested either externally, or generated within the lubrication system and then not being removed by the filter. Consequently, to provide maximum bearing component life, a concerted effort must be made to prevent contaminants/debris from gaining entry to the lubrication-system by proper sealing and then to remove any contaminants through proper filtration.

6.4.4 Bearing Contamination

Most of the different contaminants that are ingested or generated in a machine tool have serious effects on the actual service life of rolling bearings—as previously mentioned. Nonetheless, the most common form of debris comes from abrasive ingested dust (i.e. typically, Silicon dioxide, also known as silica, which is a hard chemical compound that is an oxide of silicon: SiO_2). Certain sizes of these hard and abrasive particulates can enter the bearing's contact zone and cause extreme impact pressures by bridging across the gap and then removing the EHD film. Surface features such as: scuffing; abrasive wear; polishing by the smaller particles; plus indentation by even larger particles; are among the principal causes leading to the premature demise of such bearings. Furthermore, the effect of surface polishing may cause excessive bearing clearances, which will subsequently lead to early degradation of this bearing. Additionally, the jamming action of hard particles in the bearing's contact zone may cause what is termed ligament collapse at depth (i.e. the fracture of the remaining material between two cracks, or a crack and the surface in just a few load cycles) by low-cycle fatigue, which could be quite different from the expected and normal, high-cycle fatigue based phenomena.

Such bearing indentations at the surface interface could also become stress concentration sites within the bearing and accelerate the deterioration and progression of low-cycle fatigue. Once any form of fatigue phenomena has been initiated within rolling element bearings, it will usually exacerbate its condition at an increasing rate. This undesirable action is because the particles that spall out from the surface represent yet more particles that can become jammed-in in the contact zone, causing these attrition effects to then develop exponentially.

6.5 Condition Monitoring—Of Machine Tools

Condition Monitoring[13] (CM) is an all-encompassing in-depth procedure covering a variety of plant activities, which is usually associated with the measurement of various parameters related to the mechanical condition of machinery. It embraces conditions such as the monitoring, controlling and maintenance of: vibration; bearing temperature; oil pressure; oil debris; also its performance; which makes it possible to determine whether the machinery is in a good or bad mechanical condition. If the plant's mechanical condition is in a poor state, then CM makes it possible to determine the actual cause of the problem. It is normal best practice, where a company would utilise CM in conjunction with some form of Predictive maintenance (PdM)[14] to determine a machine tool's current maintenance status—see Fig. 6.15—for a graphical interpretation of the development and rise in maintenance strategies over the years. Explicitly, one can say that any form of maintenance of machinery is based on an indication that a problem is about to occur. Accordingly, in many companies, the term Asset management[15] can also be

[13]**Condition monitoring** (**ISO/TC 108/SC 5—Condition monitoring and diagnostics of machine systems**: this relevant Maintenance Standard—being instigated in 1993) or, colloquially, **CM**: can be simply defined as: "The process of monitoring a parameter of condition in machinery (i.e. vibration, temperature, etc.), in order to identify a significant change which is indicative of a developing fault". Hence, this CM is a major component of Predictive maintenance. The use of CM allows maintenance to be scheduled, or other actions to be taken to prevent failure and avoid its consequences. Accordingly CM has a unique benefit, in that conditions that would tend to shorten a normal component's lifespan, can be addressed before they develop into a major failure. CM techniques are normally utilised on for example, the machine's rotating plant and equipment, plus other machinery sub-assemblies (i.e. such as: pumps, electric motors), while periodic inspection utilising Non-destructive testing (NDT) techniques and that of Fit for Service (FFS) evaluation—these techniques are also prevalent and common place today.

[14]**Predictive maintenance** (**PdM**): techniques have been devised that are designed to help determine the condition of in-service equipment in order to predict when maintenance should be performed. This PdM approach promises significant cost savings over that of either Routine- or Time-based preventive maintenance, because tasks are performed only when warranted. The major advantage of PdM, is to allow convenient scheduling of corrective maintenance, and to prevent unexpected equipment failures. The key phrase here is: "The right information at the right time!" By understanding which equipment/plant needs maintenance, any maintenance work can be better planned (i.e. with availability of spare parts, appropriate technical people, etc.) and what would have been unplanned stops, are then transformed to shorter and fewer more efficiently planned stops, thus increasing the overall company's plant availability. Other potential advantages of this PdM approach, includes: an increased equipment lifetime usage; improved plant safety; with fewer potential accident sites; while having a negative impact on environment; plus having an optimised spare parts handling capability.

[15]**Asset management** in **ISO 55000 Standard** (**ISO 55000:2014 Standard—**provides an overview of the subject of Asset management and the standard terms and definitions to be utilised), is where it is defined as: "The coordinated activity of an organization to realize value from assets" (The Institution of Asset Management). Thus, these Assets can be individually defined as follows: "An asset is an item, thing, or entity that has potential, or actual value to an organization". This statement is deliberately wider than that for physical assets, but these form an important focus across more types of organisations.

The quality-building & essential maintenance of Robotic equipment is indispensable for its operational performance in a Manufacturing Cell environment during its active life.

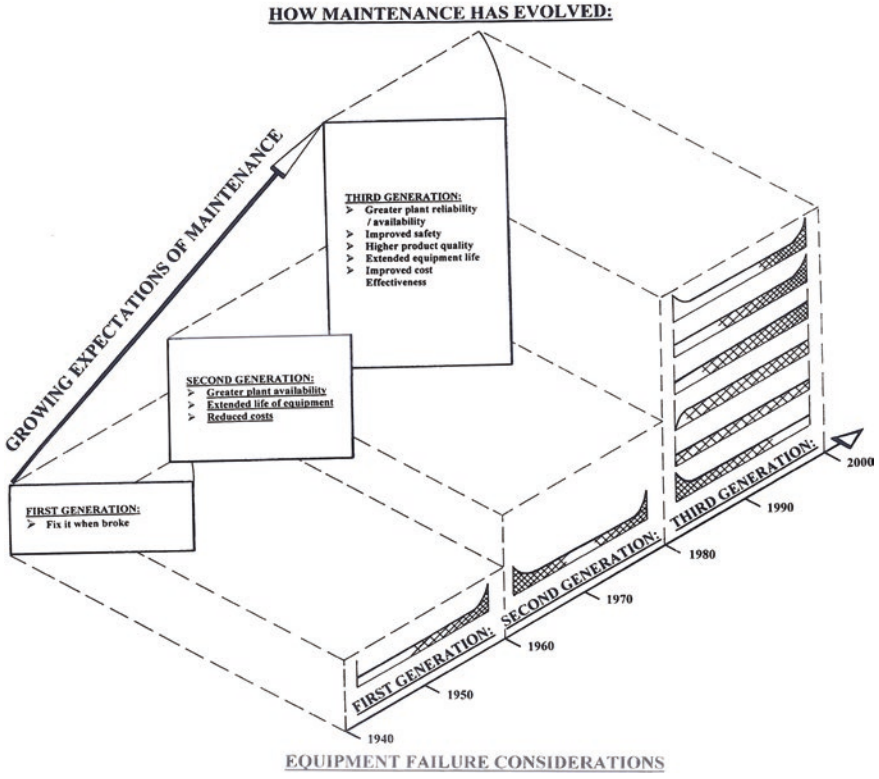

Fig. 6.15 The historical context of maintenance—an overview of maintenance and its operation (courtesy of Kuka Roboter GmbH—top image)

considered as some form of predictive maintenance, which has replaced both: Run to breakdown maintenance (i.e. the latter alternative name for the old-maintenance strategy form of, "Fix-it-when-its-broke!"—see Fig. 6.15) and Preventive maintenance (i.e. in which mechanical parts are replaced periodically at fixed time intervals, regardless of the machinery's mechanical condition). As a consequence, both

the Condition Monitoring and Predictive maintenance of machinery will:

- **avoid any unexpected catastrophic breakdowns**—that would otherwise have expensive or dangerous consequences;
- **reduce the number of overhauls on machines to a minimum**—thereby reducing maintenance costs;
- **eliminate unnecessary interventions**—with the otherwise consequent risk of introducing faults on smoothly operating machines;
- **allow spare parts to be ordered in timely manner**—thus eliminating costly inventories;
- **reduce the intervention time**—thereby minimising production loss via unanticipated time delays, because the specific fault to be repaired is known in advance, enabling any overhauls to be scheduled when it is most convenient.

6.5.1 Condition Monitoring—Historical Perspective

In engineering at large since the birth of the Industrial Revolution[16] a couple of hundred years ago, there have been significant advances and developments in industry, but perhaps the most dramatic changes have occurred within the last fifty years. These latter manufacturing and engineering changes have of course affected how industry's plant has been maintained. Consequently, prior to WWII, the

[16]The **Industrial Revolution**: this was the transition to new manufacturing processes and practices in the period dating from: ≈1760 to ≈1820–1840. This industrial transition included changing from the original and outdated hand production methods to the introduction and the use of machinery. These newly developed industrial aspects, coupled with some recently introduced methods in: iron production processes; chemical manufacturing; plus improved efficiency of water power—thereby increasing use of steam power; in conjunction with significant developments of machine tools and their usage, further and significantly advanced the nation's production capabilities. This Revolution, also included the change from the previous usage of wood and other biofuels, to that of coal usage. Textiles that were at the time, the dominant industry of the Industrial Revolution in terms of: employment; value of output; along with the capital invested, thus, Textile manufacturing in Manchester (England) was well known and documented, as being in reality, the first industry to use modern production methods. The Industrial Revolution signifies a major turning point in history, as almost every aspect of daily life was influenced by these current industrialised events—to a certain extent. Of particular note, was that the average income and its associated population began to exhibit unprecedented and sustained growth. In the words of the American economist: Robert E. Lucas, Jr. (i.e. a Nobel Prize winner—born in 1937, in: Yakima, Washington, USA), who succinctly said: "For the first time in history, the living standards of the masses of ordinary people have begun to undergo sustained growth … Nothing remotely like this economic behaviour is mentioned by the classical economists, even as a theoretical possibility". It is also well documented that this Industrial Revolution began in Great Britain, and within a few decades had spread to the rest of Western Europe and subsequently across to The United States of America. The period of time covered by the Industrial Revolution varies with different historians, where: Eric Hobsbawm (Born: June 1917, Alexandria, Egypt, died: October 2012, London) held that it "… broke out in Britain in the 1780 and was not fully felt until the 1830s, or 1840s"…, while, the English-historian: T.S. Ashton (Born: 1889, Ashton-under-Lyne, England—died: 1968, London), maintained that: "… it (i.e. the Industrial Revolution) occurred roughly between 1760 and 1830".

majority of machinery was generally quite rugged in construction and unsurprisingly it was relatively slow running, with its associated instrumentation and control systems being somewhat rudimentary and basic. This meant that any maintenance undertaken was only performed when equipment either failed, or perhaps if it needed to be replaced (i.e. re-emphasising that this form of maintenance strategy is known as, "Fix-it-when-its-broke!"—being a somewhat basic maintenance attitude)—see Fig. 6.15. In mitigation the demands of production were not overly severe, so that any plant downtime was not usually a critical issue and at that time period it was simply adequate to maintain equipment on an elementary breakdown basis. Due to the lack of sophistication of such machinery, it had the advantage of being inherently reliable and rugged. Even today, one can still envisage certain examples of the rugged machinery made during that period, which might have been worked very hard and is still essentially as good as the day it was first produced.

From the early 1950s, in conjunction with the total rebuilding of countries such as Japan and Germany after WWII who had suffered industrial decimation, a much more competitive marketplace was a perceived philosophy of cumulative intolerance to any form of downtime. Here, the cost of labour became increasingly significant, leading to greater mechanisation and automation, with the majority of machinery now being of lighter construction, and as such, running at much higher speeds. The downside of the less robust, but faster operated plant, was that it tended to wear out much more rapidly. As a result of this, premature but anticipated service life became less reliable, or alternatively perhaps, it might be that it was utilised more fully and efficiently thus affecting its longevity. This contemporary type of production strategy, really demanded the introduction of some form of enhanced maintenance programmes, which has led to the development of the principles and practice of Planned Preventative Maintenance (PPM).[17]

Sometime ago it was recognised that a Level of failure of, for instance 10 % of all machines, meant that inevitably its Probability of failure had become unacceptably high, which preordained that the majority of such machine tools should now be subject to some form of a maintenance overhaul. Nonetheless, there may be a significant loss in potential life in the remaining group of machines, but in view of the potential failure risk, this maintenance strategy was at the time considered to be justified. The maintenance planning previously occurring during this time period, often involved plant overhauls that were usually based upon a specific and planned time interval, or after its industrial usage at which time the failure rate of a group of similar machines became unacceptable. This particular form of maintenance action, has now led to the basic assumption that older machinery and equipment becomes more likely to fail with respect to time and this hypothesis has introduced

[17]**Planned Preventative Maintenance** (**PPM**): or more simply stated as: **Planned Maintenance**: which is considered as any variety of Scheduled maintenance to an actual asset, or item of equipment. More specifically, Planned Maintenance (PM), is a scheduled-service visit undertaken by a competent and suitable agent (e.g. normally a company's Service Engineer), to ensure that the equipment, or plant is operating correctly and therefore avoiding any unscheduled breakdown—with its attendant increased downtime.

the well-acknowledged supposition, being known as the Bathtub Curve[18] that indicates the plant unreliability of such events (see Fig. 6.15). Generally by manufacturing industry, there is a wide acceptance of CM, but there are also a number of limiting factors, mostly relating to the historical context of the current equipment and its application, this being seen as the response to all of maintenance's needs. In consequence, Condition Monitoring limitations, might include:

- the fact that CM is often utilised as a stand-alone maintenance concept;
- frequently CM is simply utilised for just Failure prediction, with little else being investigated or indeed expected;
- invariably CM has been seen as Management-driven—but, usually from the bottom-up approach;
- CM in isolation, does not provide for reliability of an asset;
- finally, CM does not prevent failure—it simply detects and predicts its occurrence.

By way of a practical example, typically in many machine shops around the world, a vibration history from a successful CM programme will highlight that ≈50 % more machine tools are running effectively after a period of 2 years of significant use, although with the remaining machinery it is not unusual to find the same old problems repeatedly appearing and as such the problems are not being effectively eliminated. However, often the company's maintenance strategy might be considered successful—from a failure prediction perspective—but even here maintenance might have found a lot more problems, so in this manner, the Condition Monitoring strategy was not effectively supported with an efficient defect elimination policy.

6.5.2 Types of Condition Monitoring Systems

When employed by manufacturing industries across a broad spectrum of industry, the Condition Monitoring Systems that tend to manifest themselves, are of two distinct types, these can be considered as either a:

[18]The **Bathtub curve** [The Bathtub curve is generated by plotting the product's rate of early infant mortality failures—when products are firstly introduced—which are high, while the rate of random failures—with a constant failure rate—occurs during its useful life (i.e. this being a steady-state region of its potential life), and finally the rate of wear out failures—which increases as the product, or component exceeds its anticipated design lifetime. It was recognised from the outset, that this Bathtub curve was an amalgamation of six potential failure patterns, relating to the introduction of the: Third generation of maintenance activities (i.e. see Fig. 6.15). However, now many industrial companies are entering into what is termed the: Fourth generation of maintenance, which is somewhat beyond the scope of the current text, but for more details, contact: Assetivity Pty Ltd, of: South Perth WA6151, Australia (2015)]: it is widely utilised within the discipline of Reliability engineering, where its graphical profile resembles the cross section of a Bathtub—hence its name. This Bathtub curve describes a particular form of the hazard function, that comprises three distinct parts, they are: (i) **a decreasing failure rate**—known as early failures; (ii) **a constant failure rate**—known as random failures; (iii) **an increasing failure rate**—known as wear out failures.

1. **Periodic monitoring system** (also termed an: Offline condition monitoring system)—for example, machinery vibration might be measured, or recorded and later analysed at selected time intervals in, for example, the machine shop. At this time, these advanced data analysis techniques are normally required for fault diagnosis coupled with trend analysis. This category of Intermittent monitoring, provides information at a very early stage about the potential for incipient failure and are normally utilised where: (i) an early warning of faults is a prerequisite; (ii) advanced diagnostics are necessary; (iii) data capture must be undertaken at many locations on a machine tool; (iv) where these machines are both sophisticated and complex in nature;
2. **Permanent condition monitoring system**—here, the principal function is to protect one, or more machine tools within the production facility, by providing a warning that one of the machines is either currently operating improperly and/or necessitates it to be shutdown when a preset safety limit is exceeded. Thereby such remedial action will circumvent its potential for catastrophic failure and destruction. In this situation, the measurement system is usually permanently incorporated into the plant, or it may at the very least be quasi-permanent. In the former case of a Permanent monitoring system, any CM transducers would be mounted perpetually at each key-selected measurement point. As result, such Permanent systems tend to be somewhat expensive to install, so they are habitually utilised only in critical applications, where there are: (i) no personnel that are available to perform these measurements; (ii) where it is necessary to stop the machine before a breakdown occurs in order to avoid a catastrophic accident; (iii) if an instantaneous fault occurs that requires an immediate machine shutdown; (iv) the production environment does not permit any form of human involvement—which would normally be the requirement for any intermittent measurements.

Of some note concerning this latter kind of CM system, is that prior to installing a Permanent condition monitoring system, some form of investigative preliminary measurements should normally be periodically undertaken over a specific period of time on the machine tool, so that one becomes acquainted with, for instance, the vibration characteristics of the machine under test. This type of preliminary CM procedure will ensure that it is possible to select the most appropriate: vibration measurement parameter; its frequency range; coupled with the expected normal alarm- and trip levels necessary.

In Table 6.1, is depicted a simple tabulation of some techniques in which the terminology of monitoring machinery classifications for machine tools are known.

6.5.3 Condition Monitoring Systems—Establishing a Programme

For the representative type of manufacturing plant such as machinery, a Condition Monitoring Programme can be established to simply ensure that the satisfactory

Table 6.1 Typical asset terminology for both plant and machinery classifications for condition monitoring, with their associated failure mechanisms

Machinery classification	Result of failure
Critical	Unexpected shutdown, or failure—causes significant production loss
Interrupts production	Unexpected shutdown, or failure—causes minor interruptions in production
Causes inconvenience	Inconvenience in operation, but no interruption in production
Noncritical	Production is not affected by this machinery failure

Source Courrech (2014)

operation of a stand-alone machine tool occurs. Furthermore it is customary to determine whether the operation of a number of machines need to be checked, or indeed, perhaps if all the machine tools in an entire plant require some form of CM. In the following steps, a logical progression is considered in the establishment of a typical CM-programme. Therefore, depending on the type of machine tool or metrology instrumentation being monitored and the impact of any form of plant failure regarding these machines within the production environment, the following abridged steps in establishing a Workable CM-system might be utilised. Such might be the case when, for example below, the vibration monitoring in a CM environment is the explicit requirement:

- **Step 1—determining the type of CM system necessary**—as previously described and that best meets the needs of the plant/asset in question;
- **Step 2—listing all of the machines to be monitored**—this being based upon the importance of these machine tools within the overall production line;
- **Step 3—tabulating the characteristics of these machine tools**—which are important in conducting vibration analysis of the machines (i.e. as per Step 2). Here, these characteristics are associated with its actual machine constructional elements such as the natural frequencies of: shafts; castings; columns, pedestals; with their operational and defect responses. Moreover, a tabulation of machine frequencies is important, because fault analysis is conducted by matching machine frequencies to measured frequencies appearing within a vibration spectrum;
- **Step 4—selecting the most appropriate vibration measurement parameter**—which is very important. For example, when an accelerometer is employed as the sensing device in a CM system, the resulting acceleration signal can be electronically integrated to obtain velocity, or displacement, so any one of these parameters may be utilised in its ensuing measurements;
- **Step 5—selecting one type of a particular vibration pickup**—which will best meet the requirements of Step 4. For example a displacement transducer—which is a transducer that converts an input mechanical displacement into an electrical output that is proportional to the input displacement;

- **Step 6—selecting the strategic measurement locations**—on the machine tool. Accordingly, when a periodic (i.e. offline) monitoring system is employed, the number of points at which measurements are made is limited only by the requirement for keeping measurement time to a minimum. As a general rule, typical bearing vibration measurements are normally undertaken in the radial direction on each accessible bearing and in the axial direction on thrust bearings;
- **Step 7—selecting the time interval**—between these measurements. The selection of the time interval between measurements requires knowledge of the specific machine tool. Some machines develop faults quite quickly, while others run trouble free for years. Accordingly, a compromise must be found between the safety of the system and the time taken for such measurements and analysis. Measurements should be made frequently in the initial stages of a CM-programme, to ensure that the vibration levels measured are stable and that no fault is already developing. When a significant change is detected, then the time interval between measurements should be reduced sufficiently so as not to risk a breakdown before the next measurement. The trend curve will help in determining when the next measurement should be performed;
- **Step 8—establishing an optimum sequence of data acquisition**—the sequence in which data is acquired in a CM-programme must be planned so that data can be acquired efficiently. For example, the data collection may be planned on the basis of plant layout for the type of data required, or on the sequence of components in the machine train, such as from its driver-to-driven components. Typically, low frequencies need to be acquired for subsynchronous components such as for looseness; oil whirl; faulty belt-drive; also to that of vibrations at very high frequencies for: tooth meshing frequencies; blade passing frequencies; frequencies of structural resonances excited by faulty rolling element bearings; etc. Such data detection should be applicable across the complete range of machines within a production plant, and can operate from very low-to-high speeds. This detection procedure requires the selection of equipment and analysis techniques, which cover a very broad frequency range. Measurements of absolute vibration levels of bearings provide no indication of the machine's condition, since they are influenced by the transmission path between the force and the measurement point, which may amplify some frequencies while also attenuating others. Despite the fact that bearing vibration levels may change from one measurement point to another on a given machine, since the transmission paths are different, they may also change for the same reason from machine-to-machine for measurements that are made at the same measurement point.

The early detection of faults in a diverse range of plant and machinery, or for other assets, can be carried out successfully but only by comparison with a reference spectrum. Condition monitoring techniques employed during transient operating environments of the machine (i.e. when the machine is running up to full speed, or the opposite when slowing down from full speed) differs significantly from the

techniques employed during steady-state operating conditions. For that reason, it is essential that a careful investigation is undertaken to ensure that specific condition monitoring techniques are selected, which will be appropriate for the conditions of measurement.

6.6 Thermographical Inspection

Introduction

Thermography and its associated technique of Thermographic inspection, refers to the non-destructive testing (NDT) of workpieces, materials, or complete systems, through the imaging of the thermal patterns at the object's surface. In essence, the term thermography alone, refers to all thermographic inspection techniques, regardless of the physical phenomena utilised to monitor any thermal changes. By way of a simple example, the application of a temperature-sensitive coating to a surface in order to measure its actual temperature is a thermographic inspection contact technique. This elementary NDT technique, is based upon that of heat conduction—where there is no infrared sensor involved. The term Infrared thermography, is a non-destructive form of contact mapping of thermal patterns, these are often known as thermograms on the surface of objects, via the use of an infrared detector. Moreover, there are two distinct methodologies in any form of thermographic inspection, these are:

1. **Passive inspection**—in which the specific features of interest are naturally at a higher or lower temperature than their background, typically, this passive technique is often utilised for the surveillance of people at a particular scene;
2. **Active inspection**—this is when an energy source is required to produce a thermal contrast between the feature of interest and its background. Typically, this active technique has been traditionally utilised for example, an aircraft part with its associated internal flaws, but is also utilised today for machine tool thermographical analysis.

6.6.1 Electromagnetic Spectrum—A Brief and Introductory History

Historically, the visible, or white light—as already previously described—is the acknowledged portion of the Electromagnetic spectrum that was originally recognised by the population at large, see Fig. 6.16 (top). Fundamentally, it was understood that the Ancient Greeks accepted that light travelled in straight lines and they basically studied some of its properties, including both its reflection and refraction. Since this time, the study of light has been sustained and conflicting theories developed particularly during the sixteenth- and through to the

Infrared – part of the electromagnetic spectrum

The human eyes are 'detectors' that have been designed to detect visible light, or visible radiation. Other forms of light – radiation - that occur one cannot see, thus, the eye can only perceive a very small region of the total electromagnetic spectrum. So, at a certain extreme part of the spectrum – beyond that being visible, ultraviolet light exists, which cannot be seen. While similar circumstances occur at the opposite extreme portion of this visible spectrum, being the region where infrared occurs – which cannot also be seen. Subsequently, this Infrared radiation lies between the visible and microwave portions of the electromagnetic spectrum. The primary source of infrared radiation is heat, or thermal radiation. So, any object that has a temperature above absolute zero (i.e. -273,15° Celsius, or 0 Kelvin), emits radiation in the infrared region. Even objects that one might perceive as being very cold, for example an ice-cube, will emit some infrared radiation. During one's everyday-circumstances, this infrared radiation is continuously-experienced, such as heat from: the sunlight's rays; a fire; or a radiator. Moreover, although our eyes cannot see infrared radiation, our skin can feel it as heat, with the warmer the object, the more infrared it emits.

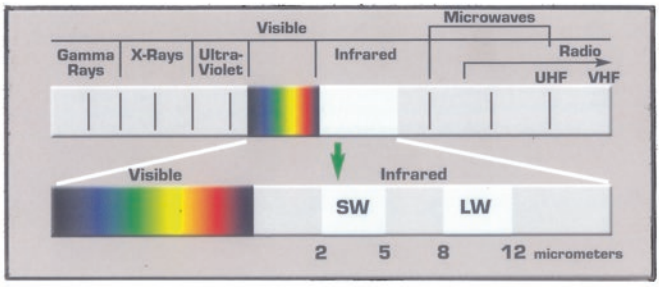

The infrared camera

Infrared energy (A) coming from an object is focussed by optics (B) onto an infrared detector (C). The detector sends the information to sensor electronics (D) for image processing. The electronics translate the data coming from the detector into an image (E) that can be viewed in the viewfinder, or on a standard video-monitor, or an LCD-screen.

Infrared thermography is the art of transforming an infrared image into a radiometric one, which allows temperature values to be read from the image. Consequently, in order to achieve this, complex algorithms are incorporated into the infrared camera.

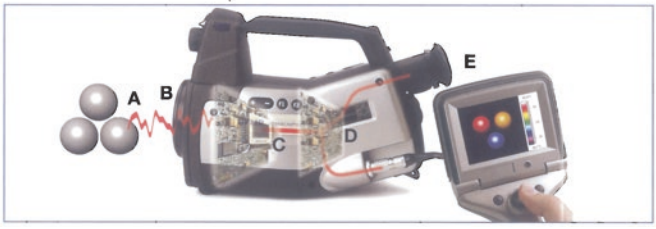

Fig. 6.16 The infrared portion of the electromagnetic spectrum and the operating principle of a thermography camera (courtesy of Flir Systems)

seventeenth centuries regarding how such light effects occurred. At that time, it was known that this light had either some form of a wave or a particle formation. Probably the foremost discovery of Electromagnetic radiation other than that known concerning visible light, occurred in 1800 with the discovery of infrared

radiation—by William Herschel.[19] Herschel studied the temperature of different colours, by moving a thermometer through light split by a prism, where he noticed that the highest temperature was 'beyond-red'. Herschel then theorised that this temperature change was due to calorific rays, which would be in effect a type of light ray—that could not actually be seen. Contrariwise, the following year (1801) Johann Ritter[20] researching at the opposite end of the visible spectrum, noticed what he called 'chemical rays', which were later renamed as ultraviolet radiation.

In 1845, electromagnetic radiation was first linked to electromagnetism, when Michael Faraday[21] noticed that the polarisation of light travelling through a transparent material responded to a magnetic field, now being noted as the Faraday effect. In the mid-1860s, James Clerk Maxwell,[22] developed four partial differential equations concerning this electromagnetic field, with just two of these equations predicting the possibility of, and behaviour of, waves in the field. So, by analysing the speed of these theoretical waves, Maxwell comprehended that they must travel at the speed of light. This directed Maxwell to make the inference that light itself must be a form of electromagnetic wave. Maxwell's equations, predicted an infinite

[19]**(Frederick) William Herschel** KH, FRS: (Born: 15 November 1738—died: 25 August 1822), was a Hanoverian born British astronomer, Technical expert and a Composer. He migrated from the Continent to Great Britain at the age of nineteen. Herschel became famous for his discovery of the planet Uranus, along with two of its major moons, Titania and Oberon, and he also discovered two moons of Saturn. In addition and more applicable here, was the fact that Herschel—in 1800—also discovered the existence of infrared radiation.

[20]**Johann (Wilhelm) Ritter**: (Born: 16 December 1776—died: 23 January 1810) was a German Chemist, Physicist and Philosopher. Ritter was born in Samitz (Zamienice), near to Haynau (Chojnów) in Silesia and later died in Munich. In 1801, after hearing about the discovery of the heat rays (i.e. infrared radiation) by William Herschel—in 1800, Ritter looked for an opposite (i.e. cooling) radiation beyond the other end of the visible spectrum. However, Ritter did not find exactly what he expected, but after a series of scientific attempts, he noticed in his experiments that silver chloride was transformed faster from white to black when it was placed at the dark region of the Sun's spectrum, close to its violet end. Later, Ritter found these so-called chemical rays, which he by now termed as: ultraviolet radiation.

[21]**Michael Faraday** (Also see: Footnote 9—for further brief information regarding some of Faraday's experimental work) FRS: (Born: 22 September 1791—died: 25 August 1867) was an exceptional English Scientist, who fully contributed to both the fields of Electromagnetism and Electrochemistry. Faraday's major discoveries also included those of: Electromagnetic induction; Diamagnetism; as well as Electrolysis. Moreover, Faraday also established that magnetism could affect rays of light, and that there was an underlying relationship between these two phenomena.

[22]**James Clerk Maxwell** FRS FRSE: (Born: 13 June 1831—died: 5 November 1879) was a truly brilliant Scottish Mathematical physicist. Maxwell's most prominent achievement was to formulate a distinct set of equations that described: Electricity; Magnetism; also for that of Optics; exhibiting them as manifestations of the same phenomenon, namely as being that of the Electromagnetic field. Maxwell's scientific achievements concerning electromagnetism have been described as the: "… [The] Second great unification in Physics …", after that of the First—initially being realised by **Sir Isaac Newton**. In 1865, with the publication of: *A Dynamical Theory of the Electromagnetic Field* by Maxwell, he demonstrated that both electric- and magnetic fields travel through space as: "… waves moving at the speed of light …". Furthermore, Maxwell also proposed that light, is in fact, undulations in the same medium that is the cause of electric and magnetic phenomena. Thus, with the: Unification of light and electrical phenomena, this led to the prediction of the existence of what we now know today, as simply: radio waves.

number of frequencies of electromagnetic waves, with them all travelling at the speed of light. This notable and fundamental research, was the first indication of the existence of the entire electromagnetic spectrum. Furthermore, Maxwell's predicted waves, also included certain waves that occurred at very low frequencies when compared to infrared, which theoretically might be created by oscillating charges in a certain type of ordinary electrical circuit of.

In 1886, Heinrich Hertz—see Footnote 12—built an apparatus to generate and detect what is now known as radio waves, whilst attempting to prove Maxwell's equations and to detect such low frequency electromagnetic radiation. Hertz then established these waves and was able to infer (i.e. by measuring their wavelength and then multiplying it by their frequency) that they travelled at the speed of light. What is more, Hertz also confirmed that this new radiation could either be reflected, or refracted by various dielectric media, in a similar fashion to that of light. Hertz's new definition of types of waves then laid the foundations for the way forward for inventions such as the wireless telegraph and then subsequently, to that of the invention of the radio.

In 1895, Wilhelm Röntgen[23] noticed a new type of radiation emitted during an experiment with an evacuated tube subjected to a high voltage. Röntgen entitled these newly found radiations as X-rays, where he established that they were capable of travelling through certain parts of the human body, but were reflected, or stopped by denser physical matter—such as bones. Subsequently and not long after this was known, this newly developed X-ray technique found considerable and varied uses in the field of medicine. Finally, the last portion of the electromagnetic spectrum was completed with the discovery of gamma rays. In 1900, Paul Villard[24] was investigating the radioactive emissions of radium, when he identified a new type of radiation that he initially believed consisted of particles similar to the known alpha- and beta particles, but with the considerably more penetrating power. However, of some significant interest was that in 1910, William Henry Bragg[25]

---

[23]**Wilhelm (Conrad) Röntgen**: (Born: 27 March 1845 in Remscheid, Germany—died: 10 February 1923 in Munich, Germany) was an eminent German Physicist, who, on 8 November 1895, produced and then detected electromagnetic radiation in a wavelength range that today is known as: X-rays, or Röntgen rays—an achievement that earned him the first Nobel Prize in Physics (1901). In honour of Röntgen's accomplishments in 2004, the International Union of Pure and Applied Chemistry (IUPAC), named after him the element 111, which is now known as: Roentgenium—this being a radioactive element with multiple unstable isotopes.

[24]**Paul (Ulrich) Villard**: (Born: 28 September 1860—died: 13 January 1934) was a significant French Chemist and a notable Physicist, from Saint-Germain-au-Mont-d'Or, Rhône, who later died in Bayonne in France. Villard was credited with discovering: gamma rays in 1900, while studying and researching into the effects of radiation emanating from that of Radium.

[25]**Sir William Henry Bragg** OM, KBE, PRS: (Born: 2 July 1862—died: 10 March 1942) was a British/Australian: Physicist; Chemist; Mathematician. Bragg (i.e. uniquely in Science) shared a Nobel Prize in Physics in 1915 with his son: William Lawrence Bragg: "… for their services in the analysis of crystal structure by means of X-rays …". Previously, their joint research work was undertaken by using an: X-ray Spectrometer—of the X-ray spectra, with that of X-ray diffraction, and investigating the atomic crystal structure, where they developed their notable scientific contributions to the field. While just ten years later, their seminal book: *X-rays and Crystal Structure* (1915)—had reached its 5th Edition. Of note, was the mineral Braggite was named after both: Bragg Snr and Jr.

demonstrated that gamma rays are an electromagnetic radiation and not simply particles. In 1914, Ernest Rutherford[26] who in 1903 had named these so-called particles gamma rays, realised that they were fundamentally different from that of the known charged alpha- and beta rays. Edward Andrade,[27] actually measured their wavelengths, and found that these gamma rays were similar to X-rays—but with shorter wavelengths and higher frequencies.

In summary, it is possible to state that the electromagnetic spectrum is, "The range of all possible frequencies of electromagnetic radiation". The electromagnetic spectrum of an object—see the diagram in Fig. 6.16 (top)—has a different meaning and is instead, the characteristic distribution of electromagnetic radiation emitted, or absorbed, by that particular object. Consequently, the electromagnetic spectrum extends from below the low frequencies utilised for modern radio communication to that of gamma radiation at the short wavelength (i.e. high frequency) end thereby achieving an all-encompassing spectrum of the wavelengths ranging from thousands of kilometres down to a fraction of the size of an atom. The upper limit for these exceedingly long wavelengths is the virtual size of the universe itself, while it is thought that the shortest wavelength limit is in the vicinity of the Planck length[28]—although in principle the spectrum is both infinite and continuous. The majority of portions of the electromagnetic spectrum are utilised in science and engineering for spectroscopic and other probing interactions for

[26]**Ernest Rutherford**—was the 1st Baron Rutherford of Nelson, OM FRS: (Born: 30 August 1871 in Brightwater, Tasman District, in New Zealand—died: 19 October 1937 in Cambridge, England), was a New Zealand-born British Physicist, who became known as simply the: "Father of Nuclear Physics". In Rutherford's early work, he discovered the concept of: radioactive half-life—proving that radioactivity involved: "… the transmutation of one chemical element to another …", moreover, Rutherford also differentiated and named alpha- and beta radiation. Rutherford performed his most famous work after he became a Nobel laureate—in 1908. In 1911 and although he could not prove that an atom's charge was either positive, or negative, Rutherford theorised that atoms have their charge concentrated in a very small nucleus, and thereby he pioneered the so-called: Rutherford model of the atom—through his discovery and interpretation of Rutherford scattering in his famous Gold foil experiment. In 1917, Rutherford was widely credited with the first: splitting of the atom—in a nuclear reaction between nitrogen and alpha particles, in which he also discovered and subsequently named the proton.

[27]**Edward (Neville da Costa) Andrade** FRS: (Born: 27 December 1887—died: 6 June 1971) was an English Physicist; writer; as well as a poet. Andrade notably told The Literary Digest—when interviewed—that his unusual name was pronounced: "… as written, that is, like air-raid, with and substituted for air". Specifically, Andrade is principally known for his fundamental research and scientific collaborative work with Ernest Rutherford, and it was where he first determined the wavelength of a type of gamma radiation.

[28]**Planck length**: in Physics, this so-called Planck length is denoted by '$\mathbf{l_P}$' which is a unit of length, equal to: $1.616199(97) \times 10^{-35}$ m. It is a base unit in the system of Planck units—developed by Physicist **Max Planck** (**Max (Karl Ernst Ludwig) Planck**, FRS: (Born: April 23, 1858 in Kiel, Duchy of Holstein, Germany—died: October 4, 1947 in Göttingen, Lower Saxony, Germany) was an eminent German Theoretical physicist, who originated Quantum theory, for which he won the Nobel Prize in Physics—in 1918). Consequently, the Planck length can be defined from three fundamental physical constants: (i) the speed of light in a vacuum; (ii) Planck's constant; (iii) the gravitational constant.

techniques utilised to study and characterise matter. In addition, radiation from various parts of the spectrum have found many other scientific uses, notably for communications and, today, in explicit manufacturing engineering applications.

6.6.2 Thermography—Further Information

In both science and engineering, thermal images, or thermograms—see Figs. 6.17 and 6.18 (middle)—are actually visual displays of the amount of infrared energy being: emitted; transmitted; also reflected; by an object under surveillance. As there are multiple sources of the infrared energy, it is somewhat challenging to get an accurate temperature of an object being investigated employing this technique. With a Thermal imaging camera—see Figs. 6.16 (bottom) and 6.17 (top-left)—this type of camera is capable of performing algorithms to interpret any thermal data and build up a representative thermographic image, granting the fact that these thermal image displays to the viewer are an approximation of the temperature at which the object is operating. At this time, the camera is actually utilising multiple sources of data, based on the areas surrounding the object to determine that value, rather than detecting the actual temperature. This variation in thermal phenomenon, may become clearer with consideration of the following expression:

$$\text{Incident energy} = \text{Emitted energy} + \text{Transmitted energy} + \text{Reflected energy}$$

where:

Incident energy = energy profile (i.e. when viewed through a thermal imaging camera);
Emitted energy = generally what is intended to be measured;
Transmitted energy = energy that passes through the subject (i.e. from a remote thermal source);
Reflected energy = amount of energy that reflects off the surface of the object from a remote thermal source.

Consequently, if an object is radiating at a higher temperature than its immediate surroundings, then a measurable power transfer will occur and this power will radiate from a warm-to-cold body, as predicted by the Second Law of Thermodynamics.[29]

[29]**Second Law of Thermodynamics** (This Second law may be expressed in many specific ways, but the first formulation was credited to the notable French Scientist: (Nicolas Léonard) in 1824, or **Sadi Carnot**—as he was invariably known. Sadi Carnot (Born: 1 June 1796 in Palais du Petit-Luxembourg—died: 24 August 1832 also in Paris), was also a distinguished French Military engineer and Physicist, often being described as the: "Father of Thermodynamics". NB **First Law of Thermodynamics**, provides the basic definition of thermodynamic energy, also termed: Internal energy this being associated with all thermodynamic systems, but it is unknown in Classical mechanics, and in its most simple of terms, it states: "The rule of the conservation of energy in nature"), states that: "The entropy of an isolated system never decreases, because isolated systems always evolve towards thermodynamic equilibrium, a state with maximum entropy". This Second law, is an empirically validated postulate of thermodynamics.

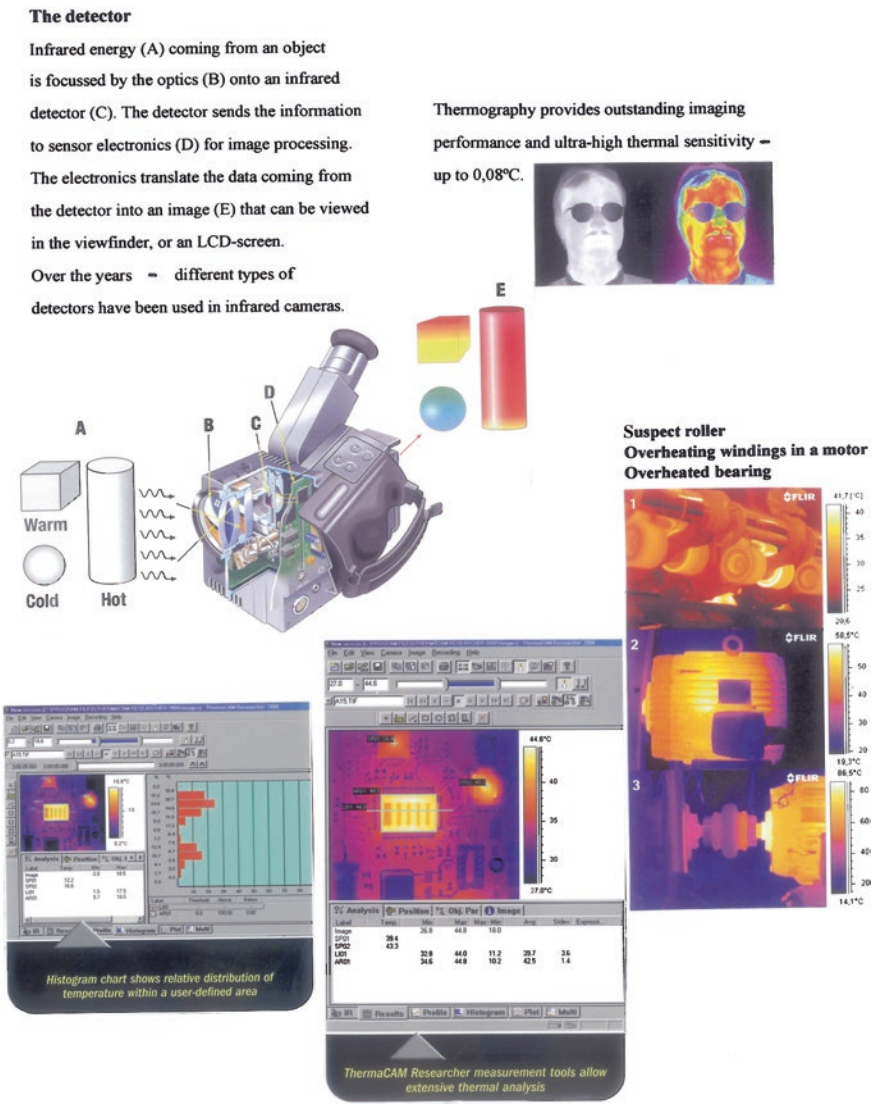

Fig. 6.17 Infrared thermography: for diagnostic assessment of industrial plant (courtesy of Flir Systems)

As a result, if there is a cool area in the thermogram, that object will absorb the radiation emitted by the warm object. The ability of a range of objects to emit, or absorb this radiation is called emissivity—see Sect. 6.6.4.

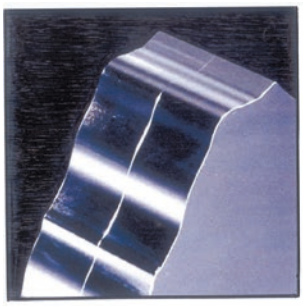

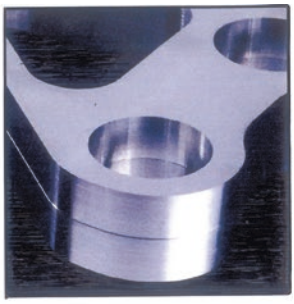

Profile of the *'Watzman mountain'* (left) using *free-form surfaces* shows a distinct dividing line where the *semi-closed-loop side milling* reference *changed* due to *thermal expansion* between milling passes.

This coupling lever (right) was milled with two passes. The semi-closed loop side of the rotary encoder shows a distinct demarcation line where *heat-induced expansion* created an offset in the dimension.

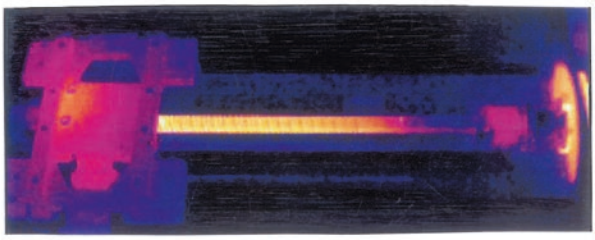

This *'thermographic snapshot'* image, shows the *heating* of a *Recirculating ballscrew* during *multi-pass milling* at 10 m min^{-1}, temperature range is depicted in the lower graph ranging up to +40°C. [Source: J. Kummetz & J. Heidenhain (Machine Design Aug. 2008)]

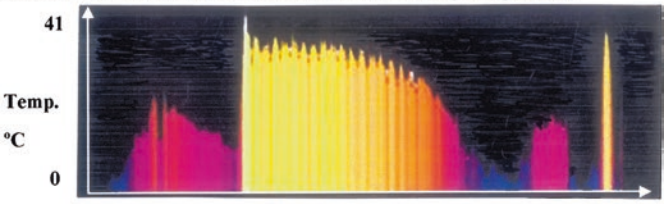

Sectional cutaway diagram of a recirculating ballscrew for a typical CNC machine tool.

[Courtesy of THK America, Inc. (Schaumberg, Il, USA)]

Fig. 6.18 The thermal effects of machine tool elements such a the *recirculating ballscrew*, will undoubtably have an *affect* on the *accuracy* and *precision* of the *machined part*

6.6.3 Thermal Imaging Cameras

A typically available commercial Thermal imaging camera—see Figs. 6.16 (bottom) and 6.17 (top-left)—will exploit a series of mathematical algorithms to determine the actual thermogram. Since the camera is only able to perceive that part of the electromagnetic radiation that is impossible to detect with the human eye, it will build up an image in the viewer and record a visible picture—such as that produced in a JPG format. As a result, in order to execute the role of a non-contact temperature recorder, the camera will change the temperature of the object being viewed with its emissivity setting. What is more, other types of algorithms can be utilised to affect the measurement, including the transmission ability of the transmitting medium (i.e. usually air) and the temperature of that transmitting medium. All of these settings will affect the ultimate output for the temperature of the object being viewed. This type of functionality ensures that the Thermal imaging camera is an excellent instrument for the maintenance of both electrical and mechanical systems in science and industry, also for applications in commerce—see Figs. 6.17 and 6.18. As a consequence, by incorporating the correct camera settings and by being mindful when capturing the thermal image, typical electrical/mechanical systems could be scanned and problems then established and afterward rectified. In the instance of energy savings, these Thermal imaging cameras can achieve somewhat more, because they can see the radiating temperature of an object together with what that object is radiating at, with the product of this thermal radiation being calculated by means of the: Stefan–Boltzmann constant.[30]

Over the past fifty years or so, the commercial application and use of thermography has steadily increased and even more dramatically of late for numerous and diverse industrial applications also for various health and safety situations. Machine tool maintenance technicians have utilised thermography to locate overheating joints, hot bearings and motors, which when excessively heated, are an immediate sign of impending failure—see Fig. 6.17 (middle-right). Thermographic cameras can detect radiation in the infrared range of the electromagnetic spectrum (i.e. here ranging from: ≈9000 to 14,000 nm, or ≈9 to 14 μm) and can produce images of that radiation, which have previously been described (above) as basically thermograms.

[30]**Stefan–Boltzmann constant** (i.e. also termed: **Stefan's constant** [The Austrian Physicist: **Josef Stefan**, formulated this constant in 1879 and it was later derived in 1884, by yet another Austrian Physicist: **Ludwig Boltzmann**—hence the joint theoretical name for this constant. Accordingly, this Stefan–Boltzmann equation can also be derived from Planck's Law]): which is a physical constant denoted by the Greek letter 'σ', which is the constant of proportionality in the Stefan–Boltzmann law, which states that: "The total intensity [Physics] radiated over all wavelengths increases as the temperature increases, of a black body which is proportional to the fourth power of the thermodynamic temperature". This explicit theory of thermal radiation underpins the current theory of: **Quantum mechanics**—by utilising the application of its Physics to relate to the: molecular; atomic; and subatomic levels—of all known substances.

As infrared radiation is emitted by all objects above the temperature of absolute zero—according to the Black-body radiation law,[31] thermography enables one to see the thermal environment with or without visible illumination. It has already been established that the amount of radiation emitted by an object increases with temperature and for that reason, thermography allows one to see variations in temperature. When viewed through a thermal imaging camera, any warm objects will be enhanced against cooler backgrounds, such that humans and other warm-blooded animals become easily visible against their environment, either by day or night—see Fig. 6.17 (top-right). Consequently, the scientific field of thermography is particularly useful to many military investigations and other users of these types of surveillance cameras. Often the live thermogram can reveal temperature variations so clearly that a photograph becomes unnecessary for thermal analysis. Non-specialised CCD- and CMOS sensors have most of their spectral sensitivity in the visible light wavelength range. Nevertheless, by utilising the trailing area of their spectral sensitivity—namely that the part of the infrared spectrum called Near-infrared (NIR)—and by utilising an off-the-shelf CCTV camera, it is possible under certain circumstances to obtain true thermal images of objects with temperatures at ≈280 °C, or even higher.

Some of the more specialised Thermal imaging cameras use Focal plane arrays (FPAs), which can respond to much longer wavelengths, namely, within the mid- and long-wavelength infrared vicinity, with the most common types tending to be: InSb; InGaAs; HgCdTe; also QWIP FPA. Additionally, with the newest technologies, these cameras can utilise low-cost, uncooled microbolometers—as their FPA sensors. Typically, their image resolution is considerably lower than that of optical cameras, mostly in the range: 160 × 120; or 320 × 240 pixels; but some are now up to 640 × 512 pixels—for the most expensive models. These commercial

[31]**Black-body radiation law** (The term Black-body was originally introduced in 1862, by the eminent German Physicist: **Gustav (Robert) Kirchhoff** (Born: 12 March 1824 in Königsberg, East Prussia (Germany)—died: 17 October 1887 in Berlin, Germany). Kirchoff was educated at the University of Königsberg, completing his studies in 1847. Kirchhoff contributed so much to our fundamental understanding of: Electrical circuits; Spectroscopy; but more specifically here, in the emission of Black-body radiation—by heated objects): this is the type of electromagnetic radiation within, or surrounding a body in thermodynamic equilibrium with its environment, or alternatively, being emitted by a black-body (i.e. this being either an opaque, or non-reflective body) which is held at constant, uniform temperature. Consequently, the radiation has a specific spectrum and intensity that depends only on the temperature of this body. Moreover, it was Kirchhoff who contributed significantly to the field of Spectroscopy, by formalising its three laws that describe the spectral composition of light emitted by incandescent objects, thus building substantially on the previous discoveries of both that of David Alter (Dr David Alter (Born: 3 December 1807 in Westmoreland County, Pennsylvania—died: 8 September 1881, in Freeport, USA), was a prominent American Inventor and Scientist of the nineteenth century. While living in Freeport: "… In the great Pittsburgh Fire of 1845 …", he found a shard of glass that had melted and solidified, which in the light, gave him the idea of the light spectrum, afterward, he went on to discover Spectral Analysis—in 1853) and Anders Jonas Ångström (Anders Jonas Ångström (Born: 13 August 1814 in Lögdö, Medelpad, Sweden—died: 21 June 1874 in Uppsala, Sweden) was a distinguished Swedish Physicist and one of the founders of the Science of Spectroscopy). Of some note was that the: **Ångström** unit (i.e. 1 Å $= 10^{-10}$ m) with which the lengths on a scale of the wavelength of light, or interatomic spacings in condensed matter is measured—was named after him—moreover, the Ångström unit is also used in both Crystallography, as well in Spectroscopy.

Thermal imaging cameras are much more expensive than their visible spectrum counterparts and the higher end models are often export-restricted—due in the main, to certain military sensitivities and their subsequent uses for such technology. Moreover, the somewhat older types of Bolometers, or more sensitive models such as InSb require cryogenic cooling, this being normally achieved by a miniature Stirling-cycle refrigerator,[32] or by liquid nitrogen.

6.6.4 Emissivity—Thermal Radiation

The term Emissivity[33] represents a material's ability to emit thermal radiation. As a consequence, each material has a different emissivity and it can be somewhat difficult to determine the appropriate emissivity for a subject currently under examination. In practice, a material's emissivity can range from a theoretical 0.00 (i.e. when completely not emitting) to an equally theoretical 1.00 (i.e. when completely emitting) which means that the emissivity often varies with temperature. By way of an example of a substance with low emissivity, this could be silver—having an emissivity coefficient of 0.02, while an example of a substance with high emissivity would be say, asphalt—with an emissivity coefficient of 0.98.

A black body—which has already previously been described—is a theoretical object which will radiate infrared radiation at its contact temperature. Hence, if a thermocouple on a black body radiator reads 50 °C, the radiation of a black body will also emit an identical temperature, namely 50 °C. Consequently, as just described, a true black body will have an emissivity of 1.00. Furthermore, a perfect black body cannot really exist—just in theory—but the infrared radiation of normal objects will appear to be less than the contact temperature. The rate (i.e. the percentage) of emission of infrared radiation will, in consequence, be a fraction of the true contact temperature. This fraction is known as its emissivity. Certain objects have different emissivities in long-wave, when compared to mid-wave emissions, also emissivities may also be subject to change as a function of temperature in some materials.

---

[32]**Stirling-cycle refrigerator**: thus, the **Stirling-cycle** is a thermodynamic cycle that describes the general class of Stirling devices, which includes the original Stirling engine that was invented, developed and patented in 1816 by the **Reverend Dr. Robert Stirling** (The Reverend Dr Robert Stirling (Born: 25 October 1790—died: 6 June 1878) was a Scottish clergyman)—with help from his brother, who was an Engineer. The cycle is reversible, meaning that if supplied with mechanical power, it can function as either a heat pump for heating, or more specifically here, for the Thermographical-applications of cryogenic cooling.

[33]**Emissivity**: of a material (i.e. which is usually written as: 'ε', or 'e'), being simply defined as: "The relative ability of its surface to emit energy by radiation". Furthermore, this emissivity is the ratio of energy radiated by a particular material to energy radiated by a black-body—at the same temperature. Consequently, a true black-body would have a $\varepsilon = 1$, while any real object would have a $\varepsilon < 1$. It should also be said, that emissivity is considered as a dimensionless quantity. For example, a high-quality mirrored surface may reflect 98 % of the energy, while absorbing just 2 % of this energy, conversely, a good black-body surface will reverse this ratio, here under these conditions, this body will absorb 98 % of the energy and reflect only 2 %.

When taking a temperature measurement of an object, the Thermographer (i.e. the user), will refer to the emissivity table to choose the emissivity value of the object, which is then entered into the camera. Once this emissivity value has been entered, the camera's algorithm will then correct the temperature by utilising its preselected emissivity to calculate a temperature that more closely matches the actual contact temperature of the object under test. Whenever possible, the Thermographer should attempt to test the emissivity of the object in question; this action, would be more accurate than attempting to determine the emissivity of the object, via an emissivity table. The normal technique—whenever possible—of testing for a subject's emissivity, is to place a material of known high emissivity in contact with the surface of the object. As a consequence, the material of known emissivity can be as complex as industrial emissivity spray—which is produced specifically for this purpose, or it can be as simple as a standard piece of black insulation tape—having a consistent emissivity of 0.97. Once emissivity has been established, a temperature reading can then be taken of the object, with the emissivity level on the imager set to the value of this test material—giving an accurate value of the temperature of the test object. Afterward, the temperature can simply be read on a part of the object not covered by the test material. If the temperature reading is different, then the emissivity level on the image can be adjusted until the object reads an identical temperature. This operation, will give the Thermographer a much more accurate emissivity reading. It should also be emphasised, that there are certain times, however, when an emissivity test is not possible due to either dangerous, or inaccessible conditions. Under such dangerous circumstances and apparent hostile situations, the Thermographer must simply rely on their emissivity tables.

6.6.5 Advantages and Limitations of Thermography

As with any form of sophisticated instrumentation, there are always going to be both certain advantages and disadvantages for Thermographic practical usage in any given industrial application, with some of the main ones being listed below:

- **Advantages of thermography**
  - it can show a visual picture so any temperatures over a large area can be compared;
  - it has the capability of catching moving targets in real time;
  - it has the ability to find deteriorating (i.e. higher temperature) components, prior to their failure;
  - the technique can be utilised to measure, or observe in areas that are either inaccessible, or hazardous for other test methods;
  - the technique is a non-destructive test (NDT) technique;
  - it can be used to find defects in a range of industrial assemblies, or parts, such as: shafts; bearings; gears; pipes; also other metals, or even for certain plastic parts;
  - it may be utilised to detect objects in dark areas;

- **Disadvantages of thermography**
  - Thermography cameras of high-quality usually also have a high price range, which means that currently they are often in the region of >$4000(US), while cheaper ones are at present limited in their sensitivities, ranging from: ≈40 × 40 to ≈120 × 120 pixels;
  - images can be difficult to accurately interpret when based upon certain objects—specifically those that might occur with either erratic, or fluctuating temperatures. Nonetheless, this interpretation problem is to a certain extent reduced by the technique of active thermal imaging;
  - sometimes accurate temperature measurements are hindered by differing emissivities and reflections from adjacent surfaces;
  - most Thermal imaging cameras have ±2 % accuracy, or worse, in measurement of temperature and as such, are not as accurate as many forms of contact methods;
  - a camera will only be able to directly detect surface temperatures (i.e. by having an actual line-of-sight condition);
  - the condition of work, depending on the particular situation, can be somewhat dramatic, when there is a: 10 °C of difference between internal/external readings; if say, there is a maximum of 10 km h^{-1} of wind occurring; in conditions of direct sunlight; or if recent rain has occurred; …etc.

6.6.6 Effects of Temperature Variation in Machine Tools

The thermal effects within a machining environment have a major influence on the structural changes in a machine tool in usage and hence, affect the machined workpiece accuracy—see Fig. 6.19. It is also a well-known fact that all materials will either expand, or contract when they are either heated up, or cooled down—specifically during the machine tool's actual working day, which subsequently changes the measured dimensional features on components—see Fig. 6.20a. Furthermore, any form of expansion and contraction will create a distortion in the machine tool and affect its actual positioning accuracy. Over the years, researchers have shown that this machine tool thermal distortion, can create between 40 and 70 % of all dimensional errors on precision machined parts. Hence, any minute temperature changes can make a significant difference in a component's machined quality; this can be demonstrably shown by the so-called Watzman mountain effect[34]—see Fig. 6.18 (top).

[34]**Watzman mountain effect** (This Watzman mountain effect was originally named after the actual Watzman mountain—as it has a distinctly similar rugged profile—that resembles an identical twin-peak effect. This actual mountain is in the Bavarian Alps, south of Berchtesgaden. Of geographical note, rather than for its technical interest, is that it is the third highest mountain in Germany, and the highest located entirely on German territory at an elevation of: 2713 m): has been coined for the machined profile that resembles this Watzman mountain when utilising and machining any free-form surfaces, which shows a distinct dividing line where the semi-closed-loop side milling reference changes, due to thermal expansion between each separate profiling–milling pass.

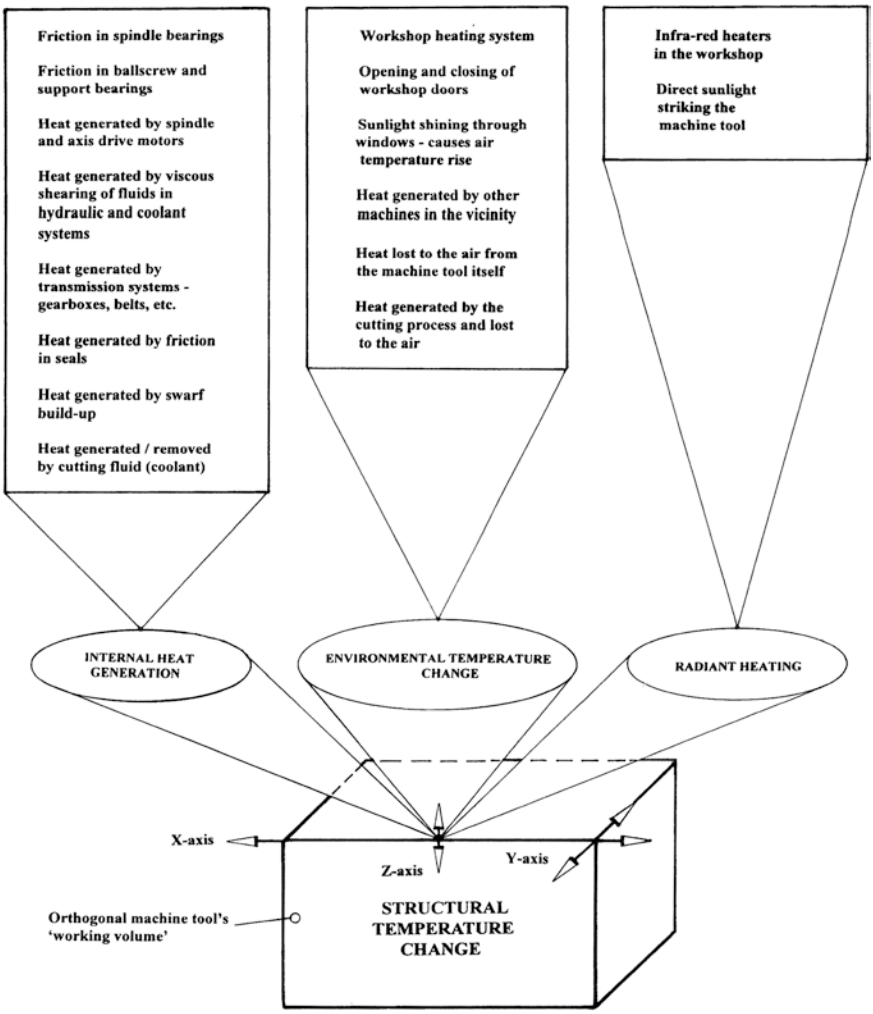

Fig. 6.19 Potential causes for structural changes in the machine tool—due to temperature effects (adapted from Postlethwaite, Allen and Ford, 1999)

By way of an example of these differing temperature effects, a 450 mm-long steel gauge will change its dimension by 0.00005 mm with an alteration of just 1⁄30 °C. Additionally, in an industrial machine shop that has experienced a 1.5 °C change on a 450 mm-long steel component will involve a dimensional size modification of: ≈0.005 mm (≈5 μm). Despite the fact that this variation may only be critical with specific tight tolerance dimensional features on items such as Precision gauges, a more extreme temperature excursion will clearly reduce overall its tolerance zone quite significantly. To press this point still further, an

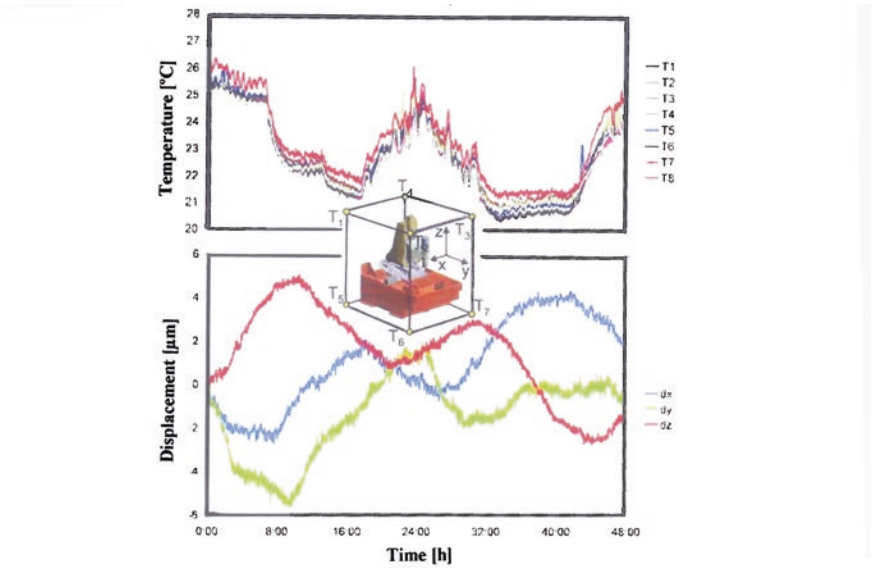

(a) **The environmental influences depend on the position of the machine tool in the shop, with the most important feature being the machine's environment. This effect is indicated by *time-dependent fluctuations* of the *air temperature* and *horizontal and vertical gradients*. The variation of the air temperature reduces the thermal steady-state of a machine tool and its associated: constant thermal behaviour. While, the same conditions apply to the speed, or load dependent influences. Due to the actual dimensions of the machine elements - especially large machine tools, they are influenced by any dissimilarities in vertical temperature gradients.**
[Source: RWTH Aachen University Germany (Nov. 2011]

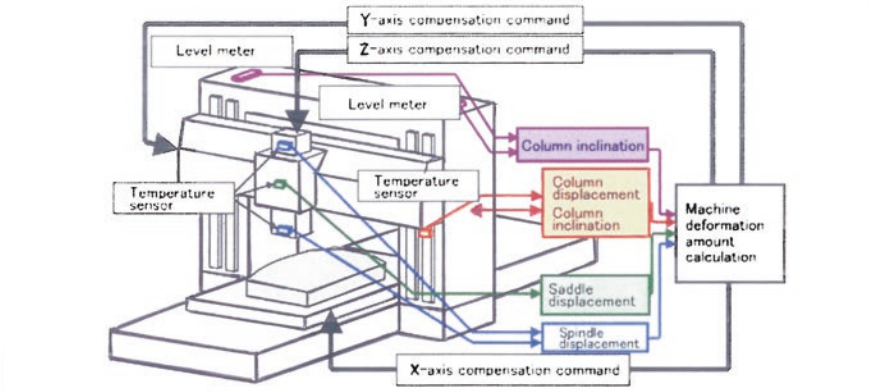

(b) **Thermal displacement prediction and compensation technology by usage of the *'Thermal analysis technology'*. By integrating three *'Advanced Thermal Displacement Suppression Systems'* (i.e. ATDS): 1. Structure; 2. Cooling system; and 3. Prediction and compensation; in a well-balanced manner based on *'Thermal analysis simulation technology'* - so here then, its effects caused by thermal displacement can be significantly reduced.**
[Source: Mitsubishi Heavy Industries, Ltd. (MHI) Japan (2014)]

Fig. 6.20 Any machine tool configuration—especially a 'C-frame' vertical machining centre, will distort if the thermal environment changes significantly

aluminium component of the same length as a steel part, will have an even greater thermally induced error of double that of the equivalent steel part, because aluminium has twice steel's coefficient of thermal expansion [e.g. 23 for pure aluminium versus the hardened steel's value of 12.4 ($\alpha \times 10^6$ °C^{-1})]. So, when the machine tool experiences an increase of 1.5 °C, the workpiece feature being produced can vary by much more than the expansion caused by this relatively small 1.5 °C increase, because the heat will thermally distort the machine's overall geometry and create an out-of-position effect of the tool, relative to that of the part's feature—see Figs. 2.8a and 6.19. In several previous applied research programmes, it has been shown that by utilising relatively simple thermal controls—see Fig. 6.20b—many machine shops can increase their machined part accuracy by >50 %. For example, in just one such study, which was undertaken at The National Taiwan University by K.C. Fan and his research associates thermally compensated for temperature changes on a 3-axis column CNC mill, reducing the spindle growth dimensional errors from: 53 μm to just 18 μm, coupled with an impressive reduction in errors in both the *X*- and *Y*-axis positions ranging from: 40 μm to only 20 μm.

In reality, there are two significant aspects of machine tool thermal control, these are:

1. **defining a temperature standard**—usually based around ambient (ideally, 20 °C). Here, the part dimensional measurements should be undertaken at a temperature that both the buyer and seller of the machine tool can agree upon—with accurate part measurements dependent on establishing the workpiece's temperature with any associated gauges at the same working temperature;
2. **controlling temperature variations**—minimising temperature fluctuations to within ±2 °C. This action requires consideration for either controlling, or compensating for all of the following: machine tool's temperature within the shop; the component's temperature; the actual room's air temperature; the floor temperature, ceiling and wall temperatures; coolant temperature; plus the removal of hot chips from the machine's working envelope. Further temperature control is also necessary for other relevant heat-sources within the workshop, including: any other machine tools; also pumps; windows; and personnel—from daytime to night shifts. Other consideration will be taken for any other variations within the machine shop, for example, noting that temperatures near the ceiling are higher than temperatures near the floor, also that temperatures near a window could be either higher, or lower—depending upon the specific season of the year.

At present, much of the existing temperature control research, is now being typically focused on providing improved and Advanced Thermal Displacement Systems (ATDS)—as shown in Fig. 6.20b—for control of machine tools to accommodate these thermal changes, with some effort being targeted upon flood coolant and its high-pressure delivery, plus the means to surround these machine tools with stable temperature envelopes.

6.6.7 Controlling Component Part Temperatures

When about to commence machining very high precision parts, it is normal working practice for them to soak in ambient air within the workshop at the desired temperature—for several hours. This explicit action, will thereby tend to reduce any potential errors that would otherwise occur when subsequently machining components, because otherwise it causes the part to become hot and later to cool when returning them once again to ambient room temperature. In order to save significant time, some industrial users place their machined parts that have not been temperature stabilised to the desired temperature, in a liquid bath (typically oil) which forces a constant temperature liquid over the part.

Even though the previous techniques are successful, yet another temperature stabilisation approach might be to employ heat-exchangers that are commercially available and can help to maintain consistency to that of both the machine tool and hence the component part's coolant temperature. Accordingly, with the details available from appropriate handbook values for known thermal coefficients of expansion for the workpiece material in question, this will enable appropriate temperature settings to be utilised. It has also been noted that these actual coefficients are affected by slight changes in their: alloying elements; previous heat treatment condition; also from the amount of cold work undertaken (i.e. the internal deformation of the crystal- and grain structures) produced when say, a steel mill rolls the metal to a predetermined cold-rolled dimensional size. This means that the average published values given, may be incorrect by up to 20 % on certain potential workpiece materials to be subsequently machined. With this in mind, research has shown that, for example, the expansion of steel may vary from: 12.4 to $\approx$14 ($\alpha \times 10^6$ °C^{-1}), depending upon the steel's hardness and its exact metallurgical composition. For that reason, when machine tools, cutting tools, or component parts are based upon several differing materials that may also come from different batches, or lots, then in reality, it is very difficult to predict with accuracy and precision, these actual dimensional component part changes.

6.6.8 Minimising Heat Sources

As already discussed, windows and doors act as significant heat sink sources in a typical machine shop and the amount of heat they either let in, or lose, will also vary throughout the day. This is why, for many advanced machine shops that are involved in the machining of very high precision and accuracy parts, they are purpose-built without windows coupled with twin sets of independent opening/closing doors—to retain a semblance of thermal stability of the actual workshop's

ambient temperature when these doors are either opened, or closed. Nevertheless, the thermal strategy of simply blacking out windows that would otherwise allow the sun to shine directly onto machines, can be effective and simply reduce the temperatures within individual machine tools by several degrees and eliminate a significant part of the daily heat cycle—see an example of these temperature variable effects in Fig. 6.20a.

By the simple expedient of locating machine tools at some distance from the workshop's radiators and also its ventilators can somewhat lessen any localised temperature variations. Furthermore, the actual movement of people within the working environment can also produce some large thermal changes in a shop. Merely by having an Operator just standing in front of a high-quality and precision machine tool will add heat within the machining vicinity. Labouring this point still further, a Machine operator may not be a significant factor on a large and high-powered machine tool currently machining massive wide-toleranced parts—but any personnel should not be allowed to be adjacent to any form of low-powered and ultrahigh accuracy/precision machines that must effectively cut to tolerances such as: <0.000025 mm. This is because such Operational personnel will add too much heat to the work envelope and in so doing, they might affect the machine's thermal stability in an uncontrolled manner.

Probably one of the least costly thermal control strategies involves the correct use and application of the machine tool's coolant supply. By the application of copious flooding of aqueous-based coolant directly onto the workpiece, its machine tool's table, the fixturing, or a chuck, within the envelope's cutting area the localised temperature hardly changes. As such, this effective coolant strategy will keep and maintain the workpiece temperatures, also its machine beds, fixtures and workpieces at a controlled and specifically defined temperature. Moreover, this effective coolant flooding of the working-envelope, will also washaway any hot chips that would otherwise retain up to 80 % of cutting energy in the form of localised and undesirable heat. In most modern-day CNC machine tools, the aqueous-based coolant supply can characteristically be controlled to very tight limits of: ±0.02 °C; by utilising specially designed heat-exchangers—in the same manner as that of oil showers, which can also achieve similar temperature control effects.

6.6.9 Temperature Control Strategies

Any form of thermal improvement strategies, require consideration of all key heat generating issues. On the other hand, not all of the items must be precisely controlled, but they should be evaluated before allocating costly additional equipment

and associated financial resources. Here, some form of Error budget tabulation[35] when attempting to determine the correct thermal-strategy, may be of some help. In many workshops one can determine the amount of machine uncertainty caused by thermal effects by utilising: laser interferometers; or touch trigger/scanning probes (see further information on these topics in Chap. 2); to either calibrate/validate the positioning accuracy over time—at various conditions and workloads.

For most machine shops, possibly the lowest form of cost improvement strategy will be to simply reduce heat coming to the machine tool from either the machine shop's windows; doors; HVAC vents; or from adjacent machines. Moreover as was previously discussed, simply by soaking large parts in temperature-controlled solutions will provide a low-cost method of bringing potential workpieces to the desired machining operational temperature that they should attain—when any machining commences. Moreover, by utilising large volumes of temperature-controlled flood coolant on the machine—also just mentioned—this is yet another inexpensive, but effective thermal control strategy.

By boxing-in the footprint of a machine tool within its strategically positioned floor space with some form of temperature-controlled airflow, this might have the effect of sometimes inhibiting its machine accessibility, while also being somewhat costly, but this type of thermal isolation can provide some degree of a steady-state production operating environment for the machine tool. While yet another approach might be to modifying the machine's spindle to reduce the heat that it generates, or that it conducts into the adjacent machine elements, but this will normally require the end-user to work closely with their machine tool/spindle suppliers. By creating some form of thermal compensation to the actual machine tool's positioning requiring a one-off cost has the added advantage of creating minimal changes to this actual plant/equipment. Nevertheless, machine shop owners must determine if the actual machine tool manufacturer has previously incorporated any of these thermal solutions, which can account for any of these undesired temperature changes. If not, then such machine tool end-users need to undertake

[35]**Error budget strategies and their tabulation**—these budgets usually include: the four primary types of error, which are: (i) Geometric-; (ii) Load-induced-; (iii) Thermal-; or (iv) Process errors. For high-precision machines, the magnitude of each of these errors will be about equal, if there is a balanced allocation of resources. During the concept phase, the development of a geometric-based error budget should be four times better than that required for the entire machine. Therefore, at this point of evaluation:

(i) one could employ Homogeneous Transformation Matrix-based (HTMs) spreadsheets—as they will enable a company to investigate the overall geometry (and spacing) of these elements;
(ii) one might also use either solid models, or FEA, to ensure that these load-induced and thermal deflections are within prescribed limits.

Such Error budgets are useful for predicting both the accuracy and repeatability of a machine tool, furthermore, they can also be useful for helping to predict the misalignment loads on bearings. Hence, for more technical information regarding these: Error budgets—and more—see and obtain these details from: **FUNdaMENTALS of Design Error Budgets**, by Alexander Slocum Pappalardo—who currently is a Professor of Mechanical Engineering at The Massachusetts Institute of Technology, USA (slocum@mit.edu), for the latest version availability.

some applied research into how to simply control thermal changes—because their machined part accuracy output could well depend on any of these vital temperature control strategies that have now been incorporated into the machining environment.

References

Journal and Conference Papers

A Better Way to Protect Machine Spindles from Collisions, in: Design World, March 2014.

Ashworth, S., *The 3 R's: Retrofit, Rebuild and Remanufacture*, Cutting Tool Eng'g. Vol. 52 (8), Aug. 2000.

Attia, M.H. & Kops, L., *Thermometric design considerations for temperature monitoring in machine tools and CMM structures*, Int. J. of Adv. Manufact. Technol., Vol. 8 (5), 311-319, 1993.

Benes, J., *Errant performer, or scapegoat* [i.e. concerning: Machine tool spindle-errors], American Machinist, 38-41, Feb. 2007.

Berg, H., *Johann Wilhelm Ritter – The Founder of Scientific Electrochemistry*, Review of Polarography, Vol. 54 (2), 99-103, 2008.

Blackshaw, M., *Don't drift into distortion* [i.e. describing: Spindle-distortion], Quality Today, Feb. 1997.

Bryan, J.B., Clouser, R. & Holland, B., *Spindle accuracy*, American Machinist, 149-164, 1967.

Chatterjee, S., *Spindle deflections in high-speed machine tools — Modelling and simulation*, The Int. J. of Adv. Manufact.Tech., Vol. 11 (4), 232-239, 1996.

Chen, J-S. & Hsu, W-Y., *Characterizations and models for the thermal growth of a motorized high speed spindle*, Int. J. of Mach. Tools and Manufact., Vol. 43 (11), 1163–1170, Sept. 2003.

Cheng, H., Keer, L. & Mura, T., *Analytical Modelling of Surface Pitting in Simulated Gear Teeth Contacts*, SAE Tech. Paper No. 841086, 4,987-4,995, 1984.

Clough, D.A., Fletcher, S., Longstaff, A.P. & Willoughby, P., *Thermal Analysis for Condition Monitoring of Machine Tool Spindles,* J. of Physics: Conference Series, 364, 2012.

Courrech, J., *New Techniques for Fault Diagnostics in Rolling Element Bearings*, Proc. 40th Meeting of the Mechanical Failure Preventive Group, National Bureau of Standards, Gaithersburg, Md., April 16–18, 1985.

Courrech, J., *Examples of the Application of Gated Vibration Analysis for the Detection of Faults in Reciprocating Machines*, Noise and Vibration '89 Conference, Singapore, August 16–18, 1989.

Cui. L., Gao. W., Zhang, D., Zhang, H. & Han, L., *Thermal error compensation for telescopic spindle of CNC machine tool based on SIEMENS 840D system*, Trans. of Tianjin University, Vol. 17 (5), 340-343 Oct. 2011.

Design World, *Machine Tool - A better way to protect machine spindles from collisions*, 16-17, Aug. 2012.

Donaldson, R.R., *A simple method for separating spindle error from test ball roundness*, Annals. of the CIRP., Vol. 21, 125-126, 1972.

Evans, C.J., Hocken, R.J. & Estler, W.T., *Self-calibration: Reversal, redundancy, error separation and 'absolute testing'*, Annals of the CIRP., Vol. 42 (2), 483-492, 1997.

Fan, K-C., *An Intelligent Thermal Error Compensation System for CNC Machining Centers*, J. of Chinese Society of Mech. Eng'rs., Vol. 28 (1), 81-90, internet accessed: May, 2014.

Fletcher, S., Postlethwaite, S.R. & Ford, D.G., *Machine tool error identification and compensation advice system*, LAMDAMAP IV Int. Conf. Proc., 323-333, WIT Press, 1999.

Fletcher, S. & Ford, D.G., *Measuring and modelling heat transfer and thermal errors on a ballscrew feed drive system*, LAMDAMAP VI Int. Conf. Proc., 349-359, WIT Press, 2003.

Ford, D.G. & Postlethwaite, S.R., *Accuracy improvement for three axis CNC machining centres by geometric, load and thermal error compensation*, LAMDAMAP IV Int. Conf. Proc., 113-124, WIT Press, 1999.

Gillespie, L.K., *Cool Quality – Understanding and controlling thermal effects can improve part quality* [i.e. in Machine Tools], Cutting Tool Eng'g., 2014.

Harris, C.G, Williams, J.H. & Davies, A., *Condition monitoring of machine tools*, Int. J. of Product. Res., Vol. 27 (9), 1445-1464, 1989.

Hertz, H., *Über die berührung fester elastischer Körper* (Translation: *On the contact of rigid elastic solids*), in: *Miscellaneous Papers* - Jones and Schott (Editors), *J. reine und angewandte Mathematik* 92, Macmillan, London, 1896.

Hoskin, M., *William Herschel*, New dictionary of Scientific Biography Scribners, Vol. 3, 289–291, 2008.

Hsieh, K-H., Chen, T-R., Chang, P. & Tang, C-H., *Thermal growth measurement and compensation for integrated spindles*, The Int. J. of Adv. Manufact. Technol., Vol. 64 (5-8), 889-901, Feb. 2013.

Jorgensen, B.R. & Shin, Y.C., *Dynamics of Machine Tool Spindle/Bearing Systems Under Thermal Growth*, *Journal of Tribology, Vol.* 119(4), 875-882, Oct. 1997.

Keer, L. & Bryant, M., *A Pitting Model for Rolling Contact Fatigue*, *J. of Lubrication Technol., Trans. of the ASME,* Vol. 105, 198-205, April 1983.

Kruth, J-P., Vanherck, P. & Van den Bergh, C., *Thermal Compensation for a CMM Based on Interferometer Measurements and Testing its Applicability with a Thermal Stable Artefact*, Proc's of the 33rd Int. MATADOR Conf., 223-228. 2000.

Kuhnell, B.T. (Monash University, Australia), *How Age and Contamination Affect Rolling Bearings and Gears*, Machinery Lubrication Magazine, Sept./Oct., 2004.

Kummetz J. & Heidenhain, J., *Secrets of Accurate Machining*, in: Machine Design, 21 *Aug., 2008.*

Marsh, E. & Grejda, R., *Experiences with the master axis method for measuring spindle error motions*, Precision Eng'g., Vol. 24, 50-57, 2000.

McNamara, A., *Compensating for Thermal Expansion to Maintain Part Accuracy*, Moldmaking Technology, May 2008.

Meier, H., Pollmann, J. & Czechowicz, A., *Design and control strategies for SMA actuators in a feed axis for precision machine tools*, Production Eng'g., Volume 7 (5), 547-553, Sept. 2013.

Mian, N.S., Fletcher, S., Longstaff A.P. & Myers, A., *Efficient thermal error prediction in a machine tool using finite element analysis*, Meas. Science and Technol., Vol. 22 (8), 2011.

Neugebauer, R., Ihlenfeldt, S. & Zwingenberger, C., *An extended procedure for convective boundary conditions on transient thermal simulations of machine tools*, Production Eng'g., Vol. 4 (6), 641-646, Dec. 2010.

Nitske, R.W., *The Life of W. C. Röntgen, Discoverer of the X-Ray*, University of Arizona Press, 1971.

Popoli, W., *High Speed Spindle Design and Construction*, Modern Machine Shop, Aug. 1998.

Sin, H. & Suh, N., *Subsurface Crack Propagation Due to Surface Traction in Sliding Wear*, *J. of Appl. Mechanics, Trans of the ASME,* Vol. 51, 317-323, June 1984.

Starodubov, V.S., *Reducing and correcting the temperature deformation of numerically controlled machine tools*, Russian Engineering Research, Vol. 28 (2), 135-143, Feb. 2008.

Tseng, P-C., *A real-time thermal inaccuracy compensation method on a machining centre*, Int. J. of Advan. Manufact. Technol., Vol. 13 (3), 182-190, 1997.

White, A.J., Postlethwaite, S.R. & Ford, D.G., *An identification and study of mechanisms causing thermal errors in CNC machine tools*, LAMDAMAP IV Int. Conf. Proc., 101-112, WIT Press, 1999.

White, A.J., Postlethwaite, S.R. & Ford, D.G., *An investigation into the relative accuracy of ball-screws and linear encoders over a broad range of application configurations and usage conditions*, LAMDAMAP IV Int. Conf. Proc., 345-355, WIT Press, 1999.

Yang, J., Zhang, D., Feng, B., Mei, X. & Hu, Z., *Thermal-Induced Errors Prediction and Compensation for a Coordinate Boring Machine Based on Time Series Analysis*, Mathematical Problems in Engineering, Vol. 2014, Article ID 784218, 13 pages, Aug. 2014.

Zhang, H., Yang, J., Zhang, Y., Shen, J. & Wang, C., *Measurement and compensation for volumetric positioning errors of CNC machine tools considering thermal effect*, Int. J. of Advan. Manufact. Technol., Vol. 55 (1-4), 275-283, July 2011.

Zitney, E., *Turning to the Health of Machine Tool Spindles - By understanding how and why spindles can fail, operators can help to mitigate poor performance and keep machines running as intended* [Adapted from: SKF's state-of-the-art Spindle Service Center - information in: Mentor, OH, USA], American Machinist, July 2011.

Books, Booklets and Guides

Alban, L., *Systematic Analysis of Gear Failures,* ASM International (Metals Park, Ohio, USA), 1985.

ANSI/ASME Standard B89.3.4 M -1985, *Axis of Rotation: Methods for Specifying and Testing*.

ANSI/ASME Standard B5.54-1992*, Methods for Performance Evaluation of CNC Machining Centers*.

ANSI/ASME Standard B5.57-1998, *Methods for Performance Evaluation of CNC Turning Centers*.

Armstrong D. & Idhammar, T., *Maintenance Planning and Scheduling Book*, [Preventive Maintenance Management Books] IDCON Pub. (USA), Jan. 2006.

ASTM G40–13 Standard – 2006, *Standard Terminology Relating to Wear and Erosion*.

Bragg, William Henry (BRG880WH), A Cambridge-Alumni Database, University of Cambridge, 2014.

BS ISO 18434-1 - 2008: *Condition monitoring and diagnostics of machines. Thermography – General procedures*.

Carvill, J., *Mechanical Engineer's Data Handbook*, Butterworth Heinemann Pub., 1997.

Cottrell, A., *Edward Neville da Costa Andrade. 1887-1971*, Biographical Memoirs of Fellows of the Royal Society - 18: 1–0, 1972.

Davis, J.R., *Surface Engineering for Corrosion and Wear Resistance*, ASM International Pub., 2001.

de Ciurana, J., Quintana, G., & Campa, F.J., *Machine Tool Spindles*, [in: Machine Tools for High Performance Machining], Springer Pub., 75-127, 2009.

Deane, P.M., *The First Industrial Revolution*, Cambridge University Press, 1979.

Ding, Y. & Kuhnell, B., *The Physical Cause of Spalling in Gears*, *Machine Condition Monitoring, The Research Bulletin of the Centre for Machine Condition Monitoring*, Vol. 9, Monash University (Australia), 1997.

Dowson, D. & Higginson, G., *Elastohydrodynamic Lubrication*, SI Ed., Pergamon Press (UK), 1977.

Elert., G., *The Electromagnetic Spectrum*, The Physics Hypertextbook, Hypertextbook.com., retrieved 2014-04-16.

Fontana, M.G. & Greene, N.D., *Corrosion Engineering*, McGraw-Hill Int. Pub., 1978.

Griffin, E., *A Short History of the British Industrial Revolution*, Palgrave Macmillan (UK), 2010.

Hamilton, J., *A Life of Discovery: Michael Faraday, Giant of the Scientific Revolution*, New York: Random House, 2004.

ISO 230 Part 3- 2007, *Test conditions for metal cutting machine tools, Evaluation of Thermal Effects*.

ISO 6781, *Thermal insulation – Qualitative detection of thermal irregularities in building envelopes – Infrared method.*

ISO 18434-1, *Condition monitoring and diagnostics of machines – Thermography – Part 1: General procedures.*

ISO 18436-7, *Condition monitoring and diagnostics of machines – Requirements for qualification and assessment of personnel – Part 7: Thermography.*

Johnson, K. L., *Contact mechanics*, Cambridge University Press, 1985.

Kuhn, T. S., *Black–Body Theory and the Quantum Discontinuity*, Oxford University Press, 1978.

Lanza, G., Werner, P., Appel, D. & Behmann, B., *Increased Trustability of Reliability Prognoses for Machine Tools*, in: Globalized Solutions for Sustainability in Manufacturing, Springer Pub., 225-228, 2011.

Loudon, R., *The Quantum Theory of Light* (3rd Ed.), Cambridge University Press, 2000 [1973].

Maldague X. P. V., Jones T. S., Kaplan H., Marinetti S. & Prystay M., in: Chapter 2, *Fundamentals of Infrared and Thermal Testing: Part 1. Principles of Infrared and Thermal Testing,* Nondestructive Handbook, Infrared and Thermal Testing, Vol. 3, 3rd Ed., Columbus, Ohio, ASNT Press, 2001.

Mehta, A., *Introduction to the Electromagnetic Spectrum and Spectroscopy*, from: Pharmaxchange.info. - retrieved: 2014-04-16.

Mobley,P.K., *An Introduction to Predictive Maintenance* (2nd Ed.), Elsevier Science (USA), 2002.

Nimmo, B. & Hinds, G., *Beginners Guide to Corrosion*, NPL Guide, Feb. 2003.

O'Connor, P., *Practical Reliability Engineering*, John Wiley & Sons, 2012.

Rabinowicz, E., *Friction and Wear of Materials*, 2nd Ed., John Wiley and Sons (New York), 1995.

Schaffer, J.P., Saxena, A., Antolovich, S.D., Sanders Jr., T.H. & Warner. S.B., *Science and Design of Engineering Materials* (2nd Ed.), WCB NcGraw-Hill (Boston), 1999.

Sier, R., *Hot air caloric and stirling engines. Vol.1, A history* (1st Ed. (Revised), by Mair, L.A., 1999.

Smith, G.T., *Cutting Tool Technology – Industrial Handbook*, Springer-Verlag (London) Pub., 2008.

Tolstoy, I., *James Clerk Maxwell: A Biography*, University of Chicago Press, 1982.

WZL- RWTH Aachen, DFG-Project: *Compensation of the Environmental Influences on the Machining Accuracy of Machine Tools*, Nov. 2011.

Chapter 7
Uncertainty of Measurement and Statistical Process Control

"Fere libenter homines id quod volunt credunt."
TRANSLATION:
"Men are nearly always willing to believe what they wish."
Gaius Julius Caesar
[100–44 BC].
(In: Book 3, Sect. 18; By—De Bello Gallico, 51 BC).

7.1 Conformance, Traceability and Measurement Uncertainty

Introduction

With the dramatic effect of globalisation of trade in the more recent decades, this has refined the world's industrial focus on demands for the conformance of components to exacting customer specifications. If a manufacturing or metrological problem in customer–supplier disagreements occurs—as to a product's-compliance—then this can be exceedingly costly to all of the interested parties involved. In the case of dimensional metrology, the latest national and international standards have addressed questions of conformance of both its respective geometric dimensioning and tolerancing (GD&T)[1] specifications, recognising the

[1]**Geometric Dimensioning and Tolerancing** (**GD&T**) (There are several international standards available worldwide that describe the symbols and define the rules utilised in typical GD&T. One such well-recognised international standard has been produced by The American Society of Mechanical Engineers, this being: (ASME) Y14.5-2009): that is, a system for defining and communicating engineering tolerances. Consequently, this Geometric Dimensioning and Tolerancing (GD&T) utilises an internationally recognised form of symbolic language on engineering drawings and computer-generated three-dimensional solid models, which explicitly describes the nominal geometry and its allowable variation.

G.T. Smith, *Machine Tool Metrology*, DOI 10.1007/978-3-319-25109-7_7

fundamental importance of measurement traceability, see Fig. 7.1a, as well as recognising the key role played by measurement uncertainty[2]—see Fig. 7.1b. Moreover, in addition to being indispensable to declarations of traceability, task-specific measurement uncertainty evaluations (see Sect. 7.2) are requisite contributions to a company's business model, which enables decisions affecting its overall profitability and their customer's perception of the establishment's product quality.

The current DMIS standard[3] (i.e. presently at 5.0-release) provides the mandatory statements to accommodate reporting of product's measurement uncertainties, together with results of the application of conformance rules to measurement data for individual component parts. Hence, GD&T requirements involve the assessment of rather complex 3-D interrelationships of critical part feature characteristics. Subsequently in order to meet this challenge, a multiplicity of tools is available to the end user, which may be generally classified as dimensional measuring equipment (DME), and the most widely applied metrology instrument now being utilised is the ubiquitous CMM—typically shown in Fig. 1.45a. The application of a CMM's bespoke-associated data analysis software enables the transformation of raw inspection sampling points taken on a component part's surfaces into significant and reportable GD&T parameters, such as that for example, for the dimensional bore spacing and parallelism of the cylinders in an engine block shown in Fig. 7.2a. A specific metrological question that must always be addressed is "How much confidence can one place in the values reported by the DME?"—this being a pertinent and valid comment and this chapter will now consider and prove enlightening concerning this particular question, while raising still other effective and relevant queries.

[2]**Measurement uncertainty**: in simplistic terms in dimensional metrology, it can be said to be "A non-negative parameter characterising the dispersion of the values attributed to a measured quantity". This potential uncertainty has a probabilistic basis that reflects incomplete knowledge of the measured quantity. Here, all measurements are subject to degree of uncertainty, and a measured value is only complete if it is accompanied by a "Statement of the associated uncertainty". Relative uncertainty is the term obtained from the actual measurement uncertainty divided by the measured value.

[3]**DMIS** (i.e. **D**imensional **M**easuring **I**nterface **S**tandard) (ISO 22093:2011 is where this standard defines "…a neutral language for communication…" between information systems and DME—thus, it is known simply as DMIS. For that reason, this DMIS is an execution language for measurement part programmes and provides an exchange format for metrology data such as for features, tolerances, as well as the measurement results); and is the definitive standard for communications of dimensional measurement programme sequences and results for manufacturing inspection. Accordingly, this dimensional measuring interface standard (DMIS) is widely utilised within CMMs, this being either as an intermediate file format between a CAD system and that of the CMM's bespoke proprietary inspection language, or as a specific programming language for direct control of the actual CMM.

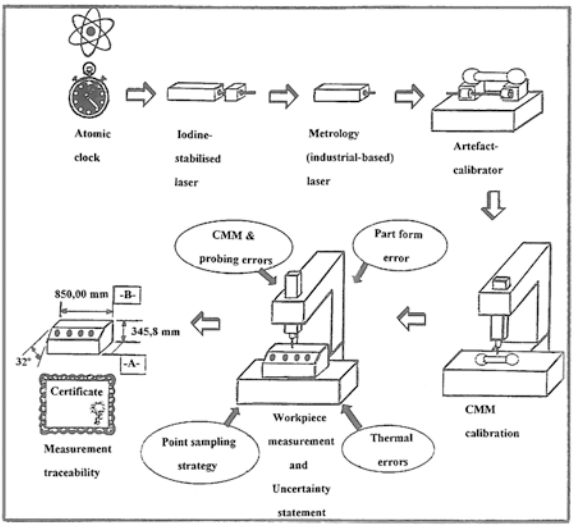

(a) CMM - Traceability: The ISO defines traceability as: *"The property of the result of a measurement or the value of a standard whereby it can be related to stated references, usually national or international standards, through an unbroken chain of comparisons all having stated uncertainties."* The prominent role of uncertainty in completing the traceability chain is evident. Simply having a CMM calibrated does not make its measurement results traceable. If the CMM-derived GD&T measurements are to be traceable, one needs to include *'defensible task-specific uncertainty evaluations'* as part of the *Traceability Report*.

[Source: CMM Quarterly, 2012/ Kim D. Summerhays,Technical Director - MetroSage, LLC]

Source of Uncertainty	Uncertainty type	Probability distribution	Sensitivity coefficient	Degrees of freedom	Standard uncertainty (µm)
M	A	Normal	1 µm	4	0,074
R_{MM3c}	B	Rectangular	1 µm	∞	1,15 E-6
R_{Laser}	B	Rectangular	1 µm	∞	0,0058
α_E	B	Rectangular	-0,0064 µm/°C	∞	-1,95 E-10
C_{Laser}	B	Rectangular	0,0064 µm/°C	∞	5,17 E-7
δT	B	Rectangular	-0,53E-7 µm/°C	∞	-1,07 E-8
ΔT	B	Rectangular	-0,139E-4 µm/°C	∞	-5,17 E-5
Combined standard uncertainty (u_c)					0,104 µm
Effective degrees of freedom (V_{eff})					4,05
Coverage factor (v_{eff} 95%)					k=2,78
Expanded uncertainty (95%)					0,289 µm

(b) Typical CMM estimation of the measurement uncertainty: volumetric error was performed, with the *law of uncertainty propagation* applied to the equations of the *CMM thermal-geometric model*, in accordance with the Guide to the expression of uncertainty in measurement. Estimation of measurement uncertainty, was necessary to estimate the uncertainty associated with each geometric error and offsets present in the equations of the model, the table presents data referring to *X* axis positioning error uncertainty estimation, at 20°C. [Source: Valdés R. A.; B. Di Giacomo; F. T. Paziani (June, 2005)]

Fig. 7.1 Tracebility and measurement uncertainty tabulation

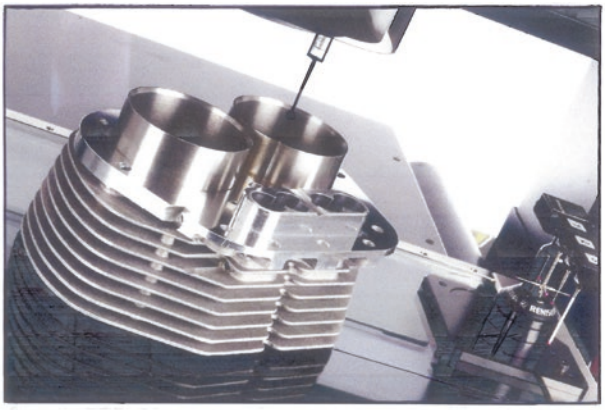

(a) Twin-cylinder barrels/bores: for motorcycles, are just some of the typical automotive parts benefiting from the ability to deploy a variety of probes & sensors in full 3-D automated measurement routines on a CMM.[Courtesy of OGP UK Ltd (Derby, UK)]

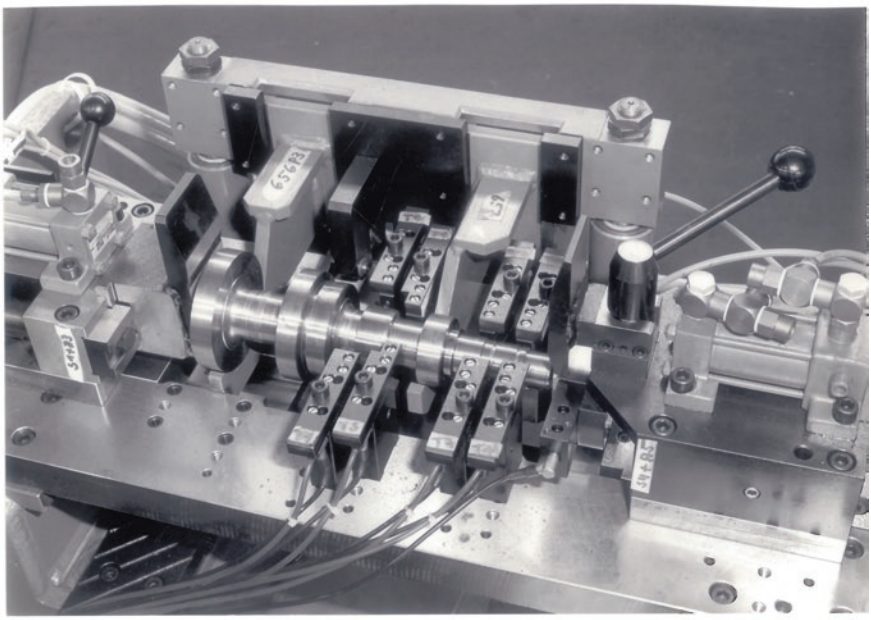

(b) A typical *Receiver-gauge fixture*: for the automated inspection of a high-quality machined part, allowing closed-loop feed-back – in real-time, for control and adjustment of a machine tool.

Fig. 7.2 Automated inspection for *statistical process control* of the volume production machined parts

7.2 Task-Specific Measurement Uncertainty

In valid information gleaned from the National Institute of Standards and Technology (NIST) within the USA (i.e. from its HQ—in Washington D.C.), their comprehensive range of documentation considers the importance of measurement uncertainty in a precise and distinct manner, with the clearly corroborated statement that says "A measurement result is complete only when accompanied by a quantitative statement of its uncertainty". Customarily, this uncertainty is expressed as a range of values where, at a specified level of confidence, the true value of the quantity measured occurs—see Fig. 7.3. Accordingly, in any form of dimensional metrology, a task-specific uncertainty for each and every GD&T parameter is essential. Characteristically, the required statements for this uncertainty might include "The uncertainty of the diameter of this individual ∅85.00 mm hole (i.e. produced under definite manufacturing conditions) is: ±0.05 mm at 95 % confidence (i.e. when determined with this particular measurement system, utilising this actual measuring protocol, under this precise set of environmental conditions)". Moreover, as this definitive statement might suggest that there are many contributing factors that can affect these task-specific measurement uncertainties, see an example of just some of these uncertainties in Fig. 7.4. Consequently, the same command and versatility that make such DMEs attractive as very useful measuring devices can also create a somewhat formidable task in assessing these particular measurement uncertainties.

7.2.1 Traceability Reporting

In the archetypical ISO standard documentation, it defines traceability as "The property of the result of a measurement, or the value of a standard whereby it can be related to stated references, usually national, or international standards, through an unbroken chain of comparisons all having stated uncertainties". The fundamental role of this uncertainty in dimensional metrology when completing the traceability chain becomes quite evident—see Figs. 1.2 (i.e. for the family tree-based traceability chart) and 7.1a (i.e. for a diagrammatic representation of a traceability flow chart). So, by simply undertaking for example, a CMM's calibration does not ensure that its obtained measurement results are traceable. This is particularly valid if traceability of a CMM-derived GD&T measurement is required, and then here, the actual instrument itself must also need to include these defensible task-specific uncertainty evaluations—as part of the company's traceability report—see Fig. 7.1a, b.

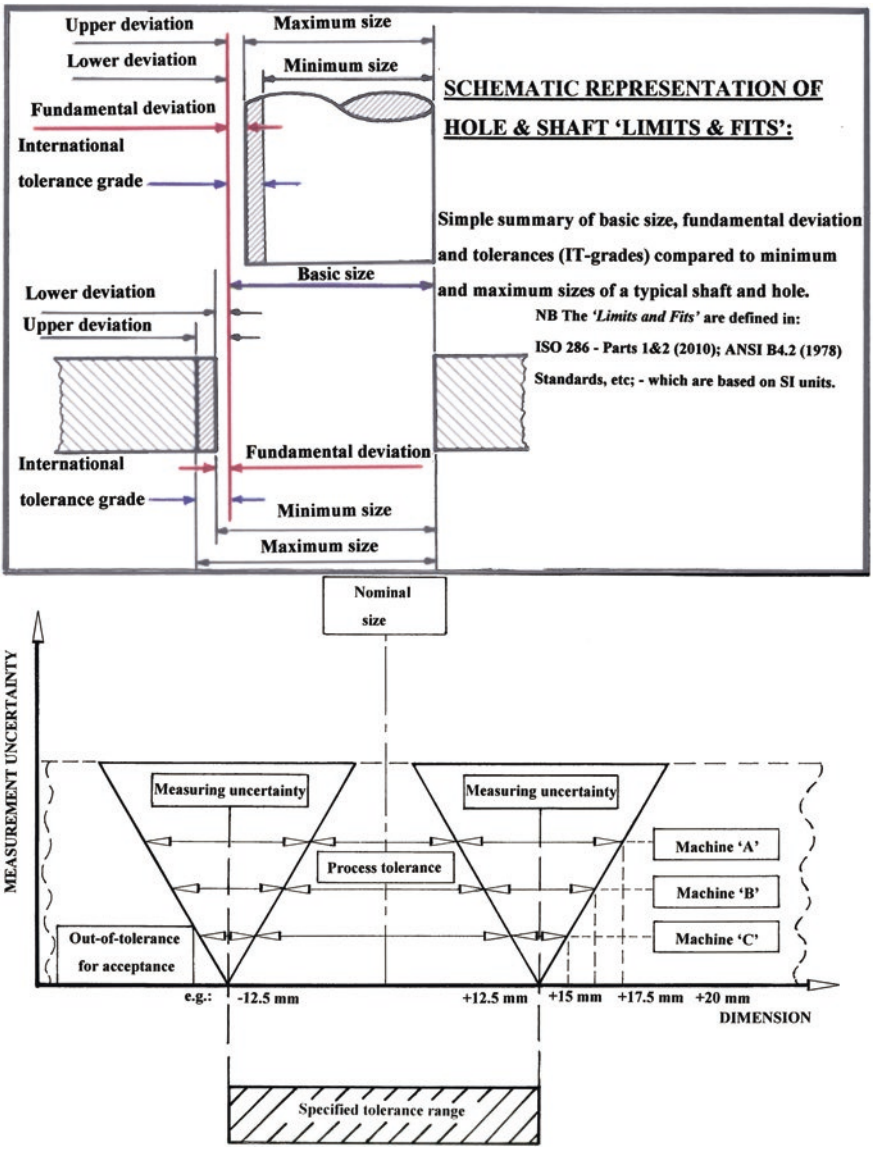

Fig. 7.3 An example of the impact of measurement uncertainty [*Source* D. Flack/NPL (2011)]

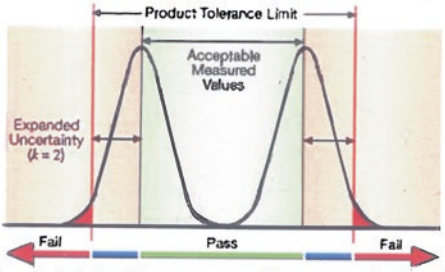

The real cost of uncertainty of measurement for a manufactured product.

[Courtesy of the OEMAGAZINE (Feb. 2005)]

PROCESS INFLUENCES:

Workpiece
- *material*
- *preshape (geometry)*

Tool
- *contouring accuracy*
- *sharpness of tool's edge*
- *wear*

Technology
- *cutting parameters*
- *coolant*
- *chip flow*

ENVIRONMENTAL INFLUENCES:

Temperature

Air pressure

Humidity

Noise

Ground vibrations

WORKPIECE ACCURACY / PRECISION:

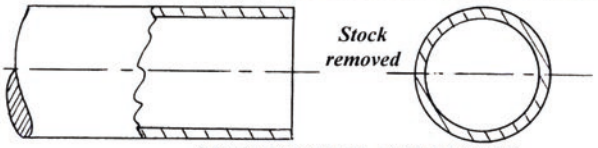

MACHINE TOOL INFLUENCES:

Geometrical behaviour
- *positional errors/uncertainties*
- *straightness errors/uncertainties*
- *angular errors/uncertainties*
- *spindle errors/uncertainties*
- *slideway parallelism*
- *slideway orthogonality*

Dynamic behaviour
- *compliance*
- *mode shape*
- *internal vibration excitation*
- *external vibration excitation*

Kinematic behaviour
- *following errors/uncertainties*
- *control errors/uncertainties*

Thermal behaviour
- *structural deformations resulting from temperature fluctuations of internal & external heat sources*

Statistical behaviour
- *stiffness*
- *deviations resulting from moved slideways*

Fig. 7.4 The sources of uncertainties influencing a component's machined quality (adapted from: Breuckmann and Langenbeck 1989)

7.2.2 Conformance Rules—for Metrological Equipment

In some of the more recent international standards, the significance of uncertainty evaluation has been further accentuated, most notably in **ISO 14253-1**, as well as in **ASME B89.7.3.1**; which offers some guidance for the formulation of decision rules to govern the acceptance or rejection of articles from that of both industry and commerce. Knowing the actual factors that contribute to a DME's measurement uncertainty—see Fig. 7.5—it can be considered fundamental to any form of traceability and conformance, enabling one to find techniques for minimising this uncertainty, which perhaps might also have an additional indirect benefit of enhancing a company's profitability.

As seen from Fig. 7.4, there are a significant number of sources that can contribute to any form of uncertainty, most notably in a CMM-based measurement of its GD&T parameter. Here, the wide range of error influences and their complexity of interactions have been duly recognised as contributing to the application of traditional error budget approaches[4] to measurement uncertainty, which tends to be somewhat largely impractical for CMMs—see Fig. 7.1b. In the **ISO 15530 series**, several alternative approaches are provided, typically being computer simulation that might offer one of the most promising responses—in terms of its versatility, economy, robustness, as well as its predictive character. At this time, the measurement of the component part's critical features is normally repeatedly simulated, under various measurement and inspection conditions. Moreover, the ranges of variability of factors such as the CMM's geometry errors, sensors utilised and potential probing errors—see Fig. 7.6—environmental conditions, and so on are utilised in a mathematical model that permits their influences to be reproduced in the resulting ranges of GD&T parameters

Commencing with DMIS—see Footnotes 3 and 5 for more details on this topic—it provides innovative statements to accommodate measurement uncertainty assessment and the anticipated conformance rules. Briefly, these statements provide the following specific functionalities being related to **Input**:

- **the designation of an uncertainty assessment algorithm**—to be employed;
- **the designation of a conformance rule**—to be engaged;
- **activation/deactivation of uncertainty assessment and optionally, the conformance rule usage**—which will be addressed herein with this release.

Thus, for its associated **Output**:

- **indication as to whether designated uncertainty assessment algorithm is supported by the DME, or not**—which needs to be considered;
- **indication as to whether designated conformance rule is supported by the DME, or not**—which also needs consideration;

[4]**Error Budget**: thus, a very basic but suitably valid definition might be "Simply a list of all error sources and their effect on component part accuracy" (Adapted from: *Precision Manufacturing*—by D.A. Dornfeld and D.-E. Lee, Springer Sci. Pub., 2008).

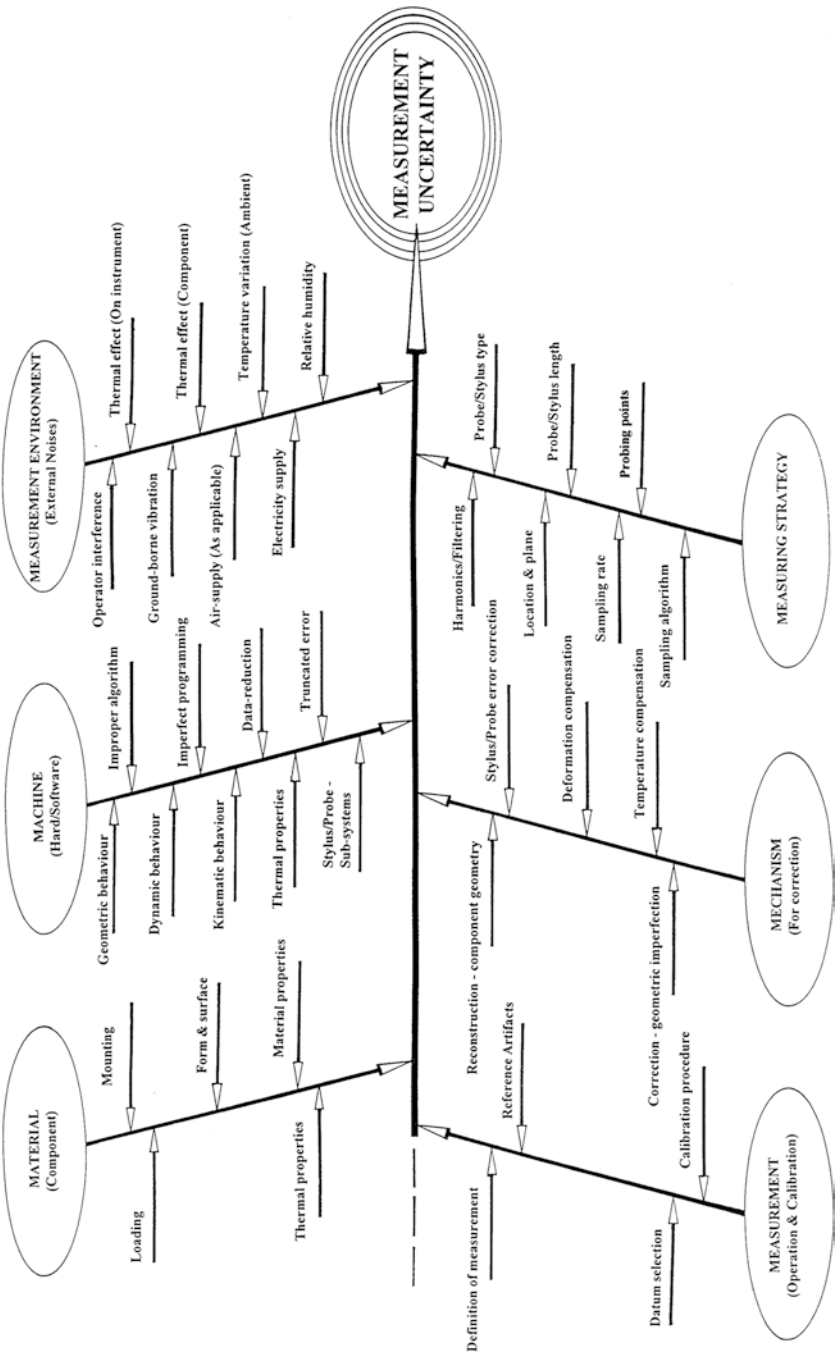

Fig. 7.5 The 'cause-and-effect' (6 m) categorisation for measurement uncertainty—generalised causation—when probing a machined component on either a machine tool, or utilising a coordinate measuring machine (CMM)

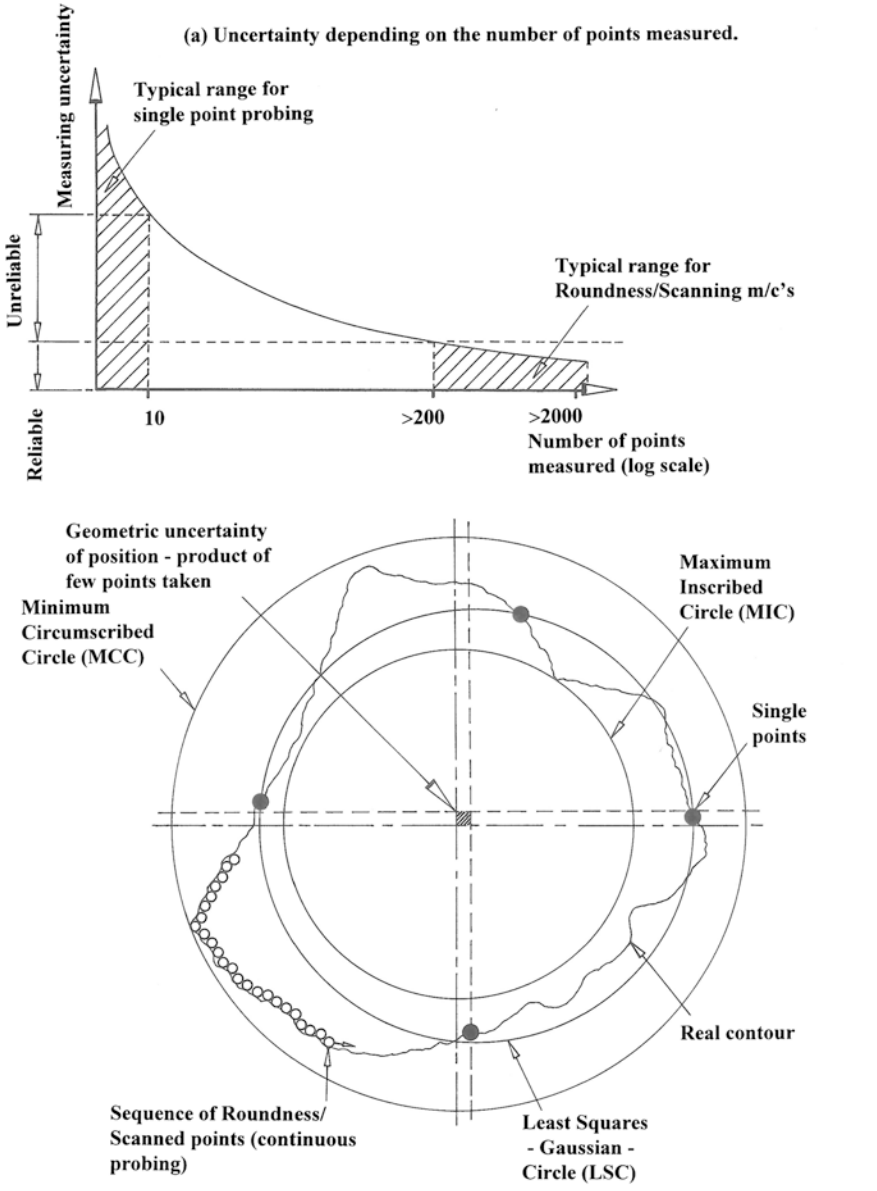

Fig. 7.6 'Probing uncertainty' arises if too few points are taken on round part features (after: Knebel/American Machinist, 1999)

- **reported conformance status in TOL output**—namely the simple format, rule-based conformance, non-conformance, or indeterminate status as well as estimated mean error, together with the expanded uncertainty of measurement.

Reference should also be made that when a desired conformance rule is not supported by a particular DME, then the DMIS[5] also permits the specific coding of the actual decision rule—within the DMIS programme itself. In the ISO standard, a sample code to illustrate this situation is provided within the actual standard. Accordingly, recognition of the importance of measurement uncertainty and its role in measurement traceability and in any conformance decisions is now being widely considered within its remit by the whole dimensional metrology community.

7.3 Measurement Uncertainty—Typically Relating to Machine Tools and CMMs

The well-known comically documented phrase, "I used to be uncertain, but now I'm not so sure?" with the key word here being uncertain, does not actually encourage any particular feeling of confidence in any Metrologist who is looking into certain aspects of measurement uncertainty. Nonetheless, when utilised in a basic technical sense as in measurement uncertainty or uncertainty of a test result, these uncertainties will now have specific meanings. Here then, a specifically measured parameter will be associated with the result of a particular measurement (e.g. a metrology instrument's calibration, or from that of a specific machine tool test) that defines the range of the values that could reasonably be attributed to the measured quantity. As a consequence, when an uncertainty value is evaluated and reported in a specified manner, it normally indicates the level of confidence that the value actually lies within the range defined by the uncertainty interval—see Fig. 7.3.

[5]**ISO 22093:**2011—**Industrial automation systems and integration—Physical device control—dimensional measuring interface standard (DMIS)**: this standard defines a neutral language for communication between information systems and dimensional measurement equipment (DME). Thus, DMIS is an execution language for measurement part programmes and provides an exchange format for metrology data such as features, tolerances, as well as for measurement results. DMIS conveys the product and equipment definitions along with the process and reporting information necessary to perform dimensional measurements which employ coordinate metrology. DMIS contains product definitions for nominal features, feature constructions, dimensional and geometric tolerances, functional datums and also for part coordinate systems. It also communicates equipment definitions for various measurement sensors, measurement resources and machine parameters. Accordingly, DMIS instructs the DME's motions and measurements for product acceptance, or verification and for manufacturing process validation and control. Furthermore, DMIS guides the analysis of coordinate data to report and tag measurement results that ascertain product/process quality. While finally, to aid in its implementation, application functional subsets of DMIS, it has been defined to ensure that successful interoperability and it can also validate DMIS conformance, while furthermore, DMIS addresses the associativity of DMIS product definitions with computer-aided design (CAD) information. NB Also see Footnote 3, for more information.

When undertaking, for example, any dimensional or angular measurements, these measurements are subject to certain imperfections. Some of these imperfections are due to random effects—such as short-term temperature fluctuations, also humidity and air pressure changes, or indeed from the result of the variability in performance of the operator/inspector. Any repeated measurements will display variation because of these random effects, while other types of imperfections are probably due to the practical limits to which correction can be made for systematic effects—such as an offset of a measuring instrument or perhaps due to its specific tool drift[6] occurring in batch machining operations (i.e. typically shown in Fig. 7.7a) that become apparent in characteristics between periodic calibrations. Furthermore, other imperfections might be caused as a result of a personal bias in the actual measurement and subsequent reading of perhaps an analogue scale, or from the uncertainty of the value of a particular reference standard, the latter of which will also introduce a small but significant degree of measurement uncertainty. It is important to know the specific reasons for this actual uncertainty arising, as it is a quantitative indication of the quality of the result. Likewise, as the following valid UKAS question has suggested, it provides an answer to the relevant question of "How well does the result represent the value of the quantity being measured?" Accordingly, it permits users of the result to assess its reliability, such as for the purposes of comparison of results from different sources, or with that of reference values. Here, by way of a typical example, the standard **ISO/IEC 17025:2005**—General requirements for the competence of testing and calibration laboratories stipulate requirements for reporting and evaluating uncertainty of measurement. The difficulties presented by these and other typical standard requirements can vary in nature and severity, depending on the technical field and whether the measurement is either a calibration activity, or an actual test procedure. For example, a calibration procedure would normally be characterised by the three following facts:

1. repetitive measurements can be undertaken;
2. uncertainty of reference instruments is provided at each successive level down the calibration chain, beginning with that country's national standard;
3. any customers are cognizant of the need for a statement of uncertainty in order to ensure that their instrument in question meets the requirements for that standard.

[6]**Tool drift**: this is a well-documented stochastic phenomenon, which occurs whilst machining, for example, a medium-to-large-sized batch of parts—see Fig. 7.10 (top)—due to its stochastic and tribological nature that is present during any type of machining operations, such as when an external turning operation is undertaken. Here, the flank insert wear on the cutting tool increases, which means the workpiece diameter will also steadily and proportionally increase—with the actual time in cut. This action necessitates that the tooling being utilised will need periodic re-calibration/adjustment, otherwise tight workpiece tolerances could be compromised—due to this incipient drifting of dimensional tolerances (see Fig. 7.11a). Of particular note is that a drilled hole produces the opposite effect. In this instance, a batch of the drilled hole diameters gets smaller, as a result of the continuous wearing on the drill's margin, or perhaps due to a boring tool's insert increasing wear rate—when undertaking such boring operations—in batches of similar parts (Sources: Smith 1989, 2001, 2008, etc.).

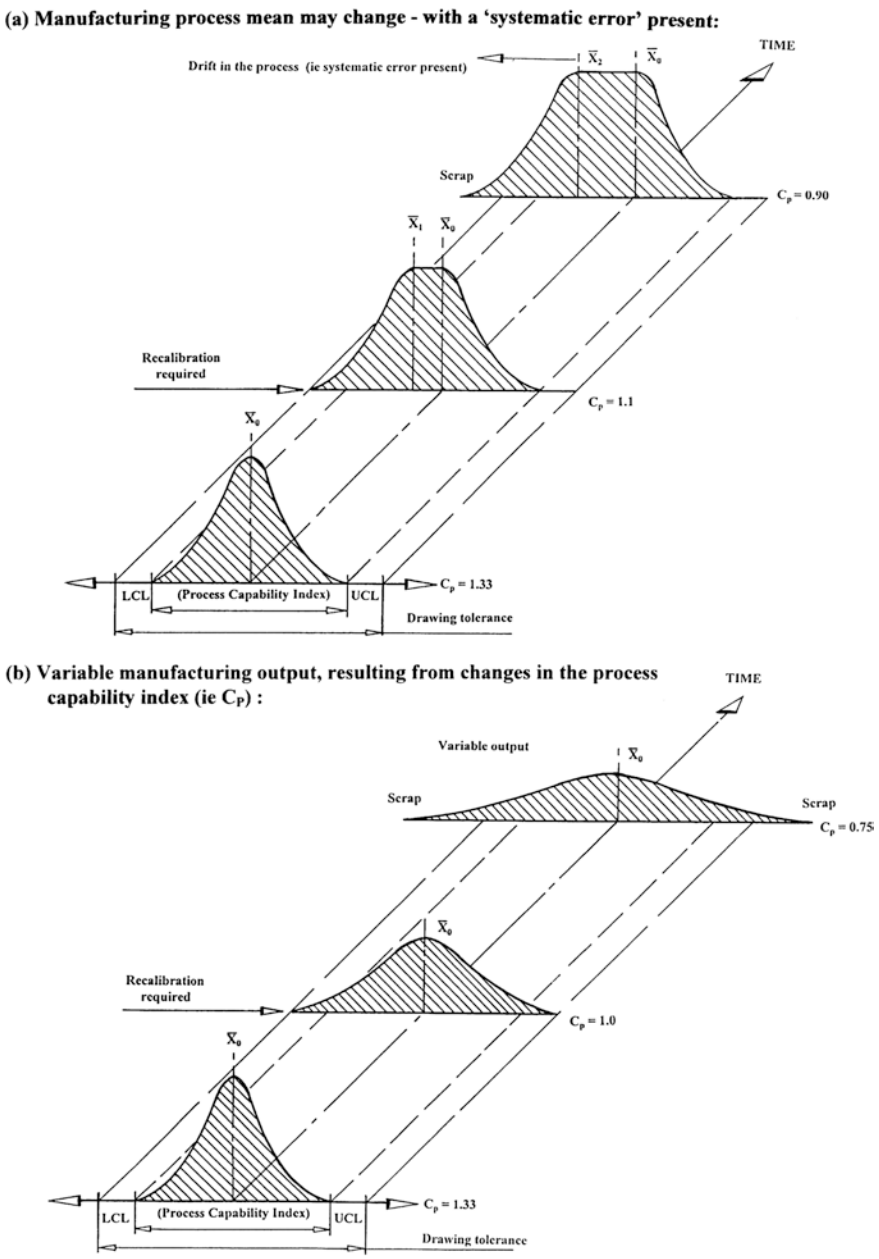

Fig. 7.7 A simple illustration of how **a** the *manufacturing process* mean *changes* with *time*; **b** a *process capability index* will also *change* with *time*, or indeed *both* these *processes/times*

For these specific reasons, accredited calibration laboratories are utilised when evaluating and reporting any form of potential and probable uncertainties. Therefore, in these accredited laboratories, anticipated uncertainty evaluation is

subject to assessment by the accreditation body and it is then quoted on the appropriate calibration certificates, which are issued by that laboratory. Nevertheless, the circumstances in many of these testing procedures are not as well developed and refined, with some notable technical difficulties being encountered. In certain circumstances, a particular test procedure may not be appropriately defined by the standard, which can lead potentially to an inconsistent application of that test and thus provide yet another source of uncertainty. To confuse these matters still further, in many such tests, there will be uncertainty components that need to be evaluated on the basis of previous data and experience, which is in addition to those evaluated from calibration certificates, manufacturer's specifications and other related documentation.

As previously stated, uncertainty is a consequence of the unknown sign of random effects and the limits to corrections, for its systematic effects. For that reason, such effects and corrections can be expressed as a quantity—being an interval about the result that is evaluated by combining a number of uncertainty components. At this instance, these components can be quantified either by evaluation of the results of several repeated measurements, or by estimation based on data from records, previous measurements, as well as knowledge of the equipment and experience of that measurement. Invariably, repeated measurement results are distributed about the average (i.e. mean) in the accustomed Gaussian/normal distribution curve—see Fig. 7.8b—in which there is an inordinate probability that the measured value will be positioned nearer to the mean than to the extremes of the specification limits. Here (i.e. in Fig. 7.8b) the evaluation from successive measurements is undertaken by applying a basic mathematical formula, which has been derived from statistical theory—based upon the standard deviation parameter (i.e. see Sect. 7.3.3).

Techniques that combine the uncertainty components are normally targeted toward producing a realistic, rather than pessimistic combined uncertainty. Such combined standard uncertainty normally means calculating the square root of the sum of the squares of the separate components (i.e. often known as the root sum square method). This combined standard uncertainty might be reported as calculated, namely at the one standard deviation level, or more usually being stated, as an expanded uncertainty. So, this is the combined standard uncertainty, which is multiplied by what is termed a coverage factor. The greater the actual factor, the larger will be the uncertainty interval and, correspondingly, the higher the level of confidence that the value will lie within this interval. Hence, for example, the measurement might be reported in the following manner for a $\approx$95 % confidence level, with a coverage factor of say, 2. As a consequence, when reporting this uncertainty, it is essential to indicate the coverage factor, or to state the level of confidence, or indeed both. The actual process of evaluation highlights those aspects of a test or calibration that produce the greatest uncertainty components and as a result designating where improvements could be advantageous. Equally, it can be established that larger uncertainty contributions could be accepted from some other sources, without significantly increasing the overall interval. This evaluation strategy may perhaps give the opportunity to use either cheaper, or less-sensitive equipment, or providing justification for extending the calibration intervals.

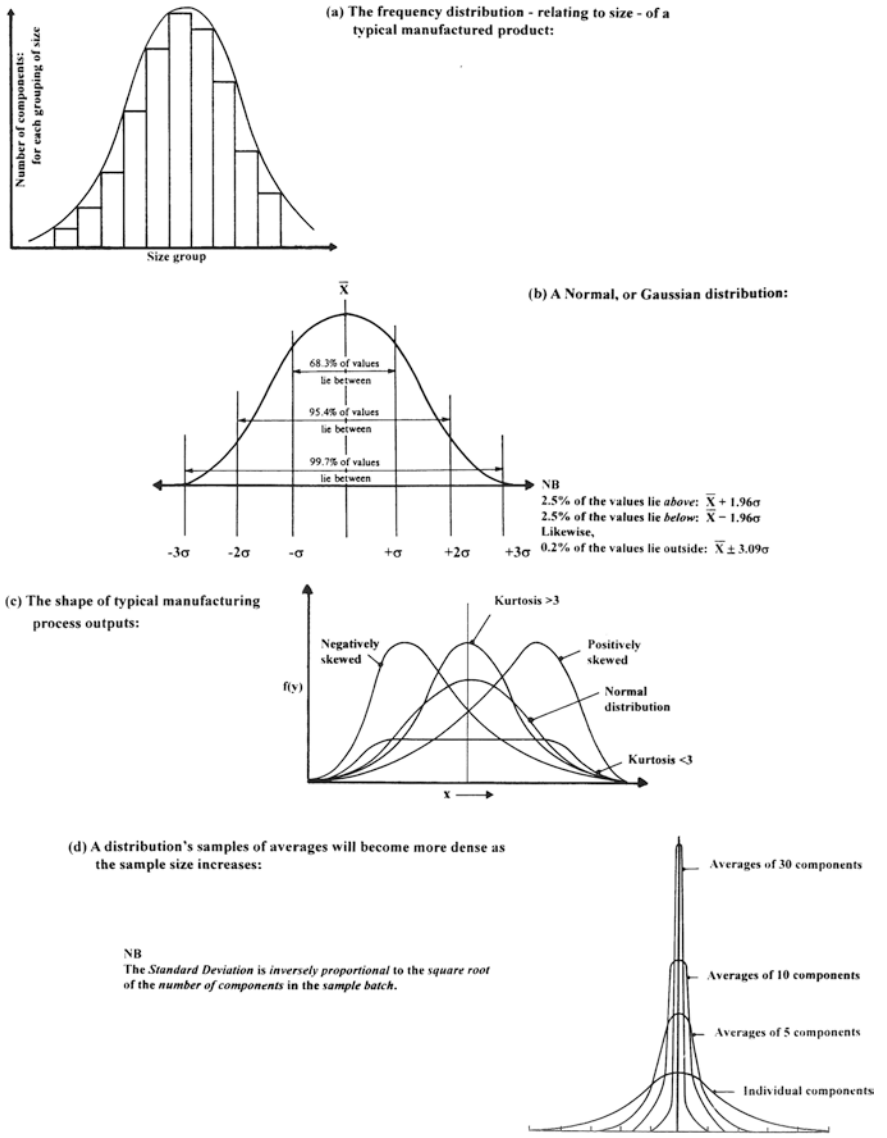

Fig. 7.8 The fundamental statistical relationships of manufactures component outputs (*Source* Oakaland, 1986)

In any event, measurement data records and the testing procedures that were undertaken during this assessment should be retained, and then displayed together with the assumptions that were made, such as concerning the distribution functions—as previously described—plus the sources of information for the estimation of component uncertainty values. These sources are typically from the calibration certificates, previous data, as well as any experience concerning the behaviour of utilising either relevant metrology processes, or any associated materials.

7.3.1 Statements of Compliance—The Effect of Uncertainty

The axiom, "Statements of compliance", relates to a somewhat problematic topic, meaning that what is to be reported must be deliberated in the context of the client's requirements. In particular, some consideration must be given to the possible consequences and attendant risks associated with a result that might be close to the specification limit. The level of uncertainty may be such as to raise some real misgivings concerning the reliability of any pass/fail statements. When uncertainty is not considered, the larger the uncertainty, the greater the chances of either passing failures, or alternatively and equally undesirably, failing passes.

It is generally accepted that a lower uncertainty is normally attained by utilising superior equipment, better control of the inspection environment and ensuring consistent performance of the actual test procedure. In the case of certain products, it may be appropriate for the end user to make a judgment of compliance, founded upon whether the result is within the specified limits, but with no allowance being made for uncertainty. This type of strategy is often referred to as a shared risk, because the end user accepts some of the risks of the product not meeting its specification, although the implications of that risk may vary noticeably. Consequently, a shared risk may be acceptable in a product's non-safety critical performance; however, when testing, for example, the majority of critical components for aerospace purposes, the user may require that the risk of the product not complying has to be negligible and would obviously need its uncertainty to be taken into account. Finally, a significant aspect of shared risk is that all of the parties concerned in this procedure must agree on the level of uncertainty that is considered acceptable and if not, then later on the prospect of industrial disputes and potential litigation may therefore arise.

7.3.2 Uncertainty Issues

An unpretentious question that is often asked in any calibration-related tasks is simply, "What is measurement uncertainty?" This uncertainty of measurement refers to the doubt that exists about any measurement and where there occurs a margin of doubt for every measurement. This expression of measurement uncertainty then raises still further two more questions; these being: (i) "How large is the margin?" and (ii) "How bad is the doubt?" For that reason and from now on within this discussion, in order to quantify this uncertainty, two specific numbers are required; these are (i) the width of the margin—termed its interval, and (ii) the confidence level. This latter value states how sure one is that the actual value occurs, within the margin. As a worked example, an inspected component part's length might be 100 ± 0.5 mm—at the 95 % confidence level. Hence, this level of uncertainty could be more characteristically expressed as follows:

Component part's length is: 100 ± 0.5 mm—at the 95 % confidence level

In reality, what this unambiguous statement is implying to any experienced Metrologist is that one must be 95 % sure that any of the component parts will lie between the stated limits of 99.5 and 100.5 mm in length. In this basic discussion, it is essential not to confuse the term uncertainty with error, as they can be distinctly and separately classified in the following manner:

- **uncertainty**—"The quantification of the doubt existing with regard to the result of this measurement";
- **error**—"The difference between the measured value and the true value of the item being inspected".

In the vast majority of metrological situations, one always tries to correct for any known errors, which is attempted by the application of corrections from appropriate certificates of calibration, although any error occurring that is not known will noticeably be a source of uncertainty. The estimation of measurement uncertainty is very important because precise and accurate quality measurements enable the Metrologist to comprehend the results without ambiguity. However, the expression of the measurement uncertainty is significant when undertaking any form of test measurements; this is principally because they may be part of

- **calibration**—where measurement uncertainty must be reported on an appropriate certificate;
- **testing**—if measurement uncertainty is required to establish either a pass, or fail condition.

Alternatively, information on measurement uncertainty can be considered indispensable, so that the component feature can hold a

- **tolerance**[7]—where the uncertainty had been previously established, prior to deciding whether a tolerance is met.

7.3.3 Statistical Measures—In Uncertainty Calculations

In order to evaluate the test data from an inspection procedure and to determine whether an adequate process control has been established, statistical measures are normally adopted. If the metrological process is not influenced by systematic, or random errors, then the process is deemed to be behaving normally and any production process output data is valid. Two statistically derived mathematical

[7]See the schematic representation of typical limits and fits for a characteristic hole and shaft—for suitable mating parts, shown in Fig. 7.6 (top), according to **ISO 286—Parts 1 and 2**, and **ANSI B4.2 (1978)**. Without the above considerations, one might need to read and comprehend the information on the calibration certificate, or written specification for a particular test/measurement. However, it is worth re-emphasising that a measurement is not traceable unless it is quoted with a valid figure of uncertainty.

expressions are merely required to define whether a manufacturing/metrological process is behaving correctly and these are the arithmetic mean[8] and its accompanying standard deviation[9]—see Fig. 7.11—together with their respective chart values in Fig. 7.9. Invariably, the arithmetic mean is shortened to just the mean, this being denoted by the symbol '$\overline{x}$'. This $\overline{x}$ value is the mean of all values of 'x' and

[8]'**Arithmetic mean**—this term being denoted by the symbol '$\overline{x}$' (i.e. stated as x-bar): invariably it is utilised in both Mathematics and Statistics. The arithmetic mean can be considered as "The sum of a collection of numbers divided by the quantity of numbers in that collection". Furthermore, this **mean** may often be confused with the **median**, **mode** or even **range**. Thus as just described, but mentioned here slightly differently, such that the **mean** is often stated as the "Arithmetic average of a set of values, or distribution". However, for skewed distributions, the **mean** is not necessarily the same as the middle value (**median**), or the most likely (**mode**), consequently the simplified calculation for this **arithmetic mean** is given by

Arithmetic mean'$\overline{x}$':

$$\overline{x} = \frac{\sum (x_1 \ldots x_n)}{n}$$

where 'n' is the number of observations.

[9]**Standard deviation** (**SD**) represented by the Greek letter sigma ('σ'), in both Statistics and Probability theory, where it shows how much variation or dispersion from the average exists. Thus, a low standard deviation indicates that the data points tend to be very close to the mean—also termed expected value—whereas a high standard deviation indicates that the data points are spread out over a large range of values. The standard deviation of a random variable, statistical population, data set or probability distribution is the "Square root of its variance". NB An inflection point—where 'σ' occurs—is a position where a Gaussian curve changes its curvature from say, convex to concave—at its point of tangency. Here, the random variable that is normally distributed will have its associated mean ('$\overline{x}$') and standard deviation ('σ'). An **unbiased estimator** for the **variance** is given by applying **Bessel's correction** (**Friedrich Wilhelm Bessel** (Born: 22 July 1784 in: Minden, Minden-Ravensberg, died: 17 March 1846 in Königsberg, Prussia, now Russia). He was a German Astronomer, Mathematician (i.e. being known as the Systematiser of these **Bessel functions**). It is worth just mentioning as an interesting aside that Bessel was the first astronomer to determine the distance from our Sun to another Star—by the method of parallax. Of particular note was that these types of functions were originally discovered by **Daniel Bernoulli** (Born: 8 February 1700; died: 17 March 1782). Bernoulli was a notable Swiss Mathematician and Physicist; he was principally known for the Bernoulli principle, also for his early work on Kinetic theory of gases and, for his excellent research work in the field of Thermodynamics), utilising '$\boldsymbol{N-1}$' instead of '$\boldsymbol{N}$' to yield the **Unbiased sample variance**, which is denoted by 's^2', thus

$$s^2 = \frac{1}{N-1}\sum_{i=1}^{N}(x_i - \overline{x})^2.$$

Although this estimator is unbiased, if the **variance** exists and the sample values are drawn independently with replacement, then the term '$\boldsymbol{N-1}$' corresponds to the number of degrees of freedom in the vector of residuals $(x_1 - \overline{x}, \ldots x_n - \overline{x})$. So, by taking square roots it reintroduces bias, and then yields the **Corrected sample standard deviation**, denoted by 's'—which is often termed the **estimated standard deviation**, thus

$$s = \sqrt{\frac{1}{N-1}\sum_{i=1}^{N}(x_i - \overline{x})^2}.$$

can be derived from the following expression (below), but also see the derivated expression in Footnote 7:

$$\bar{x} = \frac{1}{n} \sum_{i=1}^{n} x_i$$

where $\bar{x}$ = arithmetic mean; $\sum x$ = sum of x; and, n = number of readings.

NB Invariably, it is often necessary to obtain several readings which are required to be taken, where it would then modify this calculation to

$$\bar{x} = \frac{1}{n} \sum_{i=1}^{n} f_i x_i$$

where $\sum fx$ = the sum of the frequencies of x.

For example, in the following elementary metrological inspection case, the difference in a basic stock component's nominal diameter measurements for their inspected measured values was found to be thus 17, 18, 22, 18, 18, 19, 21, 19, 18 and 20 μm, respectively. Then in this metrological situation, the calculated value of $\bar{x}$ would simply be

$$\sum x = 17 + 18 + 22 + 18 + 18 + 19 + 21 + 19 + 18 + 20\,(\mu\text{m})$$

Therefore,

$$\sum x = 190\,\mu\text{m}$$

$$\bar{x} = \frac{190}{10} = 19\,\mu\text{m}$$

The spread of these readings will give an indication of the uncertainty of the actual measurements. Moreover, knowing how large the spread is enables one to form an opinion as to the quality of the inspection procedure, or for a group of measured data. The customary way to quantify this spread is by use of the Greek lower case letter 'σ' (i.e. sigma). Usually, only a moderate number of measured data is obtained and in this case, an estimate of the standard deviation can be derived, which is denoted by the letter 's', meaning the estimated standard deviation. In principle, the calculation of the term 's'—for the previous series of component diameter differences—would simply be as follows (i.e. here, rewritten once again):

$$17 + 18 + 22 + 18 + 18 + 19 + 21 + 19 + 18 + 20\,(\mu\text{m}) = 19\,\mu\text{m (mean)}$$

Consequently, the next step from this calculated mean is to find the difference between each successive reading; this is obtained in the following manner—by making the component's mean diameter value of 19 μm, then equating it to zero, changing the subsequent readings to

$$-2\ -1\ +3\ -1\ -1\ 0\ +2\ 0\ -1\ +1$$

At this time, each of these now adjusted values are then squared, as follows:

$$4\ 1\ 9\ 1\ 1\ 0\ 4\ 0\ 1\ 1$$

Next, one must sum the total, and then divide by '$n - 1$'; here, in the case of 'n' the value is 10, so '$n - 1$' will be 9; hence,

$$(4 + 1 + 9 + 1 + 1 + 0 + 4 + 0 + 1 + 1)/9 = 22/9 = 2.44\,\mu\text{m}^2$$

Thus, the **estimated standard deviation** (s) can then be simply obtained by taking the square root of the previous answer; therefore,

$$s = \sqrt{2.44}\,\mu\text{m}^2 \approx 1,6\,\mu\text{m (correct to one decimal place)}$$

The overall process of calculating the **estimated standard deviation** (s), for a series of 'n' measurements, can now be mathematically expressed in the following manner:

$$s = \sqrt{\frac{1}{n-1}\sum_{1=1}^{n}(x_i - \overline{x})^2}$$

where 'x_i' is the result of 'ith' measurement; '$\overline{x}$' is the arithmetic mean of 'n' results considered.

To ensure that the production process was correctly operating, the **estimated standard deviation** (s) can also show whether a process was in-control, or perhaps not. If plus or minus three, 's' is utilised in conjunction '$\overline{x}$' (centred-mean), then if the process is normally distributed, all the component diameter readings should fall within the upper and lower values for the component's specification tolerance, because this represents 99.7 % of the overall population—see Fig. 7.11b. Hence, the lower and upper specification limits for these basic component diameter values are

$$\begin{aligned}\overline{x} \pm 3s &= 19 \pm 3 \cdot 1.6\,\mu\text{m} \\ &= 19 \pm 4.8\,\mu\text{m} \\ &= 14.2\text{ (lower-limit) and }23.8\text{ (upper-limit) }\mu\text{m}\end{aligned}$$

Consequently, with the lowest diameter's measured reading being obtained for this set of components—being 17 μm—and the highest measured reading of 22 μm, then these readings would readily fall within, say, some pre-selected tolerance set by the engineering designer, which might be for the component diameters of perhaps,

14 and 24 μm, respectively. One further manner of expressing these batch production values for the component output is to employ its associated process capability index[10]—usually denoted by the letters 'C_p', which indicates the spread of the process. This C_p *value* can be derived in the following manner:

$$\text{Process capability } C_p = \frac{\text{overall tolerance}}{\pm 3s} \quad (\pm 3s \text{ is } 6s, \text{ or } 6\sigma)$$

Thus, in this case,

$$\text{Process capability } C_p = \frac{24 - 14}{9.6}$$

Therefore,

$$C_p = 1.04$$

NB The overall tolerance represents the width of the specification limit for this production process.

A term to denote the relationship between the tolerances and their associated process capability is known as relative precision index (RPI)[11]—see Figs. 7.7 and 7.10.

[10]**Process capability index**: thus, in case of process improvement efforts, this process capability index 'C_p', or alternatively, its process capability ratio, is a statistical measure of process capability, namely, the ability of a process to produce output within specification limits. The concept of process capability only holds meaning for processes that are in the state of statistical control. These process capability indices can actually measure how much natural variation a process experiences—relative to its specification limits—and allows different processes to be compared with respect to how well an organisation, or a company, can control them, during a particular batch, or volume production operation.

[11]**Relative Precision Index** (**RPI**): it is perhaps one of the oldest indexes which was utilised for production output capability. It is based on the ratio of the mean range of samples within the tolerance band. In order to avoid the production of defective material, the specification width must be greater than the process variation; hence,

$$2T > 6\sigma$$

$$\text{Knowing that: } \sigma = \overline{R}/d_n = \frac{\text{Mean of sample ranges}}{\text{Hartley's Constant}}$$

[**H. O. Hartley** (Born as **Herman Otto Hirschfeld** (1912–1980)), but more commonly called 'HOH'. In fact, Hartley was a German-American statistician, who developed and then refined the so-called Hartley's test—for the Equality of variances (i.e. in 1950)]

$$\text{So:} \qquad 2T > 6\overline{R}/d_n$$

$$\text{Therefore: } 2T/\overline{R} > 6/d_n$$

Thus, $2T/\overline{R}$ is known as the RPI and the value of $6/d_n$ is the minimum RPI, to avoid a generation of material outside the specification limit.
[Sources: Oakland 1989/2003].

The relationship between the tolerance and '6*s*'—in its original form—gave rise to three distinct levels of precision for a manufacturing process; these were

1. **low relative precision**—where the tolerance band is either less than or equal to 6*s* (i.e. representing the value 1);
2. **medium relative precision**—where the tolerance band is greater than to 6*s* (i.e. value 1) but less than 1.33 (i.e. a value of >1, but <1.33);
3. **high relative precision**—where the tolerance band is greater than 1.33 (i.e. representing a value of >1.33).

A manufacturing process distribution that equates to a high RPI that is centred on the mean will be most unlikely to produce scrap parts, as any small amount of potential process—drift—that has been introduced by either systematic or random errors are not likely to produce components that are out-of-tolerance—see Fig. 7.7a (i.e. with the middle value here, having a $C_p = 1.1$). Today, many companies are artificially introducing RPIs that often exceed values of, say, 2 and with these values being centred there is a very low probability that any components produced by this production process will produce scrap. This condition might change if the process has now exhibited instability and then exacerbates its condition and becomes completely out-of-control—through a fundamental change in its output—see Figs. 7.9 (Shewhart—average and range charts[12]) and 7.7a (i.e. $C_p = 0.90$), Fig. 7.11b (i.e. $C_p = 0.75$).

[12]**Shewhart charts** (**Walter Andrew Shewhart** (Born: 18 March 1891, New Canton, Illinoi—died: 11 March 1967): he was a distinguished American Physicist, Engineer and Statistician. W.A. Shewhart is invariably known as "The Father of Statistical Quality Control". Dr. Shewhart was awarded a Doctorate in Physics from The University of California, Berkeley, in 1917, where he created the basis for the control chart and the concept of a state of statistical control by carefully designed experiments. While Dr. Shewhart drew on his knowledge from pure mathematical/statistical theories, he understood that data from physical processes never produce a normal distribution curve (i.e. Gaussian distribution). Moreover, he also went on to discover that observed variation in manufacturing data did not always behave in the same manner as data in nature (i.e. often termed as the Brownian motion of particles). Thus, Dr Shewhart concluded that while every process displays some form of variation, with certain processes displaying controlled variation—that is natural to the process—while still others displayed uncontrolled variation—that is not present in the process causal system at all times. **NB** (Also see Footnote 16, for more specific details, concerning Dr Shewhart's life and work) (***X*-bar and *R* and *S* Control Charts**): accordingly, in statistical quality control (SPC), the individual/moving range chart is a type of control chart being widely utilised to monitor variable data from an industrial process, for which it is impractical to use rational subgroups. The chart is necessary in the following situations: where automation allows inspection of each unit, so rational subgrouping has less benefit, where production is slow, so that waiting for enough samples to make rational subgroup unacceptably delays its subsequent monitoring; for processes that produce homogeneous batches where repeat measurements vary primarily because of measurement error. Thus, this chart configuration actually consists of a pair of charts; these are (i) the individuals chart—for averages, which displays the individual measured values; (ii) the moving range chart, which displays the difference from one point to the next. As with some other quality control charts, these two charts enable the user to monitor a manufacturing process for shifts in the process that could potentially alter the mean, or variance of the measured statistic—see Fig. 7.8.

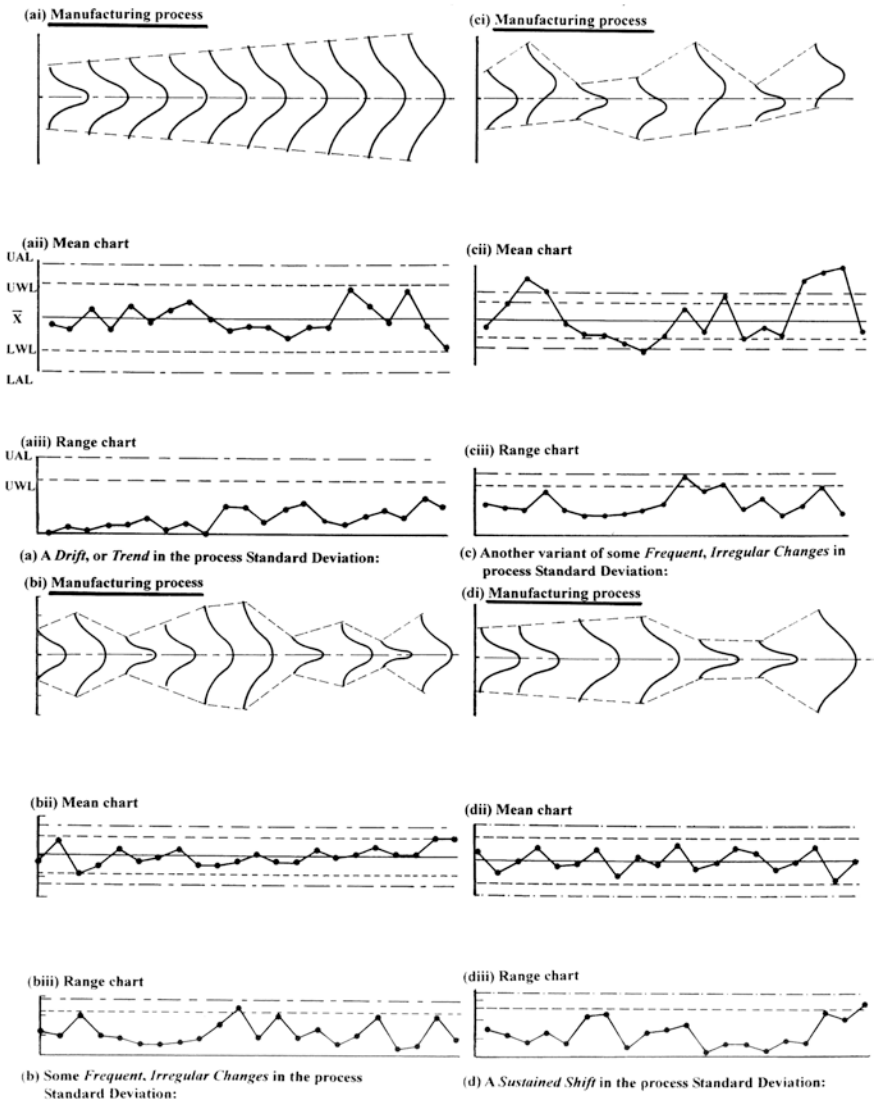

Fig. 7.9 Typical control charts utilising mean and range, for process capability trouble—shooting (*Source* Oakaland, 1986)

7.3.4 Origins of Uncertainties

There are numerous aspects that can contribute to, for instance, poor measurements with many of these measurements being easily established, while others remain more difficult types of uncertainties to determine. Due to the fact that actual measurements are never taken under ideal conditions, then any potential errors—termed their uncertainties—can be the product of a wide range of contributing factors—see Figs. 7.4 and 7.4—not least of which are the result of

- **metrological equipment**—here, the instrumental problems that can accrue are due to drift, wear, ageing and many more unanticipated problems;
- **component inspection**—which may not be stable[13] during the actual measurement task;
- **measurement process**—the practice of measuring a component may be difficult to achieve, this being particularly true if the subject of this actual measurement is in dynamic motion, whilst the real-time readings are taken;
- **imported uncertainties**—any metrological instrument has its own uncertainty and this affects the subsequent measurement which has just been taken[14];
- **operator skill**—occasionally certain measurements rely on both the operator's skill and their judgement, with some operators being more efficient and reliable than others. For example, when timing a particular trial with a stopwatch, the level of uncertainty will depend upon the individual operator's reaction time;
- **sampling concerns**—any dimensional measurements, or test data obtained, must be representative of the process being assessed[15];
- **metrological inspection**—the measuring instrument can be significantly influenced by either the component being measured or from any variations in temperature, humidity, air pressure and vibrational effects as well as many more unexpected conditions.

Of particular note is that the overall measurement uncertainty will be affected by individual uncertainties and where the error is known this factor can be derived from the instrument's calibration certificate. For example, in this instance, a suitable and specific correction can be applied to the result of the measurement.

---

[13] An often quoted analogy of the overall measurement problem, when attempting an inspection procedure, this being somewhat comically and expressly described as being: "To attempt to measure the size of an ice cube, in a warm room!"

[14] If an instrument has not been previously calibrated, then its condition will exacerbate any future measurements taken.

[15] As examples of these potential sampling issues, any temperature measurement data should be assessed close to the item being monitored and certainly not away from its local thermal environment. When selecting samples from the production line, always ensure that they do not originate in the initial start-up batch run, nor that samples were obtained from a mixed stillage—noting here in this latter circumstance that samples were taken from two separate production process runs.

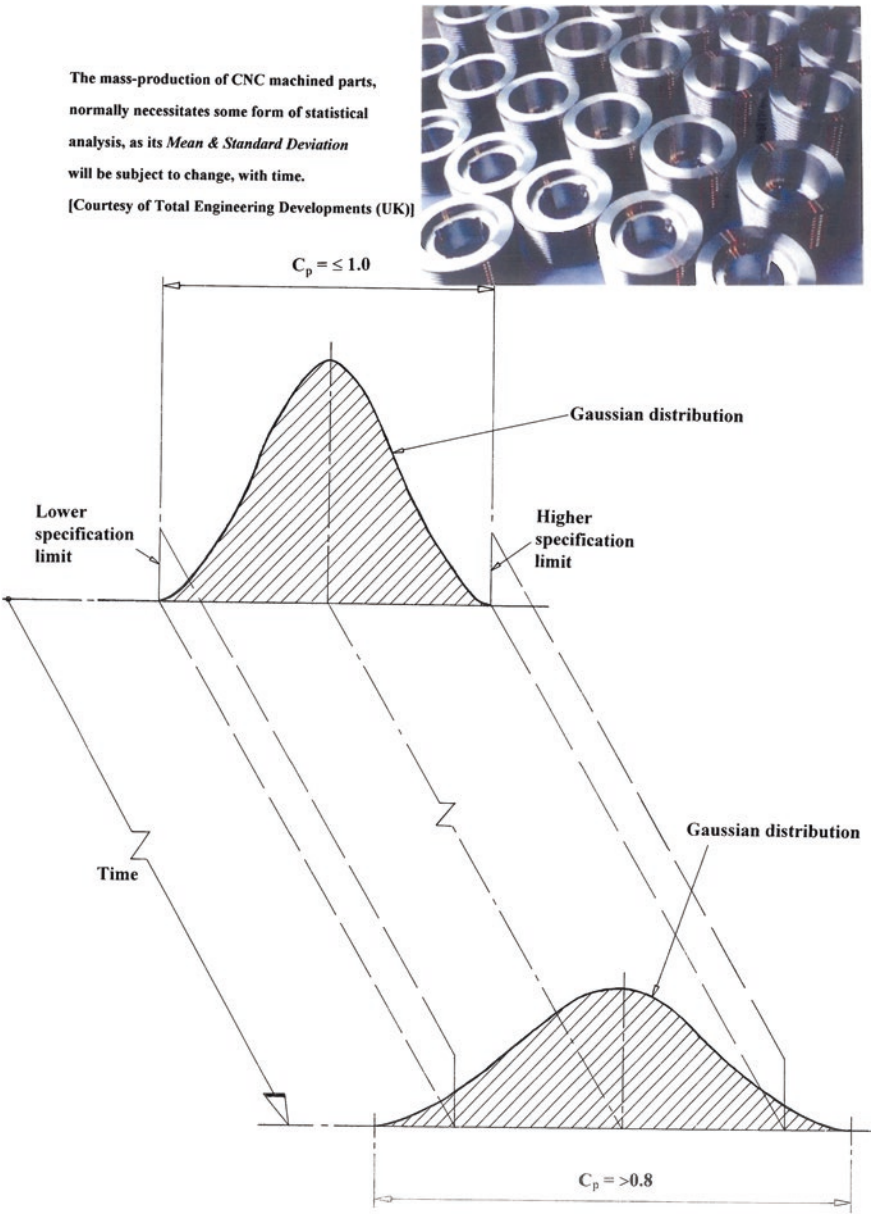

Fig. 7.10 The process capability index (i.e. C_P) may change with time

7.3.5 Calculation of Measurement Uncertainty

Prior to the calculation of measurement uncertainty, initially the sources need to be positively identified—as briefly itemised in Figs. 7.4 and 7.5. Once this task has

been performed, then an estimate of the size of the uncertainty from each source must be established. Finally, each of the individual and contributory uncertainties is then combined, to produce an overall figure for the whole uncertainty. There are two methods that are utilised to estimate these uncertainties, which are termed either Type A or Type B evaluations and in many instances the uncertainty evaluations of both types are often required, their identification being according to the following classifications:

1. **Type A evaluations**—these are estimates of uncertainty by statistical techniques, normally from repeated readings;
2. **Type B evaluations**—this concerns uncertainty estimates obtained from any relevant information, such as calibration certificates, manufacturer's specifications, published information, past experience, also from just simply common sense.

It is tempting to consider that Type A uncertainties occur by random processes and that Type B uncertainties result from systematic factors, but this logic is somewhat questionable. In Table 7.1, an attempt has been made to illustrate how to use the information from both Type A and Type B evaluations, for an overall estimate of uncertainty. Any contributions to the uncertainty must be expressed in the same units before they are combined, moreover, having matching levels of confidence. The contributing uncertainties and their respective confidence levels need to be uniform and this allows them to then be converted into standard uncertainties. What is more, a value of ± 1 standard deviation is the margin for standard uncertainty, and further, it also provides information on the uncertainty of an average and not just the spread

Table 7.1 Just some of the basic steps that can be utilised, when attempting to determine potential measurement uncertainty

Step	Procedure
1	Decide what you need from your measurements. Decide what actual measurements and calculations are needed to produce the final result
2	Carry out measurements needed
3	Estimate the uncertainty of each input quantity that feeds into the final result. Express all uncertainties in similar terms (see text)
4	Decide whether the errors of the input quantities are independent of each other, but if not, then additional calculations/information is required
5	Calculate the result of your measurement and include known corrections from previous calibration, etc.
6[a]	Find the combined standard uncertainty from each individual aspect
7[a]	Expressing uncertainty in terms of coverage factor, together with a size of uncertainty interval and state the confidence level
8[a]	Write down the measurement result and its uncertainty, stating how both were obtained

Source Beginner's G.U.M., Bell, S./The NPL (1999)
[a]To be discussed in more detail in this section

of these values. It is normal to quote standard uncertainty using the symbol 'u', or a '$u(y)$', this latter term being the standard uncertainty in 'y'.

***Type A Evaluation*—Standard Uncertainty Calculation**

Once a series of measurement readings has been obtained for a Type A evaluation, the value of '$\bar{x}$' (*mean*) and its accompanying value of 's' (i.e. the estimated standard deviation) can then be calculated. From this set of readings the estimated standard uncertainty ('u') of the mean can be calculated from the following simple expression:

$$u = \frac{s}{\sqrt{n}}$$

where $n =$ the number of measurements taken.

***Type B Evaluation*—Standard Uncertainty Calculation**

If information is somewhat scarce, typically for estimates of some Type B values, it might be possible to establish the upper and lower limits of uncertainty. If this action is taken, it could be shown that these limits might equally fall anywhere between the positions along the uniform distribution, or for that matter in a rectangular distribution. In this latter case, the standard uncertainty for a rectangular distribution will be

$$u = \frac{a}{\sqrt{(3)}}$$

where $a =$ the semi-range (half-width) between the upper and lower limits.

For a calibration certificate of a measuring instrument, it can usually be assumed that any uncertainty indicated will have been derived from a normally distributed set of statistical data, although it is not uncommon to obtain such data from either a uniform or rectangular distribution. Table 7.1 shows the simple basic steps required in determining measurement uncertainty.

Combining Standard Uncertainties

Whether the individual standard uncertainties are calculated by either Type A or Type B evaluations is not the issue, as they can be equally and validly combined by mathematical techniques known as the summation by quadrature, or more commonly termed either 'root sum of …' and denoted by the notation 'u_c', or '$u_c(y)$'.

Addition and Subtraction: Summation in Quadrature

The most elementary case for this technique is where the sum of a series of measured values—by either addition, or subtraction—is calculated. By way of illustration of the summation by quadrature method, when determining the total height of a pile of wrung together Gauge blocks—of differing sizes—then the standard uncertainty of each Gauge block could be represented by the notations a, b, c, etc. The known (i.e. measured) values are then found by squaring the individual

uncertainties, and then adding them together and then taking the square root of the total, as follows:

$$\text{Combined standard uncertainty} = \sqrt{\left(a^2 + b^2 + c^2 + \cdots + n^2\right)}.$$

Multiplication: Summation in Quadrature

In cases of more complex uncertainty problems, an approach adopted to simplify the calculations is to work in terms of either relative or fractional uncertainties. For example, in the simplest form of calculation, if a large rectangular surface area '*A*'—such as a CMM table's flat working surface—has to be established, then it is simply determined by multiplying its length '*L*' by the width '*W*', which is simply: $A = L \times W$. The fractional uncertainty in the area is established from the individual fractional uncertainties for the length and width. Consequently, in the case of its length '*L*' with an uncertainty of '*u*(*L*)', the relative uncertainty will be '*u*(*L*)/*L*', likewise for the width '*W*' the relative uncertainty is '*u*(*W*)/*W*'. Accordingly, in the table's representative area—for this CMM's surface—the relative uncertainty '*u*(*A*)/*A*' is given by

$$\frac{u(A)}{A} = \sqrt{\left(\frac{u(L)}{L}\right)^2 + \left(\frac{u(W)}{W}\right)^2}.$$

Complicated Functions: Summation in Quadrature

In many instances in the calculation of the final result, the value will be squared (e.g. 'Z^2'), with the relative uncertainty due to this squared component taking the form '2*u*(*Z*)/*Z*'.

In some instances, measurements taken are calculated utilising formulae that employ combinations of addition, subtraction, multiplication, division, etc. For example, in some uncertainty budgets—more will be said on this topic in the next section—it might be necessary in the metrology instrumentation to measure, say, the electrical resistance '*R*' and the voltage '*V*' and, then to calculate the resultant power '*P*', using the following known relationship of '$P = V^2/R$'. In this case, the relative uncertainty '*u*(*P*)/*P*'—in the value for power—would be given by the following expression:

$$\frac{u(P)}{P} = \sqrt{\left(\frac{2u(V)}{V}\right)^2 + \left(\frac{u(R)}{R}\right)^2}$$

In general for any multi-step calculations, the procedure for combining standard uncertainties in quadrature can be achieved in multiple steps, utilising the relevant form of addition, multiplication, etc., at each step. For complicated formulae, the combination of standard uncertainties is explained in much more detail elsewhere (e.g. in the relevant **UKAS Publication: M 3003**).

Correlation

The equations required to calculate the combined standard uncertainties—mentioned above—are only valid if the input values for standard uncertainties are not interrelated or correlated. As a consequence, correlation refers to the question of whether all the uncertainty contributions are independent, namely, the question raised here is "Could a large-error in one input measurement cause a similar sizeable-error in another?" Furthermore, might some outside environmental influence temperature, create a similar effect simultaneously on several aspects of uncertainty, which are either easily established, or require further investigation by the Metrologist? In many instances, these individual errors are independent, but where they are not, then some additional calculations are required.

Coverage factor ('*k*')

In the previous discussion on uncertainty, the components were invariably scaled to obtain the combined standard uncertainty. The result of the calculations for combined standard uncertainty may be thought of as equivalent to one standard deviation, but it may be necessary to obtain the overall uncertainty expressed in terms of a different level of confidence, typically at the 95 % limit. Such rescaling can be achieved by utilising a coverage factor ('*k*'). Multiplying the combined standard uncertainty ('u_c') by the coverage factor ('*k*') resulting in what is termed the expanded uncertainty, which is normally denoted by '*U*', in the following manner:

$$U = k \,.\, u_c.$$

NB A specific value of the coverage factor ('*k*') will introduce a particular confidence level for the expanded uncertainty.

In particular, if the overall uncertainty is scaled by utilising a coverage factor of '$k = 2$' to obtain an approximate level of confidence of 95 % then the '$k = 2$' value is acceptable when the combined standard uncertainty tends to be normally distributed. Some typical coverage factors for these normal distributions are

- '$k = 1$' is for a confidence level of ≈68 %;
- '$k = 2$' is for a confidence level of ≈9 %;
- '$k = 2.5$' is for a confidence level of ≈99 %;
- '$k = 3$' is for a confidence level of ≈99.7 %.

Other less popular distribution shapes have different coverage factors. As an alternative, whenever an expanded uncertainty is quoted, it can be found by reversing the process, namely by dividing this uncertainty by an appropriate coverage factor. On typical calibration certificates, the quoted expanded uncertainty—if expressed correctly—can be interrogated to obtain the required standard uncertainties. When expressing this measurement uncertainty, it should be exacting in its definition, allowing no misrepresentation. In order to achieve accurate uncertainty definitions, several important factors need to be stated; these are

- **measurement result and uncertainty figure**—for example, quoting that an artefact was 300 ± 1 mm;
- **coverage factor and confidence level**—recommended wording to minimise any possible confusion might be "The reported uncertainty is based on a standard uncertainty multiplied by a coverage factor '$k = 2$', providing a level of confidence of approximately 95 %";
- **description of how uncertainty was estimated**—reference should be made to the appropriate documentation.

7.3.6 Analysis of Uncertainty: Uncertainty Budgets

To facilitate the process of calculating uncertainty, it is often quite helpful to summarise this uncertainty analysis, in what is designated as an uncertainty budget—in a straightforward spreadsheet format, as indicated in Table 7.2.

Yet, another valued approach, which is similar in concept to that depicted in Table 7.2, is to establish the application of uncertainty budgets utilising another type of spreadsheet, as depicted in Table 7.3. Assuming here that the input quantities have been set, then the next procedure is to calculate the variation limits (i.e. 'x_i' estimates) and the uncertainty contributions, enabling one to set up an uncertainty budget. This budget can be achieved in several logical steps, as follows:

1. **calculation of estimates—**based on this case on ambient conditions, or material/product specifications, also possible variation limits that are calculated for each input quantity;
2. **application of distribution factor**—here, the type of distribution is selected (i.e. depending on the probability that the result lies within the prescribed

Table 7.2 A typical uncertainty budget— being produced here—in the form of a basic spreadsheet

Source of uncertainty	Value ± distribution	Probability	Divisor uncertainty	Standard (mm)
Calibration uncertainty	5.0	Normal	2	2.5
Resolution (size of division)	0.5 mm[a]	Rectangular	$\sqrt{3}$	0.3
Artefact not lying perfectly true and straight	10.0 mm[a]	Rectangular	$\sqrt{3}$	5.8
Standard uncertainty of mean				
10 repeated readings	0.0.7 mm	Normal	1	0.7
Combined standard uncertainty	Assumed	Normal		6.4
Expanded uncertainty	Assumed	Normal	($k = 2$)	12.8

Source Beginner's G.U.M., Bell, S./The NPL (1999)
[a]Here the (±) half-width divided by $\sqrt{3}$ is utilised

Table 7.3 An example of a typical uncertainty budget, here being tabulated for a metrology instrument

Quantity (x_i):	Type	Estimate	Distribution factor	Uncertainty contribution (μm)
Repeatability	A			1.00
Variation of zero	A			1.00
Indication error	B	1.00	0.6	0.60
Flatness	B	0.60	0.5	0.30
Straightness	B	0.60	0.5	0.30
Parallelism	B	1.00	0.5	0.50
Ambient temperature	B	0.30	0.7	0.21
Temperature difference	B	1.40	0.7	0.98
Comp. form error	B	2.00	0.6	1.20
Combined uncertainty	U_c			2.29
Expanded uncertainty	$U = 2 \times U_c$			4.58

Source Beginner's G.U.M., Bell, S./The NPL (1999)

where $U_c = \sqrt{\left(x_{1a}^2 + x_{2a}^2 + x_{1b}^2 + x_{1b}^2 + x_{2b}^2 + x_{3b}^2 + x_{4b}^2 + x_{5b}^2 + x_{6b}^2\right)}$

limits) for a rectangular distribution (i.e. 100 %), or for a normal distribution (i.e. 99.73 %).

NB As an alternative to such complex calculations, the following elementary correction factors can be utilised:

- **rectangular distribution—**multiply the limit by 0.7;
- **normal distribution (3*s*)**–multiply the limit by 0.5.

Owing to the fact that in Table 7.3 there is *no* correlation between the uncertainty components, the combined standard deviations are expressed in the form of a standard deviation. In this case, for the metrology instrument from Table 7.3, the combined uncertainty ('U_c') was established at 2.29 μm, which will need to be multiplied by the coverage factor of '$k = 2$', to ensure a 95 % probability that the measured result will lie within the uncertainty band. The metrology instrument in this case, which had a manufacturer's stated specified accuracy of 2 μm, had a measurement uncertainty of 4.58 μm (i.e. from Table 7.3) when it was used to inspect some machined shafts under workshop conditions. In any uncertainty budget calculations, the objective is to ascertain whether the measured result will be adequate for its intended purpose. By way of an example, if the measurement uncertainty is small when compared to the inspected diametral tolerance, then here, the metrology equipment can be utilised with confidence—for the stated inspection procedure. In the case cited for the uncertainty budget for the metrology instrument (Table 7.3), the analysis illustrates that $\approx$50 % of this budget is accounted for by temperature factors alone. Due to the large impact that temperature influences have on the measurement uncertainty for any critical

measured component feature on the shop floor, they must be corrected back to 20 °C. However, correcting for temperature within the production shop may lead to unforeseen practical problems being encountered. On the shop floor, the temperature could vary during the working day, as further dimensional measurements are made—see Fig. 7.11—for the various induced errors in a machine tool producing the high-quality parts. The recorded thermal history might not be correct during this time, because any thermometer readings may not be totally accurate, or there could even be some uncertainty existing concerning the actual value for the coefficient of linear expansion for the workpiece material, which leads to some dubious inspection procedures. These uncontrolled factors of inadequate temperature correction mean that more generous limits are necessary to take into account the variability introduced because of such temperature influences. At this juncture, the most obvious way to mitigate against the lack of temperature control and its adverse effect on the measurement uncertainty is to undertake the final inspection in a temperature-controlled environment that is as close as practicable to the recommended temperature of 20 °C.

Thermal-induced measurement uncertainties during metrological inspection procedures—notably the coefficient of linear expansion workpiece issues—become critical factors at the highest levels of accuracy and precision. In suitably calibrated metrological laboratories, where these thermal influences must be adequately controlled in order to minimise any potential temperature-induced errors into the measurement, the three greatest single contributors in uncertainty components are

1. **calibration of material thermometers**—ensuring that these instruments (such as the various types of temperature measurement devices) have previously been thermally error mapped;
2. **actual workpiece temperature is established**—at this temperature there will be a large influence on the coefficient of linear expansion, which must also be known;
3. **air temperature reading errors must be known** – due to air convection currents, such as lamellar flow/air turbulence/hot or cold spots within the inspection room, etc.

Other environmental factors such as humidity and air pressure can also have a significant influence on the measurement uncertainty. Particularly when a laser-based instrument's light path is employed in any calibration/measurement procedure, this problem will be exacerbated over longer laser distances, for larger plant calibrations.

In the previous tabulation and discussion of measurement uncertainty, it was seen as important that the correct conclusions were drawn from the results, which is of great significance when deciding if the values fall within or outside the component's specification limits. If both the result and its accompanying measurement uncertainty fall inside the tolerance boundary, then the process can be deemed to be compliant, in which the manufacturing operation will be capable of sustaining efficient measurement and process control. Conversely, for any form of

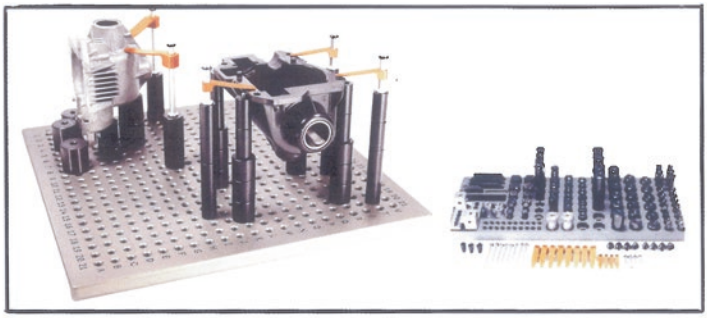

Modular fixturing designed specifically for *Coordinate Measuring Machines* (CMM's), with base plates of cast aluminium having a 'NiTuff' - a hard-coat anodised surface to resist wear. They can be utilised for measurement applications across many industries, such as aerospace, automotive and medical. Two types of 'pre-configured kits' are available depending on the part being fixture: precision-clamping – shown above; or magnetic and precision-clamping. [Courtesy of Renishaw plc]

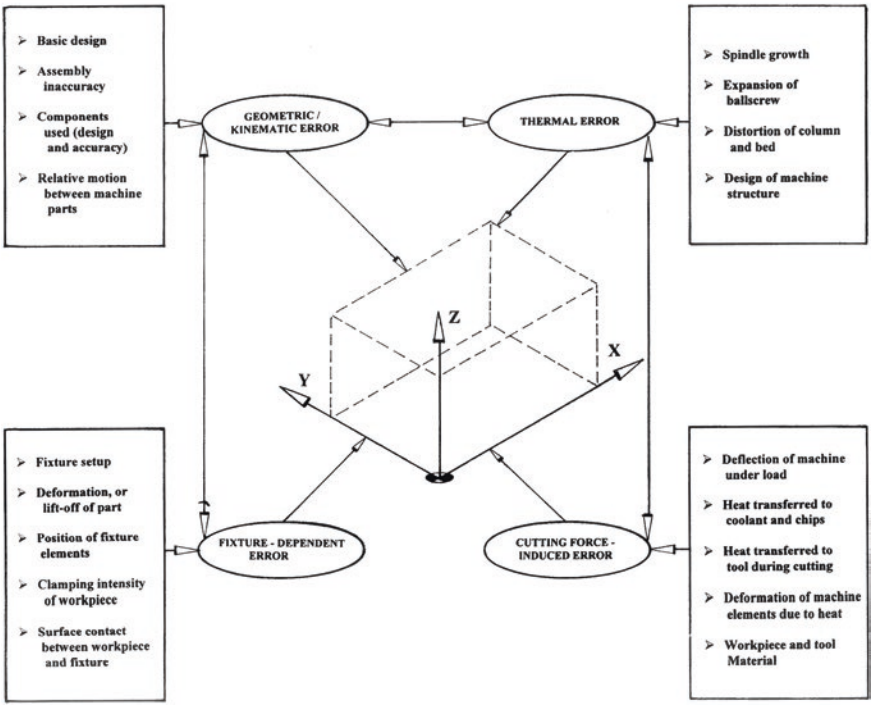

Fig. 7.11 An overview of the 'error budget' in a machine tool and some of the factors affecting the machine's structure (adapted from: Ramesh et al. 2000)

non-compliance to occur, then neither the result nor any part of the uncertainty band will fall within the specified tolerance limits. Under these circumstances, where neither the result nor any part of the uncertainty band is completely inside, or indeed outside the limits, then somewhat of a dilemma for the Inspector will occur, as no firm conclusion about the compliance state can be made. Prior to stating the compliance with any form of technical specification, it is always advisable to check the demands for this specification. By the way of illustration, sometimes a specification may incorporate factors such as attributes—these are known as non-measurable entities, such as a component's visible appearance—its interchangeability, or the ability to achieve some form of electrical connectivity and many more variations on this theme, which have no actual bearing on the measurements previously taken, but they can seriously impinge on the whole uncertainty problem.

7.3.7 Reducing Measurement Uncertainty

It is essential to remember that it is just as important to attempt to minimise uncertainties as it is to be able to quantify them. Therefore, some good metrological working practices will help to reduce measurement uncertainties, which might include the following issues:

- **calibration of instruments/equipment, or to have them calibrated by a third party**—then apply those calibration corrections which appear on the certificate;
- **compensating for any corrections**—accordingly making certain adjustments for any other significantly known errors;
- **ensuring measurements are traceable to National Standards**—employing calibrations that offer traceability via an unbroken chain of measurements to the relevant standard;
- **selecting the optimum metrology instrumentation/equipment**—normally such instruments would encompass a calibration facility with the minimum uncertainty of measurement;
- **repeating and checking measurements**—occasionally, it is advisable to allow someone other than the usual inspector to repeat these readings, or utilise a totally different method of assessment, to ensure validity of the results;
- **checking calculations and transcription of results**—here one ensures that the results are substantiated and are correctly written within the documentation;
- **utilising uncertainty budgets**—the budget will identify where the most significant uncertainties occur so that they can then be minimised;
- **awareness of problems in calibrated chains**—at every step in the chain there is the potential for uncertainty to increase.

Consequently, it is important to utilise the above-described good working practices in any form of measurements taken and therefore in this instance follow equipment manufacturer's instructions whilst this metrology equipment is operated by

experienced and relevantly trained personnel. Furthermore, one must also subsequently check and validate software—if employed—to guarantee that it operates satisfactorily, while likewise ensuring that good and appropriate record keeping of both measurements and calculations are produced at the time of this inspection procedure. Finally, it is vital to keep a written account of any other relevant and additional information, as this evidence may be useful at a later stage, should these results ever be called into doubt, or presented in a litigation dispute—sometimes many years after the actual event occurred.

Moreover, there are some additional factors that need to be considered in any dealings with uncertainty issues, particularly if they have any one or perhaps other combination of those listed below:

- **when utilising statistics for very small data sets**—normally, this type of batch size is considered to be <10 samples;
- **if one uncertainty component is considerably larger than all the others**—when involved in the calculation and tabulation of uncertainty budgets;
- **if just some inputs to the uncertainty calculation are correlated**—then this type of abridged tabulation of data needs to be singularly addressed;
- **when the distribution or spread has an unusual shape**—which is when it is obviously not normally distributed—such as is the case for either a skewed distribution (i.e. when either positively or negatively biased) or for a bi-modal hump distribution (i.e. this latter distribution may occur when two batches from different machine outputs are unintentionally merged, then inspected);
- **if the uncertainty has been obtained for other than a single result**—that is by fitting either a linear regression curve, or similar, or perhaps a line to a number of points to obtain the required information.

These explanations are by no means an exhaustive account on the somewhat complex and interrelated subject of measurement uncertainty, but they simply attempt to discuss just some of the relevant principles and practices behind the theoretical application to the problems in dimensional measurement.

7.4 Statistical Process Control (SPC)—In Production Output on Machine Tools

Introduction

The term statistical process control (SPC) relates to a technique utilised in many aspects of quality control that exploits some basic and applied statistical methods. The abbreviation to SPC is normally applied to either a batch or continuous production process, in order to monitor and control such procedures. By the successive monitoring and controlling of the manufacturing process, it will ensure that it operates at its full potential, while producing consistent high-quality parts. As

a consequence and when it is working at its full potential, this SPC process can create as much conforming product as possible, but with a minimum if not total elimination of any waste (i.e. usually the result of its subsequent rework, or in the production of unintentional scrap).

The techniques that have been developed and refined over many years of SPC usage can be applied to any process where the conforming product output (i.e. defined as a product meeting its ensuing technical specifications) can be adequately measured.

7.4.1 What is Statistical Process Control?

With the generic title of SPC in the wide spectrum of engineering disciplines, it can be considered as an analytical decision-making tool which allows one to perceive when a manufacturing process is working correctly and moreover just as importantly, when it is not. It is well known that product variability is present in any form of stochastic production process and deciding when this variation is natural and if it needs correction, it is the key element to the successful application of quality control.

In order to monitor and then control continuous production processes, control charts were originally constructed based on statistical principles previously developed by Dr Shewhart[16] and are one of the essential tools of continuous improve-

[16]**Dr. Walter Andrew Shewhart** (i.e. given here, with more in-depth treatment—also see Footnote 12): (Born: 18 March 1891 in New Canton, Il., USA—died: 11 March 1967 in Troy Hills, NJ., USA) was a significant American Physicist, Engineer and Statistician, invariably known as the "Father of Statistical Quality Control". He attended the University of Illinois obtaining both a Bachelor's (1913) and Master's (1914) degree—in Physics—before being awarded his Doctorate also in Physics from the University of California, at Berkeley—in 1917. Moreover, the original concepts of total quality management (TQM) and that of continuous improvement can be traced back to this former Bell telephone employee. He was one of W. Edwards Deming's original teachers, where at the time, he critically emphasised the importance of adapting management processes to create profitable situations for both businesses and consumers, promoting the utilisation of his own creation, this being the SPC control chart. At this time, Dr. Shewhart believed that lack of relevant information greatly hindered the efforts of control and management processes within a production environment. So, in order to assist the manager in making scientific, efficient, economical decisions, he then developed these practical statistical process control SPC techniques. Today, many of the modern ideas regarding quality-related issues owe their inspiration to the formative work by him. Furthermore, he also developed the so-called practical technique termed Shewhart Cycle Learning, which combined both creative management thinking with that of statistical analysis. This simple management Shewart cycle contains four continuous steps; these are (i) Plan, (ii) Do, (iii) Study, and (iv) Act. These steps (i.e. most commonly referred to as PDSA cycle), Shewhart believed, would ultimately lead to a total quality improvement. Here, this Shewart cycle developed its philosophical strategy from the notion that the constant evaluation of management practices—as well as the willingness of management to adopt and disregard unsupported ideas—is the key elements to the evolution of a successful commercial enterprise.

ment in quality control. As a consequence, these widely employed control charts monitor processes to demonstrate how the process is performing and in what manner this process and its capabilities are affected by changes to that process. The collected data from this charted information is then utilised to make any necessary quality improvements to the manufacturing process; further, these charts are also used to determine the capability of the process. Such charting can then help to identify either special or assignable causes for factors that might impede optimum production performance. Accordingly, control charts can obviously confirm if a process is either in-control or out-of-control and further, they can show the variance of the output of a process over time. Such a variable might be the measurement of diameter, critical length measurement, temperature fluctuations and also there are many more variable-measured quantities that can be assessed by these QC techniques.

In practise, these control charts can compare the production output variance against pre-selected upper and lower control limits, to establish if the output data for this variable being monitored fits within the expected, specific, predictable and normal variation levels. If this is so, then the process is deemed to be in control and the variance between measurements can be considered as a normal random variation—which is inherent within this stochastic process. Conversely, if this variance falls outside these prescribed limits, or has a run of non-natural points, then the process can be considered to be out-of-control. Here then the output variation is the key factor to any form of SPC charting, where the extent of this variation in a process indicates whether a process is operating as it should. Whenever the variation between the points is large enough for the process to be out-of-control, this variability is predicted to be due to non-natural or assignable (special) causes.

7.4.2 Control Chart Functions

The main purpose of utilising a control chart is to monitor, control and improve the overall process performance over time, by considering any variation and its actual source. There are a number of distinct functions that can be attributed to the use of a control chart; these are as follows:

1. centres one's attention on detecting and monitoring process variation over time;
2. provides a statistical tool for on-going control of a process;
3. differentiates the special from common causes of variation in order to act as a guide for local or management action;
4. helps to consistently improve a process, enabling it to perform and predictably achieve higher quality, lower cost and greater effective capacity;
5. serves as a common language for both engineers and metrologists—when discussing actual process performance.

Additionally, these ubiquitous control charts can offer certain other significant features and benefits—see Fig. 7.12—such as follows:

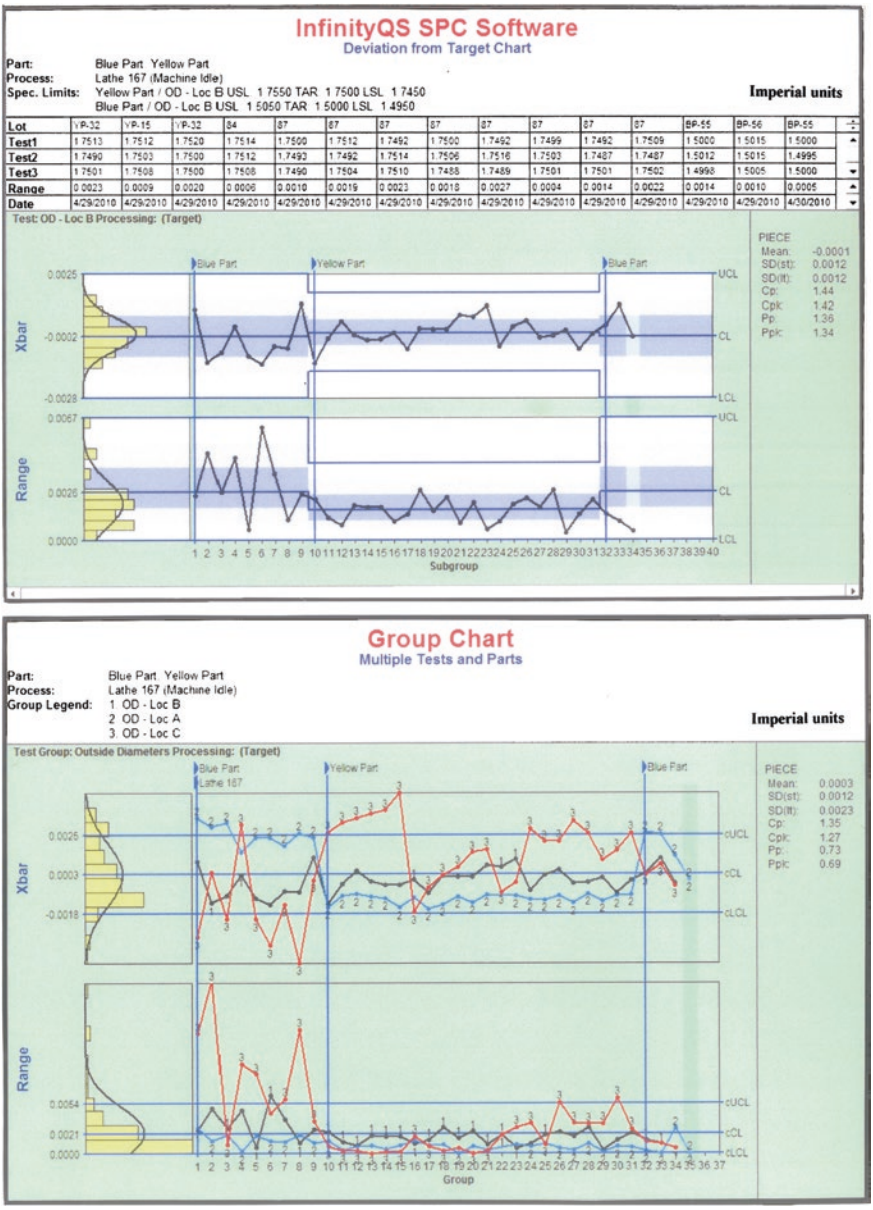

Fig. 7.12 Some 'real-time SPC software': for a typical '*averages and range chart*' for critical dimension in a volume production process—such as turning. Courtesy of InfinityQS® International, Inc. (Fairfax, FA, USA)

- data points are either averages of subgroup measurements, or more likely, individual measurements plotted on the *X*- and *Y*-axes and joined by a line, with time always being on the *X*-axis;

- the average or centreline is normally the average, or mean of the data points and is drawn across the middle section of the graph, usually as a heavy or solid line—see Fig. 7.9;
- the upper control limit (UCL)[18] is drawn above the centreline and is invariably annotated as UCL. This UCL is often termed the +3 sigma line.
- the lower control limit (LCL) (see Footnote 18) is drawn below the centreline and is normally annotated as LCL. This LCL is usually defined as the −3 sigma line. The *X*- and *Y*-axes should be labelled and a title specified for this control chart.

7.4.3 Control Chart—Background Information

As previously described, a typical manufacturing process may either be classified as in-control or out-of-control. The boundaries for these classifications are set by calculating the mean, standard deviation and also the range, for a set of process data which was collected when the process was under stable operating conditions. Once gathered, subsequent data can then be compared to the already calculated mean, standard deviation and range, to determine whether this newly acquired data will fall within acceptable constraints, namely preset limits. In the case of good and safe production control, any subsequent data collected should fall within three standard deviations of the mean. Consequently, these control charts will build on this basic idea of statistical analysis, by plotting the mean or range of subsequent data, against time. By way of example, if an industrial engineer has knowledge of the mean (i.e. Grand average) value, standard deviation and the range of a process, this information can be presented in the form of a Gaussian curve—see Fig. 7.8b—or simply as a population density function[19] (PDF).

[18]These ±3 sigma limits (i.e. see Fig. 7.8), are also practically known as upper/lower action limits (i.e. denoted by UAL and LAL, respectively, and they are nominally set at 0.001 probability, i.e. 1-in-1000 chance of occurrence), whereas the 2 sigma limits, namely the upper/lower warning limits (i.e. denoted by UWL and LWL, respectively, which are nominally set at the 0.025 probability, i.e. 1-in-40 chance of occurrence).

[19]**Population Density Function** (**PDF**) is utilised in the main, in probability and statistical theory: being the density estimation which is the construction of an estimate, based upon observed data, of an unobservable underlying probability density function. The unobservable density function is thought of as the density according to which a large population is distributed, and the data are usually considered as a random sample from that population. A variety of approaches to density estimation are utilised, including **Parzen windows**: in Statistics, is the Kernel density estimation (KDE), being a non-parametric method to estimate the PDF of a random variable. Here, the KDE is a fundamental data-smoothing problem where inferences about the population are made, based on a finite-data sample. In some research fields, it is also termed as the Parzen–Rosenblatt window method, after Emanuel Parzen (i.e. Dr Parzen is an American statistician—who has researched into signal detection theory and time series analysis) and Dr Murray Rosenblatt (i.e. who also is an American statistician—specialising in time series analysis); these active researchers are usually credited with independently creating such Windows—in their current form and there are a range of data clustering techniques, including vector quantization. Furthermore, the most basic form of density estimation is simply a rescaled histogram.

Sample Size and Subgrouping

When constructing any form of engineering-based control charts, there are a few notable conditions that must be met; these are as follows:

- the initial predictions for the manufacturing process must be made while the process is assumed to be stable; this is because future process quality will be compared to these predictions. Hence, they must be based upon a data set that is taken while the actual production operation is running in the approved manner;
- multiple subsets of data must be collected, where a subset is simply just a set of '*n*'—measurements, taken over a specific time range. The number of subsets can be represented as '*k*'. So a subset average, subset standard deviation, together with a subset range, will be computed for every single subset;
- from these computed subsets, a grand average, an average standard deviation and an average range can be calculated. This grand average is the average of all the subset averages. Further, the average standard deviation is simply the average of subset standard deviations; likewise the average range is simply the average of subset ranges.

Once this process information has been established, the upper and lower control limits for the production procedure can then be determined from this data, with future data taken to determine process stability, which can be of any size. This is because any point taken should fall within the recognised statistical predictions. It is assumed that the first occurrence of a point not falling within the predicted limits shows that the system must be unstable since it has changed from the predictive model. The subsets are simply defined, being based upon the data and the process. Finally, the population size, '*N*', is assumed to be infinite. Alternatively, if the population is finite, but the sample size is less than 5 % of the population size, one can still approximate the population to be near infinite. That is,

$$n/N \leq 0.05$$

where 'n' = the sample size, 'N' = the population size.

***X*-Bar, *R* Charts and *S* Charts**

Fundamentally, there are three types of control charts employed to determine if data is out-of-control; these are (i) *X*-bar charts, (ii) *R* charts and (iii) *S* charts. Invariably, an *X*-bar chart is often paired with either an *R* chart—see Figs. 7.9 and 7.12—or an *S* chart to produce a complete picture of the same set of data. Of note is that by utilising both the *X*-bar and *R* charts in tandem, they overcome the so-called blind spot that would otherwise be present if only the *X*-bar chart was employed. Here, the *R* chart reacts to changes in process data much faster than the *X*-bar, which alleviates this potential delay problem—to be mentioned below.

Pairing *X*-Bar with R Charts

The *X*-bar chart (i.e. average) and R chart (i.e. range) as cited above are often paired together—see Fig. 7.9 and 7.12. Here, the *X*-bar chart displays the

centreline, which is calculated utilising the grand average, coupled with the upper and lower control limits, which are calculated using the average range. Consequently, any future experimental subsets are plotted and then compared to these previous values—which demonstrates the centring effect of the subset values. The *R* chart plots the average range and the limits of the range simultaneously. Again, the future experimental subsets are plotted relative to these values, with the *R* chart displaying the dispersion of the subsets. The *X*-bar chart/*R* chart both plot subgroup averages. Of note is that these charts should only be used when such subgroups really make sense. For example, in a typical gauge R&R study when operators are testing in duplicates, this subgrouping in reality, simply, represents the same group.

Pairing *X*-Bar with *S* Charts

As an alternative, *X*-bar charts can be paired with *S* charts (i.e. standard deviation) which is typically done when the size of the subsets is large. For larger subsets, the range is an inappropriate statistical measure to estimate the distributions of the subsets and instead the standard deviation is invariably utilised. In this case, the *X*-bar chart will display process control limits that are calculated using the average standard deviation. These *S* charts are similar to that of the *R* charts; however, instead of range they track the standard deviation of multiple subsets.

Smoothing Data—With a Moving Average

Whenever it is desired to have smooth data, the moving average technique is the one relevant option. Here, this method involves taking the average of a number of points and then utilising that average for the middle data point. From this point onward, the data is treated in the same fashion as any normal group of '*k*' subsets. Although this moving average technique will produce a smoother curve, it has a distinct lag in detecting points, which may be problematic if these points are outside of the acceptable range. This time lag would keep the control system from reacting to the process problem until after the average is established. For this reason, moving average charts are only really appropriate for mainly very much slower production processes that can cope with this time lag.

7.4.4 Control Chart Limits

In many circumstances, the inherent variability of manufacturing processes is relatively small when compared to that of the actual width of the component's specification tolerance zone—see Fig. 7.3. In such circumstances, the process mean may shift from the central target value without any reject manufactured parts being made. This type of production output is partially shown in Fig. 7.7a, as the high RPI/C_p value changes from 1.33 to 1.1 and ultimately to 0.9—where at this time, some unavoidable scrap will become apparent. In this current and unstable process where drifting has occurred, a different type of control chart known as a relaxed or

modified control chart may be employed for precision class component output—as described below.

Relaxed Mean, or Modified Control Charts

Relaxed mean, or modified control charts can allow the process mean to wander away from the actual target value, until such a time as it approaches the tolerance limit—as depicted by the systematic error creating drift in Fig. 7.7a (top), with now a C_p value of 0.90. The critical question here is "How close to the tolerance boundary can one allow such a process to move?"—this questionable statement is a matter of some perceptive judgment and statistical calculation. By way of an example, if one does not accept a 0.1 % (i.e. 1-in-1000 defects) of the production output falling outside each side of the tolerance boundaries—see Fig. 7.10 (bottom) here with a $C_p > 0.80$—then one must maintain the process mean to within a distance of 3.09σ inside each tolerance limit. In order to set up the upper action limits (UAL) on the relaxed mean control chart,at '$3.09\sigma/\sqrt{n}$' above the highest allowed process mean, necessitates that the distance between the upper action limits (UAL) and the upper tolerance '$\boldsymbol{U}$' is known. This can be determined in the following manner, with the actual distance represented by '$A''_{0.001}\overline{R}$', where

$$A''_{0.001}\overline{R} = 3.09\sigma - 3.09\sigma/\sqrt{n}$$

but

$$\sigma = \overline{R}/d_n$$

therefore,

$$A''_{0.001}\overline{R} = \frac{3.09\overline{R}}{dn} - \frac{3.09\overline{R}}{dn\sqrt{n}}$$

that is,

$$A''_{0.001} = 3.09/d_n(1 - 1/\sqrt{n}).$$

Similarly, the distance between the upper warning limit (UWL) and 'U' is represented by '$A''_{0.025}\overline{R}$':
where

$$A''_{0.025} = 1/d_n(3.09 - 1.96/\sqrt{n}).$$

The actual values of both '$A''_{0.001}$' and '$A''_{0.025}$' have thankfully been previously calculated for each sample size and as such are typically available from a wide variety of reference sources, for example, in the booklets of statistical tables (Murdoch and Barnes), or from other relevant books, for example SPC (Oakland)—see Table 7.4, or alternatively, they can be obtained from relevant sources on the Internet.

Accordingly, the setting of control limits for the relaxed mean control chart, is now simply obtained by applying the appropriate expression (above), as follows:

$$\text{Upper Action Line (UAL)} = U - A''_{0.001}\overline{R}$$

Table 7.4 Constants utilised in the design of relaxed mean, or modified control charts for sample mean

Sample: size (n):	Up to 0.1 % outside tolerances		Up to 0.001 % outside tolerances	
	$A''_{0.025}$	$A''_{0.001}$	$A''_{0.025}$	$A''_{0.001}$
2	1.51	0.80	2.32	1.61
3	1.16	0.77	1.70	1.31
4	1.02[a]	0.75[a]	1.46	1.19
5	0.95	0.73	1.34	1.12
6	0.90	0,71	1.26	1.08

Source Oakland (2003)

[a]The values employed below—have been utilised—for the calculation of the action and warning limits

$$\text{Upper Warning Line (UWL)} = U - A''_{0.025}\overline{R}$$

$$\text{Lower Warning Line (LWL)} = L + A''_{0.025}\overline{R}$$

$$\text{Lower Action Line (LAL)} = L + A''_{0.001}\overline{R}$$

As a consequence in the overall production process, there being 0.1 % material outside these prescribed limits and unacceptable, and then a lower figure is required, with the A'' constants which may be adjusted accordingly—this information is also available from the appropriate statistical table.

Practical Example—Determination of Control Limits

In a typical scenario, utilising the relaxed mean control chart for establishing the control chart limits, in a rather basic production process on a turning centre, dowel steel rods of variable lengths were to be manufactured—that is parted off from a stock bar length—ranging widely from nominal lengths of 125–175 mm, having first established a precision class of '$n = 4$'; '$\overline{R} = 10.8$ mm':

$$\text{then:} \quad \text{RPI} = 2T/\bar{R}$$
$$\text{thus:} \quad = 50/10.8 = 4.63$$

By consultation with the appropriate statistical table for high relative precision this allows for the relaxed mean control chart information to be utilised. Now, assuming that one is prepared to accept just 1 in 1,000 of these rods being outside the specification (i.e. defective)—from the tables—this gives the following values:

$$A''_{0.001} = 0.75 \quad \text{and} \quad A''_{0.025} = 1.02$$

Therefore, the relaxed mean control chart limits are set to

$$\text{Upper Action Line(UAL)} = 175 - (0.75 \times 10.8) = 166.9\,\text{mm}$$

$$\text{Upper Warning Line(UWL)} = 175 - (1.02 \times 10.8) = 164.0\,\text{mm}$$

Table 7.5 A simple comparison between the conventional mean control chart (i.e. not shown) with that of the relaxed mean or modified control chart

Limit	Conventional mean chart (mm)	Relaxed control chart (mm)
Upper Action Line (UAL)	158.2	166.9
Upper Warning Line (UWL)	155.2	164.0
Lower Warning Line (LWL	145.0	136.0
Lower Action Line (LAL)	142.0	133.1

Source Oakland (2003)

$$\text{Lower Warning Line(LWL)} = 125 + (1.02 \times 10.8) = 136.0\,\text{mm}$$

$$\text{Lower Action Line(LAL)} = 125 + (0.75 \times 10.8) = 133.1\,\text{mm}.$$

NB In Table 7.5, a comparison can be made for the conventional control charts, to that of the relaxed control charts, for similar production process data.

As one might expect, the limits on the relaxed control chart are much wider than those on the conventional control chart and as a consequence allows greater relative movement of the production process mean, before any intervention/adjustment is required for the component parting off process. Furthermore, in some instances, it may be advantageous to accept a process mean moving closer toward one of the tolerance boundaries, such as the lower limit, thus allowing the process to drift toward a higher mean. Under these circumstances, the desired control may be achieved by setting up mixed control charts, utilising the relaxed lower limits in conjunction with the conventional UALs and UWLs. Here then, the mean chart could be designed to control the lengths of the parted off steel rods.

Finally of note is that the relaxed range charts have not been suggested herein as the final solution to the production process and as such, they should always be employed together with conventional range charts. This combination of mixed charting allows the process spread to increase, which invalidates the calculations of both the relative precision and relaxed mean chart control limits.

7.4.5 Reading Control Charts

As described above and shown in Figs. 7.9 and 7.12, control charts can determine whether a process is behaving in an unusual manner. Hence, the quality of the individual points of a subset is determined as unstable, if any of the following simple rules occur:

Rule 1: **any point falls beyond 3σ from the centerline**—this is normally represented by the upper and lower control limits;
Rule 2: two out of three consecutive points fall beyond 2σ—being on the same side of the centreline;

Rule 3: four out of five consecutive points fall beyond 1σ—also being on the same side of the centreline;
Rule 4: nine, or more consecutive points—falling on the same side of the centreline.

Trouble Shooting—with Control Charts

In Fig. 7.9, just a few of the wide range of variable effects of production process output are characteristically shown on the average and range charts—there are many more variants of such manufacturing outputs that could also be mentioned, but these examples clearly show how both of these control charts can be utilised for potential production line trouble shooting. As a consequence,

- **a drift or trend in the standard deviation**—in Fig. 7.9a—the pattern in the process results in an increase over the sampling period of $\approx 2^{1}/_{2}$ times the initial standard deviation. Nonetheless, the sample points on the range chart (i.e. Fig. 7.9aiii) never cross either of the control limits; however, an obvious trend in the sample range plot suggests an out-of-control process. Thus, the range chart and the mean chart (i.e. Fig. 7.9aii) have no points outside these control limits—for the same reason, with the relatively high overall process standard deviation, which has herein, necessitated quite wide control limits.
- **some frequent, irregular changes in the process standard deviation**—in Fig. 7.9b, the production process described in bi is of a frequently changing process variability, but with a constant mean. This process output results in several range chart values, either being near or crossing the warning line—depicted in biii. By careful examination of bii, it indicates the nature of the process—the mean chart points have a distribution which mirrors the process spread.
- **another variant of some frequent, irregular changes in the process standard deviation**—in Fig. 7.9c, the process varies according to ci. Both the mean (cii) and range charts (ciii)—respectively—are out-of-control and provide clear indications of a serious production process condition. In theory, it is possible to have a sustained shift in a process mean and standard deviation, or perhaps drifts or trends in both. Under these circumstances, the resultant mean and range charts would correspond to a variety of combinations of the previous charts—just mentioned.
- **a sustained shift in the process standard deviation**—in Fig. 7.9d, the process varied in di, with a constant mean, but with changes in the spread of the process sustained for periods of between six and seven sample plots. Remarkably, the range chart (diii) exhibits only one sample plot which is above the AWL, even though 'σ' has increased to virtually twice its original value. This effect is attributable to the fact that the range chart's control limits are based upon the data itself. Hence, a process showing a relatively large spread across the period of sampling will result in relatively wide control limits and further, the mean chart (dii) fails to detect the changes for a similar reason and this is the result of the process mean not changing.

7.4.6 Computerised SPC Charts

By utilising SPC software, much of the guesswork can be taken out of quality control analysis—allowing some real-time trouble shooting to occur, which is recognised as a scientific and data-driven methodology for techniques such as quality analysis and for process improvement. Today, SPC is very much an industry standard procedure for measuring and controlling quality during any manufacturing-related process. Quality data in the form of either product or process measurements is obtained in real time during continuous manufacturing activities. This data can then be simply plotted on a graph with pre-determined control limits—see Fig. 7.12. Furthermore, these control limits are established by the capability of the production process, whereas specification limits are determined by the actual end user's needs.

Establishing Control Limits on an *X*-bar and Range Charts

Any variable that has its data falling within the control limits will indicate that everything concerning the process is operating as expected and accordingly this process is deemed to be in-control. Any variation within these control limits is likely to be due to a common random cause—or systematic cause—such as the natural variation that is expected as part of the overall manufacturing process. Assuming that the data falls outside of these control limits, this will normally indicate that an assignable cause is a probable source of the product variation and something within the on-going process should be changed to rectify this issue before any potential defects occur and an out-of-control situation arises. The major advantages of utilising some form of software-driven real-time SPC is that it can

- **dramatically reduce variability and part/process scrap**—quickly and efficiently high lighting any immediate changes in the production process;
- **scientifically improve productivity**—by employing well-known and recognised statistical control measures;
- **reduce costs**—by ensuring that part scrappage is either totally eliminated from the production process, or at worst case, minimised;
- **uncover hidden process problems**—that would otherwise necessitate intimate knowledge and experience of that process, but herein is dealt with in a speedy and efficient manner;
- **instantly react to process changes**—minimising any potential out-of-control problems and conditions, allowing the process to be immediately brought back under control again;
- **make real-time decisions on the shop floor**—speedily and effectively, otherwise any such production delays would be prohibitive and potentially exceedingly costly.

Measuring the return on investment (ROI)[20]—of a real-time SPC solution—can be established and in order to be able to quantify the return on a company's SPC investment, one must start by identifying the main areas of product waste and inefficiency at the manufacturing facility. Typical common areas of such waste might include scrap, rework, over-inspection, inefficient data collection, incapable machines, equipment and/or processes, paper-based quality systems, together with perhaps some inefficient volume production lines. In order to achieve these goals, one can start to quantify the value of an SPC solution, by asking the following relevant questions:

- **"Are the quality costs really known?"**—if not, then the financial factors need to be addressed;
- **"Can current data be used to improve the processes, or is it just data for the sake of data?"**—here, much wasted time is spent looking at the wrong solutions;
- **"Are the correct kinds of data being collected in the right areas?"**—the old adage "Garbage-in, garbage-out" comes to mind;
- **"Are decisions being made based on true data?"**—if not, then control of the process will not be established;
- **"Can one easily determine the cause of quality issues?"**—this is essential trouble shooting that must be efficiently and effectively determined;
- **"Does one know when to perform preventative maintenance on machines?"**—if the process is unexpectedly out-of-control this maintenance-based problem needs to be established quickly to immediately remedy the situation;
- **"Can one accurately predict yields and output results?"**—these are important points from both a production quality output aspect, as well as from a financial viewpoint.

The advantages of utilising relevant software for SPC within the production environment has been well established over many years and industrial-based applications as to the benefits listed above, which more than cover the initial outlay cost of such software products and should be virtually mandatory in any manufacturing facility of some sophistication in today's modern industries.

[20]**Return on Investment (ROI)**: in business and commerce. The purpose of the return on investment (ROI) metric is to measure, per period, the rates of return on money invested in an economic entity in order to decide whether, or not to undertake an investment. Furthermore, it is also utilised as an indicator to compare different project investments within a project portfolio, and thus the project with best ROI is prioritised. ROI and related metrics can provide a snapshot of profitability, which is adjusted for the size of the investment assets tied up in the enterprise. Here, the ROI is often compared to expected or required rates of return on the money invested. Therefore, the ROI is not Net-present value-adjusted and most text media describe it with a Year 0 investment, but with two-to-three year's income. Marketing decisions have an obvious potential connection to the numerator of ROI (i.e. profits), but these same decisions often influence assets usage and capital requirements (e.g. receivables and inventories). Marketers should understand the position of their company and the returns expected.

7.5 Machine and Process Capability Studies

A fundamental question that should continuously be asked when reviewing any production processes will be "Is the process capable of consistently producing good parts?" If the process is capable, then one must decide what statistical controls are to be placed on the actual process. On the other hand, if the process is not capable then one must either improve the process, or implement 100 % inspection—by critically checking the relevant features of all the processed parts, but this latter action is exceedingly costly to perform.

Machine Capability Study

The production activity known as a machine capability study has in the past invariably been conducted at each machine under controlled conditions to determine whether any natural variation occurs. Normally, the person operating the machine is not allowed to alter any of the machine settings during such a study. Prior to undertaking this study on the machine, the material quality is checked/inspected beforehand to ensure component consistency. Furthermore, any metrology instrumentation and equipment to be employed in this task has to be correctly calibrated and confirmed to be repeatable, such that it has the capability to consistently record the same measurement of one specific dimension on just one specific part.

Process Capability

This process capability study is usually conducted to determine both the total variability and process stability. The study would normally include personnel, machine, as well as the material influences over a period of time. Here, time becomes an important factor as any subsequent component output quality will be influenced by any material changes and also the personnel making any corrective adjustments to cope with this and many other variables, typified by machine and room temperatures and any significant tool wear.

7.5.1 Machine and Process Capability Studies—Typical Procedure

This category of paper-based machine and process capability study may seem somewhat irrelevant in today's software-driven SPC culture, but nevertheless it may still have some relevance in machine tool investigative procedures. This type of basic study can be undertaken in a series of logical steps that are required for conducting these types of machine tool studies, as the following stages indicate:

1. **understand the component part**—determine critical dimensions and what measuring instruments are needed, while also considering the part's material and how it could influence the test results;

2. **understand the production process**—here, one must have comprehensive knowledge of the part's location, machine settings and adjustments (i.e. either manual or automatic) cycle time(s) and other factors such as any coolants required, or temperature control needed for process and if any measurements are necessary, while comprehending whether this process is to be carried out on a single or multiple workstation. This final factor is very important, because if there is more than one workstation, it may be necessary to make an actual study at each station;
3. **understand the incoming part quality**—which is being utilised in the workpiece manufacturing process;
4. **understand the inspection equipment**—with its inherent limitations of usage, which will be used for any metrological inspection procedures;
5. **understand the operating procedure**—by the person undertaking this study, during the actual production process;
6. **review any other relevant information**—obtained from either engineering, production and inspection sources, which might have an influence on the study;
7. **record test study data both accurately and succinctly with no ambiguity**—such as the machine number, its operation number and description, any tooling numbers and important machine settings, and any other relevant information.

This capability study of either the manufacturing process or a machine tool is usually expressed as a summary of the test results of the characteristic being investigated, which is then compared to say, the specified tolerance of that characteristic. These study results are then formally converted to a predicted range of variation of its anticipated six standard deviations (i.e. invariably termed just: six sigma) utilising the standard statistical measure of the normal probability distribution. Moreover, there are any number of methods by which this can be expressed, for instance:

$$\text{Capability Ratio}\,\% = (\text{6 sigma/dimension tolerance}) \times 100$$

NB This expression can be inverted to represent 'C_{pk}', which is just another way of expressing the same thing.

7.5.2 Machine Capability Study—In Detail

So that a well-organised machine capability study can be conducted effectively and efficiently, it might be a prudent approach to perhaps adopt the following step-by-step activities:

1. the capability study may be conducted at the original machine tool suppliers and then repeated later on the company's own site;
2. always utilise incoming raw material, or parts manufactured from the same batch;
3. utilise just one person to operate the machine or equipment;

4. set the machine up and do not adjust it during the course of this study;
5. prior to undertaking this study, ensure that all calibrated measuring devices, if required, have been undertaken and then do not recalibrate during the period of the study—unless it is a normal requirement;
6. judiciously record the machine details and settings, as previously outlined;
7. produce a minimum of 50 sequential parts from the process,[21] recording the order of production sequence for each part manufactured. Here, the number of parts actually studied is a matter of applying common sense. Accordingly, if the machine produces 4-off parts per minute (i.e. 240 pieces/h) or more, one should normally consider obtaining ≈200 pieces in this study. Conversely, if the machine produces <4-off parts per minute, it is quite acceptable to utilise ≈50 parts in the study;
8. from the data generated, a calculation is made for the predicted spread of six sigma and this is then compared with the total tolerance of the particular dimension under review;
9. for the machine to be considered as capable, it should be able to produce a predicted spread of six sigma—representing no more than 67 % of the total tolerance—in the instance of a newly supplied machine—and ≈75 % with an existing machine. The actual component spread should also be centrally located—centred around the nominal value within the tolerance boundaries and not simply positioned towards one end of its actual tolerance boundary;
10. the statistical calculations are usually best left to specialised computer programmes that can significantly speed up the review of results—see Fig. 7.12. This becomes a particularly important factor if the component part requires a number of features to be measured and then subsequently studied.

A factor worth consideration when undertaking a machine capability study is the influence that the tooling plays in the overall study. If one was to utilise more than one tool to undertake the same production operation, then conducting an individual study for each tool is required. Moreover, if the machine has two or more tooling stations, it is an astute measure to conduct a study on each of these separate stations. If one conducts a study, but with the combined results from a machine that has two distinct stations, then the calculated mean from each station will differ, producing a statistical curve that will now have two peaks—namely, creating a so-called bi-modal hump distribution. When setting up the ubiquitous and subsequent average and range charts—to monitor this actual process—one would be able to see a certain pattern emerging—invariably indicating some form of statistical instability being present—see Fig. 7.9. As a consequence, the knowledge

[21] **50-off sequential component parts from the production process**: here, it is normal practise when undertaking a typical capability study to obtain from this production batch, consecutive parts from the machine tool, to effectively stabilise the consistency of the overall production output. Invariably, the first-off part is often disregarded, as at that moment the production process must be stable. Moreover, statistically speaking an odd number in the inspection sample size is normally employed, thereby reducing the likelihood of the so-called flat-topped distribution from occurring; hence invariably, 49-off components are normally assessed in such capability trials—see Fig. 7.13.

gained from this machine capability study is a vital factor when attempting to both control and improve a company's plant output quality, so an unbiased output result is essential.

The logical steps in a typical process capability study are very similar to that outlined above in Sect. 7.5.2, but may vary considerably in the actual complexity and length of the study. These process-based studies are normally conducted throughout the course of a day's actual production and will take into account varying material batches, different personnels operating the plant, temperature variables, together with many other significant factors that can influence the overall part's quality. In practise, this type of process study work is somewhat time consuming and can be costly to perform. One should only undertake this type of extended study after having previously conducting a similar machine capability study and then only if it is suspected that the actual process is being subjected to certain unstable elements. At this time, identical statistical calculations are utilised and the 'C_{mk}' that was utilised in the machine capability study can invariably be replaced by 'C_{pk}'.

Of note is that many companies will now be measuring their production defects in parts per million; furthermore, one will also recall from the previous discussion that three-sigma deviations on each side of the process mean will encompass 99.73 % of the population—see Fig. 7.8b. So far, the statistical discussion has been concerned with a process capability that utilises ±3 sigma, where 99.73 % of the population of output takes place, while to provide somewhat of a safety margin, ideally ±3 sigma would be expected to fall within 75 % of the part's tolerance. This value equates to ±4 sigma at 100 % of the stated tolerance. If just the ± 3 sigma had covered the total tolerance, then 0.27 % would not be encapsulated within the spread that was utilised. This would actually equate to 2700 defective parts per million, giving 1350 parts exceeding the top limit and 1350 parts failing to reach the bottom limit. As a consequence, many companies now try for figures significantly less than this level. Finally, if a company utilises ±5 sigma instead of ±3 sigma in the statistical calculations, then one will be fairly close to 1 part per million defects—this is provided the process remains both centralised and in-control.

7.5.3 Machine Tool Capability Study—Practical Example

In Fig. 7.13, a paper-based characteristic and very basic practical example of a machine tool capability study is provided, for a machining centre, where its operation is merely slot milling a critical dimensional feature (i.e. Slot width: 40 ± 0.05 mm) in a medium-sized batch of parts. In order to complete this rudimentary chart (NB a blank copy of this chart is provided in Fig. A.28) the resulting simple and logical sequence of events should be undertaken, which might be as follows:

1. obtain 50-off slot-milled parts and measure the 40-mm slot width independently—with a suitably calibrated metrology instrument, ensuring that the consecutive machining sequence is both known and positively identified;

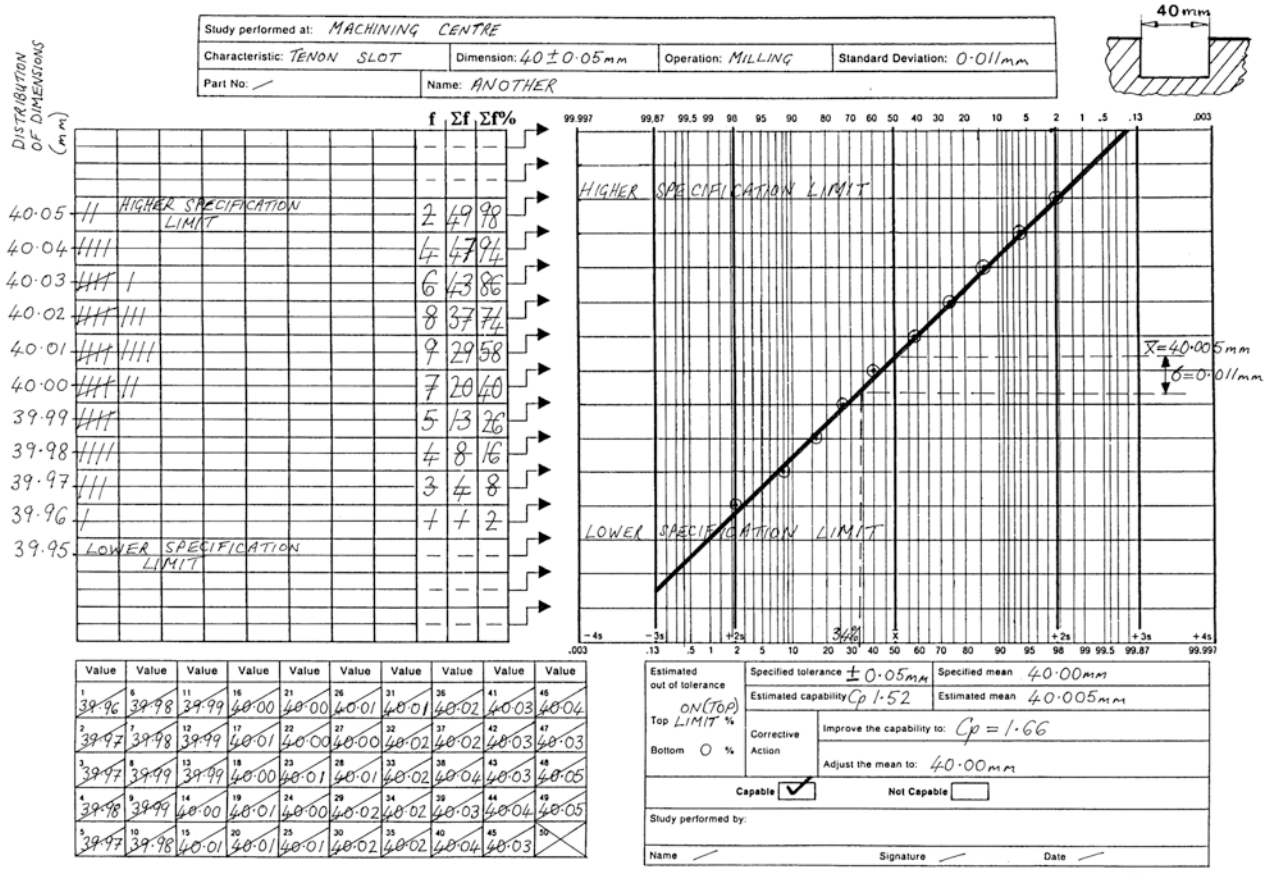

Fig. 7.13 'Capability study' (normal distribution)

2. remove the first-off milled part from this sample, ensuring both a degree of stability within this production run and utilising an odd number of parts (i.e. here, now being just: 49-off)—for the statistical reasons, mentioned previously;
3. consecutively write the components respective dimensionally measured values (i.e. their slot widths) in the appropriate numbered boxes in the bottom left-hand corner of this chart—as shown;
4. conveniently spread the sizes of the distribution of dimensions (i.e. here, ranging from 39.95 to 40.05 mm) along the left-hand side of the tally chart—as indicated;
5. simultaneously cross-off these measured values in the relevant numbered boxes, whilst concurrently marking them off in their respective tally chart positions—in the conventional manner as shown;
6. under column 'f', then tabulate their respective values of occurrence—as indicated (i.e. beginning at the bottom—with here, number '1' and ending with number '2', at the top);
7. in the adjacent column 'Σf', cumulate the respective values from column 'f', as shown (i.e. beginning at the bottom—with number '1', then adding column 'f' values to the previous value in column 'Σf' and ending with the number '49', at the top);
8. now, double these values from column 'Σf', writing them in the adjacent column 'Σf %' as shown (i.e. beginning at the bottom—with number '2' and ending with number '98', at the top);
9. plot these values on the incorporated probability paper (i.e. on the right) as illustrated then draw a straight line[22]—which is its best fit (i.e. least squares line) through these plotted points on the graph—as shown;
10. from the '$\overline{x}$' value (i.e. being obtained along the horizontal graph's axis of the probability paper) acquire a reading from this vertical line as it crosses the plotted straight line, then read-off the result—here as 40.005 mm;
11. from the 34 % value[23] (i.e. also obtained along the horizontal graph's axis of the probability paper) acquire a reading from this vertical line as it crosses the plotted straight line, this value being the difference of the values from '$\overline{x}$' to this 34 % value, giving a 'σ' value of 0.011 mm;
12. all of these estimated values from this particular machining trial can now be written in the appropriate boxes on this capability chart, allowing the 'C_p' value of 1.52 to be obtained—the method of obtaining this value being previously mentioned.

[22]If the plotted points on the probability paper occur as a straight line relationship, then this will denote that a normal/Gaussian distribution has occurred which would normally to be expected. However, if these plotted points appear as either a concave or convex curve, then it indicates a skewed distribution—either way—indicating that there is a systematic error present, which requires some further investigation, which should immediately stop this machine's production operation. Of note is that if the plotted points appear as an extended S curve on the plotted probability paper, this normally denotes a bi-modal hump distribution, meaning that either two processes have been accidently merged, or that two tools from the tooling magazine have been employed in this machining trial—possibly having different tool offsets.

[23]The difference from '$\overline{x}$' to the 34 % line, which equates to 16 %—this being the value of one standard deviation ('σ')—see Fig. 7.7b.

In summary, with this somewhat rather rudimentary paper-based form of a machine tool capability study, it has shown in this instance that the machining centre was just about capable of vertically milling this component's specific slot width and with the actual process being closely centred on the mean. Hence, all of these machined slots were proven to be just within their stated tolerance

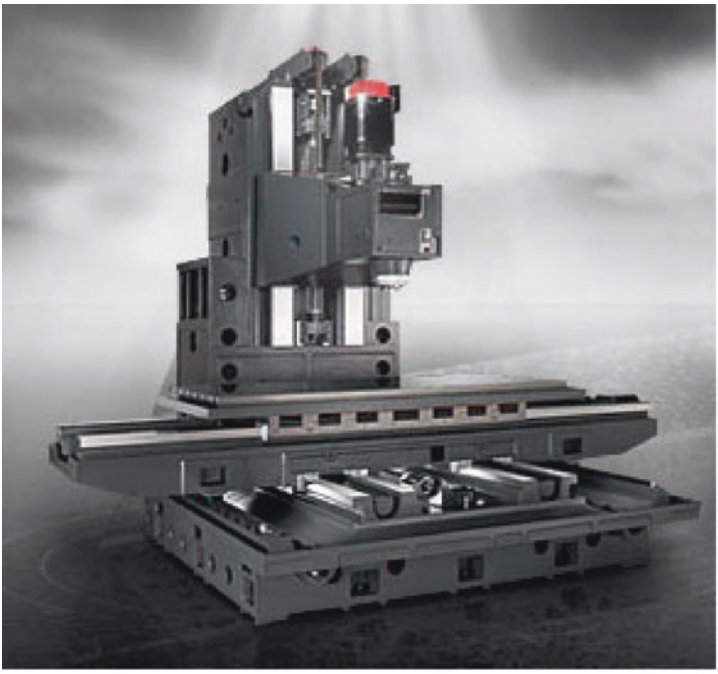

Travelling column Vertical Machining Centre – shown with guarding removed (above).

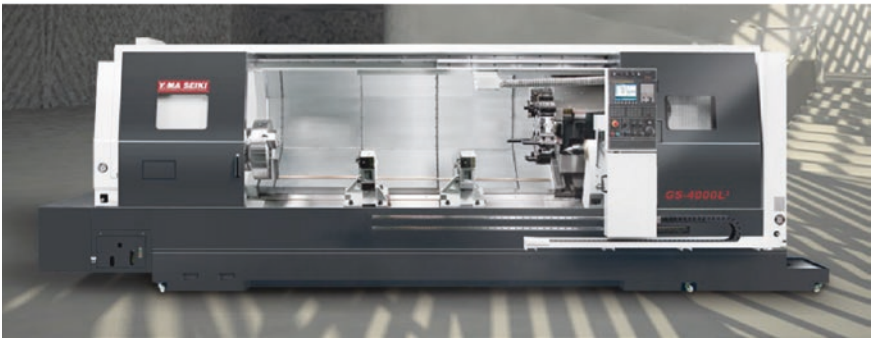

Heavy-duty Turning Centre, 30 degrees slant bed with wide box ways, with 2-speed head stock driven by a 37 kW, powerful Z-axis spindle motor, the axes rapids are 24 m/min. on X and Z axes, with FANUC motors and control.

Fig. 7.14 Two typical machining and turning centres, which are subject to periodic machine tool re-verification and process capability studies. Courtesy of Yama Seiki USA Inc. (2016)

bandwidth—admittedly slightly biased toward the top limit, and albeit, the whole process indicating somewhat of a wide dimensional spread being revealed. This latter dimensional aspect could now be statistically improved by a close examination of the reasons for this wide tolerance spread, even though the production process was shown to be just behaving normally with Fig. 7.14.

7.5.4 Final Concluding Remarks

This book on Machine Tool Metrology has endeavoured to set out to inform and explain the major reasons why, where, when and also in what manner machine calibration and artefact verification, in its widest possible form for both machine tool configurations and complementary metrology instrumentation, are considered essential today.

There are numerous differing techniques and associated artefacts that can contribute and provide possible solutions for the industrial and research-based metrologist in this endeavour, for either timely revalidation or indeed for a full calibration procedure of this critical asset within a company's manufacturing plant or laboratory. It has hopefully been established within this text that at the very least, the minimum of some form of periodic verification of such equipment is indispensable in maintaining expensive productive machines and their associated metrology-based counterparts. Ensuring that sophisticated and costly equipment and assets are suitably verified/calibrated and then certifying that they are acceptable to the relevant international standards acknowledged and utilised for this purpose for worldwide recognition is a vital activity. Such crucial metrological remedial action will confirm that these machines now duly meet the appropriate standards, with the plant traceable back to the applicable SI system of base units. This level of inherently transparent and valid traceability must be continuously maintained, in order to ensure that not only the equipment meets these mandatory standards requirements, but it is also recognised as complying, whilst being accompanied with its appropriate supportive documentary evidence. As a consequence of this level of unremitting equipment re-calibration, it will provide some actual certainty for the end user that this particular plant's calibration/verification now fully meets its correct standards, ensuring that any productive output is guaranteed to deliver and meet their customer's stringent requirements—on demand.

References

Journal and Conference Papers

Abbe, M. & Takamasu, K., *Reliability on calibration CMM*, Measurement, 359-368, 2003.

Bauman, C., De Heck, J., Leonard, E. & Merrick M., *SPC: Basic control charts: theory and construction, sample size, x-bar, r charts, s charts*, University of Michigan (USA), retrieved: May, 2014.

Bounazef, D., Chabani, S., Idir, A. & Bounazef, M., *Management Analysis of Industrial Production Losses by the Design of Experiments, Statistical Process Control, and Capability Indices*, Open Journal of Business and Management (OJBM), Vol.2 (1), Jan. 2014.

Boyles, R., *The Taguchi Capability Index*, J. of Quality Technol., Vol. 23 (1), 17-26, American Society for Quality Control Pub. (Milwaukee, Wisconsin), 1991.

Breuckmann, B. & Langenbeck, P., *In Process Interferometry By Real-Time Fringe-Analysis*, Proc. SPIE 1015 - Micromachining Optical Components and Precision Engineering, Vol. 1015, 45, April 11, 1989.

Chen, C., *Evaluation of measurement uncertainty for thermometers with calibration equations*, Accreditation and Quality Assurance, Vol. 11 (1-2), 75-82, April 2006.

Cox, M., Forbes, A., Harris, P., & Matthews, C., *Numerical Aspects in the Evaluation of Measurement Uncertainty*, Uncertainty Quantification in Scientific Computing, IFIP Advances in Information and Communication Technology, Vol. 377, 180-194, 2012.

Gibson, P,R. & Hoang, K., *Automatic statistical process control of a CNC turning centre using tool offsets and tool change*, Int. J. of Adv. Manufact. Technol., Vol. 9 (3), 147-155, 1994.

Hryniewicz, O., *Application of ISO 3951 Acceptance Sampling Plans to the Inspection by Variables in Statistical Process Control (SPC)*, Frontiers in Statistical Quality Control, Vol. 6, 80-92, 2001.

Kechagioglou, I., *Uncertainty and Confidence in Measurement*, Dept. of Applied Informatics, University of Macedonia, Ελληνικό Στατιστικό Ινστιτούτο Πρακτικά 18ου Πανελληνίου Συνεδρίου Στατιστικής σελ.441-449, 2005.

Knebel. R., *Scanning for better results*: *Scanning CMMs measure production parts more accurately than touch trigger CMMs*, *American Machinist, Nov. 1999.*

Kureková, E., Measurement Process Capability – Trends and Approaches, Measurement Science Review, Vol. 1 (1), 2001.

Leach, R., *Some issues of traceability in the field of surface topography measurement*, Wear, Vol. 257 (12), 1246–1249, Dec. 2004.

Leach, R., Chetwynd, D., Blunt, L., Haycocks, J., Harris, P., Jackson, K., Oldfield, S. & Reilly, S., *Recent advances in traceable nanoscale dimension and force metrology in the UK*, Measurement Science and Technology, Vol. 17 (3), 17, 2006.

Moona, G., Sharma, R., Kiran, U. & Chaudhary, K.P., *Evaluation of Measurement Uncertainty for Absolute Flatness Measurement by Using Fizeau Interferometer with Phase-Shifting Capability*, MAPAN – J. of Metrology Society of India, Vol. 29 (4), 261-267, Dec. 2014.

Motorcu, A.R. & Güllü, A., *Statistical process control in machining, a case study for machine tool capability and process capability*, Materials & Design, Vol. 27 (5), 364–372, 2006.

Phillips, S.D., Measurement Uncertainty and Traceability Issues: A Standards Activity Update, Precision Engineering Division, The National Institute of Standards and Technology, 2004.

Piratelli-Filho, A., *CMM uncertainty analysis with factorial design*, Precision Engineering, Vol. 27, 283-288, 2003.

Potzick, J.E., *Accuracy and traceability in dimensional measurements*, *Proc. SPIE* 3332, Metrology, Inspection, and Process Control for Microlithography XII, 471. June 8, 1998.

Prajapati, D.R., *Implementation of SPC Techniques in Automotive Industry: A Case Study*, Int. J. of Emerging Technol. and Adv. Eng'g., Vol. 2 (3), 227, Mar., 2012.

Sultana, F., Razive, N.I. & Azeem, A., *Implementation of Statistical Process Control (SPC) for Manufacturing Performance Improvement*, J. of Mech. Eng'g., Vol. 40 (1), 15-21, 2009.

Tannock, J.D.T., *Statistical process control software, data collection and computer-aided inspection*, Automating Quality Systems, 181-197, 1992.

Valdés R. A., Di Giacomo, B & Paziani, F.T., *Synthesization of thermally induced errors in coordinate measuring machines*, J. Braz. Soc. Mech. Sci. & Eng. Vol. 27 (2), Rio de Janeiro, April/June 2005.

Wang, Q., Zissler, N. & Holden, R., *Evaluate error sources and uncertainty in large scale measurement systems*, Robotics and Computer-Integrated Manufacturing, Vol. 29 (1), 1-11, Feb. 2013.

Wells, C.V., *Principles and Applications of Measurement Uncertainty Analysis in Research and Calibration*, Third Annual Infrared Radiometric Sensor Calibration Symposium September 14-17, 1992, at Utah State University - Logan, Utah, USA, NREL/TP-411-5165, UC Category: 270, DE93000034, 1992.

Zhongcheng Y., *Uncertainty analysis and variation reduction of three–dimension coordinate metrology. Part 2: uncertainty analysis*, Machine Tools & Manufact., Vol. 39, 1219-1238, 1999.

Books, Booklets and Guides

ASME B89.7.3.1-2001: *Guidelines for Decision Rules: Considering Measurement Uncertainty in Determining Conformance to Specifications*.

Bell, S., *Measurement Good Practice Guide No. 11. A Beginner's Guide to Uncertainty of Measurement*, Tech. Report, by the National Physical Laboratory (UK), 1999.

Birch, K., *Estimating Uncertainties in Testing - An Intermediate Guide to Estimating and Reporting Uncertainty of Measurement in Testing*, Measurement Good Practice Guide No. 36, British Measurement and Testing Association, 2003.

Cardelli, F., *Materials Handbook*, Springer-Verlag London Ltd., 2000.

Cox, M. G. & Harris, P. M., *Best Practice Guide No. 6, Uncertainty evaluation*, Tech. Report DEM-ES-011, National Physical Laboratory (UK), 2006.

Cox, M. G. & Harris, P. M., *Software specifications for uncertainty evaluation*, Tech. Report DEM-ES-010, National Physical Laboratory (UK), 2006.

Dieck, R.H., *Measurement Uncertainty, Fourth Edition: Methods and Applications*, ISA Pub., Dec. 2006.

Dornfeld, D.A. & Lee, D-E., *Precision Manufacturing*, Springer Science Pub., 2008.

Geometric Dimensioning and Tolerancing Handbook: Applications, Analysis & Measurement: GDT-HDBK, American Society of Mechanical Engineers (ASME), 2009.

Ghahramani, S., *Fundamentals of Probability* (2nd Ed.), Prentice Hall Pub. (New Jersey), 2000.

Grabe, M., *Measurement Uncertainties in Science and Technology*, Springer Pub., 2005.

Griffiths, B., *Engineering Drawing for Manufacture*, Kogan Page Science Pub., 2003.

Grous, A., *Applied Metrology for Manufacturing Engineering*, ISTE Ltd & John Wiley & Sons, Inc., 2011.

Imai, M., *Kaizen: The Key to Japan's Competitive Success*, McGraw-Hill/Irwin Pub., 1986.

ISO 22093:2011 - *Industrial automation systems and integration - Physical device control -Dimensional Measuring Interface Standard* (DMIS).

Leach, R., *Fundamental Principles of Engineering Nanometrology* – 2nd Ed., Elseveir Inc., 2014.

Measurement Uncertainty, United Kingdom Accreditation Service (UKAS), 2014.

Montgomery, D., *Introduction to Statistical Quality Control*, John Wiley & Sons, Inc. (New York), 2004.

Murdoch J. & Barnes, J.A., *Statistical Tables* – 2nd Ed., Macmillan Press, 1995.

Oakland, J.S., *Statistical Process Control* (5th Ed.), Butterworth-Heinemann Pub., 2003.

Salicone, S., *Measurement Uncertainty: An Approach via the Mathematical Theory of Evidence (Springer Series in Reliability Engineering)*, Springer Science Pub., Dec. 2006.

Shewhart, W. A., *Economic control of quality of manufacturing product*, Pub. by: Van Nostrand (New York), 1931.

Slocum, A.H., *Precision Machine Design*, Society of Manufacturing Engineers Pub., 1992.

Smith, G.T., *Advanced Machining – The Handbook of Cutting Technology*, IFS/Springer Verlag Pub., 1989.

Smith, G.T., *Industrial Metrology – Surface and Roundness*, Springer Verlag Pub., 2001.

Smith, G.T., *Cutting Tool Technology – Industrial Handbook*, Springer Verlag Pub., 2008.

Statistical Process Control Techniques – An Introduction, in: Statit Software, 2014.

Stigler, S.M., *The History of Statistics: The Measurement of Uncertainty Before 1900*, Belknap Press, Mar. 1990.

Stout, K., *Quality Control in Automation*, Kogan Page Pub. (London), 1985.

Study Guide for Certification of Geometric Dimensioning and Tolerancing Professionals (GDTP), American Society of Mechanical Engineers (ASME), 2013.

What is Process Capability? - NIST/Sematech Engineering Statistics Handbook, National Institute of Standards and Technology, retrieved May 2014.

Wheeler, D.J., *Understanding Statistical Process Control* (3rd Ed.), SPC Press & Statistical Process Control, Inc, 2013.

Willink, R., *Measurement Uncertainty and Probability*, Cambridge Univ. Press, March 2013.

Appendices

Appendix 1a—ISO 230 Series—Accuracy Measurement Standards (Machining Centres)

TSO 230 Machine Tool—Accuracy Measurement Standards (Machining Centres & CNC Mills)

- **ISO 230-1: 2012**
  - **Part 1:** ***Geometric accuracy of machines operating under no-load, or finishing conditions—***specifies methods for testing the accuracy of machine tools, operating either under no-load or under quasi-static conditions, by means of geometric and machining tests. The methods can also be applied to other types of industrial machines. It covers power-driven machines, which can be used for machining metal, wood, etc., by removal of chips or swarf material or by plastic deformation. It does not cover power-driven portable hand tools. ISO 230-1:2012 relates to the testing of geometric accuracy. It is not applicable to the operational testing of the machine tool (vibrations, stick-slip motion of components, etc.) or to the checking of characteristics (speeds, feeds). It does not cover the geometric accuracy of high-speed machine motions where machining forces are typically smaller than acceleration forces;
- **ISO 230-2: 2006**
  - ***Part 2: Determination of accuracy and repeatability of positioning CNC machine tools***—specifies methods for testing and evaluating the accuracy and repeatability of the positioning of numerically controlled machine tool axes by direct measurement of individual axes on the machine. These methods apply equally to linear and rotary axes. When several axes are simultaneously under test, the methods do not apply. ISO 230-2: 2006 can be used for type testing, acceptance tests, comparison testing, periodic verification, machine compensation, etc. The methods involve repeat measurements at each position. The related parameters of the test are defined and calculated. Their uncertainties are estimated as described in of ISO/TR 230- 9:2005, Annex C;

G.T. Smith, *Machine Tool Metrology*, DOI 10.1007/978-3-319-25109-7

- **ISO 230-3: 2007**
  - ***Part 3: Determination of thermal effects***—defines three tests for the determination of thermal effects on machine tools: an environmental temperature variation error (ETVE) test, a test for thermal distortion caused by rotating spindles, and a test for thermal distortion caused by moving linear axes. The test for thermal distortion caused by moving linear axes is applicable to numerically controlled (NC) machines only and is designed to quantify the effects of thermal expansion and contraction as well as the rotational deformation of structure. For practical reasons, it is applicable to machines with linear axes up to 2000 mm in length. If used for machines with axes longer than 2000 mm, it will be necessary to choose a representative length of 2000 mm in the normal range of each axis for the tests. The tests correspond to drift tests according to ISO/TR 16015 and define the evaluation and the detailed procedure for machine tools;
- **ISO 230-4: 2005**
  - ***Part 4***: ***Circular Test for CNC Machine Tools—***specifies methods of testing and evaluating the bidirectional circular deviation, the mean bidirectional radial deviation, the circular deviation and the radial deviation of circular paths that are produced by the simultaneous movements of two linear axes. Its objective is to provide a method for the measurement of the contouring performance of a numerically controlled machine tool;
- **ISO 230-5: 2000**
  - ***Part 5: Determination of the noise emission—***this part explains how, where and when noise emissions are undertaken and the levels of acceptable noise, with the techniques and equipment utilised to establish these noise levels;
- **ISO 230-6: 2002**
  - ***Part 6: Diagonal displacement test***—specifies diagonal displacement tests which allow the estimation of the volumetric performance of a machine tool. Complete testing of the volumetric performance of a machine tool is a difficult and time-consuming process. Diagonal displacement tests reduce the time and cost associated with testing the volumetric performance. A diagonal displacement test is not in itself a diagnostic test, although conclusions of a diagnostic nature may sometimes be possible from the results. In particular, when face diagonal tests are included, a direct measurement of the axes squareness is possible. Diagonal displacement tests on body diagonals may be supplemented by tests in the face diagonals, by tests parallel to the machine axes in accordance with ISO 230-2, or by the evaluation of the contouring performance in the three coordinate planes as defined in ISO 230-4. Diagonal displacement tests may be used for acceptance purposes and as reassurance of machine performance where parameters of the test are used as comparison index;
- **ISO 230-7: 2006**
  - ***Part 7: Axes of rotation—***is aimed at standardizing methods of specification and test of the geometric accuracy of axes of rotation used in machine tools. Spindles, rotary heads and rotary and swivelling tables of machine tools

constitute axes of rotation, all having unintended motions in space as a result of multiple sources of errors. ISO 230-7: 2006 covers the following properties of spindles: axis of rotation error motion; speed induced axis shifts. The other important properties of spindles, such as thermally induced axis shifts and environmental temperature variation induced axis shifts, are dealt with in ISO 230-3;

- **ISO 230-8: 2010**
  - ***Part 8: Determination of vibration values*—**is concerned with the different types of vibration that can occur between the tool-holding part and the workpiece-holding part of a machine tool. (For simplicity, these will generally be referred to as "tool" and "workpiece", respectively.) These are vibrations that can adversely influence the production of both an acceptable surface finish and an accurate workpiece. It is not aimed primarily at those who have expertise in vibration analysis and who routinely carry out such work in research and development environments. It does not, therefore, replace standard textbooks on the subject. It is, however, intended for manufacturers and users alike with general engineering knowledge in order to enhance their understanding of the causes of vibration by providing an overview of the relevant background theory. It also provides basic measurement procedures for evaluating certain types of vibration problems that can beset a machine tool:
    - vibrations occurring as a result of mechanical unbalance;
    - vibrations generated bzy the operation of the machine's linear slides;
    - vibrations transmitted to the machine by external forces;
    - vibrations generated by the cutting process including self-excited vibrations (chatter);
- **ISO 230-9: 2005**
  - ***Part 9: Estimation of measurement uncertainty for machine tool tests according to ISO 230, basic equations***—provides information on a possible estimation of measurement uncertainties for measurements according to ISO 230;
- **ISO 230-10: 2011**
  - ***Part 10: Determination of the measuring performance of probing systems of a CNC machine tool***—specifies test procedures to evaluate the measuring performance of contacting probing systems (used in a discrete-point probing mode) integrated with a numerically controlled machine tool. It does not include other types of probing systems, such as those used in scanning mode or non-contacting probing systems. The evaluation of the performance of the machine tool, used as a coordinate measuring machine (CMM), is outside the scope of ISO 230-10:2011;
- **ISO 230-11: (Not yet approved)**
  - ***Part 11: Measuring instruments & their application to machine tool geometry tests***

[Courtesy of the ISO]

Appendix 1b—ISO 13041 Series—Accuracy Measurement Standards (Turning Centres)

ISO 13041 MACHINE TOOL—ACCURACY MEASUREMENT STANDARDS (Turning Machines & Turning Centres)

- **ISO 13041-1: 2004**
  Test conditions for numerically controlled, with reference to ISO 230-1: 1996, the geometric tests on numerically controlled (CNC) turning machines and turning centres.
- **ISO 13041-2: 2008**
  Test conditions for numerically controlled turning machines and turning centre, Part 2, for geometric tests for machines with a vertical work holding spindle.
- **ISO 13041-3: 2009**
  Test conditions for numerically controlled, specifies, with reference to ISO 230-1 and ISO 230-7, Part 3: Geometric tests for machines with inverted vertical work holding spindles.
- **ISO 13041-4: 2004**
  Test conditions for numerically controlled specifies, with reference to ISO 230-2:1997, the tolerances which apply to the positioning tests for linear axes—up to 2000 mm in, Part 4: Accuracy and repeatability of positioning of linear and rotary axes.
- **ISO/CD 13041-5: 2005**
  Test conditions for numerically controlled turning machines and turning centres, Part 5: Accuracy of feeds, speeds and interpolations.
- **ISO 13041-6: 2005 (Target publication date: 2015-12-31)**
  Test conditions for numerically controlled turning machines and turning centres with reference to ISO 230-1, a series of cutting tests, under finishing conditions, of standard test pieces. Part 6: Accuracy of a finished test piece.
- **ISO 13041-7: 2004**
  Test conditions for numerically controlled turning machines and turning centres, Part 7: Evaluation of contouring performance in the coordinate planes.
- **ISO 13041-8: 2004**
  Test conditions for numerically controlled turning machines and turning centres, Part 8: Evaluation of thermal distortions.

Appendix 1c—ISO 10360 Series—Acceptance and Verification Tests (Co-ordinate Measuring Machines)

ISO 10360 Coordinate Measuring Machines (CMM'S—Acceptance & Verification Tests)

International Standard ISO 10360 covers CMM verification and this standard currently has seven parts:

- **ISO 10360-1: 2000**
  - **Geometrical Product Specifications (GPS)**—Acceptance and re-verification tests for coordinate measuring machines (CMM)—***Part 1: Vocabulary;***
- **ISO 10360-2: 2009**
  - **Geometrical product specifications (GPS)**—Acceptance and re-verification tests for coordinate measuring machines (CMM)—***Part 2: CMMs used for measuring linear dimensions;***
- **ISO 10360-3: 2000**
  - **Geometrical Product Specifications (GPS)**—Acceptance and re-verification tests for coordinate measuring machines (CMM)—***Part 3: CMMs with the axis of a rotary table as the fourth axis;***
- **ISO 10360-4: 2000**
  - **Geometrical Product Specifications (GPS)**—Acceptance and re-verification tests for coordinate measuring machines (CMM)—***Part 4: CMMs used is scanning measuring mode,***
- **ISO 10360-5: 2010**
  - **Geometrical Product Specifications (GPS)**—Acceptance and re-verification tests for coordinate measuring machines (CMM)—***Part 5: CMMs using multiple-stylus probing systems;***
- **ISO 10360-6: 2001**
  - **Geometrical Product Specifications (GPS)**—Acceptance and re-verification tests for coordinate measuring machines (CMM)—***Part 6: Estimation of errors in computing Gaussian associated features***
- **ISO 10360-7: 2011**
  - **Geometrical product specifications (GPS)**—Acceptance and re-verification tests for coordinate measuring machines (CMM)—***Part 7: CMMs equipped with imaging probing systems***

Appendix 1d—ISO 17025—General Requirements for Testing and Calibration Laboratories

ISO 17025—General Requirements for Testing and Calibration Laboratories

This Standard was first published in 1999 in May 2005 the alignment work of the ISO/CASCO committee responsible for it was completed, with the issuance of the reviewed standard. The most significant changes introduced greater emphasis on the responsibilities of senior management and, explicit requirements for continual improvement of the management system itself, and particularly, communication with the customer.

The *contents* of this ISO 17025 Standard, comprises *five* elements that are: *Scope*; *Normative References*; *Terms and Definitions,* as well as *Management Requirements and Technical Requirements.*

The two main sections in ISO 17025 are:

- ***Management Requirements—***are primarily related to the operation and effectiveness of the quality management system within the laboratory;
- ***Technical Requirements—***includes factors which determine the correctness and reliability of the tests and calibrations performed in laboratory.

Most industrial and research laboratories use ISO 17025 to implement a quality system aimed at improving their ability to consistently produce valid results. This Standard is also the basis for accreditation from an accreditation body, since the Standard is about competence, accreditation, thus, it is simply formal recognition of a demonstration of that competence. A prerequisite for a laboratory to become accredited is to have a documented quality management system, hence, the usual contents of the 'Quality manual' follow the outline of the ISO 17025 standard.

*ISO 17025 Laboratory Enclosures for—Metrological Calibration/Inspection: *Typical Laboratory Design Parameters*

- **TEMPERATURE SET POINT: ±0.01 °C to 1.0 °C;**
- **HUMIDITY SET POINT: ±1 % RH to 5 % RH;**
- **CLEAN ROOM: ISO class 1 through class 8;**
- **PRESSURE: positive, or negative:**
- **AIR VELOCITY: 1 m min^{-1} to 30 m min^{-1};**
- **LIGHTING: 50 FC, 100 FC.**

***Courtesy of Precision Environments Inc., West Chester, Ohio, USA.**

Appendix 2—Photoelectric Scanning Techniques and Linear Digital Encoders—for Machine Displacement

See Figs. A.1, A.2, A.3, A.4 and A.5.

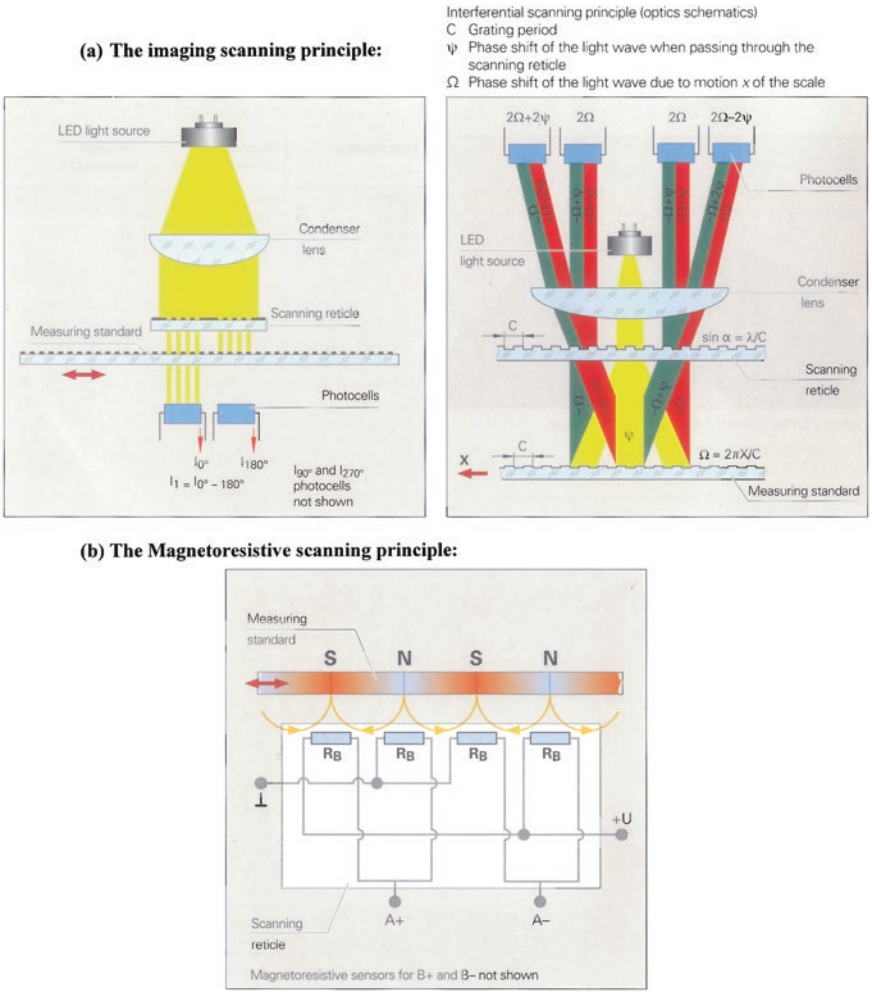

Fig. A.1 Photoelectric scanning utilising rotary/angular encoders for machines (courtesy of Heidenhain (G.B.) Limited)

(a) Block diagram: Absolute encoder with an EnDat interface:

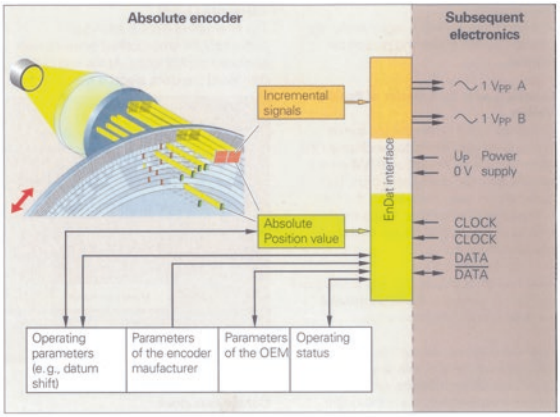

(b) Control cycles for transfer of parameters:

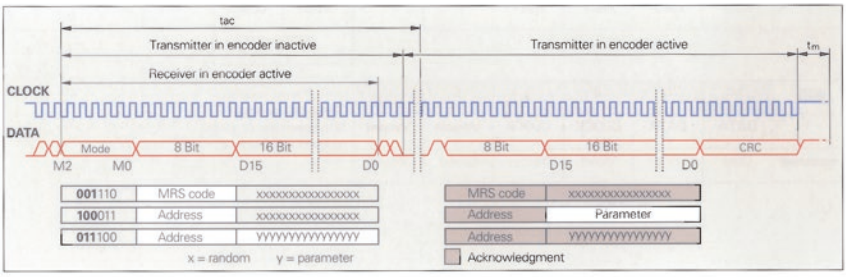

(c) Synchronization of serially transferred code value with incremental signal:

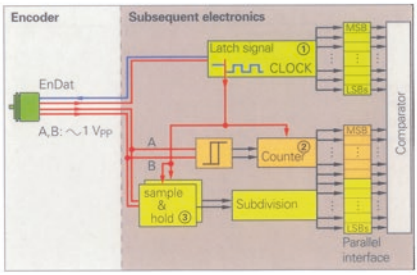

Fig. A.2 Photoelectric scanning with absolute encoders for rotary/angular applications for machines (courtesy of Heidenhain (G.B.) Limited)

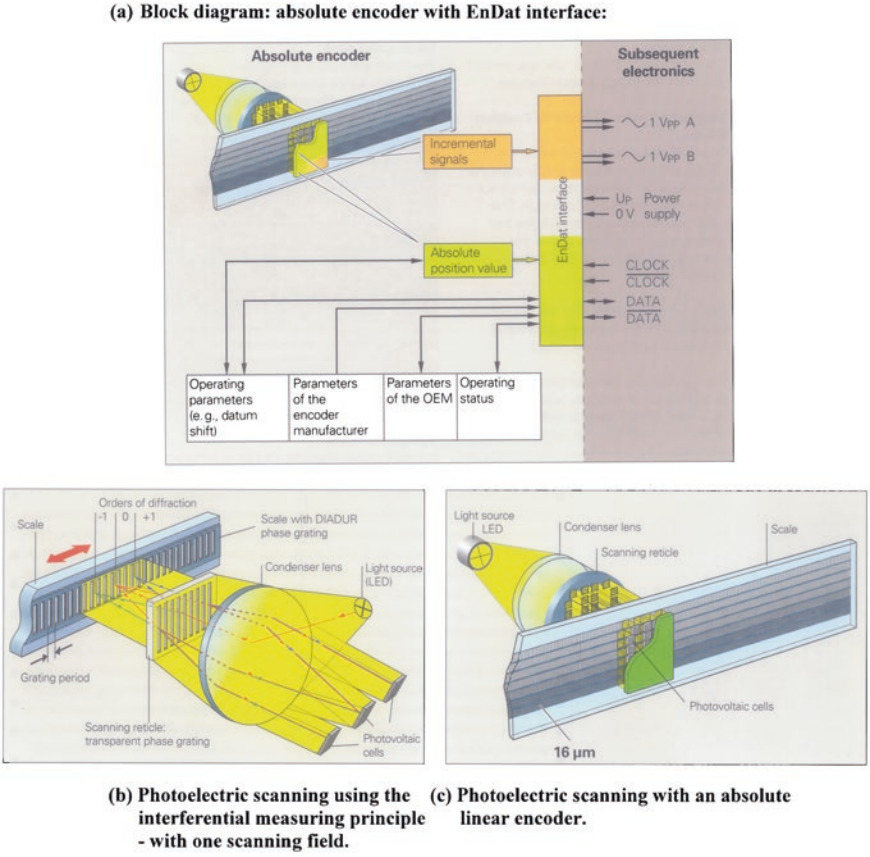

Fig. A.3 Photoelectric scanning employing inferential/absolute linear encoders for machine axis displacement. (courtesy of Heidenhain (G.B.) Limited)

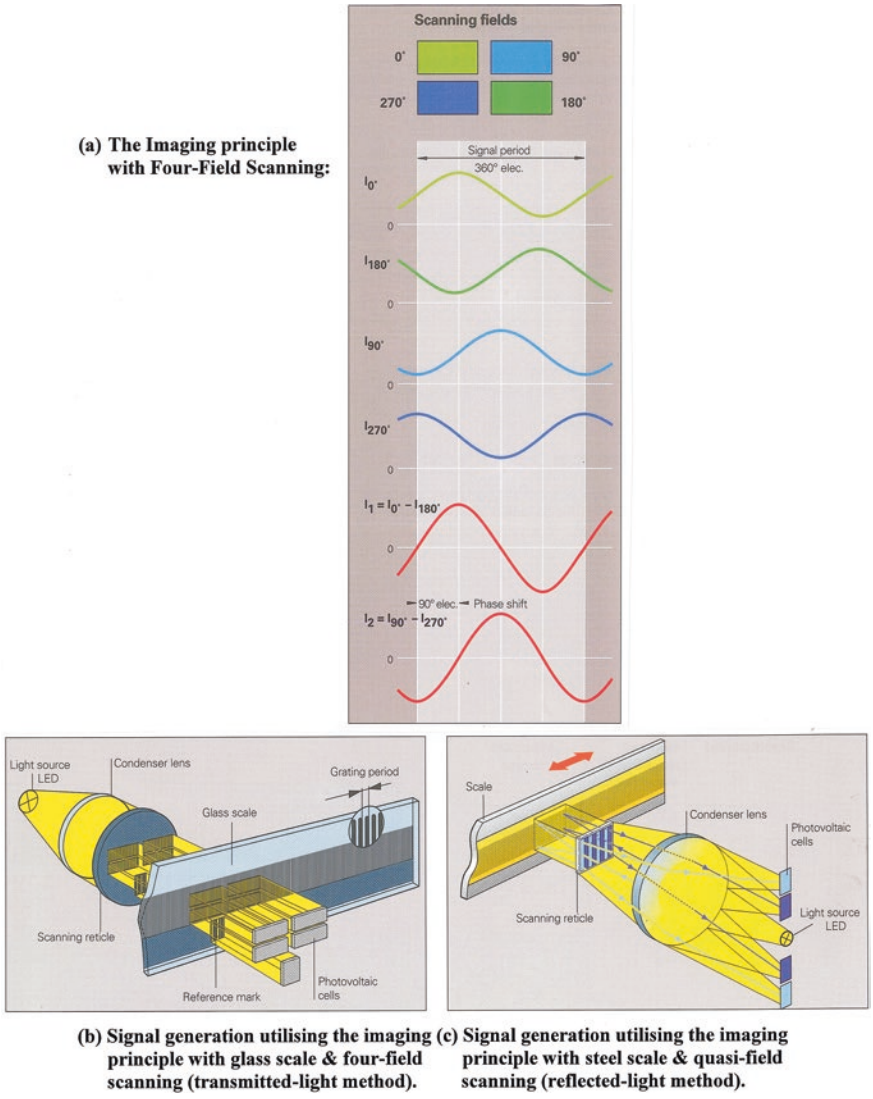

Fig. A.4 Photoelectric scanning employing incremental linear encoders for machine axis displacement (courtesy of Heidenhain (G.B.) Limited)

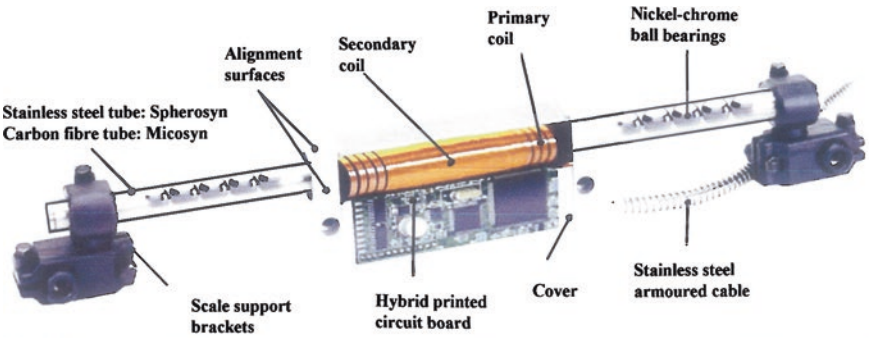

Newall Spherosyn and Microsyn encoders operate on the principle of *electromagnetic induction*. A 10kHz sinusoidal current is induced through a single drive coil within the reader head that generates an electromagnetic field. This field interacts with the nickel chrome precision balls contained in the scale. A set of four pickup coils detect variations in the induced field that are then combined and processed by the electronic circuitry to generate a signal that varies as the head moves along the scale. Depending on the position of the reader head as it passes over each ball, the phase shift of this pickup signal relative to the drive signal will vary between 0 and 360 degrees.

(i) Differential quadrature:

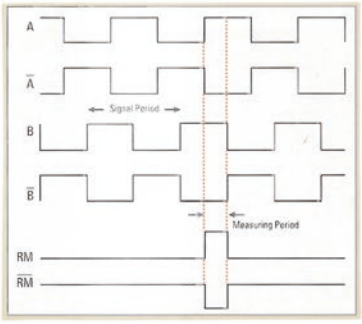

(ii) Encoder traverse rates:

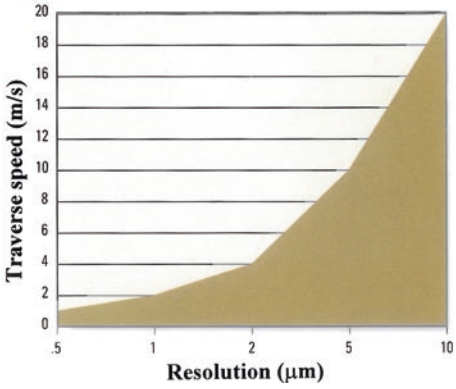

Fig. A.5 Linear digital encoders for machines—employing a high accuracy/precision stainless steel ball assembly (courtesy of Newall Measurement Systems Ltd.)

Appendix 3a—Laser Measurement—Linear Alignment and Optical Configuration

Linear Alignment and Optical Configuration

ML10 Laser system and associated optics and instrumentation—utilised in these machine tool calibration representations.
See Fig. A.6.

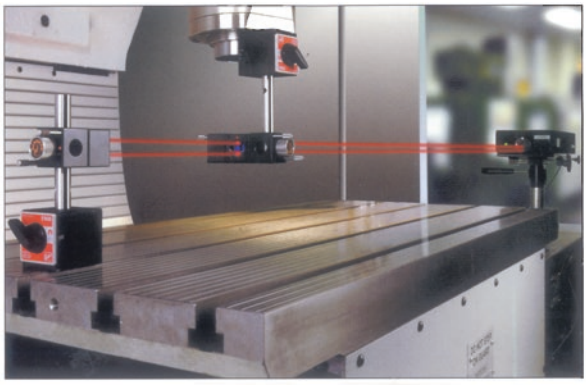

X axis linear positioning measurement on a VMC

SET-UP

The components used in this measurement comprise:

- Linear beam-splitter
- Retro-reflectors
- Targets (for easy optical alignment)

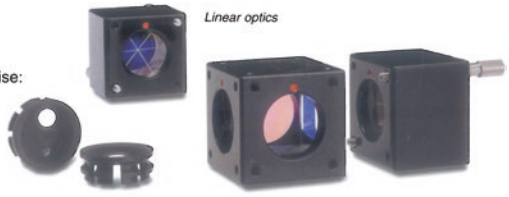

Linear optics

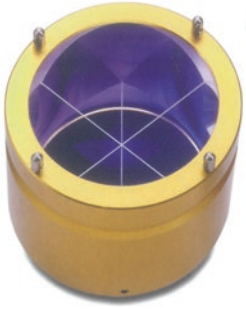

Long range retro-reflector and periscope

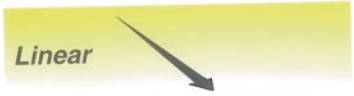

Fig. A.6 Laser and optical configuration for the linear positioning measurement on a vertical machining centre (VMC) (courtesy of Renishaw plc)

In the calibration of machine tools, the system measures linear positioning accuracy and repeatedly by comparing the position given on a machine's controller display with the true position measured by the laser. These values can then be viewed, printed and statistically analysed by the system's software to national and international standards. On many of today's machine tools, it is also possible to take this process one step further and automatically download the error data to a compensation table in the machine's controller. In this way, a download the error data to a compensation table in the machine's controller. In this way, a machine's positioning accuracy can be verified and significantly improved, quickly and easily.

Set-up

The components used in this measurement comprise:

– Linear beam-splitter;
– Retro-reflectors (2);
– Targets (for easy optical alignment).

For linear measurement, one retro-reflector is secured to the beam-splitter, to form the fixed length reference arm of the interferometer. The other retro-reflector moves relative to the beam-splitter and forms the variable length measurement arm. The laser system tracks any change in the separation between the measurement arm retro-reflector and beam-splitter.

The laser head incorporates a 'high gain' signal switch that can be used to allow linear measurements of up to 80 m. However the laser beam diverges over long distances and outgoing and incoming laser beams can interfere with one another.

Furthermore, the linear long range accessory kit provides a periscope to separate the output beam and a large retro-reflector to maintain separation and make alignment easier (kit has to be used in conjunction with standard linear measurement optics).

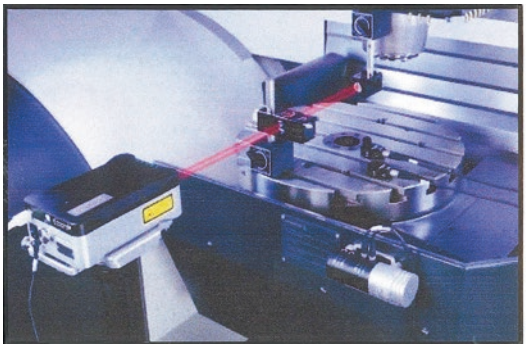

[Courtesy of Renishaw plc]

XL 80 Laser system—with is accompanying 'weather station: here depicted is the linear measurement accuracy assured ±0.5 ppm, due to a precision stabilised laser source and accurate environmental compensation. Readings can be taken at up to 50 kHz, with a maximum linear measurement speed of 4 m/s and with a linear resolution of 1 nm, even at maximum speed. All measurement optics (not just linear) are based on interferometric measurements, giving confidence in the accuracy of the data recorded.

Appendix 3b—Laser Measurement—Straightness Alignment and Optical Configuration

Straightness Alignment and Optical Configuration

See Fig. A.7.

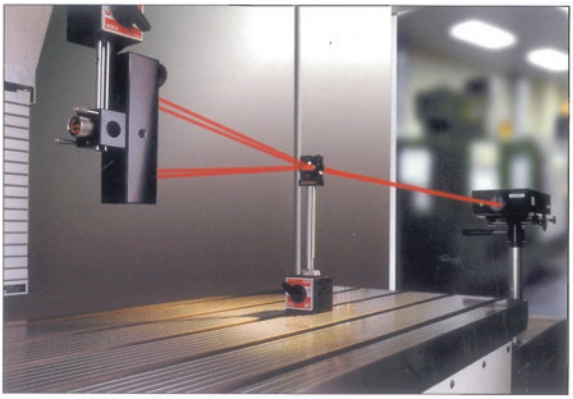

X axis straightness measurement on a moving bed VMC

SET-UP

The components used in this measurement comprise:

- Straightness beam-splitter
- Straightness retro-reflector

Short range straightness optics

Fig. A.7 Laser and optical configuration for the straightness measurement on a vertical machining centre (VMC) (courtesy of Renishaw plc)

Straightness measurements highlight any bending component or overall misalignment in the guideways of a machine.

This could be the result of wear in these guideways, an accident which may have damaged them in some way, or poor machine foundations that are causing a bowing effect on the whole machine. Straightness error will have a direct effect on the positioning and contouring accuracy of a machine.

Set-up

The components used in this measurement comprise:

– Straightness beam-splitter (Wollaston prism);
– Straightness reflector.

For measurement set-up, the straightness reflector is mounted to a fixed position on the table even if it moves. The straightness beam-splitter should then be mounted in the spindle. There are two kits available for measuring shorter axes (01–4.0 m) and longer axes (1–30 m).

When measuring vertical straightness in a horizontal axis, or straightness in a vertical axis of a machine, a straightness accessory kit is required for set-up.

[Courtesy of Renishaw plc]

Compensation unit for XL80 laser system.

Appendix 3c—Laser Measurement—Squareness Alignment and Optical Configuration

Squareness Alignment and Optical Configuration

See Fig. A.8.

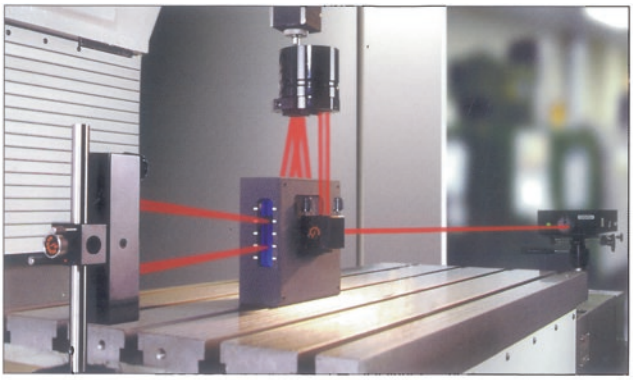

X-Z axis squareness measurement on a VMC

SET-UP

The specific component required for this measurement is:

- Optical square + bracket.

In addition to the optical square, straightness optics and a straightness accessory kit are also required for set-up (see opposite). Other set-up accessories may also be required, depending on what axes are being measured and the configuration of the machine.

Optical square

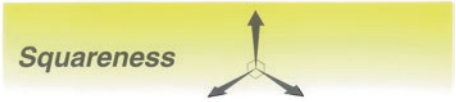

Fig. A.8 Laser and optical configuration for the squareness measurement on a vertical machining centre (VMC) (courtesy of Renishaw plc)

Squareness errors could be the result of wear in machine guideways, an accident which may have caused damage, poor machine foundations or misaligned home position sensors on gantry machines. Squareness error will have a direct effect on the positioning accuracy and contouring ability of a machine.

Set-up

The specific component required for this measurement is:

– Optical square and bracket;
– Straightness optics.

To measure squareness of horizontal to vertical axes will also require a straightness accessory kit. Other set-up accessories may also be required, depending on what axes are being measured and the configuration of the machine.

[Courtesy of Renishaw plc]

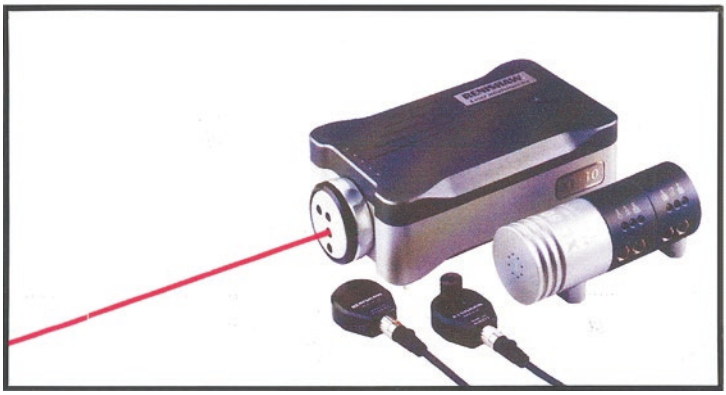

XL80 laser system with compensation unit.

XL80 Laser system—shown in physical comparison with the ML10 laser system.

Appendix 3d—Laser Measurement—Flatness Alignment and Optical Configuration

Flatness Alignment and Optical Configuration

See Fig. A.9.

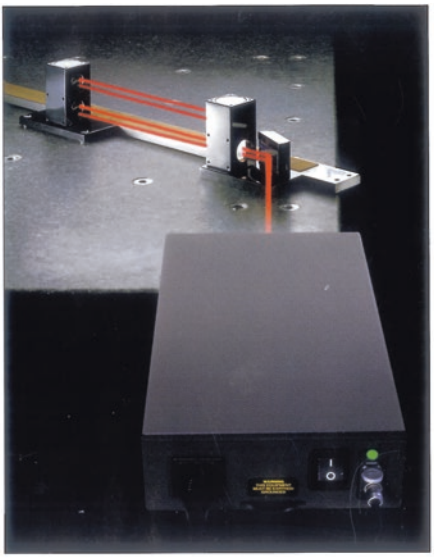

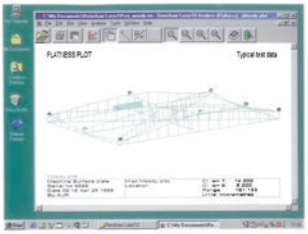

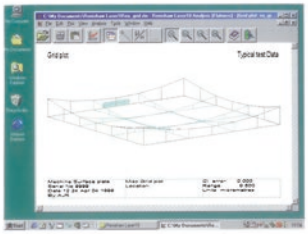

These are the typical plots obtained from a flatness measurement. The top graph shows a Moody plot type whilst the bottom shows a typical Grid plot type.

SET-UP

The specific components used in this measurement comprise:

- Base (50mm)
- Base (100mm)
- Base (150mm)
- Flatness mirrors

Angular optics

Flatness mirrors and bases

Angular measurement optics are also required to attach on top of the flatness bases.

Flatness

Fig. A.9 Laser and optical configuration for the flatness measurement on a coordinate measuring machine (CMM) (courtesy of Renishaw plc)

It determines whether any significant errors in form exist and, in turn, quantifies them. If these errors are significant to the application of the flat surface, then remedial work, such as further lapping, may be required.

Angular measurement optics are also required to attach to the top of the flatness bases. These are available separately.

The angular retro-reflector is mounted on one of three lengths of flatness foot-spacing base. The size of base used depends on the size of surface to be tested and the required number of points to be taken. The angular beam-splitter is mounted on the flatness mirror base.

Set-up

The specific components used in this measurement comprise:

– Base (50 mm);
– Base (100 mm);
– Base (150 mm);
– Flatness mirrors.

Before making any measurements, a 'map' of the measurement lines should be marked out on the surface The length of each line should be an integer multiple of the foot-spacing base selected. There are two standard methods of conducting flatness measurements.

1. ***Moody method***—in which measurement is restricted to eight stipulated lines;
2. ***Grid method***—in which any number of lines may be taken in two orthogonal directions across the surface.

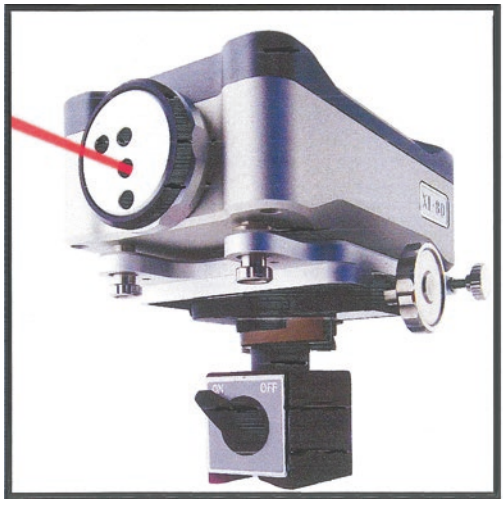

[Courtesy of Renishaw plc]

XL80 laser mounted on a magnetic base unit.

Appendix 3e—Laser Measurement—Angular Alignment and Optical Configuration

Angular Alignment and Optical Configuration

See Fig. A.10.

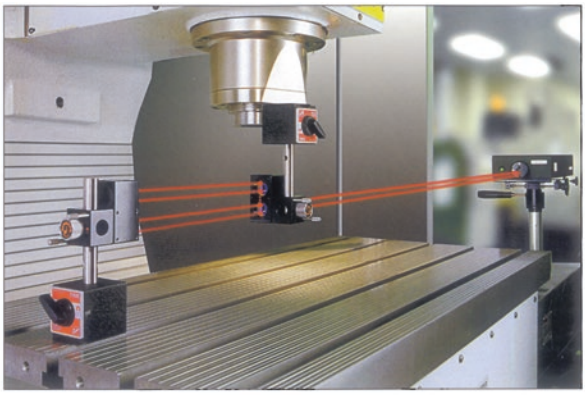

X axis pitch measurement on a moving bed VMC

SET-UP

The components used in this measurement comprise:

- Angular beam-splitter
- Angular retro-reflector
- Targets (for easy optical alignment)

Fig. A.10 Laser and optical configuration for the angular measurement on a vertical machining centre (VMC) (courtesy of Renishaw plc)

Set-up

The components used in this measurement comprise:

– Angular beam-splitter;
– Angular retro-reflector;
– Targets (for easy optical alignment).

For measurement set-up, the angular beam-splitter optic is best mounted in a fixed position on a machine, for example, the spindle on a moving bed machine tool or granite table on a CMM. The retro-reflector optic is then mounted to the moving part of the machine, for example, the moving bed of a machine tool or probe head of a CMM. The measurements are made by monitoring the change in relative angle between the beam-splitter optic and the reflector optic.

[Courtesy of Renishaw plc]

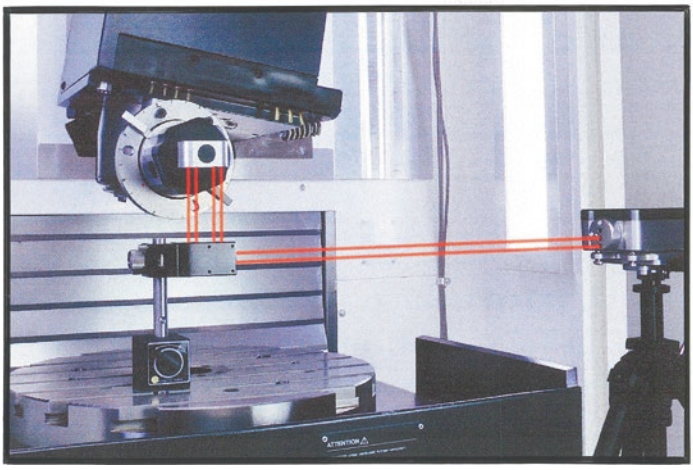

XL80 laser in conjunction with an XR20-W, which when installed with new software enables it to calibrate the rotary positioning accuracy of an axis on the different conditions of five axis machine tools. It provides users with 'detailed tools' to distinguish concerning the rotary axes with its*AxiSet*^{TM}*Check-Up system.*This machine cannot be mounted on the centre of rotation, but it allows users to test various types of machine tools using its new off-axis test ability. Moreover, it is designed for use with a rotary axis calibrator to heighten its capacity to check the pivot points, position and arrangement performance of machine tool rotary-axes.

NB Here, it features a synchronising movement method of linear and rotary axes to keep the exact alignment of the XL-80's laser beam.

Appendix 3f—Laser Measurement—Rotary Alignment and Optical Configuration

Rotary Alignment and Optical Configuration

See Fig. A.11.

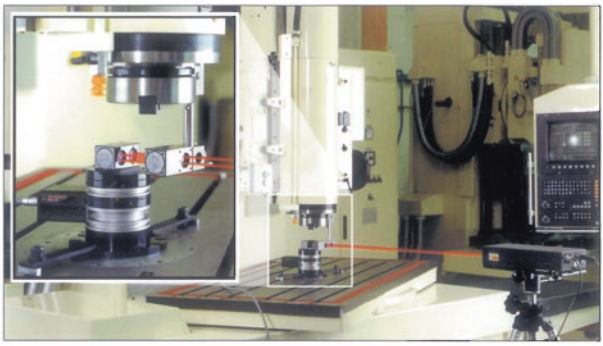

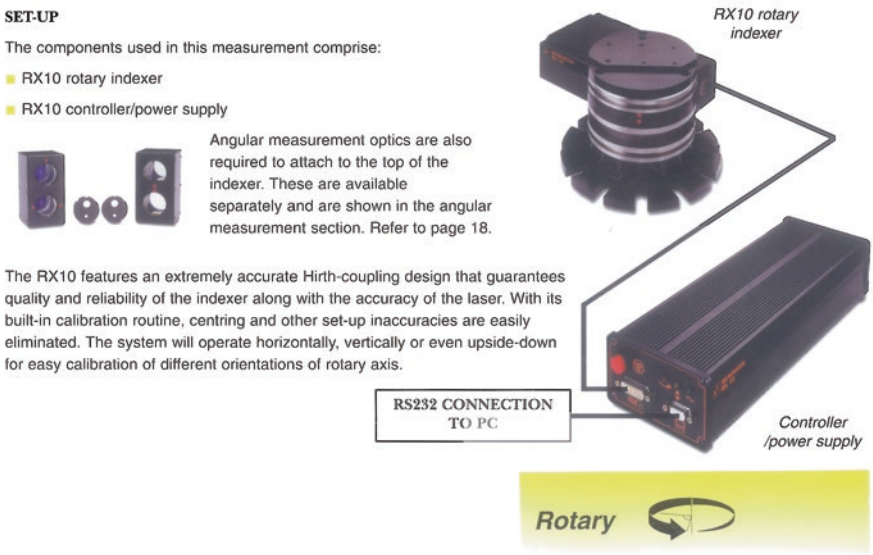

Fig. A.11 Laser and optical configuration for the rotary measurement on a multi-axis machining on a multi-axis machining machine (courtesy of Renishaw plc)

The fundamental importance of rotary axis accuracy is recognised in many national and international standards. These include strong provision for rotary axis measurement. Many CMMs also have rotary tables fitted. **NB** The *previous*-**Rotary Indexer** is shown, however, the *latest***Rotary axis calibrator** is shown in Figs. A.15 and A.16.

Set-up

The components used in this measurement comprise:

– Rotary axis calibrator;
– Angular interferometer optics.

Users may already have these as part of their angular measurement optics. Recent international standards state a rotary axis should be calibrated in a number of ways, which include:

– 0.1° increments through 5°;
– 3° intervals through 360°;
– At 0°, 90°, 180° and 270° positions and nine further random angular positions through 360°.

It is extremely difficult to complete these measurements using auto-collimators and optical polygons.

Automated testing with rotary axis calibrator enables rotary axes to be checked at any angular position and far more quickly than with any other methods.

With its integrated target and alignment optics and pre-test calibration routine, repeatable, high accuracy measurements are ensured. The system will operate horizontally, vertically or even upside-down for easy calibration of different orientations of rotary axis.

Testing an axis

A typical test (5° step size) is performed as follows:

1. The rotary axis calibrator is located on the axis under test and the laser system aligned (as shown in the diagram opposite);
2. The laser is datumed at the axis start position, data capture is started on the PC and the CNC program run;
3. After overrun the axis reaches the initial target position (laser reading equals zero) and a laser reading is triggered;
4. The axis under test then moves 5° to the target and the rotary axis calibrator rotates 5° in the opposite direction;
5. The system records the positional error in the axis under test by combining the Laser head and rotary axis calibrator readings;
6. By driving the rotary axis to a series of points it is possible to build up a picture of the overall accuracy of the axis.

Appendix 3g—Laser Measurement—Dynamic Analysis and Its Associated Software

See Figs. A.12 and A.13.

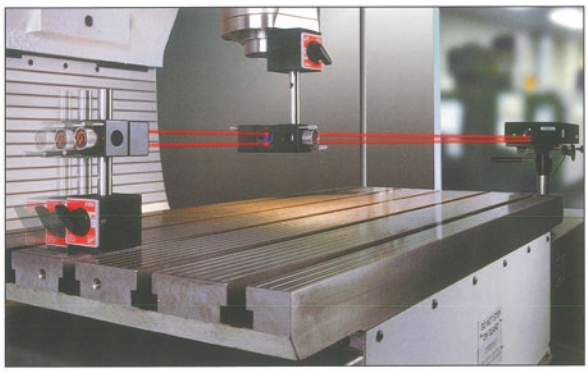

This software can be used to evaluate acceleration, vibration, velocity and servo control performance. This is extremely useful for assessing the performance of many different types of machines used in industry, not just CMMs and machine tools. Other machines that benefit from the system include:

- Robotic pick and place machines
- Surface mount machines
- Hydraulic and pneumatic systems
- Reciprocating and positioning systems
- Optical stages
- Printing presses
- PCB drilling/routing machines
- PCB printing machines

Dynamic software

This measurement capability is supplied as part of the standard laser software package and requires no additional hardware other than the optics for the specific measurement being performed.

Fig. A.12 Laser and optical configuration for the dynamic analysis on a vertical machining machine (VMC) (courtesy of Renishaw plc)

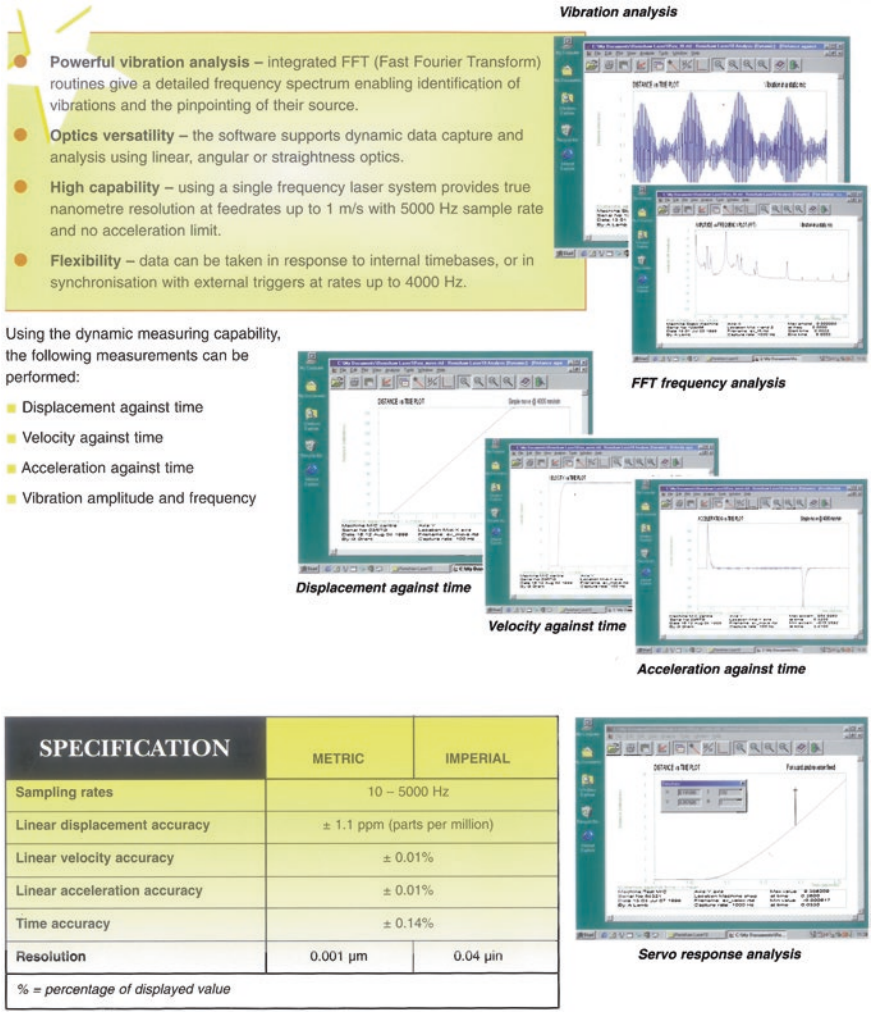

Fig. A.13 Dynamic analysis software for the condition monitoring of machines (courtesy of Renishaw plc)

Appendix 4i—Telescoping Ballbar—Axis Reversal Spikes—Circular Interpolating

See Fig. A.14.

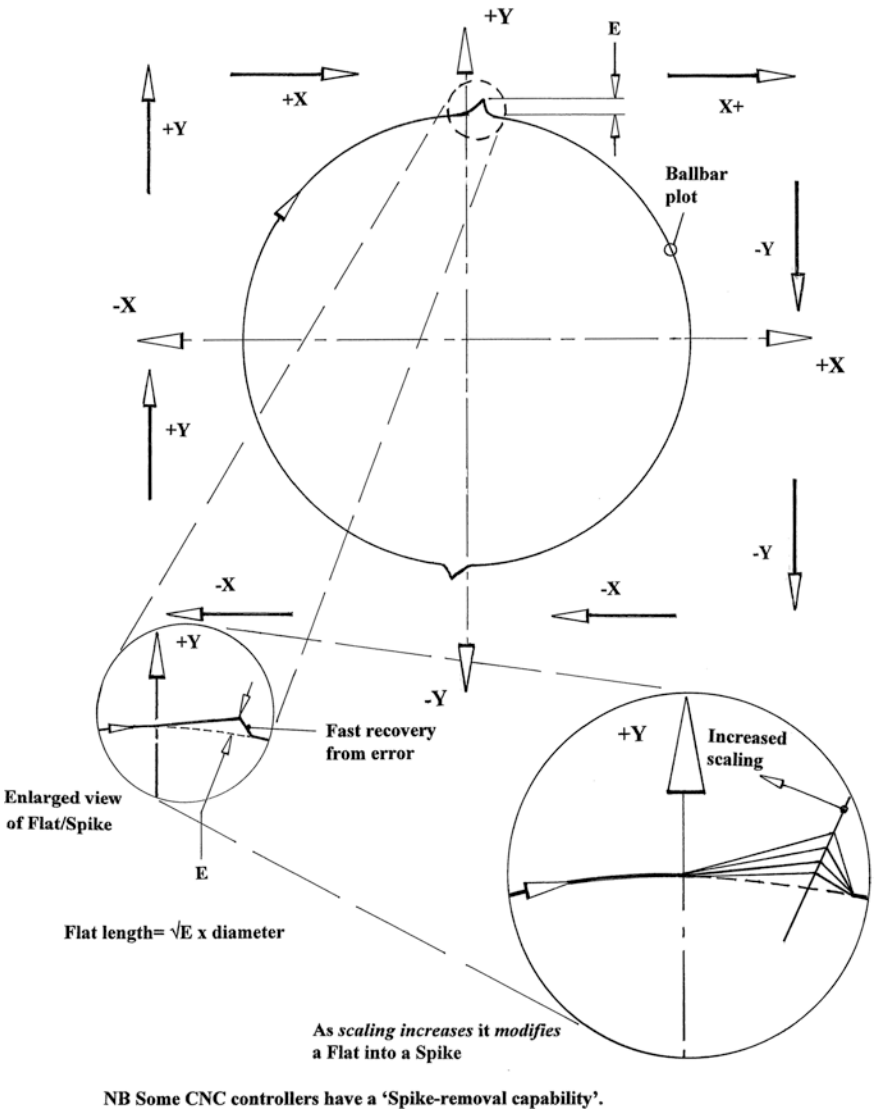

Fig. A.14 Axis reversal spikes can occur when circular interpolating (adapted from: Renishaw plc data)

Appendix 4ii—Telescoping Ballbar—Scale Mismatch—Cause and Effect

See Fig. A.15.

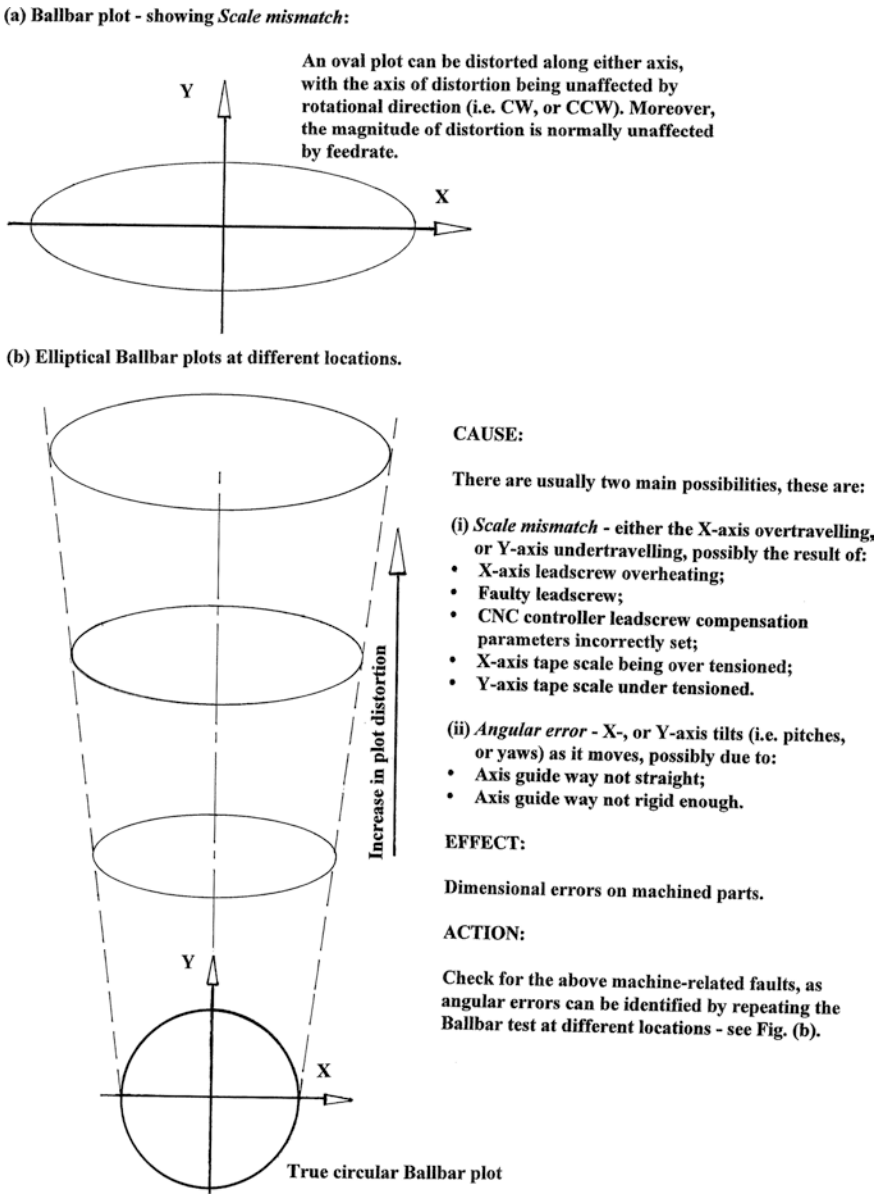

Fig. A.15 A scale mismatch Ballbar plot, with its likely: cause, effect and action (courtesy of Renishaw plc)

Appendix 4iii—Telescoping Ballbar—Backlash Step (Negative)—Cause and Effect

See Fig. A.16.

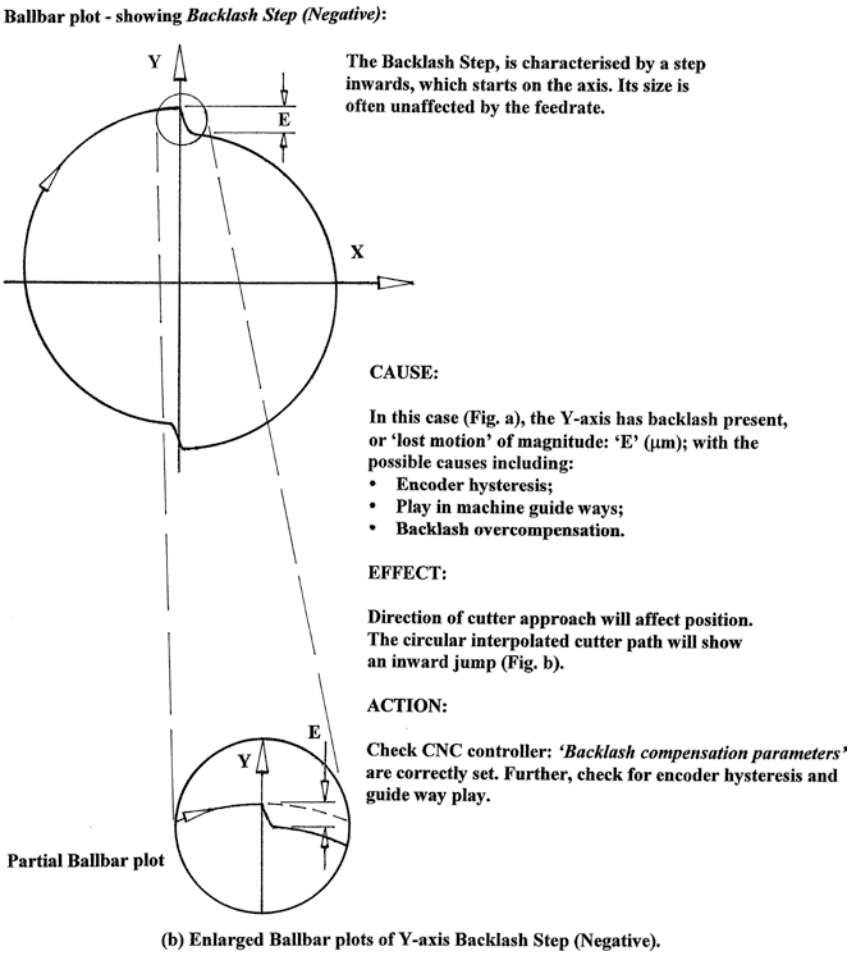

Fig. A.16 A backlash step (negative) Ballbar plot, with its likely: cause, effect and action (courtesy of Renishaw plc)

Appendix 4iv—Telescoping Ballbar—Backlash Step (Positive)—Cause and Effect

See Fig. A.17.

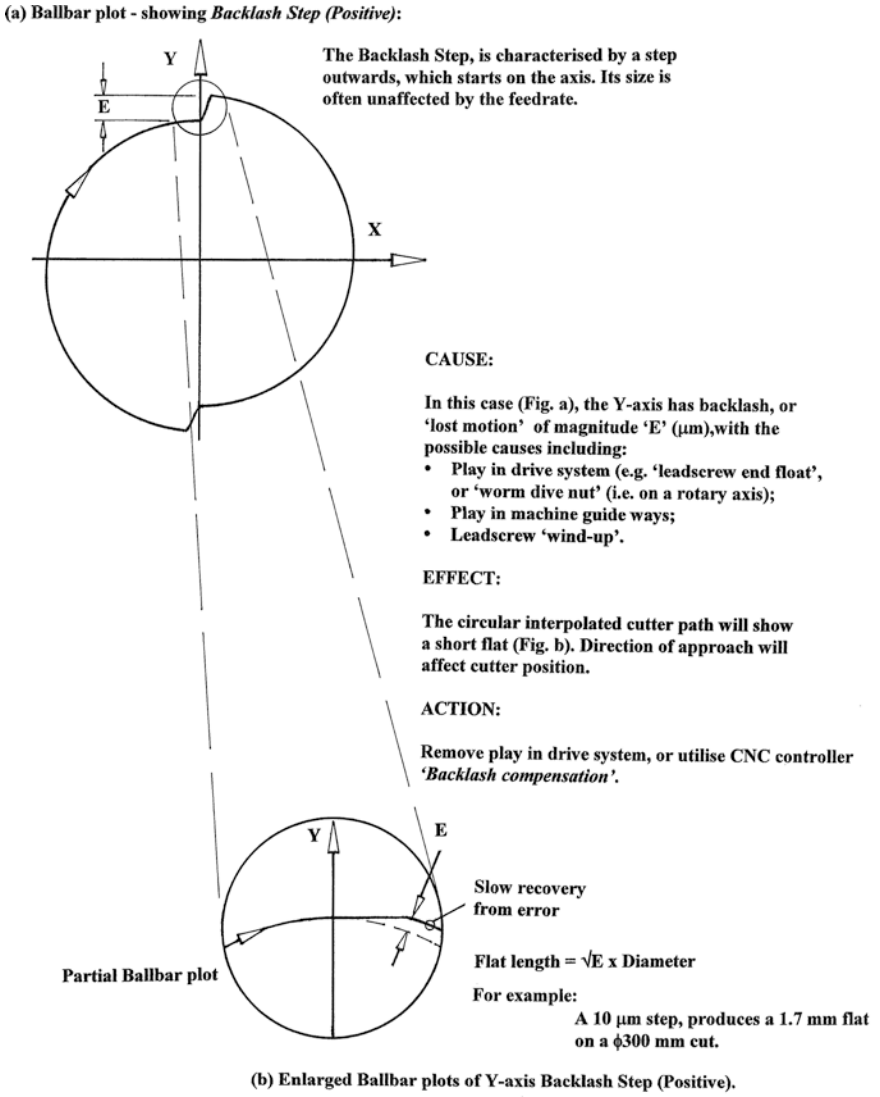

Fig. A.17 A backlash step (positive) Ballbar plot, with its likely: cause, effect and action (courtesy of Renishaw plc)

Appendix 4v—Telescoping Ballbar—Stick-Slip—Cause and Effect

See Fig. A.18.

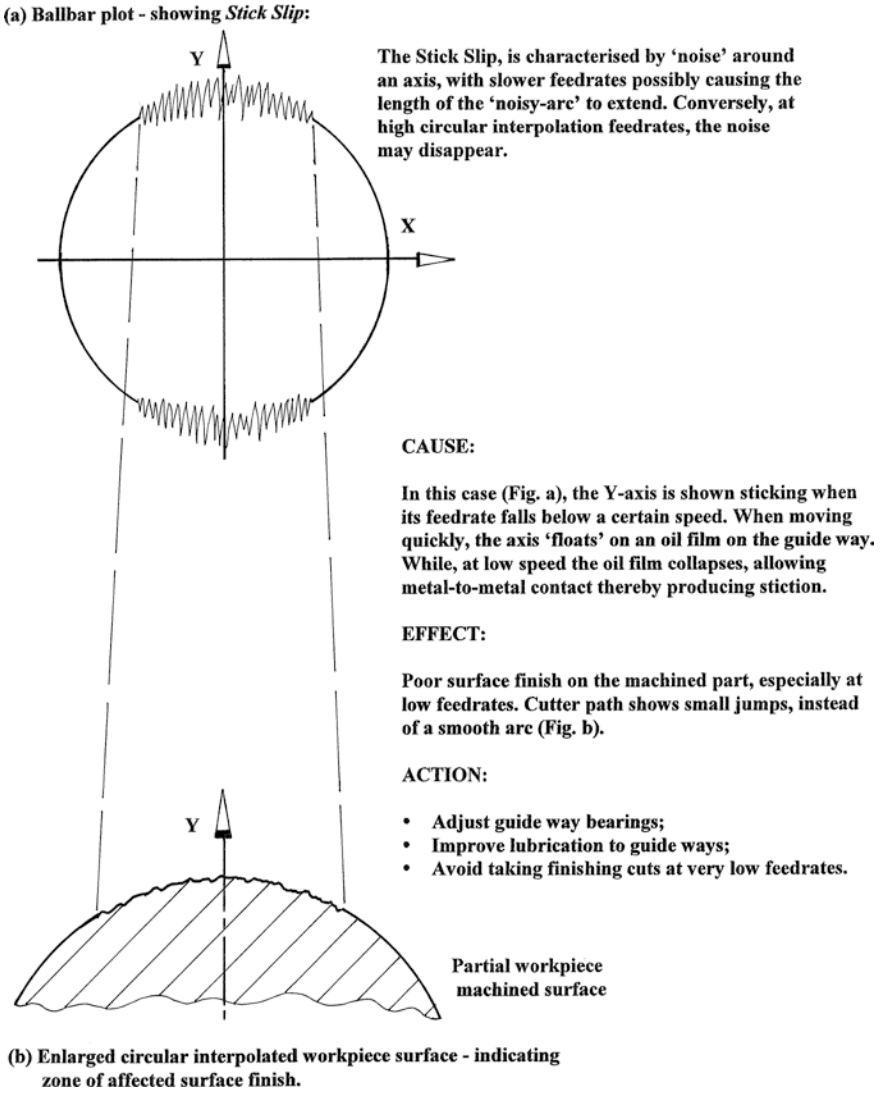

Fig. A.18 Stick slip on Ballbar plot and its affect on the machined workpiece, with its likely: cause, effect and action (courtesy of Renishaw plc)

Appendix 4vi—Telescoping Ballbar—Squareness—Cause and Effect

See Fig. A.19.

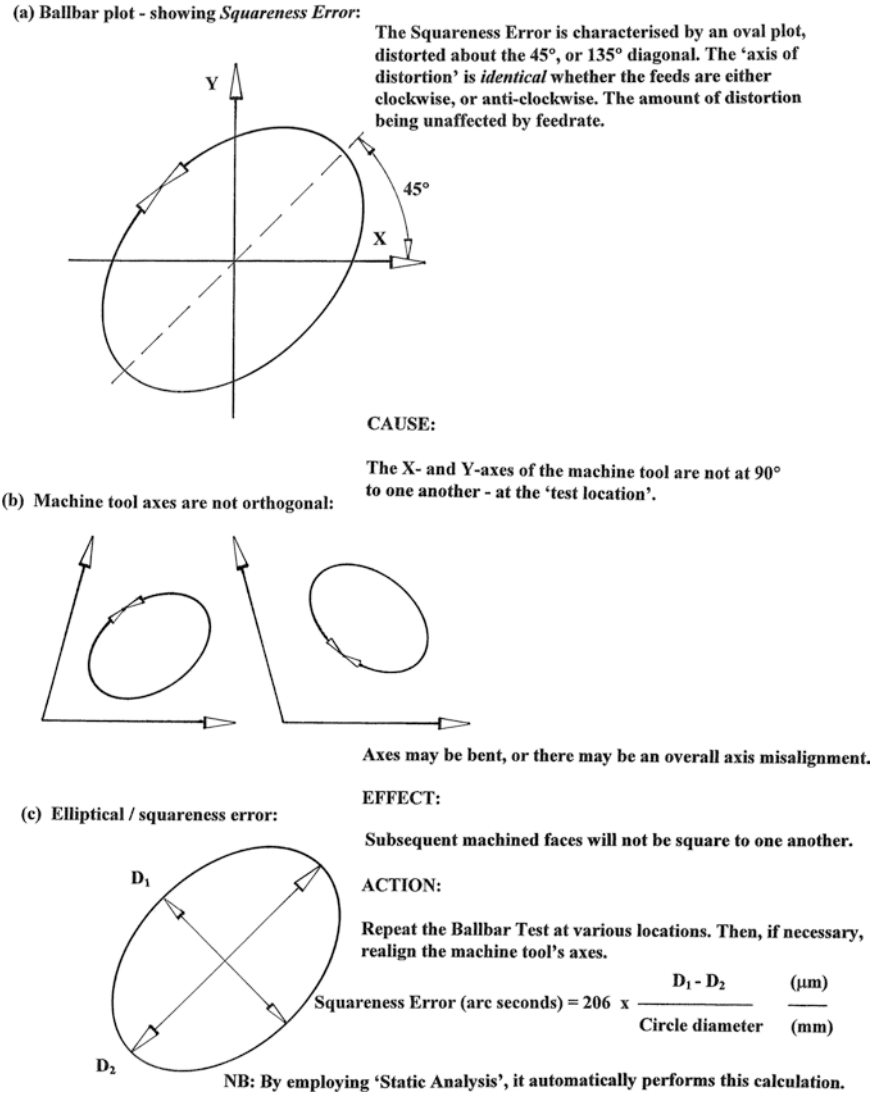

Fig. A.19 Squareness on Ballbar plot, with its likely cause, effect and action (courtesy of Renishaw plc)

Appendix 4vii—Telescoping Ballbar—Servo-Mismatch—Cause and Effect

See Fig. A.20.

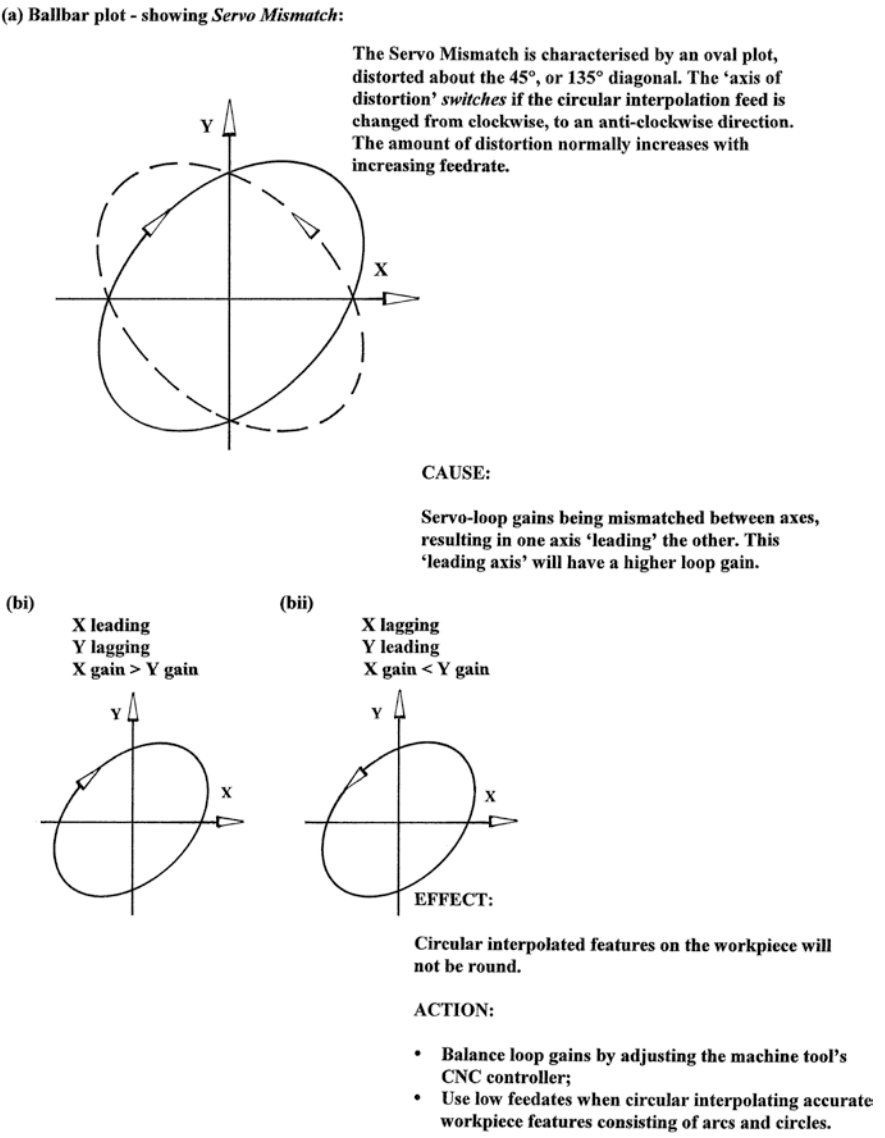

Fig. A.20 Servo mismatch on Ballbar plot, with its likely cause, effect and action (courtesy of Renishaw plc)

Appendix 4viii—Telescoping Ballbar—Cyclic Error—Cause and Effect

See Fig. A.21.

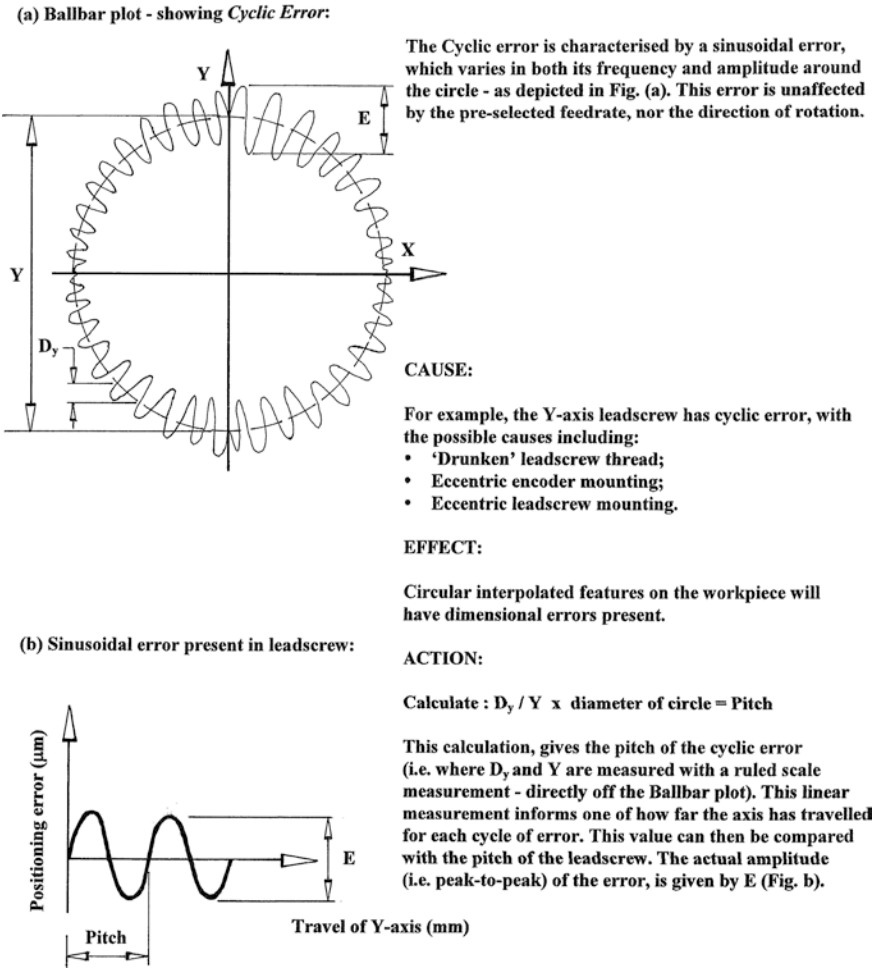

Fig. A.21 Cylic error on Ballbar plot, with its likely cause, effect and action (courtesy of Renishaw plc)

Appendix 4ix—Telescoping Ballbar—Machine Vibration—Cause and Effect

See Figs. A.22 and A.23.

Ballbar plot - showing *Machine Vibration*:

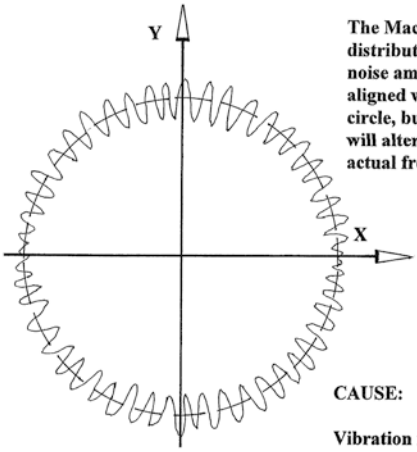

The Machine Vibration is characterised by an uneven distribution of 'noise' on the Ballbar plot. Here, the noise amplitude is at a maximum when the vibration is aligned with the Ballbar. Amplitude *varies* around the circle, but the frequency *does not.* Changing the feedrate will alter the cyclic frequency on the plot, but not the actual frequency in cycles second^{-1}.

CAUSE:

Vibration is being induced. In the example illustrated, the direction of vibration is parallel to the Y-axis. The vibration may be generated by the machine tool itself, or induced by the surrounding environment. Possibly, the main structure is resonating.

EFFECT:

Circular interpolated features on the machined workpiece will have poor surface finish.

ACTION:

Isolate the source of vibration. Tests can be undertaken by either using a 'static Ballbar procedure', or logging data when utilising the dynamic software. This action, will eliminate vibration induced from the axis drives.
So the operational procedure will be:

- **Orientate the Ballbar to the desired angle;**
- **Perform the in-feed;**
- **Stop the machine tool;**
- **Capture data (i.e. for 'dynamic data capture' - it is recommended: 300 H_Z);**
- **Analyse data.**

NB Tests can be repeated with coolant pump turned off, etc, to isolate the vibrational source.

Fig. A.22 Machine vibration on Ballbar plot, with its likely cause, effect and action (courtesy of Renishaw plc)

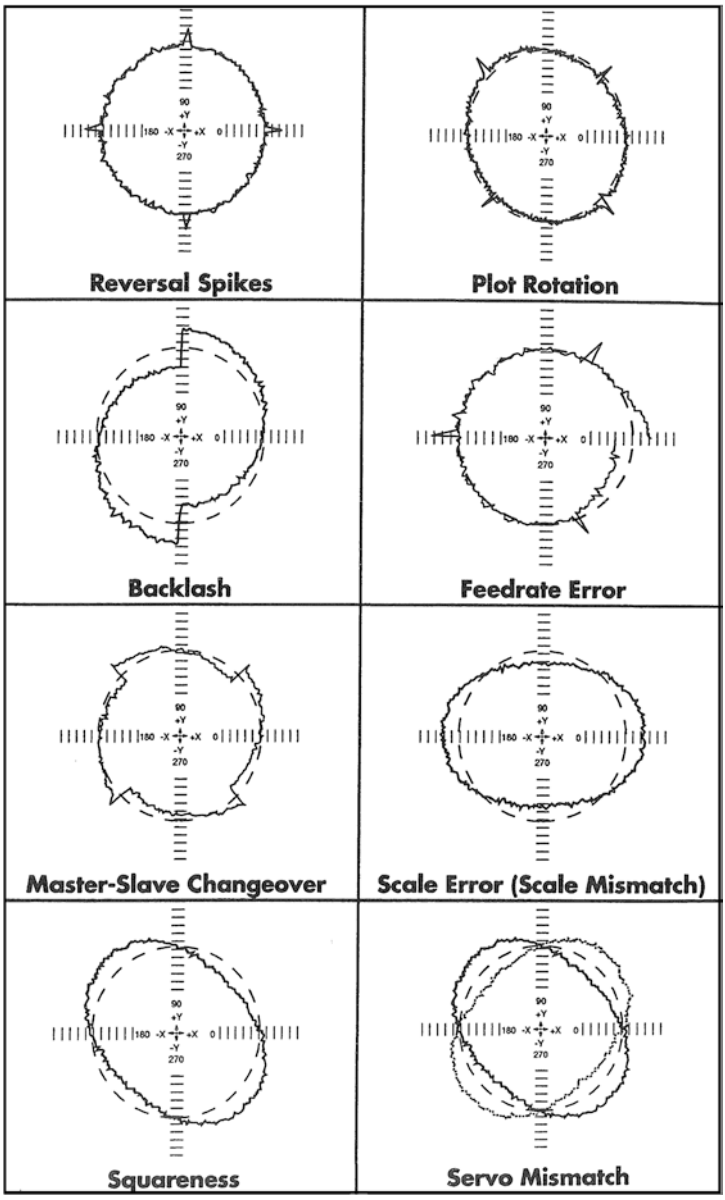

Fig. A.23 Ballbar trouble-shooting guide (courtesy of Renishaw plc)

Appendix 4x—Telescoping Ballbar—Trouble-Shooting (Visual Guide)

See Fig. A.24.

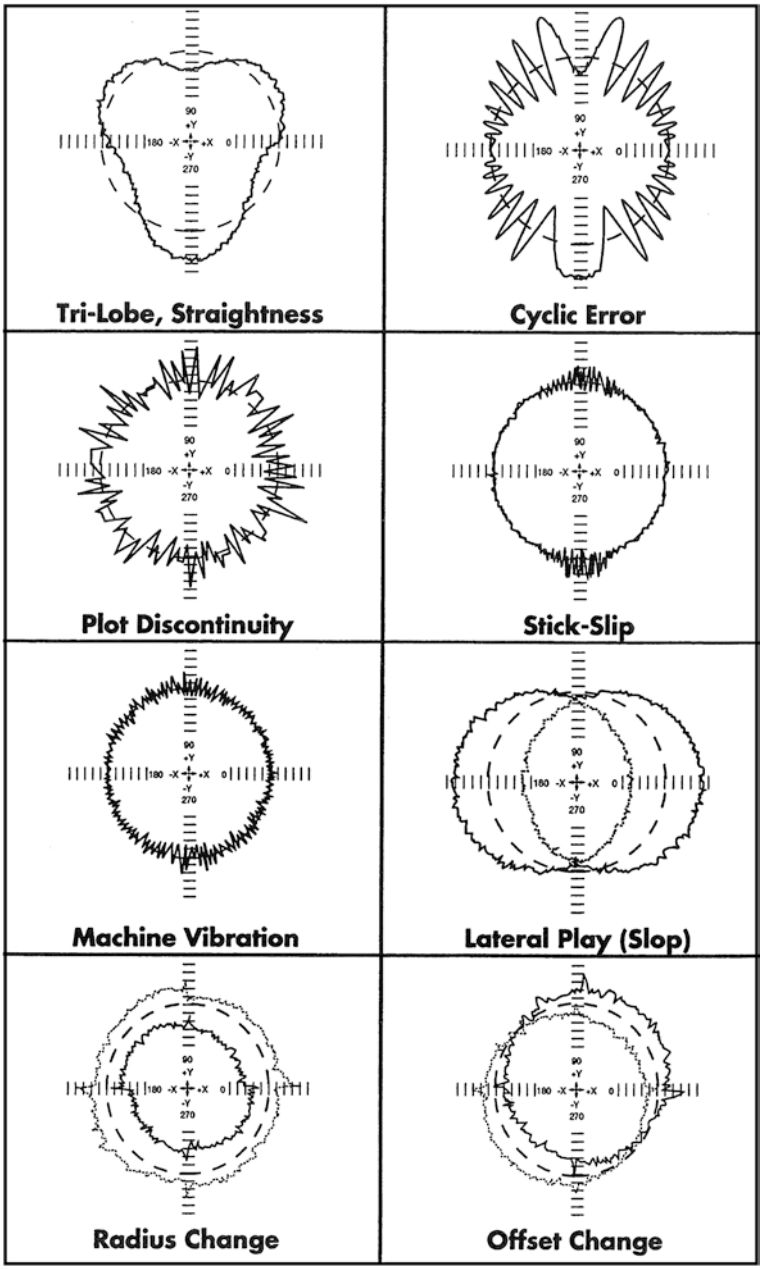

Fig. A.24 Ballbar trouble-shooting guide—continued (courtesy of Renishaw plc)

Appendix 4xi—Telescoping Ballbar—Trouble-Shooting (Visual Guide—continued)

See Fig. A.25.

QC10 (wired) Telescoping Ballbar systems—being shown in the following photographs.

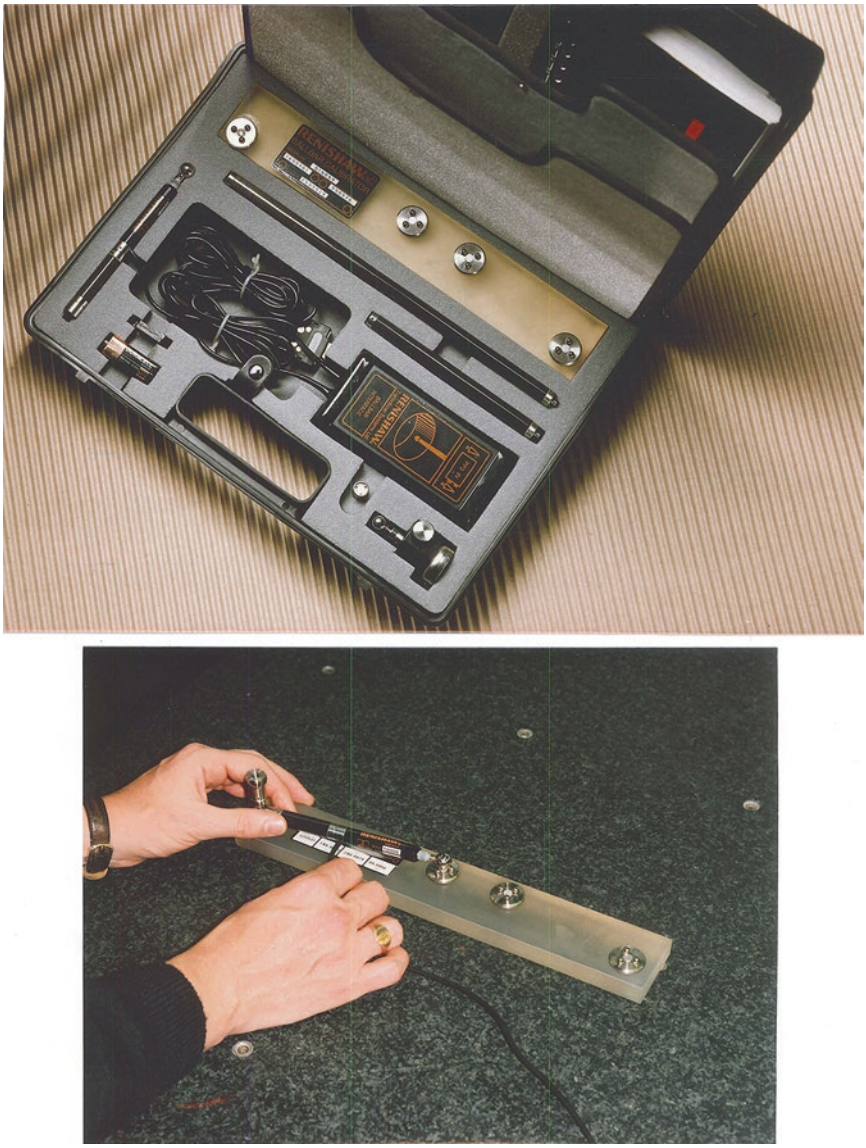

Fig. A.25 The Ballbar portable case and Zerodur™ calibrated artefact—for variable length calibration (courtesy of Renishaw plc)

Appendix 4xii—Telescoping Ballbar—Calibration Artefact

See Figs. A.26 and A.27.

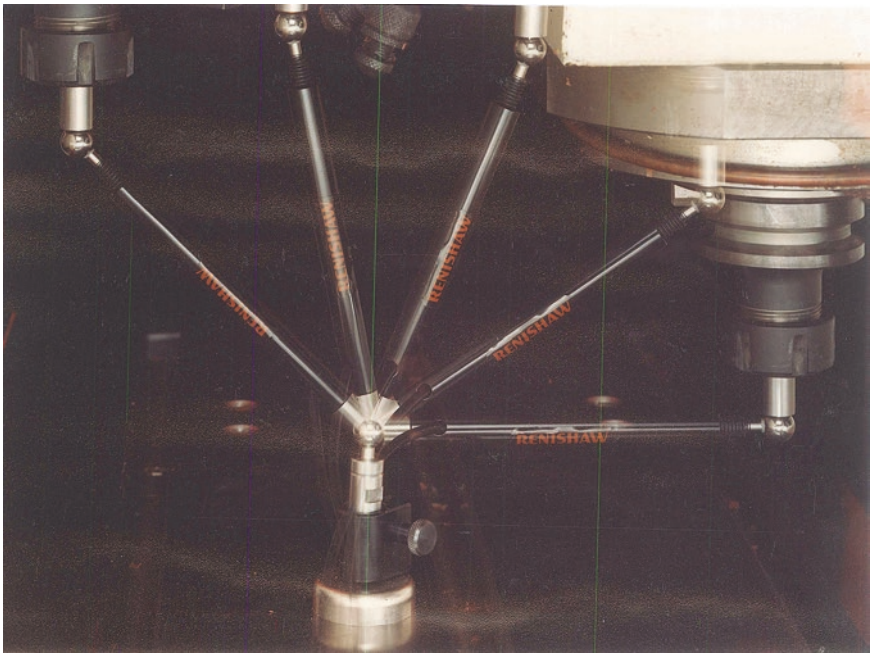

Fig. A.26 The 'static' Ballbar assessment of a vertical machining centre (courtesy of Renishaw plc)

Fig. A.27 The 'dynamic' Ballbar assessment of a vertical machining centre at an inclined plane (courtesy of Renishaw plc)

Appendix 4xiii—Telescoping Ballbar—Static and Dynamic Testing

Appendix 4xiv—Telescoping Ballbar—Calibration on: Machining and Turning Centres

See Figs. A.28 and A.29.

Fig. A.28 Quick Ballbar calibration/diagnostic assessment of a vertical machining centre—with workpiece in-situ, prior to subsequent machining (courtesy of Renishaw plc)

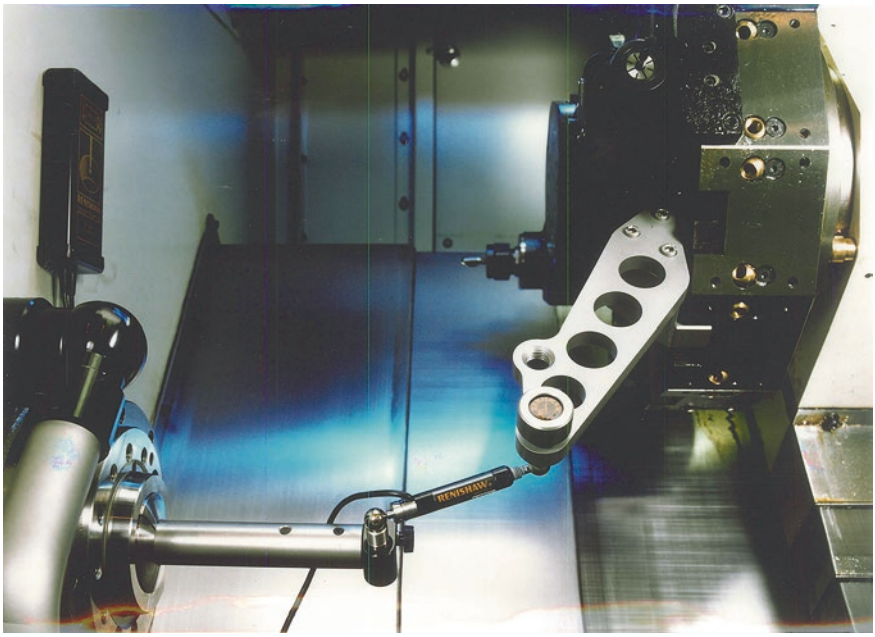

Fig. A.29 The 360° rotation of a Ballbar on a slant-bed mill/turn centre (courtesy of Renishaw plc)

Appendix 5—Capability Study

See Fig. A.30.

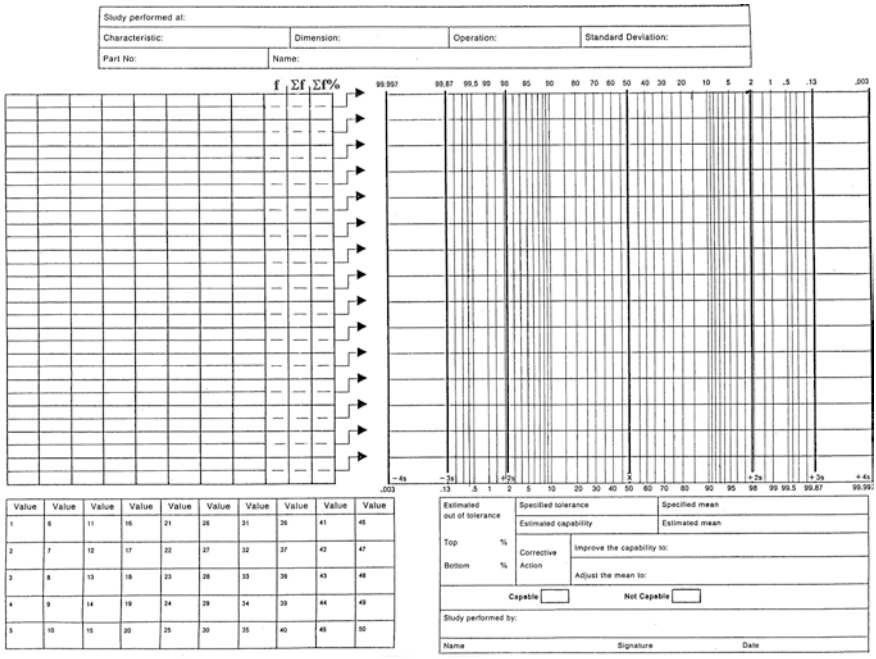

Fig. A.30 'Capability study' (normal distribution): blank sheet for an industrial process

Appendix 6a—Conversion Chart

CONVERSION CHART: English → Metric and Metric → English:

English to Metric				Metric to English					
inches (ins)	×	25.4	=	Millimetres (mm)	mm	×	0.04	=	ins
feet(ft)	×	0.3	=	Metres (m)	m	×	3.3	=	ft
yards(yds)	×	0.9	=	Metres (m)	m	×	1.1	=	yds
miles(mi)	×	1.6	=	Kilometres (km)	km	×	0.6	=	mi
sq inch(in^2)	×	6.5	=	Sq. centimetre (cm^2)	cm^2	×	0.16	=	in^2
sq feet (ft^2)	×	0.09	=	Sq. metres (m^2)	m^2	×	11	=	ft^2
sq yard(yd^2)	×	0.8	=	Sq. metres (m^2)	m^2	×	1.2	=	yd^2

English to Metric				Metric to English					
cu. in (in^3)	×	16	=	Cu. centimetres	cm^3	×	0.06	=	in^3
cu. ft (ft^3)	×	0.03	=	Cu. metres (m^3)	m^3	×	35	=	ft^3
cu. yd (yd^3)	×	0.8	=	Cu. metres (m^3)	m^3	×	1.3	=	yd^3
(liq) quart (qt)	×	0.9	=	litre (l)	l	×	1.05	=	qt
gallon (gal)	×	0.004	=	Cu. metres (m^3)	m^3	×	264.2	=	gal
(advp) ounce (oz)	×	28.3	=	Grams (g)	g	×	0.035	=	oz
(advp) pound (lb)	×	0.45	=	Kilogram (kg)	kW	×	1.34	=	hp
horsepower (hp)	×	0.75	=	Kilowatt (kW)	kg	×	2.2	=	lb
ft per second (ft/s)	×	0.304	=	Met. per second (m/s)	m/s	×	3.28	=	ft/s
ounce-force (ozf)	×	0.278	=	Newtons (N)	N	×	3.597	=	ozf
pound-force (lbf)	×	4.448	=	Newtons (N)	N	×	0.224	=	lbf
foot pounds (ft.lb)	×	1.355	=	Newtons-metres (N.m)	N.m	×	0.737	=	ft.lb
foot pounds (ft.lb)	×	1.355	=	Joules (J)	j	×	0.737	=	ft.lb
in. pounds (in.lb)	×	0.112	=	Newtons-metres (N.m)	N.m	×	8.85	=	in.lb
lb per foot (lb/ft)	×	14.59	=	Newtons-metres (N.m)	N.m	×	0.068	=	lb/ft
cycles per sec (cps)	×	1	=	Hertz (Hz)	Hz	×	1	=	cps
Brit therm unit (Btu)	×	1055	=	Joules (J)	j	×	0.0009	=	Btu

Appendix 6b—Conversion Chart

Conversion Chart: Hardness Comparisons

Hardness conversion Table approx. HV-HRC and HRC-HV-HB-HRA-HRB-Rm forcarbon/alloy steels. In accordance with Table in ASTM A 370–03a

HV	HRC	HV	HRC	HV	HRC	HV	HRC	HV	HRC
2270	*85*	*1950*	*81*	*1633*	*77*	*1323*	*73*	*1004*	*69*
2190	84	1865	80	1556	76	1245	72	940	68
2110	83	1787	79	1478	75	1160	71	920	67.5
2030	82	1710	78	1400	74	1076	70	900	67

HRC Diamond penetrator	HV Vickers 30	HB Brinell 3000 kgf	HRA Diamond penetrator	Rm N/mm^2 MPa	HRB Ball 1/16"	HV Vickers 30	HB Brinell 3000 kgf	HRA Diamond penetrator	Rm N/mm^2 MPa
68	940	–	85.6	–	100	240	240	61.5	800
67	900	–	85.0	–	99	234	234	60.9	785
66	865	–	84.5	–	98	228	228	60.2	750
65	832	739	83.9	–	97	222	222	59.5	715
64	800	722	83.4	–	96	216	216	58.9	705
63	772	706	82.8	–	95	210	210	58.3	690
62	746	688	82.3	–	94	205	205	57.6	675
61	720	670	81.8	–	93	200	200	57.0	650
60	697	654	81.2	–	92	195	195	56.4	635
59	674	634	80.7	2420	91	190	190	55.8	620
58	653	615	80.1	2330	90	185	185	55.2	615
57	633	595	79.6	2240	89	180	180	54.6	605
56	613	577	79.0	2160	88	176	176	54.0	590
55	595	560	78.5	2070	87	172	172	53.4	580
54	577	543	78.0	2010	86	169	169	52.8	570
53	560	525	77.4	1950	85	165	165	52.3	565
52	544	512	76.8	1880	84	162	162	21.7	560
51	528	496	76.3	1820	83	159	159	21.1	550
50	513	482	75.9	1760	82	156	156	20.6	530
49	498	468	75.2	1700	81	153	153	20.0	505
48	484	455	74.7	1640	80	150	150	49.5	495
47	471	442	74.1	1580	79	147	147	48.9	485
46	458	432	73.6	1520	78	144	144	48.4	475
45	446	421	73.1	1480	77	141	141	47.9	470
44	434	409	72.5	1430	76	139	139	47.3	460
43	423	400	72.0	1390	75	137	137	46.8	455
42	412	390	71.5	1340	74	135	135	46.3	450
41	402	381	70.9	1300	73	132	132	45.8	440
40	392	371	70.4	1250	72	130	130	45.3	435
39	382	362	69.9	1220	71	127	127	44.8	425
38	372	353	69.4	1180	70	125	125	44.3	420
37	363	344	68.9	1140	69	123	123	43.8	415
36	354	336	68.4	1110	68	121	121	43.3	405
35	345	327	67.9	1080	67	119	119	42.8	400
34	336	319	67.4	1050	66	117	117	42.3	395
33	327	311	66.8	1030	65	116	116	41.8	385
32	318	301	66.3	1010	64	114	114	41.4	–
31	310	294	65.8	970	63	112	112	40.9	–
30	302	286	65.3	950	62	110	110	40.4	**370**
29	294	279	64.6	930	61	108	108	40.0	–
28	286	271	64.3	900	60	107	107	39.5	–
27	279	264	63.8	880	59	106	106	39.0	360
26	272	258	63.3	860	58	104	104	38.6	–
25	266	253	62.8	850	57	103	103	38.1	350
24	260	247	62.4	820	56	101	101	37.7	–
23	254	243	62.0	810	55	100	100	37.2	340
22	248	237	61.5	790	54	–	–	36.8	–
21	243	231	61.0	770	51	–	**94**	35.5	330
20	238	226	60.5	760	49	–	92	34.6	320

Values shown in bold fall outside the ASTM table but they are still reliable Values shown in *italics* are due to passage from Tables A.2 to A.3 of ASTM A 370

Rockwell HRC diamond penetrator 120° Rockwell **HRA** diamond penetrator load 588 N (60 kgf)

Hardness load 1470 N (150 kgf) duration 30 s Hardness duration 30 s

Vickers HV diamond penetrator 136° Rockwell **HRB** ball 1/16″

Hardness load 294 N (30 kgf) duration 15 s Hardness load 980 N (100 kgf) duration 30 s

Brinell HB ball 10 mm Tensile **Rm** N/mm^2(Mpa)

Hardness load 29,400 N (3000 kgf) duration 15 s strength

Appendix 7—SI System of Units

International System of Units

[Adapted from: ***Eni Generalić***: **University of Split, Croatia—2014]**

The designation of the Système International d'Unités [International System of Units] and their abbreviation to SI, were established by: *The 11th General Conference on Weights and Measures* (CGPM)—in 1960. There are seven *base unit* quantities utilised in the SI, these are: length, mass, time, electric current, thermodynamic temperature, amount of substance, together with luminous intensity—see Table A.1. These specific *base-quantities* are by convention assumed to be *independent*. The corresponding base units of the SI were selected by the CGPM to be the: metre, kilogram, second, ampere, kelvin, mole, plus the candela—also see Table A.1. Whereas, the *derived units* of the 'SI' are then created as products of the powers of the base units, according to the algebraic relations that define the corresponding *derived quantities* in terms of their *base quantities*. So, when the product of powers includes no numerical factor other than one, then the *derived units* are termed: *coherent derived units*—see Table A.2.

The *symbols* for *quantities* are commonly *single letters* set in an *italic font*, although they may indeed be qualified by further information in: *subscripts, superscripts*, or in

Table A.1 SI *base units*

Base quantity		SI base unit	
Name of base quantity	Symbol	Name of SI base unit	Symbol
Length	*l, x, r,* etc.	Metre	m
Mass	*m*	Kilogram	kg
Time, duration	*t*	Second	s
Electric current	*I, i*	Ampere	A
Thermodynamic temperature	*T*	Kelvin	K
Amount of substance	*n*	Mole	mol
Luminous intensity	I_v	Candela	cd

Table A.2 Examples of *coherent derived units* in the SI expressed in terms of base units

Derived quantity		SI coherent derived unit	
Name	Symbol	Name	Symbol
Area	A	Square metre	m^2
Volume	V	Cubic metre	m^3
Speed, velocity	v	Metre per second	$m\ s^{-1}$
Acceleration	a	Metre per second squared	$m\ s^{-2}$
Wavenumber	σ	Reciprocal metre	m^{-1}
Density, mass density	ρ	Kilogram per cubic metre	$kg\ m^{-3}$
Surface density	ρ_A	Kilogram per square metre	$kg\ m^{-2}$
Specific volume	v	Cubic metre per kilogram	$m^3\ kg^{-1}$
Current density	j	Ampere per square metre	$A\ m^{-2}$
Magnetic field strength	H	Ampere per metre	$A\ m^{-1}$
Amount concentration, concentration	c	Mole per cubic metre	$mol\ m^{-3}$
Mass concentration	ρ, γ	Kilogram per cubic metre	$kg\ m^{-3}$
Luminance	L_v	Candela per square metre	$cd\ m^{-2}$
Refractive index	n	(The number) one	1
Relative permeability	μ_r	(The number) one	1

brackets. Of note, is that *symbols* for *quantities* are only *recommendations*, which is in contrast to *symbols* for *units* whose *style* and *form* is *mandatory*. The value of a quantity is expressed as the product of a number and a unit and, the number multiplying the unit, is the numerical value of the quantity expressed in that unit. The numerical value of a quantity depends on the choice of that unit. Consequently, the value of a particular quantity is independent of the choice of unit, although the numerical value will be dissimilar for different units (Tables A.3, A.4, A.5, A.6, A.7, A.8 and A.9).

Of note, are that the designations and symbols for decimal multiples and submultiples, for example, with the unit of mass being formed by attaching prefix names to the unit name 'gram' and, prefix symbols to the unit symbol 'g'. These 'SI-prefixes' refer strictly to powers of 10, although they should not be used to indicate powers of 2 (e.g. one kilobit *represents* 1000 bits and *not* 1024 bits). The names and symbols for the prefixes correspond to: 2^{10}; 2^{20}; 2^{30}; 2^{40}; 2^{50}; and 2^{60}; these are, respectively: kibi—Ki; mebi—Mi; gibi—Gi; tebi—Ti; pebi—Pi; and exbi—Ei. Consequently, by way of illustration, one kibibyte should be written as: $1\ KiB = 2^{10}\ B = 1024\ B$. Where: 'B' denotes a 'byte'.

Even though these prefixes are *not part* of the '*SI*', they should be utilised in the field of 'information technology'—to avoid the incorrect usage of such 'SI-prefixes'.

Table A.3 *Coherent derived units* in the 'SI'—with special names and symbols

	SI coherent derived unit			
Derived quantity	Name	Symbol	Expressed in terms of other SI units	Expressed in terms of SI base units
Plane angle	Radian	rad	1	$m\ m^{-1}$
Solid angle	Steradian	sr	1	$m^2\ m^{-2}$
Frequency	Hertz	Hz		s^{-1}
Force	Newton	N		$m\ kg\ s^{-2}$
Pressure, stress	Pascal	Pa	N/m^2	$m^{-1}\ kg\ s^{-2}$
Energy, work, amount of heat	Joule	J	Nm	$m^2\ kg\ s^{-2}$
Power, radiant flux	Watt	W	J/s	$m^2\ kg\ s^{-3}$
Electric charge, amount of electricity	Coulomb	C		$s\ A$
Electric potential difference, electromotive Force	Volt	V	W/A	$m^2\ kg\ s^{-3}\ A^{-1}$
Capacitance	Farad	F	C/V	$m^{-2}\ kg^{-1}\ s^4\ A^2$
Electric resistance	Ohm	Ω	V/A	$m^2\ kg\ s^{-3}\ A^{-2}$
Electric conductance	Siemens	S	A/V	$m^{-2}\ kg^{-1}\ s^3\ A^2$
Magnetic flux	Weber	Wb	V s	$m^2\ kg\ s^{-2}\ A^{-1}$
Magnetic flux density	Tesla	T	Wb/m^2	$kg\ s^{-2}\ A^{-1}$
Inductance	Henry	H	Wb/A	$m^2\ kg\ s^{-2}\ A^{-2}$
Celsius temperature	Degree Celsius			K
Luminous flux	Lumen	lm	cd sr	cd
Luminance	Lux	lx	lm/m^2	$m^{-2}\ cd$
Activity referred to a radionuclide	Becquerel	Bq		s^{-1}
Absorbed dose, specific energy (imparted), kerma	Gray	Gy	J/kg	$m^2\ s^{-2}$
Dose equivalent, ambient dose equivalent, Directional dose equivalent, personal dose Equivalent	Sievert	Sv	J/kg	$m^2\ s^{-2}$
Catalytic activity	Katal	kat		$s^{-1}\ mol$

Table A.4 Examples of 'SI' *coherent derived units* whose names and symbols include 'SI' *coherent derived units*—with special names and symbols

		SI coherent derived unit	
Derived quantity	Name	Symbol	Expressed in terms of SI base units
Dynamic viscosity	Pascal second	Pa s	m^{-1} kg s^{-1}
Moment of force	Newton metre	Nm	m^2 kg s^{-2}
Surface tension	Newton per metre	N/m	kg s^{-2}
Angular velocity	Radian per second	rad/s	m m^{-1} s^{-1} = s^{-1}
Angular acceleration	Radian per second squared	rad/s^2	m m^{-1} s^{-2} = s^{-2}
Heat flux density, irradiance	Watt per square metre	W/m^2	kg s^{-3}
Heat capacity, entropy	Joule per kelvin	J/K	m^2 kg s^{-2} K^{-1}
Specific heat capacity, specific entropy	Joule per kilogram kelvin	J/(kg K)	m^2 s^{-2} K^{-1}
Specific energy	Joule per kilogram	J/kg	m^2 s^{-2}
Thermal conductivity	Watt per metre kelvin	W/(m K)	m kg s^{-3} K^{-1}
Energy density	Joule per cubic metre	J/m^3	m^{-1} kg s^{-2}
Electric field strength	Volt per metre	V/m	m kg s^{-3} A^{-1}
Electric charge density	Coulomb per cubic metre	C/m^3	m^{-3} s A
Surface charge density	Coulomb per square metre	C/m^2	m^{-2} s A
Electric flux density, electric displacement	Coulomb per square metre	C/m^2	m^{-2} s A
Permittivity	Farad per metre	F/m	m^{-3} kg^{-1} s^4 A^2
Permeability	Henry per metre	H/m	m kg s^{-2} A^{-2}
Molar energy	Joule per mole	J/mol	m^2 kg s^{-2} mol^{-1}
Molar entropy, molar heat capacity	Joule per mole kelvin	J/(mol K)	m^2 kg s^{-2} K^{-1} mol^{-1}
Exposure (x- and γ-rays)	Coulomb per kilogram	C/kg	kg^{-1} s A
Absorbed dose rate	Gray per second	Gy/s	m^2 s^{-3}
Radiant intensity	Watt per steradian	W/sr	m^4 m^{-2} kg s^{-3} = m^2 kg s^{-3}
Radiance	Watt per square metre steradian	W/(m^2 sr)	m^2 m^{-2} kg s^{-3} = kg s^{-3}
Catalytic activity concentration	Katal per cubic metre	kat/m^3	m^3 s^{-1} mol

Table A.5 'Non-SI units'—Accepted for use with the International System of Units

Quantity	Name of unit	Symbol for unit	Value in SI units
Time, duration	Minute	min	1 min = 60 s
	Hour	h	1 h = 60 min = 3 600 s
	Day	d	1 d = 24 h = 86 400 s
Plane angle	Degree	°	$1° = (\pi/180)$ rad
	Minute	′	$1′ = (1/60)° = (\pi/10\,800)$ rad
	Second	″	$1″ = (1/60)′ = (\pi/648{,}000)$ rad
Area	Hectare	ha	1 ha = 1 h $m^2 = 10^4$ m^2
Volume	Litre	L, l	1 L = 1 d $m^3 = 10^{-3}$ m^3
Mass	Tonne	t	1 t = 10^3 kg

Table A.6 'Non-SI units' whose values in 'SI units'—must be obtained *experimentally*

Quantity	Name of unit	Symbol for unit	Value in SI units
Units accepted for use with the SI			
Energy	Electronvolt	eV	1 eV = 1.602 176 53(14) × 10^{-19} J
Mass	Dalton	Da	1 Da = 1.660 538 86(28) × 10^{-27} kg
	Unified atomic mass unit	u	1 u = 1 Da
Length	Astronomical unit	ua	1 ua = 1.495 978 706 91(6) × 10^{11} m
Natural units (n.u.)			
Speed, velocity	Natural unit of speed (speed of light in vacuum)	c_o	299,792,458 m s^{-1}
Action	Natural unit of action (reduced Planck constant)	$\hbar$	1.054 571 68(18) × 10^{-34} J s
Mass	Natural unit of mass (electron mass)	m_e	9.109 382 6(16) × 10^{-31} kg
Time, duration	Natural unit of time	$\hbar/(m_e c_o^2)$	1.288 088 667 7(86) × 10^{-21} s
Atomic units (a.u.)			
Charge	Atomic unit of charge, (elementary charge)	e	1.602 176 53(14) × 10^{-19} C
Mass	Atomic unit of mass, (electron mass)	m_e	9.109 382 6(16) × 10^{-31} kg
Action	Atomic unit of action, (reduced Planck constant)	$\hbar$	1.054 571 68(18) × 10^{-34} J s
Length	Atomic unit of length, bohr (Bohr radius)	a_o	0.529 177 210 8(18) × 10^{-10} m
Energy	Atomic unit of energy, hartree (Hartree energy)	E_h	4.359 744 17(75) × 10^{-18} J
Time, duration	Atomic unit of time	$\hbar/E_h$	2.418 884 326 505(16) × 10^{-17} s

Table A.7 Other 'non-SI units'

Quantity	Name of unit	Symbol for unit	Value in SI units
Pressure	Bar	bar	1 bar = 0.1 MPa = 10^5 Pa
	Millimetre of mercury	mm Hg	1 mm Hg ≈ 133.322 Pa
Length	Angström	Å	1 Å = 0.1 nm = 10^{-10} m
Distance	Nautical mile	M	1 M = 1852 m
Area	Barn	b	1 b = 100 fm^2 = 10^{-28} m^2
Speed, velocity	Knot	kn	1 kn = (1852/3600) m s^{-1}
Logarithmic ratio quantities	Neper	Np	
	Bel	B	
	Decibel	dB	

Table A.8 'Non-SI units'—associated with the 'CGS system of units'

Quantity	Name of unit	Symbol for unit	Value in SI units
Energy	Erg	erg	1 erg = 10^{-7} J
Force	Dyne	dyn	1 dyn = 10^{-5} N
Dynamic viscosity	Poise	P	1 P = 1 dyn s cm^{-2} = 0.1 Pa s
Kinematic viscosity	Stokes	St	1 St = 1 cm^2 s^{-1} = 10^{-4} m^2 s^{-1}
Luminance	Stilb	sb	1 sb = 1 cd cm^{-2} = 10^4 cd m^{-2}
Illuminance	Phot	ph	1 ph = 1 cd sr cm^{-2} = 10^4 lx
Acceleration	Gal	Gal	1 Gal = 1 cm s^{-2} = 10^{-2} m s^{-2}
Magnetic flux	Maxwell	Mx	1 Mx = 1 G cm^2 = 10^{-8} Wb
Magnetic flux density	Gauss	G	1 G = 1 Mx cm^{-2} = 10^{-4} T
Magnetic field	Oersted	Oe	1 Oe ≙ (10^3/4π) A m^{-1}

Table A.9 SI prefixes

Factor	Name	Symbol	Factor	Name	Symbol
10^1	Deca	da	10^{-1}	Deci	d
10^2	Hecto	h	10^{-2}	Centi	c
10^3	Kilo	k	10^{-3}	Milli	m
10^6	Mega	M	10^{-6}	Micro	μ
10^9	Giga	G	10^{-9}	Nano	n
10^{12}	Tera	T	10^{-12}	Pico	p
10^{15}	Peta	P	10^{-15}	Femto	f
10^{18}	Exa	E	10^{-18}	Atto	a
10^{21}	Zetta	Z	10^{-21}	Zepto	z
10^{24}	Yotta	Y	10^{-24}	Yocto	y

References

1. *The International System of Units (SI)*, Bureau International des Poids et Mesures [BIPM], Dec. 2010. <http://www.bipm.org/en/si/>.
2. *The International System of Units from NIST*, Oct 2000. The National Institute of Standards and Technology [NIST], Dec. 2010. <http://physics.nist.gov/cuu/Units/>.

Appendix 8—International Metrology Addresses

Recognised International Standards Organisations and Metrology Laboratories—an Abridged List—(i.e. non-alphabetical):

North American Region:

- ***The American National Standards Institute*** **(ANSI): 1819 L Street, NW Suite 600, Washington, DC 20036, The United States of America**.
- ***The National Institute of Standards and Technology*** **(NIST): 100 Bureau Drive, Stop 1070, Gaithersburg, MD 20899-1070, The United States of America**.
- ***Standards Council of Canada*****: 270 Albert Street, Suite 200 Ottawa, Ontario, K1P 6N7, Canada.**
- ***National Research Council Canada Institute for National Measurement Standards*****: 1200 Montreal Road, Building M-36, Ottawa, Ontario K1A 0R6, Canada**.

Central-America and Caribbean Region:

- ***Centro Nacional de Metrología*** **(CENAM): km 4,5 Carretera a Los Cués Apdo, Postal 1-100 Centro, Querétaro 76900, Mexico**.
- ***Bureau of Standards*****: # 53 Regent Street, Belize City, Belize**.
- ***Comisión Guatemalteca de Normas Ministerio de Economía*****: 8a. Avenida 10-43, zona 1, Ciudad de Guatemala, Guatemala**.
- ***Ministerio de Economía y Desarrollo*****: Direccion General de Ciencia y Technología, Del Sandy's Carretera a Masaya, 1 1/2 c. Arriba, Managua, Nicaragua**.
- ***Ministerio de Comercio e Industrias*****: Dirección General de Normas y Tecnología Industrial, Apartado Postal: 9658 Zona 4, Ciudad de Panamá, Panama**.
- ***Centro Nacional de Metrologia de Panamá*** **(CENAMEP): Secretaría Nacional de Ciencia y Tecnología (SENACYT), Apartado 7250, Zona 5 Panamá**.
- ***Departamento de Ingeniería Química Universidad Autónoma de Honduras*****: Colonia Villa Olimpica S-2, B-4, C-16 Tegucigalpa, Honduras**.
- ***Consejo Nacional de Ciencia y Technología*** **(CONACYT): Col. Medica, Ave. Dr. Emilio Alvarez, Pasaje. Dr. Guillermo Rodriguez Pacas, San Salvador, El Salvador**.

- *Jamaica Bureau of Standards*: 6 Winchester Road, P.O. Box 113, Kingston 10, Jamaica.
- *Trinidad and Tobago Bureau of Standards*: Lot 1 Century Drive, Trincity Industrial Estate, P.O. Box 467, Macoya, Tunapuna, Trinidad and Tobago.
- *Ministerio de Industria y Commercio Oficina Nacional de Normas y Unidades de Medida*: Apartado 1735-2050 Ciudad Cientifica, UCR San Pedro, Montes de Oca San José, Costa Rica.
- *Barbados National Standards Institution*: 'Flodden', Culloden Road, St. Michael, Barbados.
- *Department of Agriculture*: P.O. Box N3028, Nassau, Bahamas.
- *Antigua and Barbuda Bureau of Standards*: P.O. Box 1550, Redcliffe St. & Corn Alley, St. Johns, Antigua and Barbuda.
- *Dirección General de Normas y Sistemas de Calidad Edif. Oficinas Gubernamentales*: Juan Pablo Duarte, Piso 11 Santo Domingo, Dominican Republic.
- *Government Headquarters*: Ministry of Foreign Affairs, Trade and Marketing Commonwealth of Dominica, Dominica.
- *Grenada Bureau of Standards*: P.O. Box 2036, Lagoon Road, St. Georges, West Indies, Grenada.
- *Ministry of Development*: Planning Unit, P.O. Box 186, Government of St. Kitts, St. Kitts and Nevis.
- *Saint Lucia Bureau of Standards*: Heraldine Rock Bldg., 4th Floor, John Compton Highway, CP5412 Castries, St. Lucia.
- *St. Vincent and Grenadines Bureau of Standards*: P.O. Box 1506, Kingstown, W.I., St. Vincent and Grenadines.
- *Ministry of Commerce and Industry*: 26 Rue Legitime, Port of Prince, Haiti.

South American Region:

- *The Brazilian Standards* (INMETRO): Santa Alexandrina St, 416 Rio Comprido, Rio de Janeiro, RJ, Brazil.
- *Instituto Nacional de Tecnología Industrial* (INTI): Departmento de Físcica y Metrología,
- Av. Leandro N. Além 107, 7 piso 1001 - Buenos Aires, Argentina.
- *Bolivian Institute of Metrology* (IBMETRO): Subsecretaria de Industria Av. Camacho No. 1488 esq. Bueno La Paz, Bolivia.
- *Instituo Nacional de Normalización* (INN): Matias Cousiño #64, piso 6.
- Santiago, Chile.
- *Superintendencia de Industria y Comercio* (SIC): Avenida Carrera 50 No. 27-55, Interior 2, CAN, Bogotá D.C., Colombia.
- *Instituto Ecuatoriano de Normalizacion* (INEN):
- Baquerizo Moreno E8-29 y Diego de Almagaro, Edificio Central INEN, Casilla 17-01-3999, Quito, Ecuador.
- *Guyana National Bureau of Standards*: Sophia National Exhibition Complex, Flat 15, Sophia, P.O. Box No. 10926, Georgetown, Guyana.

- *Instituto Nacional de Tecnología y Normalización* **(INTN): A vda. Gral. Artigas 3973 c/ Gral. Roa,Asunción, Paraguay**.
- *Servicio Nacional de Metrologia***: Instituto Nacional de Defensa de la Competencia y de la Proteccion de la Propriedad Intelectual, Calle de la Prosa No. 138, P.O. Box 145, San Borja, Lima 41, Peru**.
- *Metrology Unit***: Department of Trade and Industry, P.O. Box 794, Paramaribo, Suriname**.
- *Laboratorio Tecnológico del Uruguay* **(LATU): Av. Italia, 6201, Montevideo 11500, Uruguay**.
- *Servicio Autónomo Nacional de Metrología* **(SENCAMER): Av. Francisco Javier Ustariz, Ed. Parque Residencial Bernardino, Caracas, Venezuela**.

European Region:

- *The International Organization for Standardization* **(ISO): 1, ch. de la Voie Creuse Case postale 56 CH-1211 Genève 20, Switzerland**.
- *TheInternational Bureau of Weights and Measures* [*Bureau international des poids et mesures*]**—BIPM: Pavillon de Breteuil, 12 Bis Grande Rue, 92310 Sèvres, France**.
- *Asoiciation francaise de normalizasion* **(AFNOR): 11, rue Francis de Pressensé. 93571 La Plaine Saint-Denis Cedex, France**
- *International Organization of Legal Metrology* **(OIML): Bureau International de Métrologie Légale 11, rue Turgot - 75009 Paris, France**.
- *Laboratoire National d'Essais LNE-Paris* **[hdqtrs]: 1, rue Gaston Boissier 75724 Paris Cedex 15, France**.
- *British Standards Institution* **(BSI): 389 Chiswick High Road, London W4 4AL, United Kingdom**.
- *United Kingdom Accreditation Service* **(UKAS): 21-47 High Street, Feltham, Middlesex TW13 4UN, United Kingdom**.
- *The National Physical Laboratory* **(NPL): Hampton Road, Teddington, TW11 0LW, United Kingdom**.
- **DIN—***Deutsches Institut fur Normung* **e.V. Burggrafenstrasse 6, 10787 Berlin, Germany**.
- *Physikalisch-Technische Bundesanstalt* (*PTB*)**: Bundesallee 100 D-38116 Braunschweig, Germany**.
- *The Bremen Institute for Metrology:* **Universität Bremen, Bibliothekstraße, 1 28359 Bremen, Germany**.
- *National Standards Laboratory* **(Nmi - Certin B.V.): PO Box 394, 3300 AJ Dordrecht, The Netherlands**.
- *Nederlands Meetinstituut* **(NMi): Schoemakerstraat 97, P.O. Box 654, NL 2600 AR Delft, The Netherlands**.
- *Ministry of Economic Affairs Metrology Service***: Bd E. Jacqmain 154, B-1000 Brussels, Belgium**.
- *Switzerland National Organization* **(SNV): Burglistrasse 29, 8400 Winterthur, Switzerland**.

- *Swiss Federal Office of Metrology and Accreditation*: **Lindenweg 50, CH-3003 Bern-Wabern, Switzerland**.
- *Irish Standards* **(NSAI): 1 Swift Square, Northwood, Santry, Dublin 9, Ireland**.
- *National Metrology Laboratory* **(NML): Forbairt, Glasnevin, Dublin 9, Ireland**.
- *Austrian Standards Institute* **(ON): Heinestrasse 38, 1020 Vienna, Austria**.
- **BEV -** *Federal Office of Metrology and Surveying*: **Postfach 20, Arltgasse 35 A1163 Vienna, Austria**.
- **Swedish Standards Institute (SIS): SE-118 80 Stockholm, Sweden**.
- *Swedish National Testing and Research Institute*: **Box 857, SE-50115 15 Borås, Sweden**.
- *Danish National Metrology Institute* **(DFM): Matematiktorvet 307, DK-2800 Kongens Lyngby, Denmark**.
- *Finnish Standards Association* **(SFS): Maistraatinportti 2, FI-00240 Helsinki, Finland**.
- *Centre for Metrology and Accreditation*: **P.O. Box 239, Lönnrotinkatu 37, FIN-00180 Helsinki, Finland**.
- *Norwegian Metrology and Accreditation Service*: **Fetveien 99, N-2007 Kjeller, Norway**.
- *Icelandic Metrology and Accreditation Service*: **Loggildingarstofan, Borgartun 21, 105 Reykjavik, Iceland**.
- *The Istituto Nazionale di Ricerca Metrologica* **(INRIM): Strada delle Cacce, 91-10135 Torino, Italy**.
- *Istituto Nazionale di Metrologia delle Radiaziono Ionizzanti Roma* **(ENEA)**:
- **CR Casaccia c.p. 2400, Via Anguillarese 301, 00060 Santa Maria Galeria RM, Italy**.
- *Consiglio Nazionale delle Ricerche* **(CNR): Piazzale Aldo Moro, 7 00185, Roma, Italy**.
- *Centro Español de Metrología* **(CEM): C/del Alfar 2, ES-28760 Tres Cantos (Madrid), Spain**.
- *Instituto Português da Qualidade* **(IPQ) (Portuguese Institute for Quality): Rua António Gião, 22829-513 Caparica, Portugal**.
- *Laboratório Central de Metrologia Instituto Português da Qualidade* **(IPQ): Rua C à Avenida dos Três Vales 2825, Monte de Caparica, Portugal**.
- *National Institute of Metrology*: **042 122, Bucharesti, Sos. Vitan-Bârzesti, nr. 11, Sector 4, Romania**.
- *State Committee of Ukraine for Standardization, Metrology and Certification*: **174, Gorkiy Street, 252650 GSP, Kyiv - 6, Ukraine**.
- *Polish Committee for Standardization* **(PKN): Swietokrzyska 14, 00-050 Warszawa**,
- **President's office, Poland**.
- *Central Office of Measures*: **mUl. Elektoralna 2, 00-139, Warsaw, Poland**.
- *National Office of Measures* **(OMH): H-1535 Budapest, Pf. 919, Hungary**.
- *Bulgarian Institute for Standardization*: **165 Str. Nr3-A, 'Izgrev' Complex, 1797 Sofia, Bulgaria**.

- *Czech Office for Standards, Metrology and Testing*: **Gorazdova 24, P.O.BOX 49, 128 01 Praha 2, Czech Republic**.
- *Czech Metrological Institute*: **Okruzni 31, 638 00 Brno, Czech Republic**.
- *Slovak Institute of Metrology*: **Karloveská st. 63, 842 55 Bratislava, Slovak Republic**.
- *Metrology Institute of the Republic of Slovenia*: **Kotnikova ulica 38, SI-1000 Ljubljana, Slovenia**.
- *Lithuanian Standards*: **T.Kosciuskos g. 30, LT-01100 Vilnius, Republic of Lithuania**.
- *State Metrology Service* **(VMT): Algirdo g. 31, 03219 Vilnius, Lithuania**.
- **The limited liability company Latvian Standard (LVS): 157 K.Valdemara Street, Riga LV-1013, Latvia**.
- *Recherche Physique Centre*: **Universitaire 162A, Av de la Faiencerie L-1511, Luxembourg**.
- *Laboratoire de Technologies Industrielles Technoport Schlassgoart*: **70 Rue de Luxembourg BP 144, L-4002 Esch/Alzette, Luxembourg**.
- *National Directorate of Metrology and Calibration* **(NDMC): Street 'Sami Frasheri', Nr. 33 AL–Tirana, Albania**.
- *Hellenic Organization for Standardization* **(ELOT): Acharnon 313, 111 45 Athens, Greece**.
- *Hellenic Institute of Metrology* **(EIM): Industrial Area of Thessaloniki, Block 45, 57022 Sindos, Thessaloniki, Greece**.
- *Malta Standards Authority*: **Evans Building, Merchant Street, Valletta, VLT 03, Malta**.
- *Department of Standardization and Metrology of the Republic of Moldova*: **28 E. Coca Str., 2039 Chisinau, Moldova**.
- *Tübitak Ulusal Metroloji Enstitüsü* **(UME): PK 54, 41470 Gebze-Kocaeli, Turkey**.

Russian Region:

- *State Committee of the Russian Federation for Standardization, Metrology and Certification*(**GOSSTANDART): 9, Leninsky Prospect, Moscow 117049, Russia**.
- *All-Russian Research Institute for Optical and Physical Measurements* **(VNIIOFI): 46, Ozernaya str., 119361 Moscow, Russia**.
- *D.I. Mendeleyev Institute for Metrology* **(VNIIM): 19, Moscovsky prospect, 190005 St. Petersburg, Russia**.
- *All-Russian Scientific Research Institute of Metrological Service* **(VNIIMS): 46, Ozernaya str., 19361 Moscow, Russia**.
- *Urals Scientific Research Institute of Metrology* **(UNIIM): 4, str. Krasnoarmeiskaya 620219, Ekaterinburg, GSP-824, Russia**.
- *Siberian Scientific Research Institute of Metrology* **(SNIIM): pr. Dimitrova, 4 Novosibirsk 630004, Russia**.
- *Russian Central Office*, **PromExpert-Group Office 205, Novoslobodskaya Street 58, Moscow 121170, Russia**.

Middle East Region:

- **SII—*The Standards Institution of Israel*: 42 Chaim Levanon Street, Tel Aviv 69977, Israel**.
- ***National Physical Laboratory*: Danziger A. Building, Hebrew University, Jerusalem 91904, Israel**.
- ***The Jordan Standards and Metrology Organization*: P.O. Box 941287, Amman 11194, Jordan**.
- ***Saudi Arabian Standards Organization* (SASO): Imam Saud Bin Abdul Aziz Bin Mohammed Road (West End), P.O. Box 3437, Saudi Arabia**.

Central Asian Region:

- ***State Standardization and Metrology Centre* (AZGOST): Mardanov Gardashlary, 124 BAKU - 370078, Azerbaijan**.
- ***Almaty's Center for Standardization Metrology and Certification*: The National Center of Measurement Standards Committee for Standardization, Metrology and Certification of the Republic of Kazakstan, 83 Altynsaris Avenue, 480035 Almaty, Kazakhstan**.
- ***The National Institute for Standards and Metrology of the Kyrgyz Republic 'Kyrgyzstandard'* (NISM): 197, Panfilov Street, Bishkek 720040, Kyrgyzstan**.
- ***The Agency for Standardization, Metrology and Certification of Uzbekistan* ('UZSTANDARD'): 333 'A', Farobiy str., 700049, Tashkent city, Republic of Uzbekistan**.

Southern Asian Region:

- ***Bureau of Indian Standards*: Manak Bhavan, 9 Bahadur Shah Zafar Marg, New Delhi 110 002, India**.
- ***National Physical Laboratory* (NPL): Dr. K.S. Krishnan Road, New Delhi, 110 012, India**.
- ***Pakistan Standards and Quality Control Authority* (PSQCA): Block #77, Pakistan Secretariat, PK-Karachi-74400, Pakistan**.
- ***National Physical & Standards Laboratory*: No. 16, Sector H-9, Islamabad, Pakistan**.
- ***Nepal Bureau of Standards and Metrology*: P.O. Box 985, Sundhara, Kathmandu, Nepal**.

Far-East Region:

- **JISC—*Japanese Industrial Standards Committee Information*: 1-3-1 Kasumigaseki, Chiyoda-ku, Tokyo 100-8901, Japan**.
- ***National Institute of Advanced Industrial Science and Technology* (AIST): 1-3-1, Kasumigaseki Chiyoda-ku, Tokyo 305-8561, Japan**.
- ***Standardization Administration of the People's Republic of China* (SAC): Zhichun Road No. 4, Haidian District, Beijing 100088, China**.
- ***Mongolian National Centre for Standardization and Metrology*: Peace Avenue-46A, PO Box 48, Ulaanbaatar-211051, Mongolia**.

- *Korean Agency for Technology and Standards*: 2, Jungang-Dong, Gwacheon, Gyonggi-Do, Republic of Korea 427-716, South Korea.
- *Korea Research Institute of Standards and Science* (KRISS): P.O. Box 102, Yuseong Daejon 305-600, Republic of Korea.
- *Singapore Standards*—The National Metrology Centre - is a division of 'SPRING Singapore': 2 Bukit Merah, Central Singapore 159835, Singapore.
- *SPRING Singapore National Metrology Centre* [a Division of SPRING Singapore]: 1 Science Park Drive, #02-27 Singapore 118221, Singapore.
- *Center for Measurement Standards Industrial Technology Research Institute*: 321, Kuang Fu Road, Section 2, Hsinchu 30042, Taiwan.
- *Research and Development Center for Calibration, Instrumentation and Metrology* (KIM-LIPI): Komplek PUSPIPTEK, Serpong Tangerang Banten 15314, Indonesia.
- *Standards and Industrial Research Institute of Malaysia* (SIRIM): National Measurement Center SIRIM, Berhad 1 Persiaran Dato' Menteri, Section 2, P.O. Box 7035, 40911 Shah Alam, Malaysia.
- *National Metrology Laboratory* (NMLPHIL): Industrial Technology Development Institute, DOST Compound, Gen. Santos Avenue, Bicutan, Taguig Metro Manila, Philippines.
- *National Institute of Metrology (Thailand)*: 75/7 Rama VI Road, Thungphyathai, Rajthevi, Bangkok 10400, Thailand.
- *Directorate For Standards and Technology*: Ministry of Science and Technology, No. 8 Hoang Quoc Viet Rd., Cau Giay Dist. Hanoi, Vietnam.

African Region:

- *National Institute for Standards* (NIS): Tersa Street, El-Haram-El-Giza, P.O. Box 136 Giza, Code Number 12211, Egypt.
- *Institut nacional de la Normalisation et de la Propriété Industrielle*: B.P. 23, 1012 Tunis-Belvédère, Tunisia.
- *Weights and Measures Office*: Ministry of Commerce, P.O. Box 41071, Nairobi, Kenya.
- *Ghana Standards Board*: P.O. Box M 245, Accra, Ghana.
- *Tanzania Bureau of Standards*: P.O. Box 9524, Dar es Salaam, Tanzania.
- *Uganda National Bureau of Standards*: P.O. Box 6329, Kampala, Uganda.
- *Zambia Bureau of Standards*: P.O. Box 50259, Lusaka, Zambia.
- *Scientific and Industrial Research and Development Centre*: Old Mutual Centre, 9th Floor, 3rd Street/Jason Avenue, P. Bag 7726, Causeway, Harare, Zimbabwe.
- *South African Bureau of Standards* (SABS): Private Bag X191, Pretoria 0001, South Africa.
- *National Metrology Laboratory* (CSIR): P.O. Box 395, Pretoria 0001, South Africa.

Australasia:

- ***The Commonwealth Scientific and Industrial Research Organisation*** **(CSIRO). The National Measurement Institute (NMI): 36 Bradfield Road, Lindfield, NSW 2070, Australia**
- ***Standards New Zealand*****: Level 10, 155 The Terrace, Wellington 6011, Private Bag 2439, Wellington 6140, New Zealand**.
- ***Measurement Standards Laboratory*****: Industrial Research Limited, P.O. Box 31-310, Lower Hutt, New Zealand**.

Appendix 9—International Company Addresses

A

- ***ABTech, Inc*****: 126 Monadnock Hwy, Swanzey, NH 03446, USA**.
- ***AMETEK Precitech Inc.*****: 44 Black Brook Road, Keene, NH 03431, USA**.
- ***Anaheim Automation Inc.*****: 910 E Orangefair Ln, Anaheim, CA 92801, USA**.
- ***Atomic Weapons Establishment plc,*** **Aldermaston, Reading, Berkshire RG7 4PR, U**.

B

- ***Bal-tec*****: 1550 E Slauson Ave, Los Angeles, CA 90011, USA**.
- ***Boeing Commercial Airplane*****: Seattle, Washington, USA.**
- ***BIG Kaiser Precision Tooling Inc.*****: 2600 Huntington Blvd, Hoffman Estates, IL 60192, USA.**

C

- ***Cadence Inc.*****: 9 Technology Drive, Staunton, VA 24401, USA.**
- ***Canyon Hydro*** **[HQ]: 5500 Blue Heron Lane, Deming, WA 98244, USA.**
- ***Carl Zeiss IMT/Carl Zeiss Industrielle Messtechnik GmbH*****: Carl-Zeiss-Str., 22 73446 Oberkochen, Germany.**
- ***Carl Zeiss Metrology Division*****: 4 The Mews, 53 High Street, Hampton Hill, TW12 1ND, UK.**
- ***Cranfield Precision*****: 3 Adams Close, Bedford MK42 7JE, UK.**
- ***Centre for Precision Technology*****: University of Huddersfield, Yorkshire, UK.**
- ***Chevalier Machinery Inc*****: 9925 Tabor Pl, Santa Fe Springs, CA 90670, USA.**
- ***Cincinnati Machine tools:*** **see address details for:** ***Mag IAS LLC, USA.***
- ***Cincinnati Machines Ltd*****: has become - MAG MAINTENANCE UK LIMITED, Unit 6 Maybrook Business Park Maybrook Road, B76 1ALMinworth, UK.**
- ***Citizen Machinery UK Ltd*****: 1 Park Ave, Bushey, Hertfordshire WD23 2DA, UK.**
- ***Controls s.r.l.*****: Via Aosta, 6, 20063 Cemusco s/N, (Mi), Italy.**

D

- ***DANOBATGROUP*: Arriaga kalea, 2 · P.O. Box 33, E-20870 ELGOIBAR, Spain.**
- ***Damalini AB* [Easy-Laser]: PO Box 149, SE-431 22 Mölndal, Sweden.**
- ***Davidson Optronics, Inc.*: 2223 W San Bernardino Rd, West Covina, CA 91790, USA.**
- ***Deckel Maho Gildemeister GmbH:* Gildemeisterstraße 60 Bielefeld, 33689 Germany.**
- ***Dörries Scharmann Technologie GmbH*: Hofkamp, Bielefeld 33719, Germany.**
- ***Dupont École Polytechnique*: Montreal, Quebec, Canada.**

E

- ***École de Technologie Supérieure*: 1100 Rue Notre-Dame Ouest, Montréal, QC H3C 1K3, Canada.**
- ***Eni Generalić*: University of Split, Faculty of Chemistry and Technology, Teslina 10/V, Split, Croatia.**

F

- ***FARO Technologies Inc.*: 250 Technology Park, Lake Mary, FL 32746, USA.**
- ***FLIR Systems, Inc.* [Corporate Headquarters]: 27700 SW Parkway Ave., Wilsonville, OR 97070, USA.**
- ***FLIR Commercial Systems*: FLIR Systems Trading Belgium BVBA, Luxemburgstraat 2, 2321 Meer, Belgium.**
- ***FLIR Systems GmbH*: Berner Strasse 81, D-60437 Frankfurt am Main, Germany.**
- ***FLIR Systems UK*: 2 Kings Hill Avenue, Kings Hill, West Malling, Kent, ME19 4AQ, UK.**
- ***Fuchs Lubricants (UK) plc*: New Century St, Stoke-on-Trent, Staffordshire ST1 5HU, UK.**

G

- ***Giddings & Lewis Machine Tools*: see address details for: *Mag IAS LLC, USA*.**

H

- ***Haas Automation, Inc.*: 2800 Sturgis Rd, Oxnard, CA 93030, USA.**
- ***Heidenhain*: Dr.-Johannes-Heidenhain-Straße 5, 83301 Traunreut, Germany.**
- ***Heidenhain (GB) Ltd*: 200 London Rd, Burgess Hill, West Sussex RH15 9RD, UK.**
- ***Gebr. Heller Maschinenfabrik GmbH*: Gebrüder-Heller-Straße 15, 72622 Nürtingen, Germany.**

- ***Hexagon Metrology Ltd.*: Metrology House, Halesefield 13, Telford, Shropshire TF7 4PL, England.**
- ***Hofstra Group, Ltd. Co.*: 41 Bisbee Court, Bldg. A, Unit 5, Santa Fe, NM 87508, USA.**
- ***Hyundai-Wia Machine America Corporation*: 450 Commerce Blvd, Carlstadt, NJ 07072, USA.**

I

- ***IBS Precision Engineering BV*: Industrieterrein Esp 2151, Esp 201, 5633 AD Eindhoven, Netherlands.**
- ***ICON Technologies*: Division of Hydromat Inc. (St Louis, MO, USA). Contact: The Motch & Eichele Company, LLC, 297 Ascot Parkway, Cuyahoga Falls, OH 44223, USA.**
- ***IKO Nippon Thompson America* (International Head Office): 19-19 Takanawa 2-chome Minato-ku, Tokyo 108, Japan.**
- ***IKO Nippon Thompson Europe B.V.*: Mündelheimer Weg 56, D-40472 Düsseldorf, Germany.**
- ***Index-werke GmbH & Co. KG Hahn & Tessky:* Plochinger Straße 92, 73730 Esslingen am Neckar, Germany.**
- ***InfinityQS International, Inc.*: 12601 Fair Lakes Cir #250, Fairfax, VA 22033, USA.**
- ***InnovMetric Software*: 2014 Rue Cyrille-Duquet #310, Québec, QC G1N 4N6, Canada.**
- ***Institute of Machine Tools & Manufacturing*: TH Zurich, Switzerland.**
- ***IQL Independent Quality Labs, Inc.*: PO Box 444, Ashaway, RI 02804, USA.**

J

- ***Jakob-Immobilien GmbH*: Daimlerring 42, 63839 Kleinwallstadt, Germany.**
- ***Jash Precision Tools Ltd.*: No. 87, Industrial Estate, Polo Ground Indore - 452015, Madhya Pradesh, India, Pologround Industrial Estate, Indore, Madhya Pradesh 452015, India.**
- ***JEOL (UK) Ltd.*: Silver Court Watchmead, Welwyn Garden City AL7 1LT, UK.**
- ***John Crane Orion*: 1111 Cedar Creek Road Grafton, WI 53024 262.377.2210, USA.**

K

- ***Käfer Messuruhrenfabrik GmbH & Co KG*: Hahnstrasse 11, D-78054 Villingen-Schwenningen, Germany.**
- ***Kolb & Baumann GmbH & Co. KG*: Daimlerstraße 24, 63741 Aschaffenburg, Germany.**
- ***KUKA Roboter GmbH* [Headquarters]: Zugspitzstrasse 140, 86165 Augsburg, Germany.**
- ***Kunz precision AG*: Riedtalstrasse 16, 4800 Zofingen, Switzerland.**

L

- ***Leitz/Hexagon Metrology* (GmbH): Siegmund-Hiepe-Straße 2, 35578 Wetzlar, Germany.**
- ***LK Metrology Systems, Inc.*: 12701 Grand River, Brighton, MI 48116, USA.**
- ***Luthra Engineering Works*: Luthra House, Delhi Road Sonipat-131 001, Haryana, India, Sonipat, Haryana, Haryana 131001, India.**

M

- ***Mag IAS LLC* [Giddings & Lewis, Cincinnati Machine Tools]: 142 Doty St, Fond du Lac, WI 54935, USA.**
- ***Mahr GmbH*: Carl-Mahr-Straße 1, 37073 Göttingen, Germany.**
- ***Marposs Italia Spa*: Corso Svizzera, 185, Torino, Italy.**
- **Matsuura Machinery Corporation [Headquarters]: 1-1 Urushihara Cho Fukui City, Fukui 910-8530, Japan.**
- ***Matsuura Machinery Ltd*: Garden Court, Gee Rd, Coalville, Leicestershire LE67 4NH, UK.**
- ***Mecartex Sa*: Via Industria 1, 6933 Muzzano, Switzerland.**
- ***Metrosage LLC*: 26896 Shake Ridge Rd, Volcano, CA 95689, USA.**
- ***Microlution, Inc*., 6635 W. Irving Park Road, Chicago, IL 60634, USA.**
- **Mitsubishi Heavy Industries, Ltd. (MHI): 16-5 Konan 2-chome, Minato-ku, Tokyo.**
- ***Mitsubishi Heavy Industries America Headquarters*: 630 Fifth Avenue, Suite 2650, New York, New York 10111, USA.**
- ***Mitsubishi Heavy Industries Europe Ltd*: 4th Floor, International Buildings, 71 Kingsway, London WC2B 6ST, UK.**
- ***Mitutoyo Corporation* [HQ]: 20-1 Sakado 1-chome, Takatsu-ku, 213-002 Kawasaki, Kanagawa, Japan.**
- ***Mitutoyo (UK)* [HQ]: Joule Road, West Point Business Park, Andover, Hampshire, SP10 3UX, UK.**
- ***Modern Tool Ltd.*: 70 Ave SE, Calgary, AB T2C 4Y3, Canada.**
- ***Monash University*: Faculty of Engineering, Wellington Rd, Clayton VIC 3800, Australia.**
- ***Mori Seiki*: 950 Riverside Pkwy # 90, West Sacramento, CA 95605, USA.**
- ***MRC Bearings*: 890 Forty Foot Rd., P.O. Box 352, Lansdale, PA 19446, USA.**

N

- ***Newall Measurement Systems Ltd.*: Cornwall Rd, Wigston LE18 4XH, UK**
- ***Nikon Metrology UK*: East Midlands Airport, Argosy Rd, Castle Donington, Derby DE74 2SA, UK.**
- ***Nippon Pulse*: 4 Corporate Dr, Radford, VA 24141, USA.**

O

- ***Obishi Keiki Seisakusho*: Niigata, Nagaoka, 1-1216-1 Nanyo (Nanyo Industrial Estate), Japan.**
- ***OGP UK Ltd.*: Faraday House, Woodyard Lane, Foston, Derbyshire DE65 5DJ, UK.**
- ***Optodyne, Inc.*: 1180 W Mahalo Pl, Compton, CA 90220, USA.**

P

- ***Parker Hannifin Corporation* [Parkermotion]: Electromechanical Automation Division, 5500 Business Park Drive, Rohnert Park, CA 94928, USA.**
- ***Patek Philippe*, Rue des Vieux-Grenadiers 7, 1205 Genève, Switzerland.**
- ***Peiffer Machine Services*: 7650 Lancaster Ave, Mt Aetna, PA 19544, USA.**
- ***Perry Automation* [Consulting Inc.]: 3135 39th Ave N # 7, St Petersburg, FL 33714, USA.**
- ***Pratt & Whitney Canada*: 1000 Marie-Victorin, Longueuil, QC J4G 1A1, Canada.**
- ***Premier Machinery*: 5 Monterey Rd, Dandenong VIC 3175, Australia.**

Q—n/a

R

- ***RAS Bearings Pvt. Ltd.*: 16, Abhinav Arcade, Nr. Bank of Baroda, Pritamnagar, Paldi, Ahmedabad-380006, India.**
- ***Renishaw plc* [HQ]: New Mills, Wotton-under-Edge, GL12 8JR, UK.**
- ***Retter Automation & Messtechnik GmbH*: Unter dem Malesfelsen 44, D-72458 Albstadt-Ebingen, Germany.**
- ***Rottler Manufacturing*: 8029 S 200th St, Kent, WA 98032, USA.**
- ***R T Bearings Ltd.*: Bevan Industrial Estate, Brierley Hill DY5 3TF, UK.**
- ***RWTH Aachen University*: Mechanical Engineering, Templergraben 55, 52062 Aachen, Germany.**

S

- ***Schaeffler AG*: Industriestr. 1-3, 91074, Herzogenaurach, Germany.**
- ***Schaeffler Technologies AG & Co. KG*: Inastraße 1, 91315 Höchstadt, Germany.**
- ***Scraping Community of India*: No. 6-155, Kamarajar Street, Medavakkam, Chennai - 600100, Tamil Nadu, India.**
- ***SKF Group* (Headquarters): SE-415 50, Gothenburg, Sweden.**
- ***SKF USA Inc.* [North American HQ]: 890 Forty Foot Rd., P.O. Box 352, Lansdale, PA 19446, USA.**
- ***SKF USA Inc.*: 20 Industrial Dr, Hanover, PA 17331, USA.**
- ***SKF USA Inc.* [Solution Factory]: 3443 North Sam Houston Pkwy W #100, Houston, TX 77086, USA.**
- ***SolidCAM*: 1107 Taylorsville Rd #3, Washington Crossing, PA 18977, USA.**

- ***Southampton Solent University*: Technology Faculty, East Park Terrace, Southampton, Hampshire SO14 0YN, UK.**
- ***Spear & Jackson Group*: Atlas Way, Atlas North, Sheffield, S4 7QQ, UK.**
- ***Spectrum Metrology Ltd*: 8 Ireton Avenue, Leicester LE4 9EU, UK.**

T

- ***Tampere University of Technology*: Korkeakoulunkatu 10, 33720 Tampere, Finland.**
- ***Taylor Hobson Ltd.*: 2 New Star Rd, Leicester, LE4 9JD, UK.**
- ***Tesa / Brown & Sharpe*: for contact details see - Hexagon Metrology.**
- ***Chicago THK America, Inc.* [HQ]: 200 East. Commerce Drive, Schaumburg, IL 60173, USA.**
- ***THK GmbH European Headquarters*: Hubert-Wollenberg-Strasse 13-15, D-40878 Ratingen, Germany.**
- **Total Engineering Developments (UK): 2 Lingy Close Road, Dalston, Cumbria CA5 7LB, UK.**
- ***Trapet Precision Engineering*: Berretin 10, 01139 Sarria (Alava), Spain.**

U—n/a

V—n/a

W—n/a

- ***University of Warwick*: School of Engineering, Coventry CV4 7AL, UK.**
- ***Werkzeugmaschinenlabor (WZL) der RWTH Aachen* [WZLRTHAACHEN]: Steinbachstraße 19, 52074 Aachen, Germany.**

X—n/a

Y

- ***Yama Seiki USA INC*: 5788 Schaefer Ave., Chino, CA 91710, USA.**
- ***YAMAZAKI MAZAK CORPORATION*: (Head Office) 1-131, Takeda, Oguchi-cho, Niwa-gun, Aichi 480-0197, Japan.**
- ***YAMAZAKI MAZAK UK Ltd*: Badgeworth Dr, Worcester WR4 9NF, UK.**
- ***YASDA PRECISION TOOLS K.K.* (Japan): 1160 Hamanaka, Satosho-cho, Asakuchi-gun, Okayama, 719-0303 Japan.**

Z—n/a

Index

G.T. Smith, *Machine Tool Metrology*, DOI 10.1007/978-3-319-25109-7

M

S